

Copyright  
by  
Alberto C. Marquez  
2014

**The Thesis Committee for Alberto C. Marquez  
Certifies that this is the approved version of the following thesis:**

**Finite Element Analysis of Welds Attaching Short Doubler Plates in  
Steel Moment Resisting Frames**

**APPROVED BY  
SUPERVISING COMMITTEE:**

**Supervisor:**

\_\_\_\_\_  
Michael D. Engelhardt

\_\_\_\_\_  
Todd A. Helwig

**Finite Element Analysis of Welds Attaching Short Doubler Plates in  
Steel Moment Resisting Frames**

**by**

**Alberto C. Marquez, BS**

**Thesis**

Presented to the Faculty of the Graduate School of

The University of Texas at Austin

in Partial Fulfillment

of the Requirements

for the Degree of

**Master of Science in Engineering**

**The University of Texas at Austin**

**December 2014**

## **Dedication**

I dedicate this to my family



## **Acknowledgements**

I would like to extend my deepest appreciation to Dr. Michael Engelhardt for your guidance, time and vast patience in this journey. Your “down to earth” attitude and “open door” policy have given me another life goal to aspire to, beyond this work.

A very special “thank you” is due to Dr. Todd Helwig, for the good advice, support and assistance in reading this thesis and making recommendations. Also for being one of the best teachers I have had in my life and instilling in me a huge appreciation for the stability of structures.

I dedicate this thesis to my family for the support that they have provided my entire life and in particular, I must acknowledge my wife, editor, and best friend, Emily, without whose love, encouragement and assistance, I would not have finished this thesis. I would also like to thank the Lord for my mother, my greatest example of a hard worker, and for my brothers Salva, Leo and Carlos whom I can always count on.

I would also like to acknowledge my friends Maria, Pat, and Emmey for the great conversations and the encouragement to come to graduate school. Without your motivation I would not have gotten here.

## **Abstract**

# **Finite Element Analysis of Fitted Doubler Plate Attachments in Steel Moment Resisting Frames**

Alberto C. Marquez, MSE

The University of Texas at Austin, 2014

Supervisor: Michael D. Engelhardt

A number of recent research studies have investigated the performance of panel zones in seismic-resistant steel Special Moment Resisting Frames (SMF). These recent studies investigated various options for attaching doubler plates to the column at beam-column joints in SMF for purpose of increasing the shear strength of the panel zone. This previous work was primarily focused on doubler plates that extend beyond the top and bottom of the attached beams, and considered cases both with and without continuity plates.

As an extension to this previous research, this thesis explores the situation when a doubler plate is fitted between the continuity plates. The objective of this research was to evaluate various options for welding fitted doubler plates to the column and continuity plates through the use of finite element analysis, and to provide recommendations for design. The development and validation of the finite element model are described, along with the results of an extensive series of parametric studies on various panel zone

configurations and attachment details for fitted doubler plates. Based on the results of these analyses, recommendations are provided for design of welds used for attaching fitted doubler plates in the panel zone of SMF systems.

## Table of Contents

List of Tables .....	xiii
List of Figures .....	xvi
<b>CHAPTER 1.....</b>	<b>1</b>
Introduction.....	1
1.1 Background.....	1
1.2 Statement of the Problem.....	3
1.3 Research Objectives.....	5
1.4 Outline of the Thesis.....	5
1.5 Nomenclature.....	6
<b>CHAPTER 2.....</b>	<b>8</b>
Literature Review.....	8
2.1 Overview.....	8
2.2 Previous Literature Discussed By Others .....	8
2.3 Research by Graham, J.D. et al (1959).....	8
2.4 Research by Fielding & Huang (1975).....	12
2.5 Research by Becker (1975).....	16
2.6 Research by Krawinkler (1978).....	18
2.7 Research by Popov (1987).....	21
2.8 Research by El-Tawil et Al (1999/2000).....	23
2.9 Research by Ricles et Al (2004) .....	27
2.10 Research by Shirsat (2011) .....	30
2.11 Research by Donkada (2012).....	33
2.12 Research by Gupta (2013) .....	35
2.13 Summary.....	38

<b>CHAPTER 3.....</b>	<b>43</b>
Modeling Techniques.....	43
3.1 Overview.....	43
3.2 Abaqus Program.....	43
3.2.1 Stages.....	44
3.2.2 Modules.....	45
3.2.2.1 Part Module.....	45
3.2.2.2 Property Module.....	45
3.2.2.3 Assembly Module.....	46
3.2.2.4 Step Module.....	46
3.2.2.5 Interaction Module.....	47
3.2.2.6 Load Module.....	47
3.2.2.7 Mesh Module.....	47
3.2.2.8 Job Module.....	48
3.2.2.9 Visualization Module.....	48
3.3 Structural Modeling in Abaqus.....	49
3.3.1 Element Type.....	49
3.3.2 Model Parts.....	50
3.3.3 Material Model.....	55
3.3.4 Meshing Techniques.....	59
3.3.5 Assembly.....	62
3.3.6 Time Step.....	69
3.3.7 Loading and Boundary Conditions.....	70
3.3.8 Modeling of Welds.....	72
3.3.9 Post Processing.....	75
3.3.10 Modeling Assumptions and Limitations.....	76
3.4 Abaqus Comparisons.....	76
3.4.1 Modeling of a Tension Coupon Test.....	77
3.4.1.1 Assembly & Test.....	78
3.4.1.2 Results.....	78

3.4.2 Modeling of a Shear Link .....	79
3.4.3.1 Assembly.....	80
3.4.3.2 Test.....	82
3.4.3.3 Results.....	83
3.4.4 Modeling of a DBBWWPZ Connection .....	88
3.4.4.1 Assembly.....	88
3.4.4.2 Test.....	90
3.4.4.3 Results.....	91
3.5 Chapter Summary .....	93
<b>CHAPTER 4.....</b>	<b>94</b>
Parametric Studies on Attachment Details of Doubler Plates in a W14X398 Column .....	94
4.1 Introduction.....	94
4.2 Analysis cases .....	105
4.2.1 Analysis Case 1 .....	106
4.2.2 Analysis Case 1A.....	109
4.2.3 Analysis Case 1A1 .....	119
4.2.4 Analysis Case 1C .....	132
4.2.5 Analysis Case 1C1 .....	142
4.2.6 Analysis Case 2A1 .....	155
4.2.7 Analysis Case 2C1 .....	168
4.2.8 Analysis Case 3A.....	181
4.2.9 Analysis Case 3A1 .....	191
4.2.10 Analysis Case 3C .....	204
4.2.11 Analysis Case 3C1 .....	214
4.2.12 Analysis Case 4A.....	227
4.2.13 Analysis Case 4A1 .....	237
4.2.14 Analysis Case 4C .....	250
4.2.15 Analysis Case 4C1 .....	260
4.2.16 Analysis Case 5A1 .....	271

4.2.17 Analysis Case 5C1 .....	284
4.3 Discussion of analysis results .....	297
4.3.1 Case Series 1 .....	299
4.3.2 Case Series 2 .....	301
4.3.3 Case Series 3 .....	303
4.3.4 Case Series 4 .....	304
4.3.5 Case Series 5 .....	305
4.3.6 Forces in the Welds.....	310
4.3.7 Summary .....	312
<b>CHAPTER 5.....</b>	<b>314</b>
Parametric Studies on Attachment Details of Doubler Plates in a W40X264 Column .....	314
5.1 Introduction.....	314
5.2 Analysis cases .....	315
5.2.1 Analysis Case 6.....	316
5.2.2 Analysis Case 6A.....	319
5.2.3 Analysis Case 6A1.....	329
5.2.4 Analysis Case 6C.....	342
5.2.5 Analysis Case 6C1.....	352
5.2.6 Analysis Case 7A1.....	365
5.2.7 Analysis Case 7C1.....	378
5.2.8 Analysis Case 8A.....	391
5.2.9 Analysis Case 8A1.....	401
5.2.10 Analysis Case 8C.....	414
5.2.11 Analysis Case 8C1.....	424
5.2.12 Analysis Case 9A.....	437
5.2.13 Analysis Case 9C.....	447
5.2.14 Analysis Case 10A1.....	457
5.2.15 Analysis Case 10C1.....	470
5.3 Discussion of analysis results .....	483

5.3.1 Case Comparisons.....	487
5.3.2 Forces in the Welds.....	493
5.3.3 Summary .....	501
<b>CHAPTER 6.....</b>	<b>503</b>
Summary and Conclusions .....	503
6.1 Summary .....	503
6.2 Conclusions.....	504
6.3 Future Work.....	505
Appendix A: Sample Abaqus Input File for W40x264 Column Case 8C1 .....	508
Appendix B: Matlab Code for Parsing of Large Section Force Data File .....	522
Appendix C: Abaqus Batch Job Instructions .....	524
References.....	525



## List of Tables

Table 3.1: Part meshing techniques and sizes for specimens .....	59
Table 3.2: Part constraints and contact surface discretization for W40x264 & W14x398 .....	66
Table 4.1: Force difference between DP edge and weld segments.....	100
Table 4.2: Analysis cases for W14x398 “shallow” column .....	105
Table 4.3: Panel zone shear and force on loading plate Case 1 .....	107
Table 4.4: Panel zone shear and force on loading plate Case 1A .....	110
Table 4.5: Panel zone shear and force on loading plate Case 1A1 .....	120
Table 4.6: Panel zone shear and force on loading plate Case 1C .....	133
Table 4.7: Panel zone shear and force on loading plate Case 1C1 .....	143
Table 4.8: Panel zone shear and force on loading plate Case 2A1 .....	156
Table 4.9: Panel zone shear and force on loading plate Case 2C1 .....	169
Table 4.10: Panel zone shear and force on loading plate Case 3A .....	182
Table 4.11: Panel zone shear and force on loading plate Case 3A1 .....	192
Table 4.12: Panel zone shear and force on loading plate Case 3C .....	205
Table 4.13: Panel zone shear and force on loading plate Case 3C1 .....	215
Table 4.14: Panel zone shear and force on loading plate Case 4A .....	228
Table 4.15: Panel zone shear and force on loading plate Case 4A1 .....	238
Table 4.16: Panel zone shear and force on loading plate Case 4C .....	251
Table 4.17: Panel zone shear and force on loading plate Case 4C1 .....	261
Table 4.18: Panel zone shear and force on loading plate Case 5A1 .....	272
Table 4.19: Panel zone shear and force on loading plate Case 5C1 .....	285

Table 4.20: Summary of VMS stresses and forces on column web and DP at Stg. 01 and Stg. 04. ....	297
Table 4.21: Total force transferred to DP by top horizontal weld .....	306
Table 4.22: Total force transferred to DP by left vertical weld .....	307
Table 4.23: Average force transferred by two outermost horizontal weld segments	308
Table 4.24: Average force transferred by two outermost vertical weld segments	309
Table 4.25: Relation between the horizontal force in the horizontal weld and shear strength of DP .....	310
Table 4.26: Relation between the vertical force in the vertical weld and shear strength of DP .....	311
Table 5.1: Analysis cases for W40x264 “shallow” column .....	315
Table 5.2: Panel zone shear and force on loading plate Case 6 .....	317
Table 5.3: Panel zone shear and force on loading plate Case 6A .....	320
Table 5.4: Panel zone shear and force on loading plate Case 6A1 .....	330
Table 5.5: Panel zone shear and force on loading plate Case 6C .....	343
Table 5.6: Panel zone shear and force on loading plate Case 6C1 .....	353
Table 5.7: Panel zone shear and force on loading plate Case 7A1 .....	366
Table 5.8: Panel zone shear and force on loading plate Case 7C1 .....	379
Table 5.9: Panel zone shear and force on loading plate Case 8A .....	392
Table 5.10: Panel zone shear and force on loading plate Case 8A1 .....	402
Table 5.11: Panel zone shear and force on loading plate Case 8C .....	415
Table 5.12: Panel zone shear and force on loading plate Case 8C1 .....	425
Table 5.13: Panel zone shear and force on loading plate Case 9A .....	438
Table 5.14: Panel zone shear and force on loading plate Case 9C .....	448
Table 5.15: Panel zone shear and force on loading plate Case 10A1 .....	458

Table 5.16: Panel zone shear and force on loading plate Case 10C1 .....	471
Table 5.17: Summary of VMS stresses and forces on column web and DP at Stg. 01 and Stg. 04 .....	483
Table 5.18: Total force transferred to DP by top horizontal weld .....	495
Table 5.19: Total force transferred to DP by vertical weld .....	496
Table 5.20: Average force transferred by two outermost horizontal weld segments	497
Table 5.21: Average force transferred by two outermost vertical weld segments	498
Table 5.22: Relation between the horizontal force in the horizontal weld and shear strength of DP .....	499
Table 5.23: Relation between the vertical force in the vertical weld and shear strength of DP .....	500

## List of Figures

Figure 1.1: Typical Shear and Moment Diagrams in the Column of an SMF Under Lateral Load .....	3
Figure 1.2: Typical Beam-Column Joint Region in an SMF .....	4
Figure 1.3: Extended, Fitted (clipped and unclipped) DP .....	6
Figure 2.1: Four-Way Test in Progress at Lehigh’s Fritz Lab, (Graham, 1959) .....	9
Figure 2.2: A Series Specimens - Un-Reinforced Columns, (Graham, 1959).....	10
Figure 2.3: PZ Joint Rotation for Column with Extended DP, (Graham, 1959) ...	12
Figure 2.4: Test Setup, (Fielding & Huang, 1975) .....	13
Figure 2.5: Fillet Weld Cross-Section .....	14
Figure 2.6: Specimen 1 & 3 (Becker, 1975) .....	16
Figure 2.7: Panel Zone Deformations & Forces on Joint (Krawinkler, 1978) .....	18
Figure 2.8: Web Doubler Plate Layouts (AISC 341-10) .....	21
Figure 2.9: Specimen PN3 (Popov, 1987) .....	22
Figure 2.10: Specimens 2 & 6 (Popov, 1987).....	23
Figure 2.11: Specimens with Different Web Thickness, (El-Tawil, 1999) .....	26
Figure 2.12: Specimens With and Without CP (El-Tawil, 2000).....	27
Figure 2.13: Hysteretic Response of Different PZ Strengths (Ricles, 2002).....	29
Figure 2.14: DP Arrangements Tested (Shirsat, 2011).....	31
Figure 2.15: Deep Column Specimen (Donkada, 2012).....	34
Figure 2.16: FE model of shallow column, and deep column (Gupta, 2013).....	36
Figure 2.17: Web/DP Crippling Case 2B (Gupta, 2013) .....	37
Figure 3.1: Abaqus Stages of Analysis (Abaqus 6.12.2).....	45
Figure 3.2: (a) Column, (b) Loading Plate, (c) Doubler Plate, (d) Column Profile	50

Figure 3.3 Vertical groove welds between the DP and the column flanges .....	52
Figure 3.4: Horizontal fillet welds between the DP and the column web .....	52
Figure 3.5: CJP2 and CJP3 view without column in view .....	54
Figure 3.6: Typical models of stress-strain curves, (Ho, 2010).....	55
Figure 3.7: A992 Steel tri-linear model (Okazaki, 2004).....	57
Figure 3.8: <i>Abaqus</i> A992 Steel definition (Units = Ksi, in/in).....	58
Figure 3.9: Column K-Zone where complex geometries meet.....	60
Figure 3.10: (A) Mesh without partitions, (B) Partitioning, (C) Mesh with partitions .....	61
Figure 3.11: Mesh methods used on column attachments of W14x398.....	62
Figure 3.12: Clipped DP onto W40x264 column (Part colors based on material definition).....	64
Figure 3.13: A “rigid body constraint” defines the roller BC at the top of the column .....	65
Figure 3.14: Data points for checking PZ rotation on W40x264 column.....	66
Figure 3.15: Data points used to define PZ rotation on a W14x398 column.....	68
Figure 3.16: “Section Force” surface selections on W14x398 column specimen .	69
Figure 3.17: Surface “DBL1” section force output request.....	70
Figure 3.18: Meshing, loading and boundary conditions for the W40x264 model	71
Figure 3.19: Meshing of the vertical groove weld, <b>VGW1</b> .....	72
Figure 3.20: Subdivided weld surface attached to DP .....	74
Figure 3.21: Path along the center of the column showing Von Misses stress.....	75
Figure 3.22: ASTM-A 370-08 Standard dimensions for tension coupon test .....	77
Figure 3.23: Tension coupon boundary conditions and resulting stresses.....	78
Figure 3.24: Tension coupon laboratory test vs. Abaqus model comparison.....	79

Figure 3.25: Abaqus boundary conditions for shear link model (Gupta, 2013) ....	79
Figure 3.26: Shear link assembly 12 (Ryu, 2005) .....	80
Figure 3.27: Shear link material definitions .....	81
Figure 3.28: Qualitative moment (A) and shear (B) diagrams (Ryu, 2005).....	82
Figure 3.29: “Severe” loading protocol and Lab vs. Abaqus model results .....	84
Figure 3.30: “Random” loading protocol and Lab vs. Abaqus model results .....	85
Figure 3.31: “AISC” loading protocol and Lab vs. Abaqus model results.....	86
Figure 3.32: Lab vs. Abaqus model results using “MON” load protocol (Chart and Image) .....	87
Figure 3.33: DBBWVZ Test setup (Engelhardt et al, 2000) .....	88
Figure 3.34: DBBWVZ Abaqus model (Gupta, 2013).....	89
Figure 3.35: DBBWVZ loading protocol and first 18 steps of Abaqus amplitude	90
Figure 3.36: DBBWVZ column tip displacement vs. column tip load.....	92
Figure 3.37: DBBWVZ column tip load vs. VZ rotation.....	92
Figure 3.38: DBBWVZ VMS values at .04 rad. inter-story drift .....	93
Figure 4.1: Equation J10-11 (AISC 2010) and $1.25V_{pz}$ Calculations, (Shirsat, 2011) .....	95
Figure 4.2: PEEQ and VMS values reported from center of column .....	97
Figure 4.3: Horizontal weld and groove weld attaching DP.....	98
Figure 4.4: Nodes shared by doubler plate and column web .....	99
Figure 4.5: Stresses on groove weld and left side of DP .....	101
Figure 4.6: Paths defined through center of cross-section at different levels.....	102
Figure 4.7 Global Axis used for the forces on welds, Y is parallel to applied force	104
Figure 4.8: Analysis Case 1 .....	106
Figure 4.9: Panel zone shear vs. panel zone rotation Case 1 .....	107

Figure 4.10: VMS and PEEQ in the column Case 1 .....	108
Figure 4.11: Analysis case 1A .....	109
Figure 4.12: Panel zone shear vs. panel zone rotation Case 1A .....	110
Figure 4.13: VMS and PEEQ in the column Case 1A .....	111
Figure 4.14: VMS distribution in column web at different heights Stg. 01-04 ...	112
Figure 4.14: VMS distribution in column web at different heights Stg. 01-04 ...	113
Figure 4.15: VMS and PEEQ in the DP Case 1A .....	114
Figure 4.16: Shear stress, S23 in the DP Case 1A .....	115
Figure 4.17: VMS distribution at mid-depth of DP Case 1A .....	115
Figure 4.18: Forces and stresses in vertical weld (X) .....	116
Figure 4.19: Forces and stresses in vertical weld (Y) .....	117
Figure 4.20: Forces and stresses in vertical weld (Z) .....	118
Figure 4.21: Analysis case 1A1 .....	119
Figure 4.22: Panel zone shear vs. panel zone rotation Case 1A1 .....	120
Figure 4.23: VMS and PEEQ in the column Case 1A1 .....	121
Figure 4.24: VMS distribution in column web at different heights Stg. 01-04 Case 1A1 .....	122
Figure 4.24: VMS distribution in column web at different heights Stg. 01-04 Case 1A1 .....	123
Figure 4.25: VMS and PEEQ in the DP Case 1A1 .....	124
Figure 4.26: Shear stress, S23 in the DP Case 1A1 .....	125
Figure 4.27: VMS distribution at mid-depth of DP Case 1A1 .....	125
Figure 4.28: Forces and stresses in horizontal weld, (X) Case 1A1 .....	126
Figure 4.29: Forces and stresses in horizontal weld, (Y) Case 1A1 .....	127
Figure 4.30: Forces and stresses in horizontal weld, (Z) Case 1A1 .....	128

Figure 4.31: Forces and stresses in vertical weld, (X) Case 1A1 .....	129
Figure 4.32: Forces and stresses in vertical weld, (Y) Case 1A1 .....	130
Figure 4.33: Forces and stresses in vertical weld, (Z) Case 1A1 .....	131
Figure 4.34: Analysis case 1C .....	132
Figure 4.35: Panel zone shear vs. panel zone rotation Case 1C .....	133
Figure 4.36: VMS and PEEQ in the column Case 1C .....	134
Figure 4.37: VMS distribution in column web at different heights Stg. 01-04 Case 1C .....	135
Figure 4.37: VMS distribution in column web at different heights Stg. 01-04 Case 1C .....	136
Figure 4.38: VMS and PEEQ in the DP Case 1C .....	137
Figure 4.39: Shear stress, S23 in the DP Case 1C .....	138
Figure 4.40: VMS distribution at mid-depth of DP Case 1C.....	138
Figure 4.41: Forces and stresses in vertical weld, (X) Case 1C .....	139
Figure 4.42: Forces and stresses in vertical weld, (Z) Case 1C .....	141
Figure 4.43: Analysis case 1C1 .....	142
Figure 4.44: Panel zone shear vs. panel zone rotation Case 1C1 .....	143
Figure 4.45: VMS and PEEQ in the column Case 1C1 .....	144
Figure 4.46: VMS distribution in column web at different heights Stg. 01-04 Case 1C1 .....	145
Figure 4.46: VMS distribution in column web at different heights Stg. 01-04 Case 1C1 .....	146
Figure 4.47: VMS and PEEQ in the DP Case 1C1 .....	147
Figure 4.48: Shear stress, S23 in the DP Case 1C1 .....	148
Figure 4.49: VMS distribution at mid-depth of DP Case 1C1 .....	148



Figure 4.50: Forces and stresses in horizontal weld, (X) Case 1C1 .....	149
Figure 4.51: Forces and stresses in horizontal weld, (Y) Case 1C1 .....	150
Figure 4.52: Forces and stresses in horizontal weld, (Z) Case 1C1 .....	151
Figure 4.53: Forces and stresses in vertical weld, (X) Case 1C1 .....	152
Figure 4.54: Forces and stresses in vertical weld, (Y) Case 1C1 .....	153
Figure 4.55: Forces and stresses in vertical weld, (Z) Case 1C1 .....	154
Figure 4.56: Analysis case 2A1 .....	155
Figure 4.57: Panel zone shear vs. panel zone rotation Case 2A1 .....	156
Figure 4.58: VMS and PEEQ in the column Case 2A1 .....	157
Figure 4.59: VMS distribution in column web at different heights Stg. 01-04 Case 2A1 .....	158
Figure 4.59: VMS distribution in column web at different heights Stg. 01-04 Case 2A1 .....	159
Figure 4.60: VMS and PEEQ in the DP Case 2A1 .....	160
Figure 4.61: Shear stress, S23 in the DP Case 2A1 .....	161
Figure 4.62: VMS distribution at mid-depth of DP Case 2A1 .....	161
Figure 4.63: Forces and stresses in horizontal weld, (X) Case 2A1 .....	162
Figure 4.64: Forces and stresses in horizontal weld, (Y) Case 2A1 .....	163
Figure 4.65: Forces and stresses in horizontal weld, (Z) Case 2A1 .....	164
Figure 4.66: Forces and stresses in vertical weld, (X) Case 2A1 .....	165
Figure 4.67: Forces and stresses in vertical weld, (Y) Case 2A1 .....	166
Figure 4.68: Forces and stresses in vertical weld, (Z) Case 2A1 .....	167
Figure 4.69: Analysis case 2C1 .....	168
Figure 4.70: Panel zone shear vs. panel zone rotation Case 2C1 .....	169
Figure 4.71: VMS and PEEQ in the column Case 2C1 .....	170

Figure 4.72: VMS distribution in column web at different heights Stg. 01-04 Case 2C1 .....	171
Figure 4.72: VMS distribution in column web at different heights Stg. 01-04 Case 2C1 .....	172
Figure 4.73: VMS and PEEQ in the DP Case 2C1 .....	173
Figure 4.74: Shear stress, S23 in the DP Case 2C1 .....	174
Figure 4.75: VMS distribution at mid-depth of DP Case 2C1 .....	174
Figure 4.76: Forces and stresses in horizontal weld, (X) Case 2C1 .....	175
Figure 4.77: Forces and stresses in horizontal weld, (Y) Case 2C1 .....	176
Figure 4.78: Forces and stresses in horizontal weld, (Z) Case 2C1 .....	177
Figure 4.79: Forces and stresses in vertical weld, (X) Case 2C1 .....	178
Figure 4.80: Forces and stresses in vertical weld, (Y) Case 2C1 .....	179
Figure 4.81: Forces and stresses in vertical weld, (Z) Case 2C1 .....	180
Figure 4.82: Analysis case 3A .....	181
Figure 4.83: Panel zone shear vs. panel zone rotation Case 3A .....	182
Figure 4.84: VMS and PEEQ in the column Case 3A .....	183
Figure 4.85: VMS distribution in column web at different heights Stg. 01-04 Case 3A .....	184
Figure 4.85: VMS distribution in column web at different heights Stg. 01-04 Case 3A .....	185
Figure 4.86: VMS and PEEQ in the DP Case 3A.....	186
Figure 4.87: Shear stress, S23 in the DP Case 3A .....	187
Figure 4.88: Forces and stresses in vertical weld, (X) Case 3A .....	188
Figure 4.89: Forces and stresses in vertical weld, (Y) Case 3A .....	189
Figure 4.90: Forces and stresses in vertical weld, (Z) Case 3A.....	190

Figure 4.91: Analysis case 3A1 .....	191
Figure 4.92: Panel zone shear vs. panel zone rotation Case 3A1 .....	192
Figure 4.93: VMS and PEEQ in the column Case 3A1 .....	193
Figure 4.94: VMS distribution in column web at different heights Stg. 01-04 Case 3A1.....	194
Figure 4.94: VMS distribution in column web at different heights Stg. 01-04 Case 3A1.....	195
Figure 4.95: VMS and PEEQ in the DP Case 3A1 .....	196
Figure 4.96: Shear stress, S23 in the DP Case 3A1 .....	197
Figure 4.97: VMS distribution at mid-depth of DP Case 3A1 .....	197
Figure 4.98: Forces and stresses in horizontal weld, (X) Case 3A1 .....	198
Figure 4.99: Forces and stresses in horizontal weld, (Y) Case 3A1 .....	199
Figure 4.100: Forces and stresses in horizontal weld, (Z) Case 3A1 .....	200
Figure 4.101: Forces and stresses in vertical weld, (X) Case 3A1 .....	201
Figure 4.102: Forces and stresses in vertical weld, (Y) Case 3A1 .....	202
Figure 4.103: Forces and stresses in vertical weld, (Z) Case 3A1 .....	203
Figure 4.104: Analysis case 3C .....	204
Figure 4.105: Panel zone shear vs. panel zone rotation Case 3C .....	205
Figure 4.106: VMS and PEEQ in the column Case 3C .....	206
Figure 4.107: VMS distribution in column web at different heights Stg. 01-03 Case 3C.....	207
Figure 4.107: VMS distribution in column web at different heights Stg. 01-03 Case 3C.....	208
Figure 4.108: VMS and PEEQ in the DP Case 3C .....	209
Figure 4.109: Shear stress, S23 in the DP Case 3C .....	210

Figure 4.110: VMS distribution at mid-depth of DP Case 3C.....	210
Figure 4.111: Forces and stresses in vertical weld, (X) Case 3C .....	211
Figure 4.112: Forces and stresses in vertical weld, (Y) Case 3C .....	212
Figure 4.113: Forces and stresses in vertical weld, (Z) Case 3C .....	213
Figure 4.114: Analysis case 3C1 .....	214
Figure 4.115: Panel zone shear vs. panel zone rotation Case 3C1 .....	215
Figure 4.116 VMS and PEEQ in the column Case 3C1 .....	216
Figure 4.117: VMS distribution in column web at different heights Stg. 01-04 Case 3C1 .....	217
Figure 4.117: VMS distribution in column web at different heights Stg. 01-04 Case 3C1 .....	218
Figure 4.118: VMS and PEEQ in the DP Case 3C1 .....	219
Figure 4.119: Shear stress, S23 in the DP Case 3C1 .....	220
Figure 4.120: VMS distribution at mid-depth of DP Case 3C1.....	220
Figure 4.121: Forces and stresses in horizontal weld, (X) Case 3C1 .....	221
Figure 4.122: Forces and stresses in horizontal weld, (Y) Case 3C1 .....	222
Figure 4.123: Forces and stresses in horizontal weld, (Z) Case 3C1.....	223
Figure 4.124: Forces and stresses in vertical weld, (X) Case 3C1 .....	224
Figure 4.125: Forces and stresses in vertical weld, (Y) Case 3C1 .....	225
Figure 4.126: Forces and stresses in vertical weld, (Z) Case 3C1 .....	226
Figure 4.127: Analysis case 4A .....	227
Figure 4.128: Panel zone shear vs. panel zone rotation Case 4A .....	228
Figure 4.129: VMS distribution in column wed at different heights Stg. 01-04 Case 4A.....	230

Figure 4.129: VMS distribution in column wed at different heights Stg. 01-04 Case 4A.....	231
Figure 4.130: VMS and PEEQ in the DP Case 4A.....	232
Figure 4.131: VMS distribution at mid-depth of DP Case 4A .....	233
Figure 4.132: Forces and stresses in vertical weld, (X) Case 4A .....	234
Figure 4.133: Forces and stresses in vertical weld, (Y) Case 4A .....	235
Figure 4.134: Forces and stresses in vertical weld, (Z) Case 4A.....	236
Figure 4.135: Analysis case 4A1 .....	237
Figure 4.136: Panel zone shear vs. panel zone rotation Case 4A1 .....	238
Figure 4.137: VMS and PEEQ in the column Case 4A1 .....	239
Figure 4.138: VMS distribution in column wed at different heights Stg. 01-04 Case 4A1.....	240
Figure 4.138: VMS distribution in column wed at different heights Stg. 01-04 Case 4A1.....	241
Figure 4.139: VMS and PEEQ in the DP Case 4A1.....	242
Figure 4.140 Shear stress, S23 in the DP Case 4A1 .....	243
Figure 4.141: VMS distribution at mid-depth of DP Case 4A1 .....	243
Figure 4.142: Forces and stresses in horizontal weld, (X) Case 4A1 .....	244
Figure 4.143: Forces and stresses in horizontal weld, (Y) Case 4A1 .....	245
Figure 4.144: Forces and stresses in horizontal weld, (Z) Case 4A1 .....	246
Figure 4.145: Forces and stresses in vertical weld, (X) Case 4A1 .....	247
Figure 4.146: Forces and stresses in vertical weld, (Y) Case 4A1 .....	248
Figure 4.147: Forces and stresses in vertical weld, (Z) Case 4A1 .....	249
Figure 4.148: Analysis case 4C .....	250
Figure 4.149: Panel zone shear vs. panel zone rotation Case 4C .....	251

Figure 4.150: VMS and PEEQ in the column Case 4C .....	252
Figure 4.151: VMS distribution in column web at different heights Stg. 01-04 Case 4C .....	253
Figure 4.151: VMS distribution in column web at different heights Stg. 01-04 Case 4C .....	254
Figure 4.152: VMS and PEEQ in the DP Case 4C .....	255
Figure 4.153: Shear stress, S23 in the DP Case 4C .....	256
Figure 4.154: VMS distribution at mid-depth of DP Case 4C .....	256
Figure 4.155: Forces and stresses in vertical weld, (X) Case 4C .....	257
Figure 4.156: Forces and stresses in vertical weld, (Y) Case 4C .....	258
Figure 4.157: Forces and stresses in vertical weld, (Z) Case 4C .....	259
Figure 4.158: Analysis case 4C1 .....	260
Figure 4.159: Panel zone shear vs. panel zone rotation Case 4C1 .....	261
Figure 4.160: VMS and PEEQ in the column Case 4C1 .....	262
Figure 4.161: VMS and PEEQ in the DP Case 4C1 .....	263
Figure 4.162: Shear stress, S23 in the DP Case 4C1 .....	264
Figure 4.163: VMS distribution at mid-depth of DP Case 4C1 .....	264
Figure 4.164: Forces and stresses in horizontal weld, (X) Case 4C1 .....	265
Figure 4.165: Forces and stresses in horizontal weld, (Y) Case 4C1 .....	266
Figure 4.166: Forces and stresses in horizontal weld, (Z) Case 4C1 .....	267
Figure 4.167: Forces and stresses in vertical weld, (X) Case 4C1 .....	268
Figure 4.168: Forces and stresses in vertical weld, (Y) Case 4C1 .....	269
Figure 4.169: Forces and stresses in vertical weld, (Z) Case 4C1 .....	270
Figure 4.170: Analysis case 5A1 .....	271
Figure 4.171: Panel zone shear vs. panel zone rotation Case 5A1 .....	272

Figure 4.172: VMS and PEEQ in the column Case 5A1 .....	273
Figure 4.173: VMS distribution in column web at different heights Stg. 01-04 Case 5A1 .....	274
Figure 4.173: VMS distribution in column web at different heights Stg. 01-04 Case 5A1 .....	275
Figure 4.174: VMS and PEEQ in the DP Case 5A1 .....	276
Figure 4.175: Shear stress, S23 in the DP Case 5A1 .....	277
Figure 4.176: VMS distribution at mid-depth of DP Case 5A1 .....	277
Figure 4.177: Forces and stresses in horizontal weld, (X) Case 5A1 .....	278
Figure 4.178: Forces and stresses in horizontal weld, (Y) Case 5A1 .....	279
Figure 4.179: Forces and stresses in horizontal weld, (Z) Case 5A1 .....	280
Figure 4.180: Forces and stresses in vertical weld, (X) Case 5A1 .....	281
Figure 4.181: Forces and stresses in vertical weld, (Y) Case 5A1 .....	282
Figure 4.180: Forces and stresses in vertical weld, (Z) Case 5A1 .....	283
Figure 4.182: Panel zone shear vs. panel zone rotation Case 5C1 .....	285
Figure 4.183: VMS and PEEQ in the column Case 5C1 .....	286
Figure 4.184: VMS distribution in column web at different heights Stg. 01-04 Case 5C1 .....	287
Figure 4.184: VMS distribution in column web at different heights Stg. 01-04 Case 5C1 .....	288
Figure 4.185: VMS and PEEQ in the DP Case 5C1 .....	289
Figure 4.186: Shear stress, S23 in the DP Case 5C1 .....	290
Figure 4.187: VMS distribution at mid-depth of DP Case 5C1 .....	290
Figure 4.188: Forces and stresses in horizontal weld, (X) Case 5C1 .....	291
Figure 4.189: Forces and stresses in horizontal weld, (Y) Case 5C1 .....	292

Figure 4.190: Forces and stresses in horizontal weld, (Z) Case 5C1 .....	293
Figure 4.191: Forces and stresses in vertical weld, (X) Case 5C1 .....	294
Figure 4.192: Forces and stresses in vertical weld, (Y) Case 5C1 .....	295
Figure 4.193: Forces and stresses in vertical weld, (Z) Case 5C1 .....	296
Figure 4.194: PZ Shear vs. PZ Rotation comparison.....	298
Figure 4.195: Stresses in Horizontal and Vertical Weld at 0.1 Rad for Case Series 1 .....	299
Figure 4.196: Stresses in Horizontal and Vertical Weld at 0.1 Rad for Case Series 2 .....	301
Figure 4.197: Slightly higher VMS levels on Case 2C1.....	302
Figure 4.198: Stresses in Horizontal and Vertical Weld at 0.1 Rad for Case Series 3 .....	303
Figure 4.199: Stresses in Horizontal and Vertical Weld at 0.1 Rad for Case Series 4 .....	304
Figure 4.200: VMS and PEEQ values in the “gap” in Case series 4 .....	304
Figure 4.201: Stresses in Horizontal and Vertical Weld at 0.1 Rad for Case Series 5 .....	305
Figure 5.1:W40x264 Analysis case 6 .....	316
Figure 5.2: Panel zone shear vs. panel zone rotation Case 6 .....	317
Figure 5.3: VMS and PEEQ in the column Case 6.....	318
Figure 5.4: W40x264 Analysis case 6A .....	319
Figure 5.5: Panel zone shear vs. panel zone rotation Case 6A .....	320
Figure 5.6: VMS and PEEQ in the column Case 6A.....	321
Figure 5.7: VMS distribution in column web at different heights Stg. 01-04 Case 6A .....	322



Figure 5.7: VMS distribution in column web at different heights Stg. 01-04 Case 6A .....	323
Figure 5.8: VMS and PEEQ in the DP Case 6A.....	324
Figure 5.9: Shear stress, S23 in the DP Case 6A .....	325
Figure 5.10: VMS distribution at mid-depth of DP Case 6A .....	325
Figure 5.11: Forces and stresses in horizontal weld, (X) Case 6A.....	326
Figure 5.12: Forces and stresses in horizontal weld, (Y) Case 6A.....	327
Figure 5.13: Forces and stresses in horizontal weld, (Z) Case 6A .....	328
Figure 5.14: W40x264 Analysis case 6A1 .....	329
Figure 5.15: Panel zone shear vs. panel zone rotation Case 6A1 .....	330
Figure 5.16: VMS and PEEQ in the column Case 6A1 .....	331
Figure 5.17: VMS distribution in column web at different heights Stg. 01-04 Case 6A1.....	332
Figure 5.17: VMS distribution in column web at different heights Stg. 01-04 Case 6A1.....	333
Figure 5.18: VMS and PEEQ in the DP Case 6A1.....	334
Figure 5.19: Shear stress, S23 in the DP Case 6A1 .....	335
Figure 5.20: VMS distribution at mid-depth of DP Case 6A1 .....	335
Figure 5.21: Forces and stresses in horizontal weld, (X) Case 6A1 .....	336
Figure 5.22: Forces and stresses in horizontal weld, (Y) Case 6A1 .....	337
Figure 5.23: Forces and stresses in horizontal weld, (Z) Case 6A1 .....	338
Figure 5.24: Forces and stresses in vertical weld, (X) Case 6A1 .....	339
Figure 5.25: Forces and stresses in vertical weld, (Y) Case 6A1 .....	340
Figure 5.26: Forces and stresses in vertical weld, (Z) Case 6A1 .....	341
Figure 5.27: W40x264 Analysis case 6C.....	342

Figure 5.28: Panel zone shear vs. panel zone rotation Case 6C .....	343
Figure 5.29: VMS and PEEQ in the column Case 6C .....	344
Figure 5.30: VMS distribution in column web at different heights Stg. 01-04 Case 6C .....	345
Figure 5.30: VMS distribution in column web at different heights Stg. 01-04 Case 6C .....	346
Figure 5.31: VMS and PEEQ in the DP Case 6C .....	347
Figure 5.32: Shear stress, S23 in the DP Case 6C .....	348
Figure 5.33: VMS distribution at mid-depth of DP Case 6C.....	348
Figure 5.34: Forces and stresses in vertical weld, (X) Case 6C .....	349
Figure 5.35: Forces and stresses in vertical weld, (Y) Case 6C .....	350
Figure 5.36: Forces and stresses in vertical weld, (Z) Case 6C .....	351
Figure 5.37: W40x264 Analysis case 6C1 .....	352
Figure 5.38: Panel zone shear vs. panel zone rotation Case 6C1 .....	353
Figure 5.39: VMS and PEEQ in the column Case 6C1 .....	354
Figure 5.40: VMS distribution in column web at different heights Stg. 01-04 Case 6C1 .....	355
Figure 5.40: VMS distribution in column web at different heights Stg. 01-04 Case 6C1 .....	356
Figure 5.41: VMS and PEEQ in the DP Case 6C1 .....	357
Figure 5.42: Shear stress, S23 in the DP Case 6C1 .....	358
Figure 5.43: VMS distribution at mid-depth of DP Case 6C1 .....	358
Figure 5.44: Forces and stresses in horizontal weld, (X) Case 6C1 .....	359
Figure 5.45: Forces and stresses in horizontal weld, (Y) Case 6C1 .....	360
Figure 5.46: Forces and stresses in horizontal weld, (Z) Case 6C1 .....	361

Figure 5.47: Forces and stresses in vertical weld, (X) Case 6C1 .....	362
Figure 5.48: Forces and stresses in vertical weld, (Y) Case 6C1 .....	363
Figure 5.49: Forces and stresses in vertical weld, (Z) Case 6C1 .....	364
Figure 5.50: W40x264 Analysis case 7A1 .....	365
Figure 5.51: Panel zone shear vs. panel zone rotation Case 7A1 .....	366
Figure 5.52: VMS and PEEQ in the column Case 7A1 .....	367
Figure 5.53: VMS distribution in column web at different heights Stg. 01-04 Case 7A1.....	368
Figure 5.53: VMS distribution in column web at different heights Stg. 01-04 Case 7A1.....	369
Figure 5.54: VMS and PEEQ in the DP Case 7A1 .....	370
Figure 5.55: Shear stress, S23 in the DP Case 7A1 .....	371
Figure 5.56: VMS distribution at mid-depth of DP Case 7A1 .....	371
Figure 5.57: Forces and stresses in horizontal weld, (X) Case 7A1 .....	372
Figure 5.58: Forces and stresses in horizontal weld, (Y) Case 7A1 .....	373
Figure 5.59: Forces and stresses in horizontal weld, (Z) Case 7A1 .....	374
Figure 5.60: Forces and stresses in vertical weld, (X) Case 7A1 .....	375
Figure 5.61: Forces and stresses in vertical weld, (Y) Case 7A1 .....	376
Figure 5.62: Forces and stresses in vertical weld, (Z) Case 7A1 .....	377
Figure 5.63:W40x264 Analysis case 7C1.....	378
Figure 5.64: Panel zone shear vs. panel zone rotation Case 7C1 .....	379
Figure 5.65: VMS and PEEQ in the column Case 7C1 .....	380
Figure 5.66: VMS distribution in column web at different heights Stg. 01-04 Case 7C1.....	381

Figure 5.66: VMS distribution in column web at different heights Stg. 01-04 Case 7C1 .....	382
Figure 5.67: VMS and PEEQ in the DP Case 7C1 .....	383
Figure 5.68: Shear stress, S23 in the DP Case 7C1 .....	384
Figure 5.69: VMS distribution at mid-depth of DP Case 7C1 .....	384
Figure 5.70: Forces and stresses in horizontal weld, (X) Case 7C1 .....	385
Figure 5.71: Forces and stresses in horizontal weld, (Y) Case 7C1 .....	386
Figure 5.72: Forces and stresses in horizontal weld, (Z) Case 7C1 .....	387
Figure 5.73: Forces and stresses in vertical weld, (X) Case 7C1 .....	388
Figure 5.74: Forces and stresses in vertical weld, (Y) Case 7C1 .....	389
Figure 5.75: Forces and stresses in vertical weld, (X) Case 7C1 .....	390
Figure 5.76: W40x264 Analysis case 8A .....	391
Figure 5.77: Panel zone shear vs. panel zone rotation Case 8A .....	392
Figure 5.78: VMS and PEEQ in the column Case 8A .....	393
Figure 5.79: VMS distribution in column web at different heights Stg. 01-04 Case 8A .....	394
Figure 5.79: VMS distribution in column web at different heights Stg. 01-04 Case 8A .....	395
Figure 5.80: VMS and PEEQ in the DP Case 8A.....	396
Figure 5.81: Shear stress, S23 in the DP Case 8A .....	397
Figure 5.81: VMS distribution at mid-depth of DP Case 8A .....	397
Figure 5.82: Forces and stresses in vertical weld, (X) Case 8A .....	398
Figure 5.83: Forces and stresses in vertical weld, (Y) Case 8A .....	399
Figure 5.84: Forces and stresses in vertical weld, (Z) Case 8A.....	400
Figure 5.85: W40x264 Analysis case 8A1 .....	401

Figure 5.86: Panel zone shear vs. panel zone rotation Case 8A1 .....	402
Figure 5.87: VMS and PEEQ in the column Case 8A1 .....	403
Figure 5.88: VMS distribution in column web at different heights Stg. 01-04 Case 8A1.....	404
Figure 5.88: VMS distribution in column web at different heights Stg. 01-04 Case 8A1.....	405
Figure 5.89: VMS and PEEQ in the DP Case 8A1 .....	406
Figure 5.90: Shear stress, S23 in the DP Case 8A1 .....	407
Figure 5.91: VMS distribution at mid-depth of DP Case 8A1 .....	407
Figure 5.92: Forces and stresses in horizontal weld, (X) Case 8A1 .....	408
Figure 5.93: Forces and stresses in horizontal weld, (Y) Case 8A1 .....	409
Figure 5.94: Forces and stresses in horizontal weld, (Z) Case 8A1 .....	410
Figure 5.95: Forces and stresses in vertical weld, (X) Case 8A1 .....	411
Figure 5.96: Forces and stresses in vertical weld, (Y) Case8A1 .....	412
Figure 5.97: Forces and stresses in vertical weld, (Z) Case 8A1 .....	413
Figure 5.98: W40x264 Analysis case 8C.....	414
Figure 5.99: Panel zone shear vs. panel zone rotation Case 8C .....	415
Figure 5.100: VMS and PEEQ in the column Case 8C .....	416
Figure 5.101: VMS distribution in column web at different heights Stg. 01-04 Case 8C.....	417
Figure 5.101: VMS distribution in column web at different heights Stg. 01-04 Case 8C.....	418
Figure 5.102: VMS and PEEQ in the DP Case 8C .....	419
Figure 5.103: Shear stress, S23 in the DP Case 8C .....	420
Figure 5.104: VMS distribution at mid-depth of DP Case 8C.....	420

Figure 5.105: Forces and stresses in vertical weld, (X) Case 8C .....	421
Figure 5.106: Forces and stresses in vertical weld, (Y) Case 8C .....	422
Figure 5.107: Forces and stresses in vertical weld, (Z) Case 8C .....	423
Figure 5.108: W40x264 Analysis case 8C1 .....	424
Figure 5.109: Panel zone shear vs. panel zone rotation Case 8C1 .....	425
Figure 5.110: VMS and PEEQ in the column Case 8C1 .....	426
Figure 5.111: VMS distribution in column web at different heights Stg. 01-04 Case 8C1 .....	427
Figure 5.111: VMS distribution in column web at different heights Stg. 01-04 Case 8C1 .....	428
Figure 5.112: VMS and PEEQ in the DP Case 8C1 .....	429
Figure 5.113: Shear stress, S23 in the DP Case 8C1 .....	430
Figure 5.114: VMS distribution at mid-depth of DP Case 8C1 .....	430
Figure 5.116: Forces and stresses in horizontal weld, (Y) Case 8C1 .....	432
Figure 5.117: Forces and stresses in horizontal weld, (Z) Case 8C1 .....	433
Figure 5.118: Forces and stresses in vertical weld, (X) Case 8C1 .....	434
Figure 5.119: Forces and stresses in vertical weld, (X) Case 8C1 .....	435
Figure 5.120: Forces and stresses in vertical weld, (Z) Case 8C1 .....	436
Figure 5.121: W40x264 Analysis case 9A .....	437
Figure 5.122: Panel zone shear vs. panel zone rotation Case 9A .....	438
Figure 5.123: VMS and PEEQ in the column Case 9A .....	439
Figure 5.124: VMS distribution in column web at different heights Stg. 01-04 Case 9A.....	440
Figure 5.124: VMS distribution in column web at different heights Stg. 01-04 Case 9A.....	441

Figure 5.125: VMS and PEEQ in the DP Case 9A.....	442
Figure 5.126: Shear stress, S23 in the DP Case 9A .....	443
Figure 5.127: VMS distribution at mid-depth of DP Case 9A .....	443
Figure 5.128: Forces and stresses in vertical weld, (X) Case 9A .....	444
Figure 5.129: Forces and stresses in vertical weld, (Y) Case 9A .....	445
Figure 5.130: Forces and stresses in vertical weld, (Z) Case 9A.....	446
Figure 5.131: W40x264 Analysis case 9C.....	447
Figure 5.132: Panel zone shear vs. panel zone rotation Case 9C .....	448
Figure 5.133: VMS and PEEQ in the column Case 9C .....	449
Figure 5.134: VMS distribution in column web at different heights Stg. 01-04 Case 9C.....	450
Figure 5.134: VMS distribution in column web at different heights Stg. 01-04 Case 9C.....	451
Figure 5.135: VMS and PEEQ in the DP Case 9C .....	452
Figure 5.136: Shear stress, S23 in the DP Case 9C .....	453
Figure 5.137: VMS distribution at mid-depth of DP Case 9C.....	453
Figure 5.138: Forces and stresses in vertical weld, (X) Case 9C .....	454
Figure 5.139: Forces and stresses in vertical weld, (Y) Case 9C .....	455
Figure 5.140: Forces and stresses in vertical weld, (Z) Case 9C .....	456
Figure 5.141: W40x264 Analysis case 10A1 .....	457
Figure 5.142: Panel zone shear vs. panel zone rotation Case 10A1 .....	458
Figure 5.143: VMS and PEEQ in the column Case 10A1 .....	459
Figure 5.144: VMS distribution in column web at different heights Stg. 01-04 Case 10A1.....	460

Figure 5.144: VMS distribution in column web at different heights Stg. 01-04 Case 10A1 .....	461
Figure 5.145: VMS and PEEQ in the DP Case 10A1 .....	462
Figure 5.146: Shear stress, S23 in the DP Case 10A1 .....	463
Figure 5.147: VMS distribution at mid-depth of DP Case 10A1 .....	463
Figure 5.148: Forces and stresses in horizontal weld, (X) Case 10A1 .....	464
Figure 5.149: Forces and stresses in horizontal weld, (Y) Case 10A1 .....	465
Figure 5.150: Forces and stresses in horizontal weld, (Z) Case 10A1 .....	466
Figure 5.151: Forces and stresses in vertical weld, (X) Case 10A1 .....	467
Figure 5.152: Forces and stresses in vertical weld, (Y) Case 10A1 .....	468
Figure 5.153: Forces and stresses in vertical weld, (Z) Case 10A1 .....	469
Figure 5.154: W40x264 Analysis case 10C1 .....	470
Figure 5.155: Panel zone shear vs. panel zone rotation Case .....	471
Figure 5.156: VMS and PEEQ in the column Case 10C1 .....	472
Figure 5.157: VMS distribution in column web at different heights Stg. 01-04 Case 10C1 .....	473
Figure 5.157: VMS distribution in column web at different heights Stg. 01-04 Case 10C1 .....	474
Figure 5.158: VMS and PEEQ in the DP Case 10C1 .....	475
Figure 5.159: Shear stress, S23 in the DP Case 10C1 .....	476
Figure 5.160: VMS distribution at mid-depth of DP Case 10C1 .....	476
Figure 5.161: Forces and stresses in horizontal weld, (X) Case 10C1 .....	477
Figure 5.162: Forces and stresses in horizontal weld, (Y) Case 10C1 .....	478
Figure 5.163: Forces and stresses in horizontal weld, (Z) Case 10C1 .....	479
Figure 5.164: Forces and stresses in vertical weld, (X) Case 10C1 .....	480



Figure 5.165: Forces and stresses in vertical weld, (Y) Case 10C1 .....	481
Figure 5.166: Forces and stresses in vertical weld, (Z) Case 10C1 .....	482
Figure 5.167: PZ Shear force vs PZ rotation plots for cases using a “deep” W40x264 column.....	484
Figure 5.168: Principal stress flow in column with and without CPs, near 0.1 PZ rotation .....	486
Figure 5.169: PZ and PZ shear force vs PZ rotation between Case 6A and 6A1	487
Figure 5.170: PZ and PZ shear force vs PZ rotation between Case 6C and 6C1	487
Figure 5.171: PZ and PZ shear force vs PZ rotation between Case 8A and 8A1	488
Figure 5.172: PZ shear force vs PZ rotation between Case 8C and 8C1 .....	488
Figure 5.173: PZ and PZ shear force vs PZ rotation between 6A1 and 8A.....	488
Figure 5.174 Difference in shear stresses in DPs with horizontal welds and without .....	489
Figure 5.175: Buckling of DPs at 0.1 radians (scaled 3 times).....	490
Figure 5.176: Weld stresses on case series 6 and 7 .....	491
Figure 5.177: Stress distributions for cases with highest PZ strength .....	492
Figure 5.178: Stress on horizontal weld segments due to horizontal forces.....	493
Figure 5.179: Vertical weld transfer of forces for “deep” (Left) and “shallow” (Right) columns .....	494
Figure 6.1: Abaqus PZ model with one beam attached .....	506
Figure 6.2: Abaqus PZ model with two beams attached .....	507

# CHAPTER 1

## Introduction

### 1.1 BACKGROUND

When designing a steel building for seismic resistance, one option for the lateral force resisting system (LFRS) is the use of Special Moment Frames (SMF). Steel SMF are designed to provide stiffness, strength and ductility when subject to lateral loads from earthquakes. Current U.S. requirements for the design and detailing of SMF for earthquake loading are specified in *ASCE 7-10 Minimum Design Loads for Buildings and Other Structures* (ASCE 2010) and in *AISC 341-10 Seismic Provisions for Structural Steel Buildings* (AISC 2010). SMF resist lateral loads through rigid frame action, resulting in flexure and shear in the beams and columns, which are joined using moment resisting connections. Under lateral load, large moments are developed at the ends of the clear span portions of beams and columns. As described in AISC 341-10, the primary source of ductility in SMF under severe earthquake loading is intended to be flexural yielding of the beam ends, in the region near the beam-to-column connection.

The shear in the clear span portion of the beams and columns in SMF subject to lateral load is generally quite small. However, the shear force in the portion of the column within the beam-column joint region is generally quite high. Figure 1.1 qualitatively shows the distribution of bending moment and shear force within the columns of an SMF. The portion of the column within the beam-column joint region is referred to as the *panel zone*. High shear in the column panel zone is the result of the high moment gradient within this region,

as illustrated in Figure 1.1. The high shear force in the panel zone region of columns can result in shear yielding of the panel zone under earthquake loading.

As described in AISC 341-10, limited shear yielding of the panel under earthquake loading is considered acceptable, although the primary yielding mechanism in an SMF is still required to be flexural yielding of the beam ends. Consequently, AISC 341-10 requires that the shear strength of the panel be adequate to resist the shear generated when the beam ends have achieved their fully yielded and strain hardened flexural strength. In many cases, the column by itself does not have adequate shear strength to satisfy this requirement. When this is the case, the shear strength of the panel zone can be increased by welding a *doubler plate* (DP) to the column in the panel zone region. The doubler plate serves to increase the web area of the column and therefore increases the column shear strength within the panel zone region.

Figure 1-2 shows a typical detail for a beam-column joint in an SMF. The beams are attached to column using a moment resisting connection. AISC 341-10 specifies design requirements for the beam-to-column connection in SMF, and a variety of different connection types can be used, as described in AISC 358-10. Many of the commonly used beam-to-column connection details employ complete joint penetration (CJP) groove welds between the beam flange and the column flange, as shown in Figure 1-2. In some cases, continuity plates (CP) are needed to locally reinforce the column flange or column web for the concentrated forces delivered to the face of the column by the beam flanges. AISC 341-10 specifies rules to determine when CPs are required, and rules to determine the size and welding details for CPs.

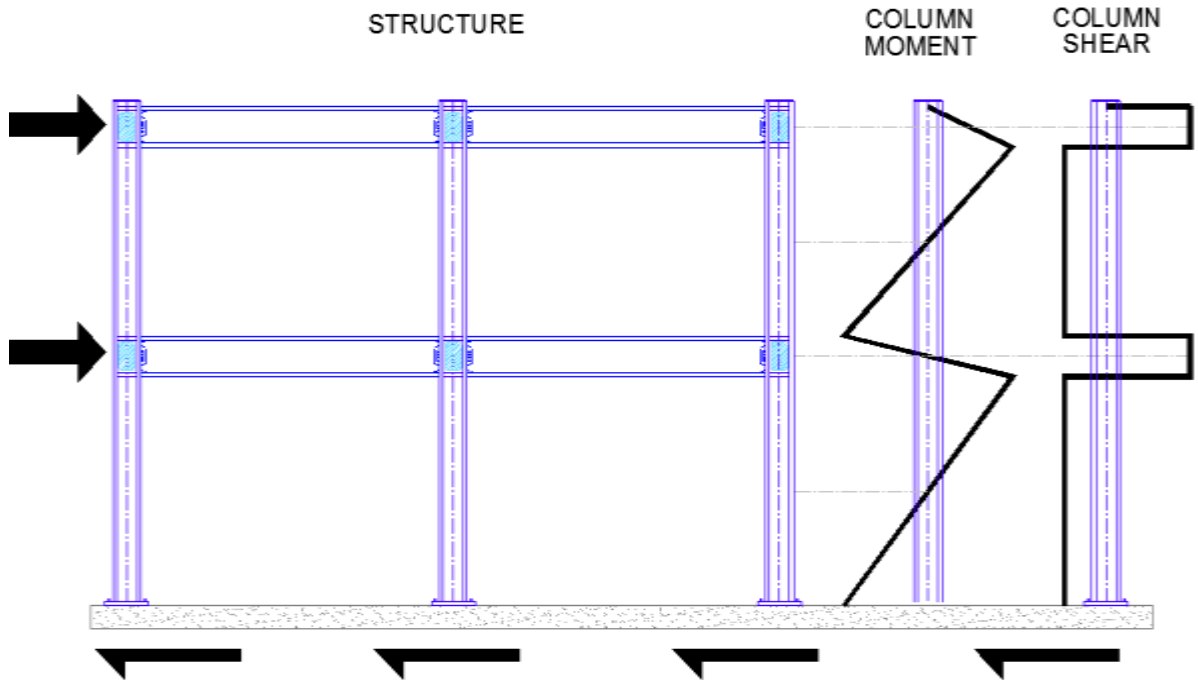


Figure 1.1: Typical Shear and Moment Diagrams in the Column of an SMF Under Lateral Load

## 1.2 STATEMENT OF THE PROBLEM

Much of the research involving the PZs in SMFs has focused on the global behavior of beam-column joints and overall performance of the SMF under earthquake loading with varying design approaches for determining the shear strength of the PZ and the effect of varying the relative strength of the PZ and the beams. However, less previous research has investigated the details of attachment of the doubler plate to the column, and how these details affect the performance of the PZ when subject to large shear forces and deformations. Recently, however, a series of research studies conducted at the University of Texas at Austin began to investigate the attachment details for DPs. This work is reported by Shirsat (2011), Donkada (2012), and Gupta (2013), who have focused on understanding the behavior of PZs reinforced by extended DPs. These three studies focused primarily on cases where the doubler plate was extended above and below the connected

beams, as shown in Figure 1-3(a), and investigated cases with and without continuity plates. The research reported in this thesis is an extension of this previous work, and more specifically will investigate the case where continuity plates are present, and the doubler plate is fitted between the continuity plates, as shown in Figure 1-3 (b) and (c).

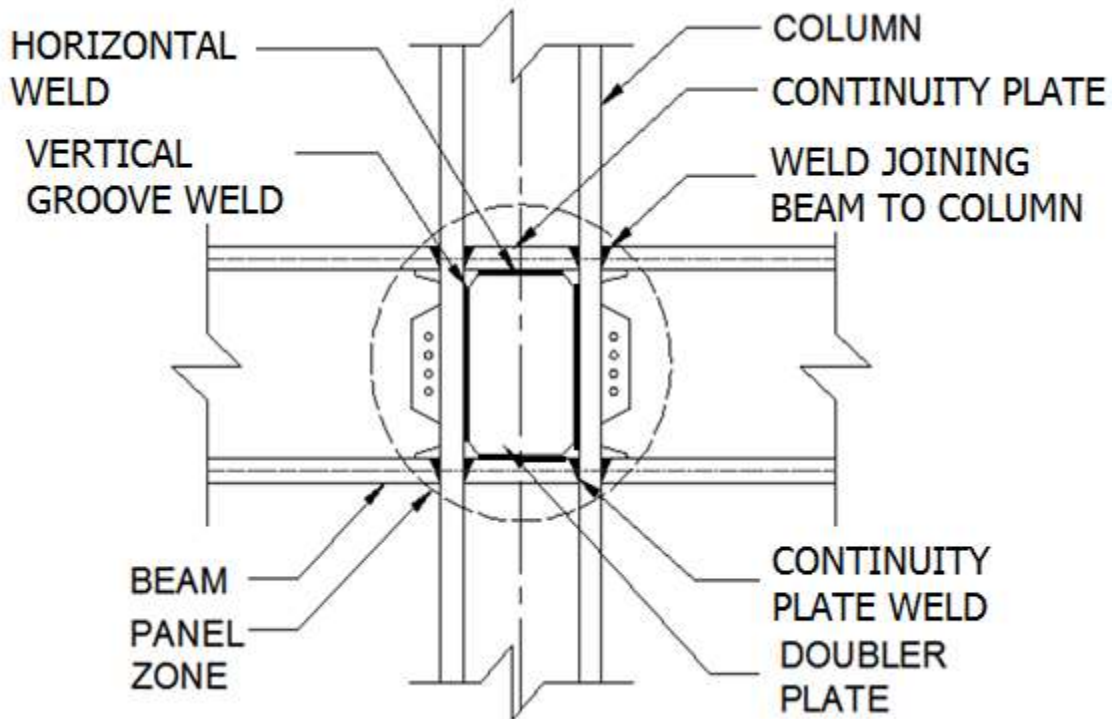


Figure 1.2: Typical Beam-Column Joint Region in an SMF

This thesis will describe the development of finite element models similar to those of the previous researchers and discuss the results of the analysis performed. Much of the focus will be placed on the effects that using a fitted DP has on the PZ and how forces flow thorough this design configuration. It will also attempt to bring design recommendations for the size and design of welds used to attach these fitted DPs.

### **1.3 RESEARCH OBJECTIVES**

The objectives of this research include the following:

- 1) Gain a better understanding of the performance of different attachment details for fitted DPs.
- 2) Study the effects that clipped corners on fitted doubler plates have in the PZ and the welds attaching it and gain a perspective of the force flow through the panel zone.
- 3) Report the forces and stresses that both horizontal and vertical welds transfer to the fitted DP and determine if both welds are necessary. Obtain a range of forces for which the welds attaching the plates should be designed for.

### **1.4 OUTLINE OF THE THESIS**

The thesis will be composed of six chapters. In Chapter 2, a literature review of past research and recent findings will be discussed. Modeling techniques and clear descriptions of settings and parameters used in the FE Software, Abaqus, will be described in Chapter 3. Meshing parameters and contact properties can have great influence in the modeling of any structural system. In addition, sources for the material models for the steel sections and the welds will be reviewed and validation exercises will be presented.

Chapter 4 will discuss the results of analysis of various DP configurations for a shallow column, specifically a W14x398. Chapter 5 will discuss similar results for analysis of a deep column, specifically a W40x264. Chapters 4 and 5 will have a detailed evaluation of the models studied and assess how the results derived from these models impact the design of welds in the panel zone. Chapter 6 will summarize all the results of this research, attempt

to provide explanation for what they mean and make recommendations intended to inform design and provide future research ideas.

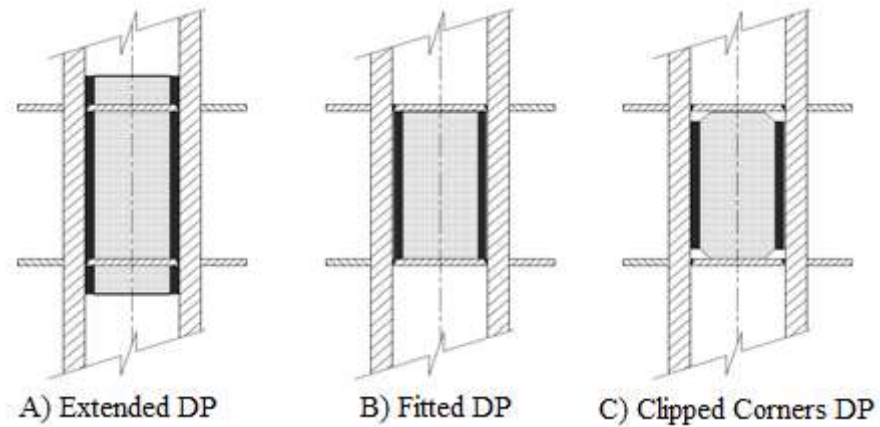


Figure 1.3: Extended, Fitted (clipped and unclipped) DP

## 1.5 NOMENCLATURE

The following abbreviations are used throughout this thesis.

<b>CJP</b>	Complete Joint Penetration Weld
<b>CJP1</b>	Complete Joint Penetration weld between column flange and DP
<b>CJP2</b>	Complete Joint Penetration weld between column flange and CP
<b>CJP3</b>	Complete Joint Penetration weld between column web and CP
<b>CP</b>	Continuity Plate
<b>DP</b>	Doubler Plate
<b>EBF</b>	Eccentrically Braced Frames
<b>FBD</b>	Free Body Diagram
<b>FE</b>	Finite Element

<b>FEM</b>	Finite Element Method
<b>LP</b>	Loading Plate
<b>VMS</b>	Von Misses Stress
<b>PEEQ</b>	Cumulative Equivalent Plastic Strain
<b>PZ</b>	Panel Zone
<b>LFRS</b>	Lateral Force Resisting System



## **CHAPTER 2**

### **Literature Review**

#### **2.1 OVERVIEW**

This literature review will discuss previous research regarding the PZ region, including how the strength and detailing of the PZ affects performance of previous research, which investigated the overall response of the PZ will be presented first. This is followed by research regarding the importance of stable ductile behavior in the PZ and how the reinforcing DPs and CPs can improve performance and increase frame strength and ductility. Other issues discussed will include how the local stress concentrations, strain hardening of the web, and column flange contributions affect the overall behavior of the PZ. Lastly, the work of Shirsat (2011), Donkada (2012) and Gupta (2013) will be discussed in detail in order to provide the background for this thesis.

#### **2.2 PREVIOUS LITERATURE DISCUSSED BY OTHERS**

For research covering FEM analysis of PZs and pertinent design considerations, see previous literature reviews of Mays (2000), Cutina and Dubina (2008), Slutter (1982) and Ye et al (2005) in theses by Shirsat (2011), Donkada (2012) and Gupta (2013).

#### **2.3 RESEARCH BY GRAHAM, J.D. ET AL (1959)**

One of the earliest researchers of PZ behavior was Lehigh's J.D. Graham. In the report "Welded interior beam-column connections", a range of tests performed on two-way setups composed of two beams joined at the column, similar to Figure 1.2, and four-way setups composed of four beams as seen in Figure 2.1, is discussed. These setups were loaded

monotonically, until the loading machine could no longer apply load or until failure by weld fracture or buckling ensued.

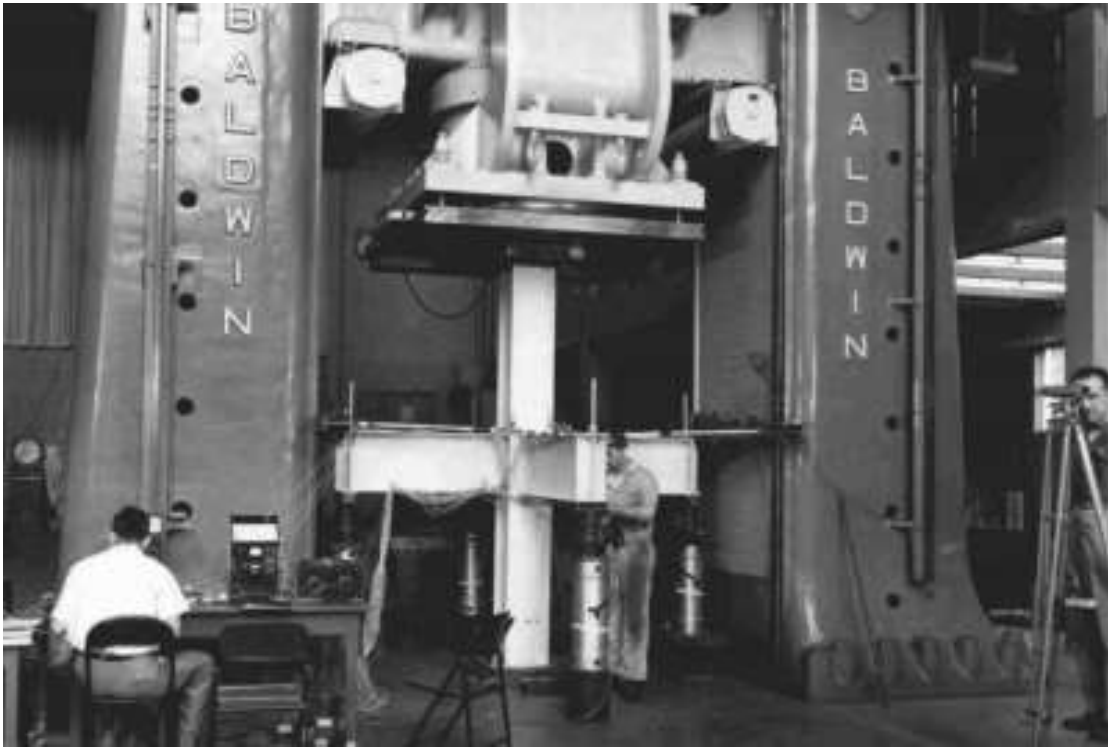


Figure 2.1: Four-Way Test in Progress at Lehigh's Fritz Lab, (Graham, 1959)

Four sets of un-reinforced columns with web thickness ranging from 1/4" to 5/8" were tested in the two-way beam-column setup. Figure 2.2 illustrates the results of the measured column PZ rotation vs. moment due to lateral force. By determining the rotation capacity relative to the amount of loading on the column, the performance and strength limits of the connection can be measured. A column that requires more force to rotate to a certain level can be said to be stiffer and stronger. This strength is necessary to resist the loads imposed by earthquakes. Although they have high strength, this does not necessarily mean that the specimens can withstand large deformations, or that they are ductile.

The results seen in Figure 2.2 show that thin webs, resulting in buckling of the column web, are not desirable. The poor performance of specimens A-1 and A-4 demonstrates this effect; because of a lack of reinforcement, the column webs buckled and the columns failed due to instability. Unlike girders, where tension field action is desired, buckling of the PZ proves ineffective in resisting lateral loads. Specimens A-2 and A-5 failed due to local buckling of the flanges.

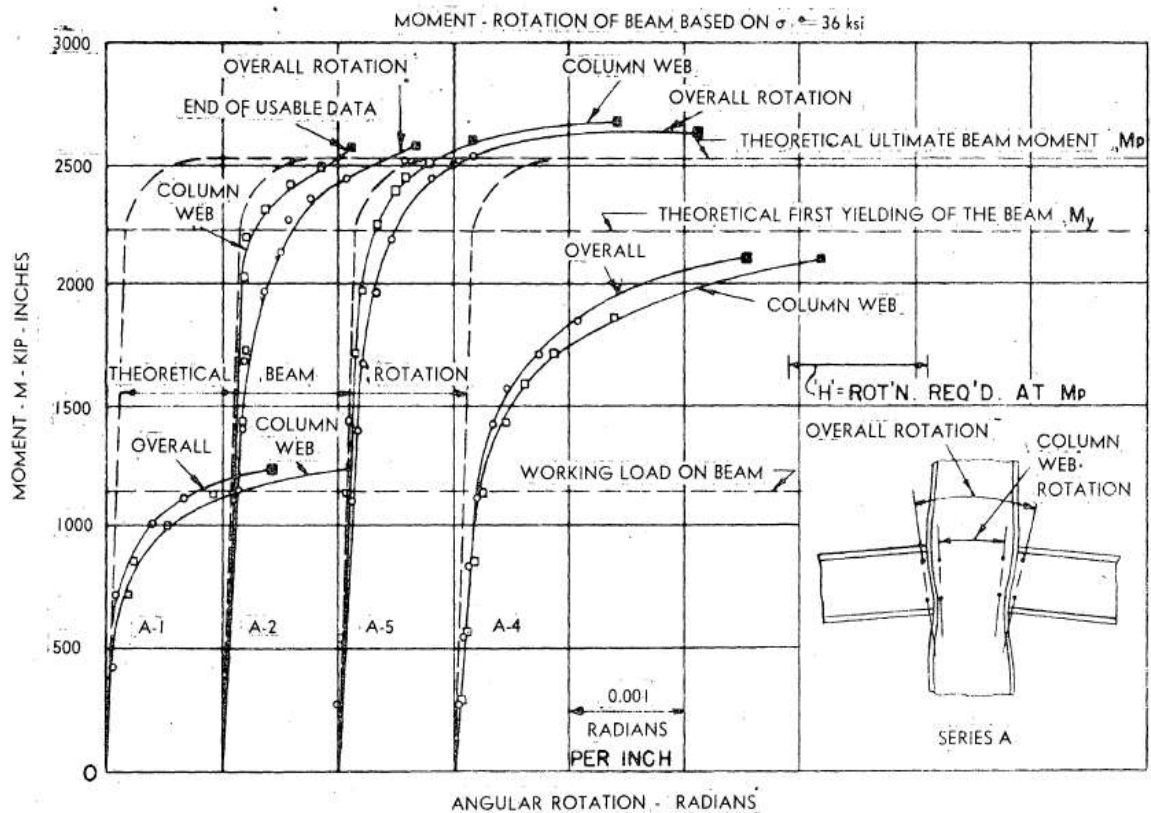


Figure 2.2: A Series Specimens - Un-Reinforced Columns, (Graham, 1959)

Other tests performed included two columns with only continuity plates as the PZ reinforcement. The results for these tests can be seen in the report, along with those of the

setups that had a DP welded a distance away from the center of the column web or a T shape with its stem welded directly to the PZ.

The specimens using CPs performed well despite slight plastic deformations seen in the column flanges. The specimens with two DPs attached near the edge of the column flanges did not perform as well. These assemblies, with a DP that was not welded up against the column web, were not very effective in providing reinforcement. This setup can be used when out of plane beams have to be framed onto the web of the column, but it places a high shear demand on the column web. Despite the DP being as thick as the column web, the column web buckled in all of the specimens using the DP spaced away from the center line. This indicated that most of the shear resisted by the PZ went to the column web and very little passed through the reinforcing DPs in this case. Failure of some the specimens was initiated by column web buckling, followed by weld failure of the butt welds in the tension flange. The case of the welded T-shape had similar results. If the intent of the design is for the DP to equally share the shear load with the column web, the results indicate performance improves when a DP is attached flush up to the column web.

Only one test with a DP, 5/16" thick, welded flush up against the column web and no CP, was tested. The results are shown in Figure 2.3. The PZ was reinforced by a DP extended beyond the bottom beam flanges. It can be surmised that the reason for not extending it beyond the top beam flange is due to the monotonic loading of the specimen. These tests show higher levels of rotation at the points of failure, an indication of higher ductility. The test was stopped due to a failure of the weld between the east beam and the column.

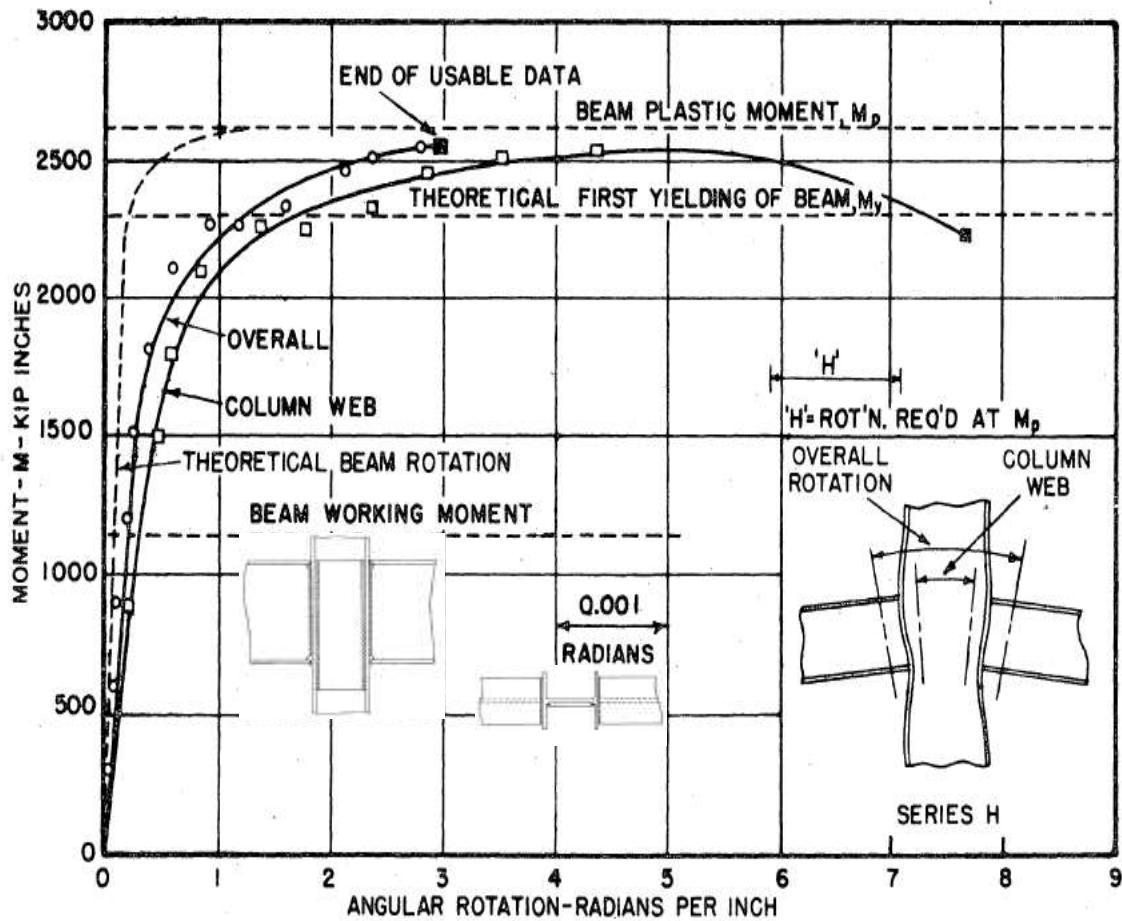


Figure 2.3: PZ Joint Rotation for Column with Extended DP, (Graham, 1959)

The work by Graham brought attention to the poor performance of thin column webs used for moment frame joints and demonstrated the importance of CPs on the behavior of the PZ. The results of the specimens reinforced by DPs demonstrated the improvement on the capacity to develop very ductile behavior and sufficient shear capacity.

#### 2.4 RESEARCH BY FIELDING & HUANG (1975)

Fielding and Huang conducted a series of tests in order to demonstrate that design suggestions for the PZ used at the time were not accurate. The inelastic behavior of the PZ,

the point beyond first yield, was not being considered when determining the strength capacity of the joint. The researchers also observed that, even though parts of the column web had reached the strain hardening stage, other segments of the joint, the column flanges, had not even yielded. This was determined to play an important role in global behavior. The studies conducted also considered the impact of axial force, combined with high shear, on moment frame joints.

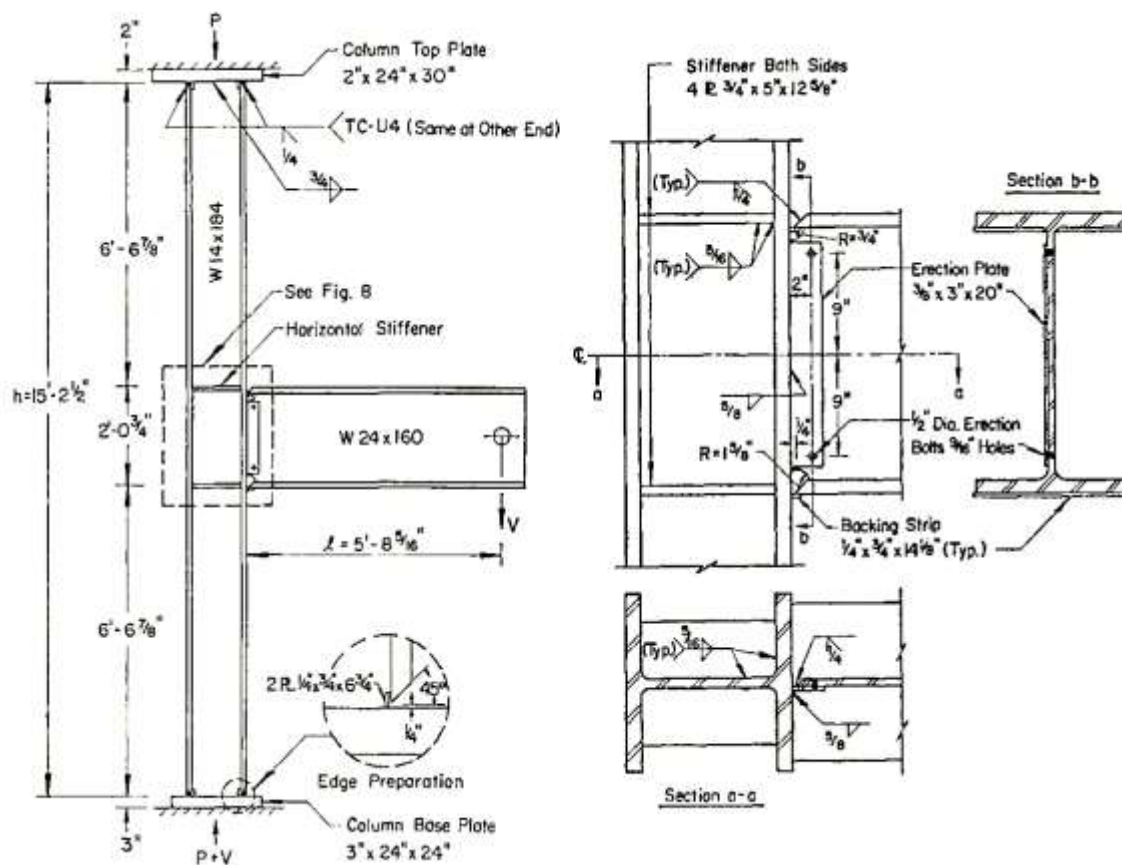


Figure 2.4: Test Setup, (Fielding & Huang, 1975)

The setup in Figure 2.4, a weak panel zone design, was sized so that failure would occur in the panel zone rather than in the attached beam, which had a plastic moment capacity

twice that of the column. Even though the specimen did not use a DP , continuity plates were used. The CPs were welded to the inside of the column flanges using fillet welds similar to Figure 2.5. The assembly was submitted to an axial load, along with anti-symmetrical moment, moment force induced on one side of the assembly instead of both, as in this thesis.

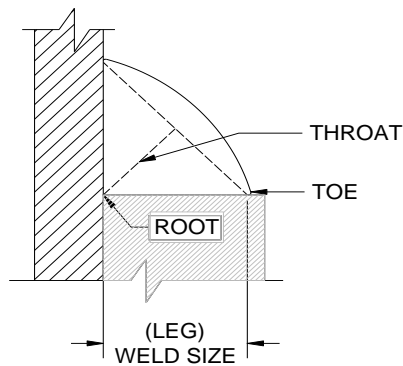


Figure 2.5: Fillet Weld Cross-Section

The procedure involved loading the column to an axial load of 819 kips,  $P/P_y = .5$ , followed by a loading of the end tip of the beam to the point of failure. These tests did not consider failure of the welds attaching the stiffeners as the stopping point for the test. During testing, one of the specimens failed due to the fracture of a fillet weld attaching the CP to the flange. The specimen was unloaded and the weld replaced by a larger weld that allowed for the full yield strength of the stiffener to be developed. Another specimen also showed failure of the weld attaching the upper beam flange to the column. This is a region where weld failures are likely due to the high curvature and stress concentrations. This weld was also cleaned, replaced and tested to ensure performance. It is important to note that three decades later, welds would prove one of the main points where fractures were initiated in the failed moment connections of Northridge.

The analysis of the data was performed in conjunction with the results from previous tests completed at Fritz Lab by J.W. Peters and G.C. Driscoll (1967). Conclusions from the work included:

- 1) Axial load on the column accelerated the yielding of the cross-section when combined with forces from the attached beam. Ultimate failure of the assemblies was not reached until the column flanges had completely yielded. Since moment frames not only resist seismic forces but also gravity loads, this was very pertinent to PZ behavior. It showed that the presence of axial load plays an important role in the rotation limits of the panel zone. It also validated the pre-supposition that yielding of the column webs was more important in the understanding of the global behavior of the joint.
  
- 2) The researchers determined that the yield point of the column web was an important point where stiffness of the connection began to decrease during testing. Along with determining the importance of the yield point of the column web, the influence of axial load needed to be considered when designing the PZ. Equations that would more accurately predict joint capacities were developed using the Von Mises criteria. These provide a better approach that considers the axial load from the gravity loads and overturning moments in the building.



## 2.5 RESEARCH BY BECKER (1975)

Becker tested three specimens fabricated with W14x61 W-shapes, to determine the effects of the PZ on the strength and stiffness of steel moment frames. Two of these specimens were reinforced with DPs that extended one inch beyond the plane of loading, defined by the flanges of the members attached to the PZ. These were also reinforced by 5/8" thick CPs, which were welded to the member flanges using full penetration welds and 1/4" fillet welds on both sides attached to the web. The key difference between the two specimens was the thickness of the DP and the types and sizes of welds attaching the DP to the PZ. One specimen used a 1/2" DP attached by vertical butt welds and 7/16" horizontal fillet welds. A thicker 5/8" web DP attached using 5/16" fillet welds all around was used in the other specimen.

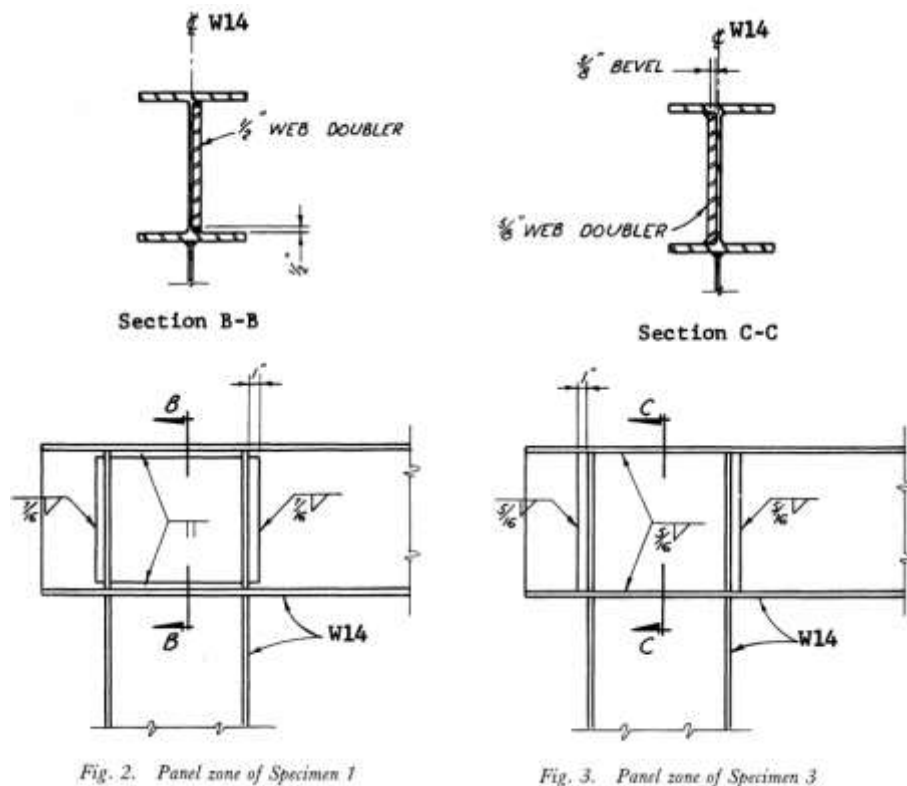


Figure 2.6: Specimen 1 & 3 (Becker, 1975)

The limits on how much capacity could be tested was determined by the limits on how much load the testing machine could apply. It is for this reason that none of the specimens failed in the sense that applying more displacement showed a decrease in load. The cyclic load used for the tests was applied in incremental steps. The un-reinforced specimen resisted the least amount of load and developed the highest strain levels. Of the three specimens, it was the only one where the PZ buckled. Specimens one and three performed similar to each other without any buckling of the panel zone or failure of welds. Specimen one, with the thinner DP but stronger butt welds, had minor local buckling in the flanges attached to these welds.

Becker's work reinforced the conclusion that DPs can substantially increase the shear capacity of PZs and the stiffness of the whole frame. It emphasized the importance of the PZ in the global behavior. An important conclusion from his work was that the DP does not resist the same amount of shear force as the column web until the strains in the PZ are three to four times the yield strains. This indicates that the addition of a DP not only becomes more important past the first yield point but its contribution to shear force resistance increases as that of the column web decreases. The PZ is a key member of the LFRS; it resists the shear force from lateral forces and in turn greatly determines the drift magnitude up the first yield point, when the DP begins to contribute more. Becker also commented on the importance of careful detailing of the welds in the PZ. In order for the DP to effectively engage in shear resistance, the welds must be capable of transferring the load from the web.

## 2.6 RESEARCH BY KRAWINKLER (1978)

Krawinkler discusses the results of previous work, along with those of three specimens loaded with monotonic and cyclic loads. Specimen A-2 was composed of a W8x24 column with two beams of 10" depth and horizontal stiffeners, CPs. Two others were composed of W8x67 columns, with one specimen using 13.72" deep beams (specimen B-2) and the other with 11.98" deep beams without any reinforcement (specimen B-3). In order to consider gravity loads, Specimen B-2 was loaded with an axial load of 40%  $P_y$ .

Specimen A-2 with a web three times thinner than that of the other two specimens had the lowest performance and developed diagonal buckling along the PZ. Between the other two similar specimens, B-2 and B-3, the one with 40%  $P_y$  axial load performed the worst. The Von Mises stress criteria, which considers both shear and axial loads, explains why the PZ yields faster and resulted in the lower performance seen in specimen B-2.

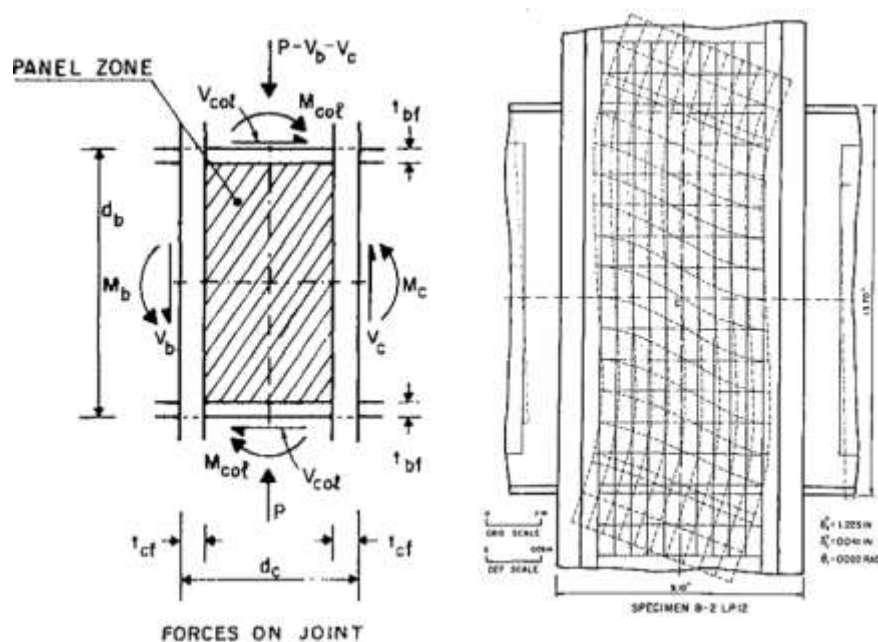


Figure 2.7: Panel Zone Deformations & Forces on Joint (Krawinkler, 1978)

The work describes how the shear stress is distributed throughout the PZ as the moment is increased. The forces applied on the PZ and the resulting shear deformations can be seen in Figure 2.7. Krawinkler commented on the important role that the PZ plays in the overall performance of the moment frame and how the stiffness of the connection starts to decrease when  $.75F_y$  of the column web is reached. This indicates that the point when the strength capacity of the moment connection begins to decrease, falls within the range of 75-100% of the yield capacity of the column web. Once the PZ has yielded, the stiffness of the joint decreases gradually until it stabilizes in a second semi-constant stiffness, which the reader is told, is due to the PZ going through strain hardening. Krawinkler's conclusion is that the column flanges and beam webs assist in resisting shear and influence the yield point of the column web. This contribution from the PZ boundary elements explains the behavior that can be seen in the two constant stiffness. As a result, Krawinkler developed Equation 2.2, which considers how the "elements surrounding the PZ" influence shear capacity.

Krawinkler also makes the recommendation to design the panel zone for the shear produced by the ultimate flexural capacity of the beams attached to the column instead of the lateral forces specified in the building code. When the research was conducted, design specifications for moment connections utilized expected lateral forces in order to determine the shear capacity required from the PZ. Equation 2.1 reflects the use of these forces amplified by 33%. The use of Equation 2.1, in conjunction with the expected lateral forces, resulted in joints that were weak and had large rotations. The beams in these designs did not contribute to energy dissipation and resulted in high drifts. It was concluded that a better design approach, which distributes the inelastic deformations between the PZ and the attached beams, has to consider the contributions from elements around the PZ and the

maximum shear that the attached beams can transfer. Equation 2.2 does this, resulting in greater ductility contributions from the beams and a closer prediction to the actual joint shear capacity. Equation 2.3 listed below adds the contribution from the addition of a DP as web reinforcement to Equation 2.2. The addition of a DP is an independent contribution to the PZ shear strength from the column web; this is the reason for the addition.

$$V_{max} = 0.53F_y d_c t \quad \text{Equation 2.1}$$

$$V_{u(col)} = 0.55F_y d_c t (1 + (3.45b_c t_{cf}^2 / d_b d_c t)) \quad \text{Equation 2.2}$$

$$V_u = V_{u(col)} + (F_y / \sqrt{3})(d_c - t_{cf})t_s \quad \text{Equation 2.3}$$

*b<sub>c</sub> = width of column*

*d<sub>b</sub> = depth of beam*

*d<sub>c</sub> = depth of column*

*t = thickness of web*

*t<sub>cf</sub> = thickness of column flange*

*t<sub>s</sub> = thickness of web stiffener (DP)*

Krawinkler's work discusses some of the details that affect the strength and stiffness of the PZ and how the importance of its contribution to the resistance of drift and stability of the LFRS is augmented after first yield. Comments throughout the writing specifically point out the importance of weld quality in the regions where plastic deformations are expected. His conclusions indicate that frame stiffness and strength greatly depend on the design of the panel zone, specifically its yield point. Along with this, a recommendation is made for a balanced design that requires the PZ to assist in force dissipation through inelastic deformations. By not considering the elements around the PZ, the designers are unintentionally forcing the deformations on the beams alone.

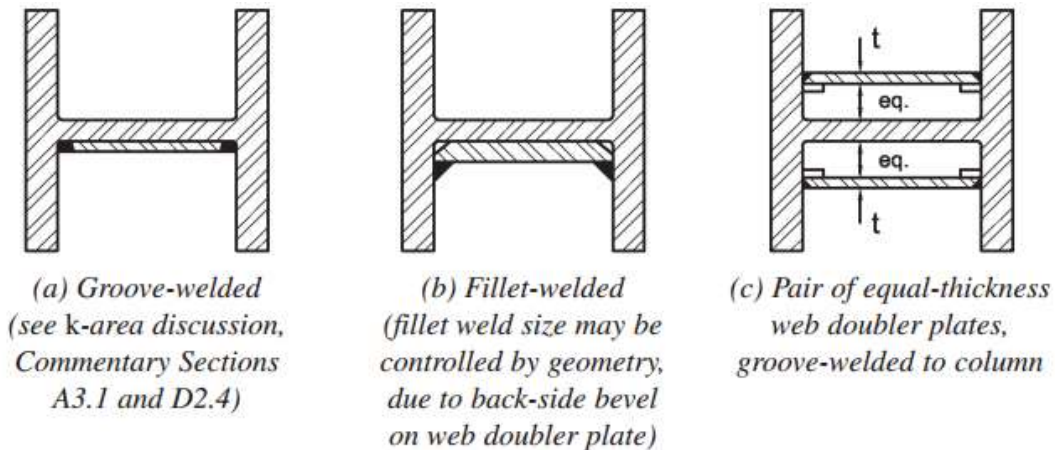


Figure 2.8: Web Doubler Plate Layouts (AISC 341-10)

## 2.7 RESEARCH BY POPOV (1987)

E.P. Popov discusses the financial and practical benefits that very ductile LFRS provide for structures subjected to wind or seismic loading. His work compares the load vs. deflection results from two moment connections attaching a W12x106 column to either a W18x50 or W24x76 beam. Two different specimens of both connections were tested, with the only difference being how the web of the beams was attached to the column; shear tab was welded or bolted. These joints were reinforced by continuity plates but lacked a doubler plate.

The W18x50 beam with the welded connection had an ultimate load capacity .7% higher and a panel zone rotation 40% higher than that of the one using bolts. Similar values were seen in the W24x76 beam setup. Load capacity was 8.9% higher and the panel zone rotation was 5.6% higher than the bolted connection. The researchers determined that the lower performance of the connection using bolts was due to slippage in the bolts.

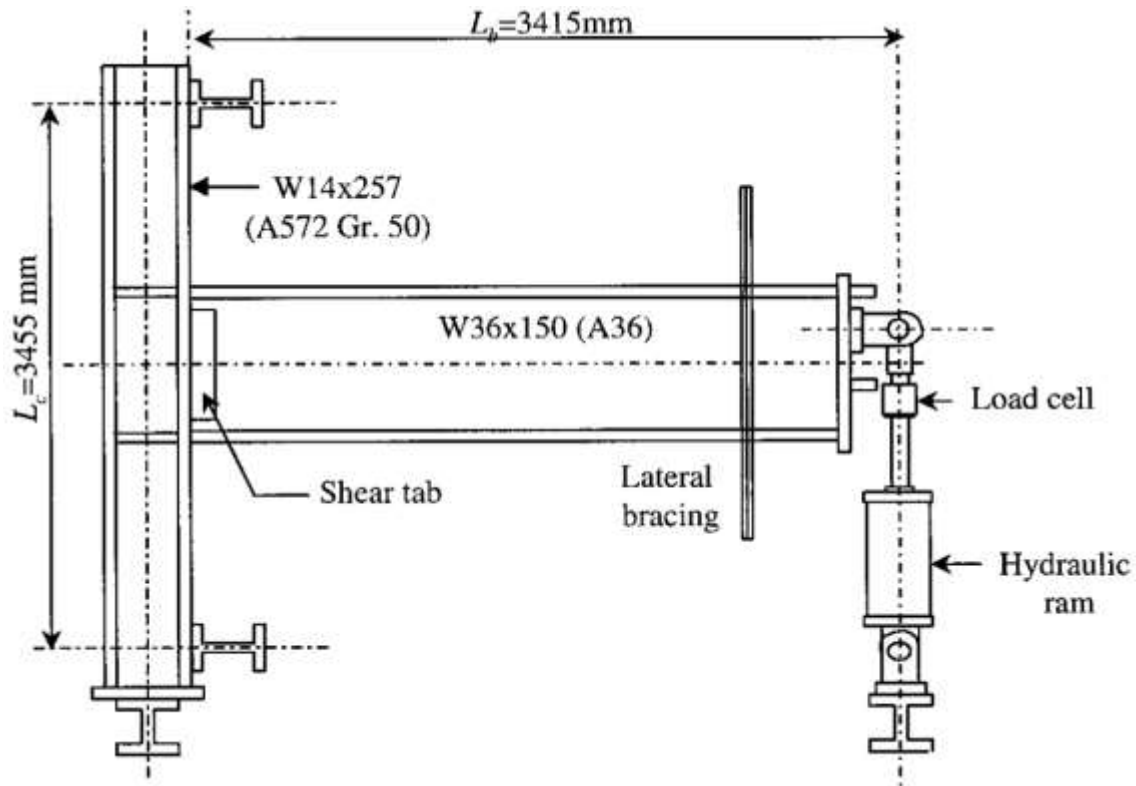


Figure 2.9: Specimen PN3 (Popov, 1987)

The work also discusses a separate set of tests that were carried out in conjunction with the previously discussed tests. Six subassemblies with varying combinations of doubler plates, stiffeners and thickness were tested. Two particular joint specimens with columns of similar depths and no CP stiffeners were tested. One of the two sub-assemblies used a column with thicker flanges, web, and doubler plate. As expected, the results indicated that the heavier assembly had a higher tip load capacity, the ability to resist moment capacity, but very low ductility. This serves as an example of the complexity in balancing the strengths and dimensions of the elements that make up the PZ while keeping the connection ductile.

High ductility in the other assemblies was attributed mostly to panel zone deformation. The results from the tests between the two setups (specimens 2 and 6), in which the difference

was the presence of a doubler plate, can be seen below in the hysteretic performance of the specimens. The results indicate that the lack of a DP in specimen 6 resulted in low ductility.

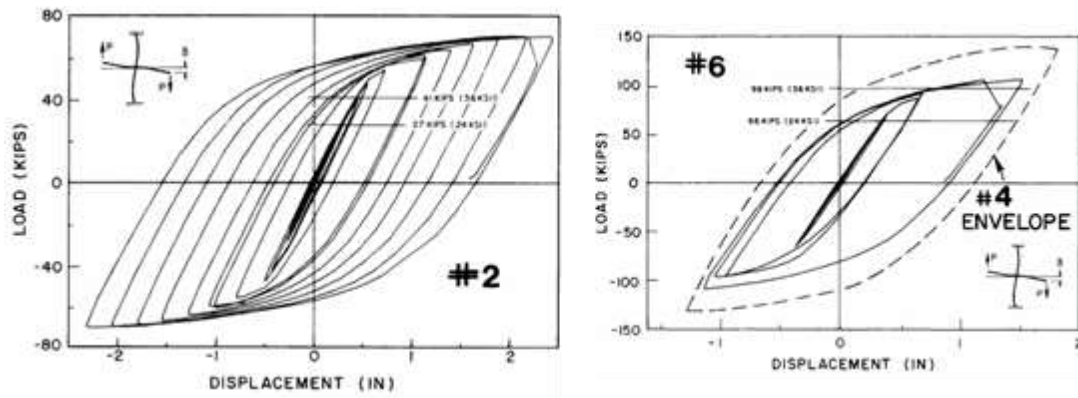


Figure 2.10: Specimens 2 & 6 (Popov, 1987)

The work by Popov covers three joint design methods, one in which the panel zone is designed to be so rigid that all the deformation and inelasticity is located in the beams attached to the column. He also mentions the opposite design approach, the weak panel zone method, in which most of the energy dissipation occurs in the column panel zone. Lastly, he mentions the balanced design method, in which both beams and column panel zone share the deformation and lateral force resistance.

## 2.8 RESEARCH BY EL-TAWIL ET AL (1999/2000)

El-Tawil et al conducted a set of FE studies on a specimen similar to PN3 from Popov (1987) (see Figure 2.9). A model of a connection attaching a W36x150 beam to a W14x257 column was made. Both beam and column were modeled using 4-node shell elements; however, the joint area where the column and beam intersect was modeled using 8-node brick elements. This combination of elements allowed for analysis of local stresses with



lower computational demands. Material nonlinearities were considered in the material definition of the members. Monotonic and cyclic loading of the sub-assemblies used isotropic strain hardening rules. Performance indicators used to analyze the results included the Pressure Index, PEEQ Index, Von Misses Stress, and Rupture Index. These all serve as measures of stress levels and tendency to fracture.

The intent of the study was to better understand the inelastic behavior of the PZ and the role it played in the fractures seen in the failed moment connections after the Northridge earthquake. Three parameters were varied in the study: column web thickness, attached beam depth, and column flange thickness. During the analysis, Equations 2.4-2.6 were used to compare PZ shear capacity against analysis results, to determine how well they predicted the shear forces.

$$V_{n1} = 0.55F_y d_c t \quad \text{Equation 2.4}$$

$$V_{u(col)} = 0.55F_y d_c t (1 + (3b_c t_{cf}^2 / d_b d_c t)) \quad \text{Equation 2.5}$$

$$V_{u(col)} = \left(\frac{0.55}{.8}\right) F_y d_c t (1 + (3b_c t_{cf}^2 / d_b d_c t)) \quad \text{Equation 2.6}$$

The results of the analyses with varying column web thickness were compared. The columns with weaker PZs due to thinner webs initially developed lower stresses than those with the thicker webs. This, however, reversed as the loading and the PZ rotation increased. At the end of the tests the principal stresses measured in the column with the weakest PZ were 15% higher than those of the column with the thickest web. As mentioned in previous work by Krawinkler, the plastic deformations in a weak PZ are much higher than those of the beams attached to it. A thinner web also results in a decrease in plastic rotation participation of the beams attached to the column. This is not only an ineffective use of

materials but can result in frame instability by forcing the column to rotate to high levels. Performance indicators indicated that, as a result of the weak PZ, the potential for fracture grew in the area where the beam flanges meet the column. This is of importance since many fractures seen in the Northridge earthquake connections occurred in the area where the beam flanges met the column web.

In order to examine the effect that column flanges had on PZ performance, specimens with decreasing column web thickness and increasing flange thickness were analyzed. By decreasing the thickness of the web, the performance of the PZ became more dependent on the flanges. The specimen with a column flange and web thickness of 1-5/16" was 12.7% stronger than one with column flanges 3-1/4" thick and a web 11/16" thick. The results of the fracture indicators seen in the specimen with the thickest flanges were similar to those of the weaker panel zones. Initially, smaller principal stresses were recorded in the beam flange-column interface of the thicker flanged specimens but rose by 28.6%, whereas the column with the thinner flanges but thicker web rose only 4.6%. This seemed to indicate that PZ performance was highly dependent on column web thickness and less dependent on column flange thickness.

When evaluating the provisions listed in Equations 2.4-2.5, it was noted that Eq. 2.4 was successful in defining the first yield point of the PZ. Determining the first yield point of the PZ is important since the PZ and the elements surrounding it begin to strain-harden at this point. It is during this stage that the role of the DP in dissipating energy increases substantially compared to that of the column web. Once the strain hardening range has been reached, Eq. 2.5 serves as more accurate method of determining the shear strength capacity of the PZ. Eq. 2.5, previously covered in Krawinkler, considers the participation of

elements surrounding the PZ. It is necessary to note that both the results of this research and Krawinkler's comment on the possible inaccuracies involved with using this equation on columns with thick flanges. As seen in Figure 2.11, the PZ curvature resulting from applied shear on a column with thicker flanges appears more evenly distributed. The localized "kinks" developed in columns with thinner flanges were used to develop Equation 2.5.

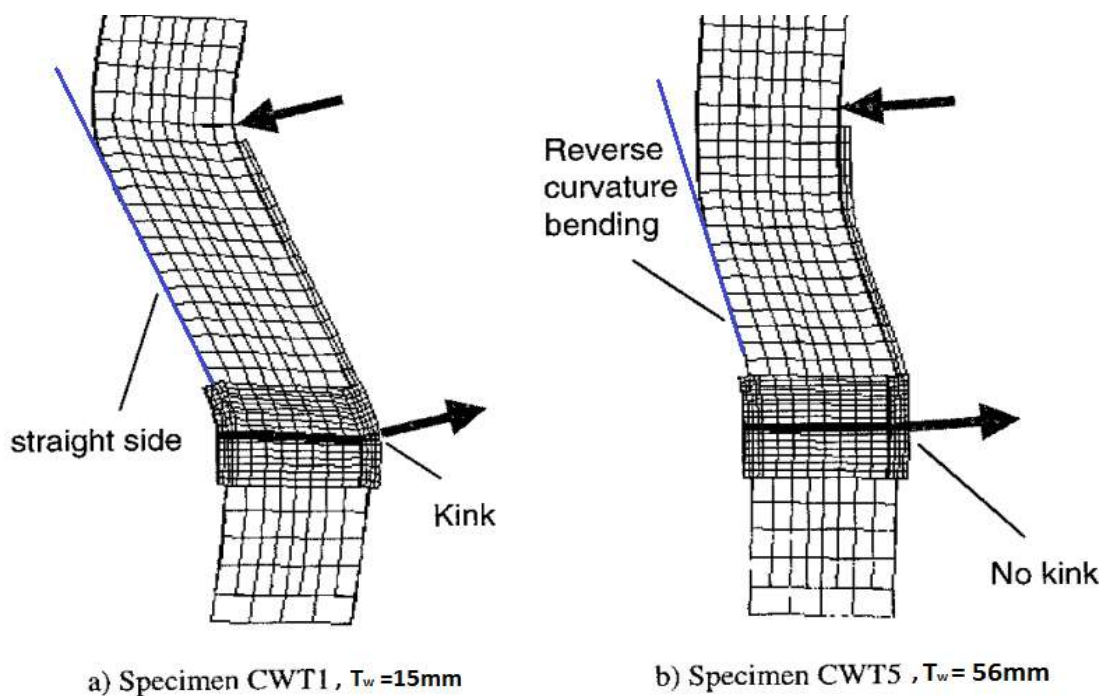


Figure 2.11: Specimens with Different Web Thickness, (El-Tawil, 1999)

El-Tawil also discusses other factors that may have affected the performance of the failed Northridge connections. Some of these include: the yield to ultimate stress ratio of the A36 steel that was used during that time period, access-hole geometry and continuity plates. CPs are said to be beneficial in resisting local failures in the form of flange local bending, web crippling, local yielding or compression buckling. The effectiveness of PZs to resist

high levels of shear is interrupted by these lower strength modes of connection failure. Other reports by Graham, Fielding and Becker alluded to the benefits of using CPs. Joints with CPs were the most successful and had fewer connection failures during testing. El-Tawil concludes that the thickness of CPs does not affect the performance of the PZ as much as their presence does. The FE models in Figure 2.12 visibly show how the lack of CPs resulted in higher local bending of the column flanges, along with an increase of 44% in principal stresses and 53% higher PEEQ at the beam-column interface. El-Tawil recommends a reduction of unrequired and conservative CP thickness requirements. Economic benefits from less material consumption and possible detrimental effects were mentioned in support of this recommendation.

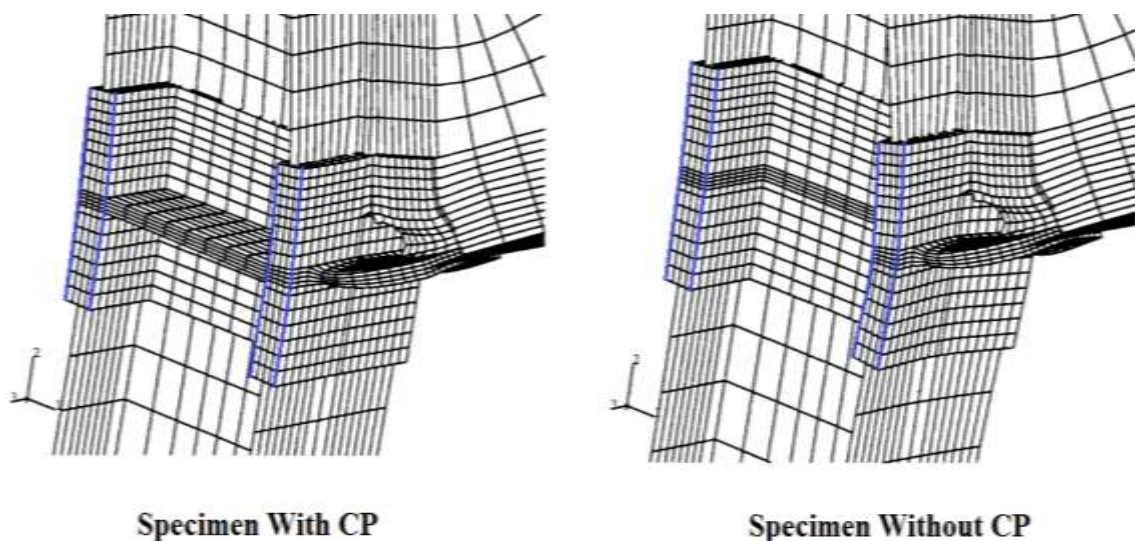


Figure 2.12: Specimens With and Without CP (El-Tawil, 2000)

## **2.9 RESEARCH BY RICLES ET AL (2004)**

Ricles et al conducted a series of studies of deep columns in order to develop seismic guidelines for steel moment connections. Two different finite element models with different mesh sizes and levels of accuracy were used to conduct the parametric studies.

To capture the overall behavior of a reduced beam section, RBS moment connection, Ricles used a global model composed of two W36x150 beams and either a W36x230 or W27x194 column using four node shell elements in Abaqus. The intent of the global model was to capture torsional effects from unsymmetrical loading and buckling of plate elements such as flanges and webs. A more “precise” sub model was used, which characterized the area where the beam lower flange connects to the column flange. This area, which also includes the K-zone of the column, required a smaller but more rigorous model since the geometries of this region are complex. The elements that participate in PZ shear resistance and meet at this point are CPs, Column Webs, DPs, and welds. This region has been studied extensively due to the complex stresses that concentrate here. It is these tri-axial stresses that increase the propensity to fracture and as a result, cracks are often initiated here. The sub-model was made up of eight-node brick elements and a more refined mesh. The resultant forces from the global model were applied to the sub-model in order to obtain more accurate levels of stresses. Material inelasticities were considered in the model, as well as strain hardening. The loading protocol was based on the 2002 AISC provisions which were used in the SAC research. The results from the models were validated against similar tests conducted at the lab.

Doubler plates have a large influence on the strength of the PZ. By varying the thickness of the attachment and providing welds strong enough to transfer the forces, a designer can determine the level of PZ performance which can range from weak, to balanced, to strong. A measure that delineates the difference between these designs is panel zone strength to panel zone shear capacity,  $R_v/V_{pz}$ , with values of 0.83, 1.09, and 1.34 for weak, balanced, and strong designs, respectively. A weak PZ design will result in a concentration of the plastic deformation in the column and almost none in the attached beams. This design

approach also seems to increase the Rupture Index values measured in the joint. As seen in Figure 2.13, a weak PZ provided strength values below the balanced or strong PZ designs in this test. When connections are welded properly, deterioration in strength of balanced and strong PZ designs results from local web and flange buckling of the attached beams. This places a stronger dependence on the use of CPs to keep the column web from failing due to the high levels of shear required to reach these failure modes.

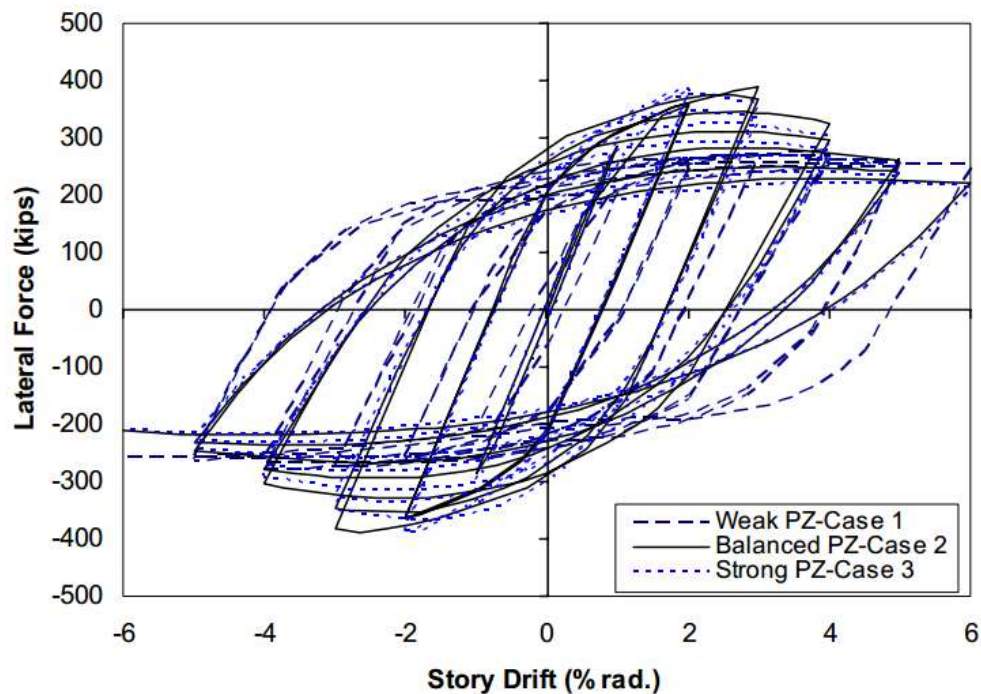


Figure 2.13: Hysteretic Response of Different PZ Strengths (Ricles, 2002)

Ricle's work also compared two specimens in which the thickness of the CPs varied from the same thickness of the column flange to  $\frac{1}{2}$  of that value. The results indicated that the fracture potential of the connection increases as the CP thickness is reduced. His research and recommendations highlighted the dependence of PZ performance on the reinforcement from DPs and CPs. When considering the level of performance expected from the column

PZ, the reinforcement used in design plays a substantial role in attaining the capacities required.

## **2.10 RESEARCH BY SHIRSAT (2011)**

Shirsat conducted finite element analysis of a variety of column specimens using Abaqus. Her models were composed of a W14x398 or a W33x263 column with two 1” thick loading plates applying a monotonic load. Using loading plates is a common simplification that simulates the flanges of beams, applying a lateral force on the PZ. This simplification assumes that the contribution from the beam web is minimal when compared to that of the beam flanges. As seen in Figure 2.14, a variety of parameters were changed with the intent to obtain knowledge regarding the following questions.

- 1) Which welds attaching the DP to the column web are necessary? Are both vertical and/or horizontal welds needed?
- 2) What are the benefits of using extended DP in moment frame connections and what welds are necessary for these as well?
- 3) How effective is the substitution of two thin DPs on each side of a column web instead of one thicker DP on one side as is typically seen? (See Figure 2.8-c)
- 4) Can we gain understanding on how and what levels of forces are transferred through the welds in the different layouts?

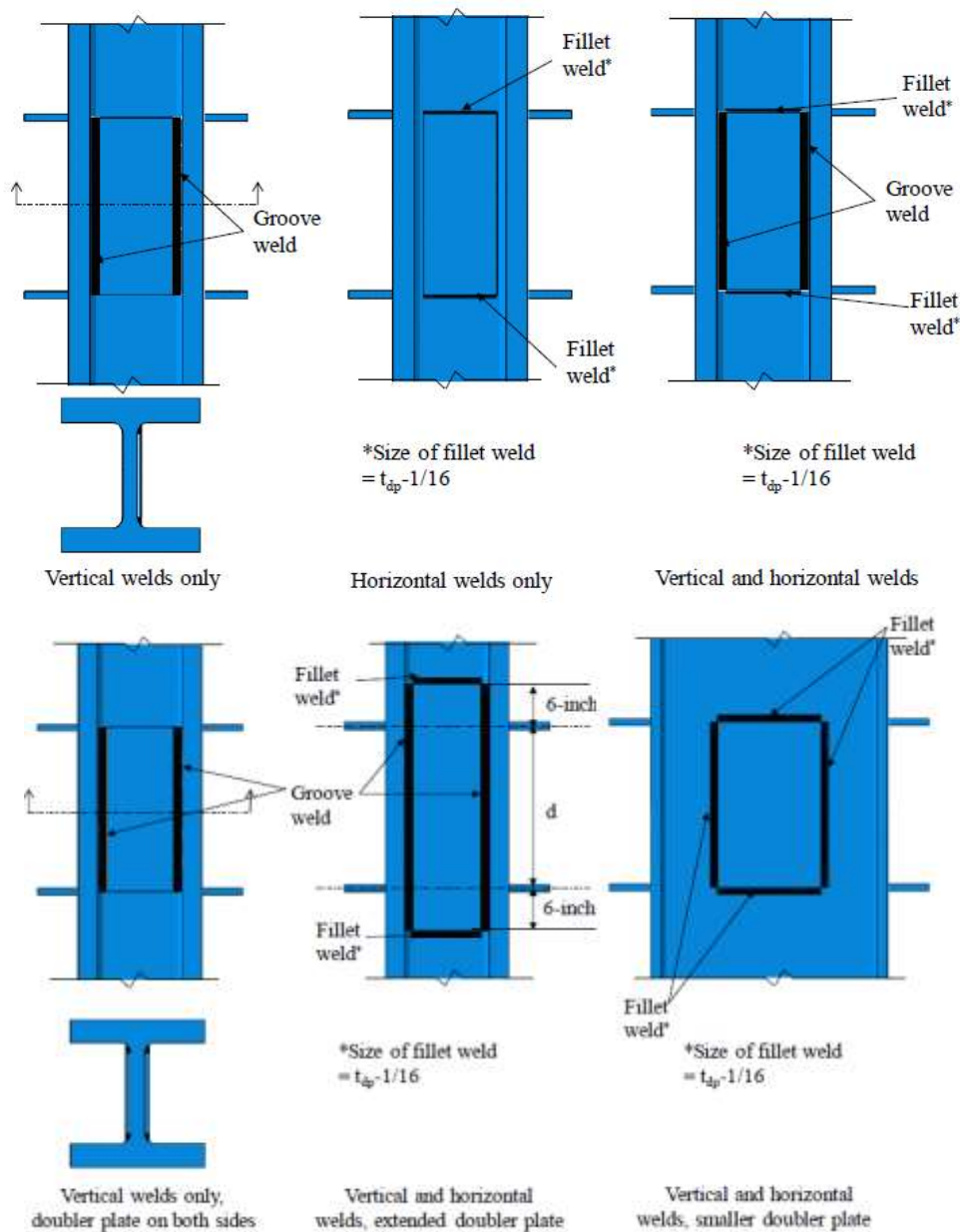


Figure 2.14: DP Arrangements Tested (Shirsat, 2011)

Twenty-one model variations were used in this work. Measurements for comparison of results were made along the four points of the load application. One of the key observations of his study was that the use of welds at the top and bottom of the DP alone were ineffective. When used as the only method of attaching the DP to the PZ, these horizontal welds were



unable to transfer the shear force from the column onto the DP. Therefore, the vertical welds are deemed necessary in order to cause the DP to perform as designed. The results also seemed to imply that horizontal welds were un-necessary for the DP to resist shear. The data showed similar shear resistance by the DP when the vertical welds were used with and without horizontal welds at the top and bottom. This was especially evident when the DPs were extended beyond the loading plates. Despite the focus of the thesis not being on how buckling of the DP affected its performance, Shirsat made an important observation. Even though the results indicated that top and bottom welds were un-necessary, thinner DPs would benefit from the use of both horizontal and vertical welds, in order to delay the buckling which permits higher stiffness/strength of the joint.

The shallow column models also seemed to indicate that extending the DP beyond the beam flanges did not provide a large benefit. However, the deeper column showed great improvement in strength when the results of an extended DP were compared to those of one without the extension. It is also worth noting that Shirsat's models did not use CPs.

Better performance by two thinner DPs, instead of one, attached flush to the column web failed to materialize in the analysis. Despite the possible economical and fabrication benefits from using thinner web reinforcement, this particular study found no benefits. A possible decrease in performance due to a higher propensity of the thinner DPs to buckle was also mentioned. When a DP does not meet thickness requirements, the seismic design code specifies the use of plug welds to prevent buckling of the reinforcement. In the case of the use of narrower web reinforcement, when the DP was half as wide as the columns depth, no benefits were found. The area where the DP overlapped the column web showed

less shear stress, but the areas surrounding the DP yielded faster and had higher levels of stress than that of the column without any reinforcement.

### **2.11 RESEARCH BY DONKADA (2012)**

Donkada's work was a continuation of the studies conducted by Shirsat. Her research reported on the results of some FEA performed on two column models as well. Monotonic displacement, strictly increasing movement of the loading plates, was applied to the loading plates up to a PZ rotation of .05 radians. SMF systems must be capable of providing a story drift angle rotation of .04 rad (AISC 341-10). The analysis performed on the shallow column, a W14x398, and the deep column, a W40x264, had results which could be reasonably expected in a SMF providing the level of rotation capacity required.

Substantial research following Northridge focused on the fracture potential that individual elements of moment connections had on locations where high stresses accumulated. Donkada's work also emphasized the advantages and disadvantages that the tested aspects had on fracture potential. Horizontal fillet welds attaching the DP to the column web, extended doubler plates, continuity plates and flange thickness variations were some of the factors varied in the analysis. The elements used in the Abaqus modeling of the specimen were 8-node 6-sided solid brick elements. Similar to Shirsat, a tri-linear material model developed by Okazaki was utilized to represent A992 steel.

One of the conclusions from Donkada's work is that it may not be necessary to weld all four sides of a DP. The data analysis indicated that there was little advantage to using horizontal welds at the top and bottom on the DP. Even though stress and strain levels on

the vertical welds attaching the DP to the K-zone went up, the fracture indices used indicated properly made welds would not fracture.

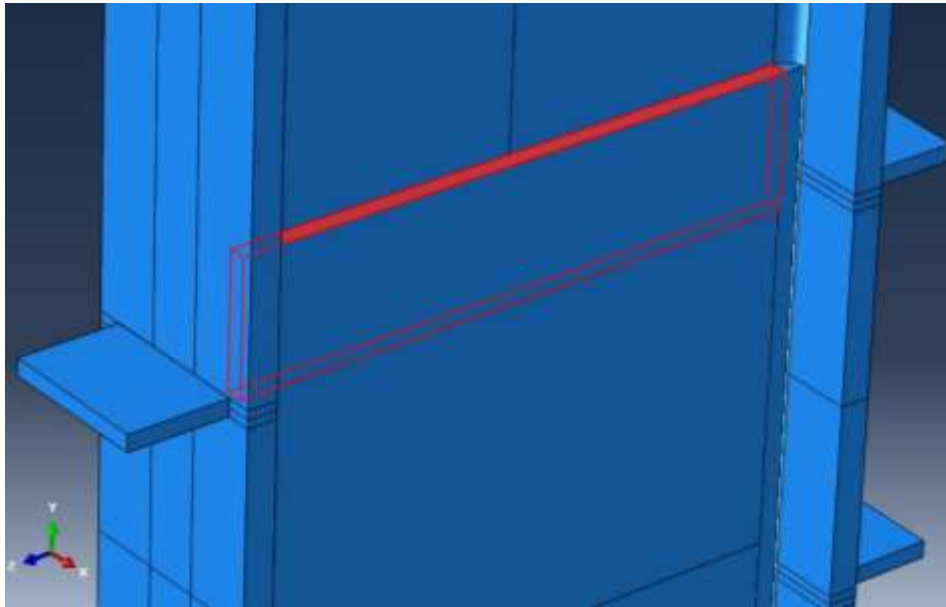


Figure 2.15: Deep Column Specimen (Donkada, 2012)

Donkada also found the extension of the DP beyond the PZ to be inefficient in increasing the strength of the PZ on the shallow column. However, one great benefit to extending the DP was found: the fracture potential was reduced in this specimen. The results for the deep column (Figure 2.15) were different. The extension of the DP increased the strength of the PZ by 10% but no decrease in fracture potential was seen. Donkada also points out the importance that a properly sized DP has on the overall behavior of the PZ. This was especially evident in the performance of the deeper column.

The data suggested that CPs do not contribute to the overall shear capacity of the PZ but do allow the joint to perform as designed, by keeping the column from failing in other

modes such as local flange bending, local web yielding, web compression buckling and web crippling. The attachment of continuity plates to the DP was also found to not increase the stresses of the DP. The use of CPs was found to reduce the level of stresses on the vertical welds attaching the DP to the PZ. It was assumed that the presence of the CP allowed for some of the forces to flow from the flanges into the CP instead of going through the DP. The presence of CPs was also found to be a critical element in both deep and shallow columns with thin flanges. The target loading level for the tests was determined to be at .05 radians. At target loading level, the load transferred through the CPs in the shallow column with thin flanges was 60% of the load being applied. The value recorded in the deeper column was 20-30% of load applied. The values recorded for the same specimens, but with flanges more than twice as thick, were 10-20% from the shallow column, a W14x398, and 20-30% from the deep column, a W40x264. The dependence of performance on CPs rises in shallow columns as the flange thickness decreases. This same dependence seems to be the same in deep columns with thick or thin flanges.

## **2.12 RESEARCH BY GUPTA (2013)**

Gupta's research continued to verify the benefits that extended DPs had on PZ performance and how other factors had influence. Research objectives of his work included determining the benefits from the horizontal welds that attach the DP to the column at the top and bottom. Variations of the length of DP were considered for this. The benefits from using CPs and how an extended DP affects the flow of forces through these, were also studied. Other objectives were to gain knowledge on the effect on the weld stresses resulting from the different setups and to gain a clearer definition of the limiting strength states in deep and shallow columns used, as seen in Figure 2.16.

Gupta's work also used solid brick elements modeled in Abaqus, (Figure 2.16). However, his work did not utilize the same inelastic monotonic material model that was used in previous research. The non-linear kinematic material model, utilized for the definition of A992 steel exposed to cyclic loads, was validated against existing lab results in similar ways as the previous thesis. Cyclic material test data for weld metal was not available for the modeling; hence a similar model was developed using considerable judgment (Gupta). Cyclic loading of the specimens, a simplification of the motions expected on a structure from an earthquake, were applied in the form of displacements with increasing amplitudes. Data points selected for the data comparison were at .01, .02, .03 and .05 radians. These were recorded at the last hysteretic cycle when the PZ rotation matched the rotation level.

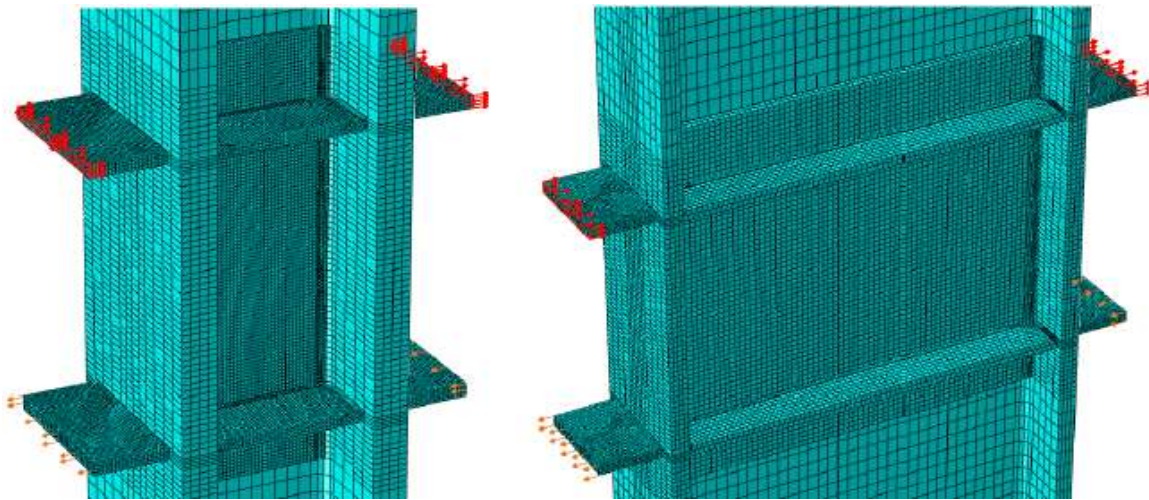


Figure 2.16: FE model of shallow column, and deep column (Gupta, 2013)

The main parameters that were varied in Gupta's work included: column flange thickness, DP extension of 6 inches above loading plates and inclusion of CPs in the models. The modeling of the PZ usually involves elements yielding and becoming inelastic due to the forces being transferred. Once the material is in the strain hardening region, the increase in

load resistance decreases substantially. As the material strain hardens, the rise in stress levels also becomes smaller and the effects of load variance become less evident. It is at this point that plastic equivalent strain, PEEQ, can be used to see how the PZ is locally affected by the increase in load. The PEEQ parameter is the measurement of strain equivalent that the Von Mises Stress is for stress measurements. Once the PZ has yielded, the measured strains grow as the load applied is increased. The model used by Gupta is loaded cyclically, which reduces the recorded PEEQ as the load is reversed. It is for this reason that a different form of strain measurement was used - plastic strain magnitude, or PEMAG. This measurement maintains a continuous accumulation of the strains as the PZ goes back and forth.

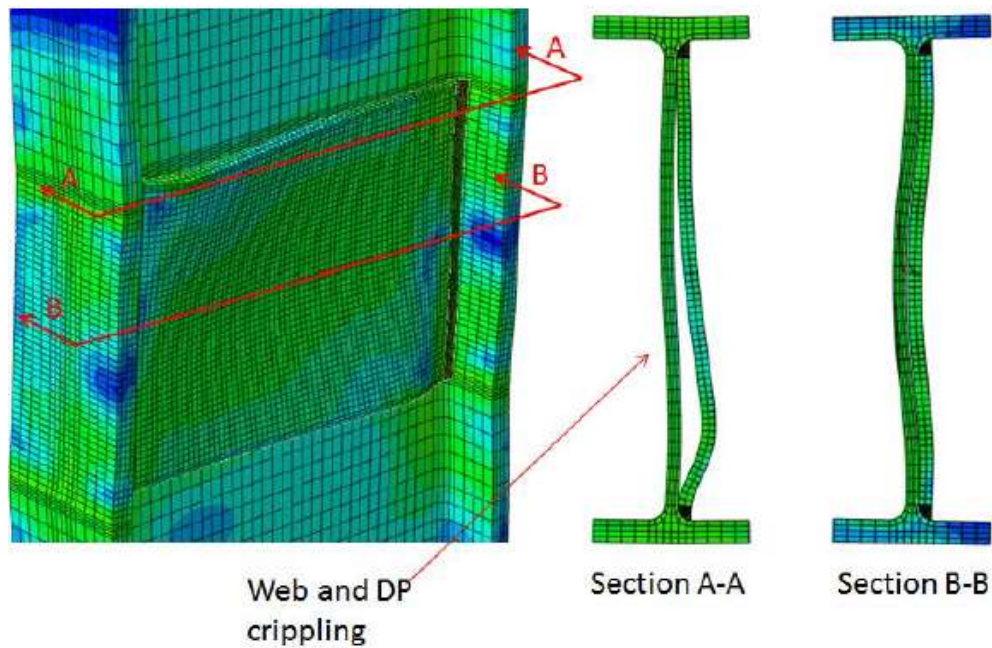


Figure 2.17: Web/DP Crippling Case 2B (Gupta, 2013)

The results from this modeling re-enforced the previous research by Donkada and Shirsat; the shallow column showed no increase in panel zone strength when all four sides of the

PZ were welded. The use of welds at the top and bottom of the DP also resulted in lower stresses in the vertical welds. A strength gain of 10% in the deep column specimen was obtained by the use of the horizontal welds along with vertical welds. It was suggested that this gain in capacity was due to the propensity for the DPs in deeper columns to fail in buckling modes. The attachment of DPs to a deep column PZ by horizontal welds, in addition to vertical welds, seemed to prevent failure due to doubler plate/column web crippling (see Figure 2.17).

Gupta's results showed that the extension of the DP by 6 inches did not increase PZ strength of the shallow column but did increase that of the deep column by 12-18%. The extension of the DP also reduced the stresses throughout the vertical groove welds. This is likely due to more weld material partaking in transferring the load to the DP. Gupta reports that the vertical groove weld carries mostly horizontal normal stress. The extension of the DP was also found to reduce the tendency of buckling and crippling by the DP.

The results also indicated that CPs do not increase the PZ strength of either shallow or deep columns but do allow the columns to reach full shear strength, especially for columns with thinner flanges. The attachment of CPs to the DP did not add significant stresses to the DP but managed to reduce the stresses in the groove welds of the shallow column.

## **2.13 SUMMARY**

This literature review covered research conducted in the 1950's, when researchers began testing the performance of moment resisting joints and the contributions the PZ made to the overall connection. It was determined that the PZ is capable of resisting high levels of

shear stress and had a large capacity to deform, meaning it was very ductile. These are important properties of the PZ, since lateral forces applied by the beam flanges distribute in the form of shear force. Ductility of the resisting member is necessary in any LFRS that will be cyclically loaded. Thin column webs were found to reduce the strength of the connection and result in early failure. The reinforcing/thickening of the column web, by the addition of a DP, greatly improved performance of the connection. These tests were early indications of how continuity plates can assist PZs in reaching full shear resistance.

It was later found that the stiffness of the joint began to decrease once the PZ had reached its yield point. This meant that once most of the material in the column web had reached the yield stress, the effectiveness of supporting any increasing load decreased. These results made the importance of the PZ contribution to lateral force resistance more obvious. Because the columns of the LFRS are also responsible for support of gravity loads, the influence of axial load on the PZ was tested. The yielding of the PZ was expedited by the presence of axial loads in the column, along with moment from a lateral force. Since gravity loads are always present, it became more important to develop design recommendations for these systems. The Von Mises yield criterion was found to be very helpful in developing these recommendations. A good understanding of the behavior of the panel zone was determined to be important since story drift levels are highly dependent on the rotations experienced in the PZ.

When researchers looked closely at the range when the performance of the PZ began to greatly influence global response of the LFRS, they found the turning point to be between 75 to 100% of the column web yield point. Once the PZ yielded, researchers also found that contributions from elements surrounding the PZ were substantial and needed to be



considered in design calculations. Determining ultimate load capacities and how these will be managed by structural members in moment frames is particularly important in LFRS. The resulting deformations, if not managed, can cause a structure to collapse.

As a way to reinforce the PZ, structural designers began to attach web doubler plates to thin column webs in order to strengthen these column webs. The results from the testing of the reinforced web showed that DPs were a very effective method of increasing the load capacity of the PZ. The tests also revealed that once the column web had yielded and as a result stiffness began to decrease, the DP contribution to shear resistance increased. Up to the yield point, most of the shear had been resisted by the column web. Commonly used steel shapes have typical sizes. When expected lateral forces are higher than what the selected column web can handle, a DP can be effectively used to increase load capacity.

Three approaches to the design of moment connections and PZ were being researched. The benefit of testing weak, balanced or strong PZs is understanding which one would provide safer options. Their research turned to the benefits that possible design features such as thinner webs, thicker flanges or thicker continuity plates could contribute. The result of a thinner column web is a design in which the PZ is the weak point. Most of the deformations are focused on this area and the attached beams do not contribute. Some research indicates that weak panel zones can potentially increase the propensity of the welds at the beam flange column web to fracture. When testing whether the use of thicker column flanges could improve performance of the PZ, it was found that the performance did not improve substantially. The use of thicker flanges did result in more complex stress conditions at the column beam interface and an increased difficulty predicting shear capacity of the PZ.

From the tests covered in this review, CPs were found to be extremely beneficial in preventing buckling of the plate elements in the PZ. These modes of failure resulted in lower design strength and early test failures. It was found that the use of CPs was far more important than their thickness, although some researchers suggested that thinner CPs can increase the fracture potential of the PZ. CPs were found to be especially useful when used in shallow columns with thin flanges. The use of these in deep columns was most beneficial in preventing buckling of the members.

The failed connections found after the Northridge earthquake brought a rise in research. In these tests, much focus was centered on how the members in moment connections were attached. One of the resulting observations from this was the realization that bolts were not as effective in transferring lateral loads as were welds. The connections using bolts to attach the beam webs to columns were observed to be less ductile as well. Other than buckling of the members, a more characteristic form of failure that reduces the performance of PZ is failure of the welds. Most of the research covered made comments regarding the need for quality welding practices.

The elements that attach the beams, CPs, and DPs, welds and the forces are of great importance. Welds are also very expensive and laborious. The panel zone's complex geometry makes it difficult to weld reinforcements onto it. Previous work attempted to find out which welds were necessary and if there were other ways to reduce the number of welds. Research by Shirsat, Donkada and Gupta has shown that one way to do this is by extending the DP beyond the beam flanges. In shallow columns, this results in reduced stresses in the vertical welds and seems to make the weld at the top and bottom of the doubler plate unnecessary. In deep columns, the extended doubler plate resulted in an

increase in PZ strength and reduction of buckling failure. The data also showed that the extension of the DP promotes ductile behavior and reduces stresses overall, resulting in a reduction of fracture potential. The necessity of the weld at the top and bottom of the unextended doubler plate was not made clear, since some benefits for it could be found.

As covered by this review, much research has been conducted regarding the overall performance of the PZ and how individual parameters affect the stresses at the beam-column interface. There is very little research regarding the attachments that reinforce the PZ and allow it to reach its full shear capacity. Some of the latest research at the University of Texas at Austin has considered the local effects that extended doubler plates, other attachments and welds have on the PZ. The purpose of this research has been to make recommendations for simpler, more effective PZ design configurations. It is for this reason that this thesis covers the situation in which a doubler plate is fitted inside the PZ. No information currently exists regarding this particular design configuration, which is necessary at times.

## **CHAPTER 3**

### **Modeling Techniques**

#### **3.1 OVERVIEW**

The purpose of this thesis is to investigate the behavior of panel zones reinforced by fitted doubler plates and the attachments used to reinforce them. This was completed using the finite element analysis package, Abaqus, to conduct the computational simulations of two specimens. This chapter provides an overview of the modeling done in Abaqus and its modules. The assembly of the models, the materials and the properties that define these will be covered, along with key modeling techniques, assumptions, simplifications, and data processing. A discussion of the validation of the models will also be covered, with comparisons to lab tests performed previously. The modeling completed in this thesis is similar to those previously done by Shirsat (2011), Donkada (2012), and Gupta (2013).

#### **3.2 ABAQUS PROGRAM**

When analyzing a structural problem, the finite element method is employed to take the geometry and break it down, into smaller, simpler shapes, elements. After the discretization, a load or displacement is applied to the model. The equations that model their response are solved and the elements are then reassembled in order to define the behavior over the entire problem. The software Abaqus Version 6.12-2 was used to model two specimens of a W14x398 and a W40x 264 column and their attachments. Abaqus is a general purpose finite element analysis program suite used by engineers in the automotive, aerospace, industrial and structural engineering industries. It was initially developed to address non-linear physical behavior and as a result, has an extensive material library with pertinent constitutive laws and the ability to model their physical properties. Abaqus is

composed of five different core products: Abaqus/CAE, Abaqus/Standard, Abaqus/Explicit, Abaqus/CFD and Abaqus/Electromagnetic. The products used in this thesis were the Abaqus/CAE, which served as a graphical interface for visual assembly, job management and result visualization, and Abaqus/Standard, which uses the model input to analyze problems with static or low-speed dynamic loads. Although earthquakes are a dynamic load that involves inertial forces amplified by the structure, Abaqus/Standard can be utilized to model the behavior and obtain the forces experienced by the PZ.

### **3.2.1 Stages**

Every complete FE analysis consists of three stages: pre-processing/modeling, processing/simulating and post-processing/result analysis (See Figure 3.1). In the modeling stage individual elements (columns, stiffeners, plates and welds) are shaped using a variety of geometric tools. Linear and nonlinear material properties are attached to the parts and an assembly is put together. It is during this stage that the points and surfaces where data will be collected, and the increments at which they are collected, are defined. During the simulation stage, actual analysis of the model occurs; modeling assumptions and simplifications determine the time period for the analysis. The analysis of a model can be very computationally demanding and time-consuming relative to its complexity. The post-processing stage displays the resulting stresses and strains of the model. The data can be analyzed and manipulated in order to provide results for the structural problem.

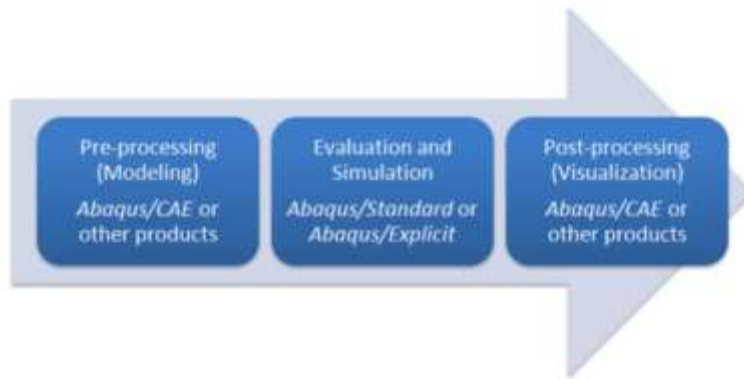


Figure 3.1: Abaqus Stages of Analysis (Abaqus 6.12.2)

### **3.2.2 Modules**

Abaqus/CAE is divided into 10 modules, 8 of which were used in this work. Some of the aspects defined in the modules include geometry, material properties and the boundary conditions. As the different modules are used to create the specimen to be analyzed, an input file to be submitted in Abaqus/Standard is generated.

#### ***3.2.2.1 Part Module***

This module is used to create or import the geometry of the individual parts. The elements used for the model are selected from solids, shells, wires, or beam elements. Geometries that will make up the parts are drawn and extrusions, fillets and profile definitions that will help define the shapes can be applied to create the parts. These parts can be subdivided into sections and the surfaces of these sections, whether internal or external, can be selected and defined in order to be used for data collecting.

#### ***3.2.2.2 Property Module***

The property module is used to define and attach material properties to the parts created. Some of the extensive material properties that can be edited include material density weight, ductility, damping, conductivity, and magnetic permeability. In general, this

module allows for physical properties to be defined for the model. Although Abaqus has its own material libraries and definitions, users are able to define their own materials using data acquired from testing done at labs.

### ***3.2.2.3 Assembly Module***

In this module, the parts are assembled to create a model to be analyzed. Even if a model is composed of one individual part, an assembly has to be completed in order for the part to be used by the software. Each individual part, which has its own local coordinate system, is brought in and positioned relative to each other in a global coordinate system. Some of the tools that are available in this module include tools for: rotating, translating and merging parts.

### ***3.2.2.4 Step Module***

It is in the step module where one selects the type of analysis that will run on the model. Thermal analysis, dynamic analysis, static analysis and buckling analysis are some of the choices that can be selected. Increments are set that will define the rate and sequence of loading or data recording during the processing of the model. If time-dependent properties were defined in the material module, the rate of loading would be specified in this module. It is here that the Nlgeom option is turned on or off, which determines if non-linear geometries are used by the equation solver. Linear geometry does not update the geometric dimensions as the load changes. The Nlgeom feature captures instabilities and effects from large displacements since it updates the element geometry at each load increment and has the ability to recognize that the element size/shape/position is different than initially

defined. Output requests of results for individual nodes, surfaces or parts can be defined here, along with the frequency of the recording of these.

### ***3.2.2.5 Interaction Module***

An assembled model requires definitions for how and what its surfaces are attached to and how they interact with each other. The interaction module is used to characterize mechanical, thermal and other interactions between the parts of the model and their surroundings, along with the methods connecting these. Two methods of defining how surface in the model behave are constraints and interactions. Constraints partially or fully eliminate degrees of freedom from selected groups of nodes or surfaces and their motion is coupled to a master node. Interactions, which define the way other parts of the model interact with each other, can also be defined in this module. These contact interactions are very important for the analysis as they represent the actual behavior expected in a real life specimen.

### ***3.2.2.6 Load Module***

Predefined fields, loads and boundary conditions are introduced and applied to the model in this module. There is a variety of load conditions that can be applied to a system including: pressure, gravity, thermal, heat flux, point and static loads. These are step dependent, meaning the user must define when and how a load is applied, which is done by the definition of an amplitude for rate of load application.

### ***3.2.2.7 Mesh Module***

In order to analyze a model it has to be subdivided into smaller sections. These sections must be uniform and with similar ratios in order for the results to be accurate. These subdivisions are done through the definition of a mesh that can be associated with the



model in this module. A mesh must smoothly change in size near complex regions and in sensitive spots. When meshing, holes, edges and other features of the geometry must be accommodated in order for the results of the model to be accurate. One method of obtaining accurate results is to decrease the size of the mesh, making it denser, which results in a large number of smaller elements. This can quickly become computationally expensive and can substantially increase the analysis time as well. A mesh refinement study can assist the user in identifying the optimal size of the mesh. Abaqus has tools that allow for the user to verify the quality of the mesh and define an optimal size for speed and accuracy.

#### ***3.2.2.8 Job Module***

In the job module, the user can create and define a job. Important parameters as to how many processors are used for the modeling can be defined here. As previously mentioned, complex models can take a substantial amount of time to complete. By using parallelization, symmetry and GPU acceleration, options in the job module, the time required to complete an analysis can be reduced. This is also where the job manager, which allows the user to monitor the process, is located.

#### ***3.2.2.9 Visualization Module***

The visualization module provides a visual method for the user to query and review the results of the analysis. Graphical representations of the deformations, stresses, displacements, and forces experienced by the elements are displayed. Data output can also be requested and plotted in this module.

### 3.3 STRUCTURAL MODELING IN ABAQUS

The following section details a description of the specimens modeled in this thesis, dimensions, simplifications, assumptions and other key parameters.

#### 3.3.1 Element Type

Abaqus has a wide range of elements from which to select when modeling structural analysis problems. Precedent research associated with this thesis used a C3D8R brick element; this work will do the same. The Abaqus element designation stands for **Continuum 3-D 8-node Reduced Integration**. This means that the model is composed of solid (C), **3D** elements made up of **8** nodes with 6 degrees of freedom each analyzed using **reduced** integration. The reduced integration reduces the computing necessary for the analysis. Some of the benefits associated with this element include: boundary conditions of both forces and displacements can be more realistically modeled, and it visually resembles the modeled system better than other models using different elements. One of the issues involved in using these elements involves complex meshing issues in regions with complex geometry such as tight radiuses or angles where a tetrahedral element might fit better. Another issue typically encountered is high computing and post-processing effort resulting from difficulties in converging of the equations. This is due to the cut in time step that Abaqus automatically does in order to attempt to resolve the issues. As is the case with smaller, more refined meshes, a model using solid elements has a higher likelihood of encountering mesh penetration issues, resulting in longer analysis periods and aborts of analysis. Node penetrations occur when the master surface mesh does not align with the slave surface mesh and because of deformations incurred during the analysis, its nodes penetrate the slave surface.

### 3.3.2 Model Parts

Two specimens were modeled in Abaqus (see Figures 3.2 – 3.3). The part module was utilized to define the geometries of the individual parts before they were assembled; these are as listed:

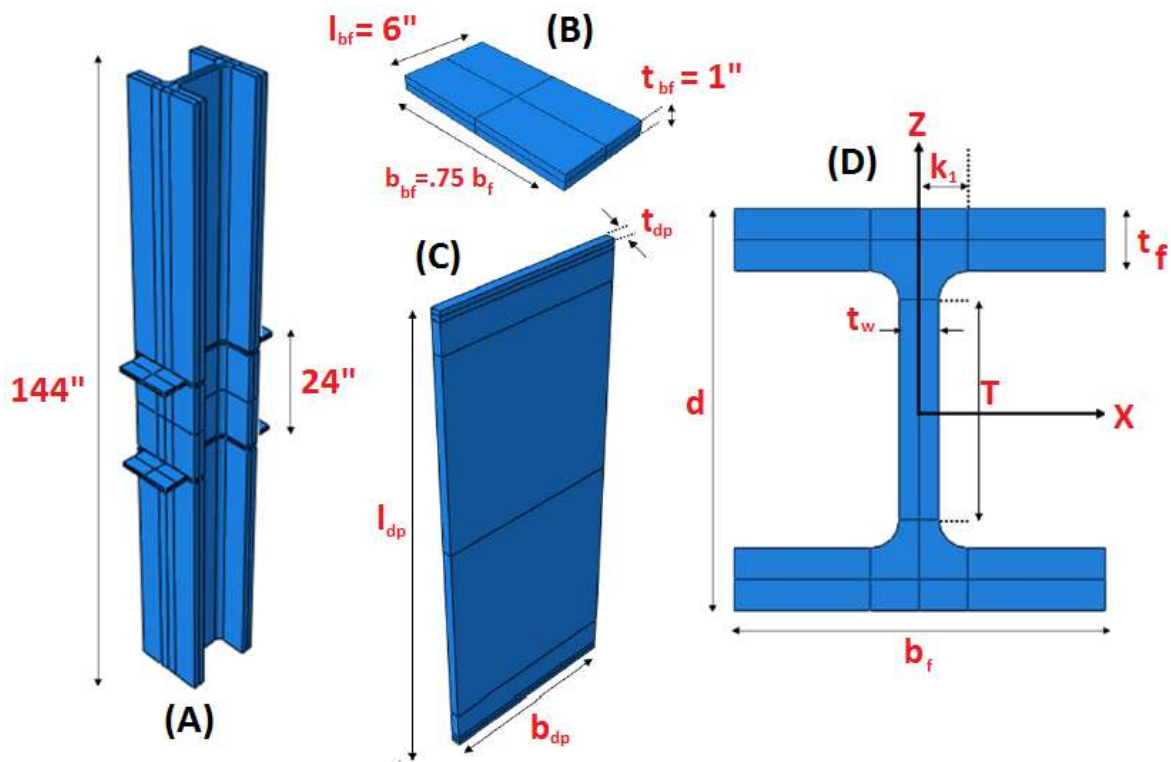


Figure 3.2: (a) Column, (b) Loading Plate, (c) Doubler Plate, (d) Column Profile

- **Column** – Two 144 inch long column segments were used. A W14x398 represented the shallow column and a W40x264 represented the deep column. For profile dimensions of these please refer to the *AISC Steel Construction Manual* (AISC 2010)
- **Loading Plate** – Four 6” x 1” x .75b<sub>f</sub> (Column Flange Width) steel plates were used to represent the top and bottom flanges from the beams that would be attached

to the column. These were placed 24” apart center to center on both sides of the column. Loads were applied to the PZ through displacement increments of the loading plates.

- **Doubler Plate (DP)** – The PZ was reinforced by a fitted DP which ranged from 21” to 24” tall for both the shallow and deep column specimens. The DP used in the shallow column was 10” wide and 1/2” thick and that of the deep column was 34” wide and 1” thick. Due to the congested region in the corners of the PZ, fitted DPs have clipped corners. These clips were done with a corner cut of 1.5” both ways, Figure 3.4.
- **Vertical Groove Welds** that “filled” in the gap between the DP and the column flanges (VGW1) were utilized in order to attach the doubler plate to the column. The forces and resultant stresses in these welds are of particular interest since they are indicative of the shear forces being applied on the DP. Because Abaqus will not allow the job to run when a node is attached to two separate surfaces, the corner of the weld where the edge of the DP and the K-Zone meet is chamfered, as seen below. This chamfer must also be done with mesh quality in consideration, since the clipping in this location will create a complicated section to be meshed. A chamfer that is very small will result in very sharp corners where a uniform mesh can’t be applied. It is better to apply a longer chamfer that matches the contour of the exterior radius.

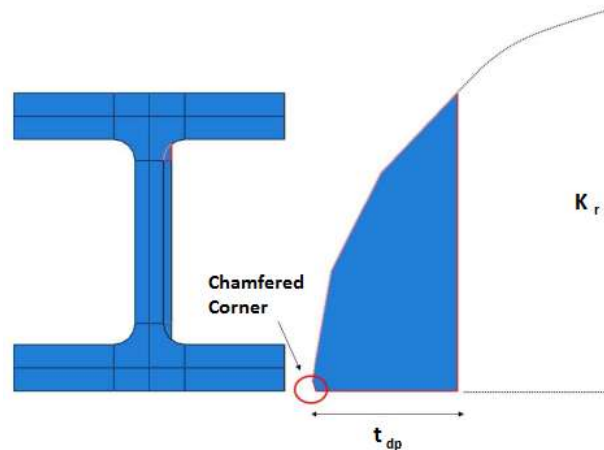


Figure 3.3 Vertical groove welds between the DP and the column flanges

- **Horizontal Fillet Welds** between the DP and the column web are as thick as the DP on both sides. The corner edge of the weld, where the top edge of the DP and the column web meet, is chamfered for the same reason as that of the vertical groove weld.

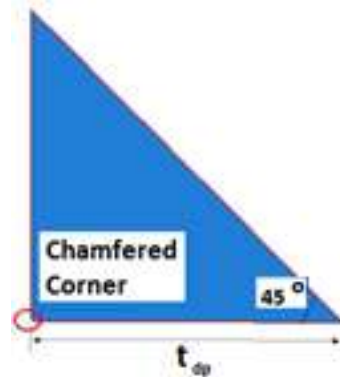


Figure 3.4: Horizontal fillet welds between the DP and the column web

- **Continuity Plates**, (CP) were used for all the models that used DPs. The plates' thickness is required to be no less than half the thickness of the attached beam's flange per *AISC Seismic Provisions*, (AISC 2010) (de a reference to the 2010 AISC Seismic Provisions) Hence, all CPs were 1" thick for the analysis to match the thickness of the loading plates. The width of the continuity plates was selected to

match the width of the loading plates as shown in Figure 3.4. The clipped corners in Figure 3.4 were dimensioned per the *AISC Seismic Provisions* (AISC 2010). For a discussion on how CPs affect PZs of columns with varying column flange thickness, see Donkada (2012).

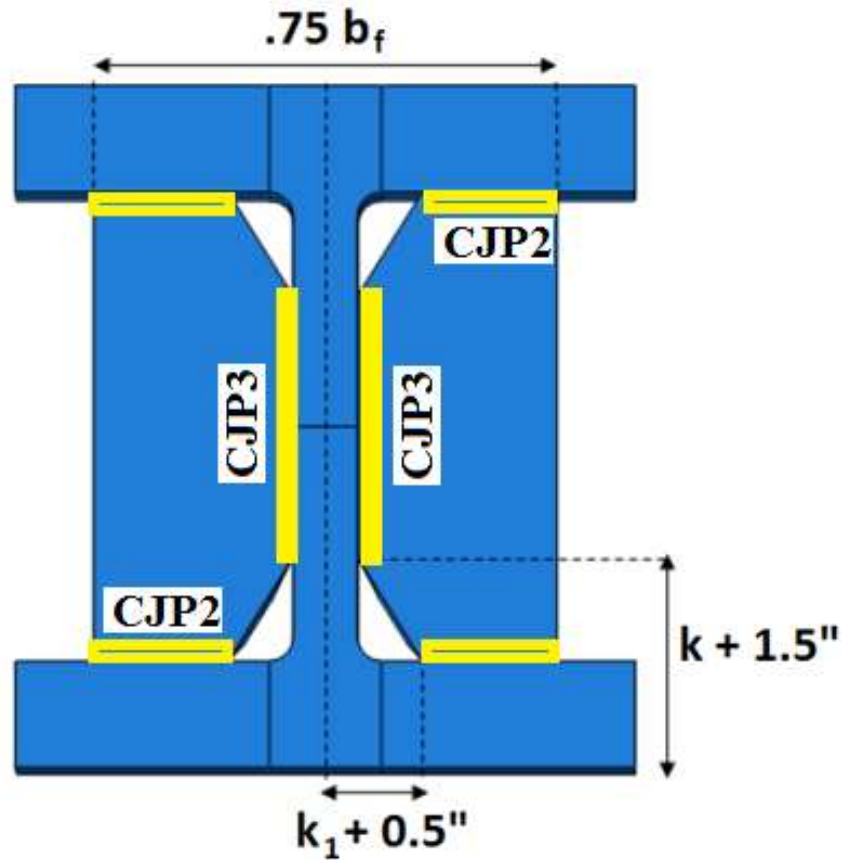


Figure 3.4: Column section cut with continuity plate dimensions

- **Single Bevel Full Penetration Weld** between the CP and the column flanges (CJP2) and **Single Bevel Full Penetration Weld** between the CP and column web (CJP3). The CP plates were attached by complete joint penetration groove welds

as seen in Figures 3.4 and 3.5. These were formed by the 30 degree single bevel in the CPs. The bottom corner of these was also chamfered.

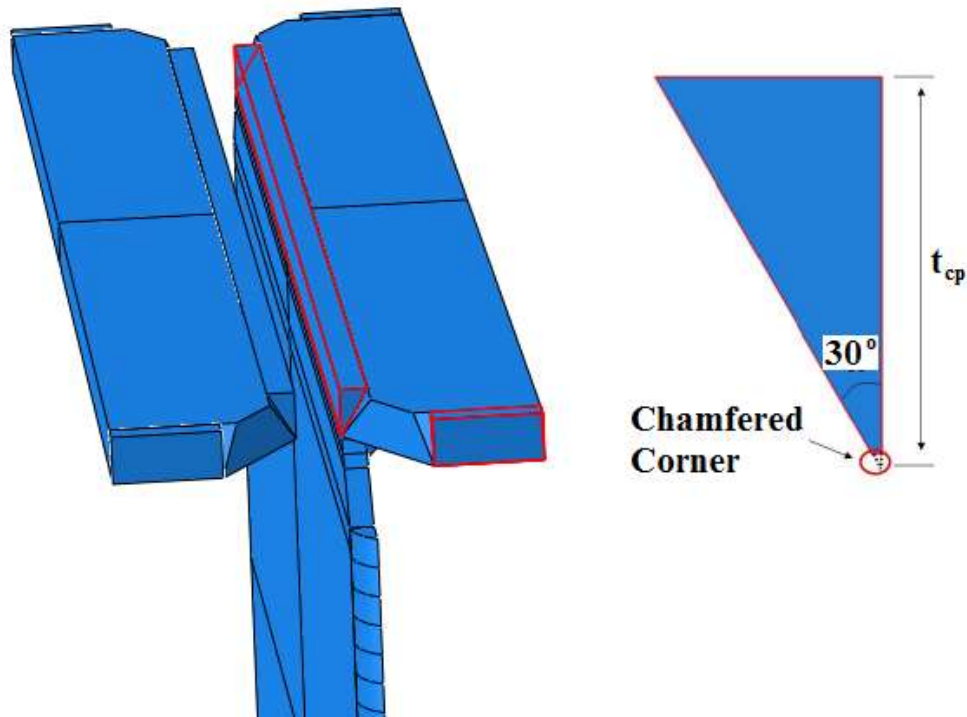


Figure 3.5: CJP2 and CJP3 view without column in view

Abaqus allows for the definition of multiple iterations of the same model in one file. A typical reason for this would be a change in geometry or an omission of a weld or part. Some of the welds modeled had 60 different surface definitions that would have had to be redefined every time a new iteration of the model was defined. Great time savings can be accomplished by editing the existing lines defining the section sketch of the part, rather than redefining a new one. This will keep all previously defined attributes and surfaces for the new model.

### 3.3.3 Material Model

Although Abaqus contains a vast library of material definitions, it provides the ability to define any material using test data. This data input is in the form of a stress-strain curve similar to those in Figure 3.6. These stress-strain curves define the elastic behavior up to the yield point of the material,  $f_y$ , and the plastic behavior afterwards. Two idealizations were used for the behavior of its parts. To keep yielding within the PZ, the loading plates used a continuously elastic material definition. This prevented local yielding in the loading plate. All other parts used a multi linear material model approximated by a curve similar to Figure 3.6(d), but composed of three segments. Different yield points and strain hardening values were selected for the three types of steel used. It is important to note that the thesis by Gupta (2013) used a material model curve similar to Figure 3.6(d), but the results of the analysis of the PZ behavior were similar to those of Donkada (2012) and Shirsat (2011), yet the analysis time was increased greatly.

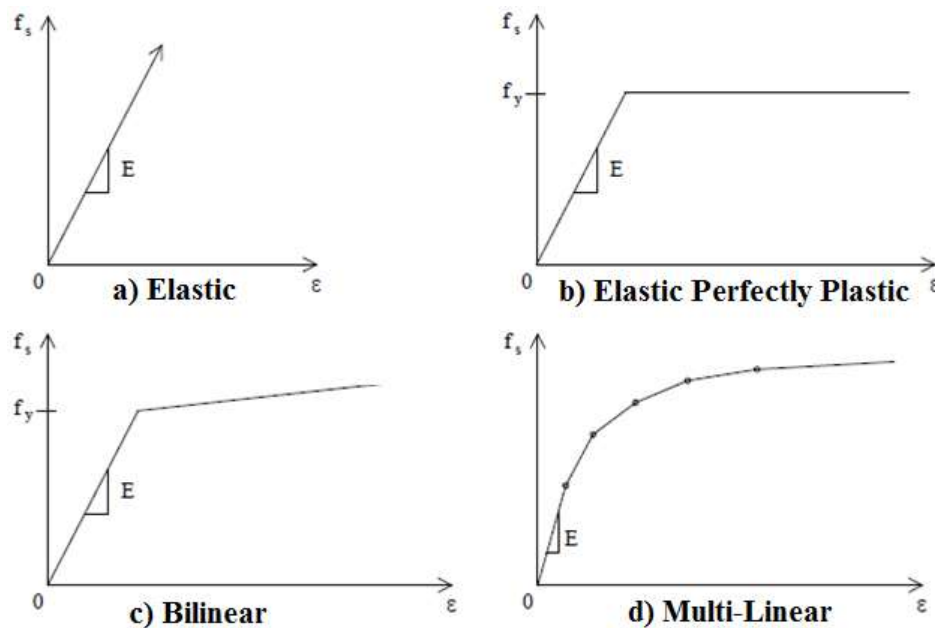


Figure 3.6: Typical models of stress-strain curves, (Ho, 2010)



The input of the material stress-strain curve is done in the Abaqus Material Module. Abaqus does not have a built-in unit system and as a result, all input and output must be specified using consistent units. In order to enter a material definition, the user must enter the edit material tab where the elastic and plastic stress strain data can be entered. The elastic range of the material is defined under the elasticity tab by Young's modulus and Poisson's ratio. The plastic part of the material definition is entered in the plasticity option under the mechanical tab. This is also the location where the user can define the type of strain hardening that the material goes through, past the point of yielding. Some of the types of rules available are kinematic, isotropic and combined.

In order to obtain a stress strain curve in a laboratory, a material coupon must be cut in a standard shape and pulled by a machine at a certain rate. As the load increases, the change in distance between two predefined points in the coupon is recorded. The difference between the measurement,  $dl$ , and the original length,  $l_0$ , is referred to as engineering strain. The matching engineering stress is defined by the force being applied,  $F$ , divided over the original cross-sectional area,  $A_0$ . This stress is not necessarily accurate, since the cross-sectional area of the coupon is decreasing, as explained by Poisson's effect. It is because of this that Abaqus does not utilize engineering stress and strain. The input must be in terms of true (Cauchy) stress,  $\sigma_{nom}$ , and true (logarithmic) strain,  $\epsilon_{nom}$ , as defined in the equations below (from *Abaqus User's Manual, Section 20.1.1*).

Relationships Between Engineering and True Stress, Strain Values:

$$\sigma_T = \sigma_{nom}(1 + \epsilon_{nom}) \quad \epsilon_T = \ln(1 + \epsilon_{nom}) \quad \epsilon_T^{pl} = \epsilon_T - \frac{\sigma_T}{E} = \ln(1 + \epsilon_{nom}) - \frac{\sigma_T}{E}$$

**Engineering Stress:**  $\sigma_{nom} = \frac{F}{A_0}$

**Engineering Strain:**  $\varepsilon_{nom} = \frac{dl}{l_0}$

**True Stress:**  $\sigma_T = \frac{F}{A}$

**True Strain:**  $\varepsilon_T = \int_{l_0}^l \frac{dl}{l} = \ln\left(\frac{l}{l_0}\right)$

The material model utilized for this thesis is similar to that of Shirsat (2011), and Donkada (2012), Figure 3.7. The inelastic material model was developed by Okazaki (2004) for the A992 steel used in his FE modeling. Coupon tests were performed on the webs and flanges of columns used in his experiments. Since the focus of the research is based on PZ behavior, the data from the web tension coupon was used for the model.

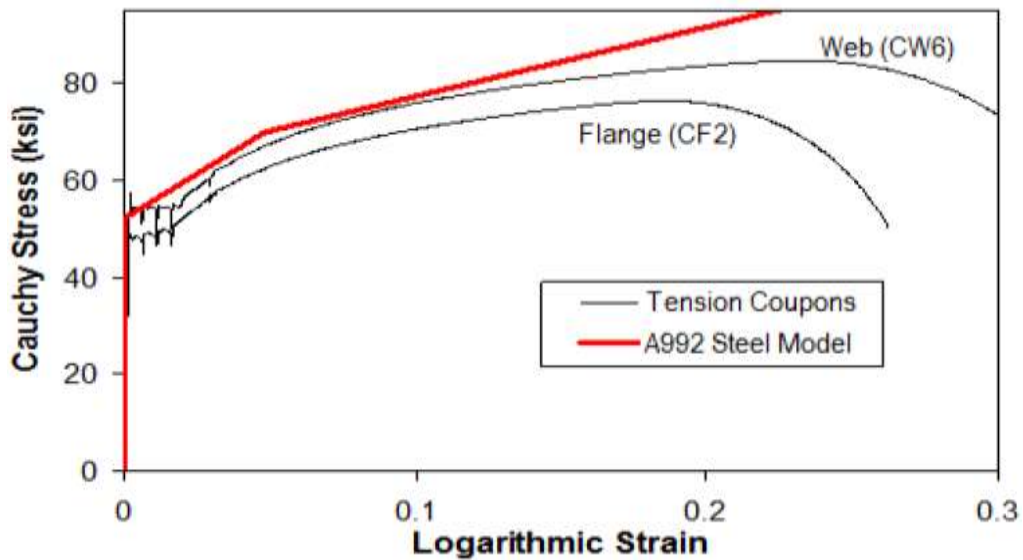


Figure 3.7: A992 Steel tri-linear model (Okazaki, 2004)

Although Okazaki’s experiments were cyclic in nature, the “Okazaki Trilinear Steel” material model was developed for monotonic loading of finite element models. The “Okazaki” material curve for steel, as defined in the Abaqus job definition file on Figure 3.8, was used to define all of the W-shape columns and beams in this thesis. Due to the similarities between A992 and A572 Gr. 50 steel, it was also used to define all plate elements including stiffeners, continuity plates and doubler plates. All welds modeled in this work used the material definition “Okazaki Trilinear Weld”, developed by Okazaki, which is based on data reported by Kauffman (1997). Figure 3.8 displays the input command lines, accessible in the “edit keywords” tab, that define the material models used by Abaqus to model the specimens used in the research.

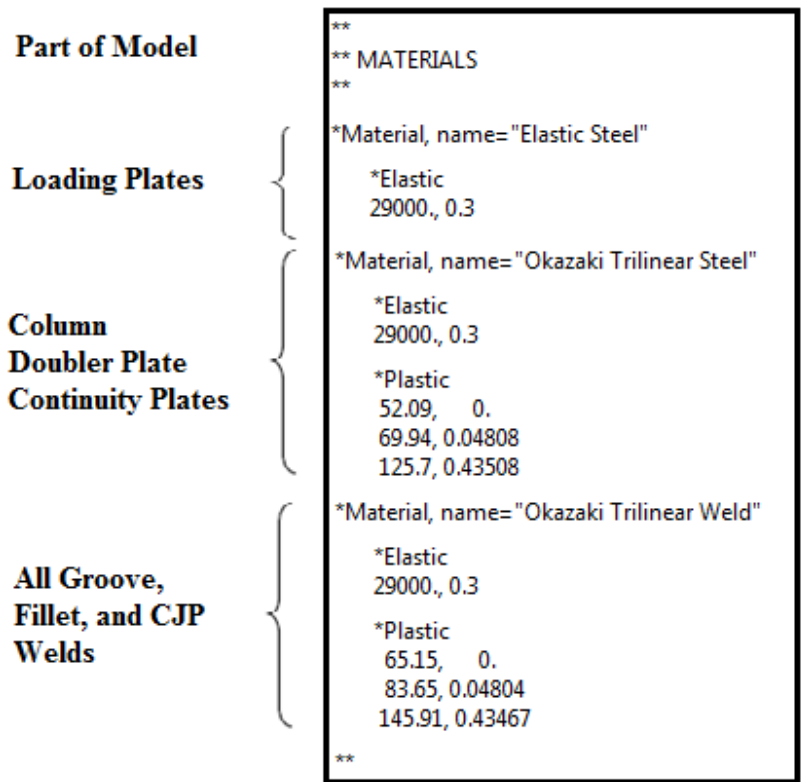


Figure 3.8: Abaqus A992 Steel definition (Units = Ksi, in/in)

To define a new material, the user must enter the “create a new material” feature and define the elastic behavior of the material using the elastic modulus of 29,000 ksi and Poisson’s ratio, 0.3. The individual values defining the inelastic part of the material definition are recorded by the user. Notice the first strain point of the plastic definition of either “Okazaki” materials lets the software know that once an element has reached the yield stress point, its plastic strains start from zero and follow the defined curve. Because the material model is based on monotonically loaded coupon tests, there is no information on the type of cyclic strain hardening rules; therefore, an isotropic strain hardening rule is assumed. Validation exercises are discussed at the end of this chapter, comparing FE results to real lab experiments where specimens were loaded into the inelastic region in flexure and shear. For a review of the development of a material model used for modeling of specimens loaded in cyclic manner, read Gupta (2013), Chapter 3.

### 3.3.4 Meshing Techniques

Part	Meshing Technique	W14 X 398 Mesh Seed Size (in)	W40x264 Mesh Seed Size (in)
Column (PZ region)	Structured	0.5	0.5
Column (Outside PZ region)	Structured	1.5	1.5
Continuity Plate, CP	Sweep with medial axis algorithm	0.5	0.5
Doubler Plate, DP	Structured	0.5	0.5
Fillet Welds	Sweep with medial axis algorithm	0.1	0.1
Groove Weld, (CJP2)	Structured	0.1	0.1
Groove Weld, (CJP3)	Structured	0.1	0.1
Loading Plate	Structured	0.25	0.25
Vertical Groove Weld, (VGW1)	Sweep with medial axis algorithm	0.1	0.1

Table 3.1: Part meshing techniques and sizes for specimens

As mentioned in section 3.2.2.7, the meshing of the model is one of the most important aspects of the process. The types of elements selected, the density, and ability to smoothly

define shapes not only determines if the job will be analyzed completely but also the speed and accuracy of results. For the specimens modeled, a hexahedral mesh was selected because these elements are robust and result in fewer convergence problems, which cause the early termination of the job. Previous mesh refinement studies by Donkada (2012), as well as work by Gupta (2013), influenced the mesh size for the individual parts seen in Table 3.1.

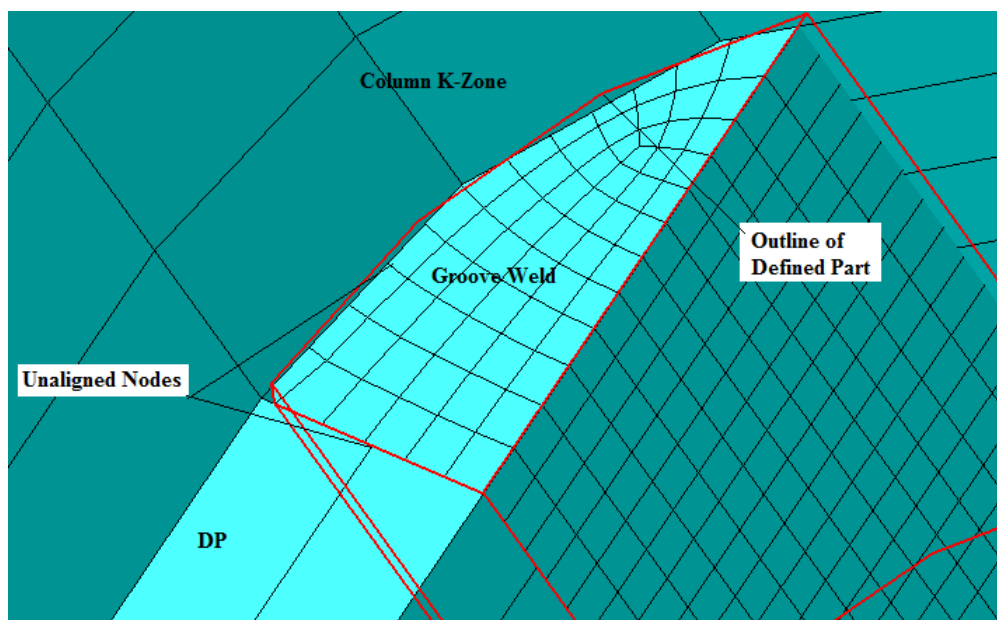


Figure 3.9: Column K-Zone where complex geometries meet

The density of the mesh is not the only characteristic that makes an analysis more time consuming; the errors that are encountered as the loads are applied also cause delays. As pictured in Figure 3.9, many parts with complex geometries meet in the PZ, in particular the K-zone of the column. Note that the user-defined groove weld, outlined by the red perimeter lines, varies from the meshed geometry, which is what is analyzed by Abaqus. The mesh sizes of the parts are not often identical to each other and because the NIgeom

option is selected, a denser mesh is able to penetrate the larger mesh. Where and how often these penetrations occur is managed by the surface discretization method, along with the Master-Slave surface definition used, Figure 3.12. When deep node penetrations occur, Abaqus stops the analysis increment and begins a new iteration but cuts the time step in half in an attempt to get a converged solution. If non-convergence continues, Abaqus will continue to cut the time in half until convergence or it aborts the job after 10 tries. These discretizations of analysis time, due to mesh issues increase time requirements substantially.

A method used to improve the quality of the mesh while modeling of the specimens is the use of partitions. Partitions can separate areas that need a denser mesh or special meshing algorithms as well as define surfaces that can be used for the query of stresses. An example of how subdividing improved the mesh of the model is pictured in Figure 3.10. Without the partitions on the column, Figure 3.10 (A), the results of the analysis would have been less accurate. Abaqus also provides a tool to check the quality of a mesh by determining the aspect ratio, the maximum or minimum value of corner angles and other size metrics. Once utilized, it will create a set highlighting the poor quality elements.

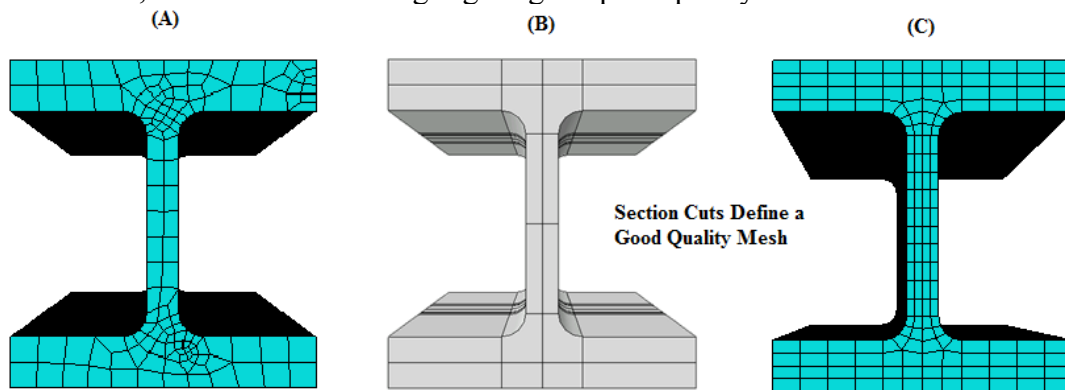


Figure 3.10: (A) Mesh without partitions, (B) Partitioning, (C) Mesh with partitions

Abaqus also provides different meshing techniques and algorithms which include medial axis and advancing front algorithms. These can help define a mesh that will provide good, accurate results; Table 3.1 and Figure 3.11 show the techniques and algorithms used for the individual parts of the specimens modeled. Many difficulties in completing the jobs were encountered in the deep column specimen. As mentioned previously, node penetrations prevent the job from completing, an issue encountered mostly in the finishing stages of the job progress. The larger DP is more prone to buckling issues, which cause node penetrations on the welds and on the DP as well. Abaqus offers a Job Diagnostics tool in the Visualization Module where these issues can be reviewed and resolved.

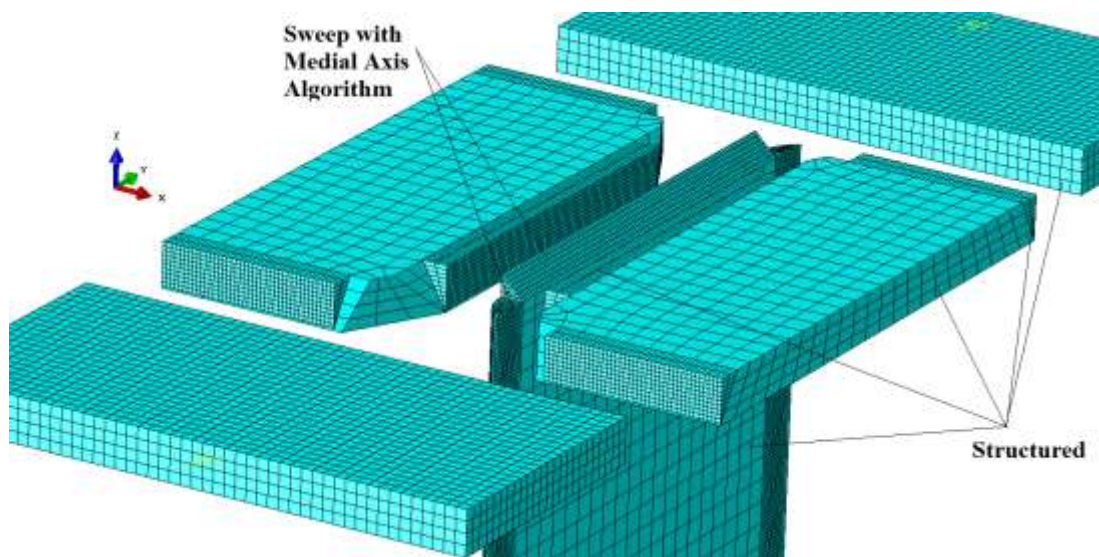


Figure 3.11: Mesh methods used on column attachments of W14x398

### 3.3.5 Assembly

Once the individual parts have been defined and appropriate physical and material properties have been attached to the parts, the model is then put together in the assembly module. Multiple copies of each element are brought in, rotated and translated into place relative to the global axis of the model. All surfaces that come into contact must be defined

as contact pairs and the nature of the interaction defined. A constraint is defined by selecting a type of constraint and defining a master and slave surface. Figure 3.12 exemplifies the use of master and slave surfaces to define a constraint. One of the recommendations for surface definition is to specify the part with the coarser mesh as the “master surface” and the one with the denser mesh as the “slave surface” (*from Abaqus Analysis User’s Manual, Section 31.3.1*). It should be noted that this is not always the case, as can be seen in the difference of surface definition for the DP and the deep column web between Gupta (2013) and this work.

The three types of constraint methods used for the model were: the tie constraint, hard contact and rigid surface constraints. The tie constraint defines two surfaces that are perfectly bonded and whose nodes are tied to each other. This constraint was used to model the binding that would be expected from welds or parts that are welded together. Similar to a real life weld, the joined parts behave in unison and stay “tied” through the whole analysis. Another type of constraint used was the “hard contact” constraint, which was defined by creating an interaction property and selecting the “Normal” behavior option in the mechanical tab. The “allow separation after contact” option was also selected in order to permit the surfaces to separate once the force between them was zero. This contact definition was used to define the actual behavior between the doubler plate and the column web (see figure 3.12). When loads are applied, the DP mesh deforms and attempts to penetrate the surface of the column web. Because of the hard contact interaction, the surfaces are prevented from penetrating each other and then are allowed to separate after the load is removed. This behavior can and does cause mesh issues in the K-zone as well, due to the complex geometry in the region. This is of particular importance to the deep column specimen, since the DP in this specimen is more prone to buckling.



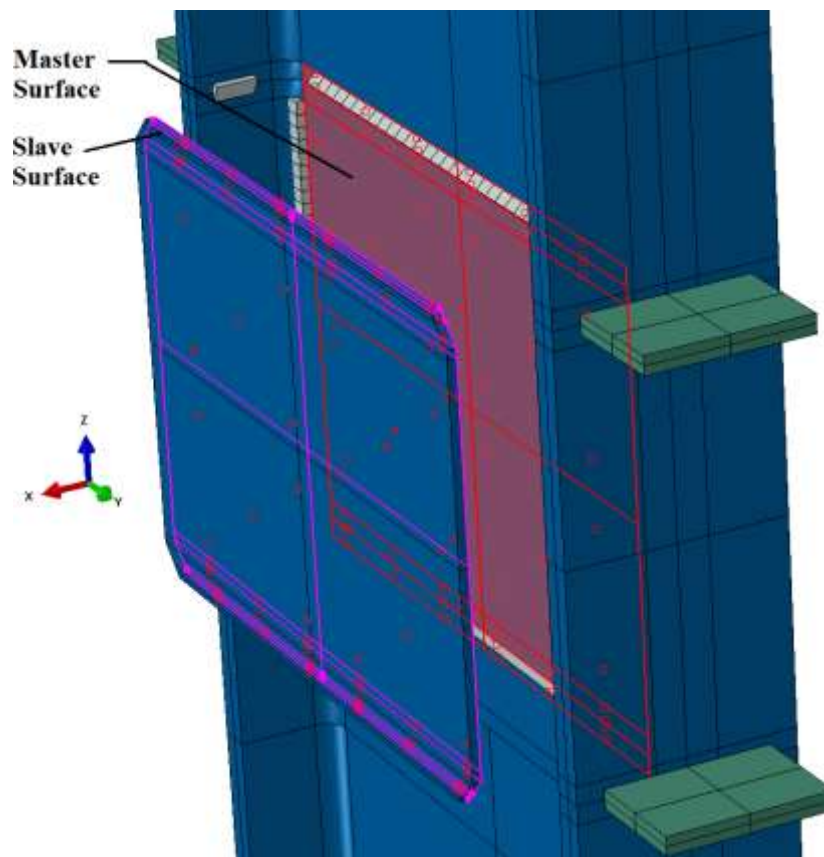


Figure 3.12: Clipped DP onto W40x264 column (Part colors based on material definition)

Initial over-closure occurs when nodes in one surface are penetrating other surfaces without any force being applied. Abaqus provides settings that can adjust the initial over-closure and keep the job from aborting. As mentioned in the section covering the definition of analysis steps, a short initial increment can help correct initial over-closure problems. Along with good meshing techniques, another tool that can be employed in regions with complex geometry is surface discretization. Two methods that Abaqus provides are: the node-to-surface or surface-to-surface discretization methods. The node-to-surface method defines contact conditions between each slave node and the master surface. The surface-to-surface discretization method considers the shape of both the master and slave surfaces when defining the constraints (from *Abaqus Analysis User's Manual, Section 12.4.3*).

Table 3.2 defines the master-slave surface definitions between the contact surfaces of the W40x264, along with the type of constraints and surface discretization methods used. The W14x398 specimen utilized the same settings except the discretization methods selected for all surfaces was the analysis default, which is surface-to-surface.

The third type of constraint used is the “rigid body” constraint, which ties a selected surface to the displacement and rotation of an individual node (*Abaqus 6.12 Analysis User’s Manual, section 2.4.10*). To define this constraint a reference point/node is defined on the model and a “rigid body” constraint is tied to this node. This will enforce the same displacement and rotation that the selected node exhibits onto the rest of the defined surface. This type of constraint was used to model a boundary condition in which the ends of a member are able to rotate and behave as one rigid surface. Both the pin and roller boundary conditions of the specimens modeled used a rigid body constraint, pictured in Figure 3.13.

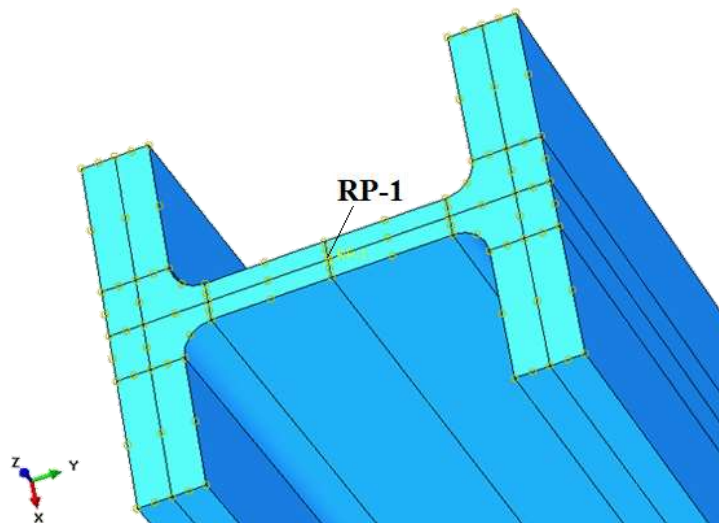


Figure 3.13: A “rigid body constraint” defines the roller BC at the top of the column

Master Surface	Slave Surface	Type of Constraint	Discretization Method
Column Flange	Loading Plate	Tie Constraint	Analysis Default
Column K-Zone	Vertical Groove Weld VGW1	Tie Constraint	Node to Surface
Column Flange	Groove Weld CJP2	Tie Constraint	Node to Surface
Column Web	Groove Weld CJP3	Tie Constraint	Analysis Default
Column Web	Horizontal Fillet Weld to DP	Tie Constraint	Node to Surface
Continuity Plate	Groove Weld CJP2	Tie Constraint	Analysis Default
Continuity Plate	Groove Weld CJP3	Tie Constraint	Analysis Default
Doubler Plate	Vertical Groove Weld VGW1	Tie Constraint	Analysis Default
Doubler Plate	Horizontal Fillet Weld (Top & Bott.)	Tie Constraint	Analysis Default
Doubler Plate	Column Web	Hard Contact	Node to Surface

Table 3.2: Part constraints and contact surface discretization for W40x264 & W14x398

Once a model is defined and assembled, the user can define the surfaces and nodes that will be used to obtain data from the analysis. Although Abaqus provides a large amount of data from the job once the analysis terminates, it is often necessary to define the rate, type and location of data acquisition. Figures 3.14 and 3.15 illustrate the definition of the panel zone and the nodes selected to calculate the PZ rotation as the specimen was being loaded.

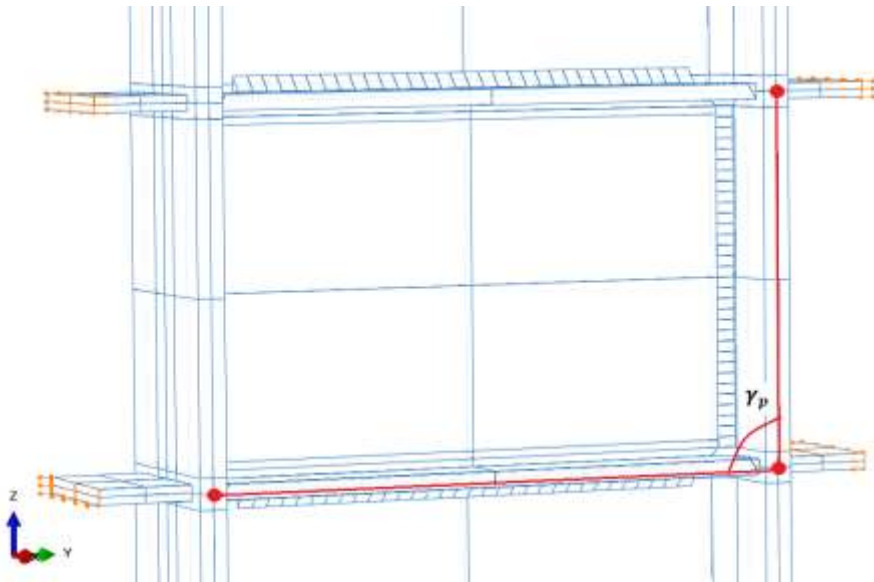


Figure 3.14: Data points for checking PZ rotation on W40x264 column

The reference points used to define the rigid surface boundary conditions as well as the nodes defining the PZ were utilized for data collecting. The PZ rotation,  $\gamma_p$ , was calculated by subtracting the difference in horizontal displacement of the top right node,  $H_t$ , from the bottom right node,  $H_r$ , and dividing the difference by the depth of the PZ (Equation 3.1). Panel zone shear was calculated using Equation 3.2, with the reaction force data recorded from the reference point at the top or bottom column rigid constraints.

$$\gamma_p = \frac{(H_t - H_r)}{d} \quad \text{Equation 3.1}$$

$$V_p = \frac{R_f(l - d)}{d} \quad \text{Equation 3.2}$$

$V_p$  = Panel zone shear

$\gamma_p$  = Panel zone rotation

$R_f$  = Reaction at bottom of column (from defined reference point)

$L$  = Length of the column (144 inches)

$d$  = Distance between the loading plates (24 inches)

$H_r$  = Horizontal displacement of the bottom right node

$H_t$  = Horizontal displacement of the top right node

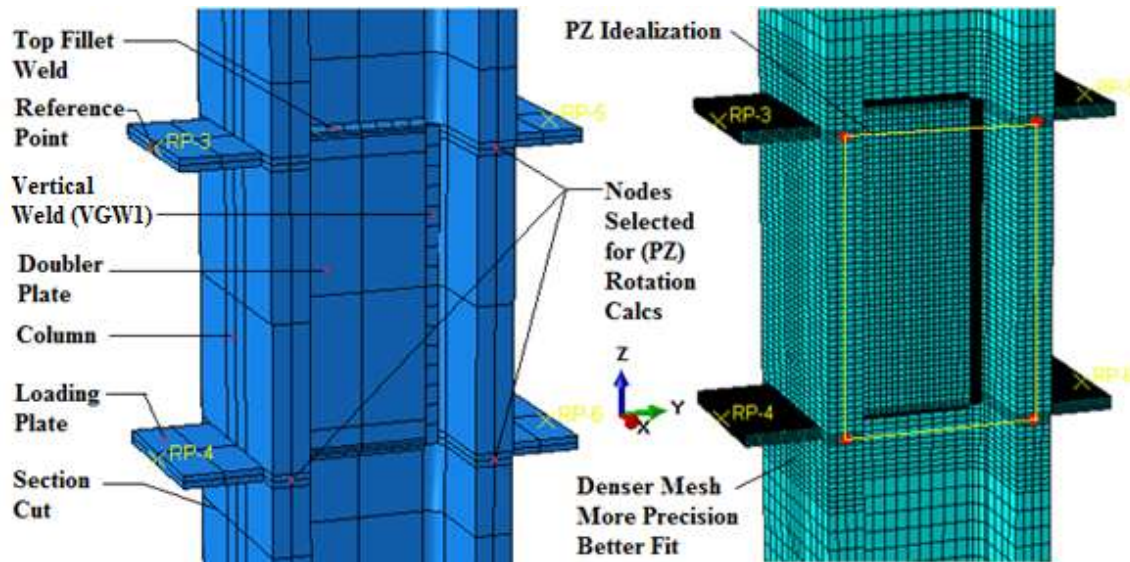


Figure 3.15: Data points used to define PZ rotation on a W14x398 column

The results from the analysis are presented in the form of stresses, but Abaqus offers the option to define a surface and record the forces and moments on the surface on all three X, Y, and Z axis. This option was utilized to obtain the normal and shear forces through the column and DP as well as surface loads being transferred by the welds attaching the DP to the column (Figure 3.16). The user defines a surface on the part, enters the edit keywords option in the Model toolbar, and types the section force command under the “\*\*OUTPUT REQUEST” line (Figure 3.17). This command will not only provide the forces from all principal global axis, if the “SOF” is typed, but also the moment forces summed about the center of the surface cut by typing “SOM” also. Abaqus will record the sum of the forces from all the nodes that define the selected surface for every increment of the load application. The results are reported in large text and data files that can be parsed by a self-written program routine. The Matlab code used to parse the section force data output from the 60 different defined surfaces is attached at the end of this thesis.

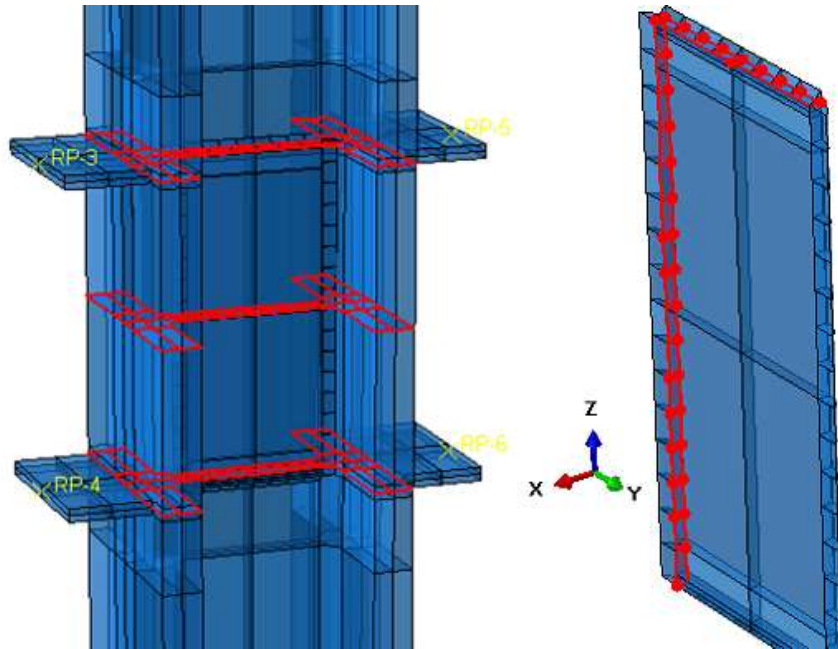


Figure 3.16: “Section Force” surface selections on W14x398 column specimen

### 3.3.6 Time Step

After assembly of the model and the definition of data collecting surfaces and nodes, a time step is defined for the application of load. Abaqus defines an initial time step by default, but the user must define another step for loading to occur. It is here that the use of nonlinear geometry can be applied to the model by turning the “Nlgeom” option on. Time step, initial increment size, as well as maximum and minimum time increment size for load application have to be defined here. As will be discussed in section 3.3.7 the rate of loading of the specimen was done using an amplitude definition. Because the loading amplitude used in the modeling had 60 increments, the time period selected for the force step had to match the amplitude with 60 increments also. The initial, minimal and maximum increment sizes were:  $1 \times 10^{-5}$ ,  $1 \times 10^{-15}$  and 0.2, respectively. The job was allowed to run for 20000 increments allowing Abaqus to make as many discretizations as needed to complete the analysis. Increment size boundaries for the time steps are important, since too large of an

increment size results in fewer points of data acquisition, which can make it possible to miss key events of the response of the model. The 0.2 max increment size defined in the step module proved to show a clear definition of the behavior of the model. A too small increment size definition will result in accurate but much longer analysis time. As covered earlier in the discussion regarding meshing, a small initial increment size can help alleviate initial over-closure issues, allowing for completion of the job and in some instances preventing the job from aborting within the first increment; hence why a value of  $1 \times 10^{-5}$  was used.

```
** OUTPUT REQUESTS
**
*section print,name=DBL1, surface=DBL1
SOF
```

Figure 3.17: Surface “DBL1” section force output request

### 3.3.7 Loading and Boundary Conditions

To apply load on a model, Abaqus subdivides the load into increments and applies at this rate. It is sometimes necessary to define a loading rate that is not only slower but will create more data collection points in order to get a good idea of behavior. The load rate definition is done through the use of the Amplitude option, which involves defining an amplitude protocol and attaching it to the load. The amplitude protocol serves as a load multiplier, which allows for a definition of many loading conditions such as ramp loading and cyclic loading. The amplitude used in the analysis used 60 steps at .0125 amplitude increments to reach the desired loading. Abaqus allows for two ways to apply loading to a model, the displacement controlled method and the loading controlled method. When using the loading controlled method a load is applied to a surface and the internal forces and resulting moments are calculated along with the displacements. This approach can make the analysis



of a complex model: difficult to complete. It is for this reason that the displacement controlled method, was utilized in the modeling, with the load derived using Equation 3.3. Since the PZ rotation of .05 radians was required and the PZ height of all models was 24 inches, the displacement applied at each of the loading plates was .6 inches. Notice that the applications of the load on the top and bottom loading plates were opposite from each other (Figure 3.14).

$$\text{Displacement Load} = \frac{(\text{Desired PZ Rotation (rad)} - \text{PZ Height (in)})}{2} \quad \text{Equation 3.3}$$

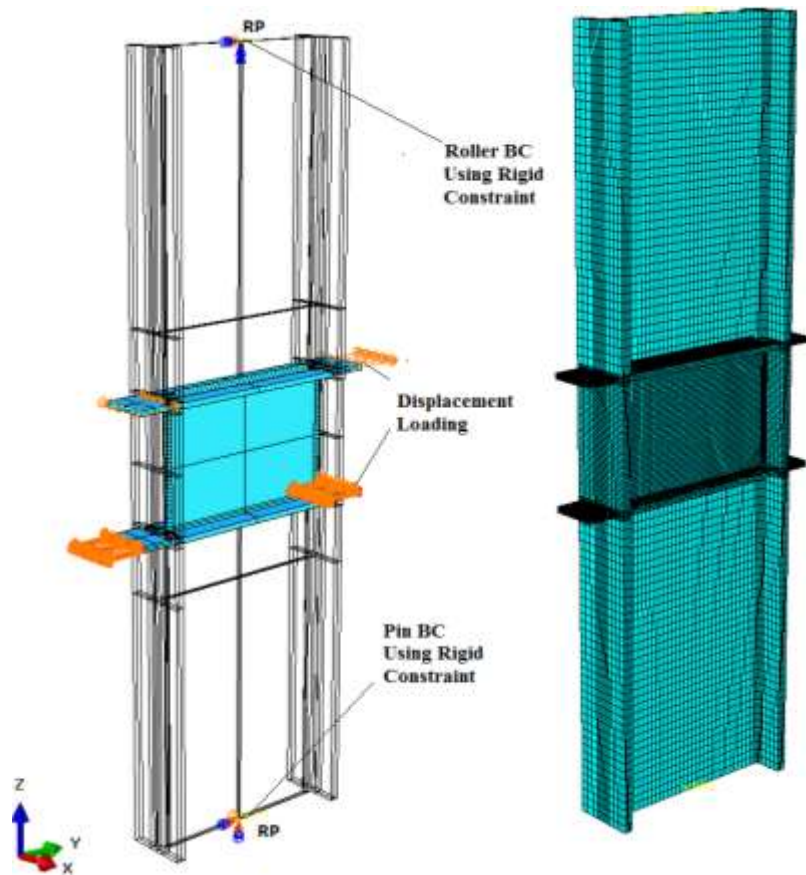


Figure 3.18: Meshing, loading and boundary conditions for the W40x264 model



The application of displacement or force loads can be completed using pressure, linear or point loads as well as through the use of a “rigid body constraint”. The latter option can be used to obtain an idea of the force being applied as well as to ensure that the load is evenly applied throughout the surface.

### 3.3.8 Modeling of Welds

The welds were carefully meshed in order to obtain the best quality mesh that was possible. As can be seen in Figure 3.19, sharp edges and radiuses can be difficult to properly subdivide. Although a decrease in mesh size can assist in increasing the quality, this is not the best solution. The use of a very dense mesh on the multiple welds of the specimen would increase the analysis time substantially. A study of the welds alone would require two models - a global model such as the one used, and a local model of the weld alone. The forces from the global model could be applied to a weld with a much denser mesh.

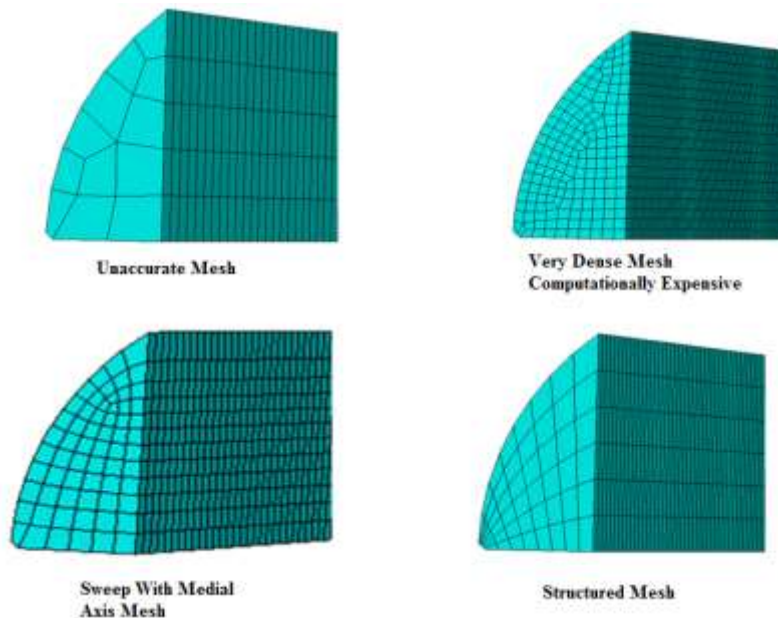


Figure 3.19: Meshing of the vertical groove weld, **VGW1**

The forces reported were obtained using the Abaqus “section force” command. The section surfaces were created using datum planes to subdivide the vertical groove weld and the fillet welds used to attach the DP to the column web, in 32 evenly spaced segments. Each segment of the surface was named and the global X, Y, and Z forces were requested using the “section force” command. As mentioned, Abaqus obtains these forces by summing up the reactions from each node that defines the selected surface. The summing of the nodes can present an issue of inaccuracy, since it is possible to double count the nodes, when the boundary dividing surfaces is counted in the summing of the forces, unless a smaller subdivision is created between the subdivisions. This is done by dividing the weld segments with two partitions relatively close to each other and not selecting the surface between these. The surfaces will not share nodes and the forces reported will be only for the nodes that define the selected surface.

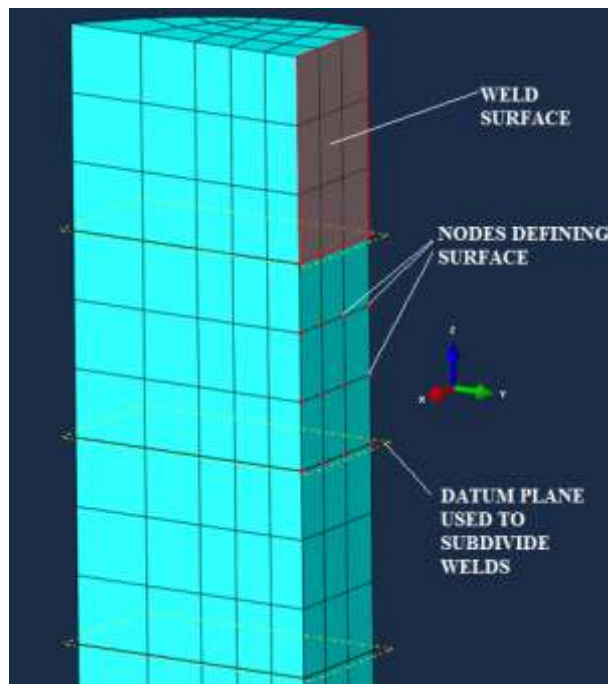


Figure 3.19: Surfaces used to collect force data & nodes that define these

To obtain the forces transferred to the DP, the weld surface of DP-weld interface was subdivided. The forces were reported in the X, Y, Z or 1, 2, 3 axis respectively. As can be seen in Figure 3.20, a force reported in the Y or 2 axis would be normal to the surface between the DP and the groove weld. This force would also be parallel to that being applied at the loading plates. A similar force on the Y axis, being reported at the top or bottom fillet weld, would represent a shear force along the length of the weld and the surface of the DP.

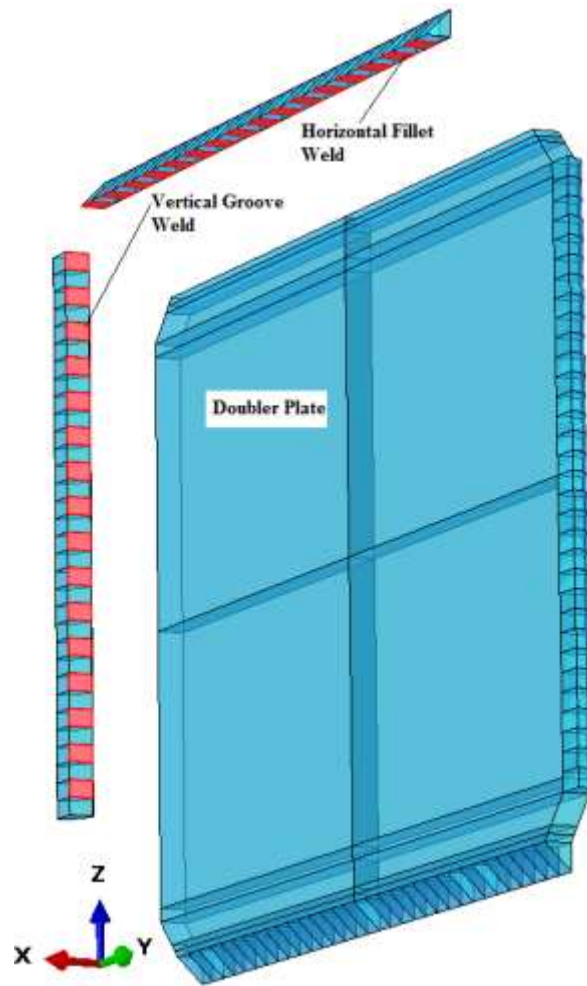


Figure 3.20: Subdivided weld surface attached to DP

### 3.3.9 Post Processing

Once properly defined, as covered in section 3.3 of this chapter, the model can be run in the Abaqus job module. The process of the analysis can be viewed from the job monitor as well as a report of warnings and modeling errors. Once complete, the results can be viewed in the Abaqus CAE and the forces from the “section force output” .DAT file can be parsed. The Matlab routine utilized to parse the large data file is attached at the end of the thesis. Another method of data collecting that was utilized after the analysis was complete was the use of paths. A path definition of the Abaqus model is a selection of nodes in a particular path. The paths defined for this thesis all ran along the center of the column from left flange to right flange at different elevations along the PZ (Figure 3.21). The user can request data values from the nodes that define the path such as: equivalent plastic strain (PEEQ,) principal stress values, Von Misses stress values, strains and Rupture Index values.

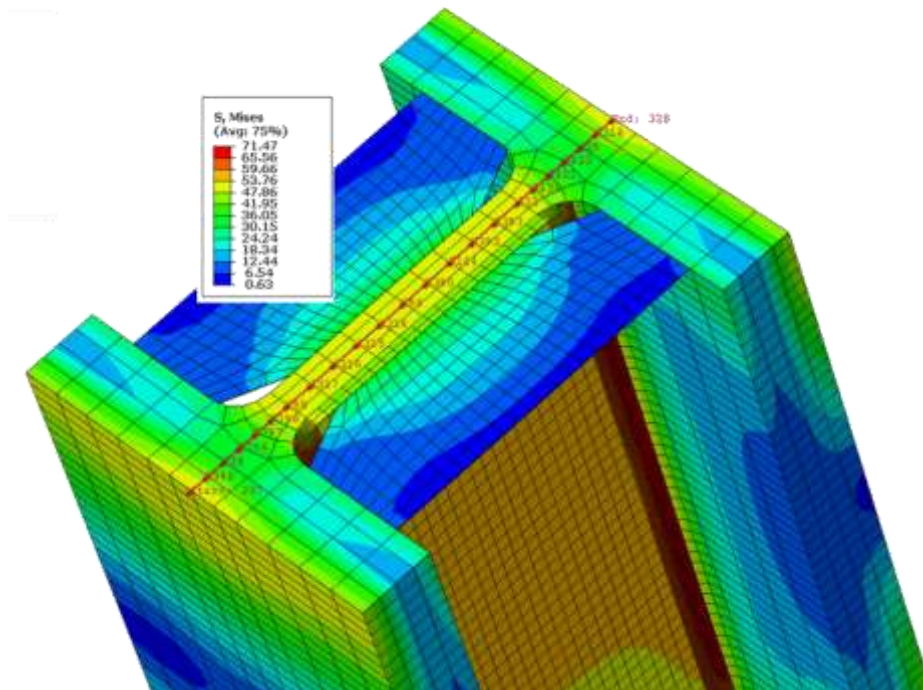


Figure 3.21: Path along the center of the column showing Von Misses stress

### **3.3.10 Modeling Assumptions and Limitations**

The model used in this thesis assumes that a 12 foot long column segment can represent the boundary conditions of a PZ of a moment connection on a typical moment frame column. The presumption that the points of inflection, where zero moment is expected to occur between floors of a moment frame, is often made in design, although in reality this is not exactly true. The model also utilized loading plates to apply the load on the PZ, when in reality the beam's web could influence the behavior because it is also attached to the column's web. Some of the limitations to the modeling of the specimens included the ability to model fracture as a form of failure. Because the models were loaded past the material yielding point, fracture, along with buckling of the stiffeners, often determines the failure of the connection. As recommended by the researchers covered in the literature review, good quality welds and weld material with proper strength can alleviate most of the fracture issues. Monotonic loading was also utilized despite the fact that the nature of seismic loading is cyclic. The intent of the modeling is to obtain an idea of how lateral forces are transferred through a simplified model, in order learn about the behavior and make design recommendations. The assumptions made are needed in order to make multiple analyses of variations of a specimen more practical, instead of an extremely long analysis of a whole frame system.

### **3.4 ABAQUS COMPARISONS**

Material definitions and methods used in this and previous FE modeling were developed and verified by modeling experiments. The following section will cover some of these analysis and their results. For more information covering the experiments, please turn to Engelhardt et al (2000), Ryu (2005), Shirsat (2011), Donkada (2012) and Gupta (2013).

### 3.4.1 Modeling of a Tension Coupon Test

In order to develop understanding of proper material definitions in Abaqus, along with the ability to model physical behavior, a tension coupon test was modeled. A 2 inch coupon was generated using the ASTM A370 standard dimensions and gauge distance. Data was obtained from a real tension coupon test, completed at the laboratory, and because it was recorded using engineering stress and strain, it was converted into real stress and strain values. Although the lab data had hundreds of data points, only 20 of these were used in the plastic stress-strain definition for the steel material of the coupon. This was done in order to keep Abaqus from aborting the project, since a definition of plastic behavior using a large set of points would result in its termination.

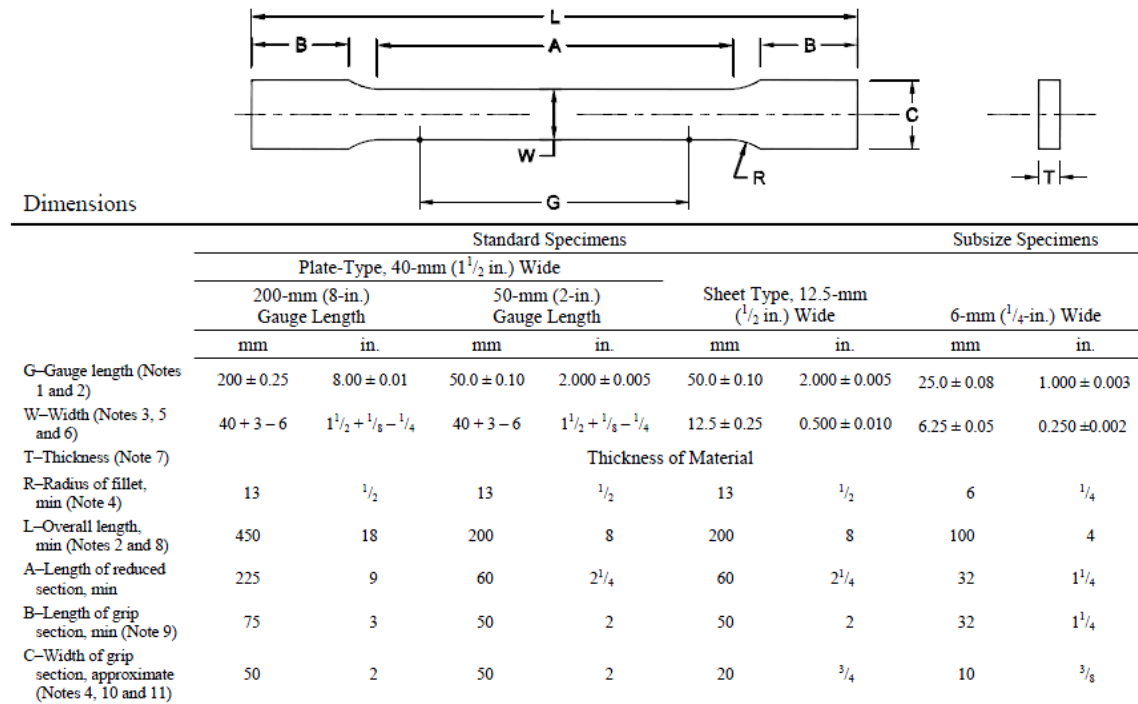


Figure 3.22: ASTM-A 370-08 Standard dimensions for tension coupon test

### 3.4.1.1 Assembly & Test

The model of the coupon used the same C3D8R brick elements as discussed previously. A fixed boundary condition was defined on one of the ends of the coupon while a 2 inch displacement load was applied at the other end. A 50 increment load amplitude was used, resulting in .04 inches of displacement application on the coupon per increment. Nonlinear geometry was applied by turning the “Nlgeom” option on. The seed size for the mesh definition used was .1 inches.

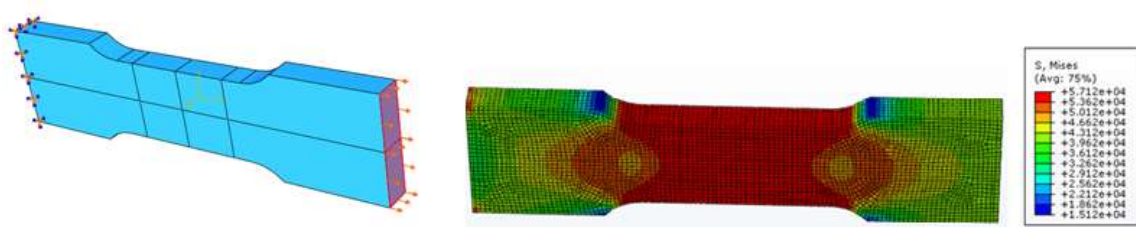


Figure 3.23: Tension coupon boundary conditions and resulting stresses

### 3.4.1.2 Results

The tension coupon test was modeled in order to develop the ability to model tension on a member and to determine the ability of the software to model this physical behavior. A steel material definition was attached on a coupon with standard geometry and dimensions. The material was defined using a “true” stress-strain curve converted from the “engineering” values from the laboratory experiment. As seen in Figure 3.24, Abaqus was able to use a defined material profile and reproduce stress-strain results that mirror those measured in the lab. Notice that the results differ once the “real” tension coupon starts necking, which is the reduction of the cross-sectional area. To model the coupon necking, the user has to use element elimination techniques, which is not the intent of this work.

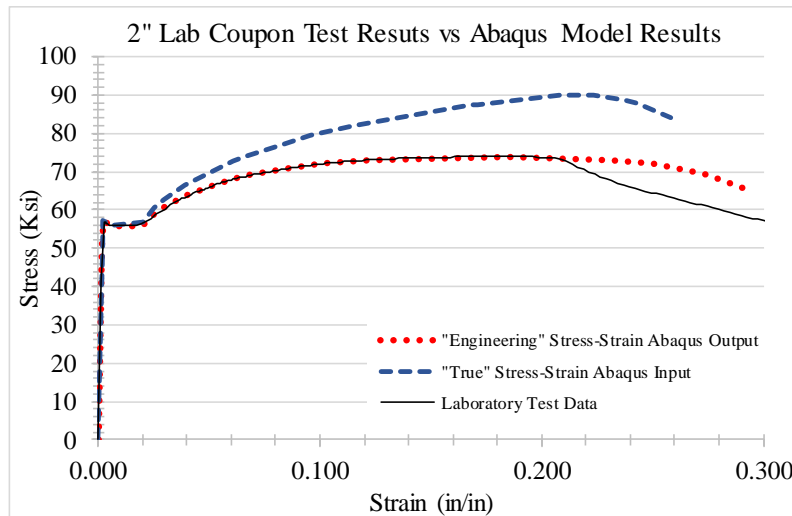


Figure 3.24: Tension coupon laboratory test vs. Abaqus model comparison

### 3.4.2 Modeling of a Shear Link

Shear in the PZ is one of the most important aspects of the research; for this reason, the ability to properly model it, was crucial. Lab experiments of a shear link performed by Ryu (2005) were used to compare and validate the material model and techniques used. An Abaqus shear link model was developed and a variety of loading protocols were applied to it.

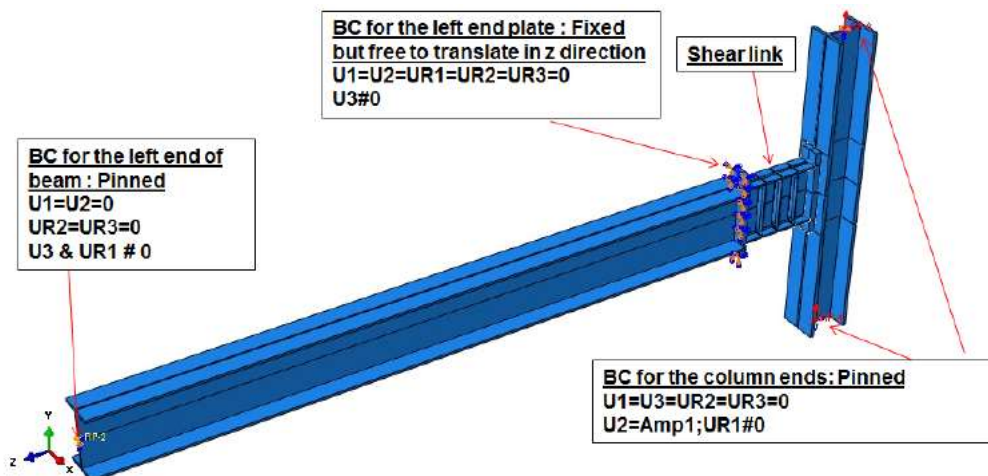


Figure 3.25: Abaqus boundary conditions for shear link model (Gupta, 2013)



### 3.4.3.1 Assembly

The experiment was composed of a 200 inch long W18x76 beam, a 96 inch high W12x120 column and a 23 inch long W18x40 long reinforced link. As pictured in Figure 3.26, the shear link was fabricated by attaching three 3/8 inch thick stiffeners to one side and spacing them 5 3/4 inches on center. Two 2 inch by 26 inch deep plates were attached to each end of the link beam.

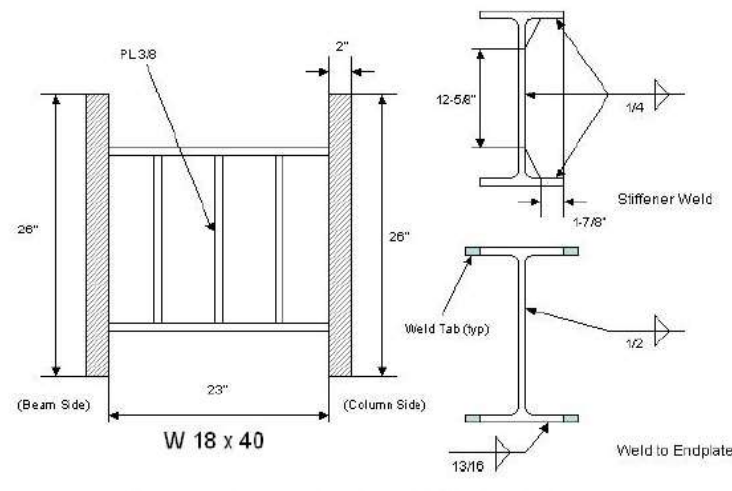


Figure 3.26: Shear link assembly 12 (Ryu, 2005)

The parts for the model were created and assembled in the part module using the dimensions provided in Ryu (2005) for specimen 12. The C3D8R brick elements used for the specimen were seeded and meshed using a “structured” mesh for all parts. In order to speed up the model and because the focus of the analysis was the shear link, a coarse mesh of 5 inches and 2.4 inches was used for the beam and column, respectively. The mesh size used for the link itself was .4 inches and 1 inch for the stiffeners and the end plates on either side of the link. It is important to note that Abaqus will not automatically subdivide the thin edge in a thin plate and will define the stiffeners using a one element thick mesh. The user must intentionally subdivide the stiffener and the link to match the subdivisions,

in order to capture accurate buckling behavior expected from the high levels of shear. Due to the expected buckling of the stiffeners and for accuracy of results, non-linear geometry was utilized by applying the “Nlgeom” option. The material definition used for all elements except for the link and stiffeners was an elastic one. The elastic modulus of 29,000 ksi, along with Poisson’s ratio of .3, was used to define the material without a definition for a yield point. Because the loading that would be applied to the link would be cyclic, the material stress-strain curve used by Gupta (2013) was used to define the plasticity of the shear link and stiffeners. As can be seen in Figure 3.27, the “combined” strain hardening method was selected, as well as the option to define 6 back-stresses for Abaqus to consider. These settings better approximate the strain hardening on a model that will be exposed to cyclic loading.

```
**
** MATERIALS
**
*Material, name=Elastic_steel
*Elastic
29000., 0.3
*Material, name=Plastic_steel
*Elastic
29000., 0.3
*Plastic, hardening=COMBINED, datatype=STABILIZED, number
backstresses=6
  0.001, 0.
 17.8433, 0.00135927
 37.2603, 0.00410534
 55.2118, 0.0131522
 64.5, 0.0358959
 70.2, 0.07492
```

Figure 3.27: Shear link material definitions

No welds were explicitly modeled in this analysis and thus tie constraints were utilized to connect all member surfaces. Rigid body constraints were used in the free ends of the beam and column in order to define the boundary conditions and allow the surfaces to rotate as they would in an experiment. These constraints were attached to reference points at the center of those surfaces and loading protocols as well as boundary conditions were defined

using these reference points. The roller at the left end of the beam was defined by placing a zero value in the U1/X, U2/Y, UR2/(rotation about Y), and UR3/(rotation about Z) lines and leaving the other lines of the boundary definition blank, as described in Figure 3.25. A similar application of boundary conditions was utilized in the column ends, with the exception that a displacement of 1 inch in the Y direction was applied to **both** top and bottom reference points. Notice the boundary condition that was applied to the link end attached to the beam. This boundary condition reflects the one used in the experiment to keep the link from rotating in the out of plane axis.

### 3.4.3.2 Test

The experiment utilized several different loading protocols of the same specimen. Three cyclic and one monotonic loading protocol were used to validate the modeling techniques and material in this thesis. These loading protocols were expected to result in high localized levels of shear and moment in the link beam (Figure 3.28). For a detailed explanation of the loading protocols and other links tested, turn to Ryu (2005)

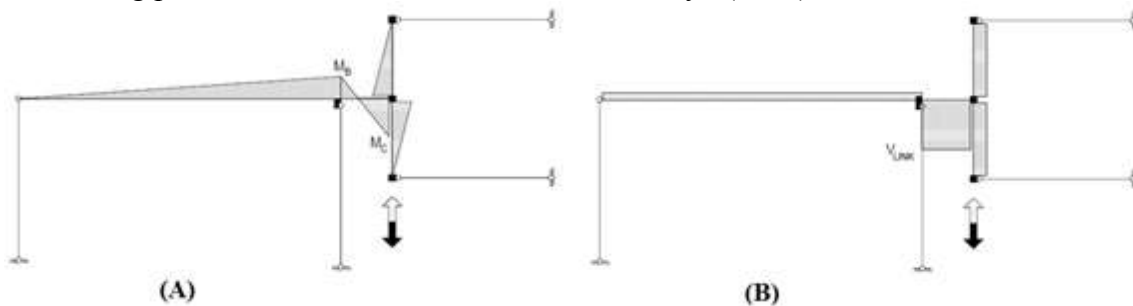


Figure 3.28: Qualitative moment (A) and shear (B) diagrams (Ryu, 2005)

The loading protocols shown in figures 3.29 – 3.31 were applied at the reference points of the column using a 1 inch displacement load. The direction and magnitude of the load application was defined using negative or positive amplitude values that increased or

decreased as necessary. The three cyclic loading protocols used for the validation exercises were '12SEV', '12RAN' and '12AISC' along with the '12MON' monotonic loading protocol, Figures 3.29 -3.32. Data collected for the results included a “History Output Request” of the Y-axis reaction force, or “RF2”, of the top and bottom reference points. These reaction forces were **combined** to determine the total force applied to the column ends in order to obtain the forces applied. This force, which was the shear that the link had to resist, was compared to the total rotation that the link experienced during the analysis. This rotation,  $\gamma$ , was determined by defining a node at the center of each end of the shear link and asking Abaqus to record the Y displacements for these as the load is being applied. Once the analysis was complete, the difference between the node displacements was divided by the length of the shear link, 23 inches, to determine the total rotation,  $\gamma$ , of the link.

#### ***3.4.3.3 Results***

Comparisons of the results from Ryu (2005) and the Abaqus models are shown in Figures 3.29 – 3.32. The comparison plots of the shear vs. rotation experienced by the link show that the models were able to capture the strain hardening behavior and ductility of the overall specimen quite well, with the exception of the specimen with the random loading protocol. The 12RAN Abaqus model underestimated the strength of the shear link by about 20%. This becomes an issue with loading protocols that are random in nature but the work done uses monotonic loading. Many of the laboratory experiments failed due to fracture of welds, something that was not part of the modeling of any specimens in this work. The failure mode that occurred in the lab, and which the Abaqus models were able to capture,

was buckling of the stiffeners (Figure 3.32). The monotonic loading of both the real and computer specimens caused buckling in the stiffeners, flanges and link web.

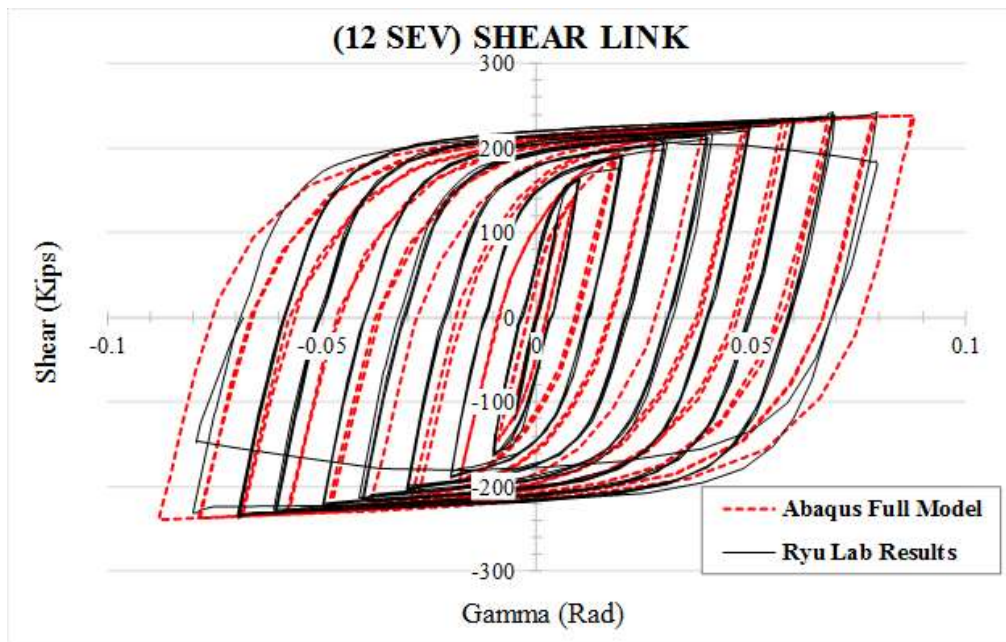
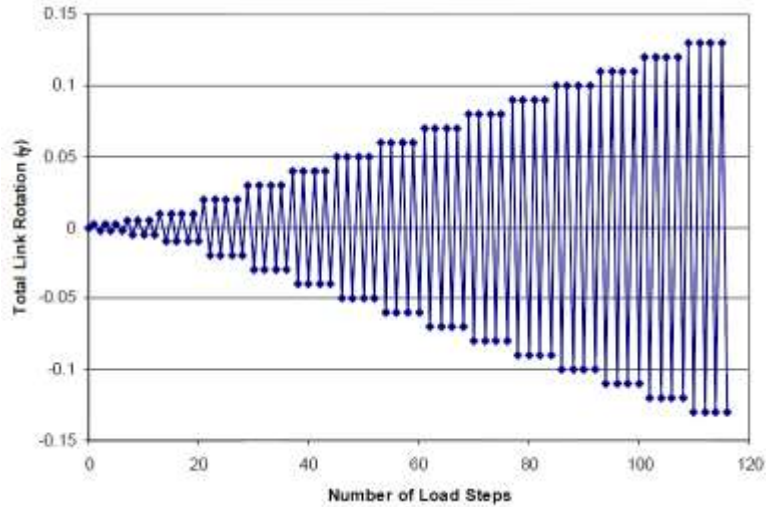


Figure 3.29: “Severe” loading protocol and Lab vs. Abaqus model results

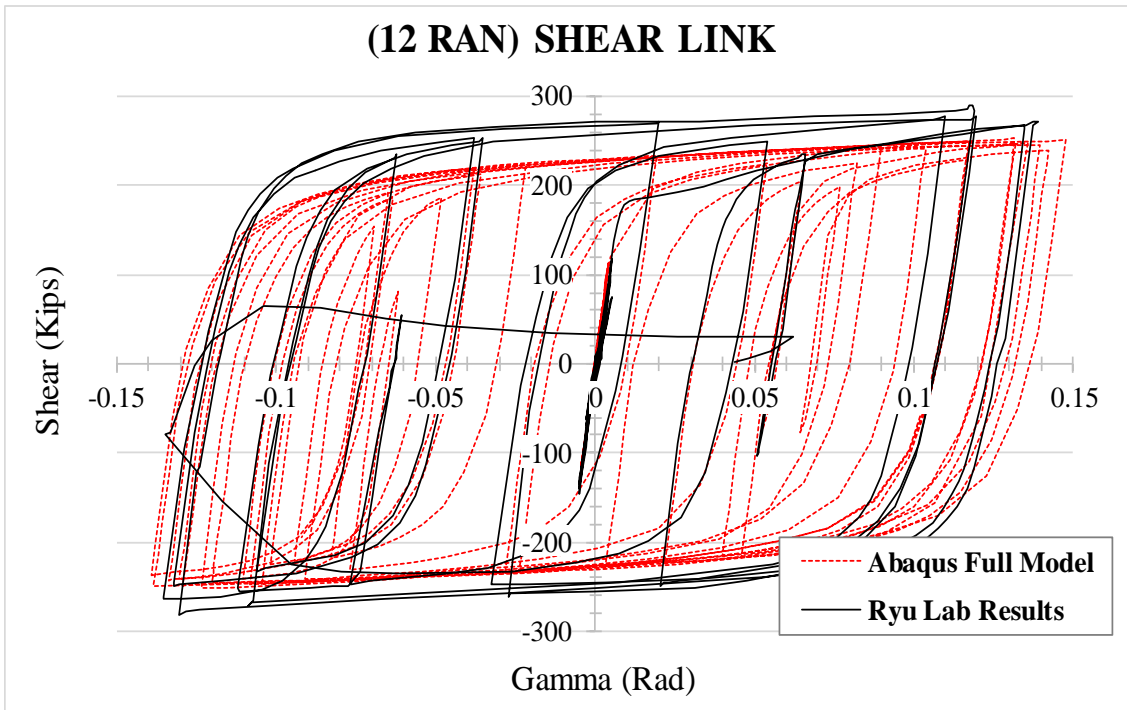
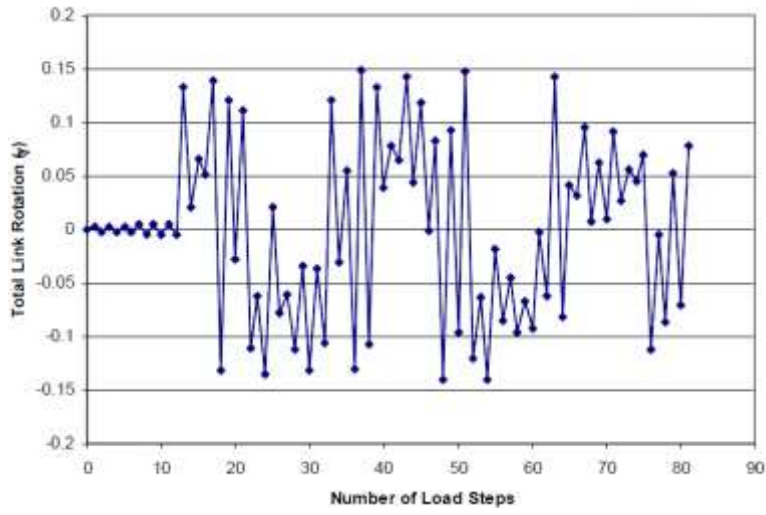


Figure 3.30: "Random" loading protocol and Lab vs. Abaqus model results

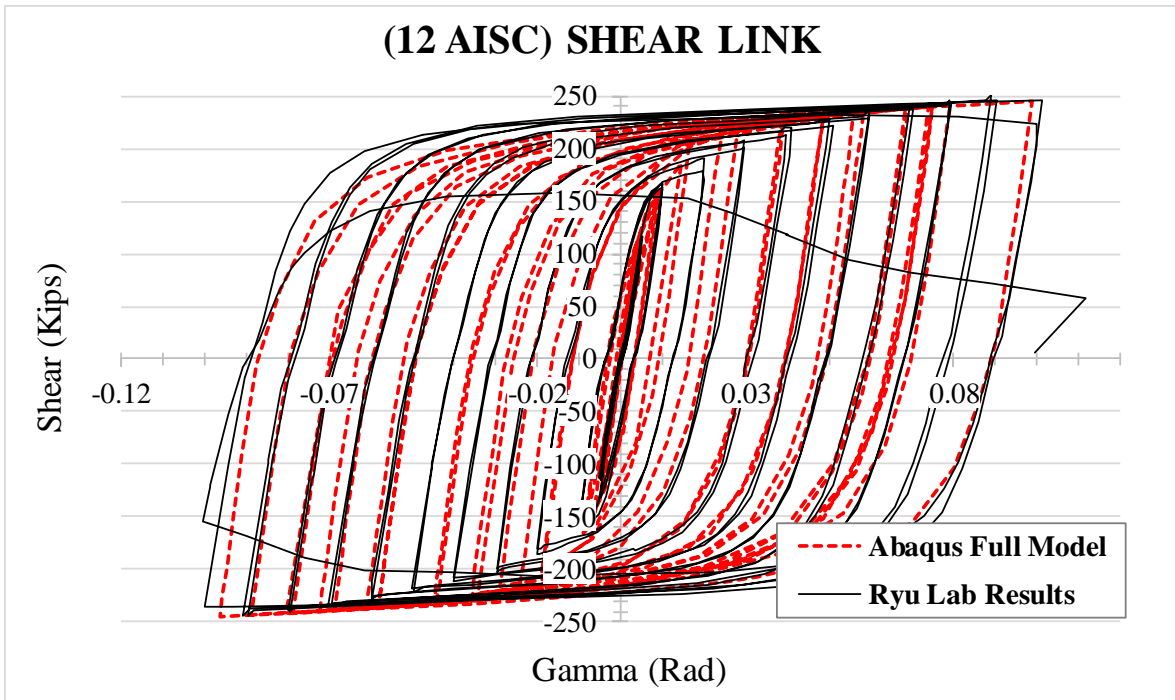
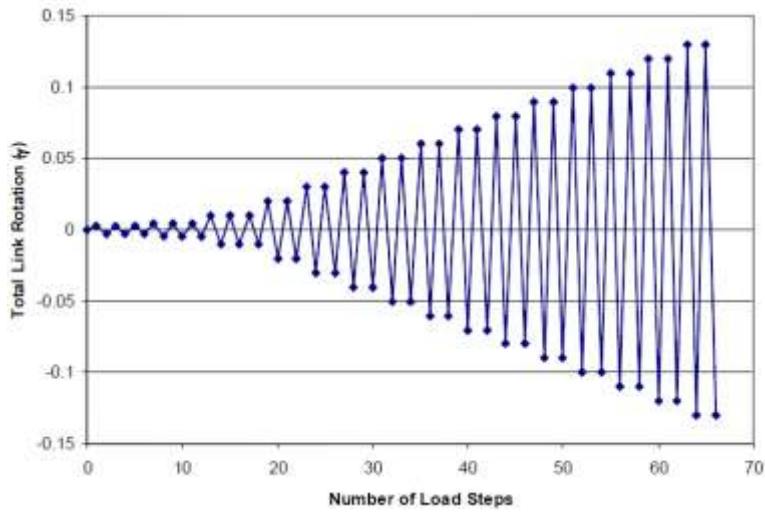


Figure 3.31: “AISC” loading protocol and Lab vs. Abaqus model results

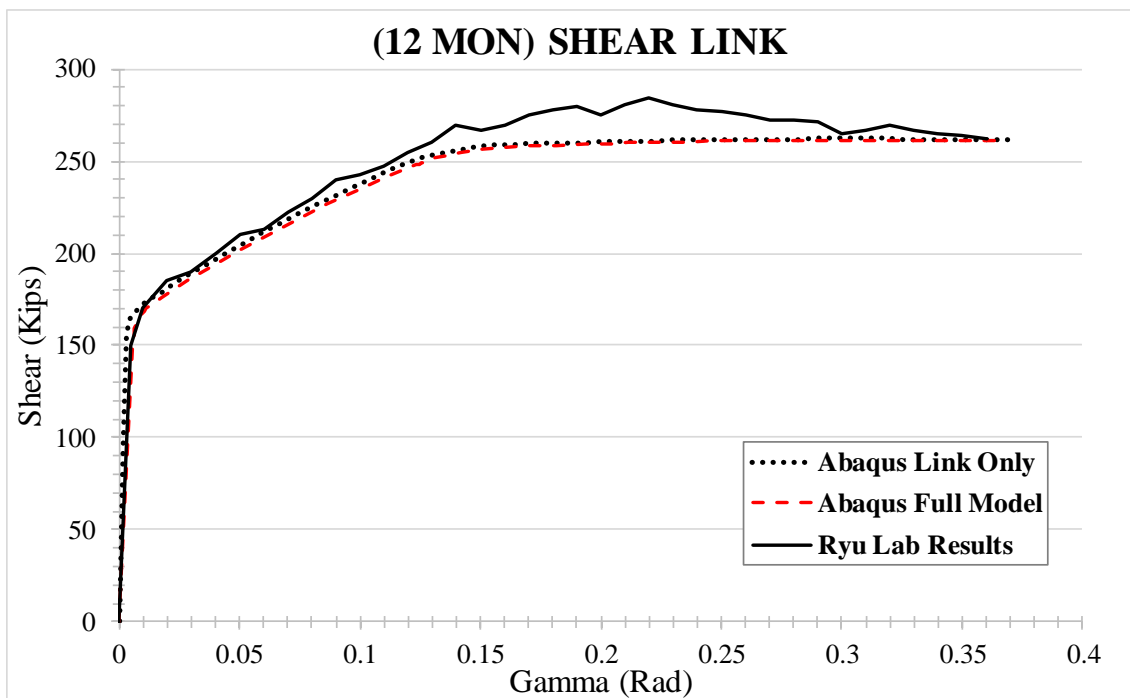
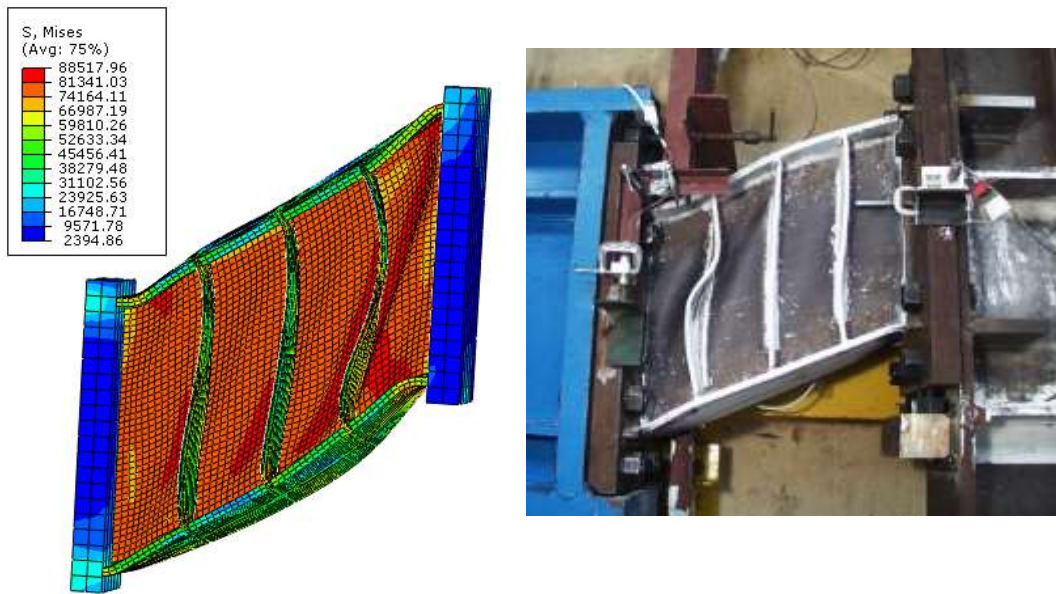


Figure 3.32: Lab vs. Abaqus model results using “MON” load protocol (Chart and Image)



### 3.4.4 Modeling of a DBBWWPZ Connection

As part of the research conducted after the Northridge earthquake, the SAC Joint Venture program tested a variety of beam-to-column connections. One of the many tested was the DBBWWPZ (Dog Bone Bolted Web Weak Panel Zone), which is discussed in Engelhardt et al (2000). This experiment was modeled in Abaqus due to the similarities in testing and data collecting that was done on the weak panel zone of the specimen. The nature of the test, which focused the plastic deformations on the PZ, served as a perfect situation for the validation of Abaqus modeling techniques used.

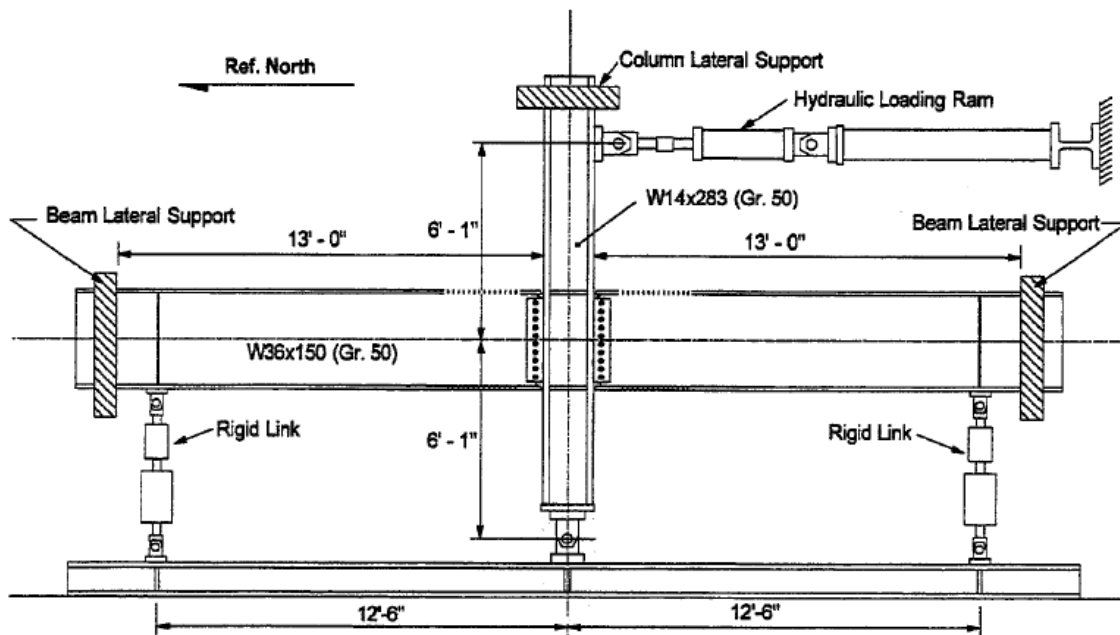


Figure 3.33: DBBWWPZ Test setup (Engelhardt et al, 2000)

#### 3.4.4.1 Assembly

The assembly was composed of two W36x150, 150 inch long beams attached with moment connections to a 146 inch long W14x238 column section. These members were formed in the Abaqus part module and meshed using a global seed size of 1.5 inches. The column PZ

region was subdivided and meshed with a finer .8 inch seed size. The model also used CP plates to reinforce the panel zone and the mesh for these was .3 inches. End plates for the columns and beams were modeled using a mesh size of 1 inch. The “structured” mesh algorithm was used for all parts of the model, and because no welds were modeled, all these were joined using tie constraints. Columns and beams were subdivided in order to define a quality mesh that would provide accurate results (see Figure 3.10).

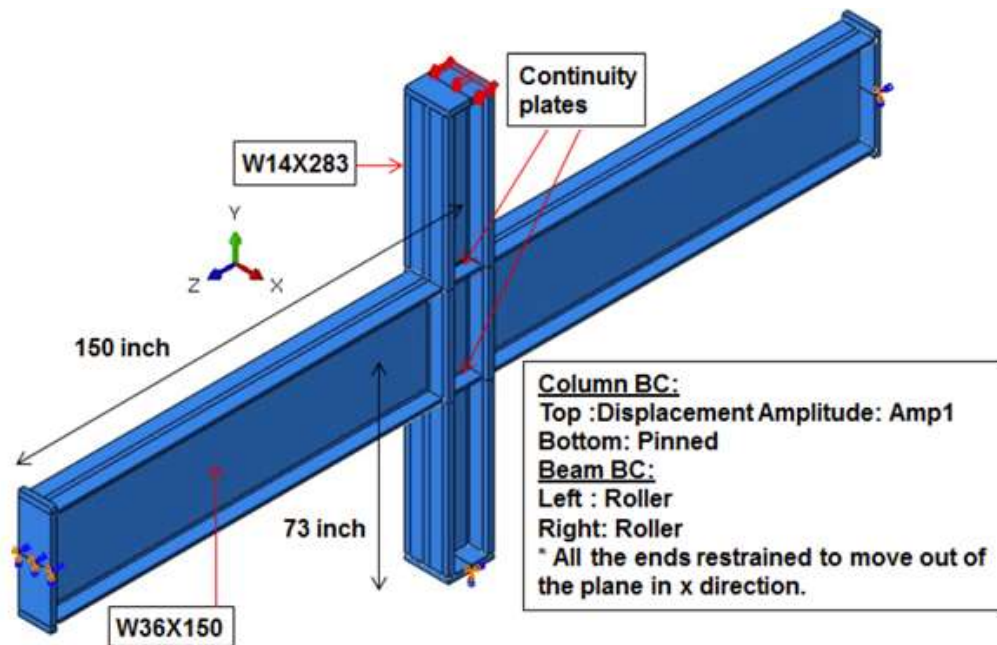


Figure 3.34: DBBWPPZ Abaqus model (Gupta, 2013)

The material definition used for the beams, column and CPs was the same as that used for all specimens with cyclic loading (see “Plastic Steel” Figure 3.27). All end plates were modeled using a continuously elastic material definition. Geometric non-linearity was also considered by activating the “Ngleom” option. As pictured in Figure 3.34, the left and right roller ends’ boundary conditions of the model were set to have zero X, Y displacement as

well as no rotations about the Y and Z axis. A rigid body constraint was used to model the pin at the bottom of the column.

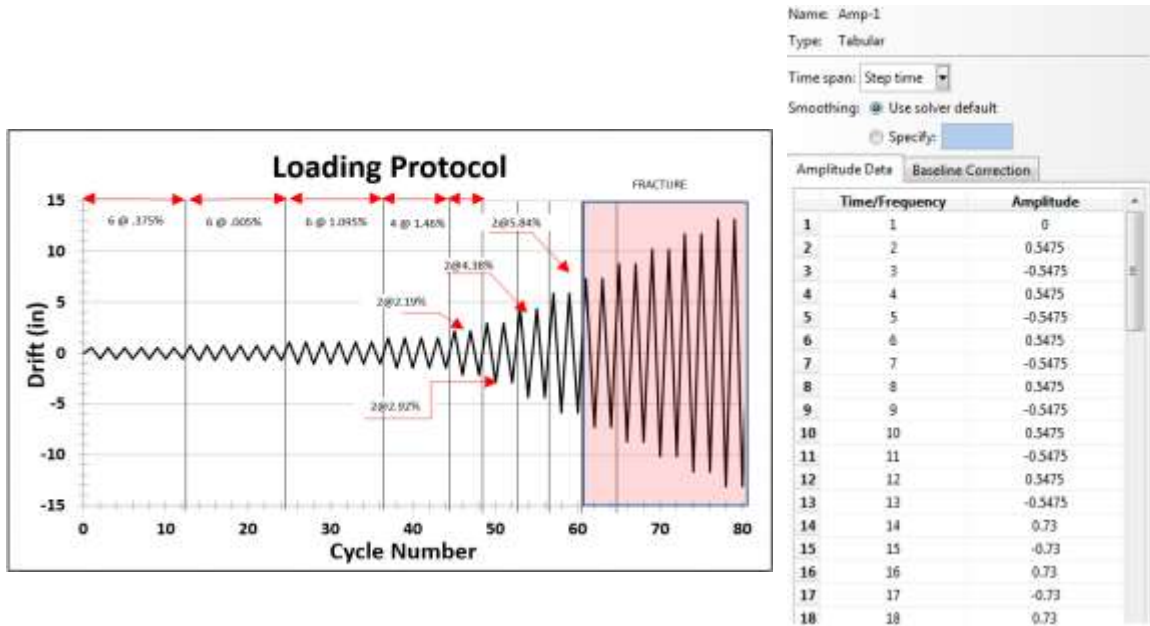


Figure 3.35: DBBWWPZ loading protocol and first 18 steps of Abaqus amplitude

#### 3.4.4.2 Test

A unit displacement load was applied at the top plate of the column. Although Figure 3.34 shows the load being applied at the edge of the plate, it can also be applied using a reference point and a rigid surface constraint at the top end of the plate. Load was amplified and given a direction by an amplitude definition, with the first 18 steps pictured next to the loading protocol (Figure 3.35). The loading protocol used in the experiment is described in section K2 of *Seismic Provisions for Steel Structural buildings* (AISC 2010b). The loading is defined in incremental steps of drift angle, which were converted into displacements by multiplying the column height by the drift angle. The time period used in the step definition matched that of the steps required for the loading amplitude.

The nodes at the top of the column to which the load was applied were grouped together and the displacement and load magnitude were recorded with the “History Output Request” tool. Panel zone gamma/rotations were calculated using nodes placed in the corners of the column flanges as seen in Figure 3.14, and their horizontal displacements divided by the PZ height (Equation 1).

#### ***3.4.4.3 Results***

Although the overall load-deflection response of the Abaqus model matched that of the experiment, some differences were noted. The hysteretic curve of the column tip displacement vs. column tip load, Figure 3.36, indicates that the Abaqus model was weaker than the real life specimen. This could possibly be due to the material definition of the FE model. Coupon data from the SAC specimen was not available and an approximation of the strain hardening behavior was carried out with the selected parameters. The column tip load vs. panel zone rotation seemed to more closely match the laboratory results. Peak load differences at a .04 rad. PZ rotation were within 5-10 kips. This seems to indicate that the material definitions and modeling techniques can make acceptable approximations to lab experiments. The experiments by Engelhardt et al (2000) reported fractures at the south beam’s bottom flange between the column-beam interfaces at a PZ rotation of about .03 radians. Since fracture modeling is not part of any of the models covered, this failure was not captured and as a result, the analysis had to be cut off at the point of failure of the real specimen. Despite this, Abaqus was able to capture high stress levels at the expected locations (Figure 3.38). The complete yielding of the PZ region, as well as the high stress concentrations at the beam flange-column interface, were captured in the specimen at a PZ rotation of .04 (rad).

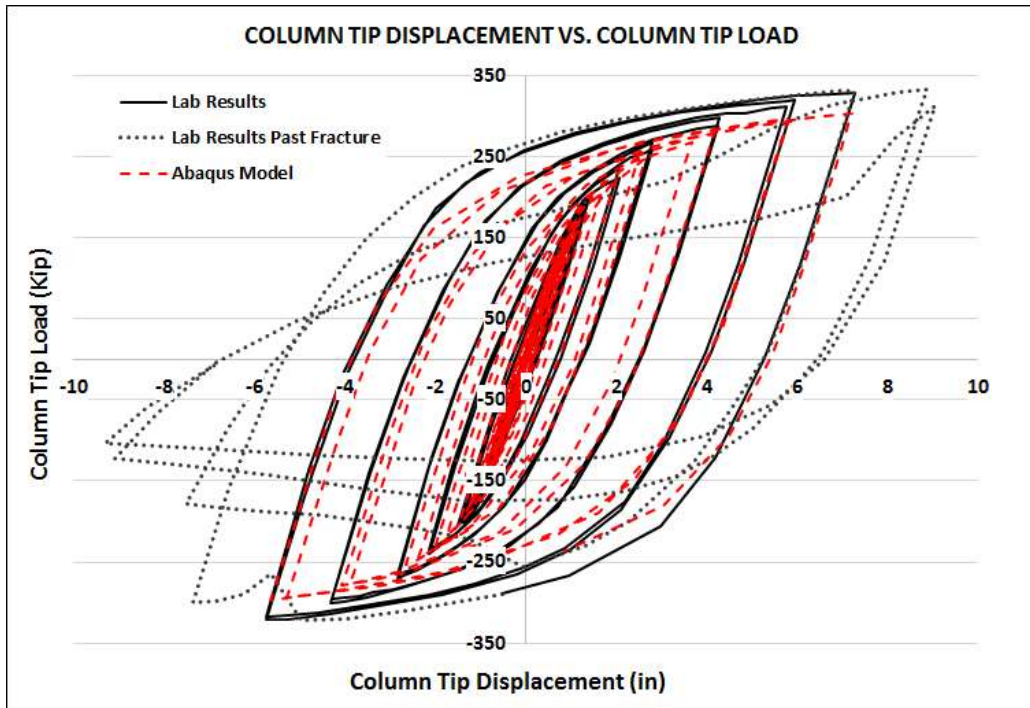


Figure 3.36: DBBWWPZ column tip displacement vs. column tip load

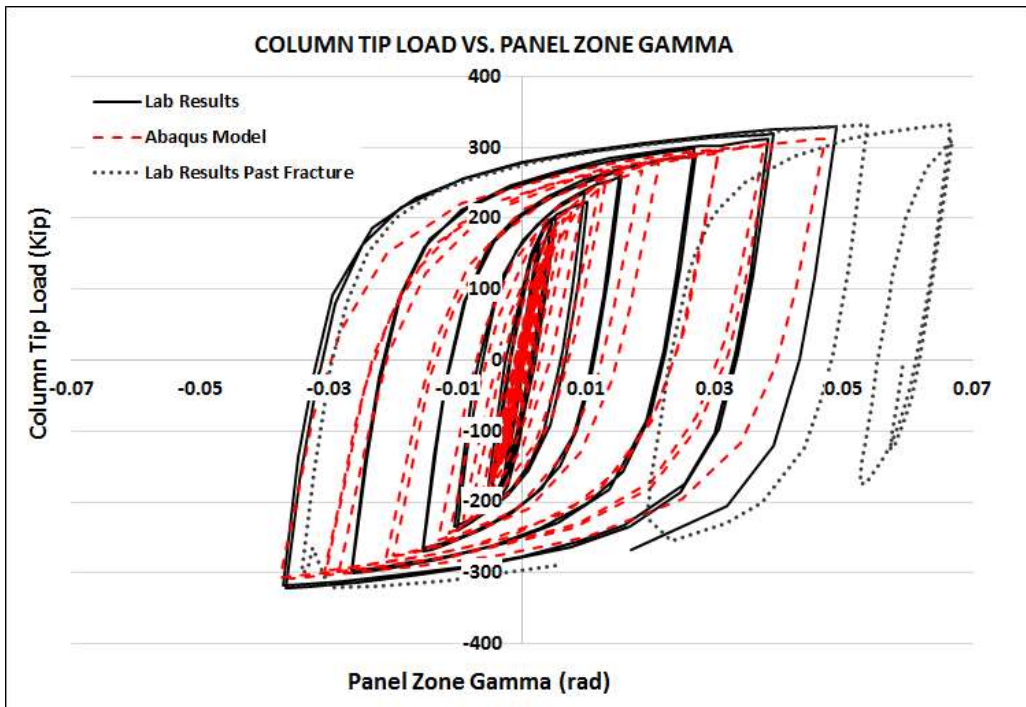


Figure 3.37: DBBWWPZ column tip load vs. PZ rotation

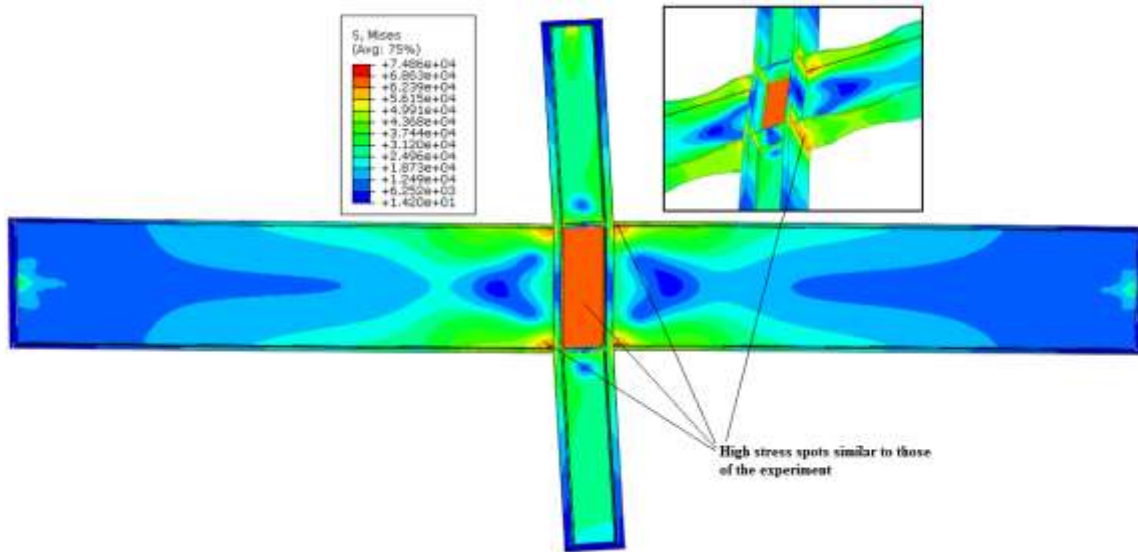


Figure 3.38: DBBW WPZ VMS values at .04 rad. inter-story drift

### 3.5 Chapter Summary

This chapter discussed the finite element analysis software, Abaqus, which was used to model two column specimens in this thesis. Its modules, tools for assembly and methods of analysis were covered as well as assembly details of the models used for the research. Material definitions, modeling assumptions and simplifications used in the analysis were also explained. Lastly, the chapter presented comparisons between model predictions and experimental observations for model validation. Abaqus model input files, model batch processing code and data parsing programs are included as appendices.

## CHAPTER 4

### **Parametric Studies on Attachment Details of Doubler Plates in a W14X398 Column**

#### **4.1 INTRODUCTION**

This chapter presents the results from the modeling of a W14x398 “shallow” column and the attachments that were used to test the performance of the panel zone. The different configurations of the PZ that were modeled used a “fitted” doubler plate, attached by vertical groove welds. In order to determine the influence that a horizontal weld at the top of the doubler plate had on the performance of the PZ and the stresses in the vertical groove welds, a weld at the top of the DP was included in some of the analyses. Other variations that were used to analyze the PZ included the use of continuity plates as well as DPs of different dimensions.

The specimens were monotonically loaded through a displacement amplitude that would cause a panel zone rotation of 0.1 radians. Because seismic loading is cyclic in nature and the rotation requirements of the PZ in a special moment frame are 0.04 radians, the 0.1 radian value was assumed to be appropriate for the evaluation of forces at peak force resisting limits of the PZ. As discussed in Chapter 3, the roller and pin boundary conditions of the specimens were defined using a “rigid” constraint to which two reference points were attached. From these points the reaction forces used for the analysis were obtained and utilized to determine the PZ shear. The displacements of two corner nodes from the PZ region were also used to determine the PZ rotation of the specimens. In order to compare performance between specimens, five stage points of the analysis were selected. Similar to Shirsat (2011), the first stage and third stage points selected were the first and second yield point of the PZ rotation vs. PZ shear plots. The first stage point was defined by the first

point in which the linear behavior in the curves ended. The third stage point was chosen as the initial point where linear behavior resumed in the specimens, after the first yield point in the same plot. Stage two and stage five points were defined by the PZ rotation values of 0.02 radians and 0.1 radians, respectively. A target loading point was selected for stage four similar to that of Shirsat (2011). This peak loading point selected was based on equation (J10-11) of the *AISC Specification for Structural Steel Buildings* (2010). The stage four target value for the “shallow” column specimen was  $1.25V_{pz}$  for an unreinforced column, as shown in the calculations below. This value provided a “relatively large panel zone shear force that might be representative of the panel zone shear developed under seismic loading” (Shirsat 2011).

$$V_n = 0.6F_y d_c t_w \left( 1 + \frac{3b_{cf} t_{cf}^2}{d_b d_c t_w} \right)$$

Calculation of F for W14x398 with d= 24in

$$V_n = 0.6 * 52 * 18.25 * 1.75 \left( 1 + \frac{3 * 16.6 * 2.85^2}{24 * 18.25 * 1.75} \right) = 1522 kips$$

$$V_{pz} = 1.25 * 1522 = 1903 kips$$

$$F = \frac{1522 * 144}{144 - 24} = 2283 kips$$

Figure 4.1: Equation J10-11 (AISC 2010) and  $1.25V_{pz}$  Calculations, (Shirsat, 2011)

Along with the reaction forces and displacements of the selected nodes, data used from the output quantities that Abaqus provides included: S23, VMS, PEEQ, and Section Forces. The S23 values were utilized to report the shear stresses on the specimens, parallel to the force being applied. Because the only forces being applied on the model were at the loading plates, this quantity can be used to compare the response of the DP to the shear being



imposed. The definitions for VMS and PEEQ are defined in section 4.2.1 of *Abaqus 6.14 Analysis User's Manual* (2014) and can be seen in equations 4.1 and 4.2 below.

VMS, equivalent misses stress; 
$$VMS = \sqrt{\frac{3}{2} S_{ij}S_{ij}} \quad \text{Equation (4.1)}$$

PEEQ, cumulative equivalent plastic strain; 
$$PEEQ = \varepsilon^{-pl}|_0 + \int_0^t \dot{\varepsilon}^{-pl} \quad \text{Equation (4.2)}$$

$S_{ij} = \text{Deviatoric Stress Tensor}$

$\varepsilon^{-pl}|_0 = \text{Initial Equivalent Plastic Strain}$

It should be noted that these two quantities were used with a holistic perspective of the model. Although the meshing techniques and densities used were intended to be of good quality, the complex geometries of the individual parts and a large “global” model with many contact definitions make points of inaccurate high stress concentrations or plastic strains possible. An example of how a simplification used in the modeling can make this possible is the point where the loading plates apply force on the column. Because the loading is being applied in such a concentrated area, the weld where the beam flanges and column meet often experiences fracture issues. This was reported in many of the tests covered in the literature review. However, the intent of the work is to understand how the attachments would respond to the forces expected at levels of rotation up to 0.1 radians. It is for this reason that VMS and PEEQ values will be based on the average value recorded over the whole cross section. An example of this would be reporting the average VMS value in a column web instead of the point on the outer flanges where the loading is being applied, or the VMS average value in the welds instead of the concentrations that occur when the geometry of the weld becomes sharp. Along with this, the center section cut of the column will be used to report values in the column (Figure 4.2). The values seem to be

more indicative of the stresses and strains occurring in the PZ, since the flanges of the column do not experience high shear stress parallel to the load being applied.

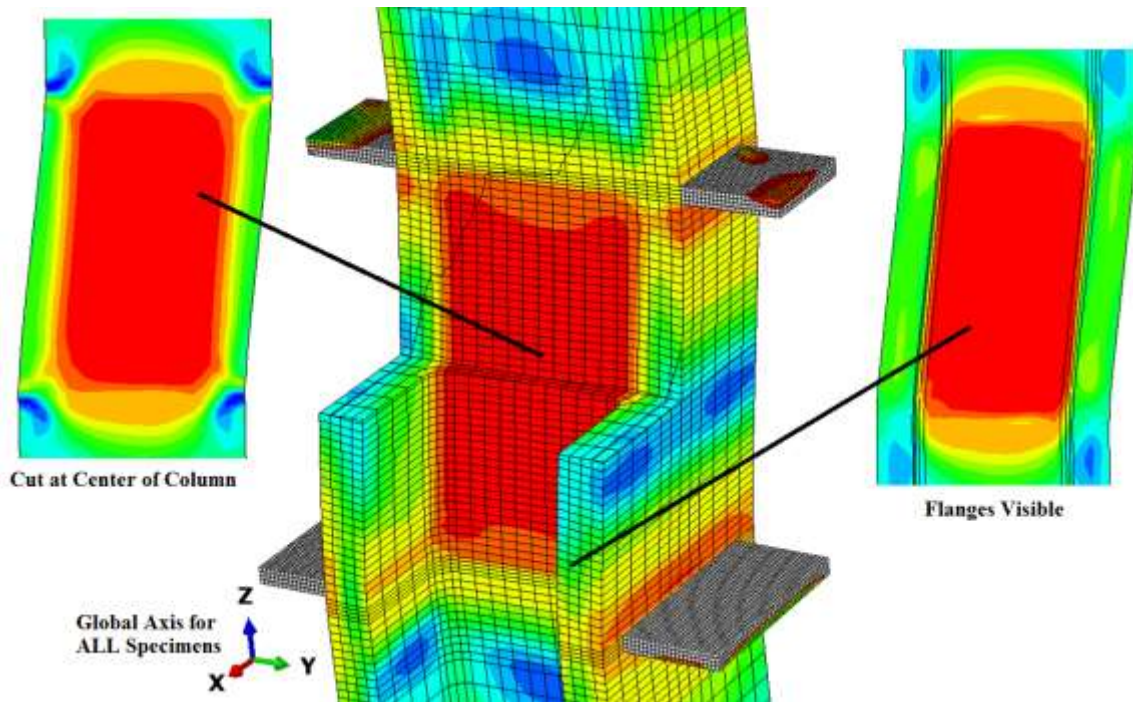


Figure 4.2: PEEQ and VMS values reported from center of column

One main interest in the thesis is the understanding of forces through the welds into the DP. For the “shallow” specimen, the top weld and vertical groove weld were subdivided into 8 and 17 sections, respectively (Figure 4.3). The length of the individual sections was of equal value but varied in the different cases since the lengths of the welds changed, due to the dimension changes of the DP edges. It should be emphasized that the sections were separated by smaller subdivisions that prevented the sections from sharing nodes, as covered in Chapter 3. The forces used in the thesis were recorded using the “Section Force” Abaqus command, which records the reaction force in all the nodes that make up a predefined section. It is for this reason that the sharing or omission of nodes, in the

definition of the individual surfaces of the weld segments in the DP and weld interface, is avoided. The sharing of nodes would result in the double counting of force, and omitting a node would result in a smaller force than actual. The sum of the forces for each of the nodes that make up a surface is then summed and reported as the force experienced by the individual section. These forces are reported using the X/1, Y/2, Z/3 global axis definition. As seen in Figure 4.3, the forces reported in the Y direction are parallel to the force being applied by the loading plates and are especially important at the top and bottom of the vertical groove welds because of the proximity to the loading plates. A force reported in the X direction would likely be a result of the buckling of the DP or the column web. A force in the Z direction would be a result from the rotation of the PZ.

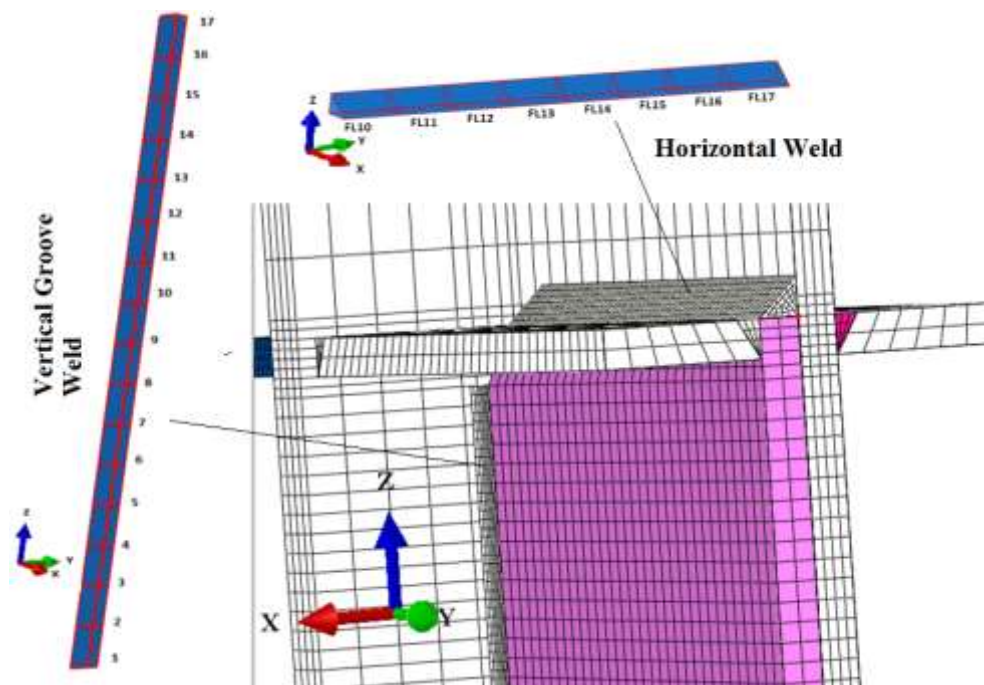


Figure 4.3: Horizontal weld and groove weld attaching DP

Previous studies on other works have reported the section forces at the edge surfaces of the DPs. The intent of this work is to report the forces transferred by the welds into the DP. Although the total force recorded at the edge surface of the DP is similar to that transferred by the welds, it is not the same. This is due to the node that the edge surface of the DP and the column web share, as shown in Figure 4.4. Because this node applies force on the DP, particularly in the out of plane axis, when the web tries to buckle, the transferred forces do not match the DP surface forces. The “hard contact” definition used between the DP and the column web also allows for the transfer of force in the Y and Z planes as well. An Abaqus requirement for parts that have two contact definitions such as the welds, is that a chamfer be used between the surface attached to the DP and the surface attached to the column web. This not only separates the different contact surfaces but also serves as a way to differentiate the forces being transferred between the DP and the welds.

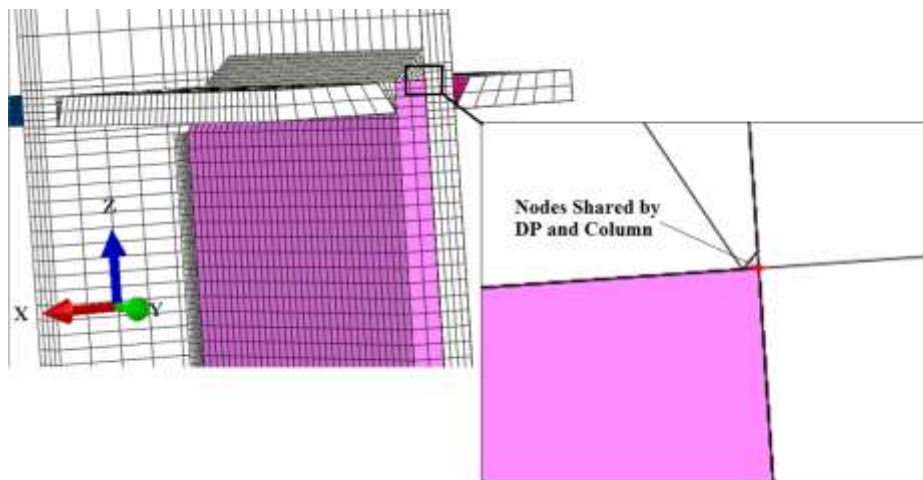


Figure 4.4: Nodes shared by doubler plate and column web

Table 4.1 shows how the forces reported on the surface interface between the weld and the DP vary between the sum of the weld segments and the entire edge of the DP. This table

shows the difference between the values of the surface defining the total DP outer surface and the sum of the forces of all the individual welds. The surface forces of the DP edges were not reported in this work; however, they were used to verify that the DP was in equilibrium and to validate that the sum of the forces of the individual weld segments was consistent with that seen in the values reported by the total DP surface. The forces reported in this work will be those from the individual surface definitions of the weld segments.

Case		Stage 01			Stage 02			Stage 03			Stage 04		
		X	Y	Z	X	Y	Z	X	Y	Z	X	Y	Z
6A1	DP Edge Section Force	5.3	-1.0	-428.4	10.6	-4.0	-567.0	10.8	-4.1	-564.6	21.3	-26.3	-710.8
	Sum of Weld Forces	-11.6	1.0	426.4	-19.3	3.5	561.9	-19.8	3.3	559.6	-36.8	24.0	702.9
8A1	DP Edge Section Force	8.7	-3.3	-563.9	13.5	-12.5	-652.1	12.0	-16.9	-678.2	13.5	-85.5	-872.8
	Sum of Weld Forces	-17.0	4.4	569.0	-29.9	13.6	655.3	-26.6	18.5	680.6	-28.3	93.7	872.9

Table 4.1: Force difference between DP edge and weld segments

It should also be noted that the forces reported were not uniform, as one might expect. The plots show jagged increases in forces being transferred by the welds. This can be explained by the subdivisions used for the welds and the way the forces are summed up (Figure 4.5). Although the force being applied to the specimens is vertical, this force does not seem to increase or decrease uniformly throughout the different specimens. Hence the force entering the doubler plate through the welds does not match the weld subdivisions, resulting in the uneven jumps on the weld force plots. As seen in Table 4.1, the sum of the forces transferred into the DP through the weld is close to that recorded on the DP surface edges. This was used to validate the assumption that the individual welds were indeed transferring the total force in the DP, but at varying values. These peaks in force and the lack of a more refined “local” model of the weld were taken into consideration when making recommendations for design.

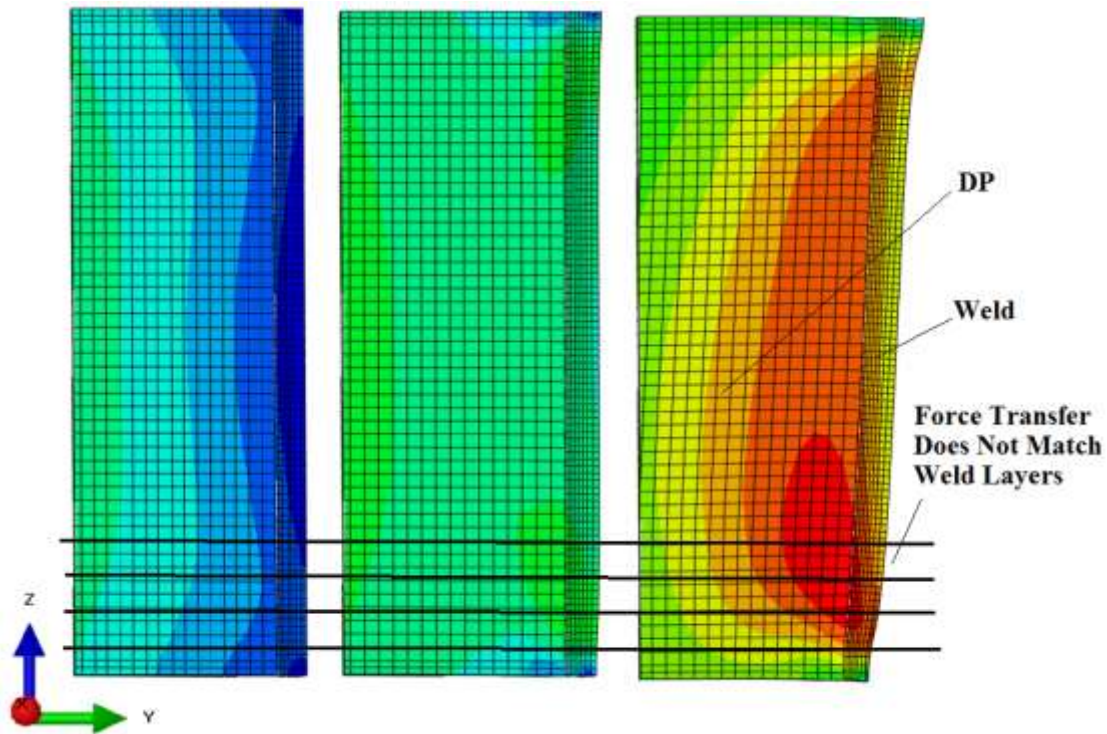


Figure 4.5: Stresses on groove weld and left side of DP

In order to express the force, results in stress from the individual forces reported in the weld segment were divided by the surface area in contact with the DP. To determine the surface area, the value of the total length of the weld, divided by the number of segments, was multiplied by the thickness of the DP. In the case of the top weld, the length was divided by 8 and in the vertical weld, it was divided by 17. Although the “true” area is slightly smaller because of the “chamfer” that separates the surfaces on the weld, the area used is a good approximation.

As covered in Chapter 3, node paths were utilized to report the Von Mises stress values at the center of the column web through the different stages of loading (Figure 4.6). These “paths” were defined +2 inches above the center of the loading plates where the load was being applied to the specimen. Center of the loading plate was defined as the 0 value for



the remaining paths. Other paths were defined -0.5, -1, -1.5, and 2 inches below the center line of the loading plate. Paths were also defined in center of the column web and on the DP at mid-height between the top and lower loading plates.

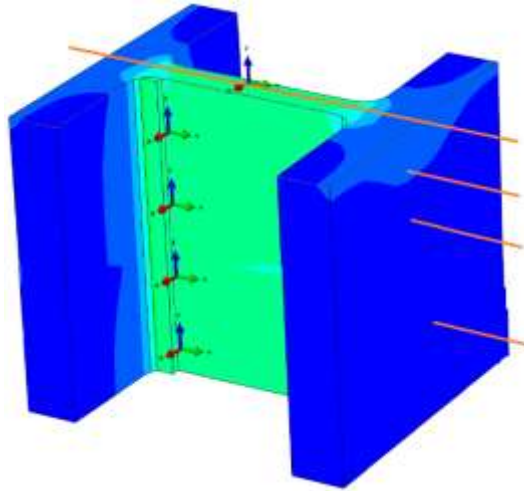


Figure 4.6: Paths defined through center of cross-section at different levels

The results from the analysis completed were helpful in completing the objectives of the thesis, which are:

- 4) To gain a better understanding of the performance of different attachment details for fitted DPs.
- 5) To study the effects that clipped corners on fitted doubler plates have in the PZ and the welds attaching it and to gain a perspective of the force flow through the panel zone.

- 6) To report the forces and stresses that both horizontal and vertical welds transfer to the fitted DP and to determine if both welds are necessary. To obtain a range of forces for which the welds attaching the plates should be designed.

All outputs of the structural response are presented in the 5 stages selected, in the following order: First yield point, Second yield point, .02 PZ rotation, PZ Shear Force=1903 Kips, and PZ rotation of .01 radians. The result for each analysis case includes one or more of the following outputs:

1. Details and dimensions of the model being analyzed
2. Shear,  $V_{pz}$ , versus Rotation,  $\gamma_{pz}$ , of the panel zone, up to 0.1 radians
3. The Von Mises Stress (VMS) and equivalent plastic strain ( PEEQ) in the column center cross section and the doubler plate at the five selected stages.
4. The shear stress (S23) of the doubler plate at the five stages.
5. The VMS values reported on the node paths, defined by varying heights from PZ mid-height to 2 inches above the top loading plates, in stages 1, 3 and 4.
6. The VMS values reported at mid-height of the DP in stages 1-5.
7. Forces and stresses reported on the weld segments of both vertical and horizontal welds in the: X, Y, Z axis, Figure 4.7. “All” forces in this thesis use the same global axis for the reporting of forces.



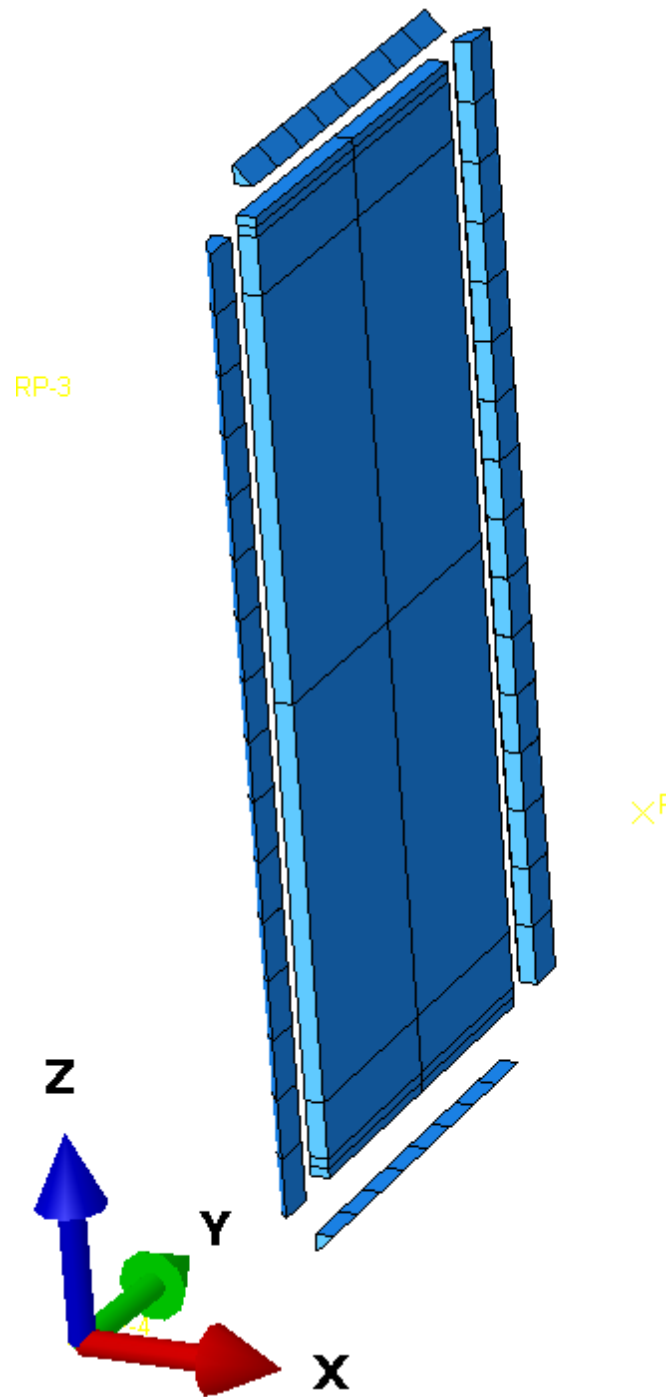


Figure 4.7 Global Axis used for the forces on welds, Y is parallel to applied force

## 4.2 ANALYSIS CASES

The following cases were performed in order to answer the objectives of the thesis. Details of the different arrangements as well as plots of the FEA results are presented in the following section. A discussion of the results is followed at the end of the chapter.

Case	$t_{dp}$ (in)	$l_{dp}$ (in)	$b_{dp}$ (in)	CP	Vertical Weld Length (in)	Horizontal Weld Length (in)
<b>1</b>	-	-	-	-	-	-
<b>1A</b>	1/2	25	-	-	25	-
<b>1A1</b>	1/2	25	10	-	25	10
<b>1C</b>	1/2	25	10	-	25	-
<b>1C1</b>	1/2	25	10	-	22	7
<b>2A1</b>	1/2	25	10	Y	25	10
<b>2C1</b>	1/2	25	10	Y	22	7
<b>3A</b>	1/2	22 7/8	10	Y	22 7/8	-
<b>3A1</b>	1/2	22 7/8	10	Y	22 7/8	10
<b>3C</b>	1/2	22 7/8	10	Y	19 7/8	-
<b>3C1</b>	1/2	22 7/8	10	Y	19 7/8	7
<b>4A</b>	1/2	21	10	Y	21	-
<b>4A1</b>	1/2	21	10	Y	21	10
<b>4C</b>	1/2	21	10	Y	18	-
<b>4C1</b>	1/2	21	10	Y	18	7
<b>5A1</b>	1/2	22	10	Y	22	10
<b>5C1</b>	1/2	22	10	Y	19	7

*Notes*

- 1) A "C" in case name indicates "clipped" doubler plate corners
- 2) A "1" after the letter designation indicates fillet welds were used at the top of DP
- 3) Cases 1-1C1 used no CPs

Table 4.2: Analysis cases for W14x398 "shallow" column

### 4.2.1 Analysis Case 1

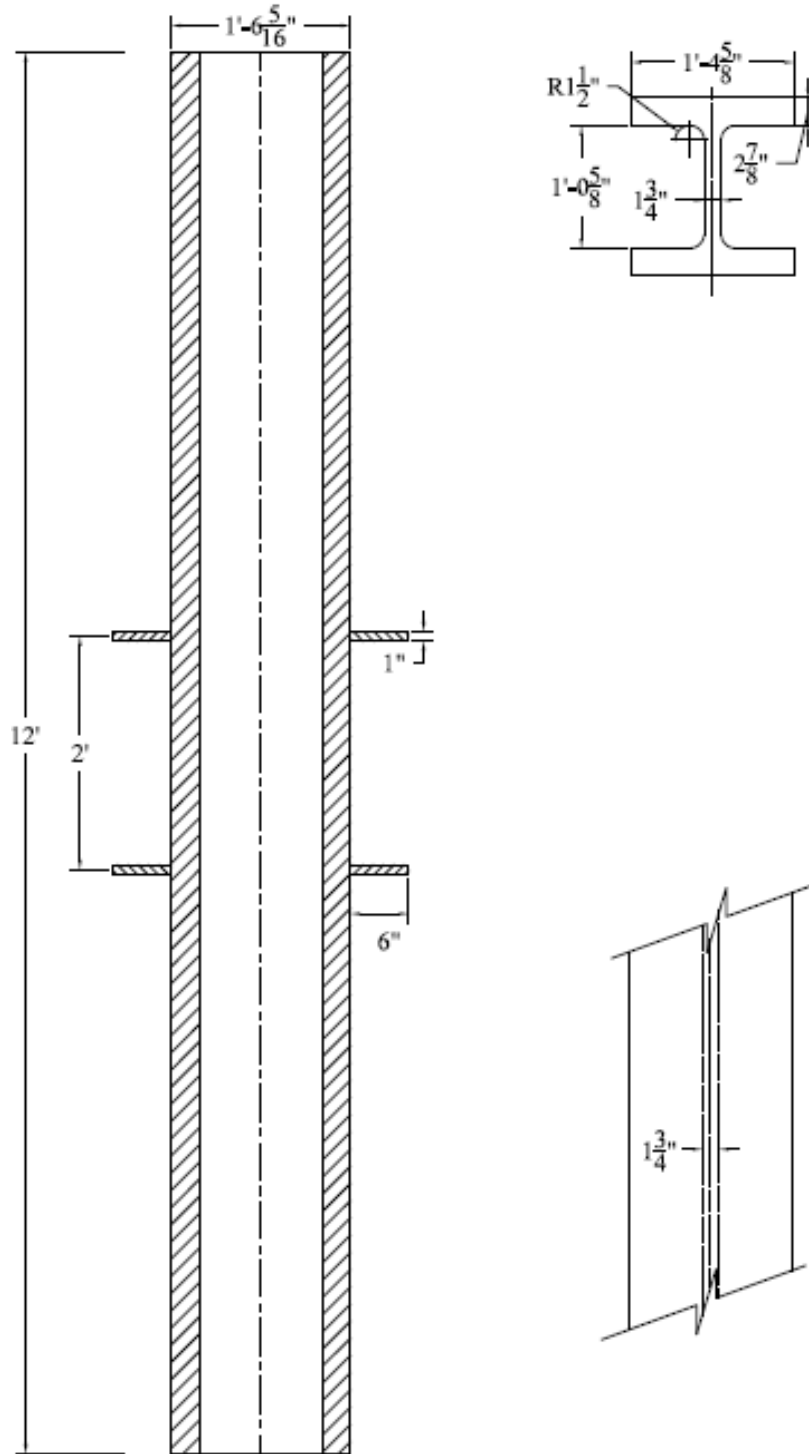


Figure 4.8: Analysis Case 1

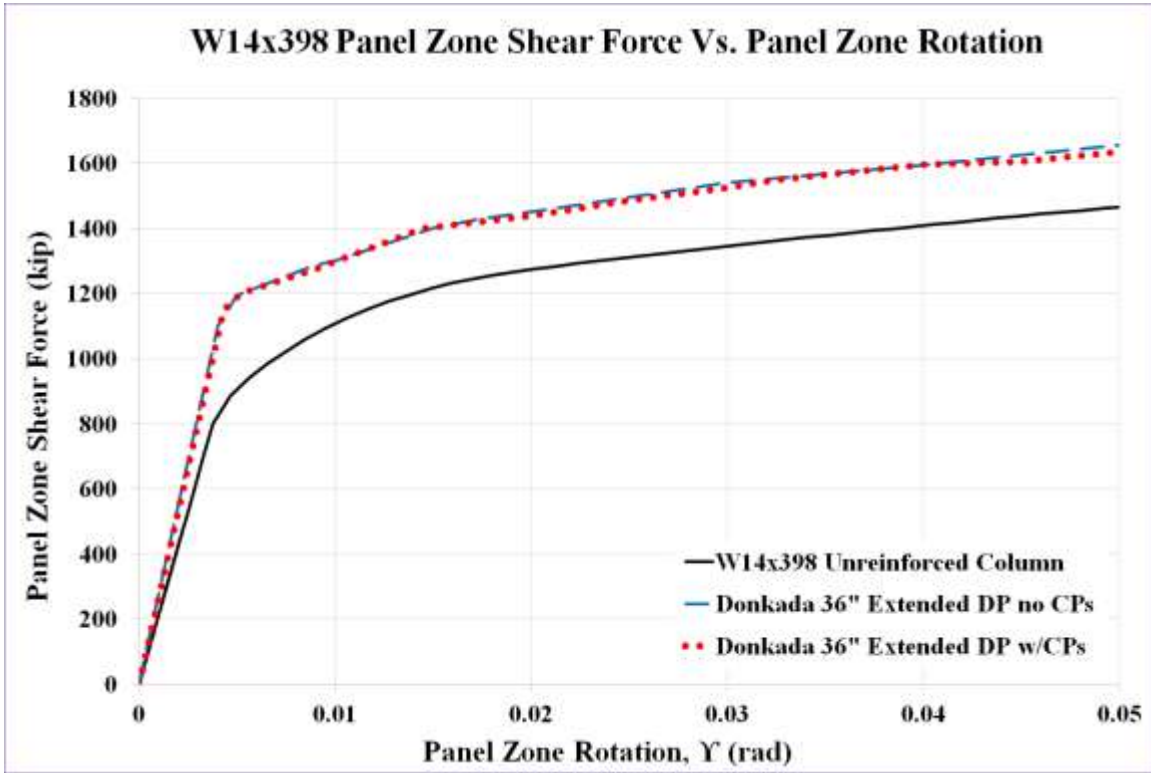


Figure 4.9: Panel zone shear vs. panel zone rotation Case 1

Stage	Applied Force/Loading Plate (Kip)	Panel Shear Force (Kip)		Panel Zone Rotation (rad)
1	530	884		0.005
2	749	1,248		0.017
3	767	1,278		0.020
4	#N/A	#N/A		#N/A
5	989	1,649		0.100

Table 4.3: Panel zone shear and force on loading plate Case 1

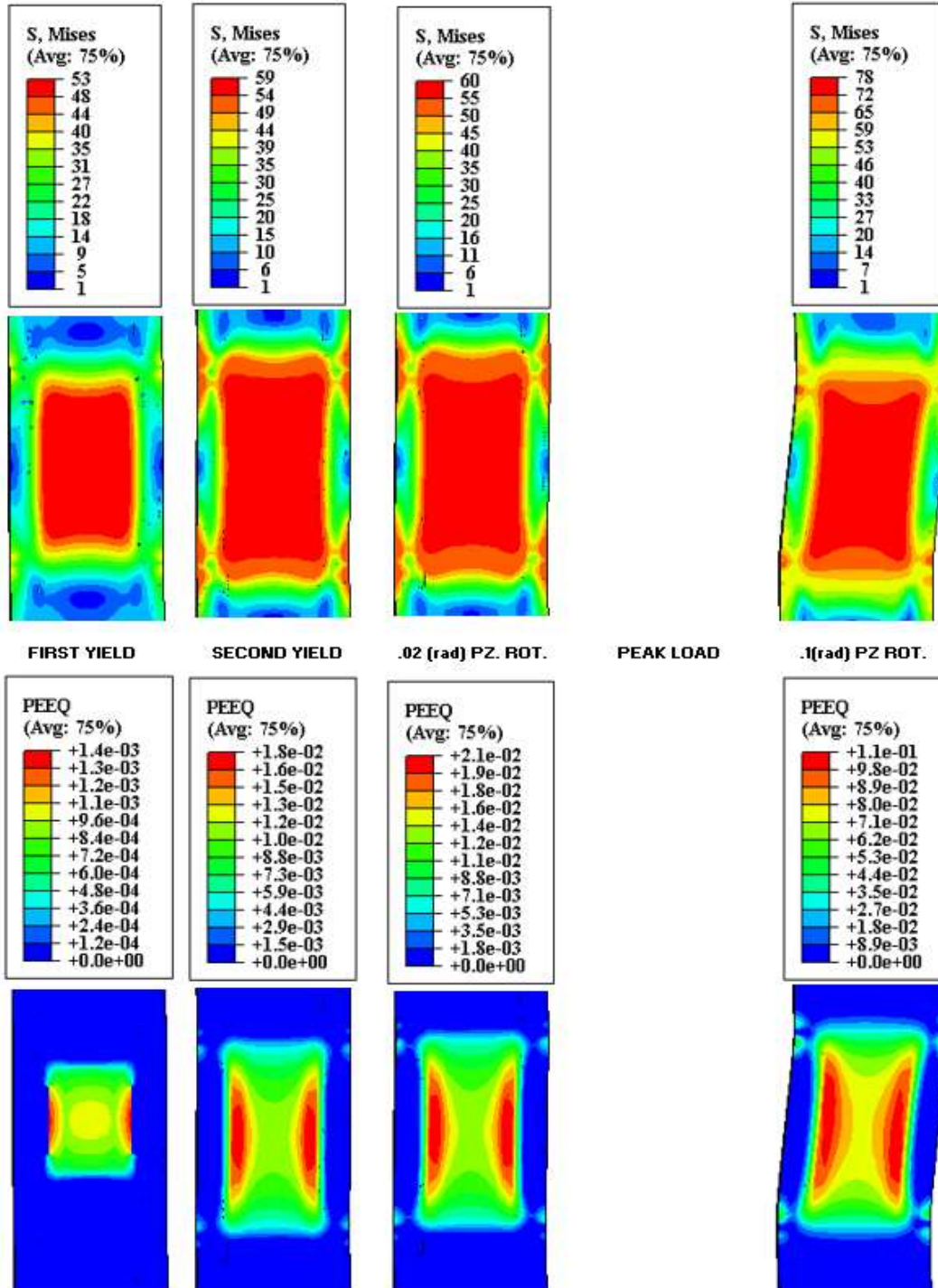


Figure 4.10: VMS and PEEQ in the column Case 1

### 4.2.2 Analysis Case 1A

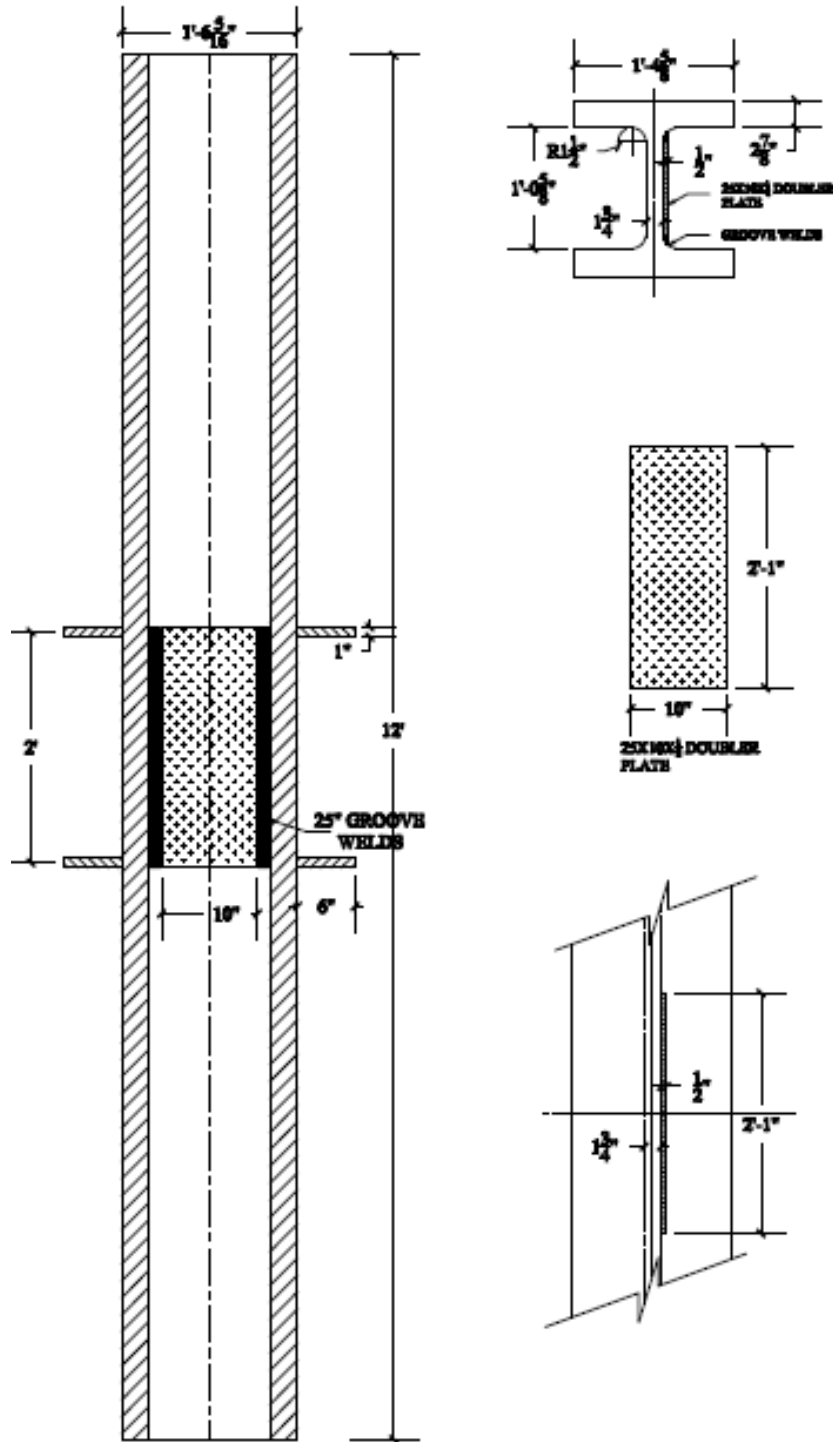


Figure 4.11: Analysis case 1A

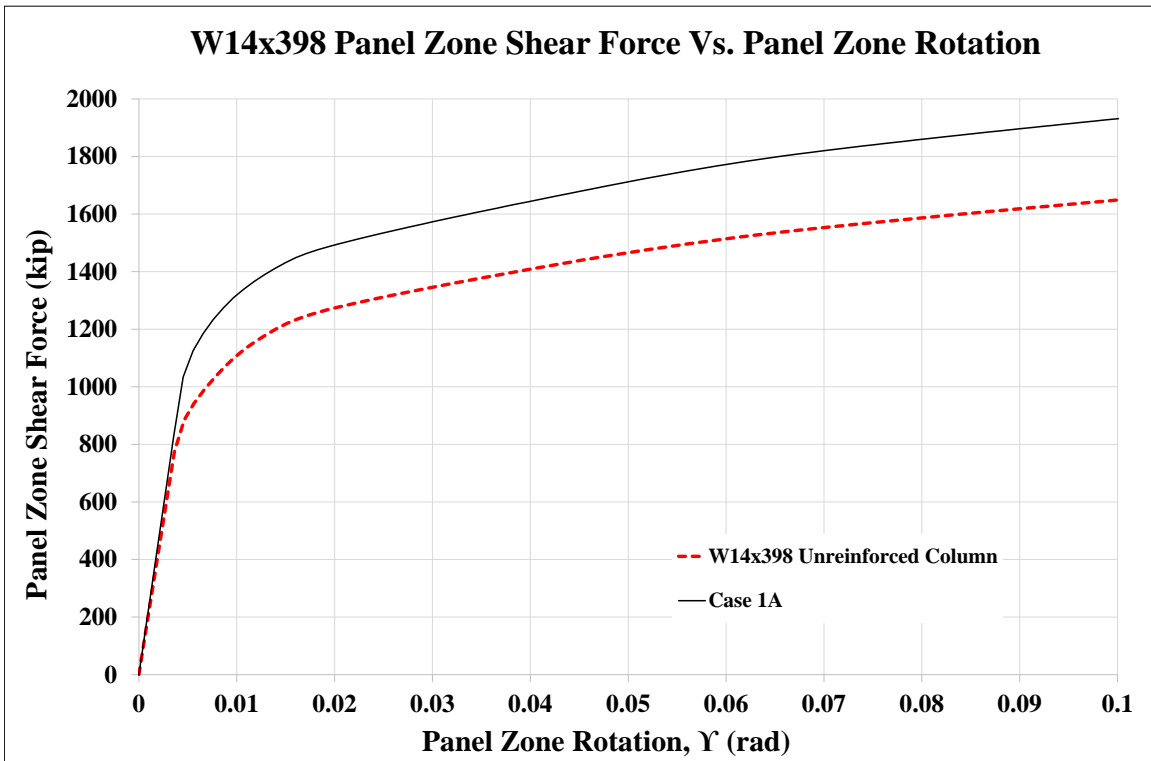


Figure 4.12: Panel zone shear vs. panel zone rotation Case 1A

Stage	Applied Force/Loading Plate (Kip)	Panel Shear Force (Kip)	% Higher than unreinforced Col.	Panel Zone Rotation (rad)
1	620	1,034	117%	0.005
2	869	1,449	116%	0.016
3	898	1,496	117%	0.020
4	1,140	1,900		0.091
5	1,158	1,930	117%	0.100

Table 4.4: Panel zone shear and force on loading plate Case 1A

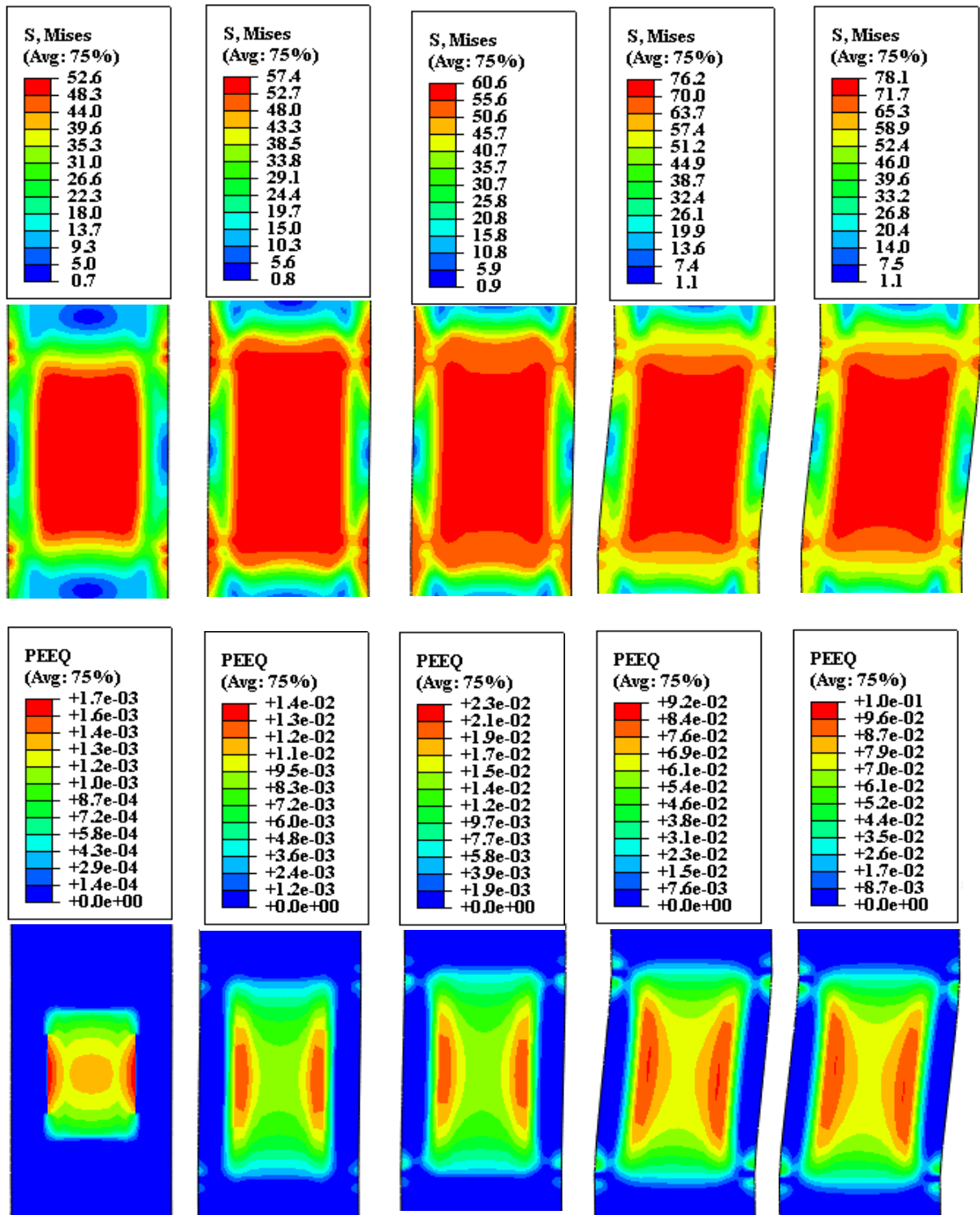
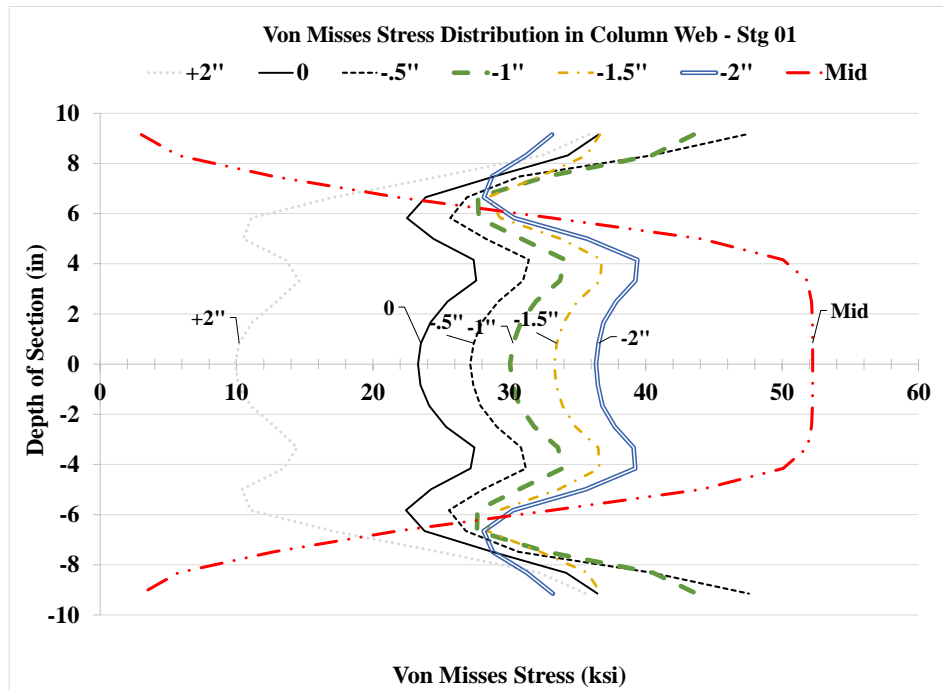
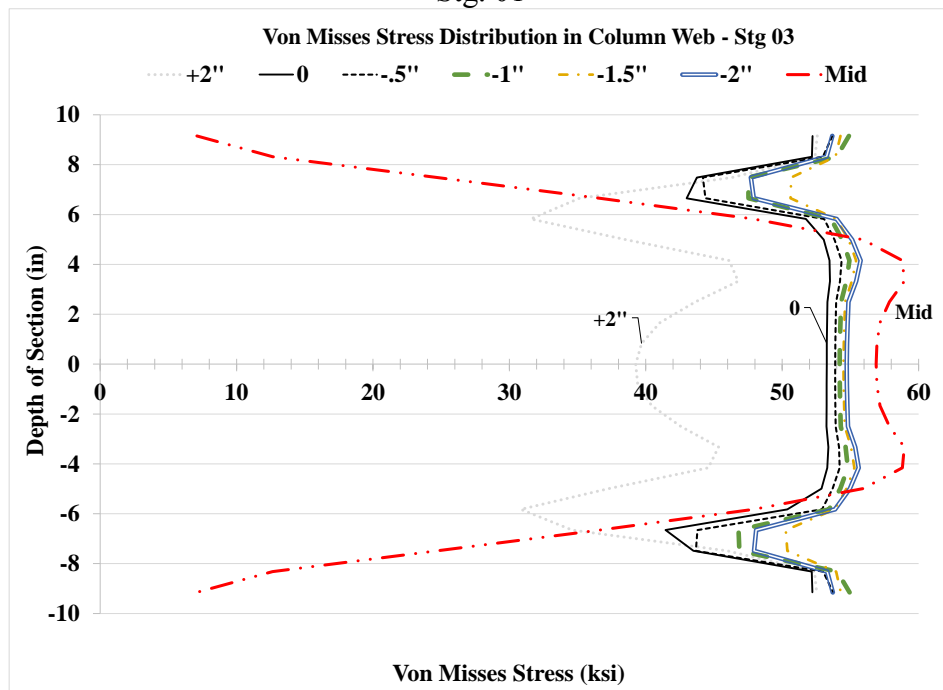


Figure 4.13: VMS and PEEQ in the column Case 1A



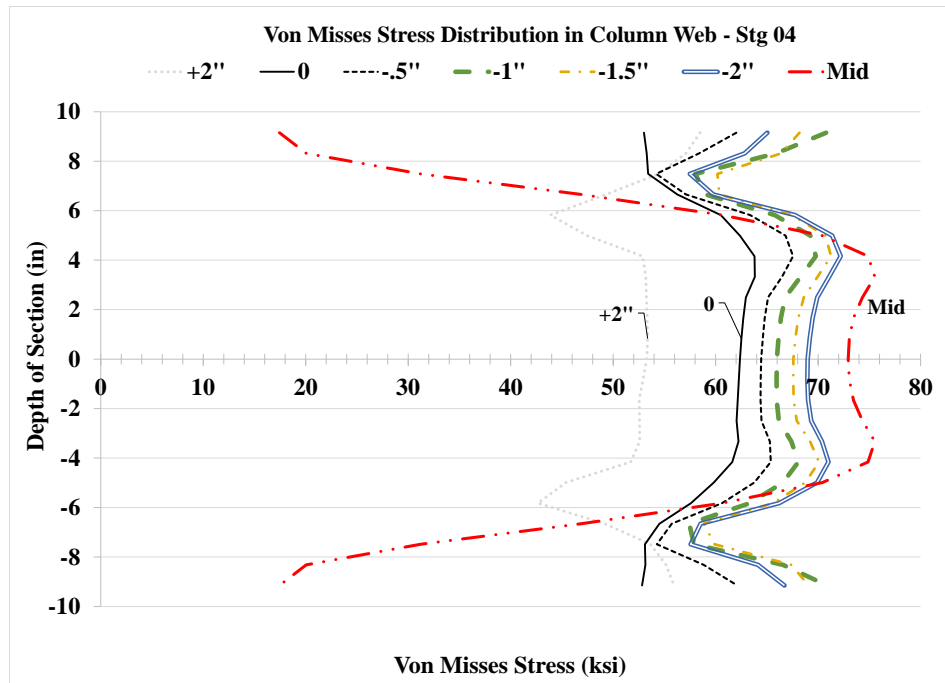


Stg. 01



Stg. 03

Figure 4.14: VMS distribution in column web at different heights Stg. 01-04



Stg. 04

Figure 4.14: VMS distribution in column web at different heights Stg. 01-04

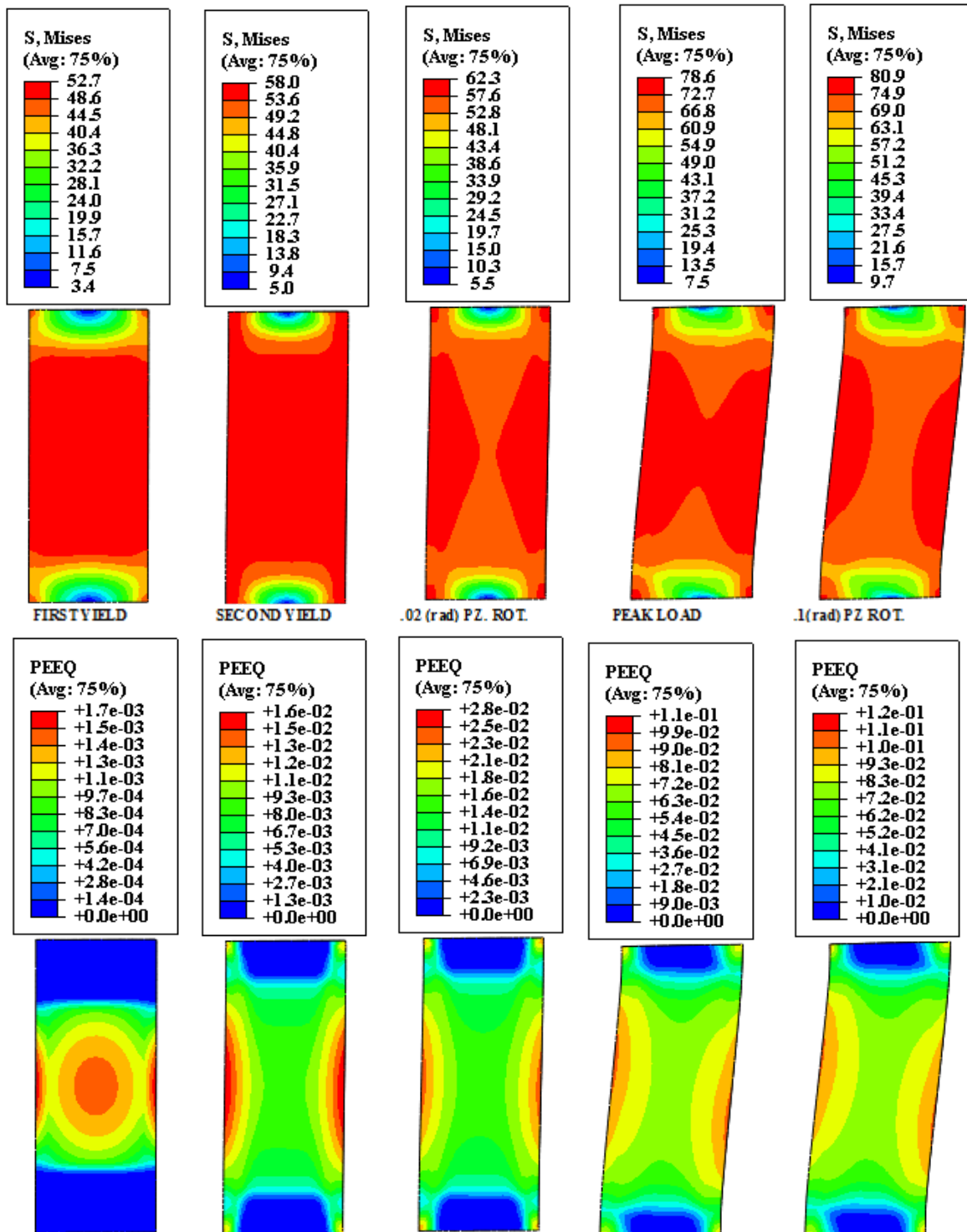


Figure 4.15: VMS and PEEQ in the DP Case 1A

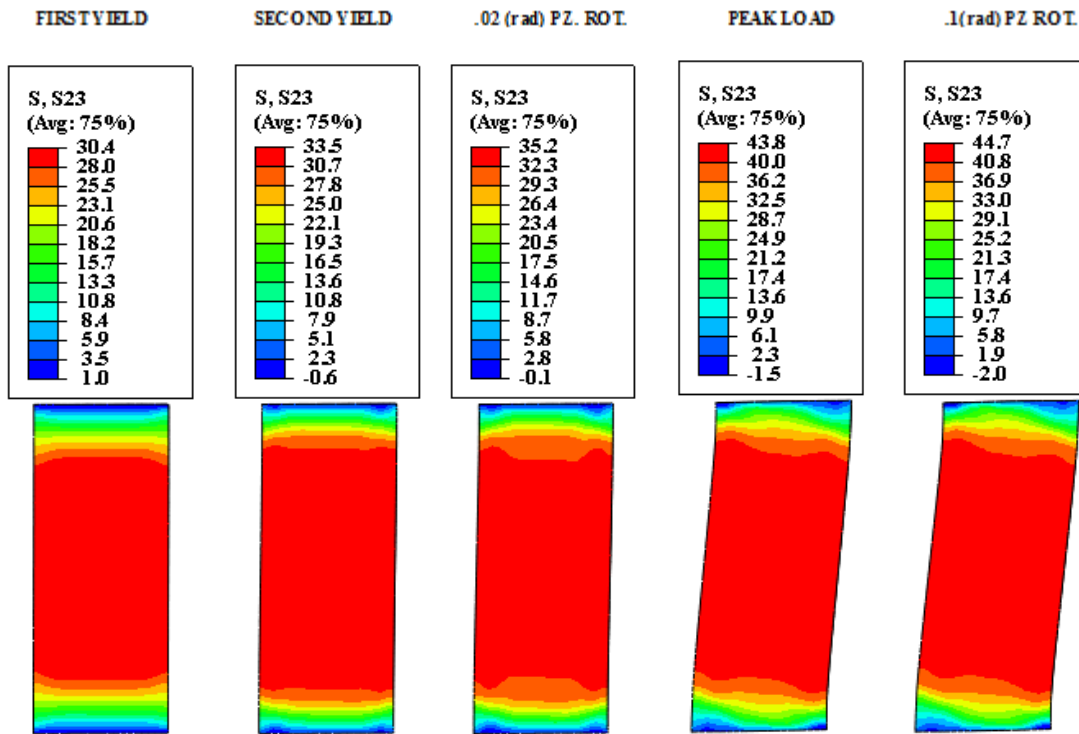


Figure 4.16: Shear stress, S23 in the DP Case 1A

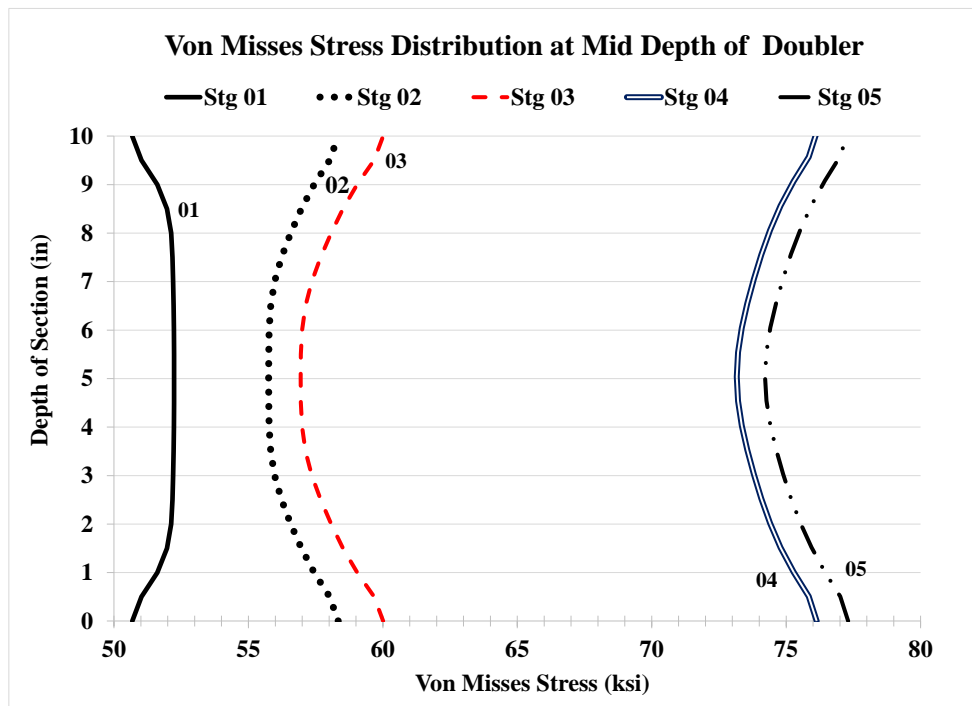


Figure 4.17: VMS distribution at mid-depth of DP Case 1A

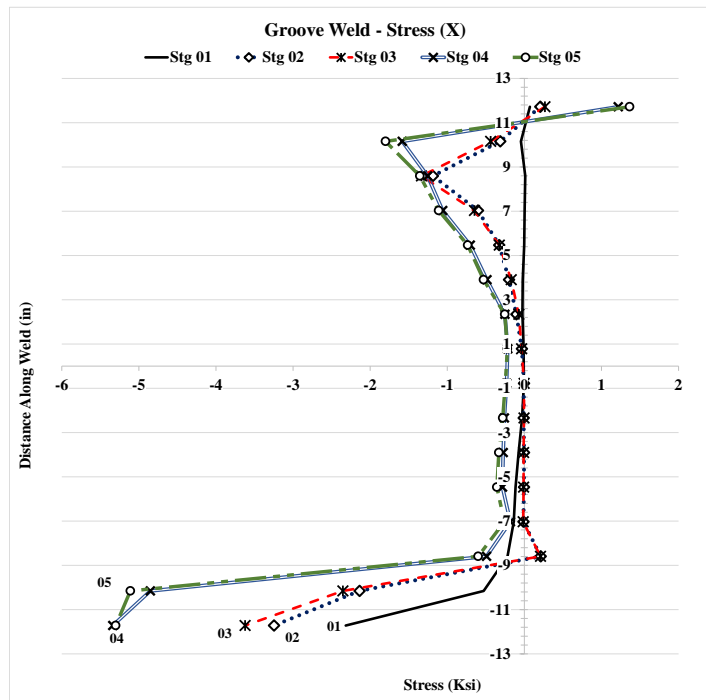
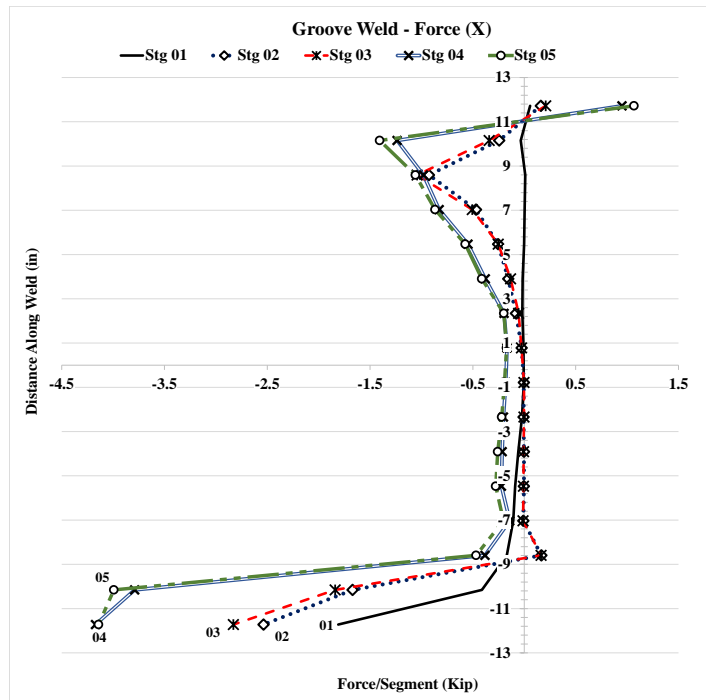


Figure 4.18: Forces and stresses in vertical weld (X)

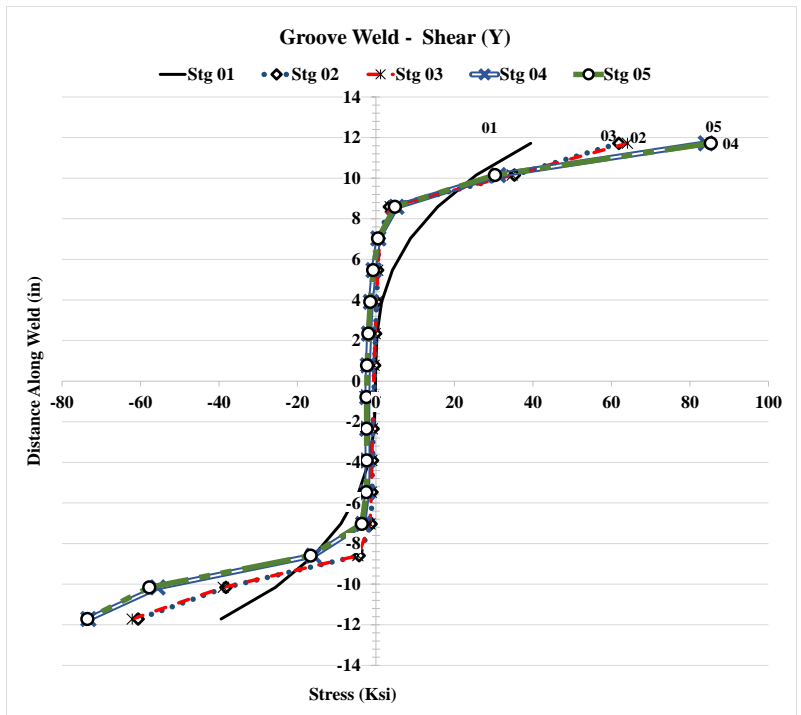
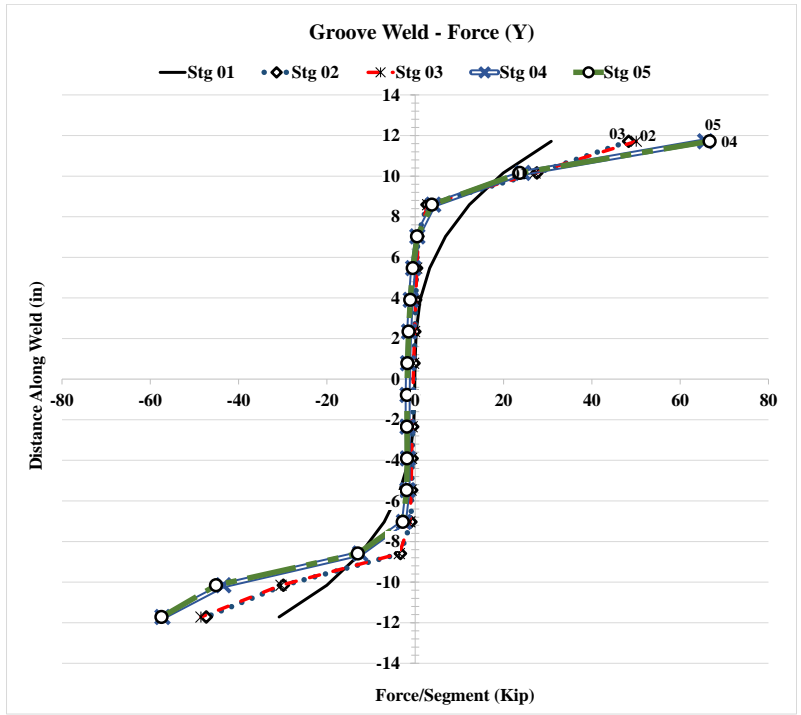


Figure 4.19: Forces and stresses in vertical weld (Y)

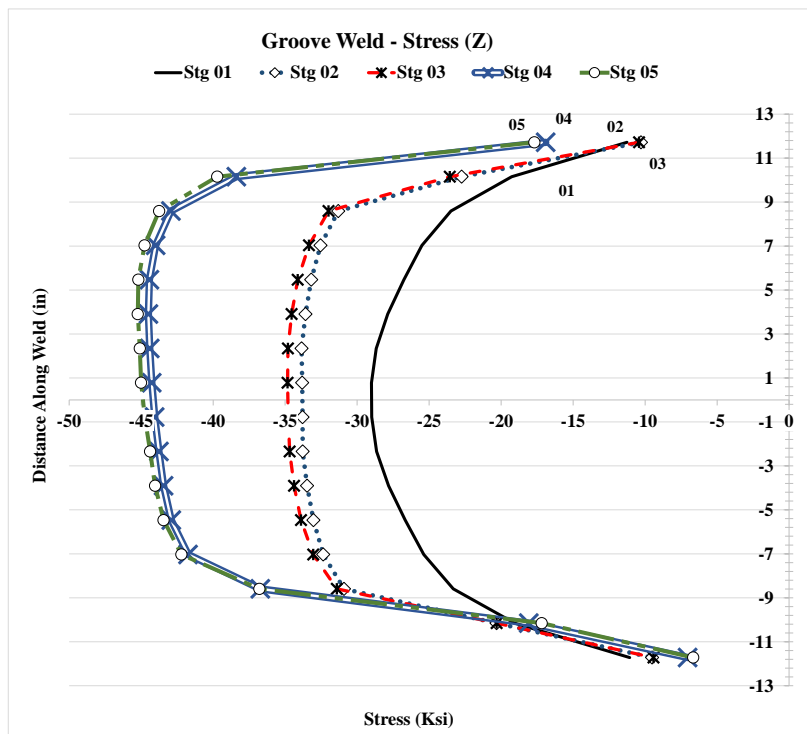
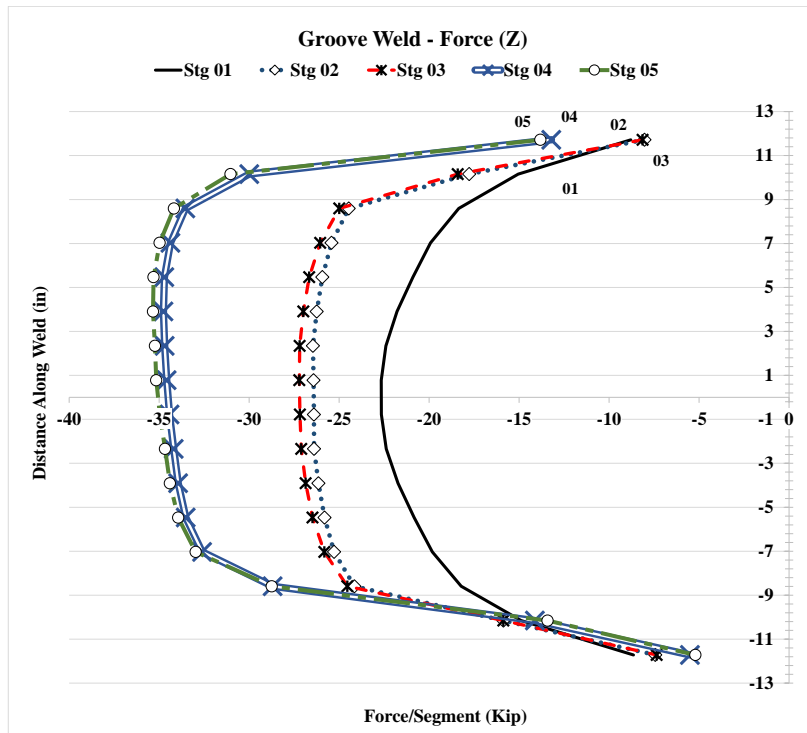


Figure 4.20: Forces and stresses in vertical weld (Z)

### 4.2.3 Analysis Case 1A1

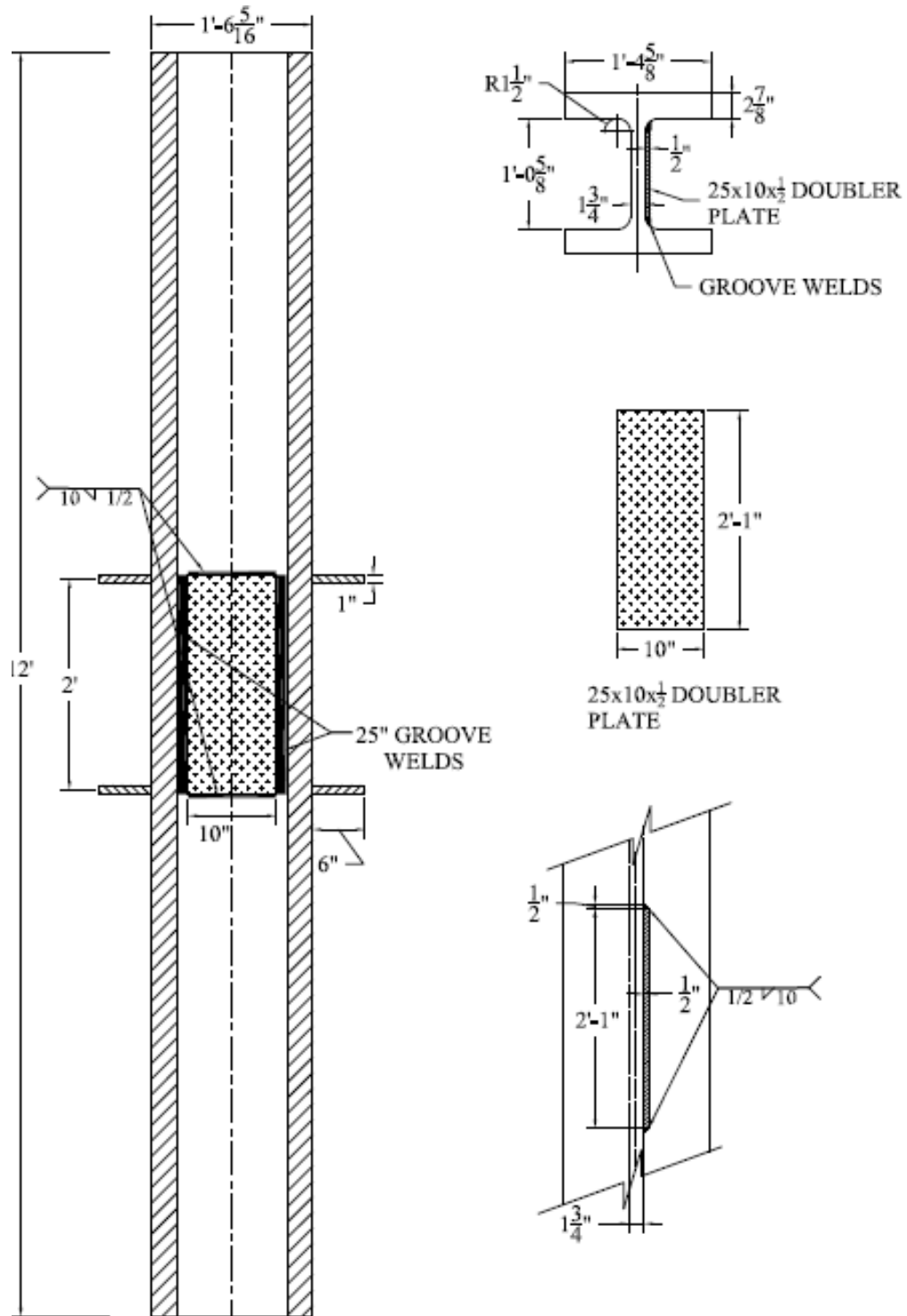


Figure 4.21: Analysis case 1A1



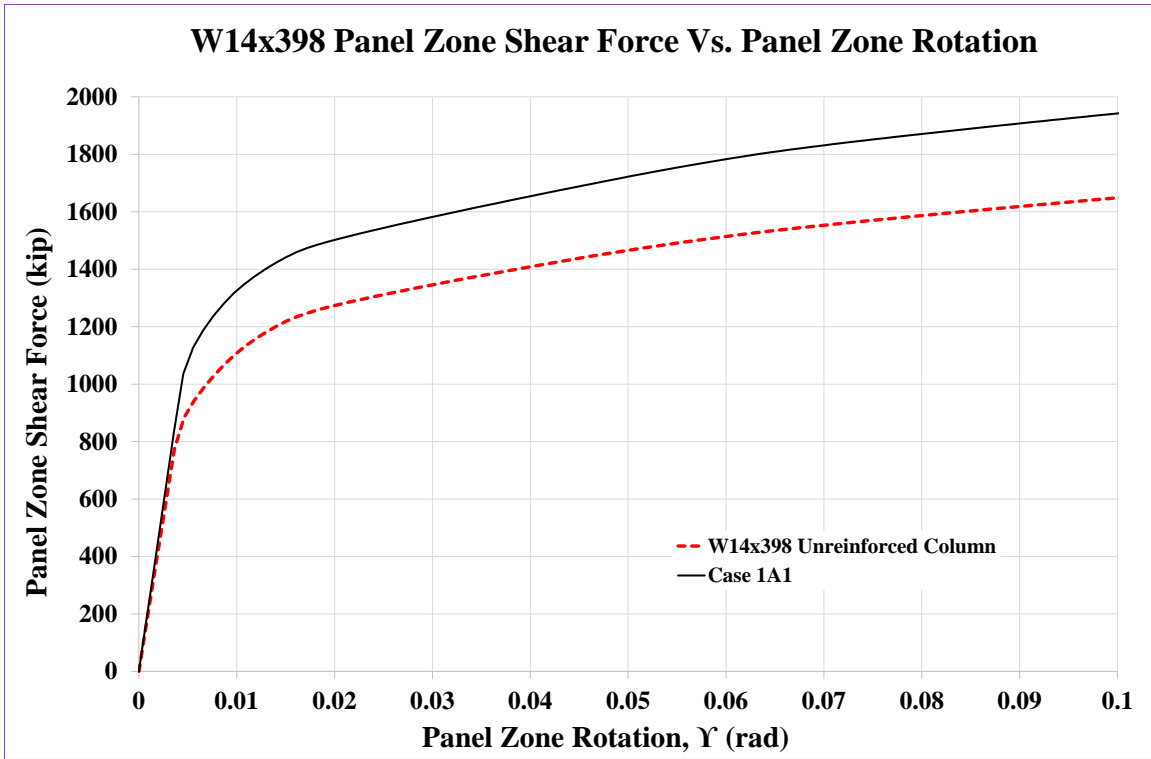


Figure 4.22: Panel zone shear vs. panel zone rotation Case 1A1

Stage	Applied Force/Loading Plate (Kip)	Panel Shear Force (Kip)	% Higher than unreinforced Col.	Panel Zone Rotation (rad)
1	677	1,128	128%	0.006
2	865	1,442	116%	0.015
3	915	1,524	119%	0.023
4	1,142	1,904		0.089
5	1,167	1,945	118%	0.101

Table 4.5: Panel zone shear and force on loading plate Case 1A1

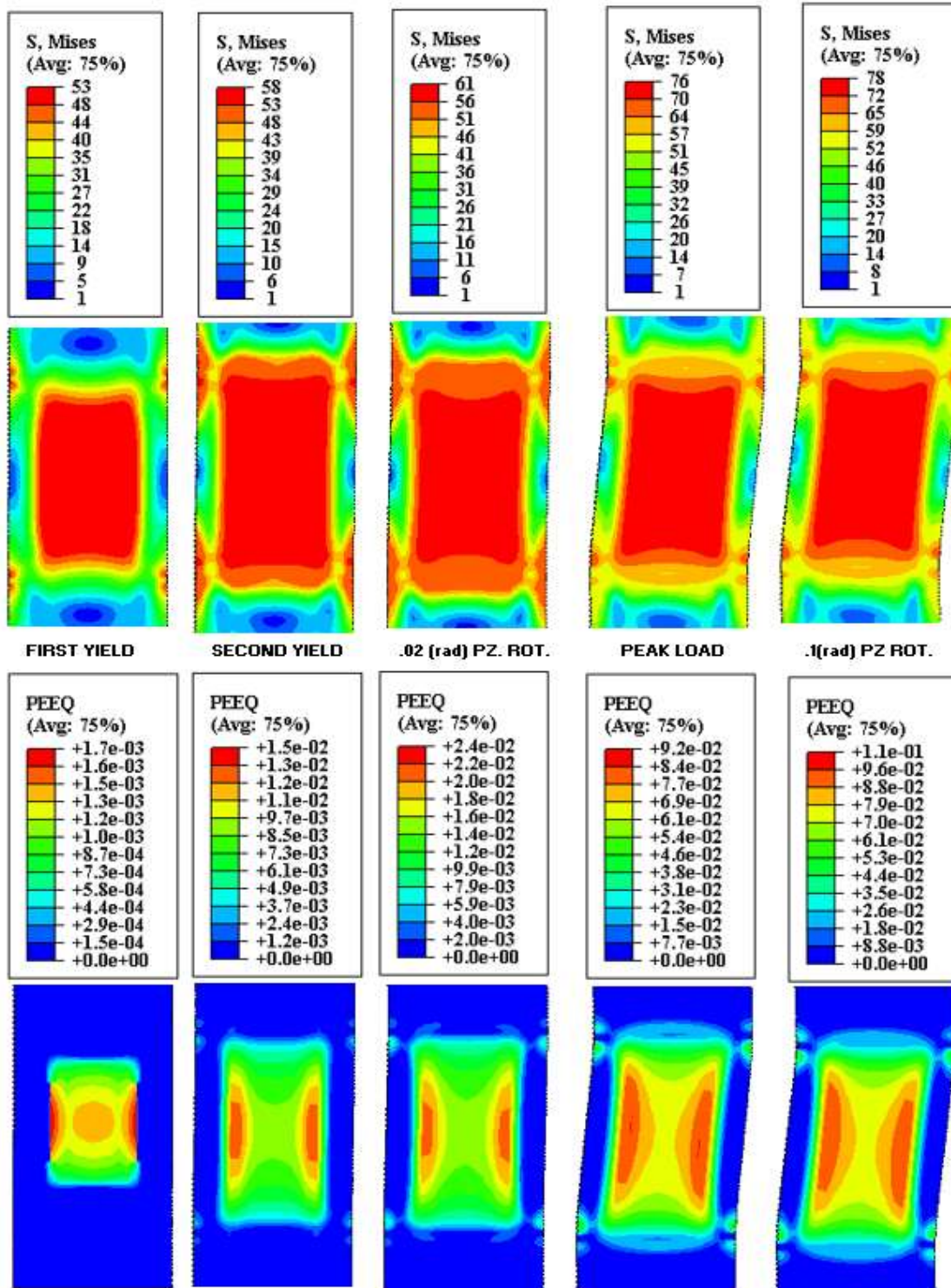
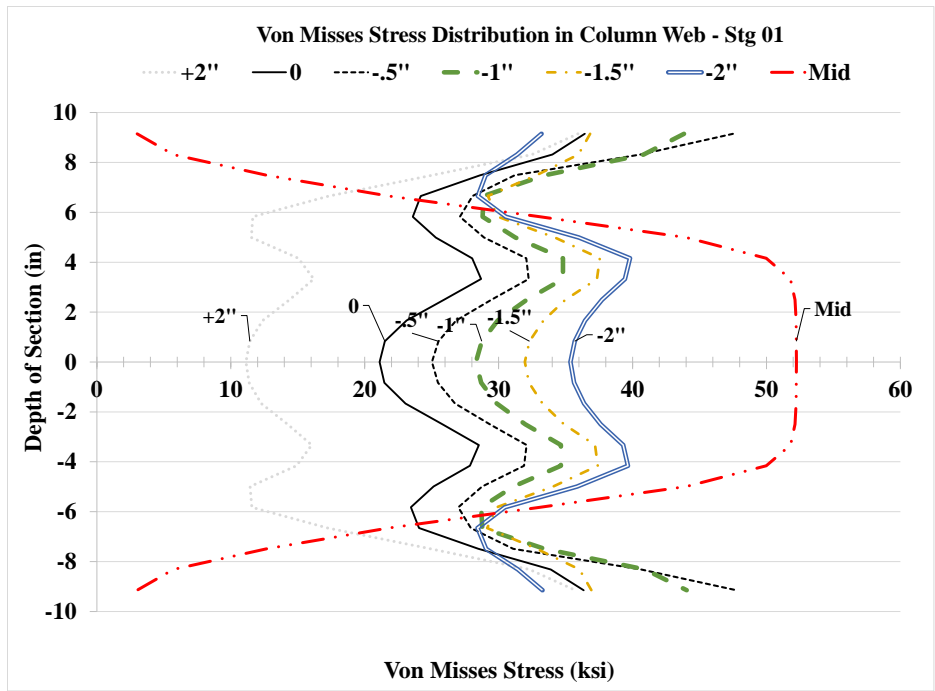
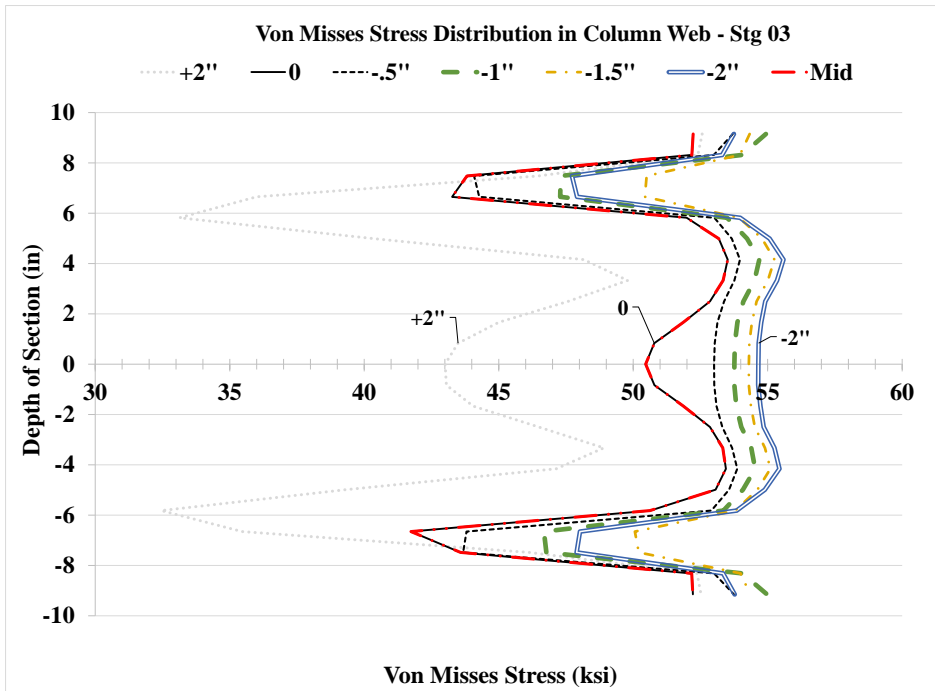


Figure 4.23: VMS and PEEQ in the column Case 1A1



Stg. 01



Stg. 03

Figure 4.24: VMS distribution in column web at different heights Stg. 01-04 Case 1A1

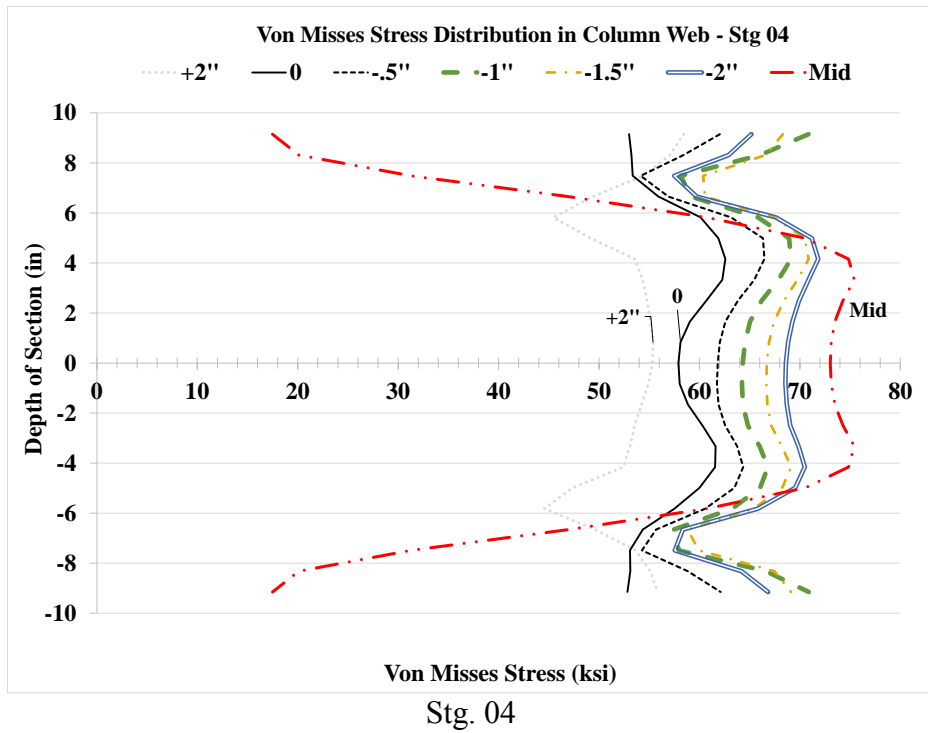


Figure 4.24: VMS distribution in column web at different heights Stg. 01-04 Case 1A1

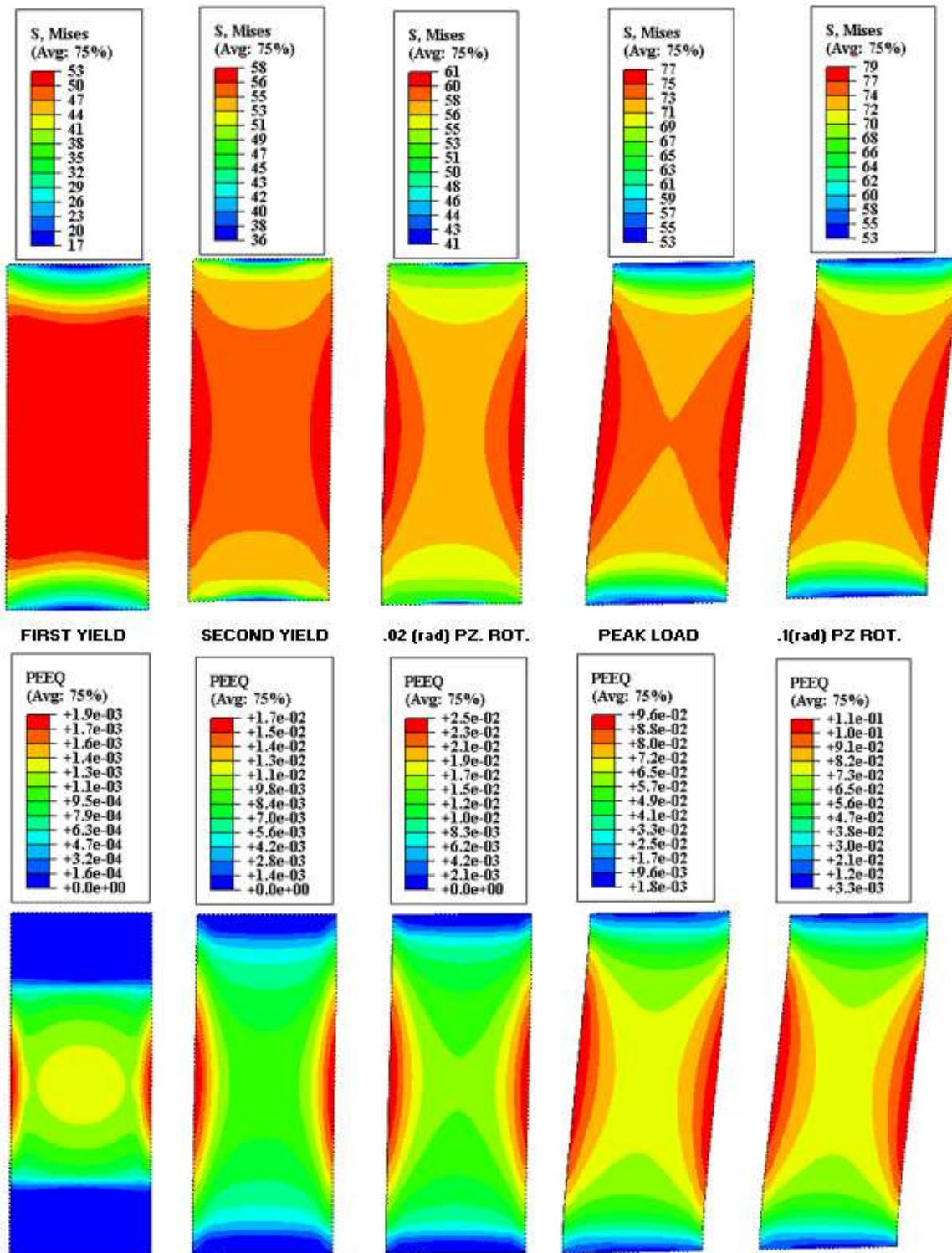


Figure 4.25: VMS and PEEQ in the DP Case 1A1

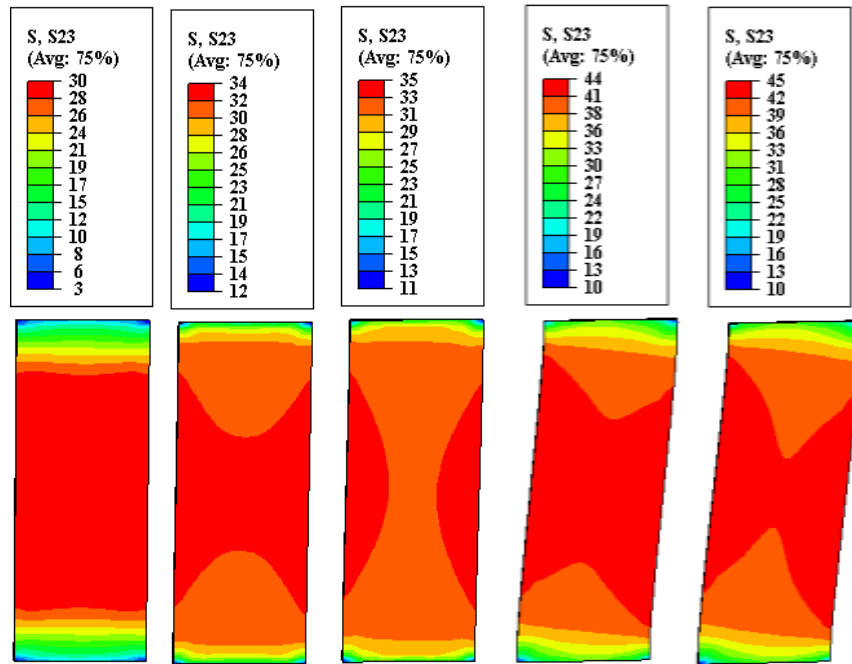


Figure 4.26: Shear stress, S23 in the DP Case 1A1

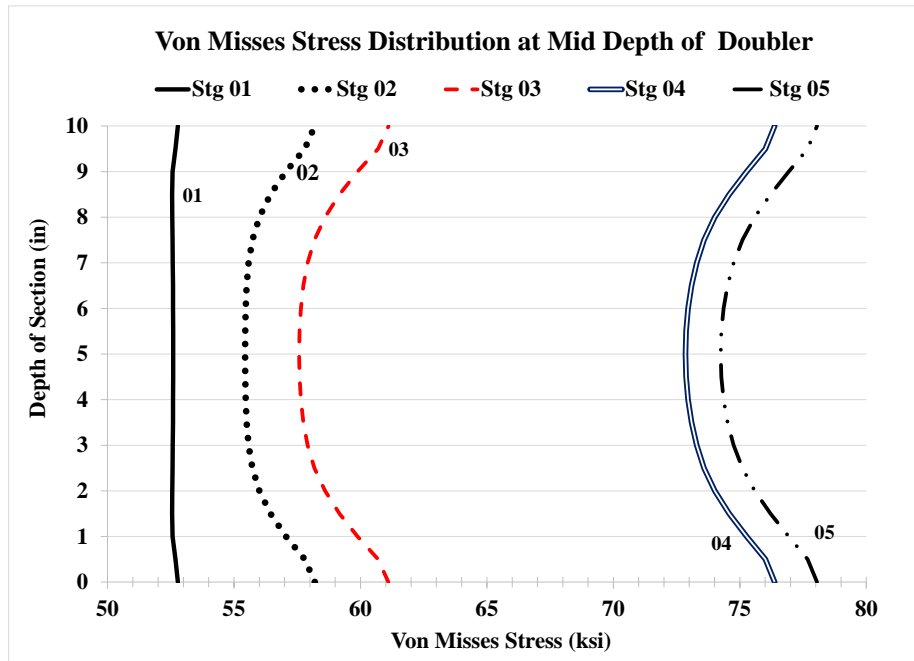


Figure 4.27: VMS distribution at mid-depth of DP Case 1A1

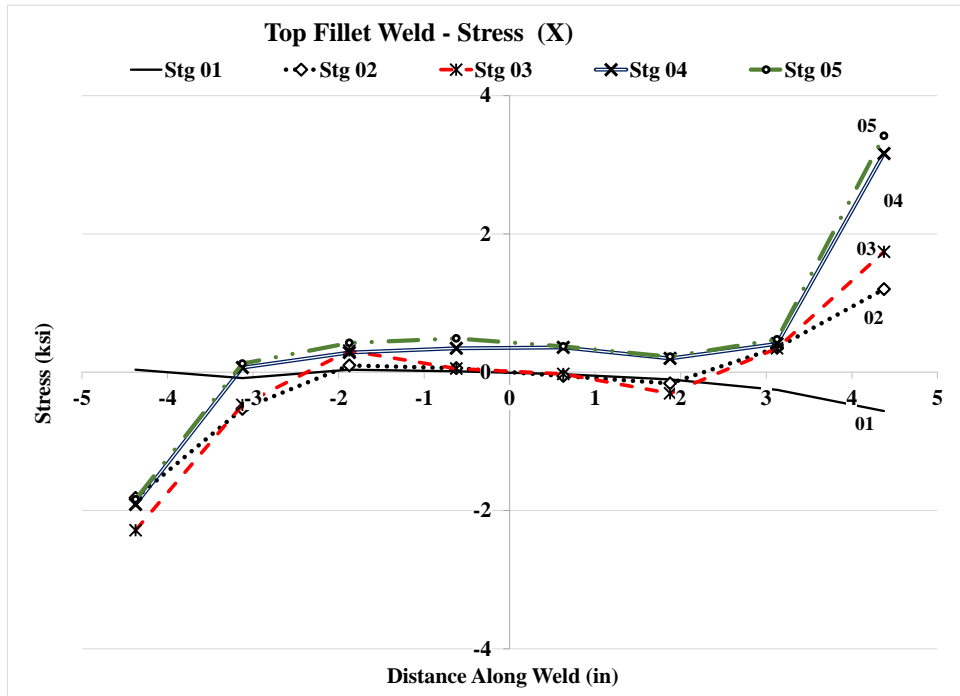
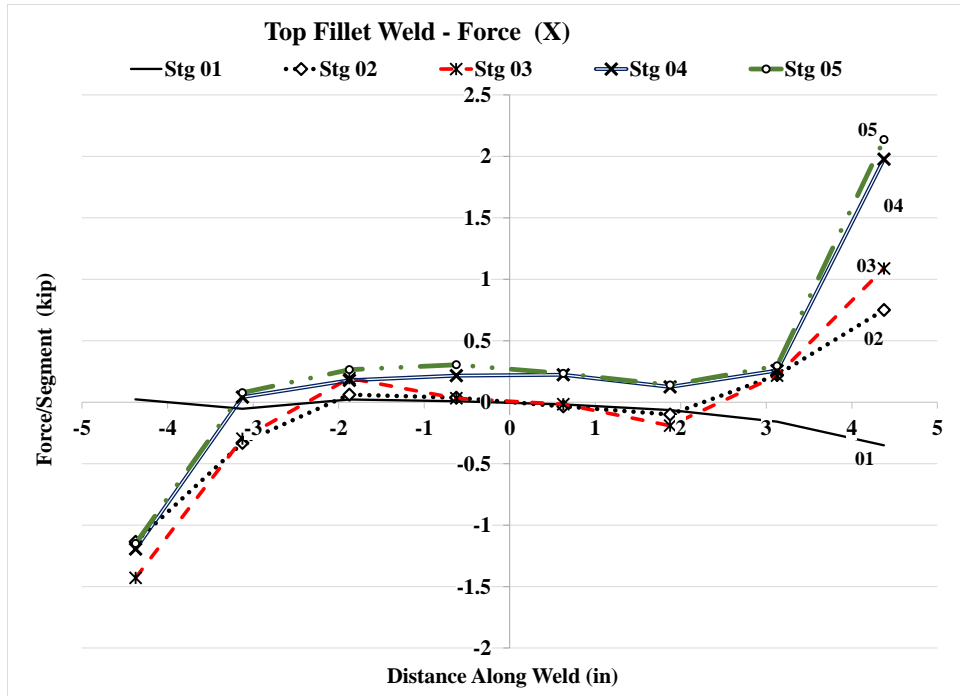


Figure 4.28: Forces and stresses in horizontal weld, (X) Case 1A1

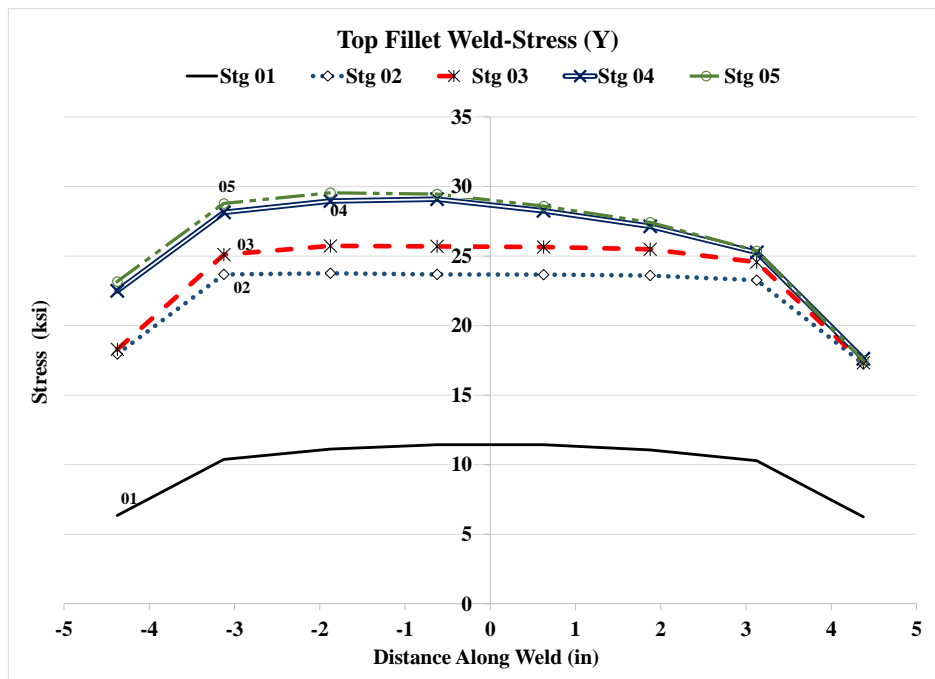
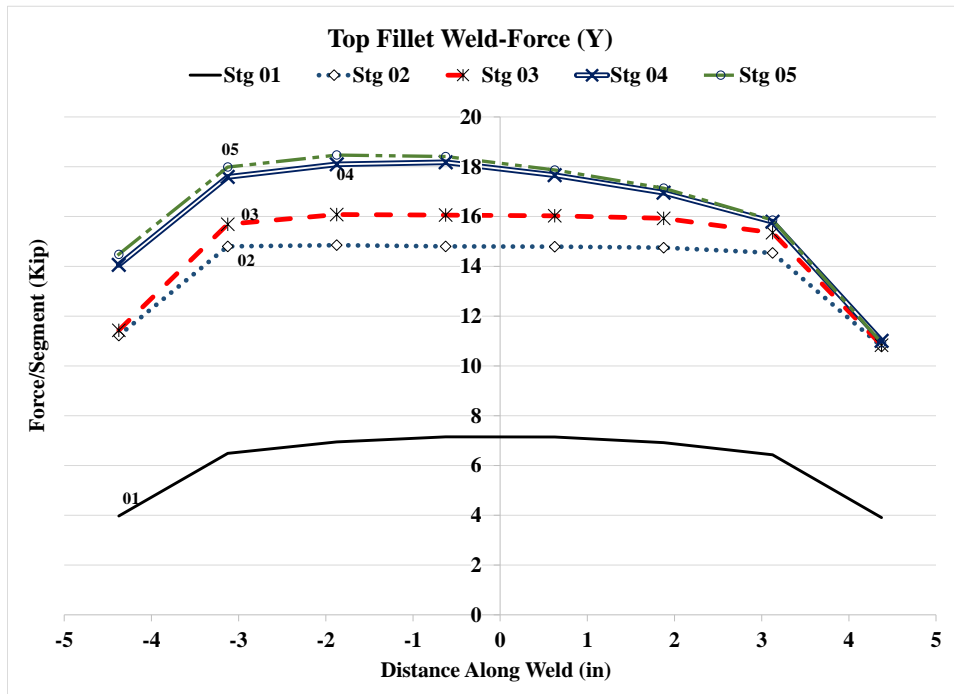


Figure 4.29: Forces and stresses in horizontal weld, (Y) Case 1A1



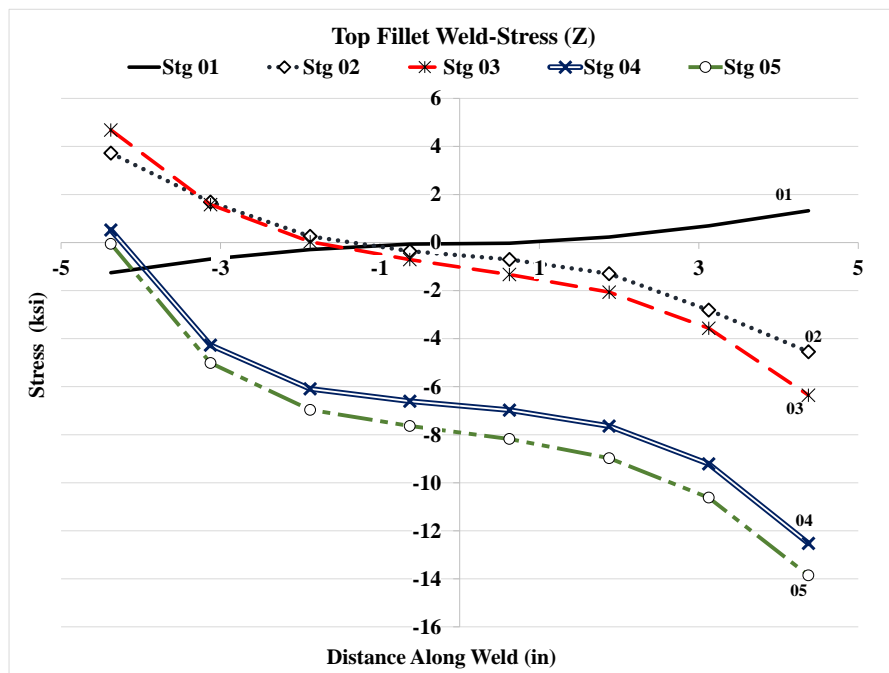
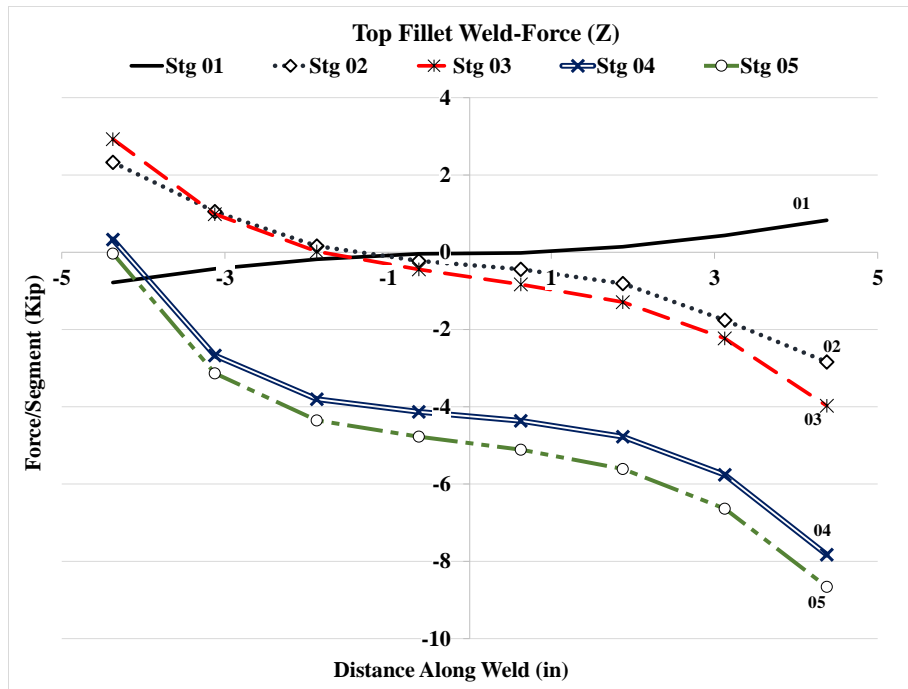


Figure 4.30: Forces and stresses in horizontal weld, (Z) Case 1A1

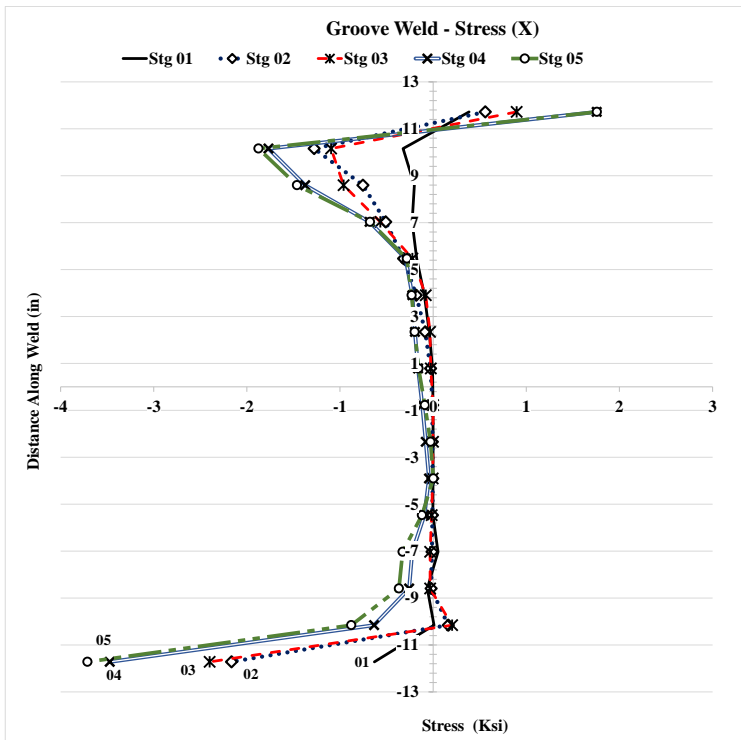
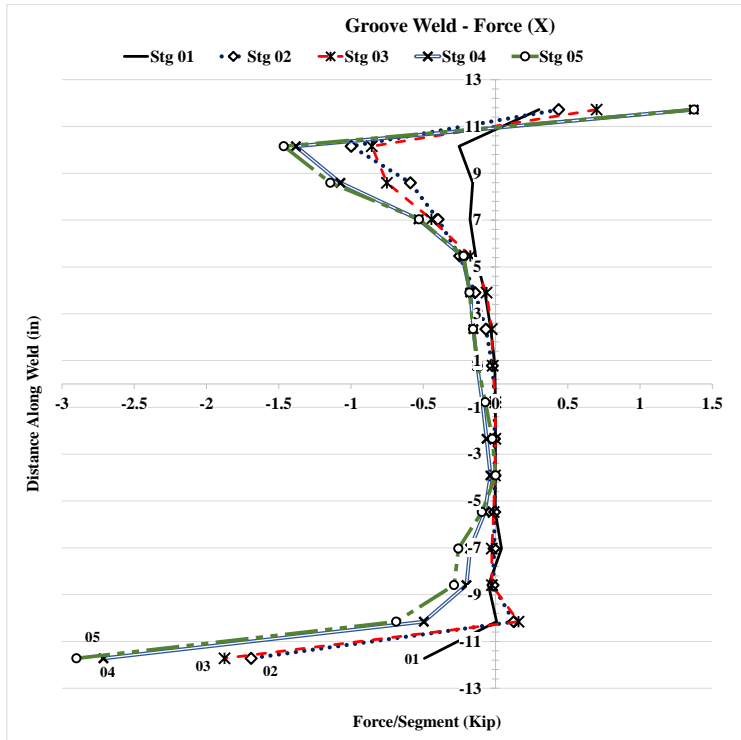


Figure 4.31: Forces and stresses in vertical weld, (X) Case 1A1

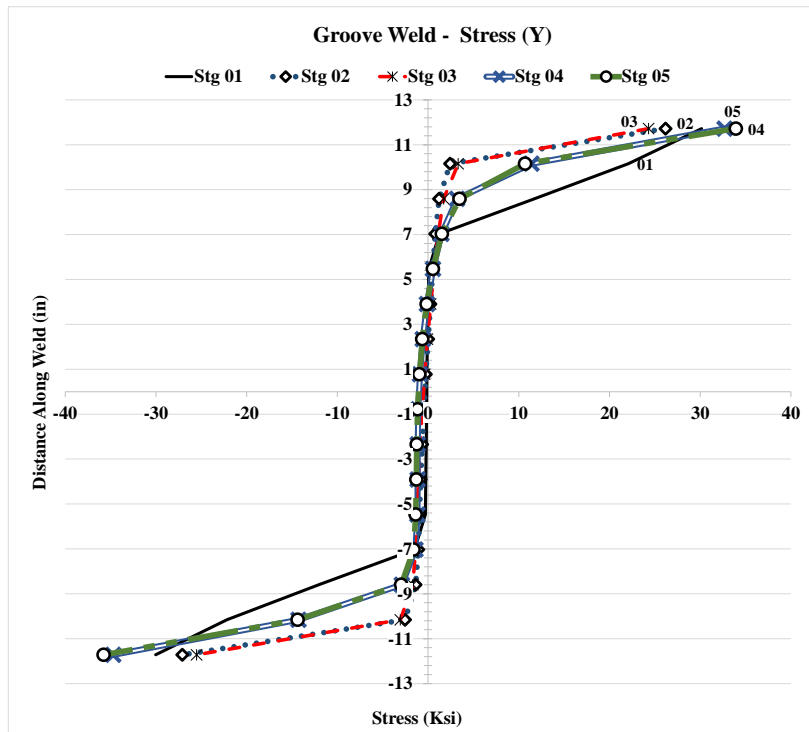
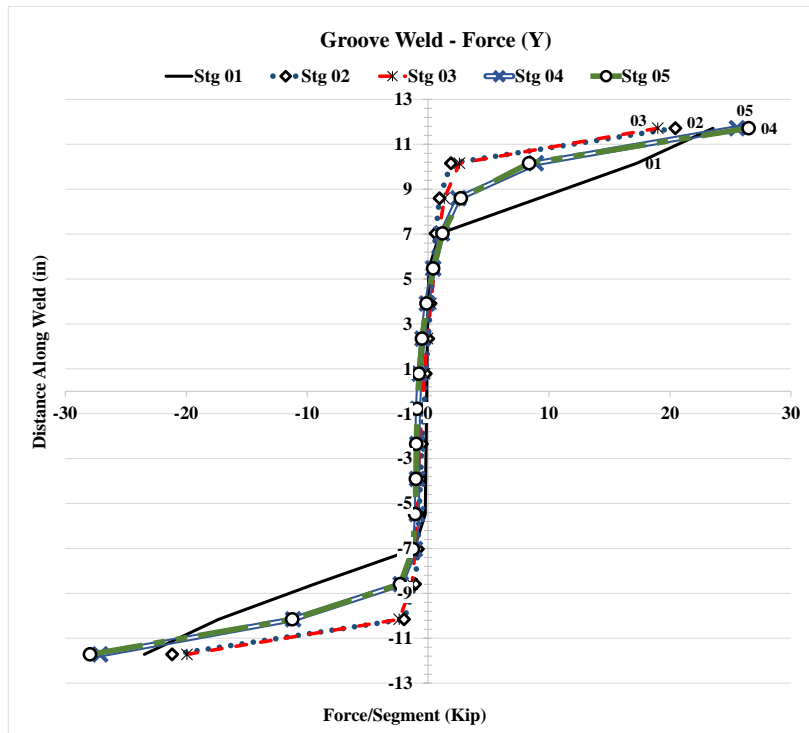


Figure 4.32: Forces and stresses in vertical weld, (Y) Case 1A1

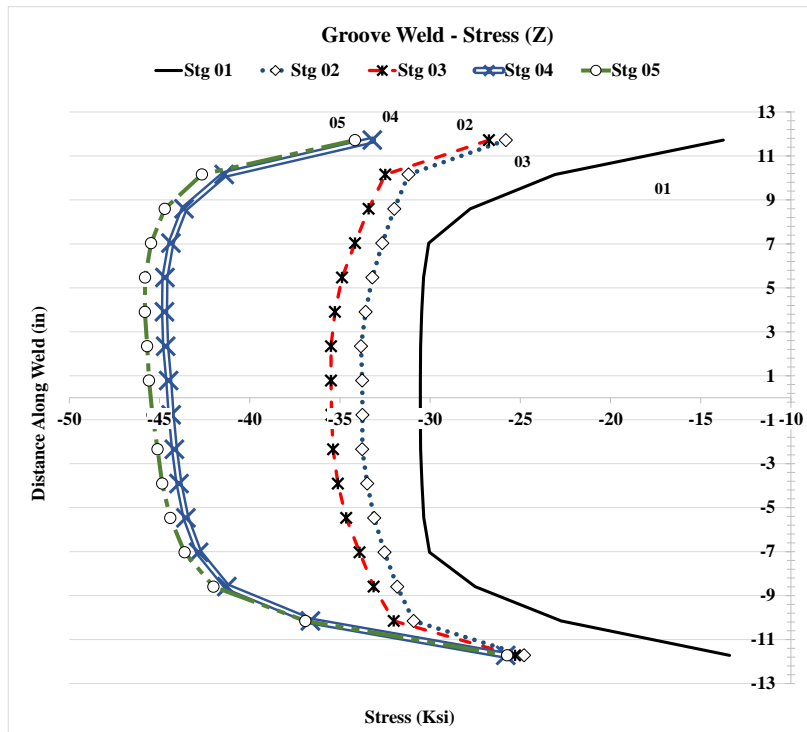
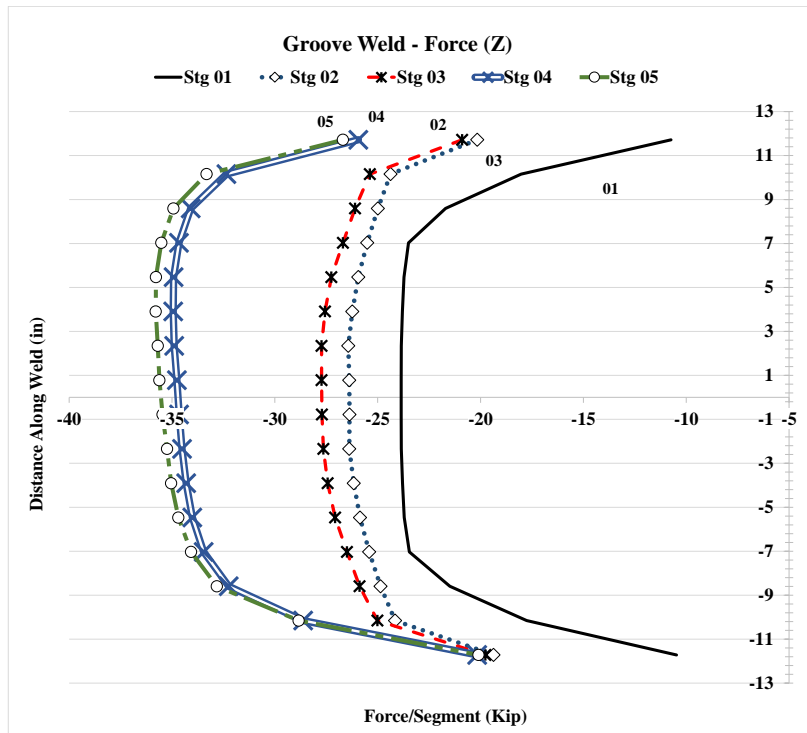


Figure 4.33: Forces and stresses in vertical weld, (Z) Case 1A1

### 4.2.4 Analysis Case 1C

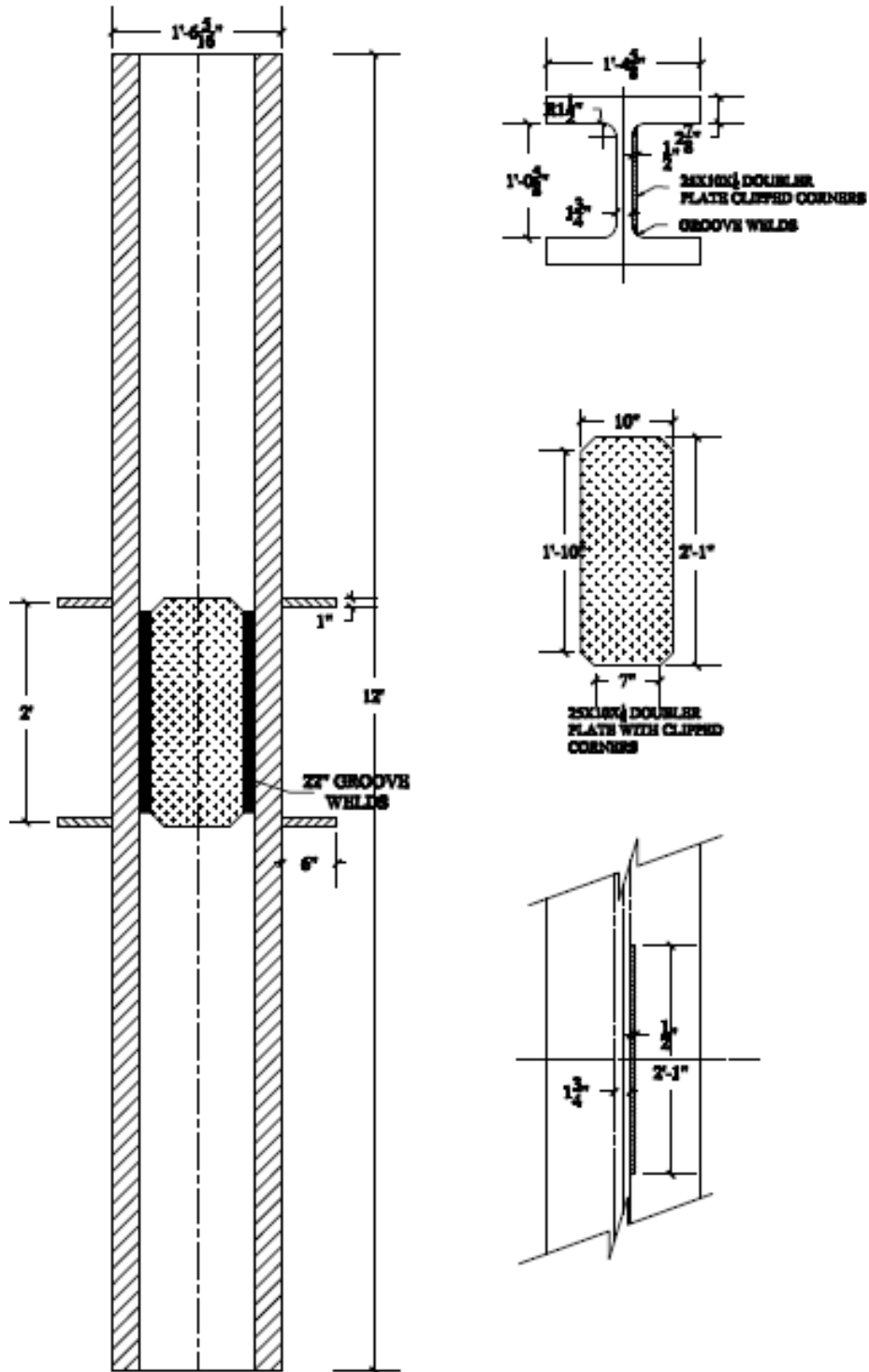


Figure 4.34: Analysis case 1C

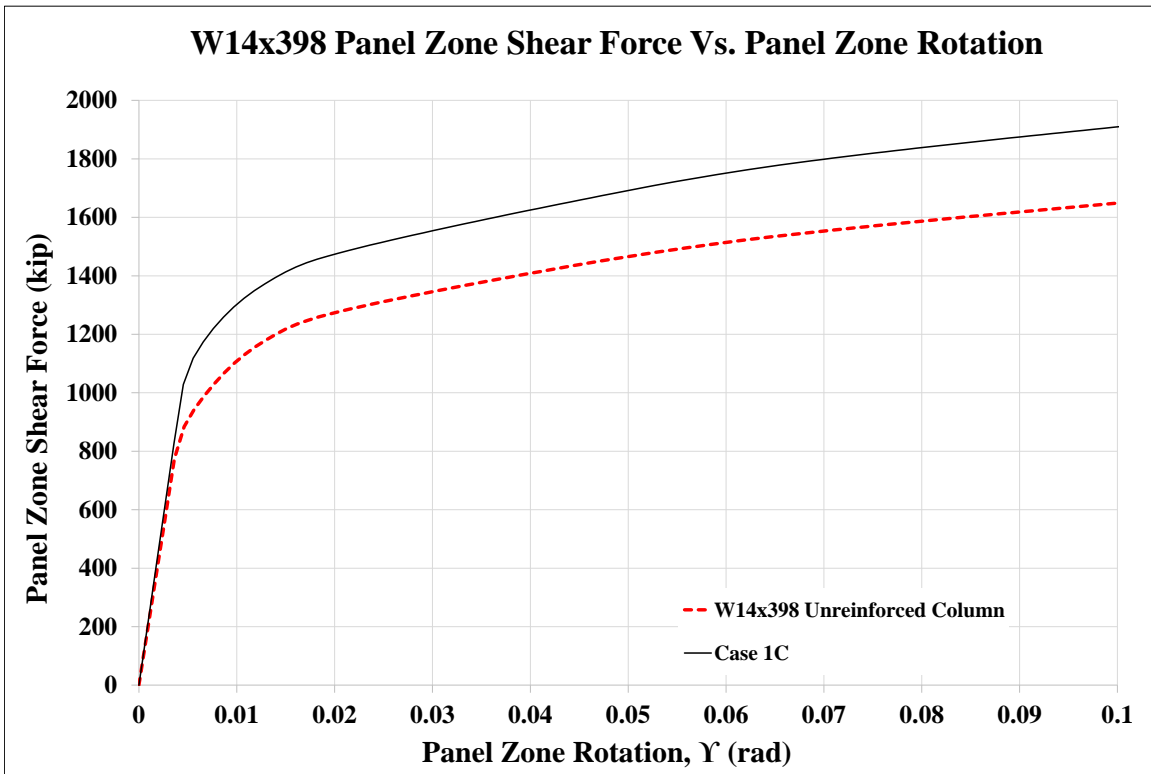


Figure 4.35: Panel zone shear vs. panel zone rotation Case 1C

Stage	Applied Force/Loading Plate (Kip)	Panel Shear Force (Kip)	% Higher than unreinforced Col.	Panel Zone Rotation (rad)
1	617	1,028	116%	0.005
2	848	1,413	113%	0.015
3	886	1,477	116%	0.020
4	1,141	1,901		0.098
5	1,147	1,912	116%	0.101

Table 4.6: Panel zone shear and force on loading plate Case 1C

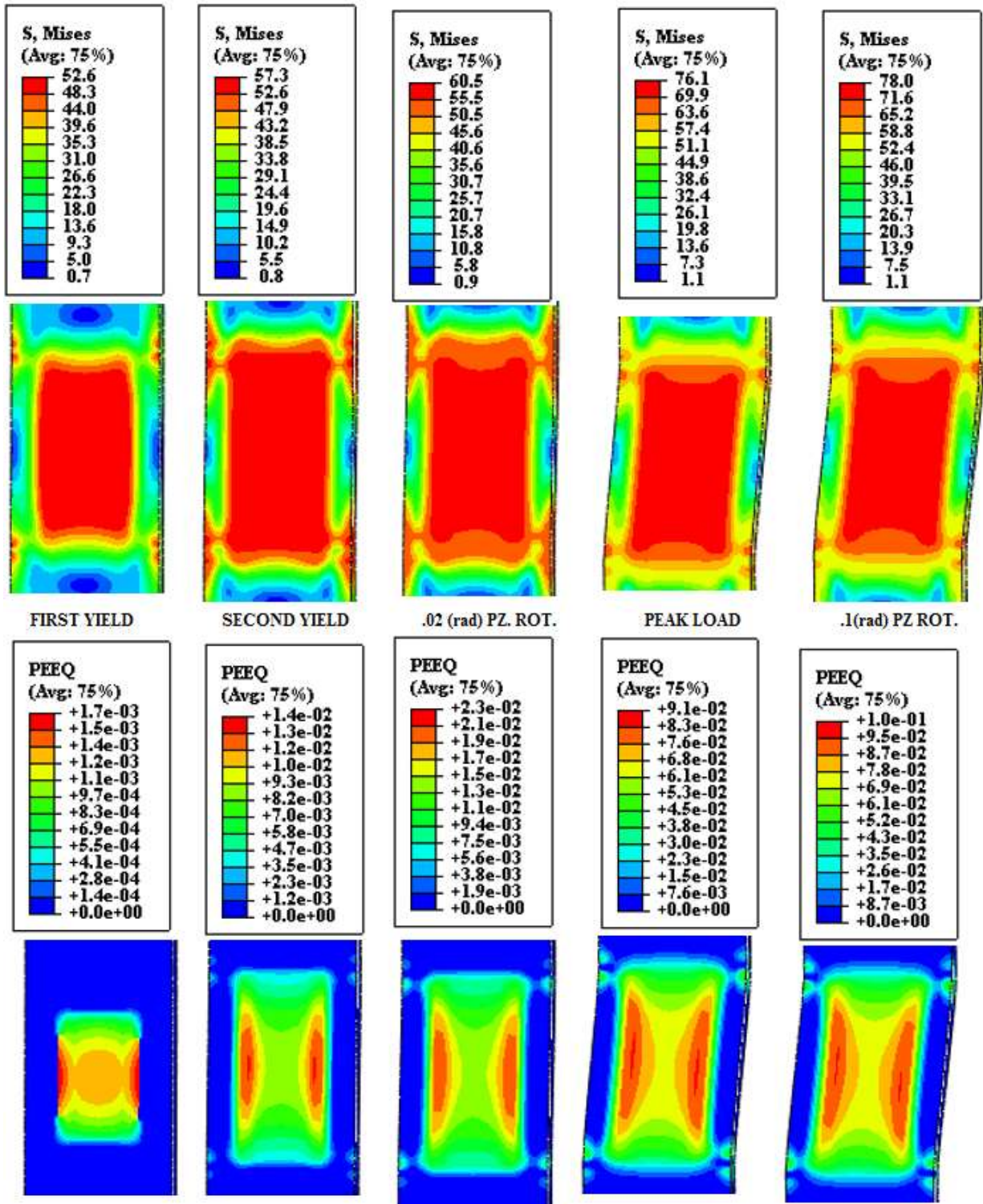
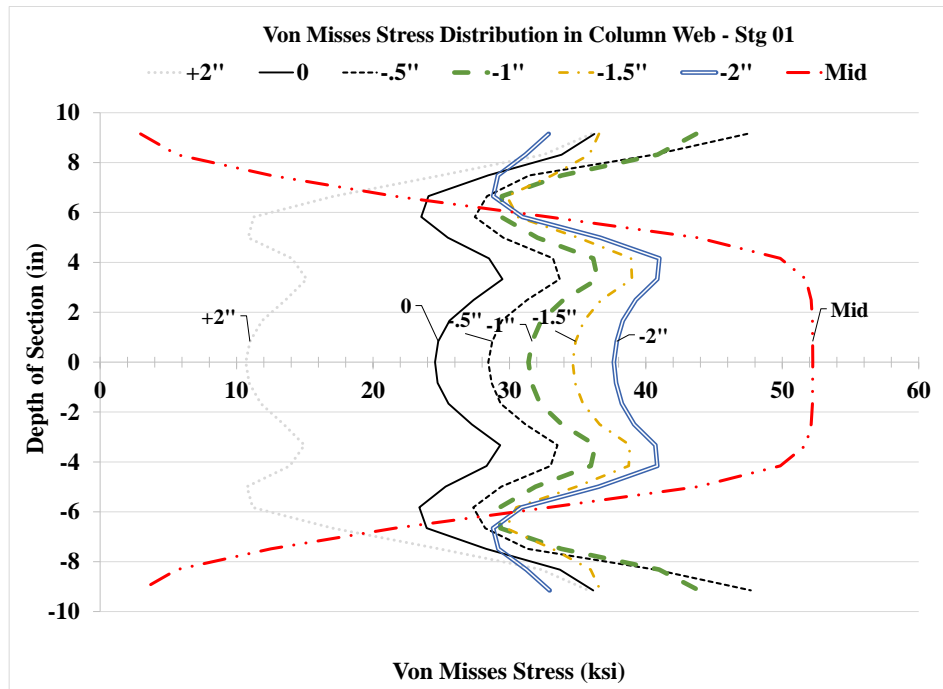
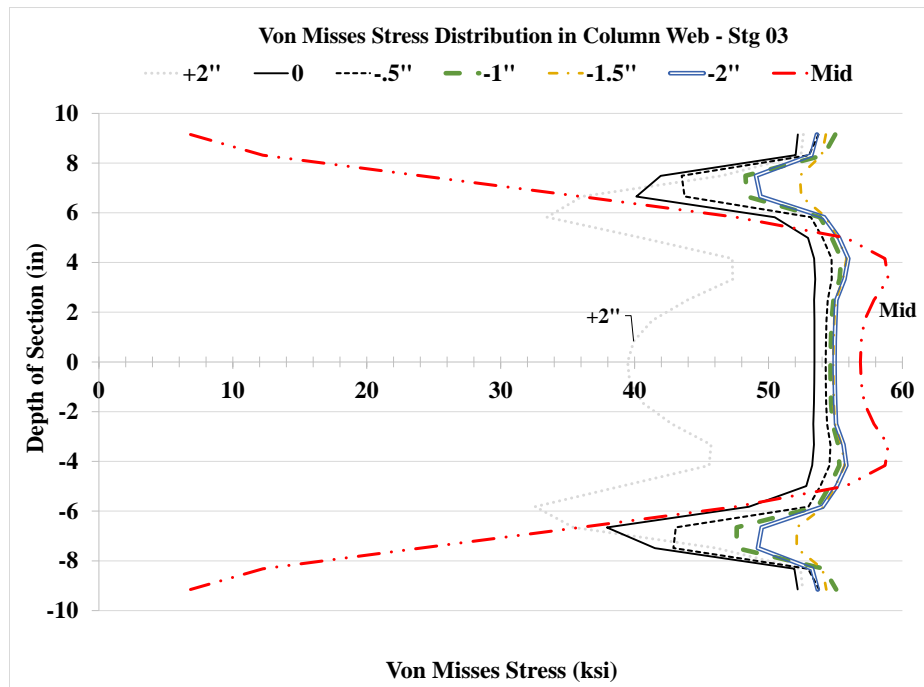


Figure 4.36: VMS and PEEQ in the column Case 1C



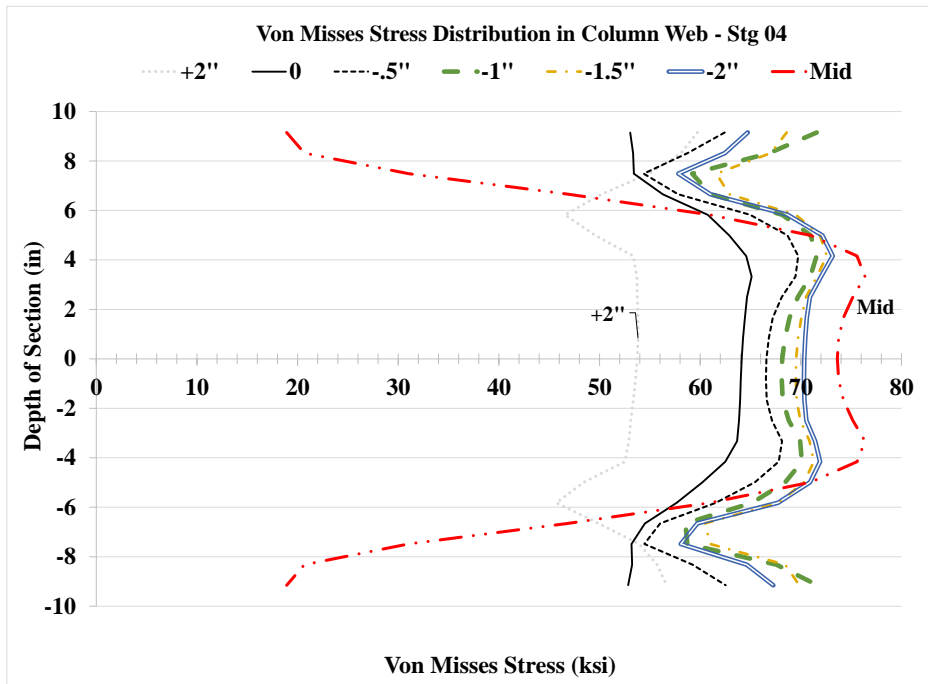
Stg. 01



Stg. 03

Figure 4.37: VMS distribution in column web at different heights Stg. 01-04 Case 1C





Stg. 04

Figure 4.37: VMS distribution in column web at different heights Stg. 01-04 Case 1C

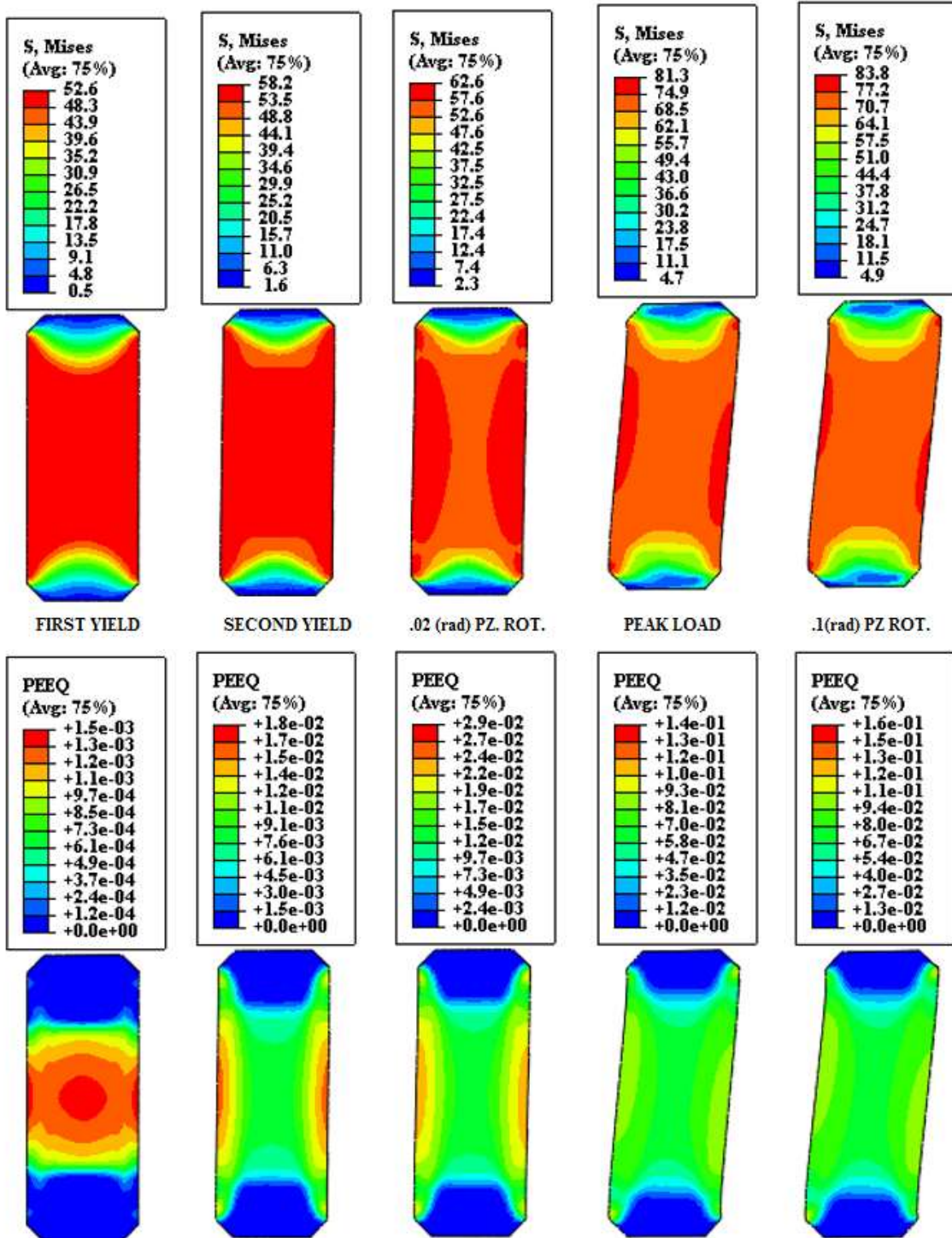


Figure 4.38: VMS and PEEQ in the DP Case 1C

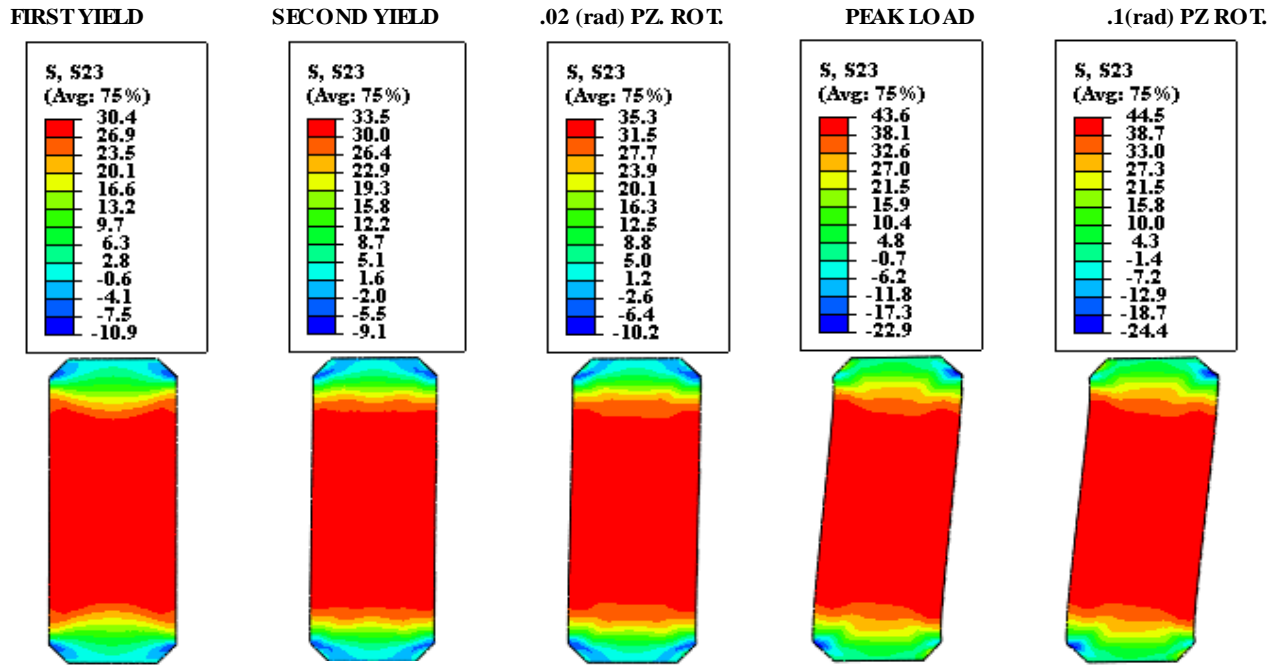


Figure 4.39: Shear stress, S23 in the DP Case 1C

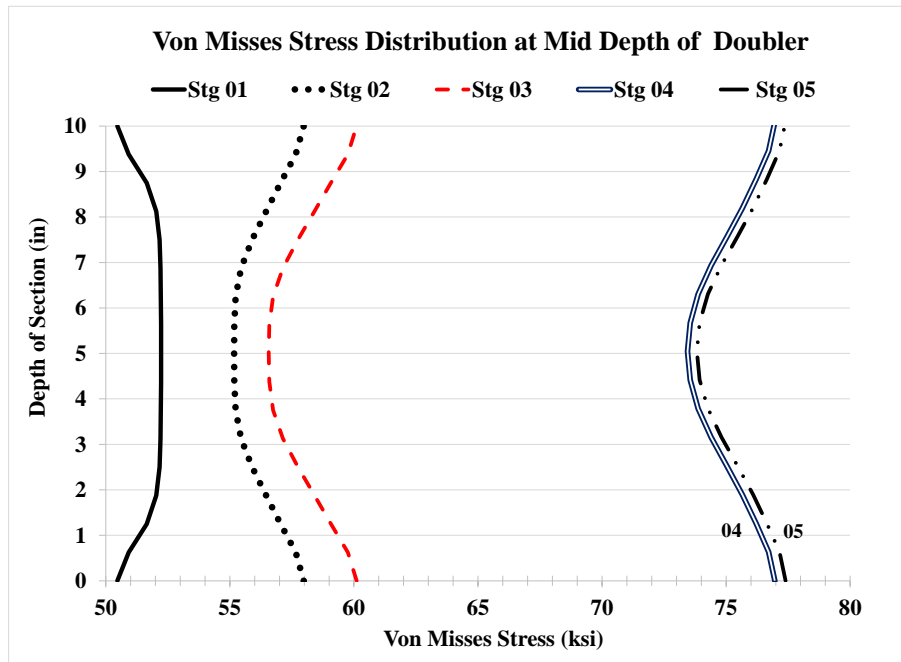


Figure 4.40: VMS distribution at mid-depth of DP Case 1C

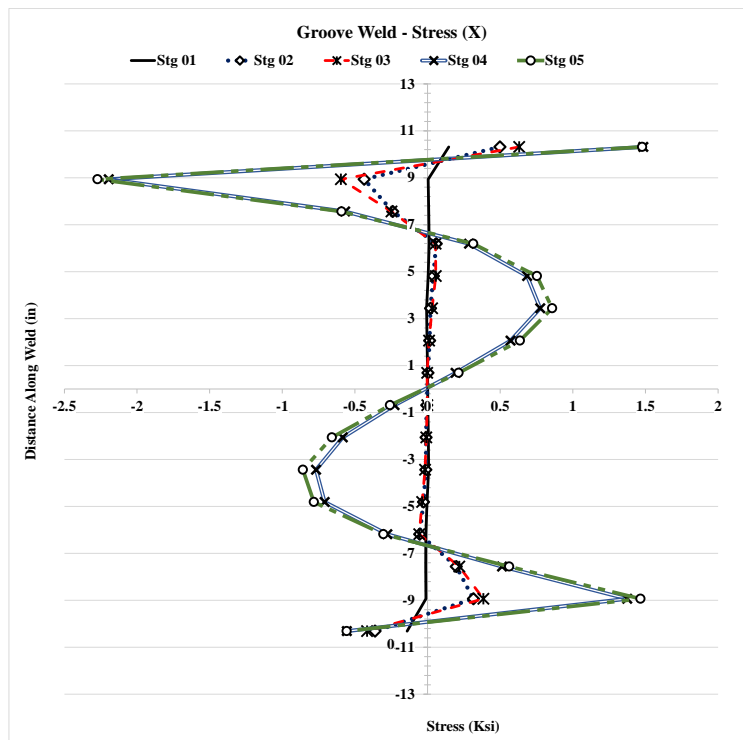
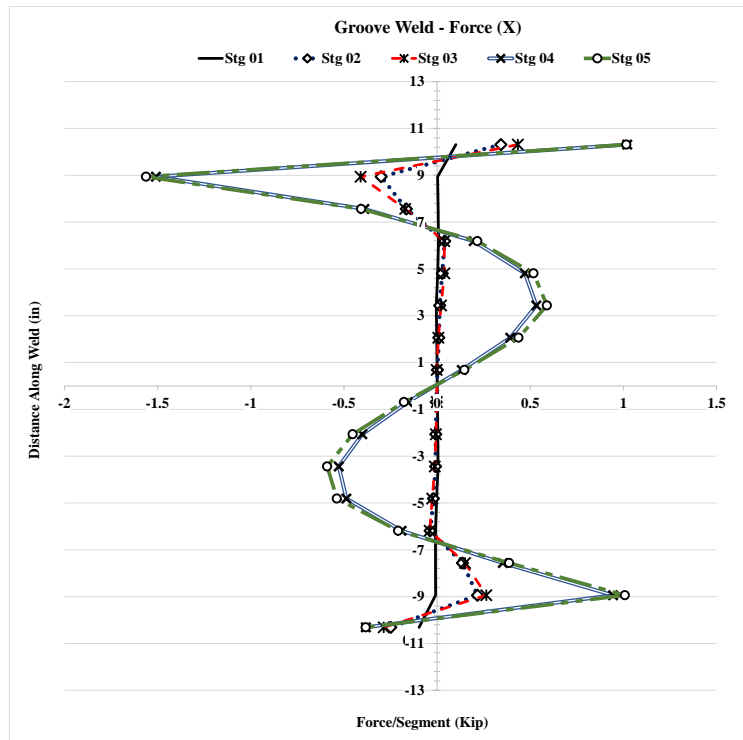


Figure 4.41: Forces and stresses in vertical weld, (X) Case 1C

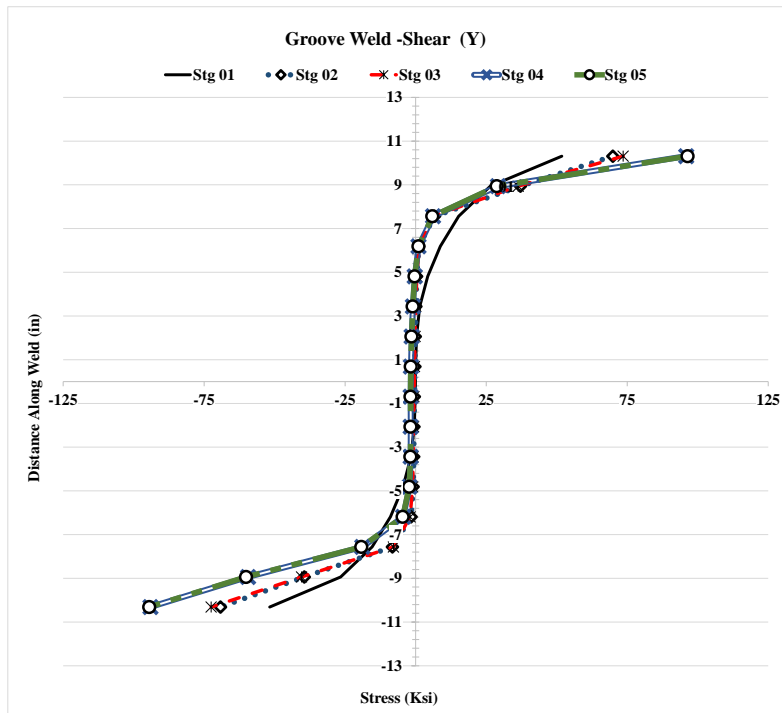
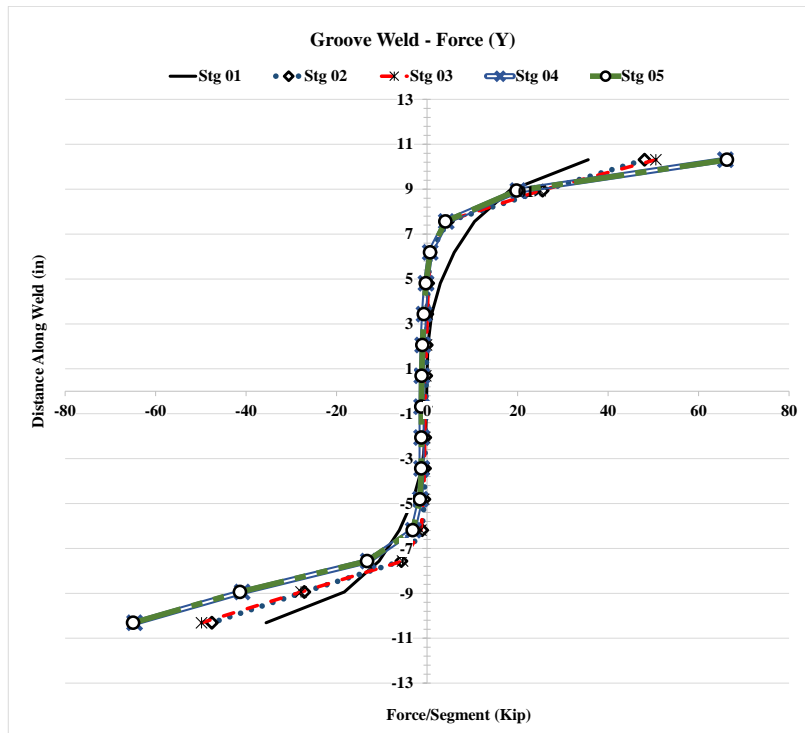


Figure 4.42: Forces and stresses in vertical weld, (Y) Case 1C

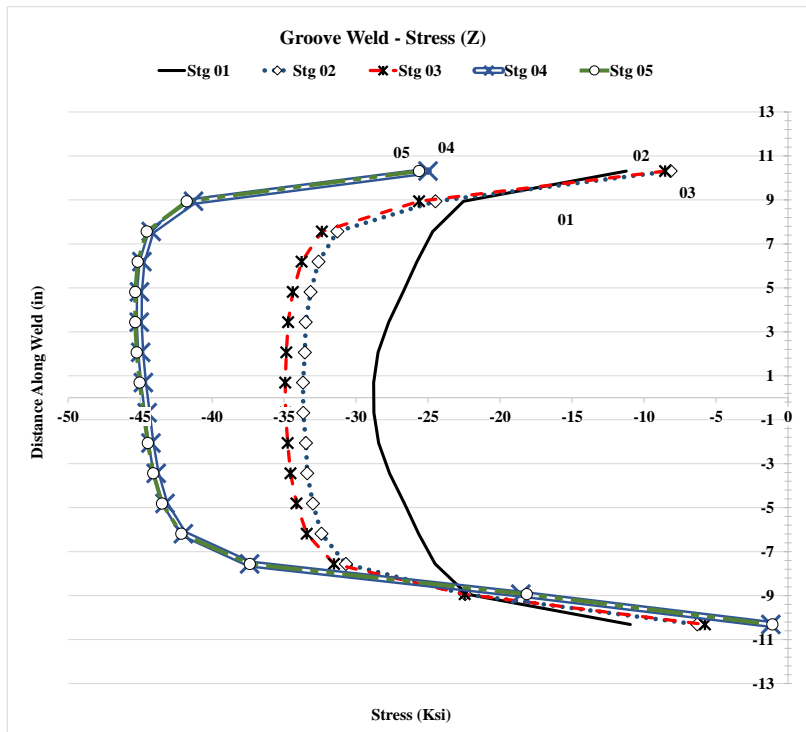
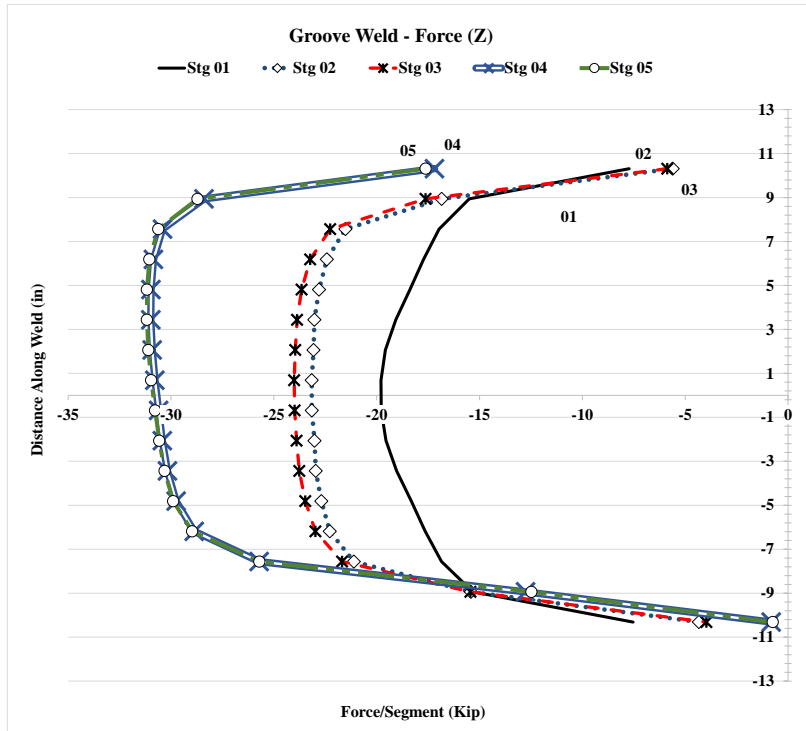


Figure 4.42: Forces and stresses in vertical weld, (Z) Case 1C

### 4.2.5 Analysis Case 1C1

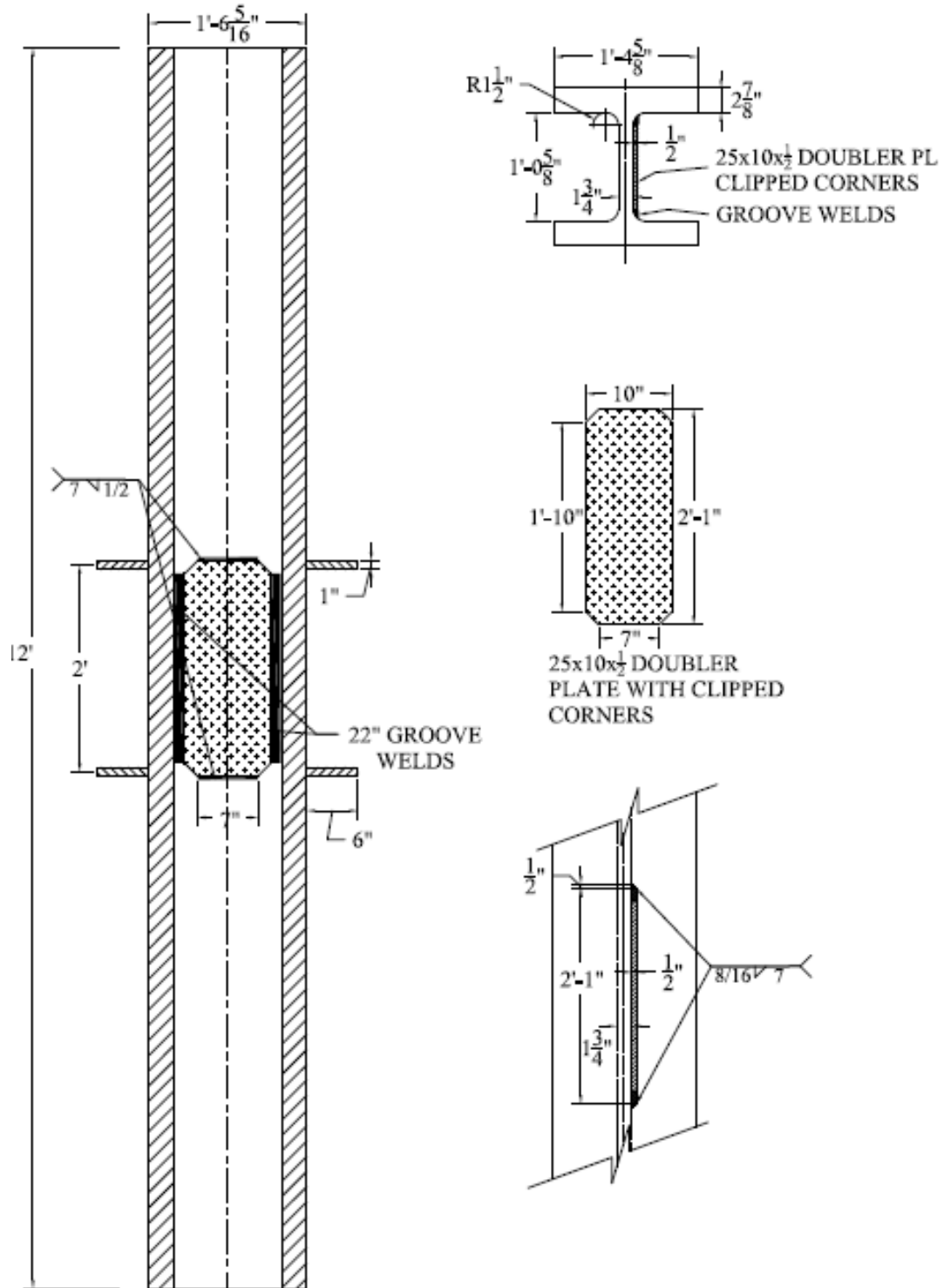


Figure 4.43: Analysis case 1C1

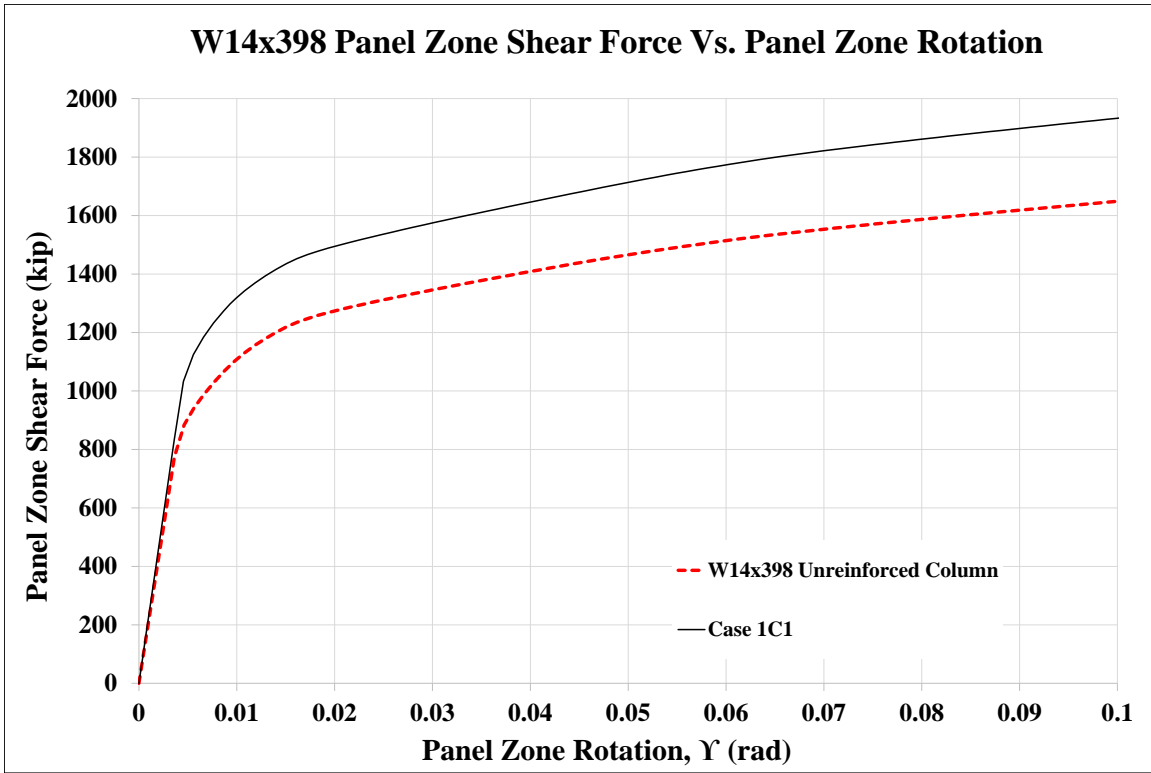


Figure 4.44: Panel zone shear vs. panel zone rotation Case 1C1

Stage	Applied Force/Loading Plate (Kip)	Panel Shear Force (Kip)	% Higher than unreinforced Col.	Panel Zone Rotation (rad)
1	620	1,033	117%	0.005
2	880	1,467	118%	0.017
3	910	1,517	119%	0.023
4	1,142	1,903		0.091
5	1,162	1,936	117%	0.101

Table 4.7: Panel zone shear and force on loading plate Case 1C1



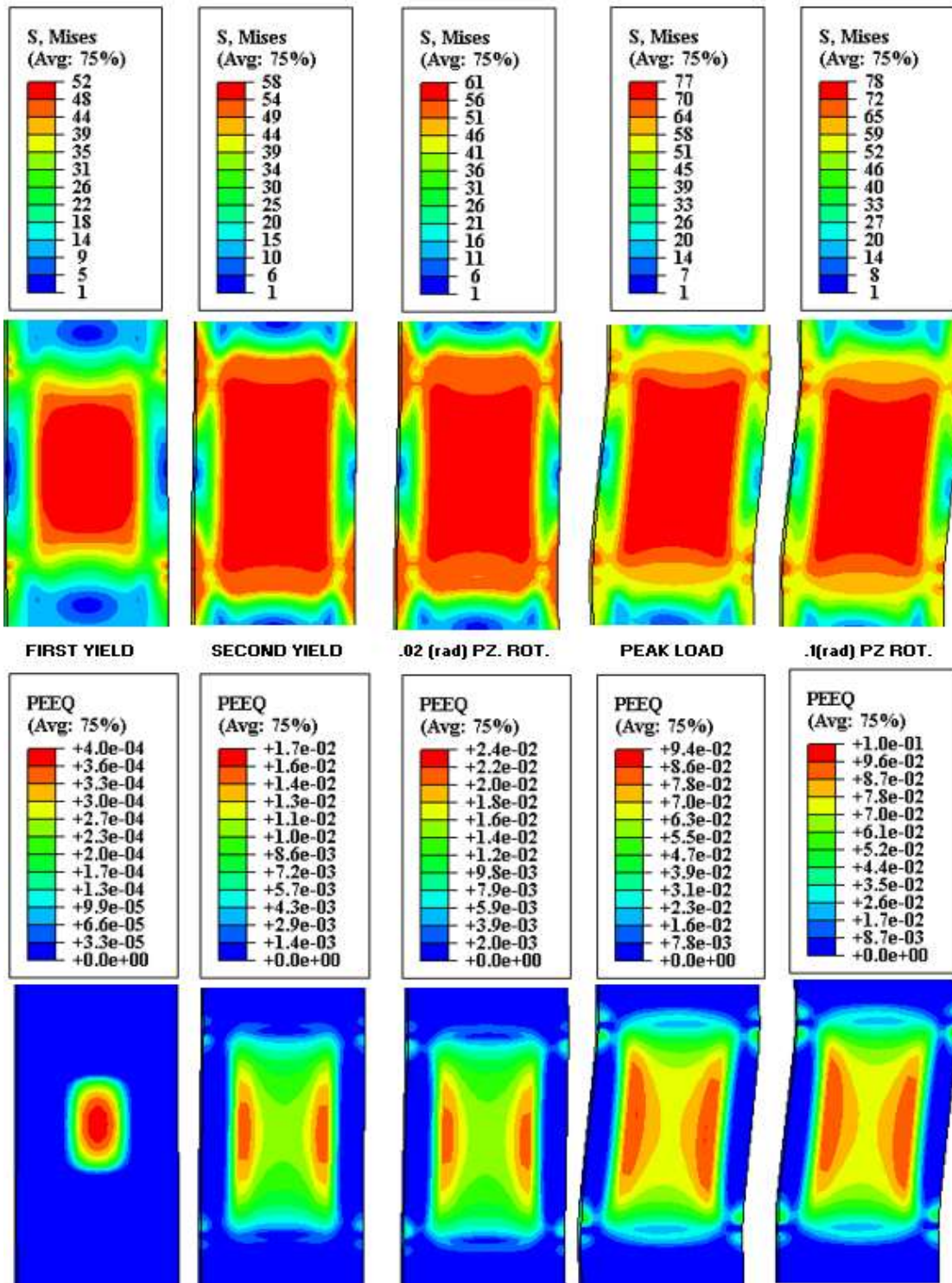


Figure 4.45: VMS and PEEQ in the column Case 1C1

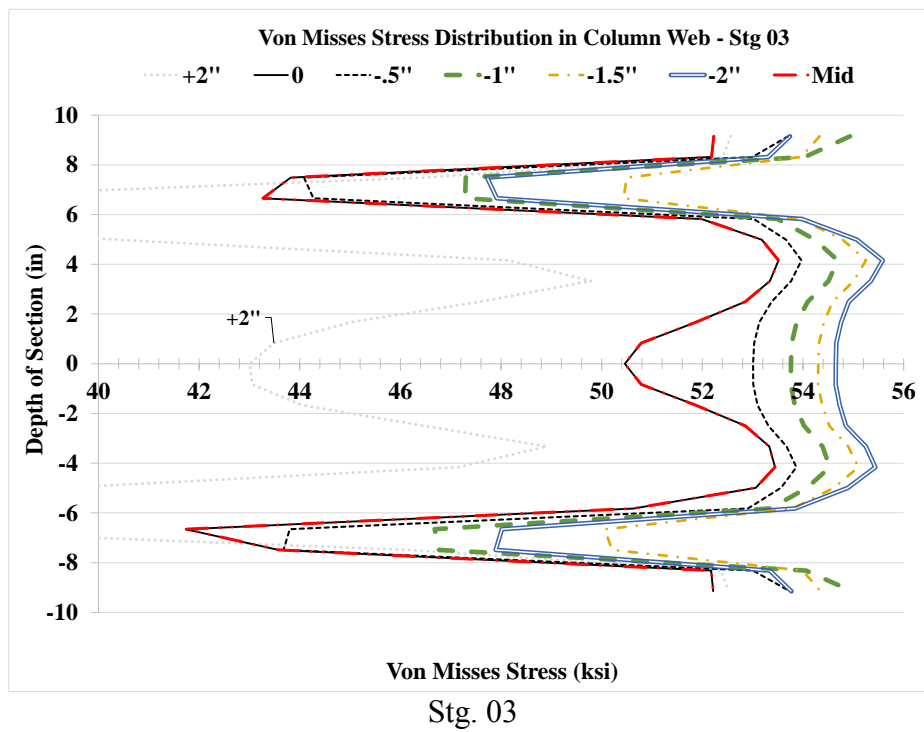
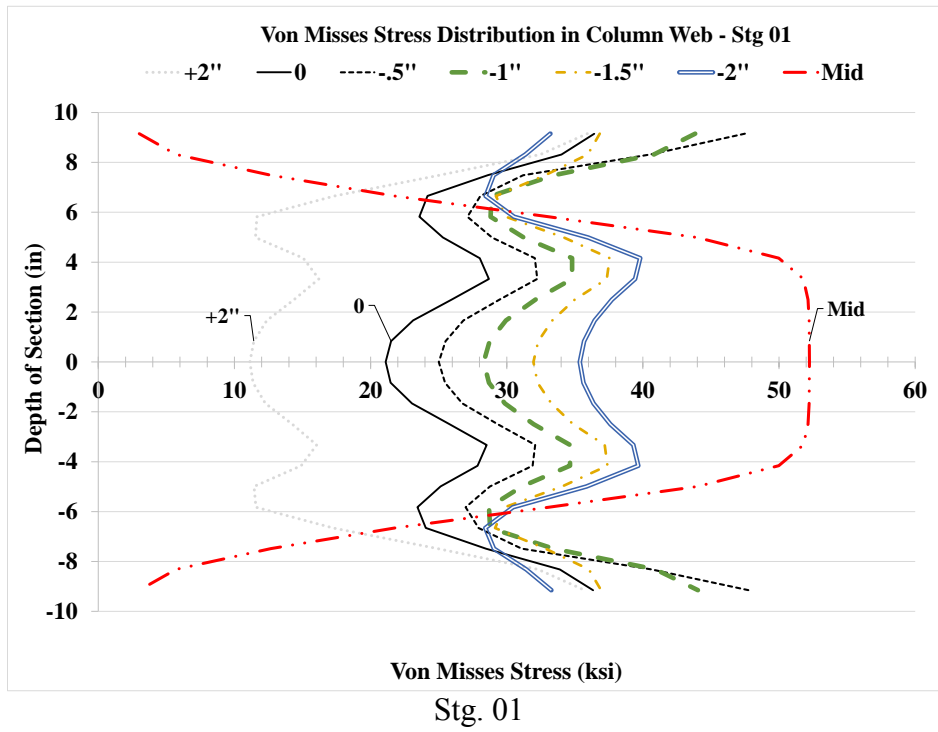


Figure 4.46: VMS distribution in column web at different heights Stg. 01-04 Case 1C1

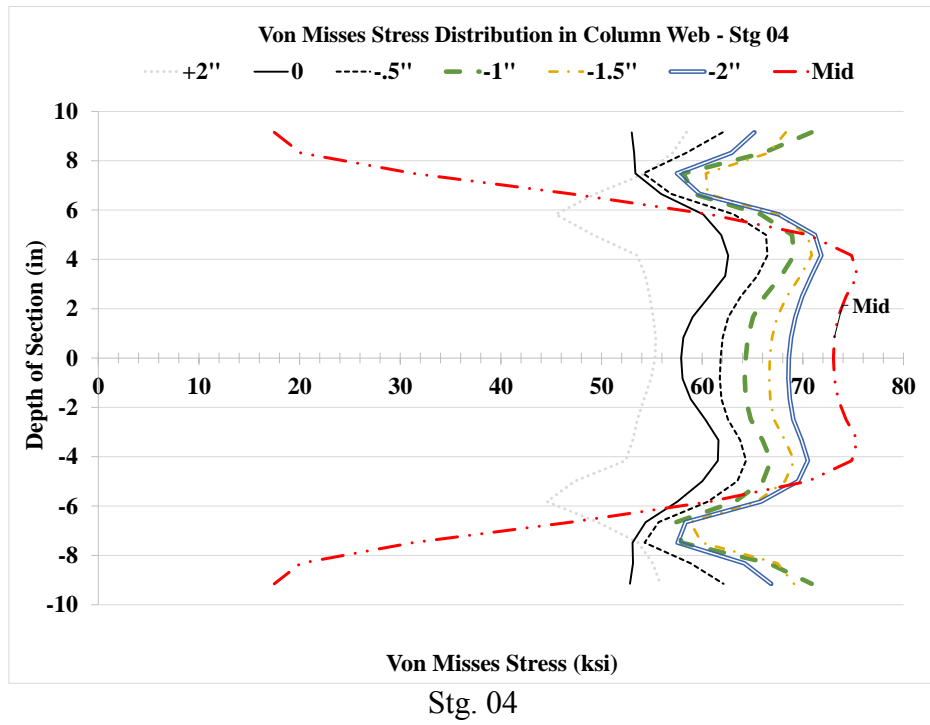


Figure 4.46: VMS distribution in column web at different heights Stg. 01-04 Case 1C1

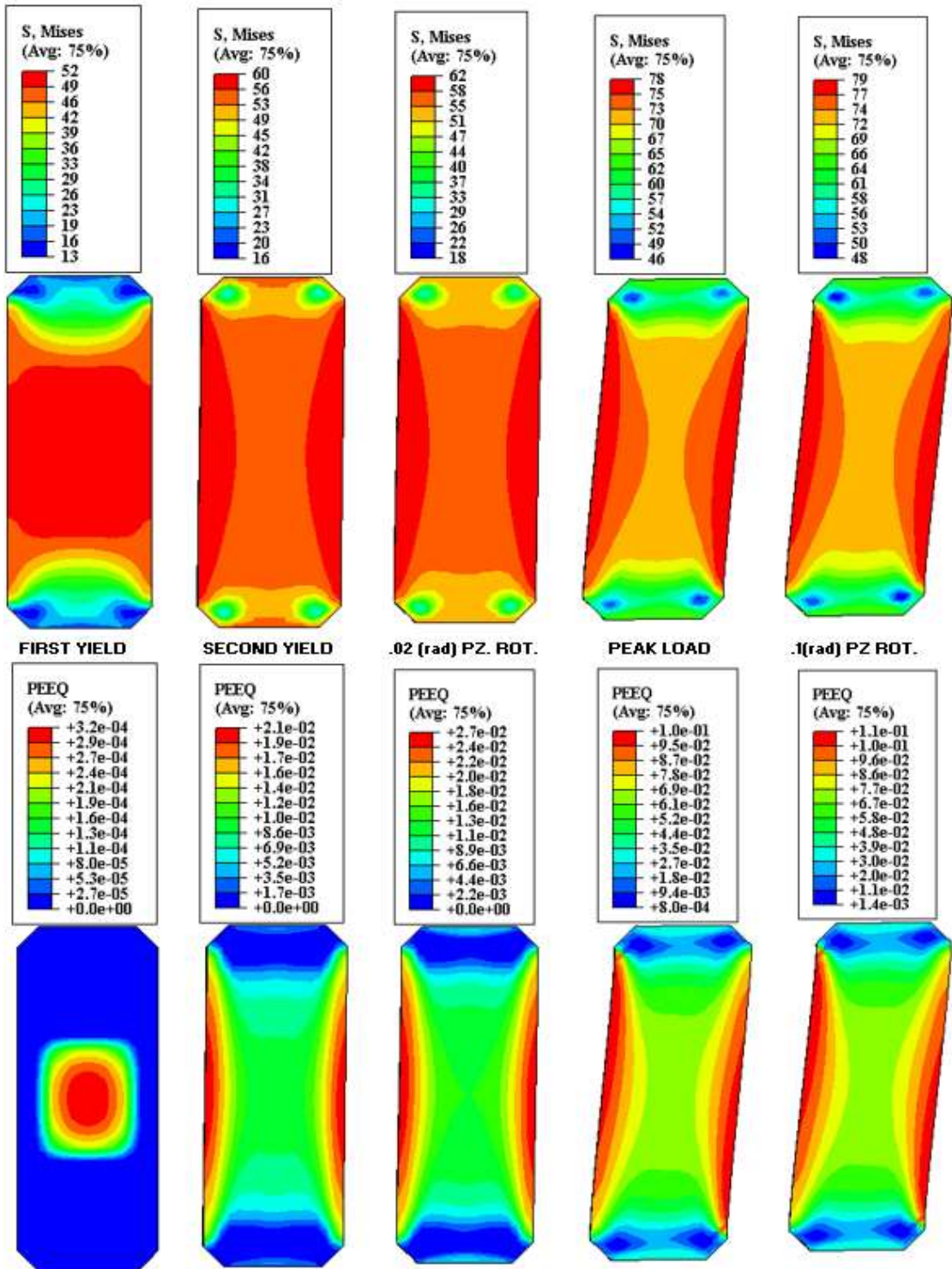


Figure 4.47: VMS and PEEQ in the DP Case 1C1

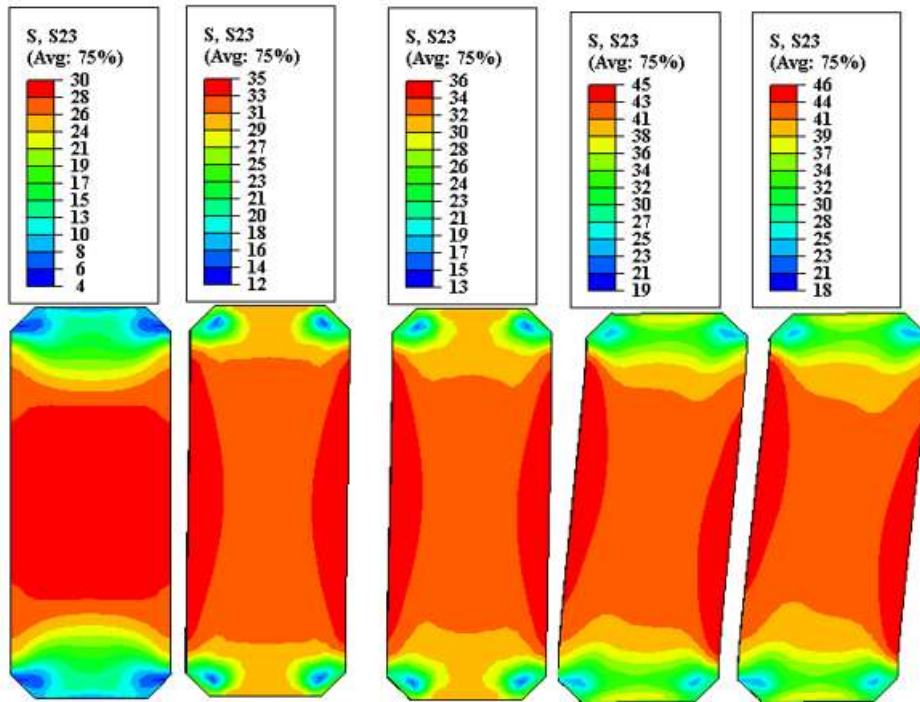


Figure 4.48: Shear stress, S23 in the DP Case 1C1

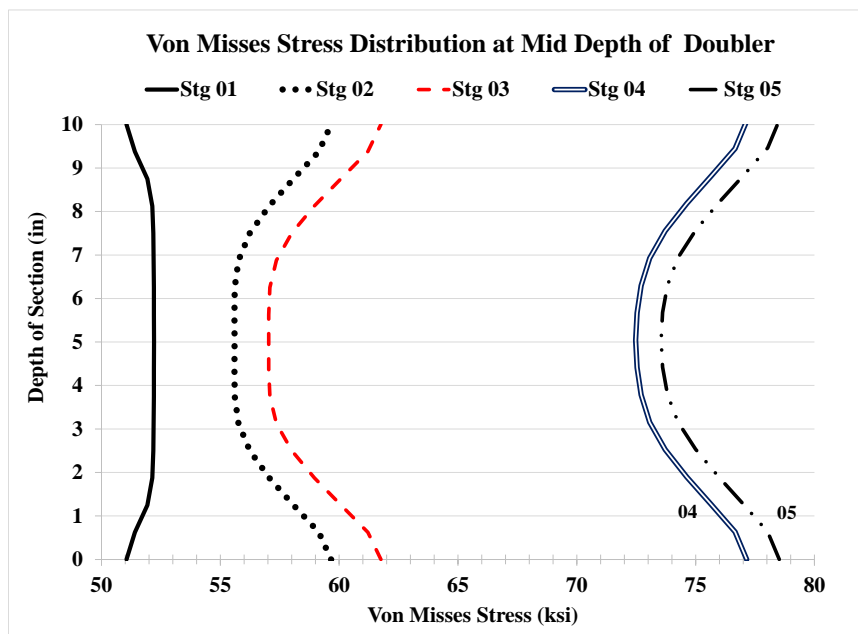


Figure 4.49: VMS distribution at mid-depth of DP Case 1C1

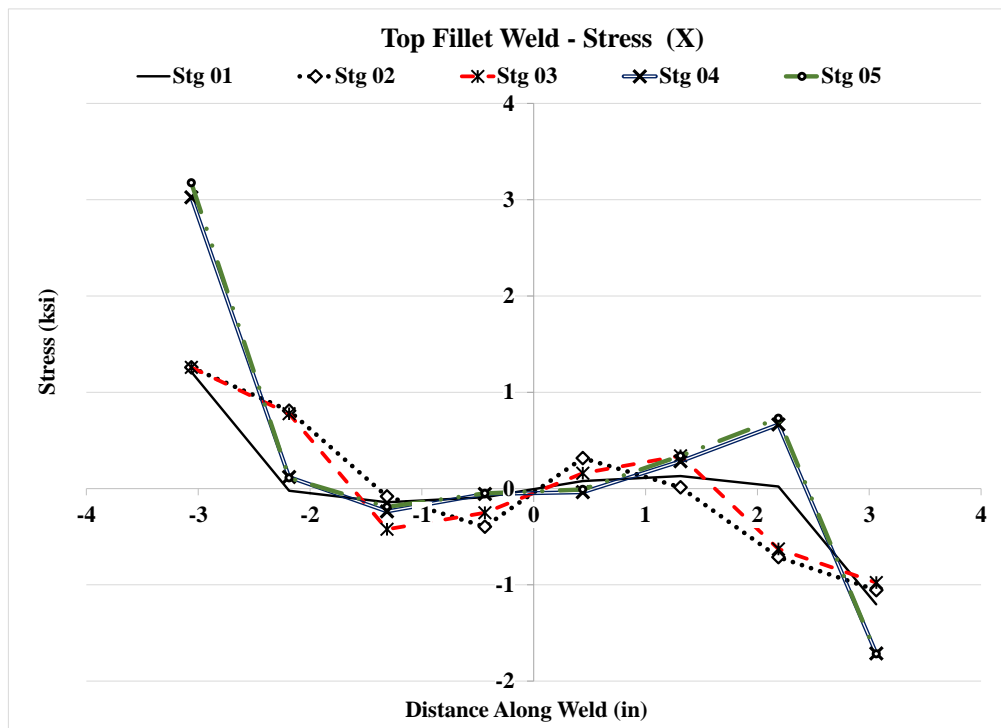
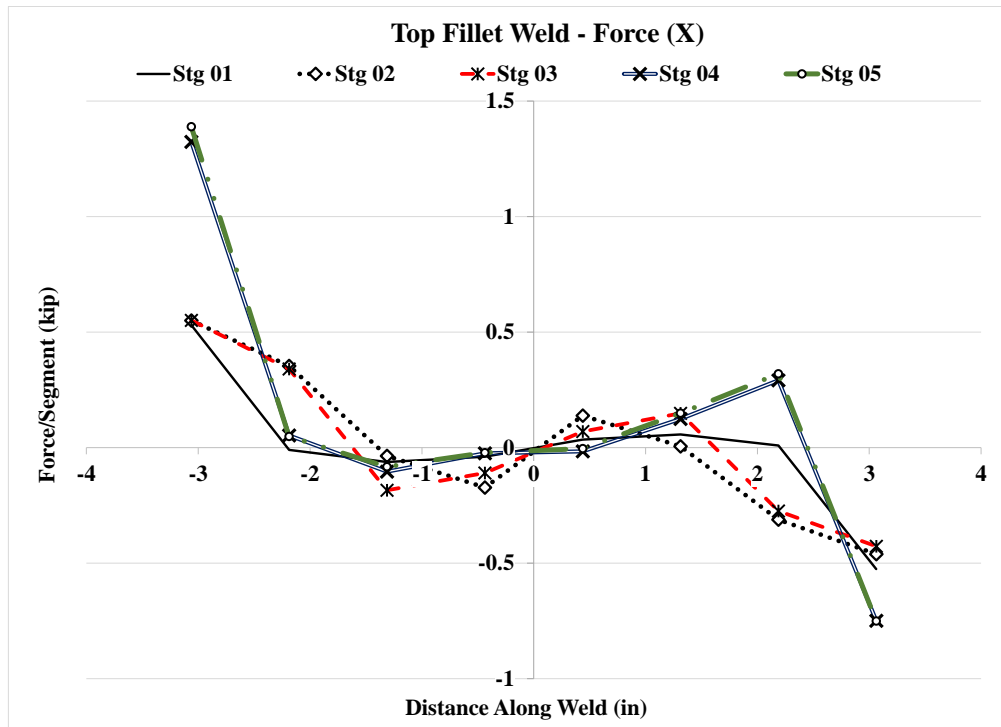


Figure 4.50: Forces and stresses in horizontal weld, (X) Case 1C1

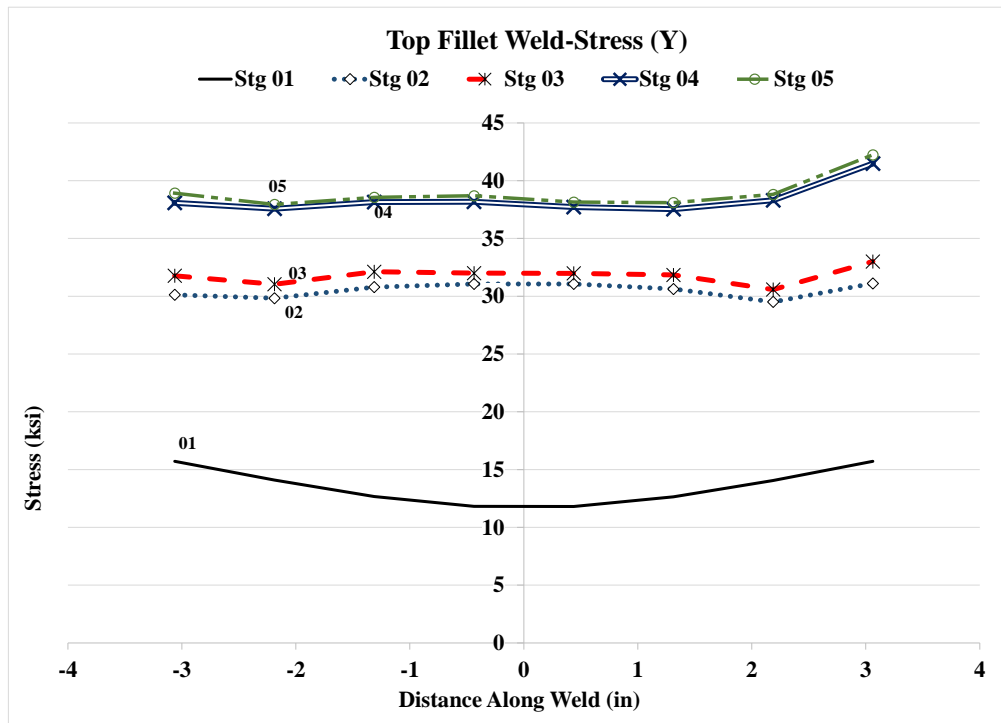
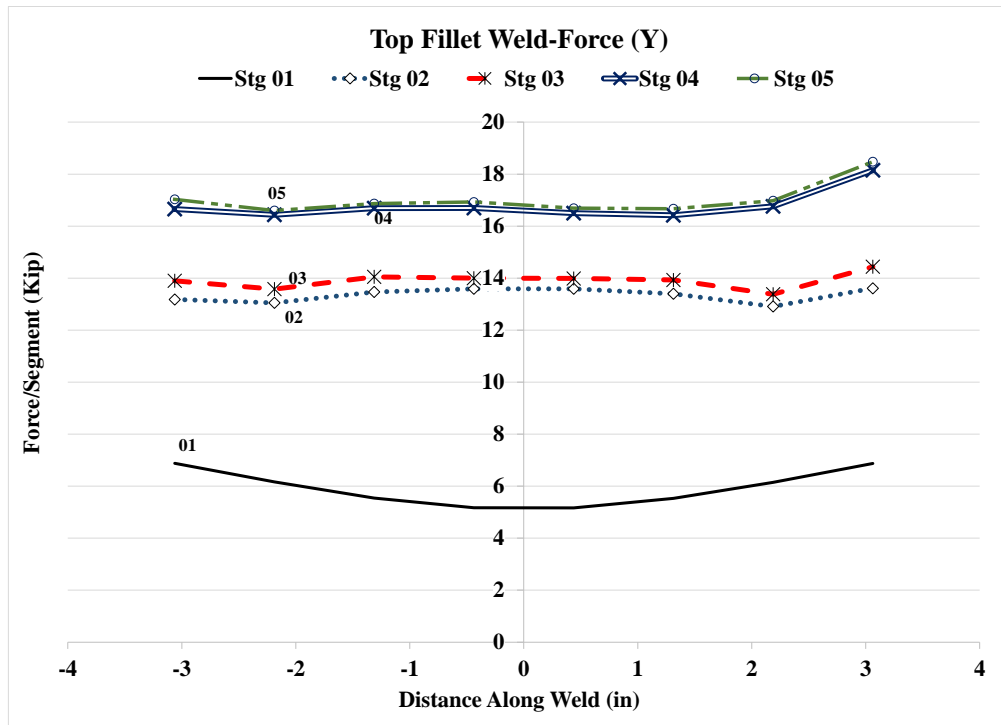


Figure 4.51: Forces and stresses in horizontal weld, (Y) Case 1C1



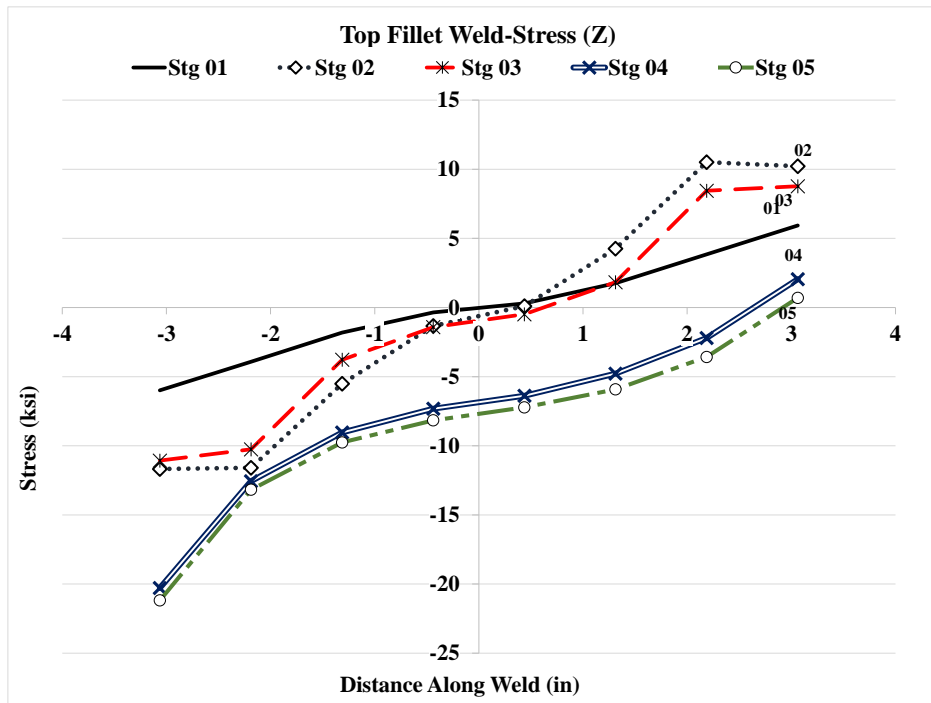
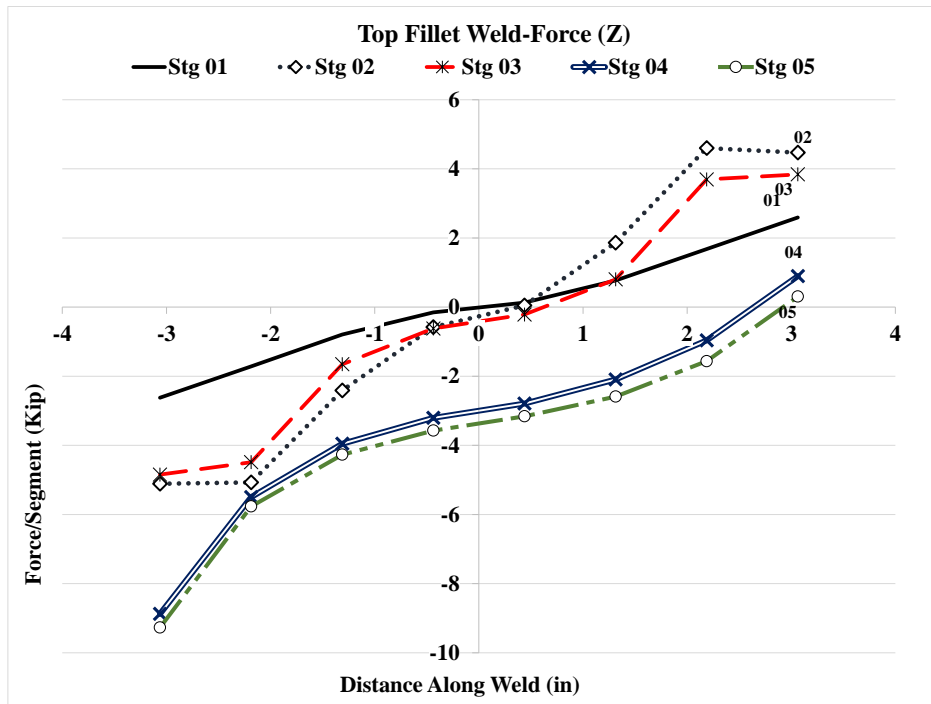


Figure 4.52: Forces and stresses in horizontal weld, (Z) Case 1C1



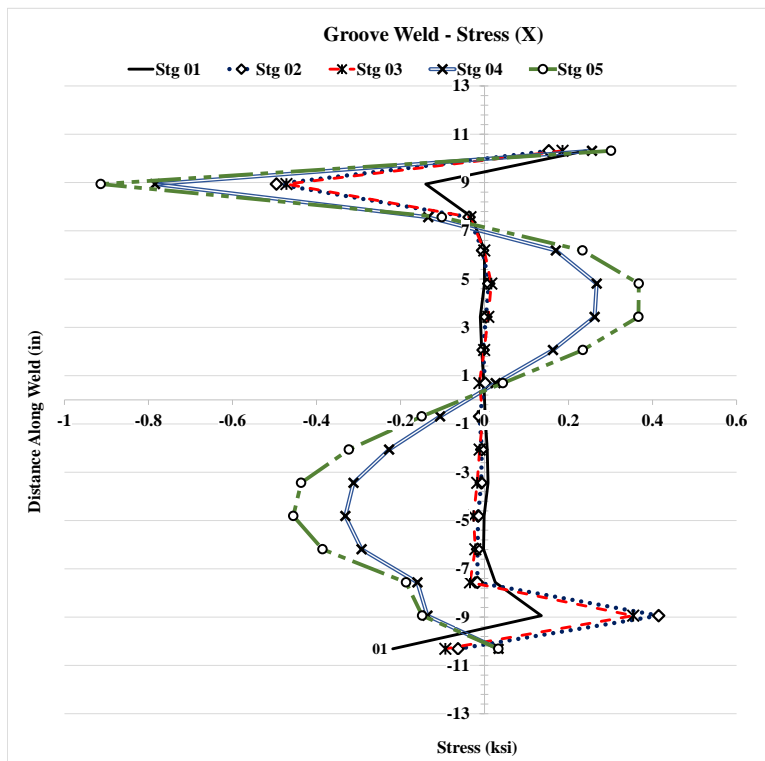
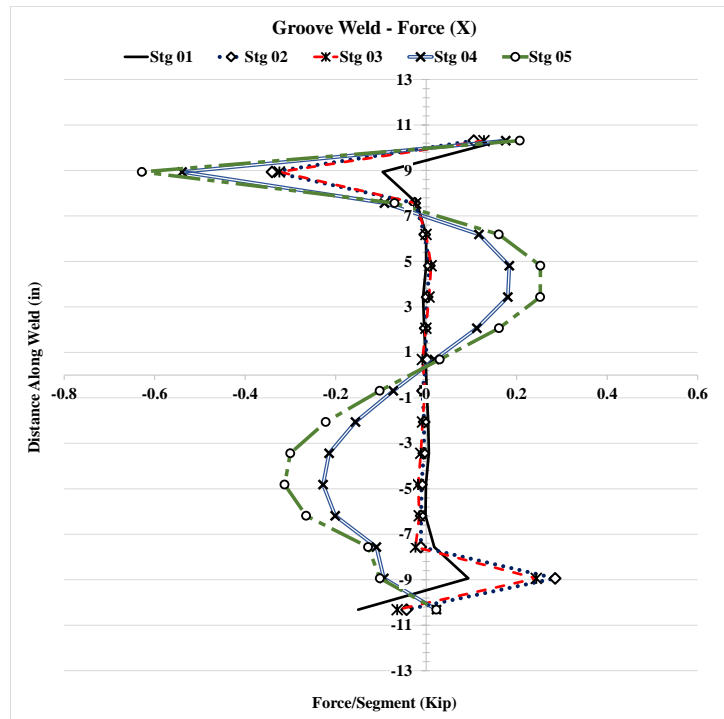


Figure 4.53: Forces and stresses in vertical weld, (X) Case 1C1

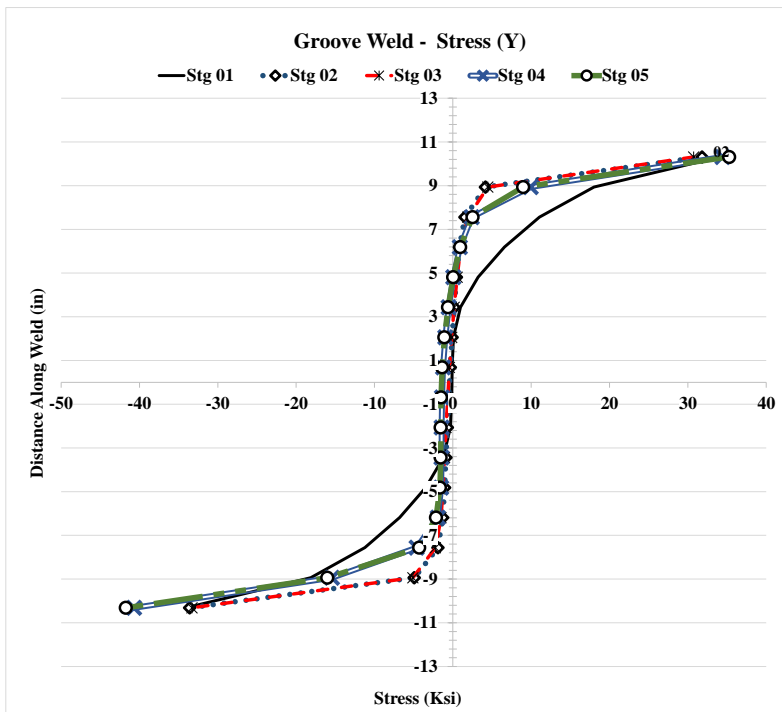
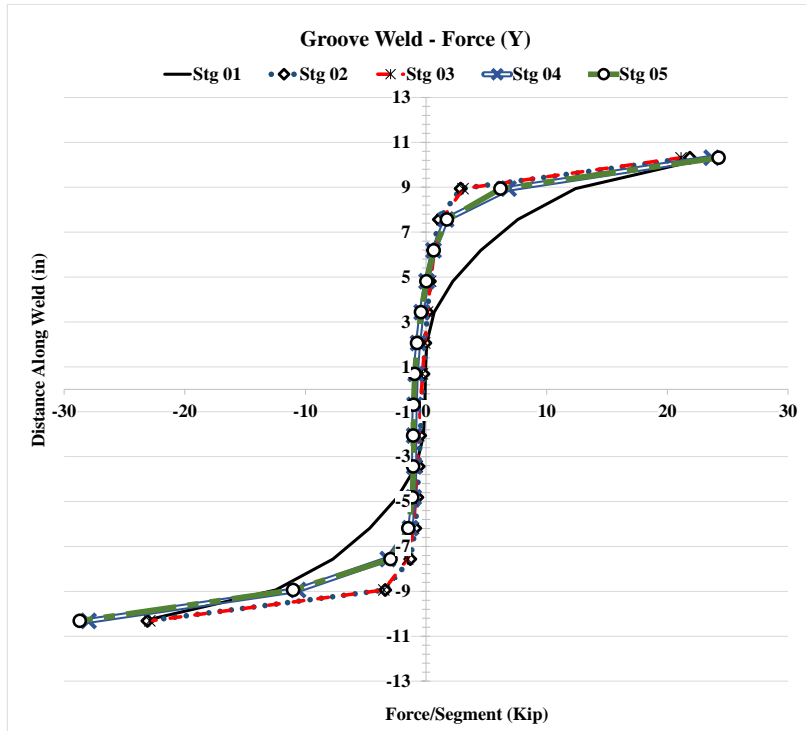


Figure 4.54: Forces and stresses in vertical weld, (Y) Case 1C1

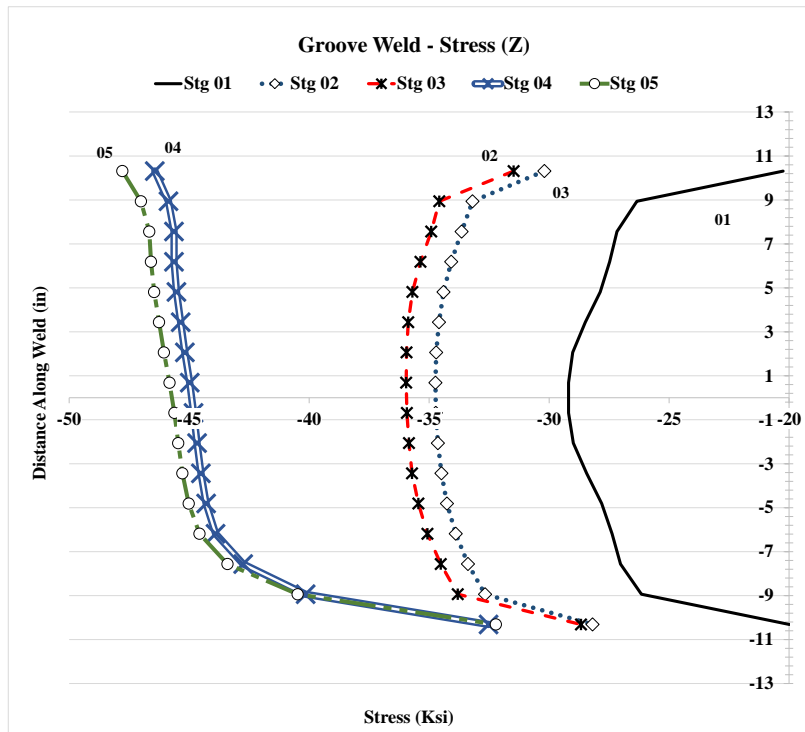
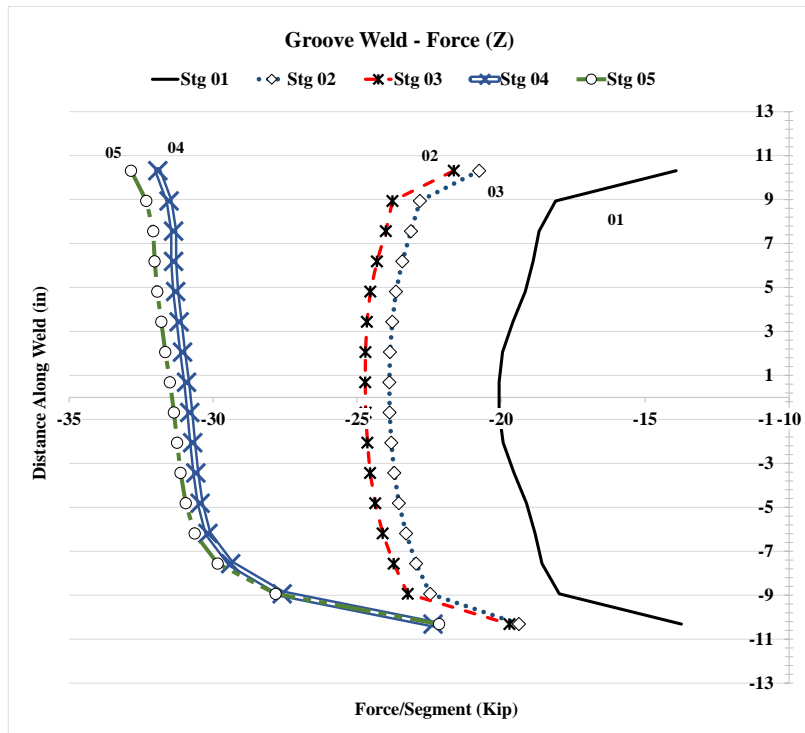


Figure 4.55: Forces and stresses in vertical weld, (Z) Case 1C1

### 4.2.6 Analysis Case 2A1

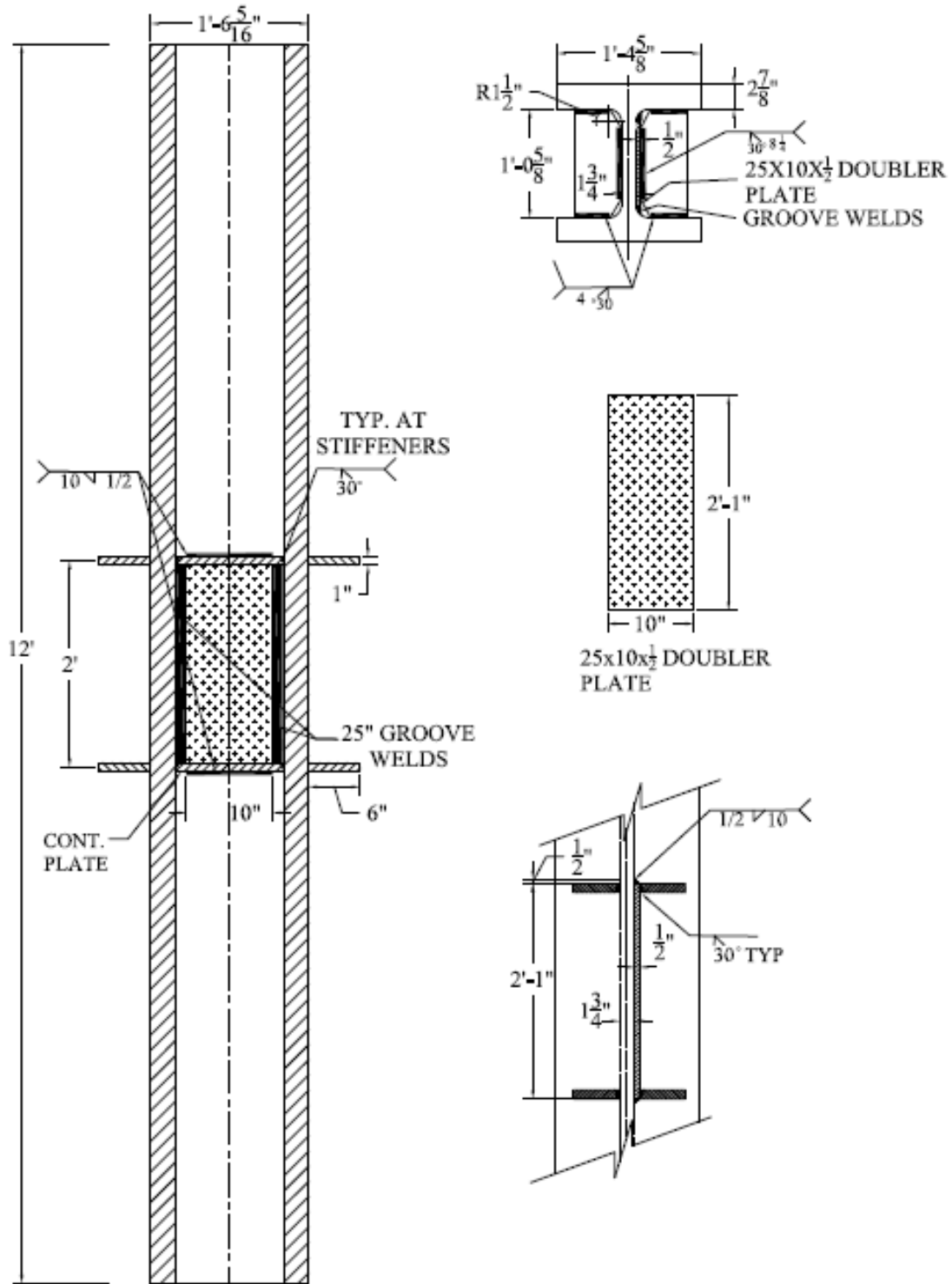


Figure 4.56: Analysis case 2A1

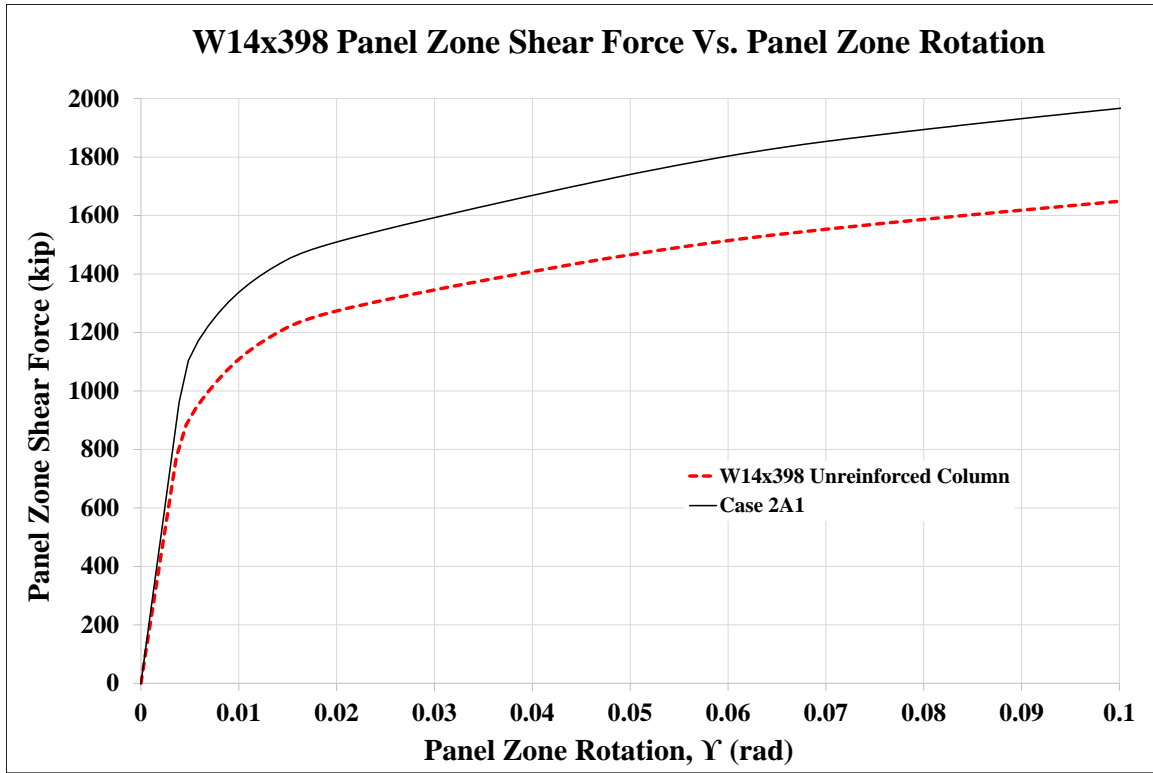


Figure 4.57: Panel zone shear vs. panel zone rotation Case 2A1

Stage	Applied Force/Loading Plate (Kip)	Panel Shear Force (Kip)	% Higher than unreinforced Col.	Panel Zone Rotation (rad)
1	662	1,104	125%	0.005
2	882	1,470	118%	0.016
3	909	1,515	119%	0.021
4	1,140	1,901		0.082
5	1,182	1,970	119%	0.101

Table 4.8: Panel zone shear and force on loading plate Case 2A1

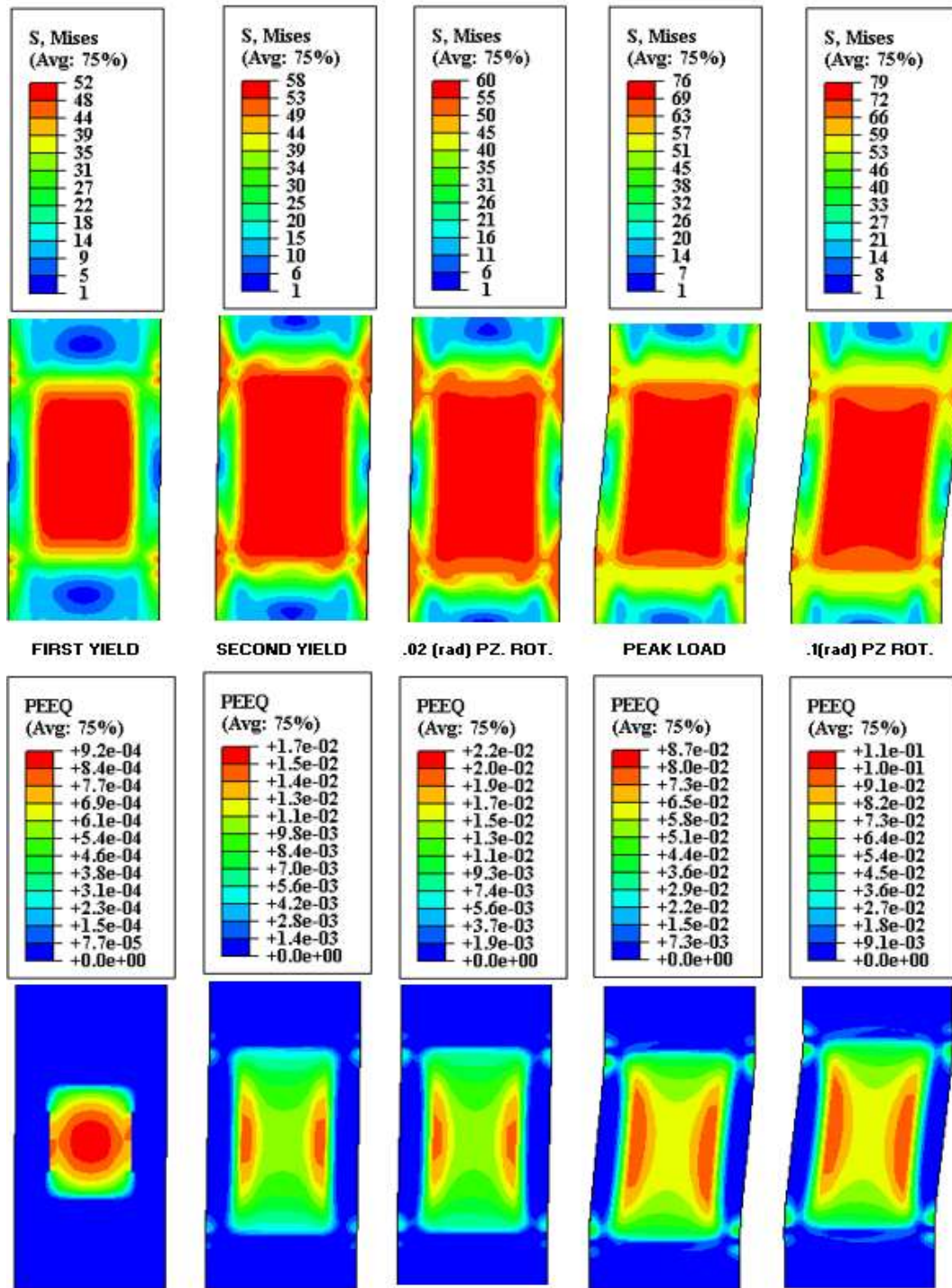


Figure 4.58: VMS and PEEQ in the column Case 2A1

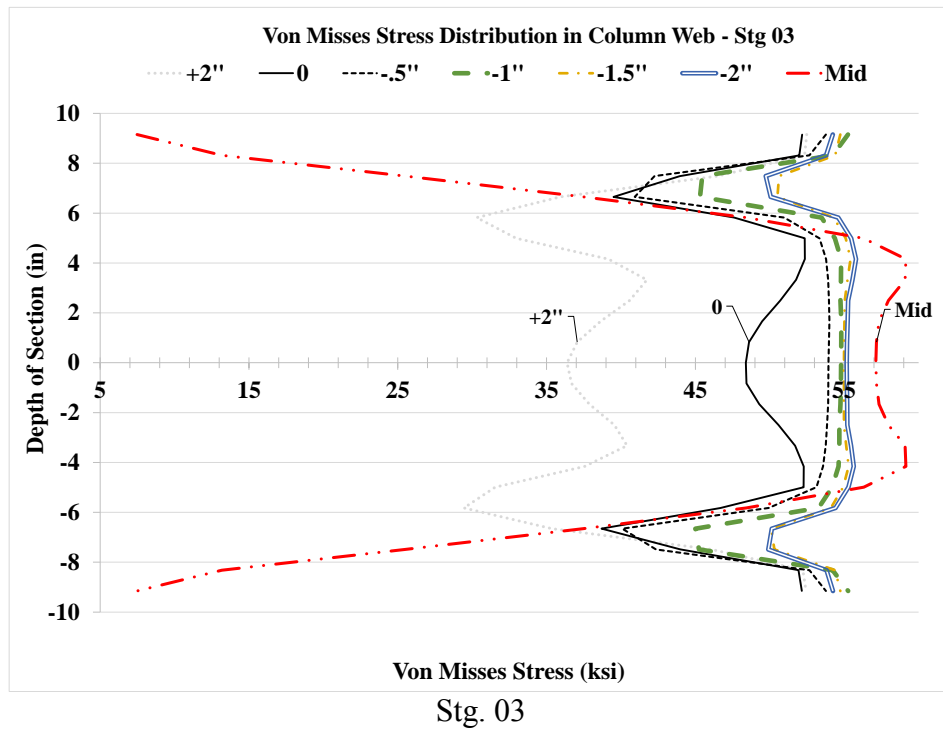
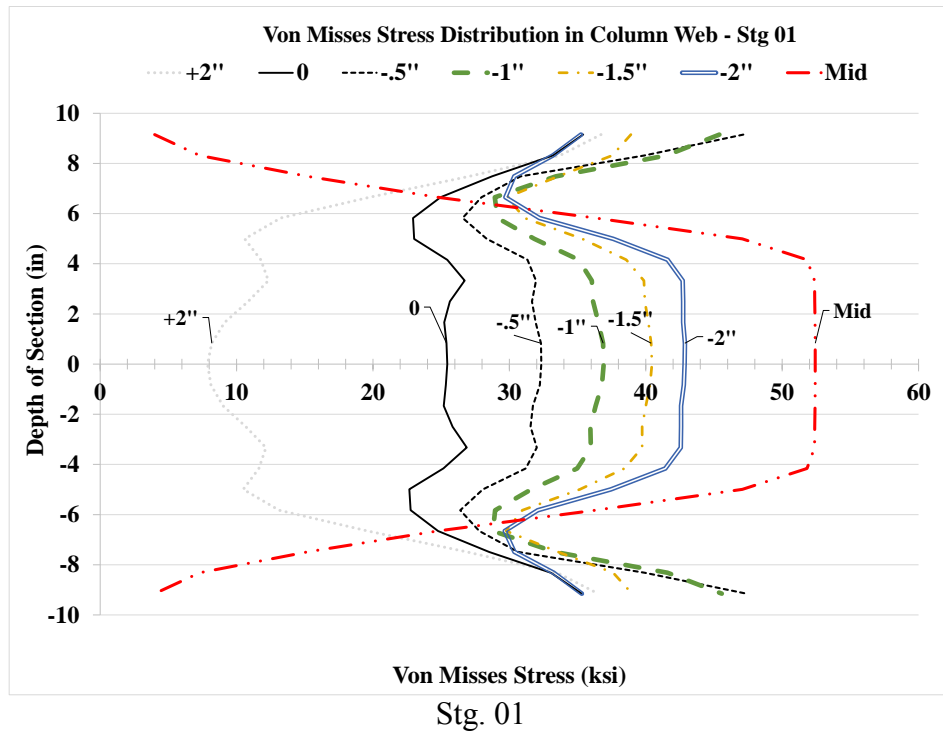


Figure 4.59: VMS distribution in column web at different heights Stg. 01-04 Case 2A1

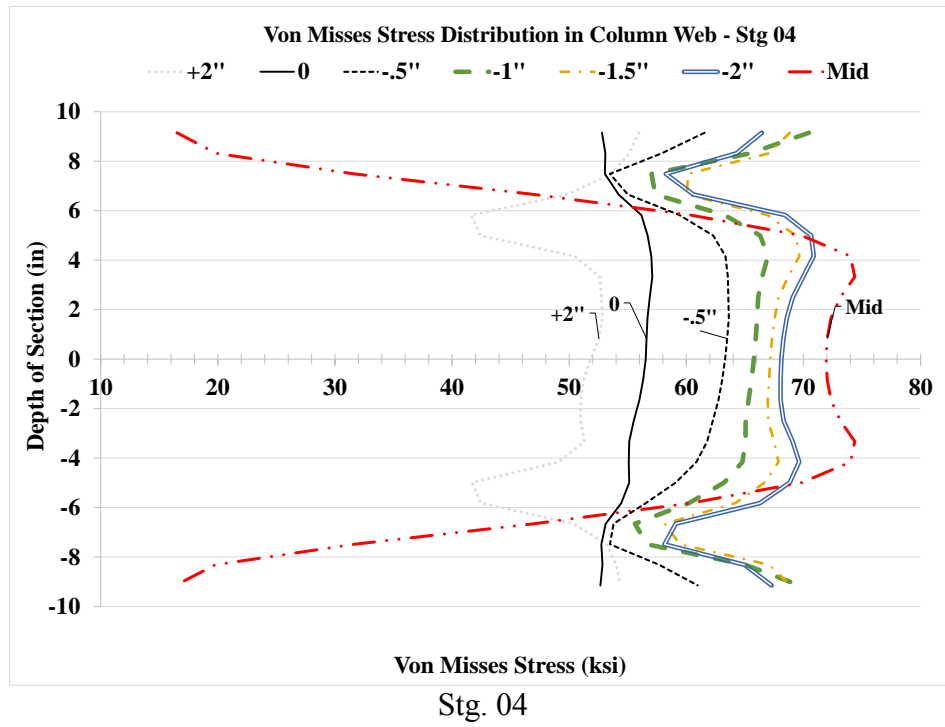


Figure 4.59: VMS distribution in column web at different heights Stg. 01-04 Case 2A1



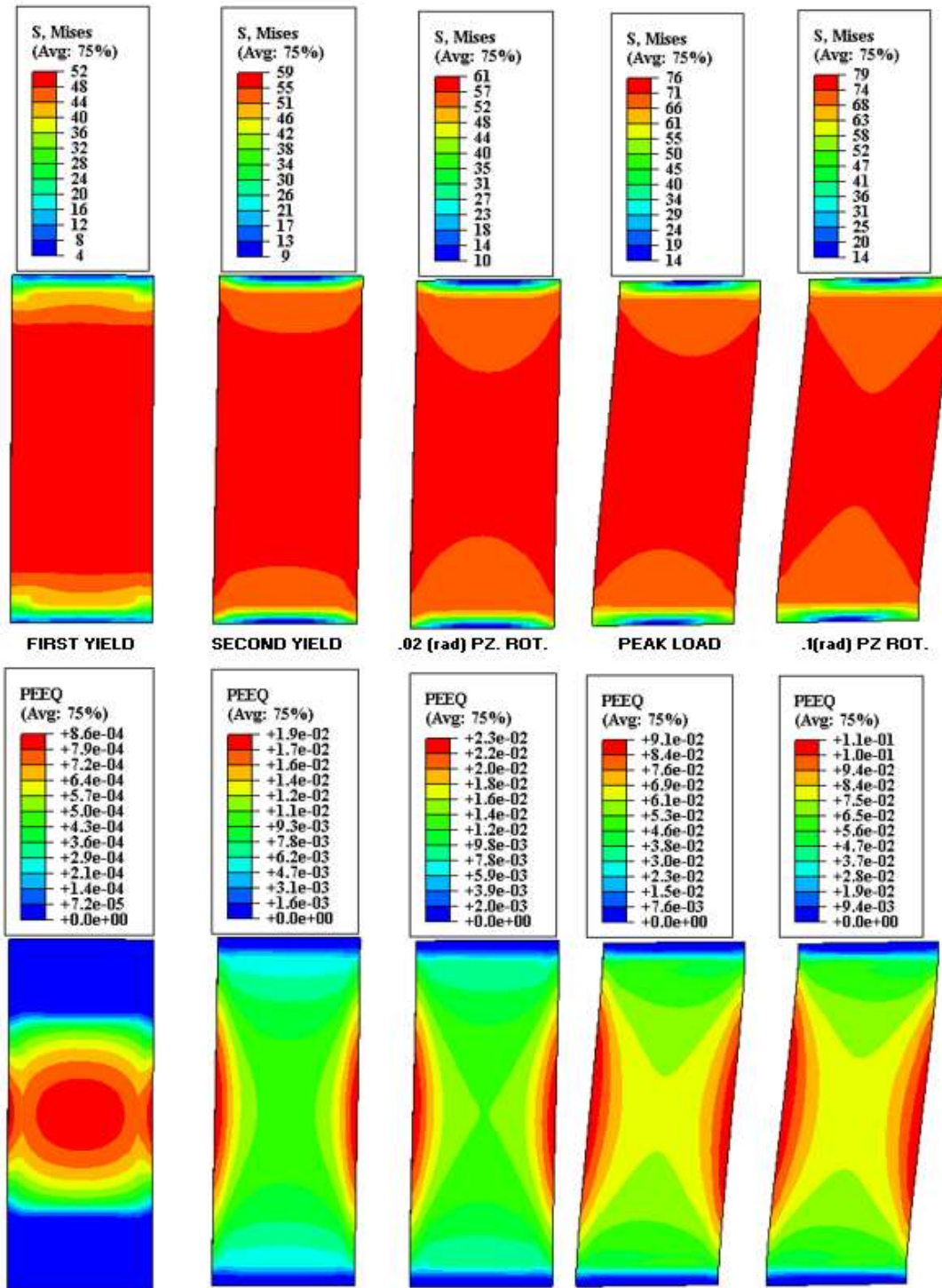


Figure 4.60: VMS and PEEQ in the DP Case 2A1

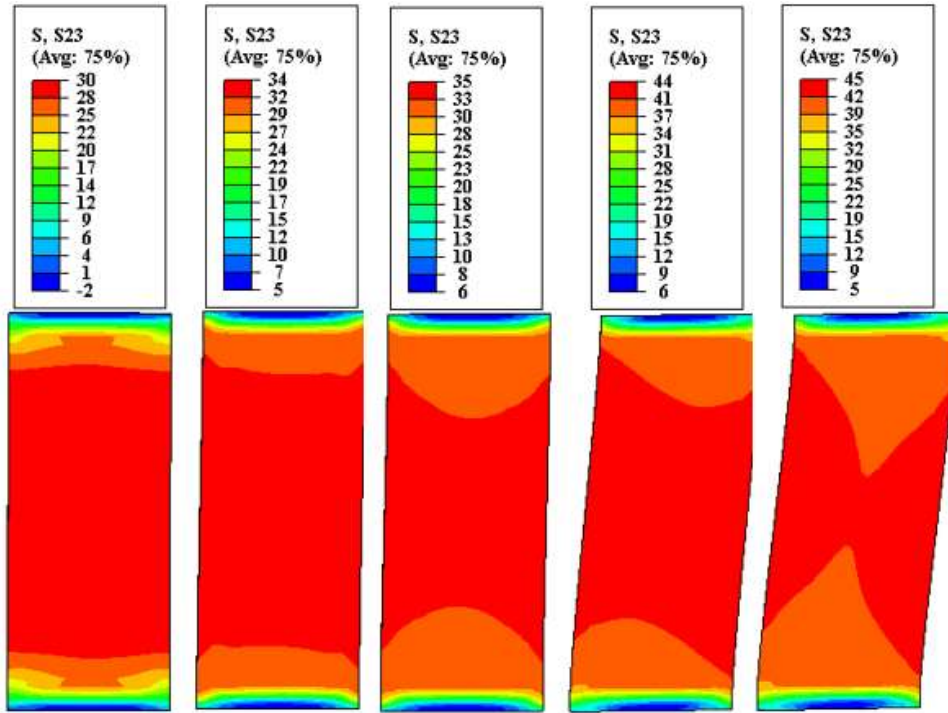


Figure 4.61: Shear stress, S23 in the DP Case 2A1

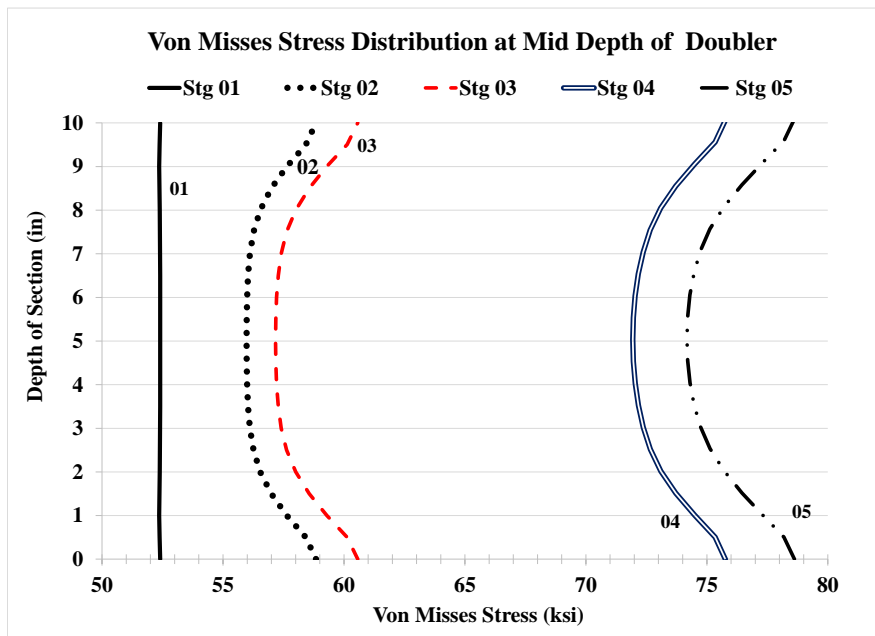


Figure 4.62: VMS distribution at mid-depth of DP Case 2A1

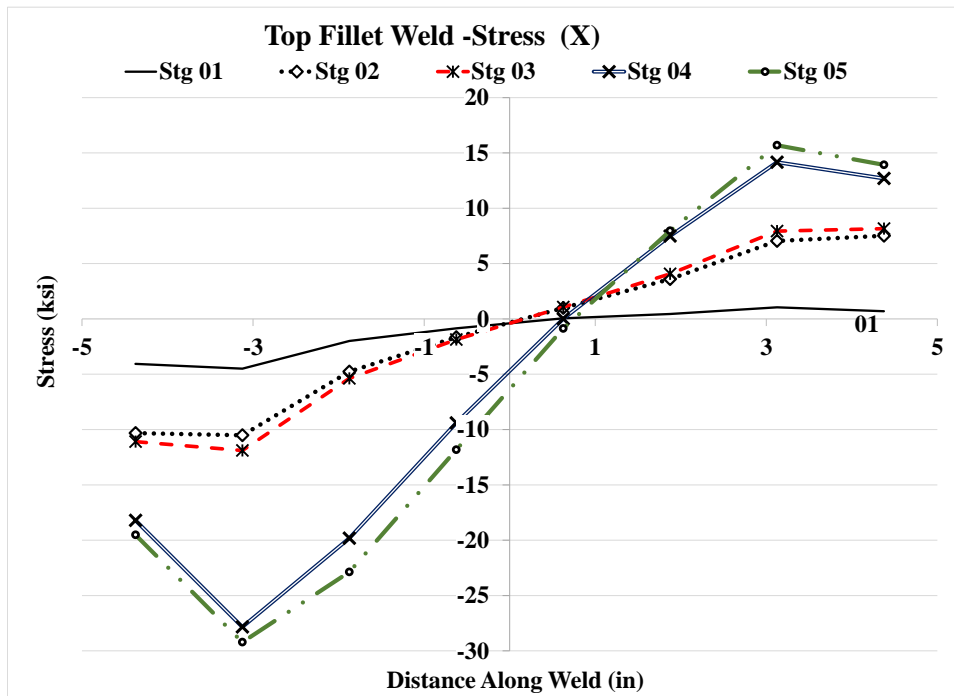
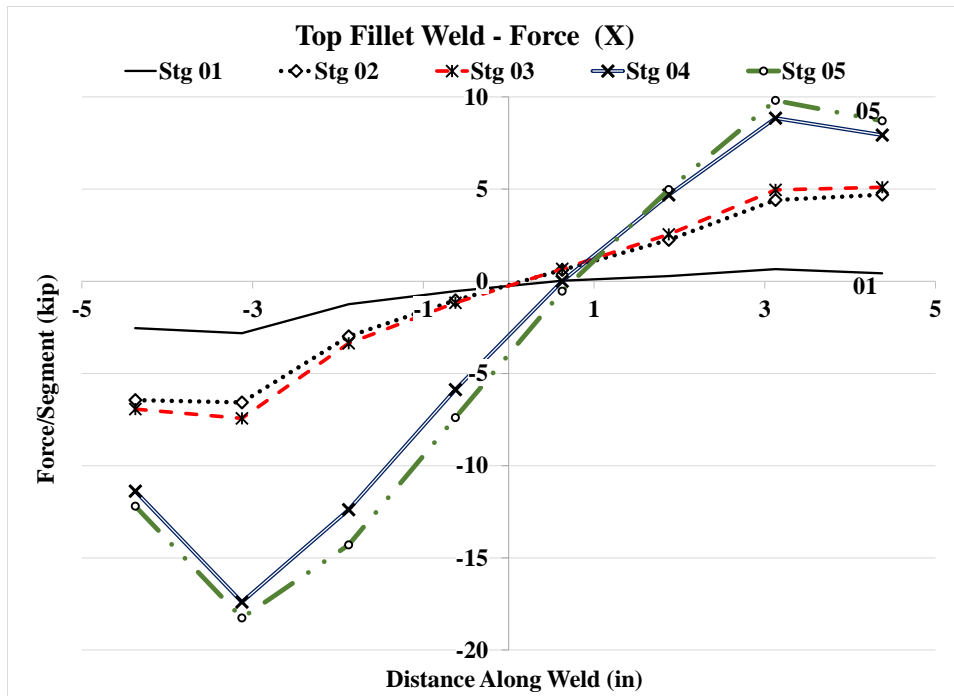


Figure 4.63: Forces and stresses in horizontal weld, (X) Case 2A1

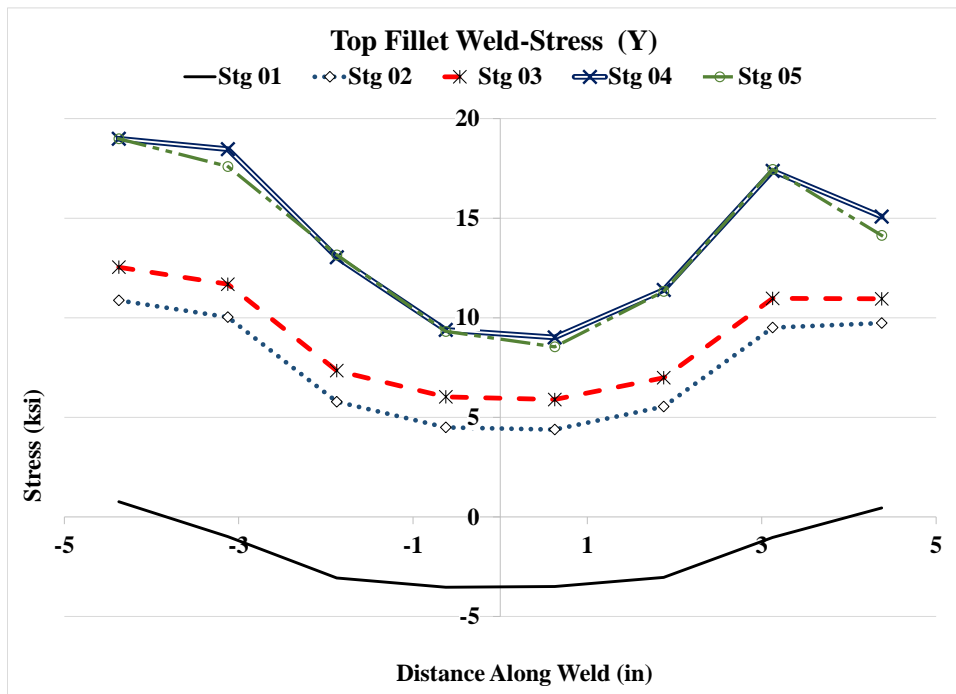
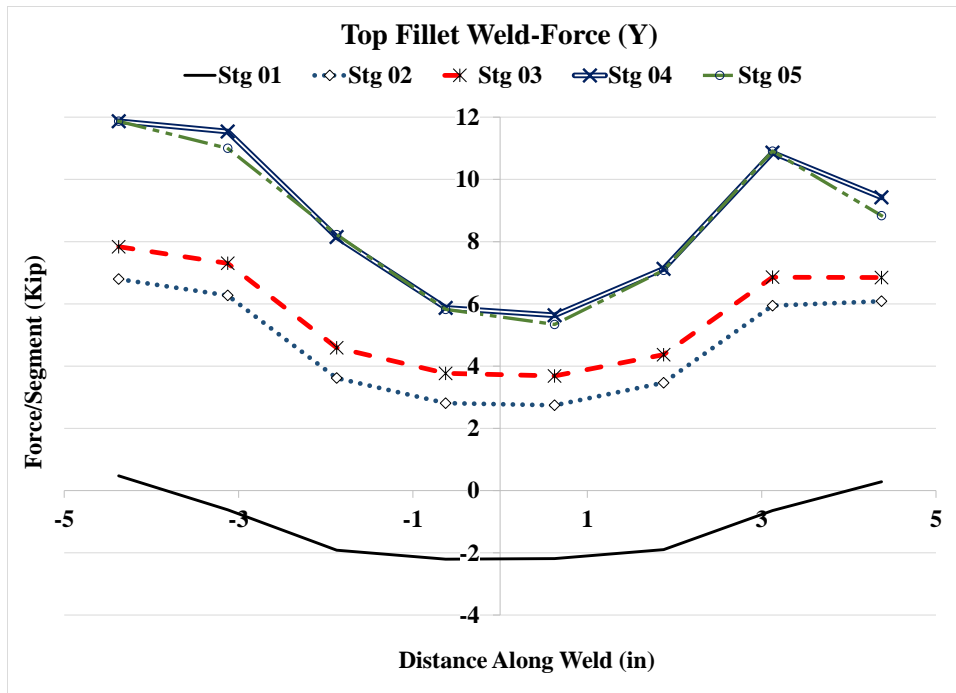


Figure 4.64: Forces and stresses in horizontal weld, (Y) Case 2A1

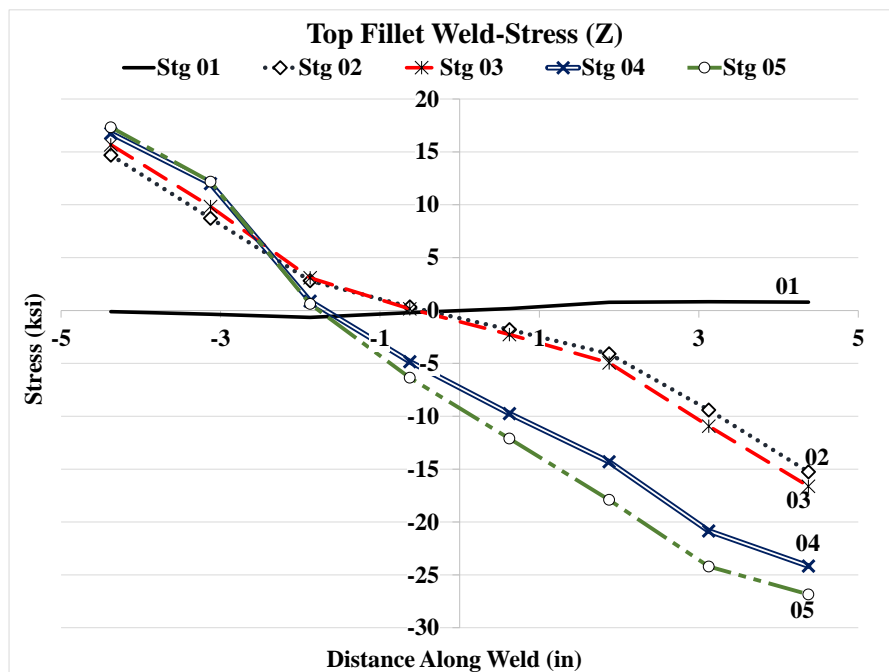
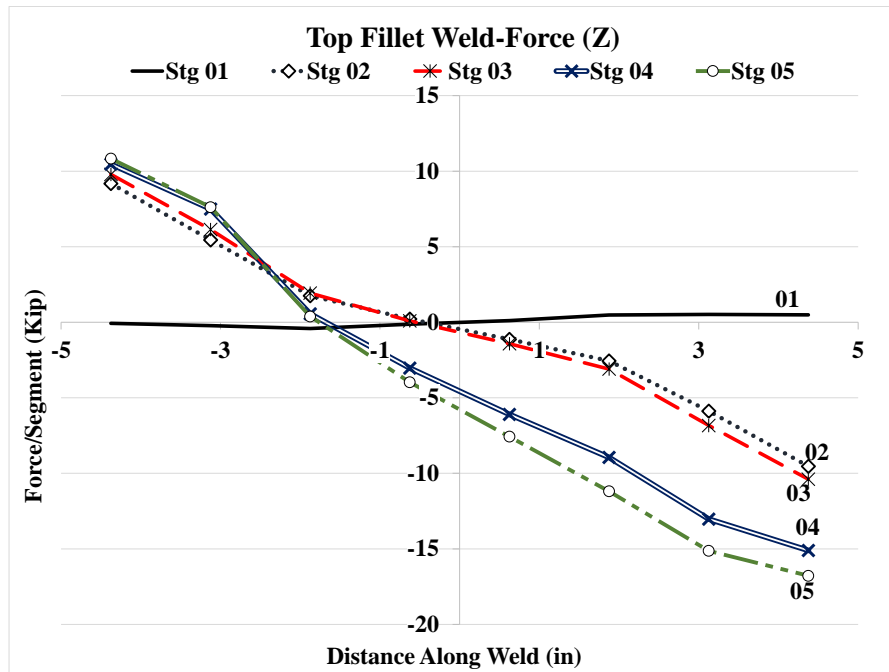


Figure 4.65: Forces and stresses in horizontal weld, (Z) Case 2A1

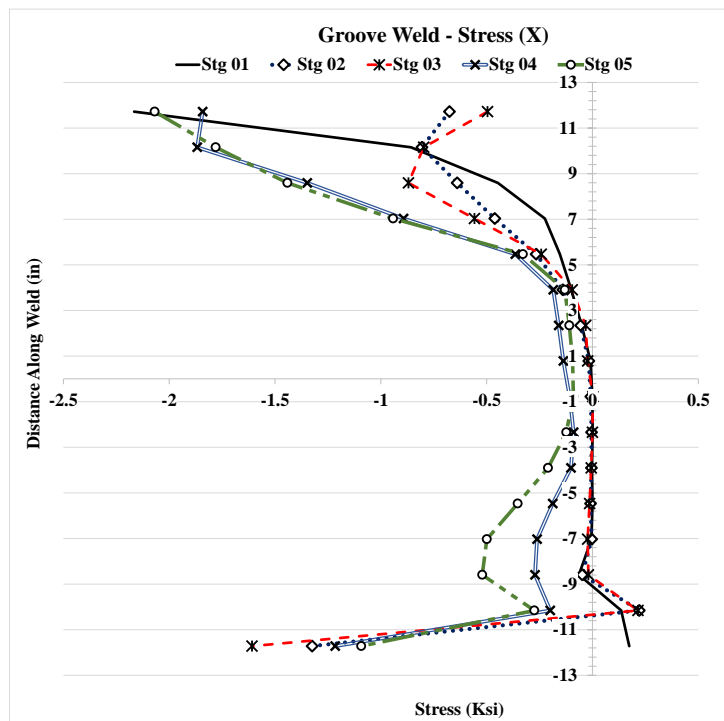
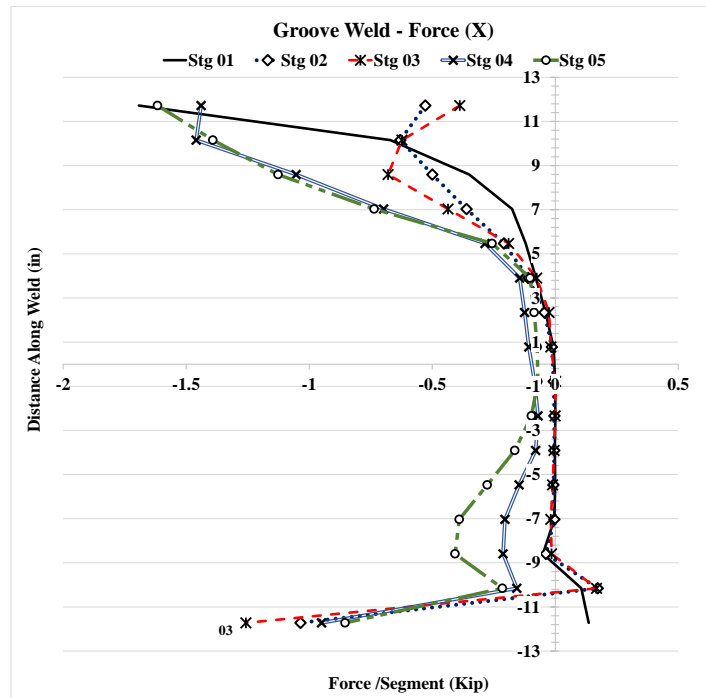


Figure 4.66: Forces and stresses in vertical weld, (X) Case 2A1

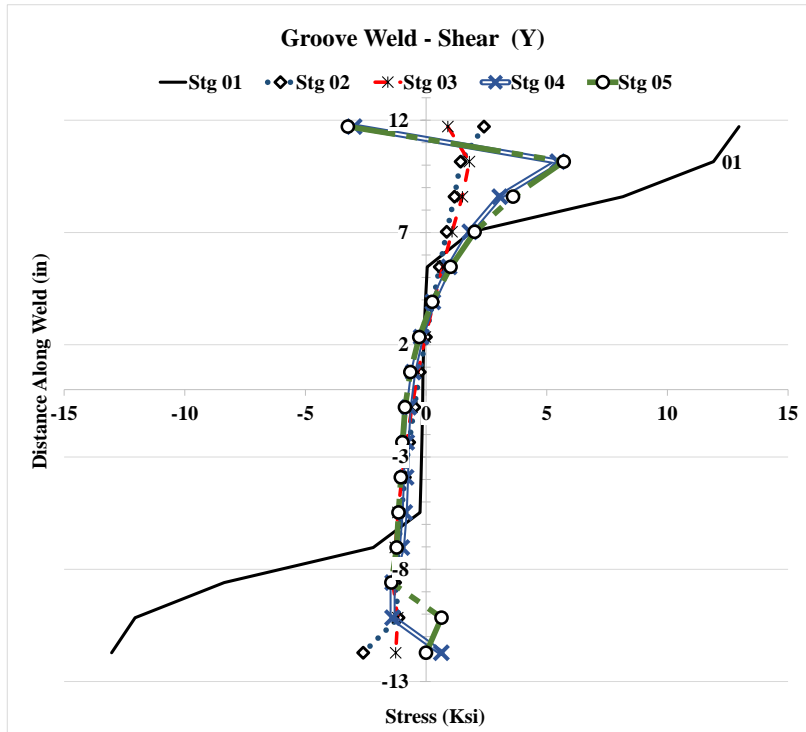
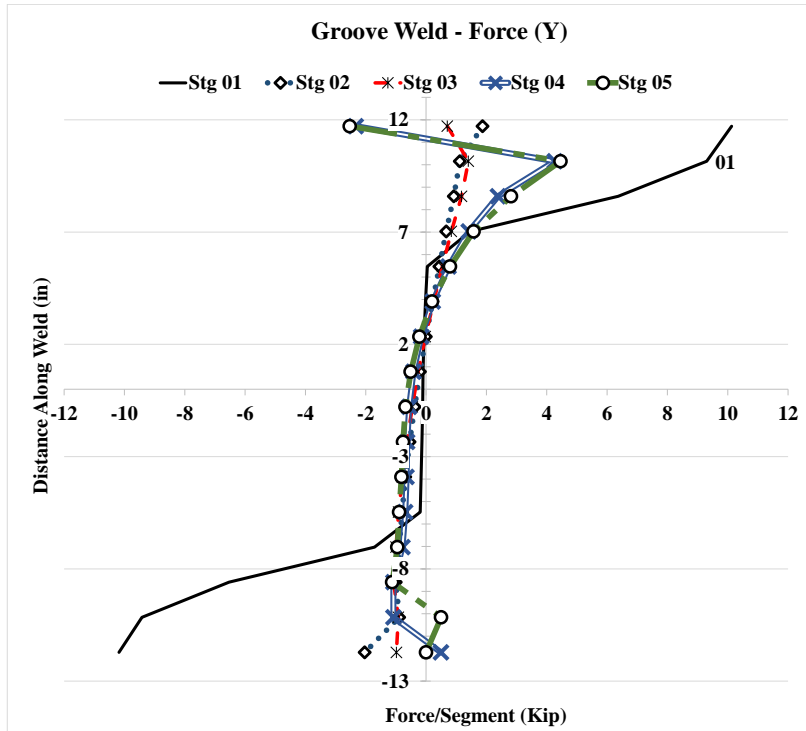


Figure 4.67: Forces and stresses in vertical weld, (Y) Case 2A1

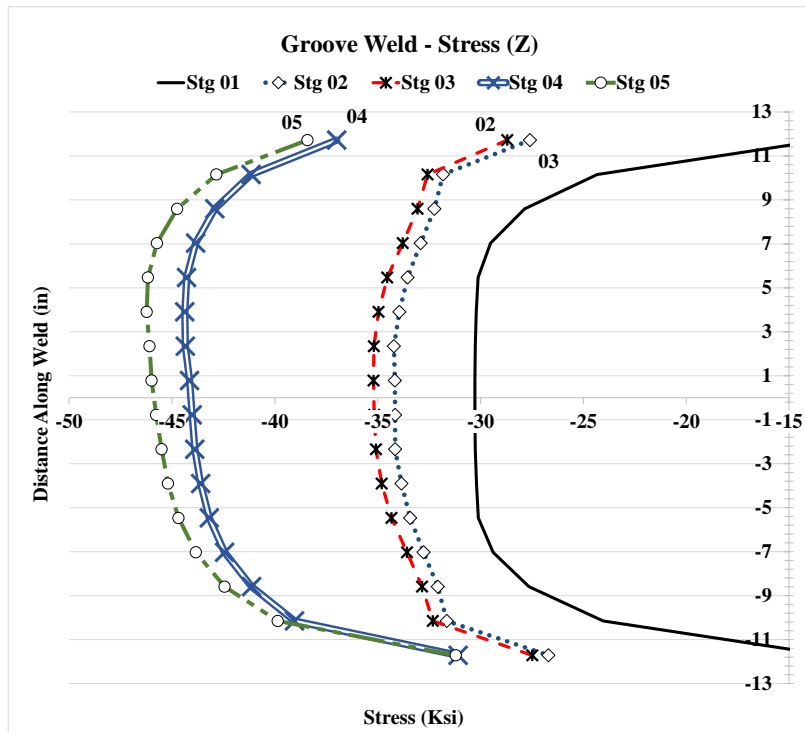
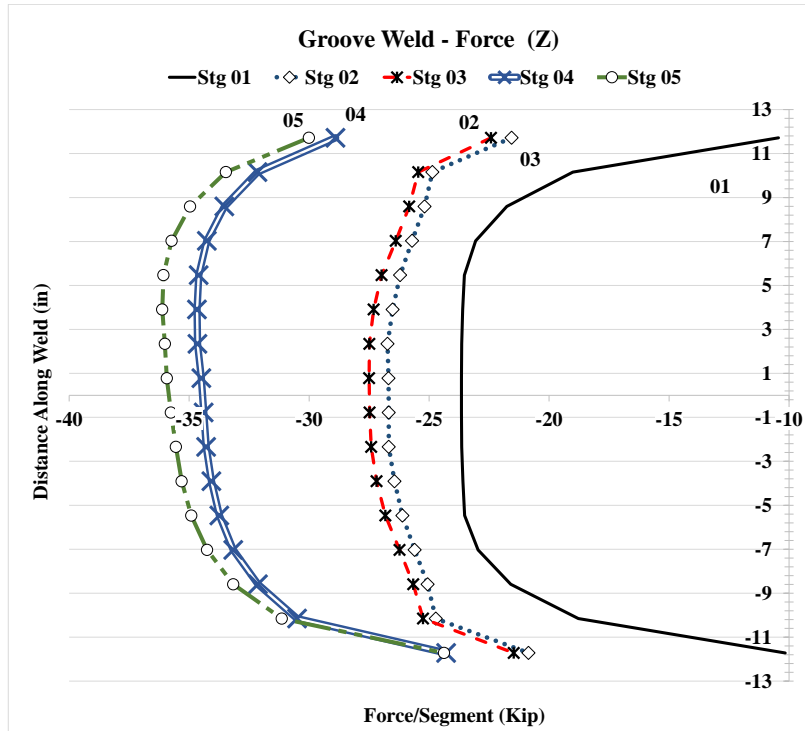


Figure 4.68: Forces and stresses in vertical weld, (Z) Case 2A1



### 4.2.7 Analysis Case 2C1

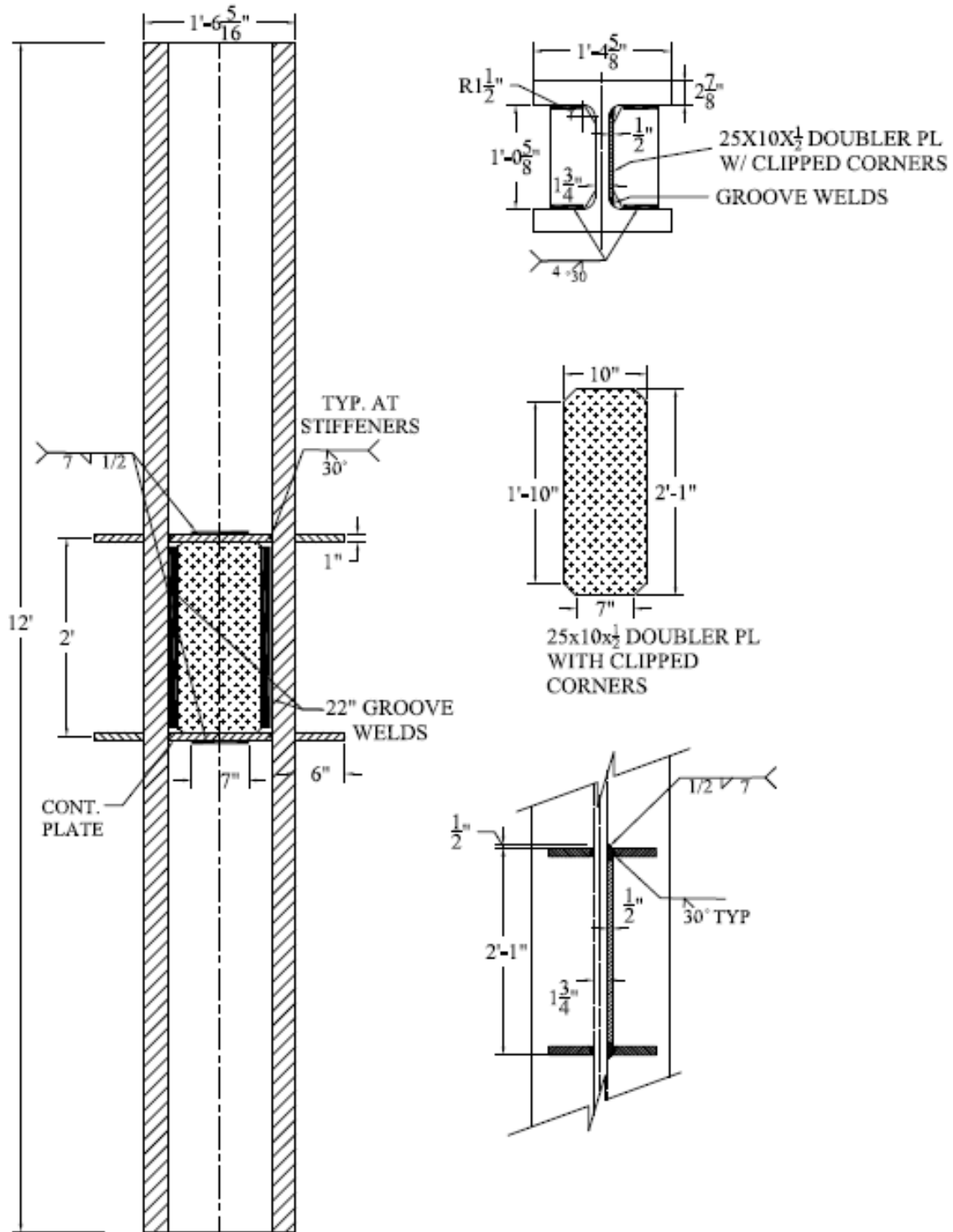


Figure 4.69: Analysis case 2C1

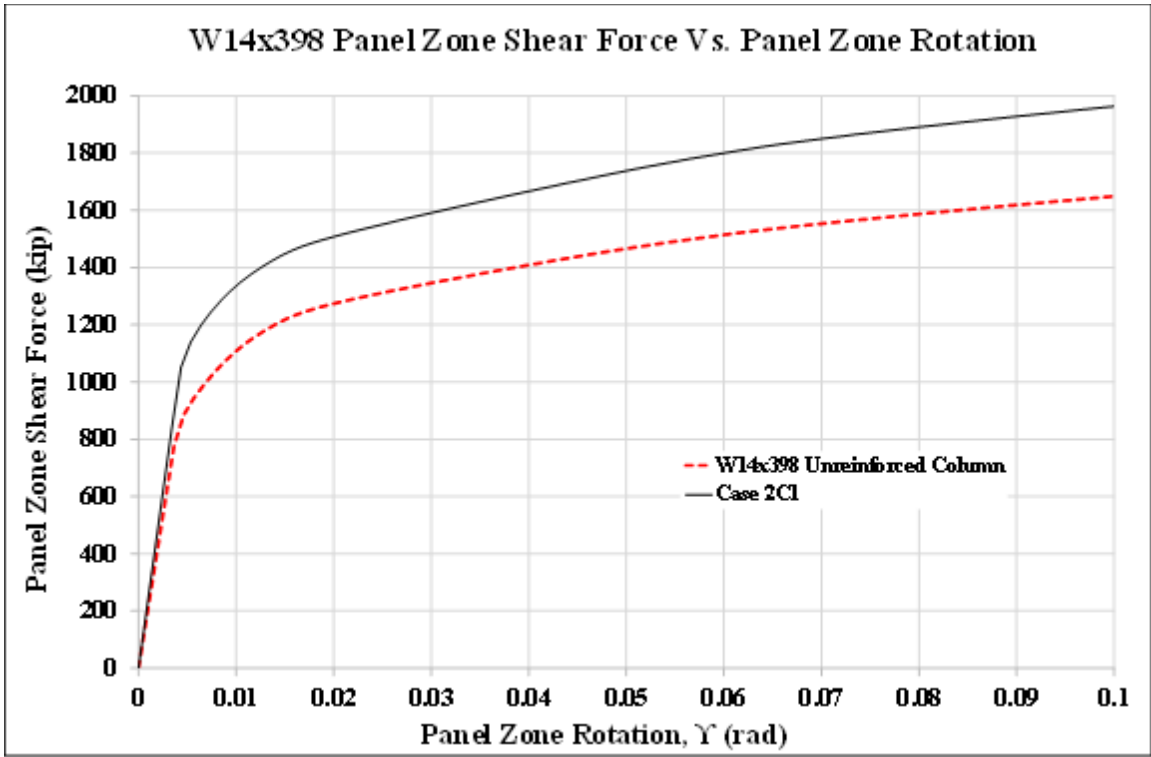


Figure 4.70: Panel zone shear vs. panel zone rotation Case 2C1

Stage	Applied Force/Loading Plate (Kip)	Panel Shear Force (Kip)	% Higher than unreinforced Col.	Panel Zone Rotation (rad)
1	631	1,052	119%	0.004
2	899	1,498	120%	0.019
3	905	1,508	118%	0.020
4	1,141	1,902		0.083
5	1,178	1,963	119%	0.100

Table 4.9: Panel zone shear and force on loading plate Case 2C1

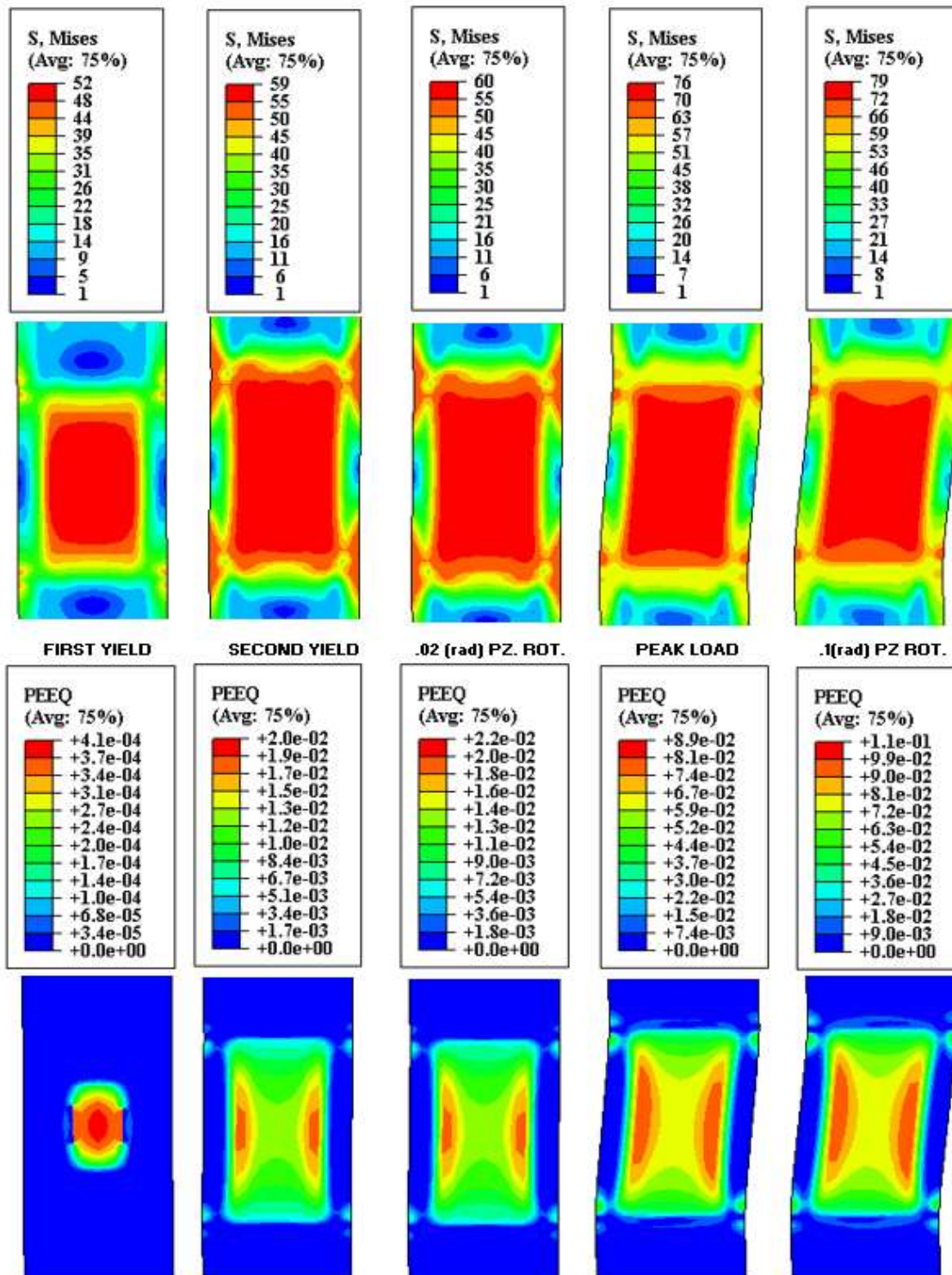
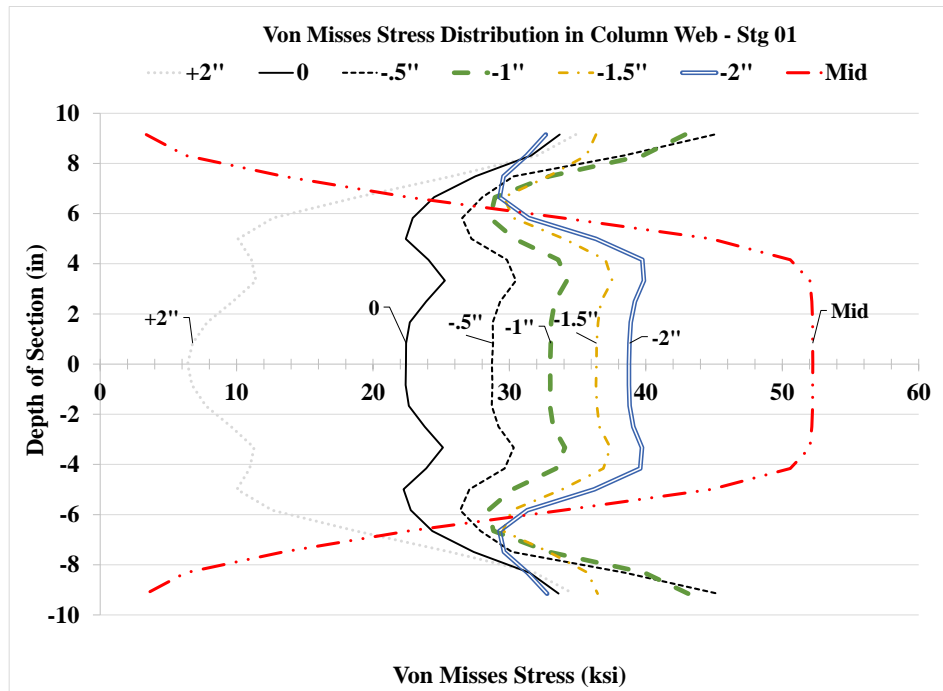
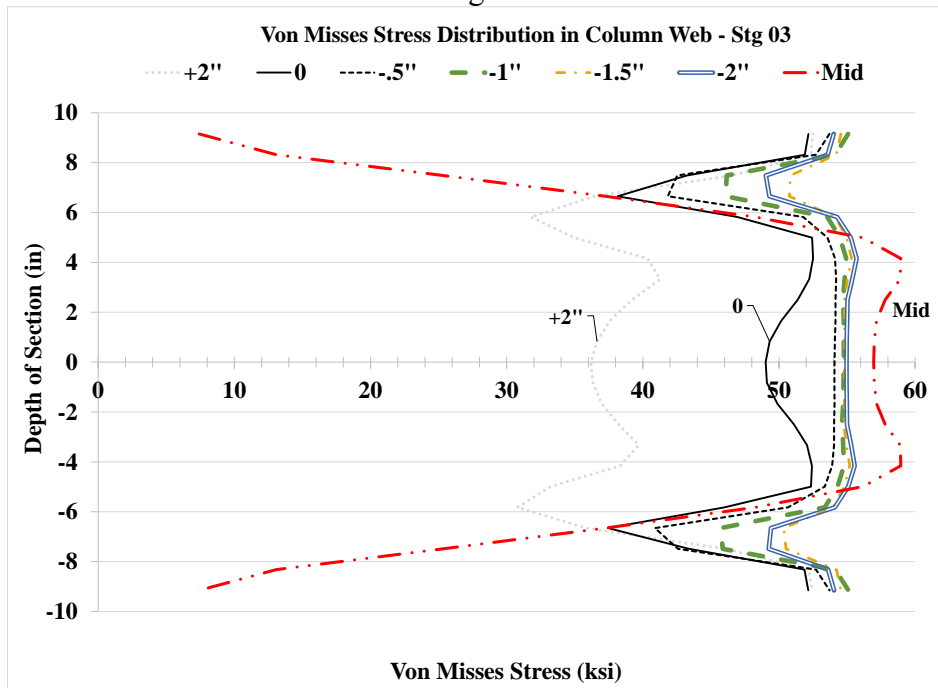


Figure 4.71: VMS and PEEQ in the column Case 2C1

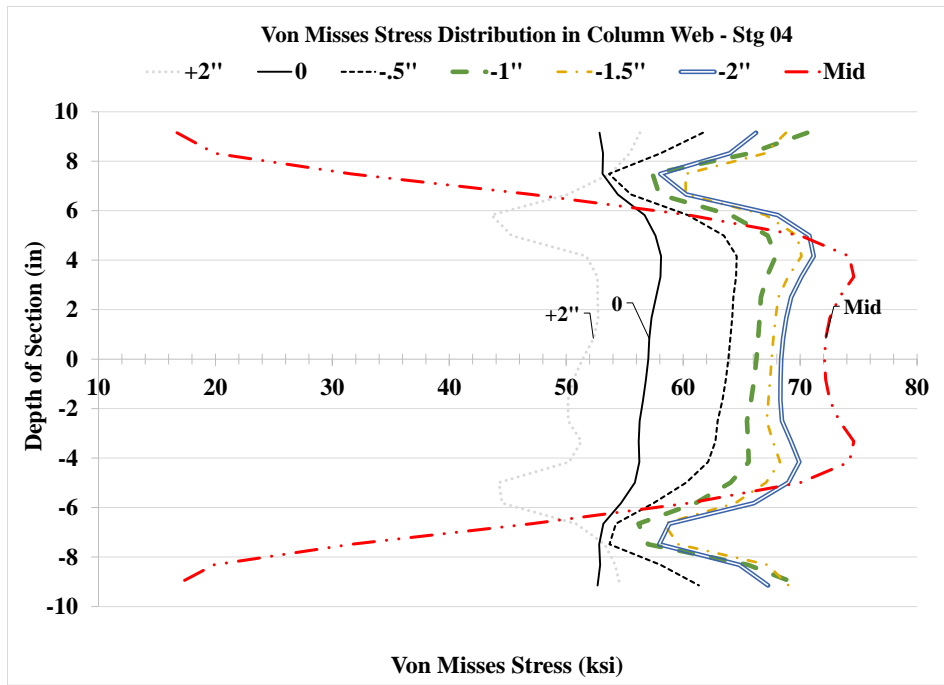


Stg. 01



Stg. 03

Figure 4.72: VMS distribution in column web at different heights Stg. 01-04 Case 2C1



Stg. 04

Figure 4.72: VMS distribution in column web at different heights Stg. 01-04 Case 2C1

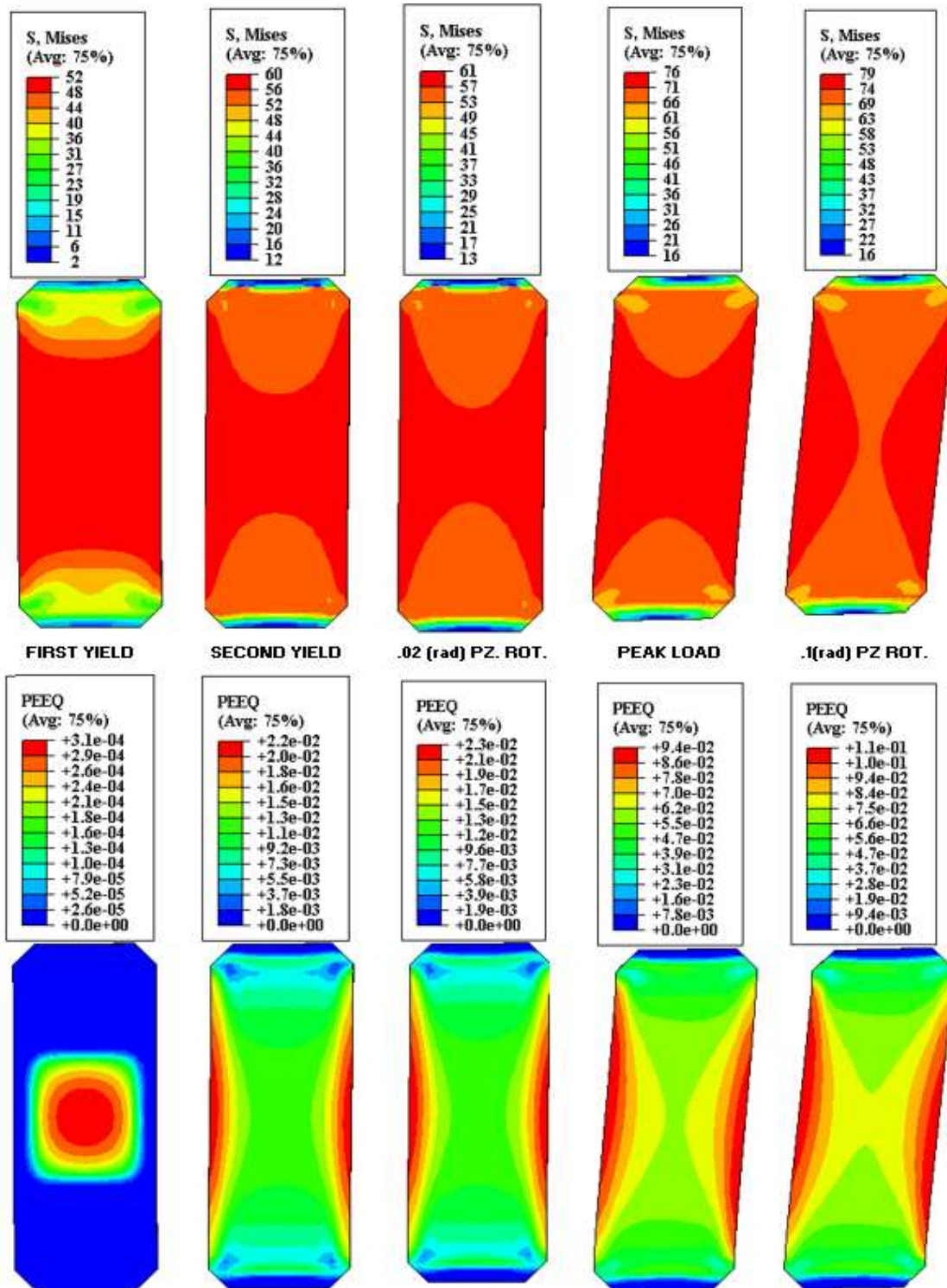


Figure 4.73: VMS and PEEQ in the DP Case 2C1

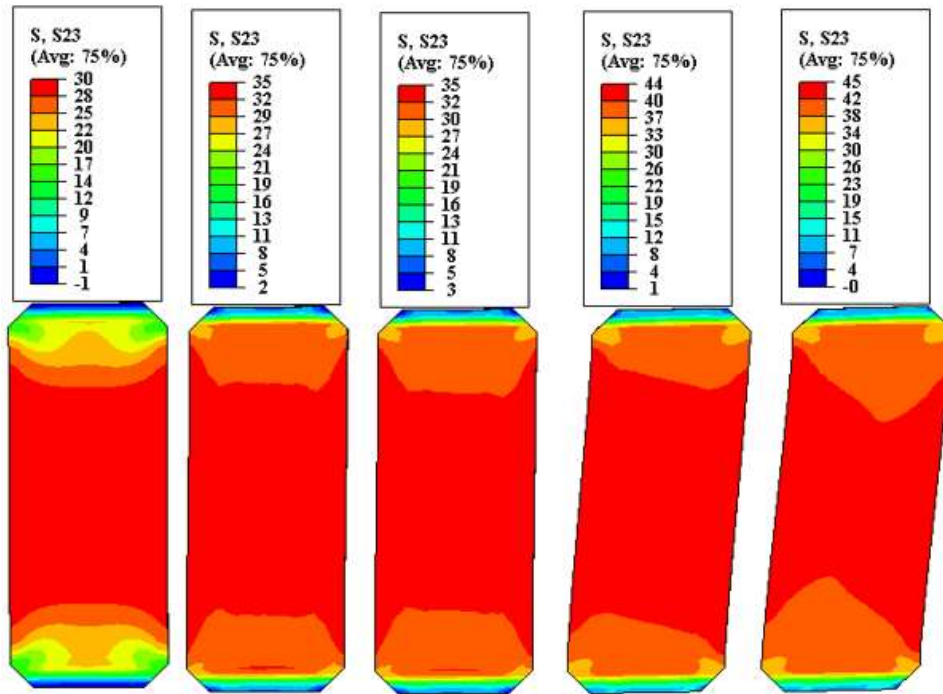


Figure 4.74: Shear stress, S23 in the DP Case 2C1

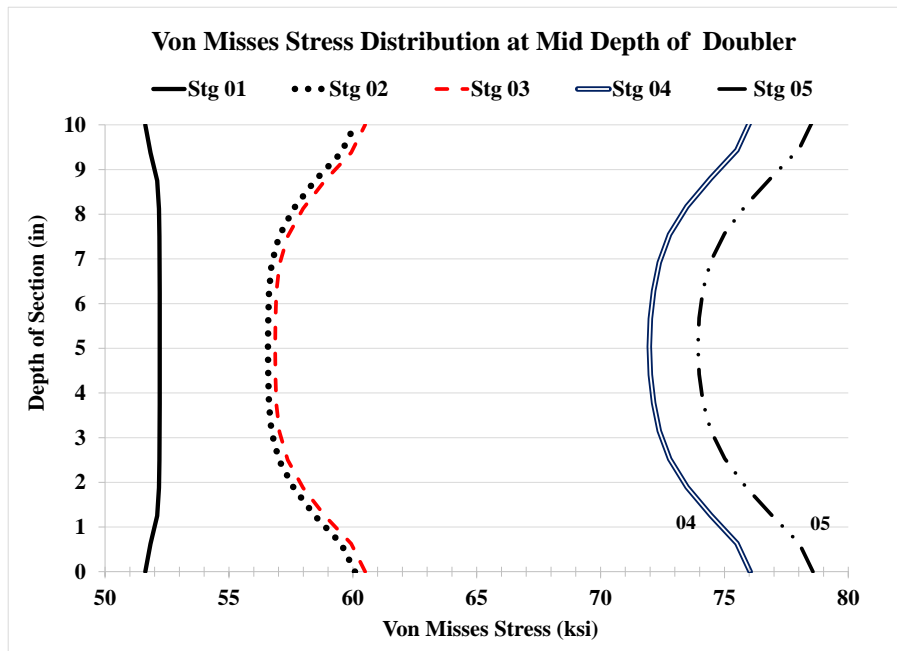


Figure 4.75: VMS distribution at mid-depth of DP Case 2C1

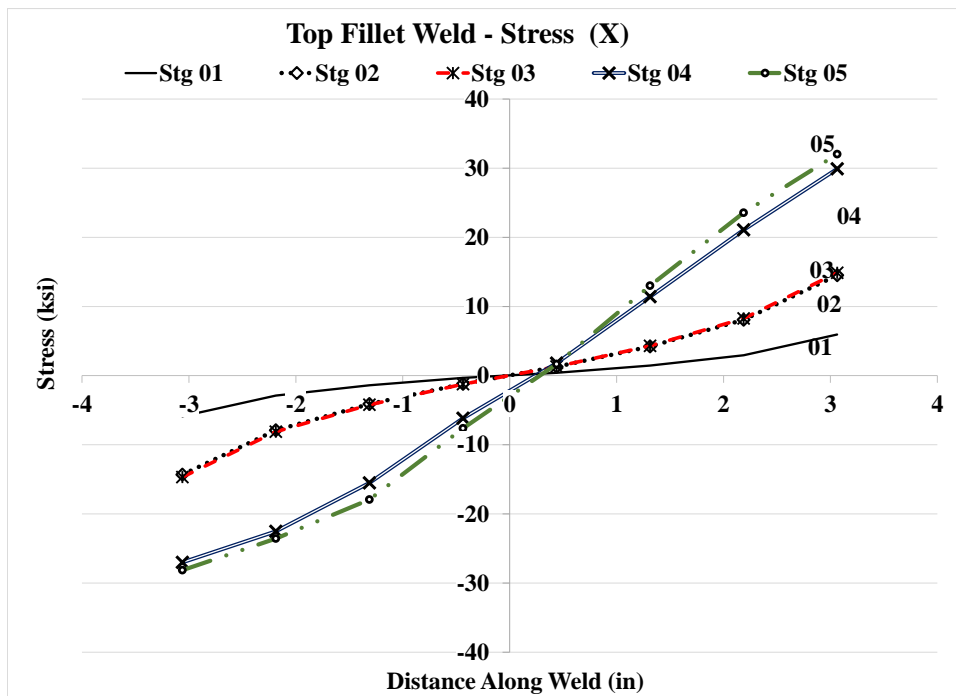
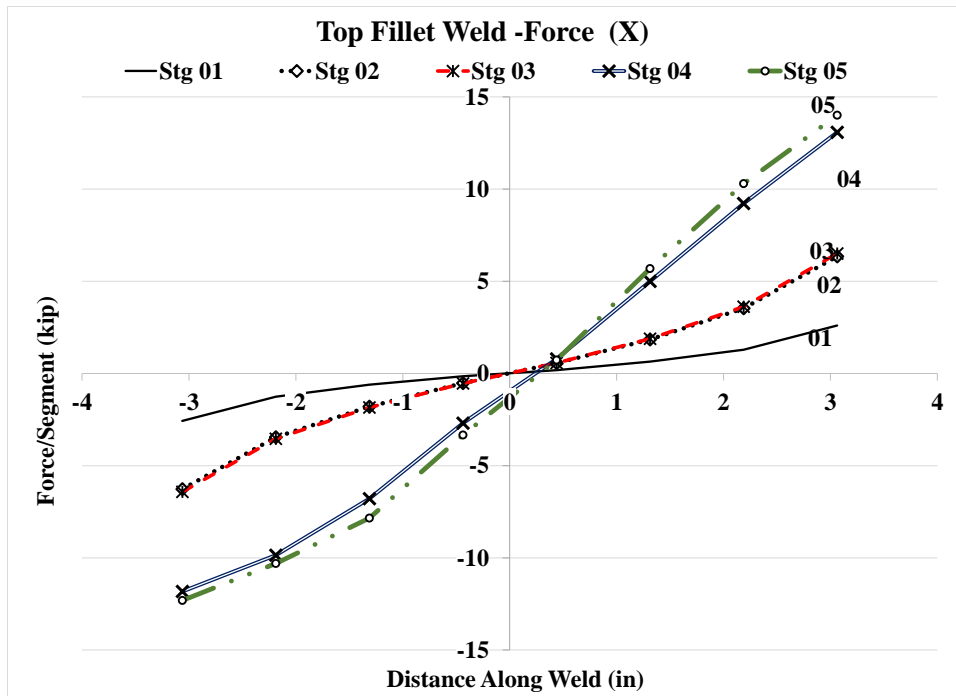


Figure 4.76: Forces and stresses in horizontal weld, (X) Case 2C1



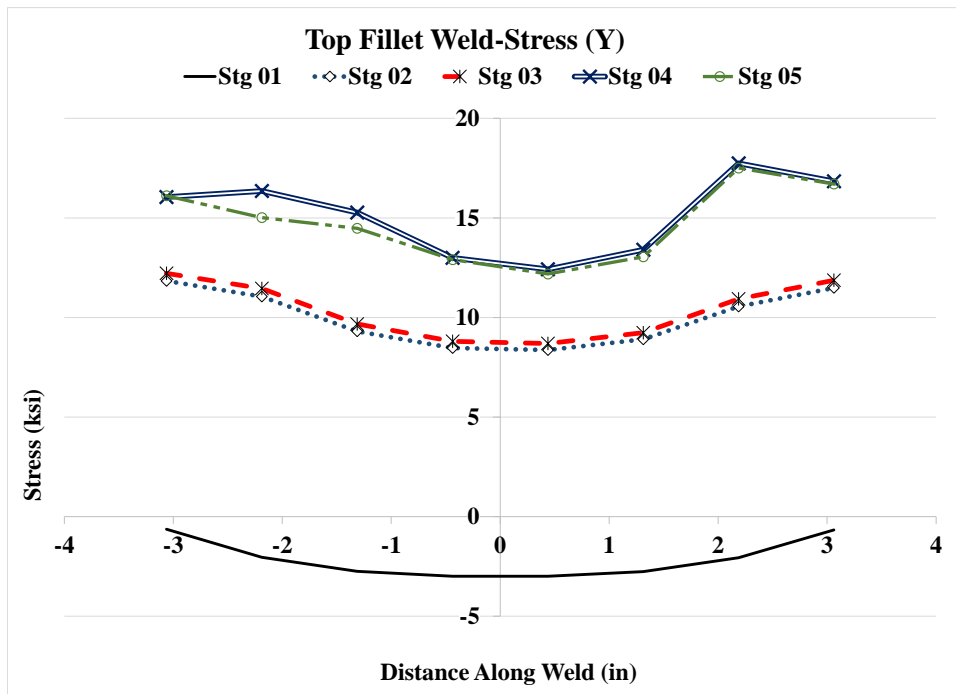
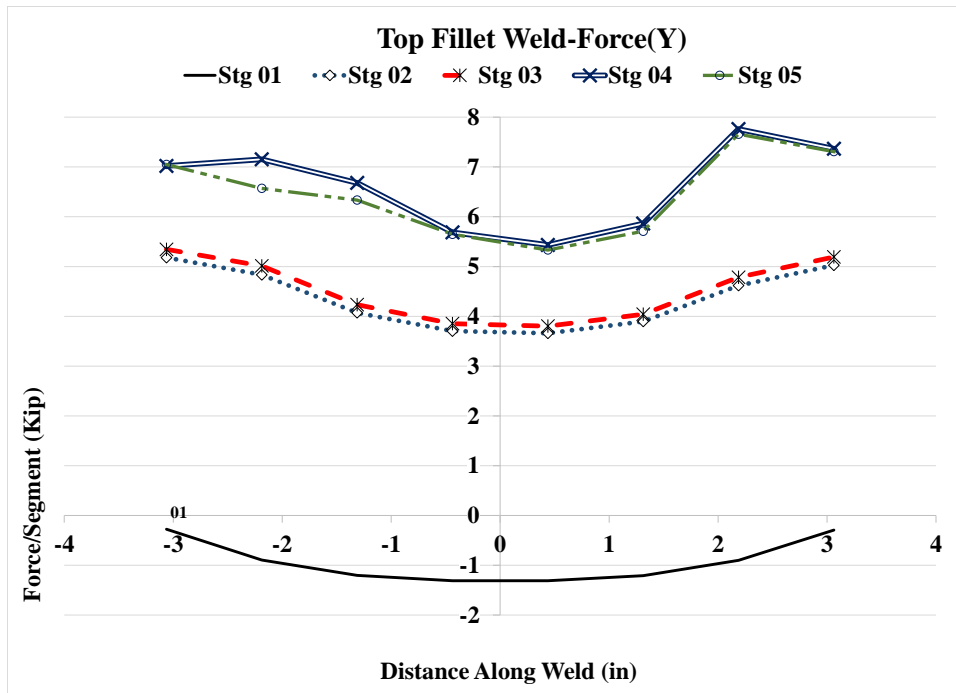


Figure 4.77: Forces and stresses in horizontal weld, (Y) Case 2C1

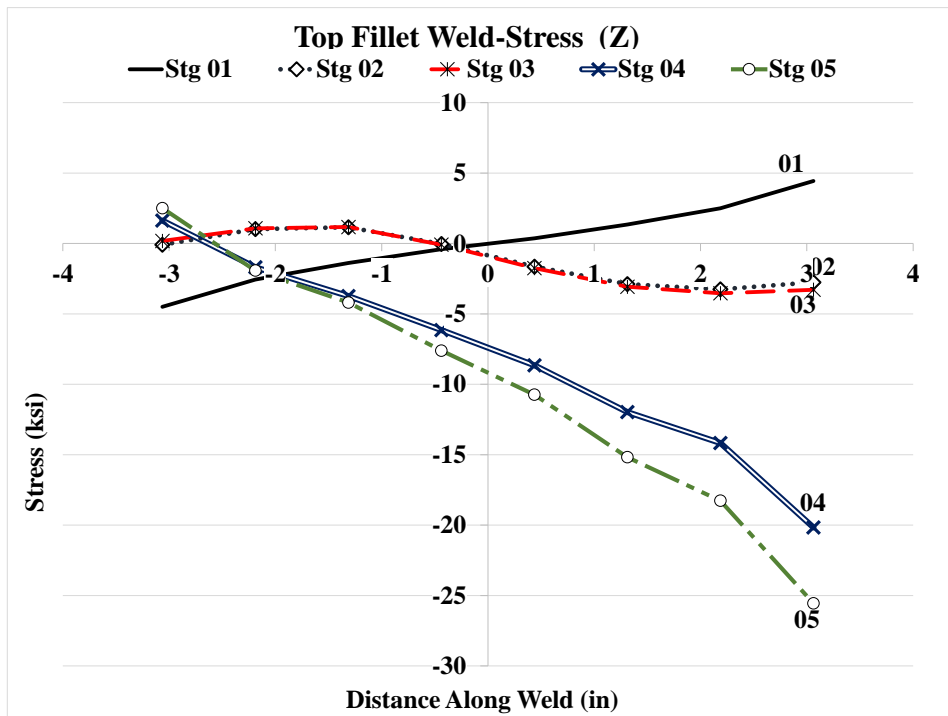
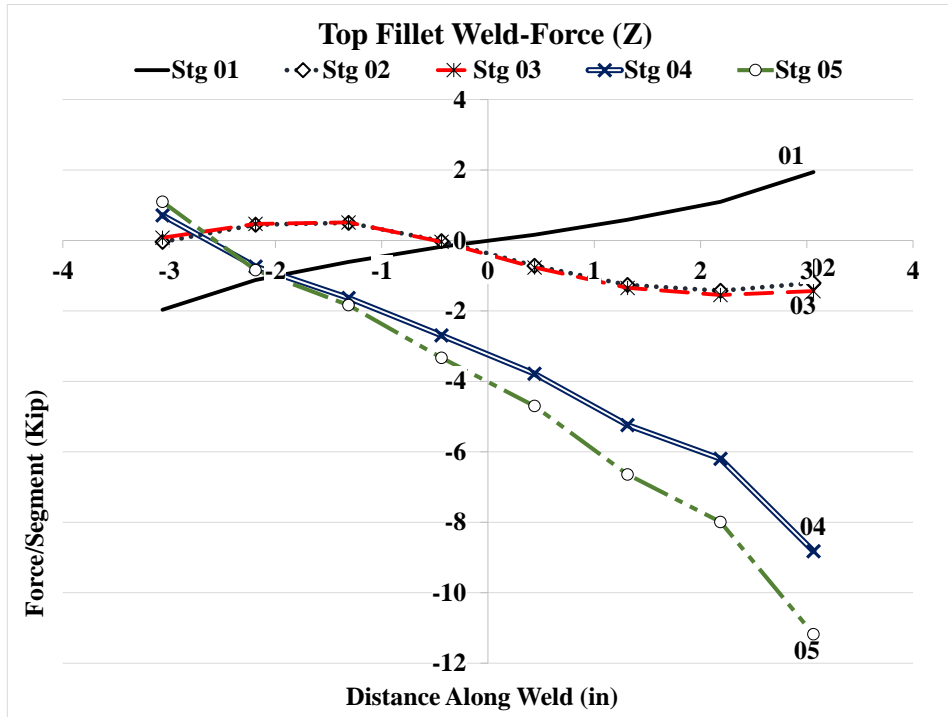


Figure 4.78: Forces and stresses in horizontal weld, (Z) Case 2C1

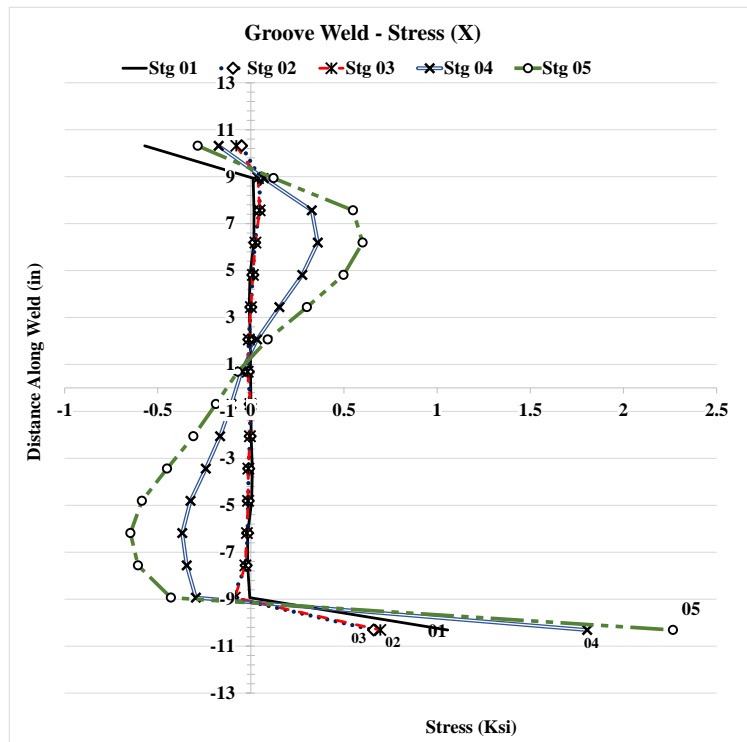
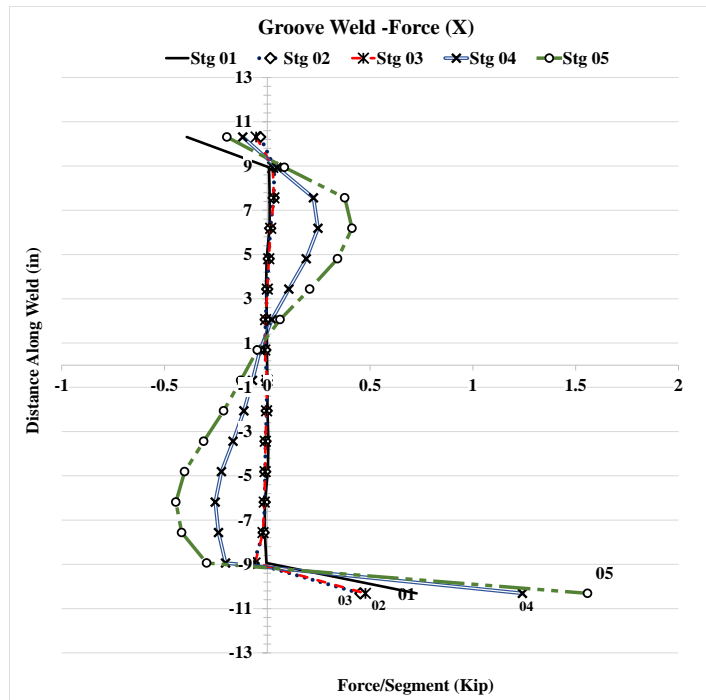


Figure 4.79: Forces and stresses in vertical weld, (X) Case 2C1

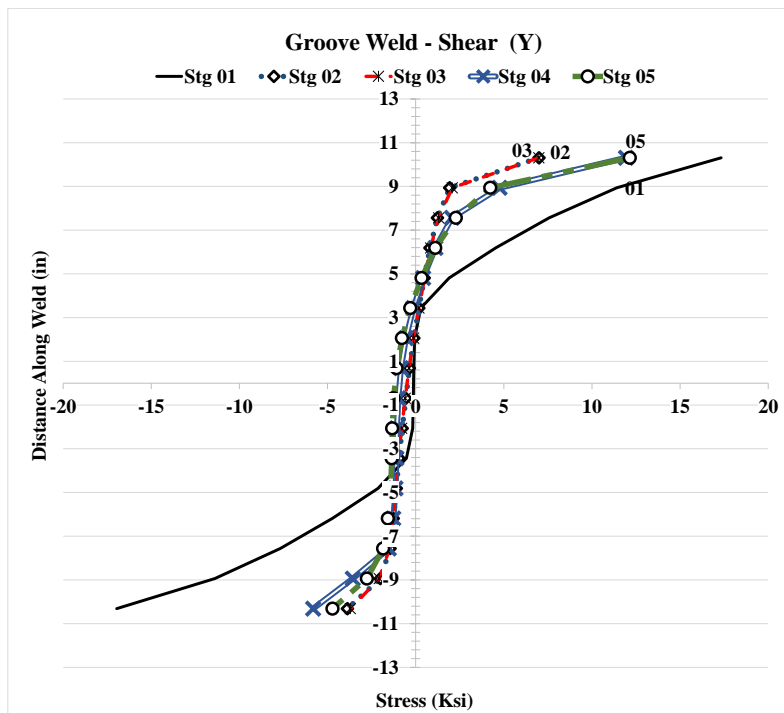
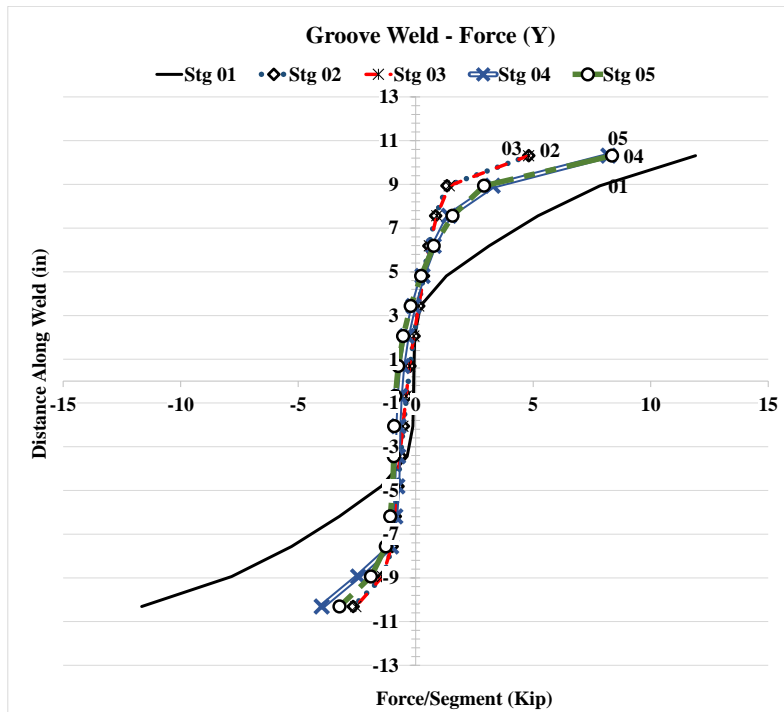


Figure 4.80: Forces and stresses in vertical weld, (Y) Case 2C1

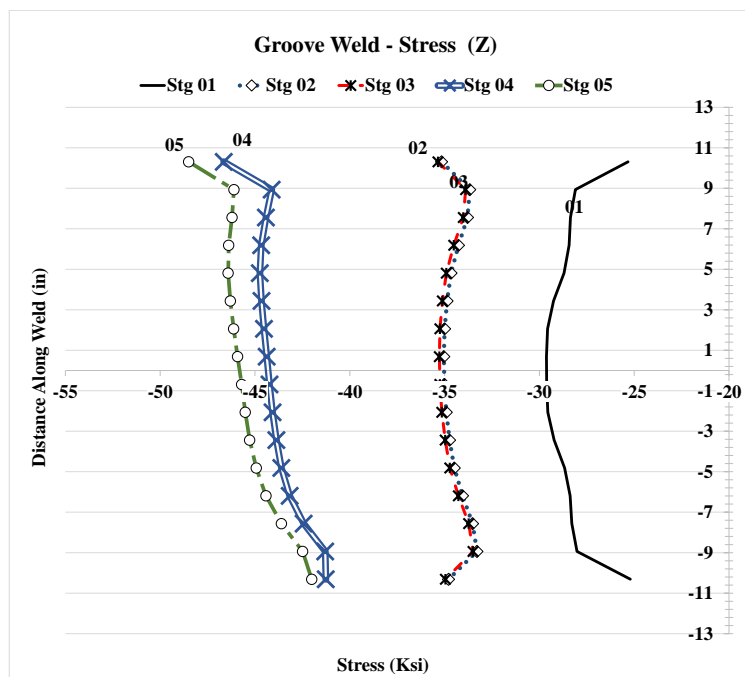
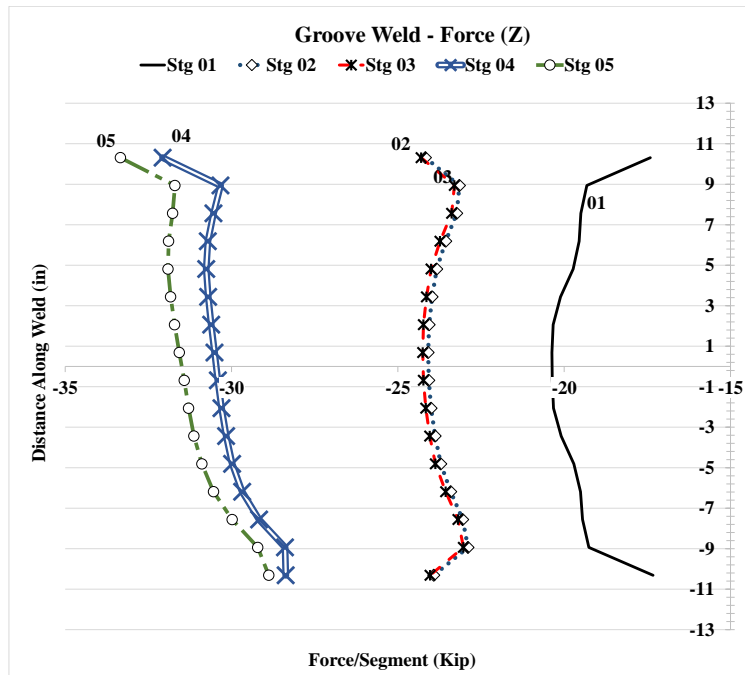


Figure 4.81: Forces and stresses in vertical weld, (Z) Case 2C1

### 4.2.8 Analysis Case 3A

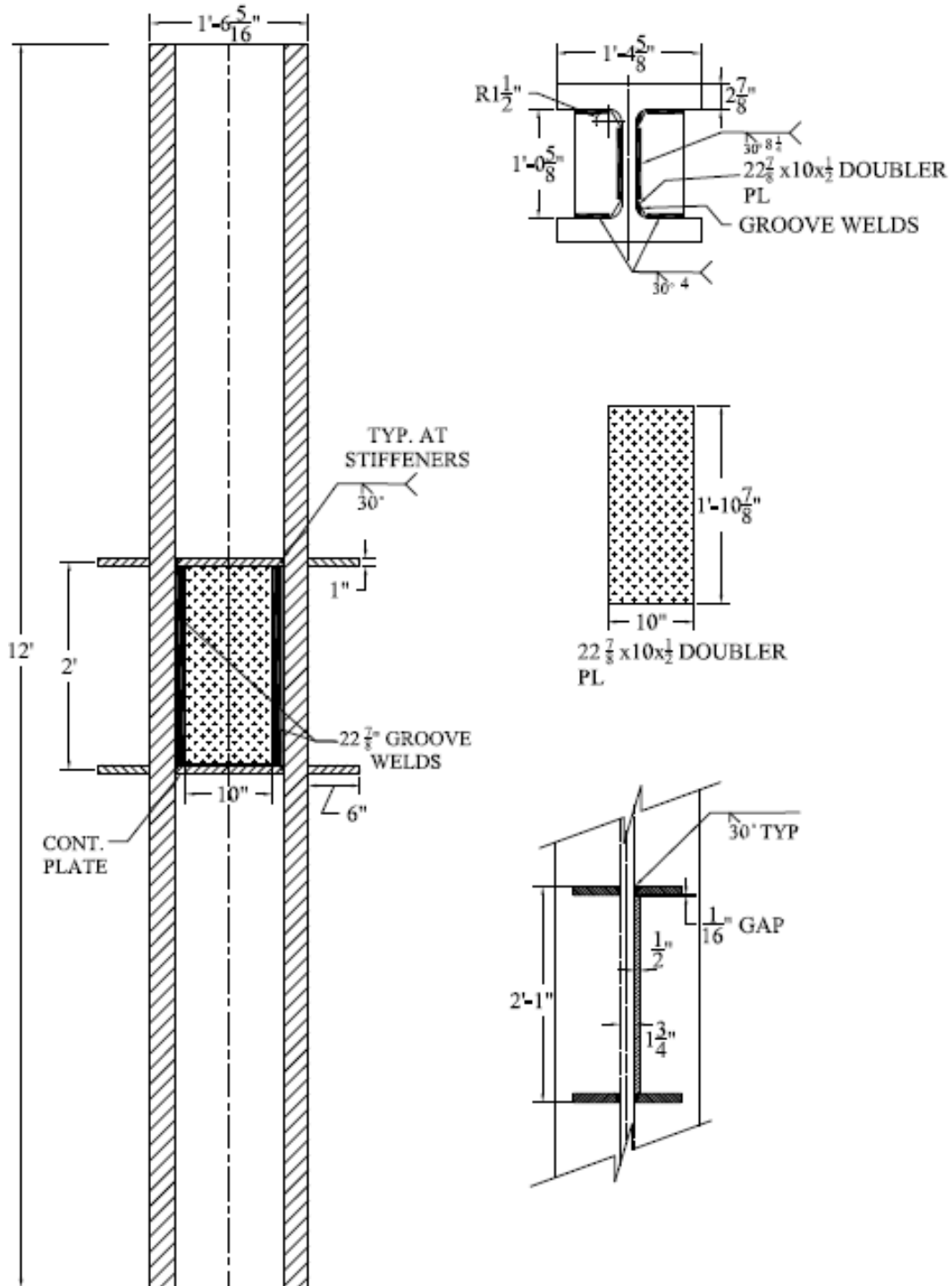


Figure 4.82: Analysis case 3A

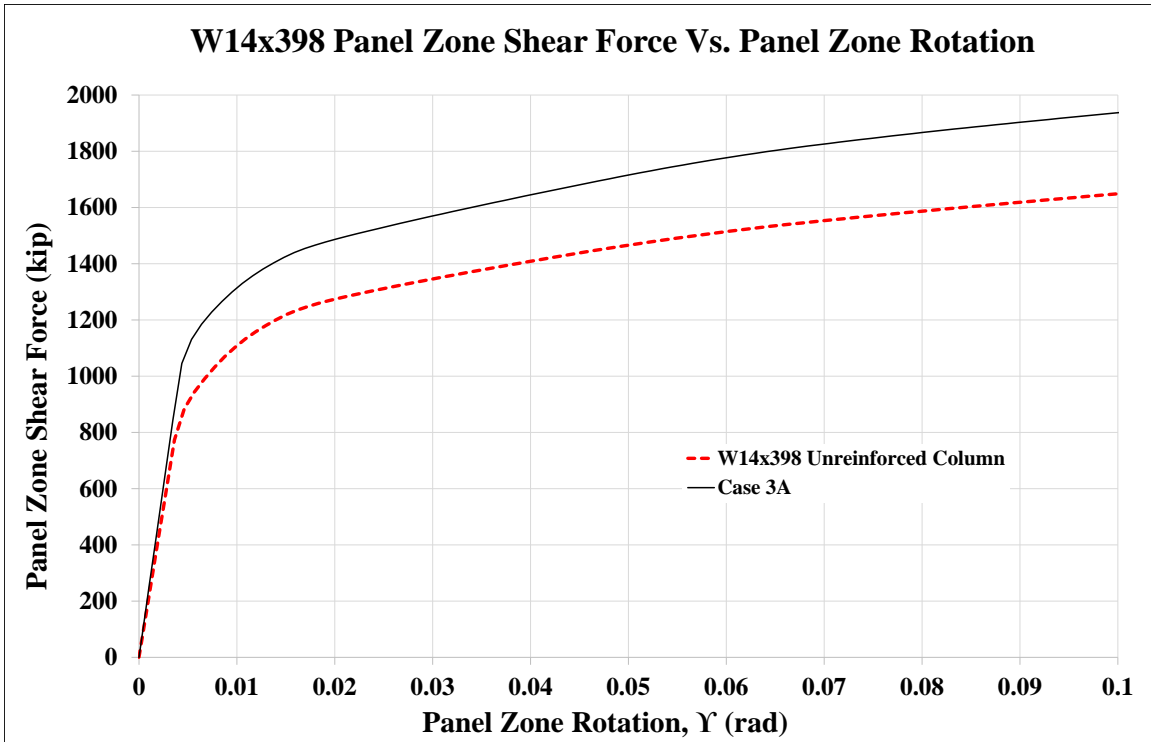


Figure 4.83: Panel zone shear vs. panel zone rotation Case 3A

Stage	Applied Force/Loading Plate (Kip)	Panel Shear Force (Kip)	% Higher than unreinforced Col.	Panel Zone Rotation (rad)
1	627	1,045	118%	0.004
2	864	1,440	115%	0.016
3	893	1,488	116%	0.020
4	1,141	1,902		0.090
5	1,163	1,939	118%	0.100

Table 4.10: Panel zone shear and force on loading plate Case 3A

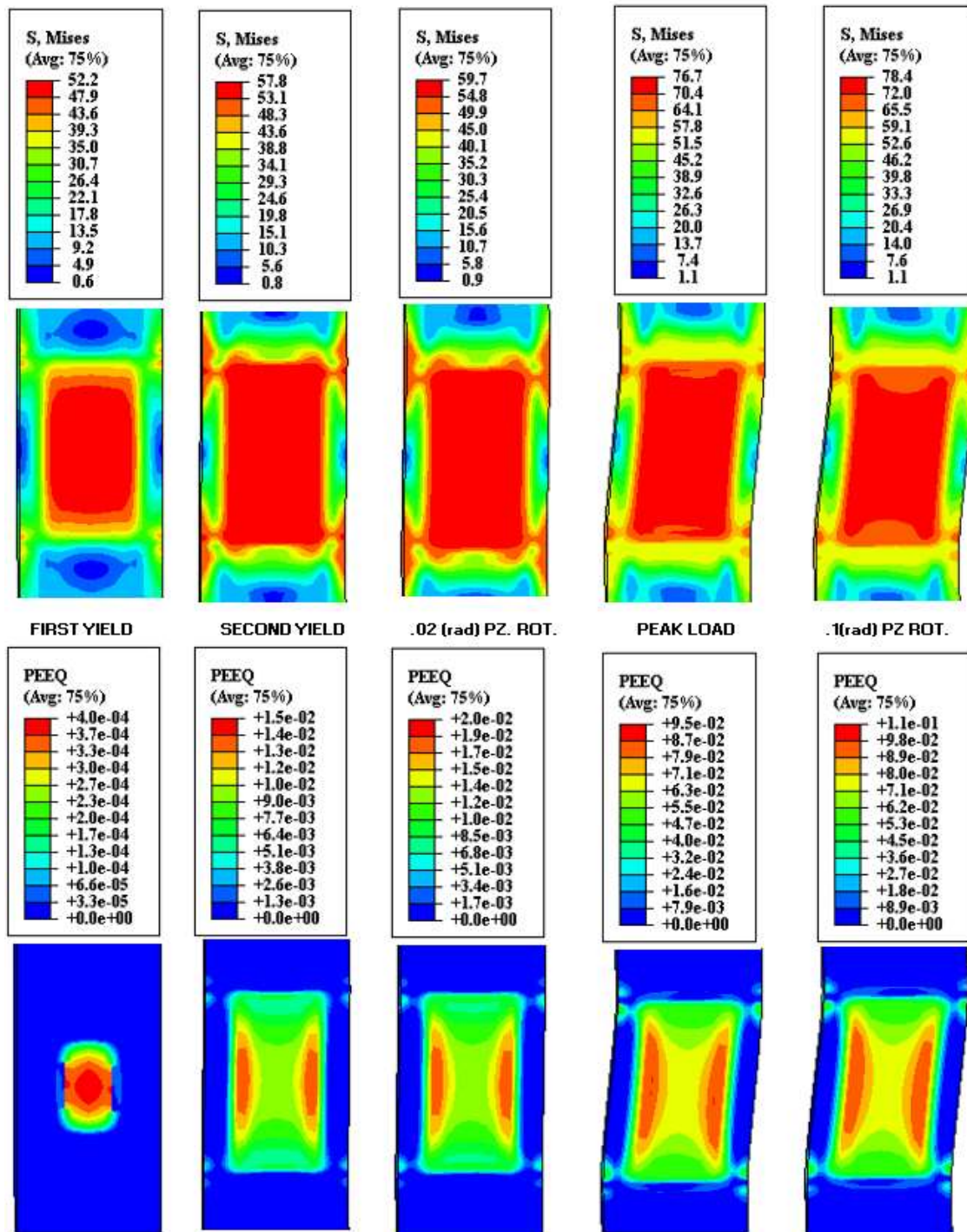
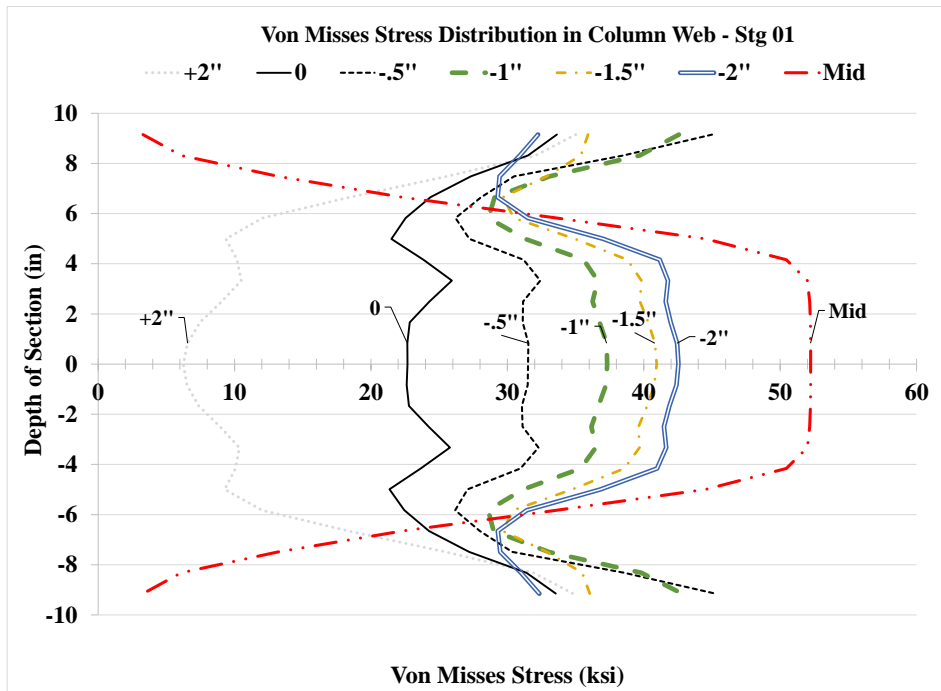
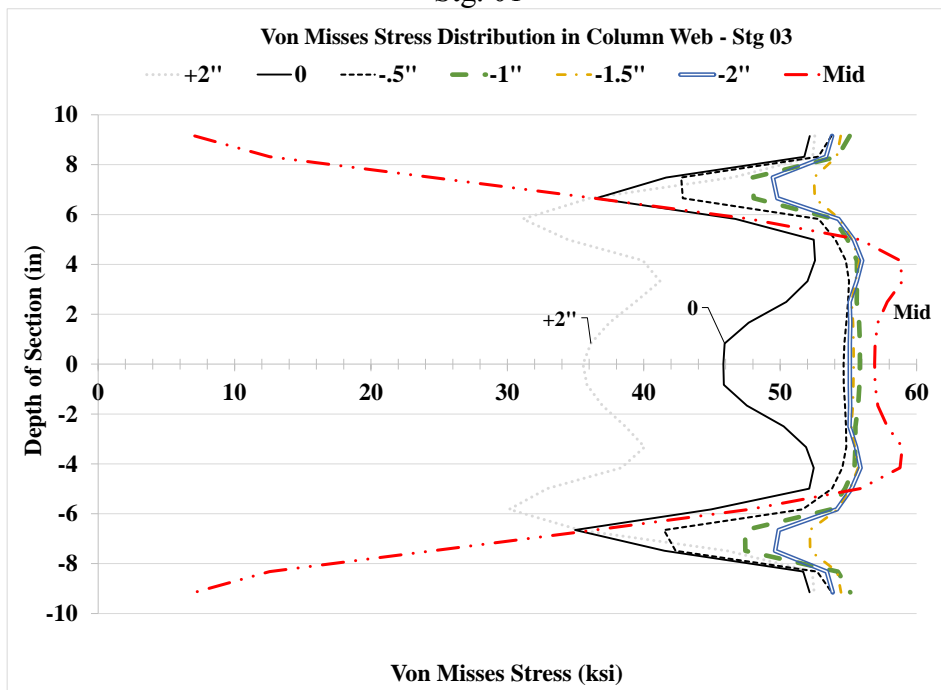


Figure 4.84: VMS and PEEQ in the column Case 3A



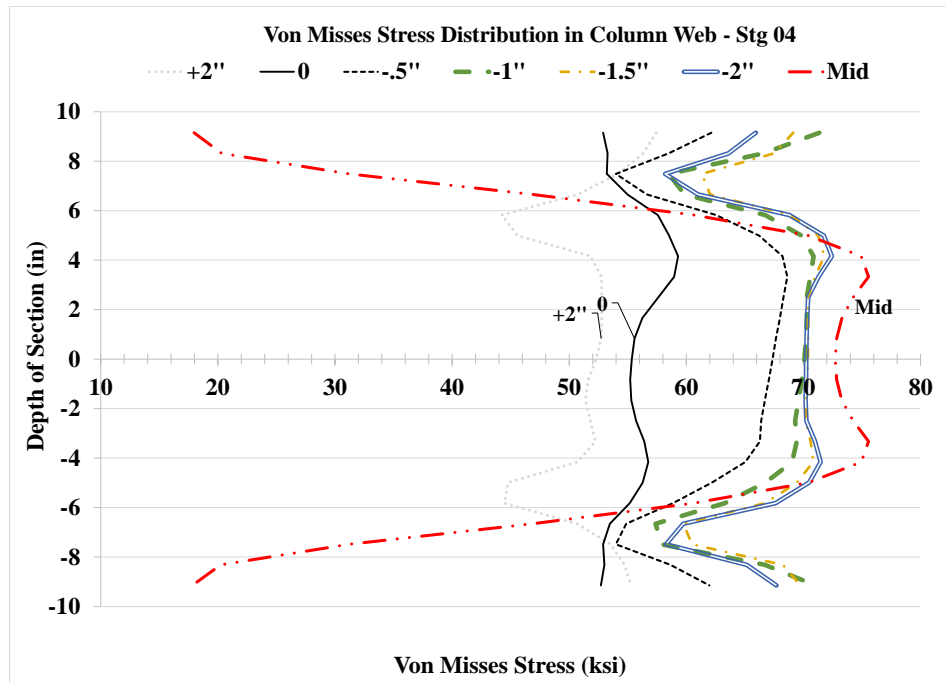


Stg. 01



Stg. 03

Figure 4.85: VMS distribution in column web at different heights Stg. 01-04 Case 3A



Stg. 04

Figure 4.85: VMS distribution in column web at different heights Stg. 01-04 Case 3A

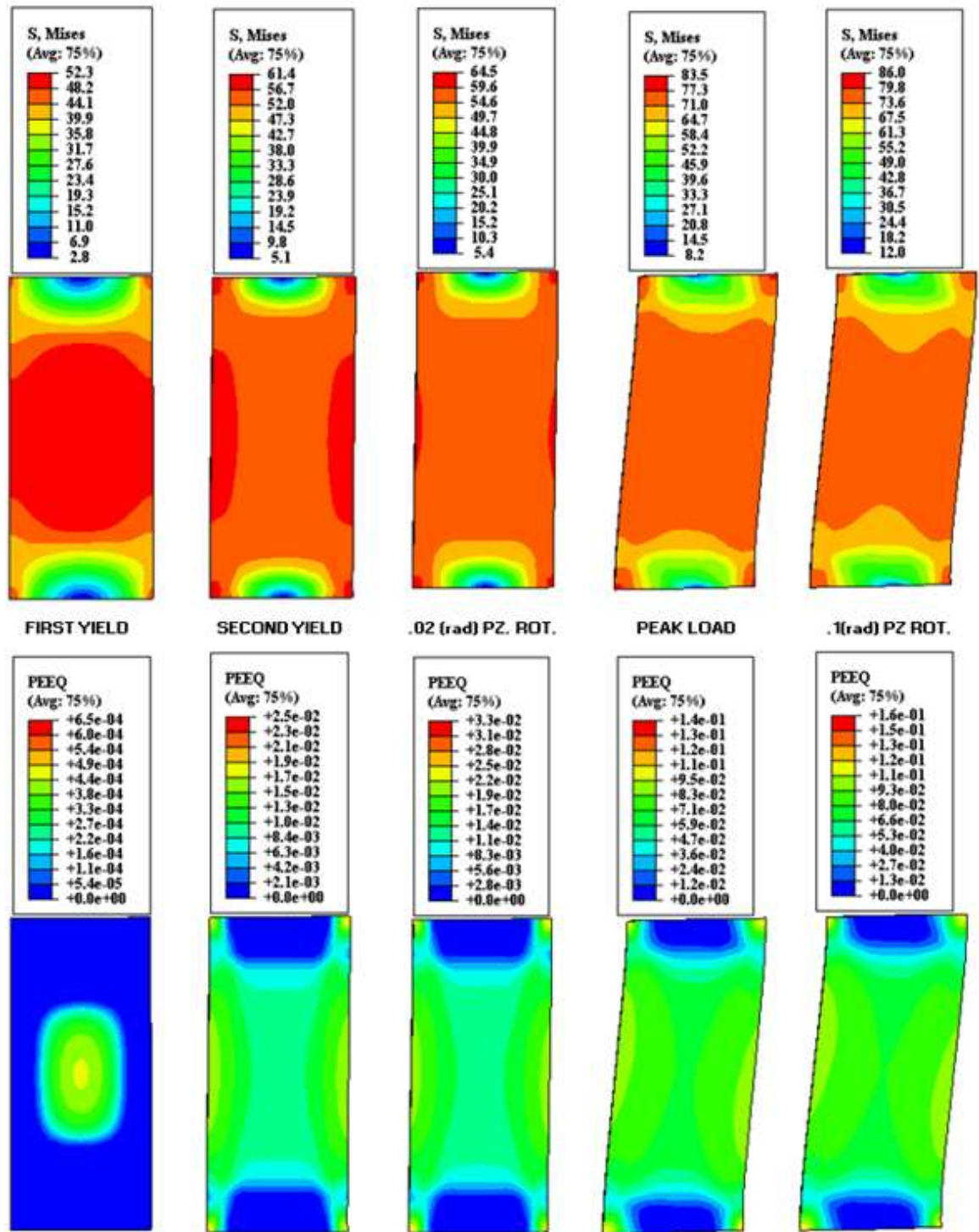


Figure 4.86: VMS and PEEQ in the DP Case 3A

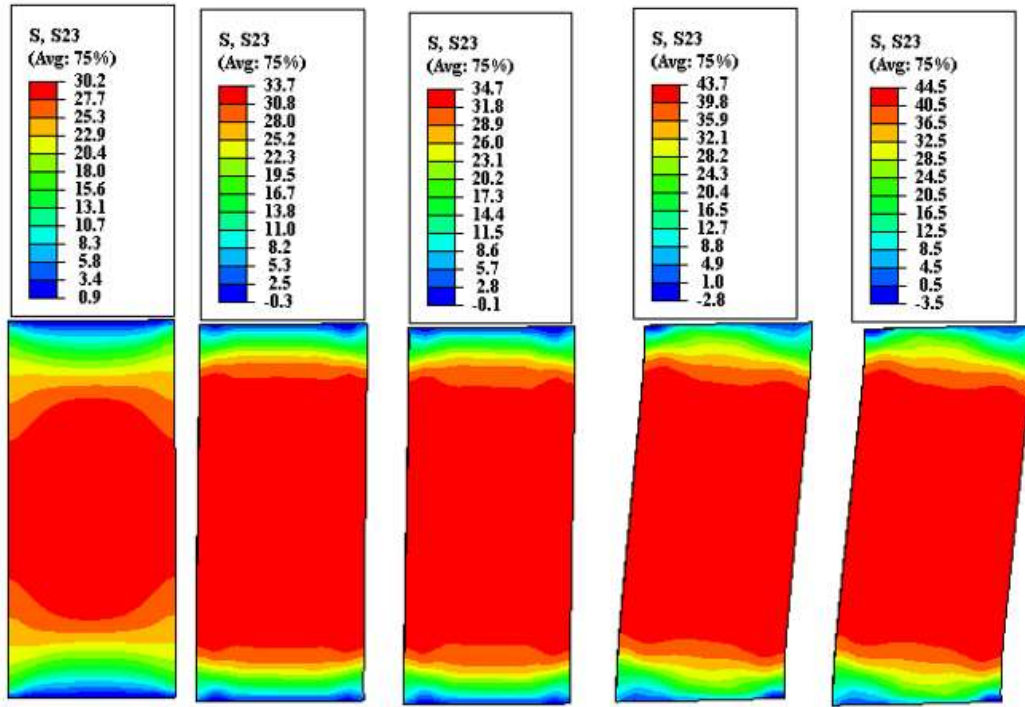


Figure 4.87: Shear stress, S23 in the DP Case 3A

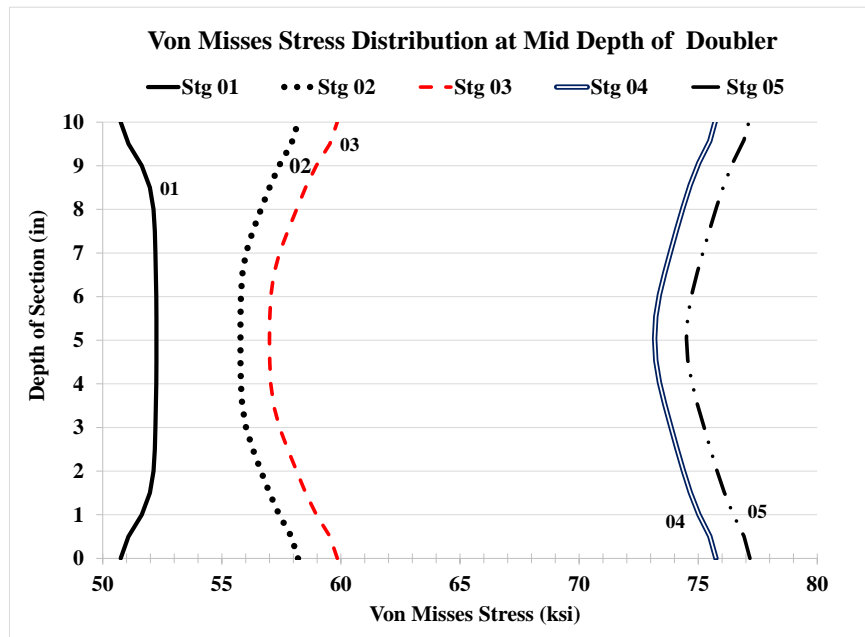


Figure 4.88: VMS distribution at mid-depth of DP Case 3A

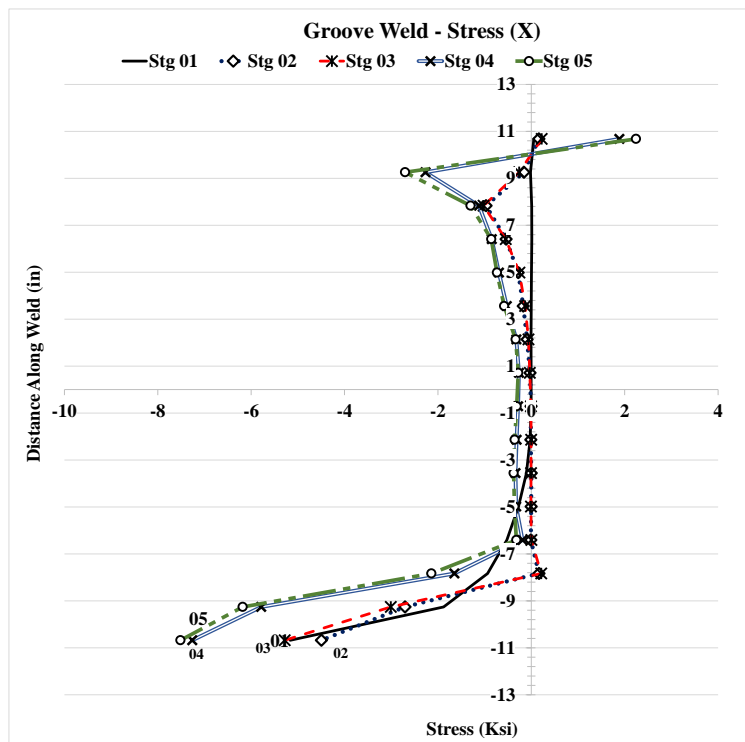
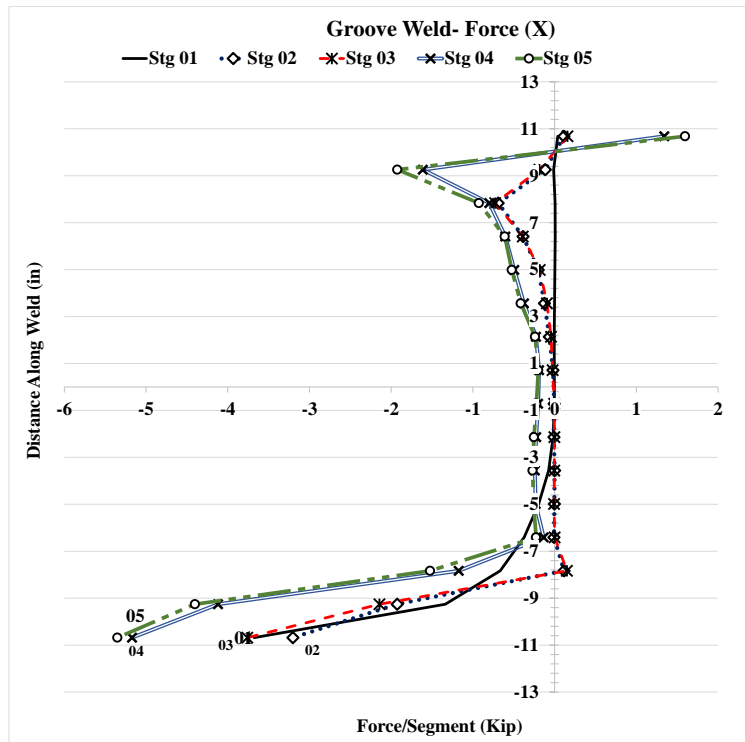


Figure 4.88: Forces and stresses in vertical weld, (X) Case 3A

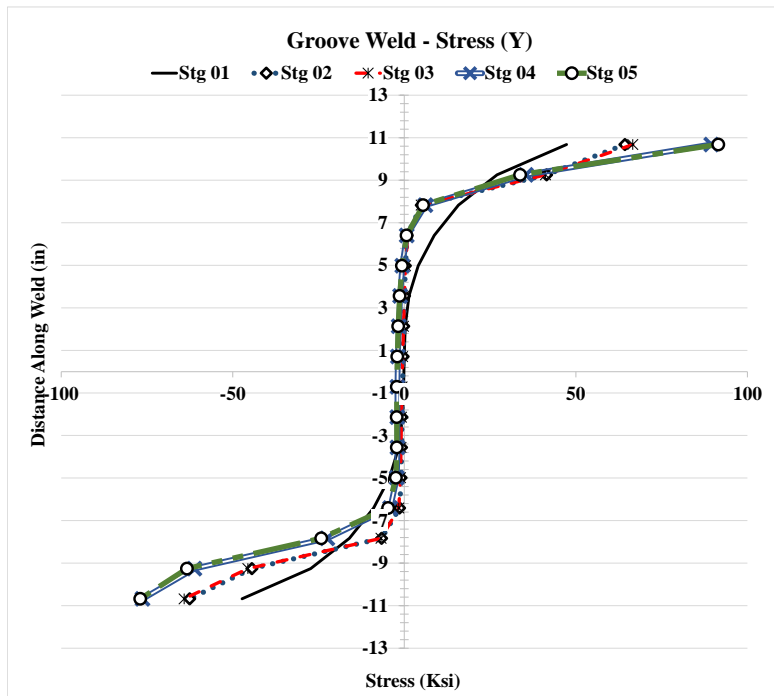
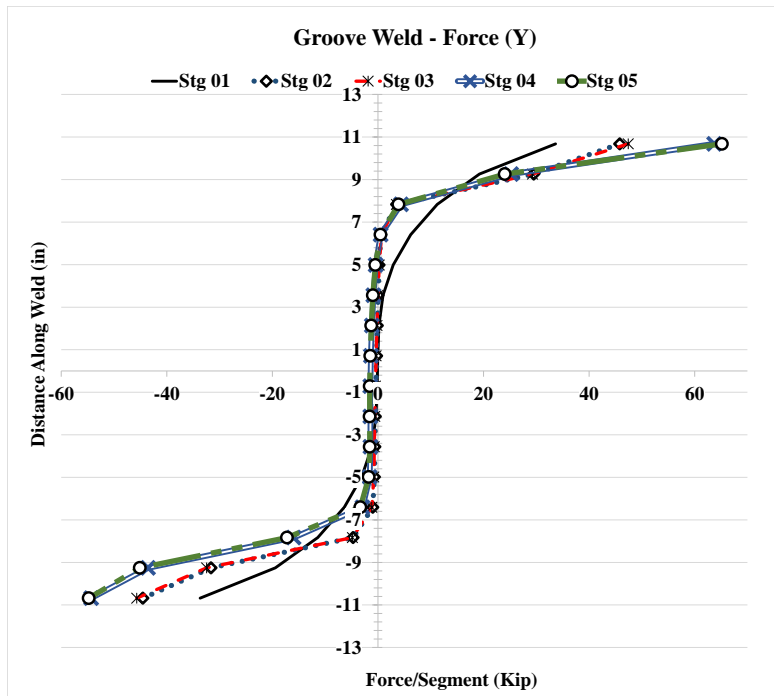


Figure 4.89: Forces and stresses in vertical weld, (Y) Case 3A

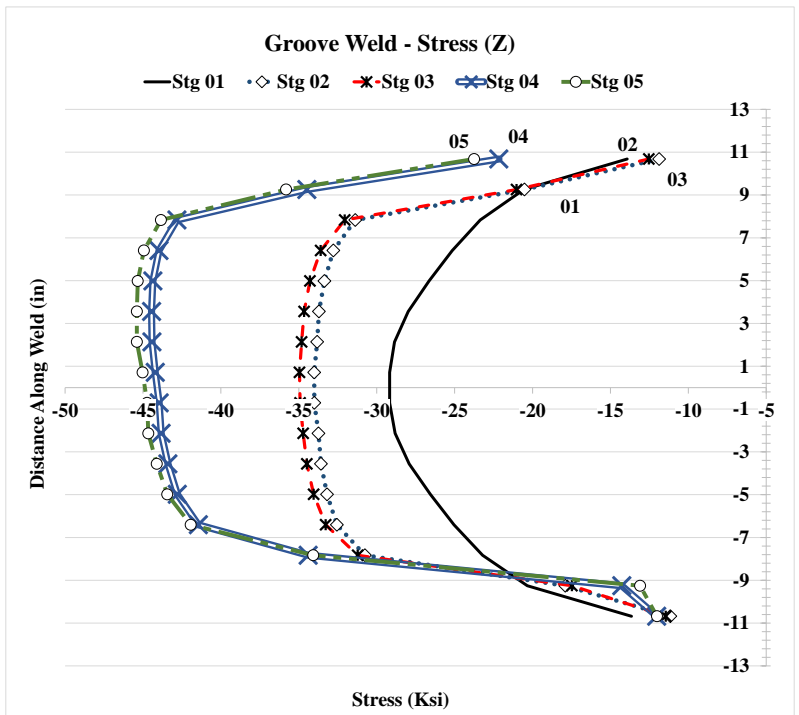
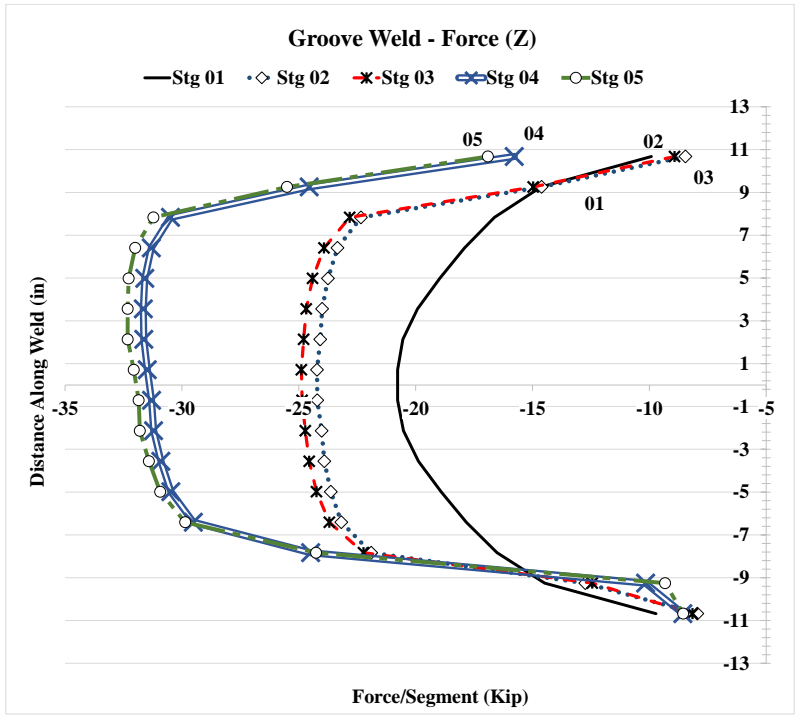


Figure 4.90: Forces and stresses in vertical weld, (Z) Case 3A

### 4.2.9 Analysis Case 3A1

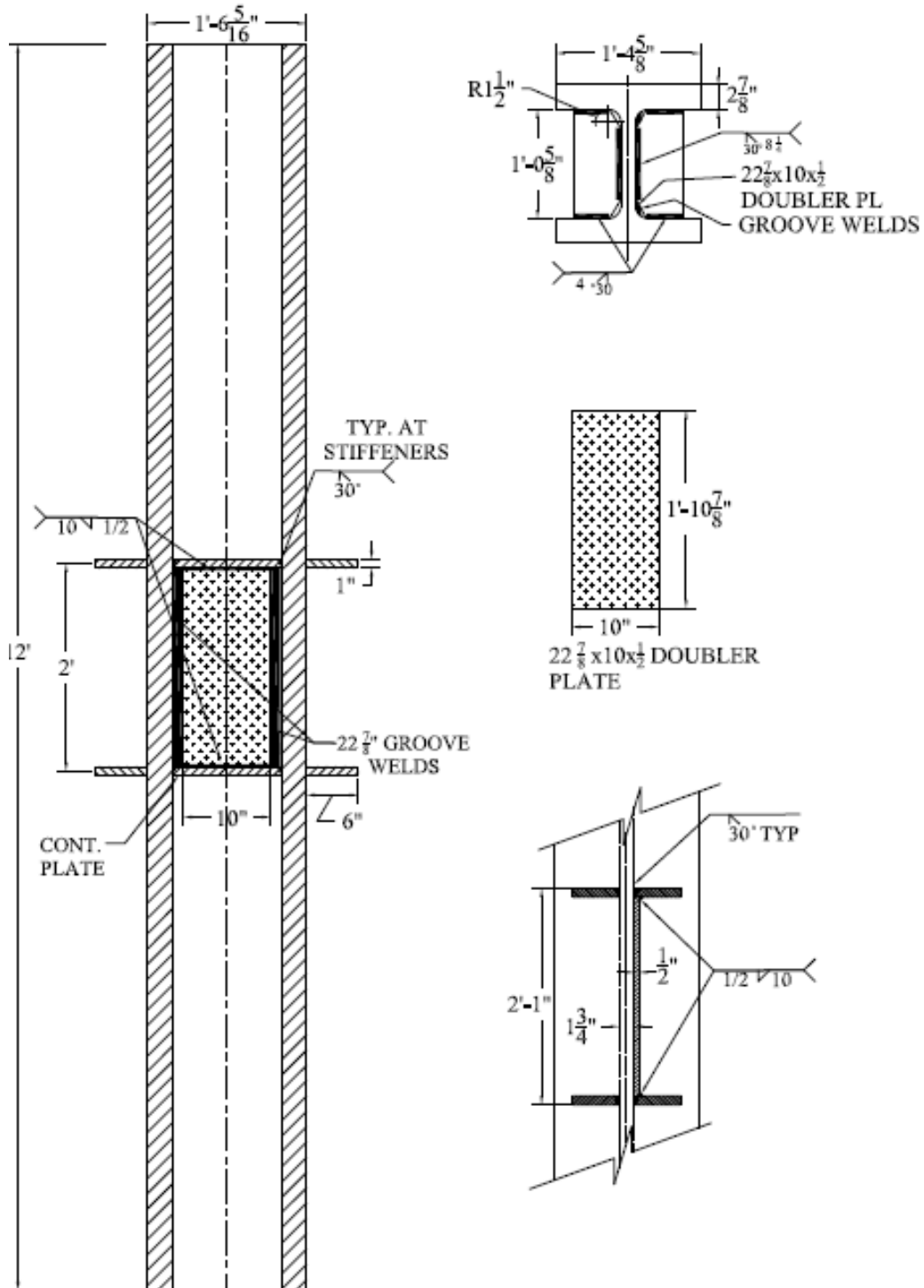


Figure 4.91: Analysis case 3A1



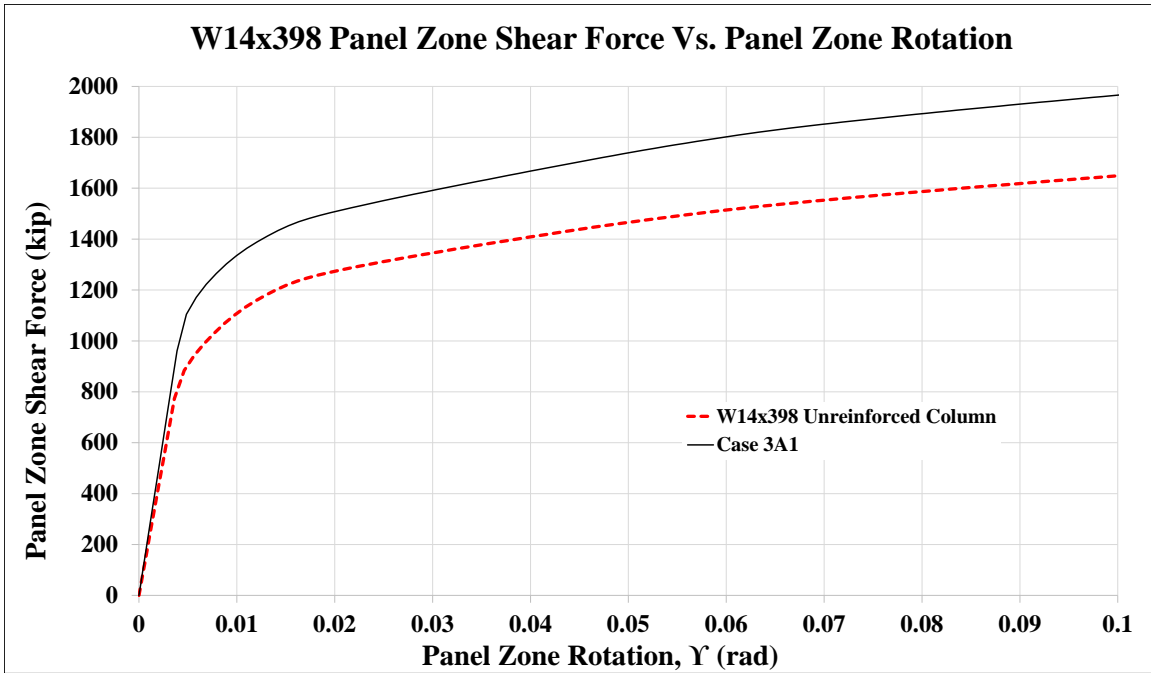


Figure 4.92: Panel zone shear vs. panel zone rotation Case 3A1

Stage	Applied Force/Loading Plate (Kip)	Panel Shear Force (Kip)	% Higher than unreinforced Col.	Panel Zone Rotation (rad)
1	663	1,104	125%	0.005
2	896	1,493	120%	0.018
3	908	1,513	118%	0.021
4	1,141	1,902		0.083
5	1,181	1,968	119%	0.101

Table 4.11: Panel zone shear and force on loading plate Case 3A1

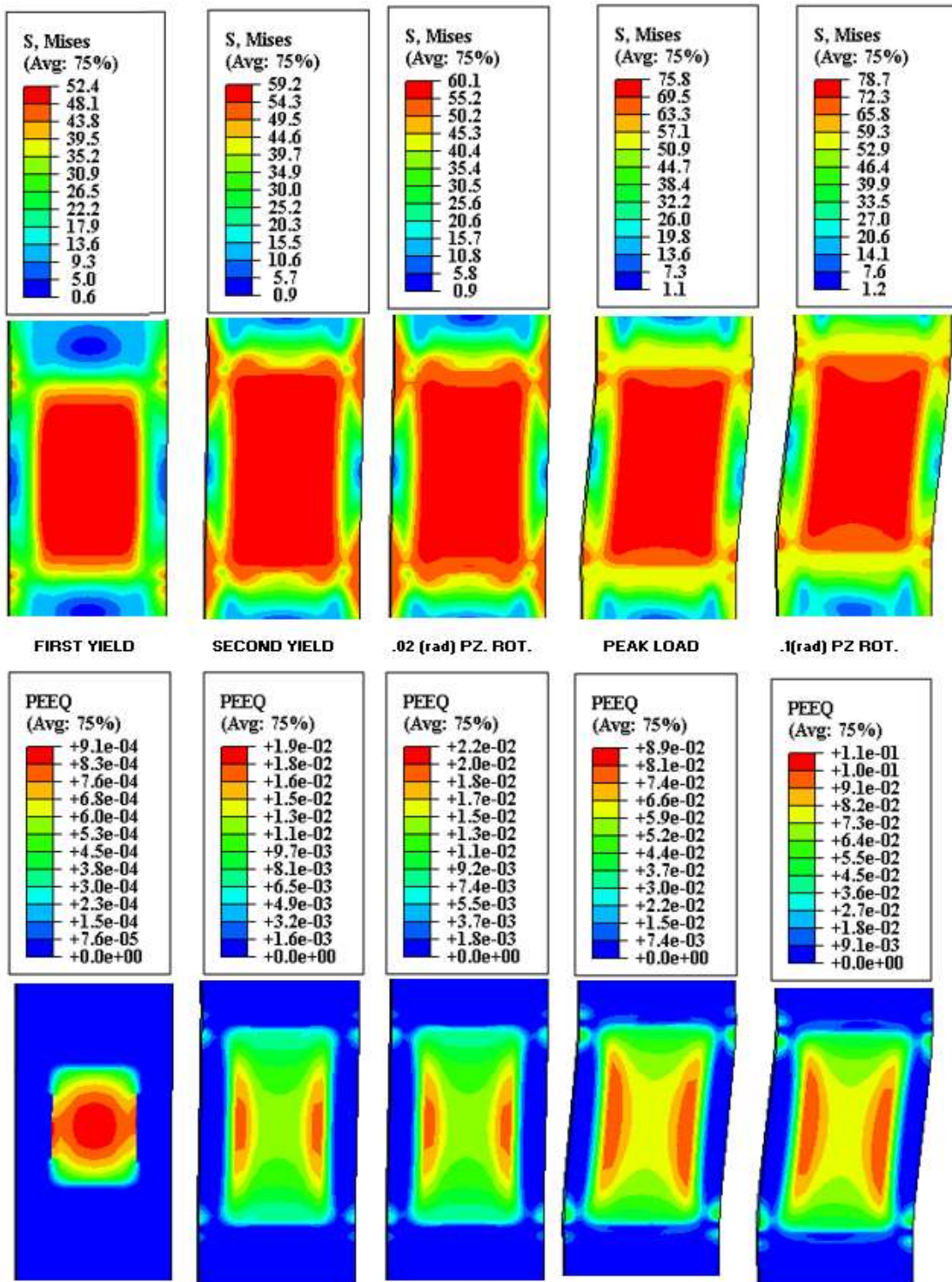
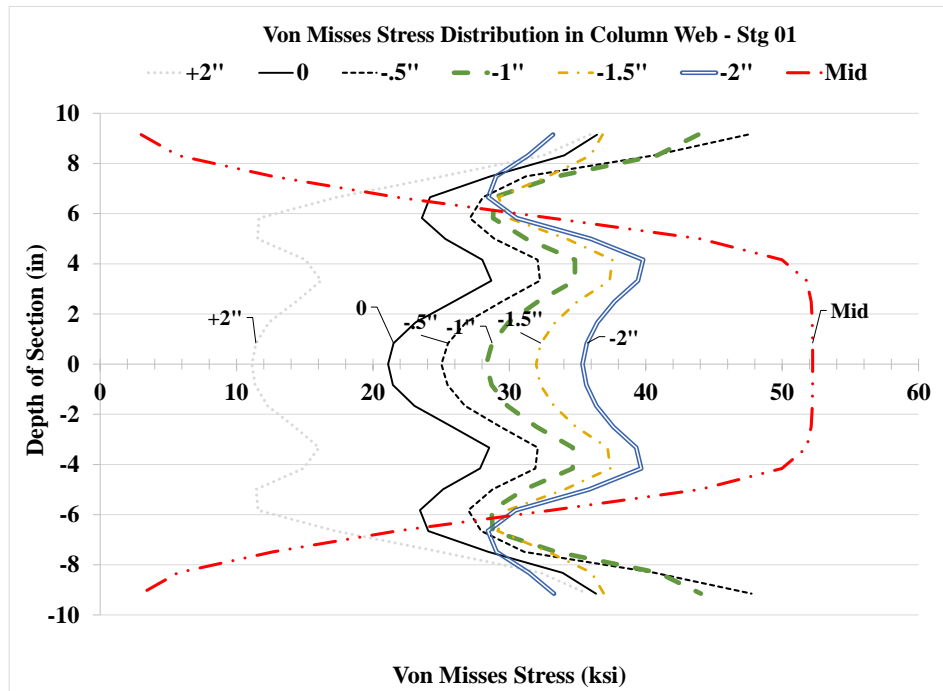
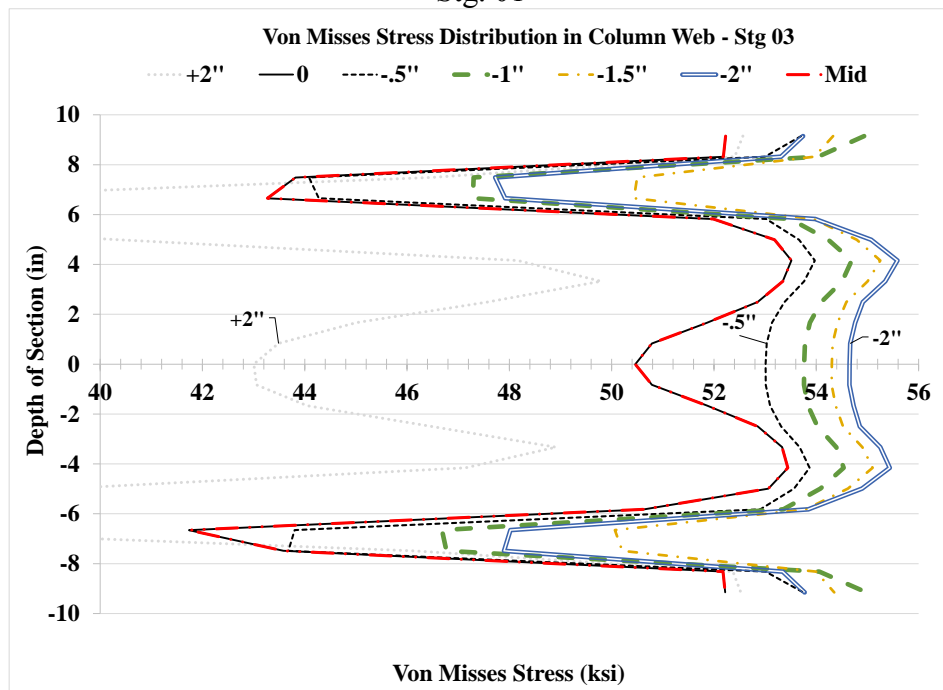


Figure 4.93: VMS and PEEQ in the column Case 3A1

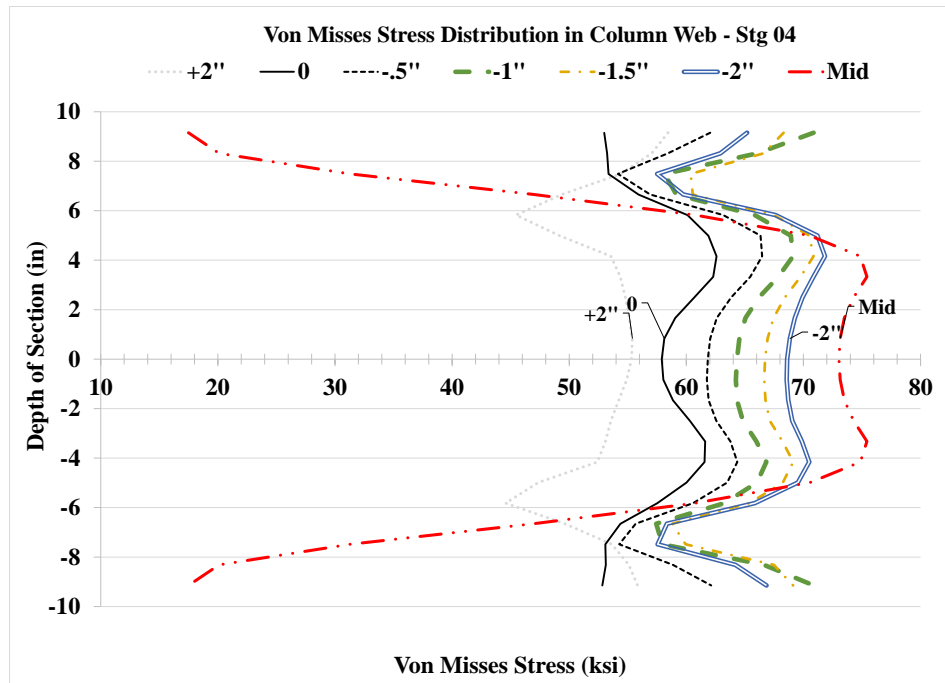


Stg. 01



Stg. 03

Figure 4.94: VMS distribution in column web at different heights Stg. 01-04 Case 3A1



Stg. 04

Figure 4.94: VMS distribution in column web at different heights Stg. 01-04 Case 3A1

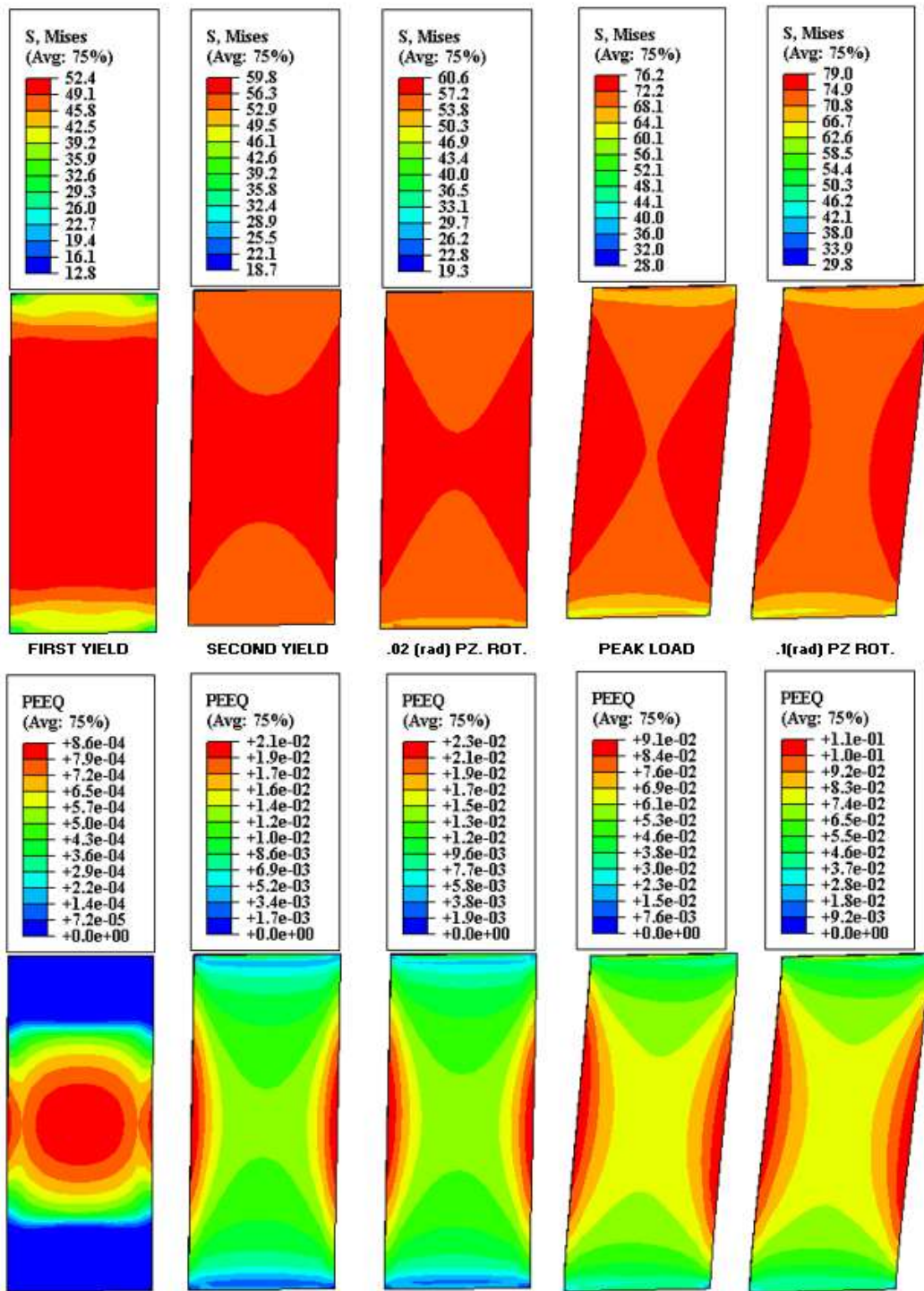


Figure 4.95: VMS and PEEQ in the DP Case 3A1

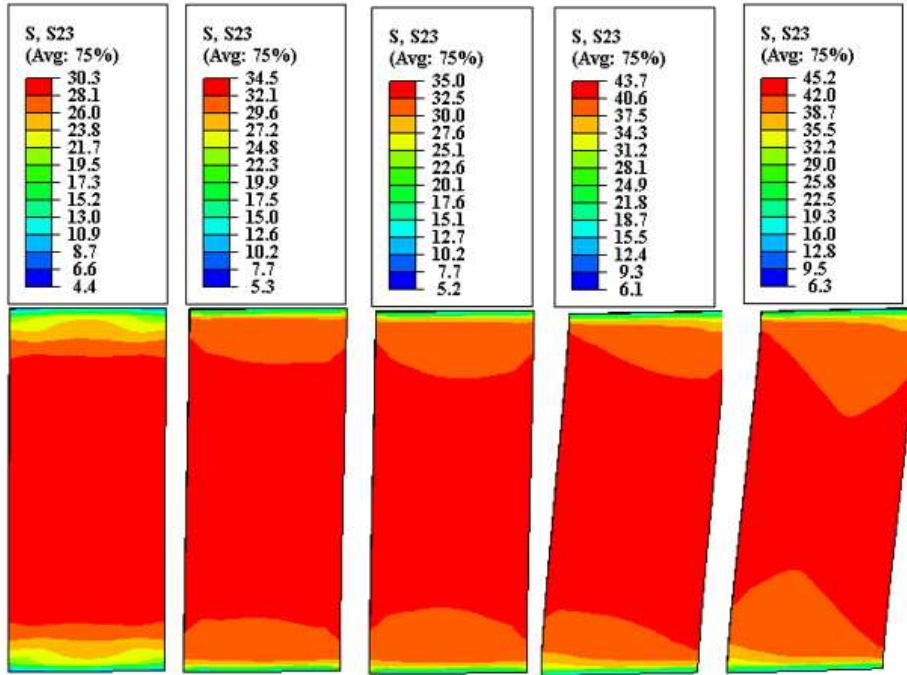


Figure 4.96: Shear stress, S23 in the DP Case 3A1

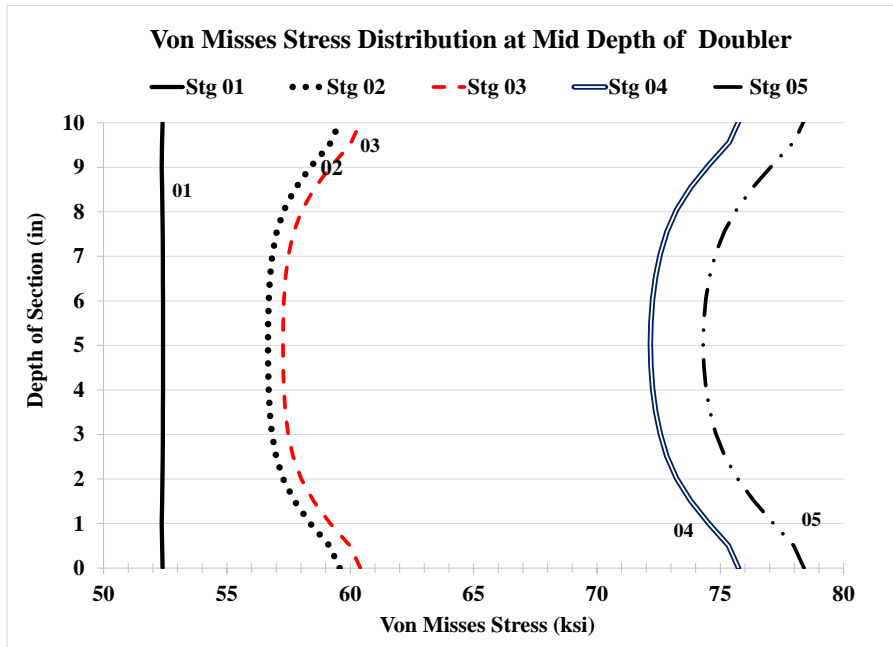


Figure 4.97: VMS distribution at mid-depth of DP Case 3A1

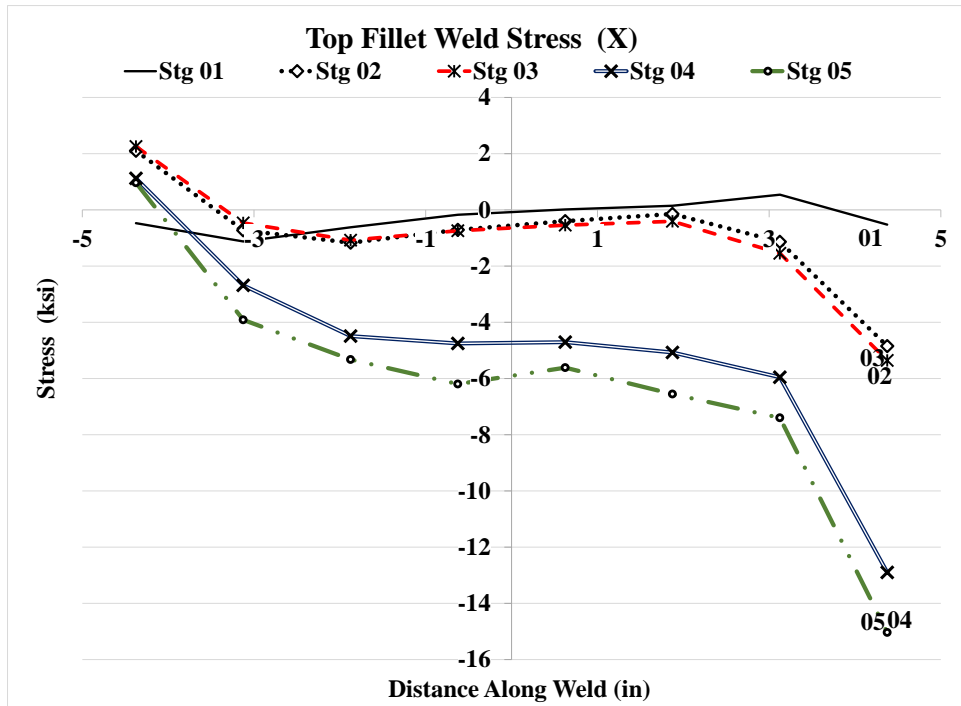
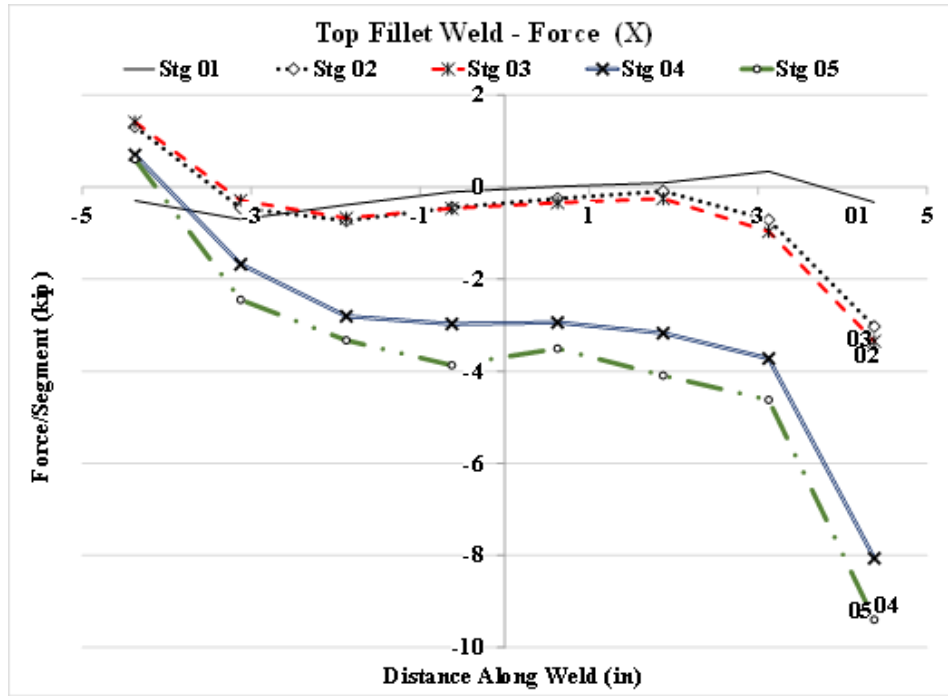


Figure 4.98: Forces and stresses in horizontal weld, (X) Case 3A1

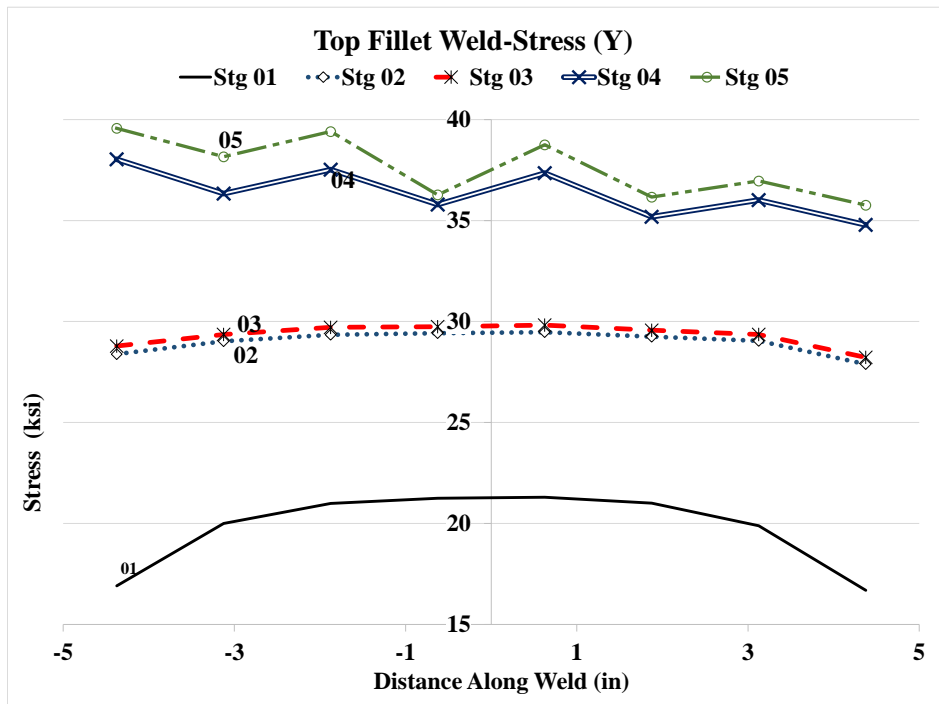
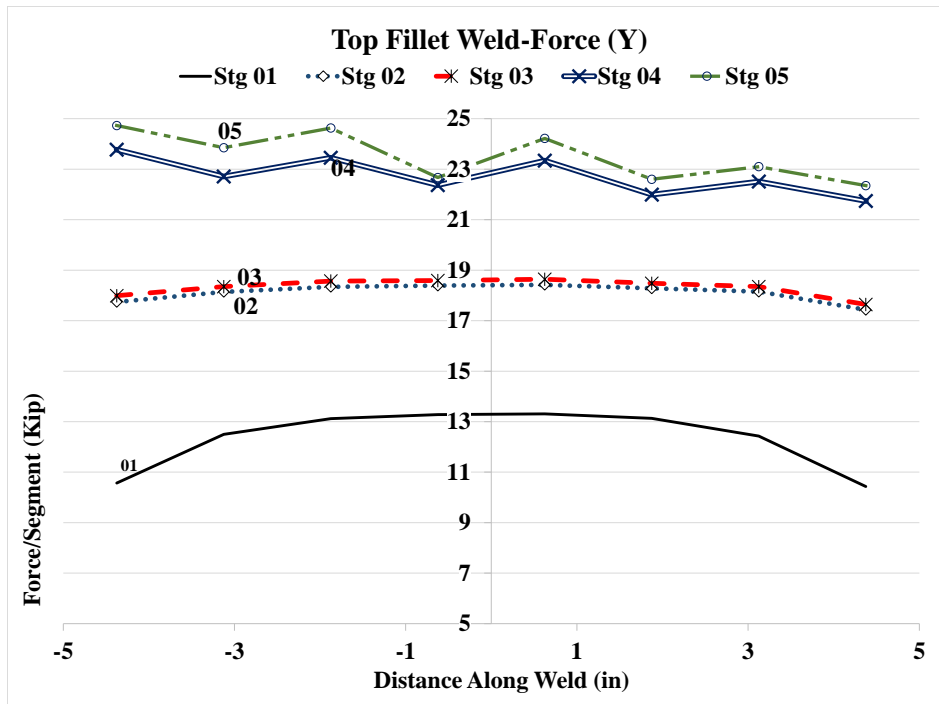


Figure 4.99: Forces and stresses in horizontal weld, (Y) Case 3A1



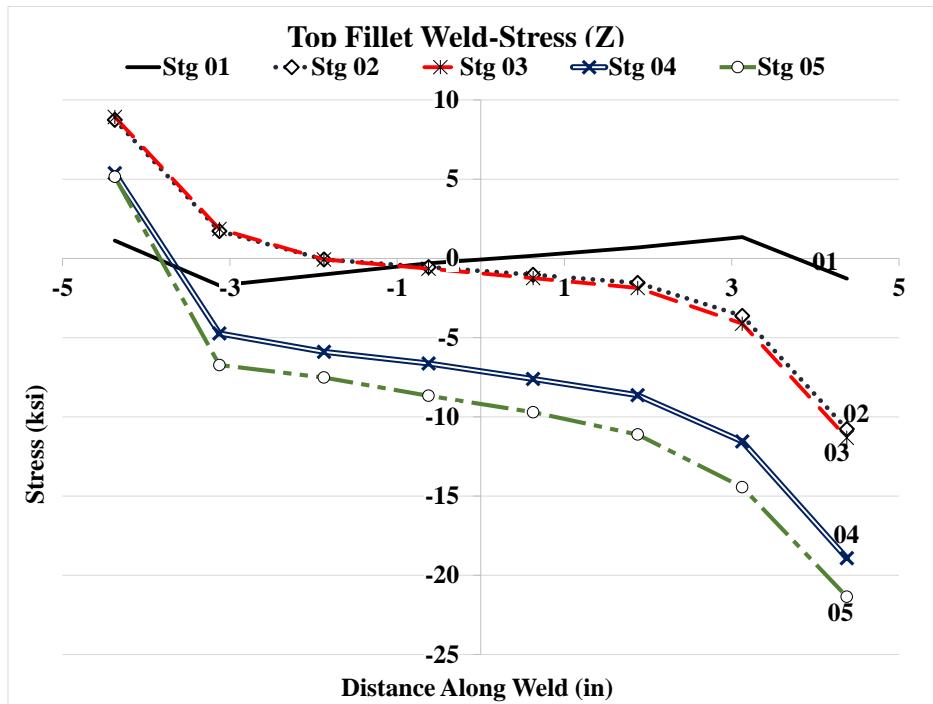
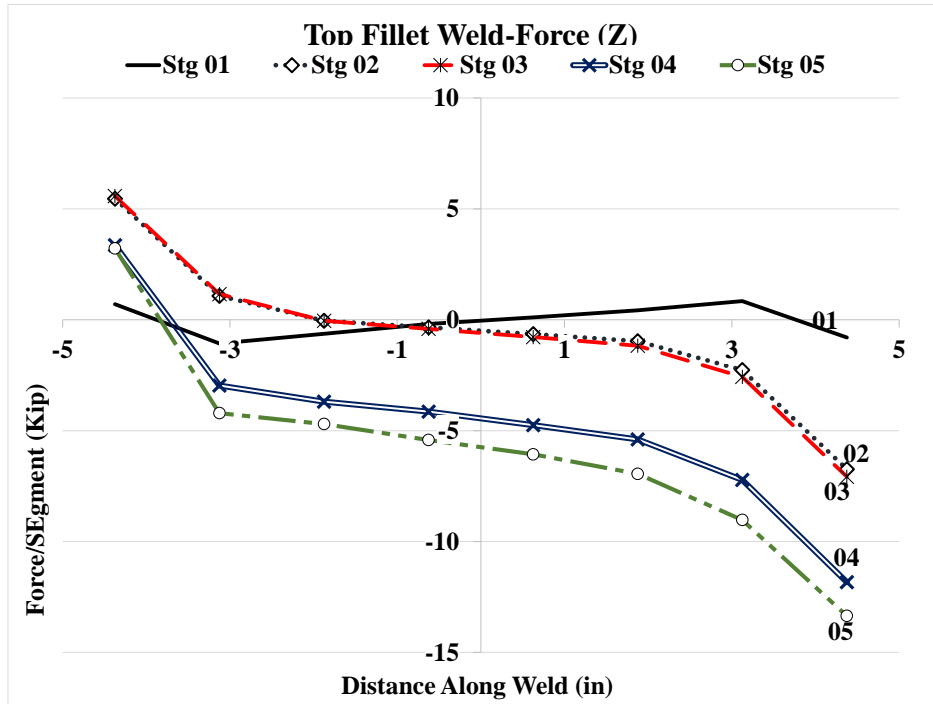


Figure 4.100: Forces and stresses in horizontal weld, (Z) Case 3A1

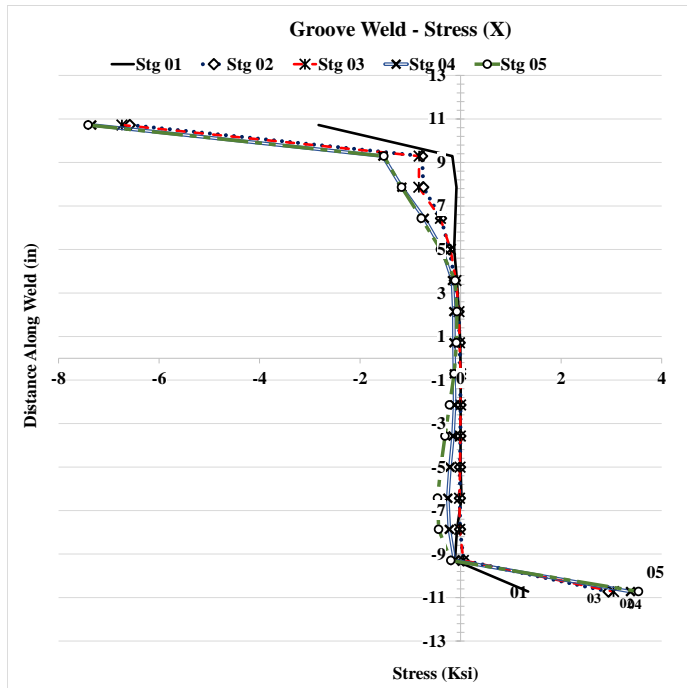
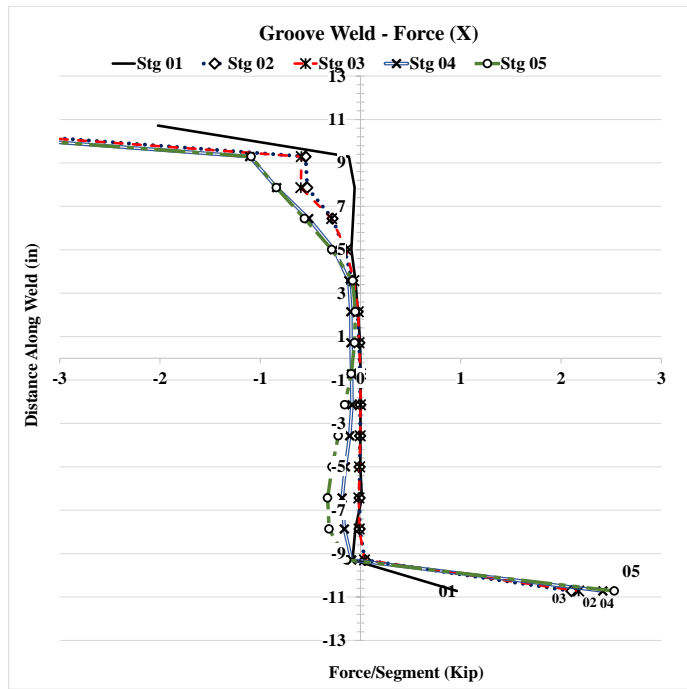


Figure 4.101: Forces and stresses in vertical weld, (X) Case 3A1

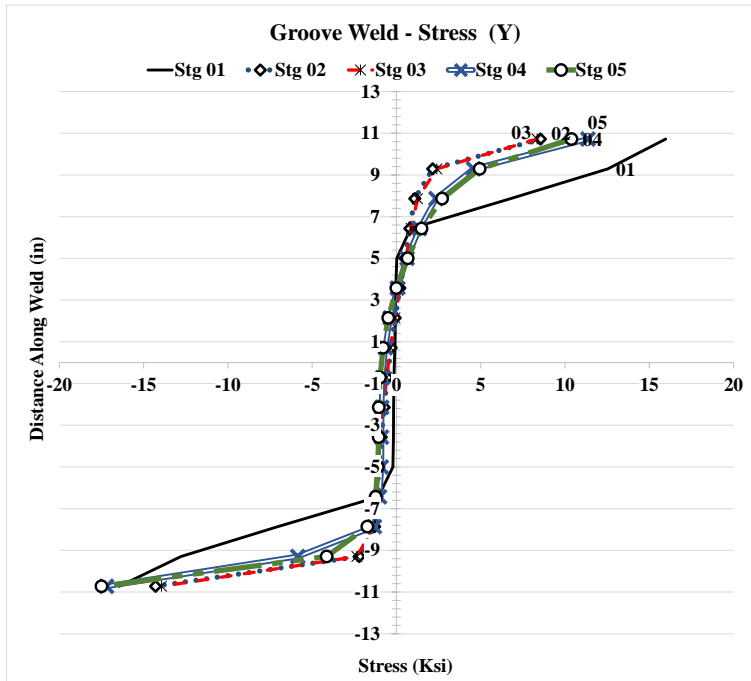
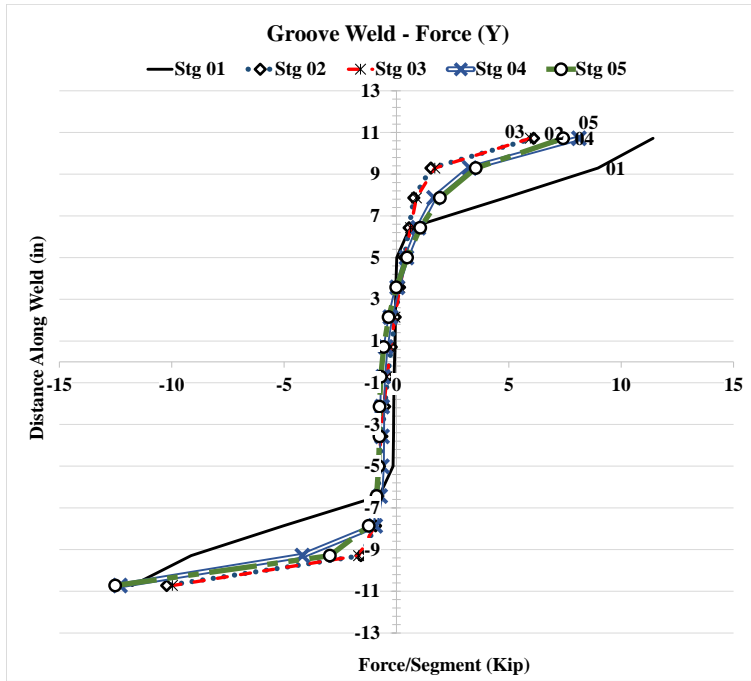


Figure 4.102: Forces and stresses in vertical weld, (Y) Case 3A1

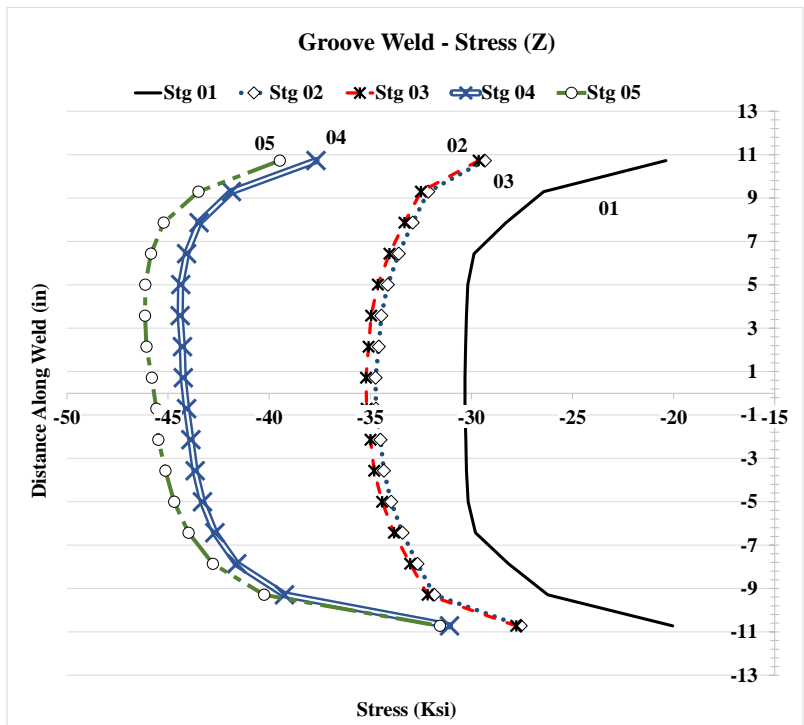
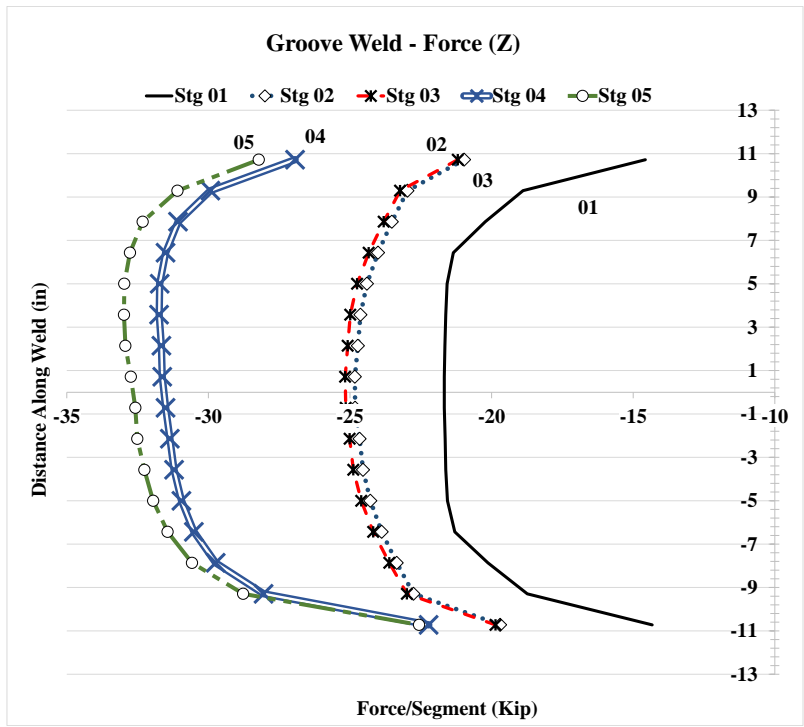


Figure 4.103: Forces and stresses in vertical weld, (Z) Case 3A1

### 4.2.10 Analysis Case 3C

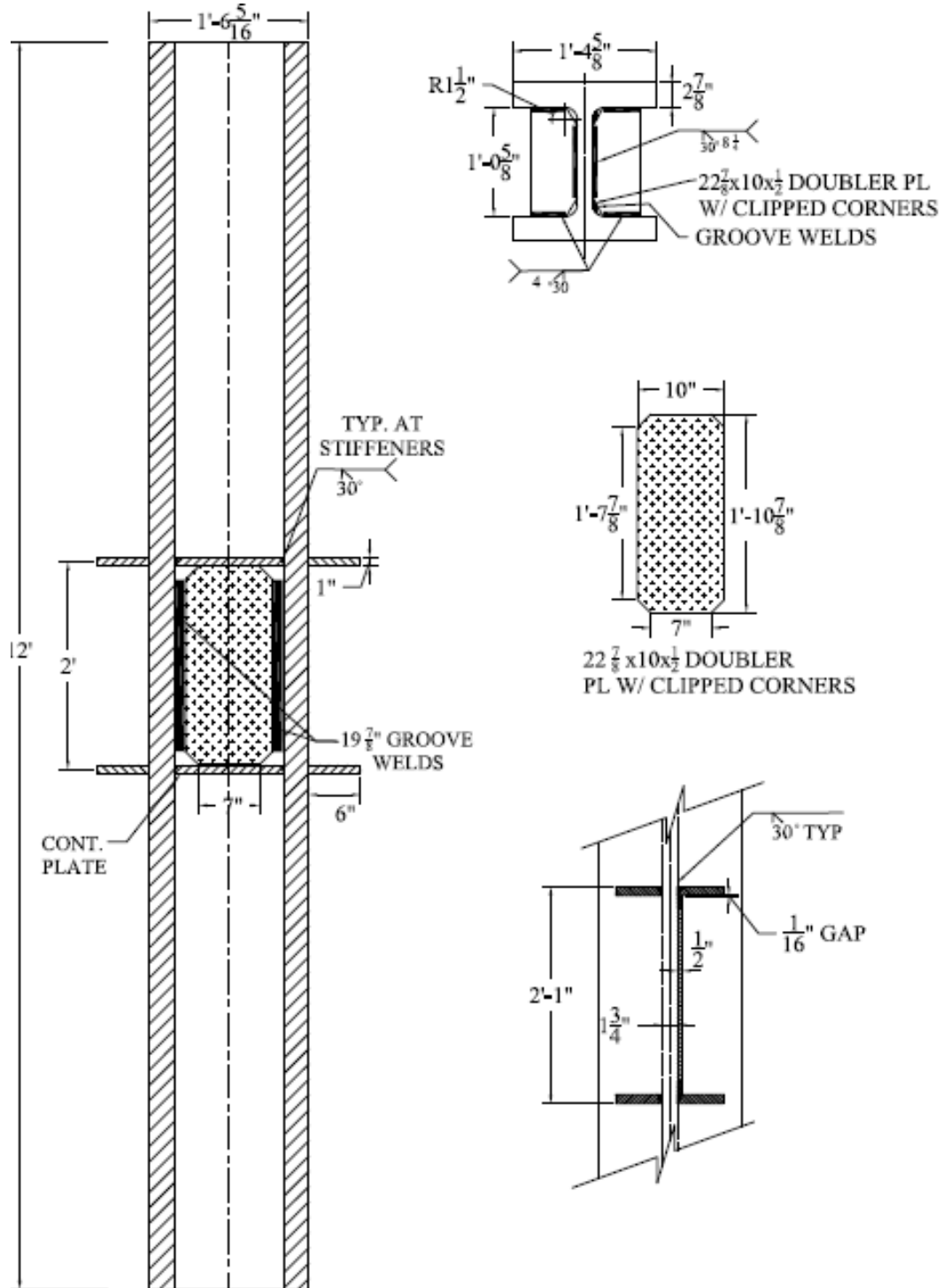


Figure 4.104: Analysis case 3C

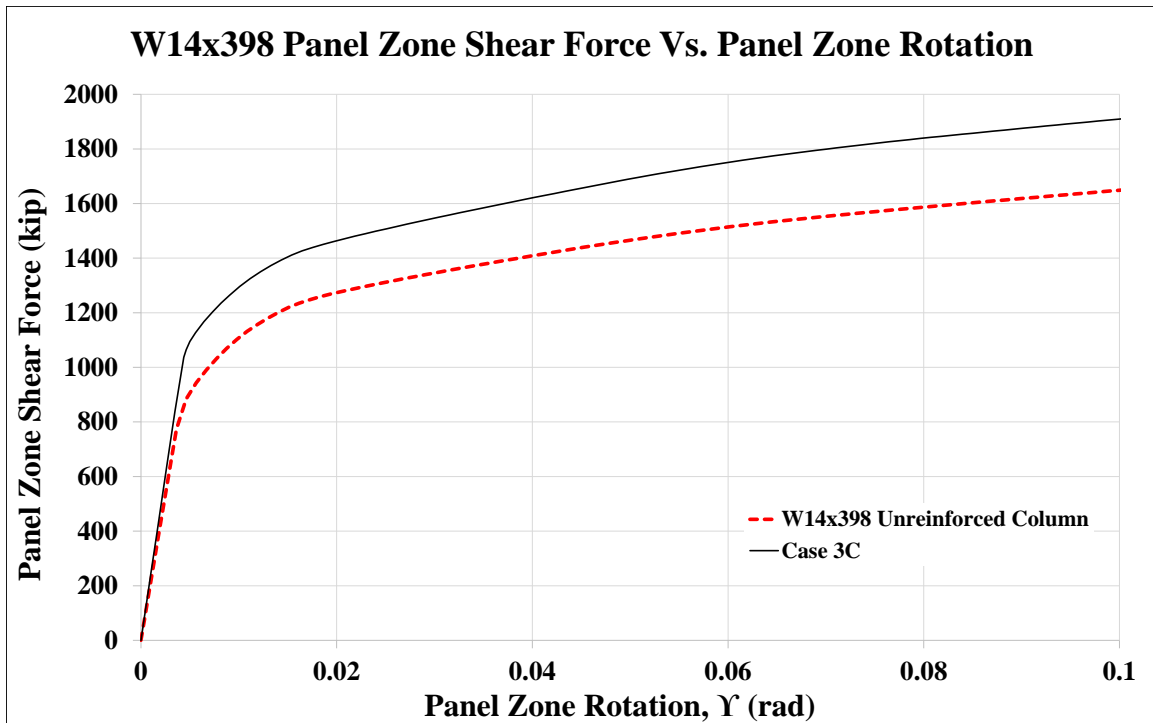


Figure 4.105: Panel zone shear vs. panel zone rotation Case 3C

Stage	Applied Force/Loading Plate (Kip)	Panel Shear Force (Kip)	% Higher than unreinforced Col.	Panel Zone Rotation (rad)
1	622	1,037	117%	0.004
2	856	1,427	114%	0.016
3	877	1,461	114%	0.020
4	1,144	1,906		0.099
5	1,146	1,909	116%	0.100

Table 4.12: Panel zone shear and force on loading plate Case 3C

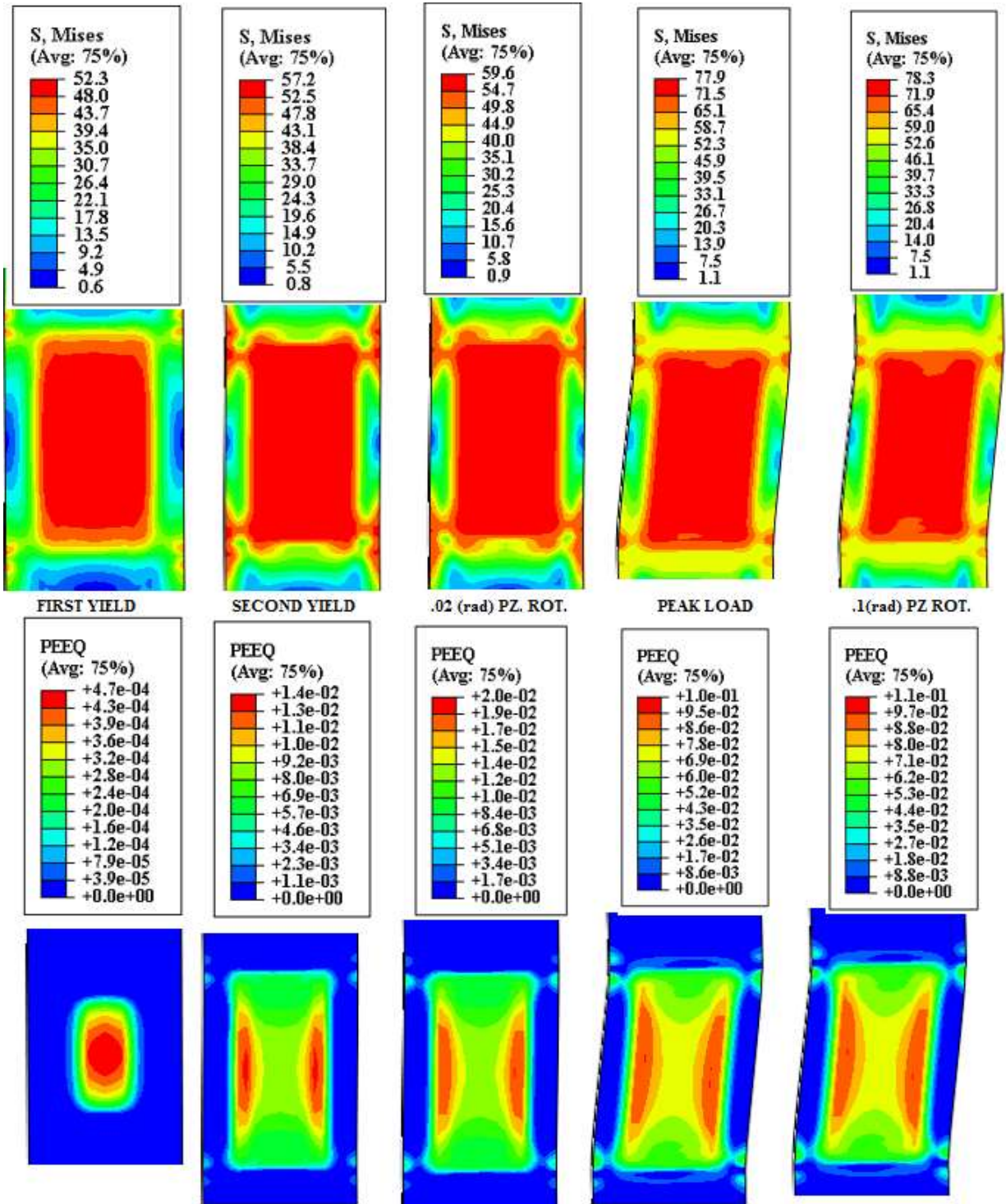
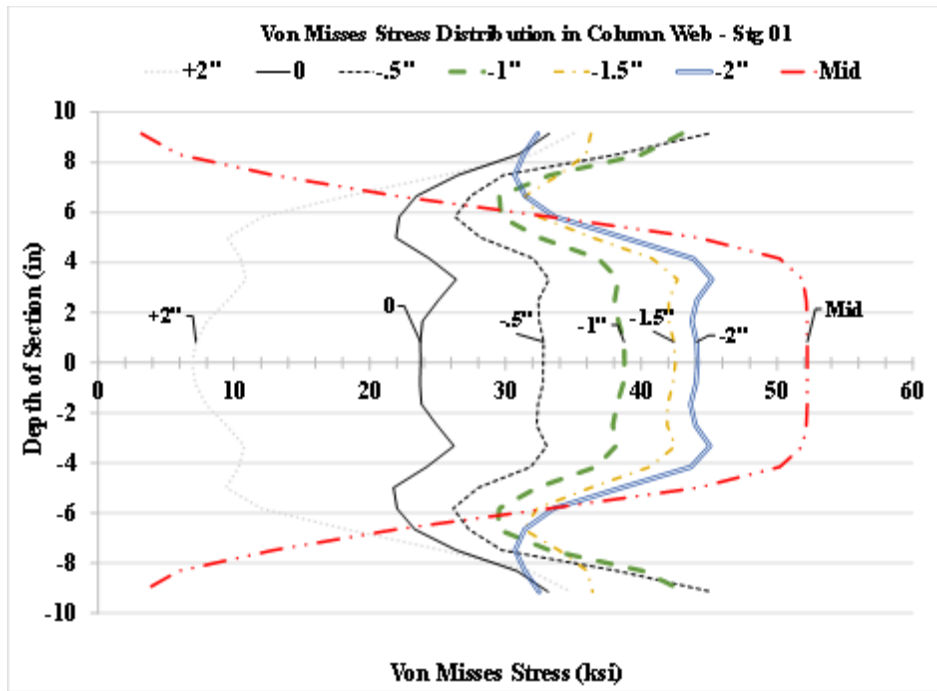
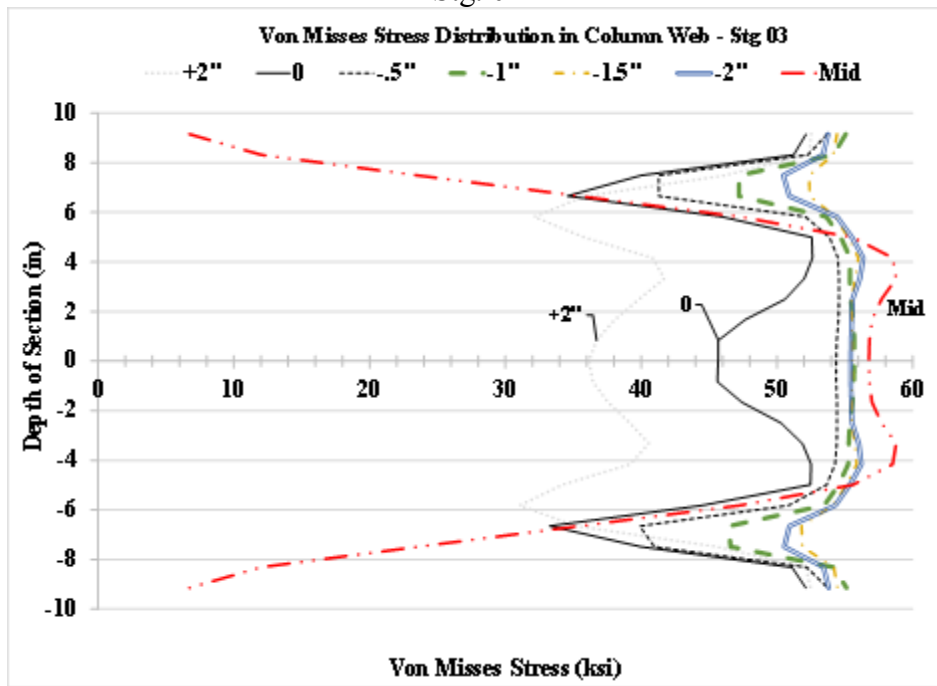


Figure 4.106: VMS and PEEQ in the column Case 3C



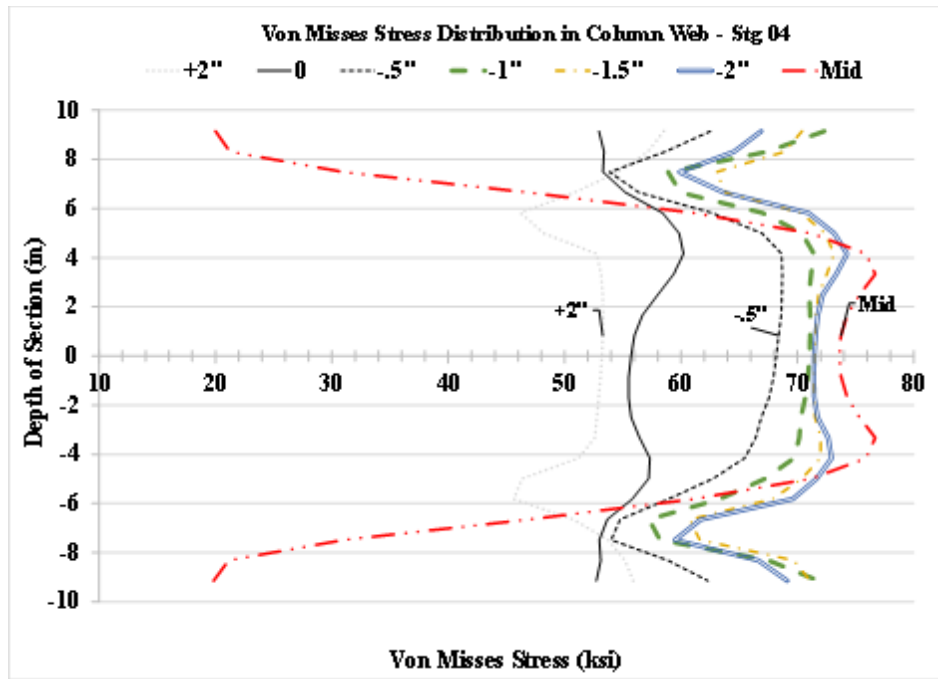
Stg. 01



Stg. 02

Figure 4.107: VMS distribution in column web at different heights Stg. 01-03 Case 3C





Stg .03

Figure 4.107: VMS distribution in column web at different heights Stg. 01-03 Case 3C

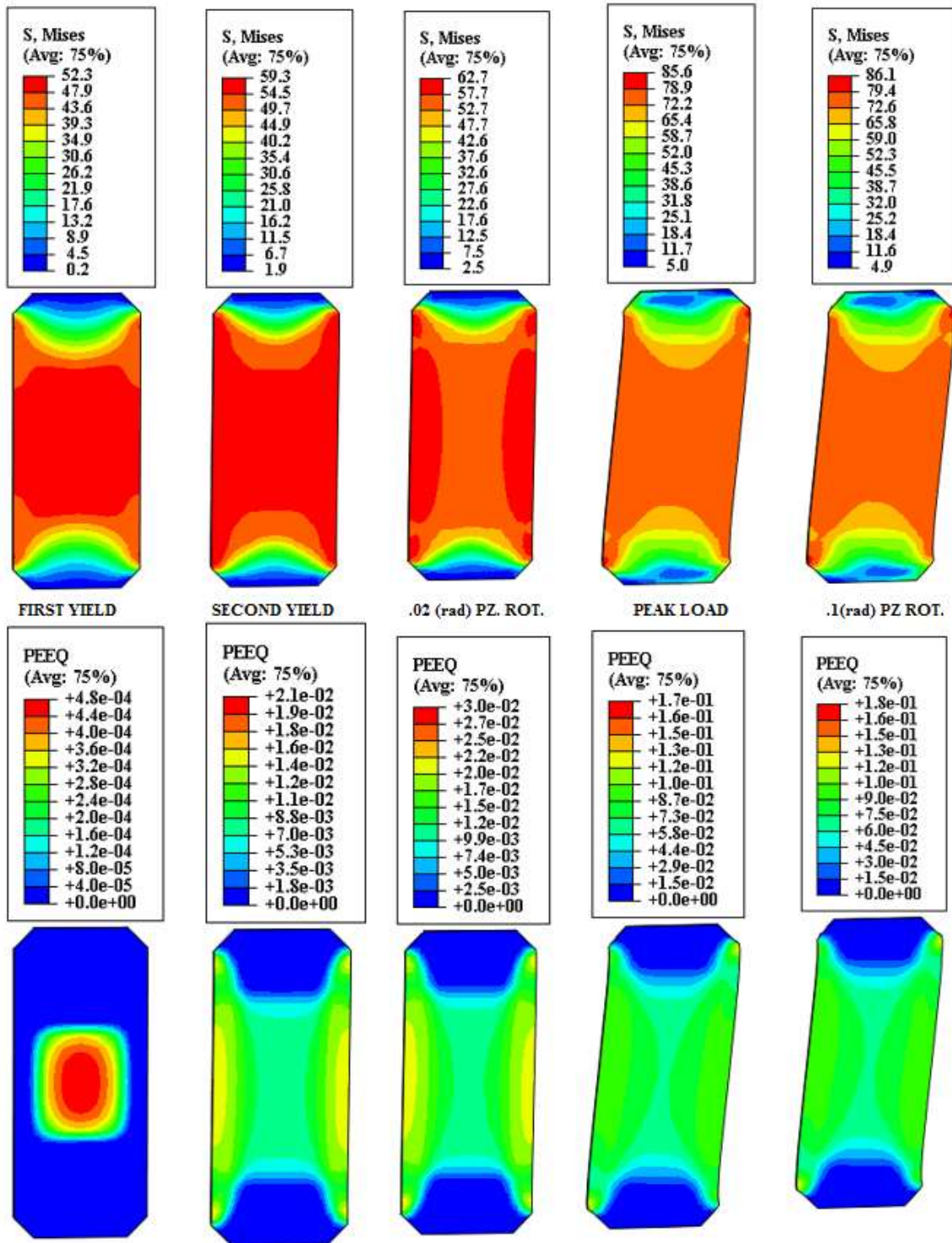


Figure 4.108: VMS and PEEQ in the DP Case 3C

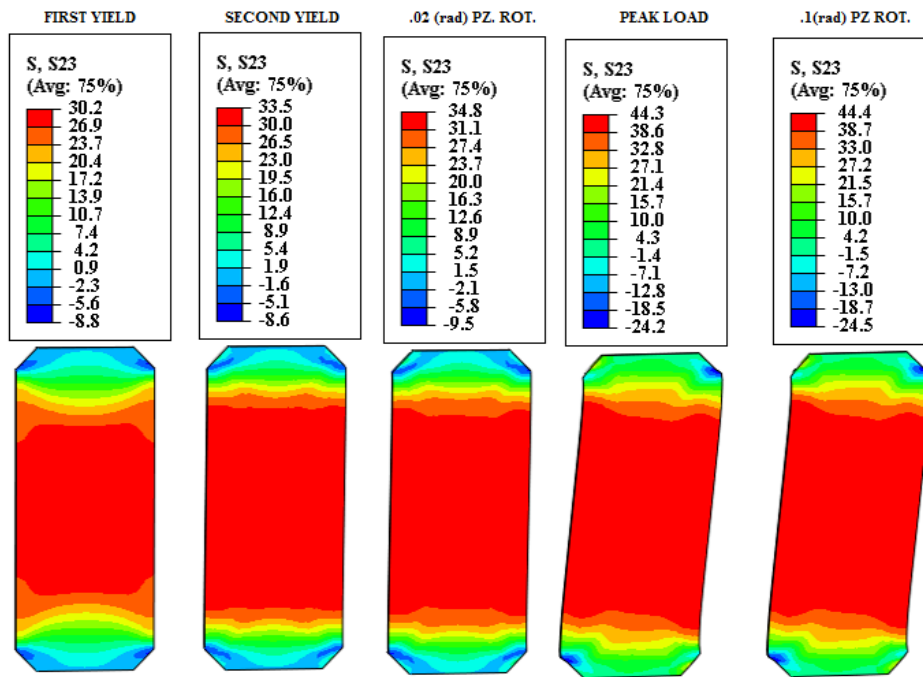


Figure 4.109: Shear stress, S23 in the DP Case 3C

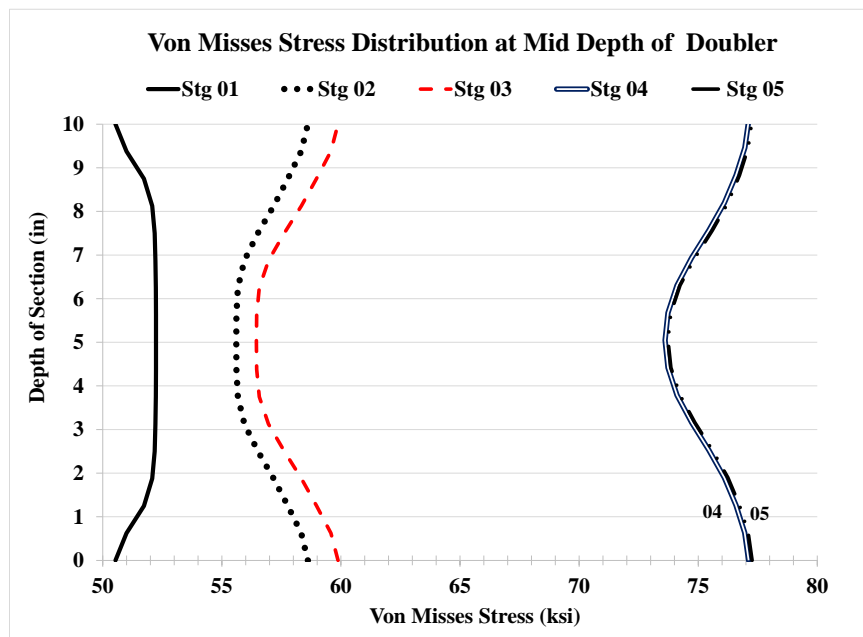


Figure 4.110: VMS distribution at mid-depth of DP Case 3C

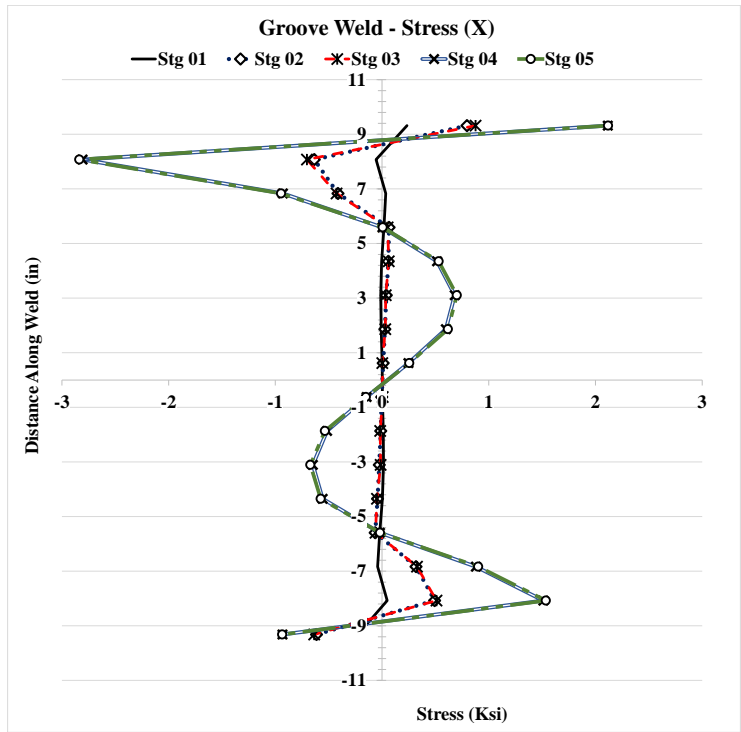
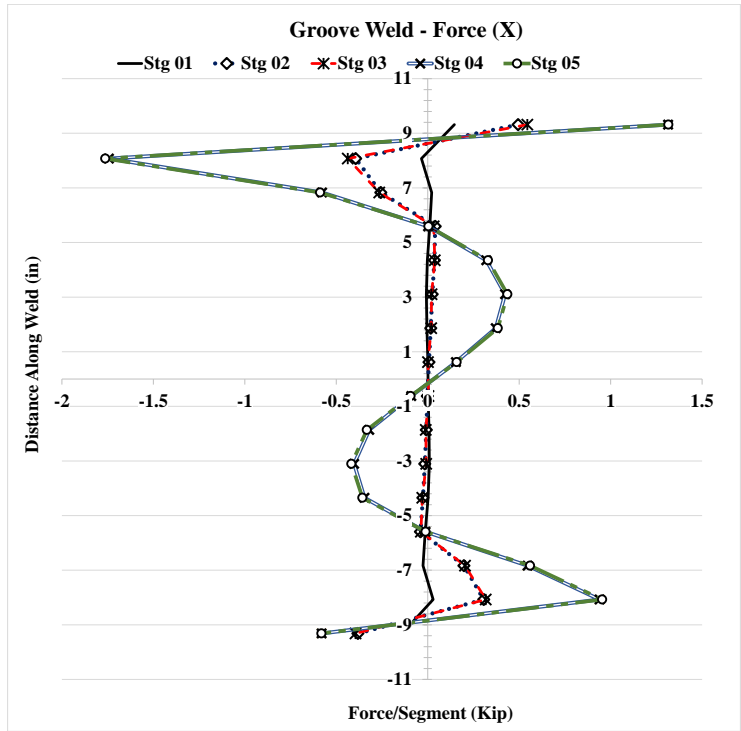


Figure 4.111: Forces and stresses in vertical weld, (X) Case 3C

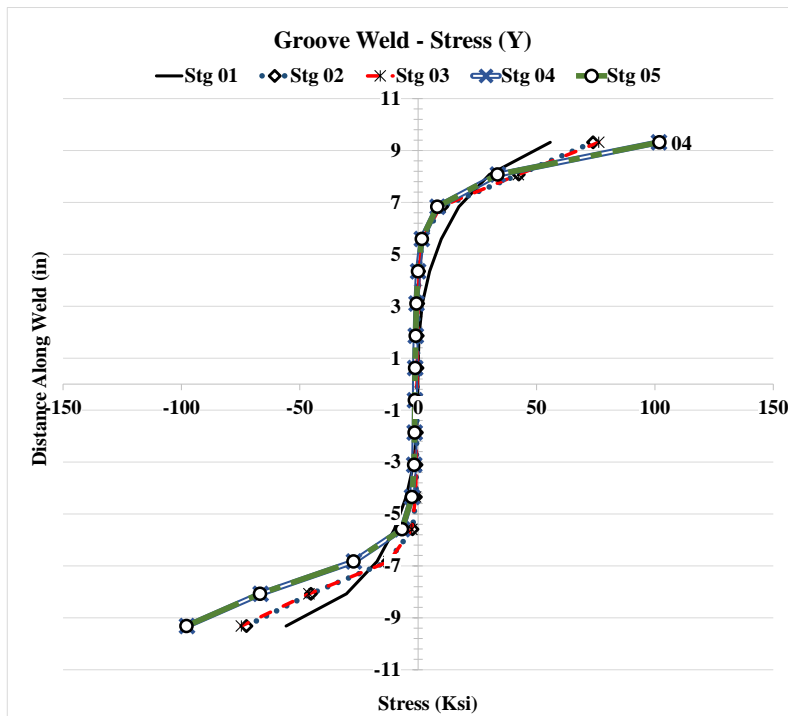
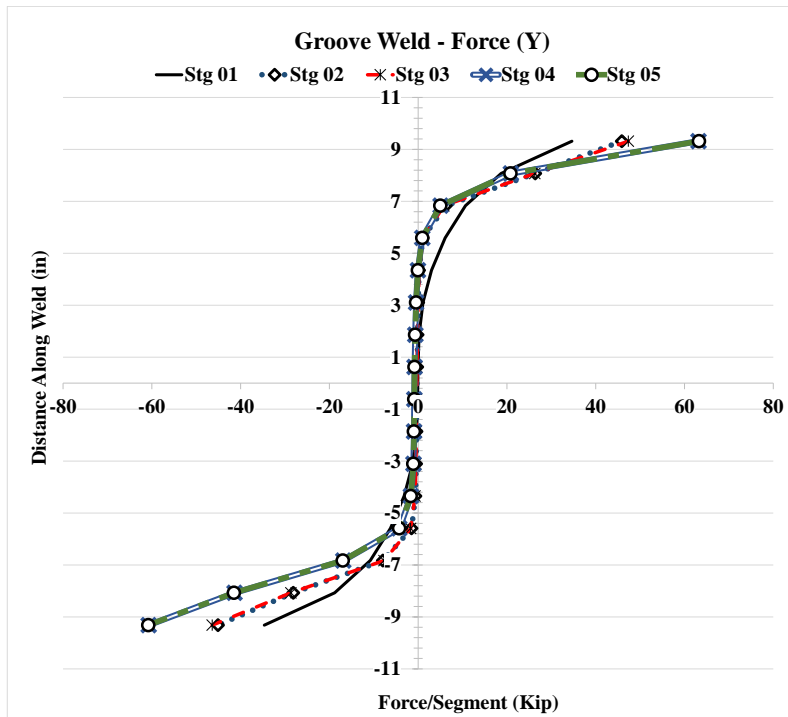


Figure 4.112: Forces and stresses in vertical weld, (Y) Case 3C

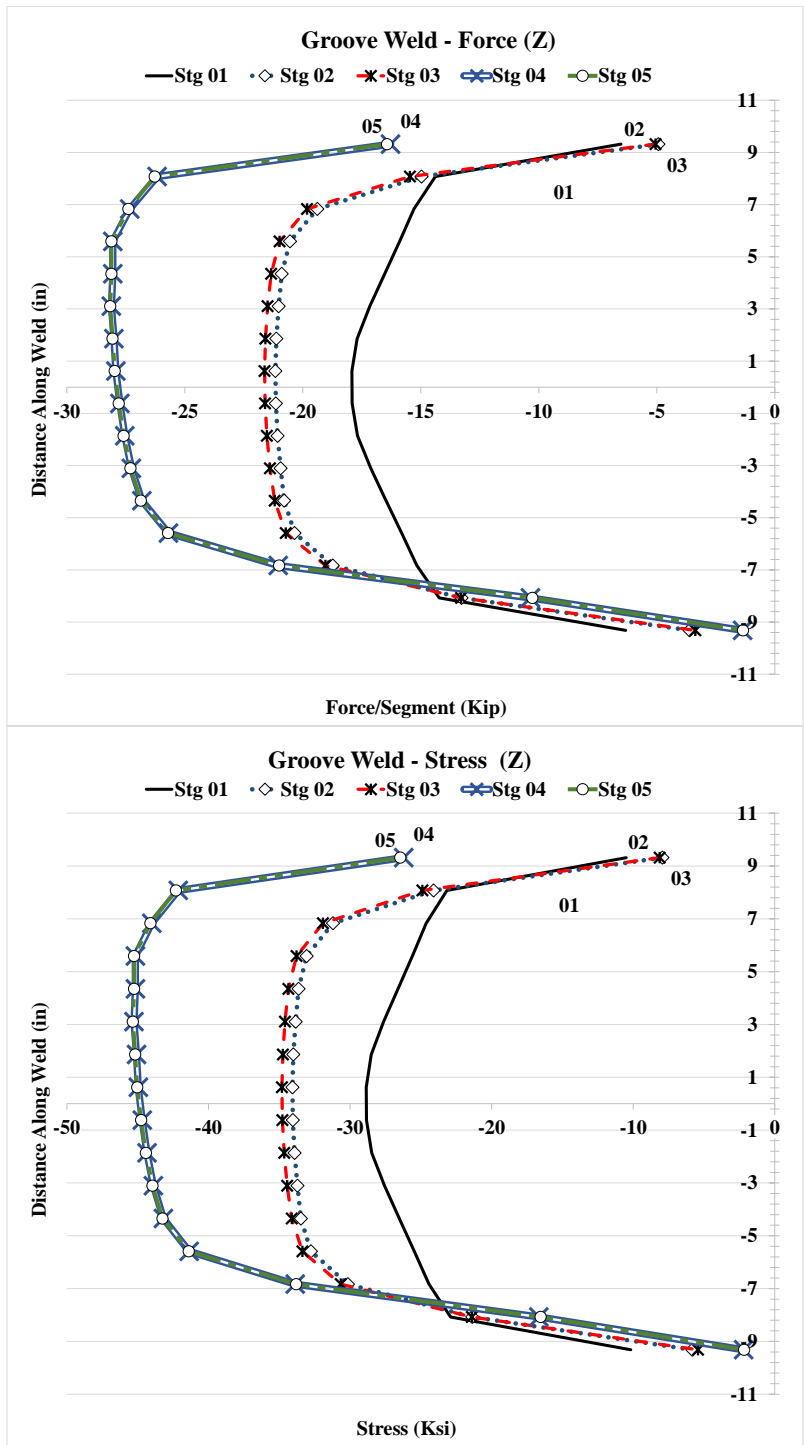


Figure 4.113: Forces and stresses in vertical weld, (Z) Case 3C

### 4.2.11 Analysis Case 3C1

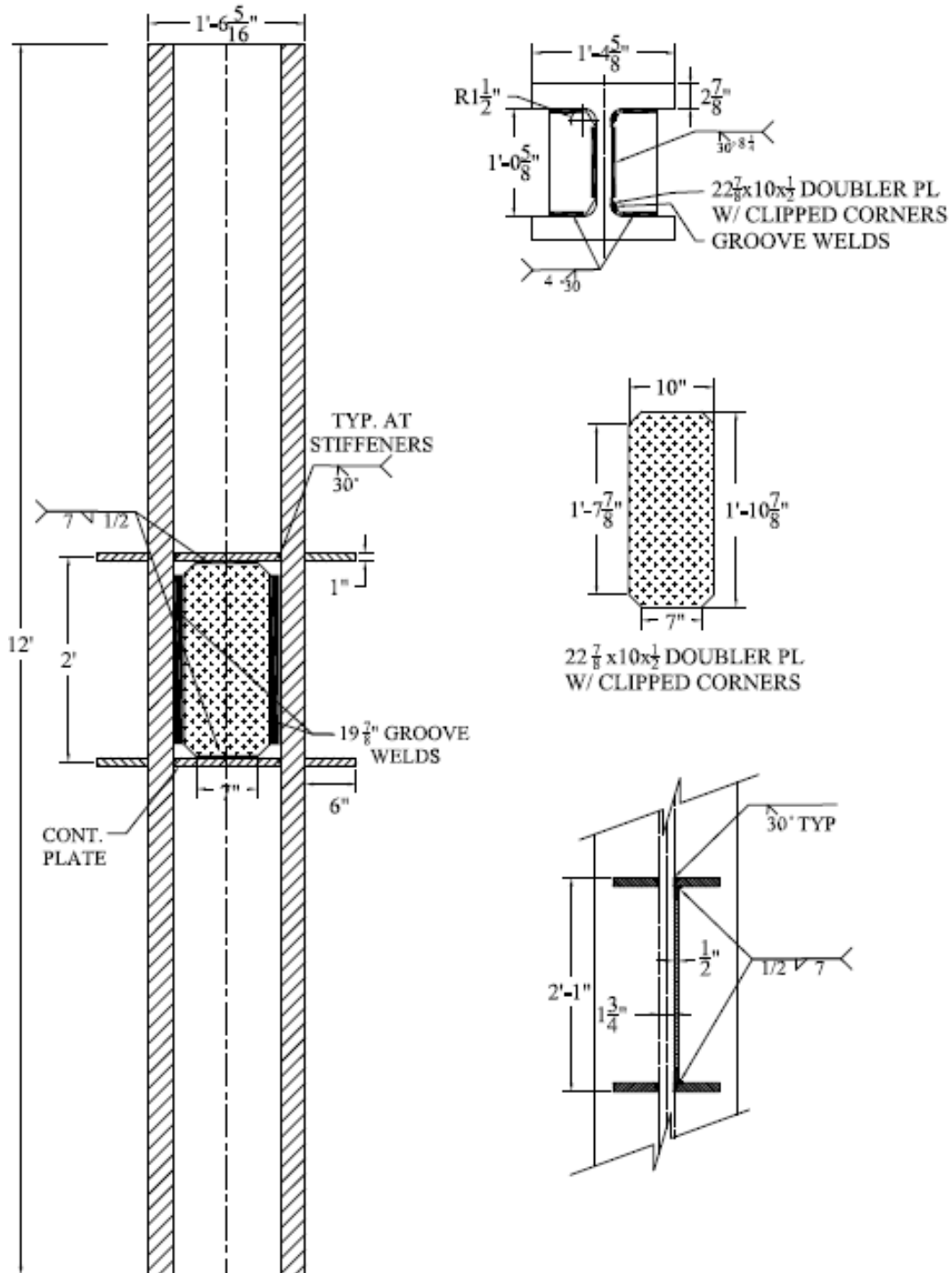


Figure 4.114: Analysis case 3C1

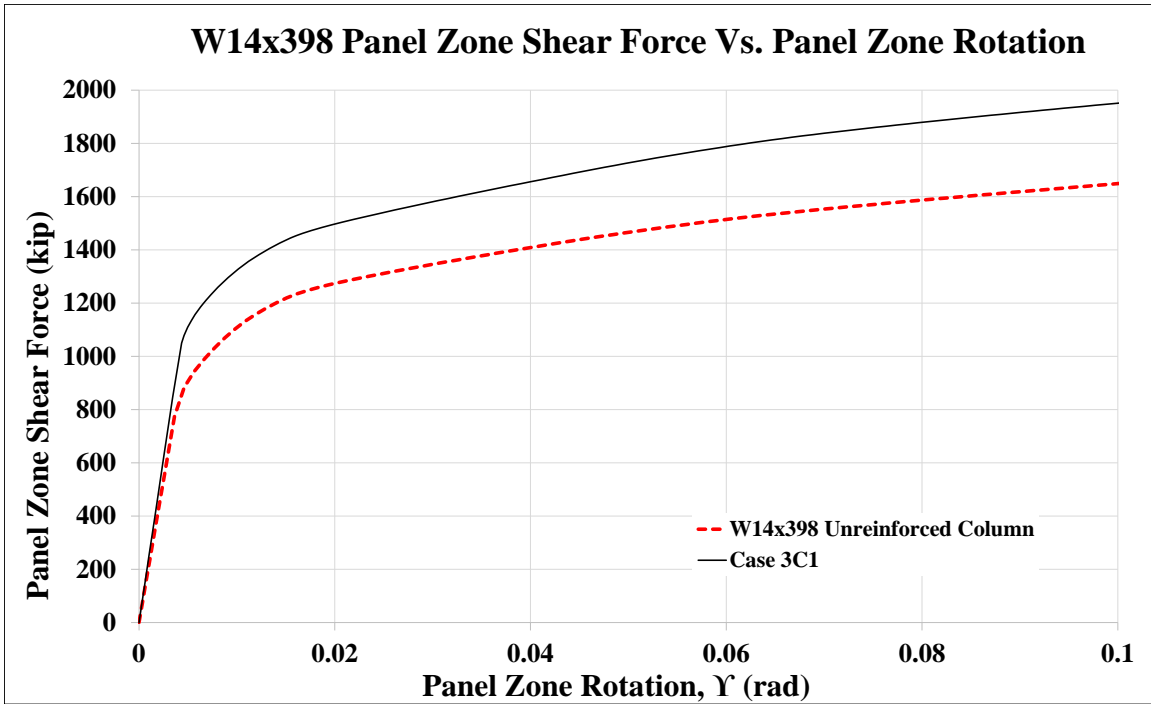


Figure 4.115: Panel zone shear vs. panel zone rotation Case 3C1

Stage	Applied Force/Loading Plate (Kip)	Panel Shear Force (Kip)	% Higher than unreinforced Col.	Panel Zone Rotation (rad)
1	630	1,050	119%	0.004
2	877	1,462	117%	0.017
3	897	1,495	117%	0.020
4	1,141	1,902		0.086
5	1,173	1,954	119%	0.101

Table 4.13: Panel zone shear and force on loading plate Case 3C1



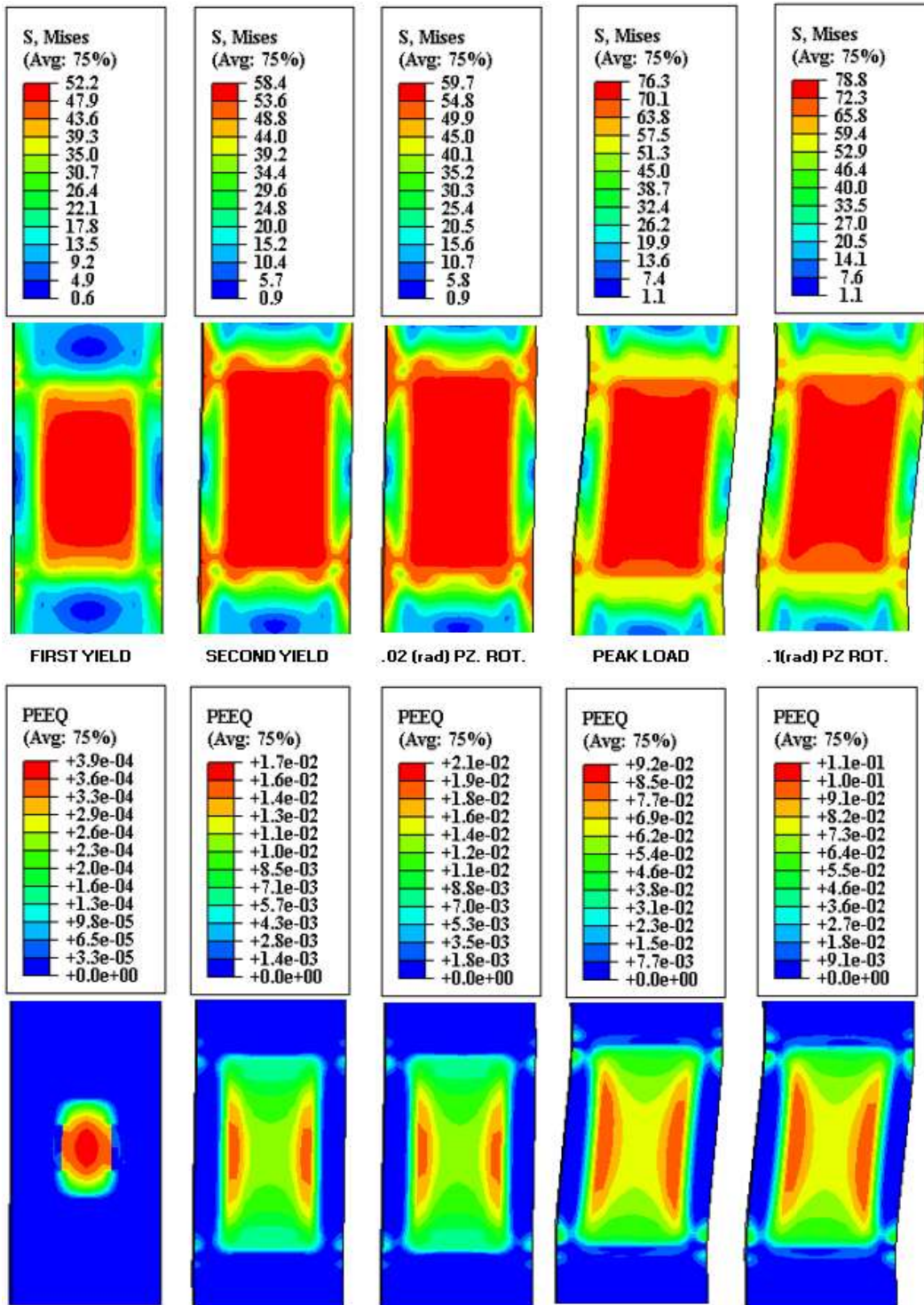
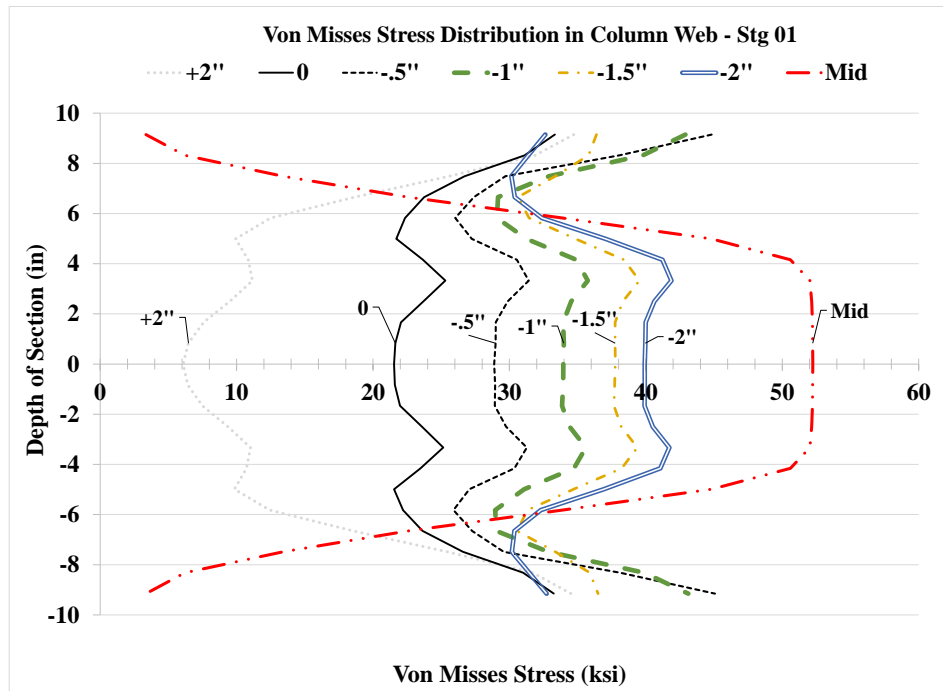
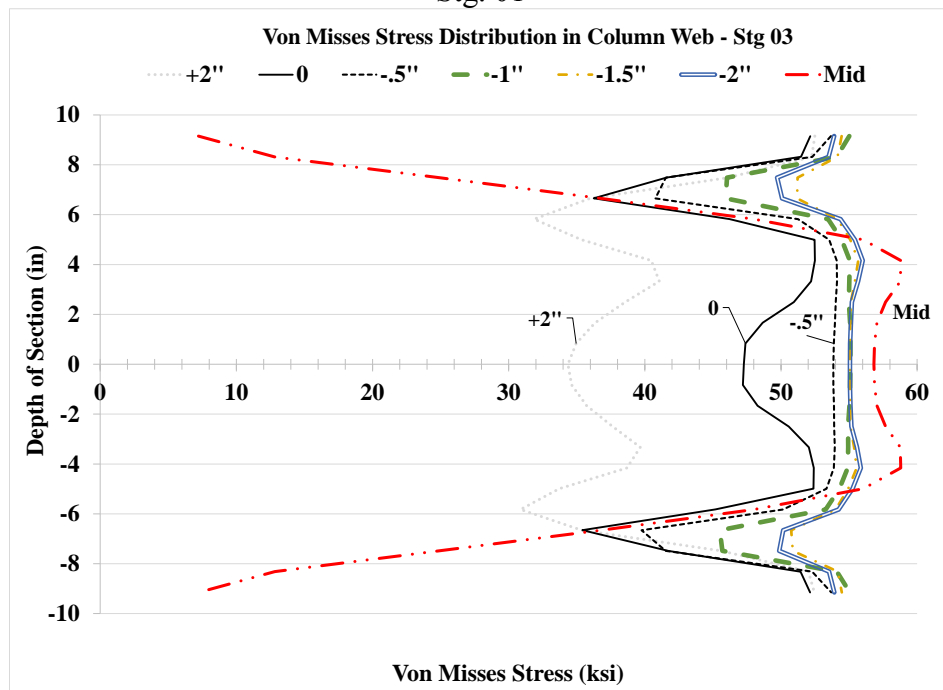


Figure 4.116 VMS and PEEQ in the column Case 3C1



Stg. 01



Stg. 03

Figure 4.117: VMS distribution in column web at different heights Stg. 01-04 Case 3C1

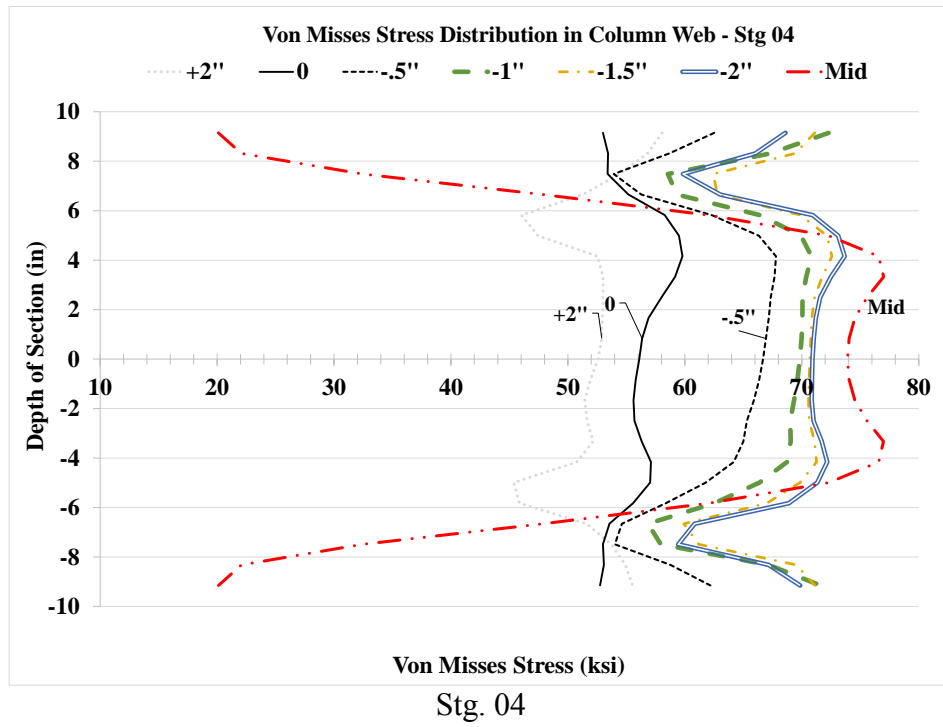


Figure 4.117: VMS distribution in column web at different heights Stg. 01-04 Case 3C1

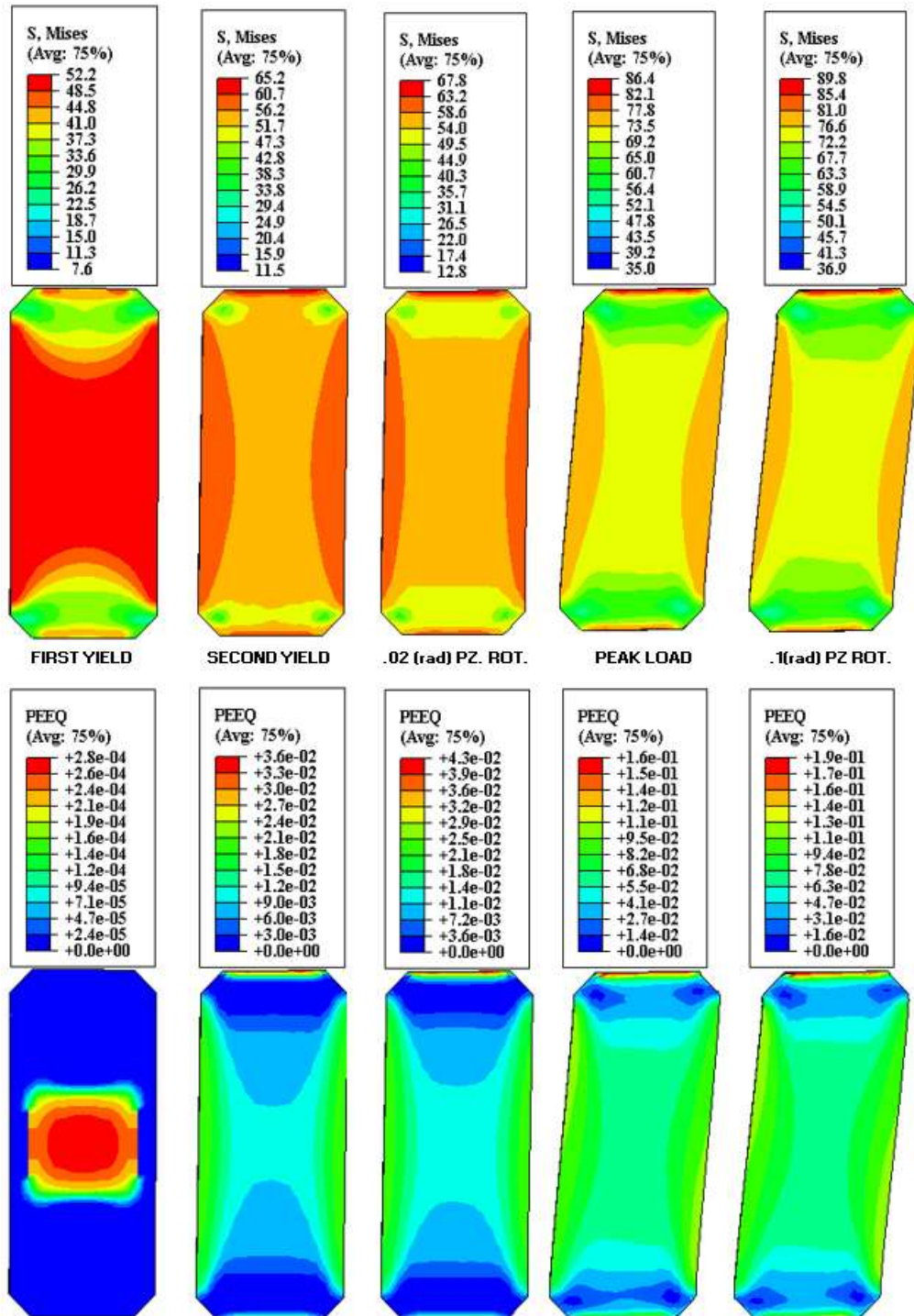


Figure 4.118: VMS and PEEQ in the DP Case 3C1

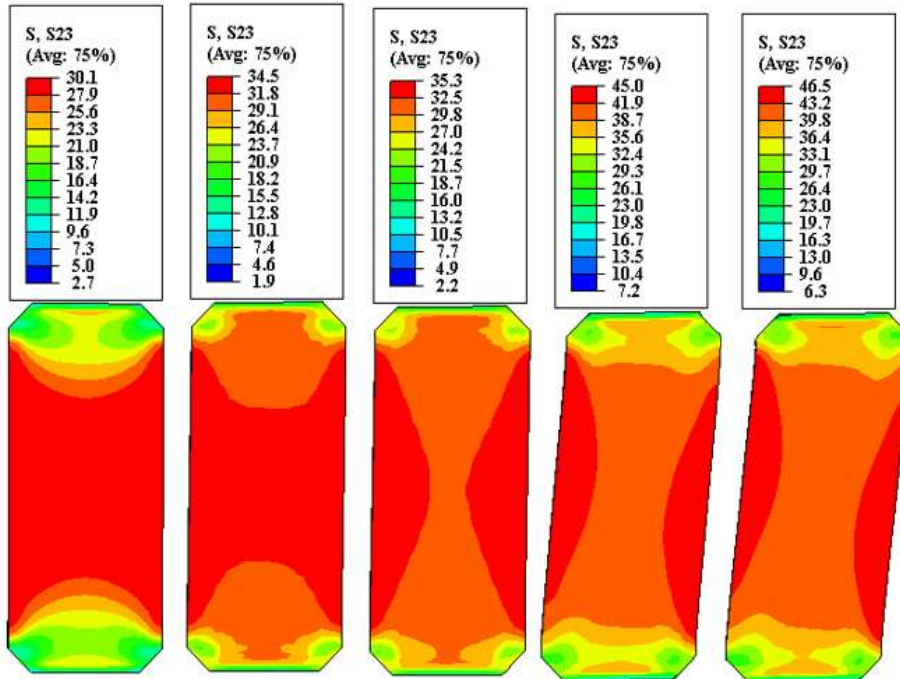


Figure 4.119: Shear stress, S23 in the DP Case 3C1

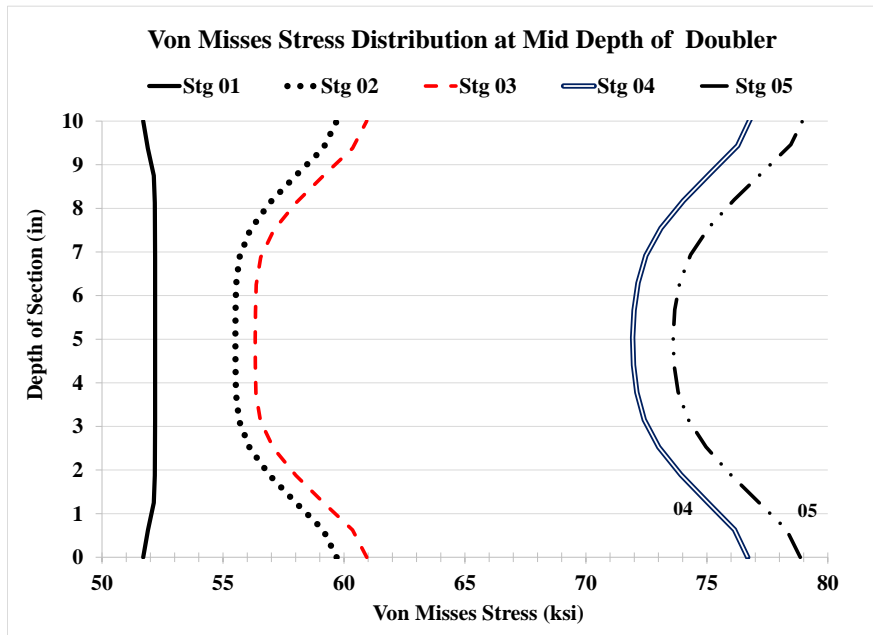


Figure 4.120: VMS distribution at mid-depth of DP Case 3C1

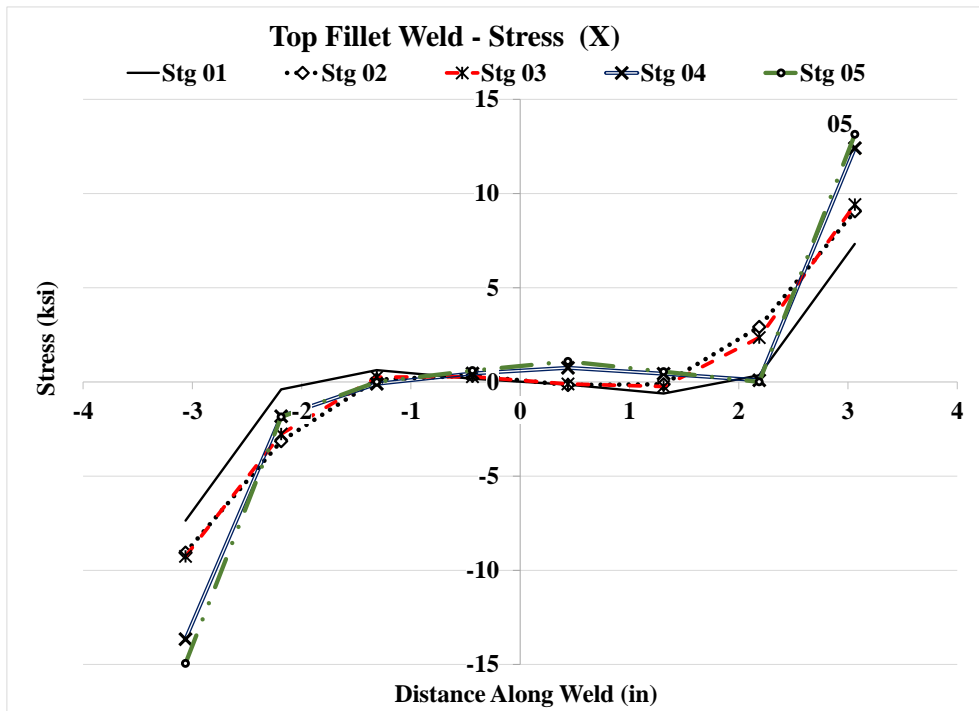
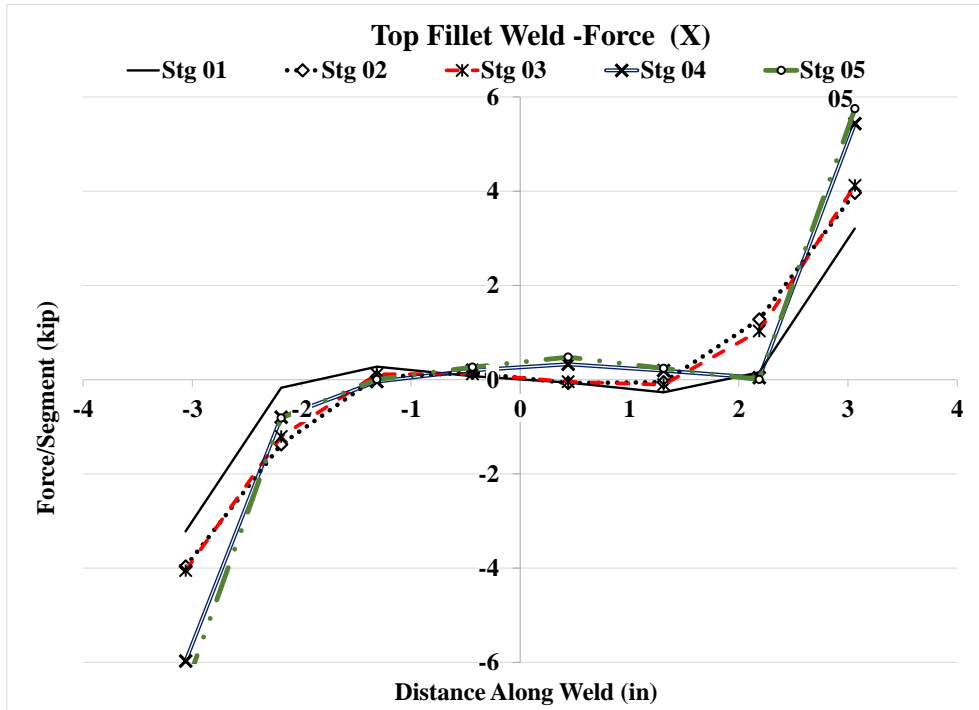


Figure 4.121: Forces and stresses in horizontal weld, (X) Case 3C1

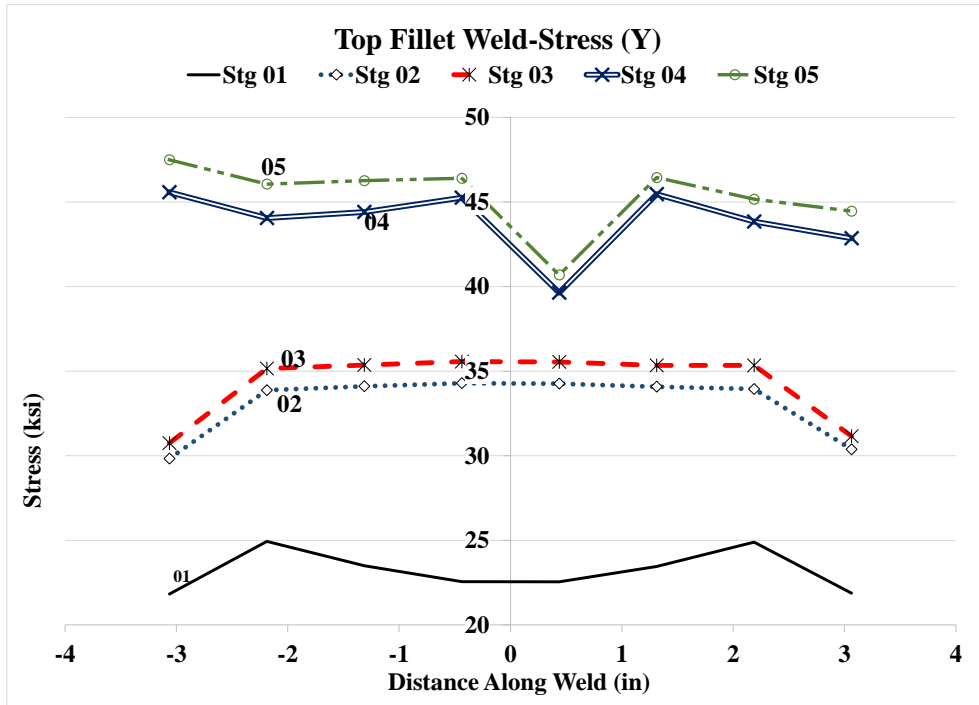
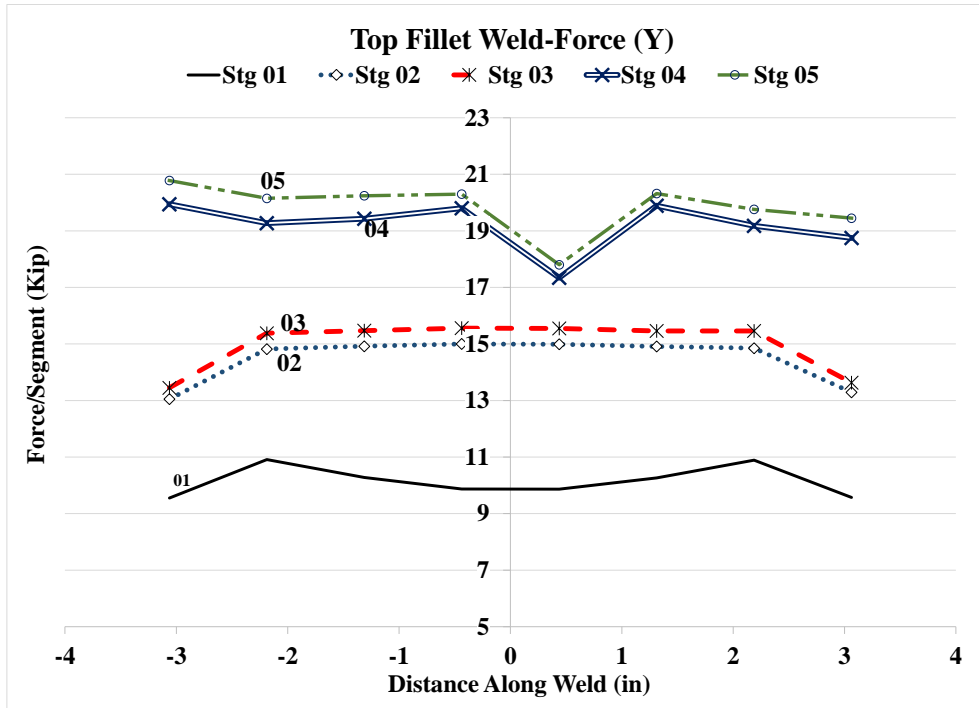


Figure 4.122: Forces and stresses in horizontal weld, (Y) Case 3C1

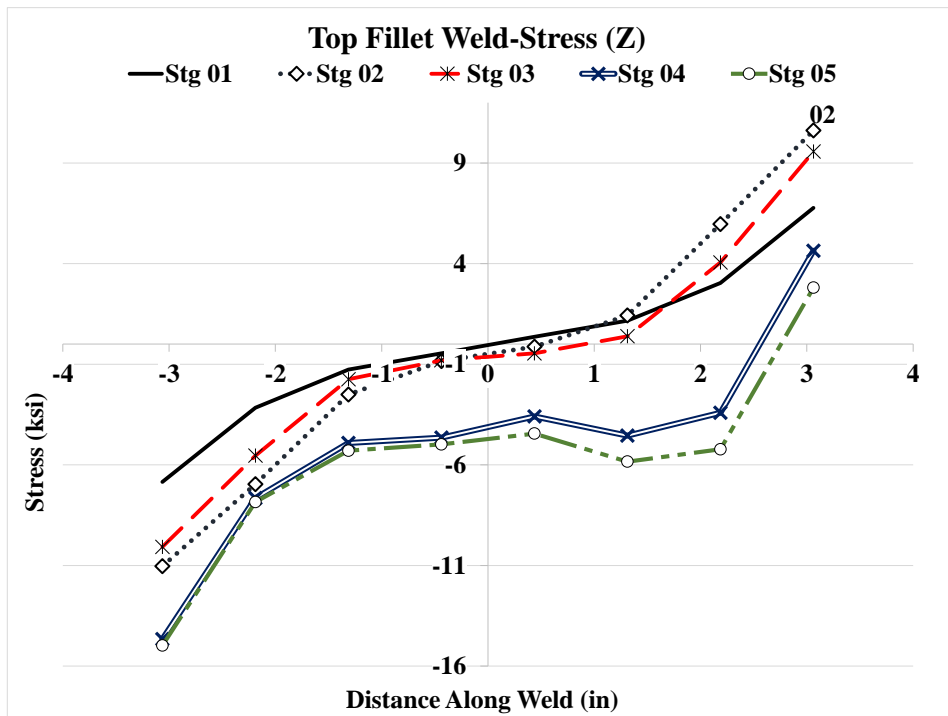
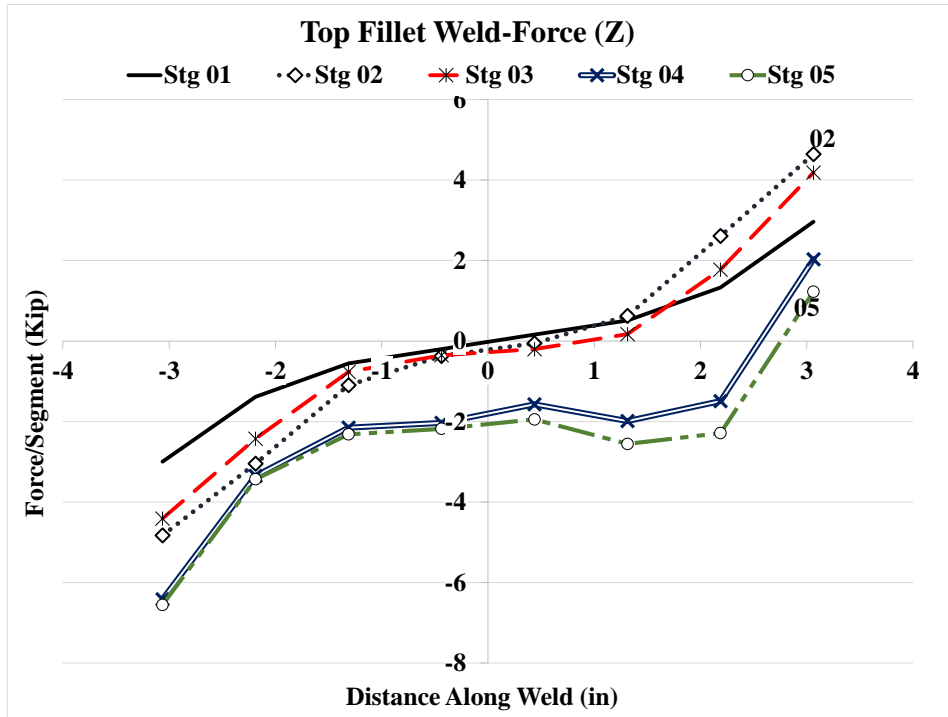


Figure 4.123: Forces and stresses in horizontal weld, (Z) Case 3C1



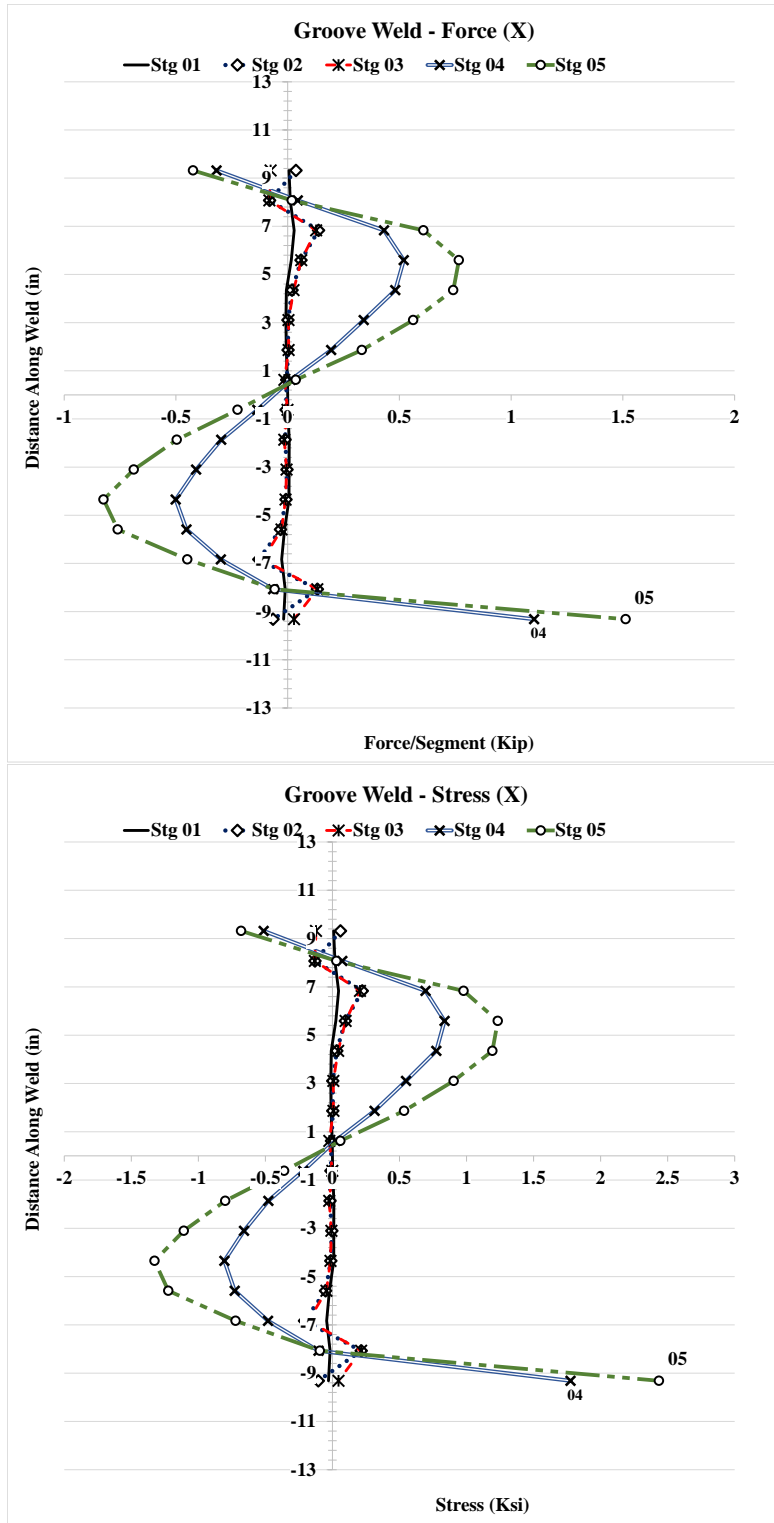


Figure 4.124: Forces and stresses in vertical weld, (X) Case 3C1

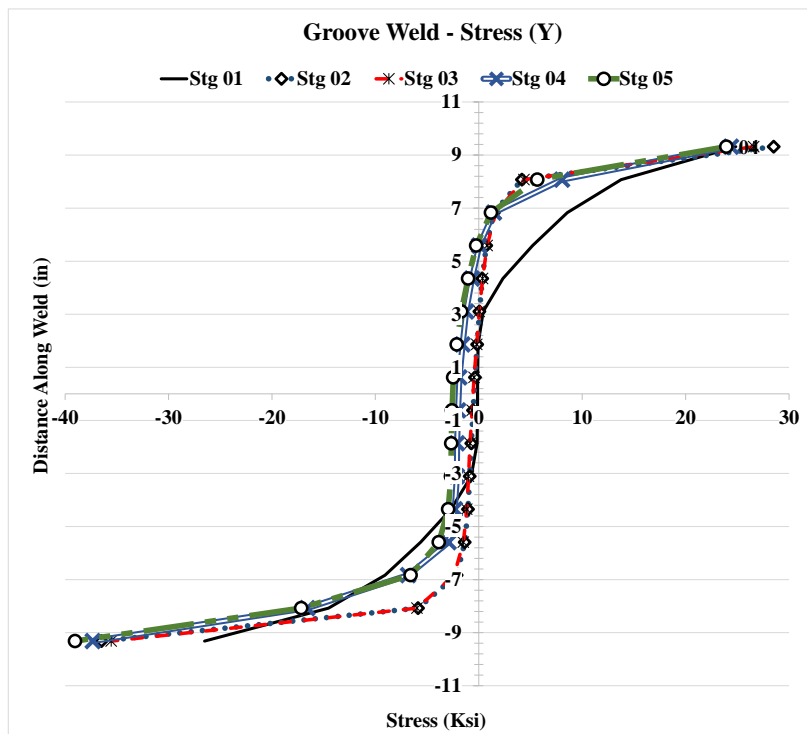
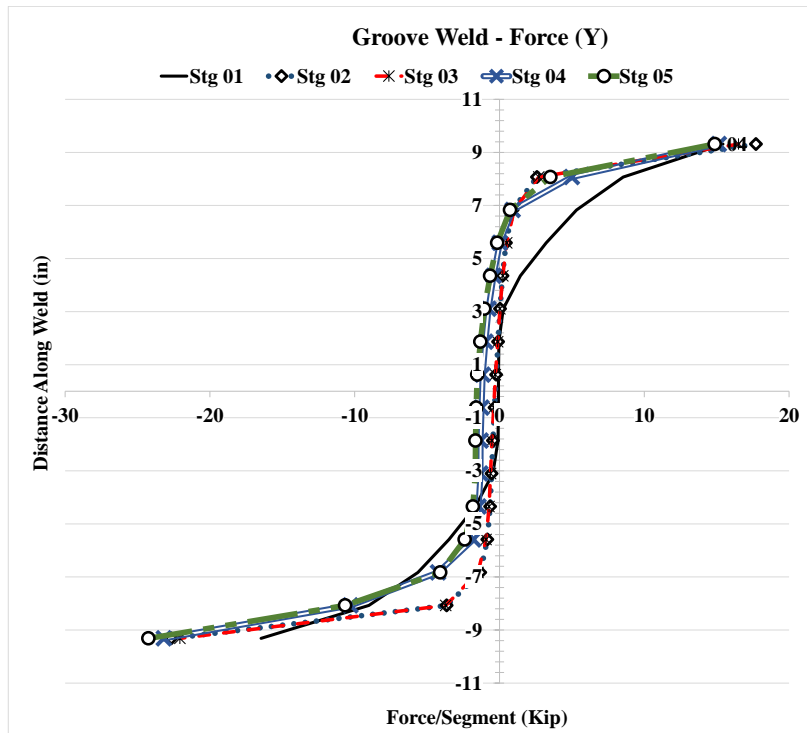


Figure 4.125: Forces and stresses in vertical weld, (Y) Case 3C1

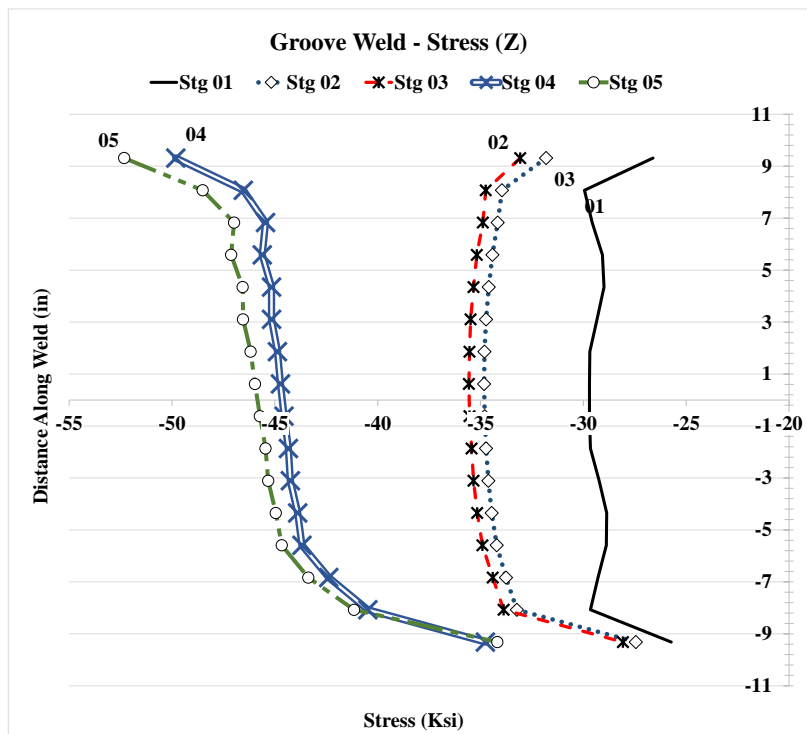
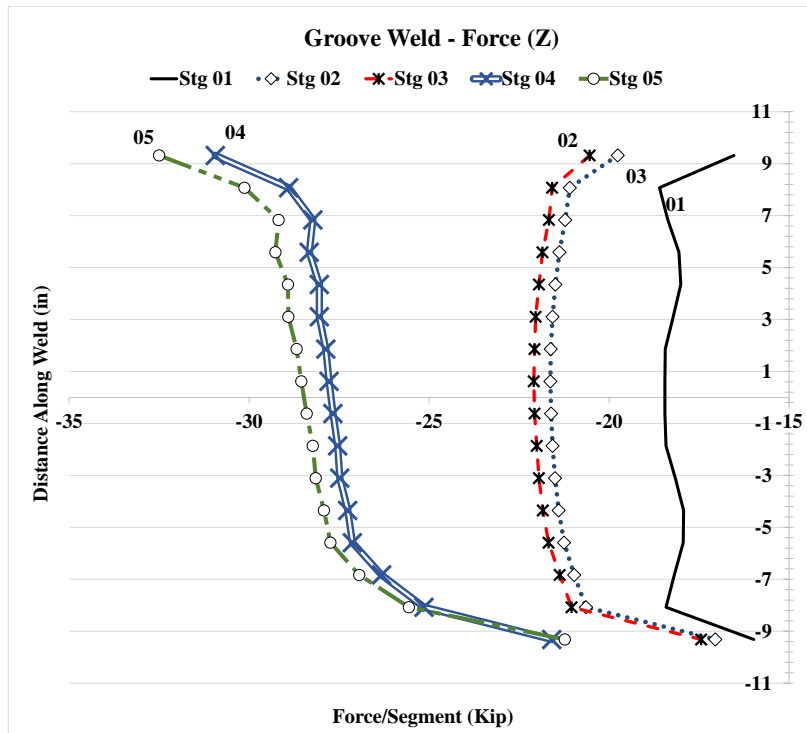


Figure 4.126: Forces and stresses in vertical weld, (Z) Case 3C1

#### 4.2.12 Analysis Case 4A

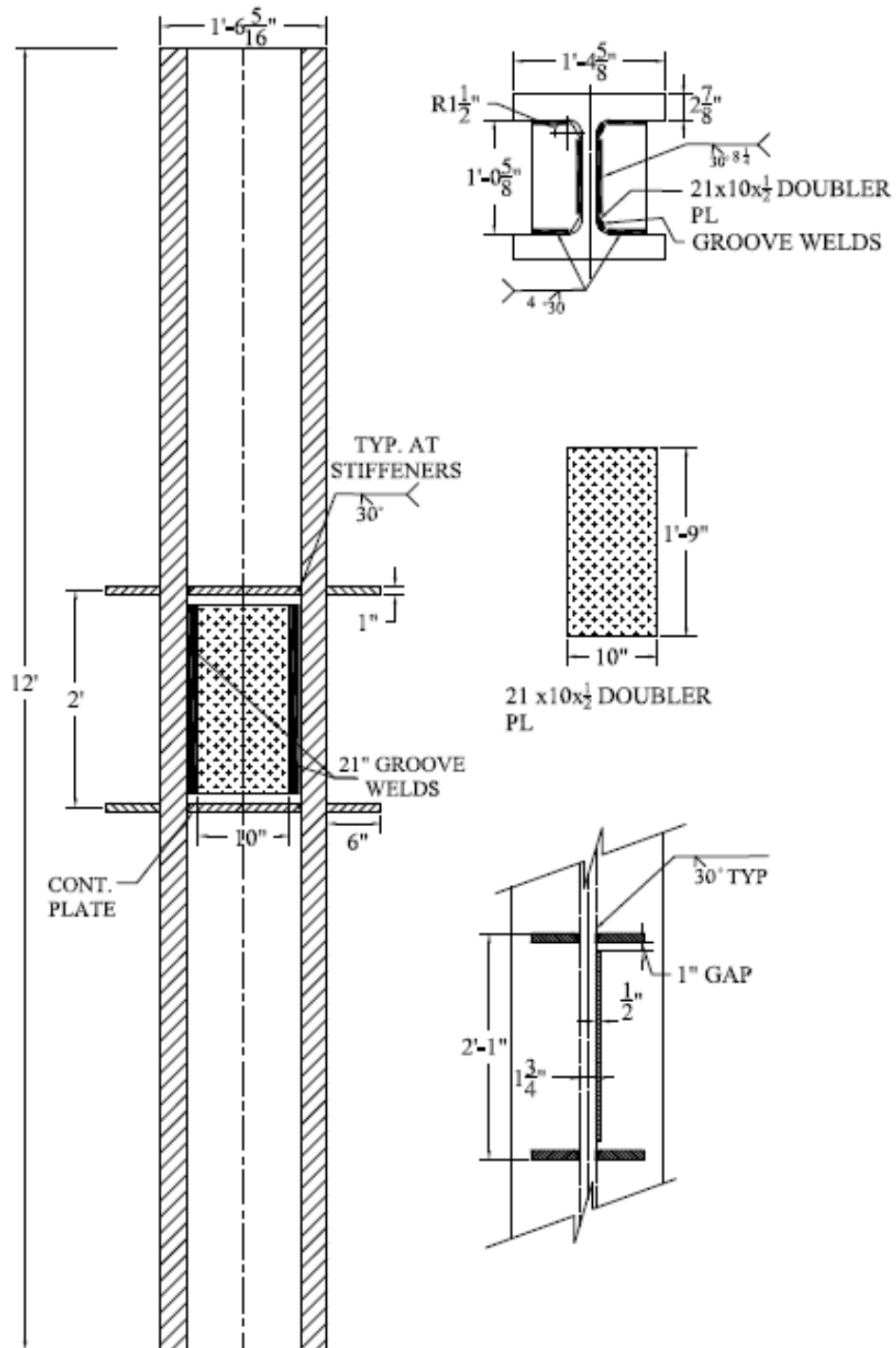


Figure 4.127: Analysis case 4A

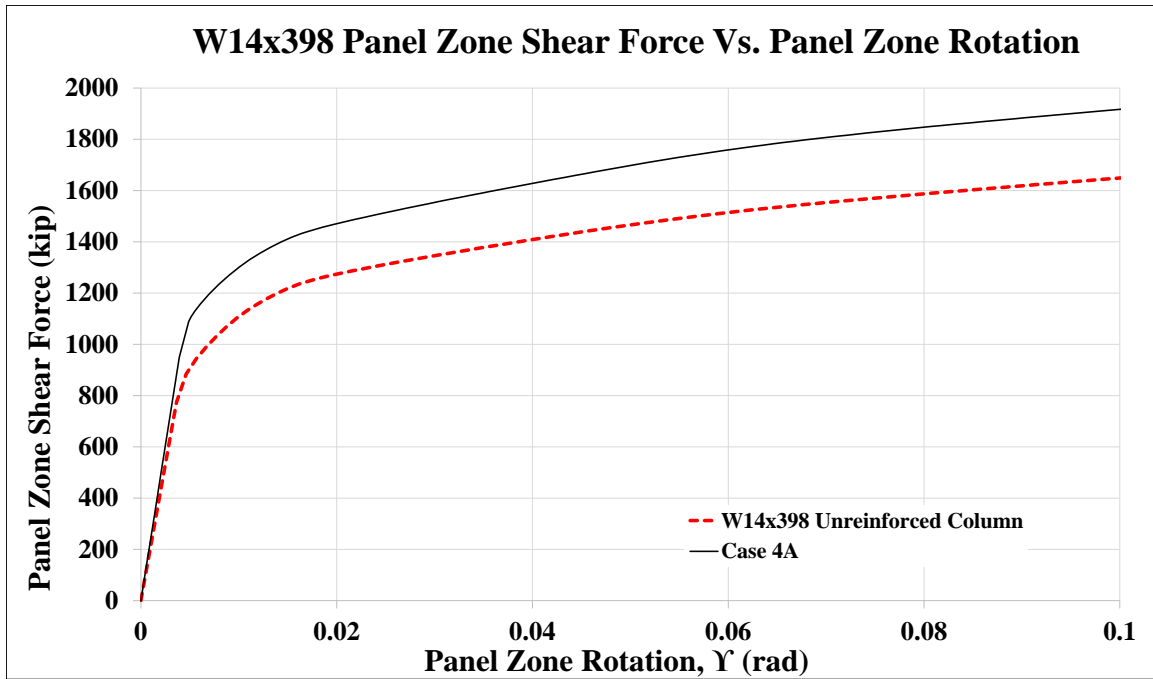


Figure 4.128: Panel zone shear vs. panel zone rotation Case 4A

Stage	Applied Force/Loading Plate (Kip)	Panel Shear Force (Kip)	% Higher than unreinforced Col.	Panel Zone Rotation (rad)
1	654	1,089	123%	0.005
2	867	1,446	116%	0.018
3	886	1,477	116%	0.021
4	1,141	1,902		0.096
5	1,150	1,917	116%	0.100

Table 4.14: Panel zone shear and force on loading plate Case 4A

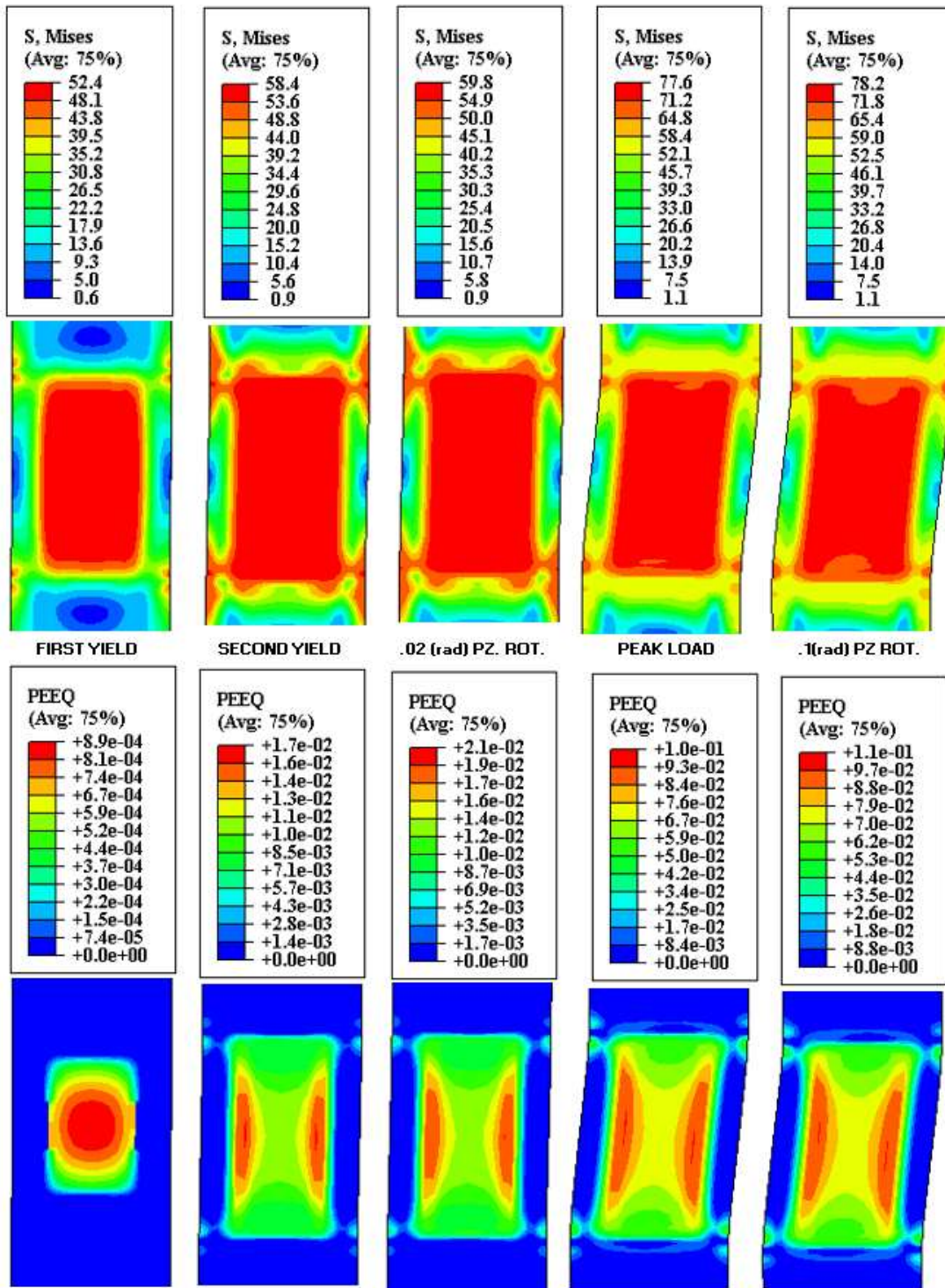
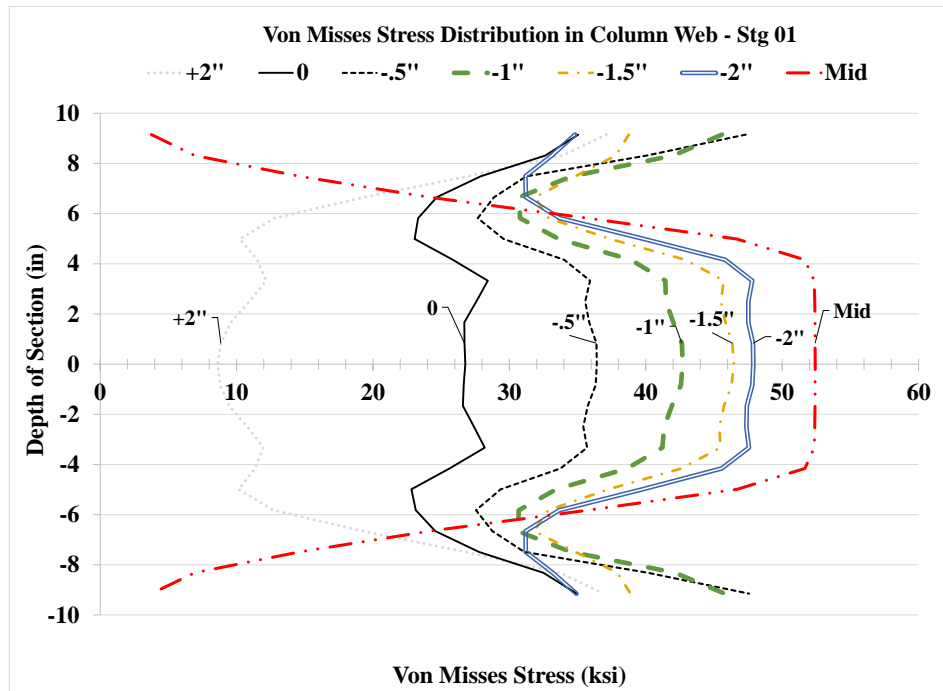
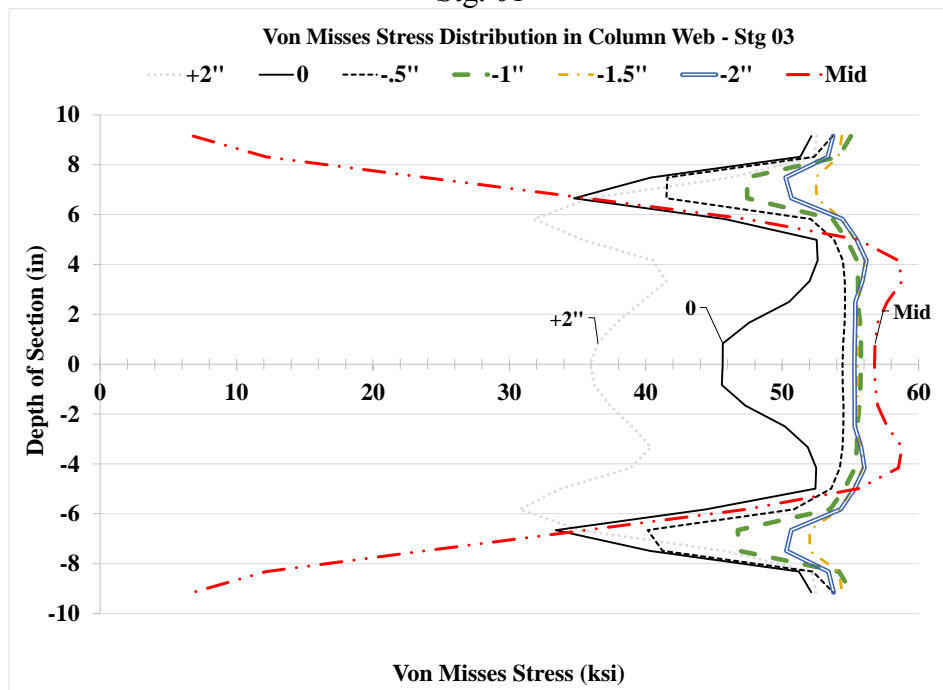


Figure 4.128: VMS and PEEQ in the column Case 4A



Stg. 01



Stg. 03

Figure 4.129: VMS distribution in column web at different heights Stg. 01-04 Case 4A

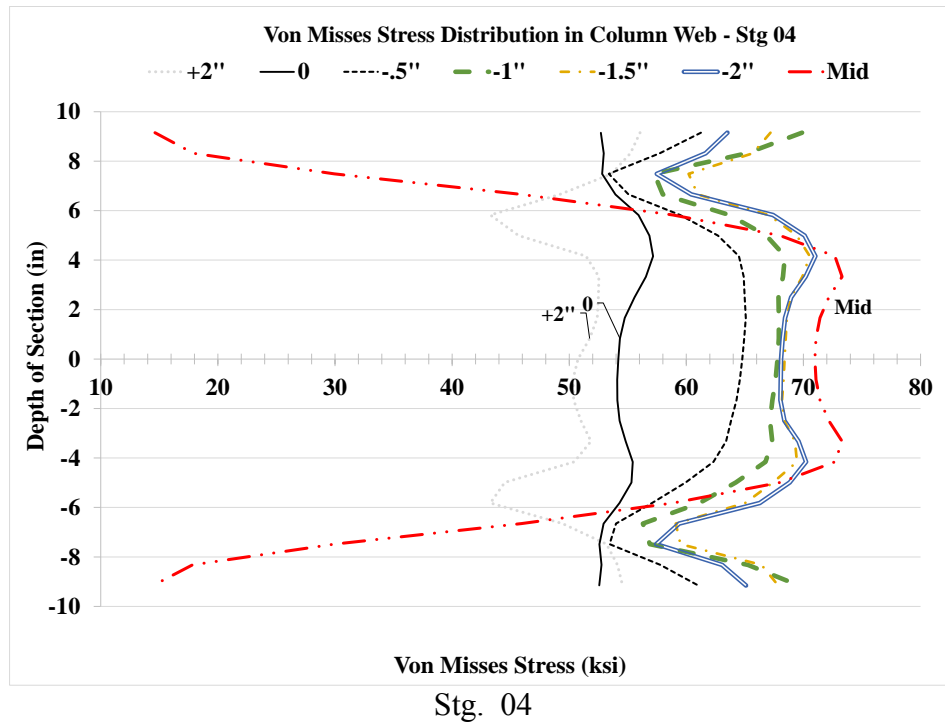


Figure 4.129: VMS distribution in column wed at different heights Stg. 01-04 Case 4A



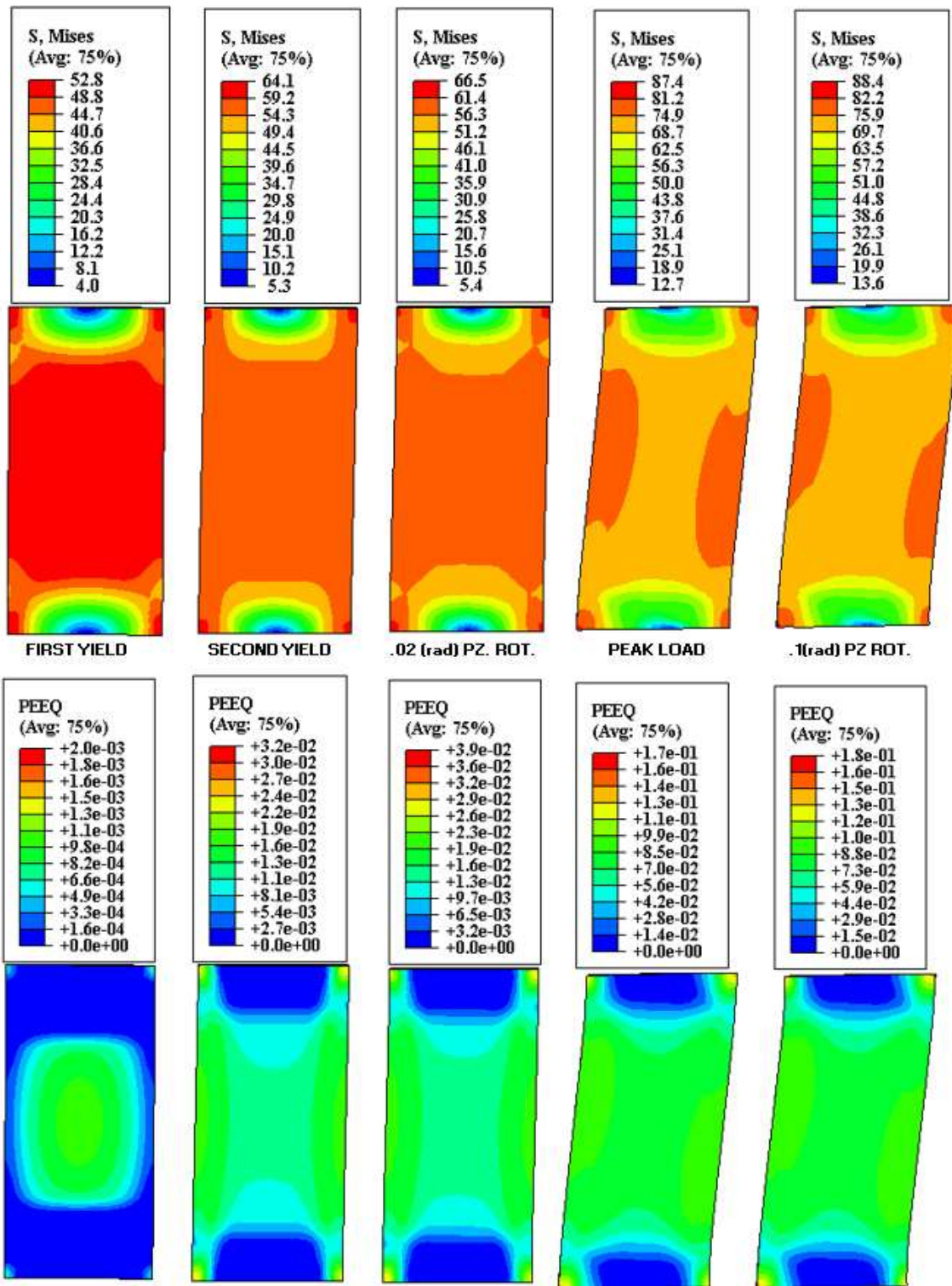


Figure 4.130: VMS and PEEQ in the DP Case 4A

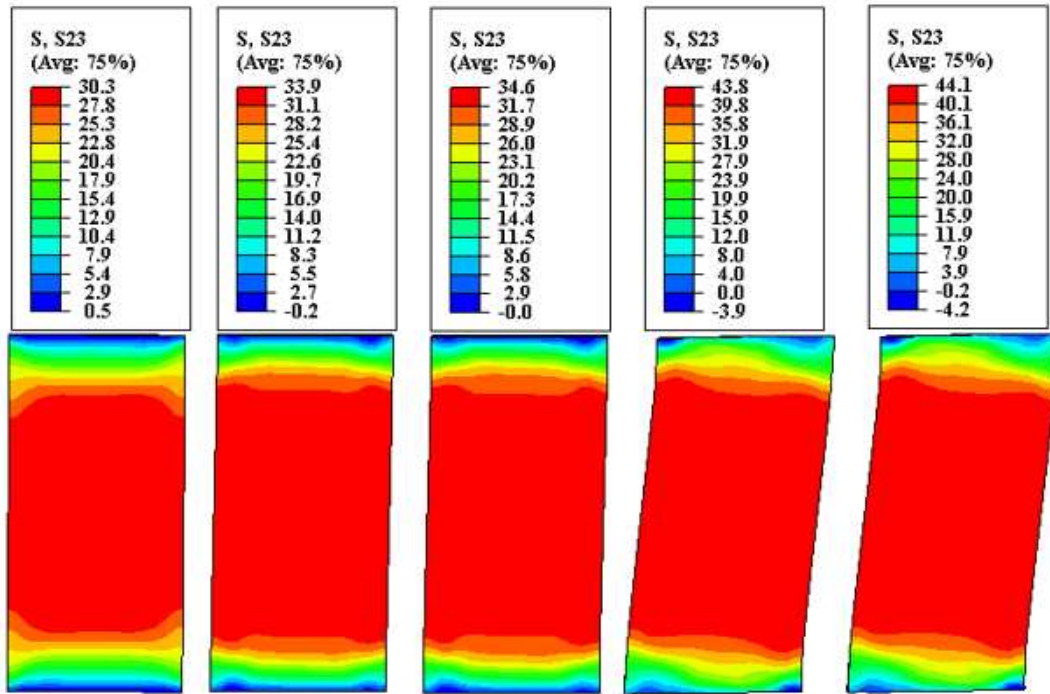


Figure 4.130: Shear stress, S23 in the DP Case 4A

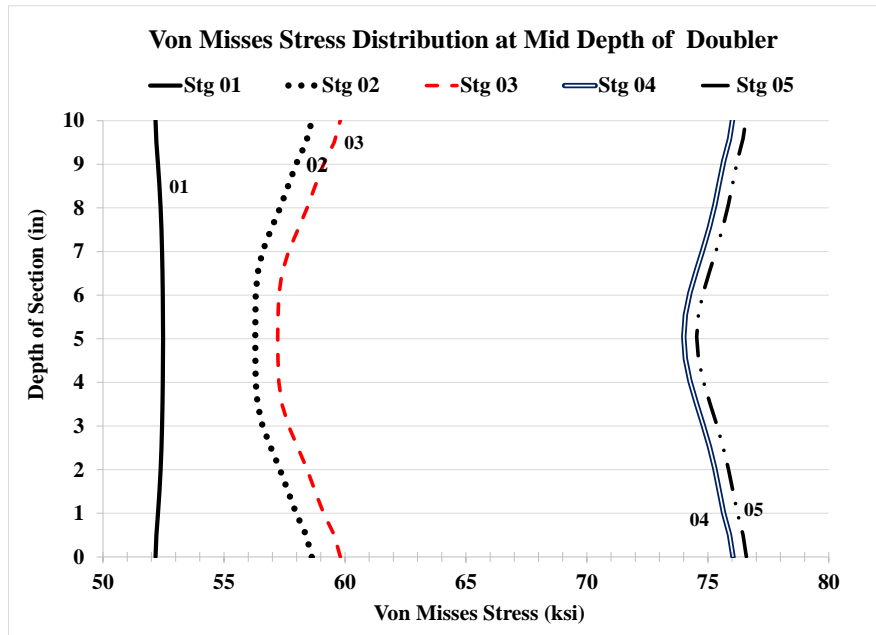


Figure 4.131: VMS distribution at mid-depth of DP Case 4A

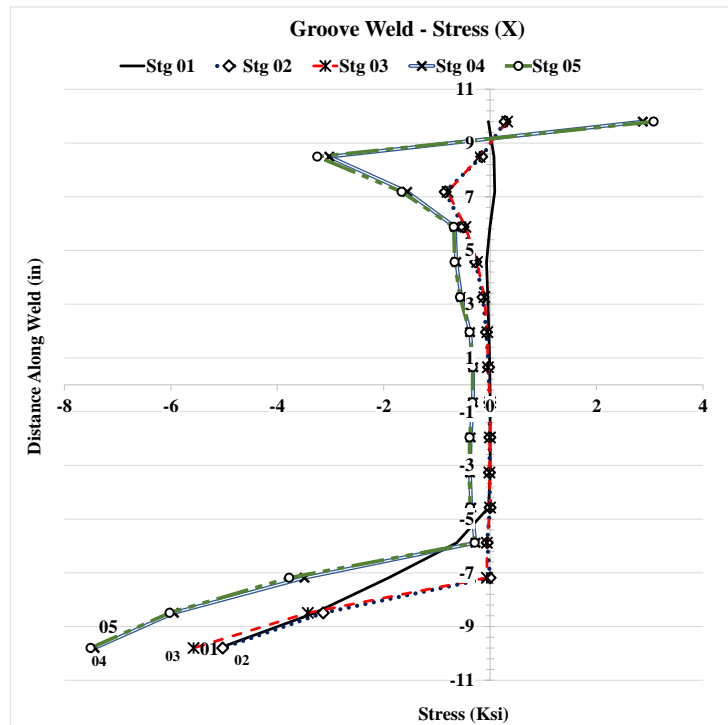
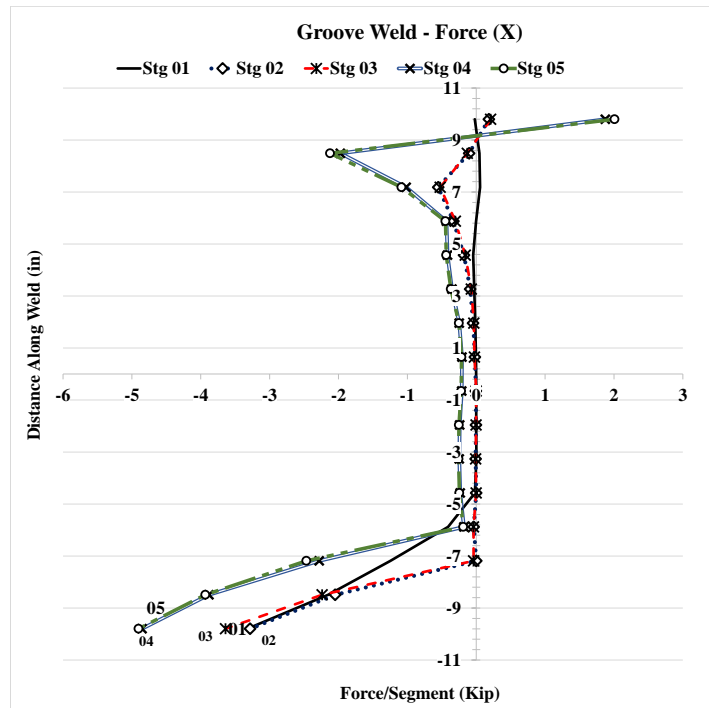


Figure 4.132: Forces and stresses in vertical weld, (X) Case 4A

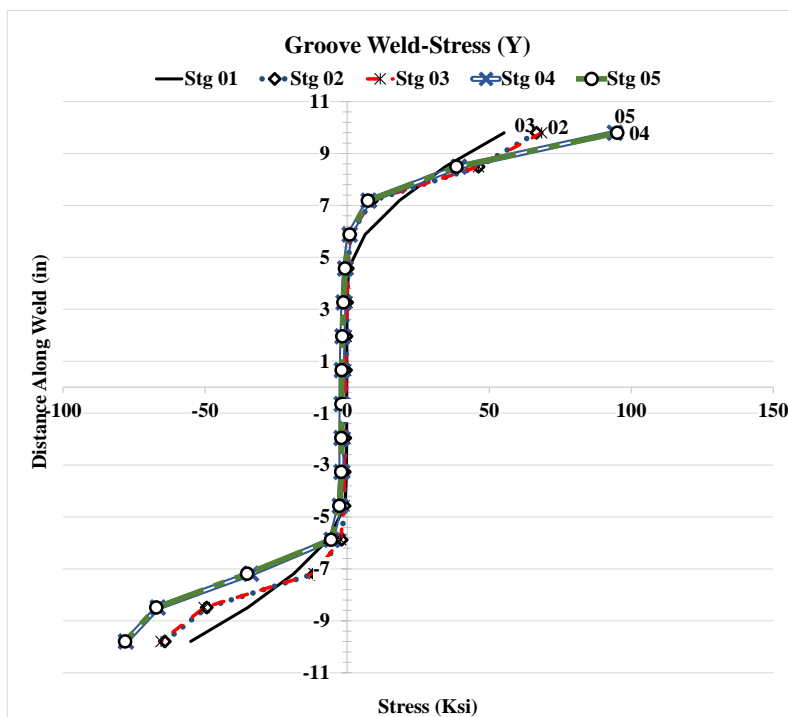
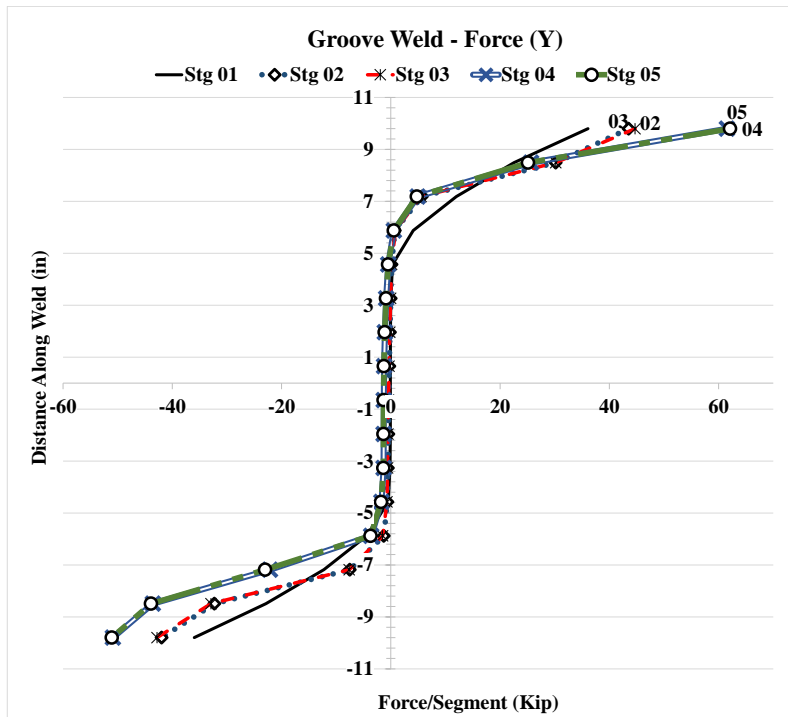


Figure 4.133: Forces and stresses in vertical weld, (Y) Case 4A

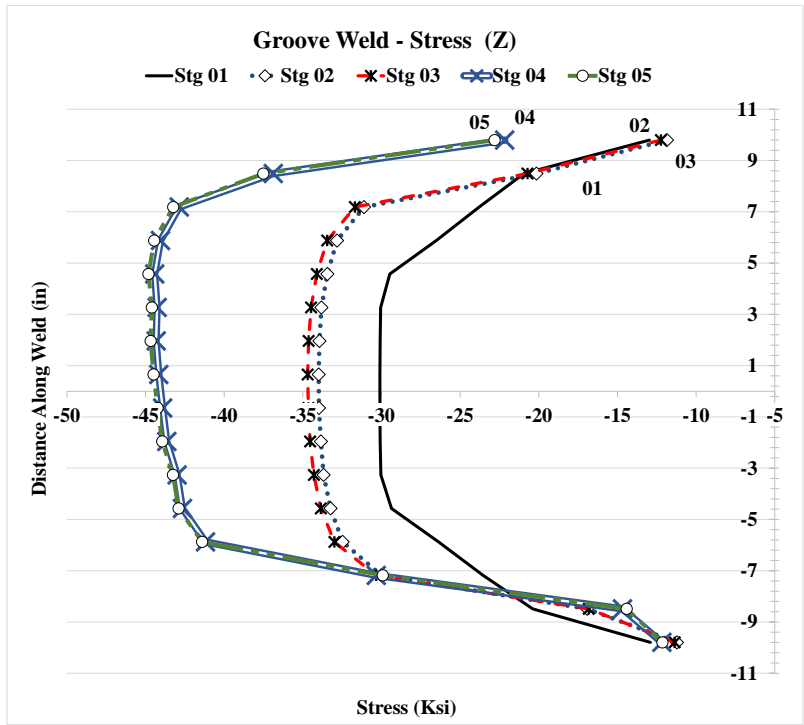
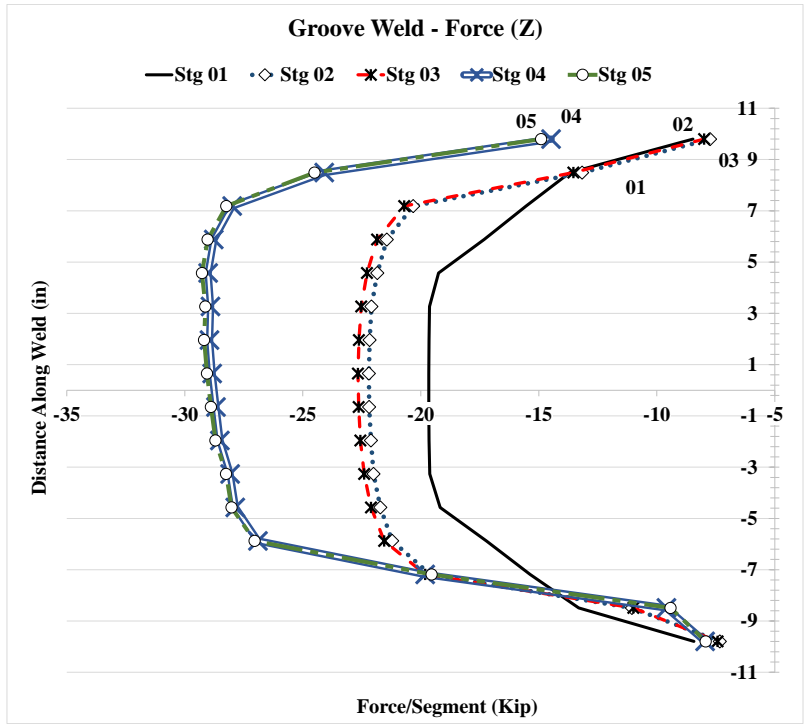


Figure 4.134: Forces and stresses in vertical weld, (Z) Case 4A

### 4.2.13 Analysis Case 4A1

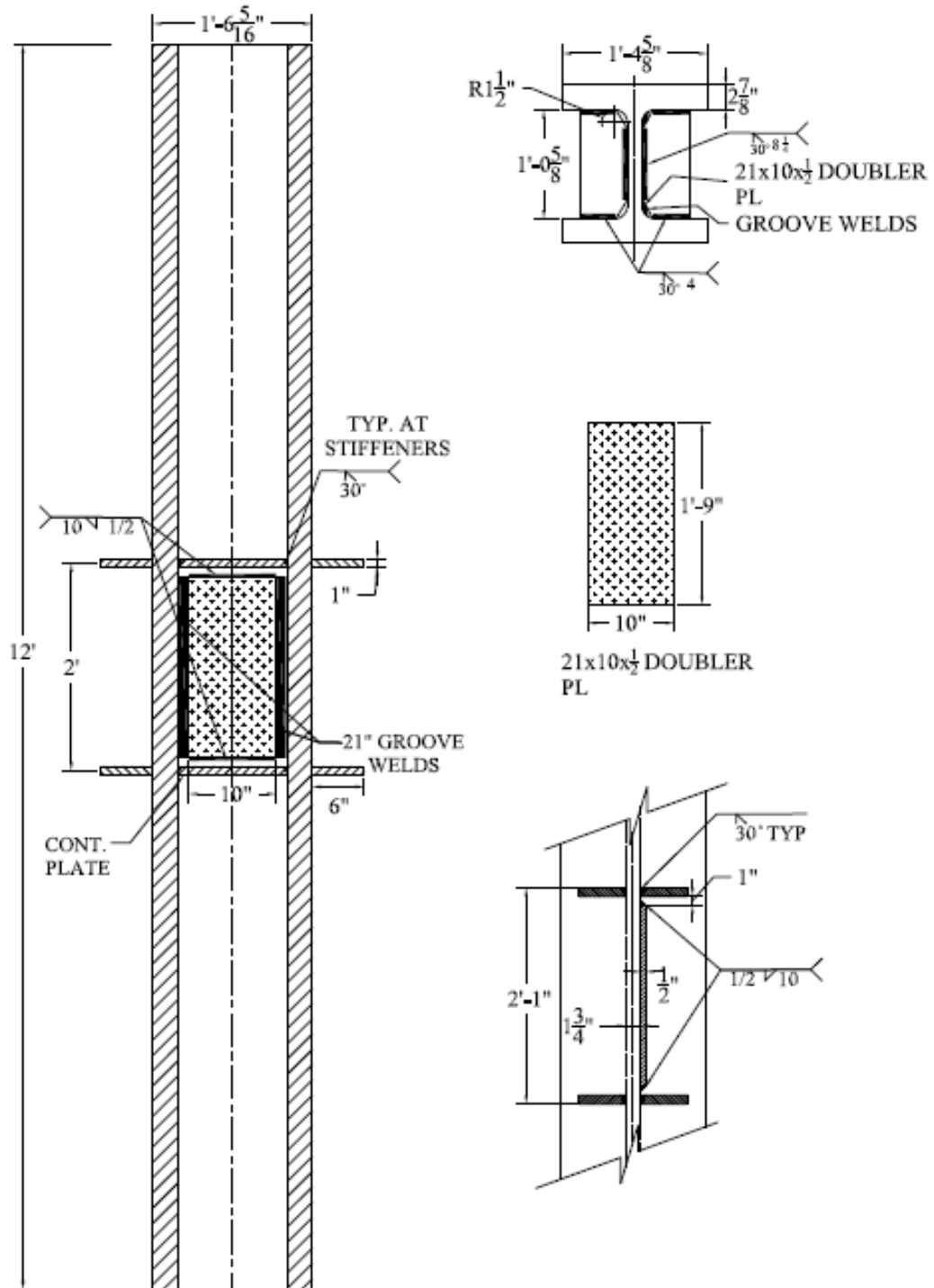


Figure 4.135: Analysis case 4A1

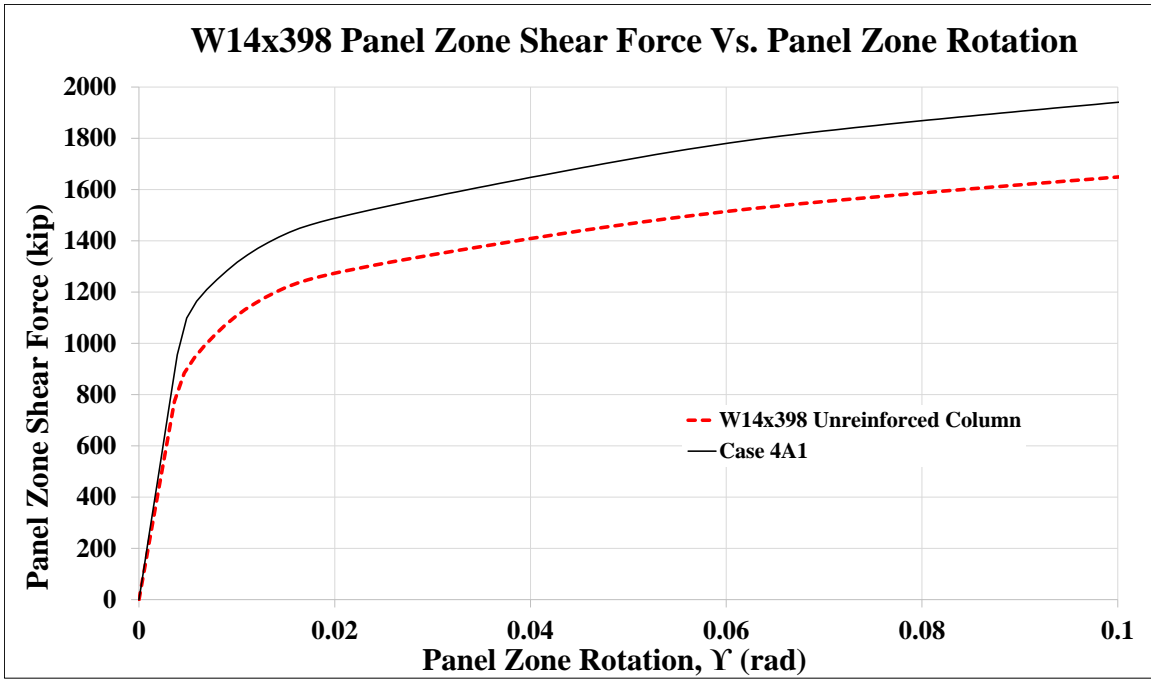


Figure 4.136: Panel zone shear vs. panel zone rotation Case 4A1

Stage	Applied Force/Loading Plate (Kip)	Panel Shear Force (Kip)	% Higher than unreinforced Col.	Panel Zone Rotation (rad)
1	659	1,099	124%	0.005
2	891	1,485	119%	0.020
3	897	1,495	117%	0.021
4	1,141	1,902		0.089
5	1,164	1,940	118%	0.100

Table 4.15: Panel zone shear and force on loading plate Case 4A1



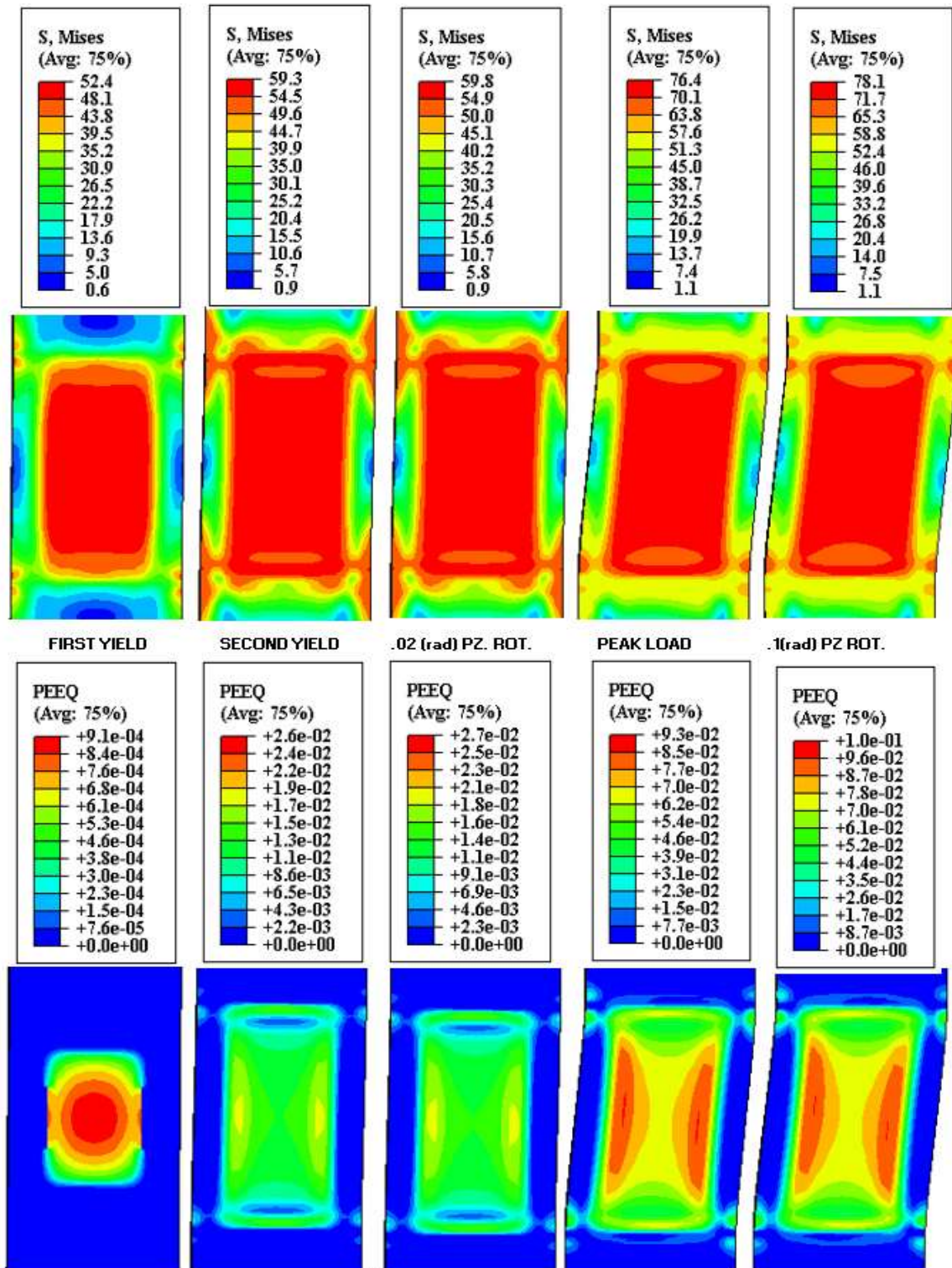
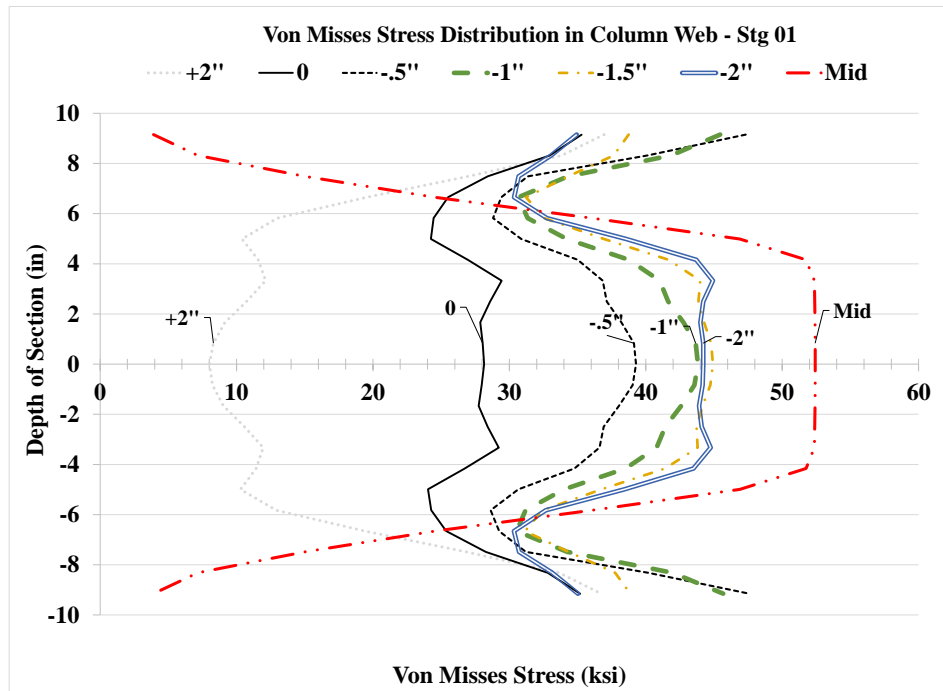
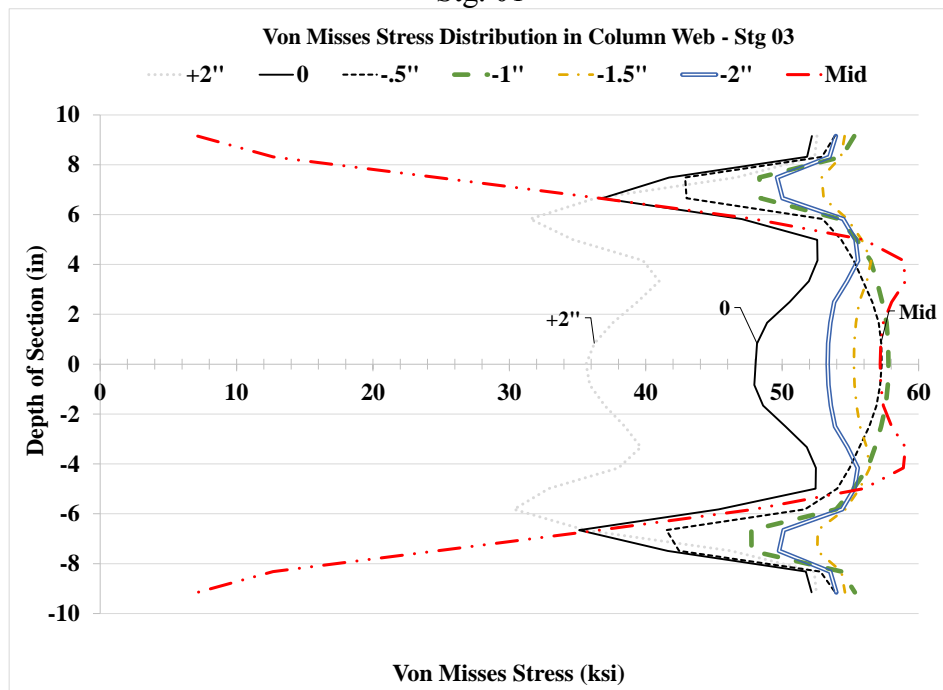


Figure 4.137: VMS and PEEQ in the column Case 4A1



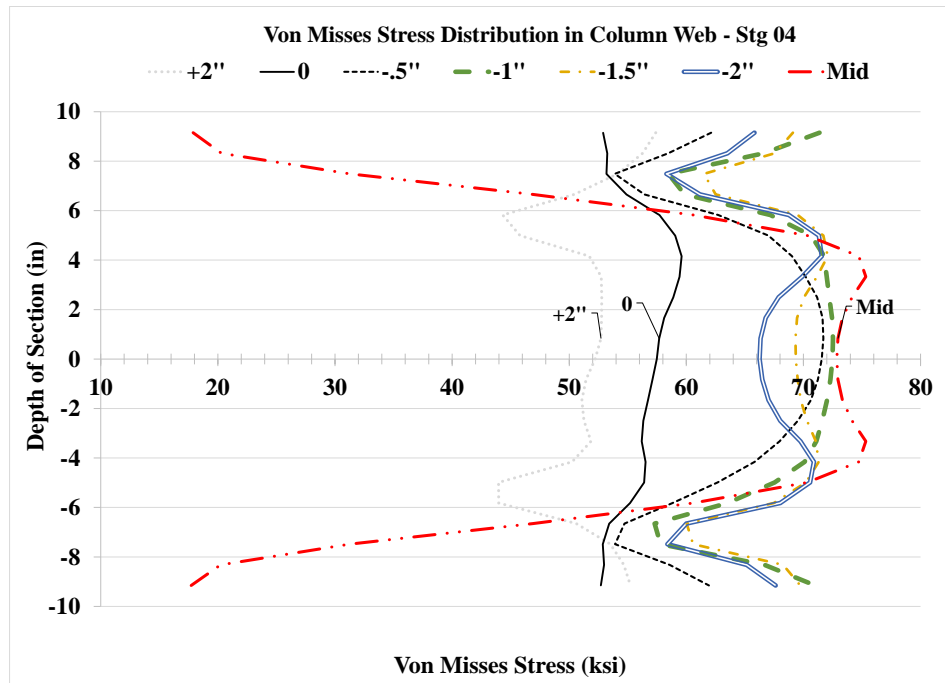


Stg. 01



Stg. 03

Figure 4.138: VMS distribution in column wed at different heights Stg. 01-04 Case 4A1



Stg. 04

Figure 4.138: VMS distribution in column wed at different heights Stg. 01-04 Case 4A1

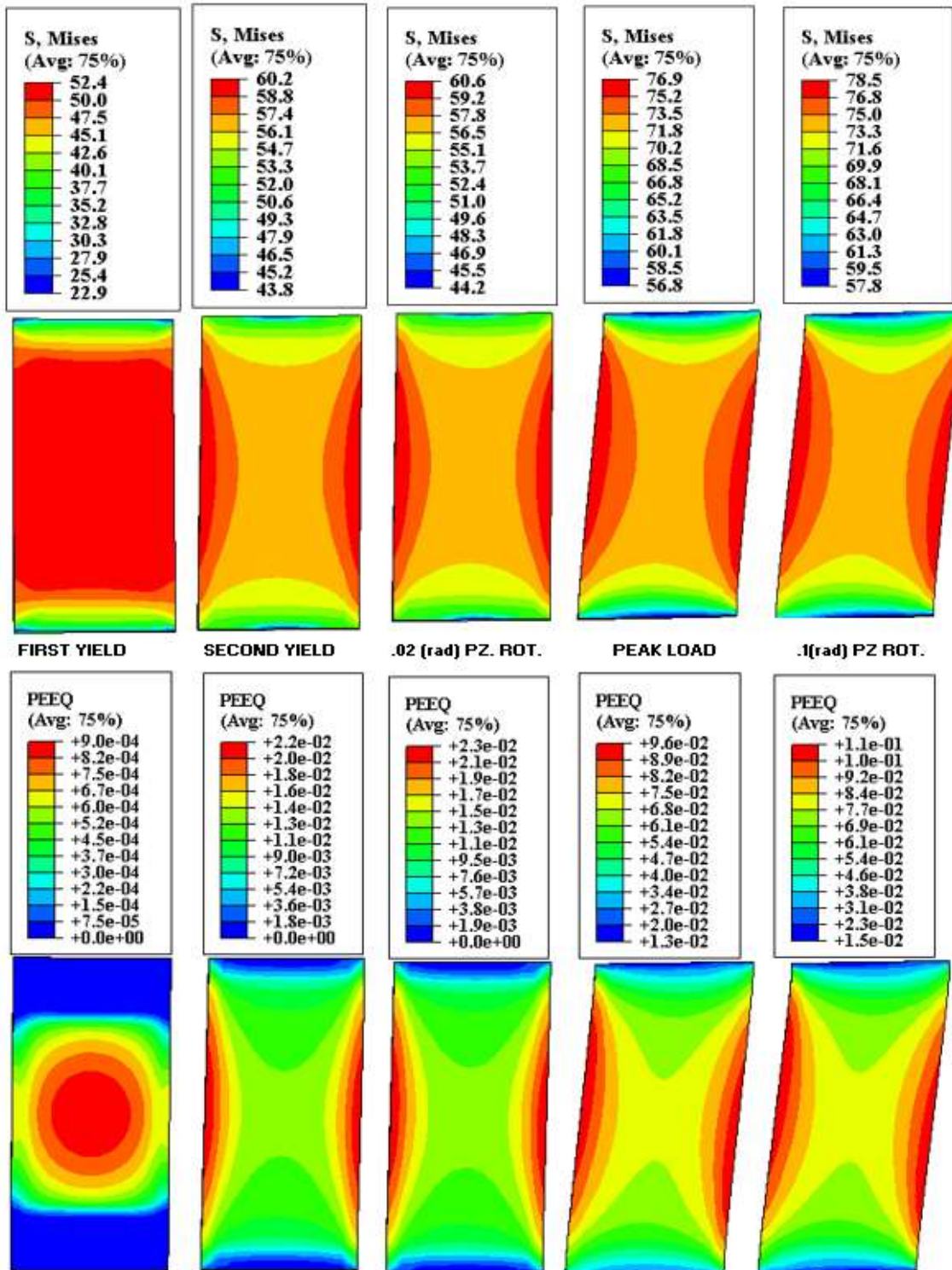


Figure 4.139: VMS and PEEQ in the DP Case 4A1

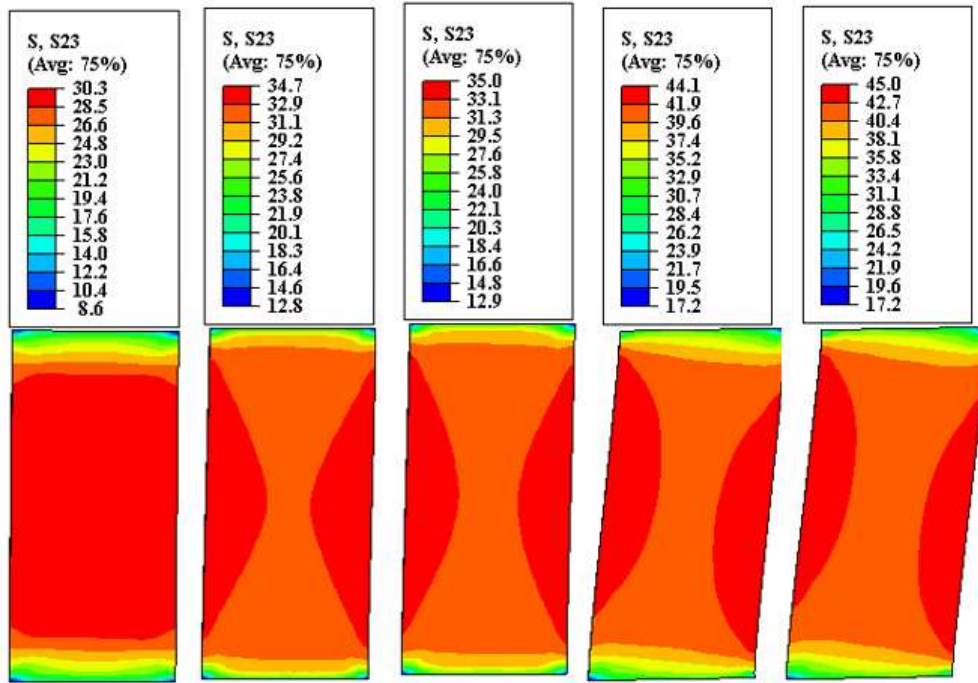


Figure 4.140 Shear stress, S23 in the DP Case 4A1

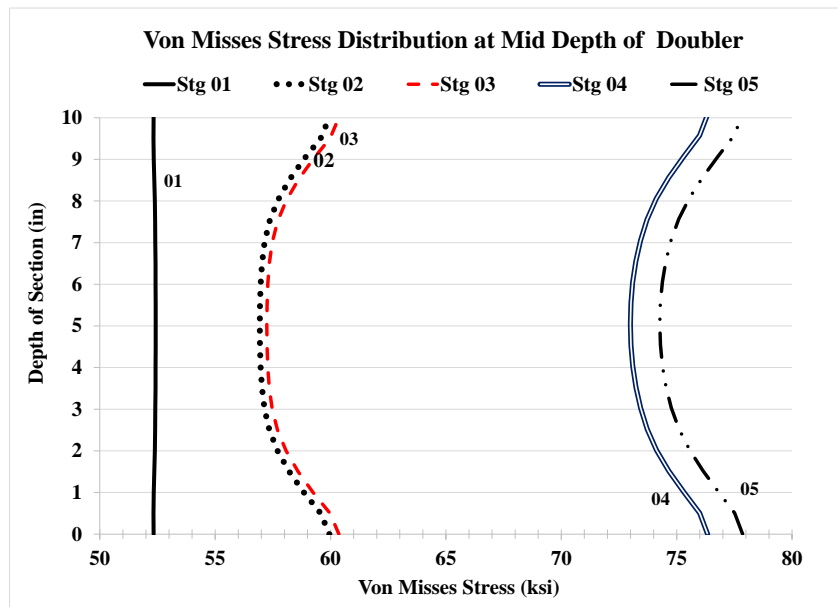


Figure 4.141: VMS distribution at mid-depth of DP Case 4A1

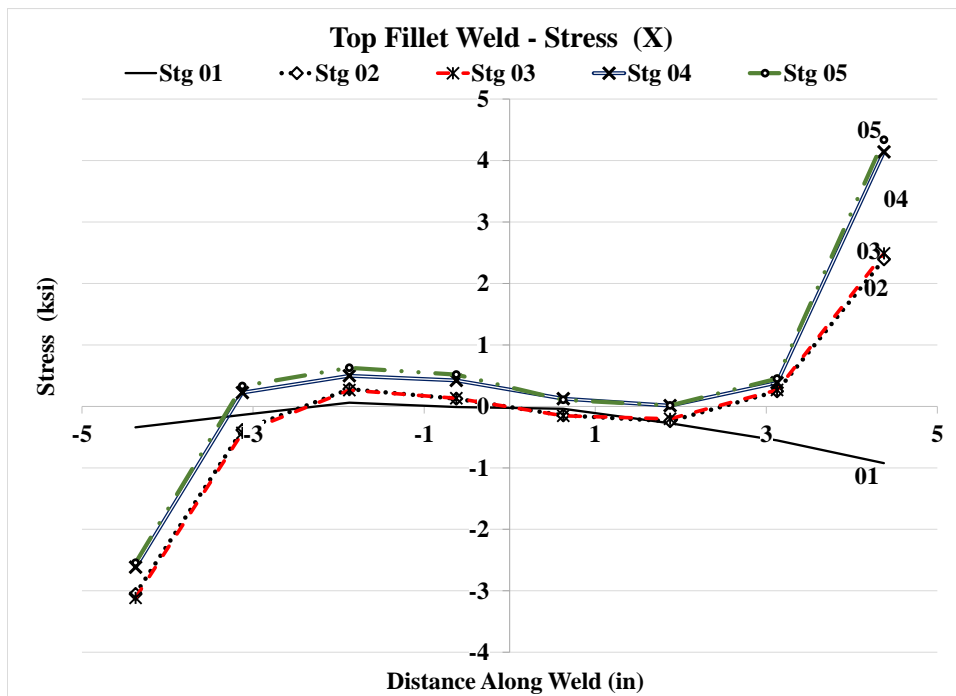
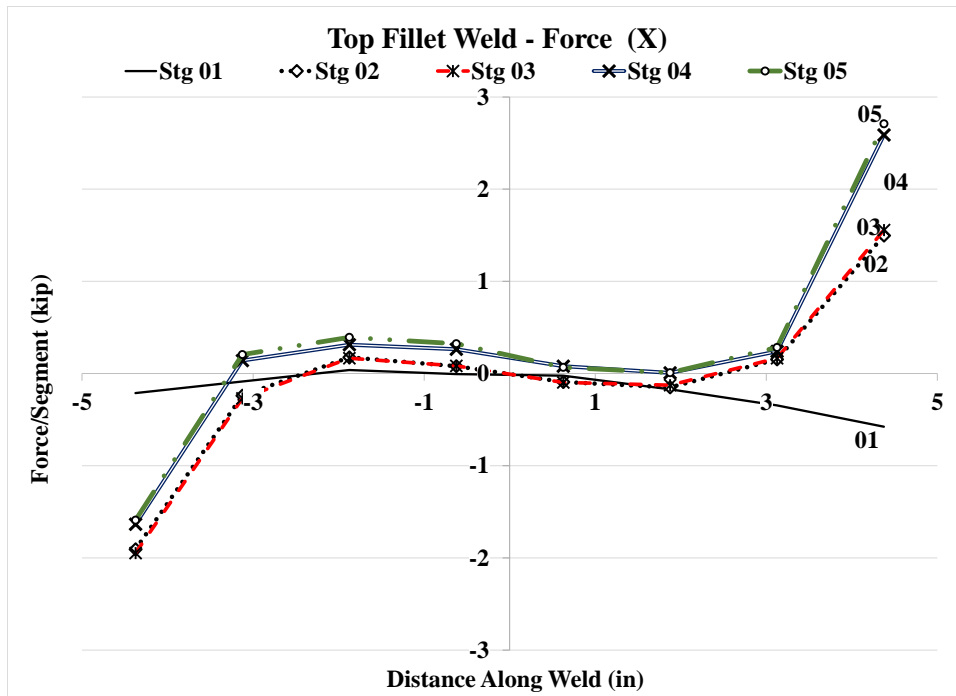


Figure 4.142: Forces and stresses in horizontal weld, (X) Case 4A1

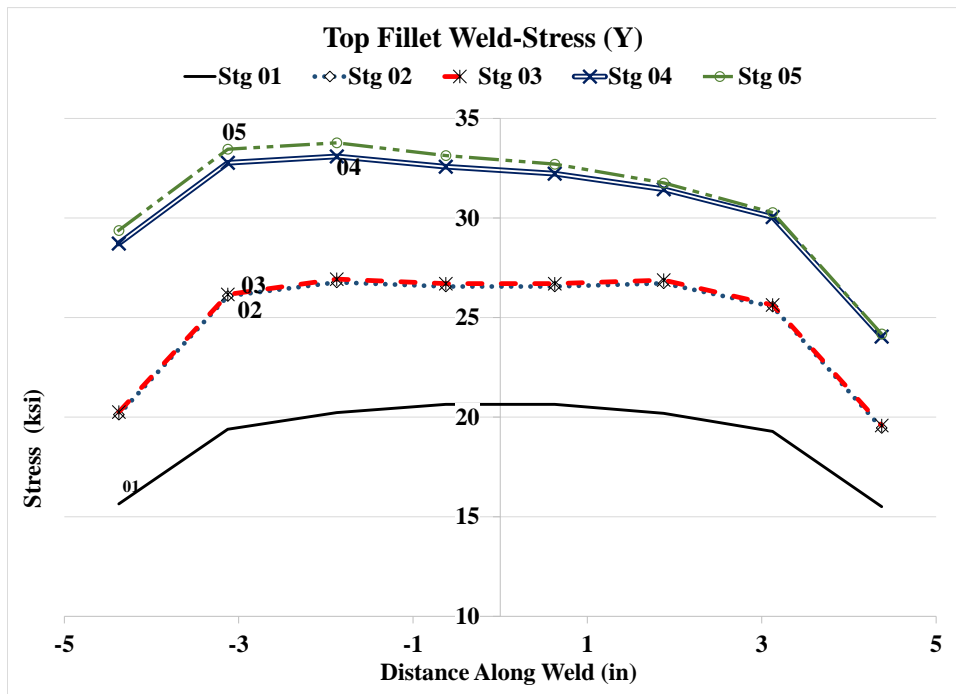
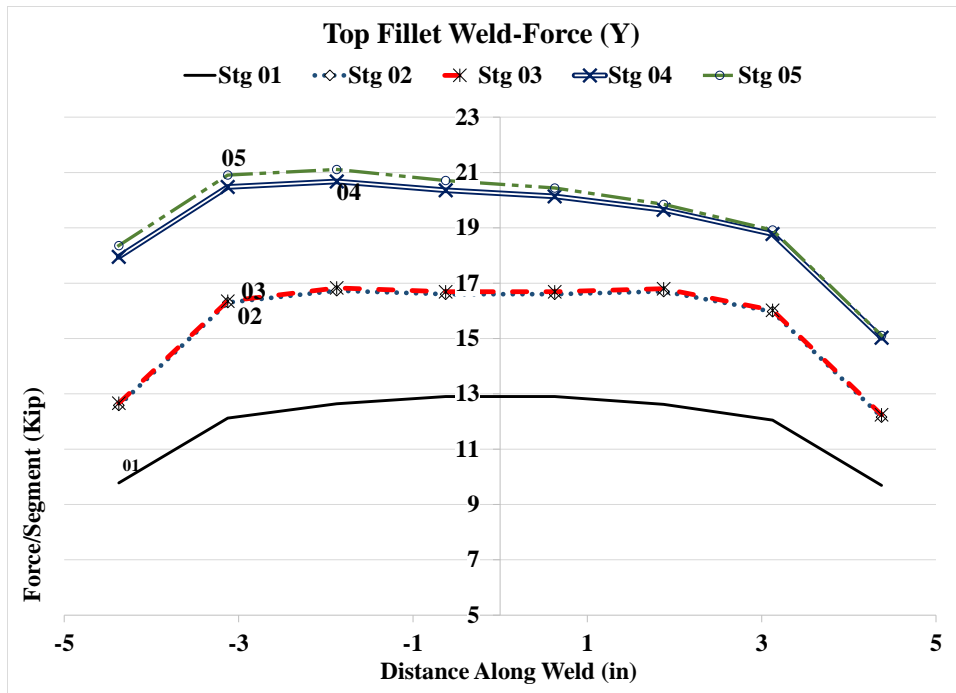


Figure 4.143: Forces and stresses in horizontal weld, (Y) Case 4A1

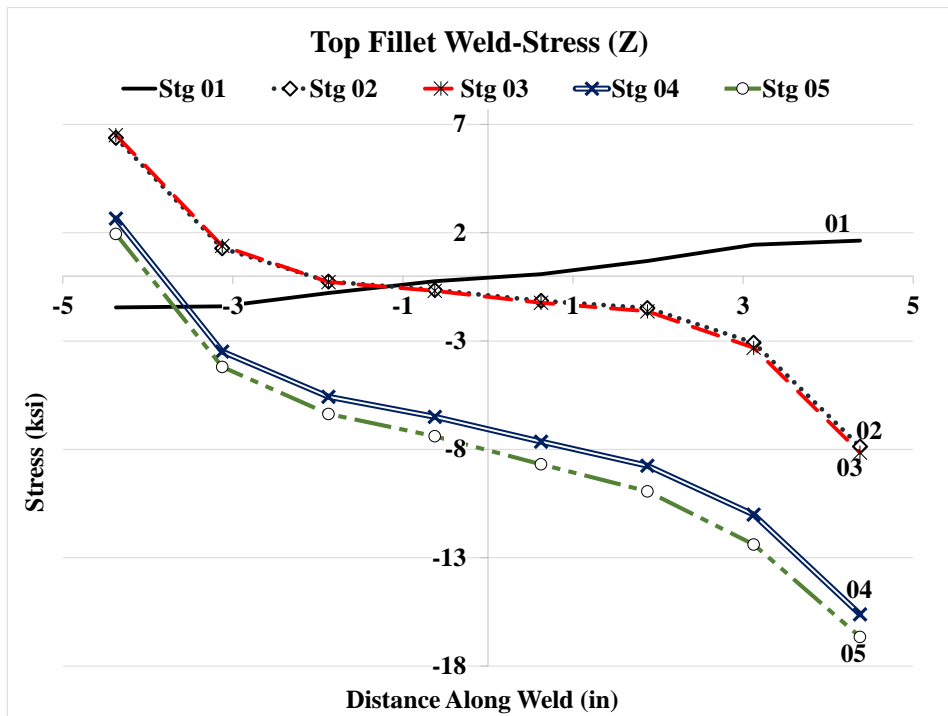
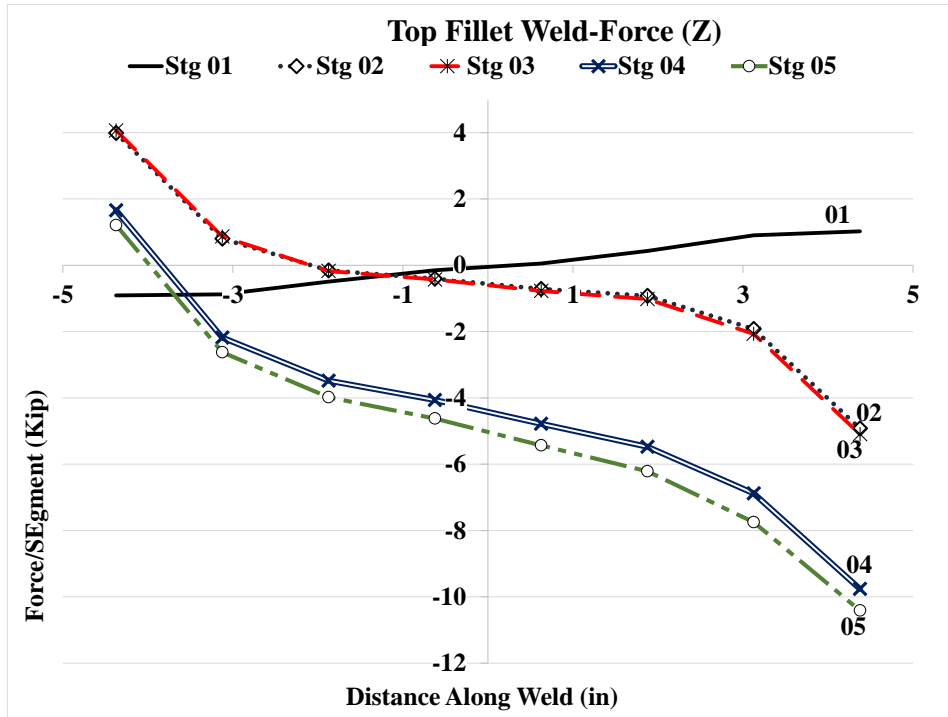


Figure 4.144: Forces and stresses in horizontal weld, (Z) Case 4A1

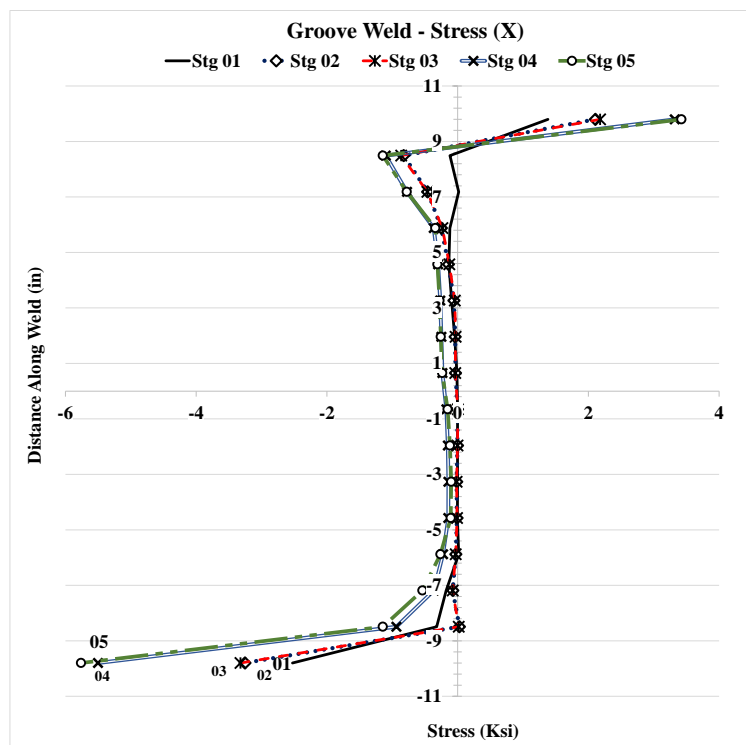
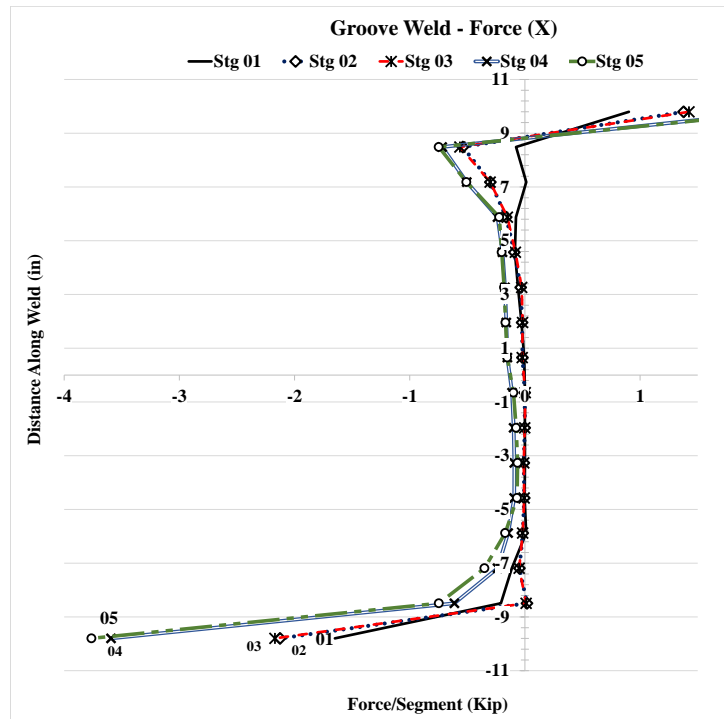


Figure 4.145: Forces and stresses in vertical weld, (X) Case 4A1



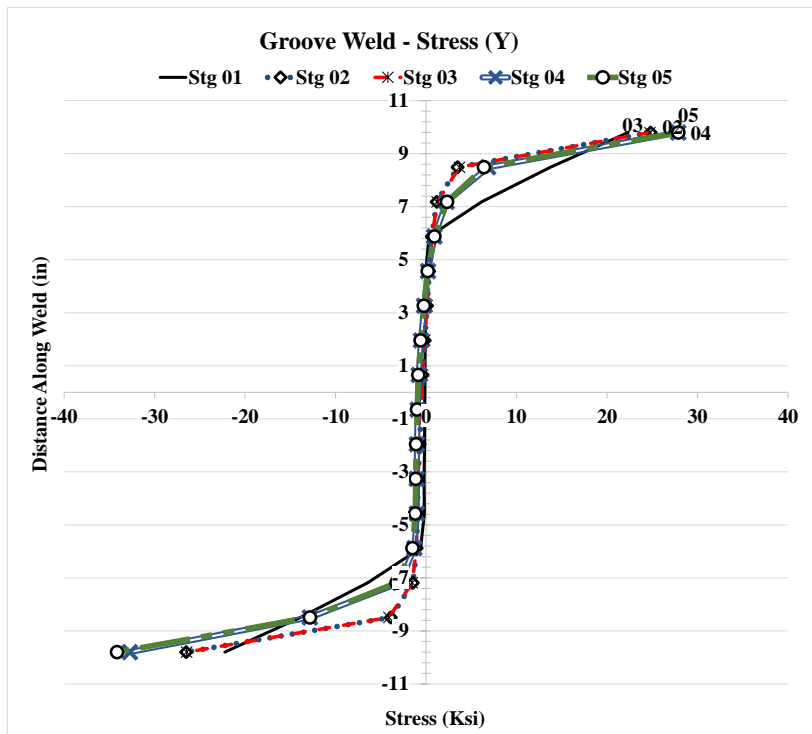
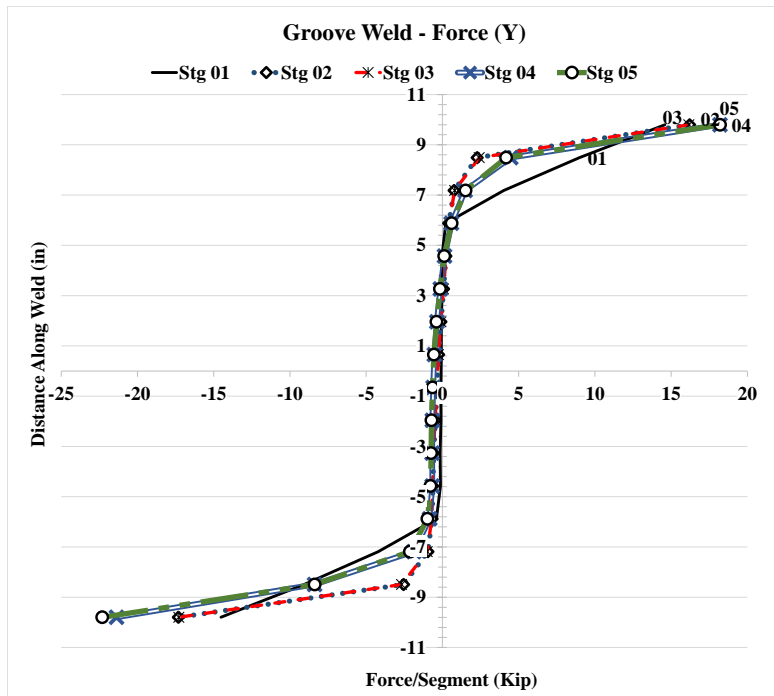


Figure 4.146: Forces and stresses in vertical weld, (Y) Case 4A1

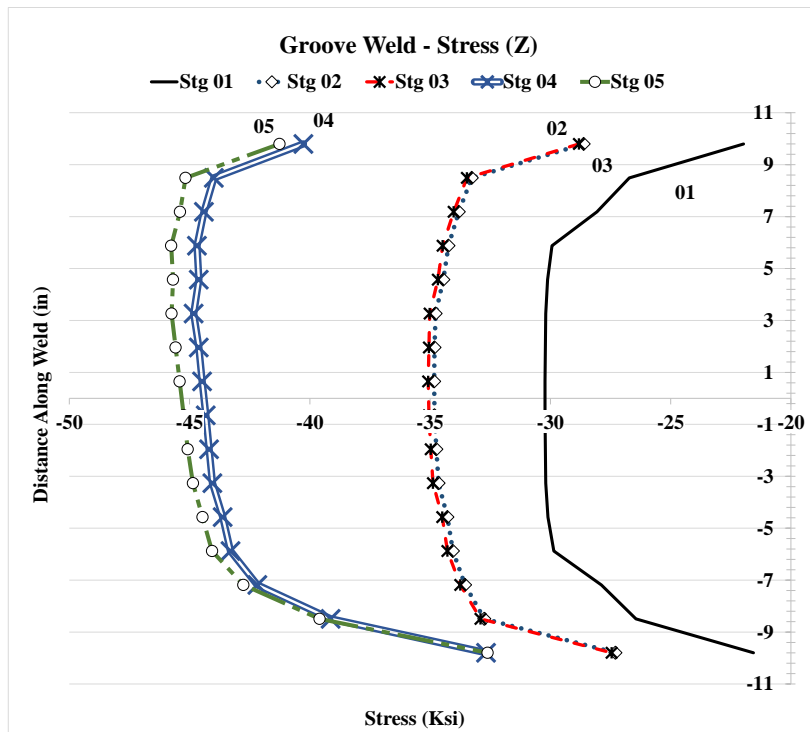
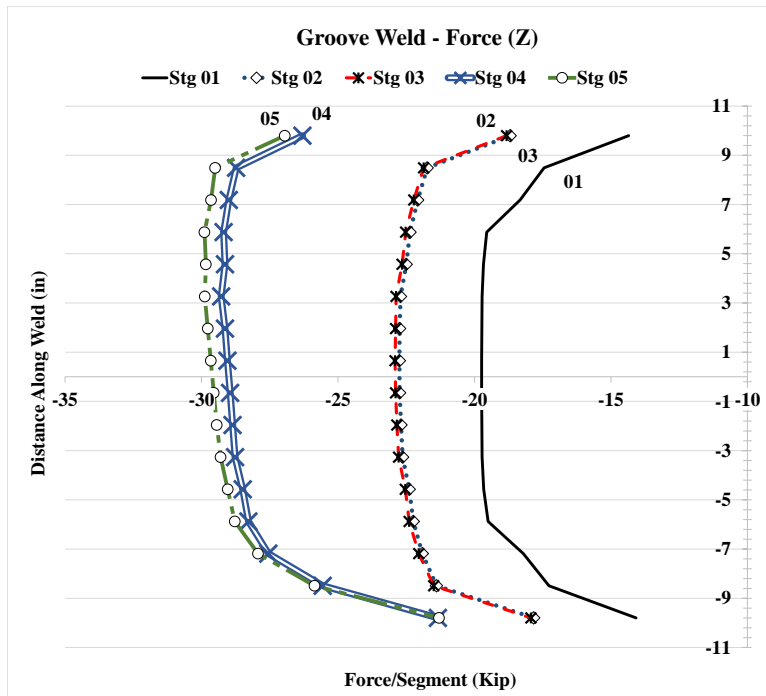


Figure 4.147: Forces and stresses in vertical weld, (Z) Case 4A1

### 4.2.14 Analysis Case 4C

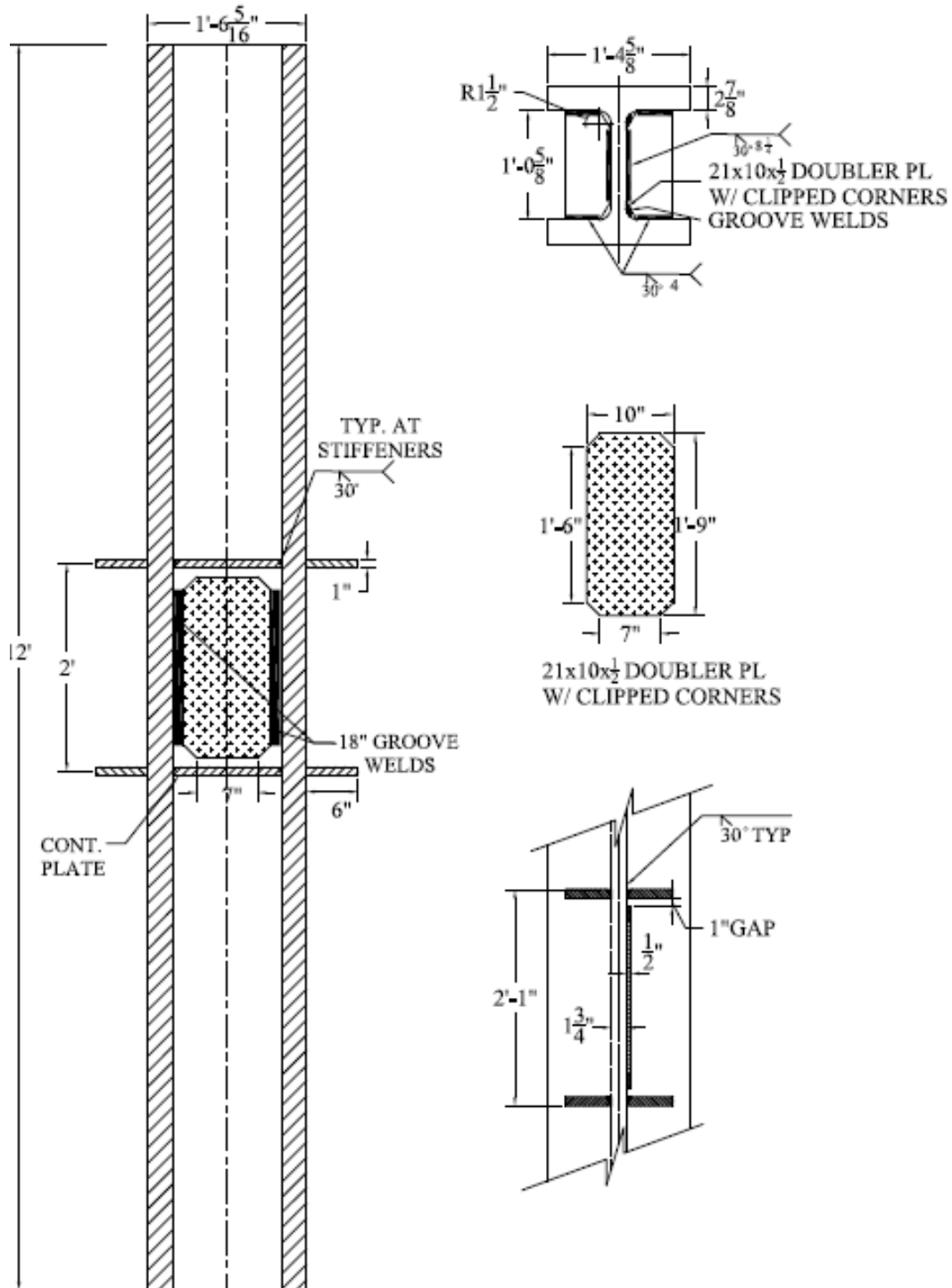


Figure 4.148: Analysis case 4C

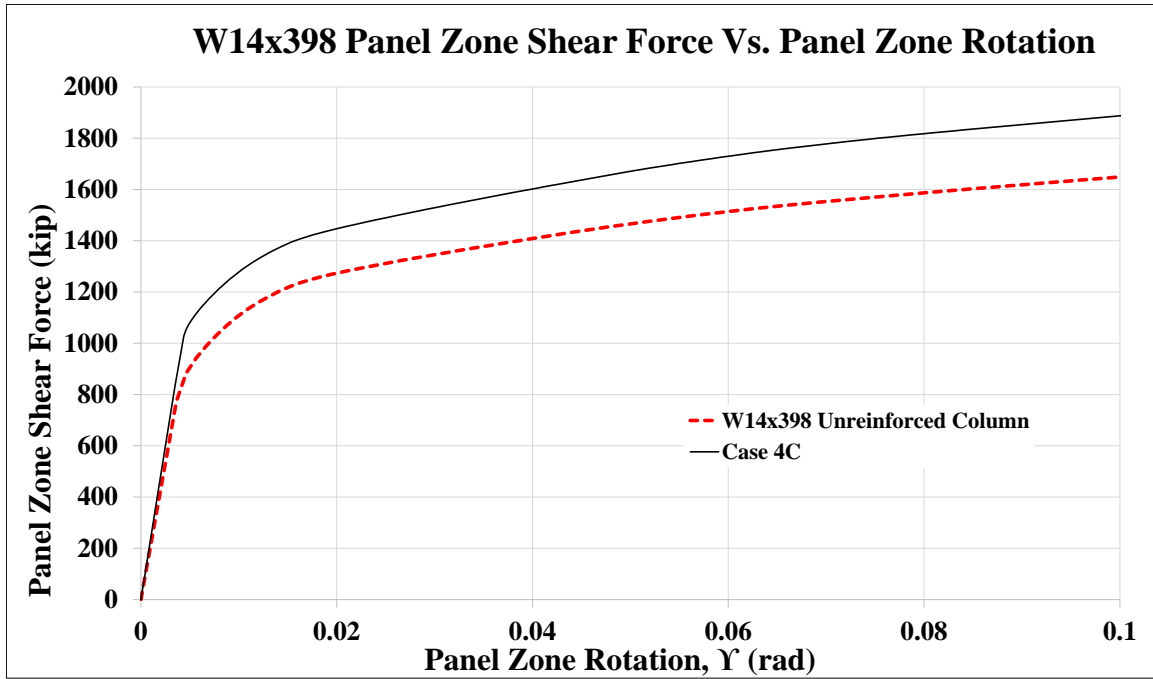


Figure 4.149: Panel zone shear vs. panel zone rotation Case 4C

Stage	Applied Force/Loading Plate (Kip)	Panel Shear Force (Kip)	% Higher than unreinforced Col.	Panel Zone Rotation (rad)
1	617	1,029	116%	0.004
2	838	1,396	112%	0.015
3	872	1,454	114%	0.021
4	1,141	1,902		0.104
5	1,132	1,887	114%	0.100

Table 4.16: Panel zone shear and force on loading plate Case 4C

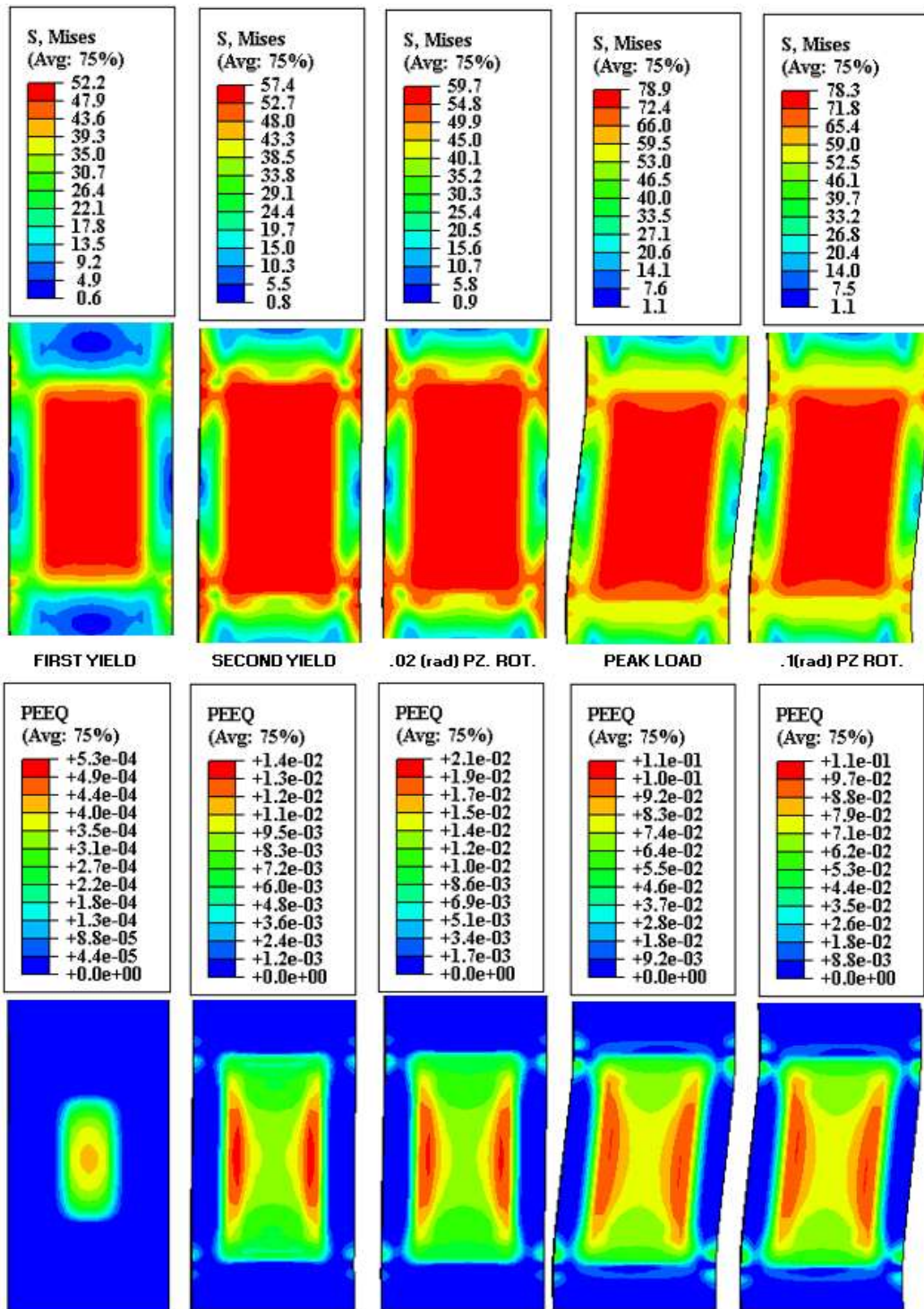


Figure 4.150: VMS and PEEQ in the column Case 4C

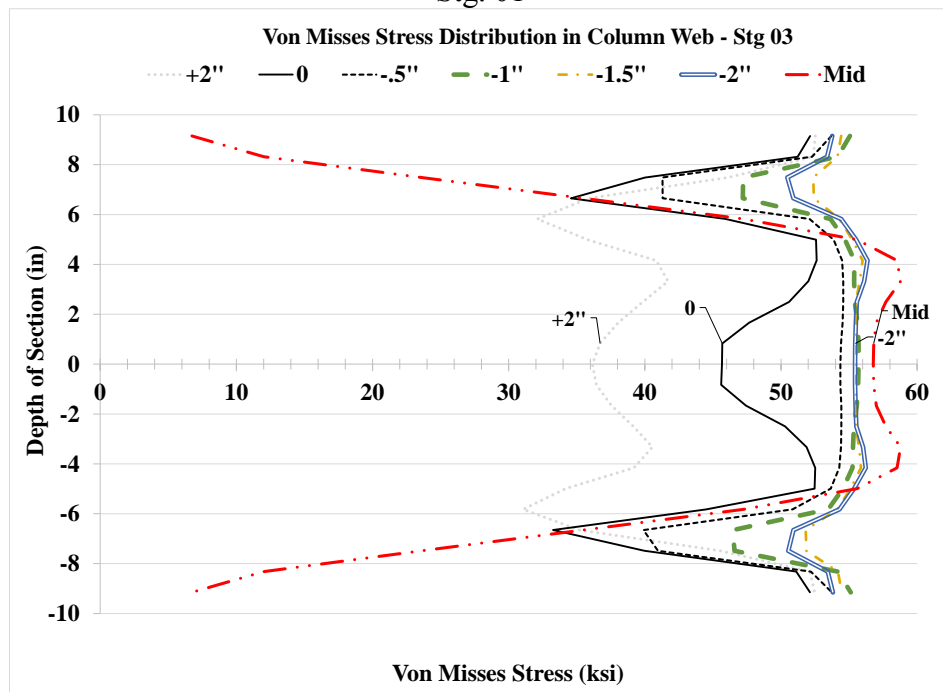
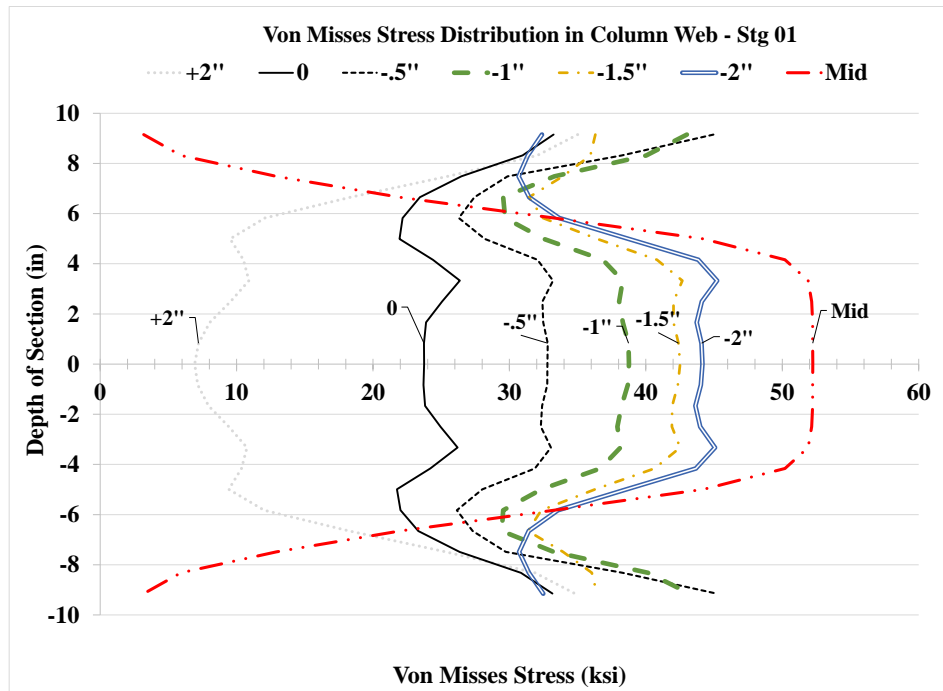
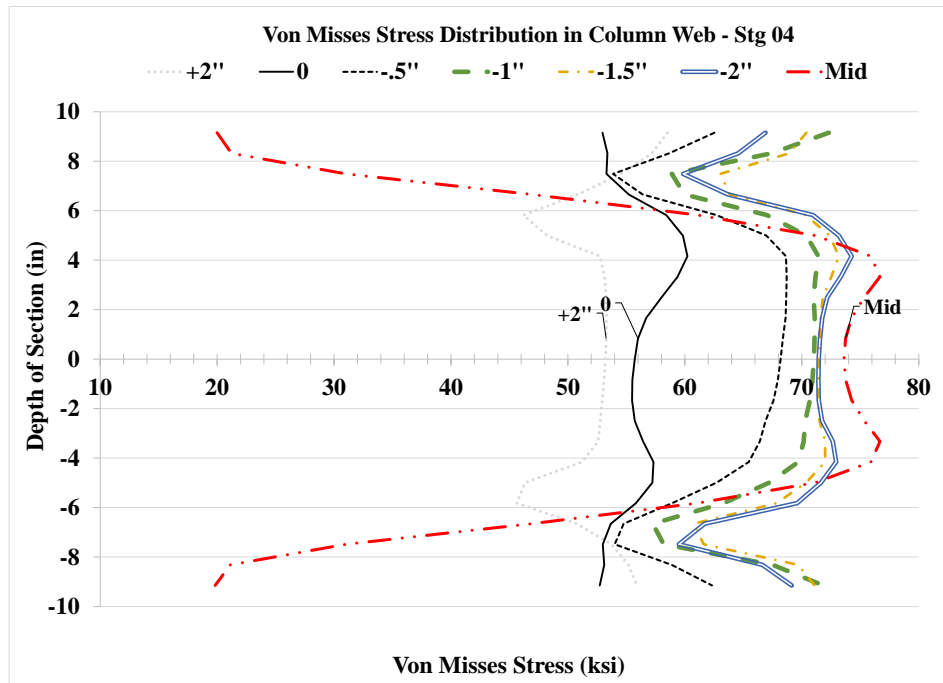


Figure 4.151: VMS distribution in column web at different heights Stg. 01-04 Case 4C



Stg. 04

Figure 4.151: VMS distribution in column web at different heights Stg. 01-04 Case 4C

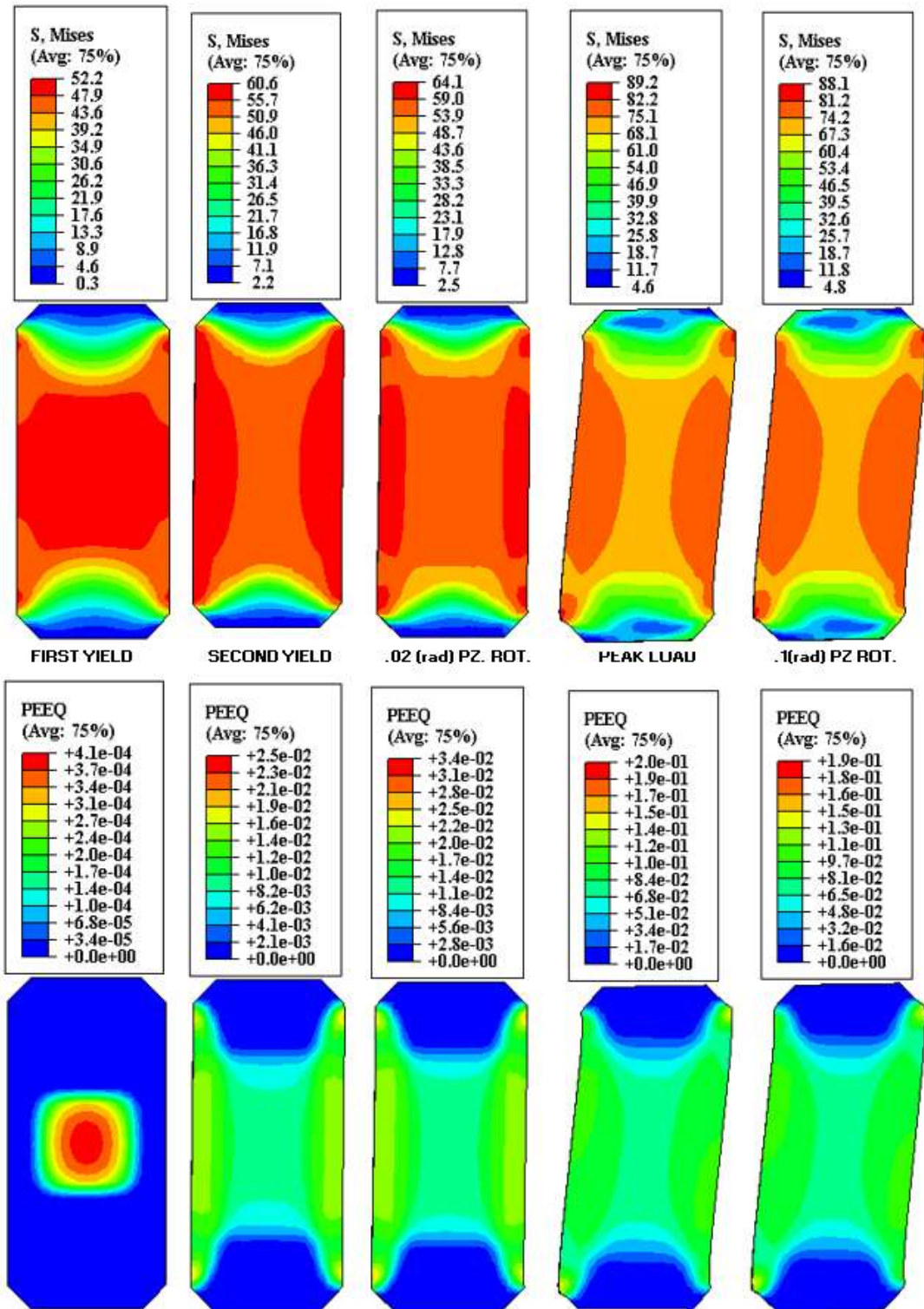


Figure 4.152: VMS and PEEQ in the DP Case 4C



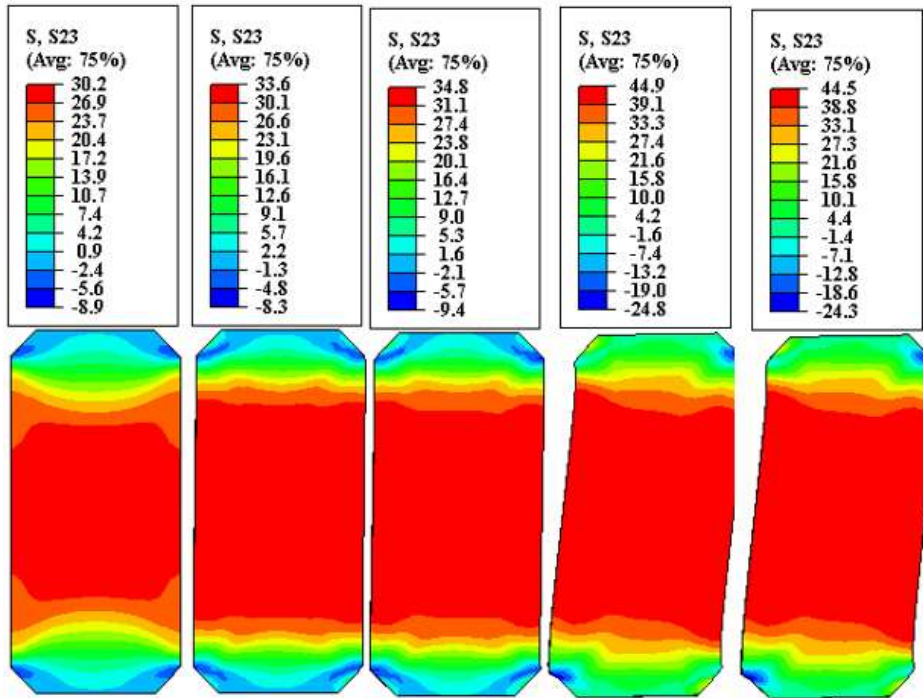


Figure 4.153: Shear stress, S23 in the DP Case 4C

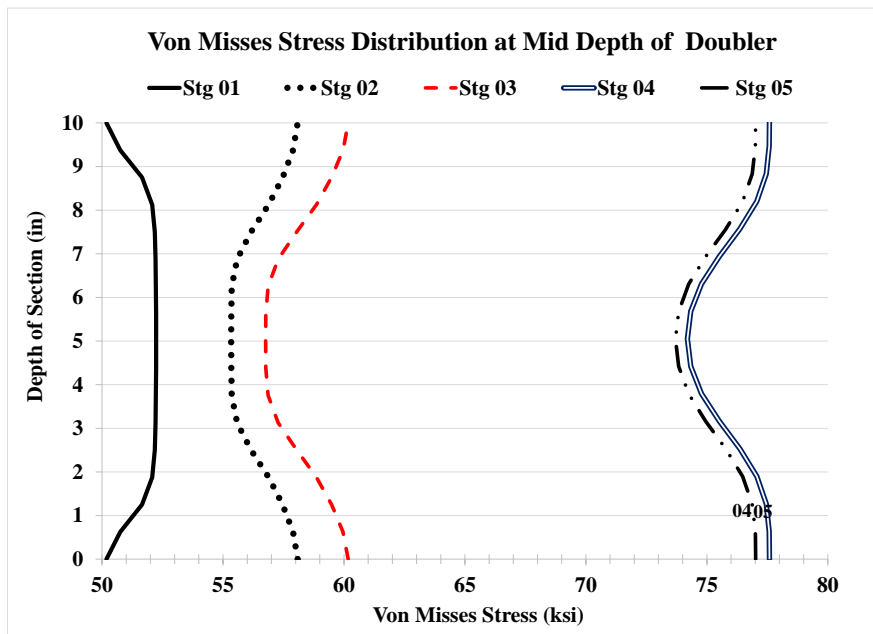


Figure 4.154: VMS distribution at mid-depth of DP Case 4C

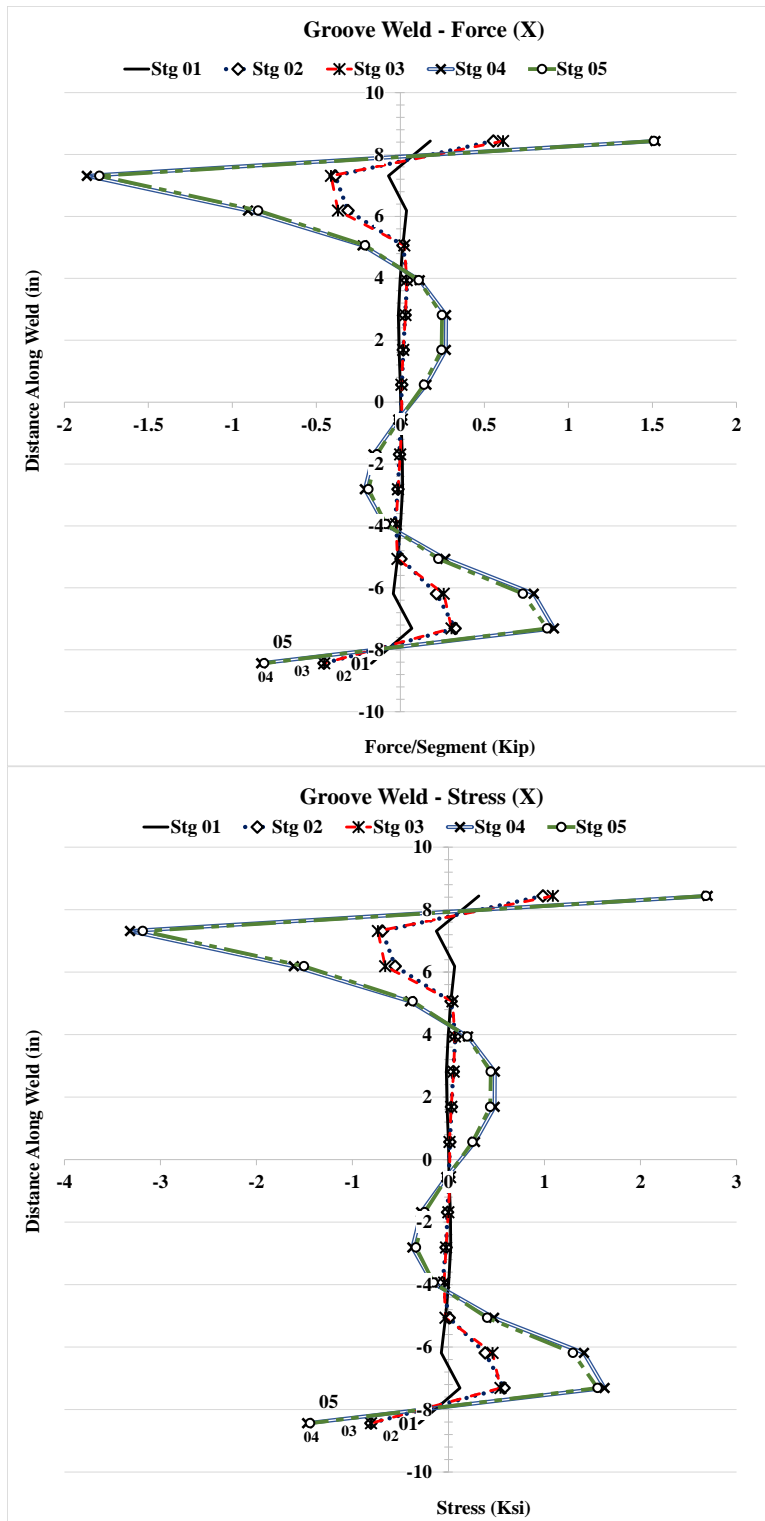


Figure 4.155: Forces and stresses in vertical weld, (X) Case 4C

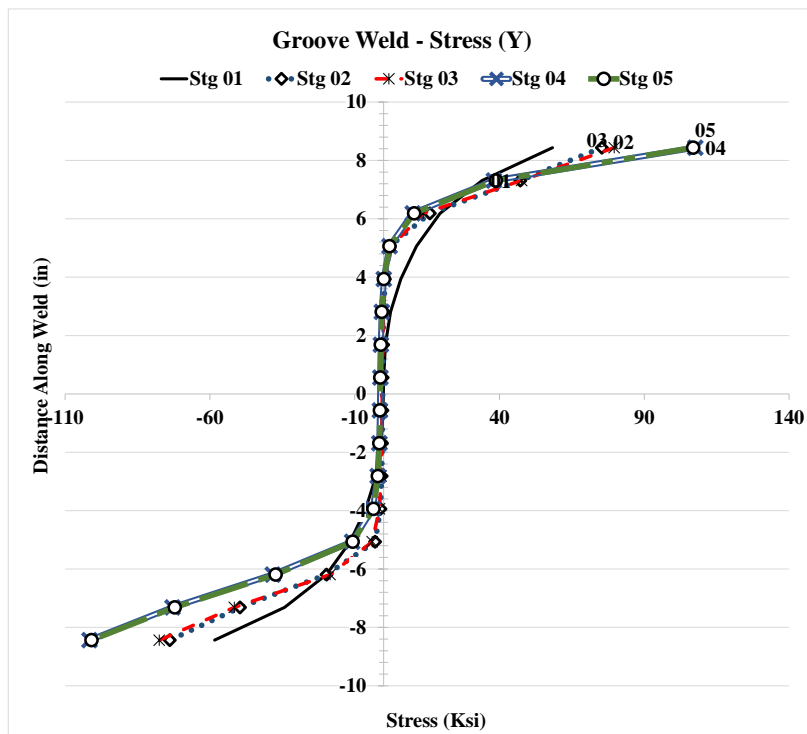
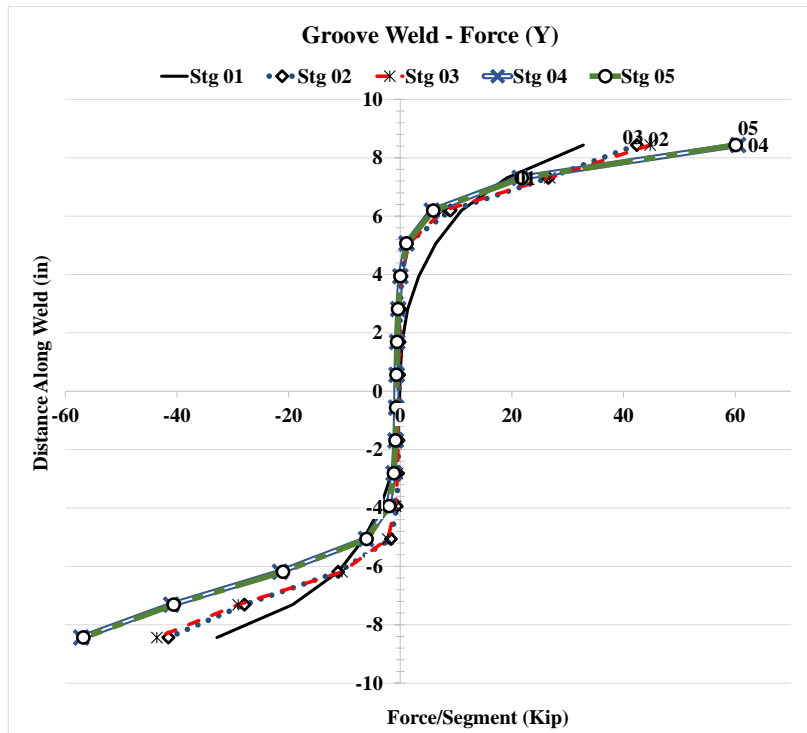


Figure 4.156: Forces and stresses in vertical weld, (Y) Case 4C

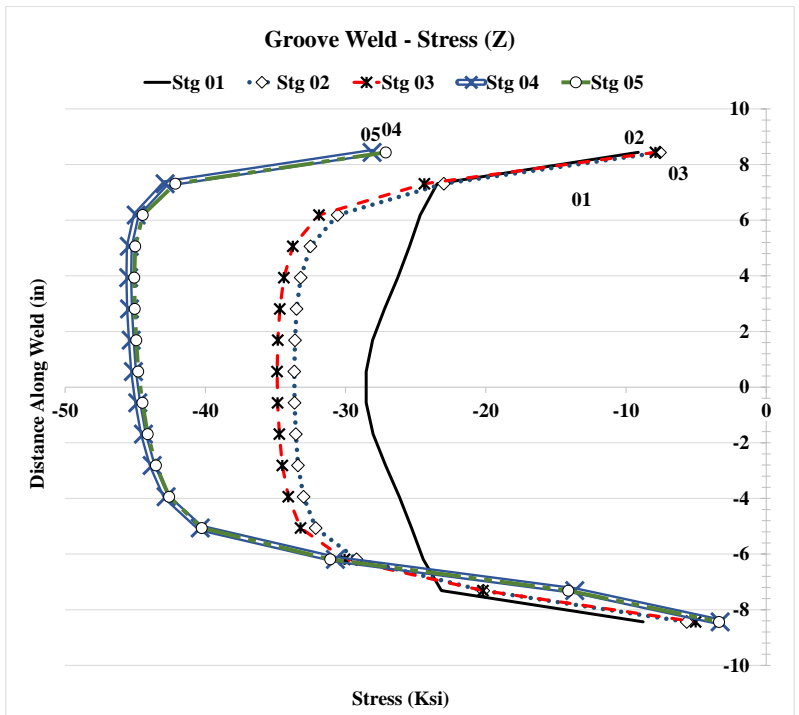
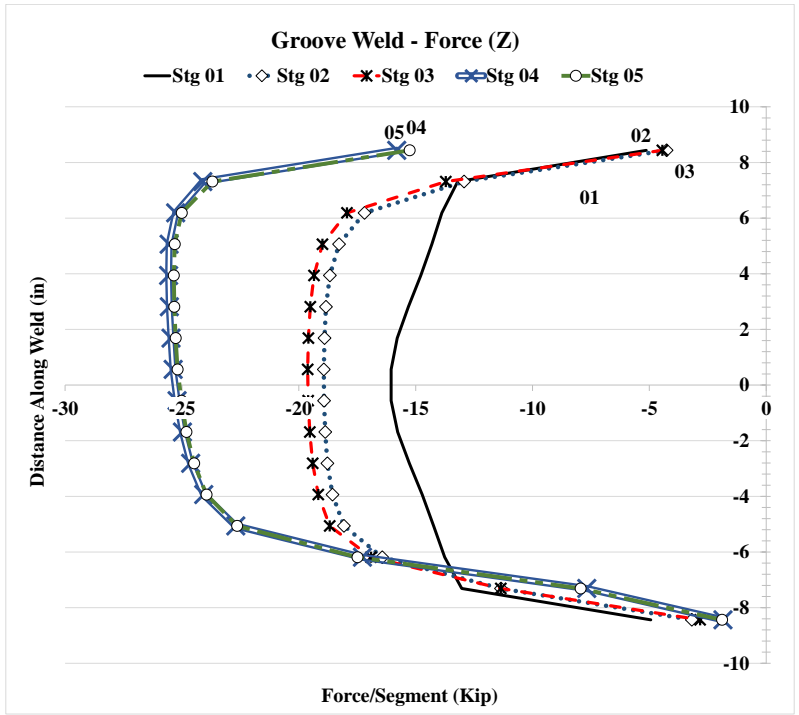


Figure 4.157: Forces and stresses in vertical weld, (Z) Case 4C  
259

### 4.2.15 Analysis Case 4C1

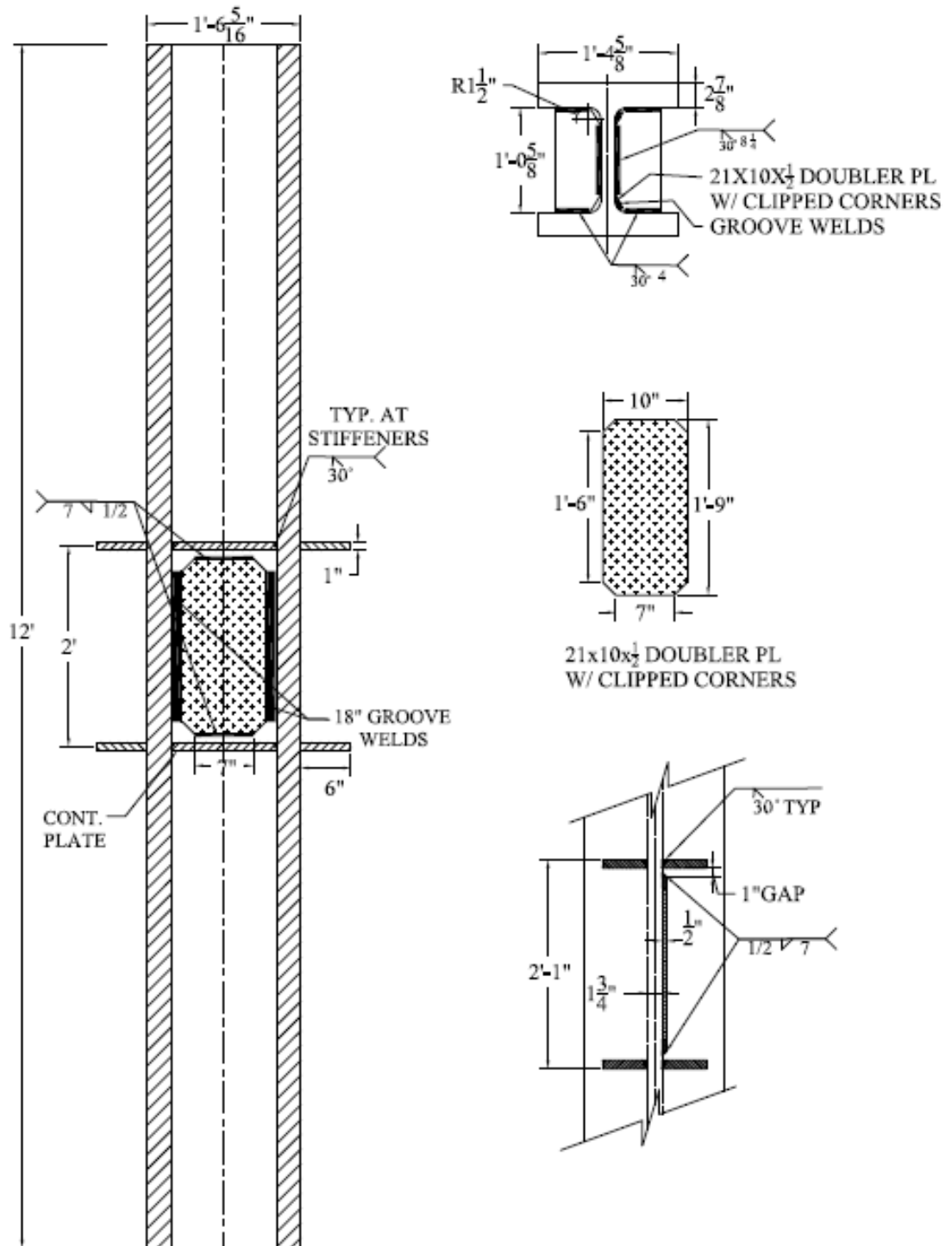


Figure 4.158: Analysis case 4C1

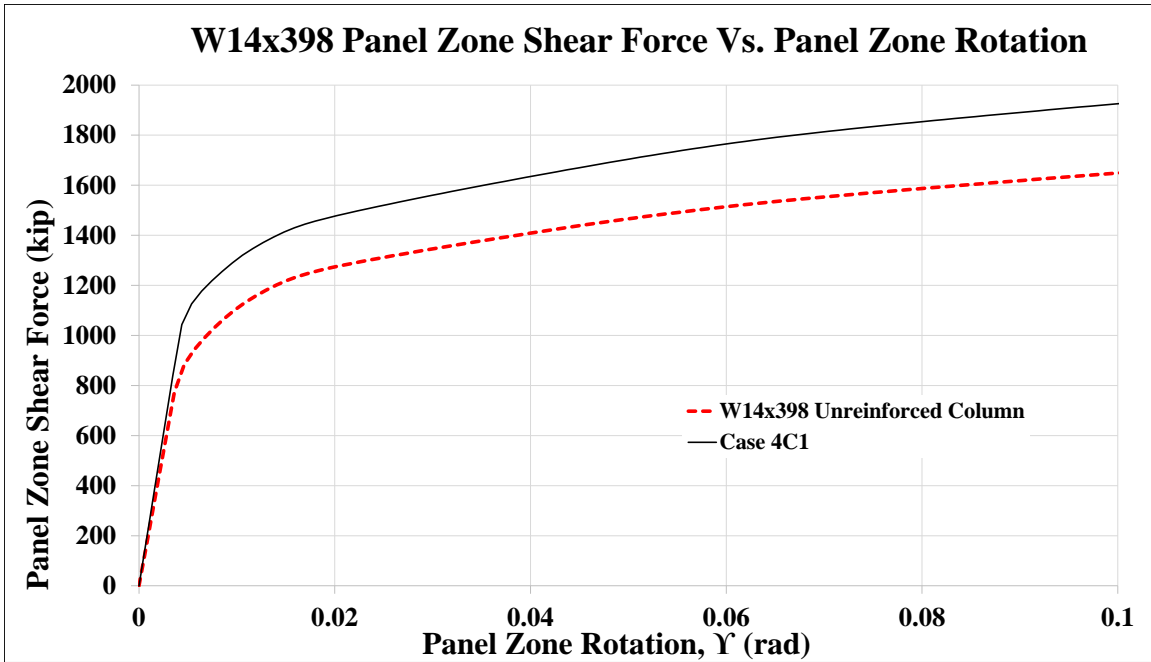


Figure 4.159: Panel zone shear vs. panel zone rotation Case 4C1

Stage	Applied Force/Loading Plate (Kip)	Panel Shear Force (Kip)	% Higher than unreinforced Col.	Panel Zone Rotation (rad)
1	626	1,043	118%	0.004
2	867	1,444	116%	0.017
3	887	1,478	116%	0.020
4	1,141	1,901		0.093
5	1,156	1,927	117%	0.100

Table 4.17: Panel zone shear and force on loading plate Case 4C1

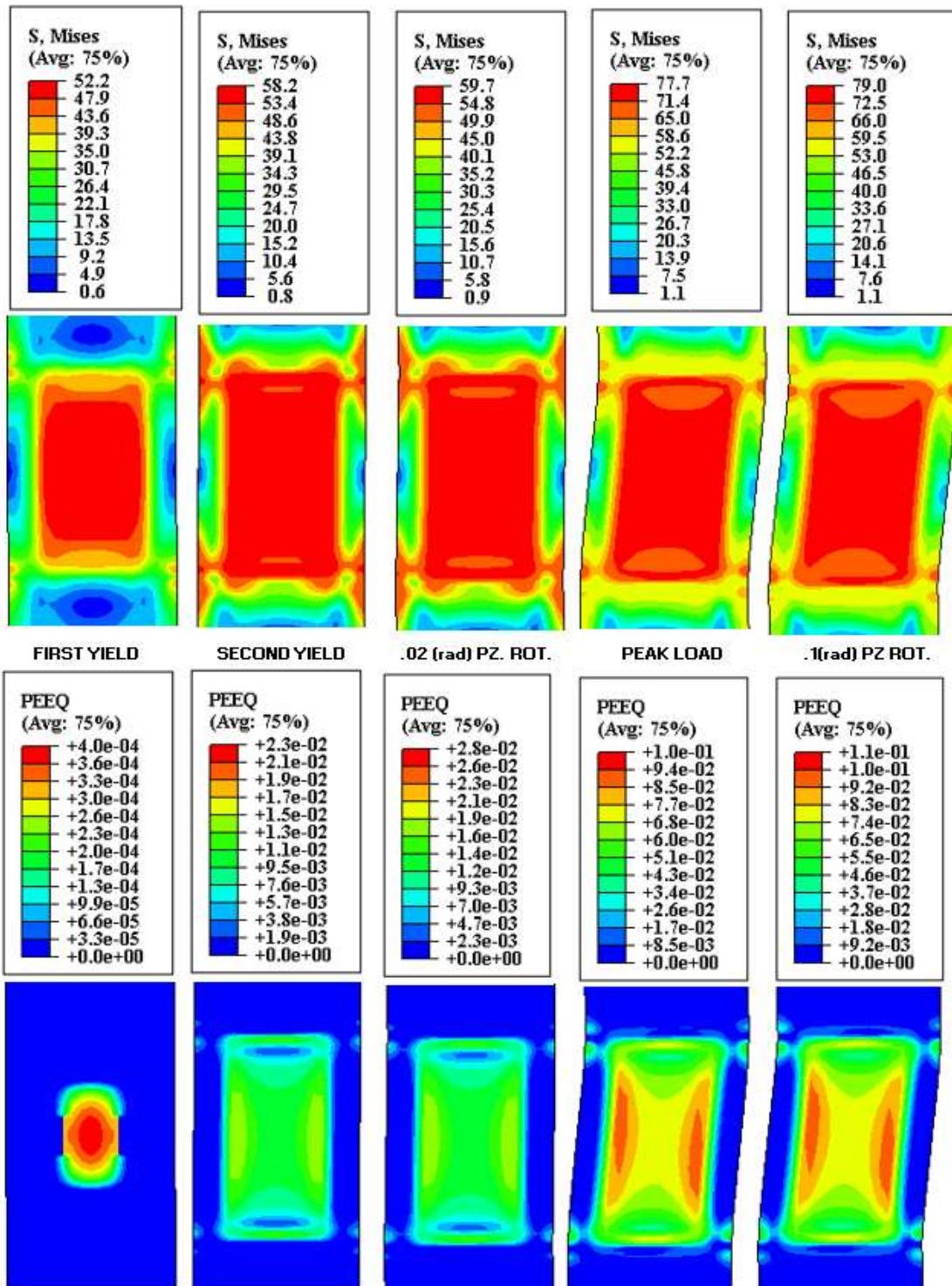


Figure 4.160: VMS and PEEQ in the column Case 4C1



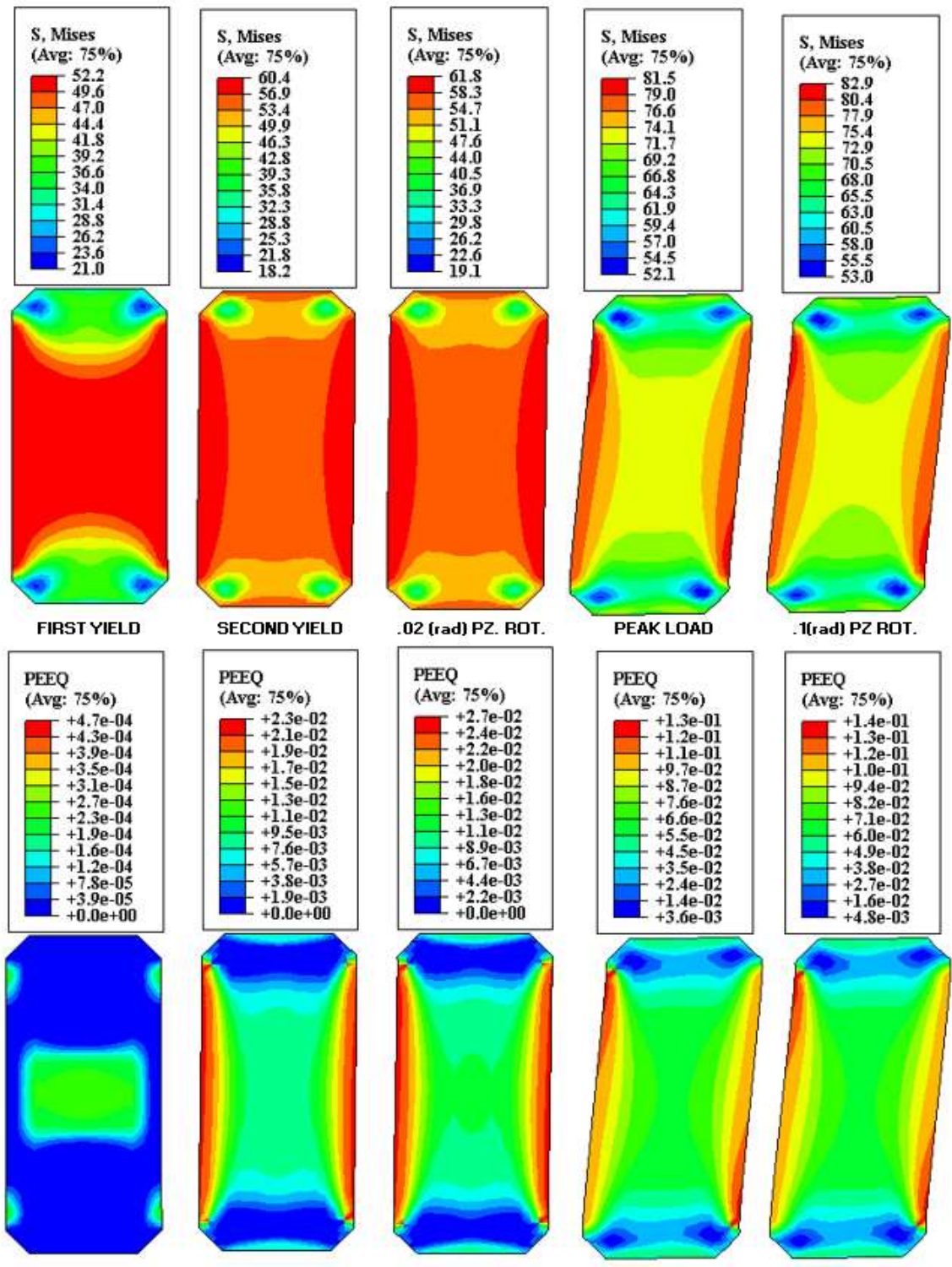


Figure 4.161: VMS and PEEQ in the DP Case 4C1



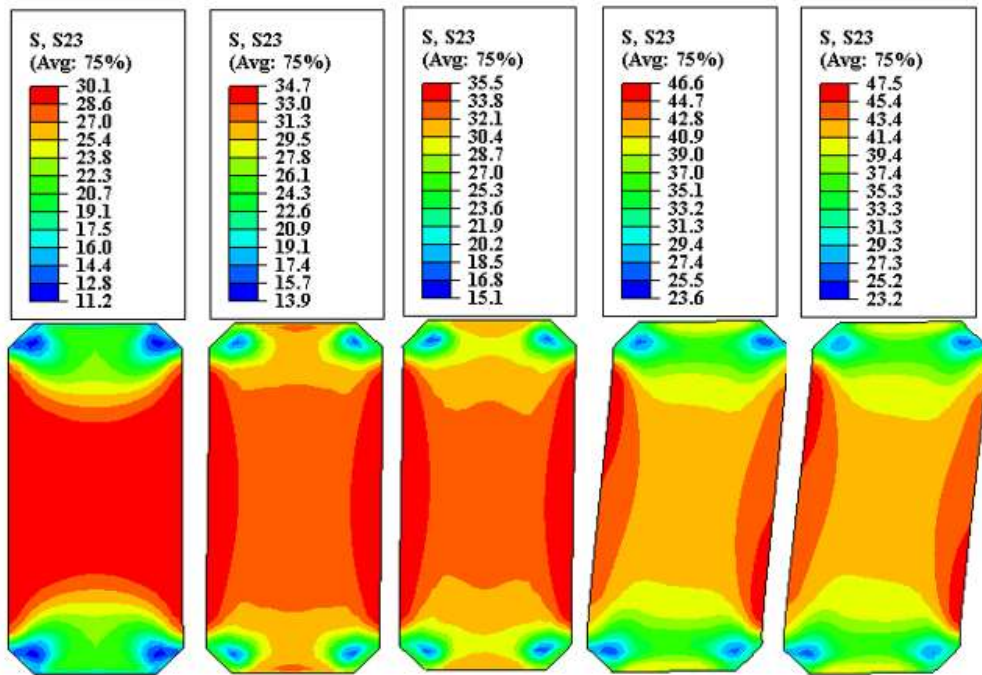


Figure 4.162: Shear stress, S23 in the DP Case 4C1

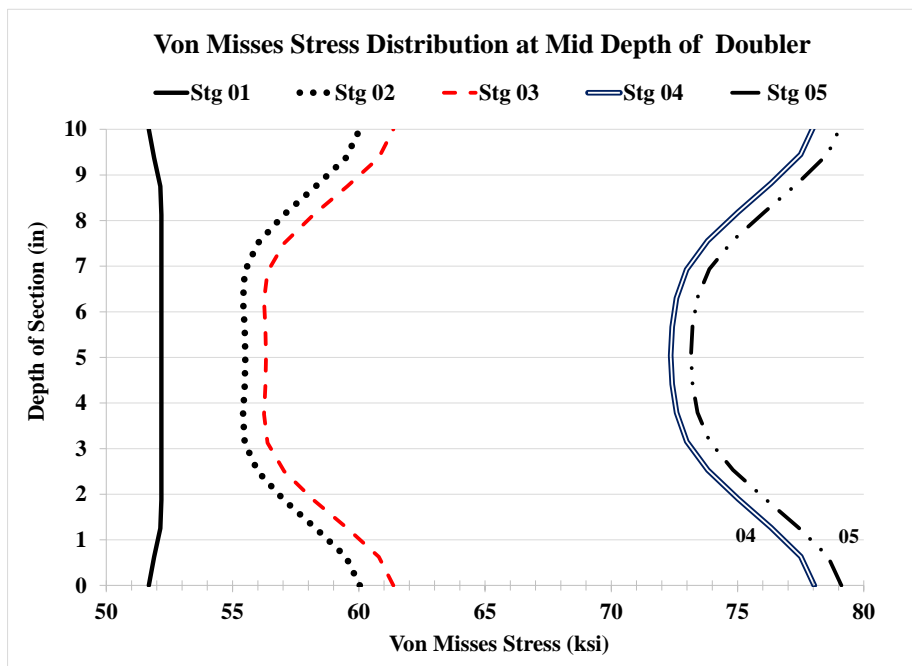


Figure 4.163: VMS distribution at mid-depth of DP Case 4C1

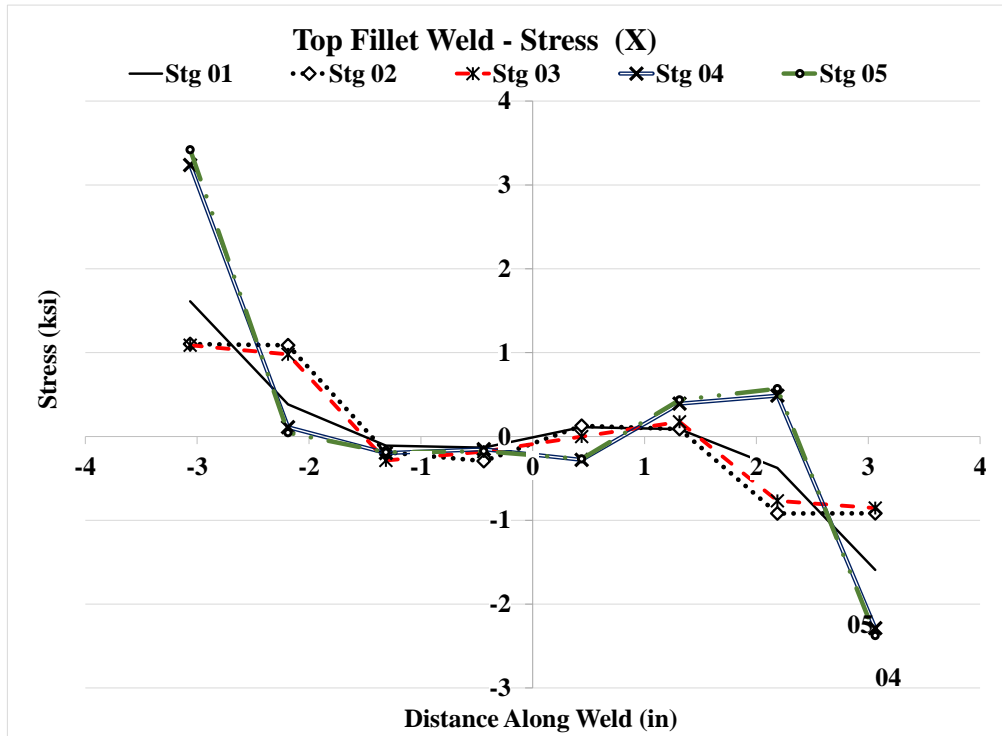
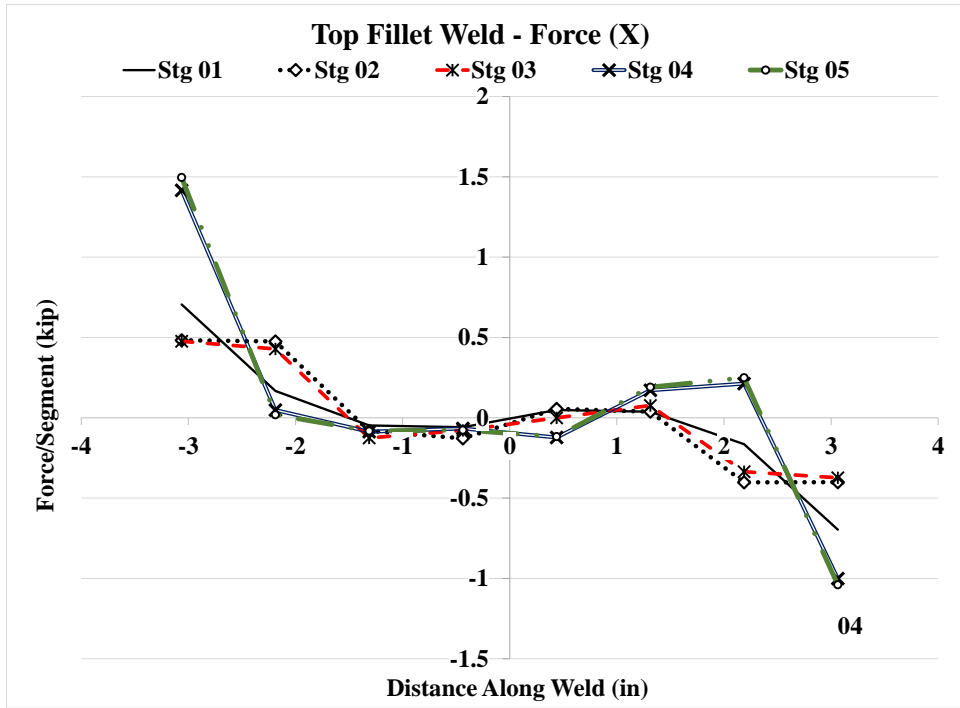


Figure 4.164: Forces and stresses in horizontal weld, (X) Case 4C1

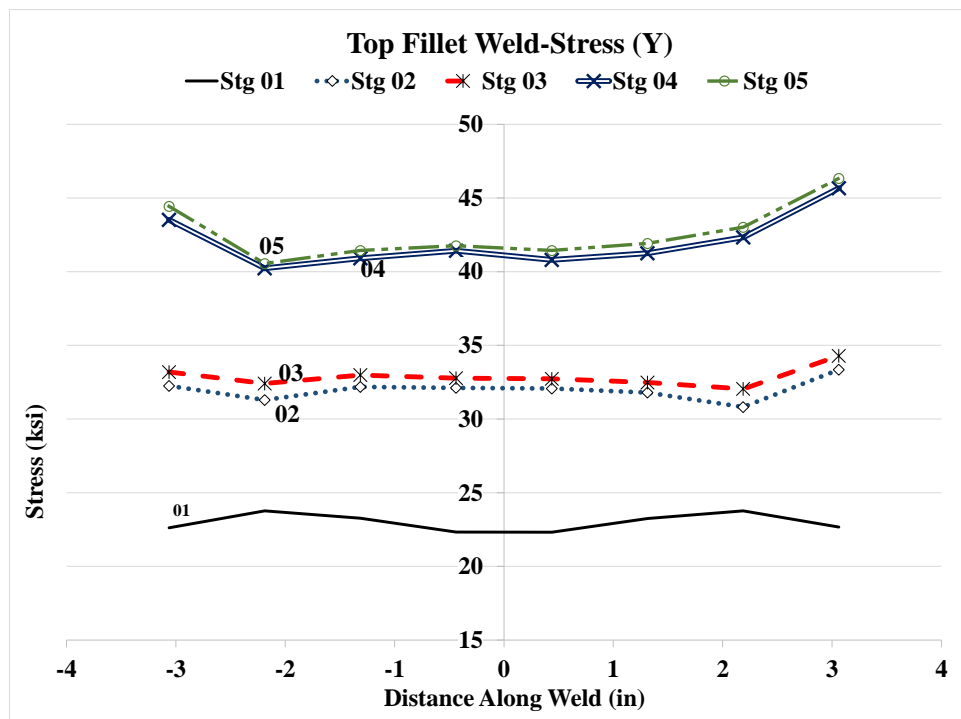
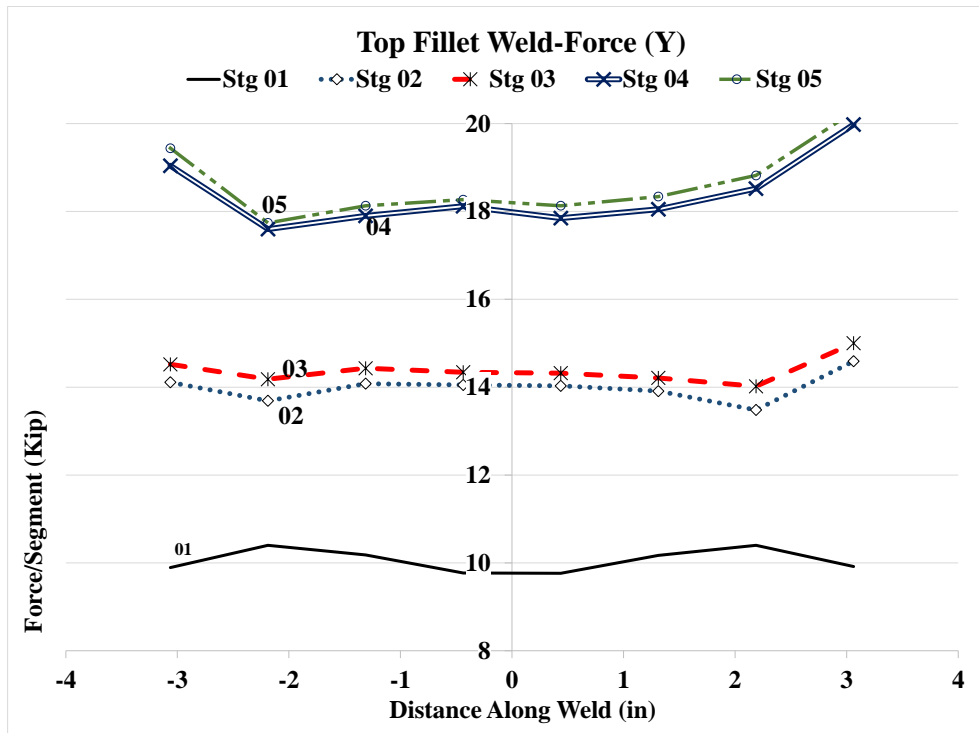


Figure 4.165: Forces and stresses in horizontal weld, (Y) Case 4C1

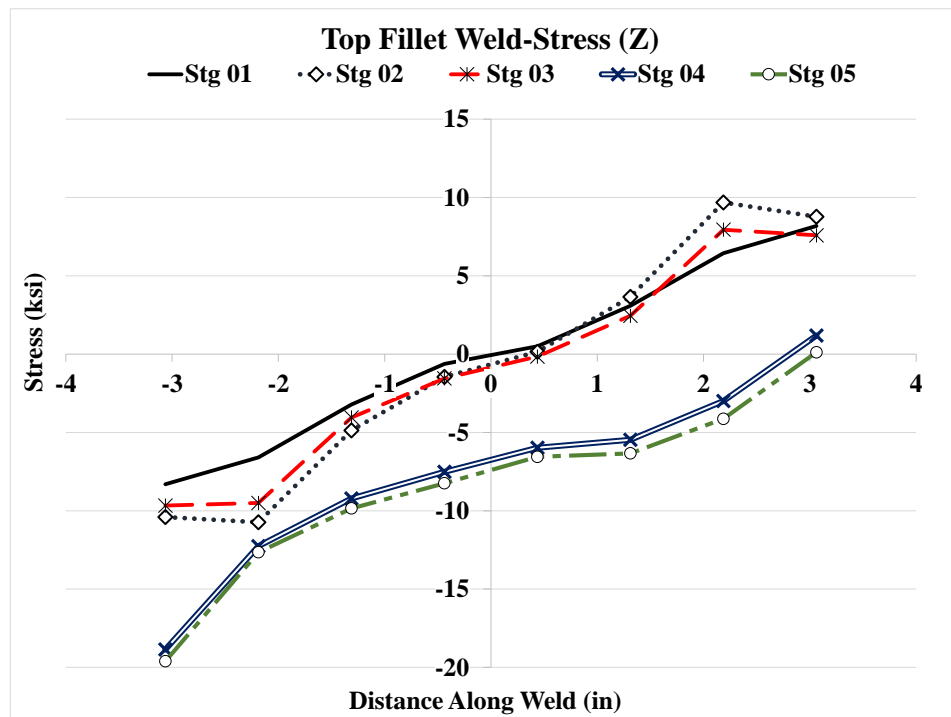
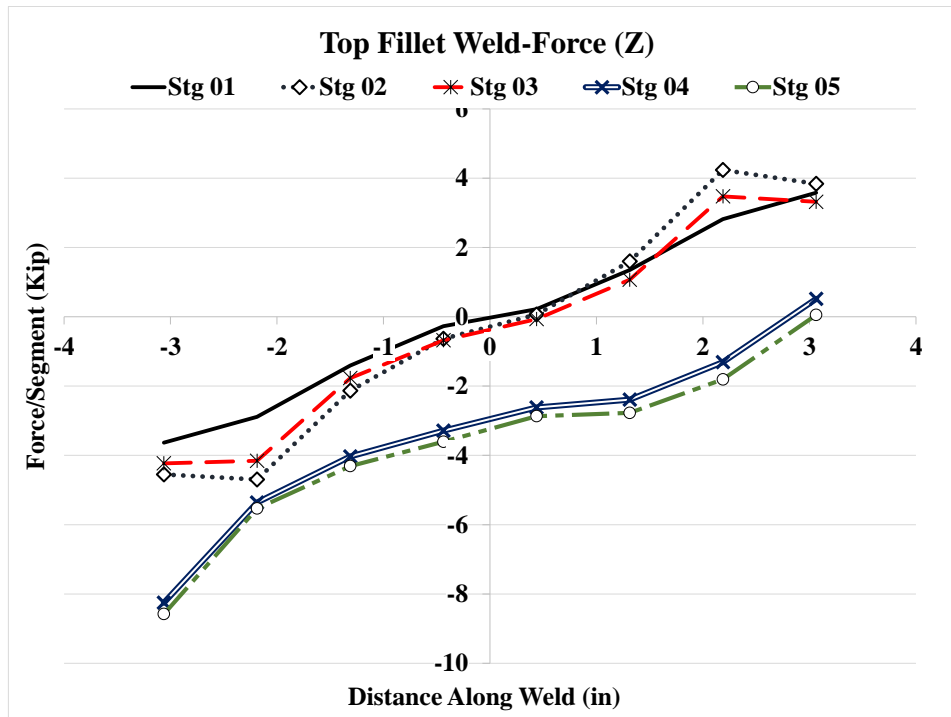


Figure 4.166: Forces and stresses in horizontal weld, (Z) Case 4C1

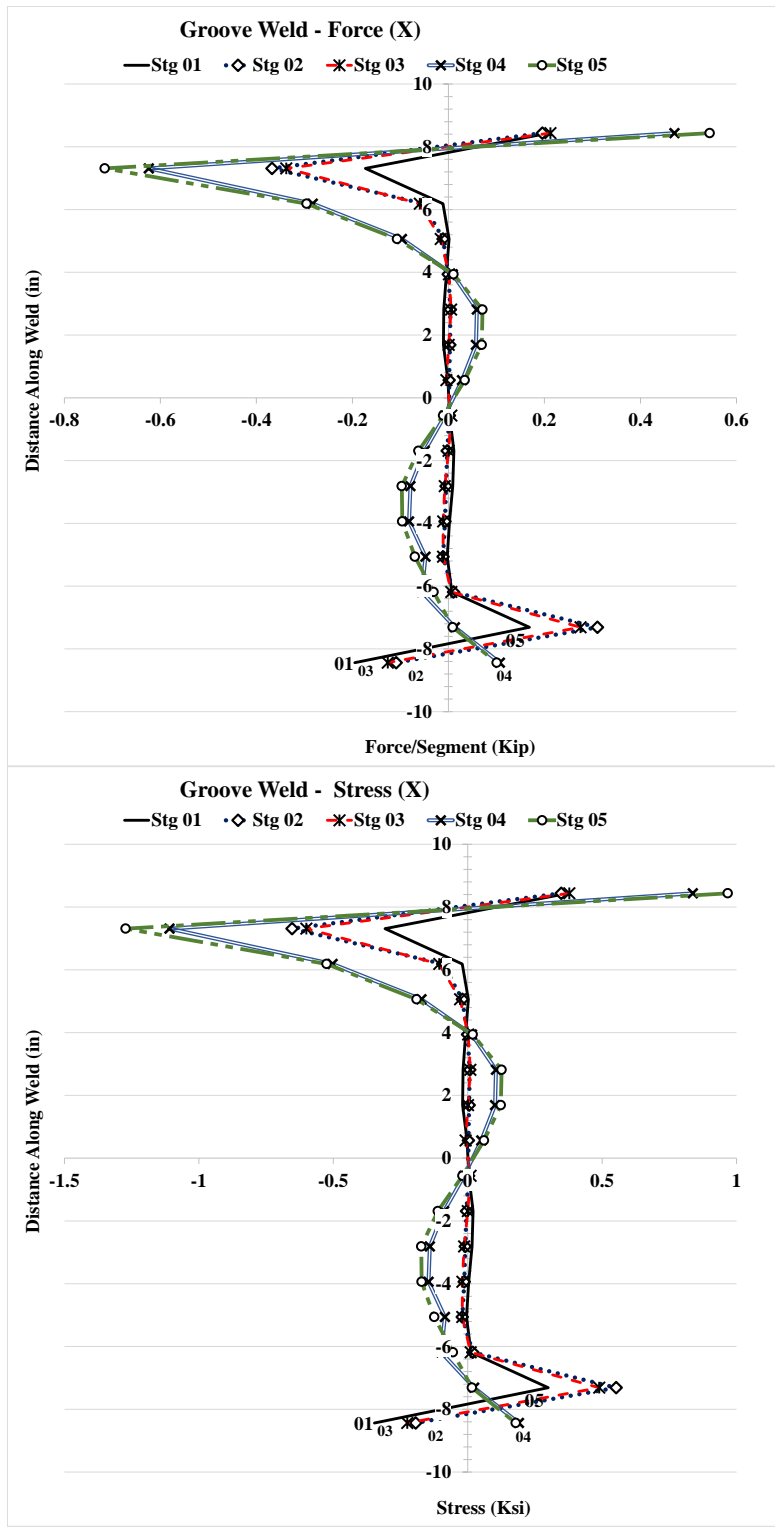


Figure 4.167: Forces and stresses in vertical weld, (X) Case 4C1

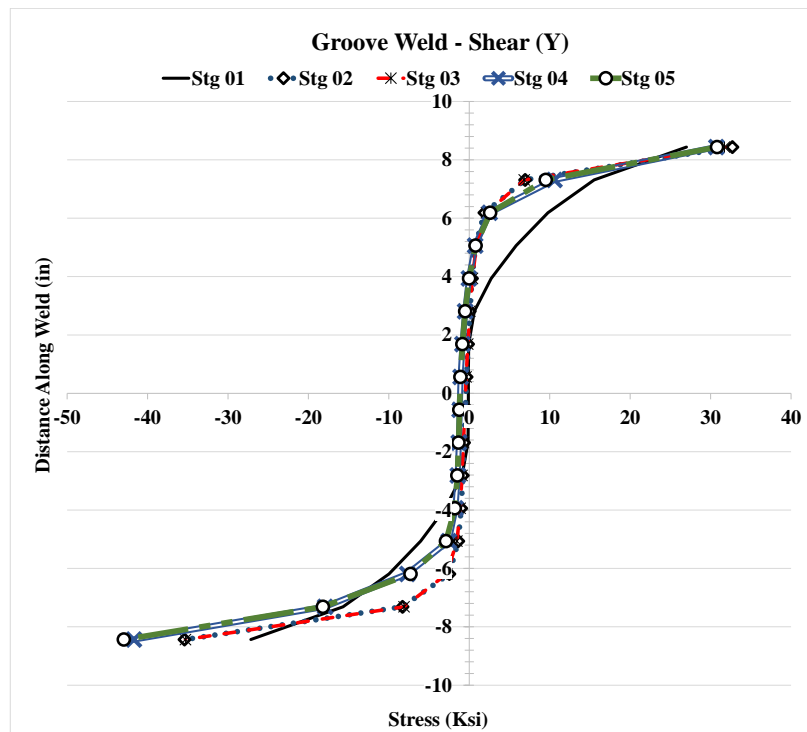
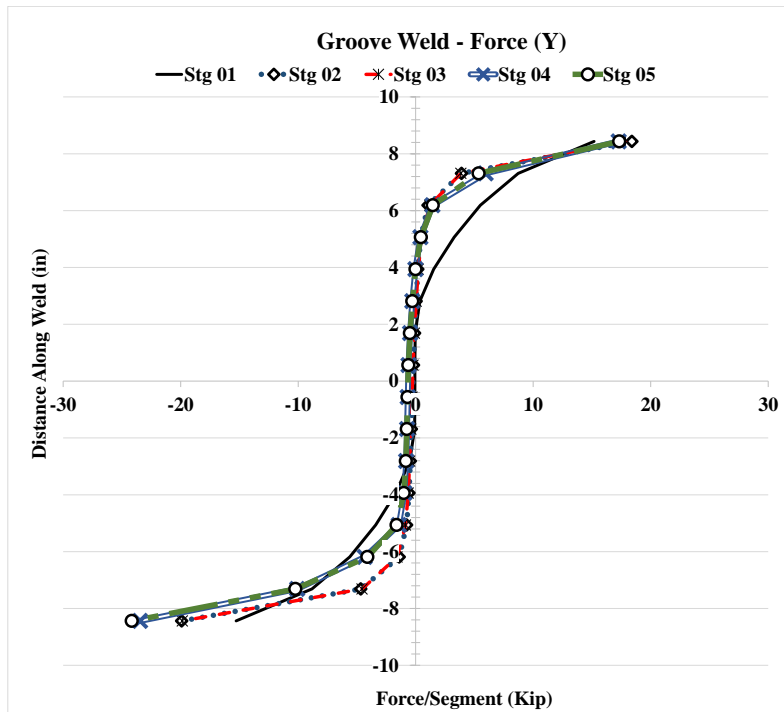


Figure 4.168: Forces and stresses in vertical weld, (Y) Case 4C1

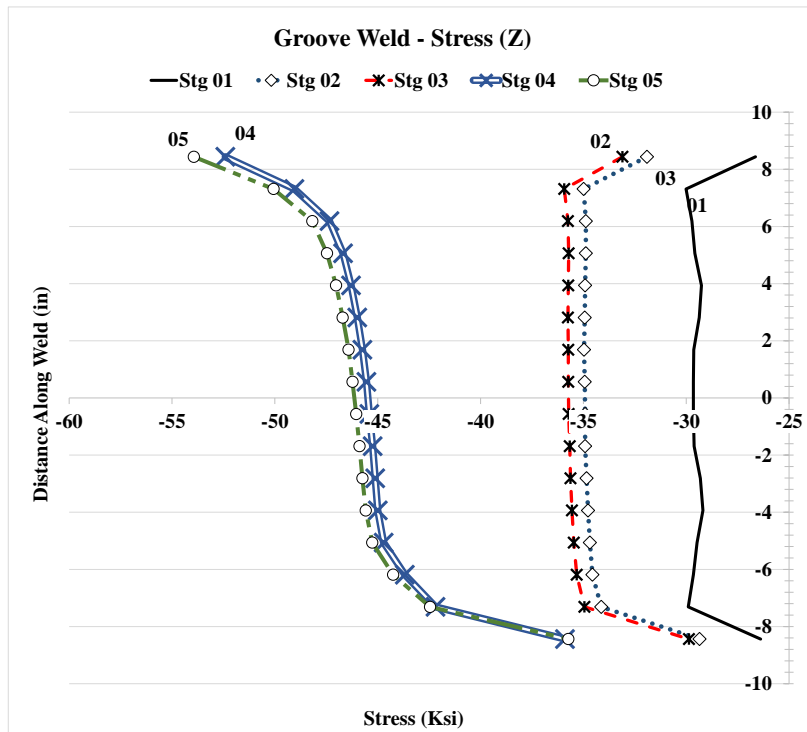
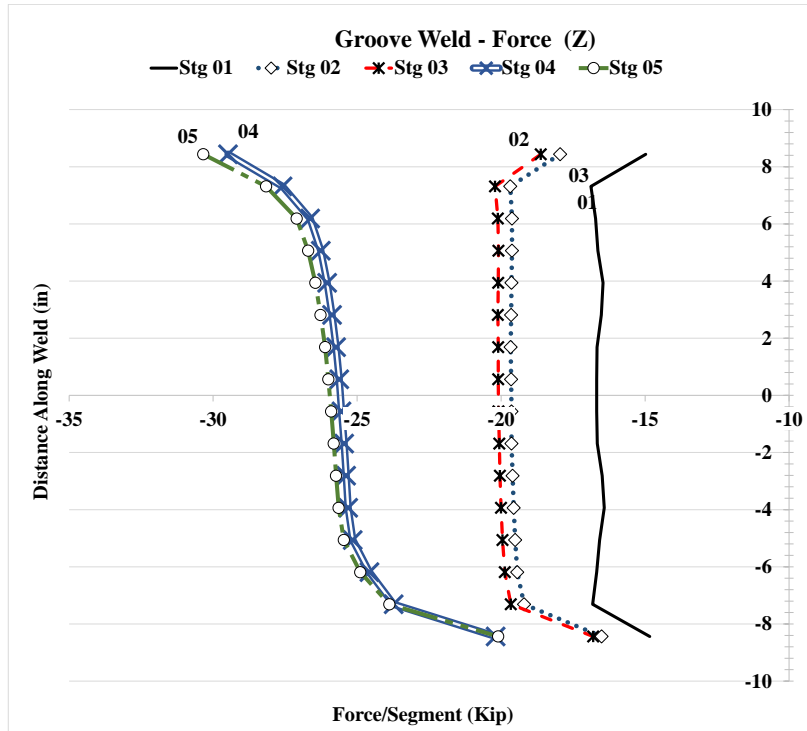


Figure 4.169: Forces and stresses in vertical weld, (Z) Case 4C1

### 4.2.16 Analysis Case 5A1

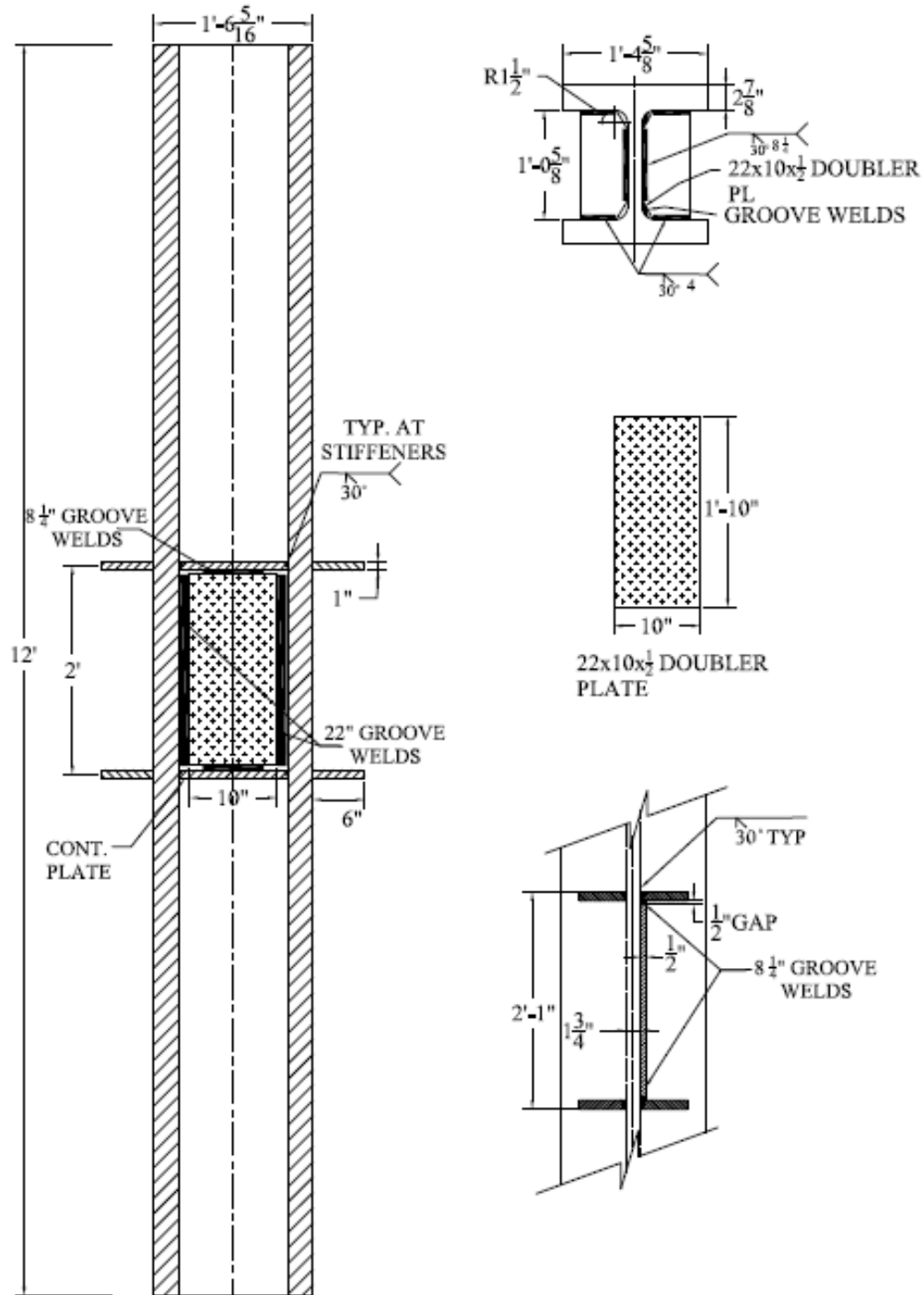


Figure 4.170: Analysis case 5A1



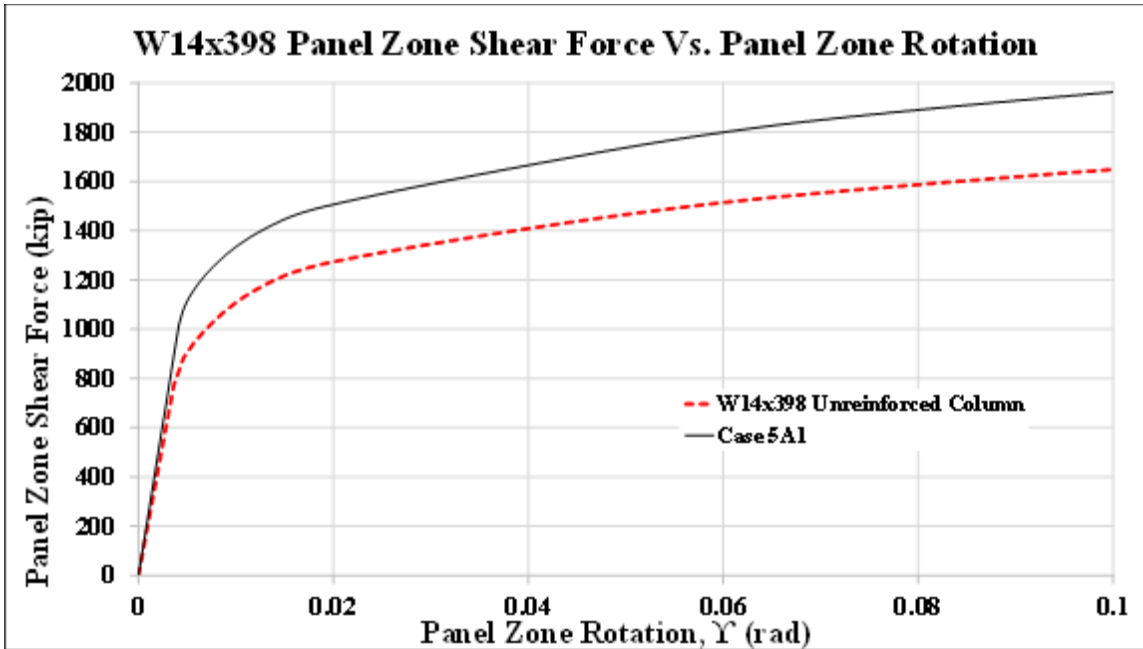


Figure 4.171: Panel zone shear vs. panel zone rotation Case 5A1

Stage	Applied Force/Loading Plate (Kip)	Panel Shear Force (Kip)	% Higher than unreinforced Col.	Panel Zone Rotation (rad)
1	611	1,018	115%	0.004
2	897	1,495	120%	0.019
3	904	1,507	118%	0.020
4	1,143	1,905		0.084
5	1,179	1,964	119%	0.100

Table 4.18: Panel zone shear and force on loading plate Case 5A1

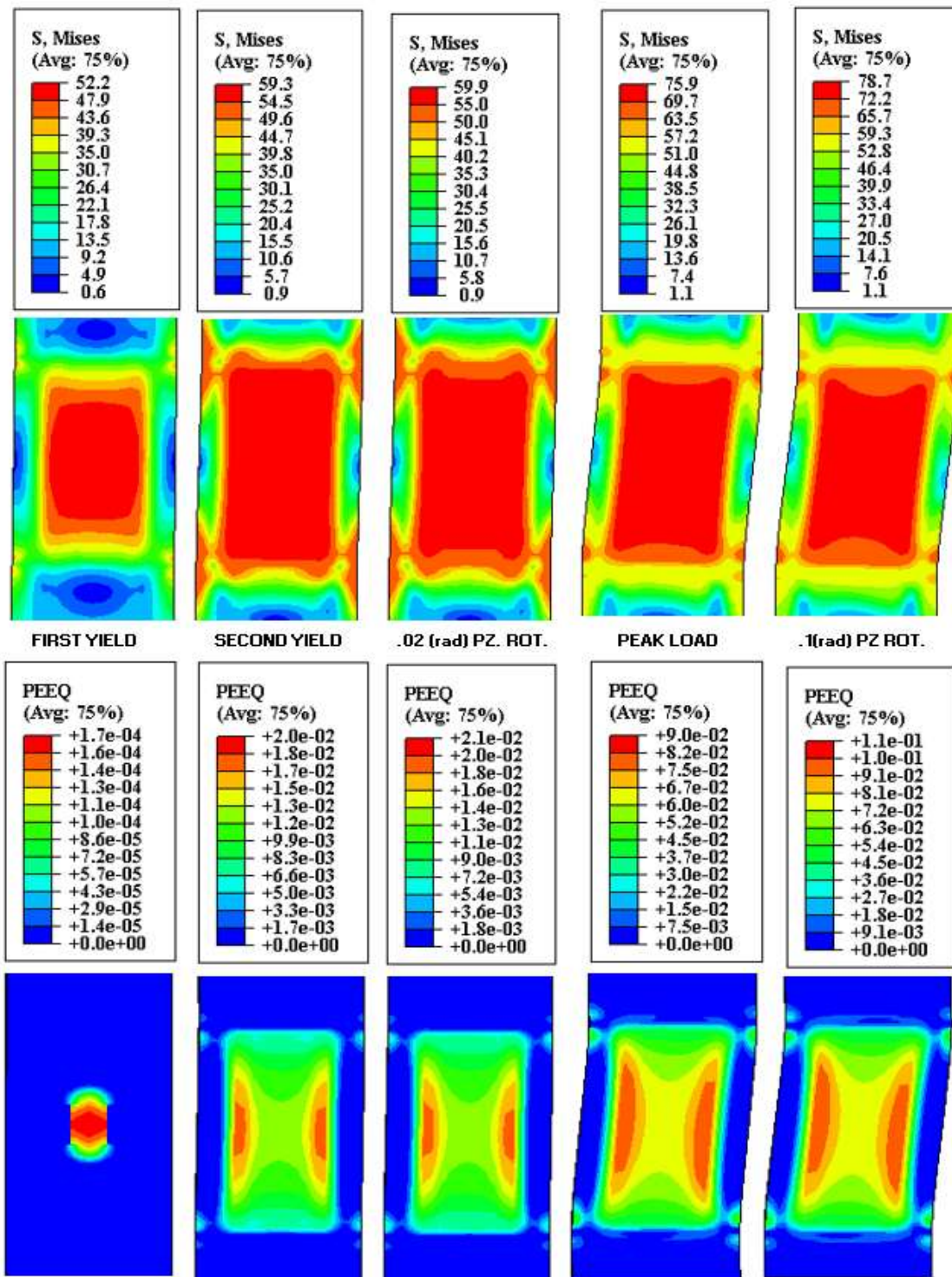
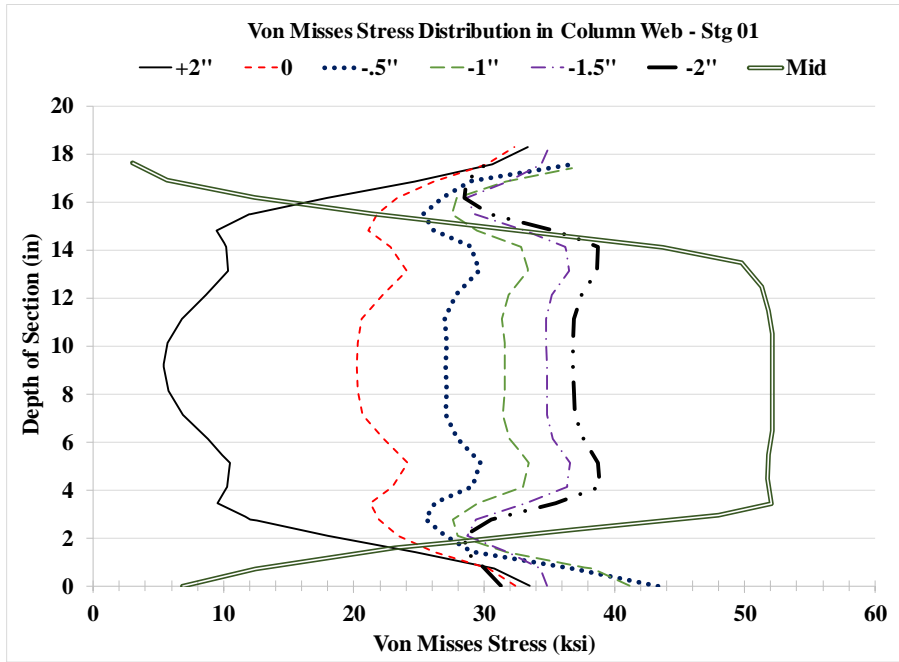
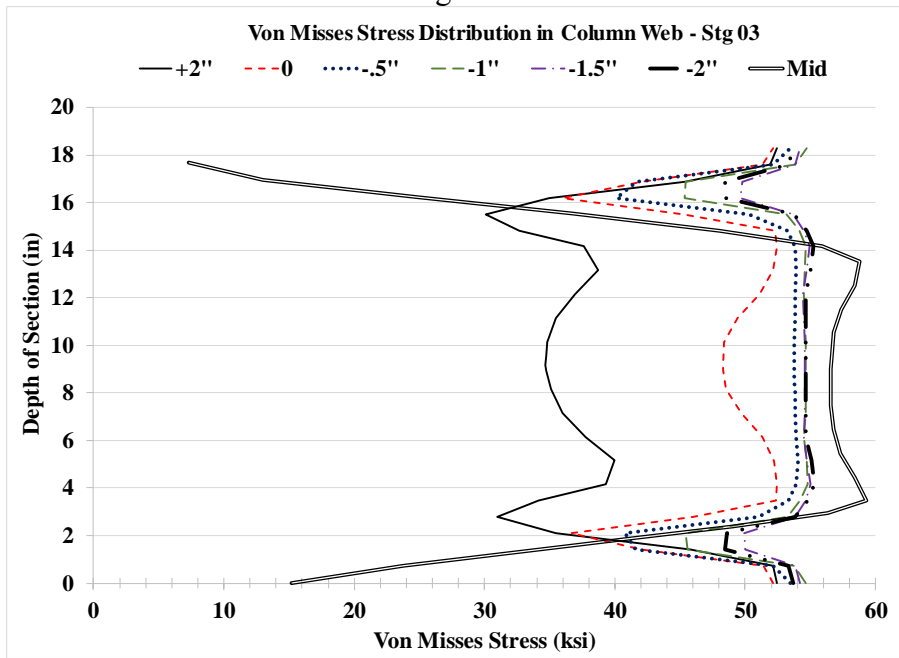


Figure 4.172: VMS and PEEQ in the column Case 5A1

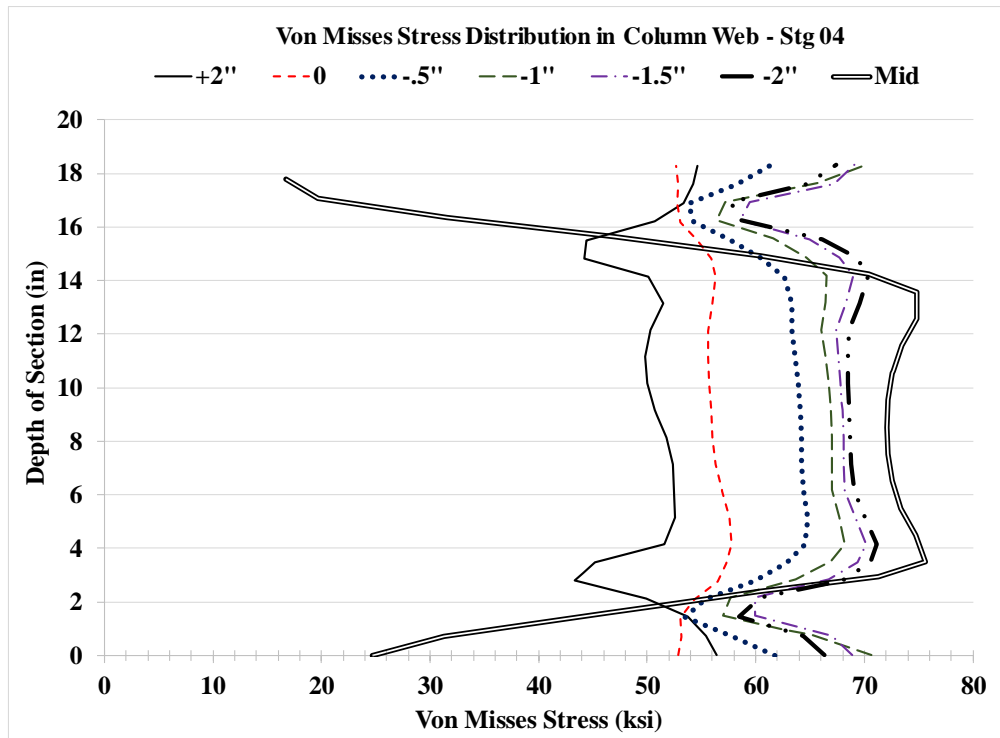


Stg. 01



Stg. 03

Figure 4.173: VMS distribution in column web at different heights Stg. 01-04 Case 5A1



Stg. 04

Figure 4.173: VMS distribution in column web at different heights Stg. 01-04 Case 5A1

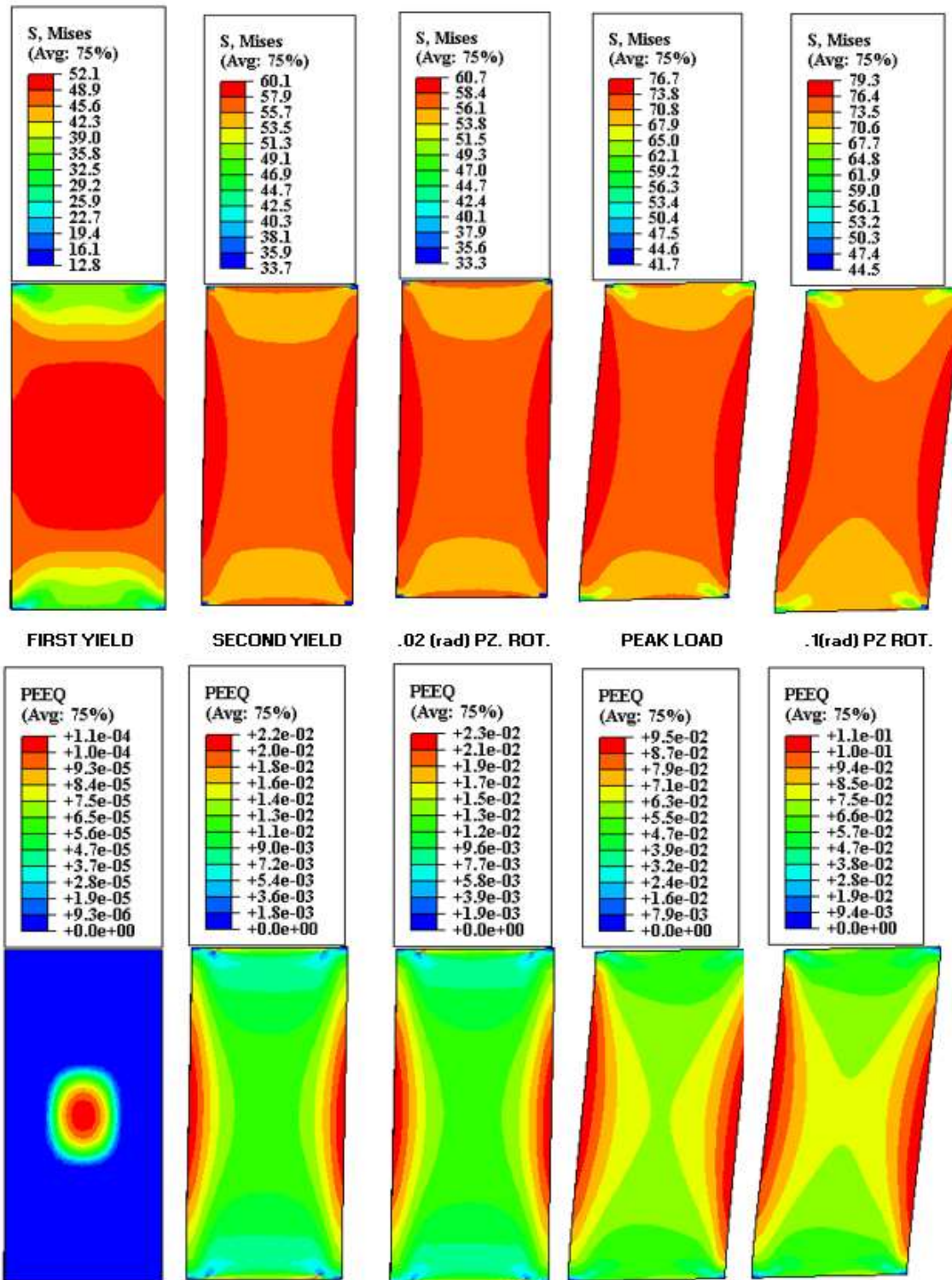


Figure 4.174: VMS and PEEQ in the DP Case 5A1

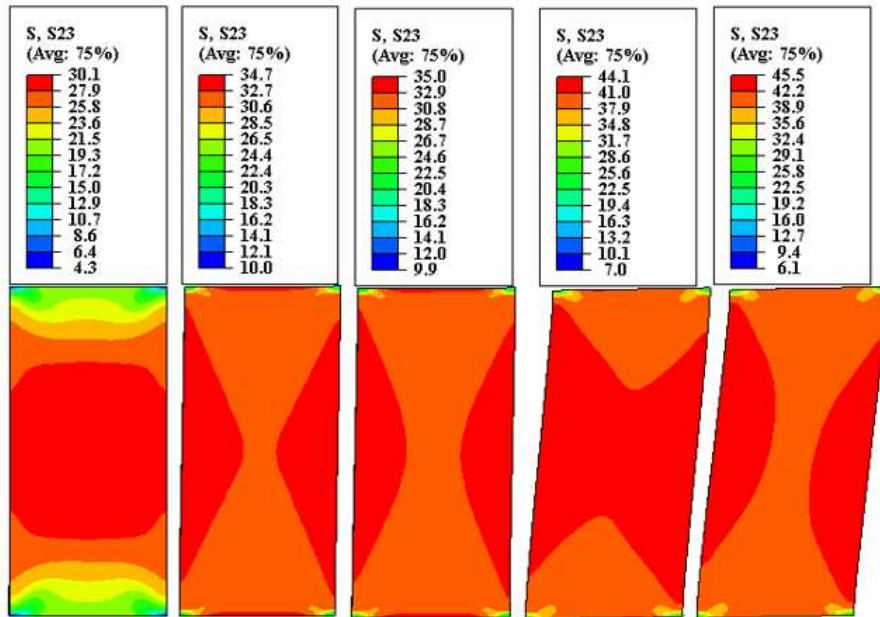


Figure 4.175: Shear stress, S23 in the DP Case 5A1

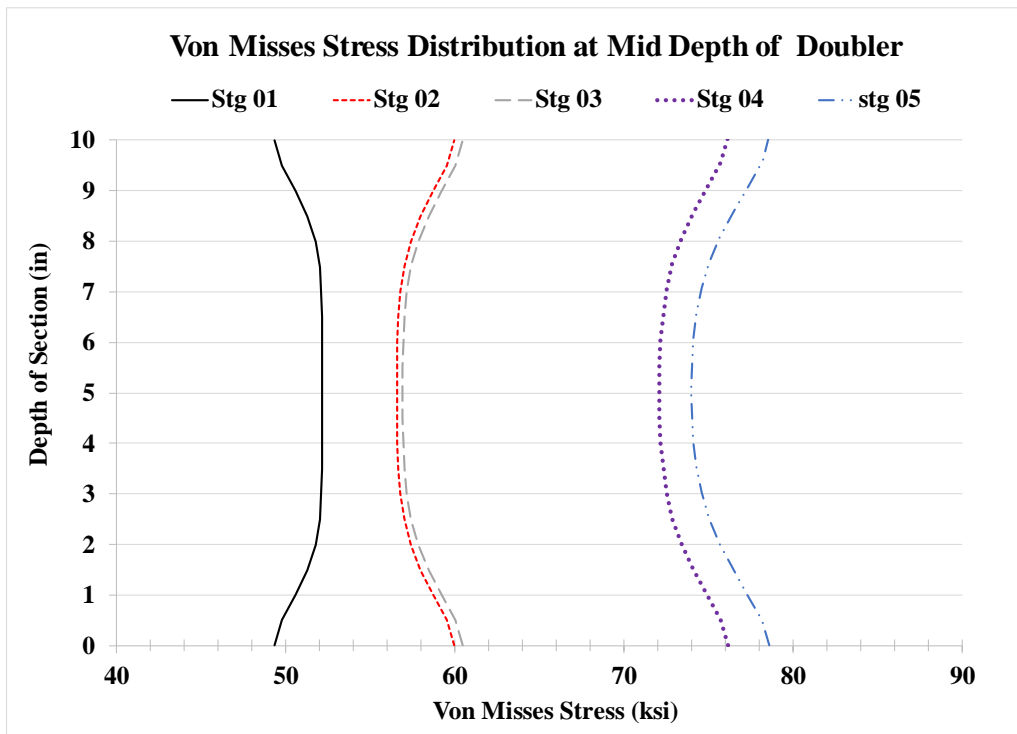


Figure 4.176: VMS distribution at mid-depth of DP Case 5A1

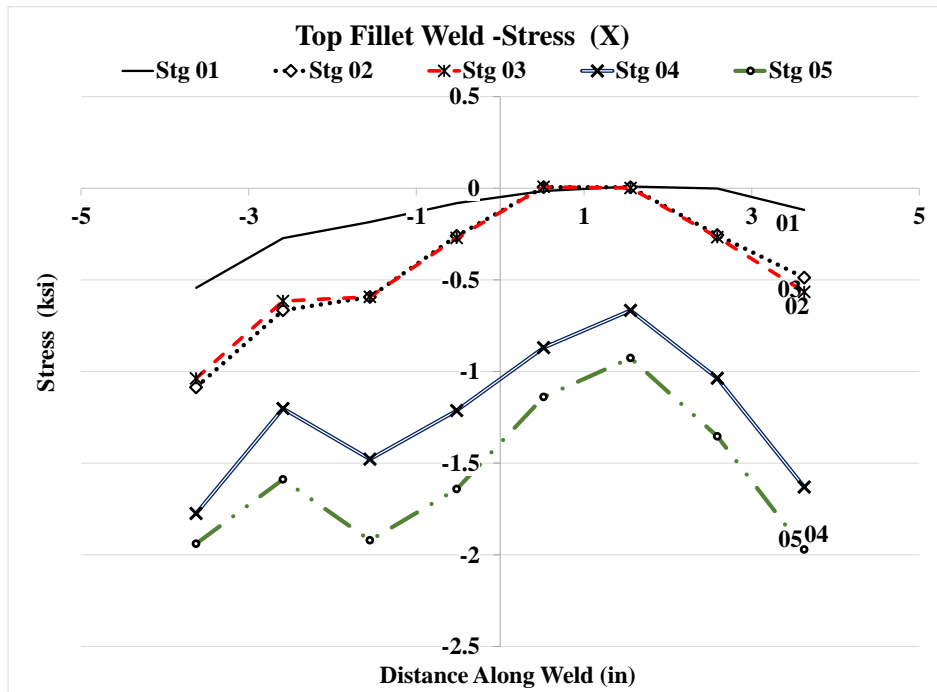
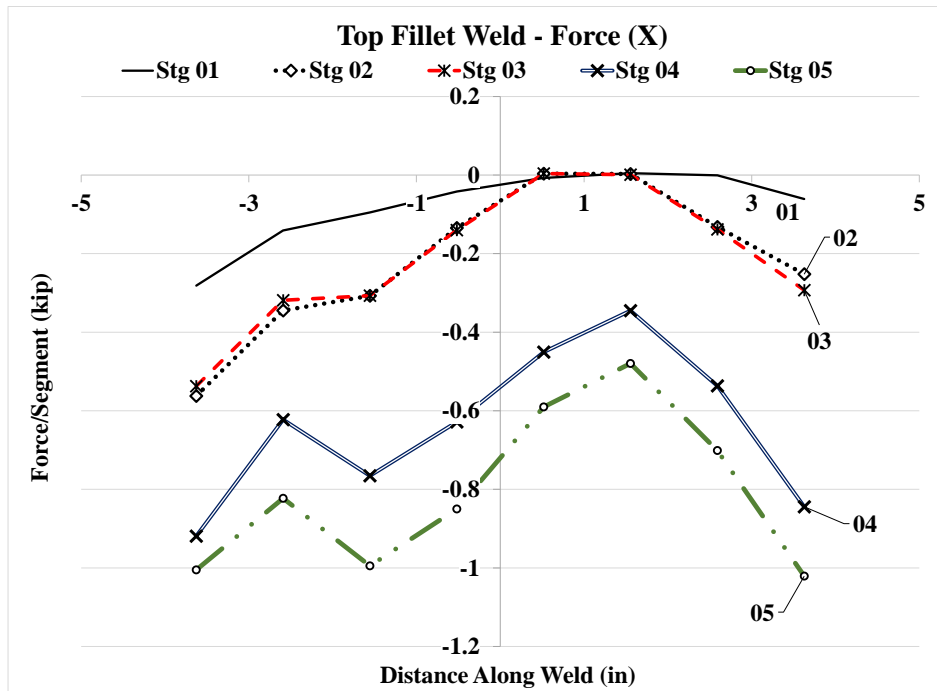


Figure 4.177: Forces and stresses in horizontal weld, (X) Case 5A1



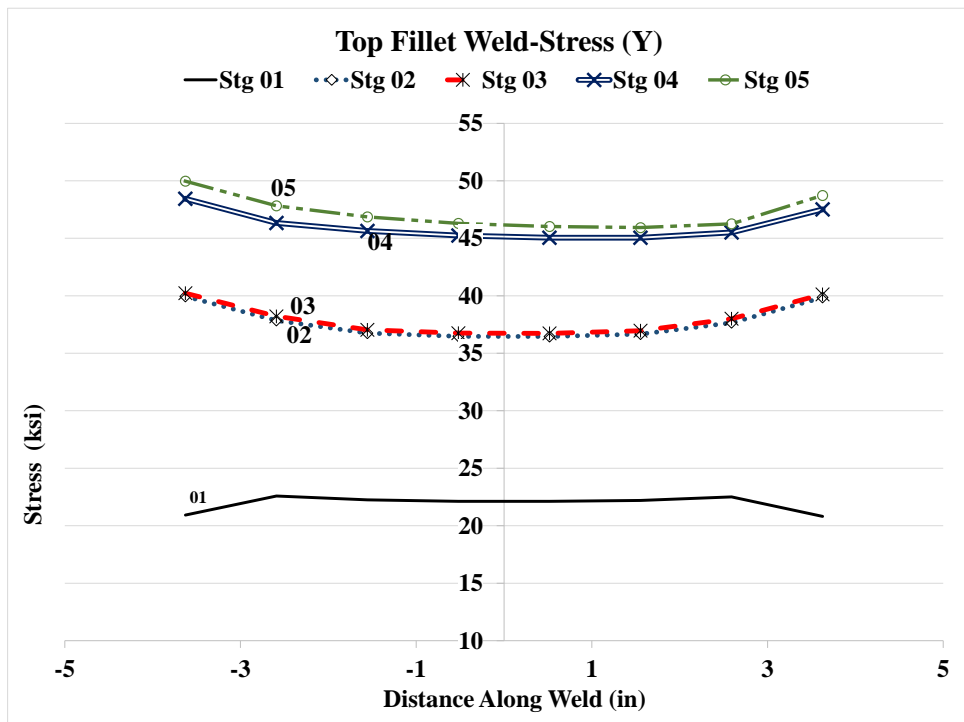
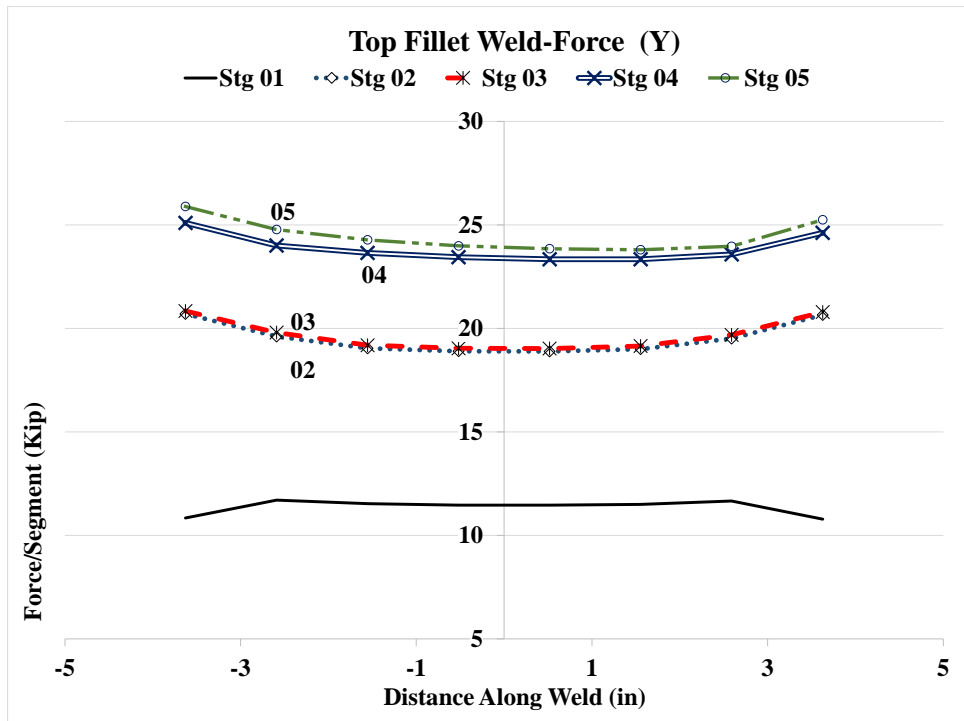


Figure 4.178: Forces and stresses in horizontal weld, (Y) Case 5A1



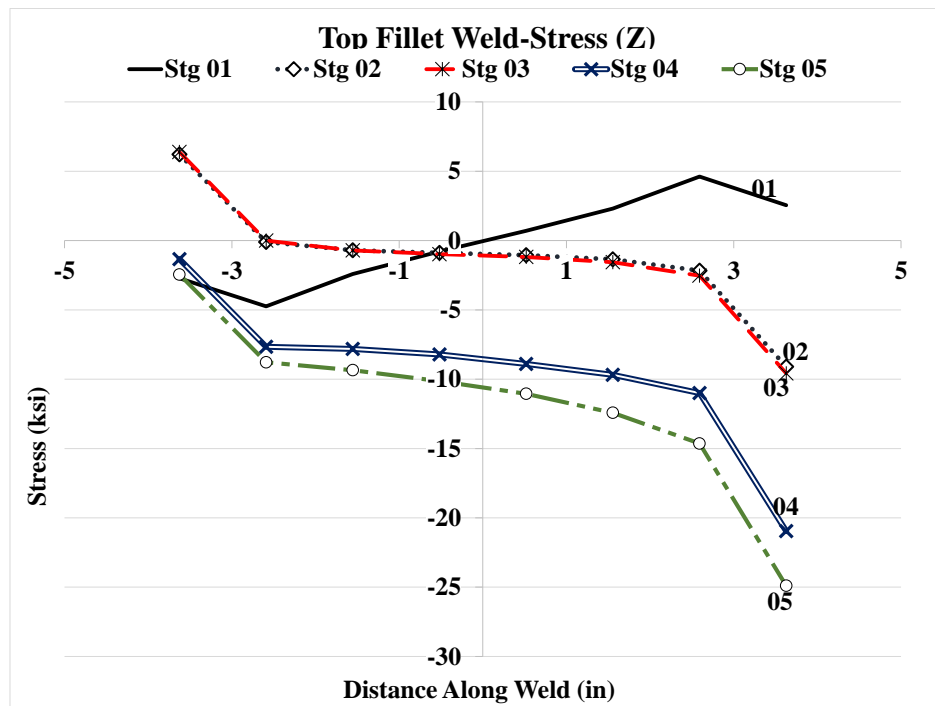
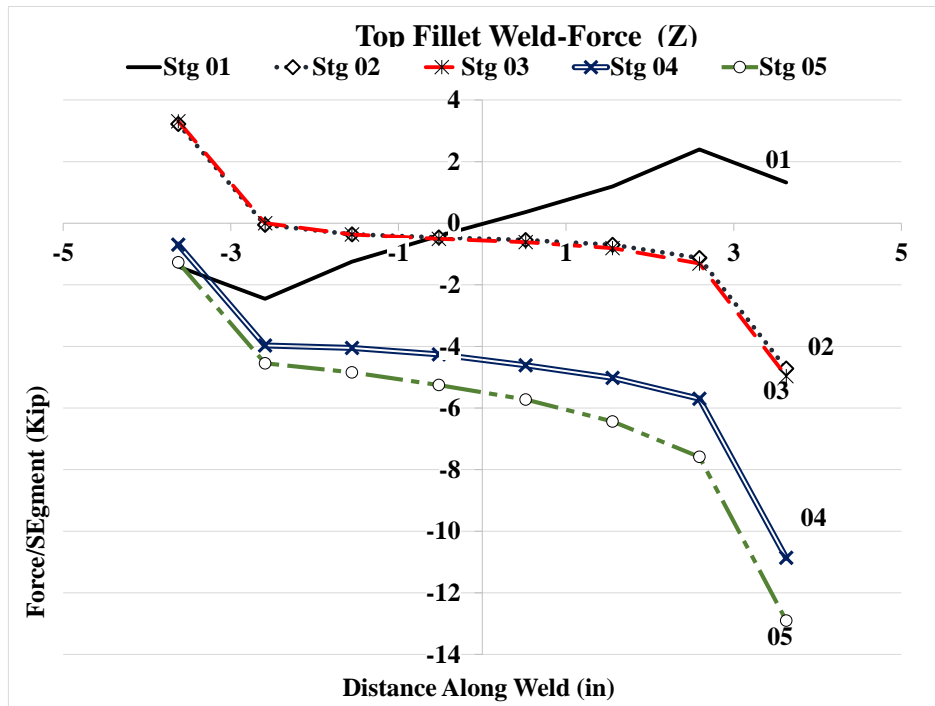


Figure 4.179: Forces and stresses in horizontal weld, (Z) Case 5A1

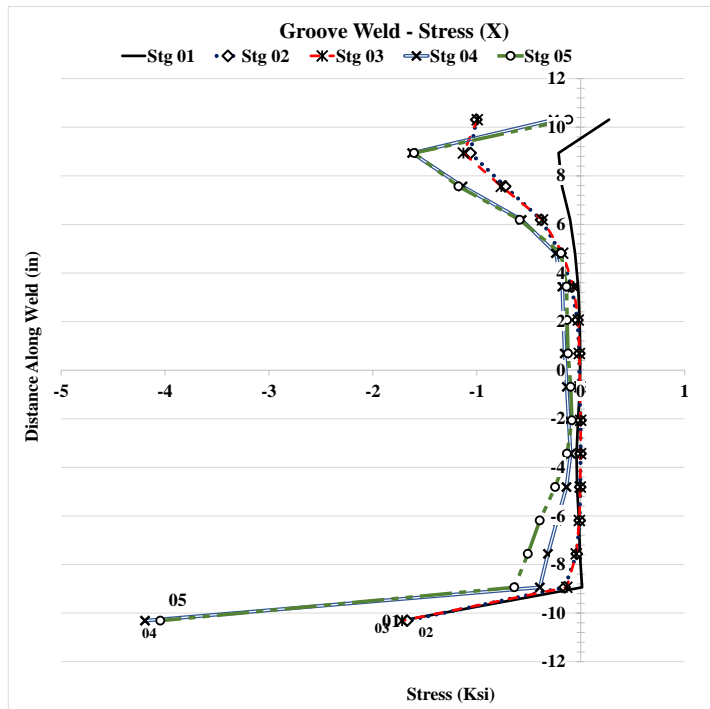
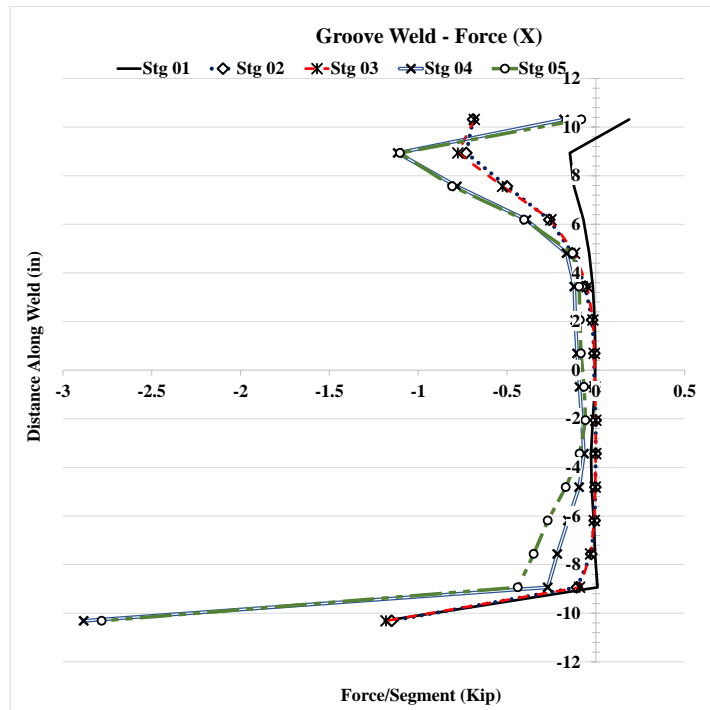


Figure 4.180: Forces and stresses in vertical weld, (X) Case 5A1

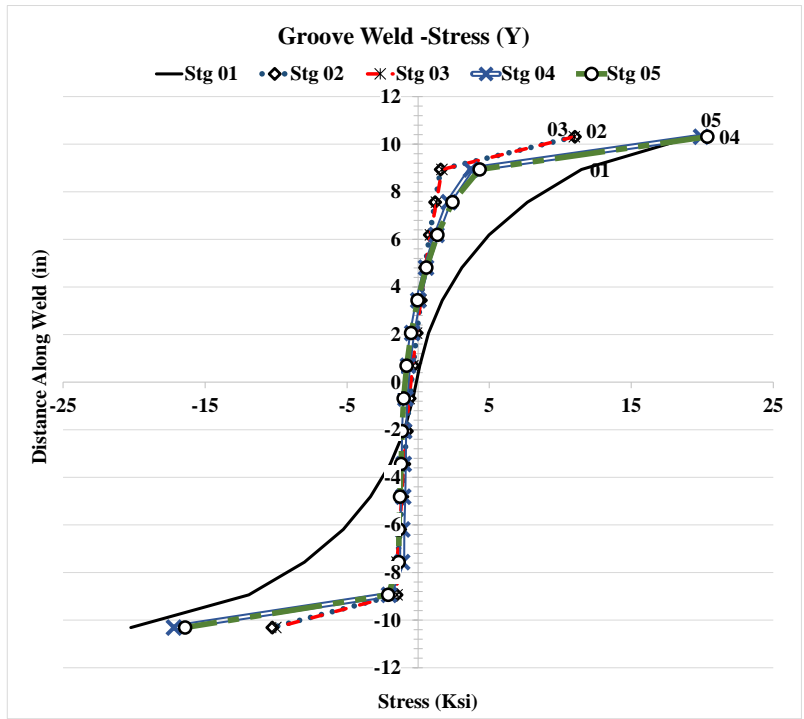
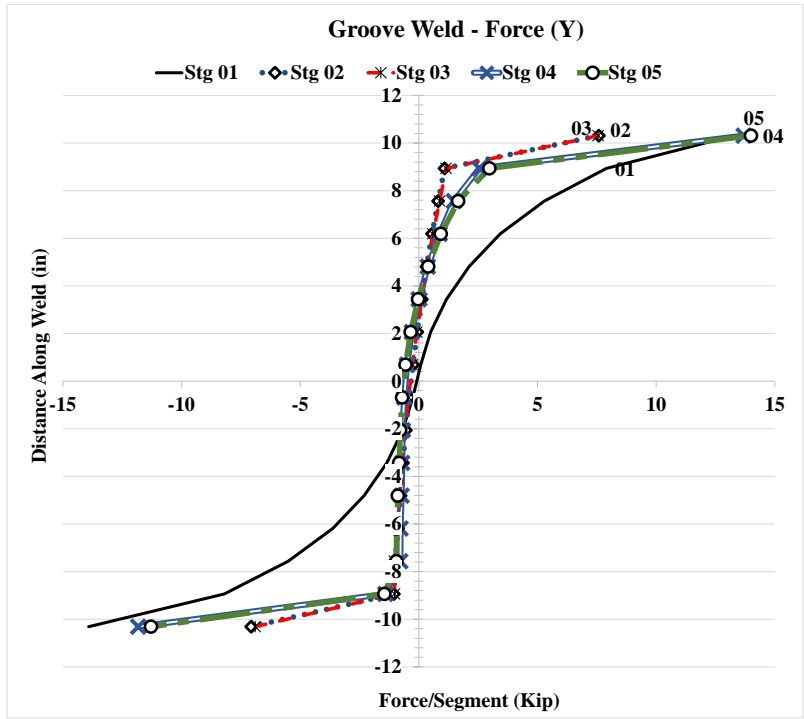


Figure 4.181: Forces and stresses in vertical weld, (Y) Case 5A1

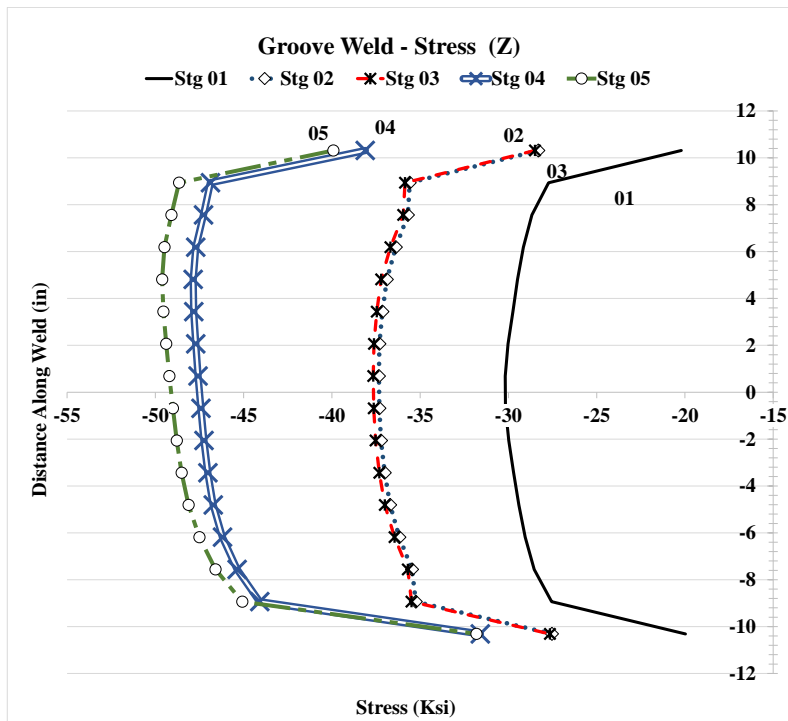
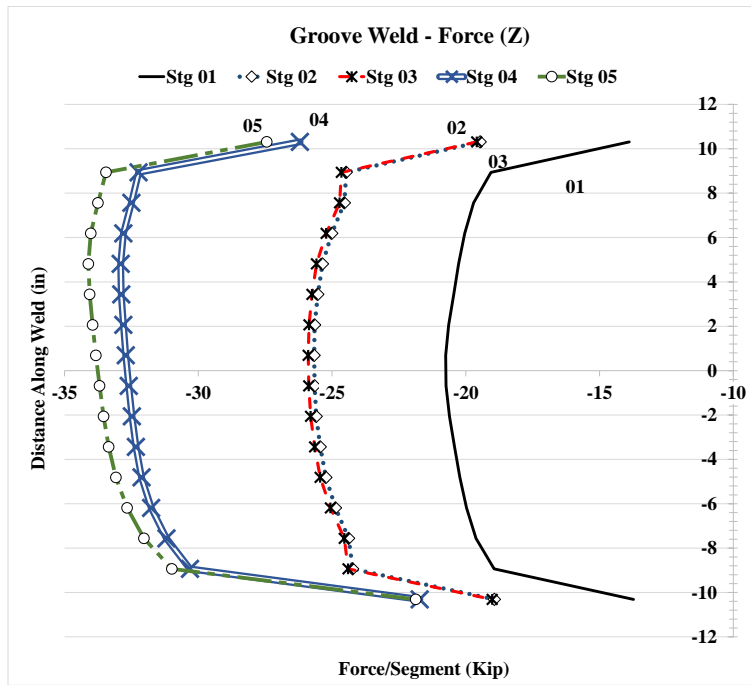


Figure 4.180: Forces and stresses in vertical weld, (Z) Case 5A1

### 4.2.17 Analysis Case 5C1

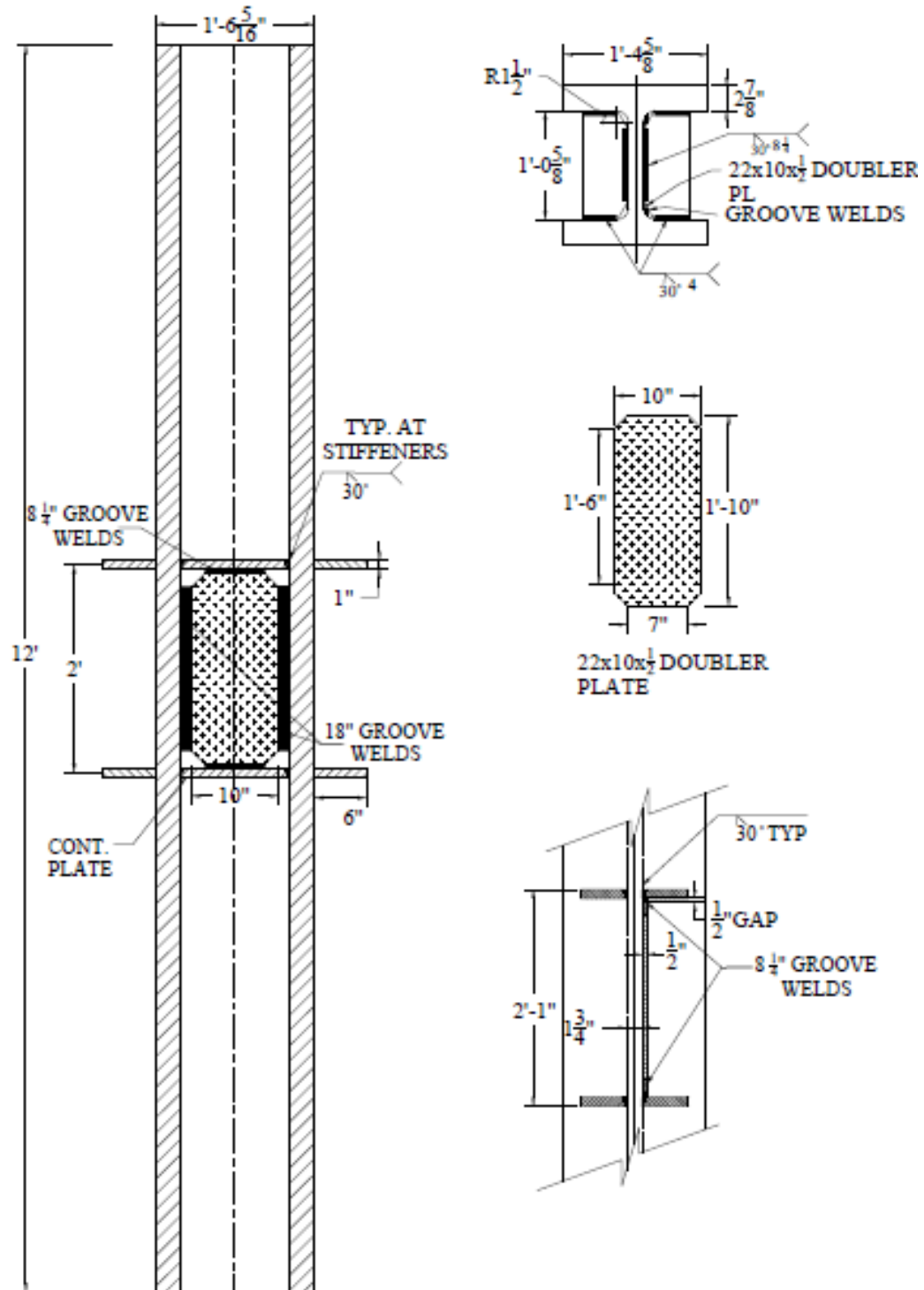


Figure 4.181: W14x398 Analysis case 5C1

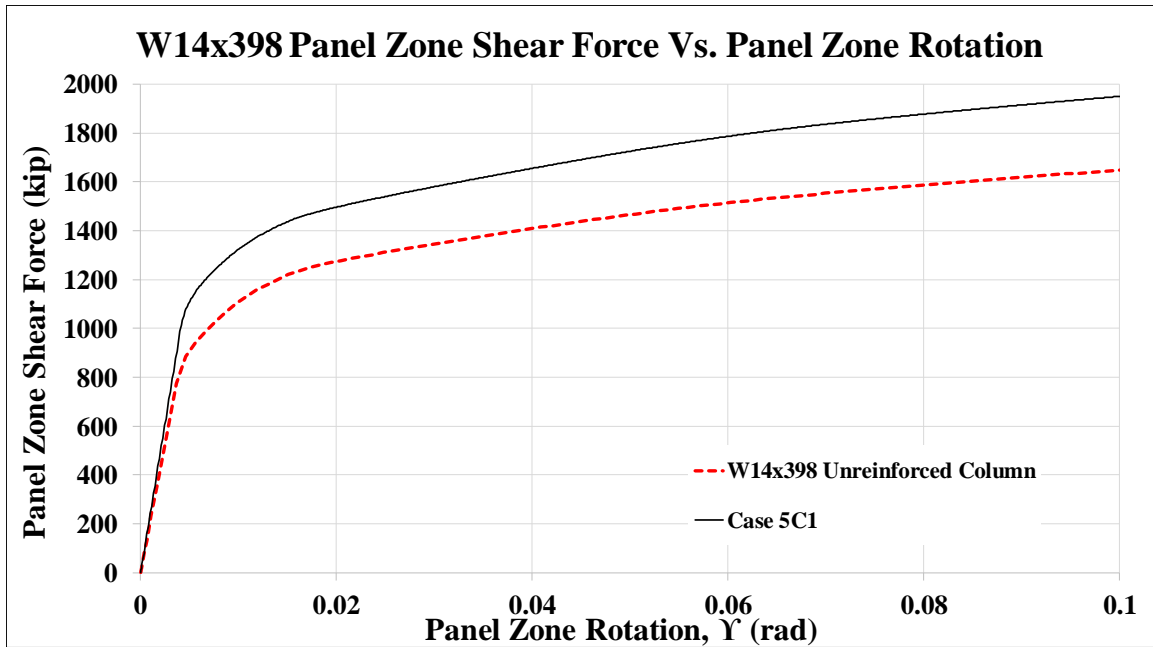


Figure 4.182: Panel zone shear vs. panel zone rotation Case 5C1

Stage	Applied Force/Loading Plate (Kip)	Panel Shear Force (Kip)	% Higher than unreinforced Col.	Panel Zone Rotation (rad)
1	608	1,014	115%	0.004
2	869	1,449	116%	0.016
3	898	1,497	117%	0.020
4	1,142	1,903		0.087
5	1,170	1,950	118%	0.100

Table 4.19: Panel zone shear and force on loading plate Case 5C1

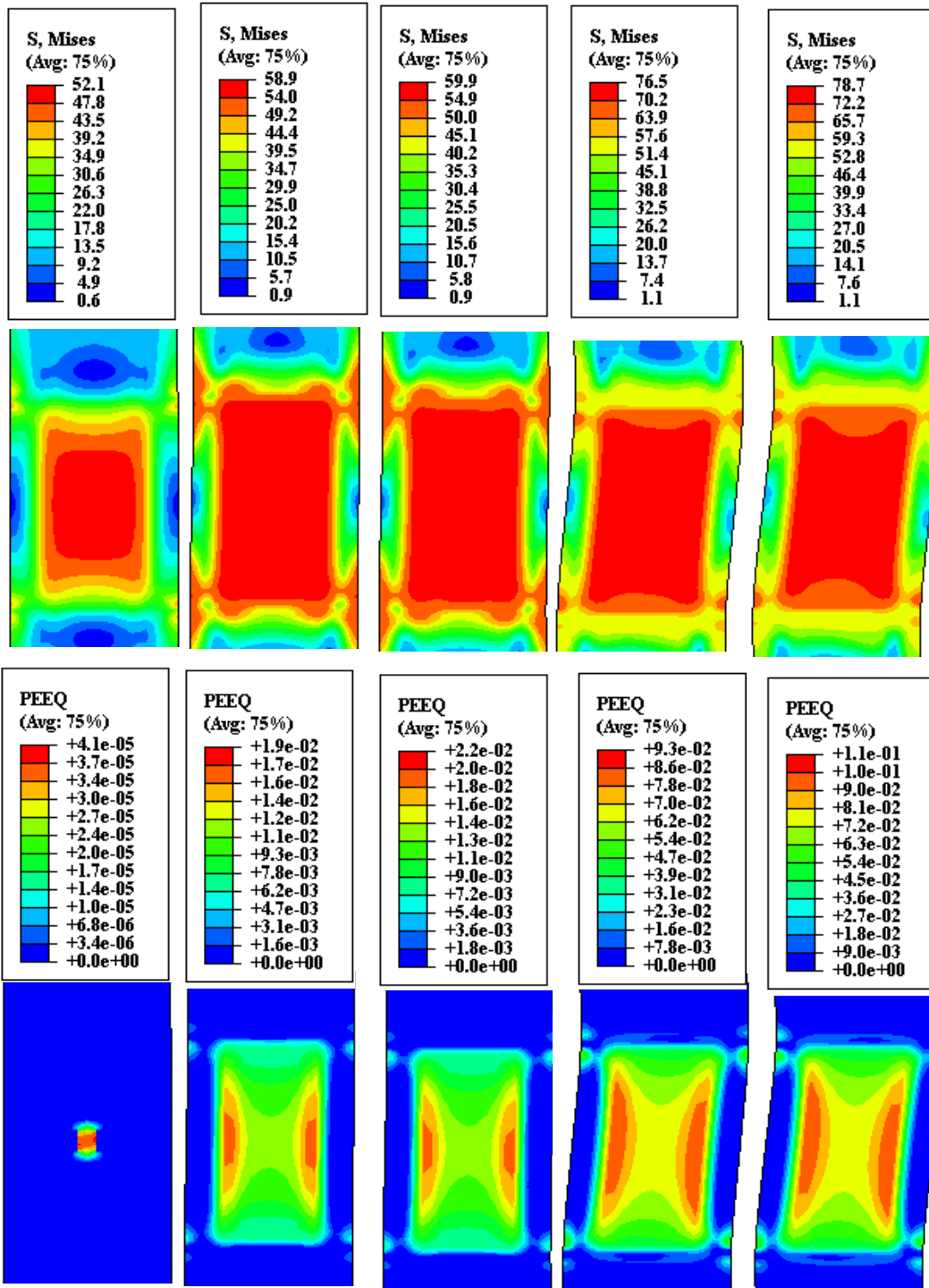
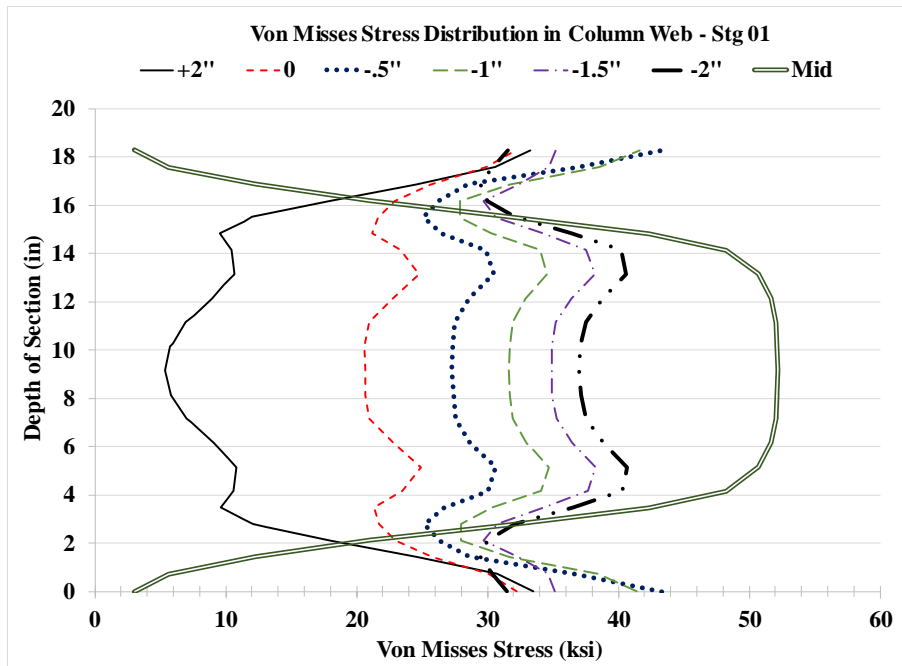
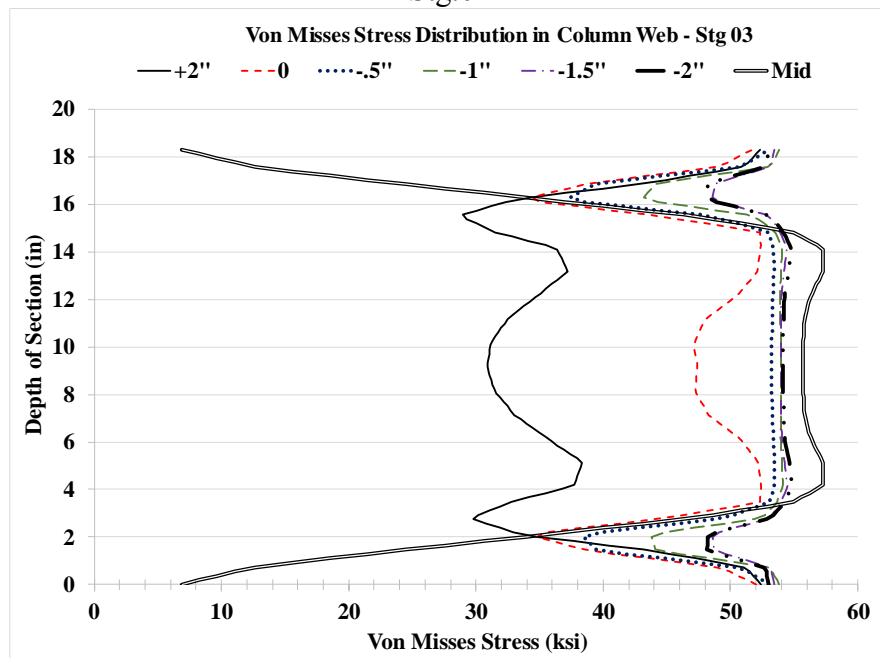


Figure 4.183: VMS and PEEQ in the column Case 5C1



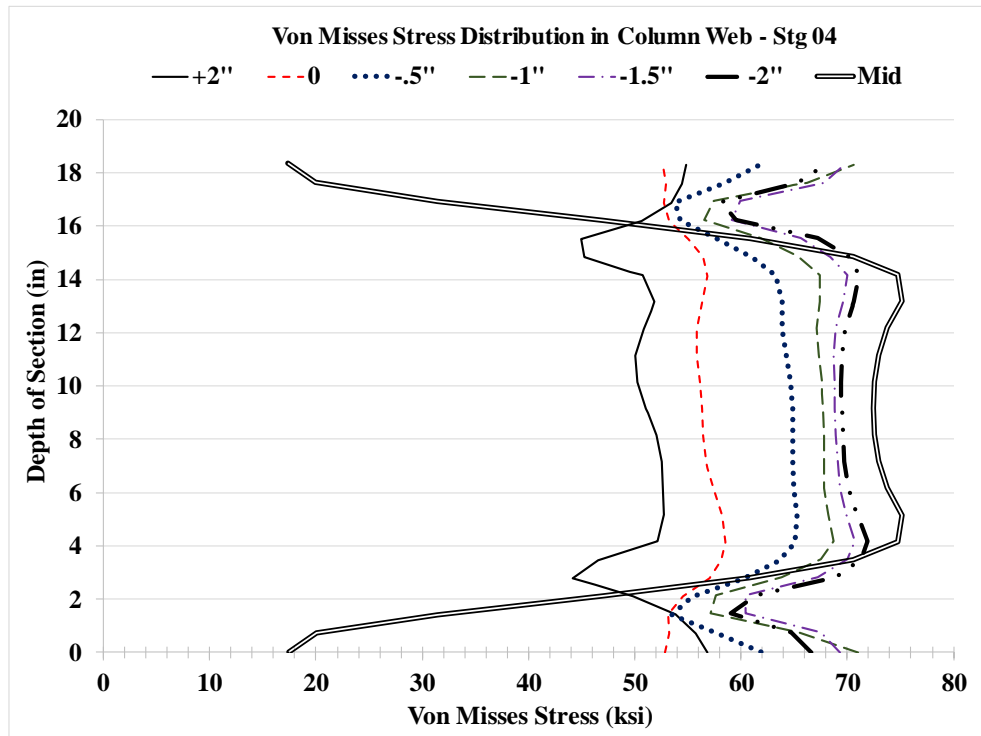
Stg.01



Stg. 03

Figure 4.184: VMS distribution in column web at different heights Stg. 01-04 Case 5C1





Stg. 04

Figure 4.184: VMS distribution in column web at different heights Stg. 01-04 Case 5C1

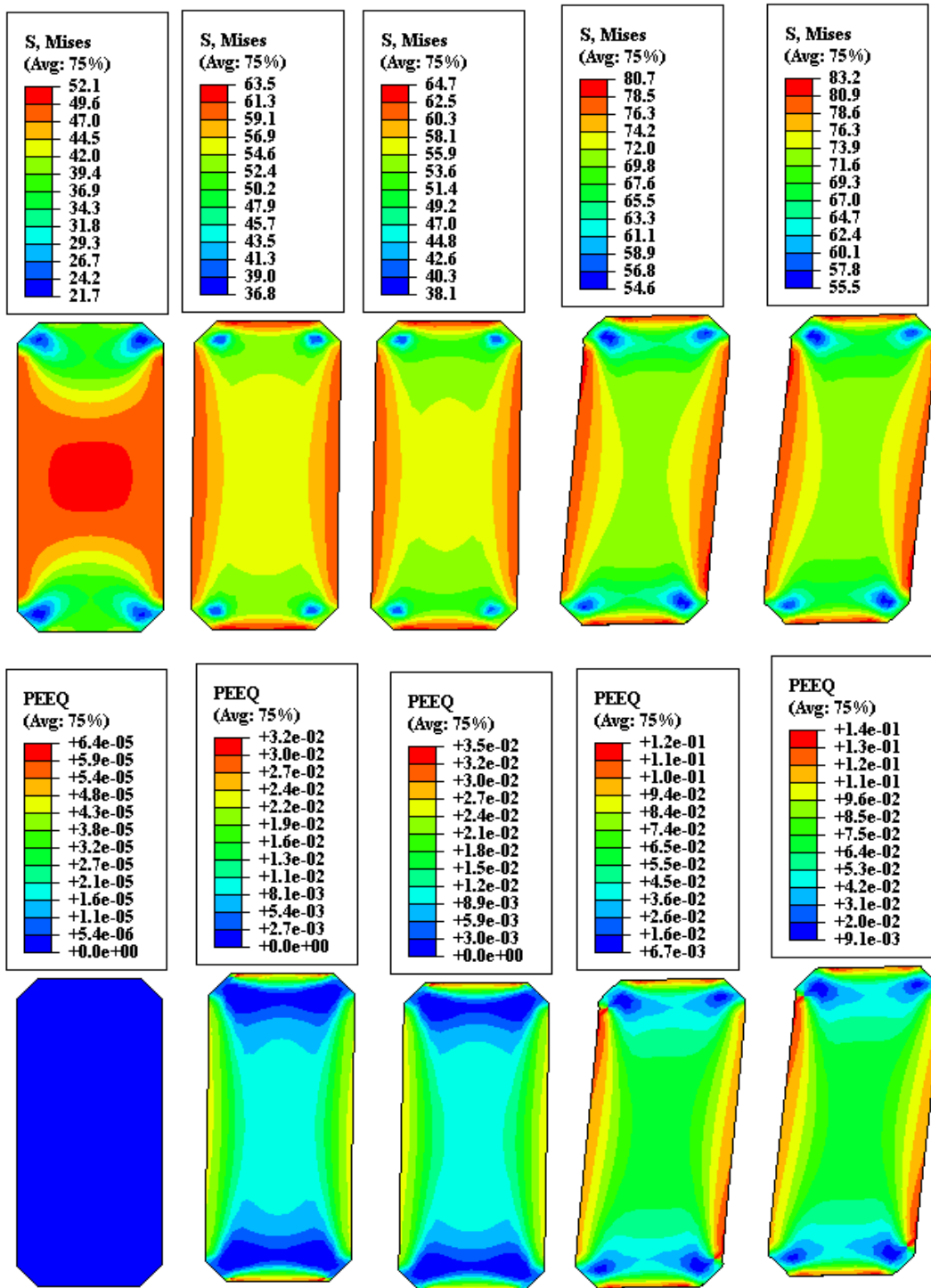


Figure 4.185: VMS and PEEQ in the DP Case 5C1

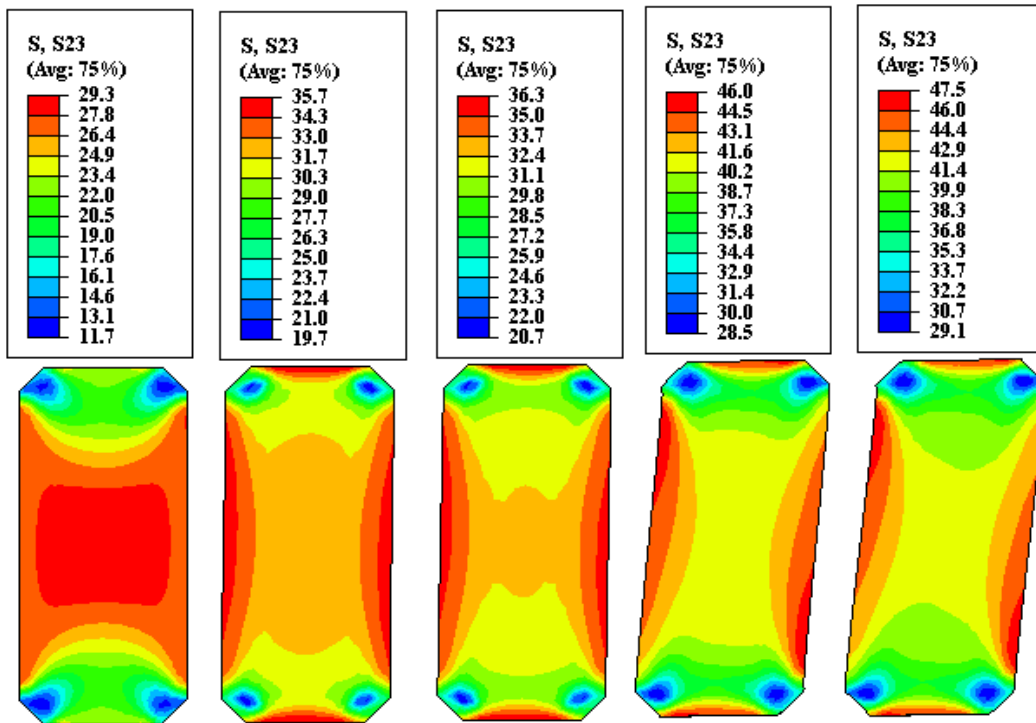


Figure 4.186: Shear stress, S23 in the DP Case 5C1

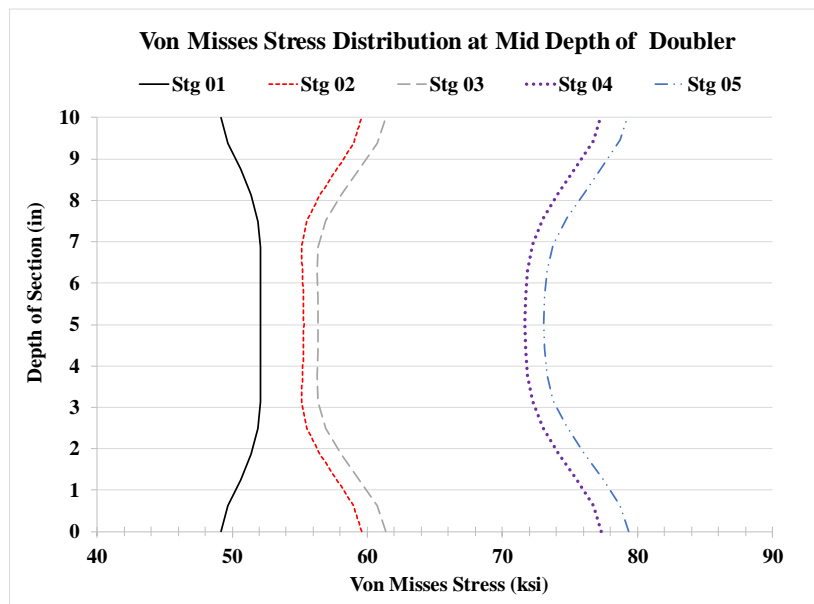


Figure 4.187: VMS distribution at mid-depth of DP Case 5C1

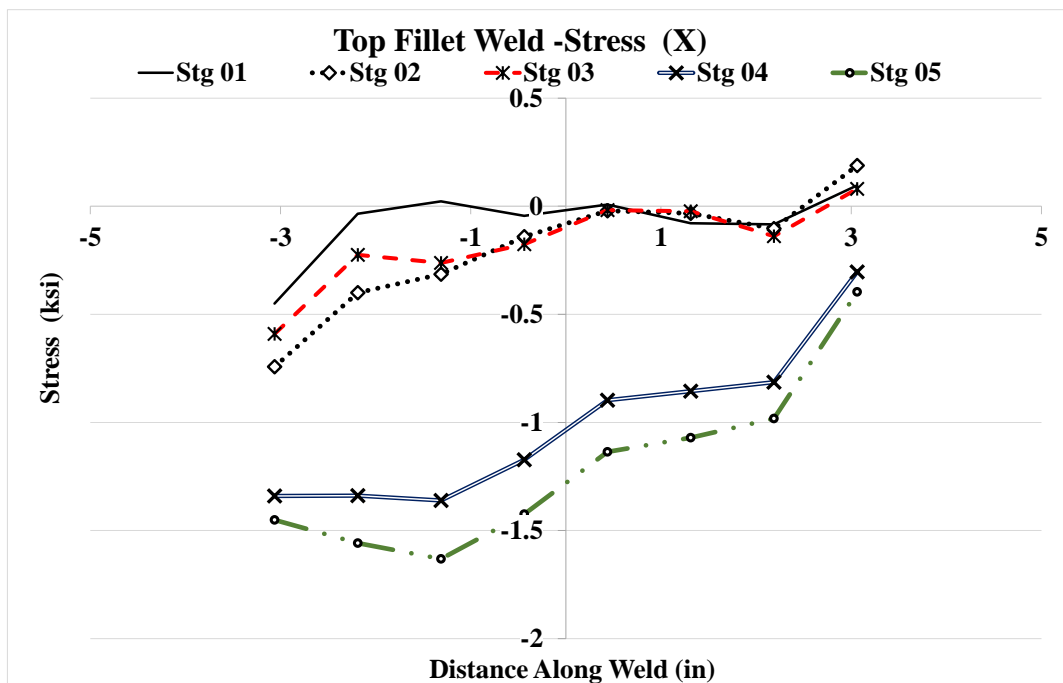
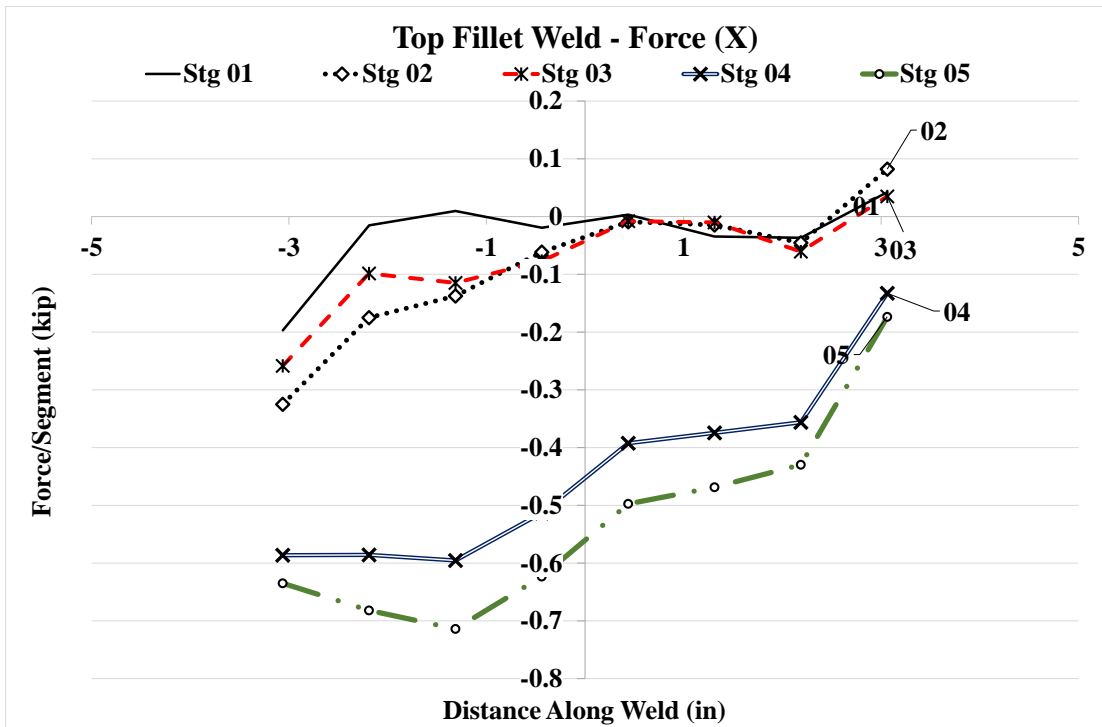


Figure 4.188: Forces and stresses in horizontal weld, (X) Case 5C1

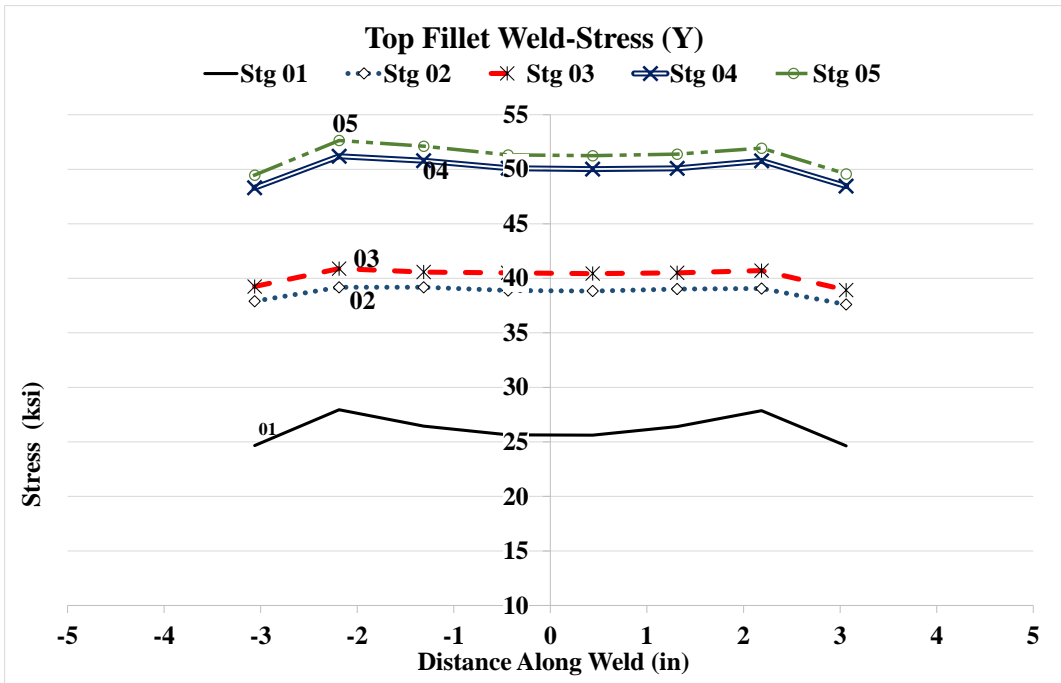
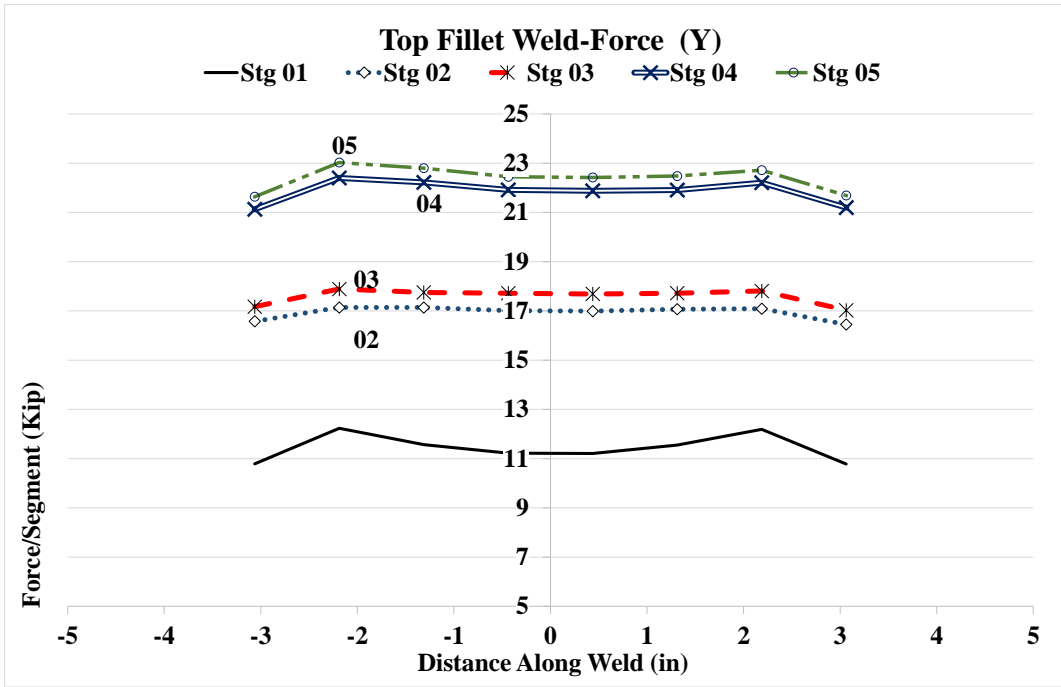


Figure 4.189: Forces and stresses in horizontal weld, (Y) Case 5C1

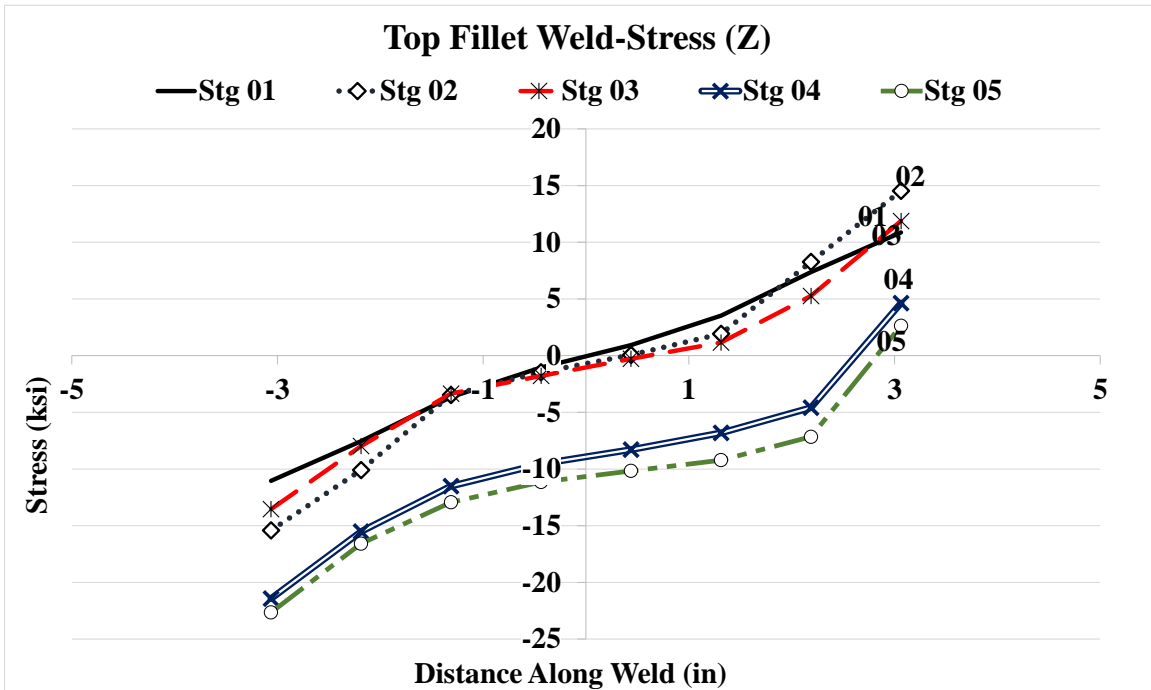
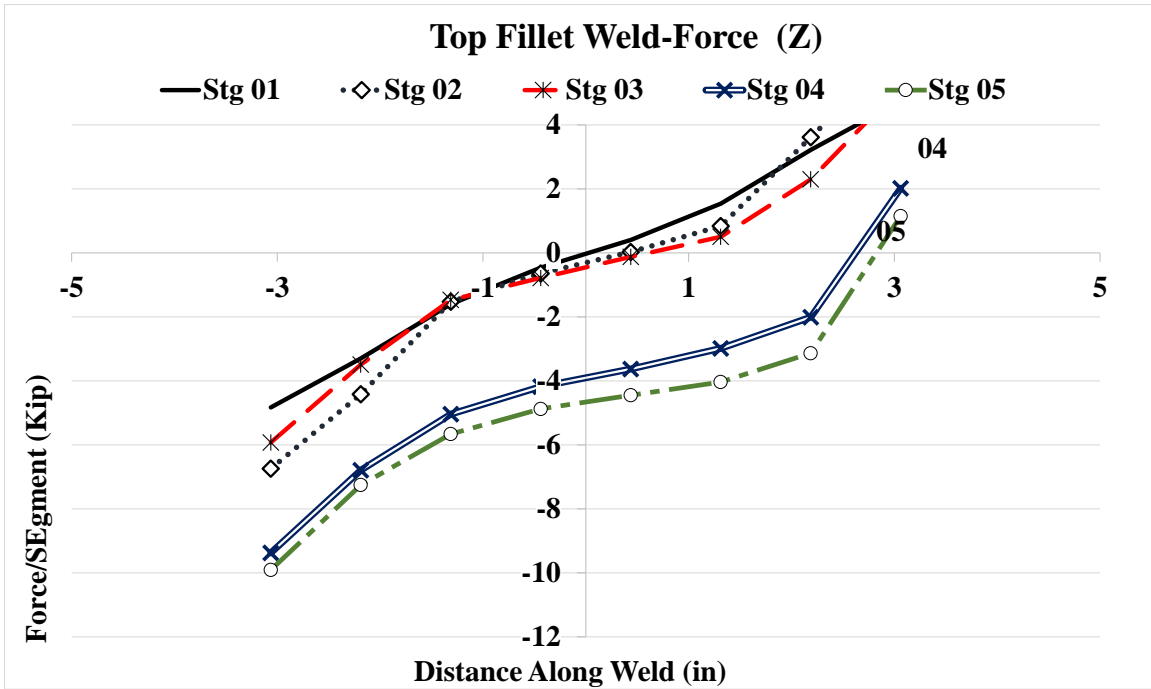


Figure 4.190: Forces and stresses in horizontal weld, (Z) Case 5C1

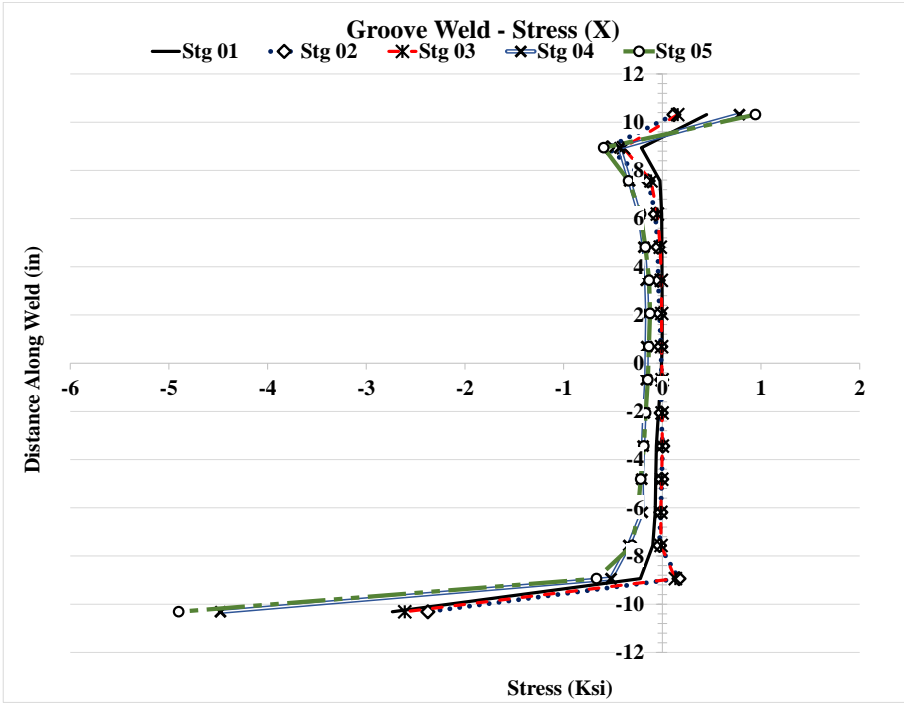
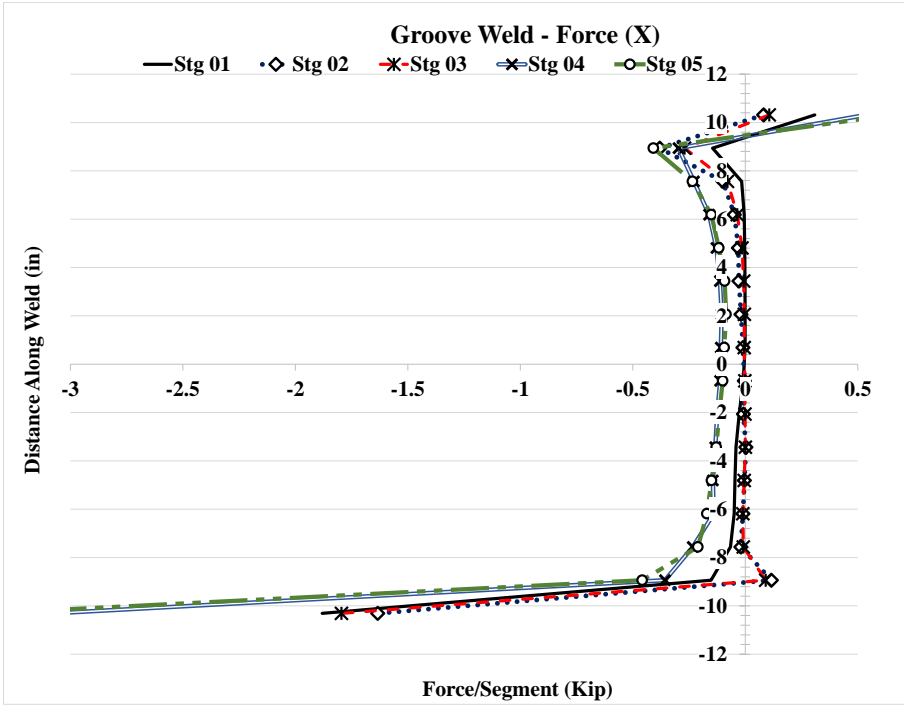


Figure 4.191: Forces and stresses in vertical weld, (X) Case 5C1

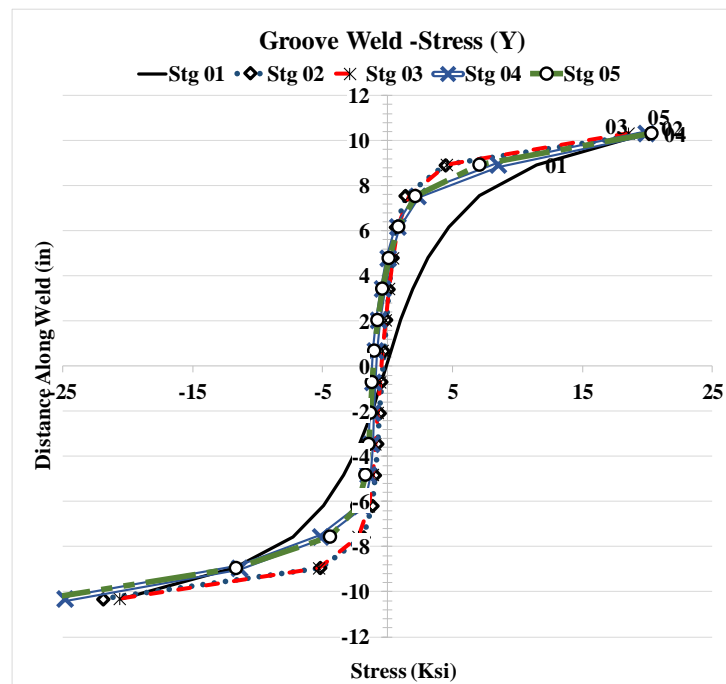
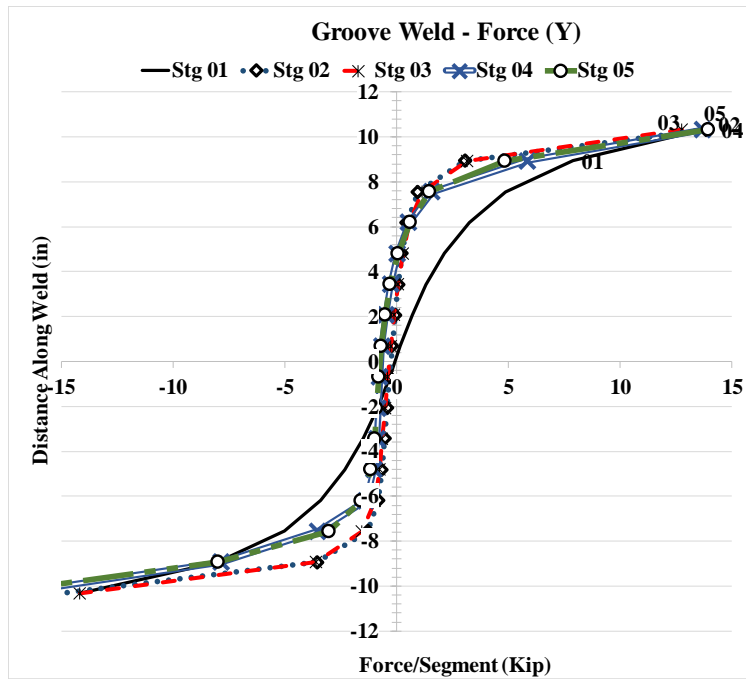


Figure 4.192: Forces and stresses in vertical weld, (Y) Case 5C1



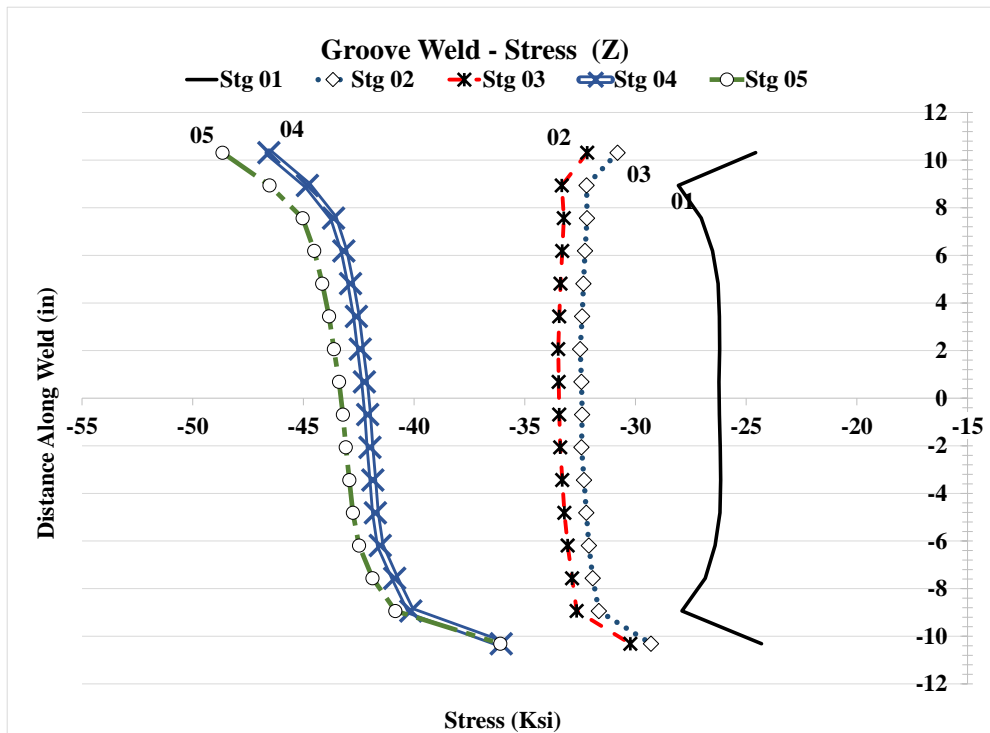
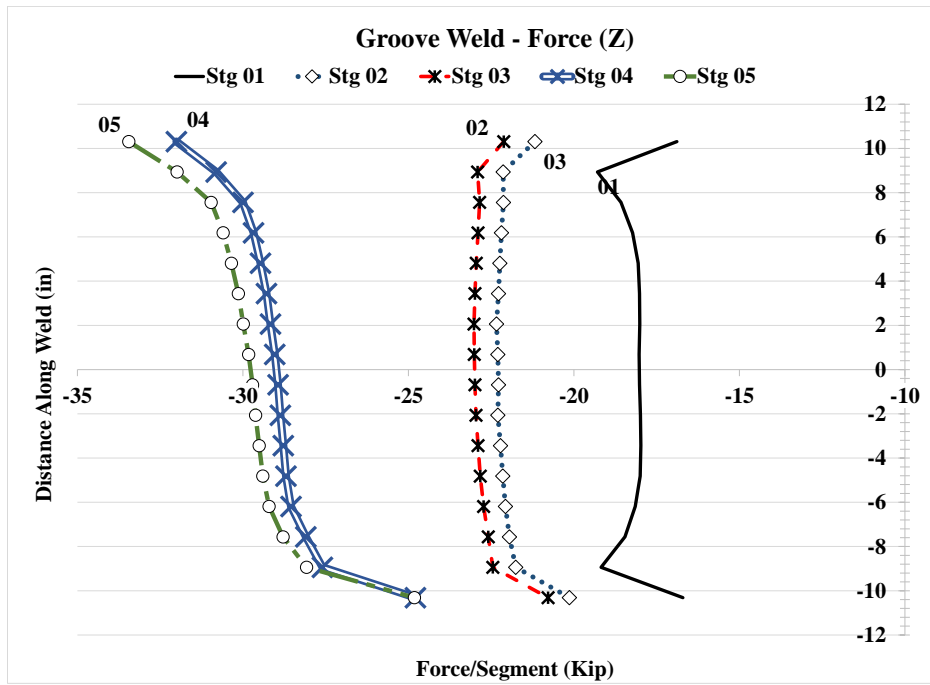


Figure 4.193: Forces and stresses in vertical weld, (Z) Case 5C1

### 4.3 DISCUSSION OF ANALYSIS RESULTS

Case	VMS in Column Web (ksi)		VMS in DP (ksi)		S23 in DP (ksi)		Shear at mid-height of DP (kip)		Total PZ Shear (kip)	
	Stg 01	Stg 04	Stg 01	Stg 04	Stg 01	Stg 04	Stg 01	Stg 04	Stg 01	Stg 04
<b>1</b>	53.0	78.0	-	-	-	-	-	-	884	1,900
<b>1A</b>	52.6	76.2	52.7	78.6	30.4	43.8	149.9	212.7	1,034	1,904
<b>1A1</b>	53.0	76.0	53	77	30.4	43.8	151.8	211.8	1,128	1,901
<b>1C</b>	52.0	76.1	52.6	81.3	30.4	43.6	149.7	214.7	1,028	1,903
<b>1C1</b>	52.0	77.0	52	78	30.4	44.8	150.1	212.3	1,033	1,901
<b>2A1</b>	52.0	76.0	52	76	30.3	44.3	151.2	209.6	1,104	1,902
<b>2C1</b>	52.2	76.0	52	76	30	44	150.4	210.1	1,052	1,902
<b>3A</b>	52.4	76.7	52.3	83.5	30.2	43.7	150.0	212.6	1,045	1,902
<b>3A1</b>	52.3	75.8	52.4	76.2	30.3	43.7	151.2	210.0	1,104	1,906
<b>3C</b>	52.2	77.9	52.3	85.6	30.2	44.3	149.8	215.7	1,037	1,902
<b>3C1</b>	52.4	76.3	52.2	77.8	30.1	45	150.4	210.9	1,050	1,902
<b>4A</b>	52.4	77.6	52.8	81.2	30.3	43.8	151.2	214.8	1,089	1,902
<b>4A1</b>	52.2	76.4	52.4	76.9	30.3	44.1	151.2	212.2	1,099	1,902
<b>4C</b>	52.2	78.9	52.2	82.2	30.2	44.9	149.6	217.9	1,029	1,902
<b>4C1</b>	52.2	77.7	52.2	81.5	30.1	46.6	150.4	213.2	1,043	1,902
<b>5A1</b>	52.2	75.9	52.1	76.7	30.1	44.1	148.5	210.3	1,018	1,901
<b>5C1</b>	52.1	76.5	52.1	72	29.3	46.1	148.1	211.1	1,014	1,905
<b>Case 18</b>	52.26	75.2	52	72	Not Reported		150.2	209.8	1,037	1,887
<b>Case 5A</b>		71.8		72.8						1,841

Notes:

Case 18 from Shirsat (2011) reported for same column, but no CPs and an 36" DP instead of 24"

Case 5A from Gupta (2013) reported for same column at .05 rad.of cyclic loading

Table 4.20: Summary of VMS stresses and forces on column web and DP at Stg. 01 and Stg. 04.

As summary of the results from the analysis cases for the “shallow” W14x398 column specimen can be seen on Table 4.20. Because all The VMS results for the specimens seem to fall within close range, it might be assumed that most of the benefits in varying the arrangements of the PZ attachments would likely be seen in the welds that attach the DP to the column. This could be a result of the column being able to redistribute the load as necessary to accommodate the force being applied. Five sets of configurations were modeled in order to see what benefits each would have relative to performance of the PZ.

Table 4.20 reports the average peak VMS values recorded in the column and DP at the stages 1 and 4 of the analysis. The VMS values at peak load, stg. 4, in the column fall below 78 ksi which was the value of the unreinforced column at 0.1 radians. One exception to this was Case 4C which was supposed to determine what the effect of increasing the space between the bottom of the CP and the top and bottom edges of the DP. Figure 4.194 shows Case 4C as the reinforced specimen that required the least amount of load for the PZ to rotate up to 0.1 radians. Case 4 which did not use a fillet weld to attach the DP at the top and bottom surface, had lower PZ rotation performance and higher stresses on both the DP and the column.

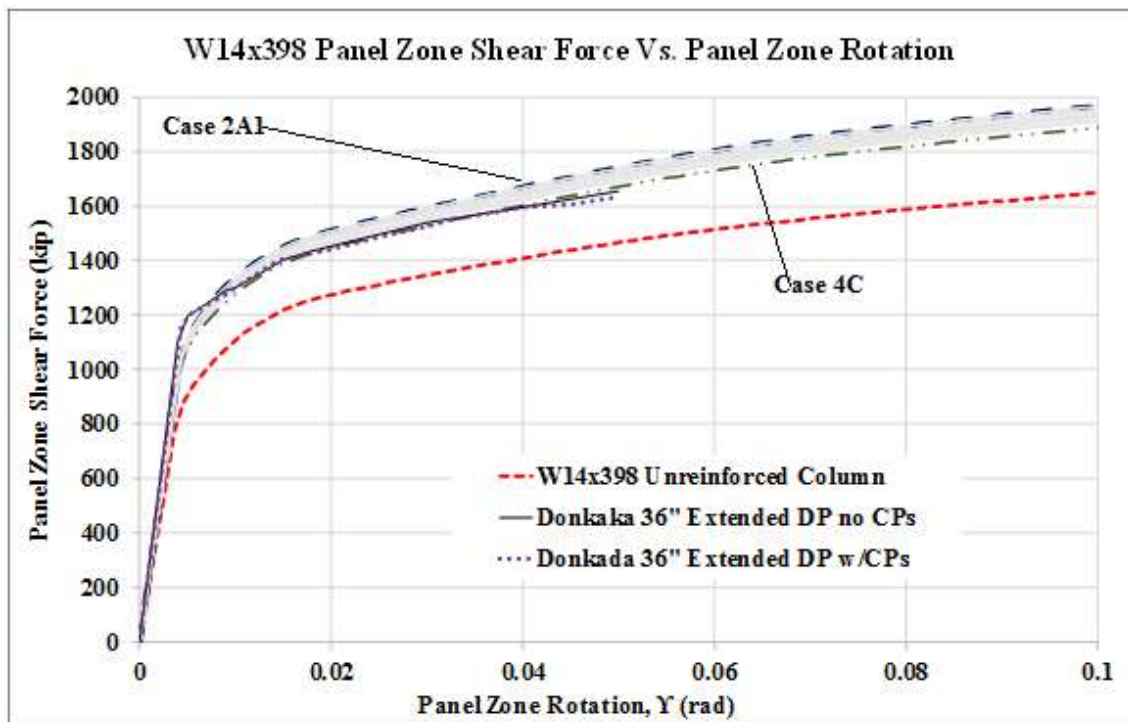


Figure 4.194: PZ Shear vs. PZ Rotation comparison

In order to evaluate the performance of the “fitted” DP relative to an “extended” DP, Case 18 from Shirsat (2011) was selected because it utilized the same column but no CPs, no top weld and a similar DP that was extended 6 inches above the loading plates. When comparing the reported VMS values for the DP and the column, no reduction in the values of the specimens with the extended DP were seen. Case 5A from Gupta (2013) was also compared in order to see if there was much difference in the VMS values at peak load levels. Case 5A was exactly like that of Shirsat, but used a different material model and the specimen was loaded cyclically. The peak loading point of .05 radians from Case 5A was selected because the total rotation of the PZ was the closest to that of stage 4. Similar VMS values were also reported in both the column and the DP. A comparison of the peak shear stress values and the total shear force at mid-height of the DP also shows very little difference between the specimens. This comparison would seem to indicate that both extended and fitted DPs provide similar benefits to the “overall” performance of the PZ and result in VMS stress values in the DP and the column web that are similar.

### 4.3.1 Case Series 1

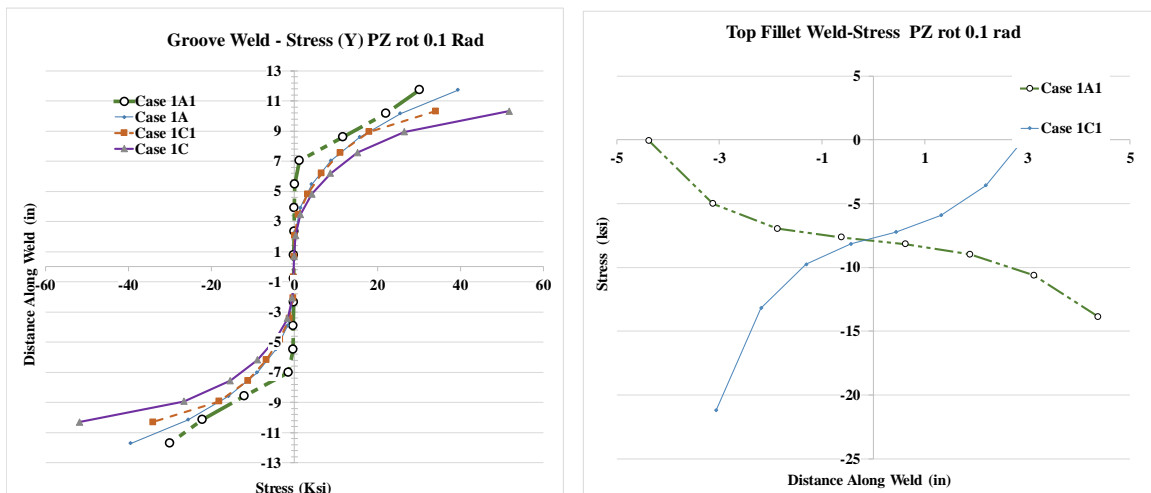


Figure 4.195: Stresses in Horizontal and Vertical Weld at 0.1 Rad for Case Series 1

The case series 1A, 1A1, 1C, and 1C1 did not use CPs in order to evaluate the effect that these have on the VMS values. Although an increase in VMS or shear stress values was not seen, the lack of CPs revealed how the use of a weld at the top and bottom of the DP helped reduce the stress levels on the vertical weld. Tables 4.21 and 4.22 report the total forces transferred by both vertical and horizontal welds for all specimens in this chapter. In Case 1A1 with the unclipped DP, at a PZ rotation of 0.1 rad., the vertical weld was able to transfer 529 kips of force into the DP when a horizontal weld was used. This value was 11% higher than that of Case 1A which did not use a horizontal weld. When this comparison is done between Case 1C which uses a DP with clipped corners the vertical weld is able to transfer 16% more load into the DP. This increase in load transfer when a weld is used at the top and bottom of the DP is not unique to this series but the lack of CPs means that the increase in performance is due to the ability of the welds to transfer the shear force to the DP alone. A look at the forces in the vertical weld will reveal that as demand increases in the Y direction, because of the lack of a horizontal weld, the ability to transfer force in the Z axis decreases. This is particularly evident in stages 4 and 5 of the analysis when the highest loads are being applied.

As can be seen in weld force and stress plots, the outermost welds segments seem to transfer the highest levels of force. To understand how much higher the demands on these segments was the forces recorded in the two outermost segments was separated and an average force for these outer weld segments was reported on, Tables 4.23 and 4.24. An example of how these values reveal the benefits of a horizontal weld can be seen when comparing the individual segment forces at 0.1 radians. In case series 1 which used no CPs, the two outermost weld segments of the vertical weld had to transfer about 2.5 times more load per segment. When no horizontal weld was present the force in each of the two

outermost weld segments was 45 kips. This value was reduced to 17 kips when a horizontal weld was used. One of the reasons for the high levels of force at the corner welds of the DP seems to be the proximity to the points of loading. The applied shear enters the column web and the weld segments in the extremities transfer much of the force into the DP.

### 4.3.2 Case Series 2

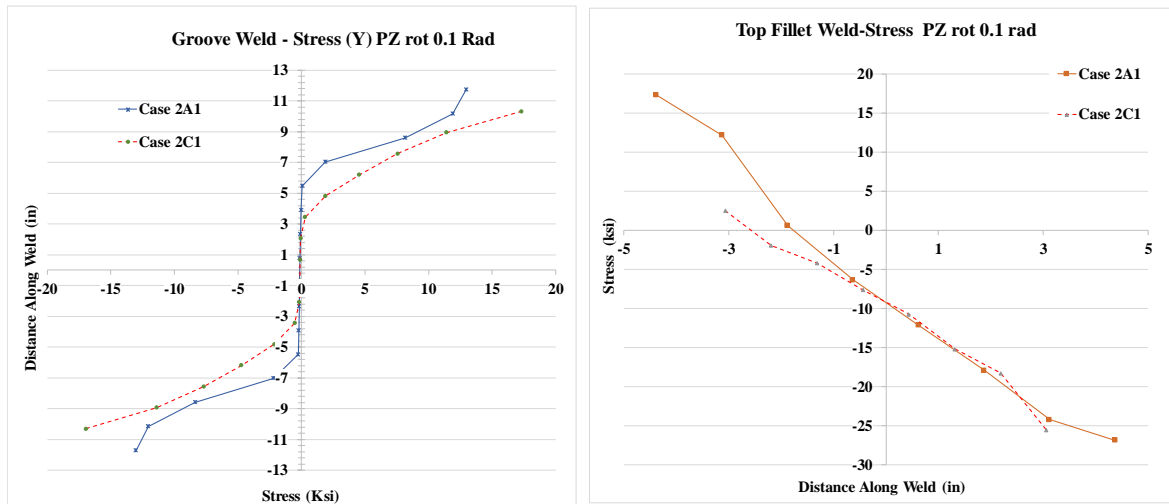


Figure 4.196: Stresses in Horizontal and Vertical Weld at 0.1 Rad for Case Series 2

Case series 2 used a fitted DP that was extended the most from all the other specimens. It terminated immediately behind the continuity plate at the same level as the top of the loading plated. Unlike the other cases the continuity plate was welded to the DP instead of being attached to the column web. Because the specimens in this case series required the most force to rotate up to 0.01 radians, this arrangement was determined to be one of the best performing ones. Similar to the benefits reported for the specimens with the extended DPs in Shirsat (2011) and Donkada (2012), this series seemed to benefit for the same reason; extra material and more edge surface area to transfer the load. The benefits from increasing the amount of vertical weld can be seen when looking at the reduction of total

force transferred in the direction parallel to the load application. The welds at the top of the DP in cases 2A1 and 2C1 transferred 69.1 and 51.6 kips of force onto the DP at 0.1 radians. These values were more than 50% lower than the other specimens which showed values ranging from 131-188 kips.

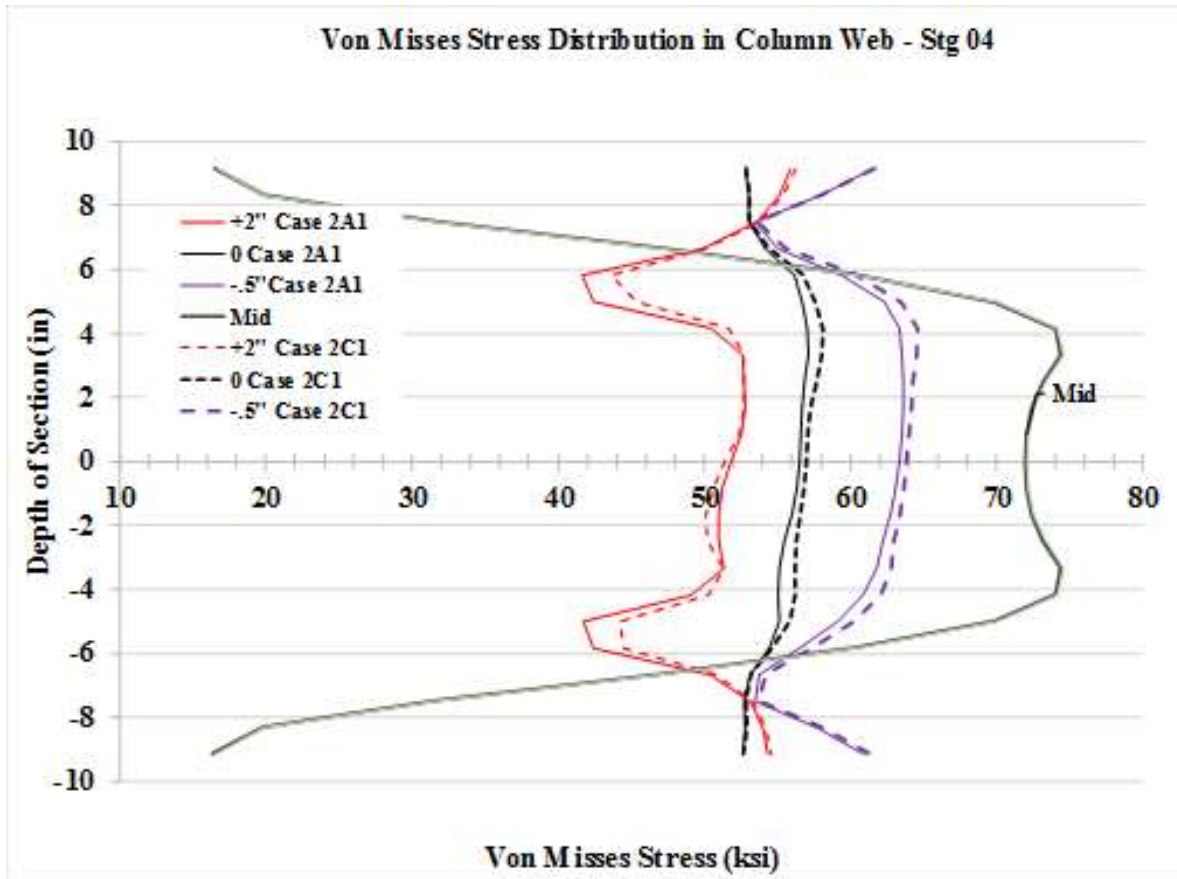


Figure 4.197: Slightly higher VMS levels on Case 2C1

Figure 4.197 also shows a trend that was noticed in the specimens with the clipped DPs. When comparing the VMS stress values at the center of the columns from a level 2 inches above the center of the loading plane to the mid-height of the DP, slightly higher stresses

were recorded in the columns with the “clipped” DPs. This effect decreased as the path were the values were collected got closer to the mid-height level of the PZ.

### 4.3.3 Case Series 3

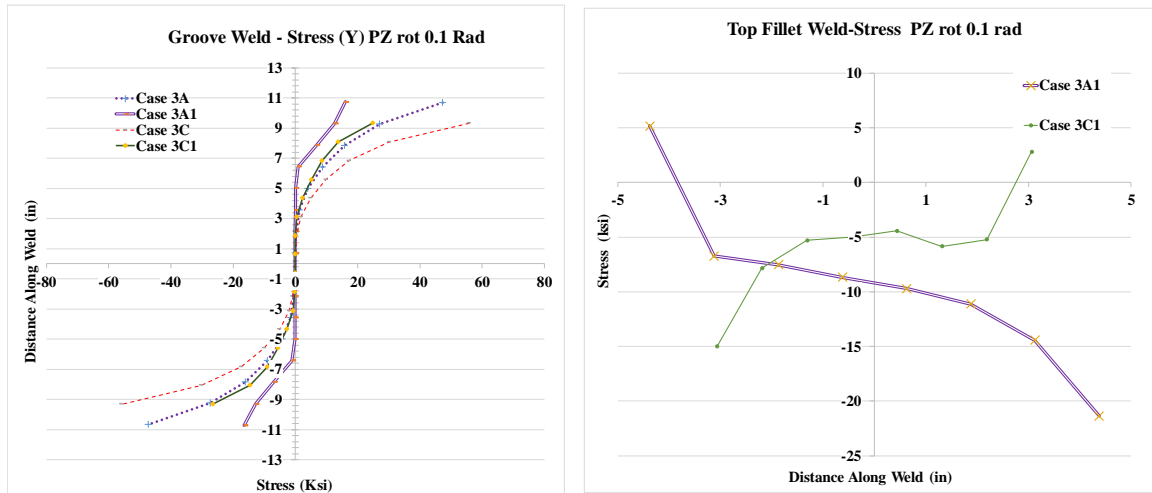


Figure 4.198: Stresses in Horizontal and Vertical Weld at 0.1 Rad for Case Series 3

Case series 3 used an arrangement in which the top and bottom edges of the DP were welded to the CPs. As seen in Figure 4.198 the stress levels recorded in the cases without horizontal welds at the top and bottom of the DP were substantially higher when the PZ had rotated 0.1 radians. As reported on Table 4.24 this was more evident in the edge segments of the vertical welds. When a horizontal weld was not used at the top of the DP, the average force in each of the weld segments in the Y direction increased from 5.48 kips to 44.61 kips in cases 3A and 3A1. Similar results can be seen in cases 3C and 3C1. This is of particular interest since the total sum of the force transferred by all the vertical weld segments reported on Table 4.22 is in the 30 kip range. These small discrepancies in reported forces can be missed when looking at the entire surface rather than the segments.



### 4.3.4 Case Series 4

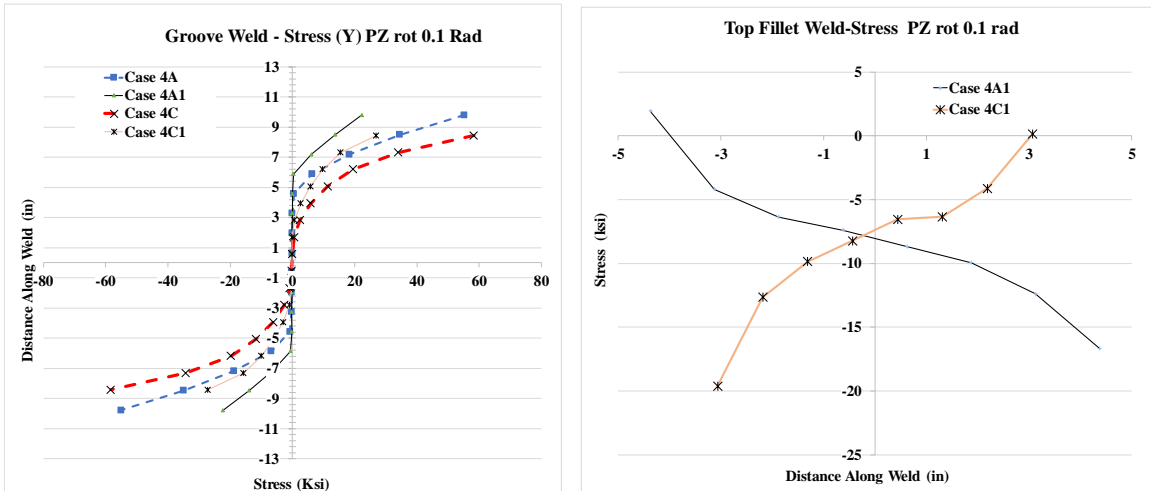


Figure 4.199: Stresses in Horizontal and Vertical Weld at 0.1 Rad for Case Series 4

Case series 4 was used to evaluate the benefits that increasing the space between the CPs and the top and bottom edges of the DP. The intent of this was to allow more space for filed welding but the 1 inch gap between the DP and the CPs resulted in a decrease of performance of the PZ. As seen in Figure 4.200 the reduced cross-sectional area experienced higher stresses and plastic strains at lower load levels than other specimens which had the DP reaching up to the CPs.

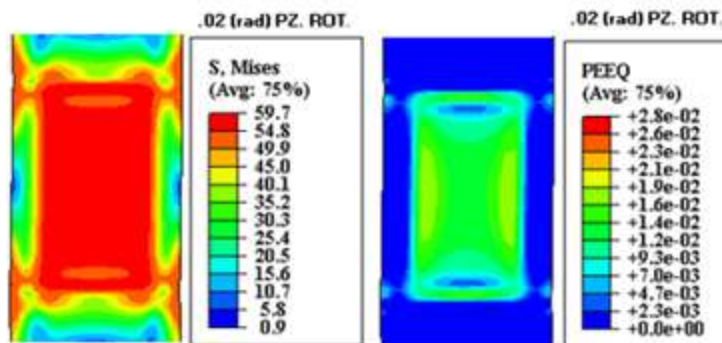


Figure 4.200: VMS and PEEQ values in the “gap” in Case series 4

### 4.3.5 Case Series 5

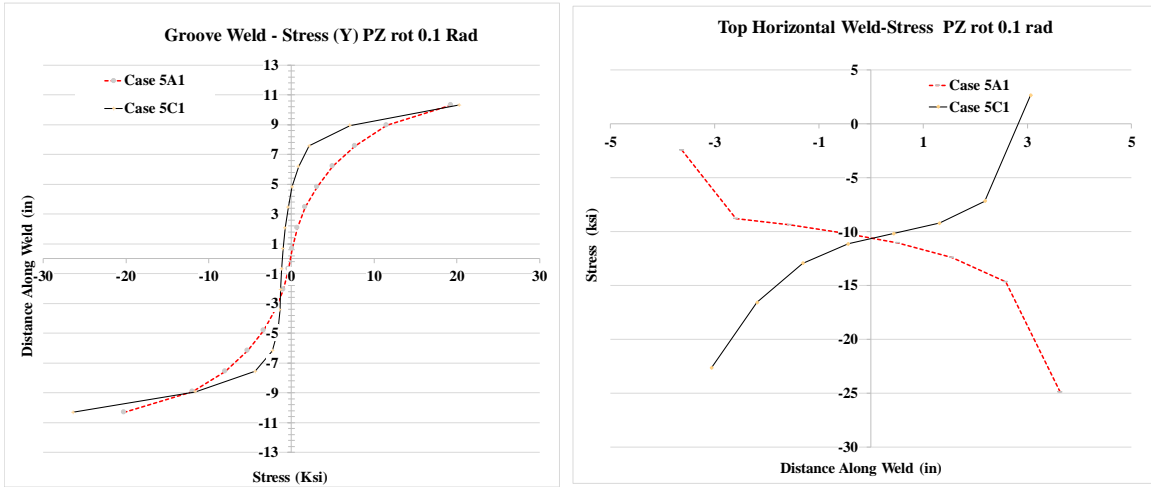
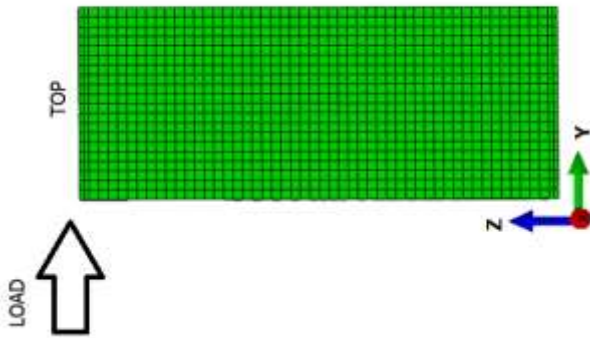


Figure 4.201: Stresses in Horizontal and Vertical Weld at 0.1 Rad for Case Series 5

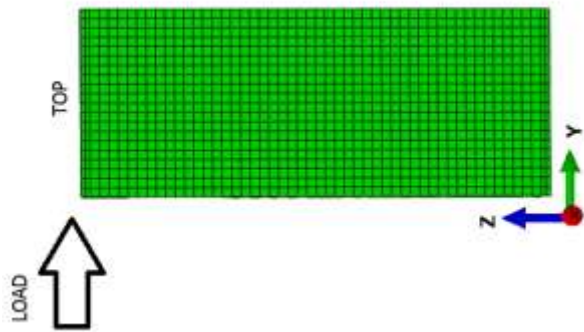
Case series 5 used groove welds on all edges to attach the DP to the column. All other specimens that used a weld at the top and bottom of the DP, used a fillet weld. Based on the VMS stresses and the force required to rotate the PZ in this arrangement, it was determined that this was also one of the best arrangements. In case 5A1 at peak load levels the groove weld transferred a total on 195 kips to the DP in the direction parallel to the loading. This force was among the highest transferred by the top weld in all of the specimens covered in this chapter. This resulted in a reduction in the contribution by the vertical weld and better PZ performance. It should be noted that the recorded shear at the mid-height of the DP was 210.3 kips. Indicating that most of the load was applied by the groove welds at the top and bottom of the DP. It should also be noted that the values for the average force applied by each of the 2 outer welds was close to 25 kips. When compared to the shear strength of a 1 inch segment of DP, these high values might indicate that a fillet weld might not be appropriate for the attachment of the DP at the top of the DP.

$$.6F_y(1/2")(1") = 15 \text{ kip}$$



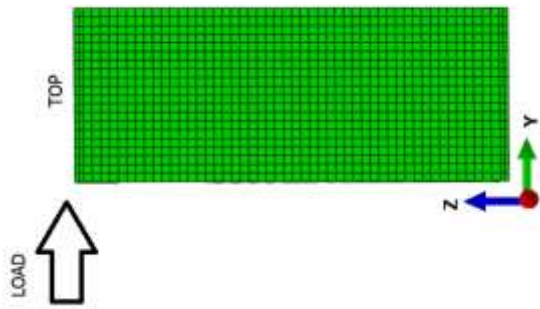
Case	Sum of Load Transferred by all Horizontal Weld Segments																							
	Stage 01			Stage 02			Stage 03			Stage 04			Stage 05											
	X	Y	Z	X	Y	Z	X	Y	Z	X	Y	Z	X	Y	Z									
1A																								
1A1	-0.59	49.0	-0.05	-0.53	110.5	-2.53	-0.40	117.4	-4.83	1.82	129.4	-33.00	2.30	131.2	-38.31									
1C																								
1C1	-0.01	47.5	-0.10	0.06	106.8	-2.19	0.11	111.3	-3.49	0.90	134.3	-26.48	1.04	136.3	-29.89									
2A1	-5.73	-8.7	0.78	-5.07	37.7	-2.50	-5.62	45.3	-3.78	-25.58	70.5	-27.68	-29.20	69.1	-35.81									
2C1	0.13	-7.4	-0.09	0.24	35.0	-3.72	0.22	36.3	-4.07	-3.08	53.0	-28.40	-3.07	51.6	-35.42									
3A																								
3A1	-1.37	98.8	-0.61	-4.39	144.9	-4.45	-4.92	146.6	-5.32	-24.64	181.9	-36.63	-30.66	188.2	-46.50									
3C																								
3C1	-0.01	81.2	-0.17	-0.03	115.8	-1.53	-0.02	120.0	-2.03	-0.63	153.6	-16.97	-0.62	158.8	-20.05									
4A																								
4A1	-1.38	94.7	-0.01	-0.48	123.6	-4.25	-0.47	124.3	-4.62	2.00	153.1	-34.95	2.40	155.4	-39.81									
4C																								
4C1	-0.01	80.5	-0.23	0.04	111.9	-2.27	0.07	115.0	-3.04	0.57	147.1	-26.73	0.64	149.1	-29.43									
5A1	-0.62	90.9	-0.25	-1.73	156.3	-4.74	-1.73	157.5	-5.25	-5.11	191.1	-39.16	-6.47	195.8	-48.56									
5C1	-0.25	91.5	-0.27	-0.69	135.5	-2.47	-0.59	140.8	-3.78	-3.54	174.9	-31.97	-4.22	179.2	-38.16									
Case 18		14.55	0.3588											2.265	12.47									

Table 4.21: Total force transferred to DP by top horizontal weld



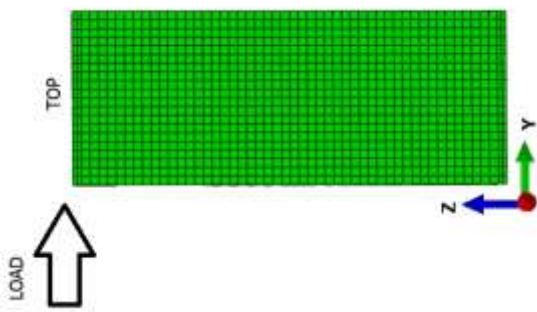
Case	Sum of Load Transferred by all Vertical Weld Segments																	
	Stage 01			Stage 02			Stage 03			Stage 04			Stage 05					
	X	Y	Z	X	Y	Z	X	Y	Z	X	Y	Z	X	Y	Z			
1A	-2.68	-1.08	-299.0	-6.06	-4.64	-358.2	-6.69	-5.95	-366.8	-12.69	-32.44	-466.8	-13.37	-36.14	-473.3			
1A1	-1.03	-1.20	-337.6	-3.64	-2.93	-398.6	-3.42	-3.47	-416.3	-6.15	-7.88	-518.5	-6.75	-8.83	-529.6			
1C	0.00	-0.99	-268.8	0.00	-4.26	-313.4	0.00	-6.16	-323.7	0.00	-38.79	-419.6	0.00	-40.36	-421.8			
1C1	0.01	-0.99	-296.2	-0.06	-4.33	-368.3	-0.11	-5.31	-381.4	-0.90	-16.07	-482.8	-1.04	-17.68	-491.3			
2A1	-2.95	-1.34	-336.6	-3.32	-2.20	-405.6	-3.57	-2.14	-416.9	-7.21	1.14	-523.8	-7.86	1.86	-542.8			
2C1	0.34	-0.59	-312.4	0.37	-0.53	-379.0	0.37	-0.43	-381.4	0.66	1.60	-482.7	0.59	1.18	-499.1			
3A	-6.31	-1.26	-277.9	-6.52	-4.59	-326.3	-7.26	-5.92	-334.3	-14.45	-32.46	-425.1	-15.74	-37.32	-432.6			
3A1	-1.60	-1.52	-322.5	-4.24	-6.66	-378.0	-4.37	-6.52	-382.8	-6.72	-6.89	-481.8	-7.26	-7.07	-498.7			
3C	0.00	-1.02	-242.1	0.00	-4.88	-283.9	0.00	-5.94	-289.5	0.00	-39.43	-377.7	0.00	-39.91	-378.4			
3C1	-0.01	-2.82	-288.2	0.05	-8.87	-335.8	0.04	-9.86	-343.2	0.65	-27.05	-438.3	0.66	-33.72	-450.3			
4A	-7.16	-1.43	-265.6	-6.52	-5.16	-298.2	-7.01	-6.17	-303.6	-14.90	-36.68	-388.4	-15.37	-38.62	-391.1			
4A1	-1.39	-1.08	-296.5	-1.99	-3.89	-349.4	-1.99	-4.00	-351.6	-4.96	-11.20	-447.6	-5.28	-13.12	-456.3			
4C	0.00	-1.02	-216.2	0.00	-4.49	-252.2	0.00	-6.37	-260.6	0.00	-43.31	-341.1	0.00	-41.27	-338.6			
4C1	0.00	-1.04	-262.7	-0.04	-4.66	-308.6	-0.07	-5.40	-315.9	-0.58	-18.80	-408.5	-0.65	-20.19	-414.5			
5A1	-1.49	-2.09	-309.1	-3.71	-2.19	-390.0	-3.75	-2.03	-393.0	-6.83	0.70	-499.5	-7.02	1.25	-515.8			
5C1	-2.14	-1.59	-289.6	-2.10	-4.20	-351.7	-2.04	-5.04	-363.0	-4.93	-12.93	-463.8	-5.24	-15.03	-476.5			
Case 18			<b>0.8693</b>			<b>-317.8</b>									<b>2.177</b>			<b>-587.4</b>

Table 4.22: Total force transferred to DP by left vertical weld



Case	Segment Length (in)	Average Force Transferred by Each of the 2 Outermost Horizontal Weld Segments (kip)																							
		Stage 01			Stage 02			Stage 03			Stage 04			Stage 05											
		X	Y	Z	X	Y	Z	X	Y	Z	X	Y	Z	X	Y	Z									
1A		-0.02	5.2	-0.6	-0.73	13.0	1.7	-0.86	13.6	2.0	-0.58	15.8	-1.2	-0.54	16.2	-1.6									
1C1	1 1/4	0.26	6.5	-2.2	0.45	13.1	-5.1	0.45	13.7	-4.7	0.69	16.6	-7.2	0.72	16.8	-7.5									
2A1	7/8	-2.68	-0.1	-0.1	-6.51	6.5	7.3	-7.18	7.6	8.0	-14.39	11.7	9.0	-15.23	11.4	9.2									
2C1	1 1/4	-1.92	-0.6	-1.5	-4.86	5.0	0.2	-4.99	5.2	0.3	-10.84	7.1	0.0	-11.31	6.8	0.1									
3A	7/8																								
3A1	1 1/4	-0.50	11.5	-0.2	0.43	17.9	3.3	0.56	18.2	3.4	-0.49	23.2	0.2	-0.92	24.3	-0.5									
3C	7/8																								
3C1	1 1/4	-1.6951	10.2	-2.19	-2.671	13.9	-3.938	-2.63	14.4	-3.418	-3.3858	19.6	-4.8825	-3.6768	20.5	-4.994									
4A	7/8																								
4A1	1 1/4	-0.15	10.9	-0.9	-1.07	14.4	2.4	-1.11	14.5	2.5	-0.75	19.2	-0.3	-0.69	19.6	-0.7									
4C	7/8																								
4C1	1 1/4	0.44	10.1	-3.3	0.48	13.9	-4.6	0.45	14.4	-4.2	0.73	18.3	-6.8	0.76	18.6	-7.1									
5A1	7/8	-0.21	11.3	-1.9	-0.45	20.2	1.6	-0.43	20.3	1.7	-0.77	24.6	-2.3	-0.91	25.3	-2.9									
5C1	1 1/4	-0.11	11.5	-4.1	-0.25	16.9	-5.6	-0.18	17.5	-4.7	-0.59	21.8	-8.1	-0.66	22.3	-8.6									

Table 4.23: Average force transferred by two outermost horizontal weld segments



Case	Segment Length (in)	Average Force Transferred by Each of the 2 Outermost Vertical Weld Segments (kip)																							
		Stage 01			Stage 02			Stage 03			Stage 04			Stage 05											
		X	Y	Z	X	Y	Z	X	Y	Z	X	Y	Z	X	Y	Z									
1A	1 4/7	0.01	25.4	-11.9	-0.04	38.0	-12.9	-0.07	38.6	-13.3	-0.14	45.0	-21.6	-0.17	45.2	-22.4									
1A1	1 4/7	0.02	20.4	-14.4	-0.28	11.2	-22.3	-0.08	10.8	-23.1	0.00	17.2	-29.1	-0.05	17.4	-30.0									
1C	1 3/8	0.05	26.9	-11.6	0.02	36.8	-11.2	0.01	37.8	-11.7	-0.24	43.0	-22.8	-0.27	43.0	-23.2									
1C1	1 3/8	0.03	17.9	-16.0	-0.12	12.4	-21.8	-0.10	12.1	-22.7	-0.18	15.3	-31.7	-0.21	15.2	-32.6									
2A1	1 4/7	-1.18	9.7	-14.7	-0.58	1.5	-23.2	-0.51	1.1	-23.9	-1.45	1.0	-30.5	-1.50	1.0	-31.7									
2C1	1 3/8	-0.19	9.9	-18.4	0.00	3.1	-23.7	-0.01	3.1	-23.8	-0.04	5.7	-31.2	-0.06	5.6	-32.5									
3A	1 3/7	0.01	26.4	-12.3	0.00	37.7	-11.5	-0.01	38.4	-11.9	-0.14	44.5	-20.2	-0.16	44.6	-21.2									
3A1	1 3/7	-1.07	10.2	-16.7	-2.63	3.8	-22.0	-2.70	3.8	-22.2	-3.18	5.7	-28.4	-3.19	5.5	-29.7									
3C	1 1/4	0.06	26.7	-10.4	0.05	36.1	-9.9	0.05	36.8	-10.3	-0.21	42.0	-21.2	-0.22	42.0	-21.4									
3C1	1 1/4	0.01	12.0	-17.6	-0.02	10.2	-20.4	-0.08	9.6	-21.1	-0.14	10.1	-29.9	-0.20	9.2	-31.3									
4A	1 1/3	0.01	29.3	-11.1	0.04	36.9	-10.5	0.04	37.5	-10.8	-0.05	43.6	-19.3	-0.06	43.6	-19.7									
4A1	1 1/3	0.41	11.8	-15.9	0.42	9.2	-20.2	0.43	9.3	-20.3	0.73	11.3	-27.5	0.74	11.2	-28.2									
4C	1 1/8	0.05	26.0	-9.2	0.08	34.5	-8.6	0.10	35.8	-9.1	-0.17	41.0	-20.0	-0.14	41.0	-19.5									
4C1	1 1/8	0.02	12.0	-15.9	-0.09	11.2	-18.8	-0.06	10.8	-19.4	-0.08	11.6	-28.5	-0.09	11.3	-29.3									
5A1	1 3/8	0.02	10.6	-16.5	-0.71	4.3	-22.0	-0.73	4.4	-22.1	-0.65	8.1	-29.2	-0.59	8.5	-30.4									
5C1	1 3/8	0.08	10.8	-18.1	-0.15	8.4	-21.7	-0.08	7.9	-22.5	0.12	9.8	-31.4	0.12	9.4	-32.7									

Table 4.24: Average force transferred by two outermost vertical weld segments

### 4.3.6 Forces in the Welds

The total forces applied by both vertical and horizontal welds were divided by the DP shear strength and presented in Tables 4.25 and 4.26.

$$S_v = .6F_y t_{dp} l_{dpv} = .6 * 50ksi * \frac{1}{2} inch * 24 inch = 360 kip$$

$$S_h = .6F_y t_{dp} l_{dph} = .6 * 50ksi * \frac{1}{2} inch * 10 inch = 150 kip$$

Case	Horizontal Weld Force in Y direction/DP shear strength, $S_h$				
	Stage 01	Stage 02	Stage 03	Stage 04	Stage 05
	Y	Y	Y	Y	Y
<b>1A</b>					
<b>1A1</b>	0.3	0.7	0.8	0.9	0.9
<b>1C</b>					
<b>1C1</b>	0.3	0.7	0.7	0.9	0.9
<b>2A1</b>	0.1	0.3	0.3	0.5	0.5
<b>2C1</b>	0.0	0.2	0.2	0.4	0.3
<b>3A</b>					
<b>3A1</b>	0.7	1.0	1.0	1.2	1.3
<b>3C</b>					
<b>3C1</b>	0.5	0.8	0.8	1.0	1.1
<b>4A</b>					
<b>4A1</b>	0.6	0.8	0.8	1.0	1.0
<b>4C</b>					
<b>4C1</b>	0.5	0.7	0.8	1.0	1.0
<b>5A1</b>	0.6	1.0	1.1	1.3	1.3
<b>5C1</b>	0.6	0.9	0.9	1.2	1.2

Table 4.25: Relation between the horizontal force in the horizontal weld and shear strength of DP

Case	Vertical Weld Force in Z direction/DP shear strength, $S_v$				
	Stage 01	Stage 02	Stage 03	Stage 04	Stage 05
	Z	Z	Z	Z	Z
1A	0.8	1.0	1.0	1.3	1.3
1A1	0.9	1.1	1.2	1.4	1.5
1C	0.7	0.9	0.9	1.2	1.2
1C1	0.8	1.0	1.1	1.3	1.4
2A1	0.9	1.1	1.2	1.5	1.5
2C1	0.9	1.1	1.1	1.3	1.4
3A	0.8	0.9	0.9	1.2	1.2
3A1	0.9	1.1	1.1	1.3	1.4
3C	0.7	0.8	0.8	1.0	1.1
3C1	0.8	0.9	1.0	1.2	1.3
4A	0.7	0.8	0.8	1.1	1.1
4A1	0.8	1.0	1.0	1.2	1.3
4C	0.6	0.7	0.7	0.9	0.9
4C1	0.7	0.9	0.9	1.1	1.2
5A1	0.9	1.1	1.1	1.4	1.4
5C1	0.8	1.0	1.0	1.3	1.3

Table 4.26: Relation between the vertical force in the vertical weld and shear strength of DP

The values on Table 4.25 would seem to indicate that the horizontal weld at the top and bottom of the DP, should be designed to provide the full strength of the DP when using a “fitted” DP. Cases 2A1 and 2C1 seem to require lower strengths but this is likely due to the placement of the top horizontal weld. The top fillet weld sits at a 1 inch distance above the center of the loading plate. As seen in all of the plots that show the VMS measured 2 inches above the PZ, the shear force is transferred “into” the PZ. Although cases 5A1 and 5C1 seemed to perform great the values reported on Table 4.25 at peak load levels and PZ rotation of 0.1 radians are the highest of all other cases.



#### 4.3.7 Summary

Key observations from this chapter can be summarized as follows:

- The use of “fitted” DP in the “shallow” column does not seem to increase or decrease the overall structural performance of the panel zone when compared to the specimens from Shirsat (2011) and Donkada (2012) which used DPs extended 6 inches beyond the top and bottom loading plates.
- The use of the clipped corners did not result in substantial performance deficits and only seemed to affect the stress levels within the first 2 inches away from the loading plates slightly.
- One of the cases series that showed the best performance was case series 2. This performance is assumed to be due to the longer DP which provided more reinforcement and weld. It also used both vertical and horizontal welds.
- Case series 5 was also very effective in transferring forces to the DP. It is for this reason that more force was required to cause a PZ rotation value of 0.1 radians. The modeling of groove welds at the top and bottom of the DP, as well as on the sides seemed to be the reason for the improvement in performance. The horizontal weld transferred most of the shear force reported at mid-height of the DP. This reduced the force requirement in the Y direction of the groove weld allowing it to provide more force in the Z direction.

- The outer most segments of the welds transfer much higher forces than those near the center of the weld. This was evident in all variations of the “fitted” DP especially in the vertical weld when no weld was used to attach the top and bottom of the DP.
- Tables 4.25 and 4.26 would seem to indicate that a weld strength of 80% of the shear strength of the DP is required for the weld to accommodate a PZ rotation of 0.02 radians and higher to reach PZ rotation of 0.1 radians. Based on the performance of case series 5, the use of a groove weld to attach the top and bottom of a “fitted” DP would seem to be more appropriate.

## CHAPTER 5

### Parametric Studies on Attachment Details of Doubler Plates in a W40X264 Column

#### 5.1 INTRODUCTION

This chapter presents the results from analysis performed on a “deep” W40x264 column specimen. The cases in this chapter are similar to those covered in Chapter 4 and the same plots were reported. The points at which these were reported were reduced to four. The four stages used for the reporting of values were in the following order, first yield point, second yield point, PZ rotation of 0.02 radians and 0.1 radians. The previous chapter reported the values at a peak load of 1.25  $P_z$ , similar to that used by Shirsat (2011). This column was not modeled in that work and for this reason only four stages were used.

A DP thickness of 1 inch was used for the models in the “deep” W40x264. This was determined using equation E3-7 from *Provisions for Steel Structural Buildings* (AISC 2010)

$$t \geq \frac{d_z + w_z}{90}$$

$d_z$  = panel zone depth between continuity plates (in)

$t$  = thickness of the doubler plate (in)

$w_z$  = panel zone width between column flanges (in)

It should be noted that both horizontal and vertical welds in this chapter were divided into 32 segments each. This is a key difference from those modeled in Chapter 4 and the main reason for this is the substantial increase in length of the horizontal weld. Another key observation that was made in both “shallow” and “deep” column was the large variation in

force transfer between segments. As explained previously, this is due to the misalignment between the force flow through the welds and the way the welds were layered. This is especially evident in the outer segments of the vertical groove weld which transfer some of the highest levels of force into the DP because of the proximity to the loading force entering the PZ.

## 5.2 ANALYSIS CASES

Analysis Cases For the W40x264

Case	$t_{dp}$ (in)	$l_{dp}$ (in)	$b_{dp}$ (in)	CP	Vertical Weld Length (in)	Horizontal Weld Length (in)
<b>6</b>	-	-	-	-	-	-
<b>6A</b>	1	25	34	-	25	-
<b>6A1</b>	1	25	34	-	25	34
<b>6C</b>	1	25	34	-	22	-
<b>6C1</b>	1	25	34	-	22	31
<b>7A1</b>	1	25	34	Y	25	34
<b>7C1</b>	1	25	34	Y	22	31
<b>8A</b>	1	22 7/8	34	Y	22 7/8	-
<b>8A1</b>	1	22 7/8	34	Y	22 7/8	34
<b>8C</b>	1	22 7/8	34	Y	19 7/8	-
<b>8C1</b>	1	22 7/8	34	Y	19 7/8	31
<b>9A</b>	1	21	34	Y	21	-
<b>9C</b>	1	21	34	Y	18	-
<b>10A1</b>	1	22	34	Y	21	34
<b>10C1</b>	1	22	34	Y	18	31

Notes

- 1) A "C" in case name indicates "clipped" doubler plate corners
- 2) A "1" after the letter designation indicates fillet welds were used at the top of DP
- 3) Cases 1-1C1 used no CPs

Table 5.1: Analysis cases for W40x264 "shallow" column

5.2.1 Analysis Case 6

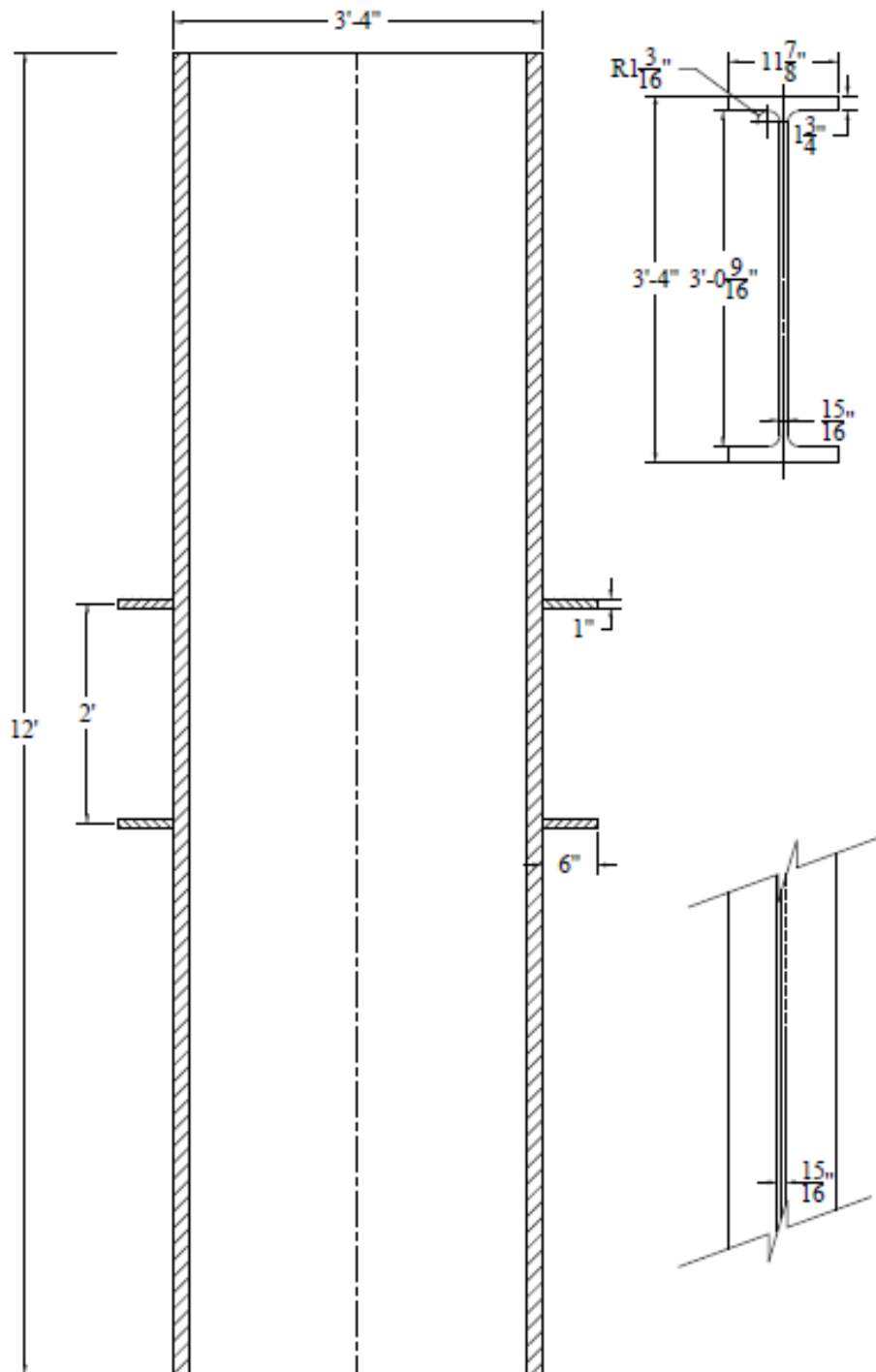


Figure 5.1:W40x264 Analysis case 6

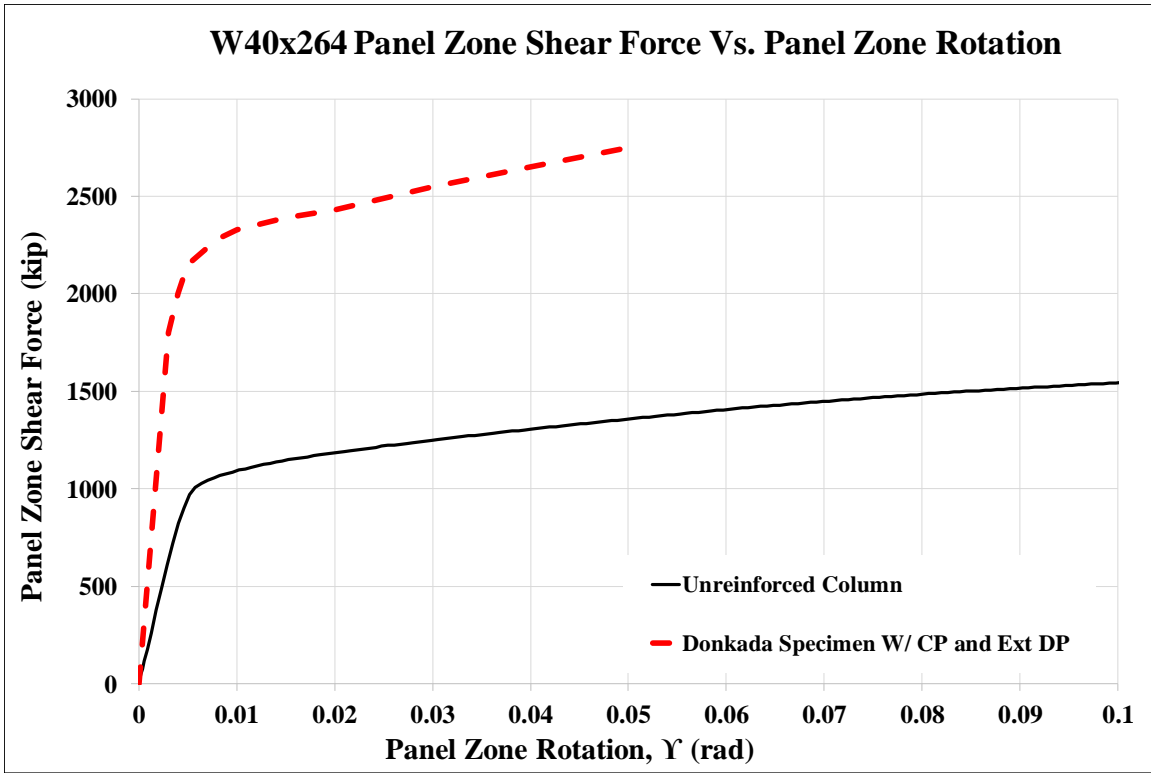


Figure 5.2: Panel zone shear vs. panel zone rotation Case 6

Stage	Applied Force/Loading Plate (Kip)	Panel Shear Force (Kip)	Panel Zone Rotation (rad)
1	582	970	0.005
2	678	1,130	0.013
3	712	1,187	0.020
4	927	1,545	0.100

Table 5.2: Panel zone shear and force on loading plate Case 6

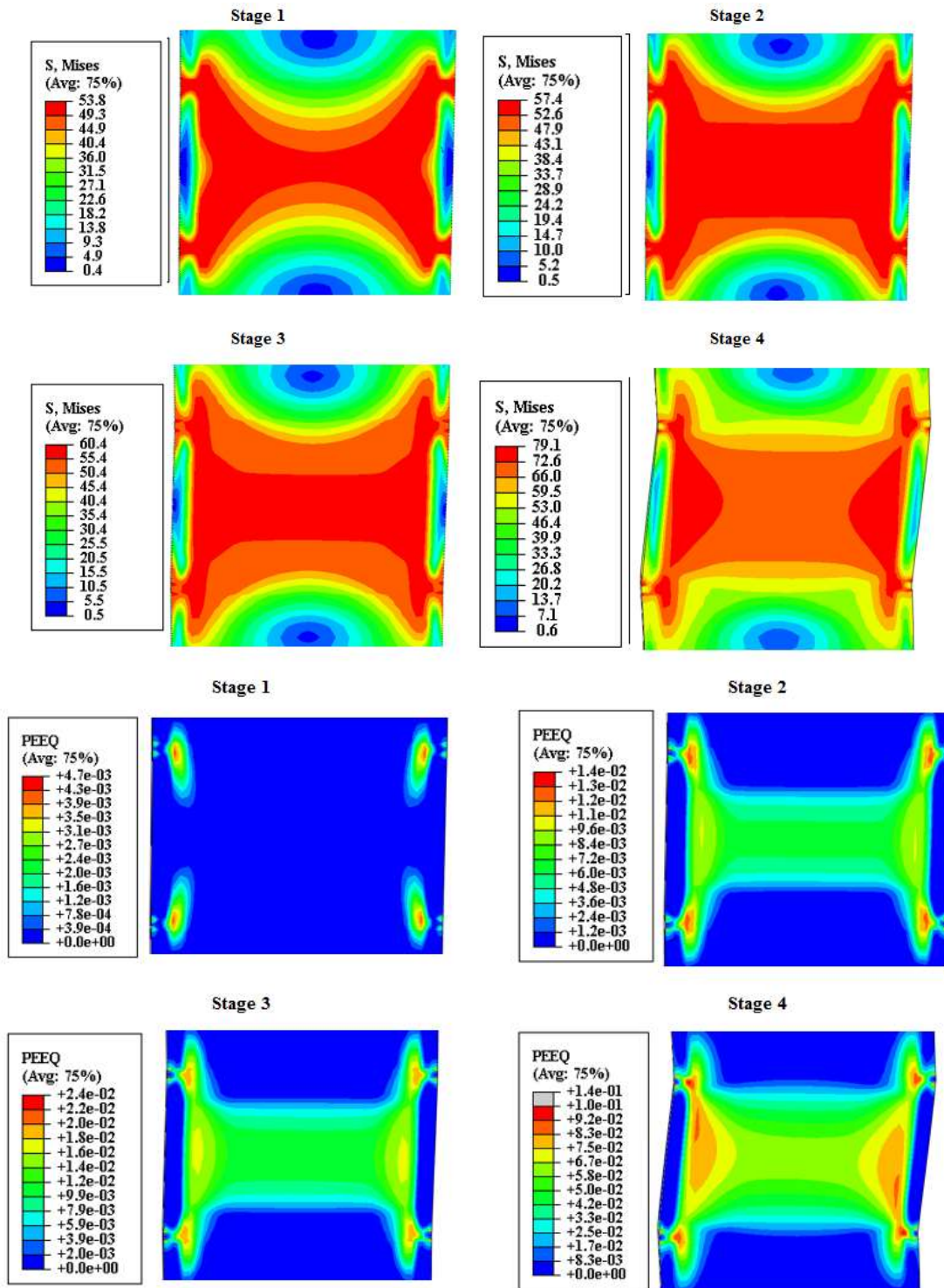


Figure 5.3: VMS and PEEQ in the column Case 6

### 5.2.2 Analysis Case 6A

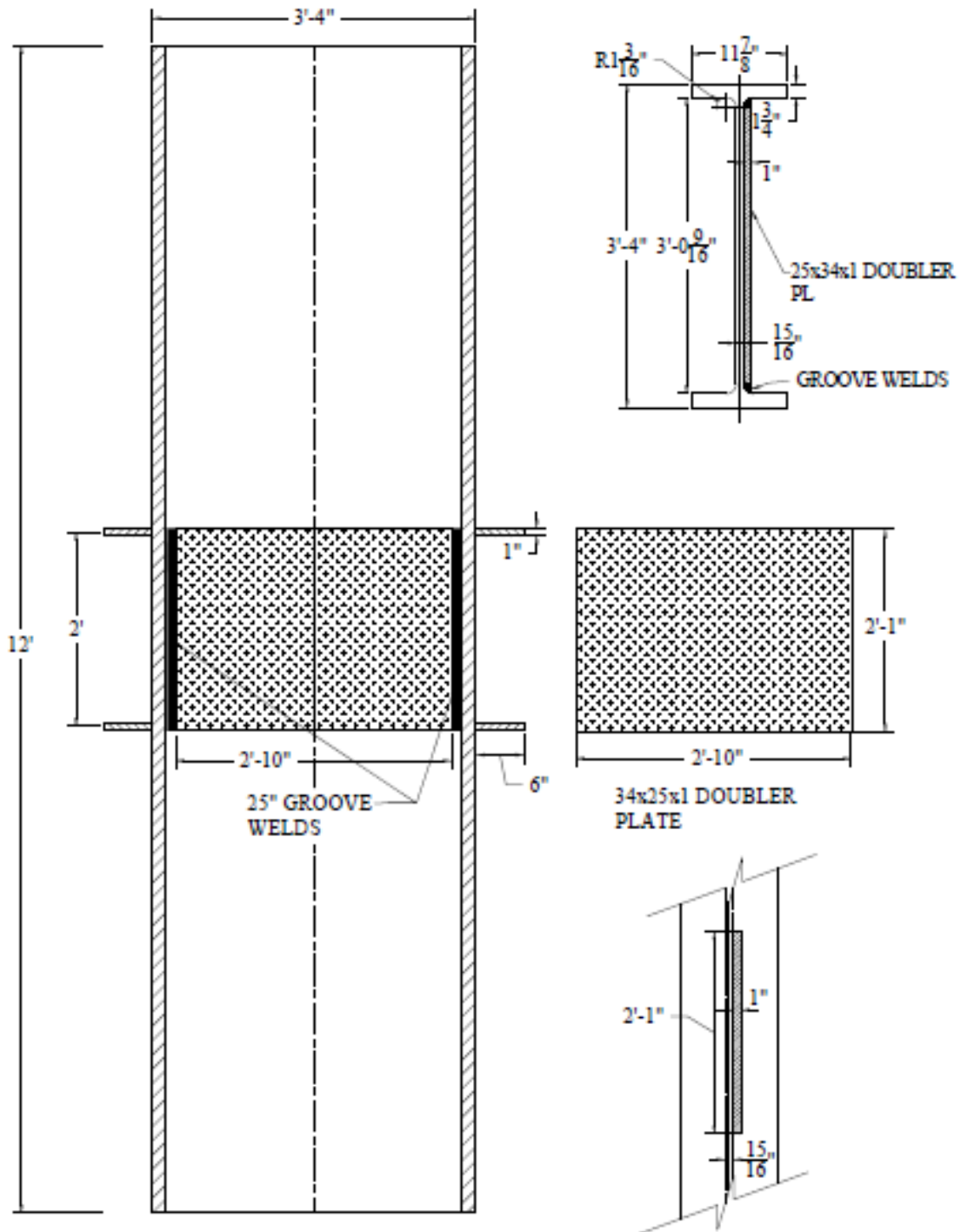


Figure 5.4: W40x264 Analysis case 6A



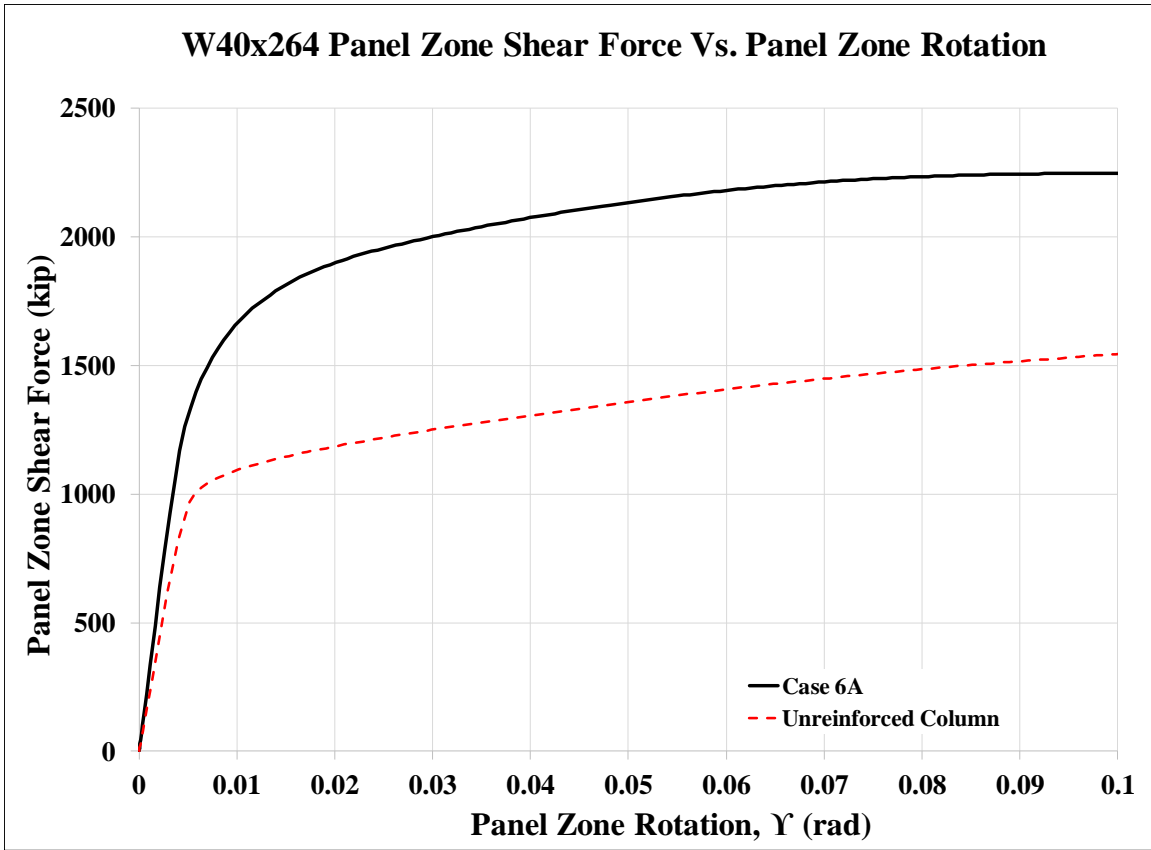


Figure 5.5: Panel zone shear vs. panel zone rotation Case 6A

Stage	Applied Force/Loading Plate (Kip)	Panel Shear Force (Kip)	% Higher Than Unreinforced Col.	Panel Zone Rotation (rad)
1	757	1,262	130%	0.005
2	1,124	1,873	166%	0.018
3	1,139	1,899	160%	0.020
4	1,348	2,246	145%	0.100

Table 5.3: Panel zone shear and force on loading plate Case 6A

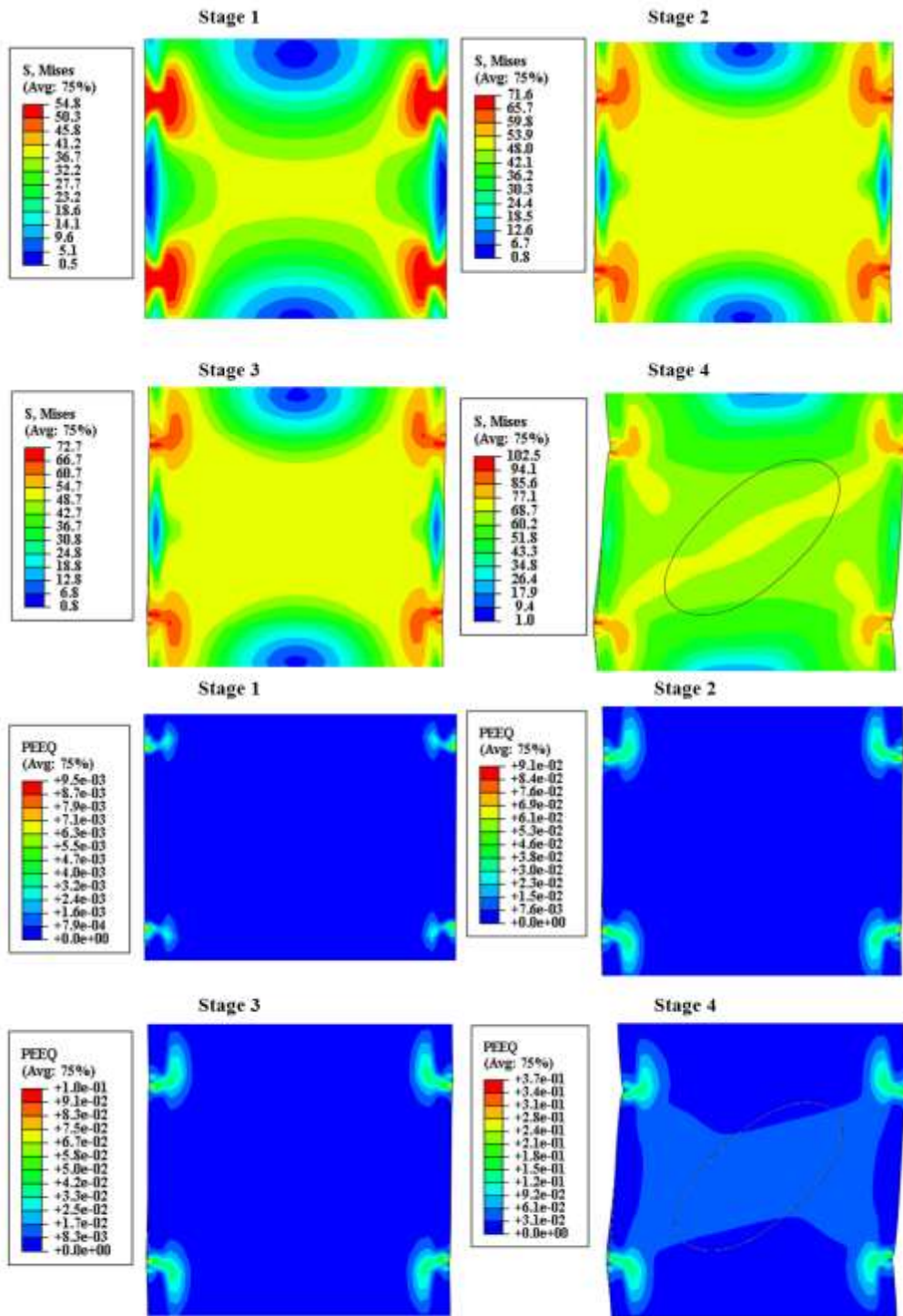


Figure 5.6: VMS and PEEQ in the column Case 6A

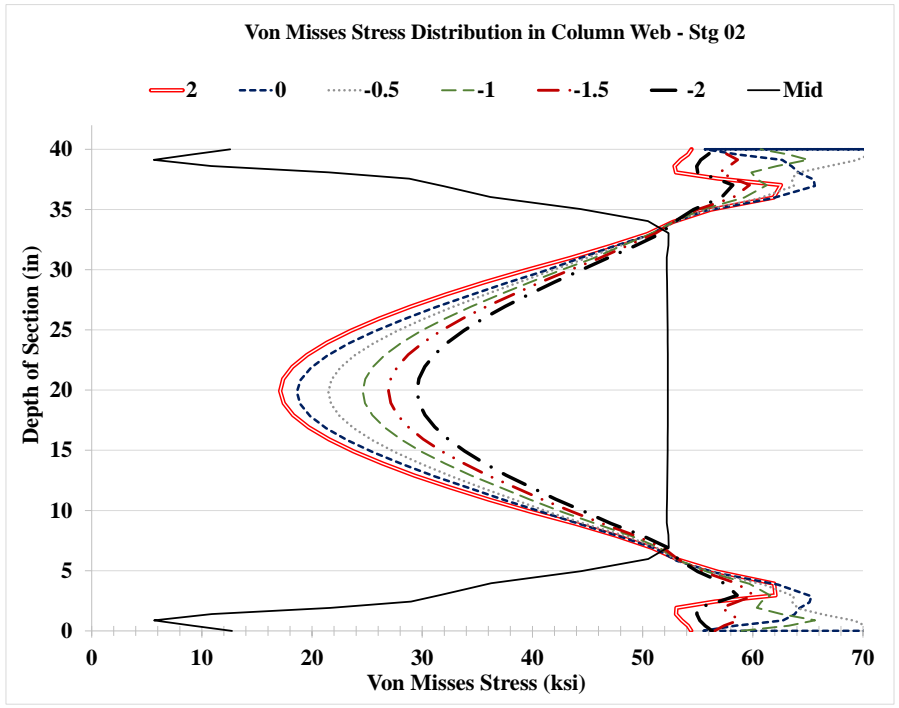
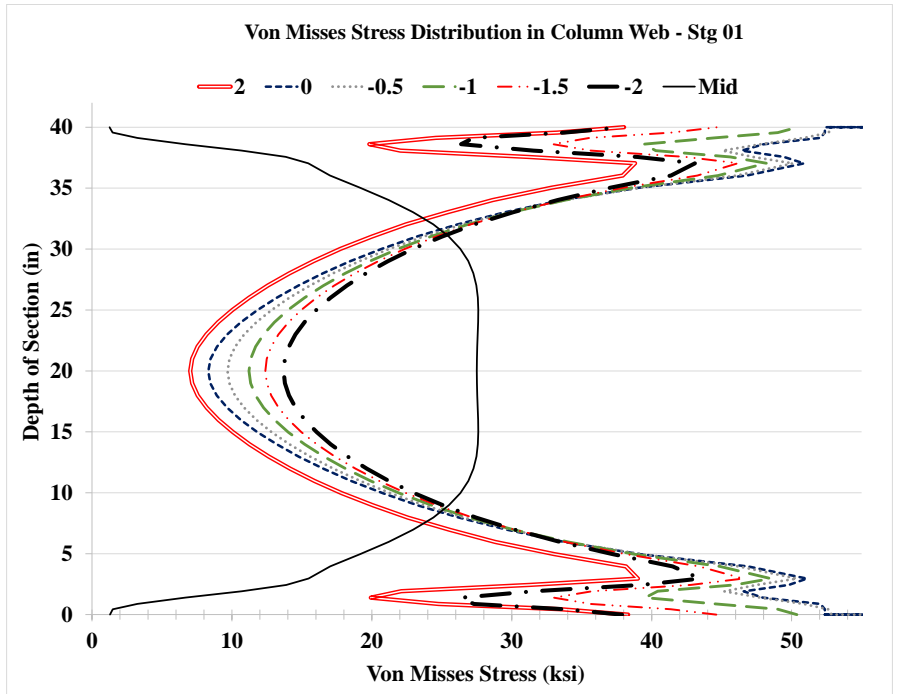


Figure 5.7: VMS distribution in column web at different heights Stg. 01-04 Case 6A

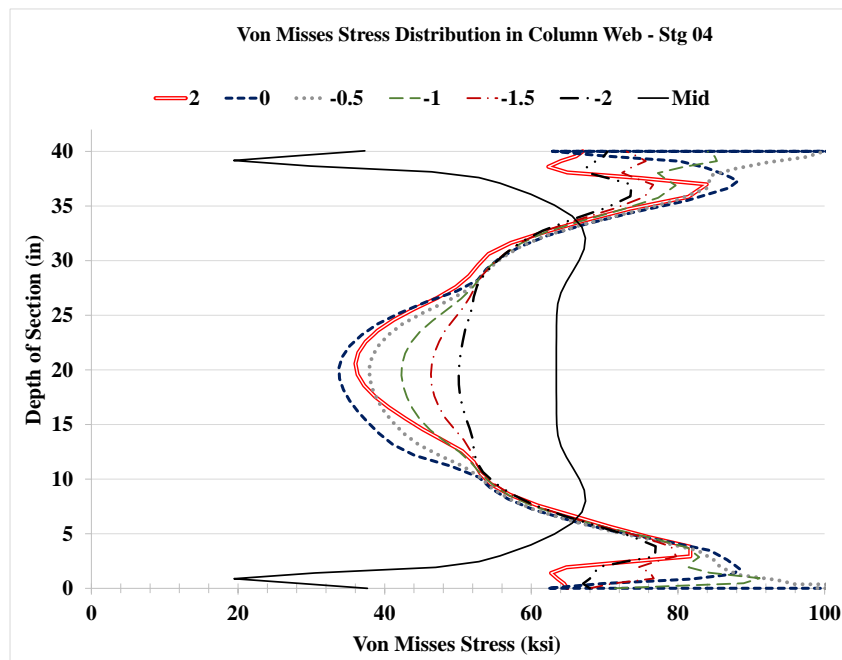
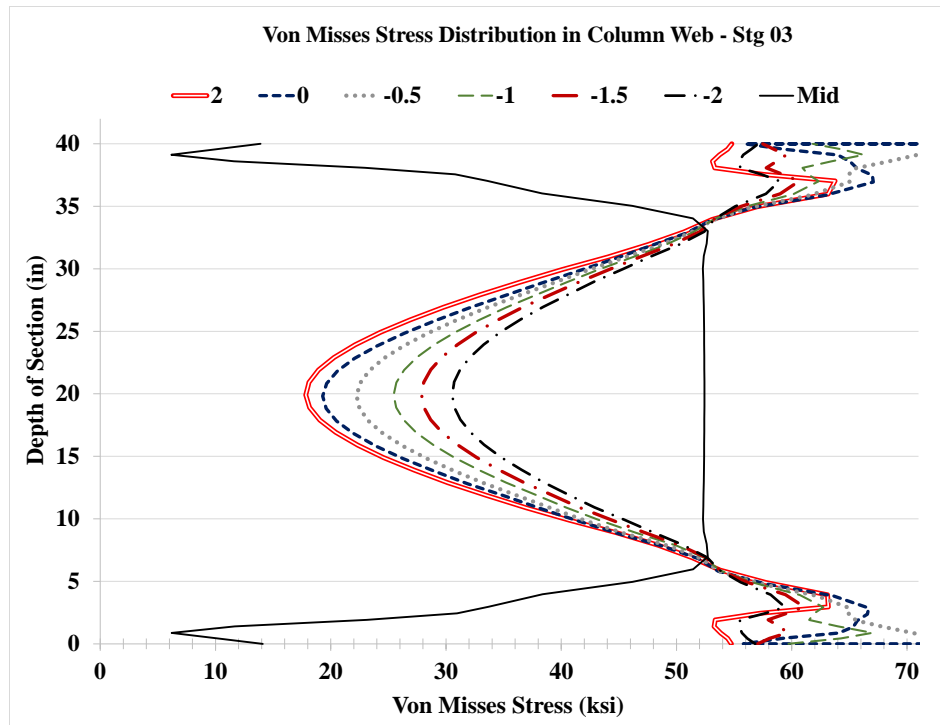


Figure 5.7: VMS distribution in column web at different heights Stg. 01-04 Case 6A

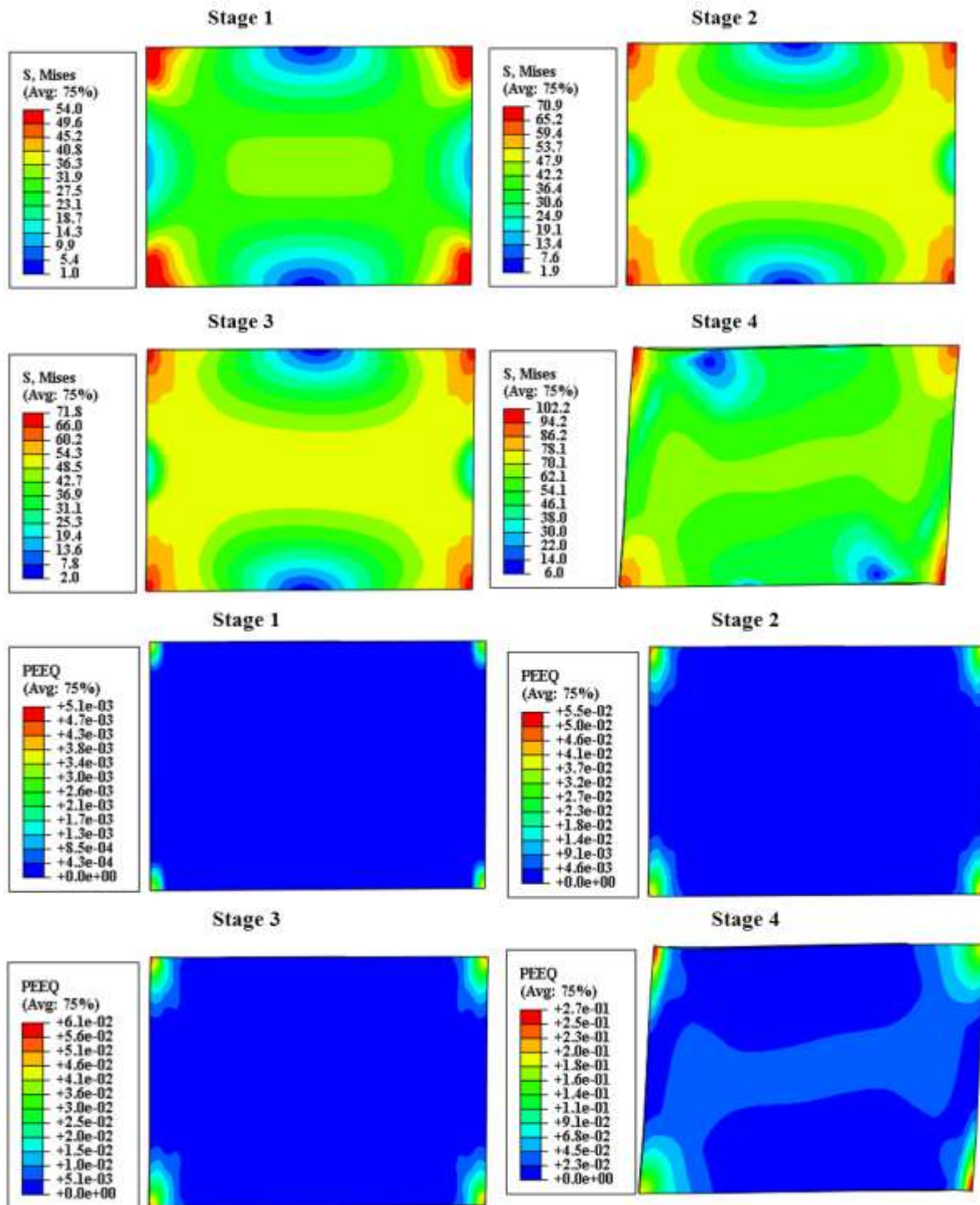


Figure 5.8: VMS and PEEQ in the DP Case 6A

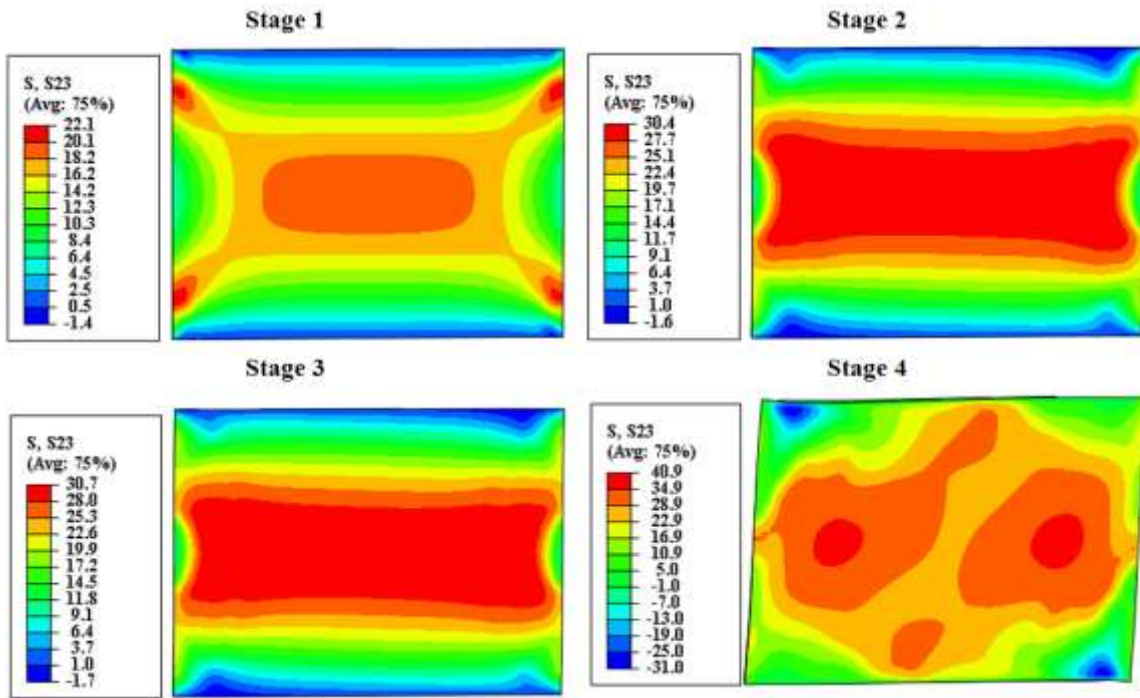


Figure 5.9: Shear stress, S<sub>23</sub> in the DP Case 6A

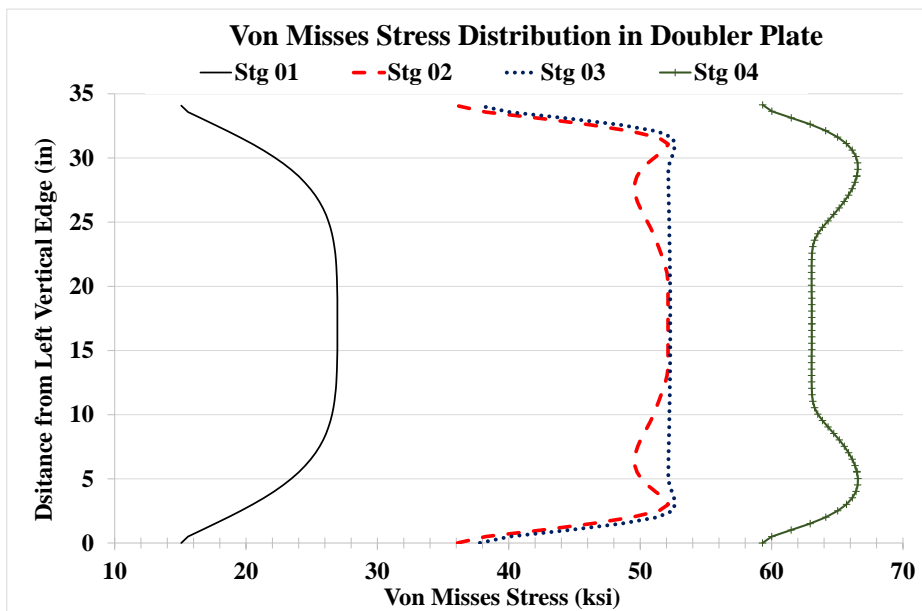


Figure 5.10: VMS distribution at mid-depth of DP Case 6A

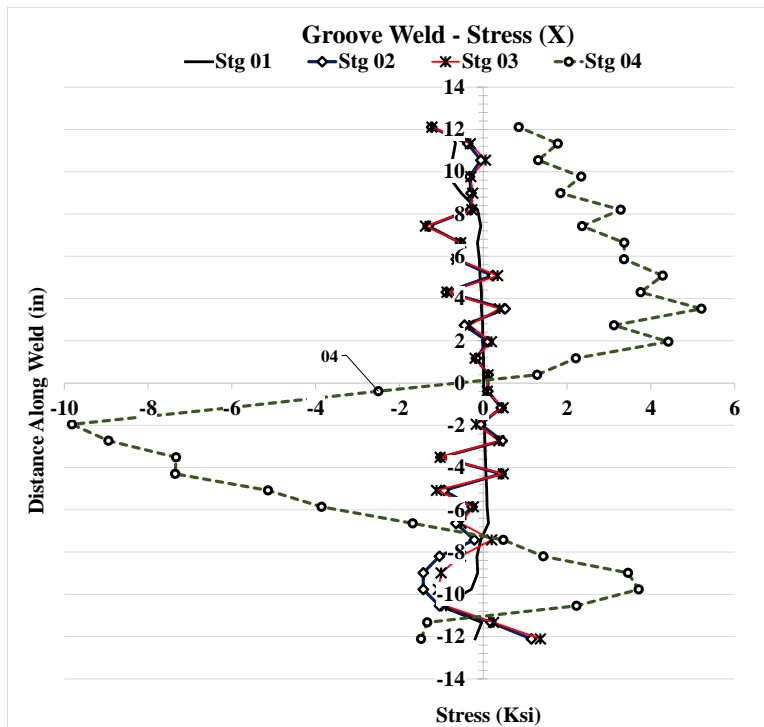
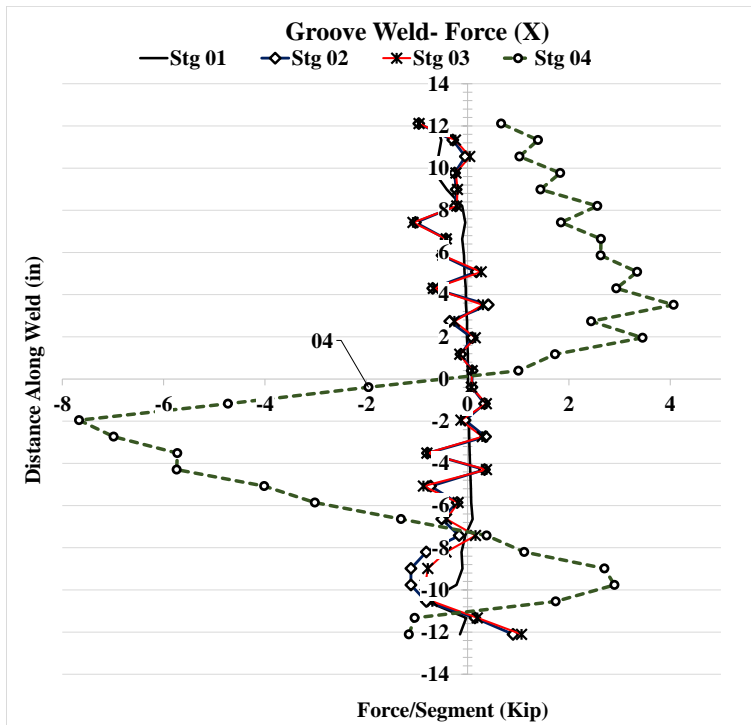


Figure 5.11: Forces and stresses in horizontal weld, (X) Case 6A

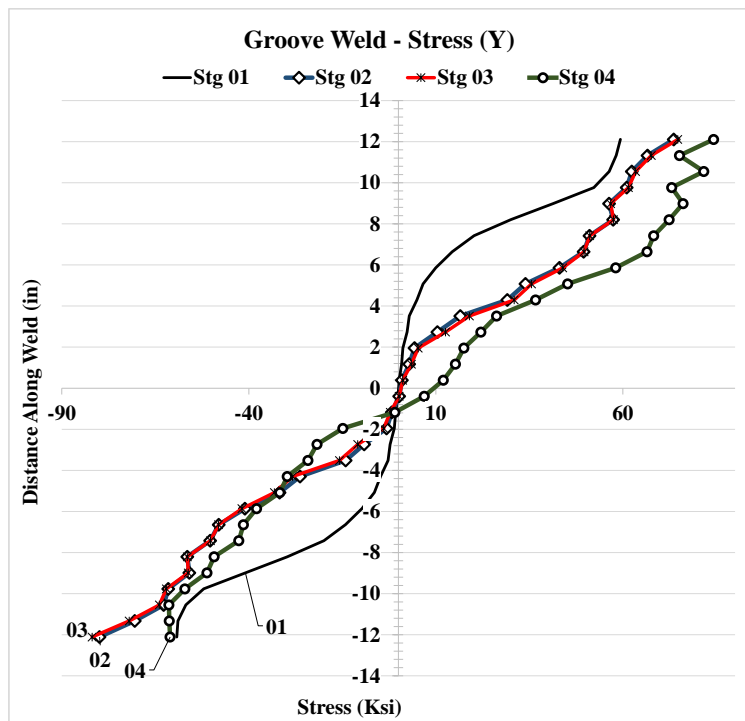
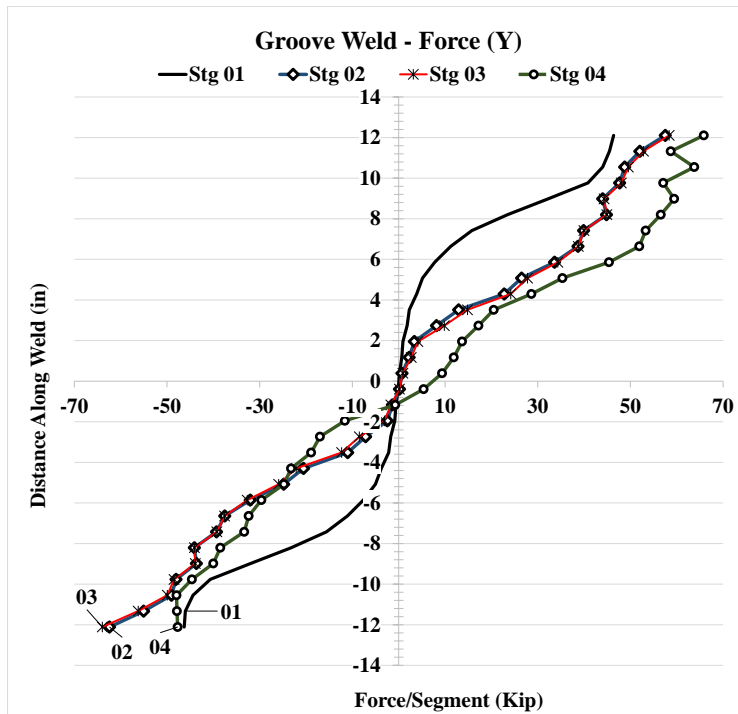


Figure 5.12: Forces and stresses in horizontal weld, (Y) Case 6A



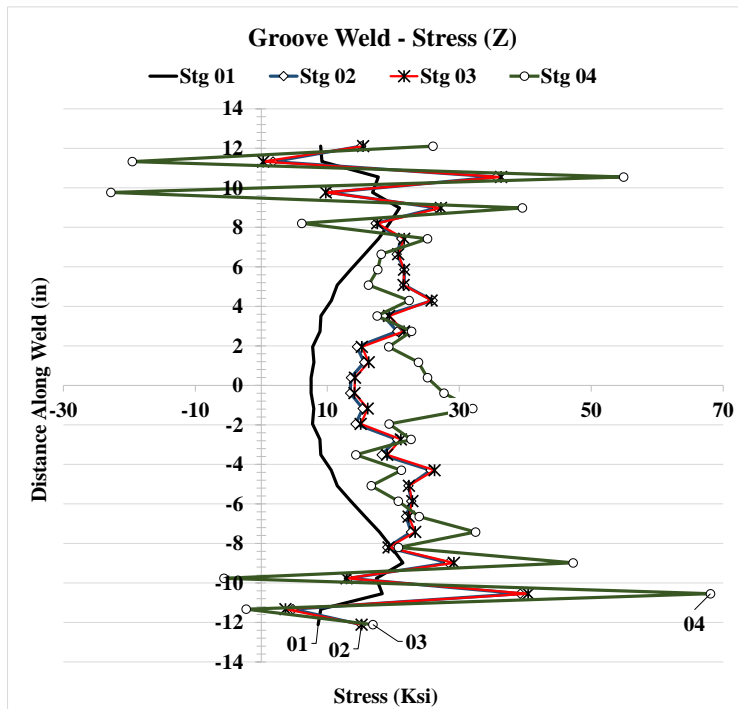
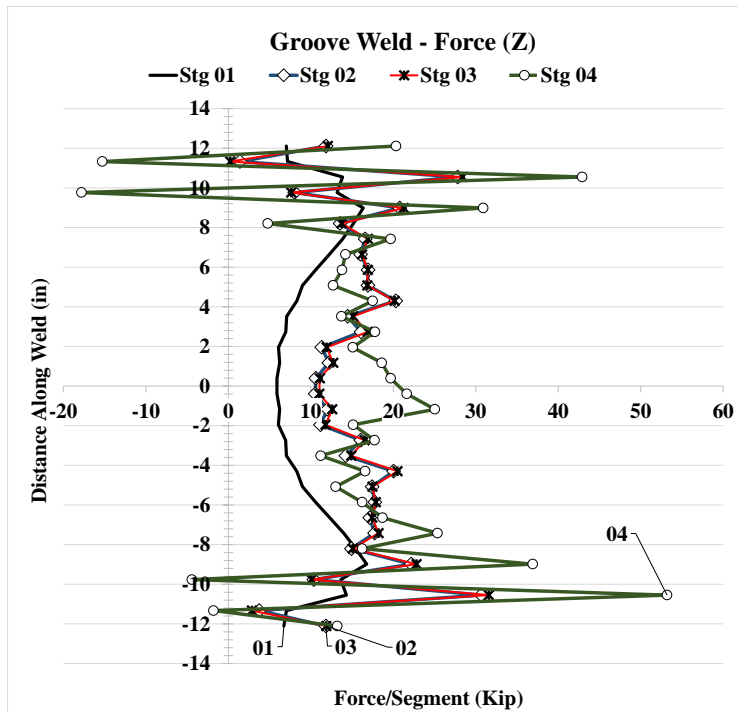


Figure 5.13: Forces and stresses in horizontal weld, (Z) Case 6A

### 5.2.3 Analysis Case 6A1

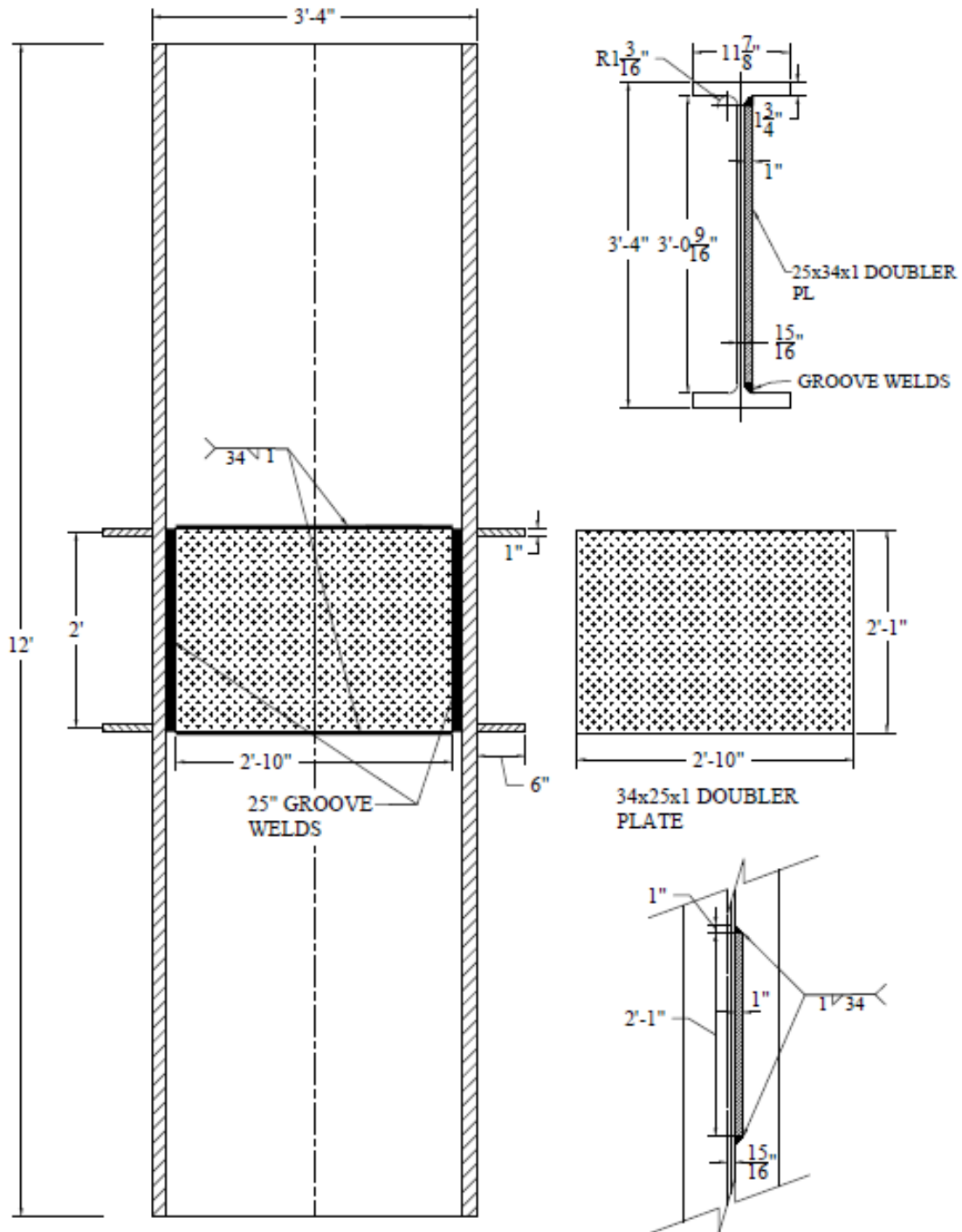


Figure 5.14: W40x264 Analysis case 6A1

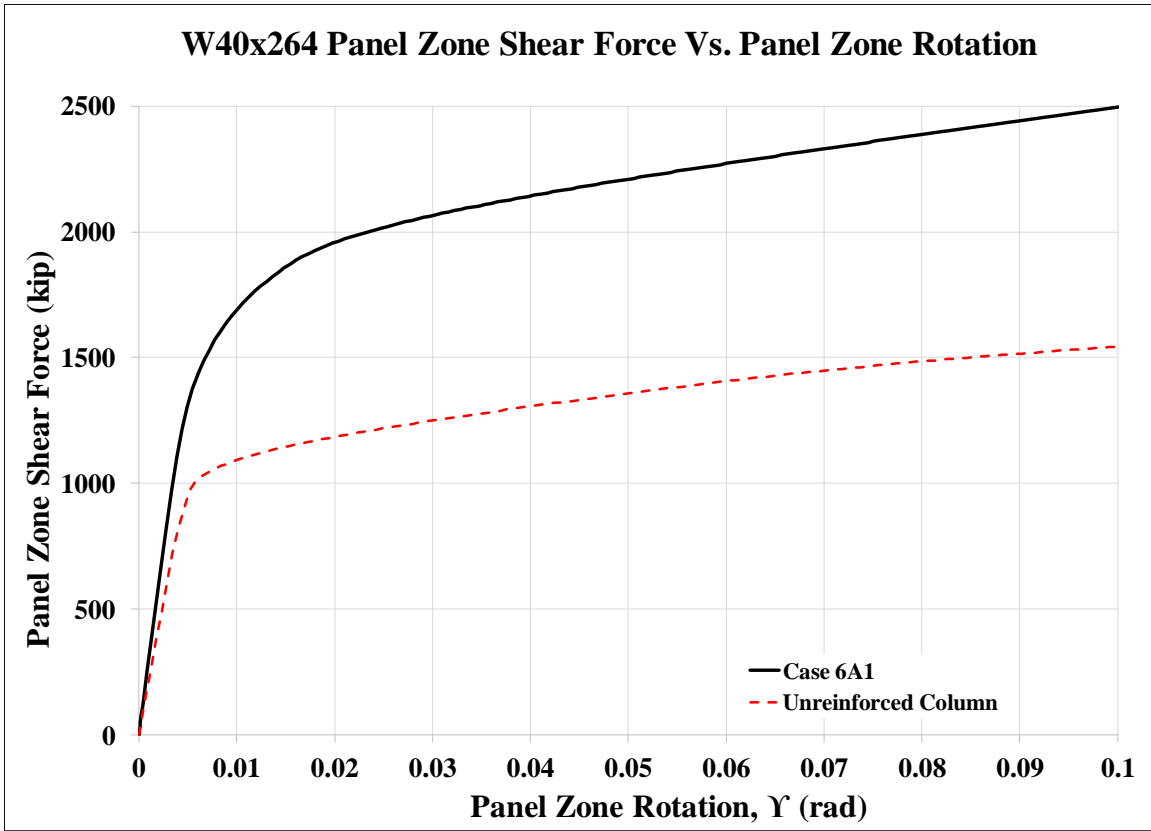


Figure 5.15: Panel zone shear vs. panel zone rotation Case 6A1

Stage	Applied Force/Loading Plate (Kip)	Panel Shear Force (Kip)	% Higher Than Unreinforced Col.	Panel Zone Rotation (rad)
1	827	1,378	142%	0.005
2	1,188	1,979	175%	0.022
3	1,178	1,963	165%	0.020
4	1,498	2,497	162%	0.100

Table 5.4: Panel zone shear and force on loading plate Case 6A1

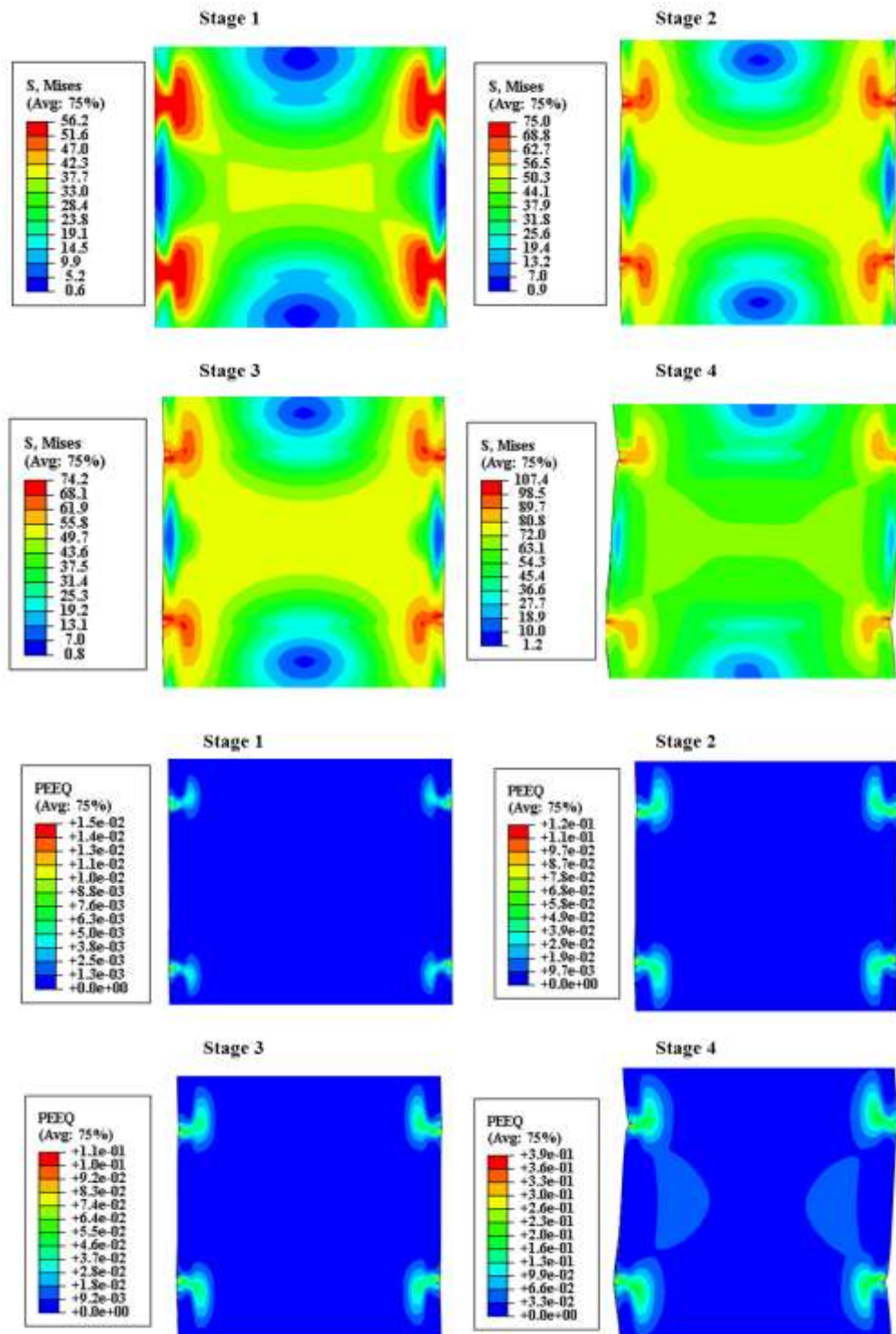


Figure 5.16: VMS and PEEQ in the column Case 6A1

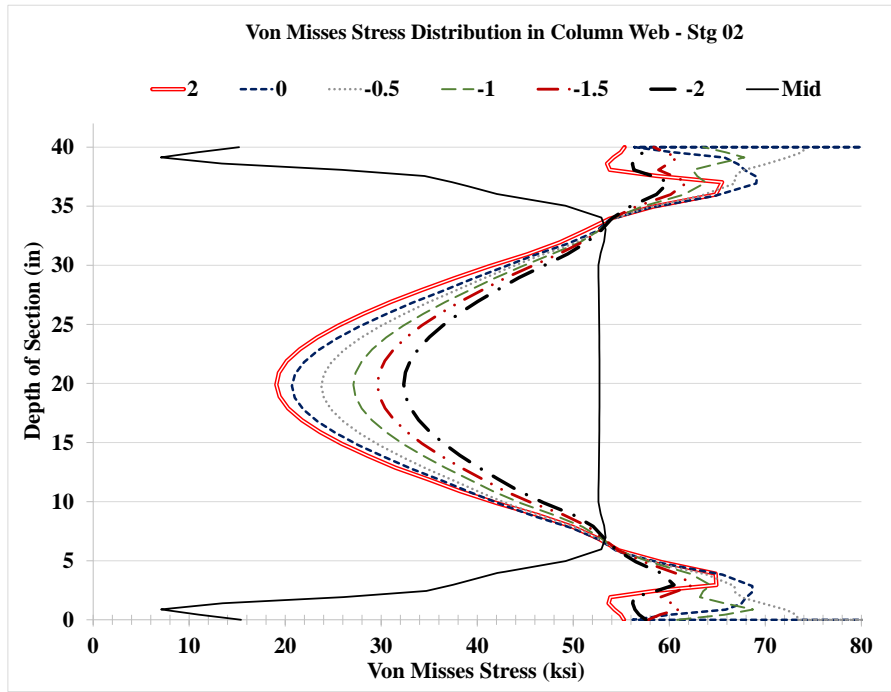
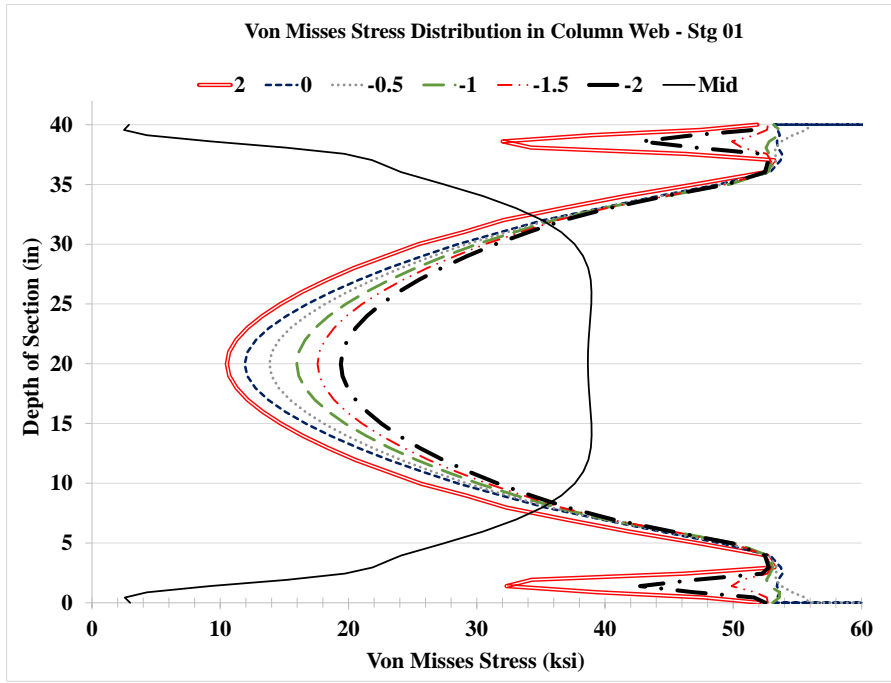


Figure 5.17: VMS distribution in column web at different heights Stg. 01-04 Case 6A1

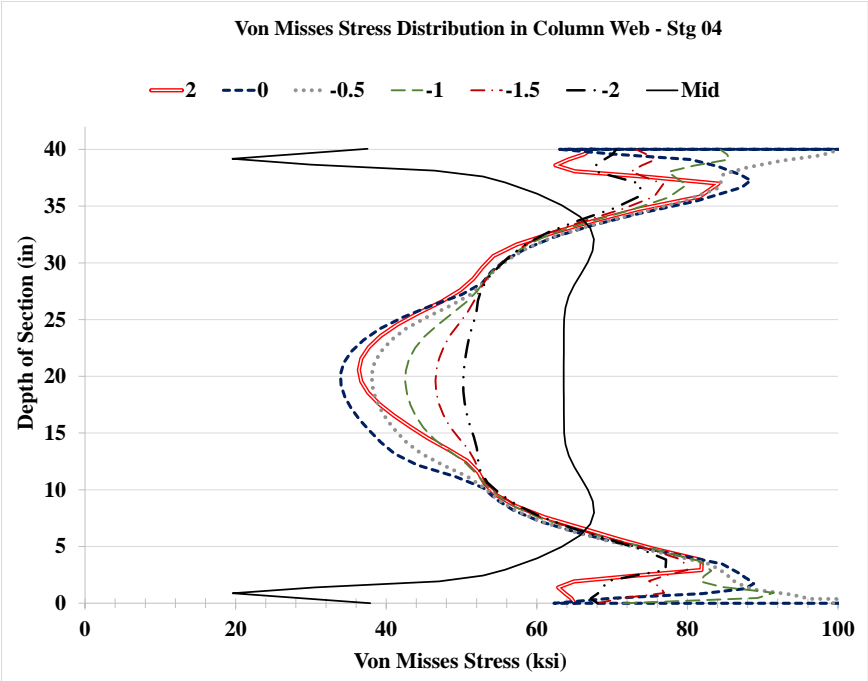
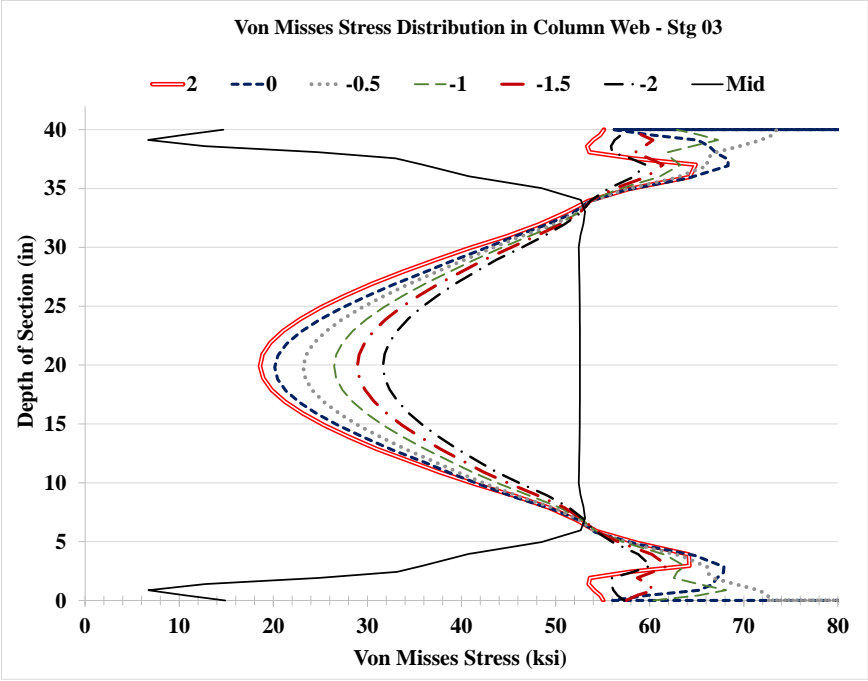


Figure 5.17: VMS distribution in column web at different heights Stg. 01-04 Case 6A1

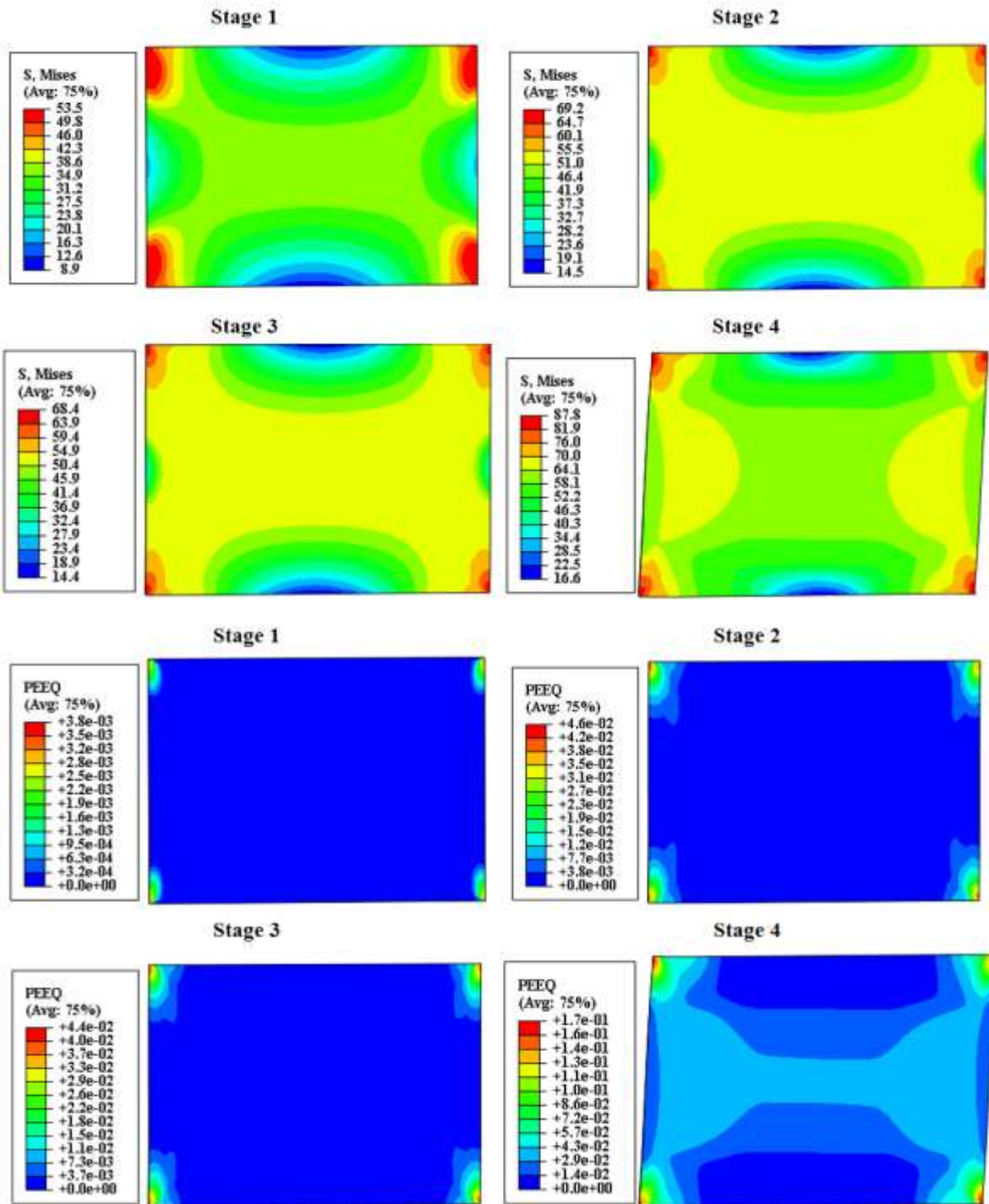


Figure 5.18: VMS and PEEQ in the DP Case 6A1

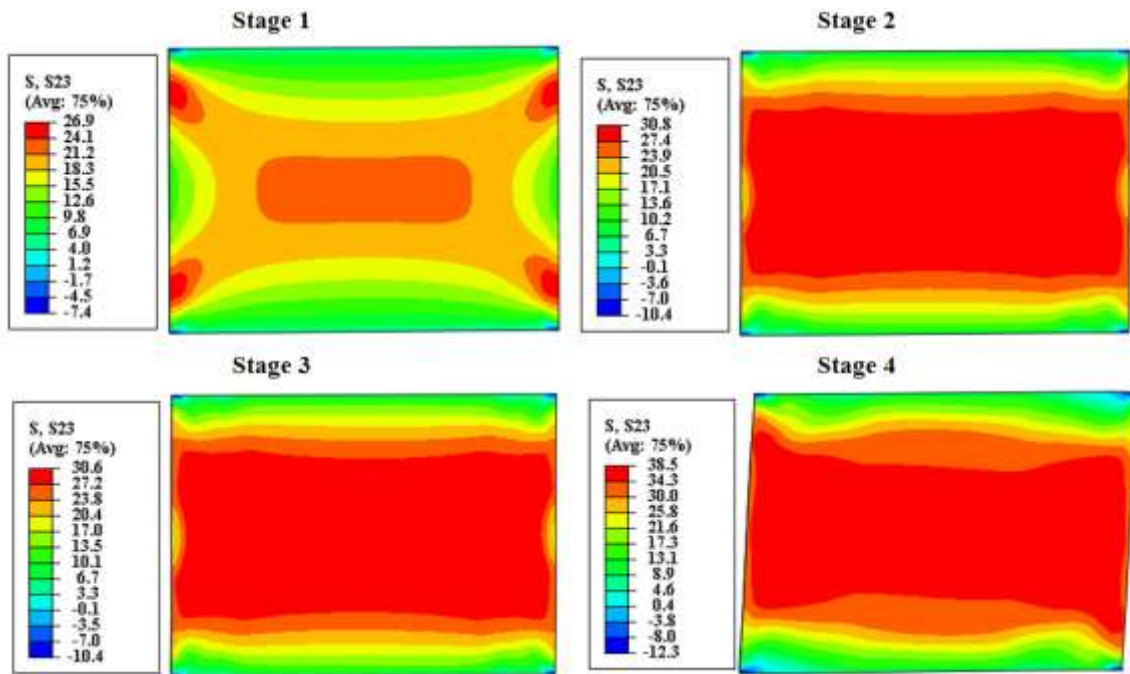


Figure 5.19: Shear stress, S<sub>23</sub> in the DP Case 6A1

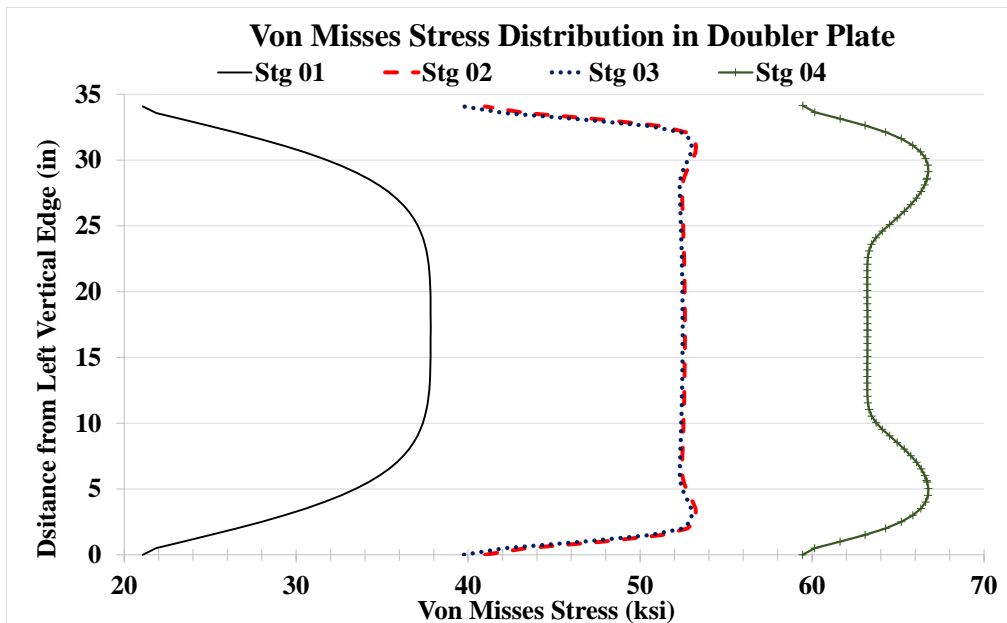


Figure 5.20: VMS distribution at mid-depth of DP Case 6A1



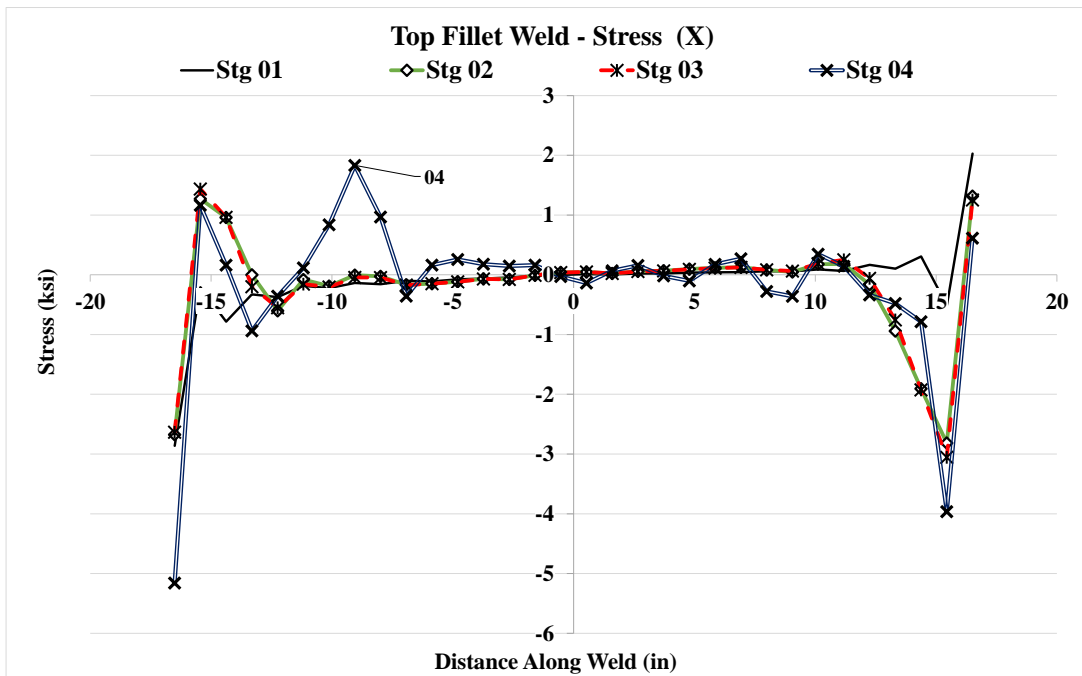
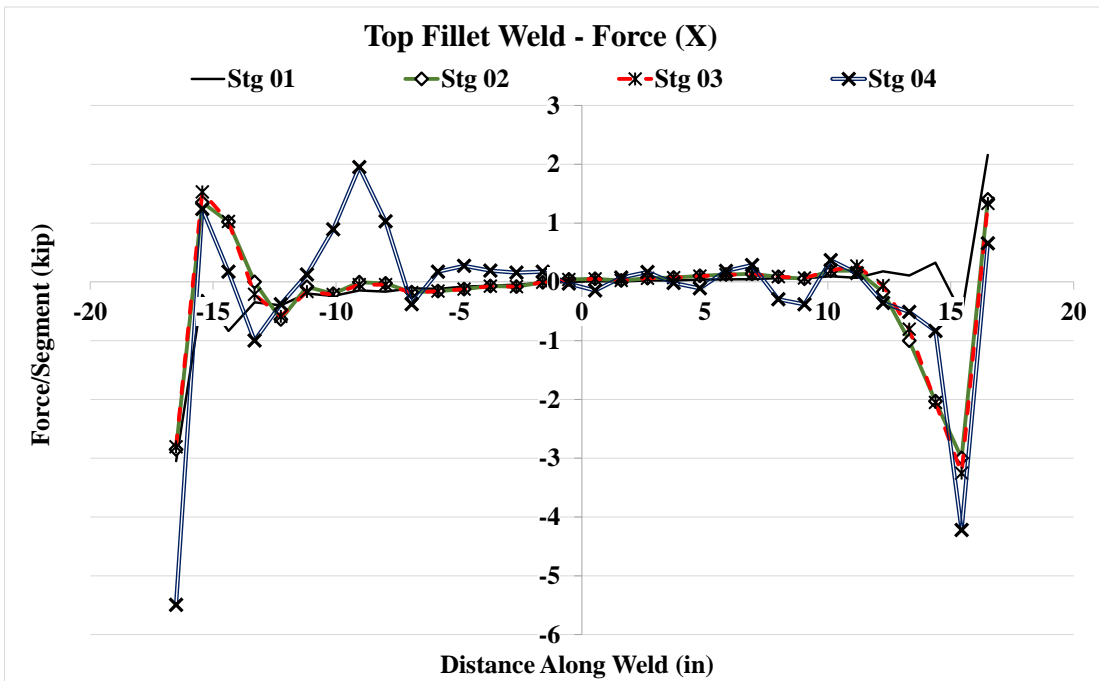


Figure 5.21: Forces and stresses in horizontal weld, (X) Case 6A1

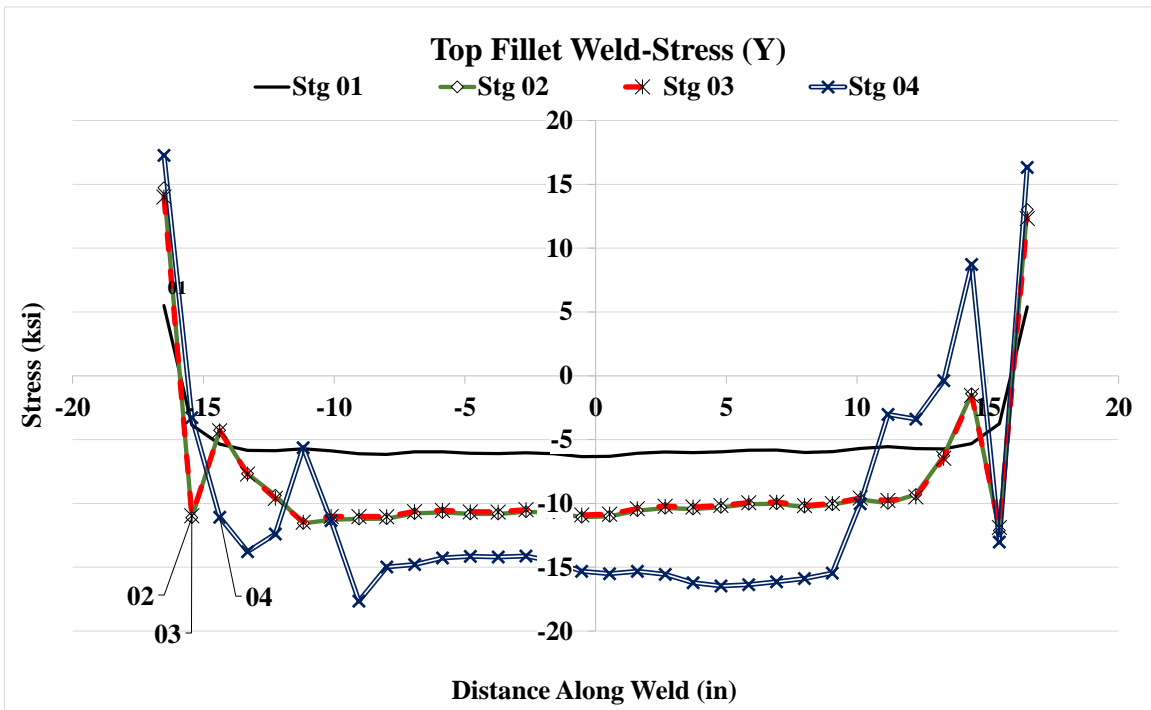
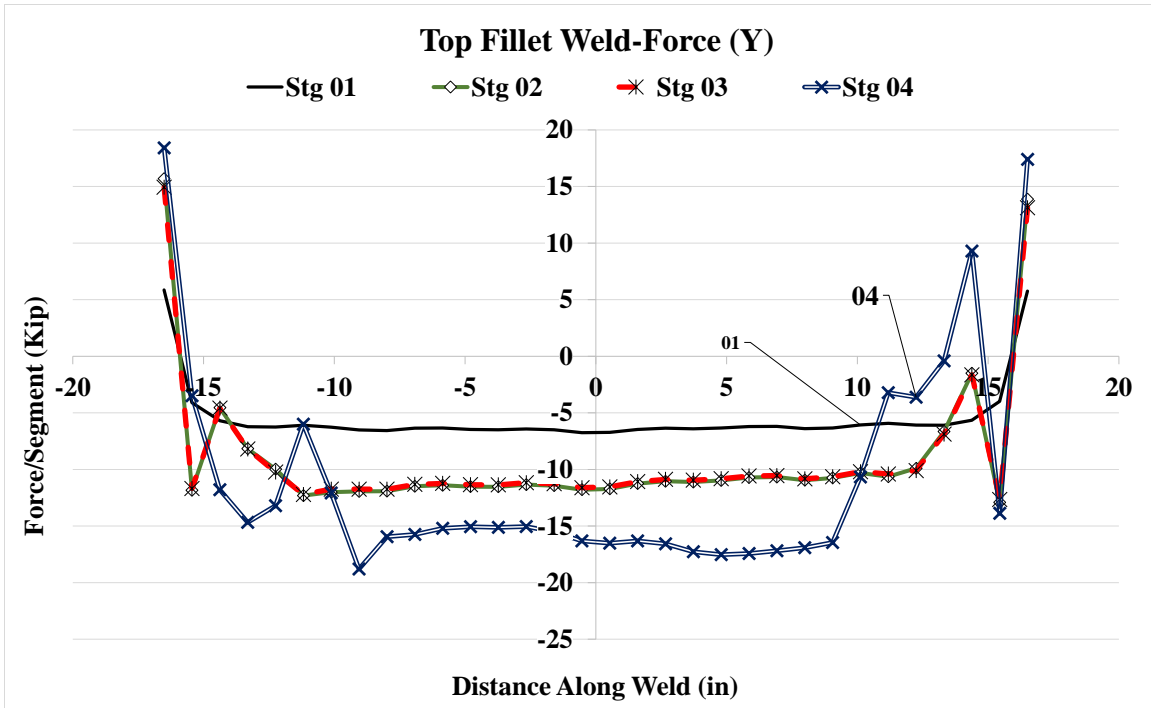


Figure 5.22: Forces and stresses in horizontal weld, (Y) Case 6A1

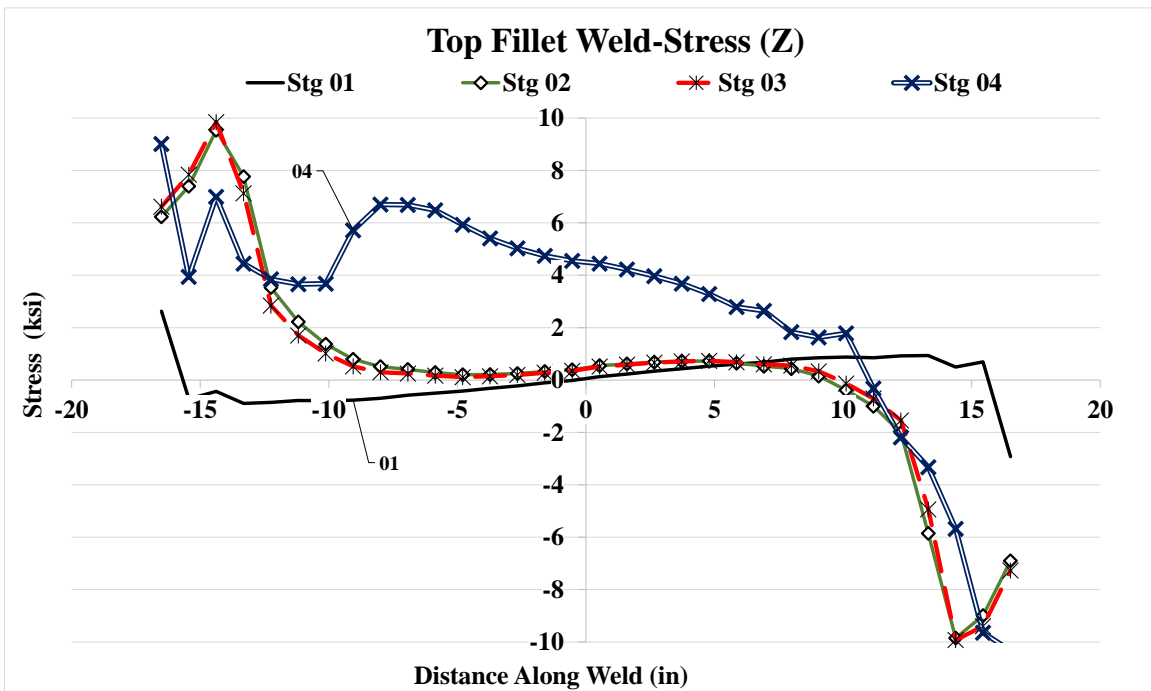
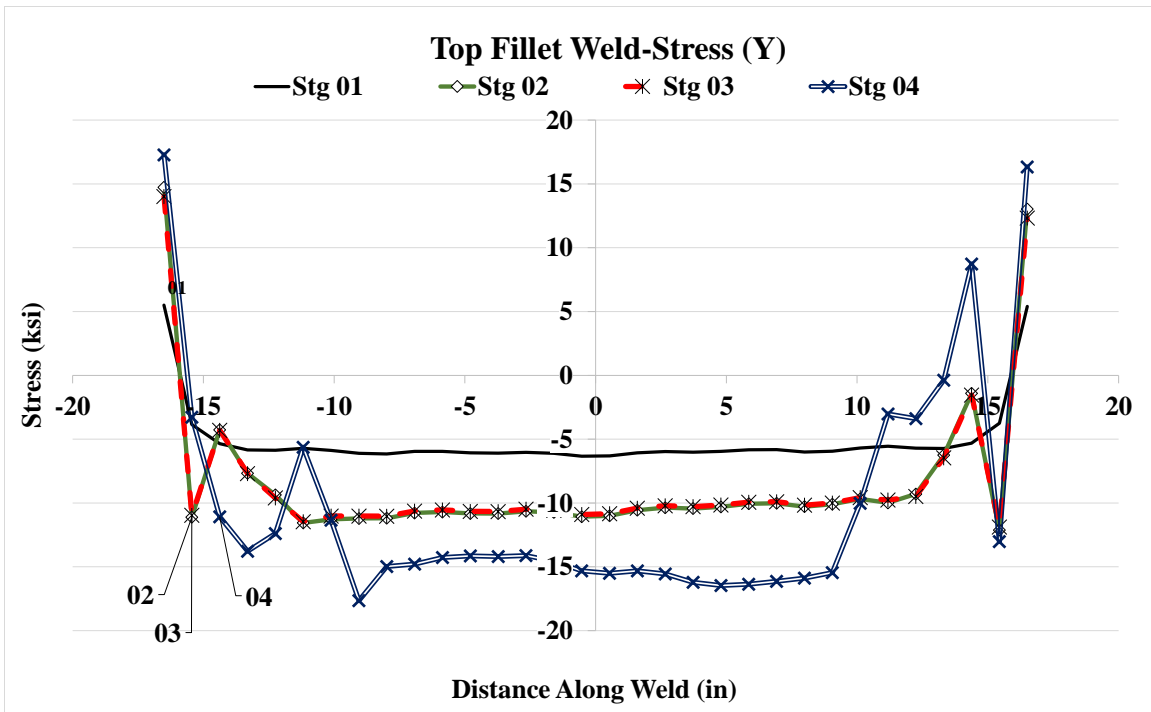


Figure 5.23: Forces and stresses in horizontal weld, (Z) Case 6A1

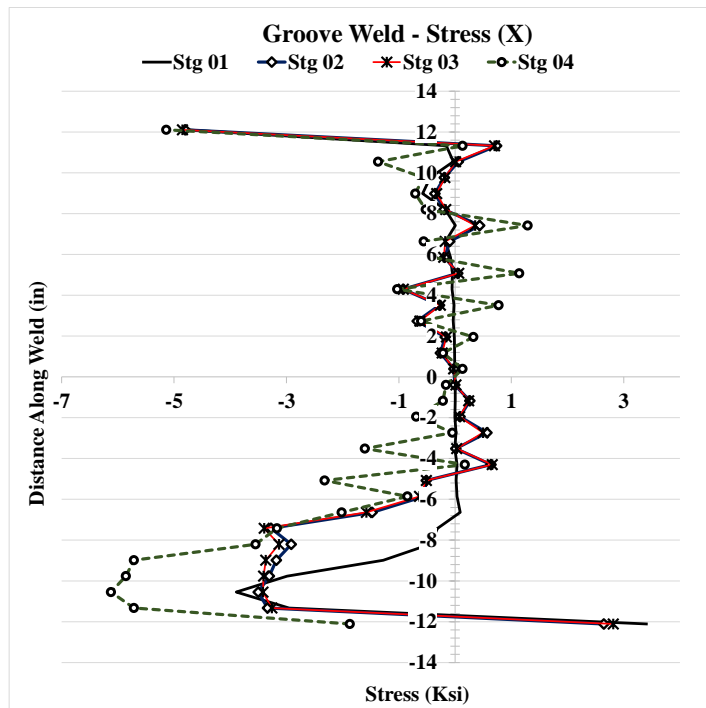
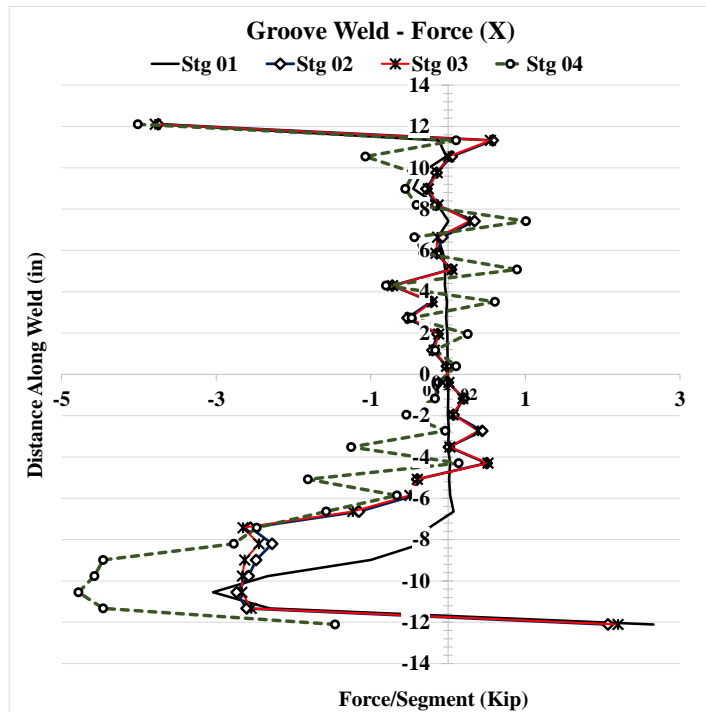


Figure 5.24: Forces and stresses in vertical weld, (X) Case 6A1

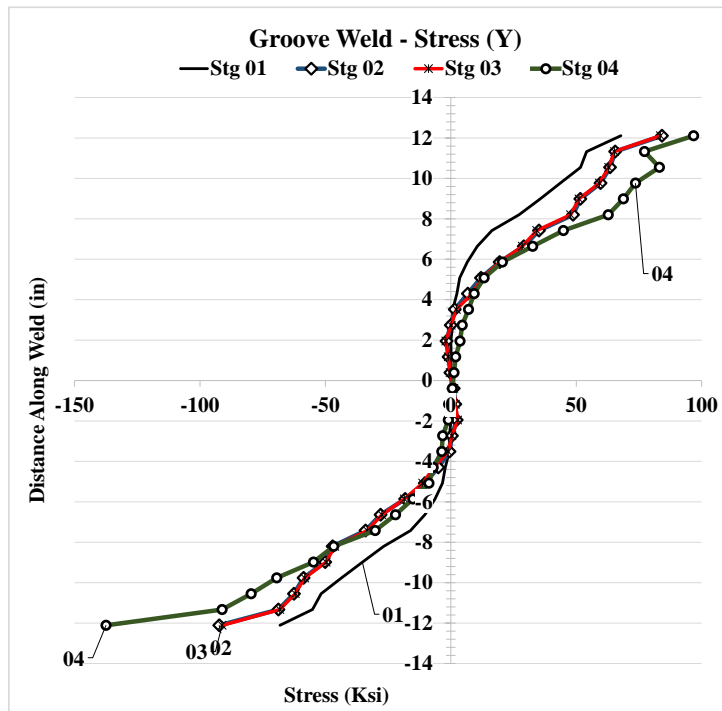
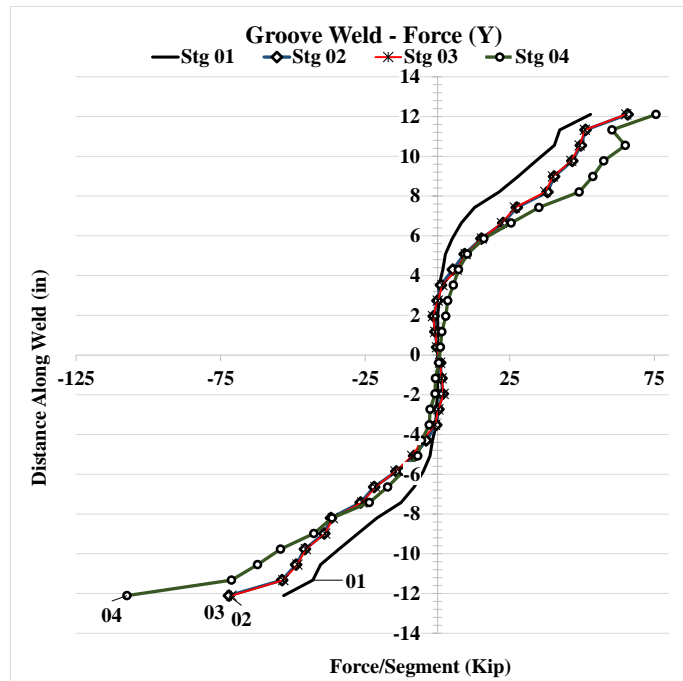


Figure 5.25: Forces and stresses in vertical weld, (Y) Case 6A1

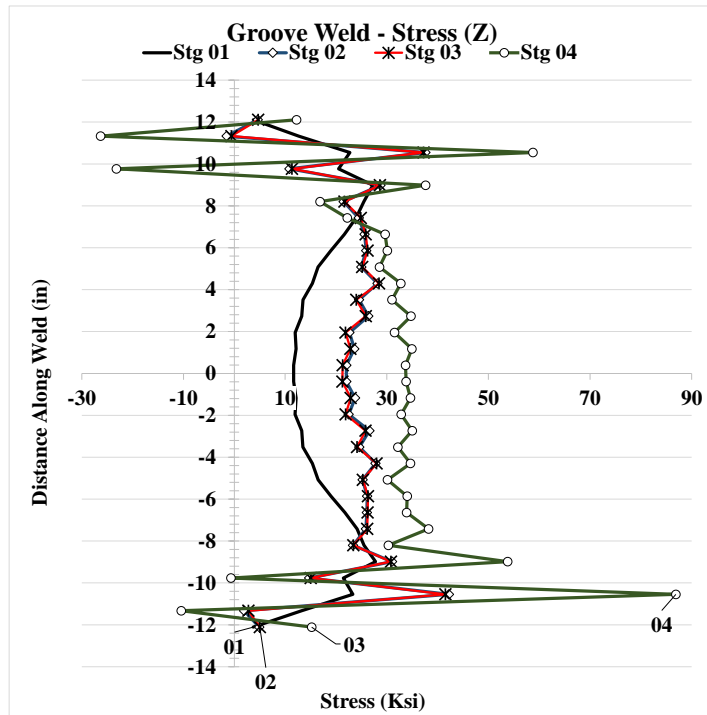
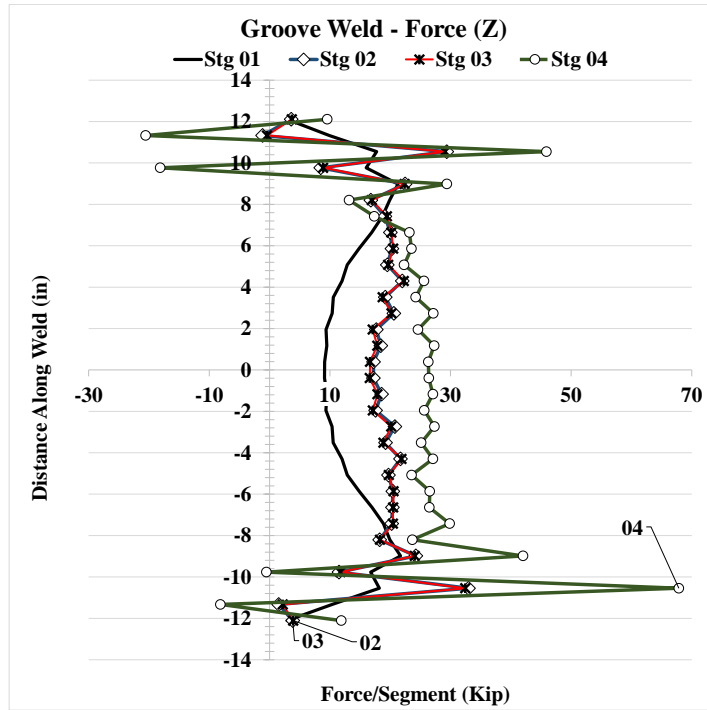


Figure 5.26: Forces and stresses in vertical weld, (Z) Case 6A1

### 5.2.4 Analysis Case 6C

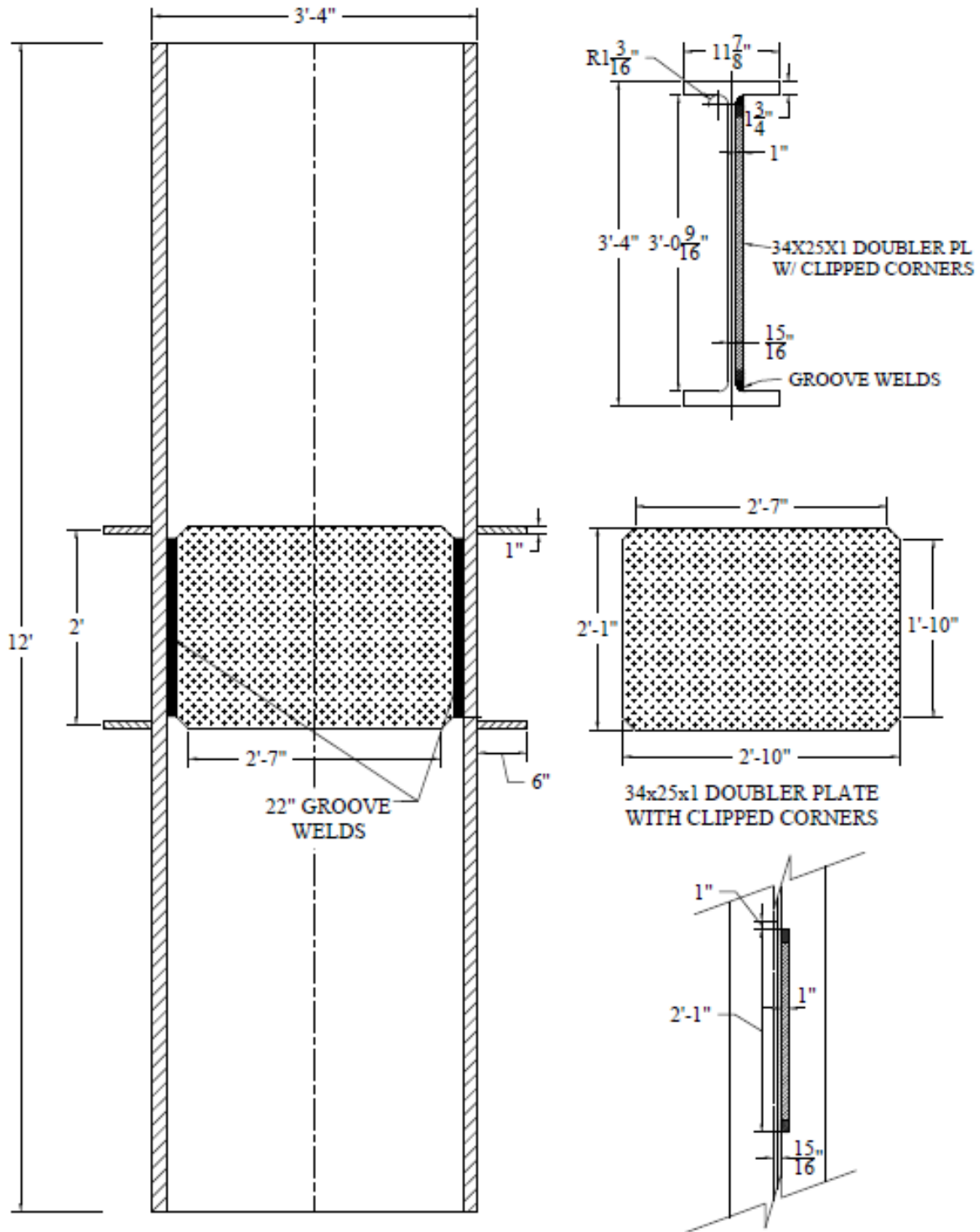


Figure 5.27: W40x264 Analysis case 6C

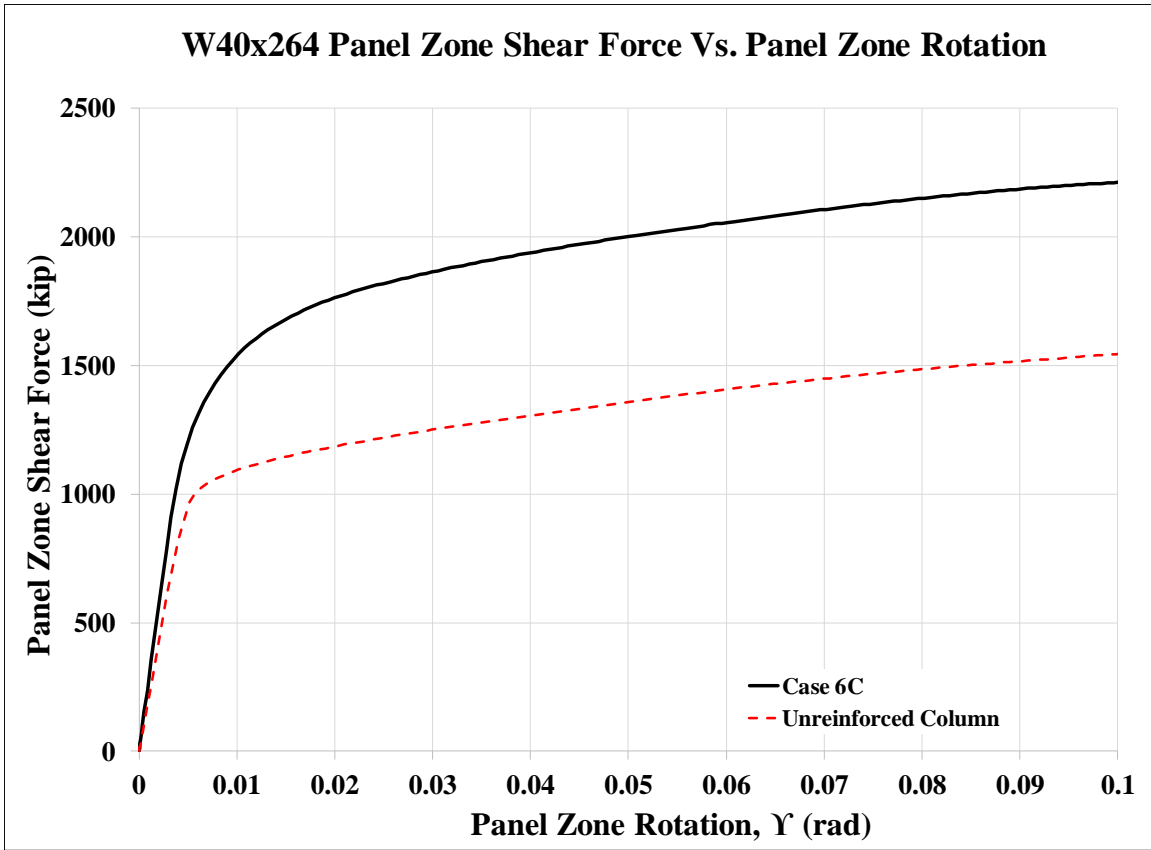


Figure 5.28: Panel zone shear vs. panel zone rotation Case 6C

Stage	Applied Force/Loading Plate (Kip)	Panel Shear Force (Kip)	% Higher Than Unreinforced Col.	Panel Zone Rotation (rad)
1	717	1,195	123%	0.005
2	1,052	1,753	155%	0.019
3	1,062	1,770	149%	0.021
4	1,327	2,211	143%	0.100

Table 5.5: Panel zone shear and force on loading plate Case 6C



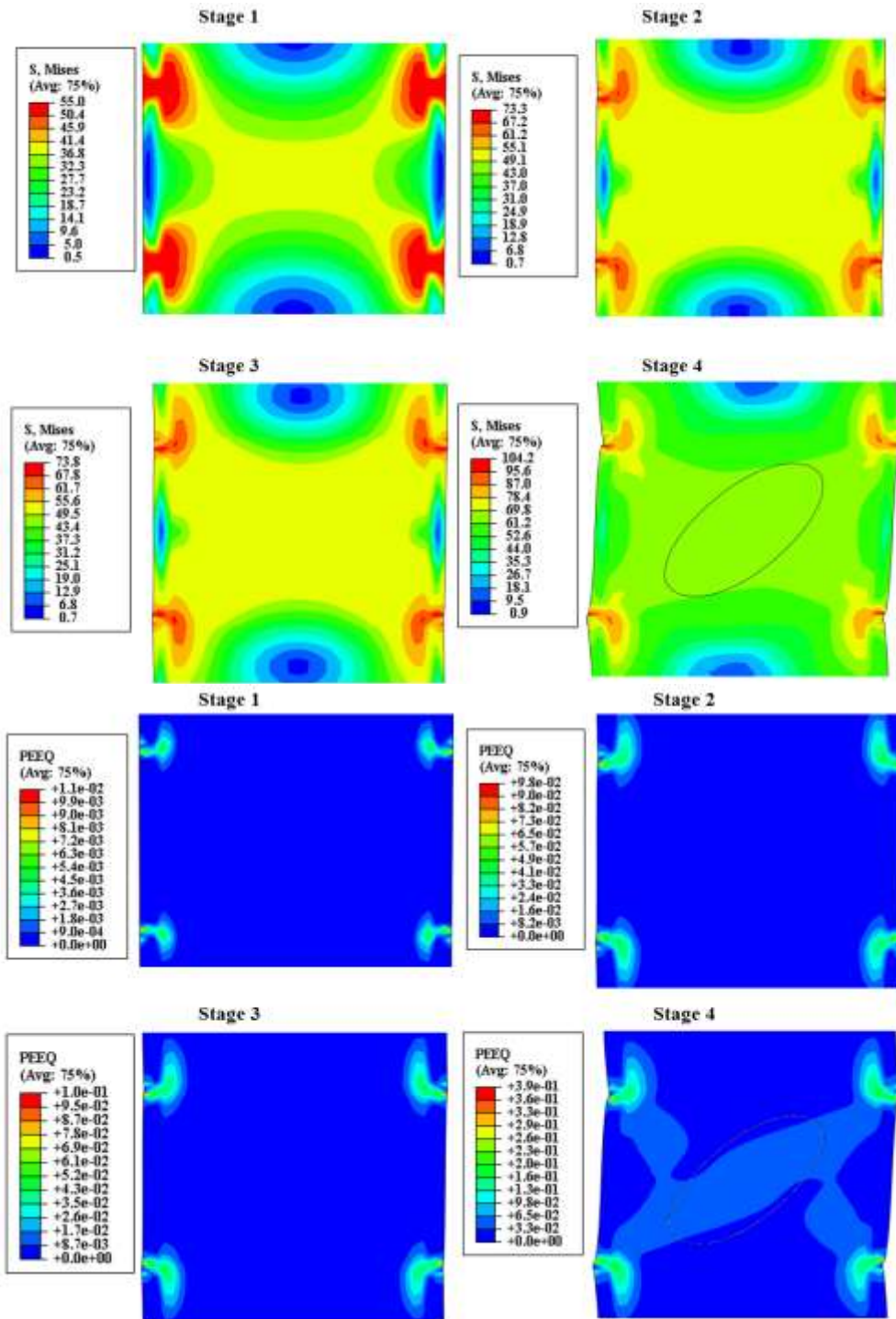


Figure 5.29: VMS and PEEQ in the column Case 6C

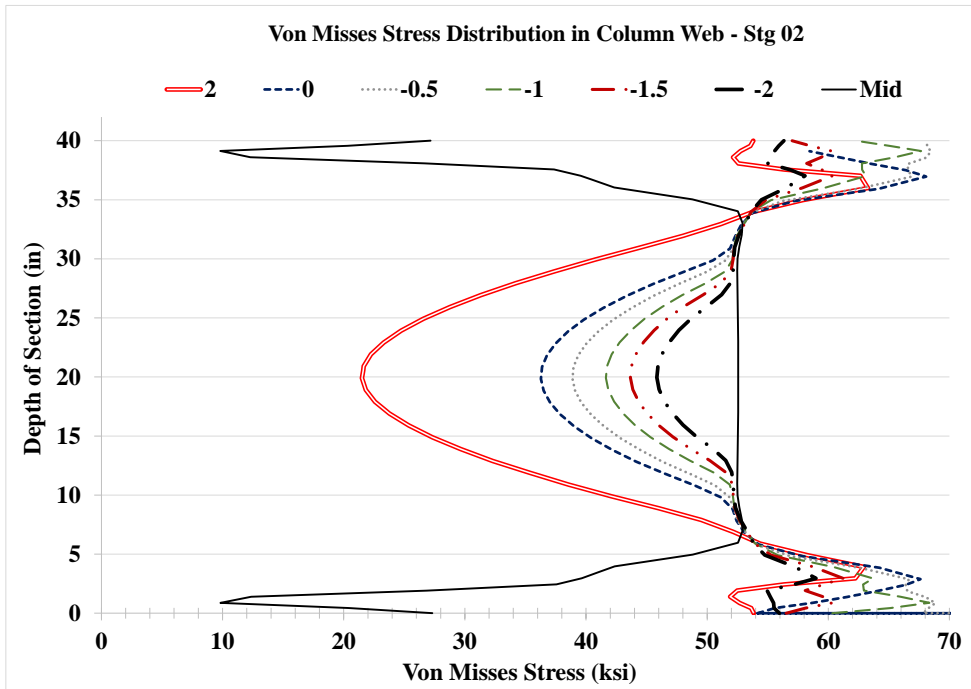
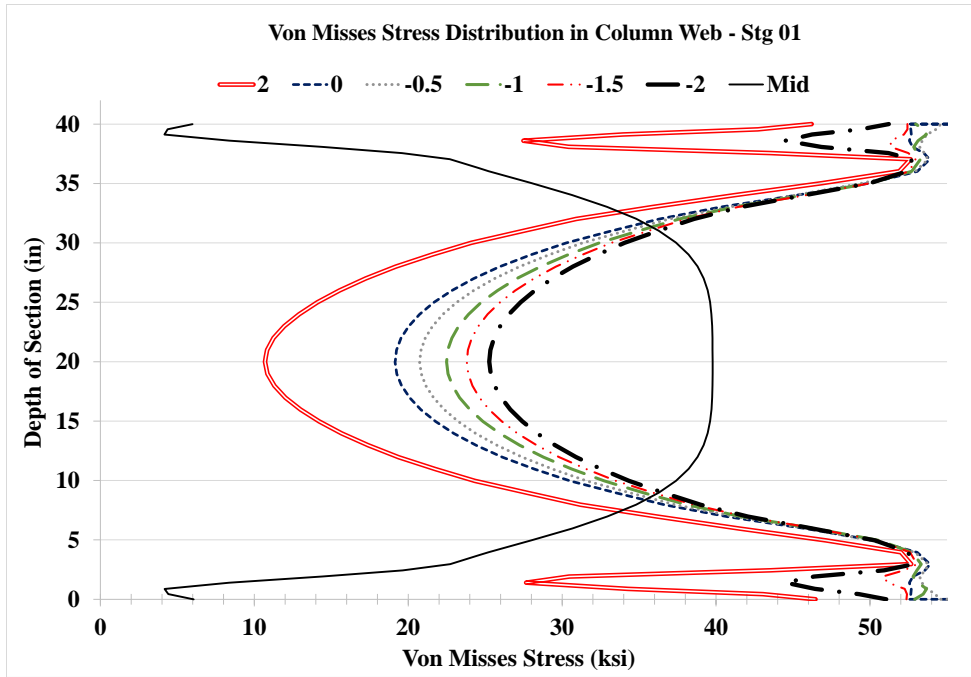


Figure 5.30: VMS distribution in column web at different heights Stg. 01-04 Case 6C

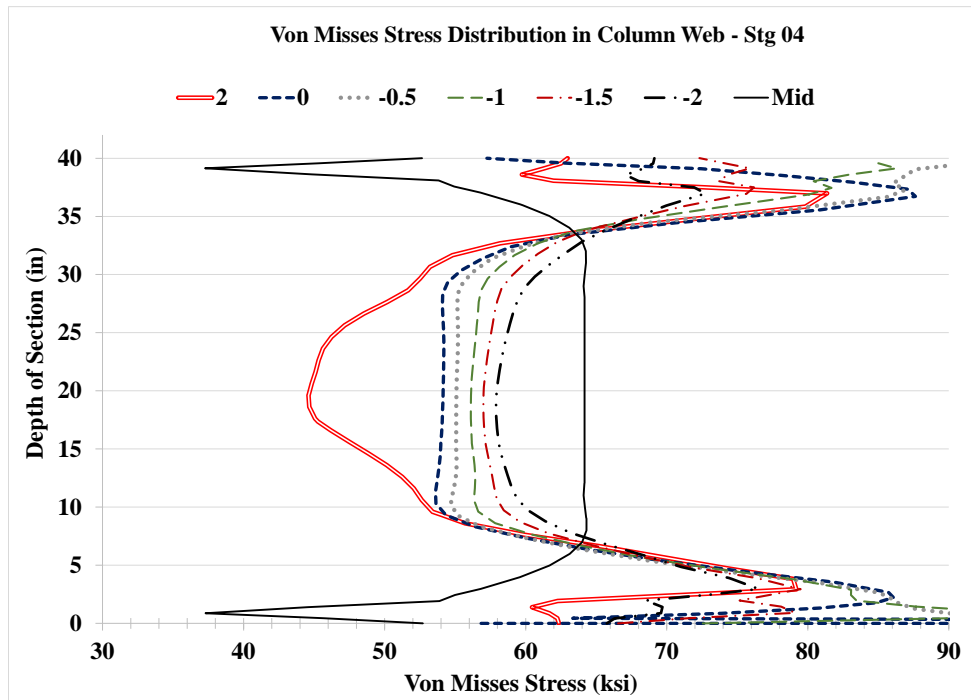
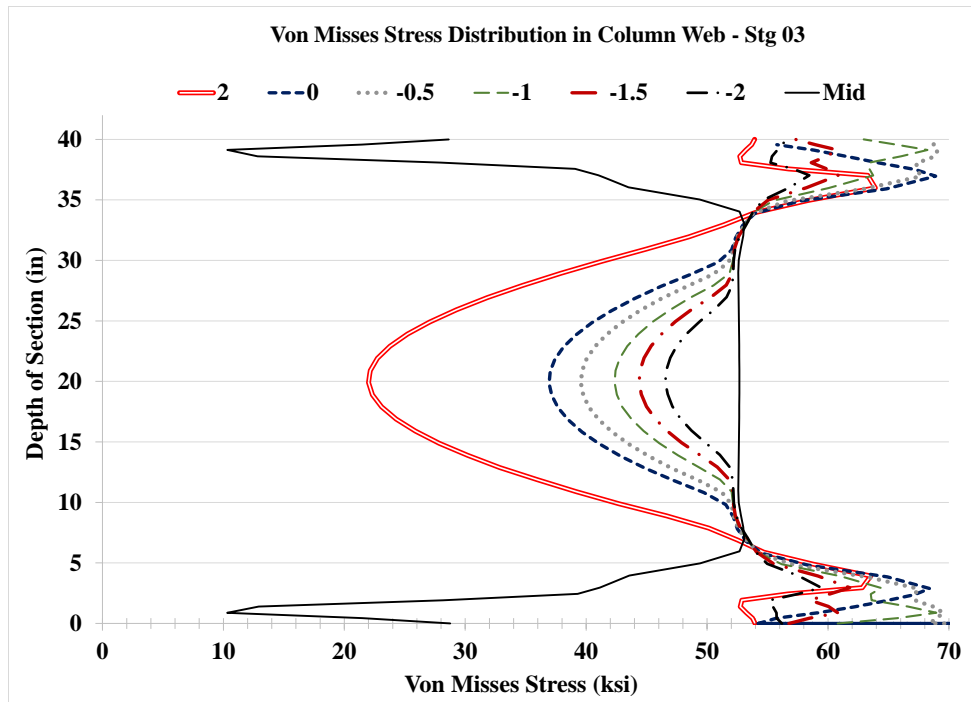


Figure 5.30: VMS distribution in column web at different heights Stg. 01-04 Case 6C

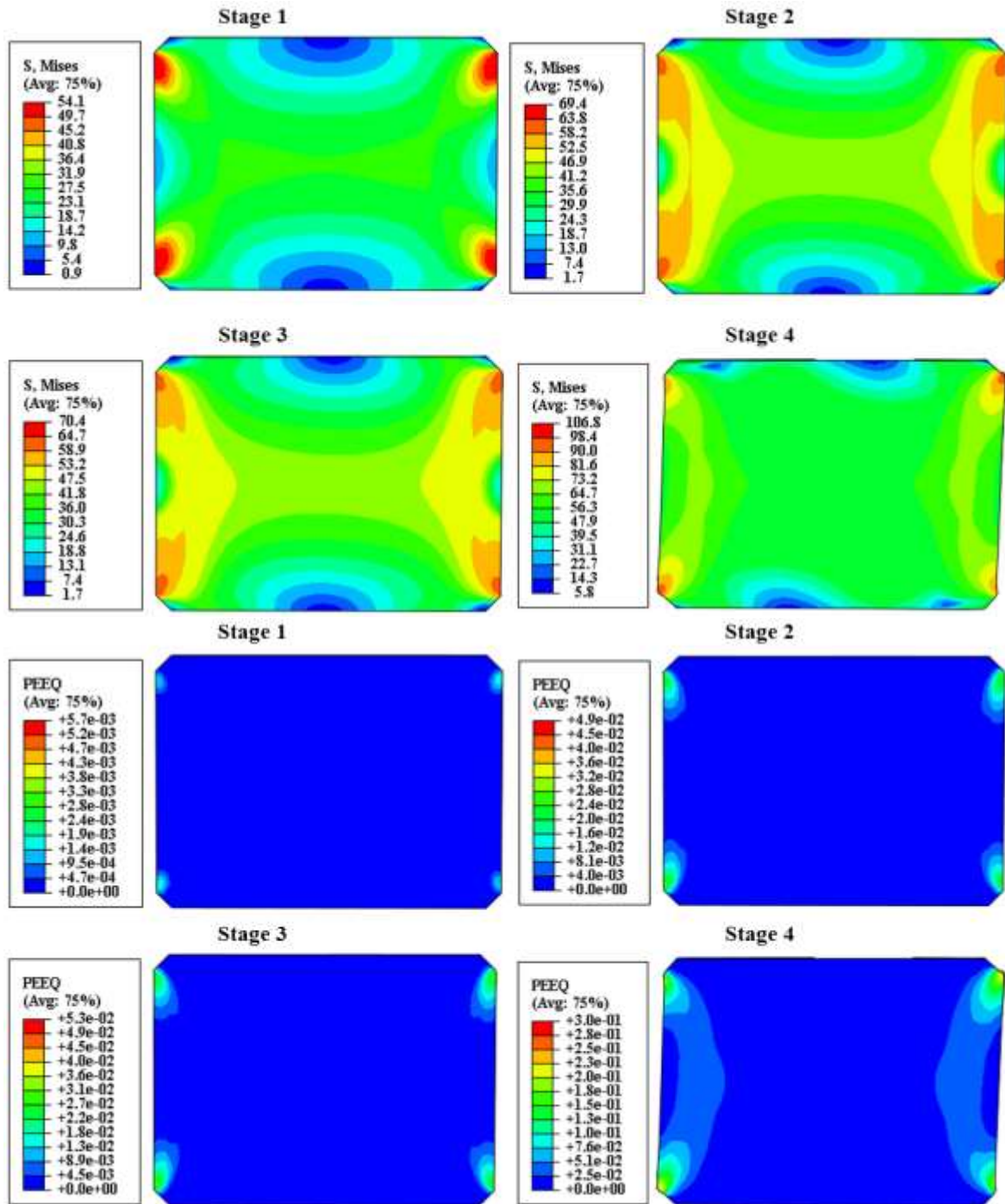


Figure 5.31: VMS and PEEQ in the DP Case 6C

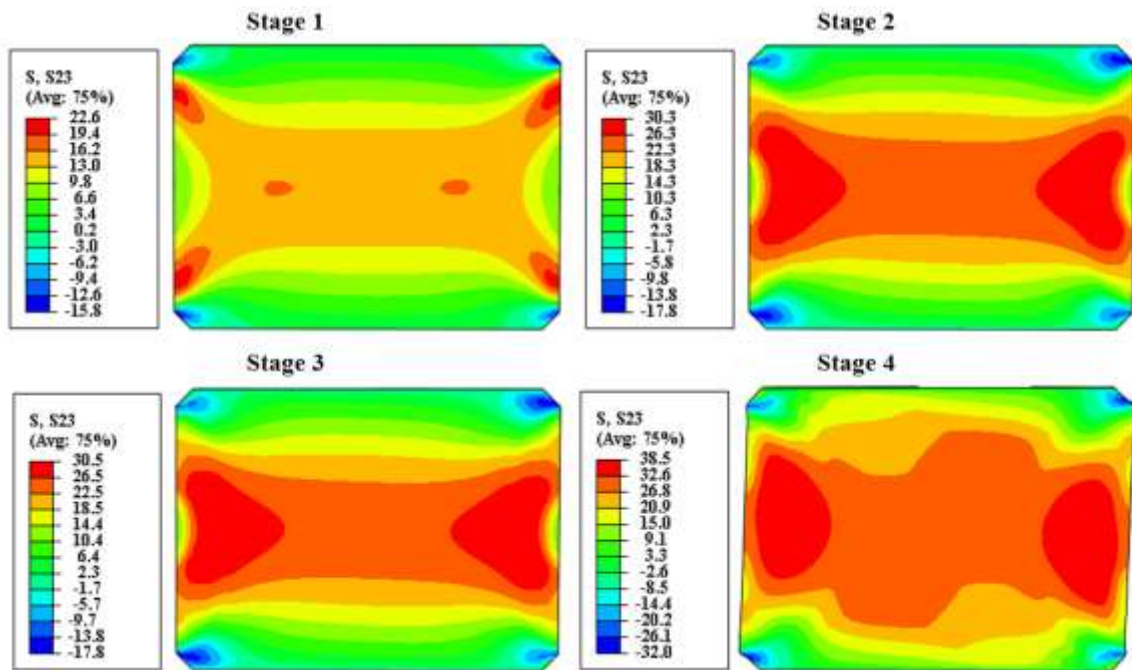


Figure 5.32: Shear stress, S23 in the DP Case 6C

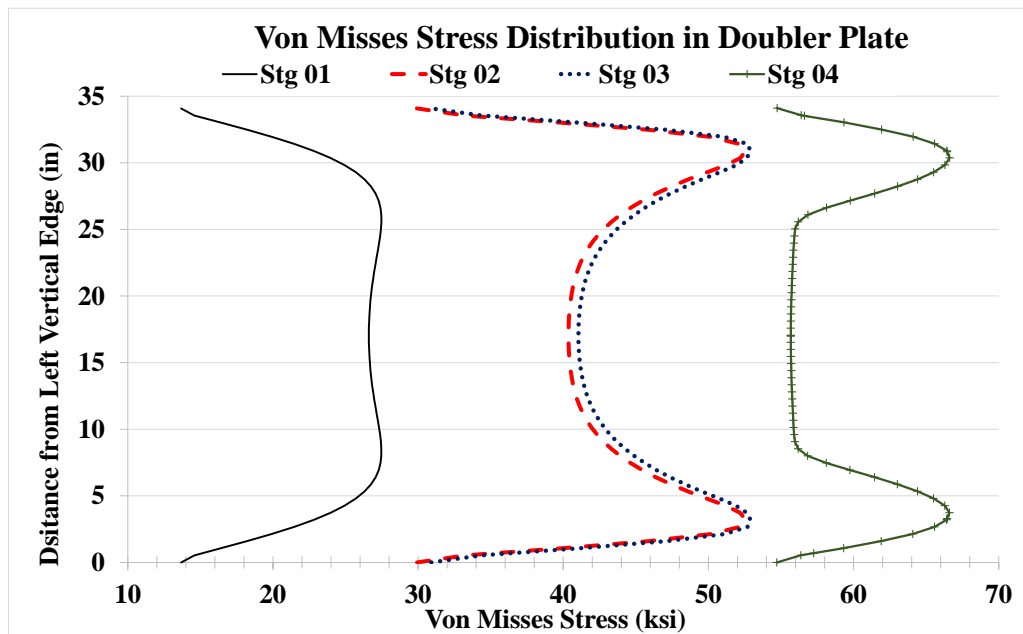


Figure 5.33: VMS distribution at mid-depth of DP Case 6C

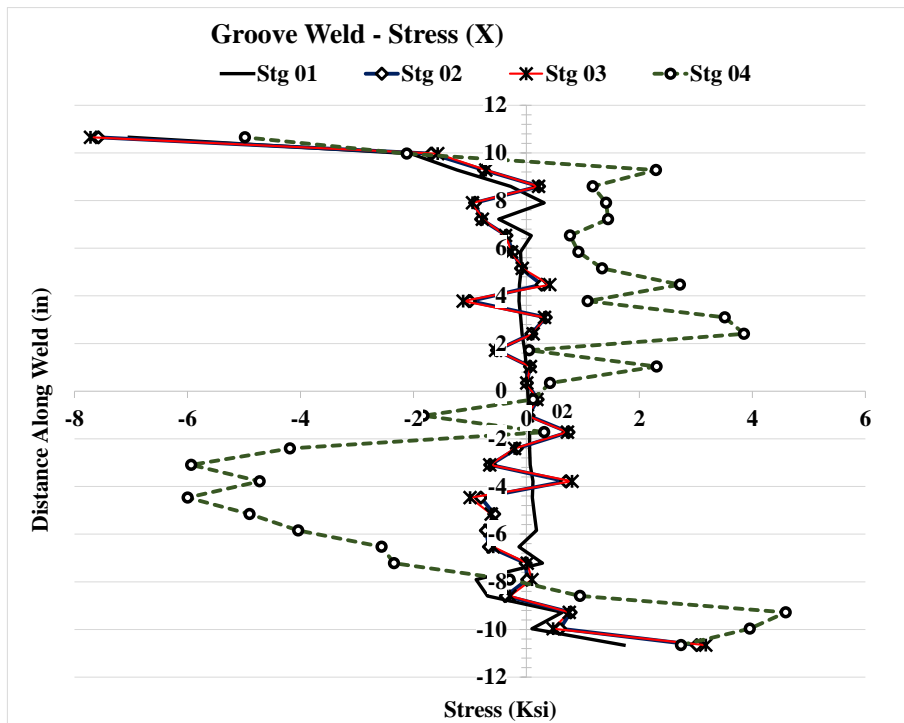
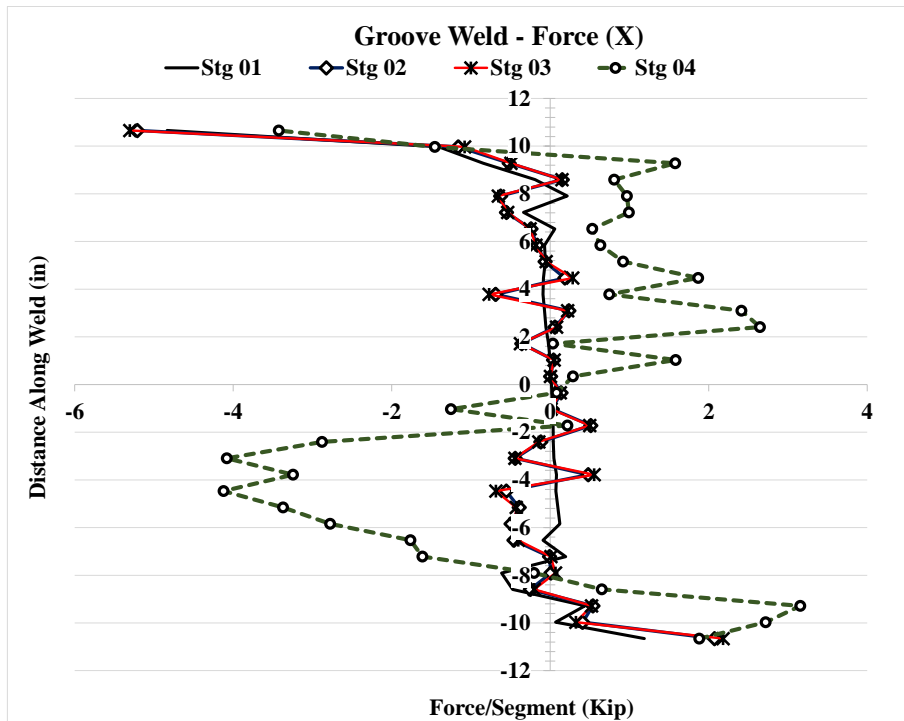


Figure 5.34: Forces and stresses in vertical weld, (X) Case 6C

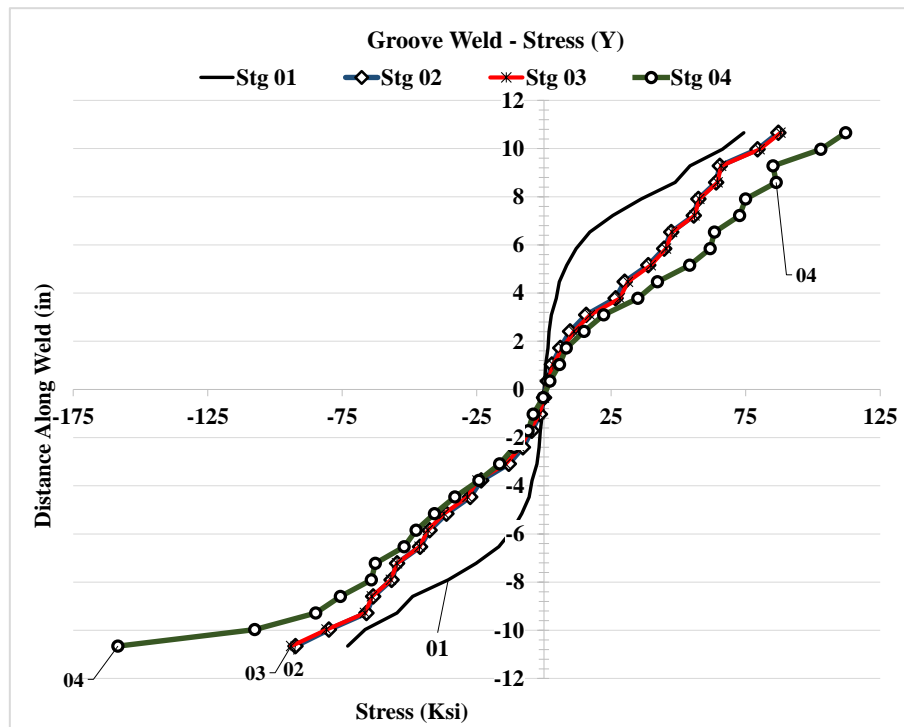
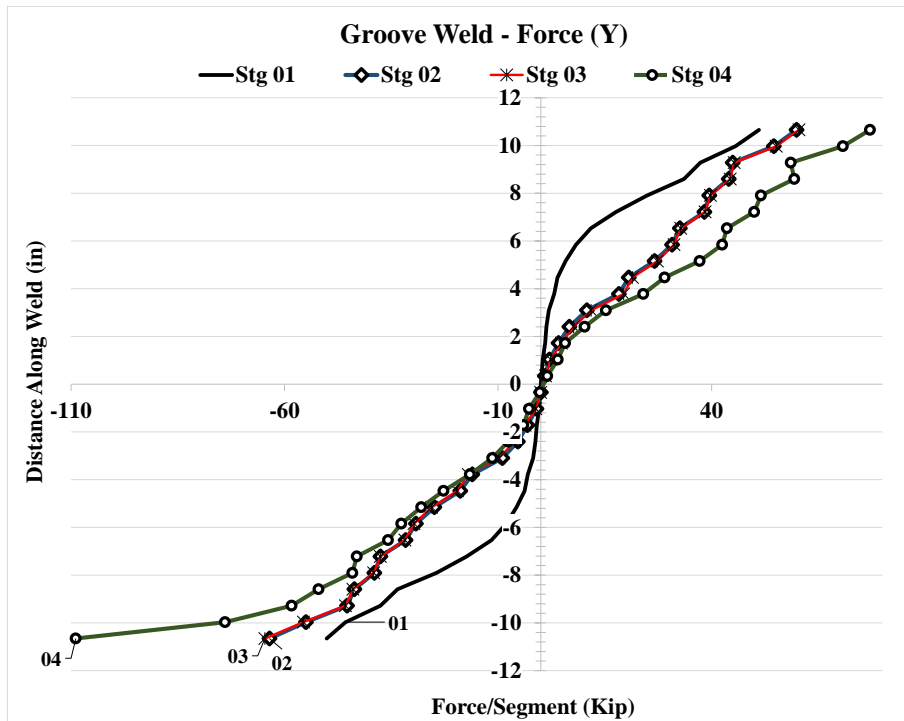


Figure 5.35: Forces and stresses in vertical weld, (Y) Case 6C

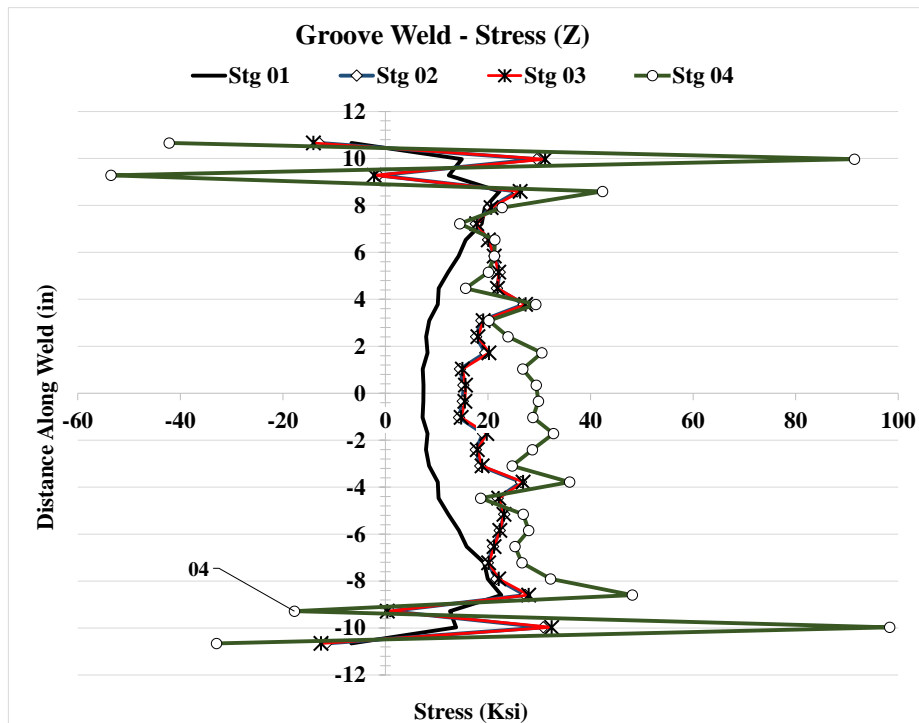
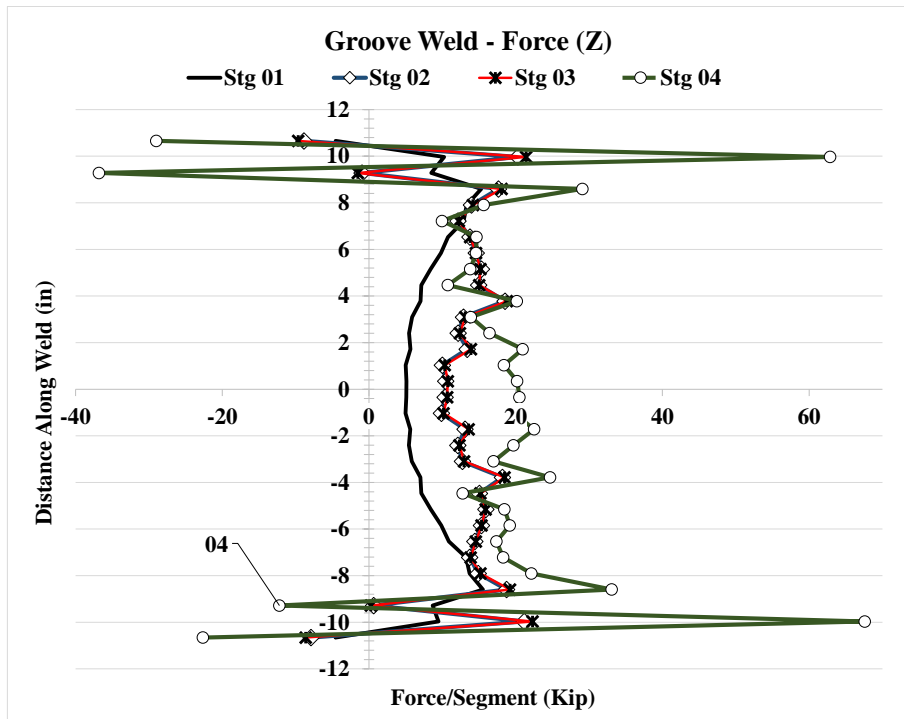


Figure 5.36: Forces and stresses in vertical weld, (Z) Case 6C



### 5.2.5 Analysis Case 6C1

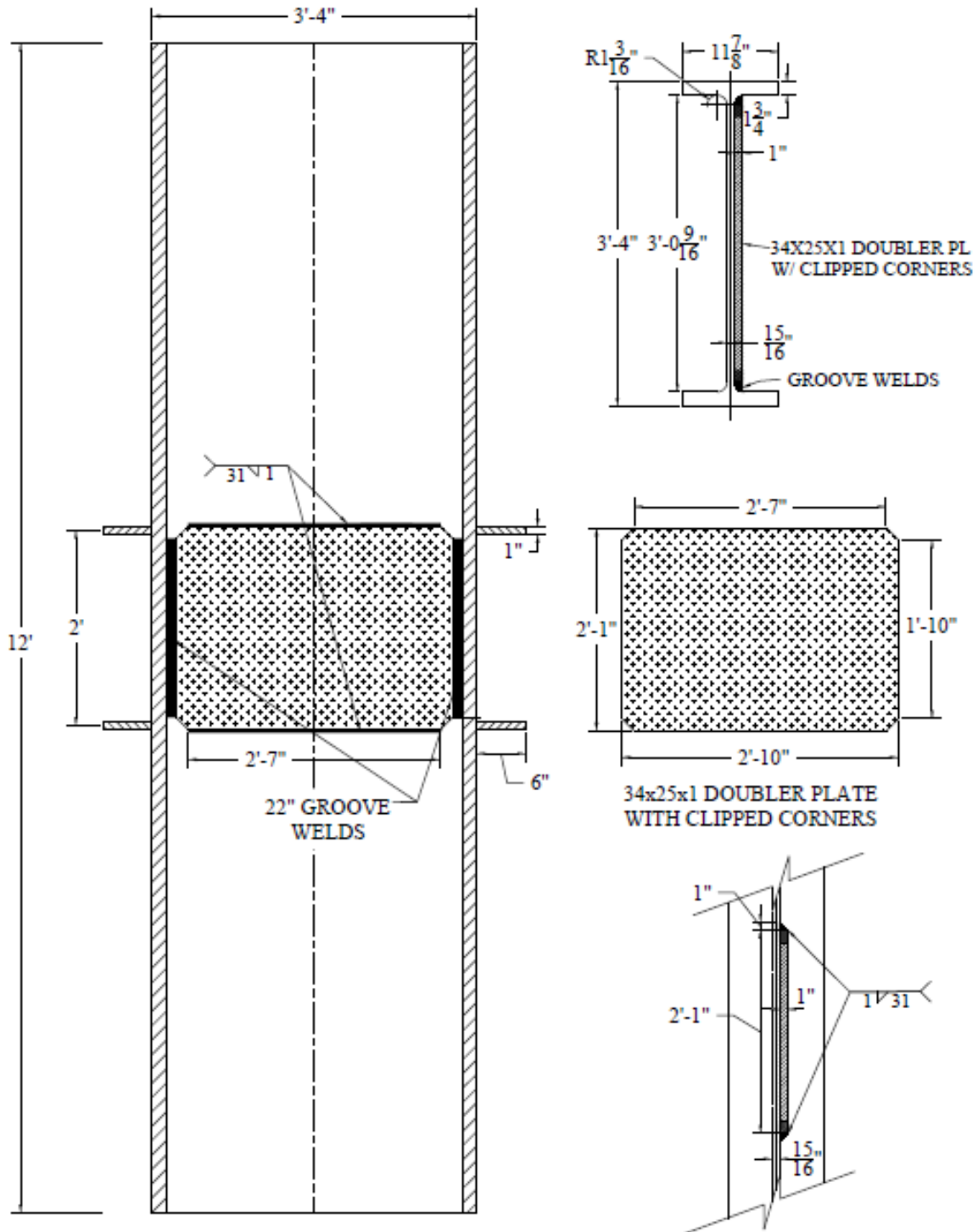


Figure 5.37: W40x264 Analysis case 6C1

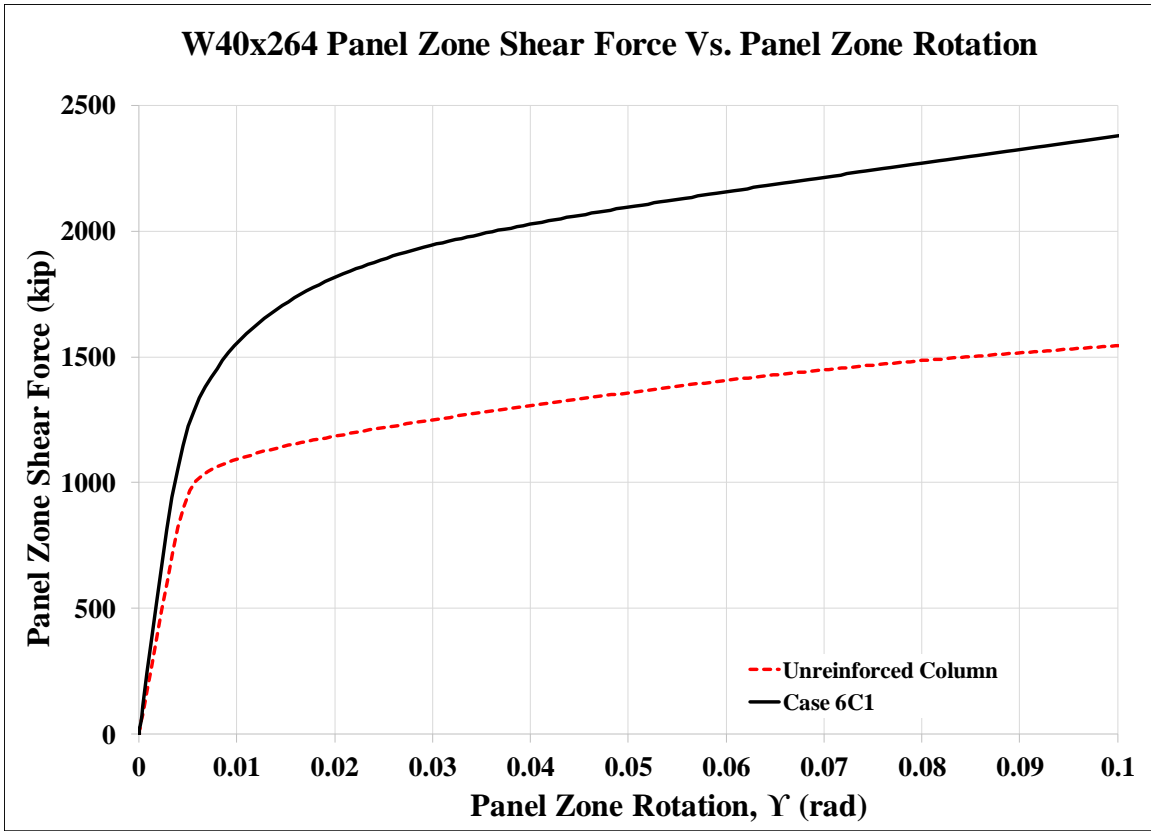


Figure 5.38: Panel zone shear vs. panel zone rotation Case 6C1

Stage	Applied Force/Loading Plate (Kip)	Panel Shear Force (Kip)	% Higher Than Unreinforced Col.	Panel Zone Rotation (rad)
1	771	1,285	132%	0.006
2	1,136	1,893	167%	0.025
3	1,092	1,820	153%	0.020
4	1,427	2,378	154%	0.100

Table 5.6: Panel zone shear and force on loading plate Case 6C1

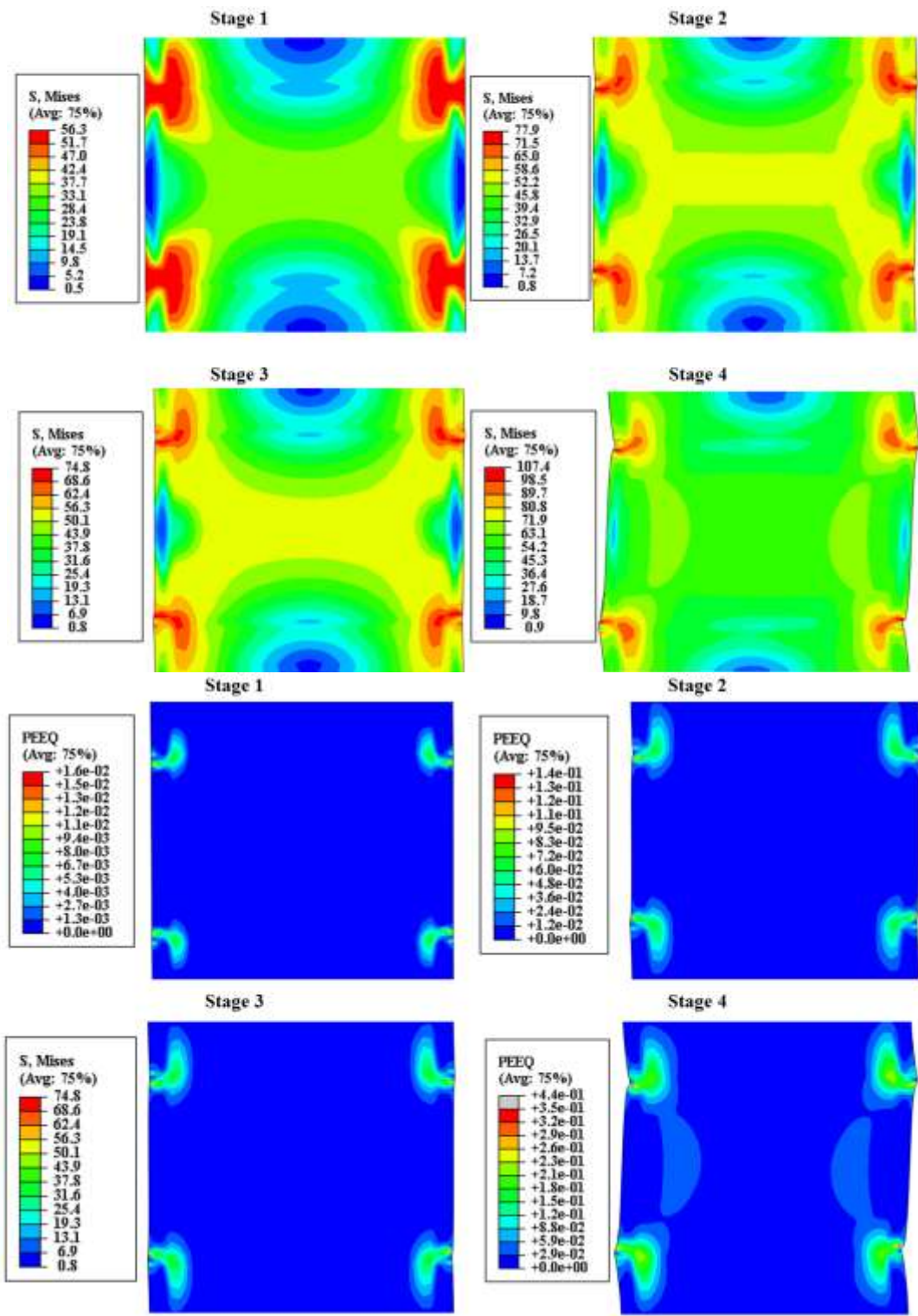


Figure 5.39: VMS and PEEQ in the column Case 6C1  
354

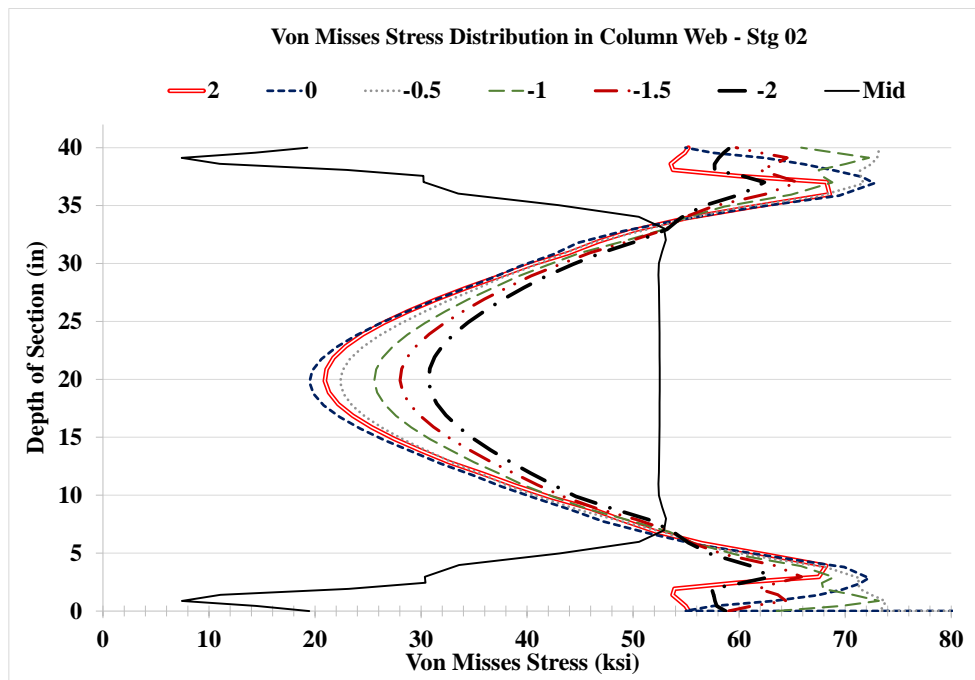
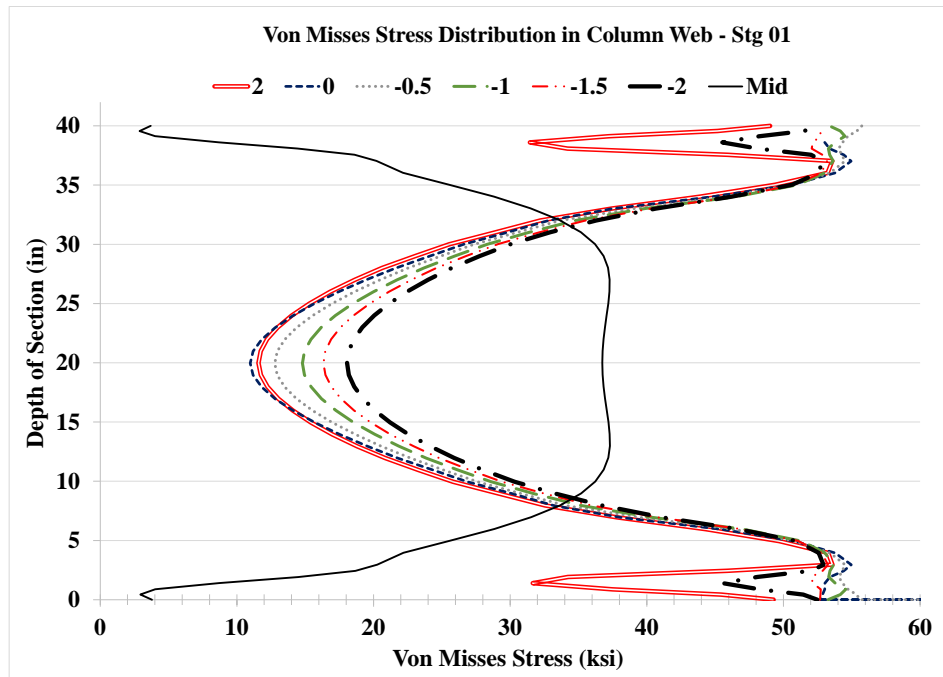


Figure 5.40: VMS distribution in column web at different heights Stg. 01-04 Case 6C1

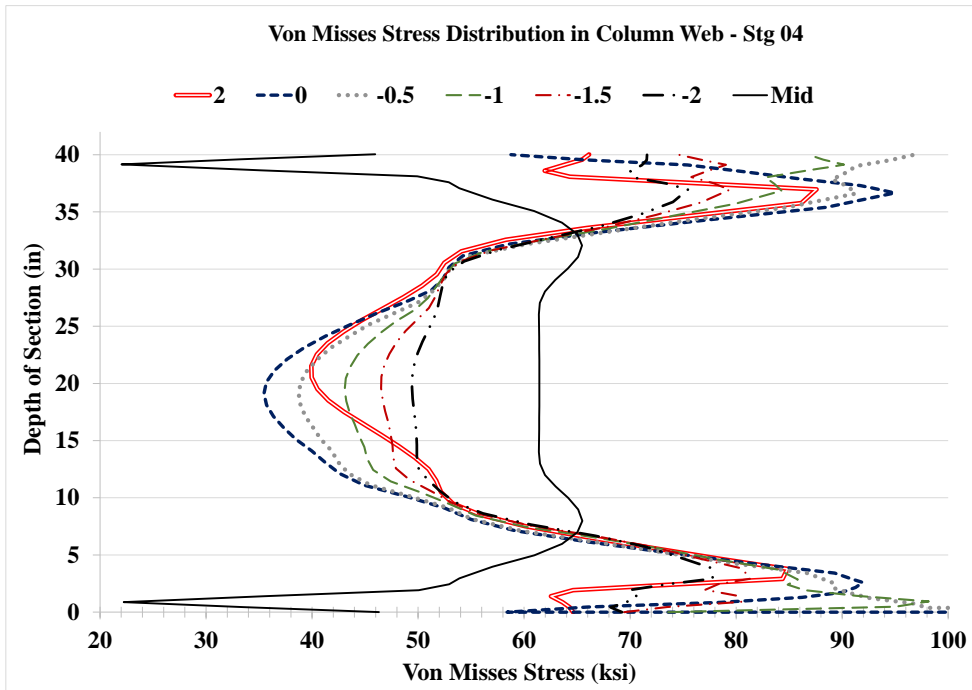
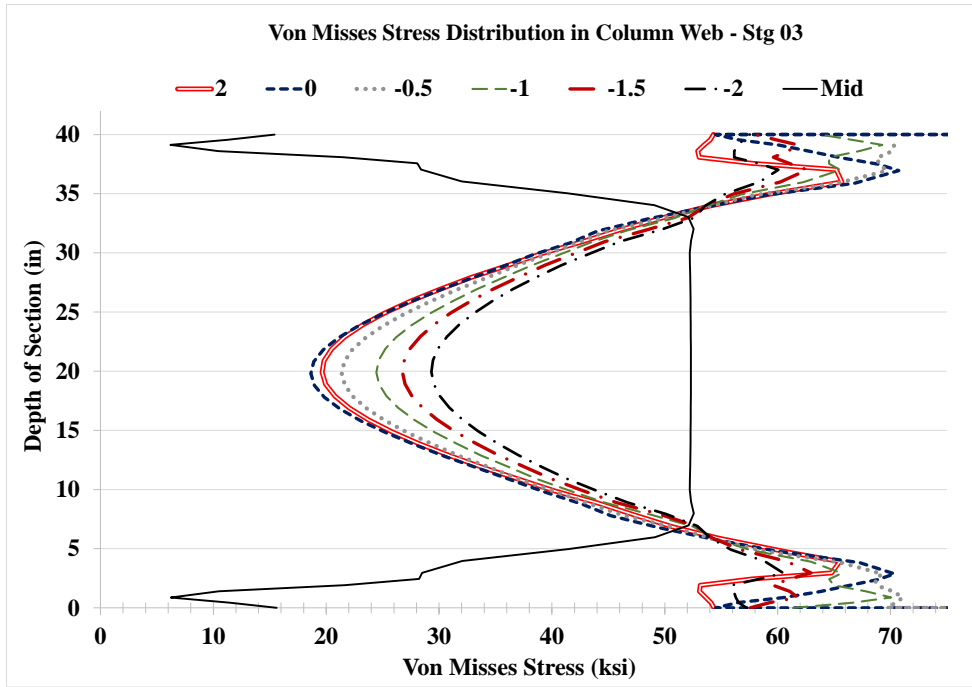


Figure 5.40: VMS distribution in column web at different heights Stg. 01-04 Case 6C1

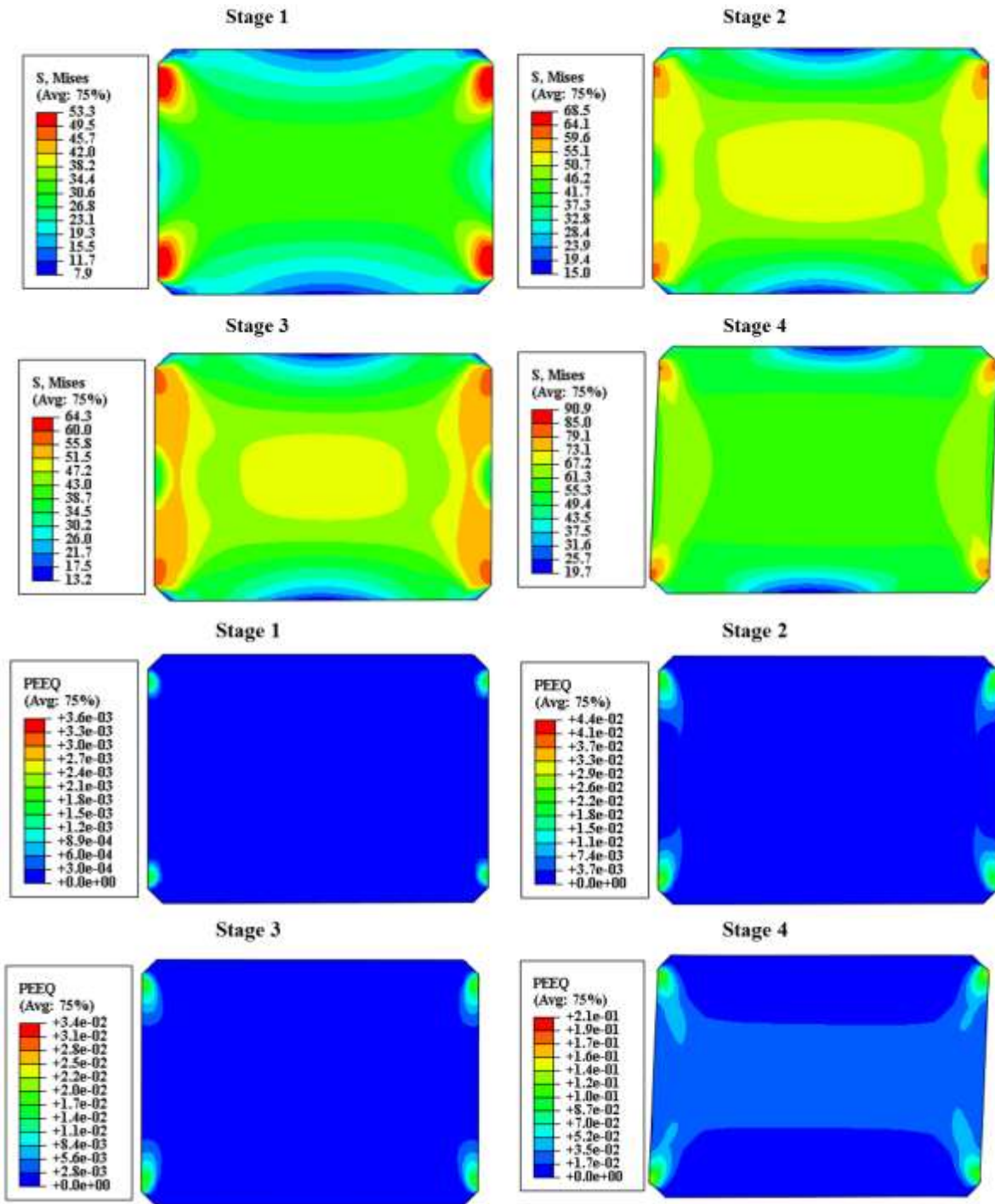


Figure 5.41: VMS and PEEQ in the DP Case 6C1

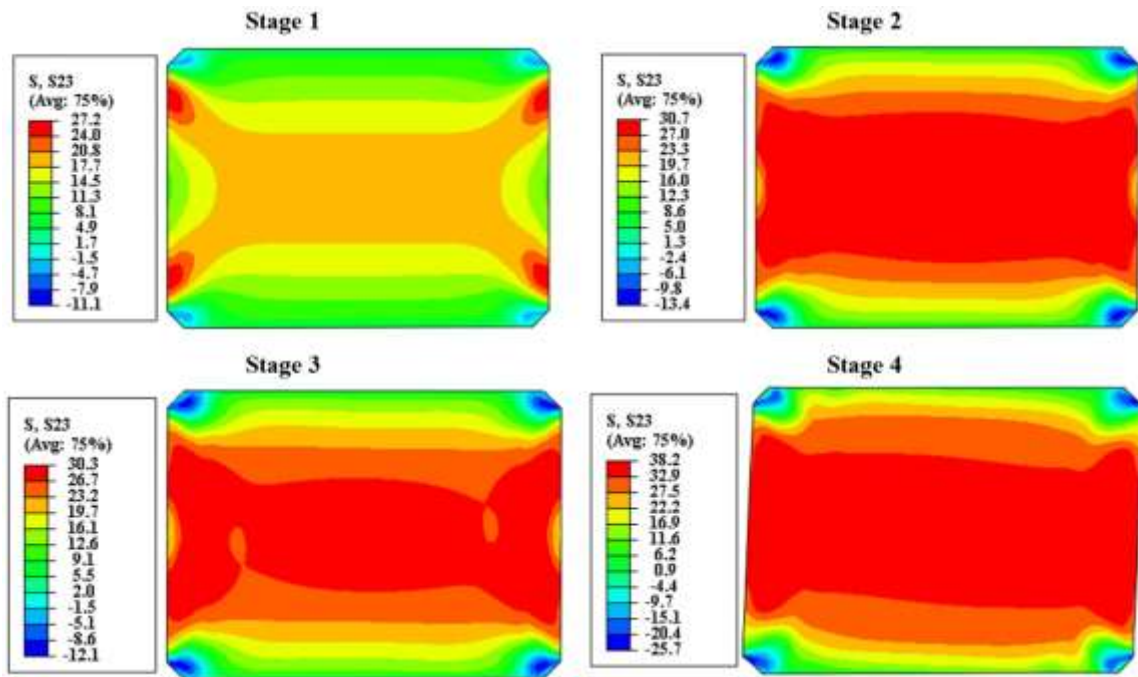


Figure 5.42: Shear stress, S23 in the DP Case 6C1

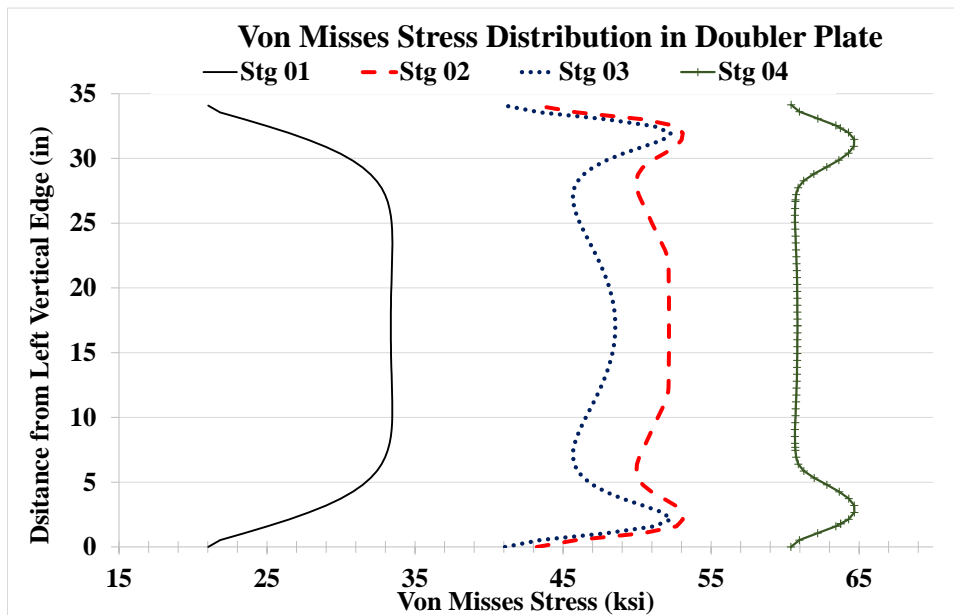


Figure 5.43: VMS distribution at mid-depth of DP Case 6C1



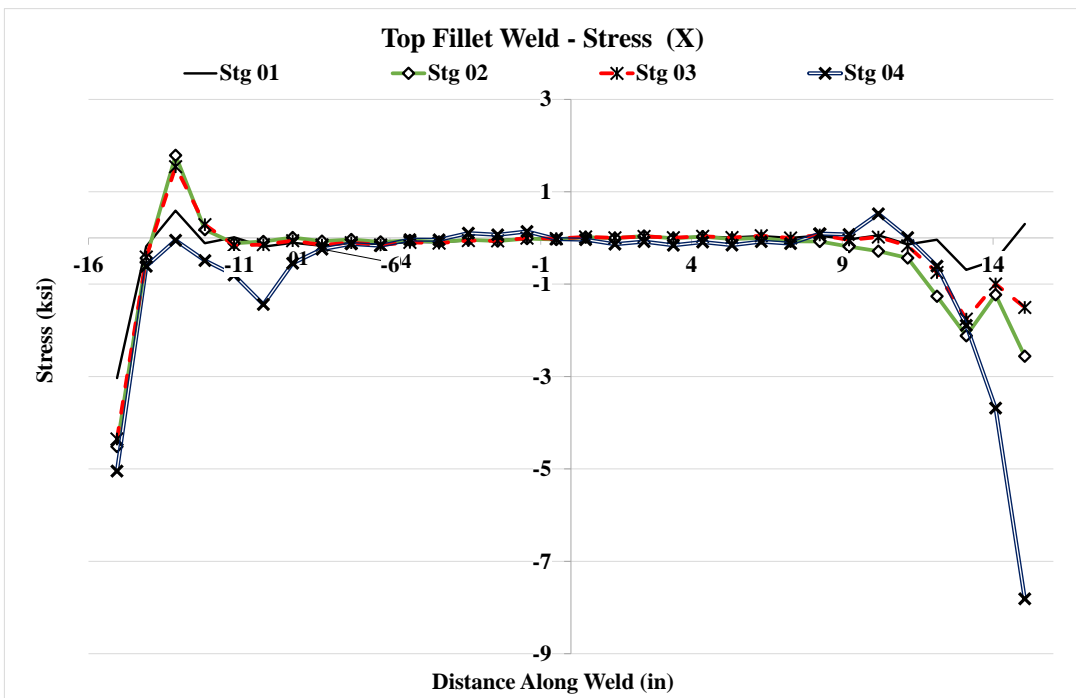
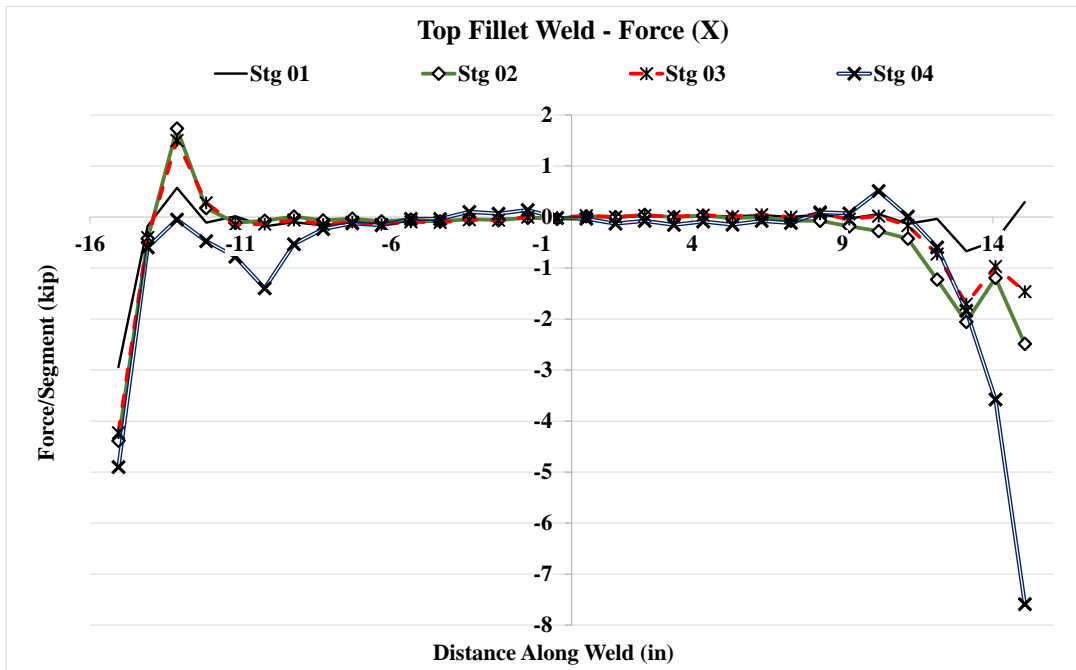


Figure 5.44: Forces and stresses in horizontal weld, (X) Case 6C1



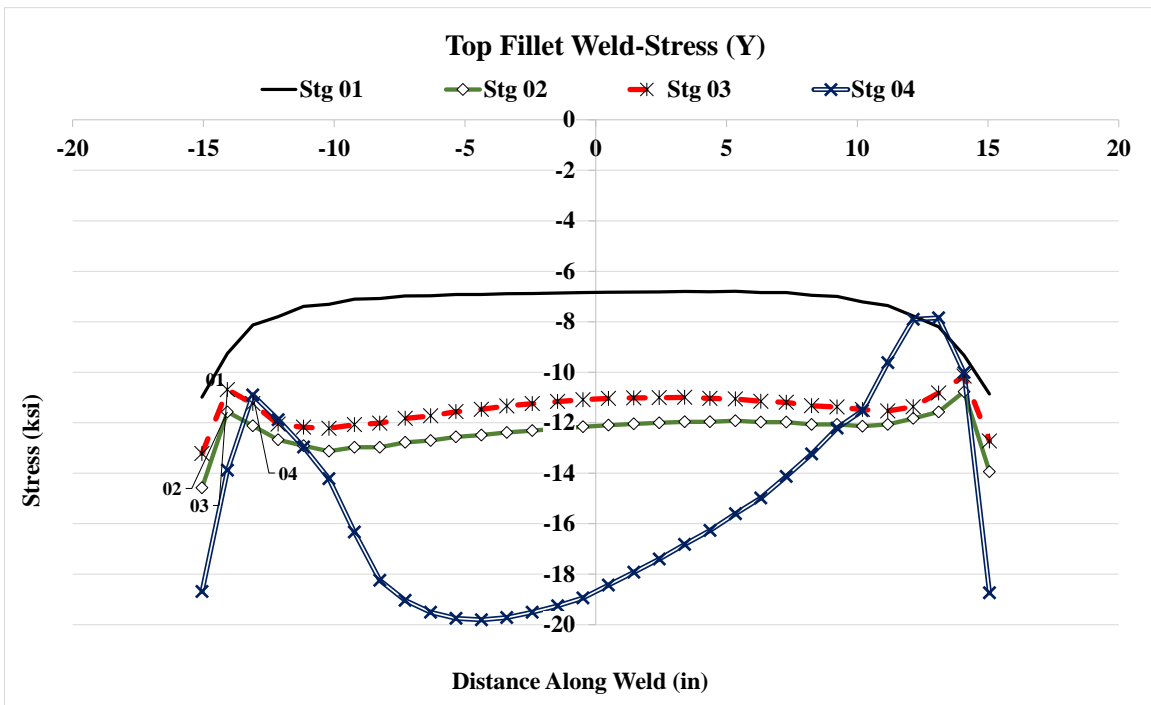
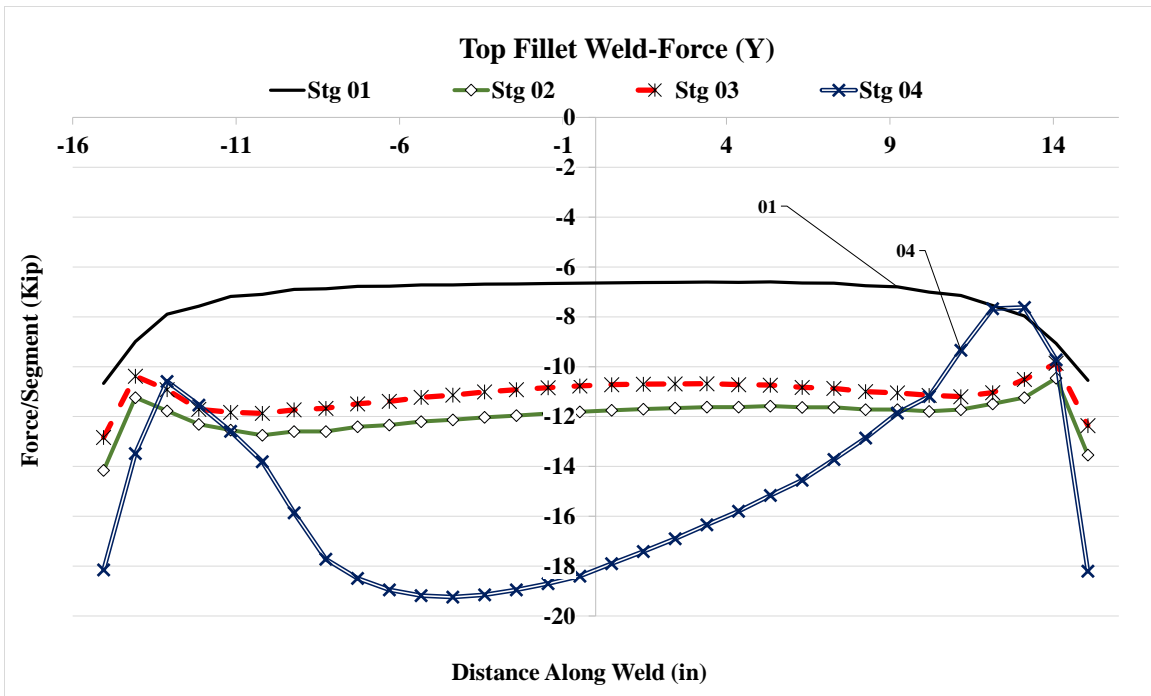


Figure 5.45: Forces and stresses in horizontal weld, (Y) Case 6C1

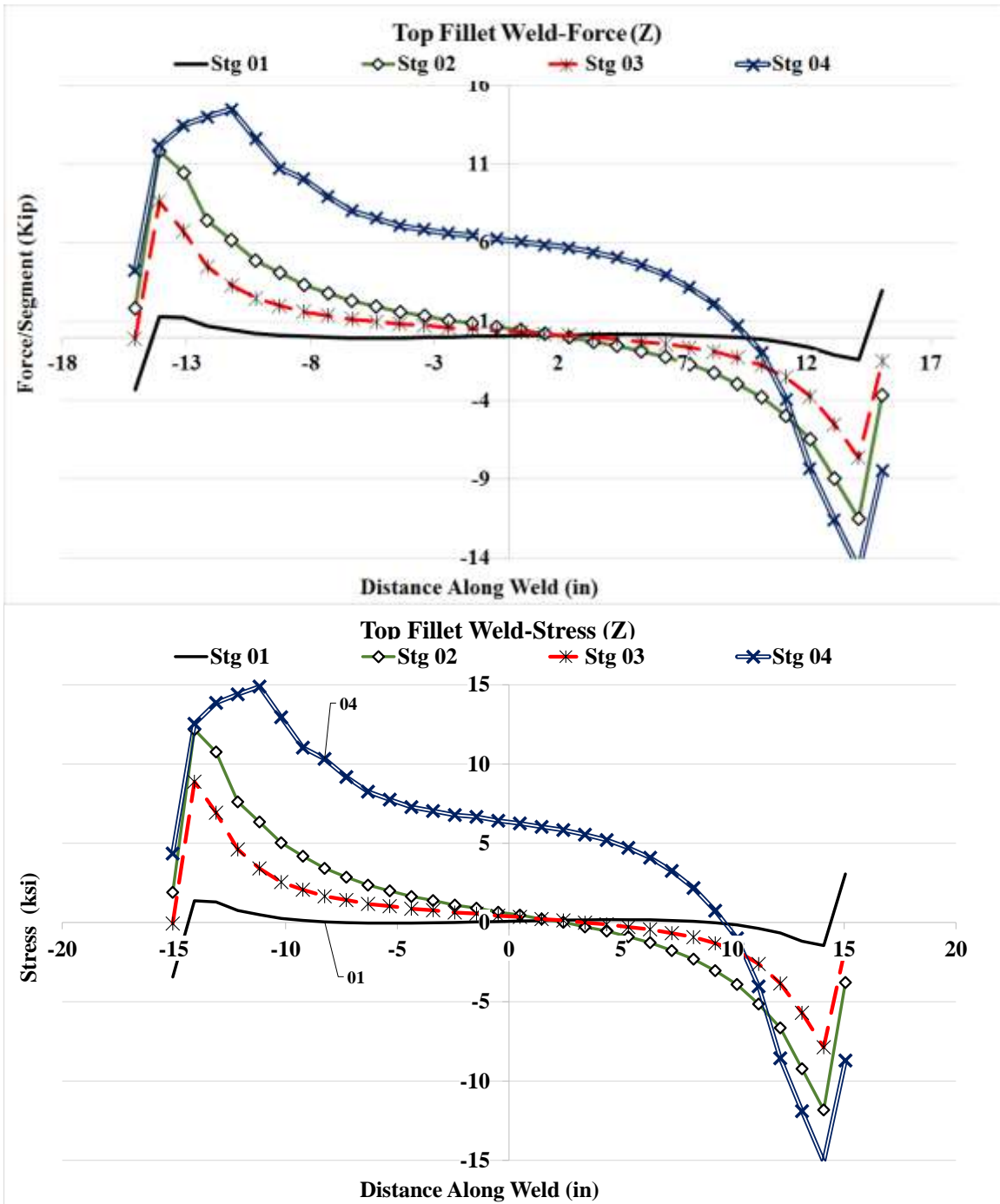


Figure 5.46: Forces and stresses in horizontal weld, (Z) Case 6C1

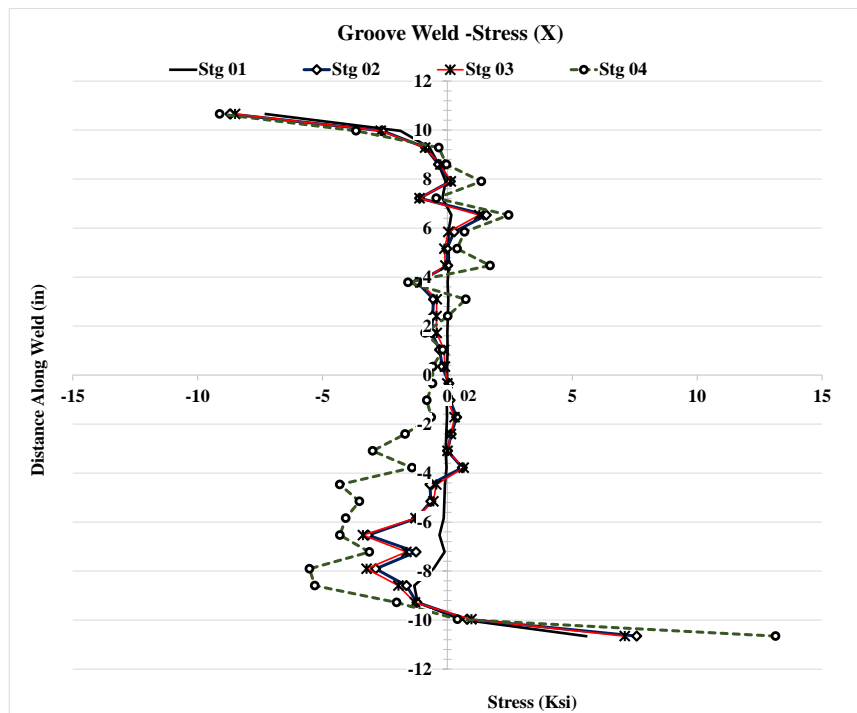
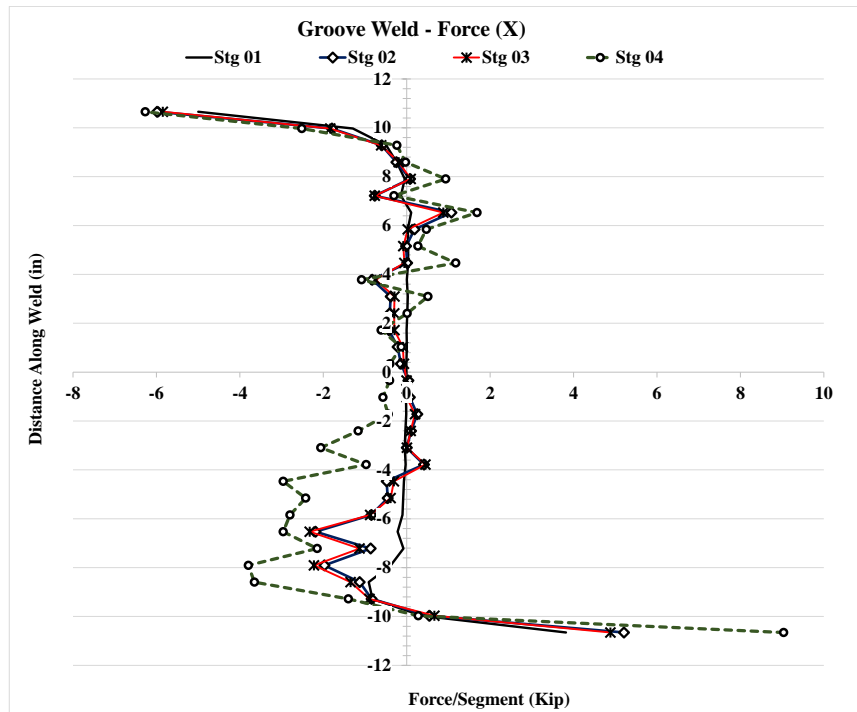


Figure 5.47: Forces and stresses in vertical weld, (X) Case 6C1

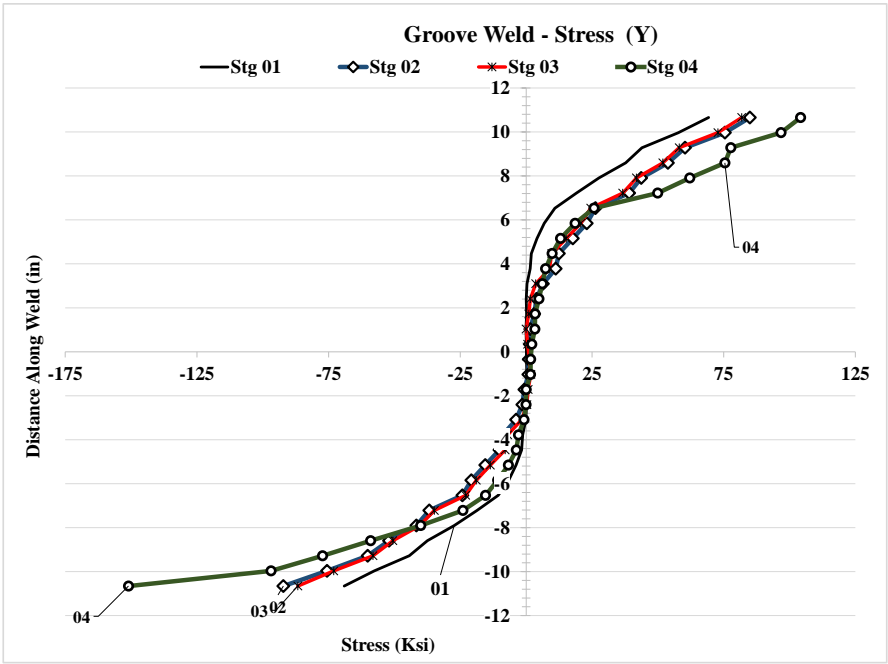
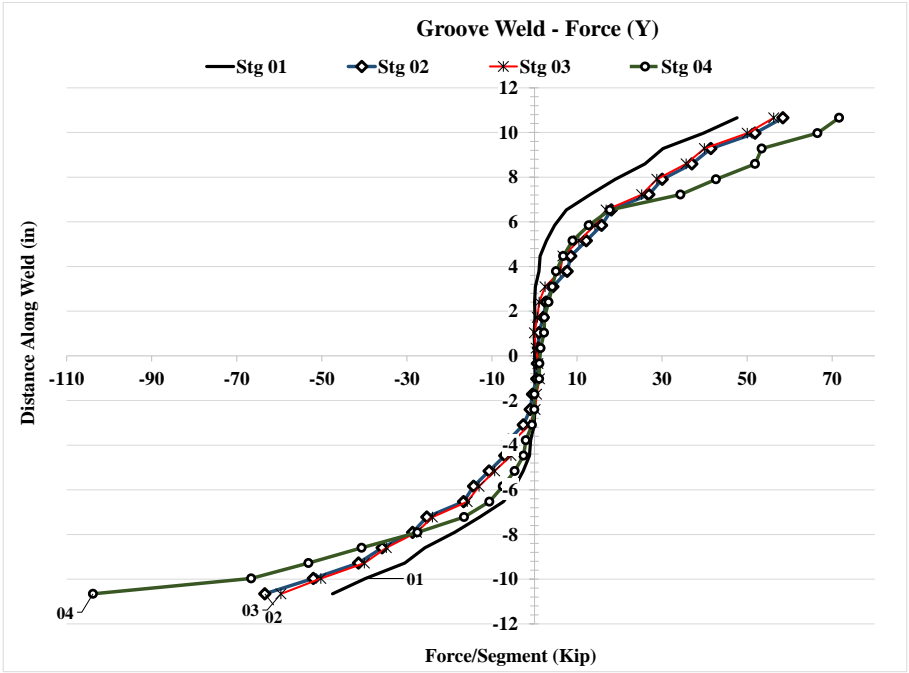


Figure 5.48: Forces and stresses in vertical weld, (Y) Case 6C1

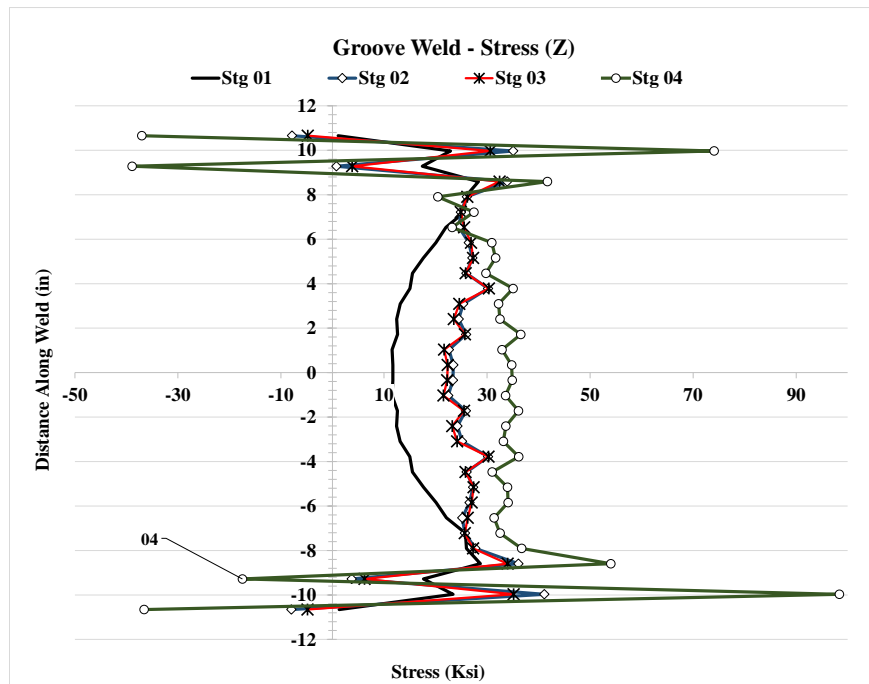
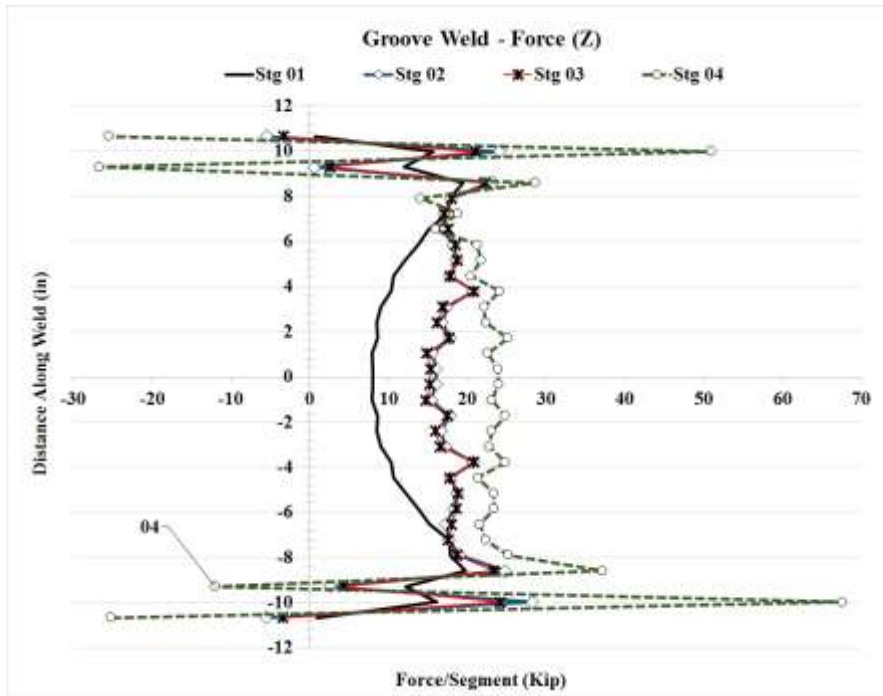


Figure 5.49: Forces and stresses in vertical weld, (Z) Case 6C1

### 5.2.6 Analysis Case 7A1

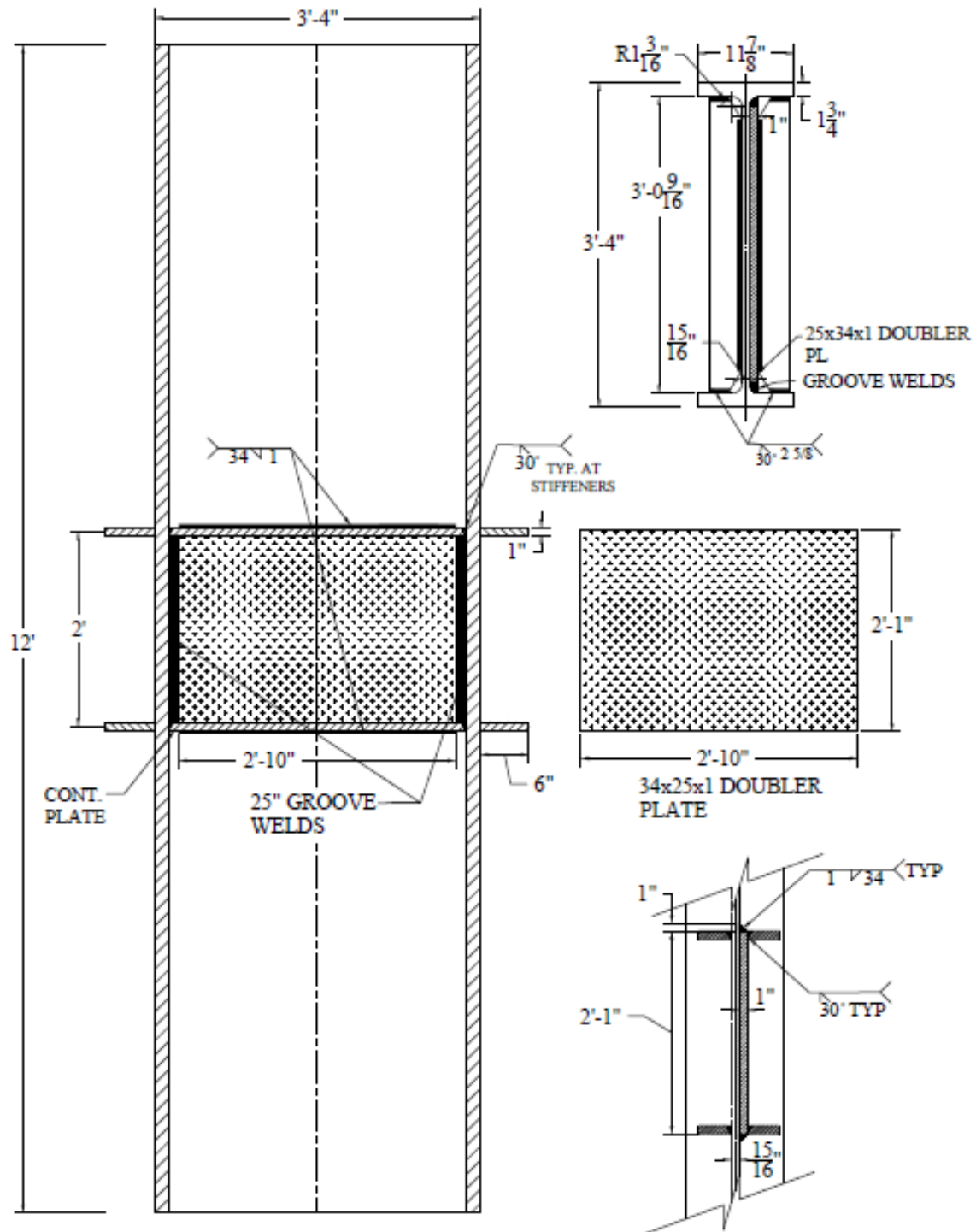


Figure 5.50: W40x264 Analysis case 7A1

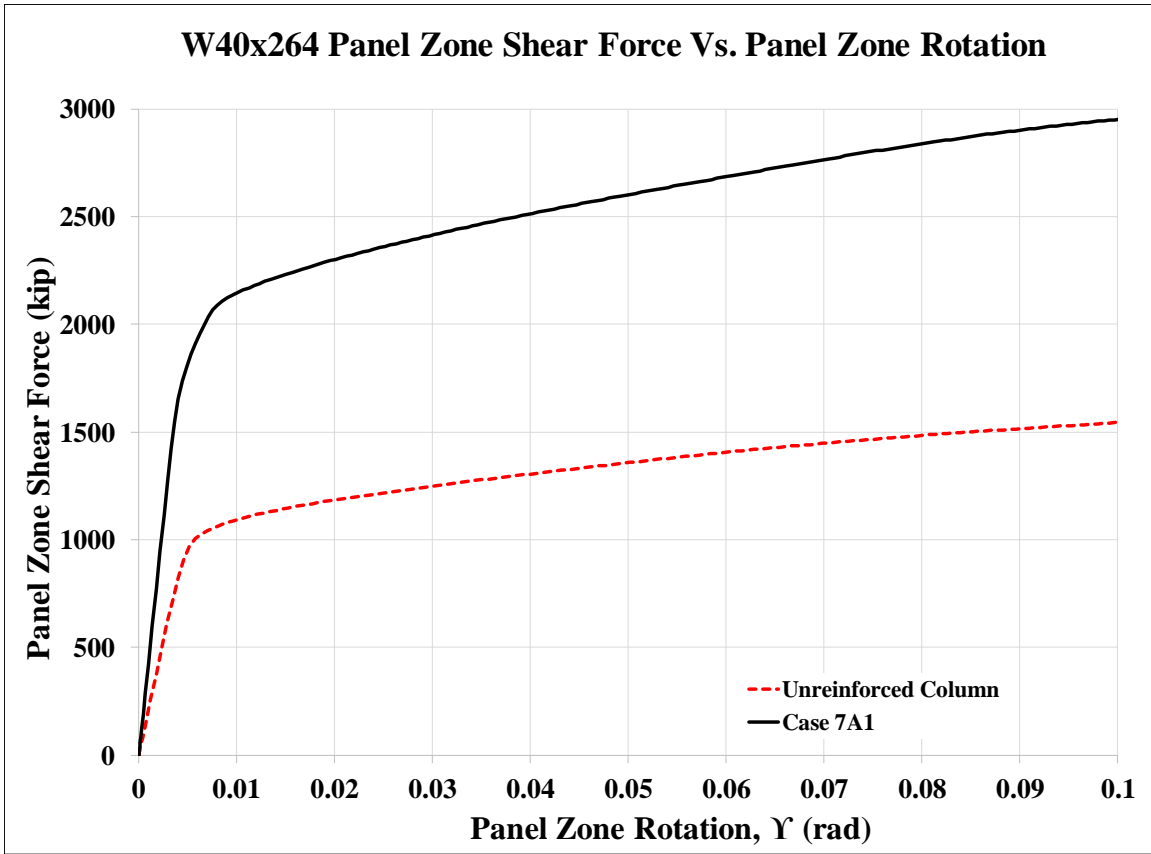


Figure 5.51: Panel zone shear vs. panel zone rotation Case 7A1

Stage	Applied Force/Loading Plate (Kip)	Panel Shear Force (Kip)	% Higher Than Unreinforced Col.	Panel Zone Rotation (rad)
1	1,042	1,736	179%	0.004
2	1,330	2,217	196%	0.014
3	1,381	2,302	194%	0.020
4	1,772	2,953	191%	0.100

Table 5.7: Panel zone shear and force on loading plate Case 7A1

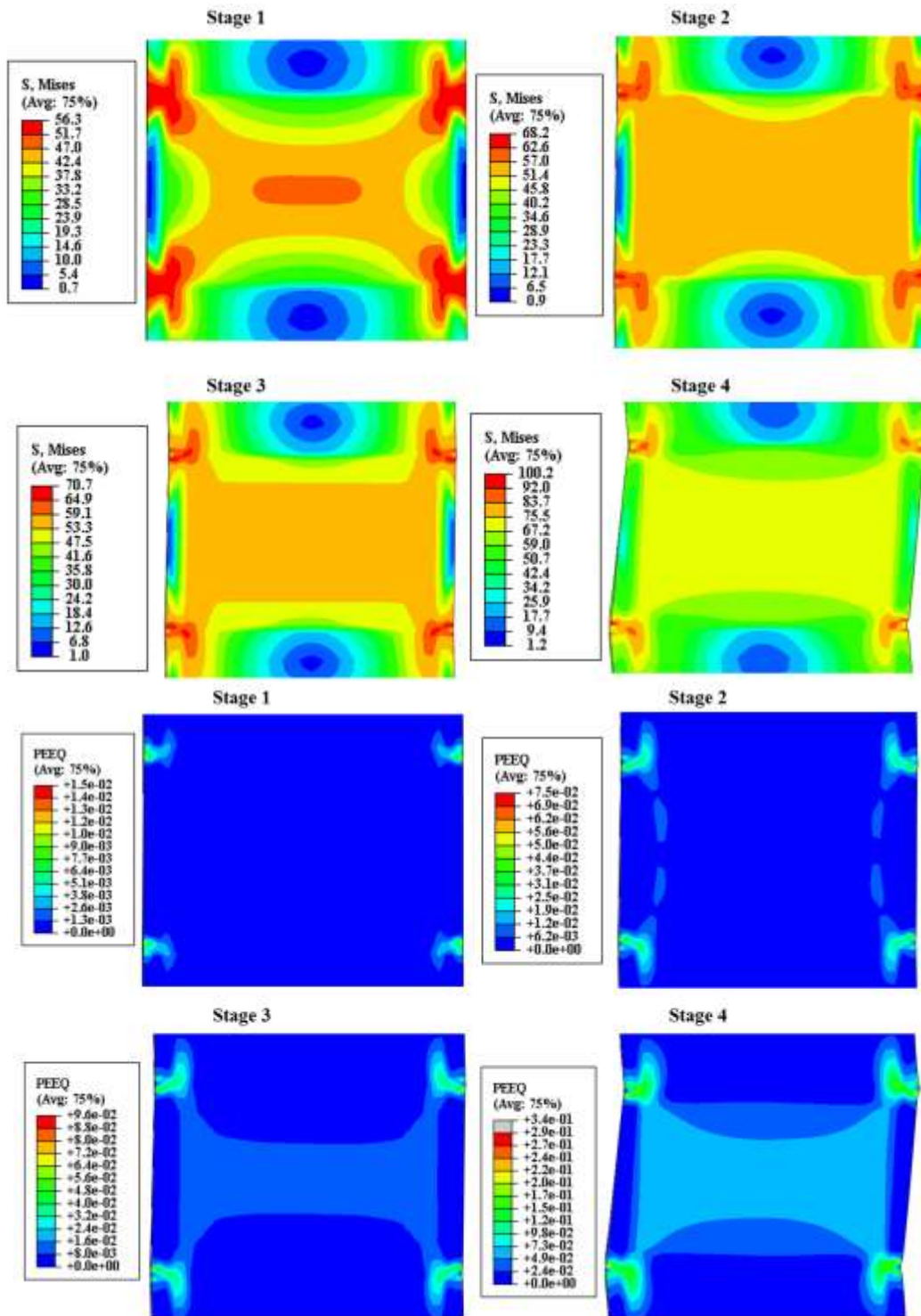


Figure 5.52: VMS and PEEQ in the column Case 7A1



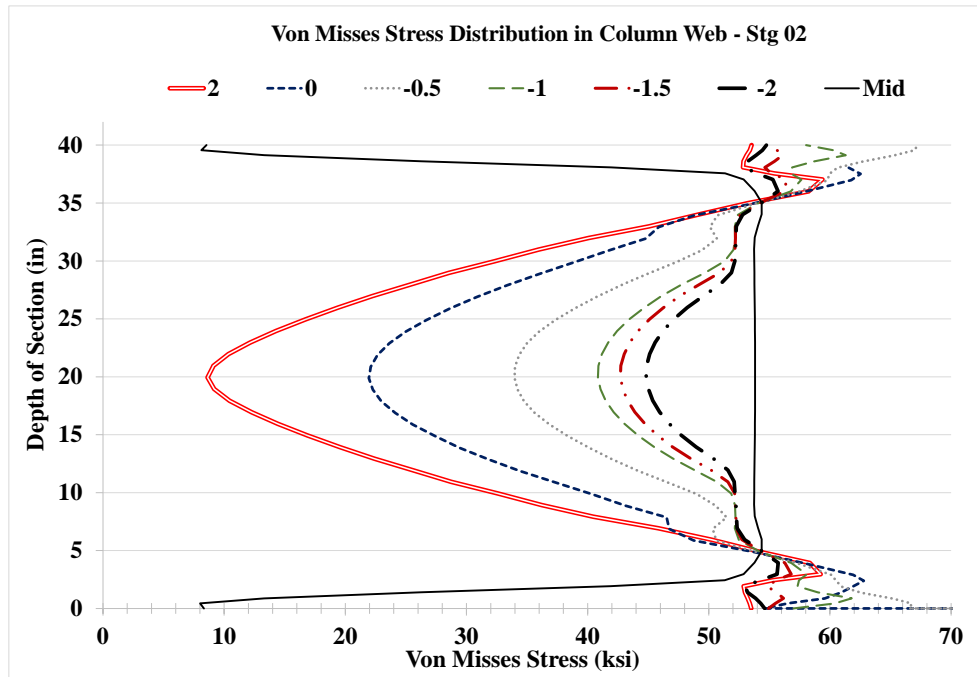
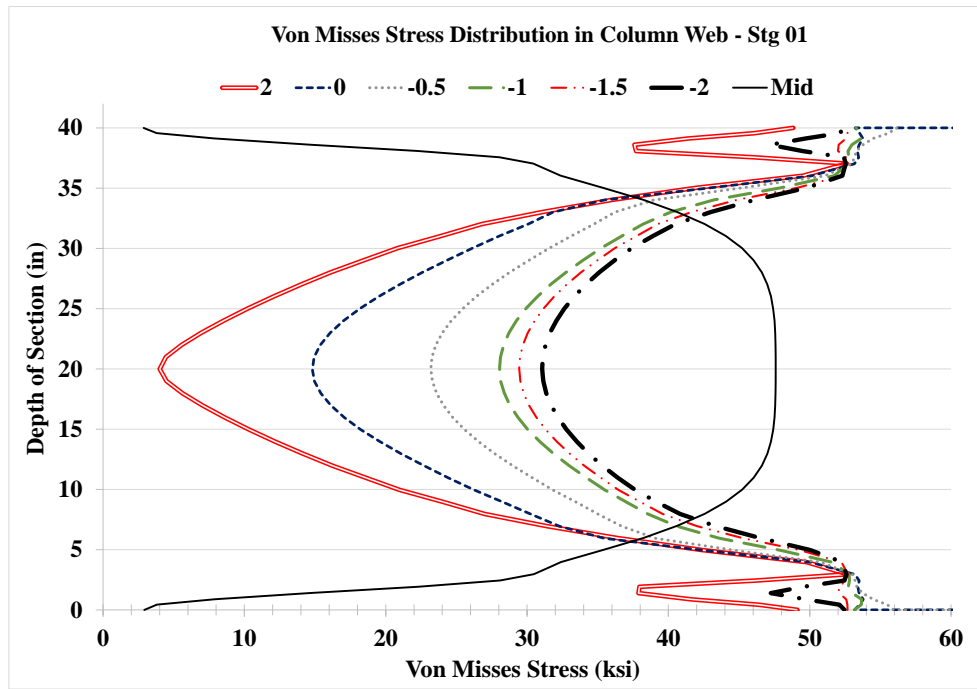


Figure 5.53: VMS distribution in column web at different heights Stg. 01-04 Case 7A1

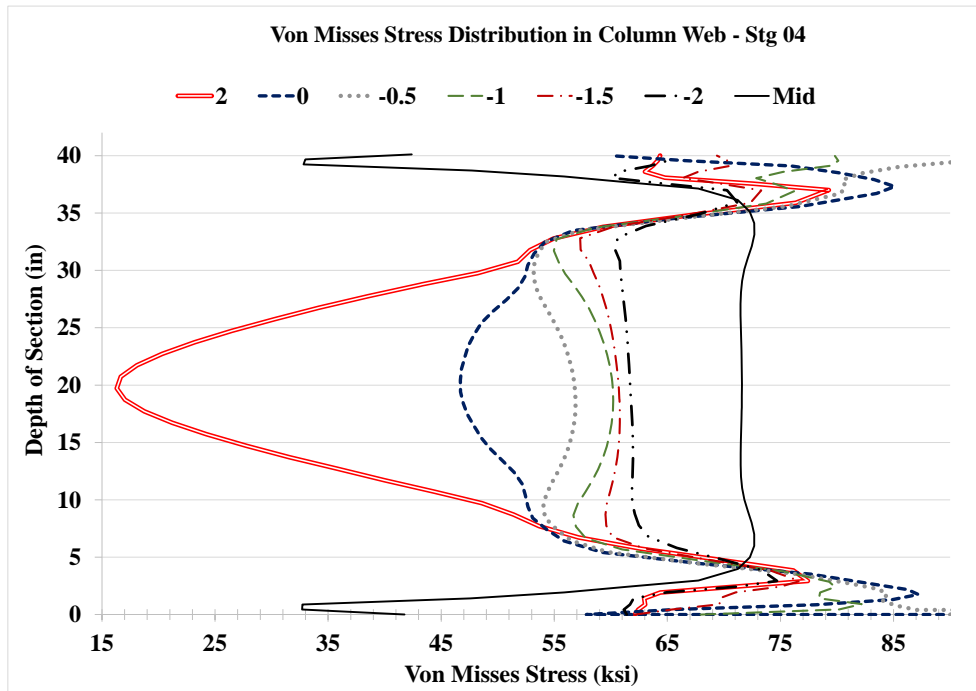
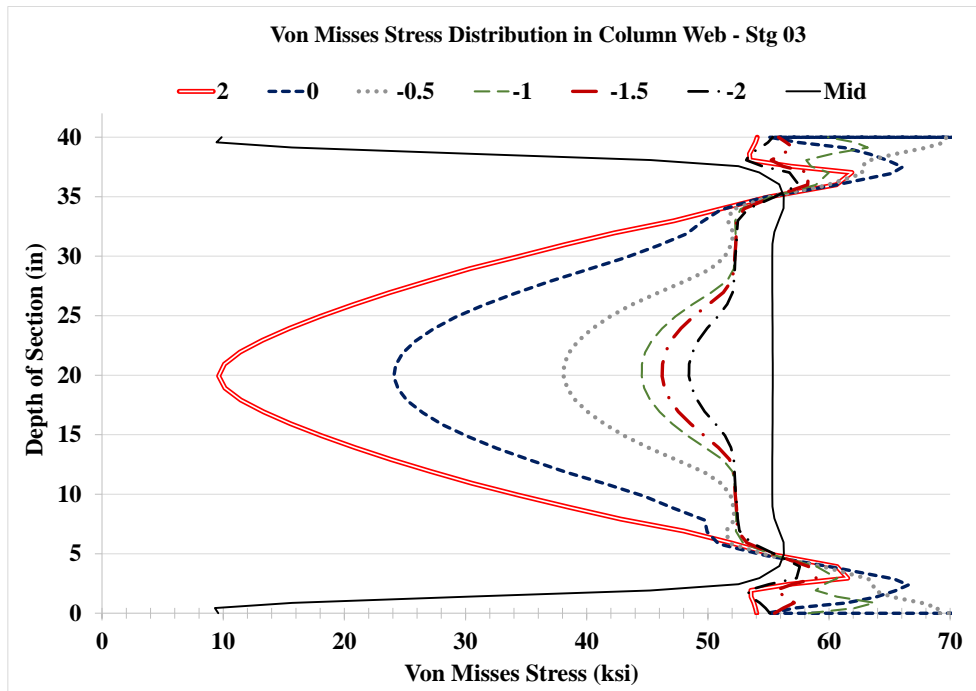


Figure 5.53: VMS distribution in column web at different heights Stg. 01-04 Case 7A1

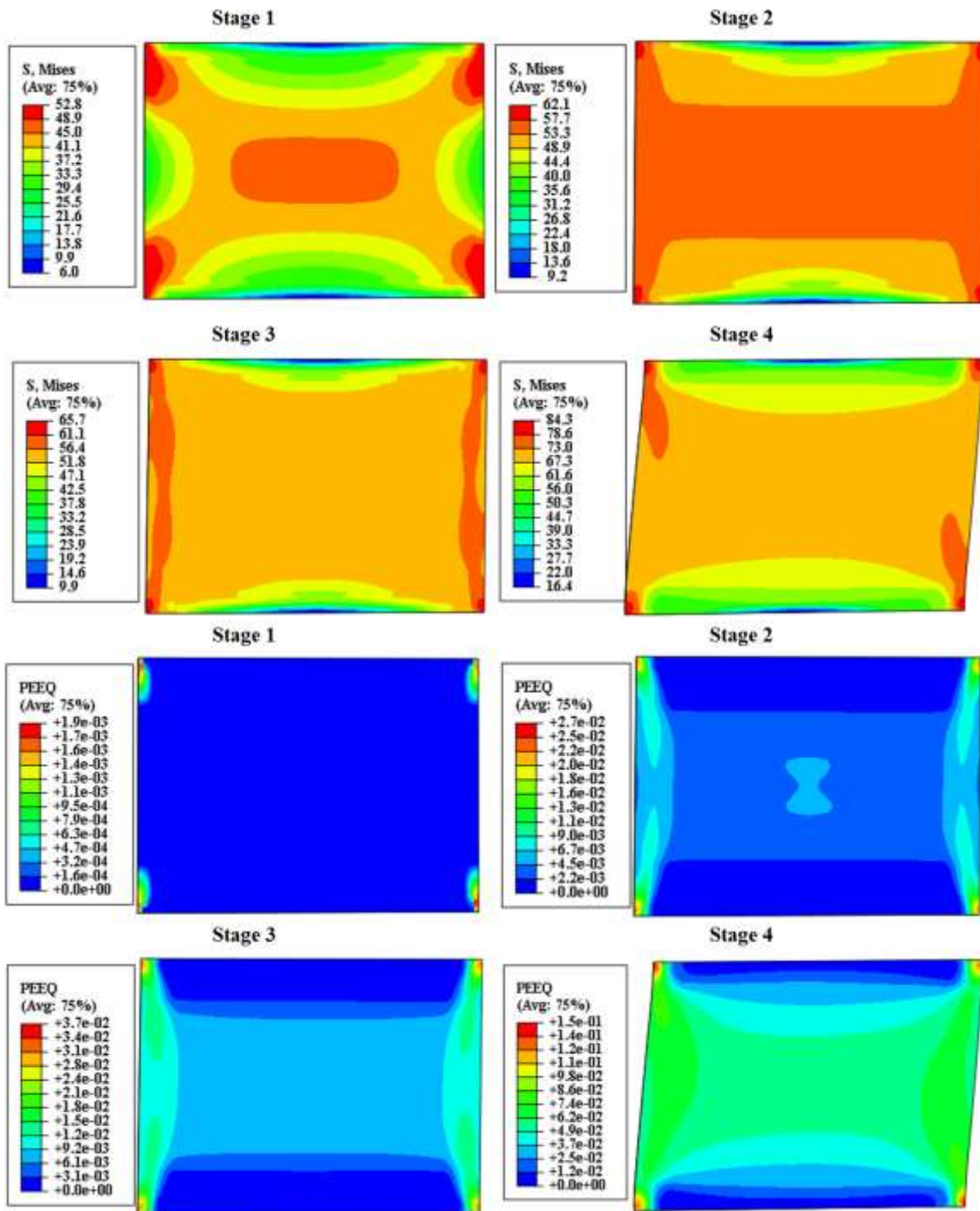


Figure 5.54: VMS and PEEQ in the DP Case 7A1

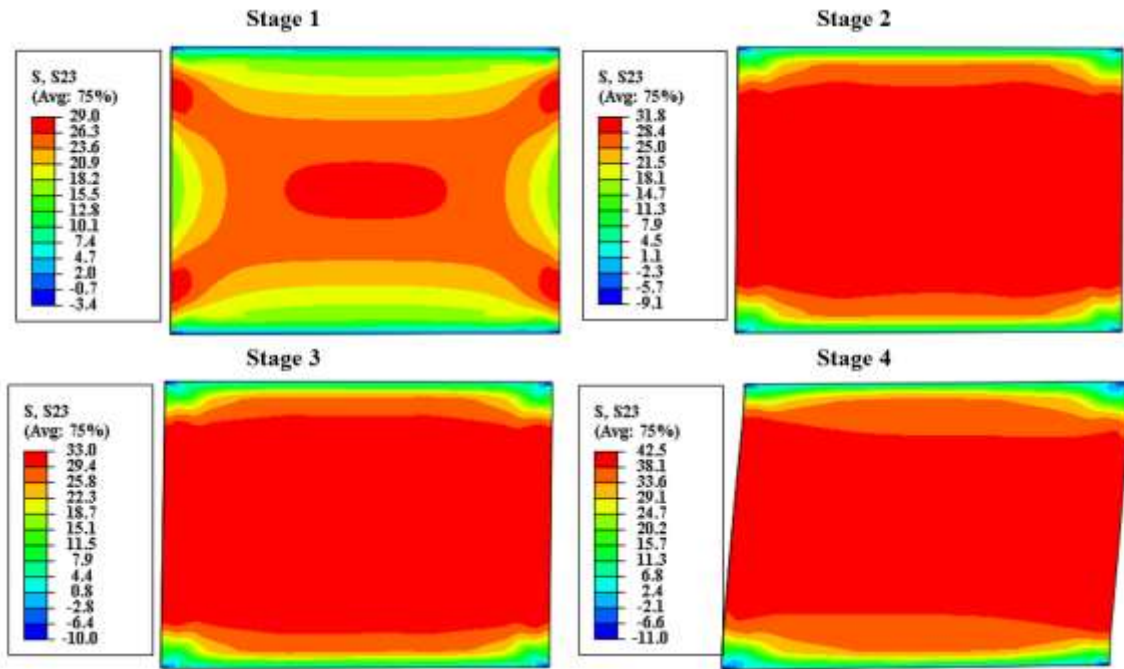


Figure 5.55: Shear stress, S23 in the DP Case 7A1

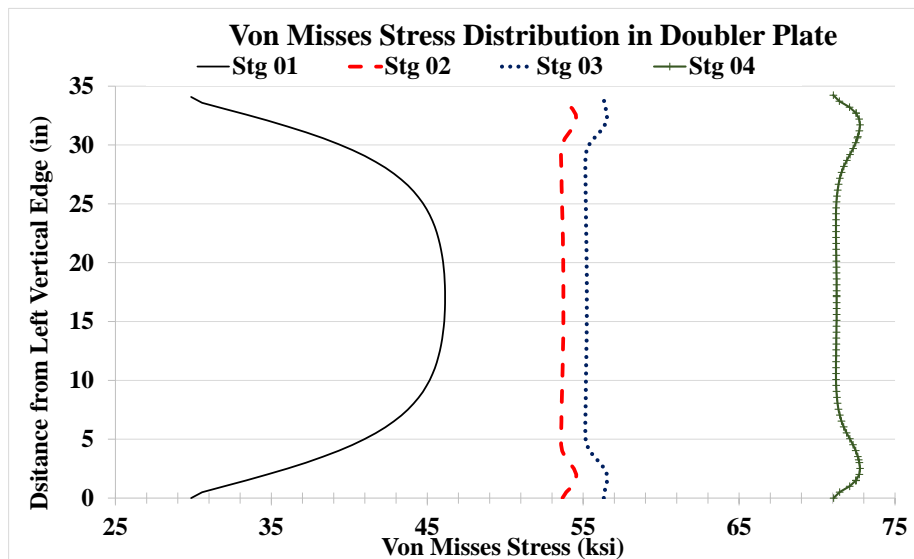


Figure 5.56: VMS distribution at mid-depth of DP Case 7A1

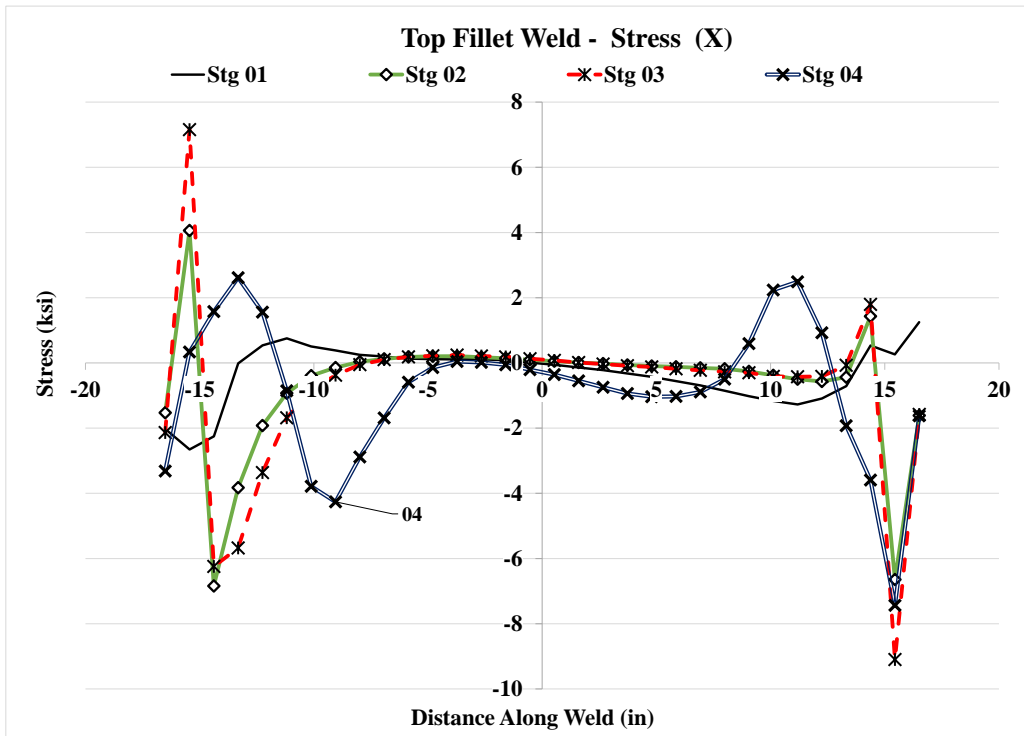
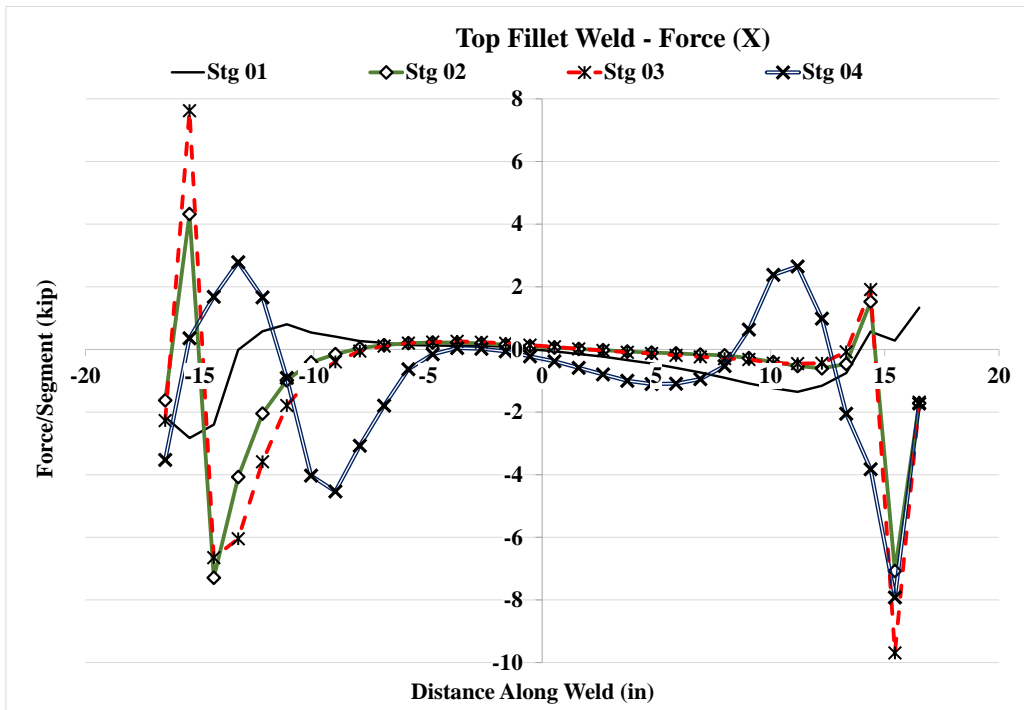


Figure 5.57: Forces and stresses in horizontal weld, (X) Case 7A1

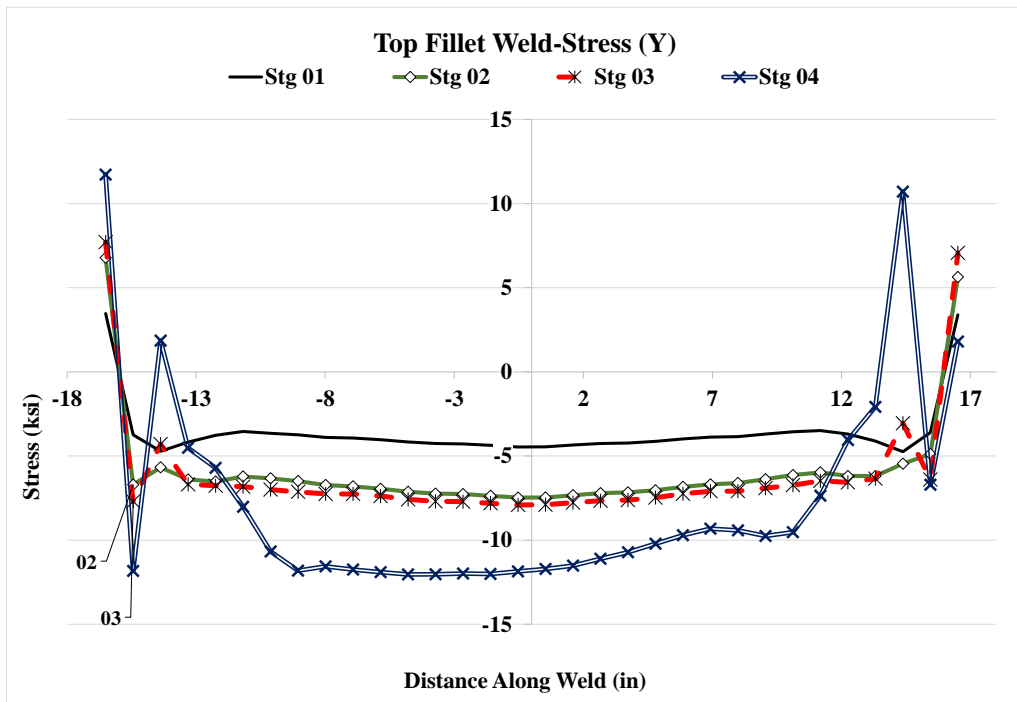
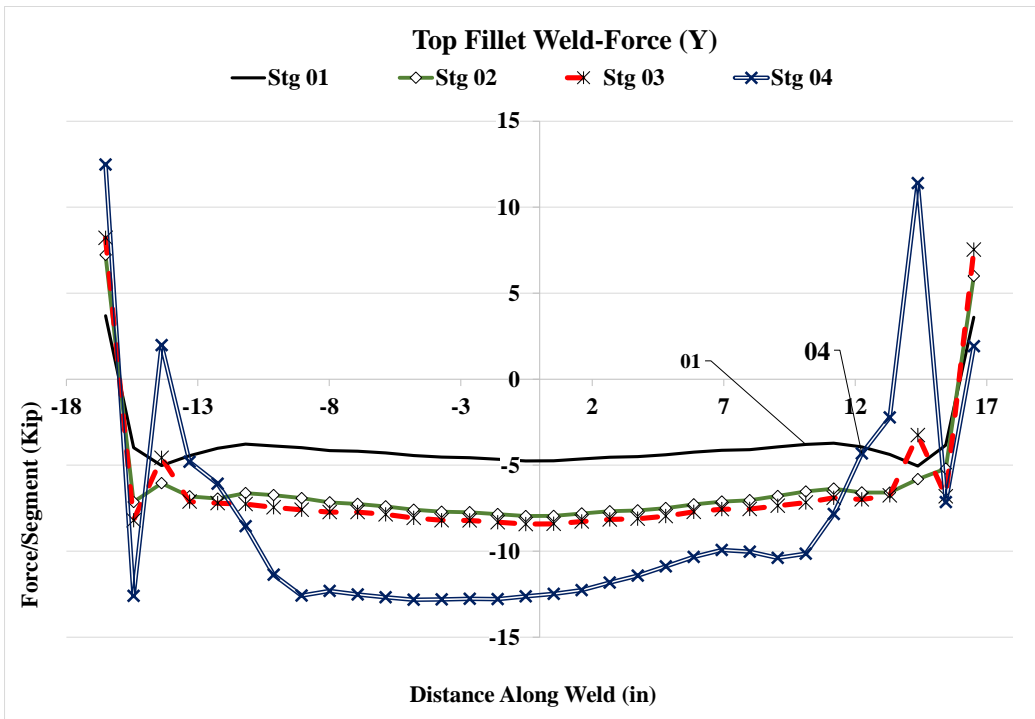


Figure 5.58: Forces and stresses in horizontal weld, (Y) Case 7A1

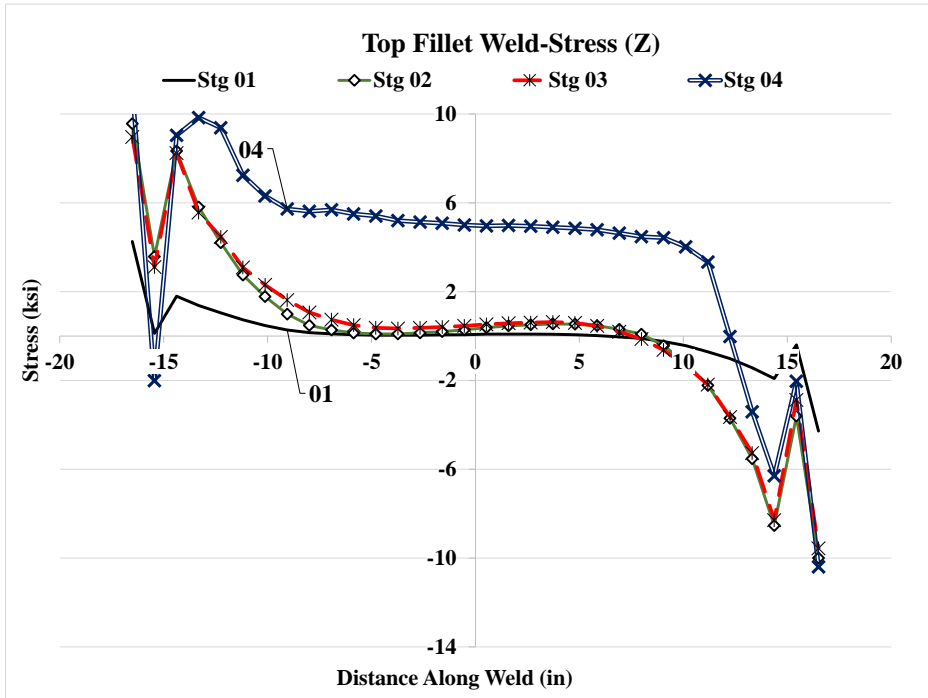
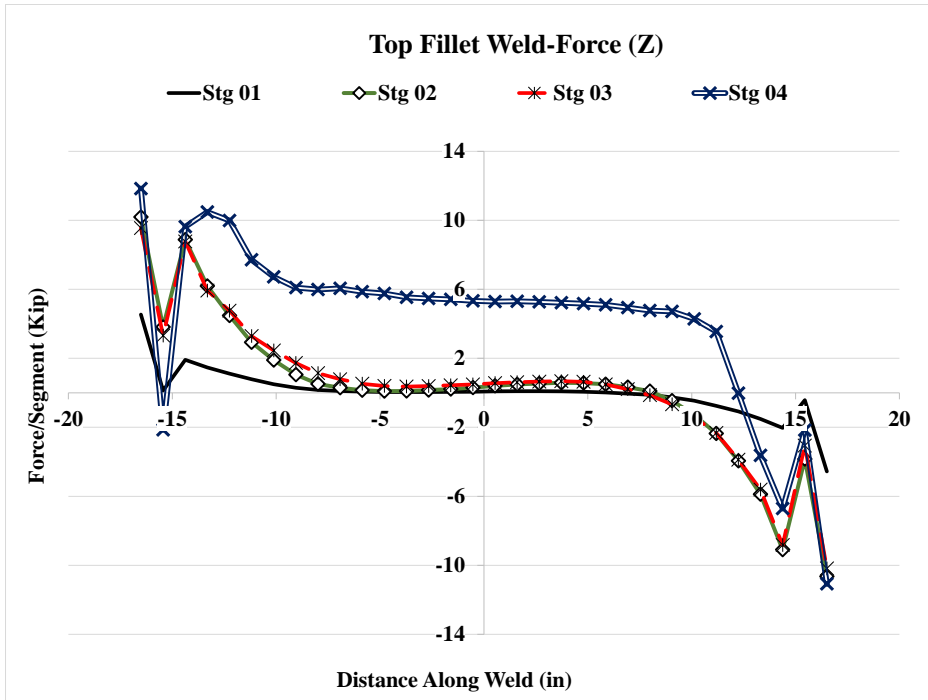


Figure 5.59: Forces and stresses in horizontal weld, (Z) Case 7A1

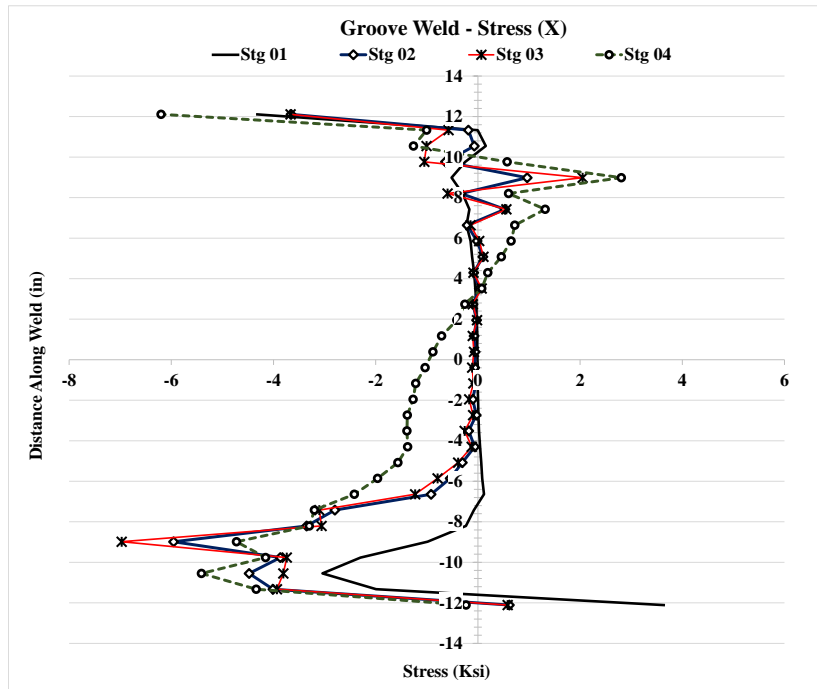
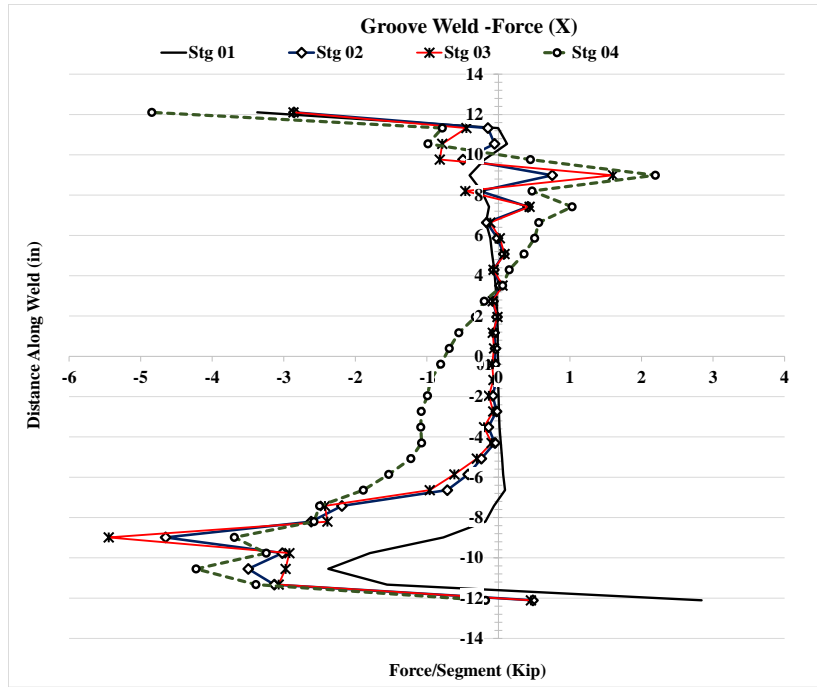


Figure 5.60: Forces and stresses in vertical weld, (X) Case 7A1



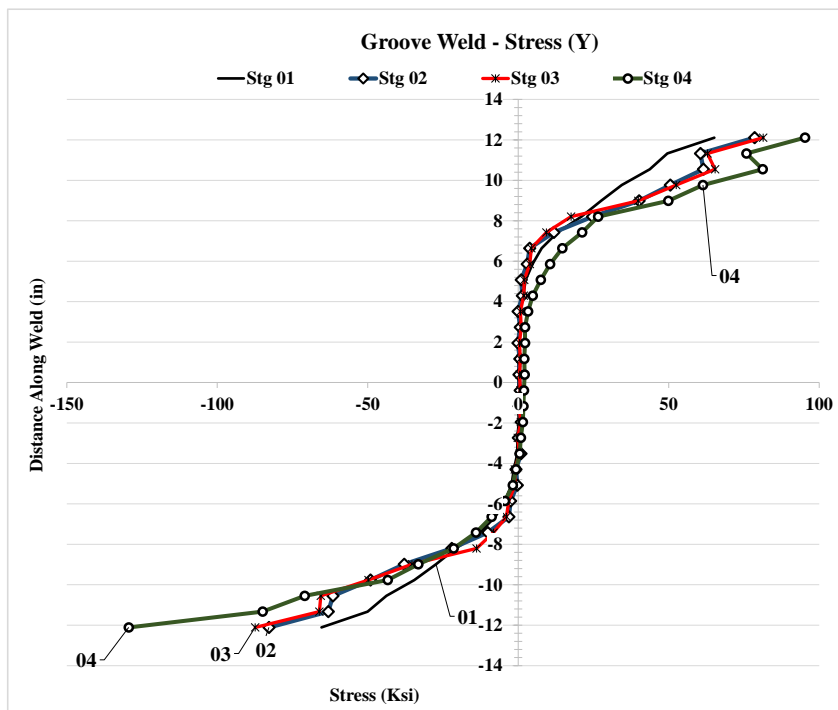
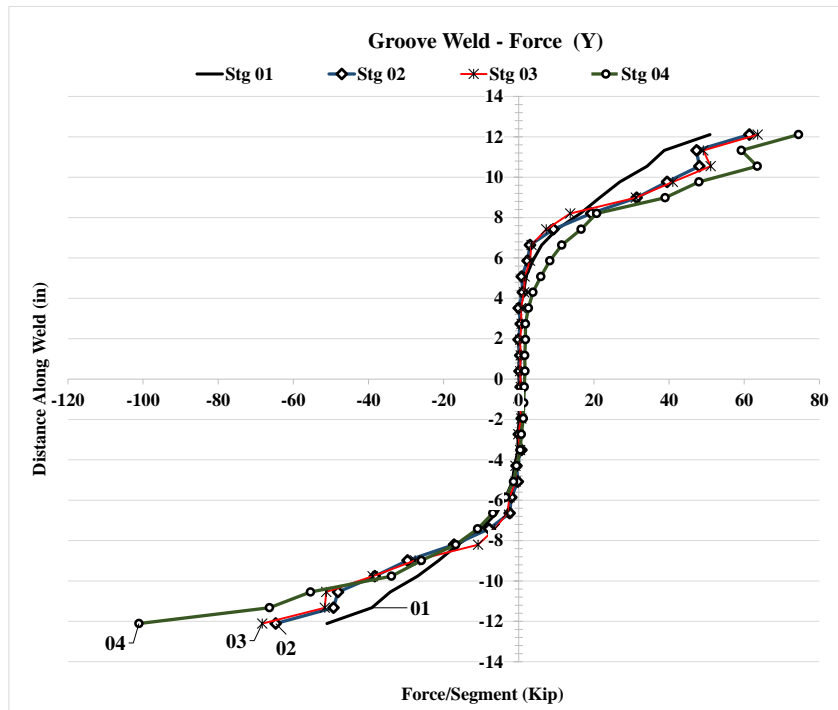


Figure 5.61: Forces and stresses in vertical weld, (Y) Case 7A1

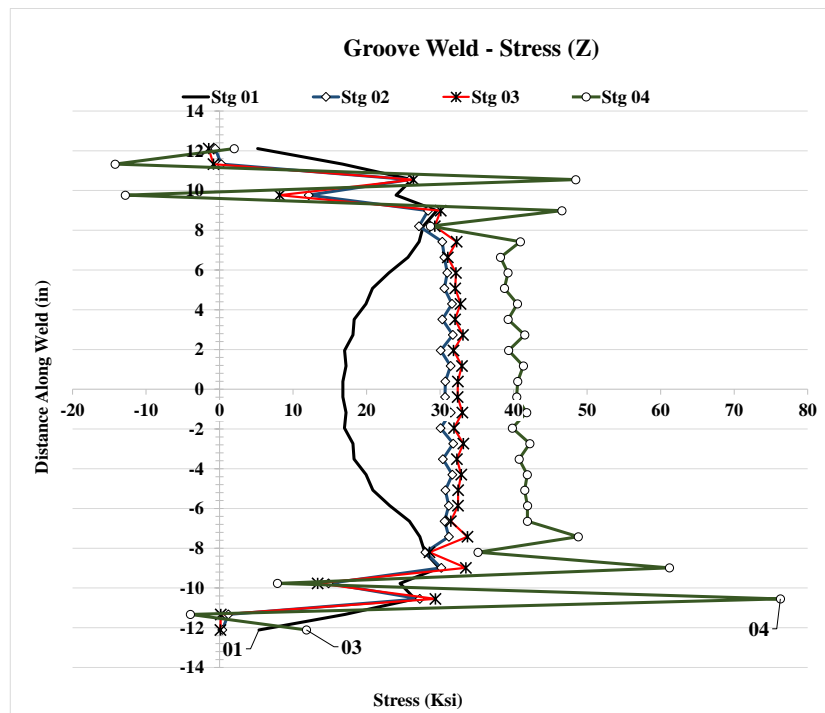
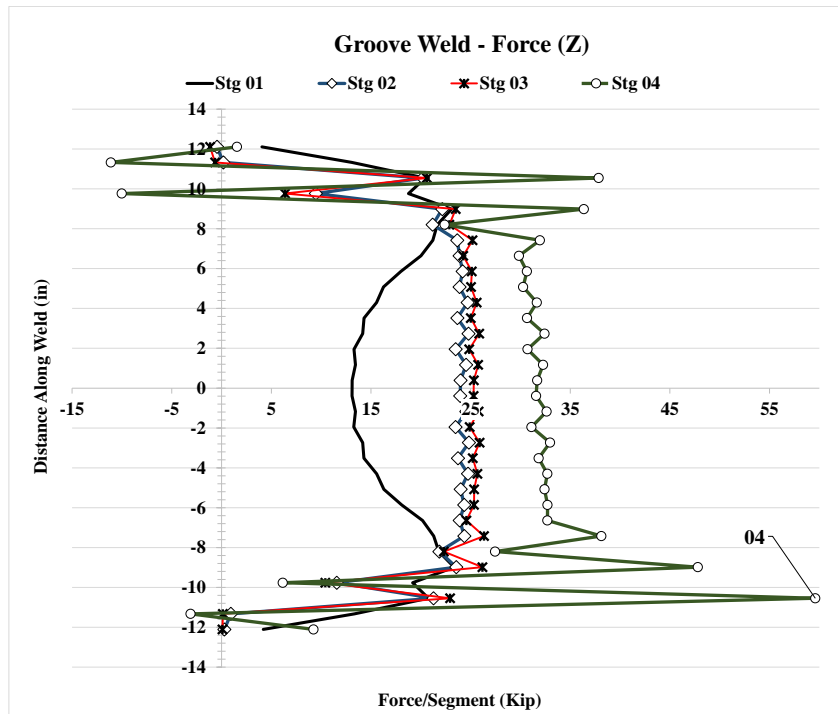


Figure 5.62: Forces and stresses in vertical weld, (Z) Case 7A1

5.2.7 Analysis Case 7C1

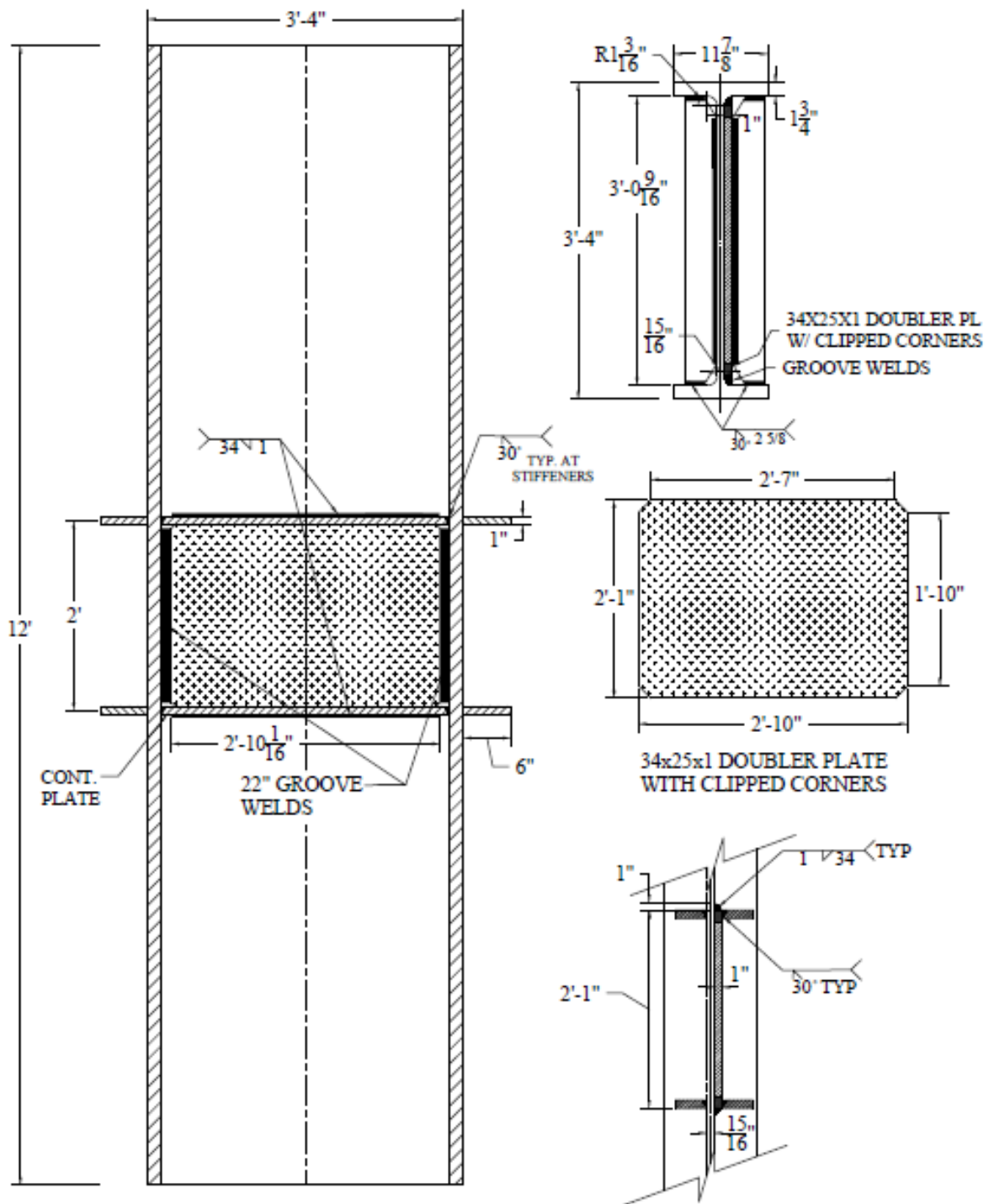


Figure 5.63: W40x264 Analysis case 7C1

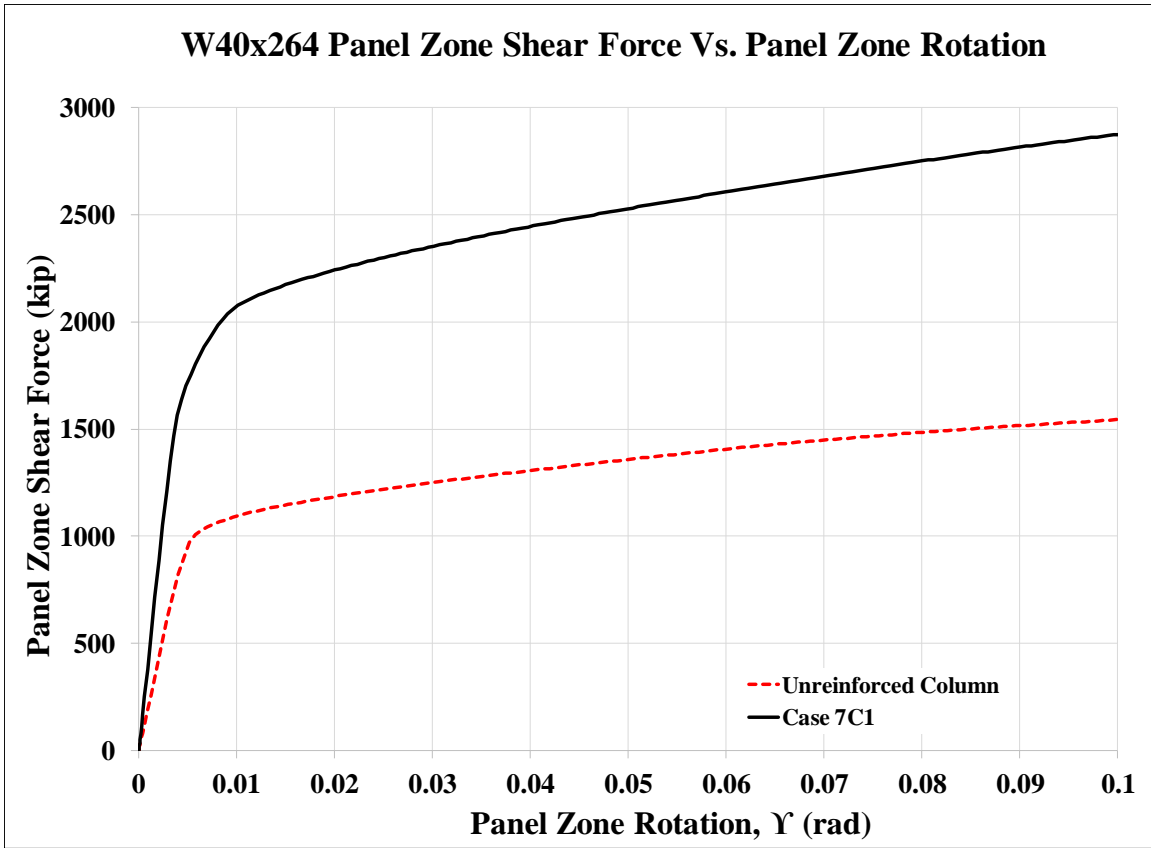


Figure 5.64: Panel zone shear vs. panel zone rotation Case 7C1

Stage	Applied Force/Loading Plate (Kip)	Panel Shear Force (Kip)	% Higher Than Unreinforced Col.	Panel Zone Rotation (rad)
1	938	1,564	161%	0.004
2	1,319	2,198	194%	0.017
3	1,345	2,242	189%	0.020
4	1,725	2,876	186%	0.100

Table 5.8: Panel zone shear and force on loading plate Case 7C1

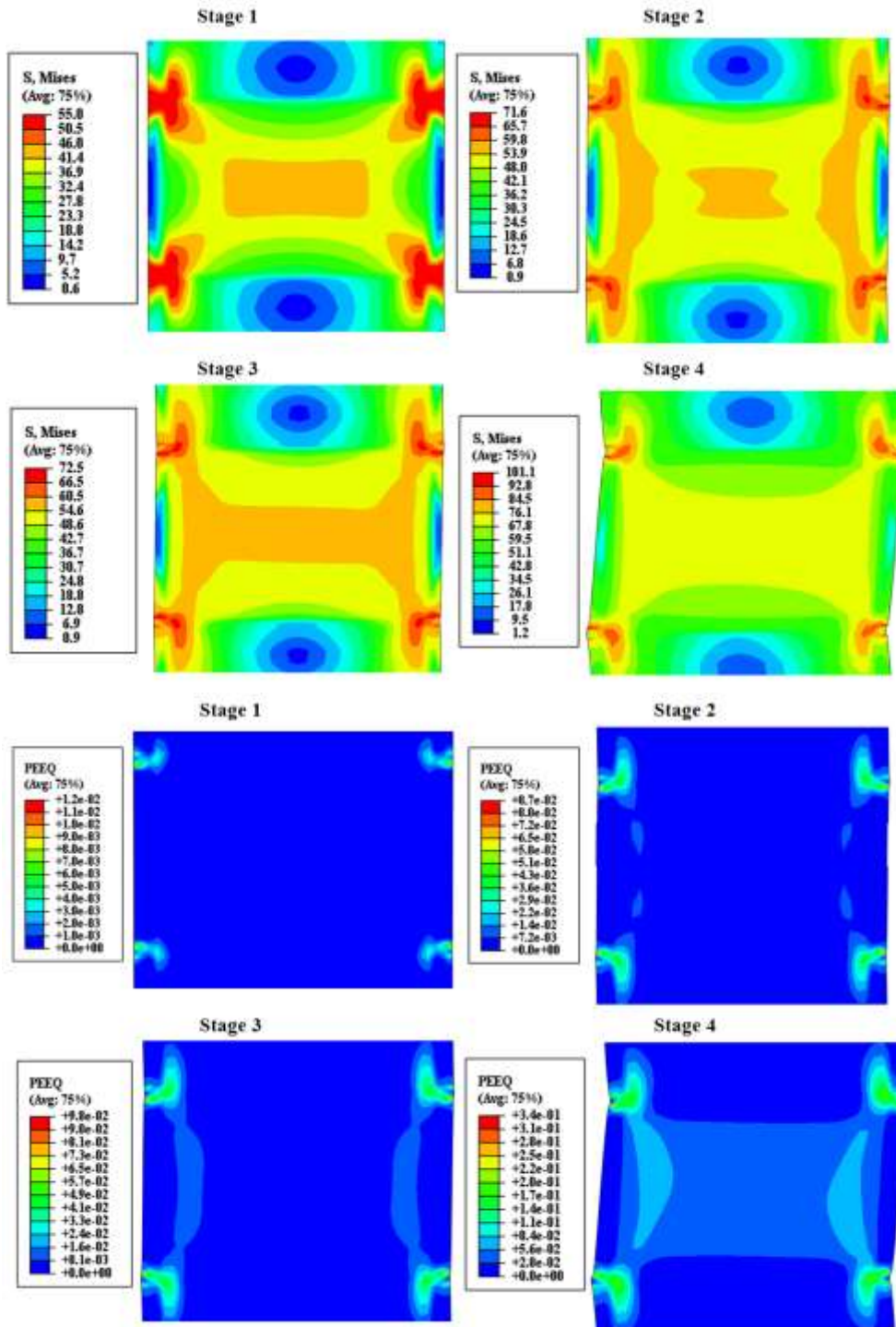


Figure 5.65: VMS and PEEQ in the column Case 7C1

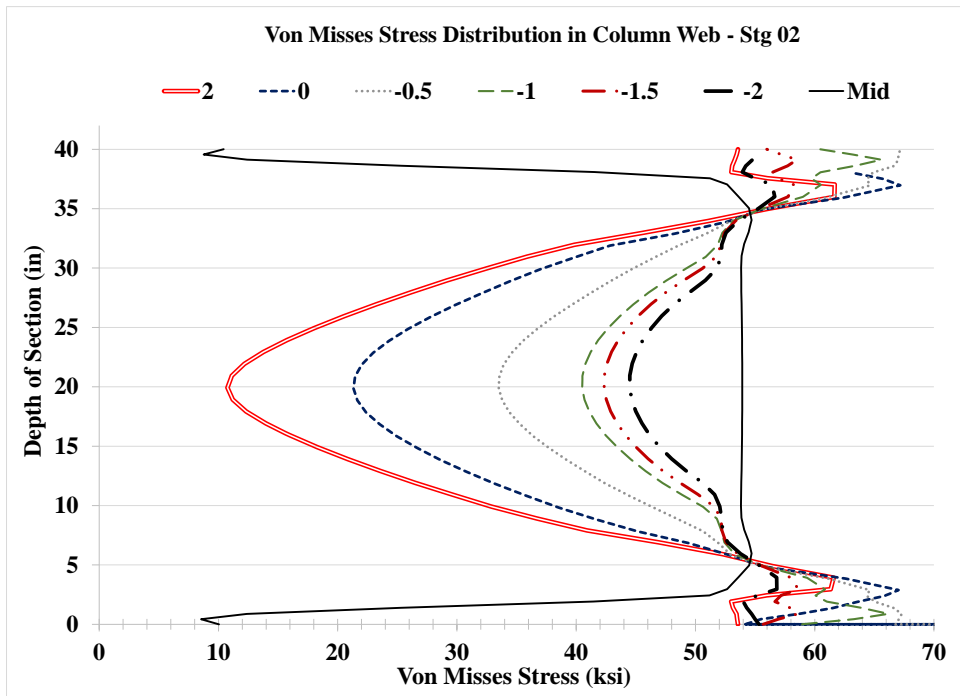
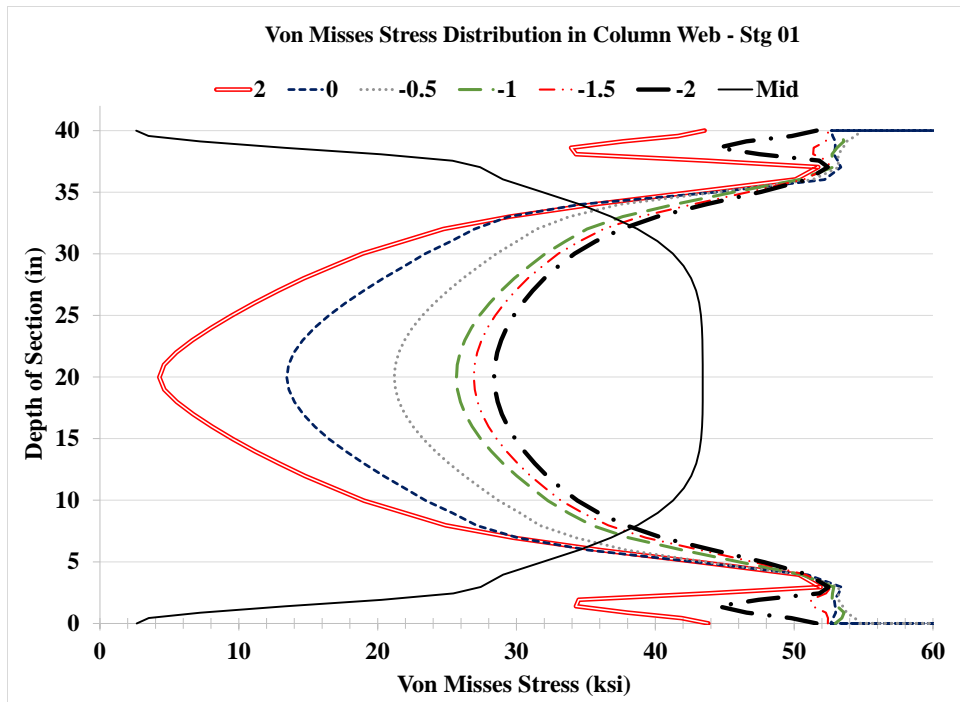


Figure 5.66: VMS distribution in column web at different heights Stg. 01-04 Case 7C1

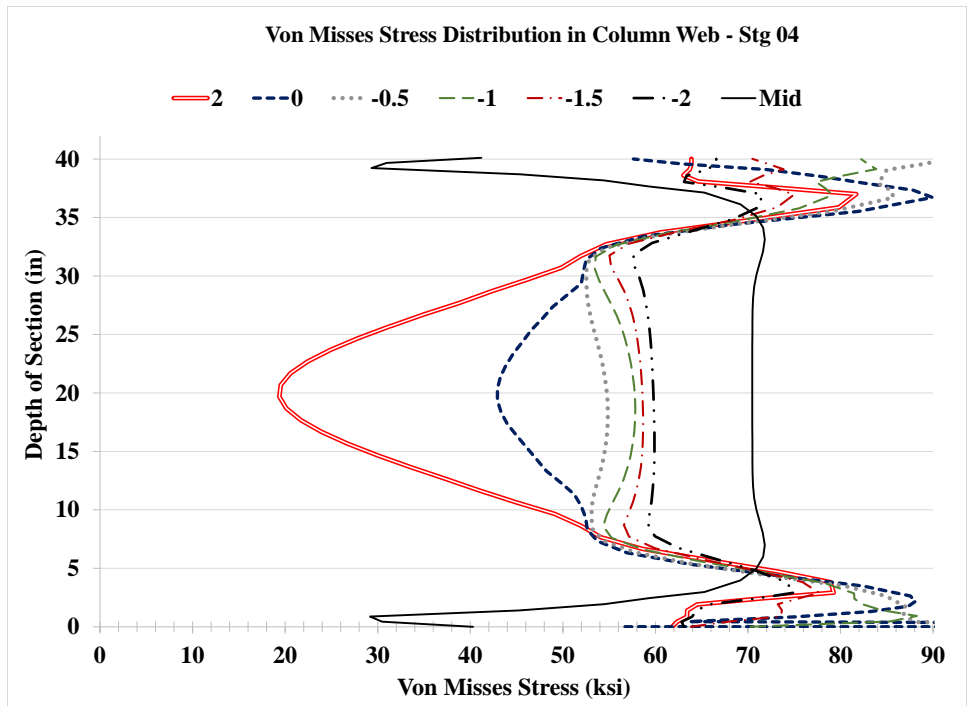
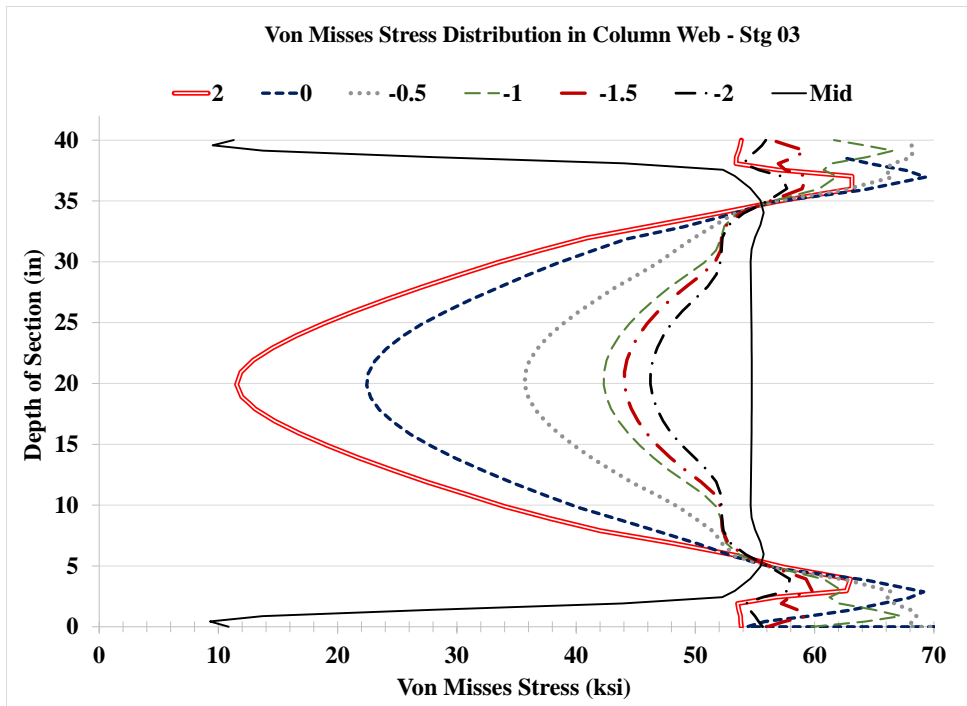


Figure 5.66: VMS distribution in column web at different heights Stg. 01-04 Case 7C1

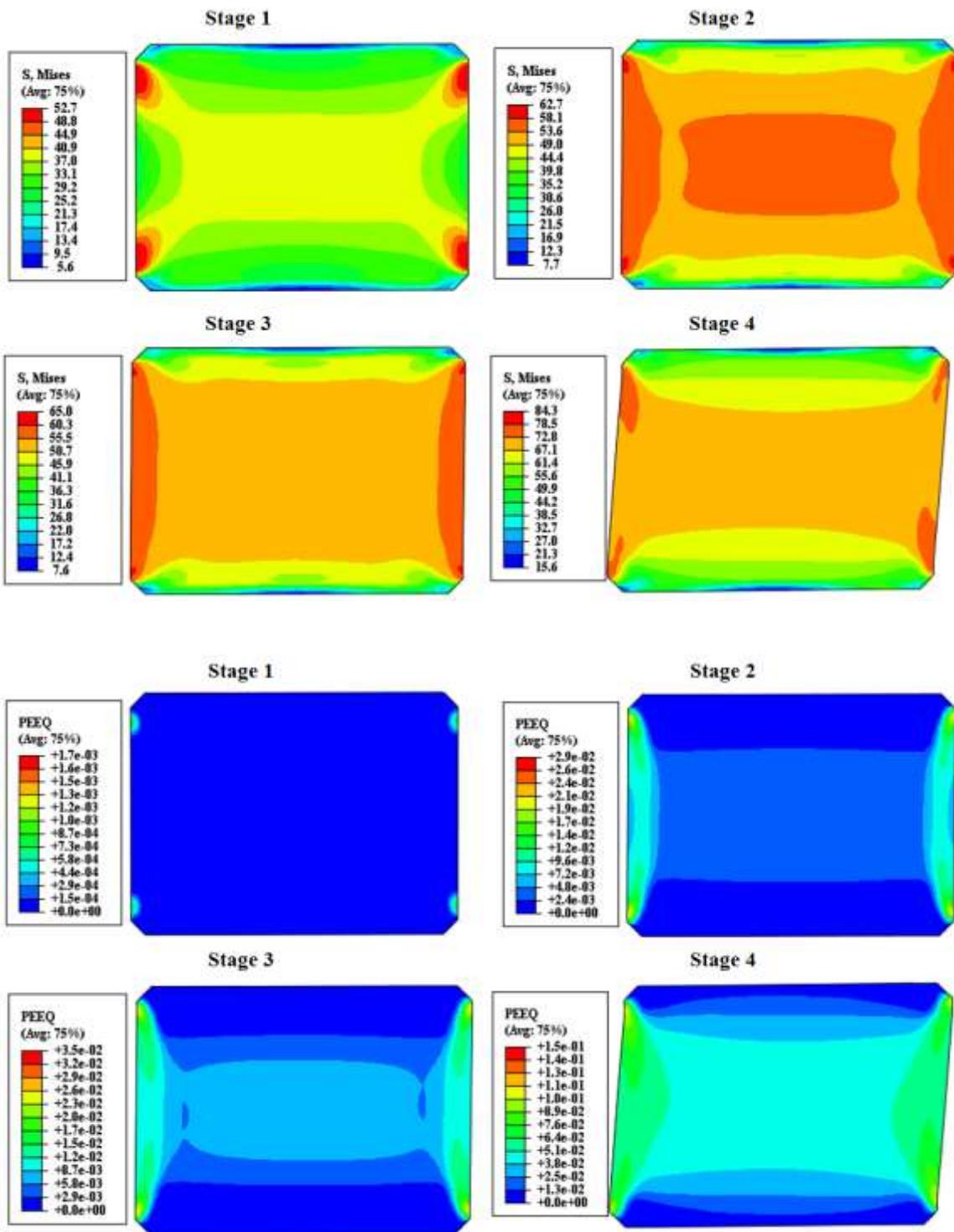


Figure 5.67: VMS and PEEQ in the DP Case 7C1



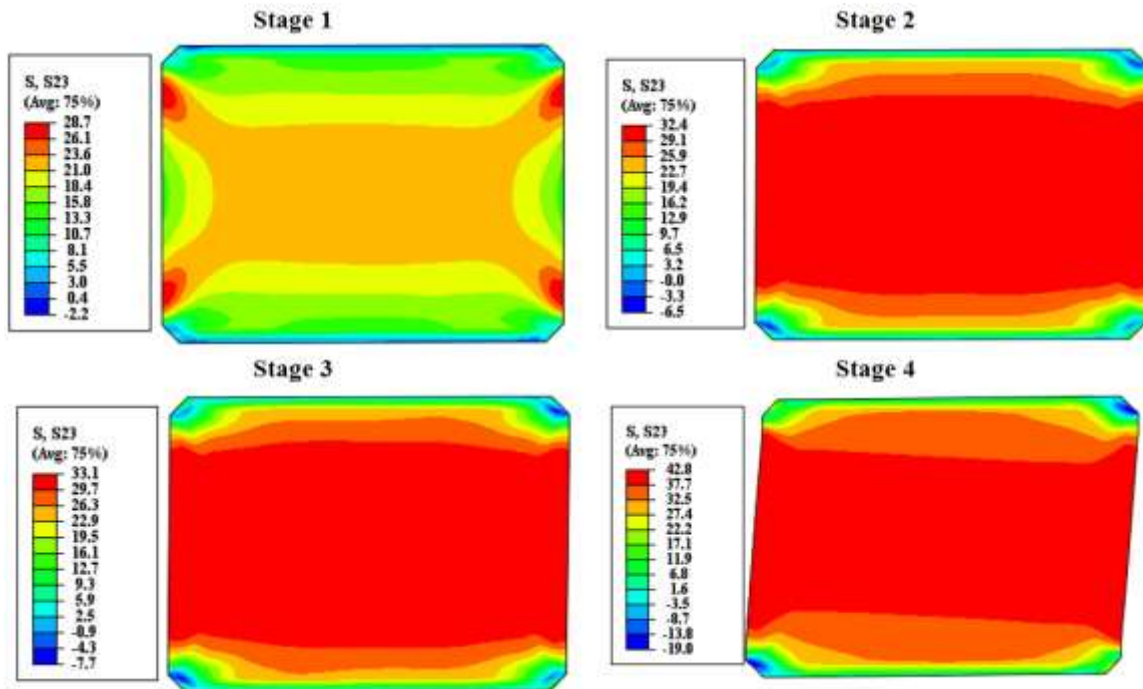


Figure 5.68: Shear stress, S23 in the DP Case 7C1

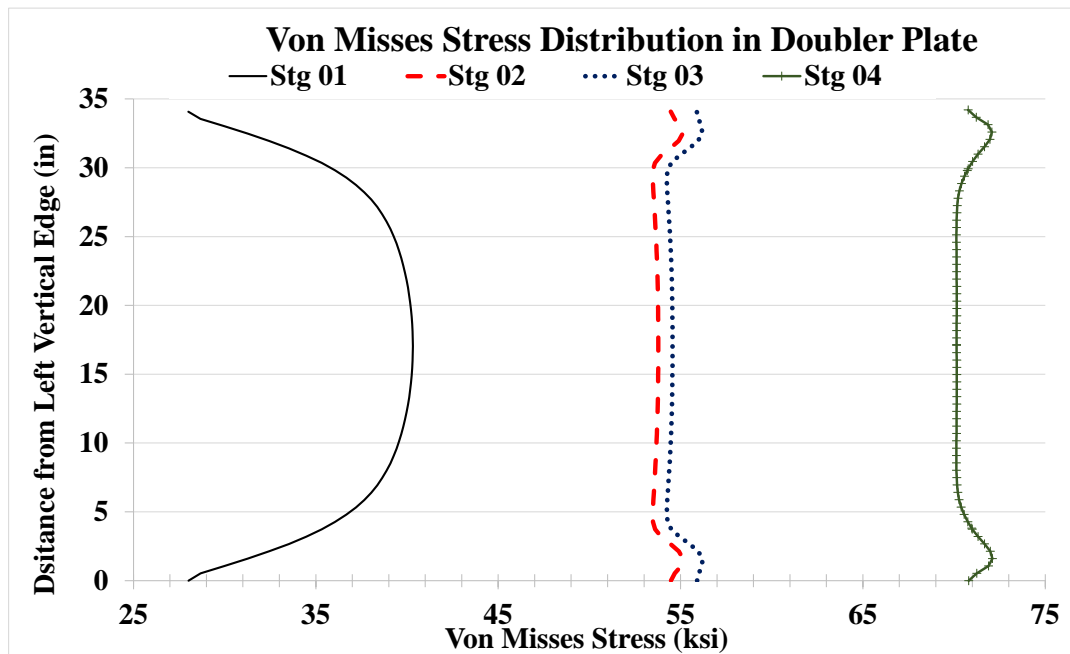


Figure 5.69: VMS distribution at mid-depth of DP Case 7C1

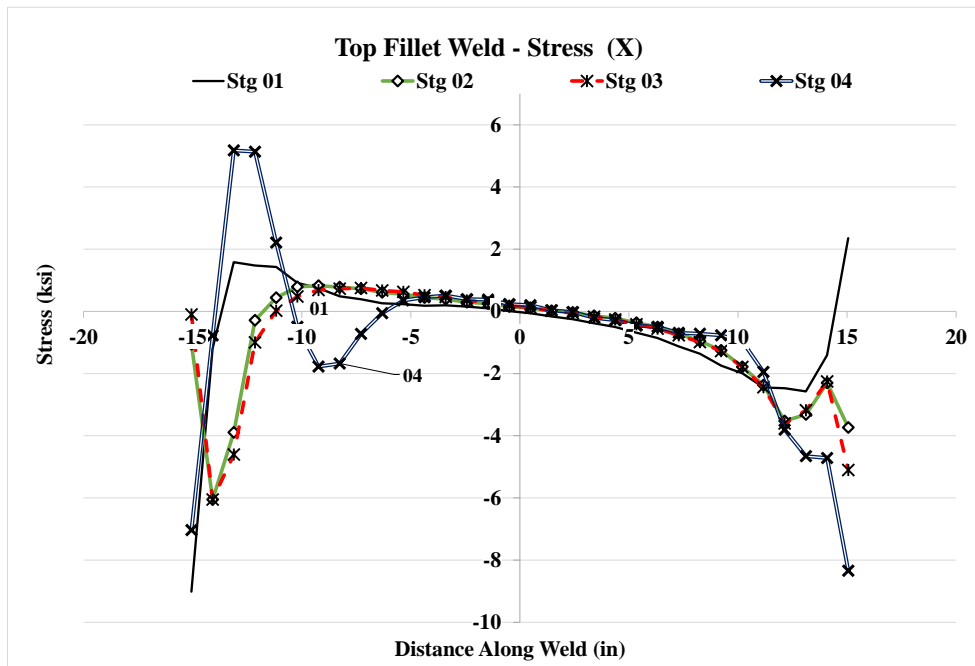
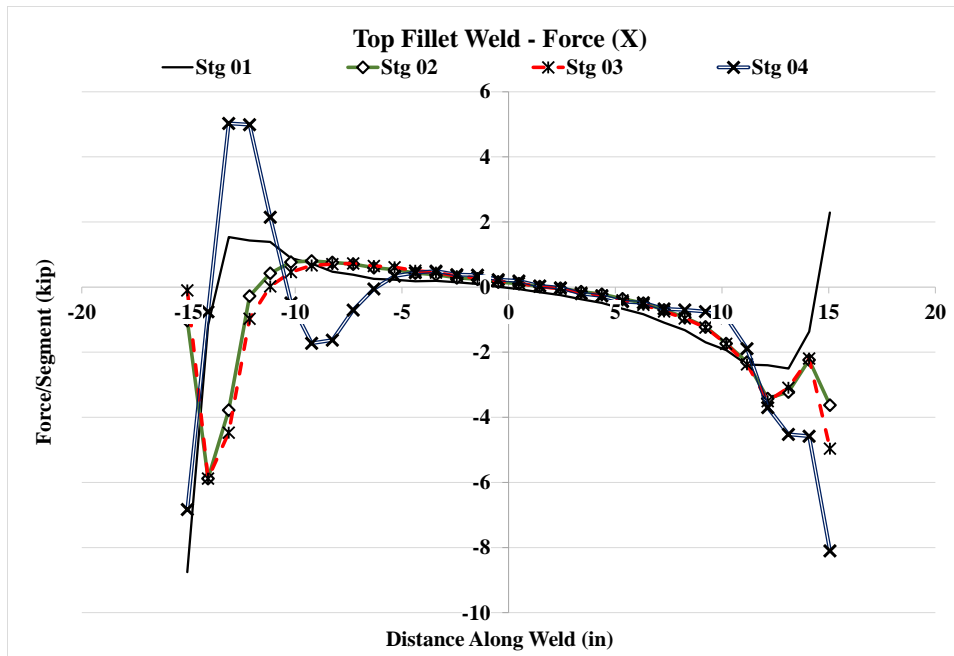


Figure 5.70: Forces and stresses in horizontal weld, (X) Case 7C1

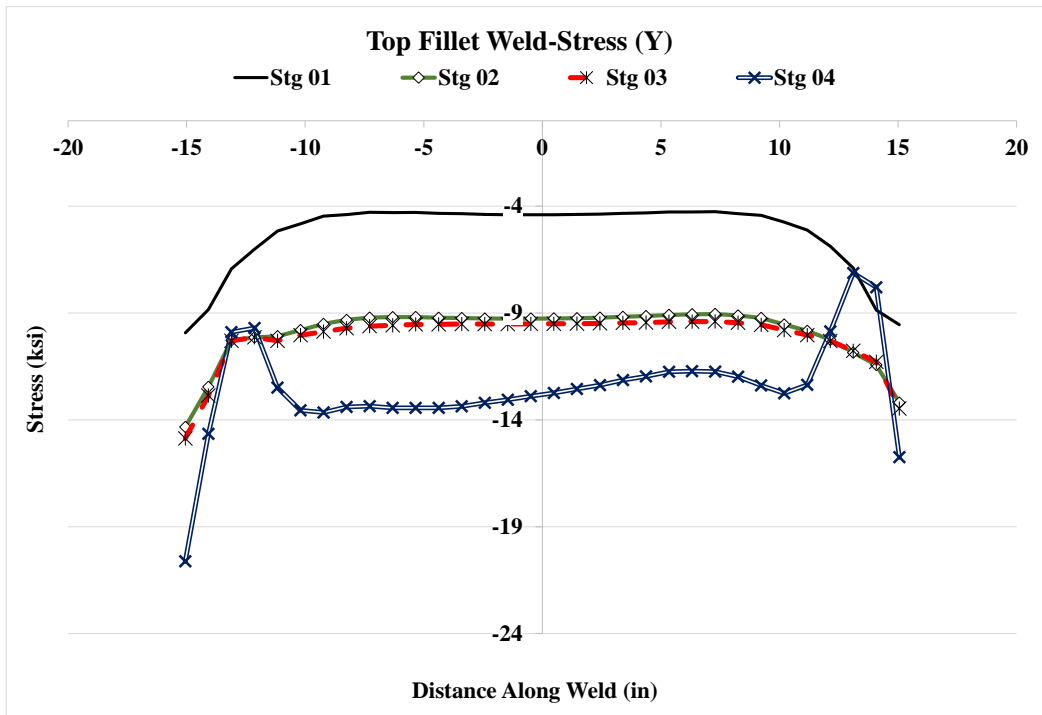
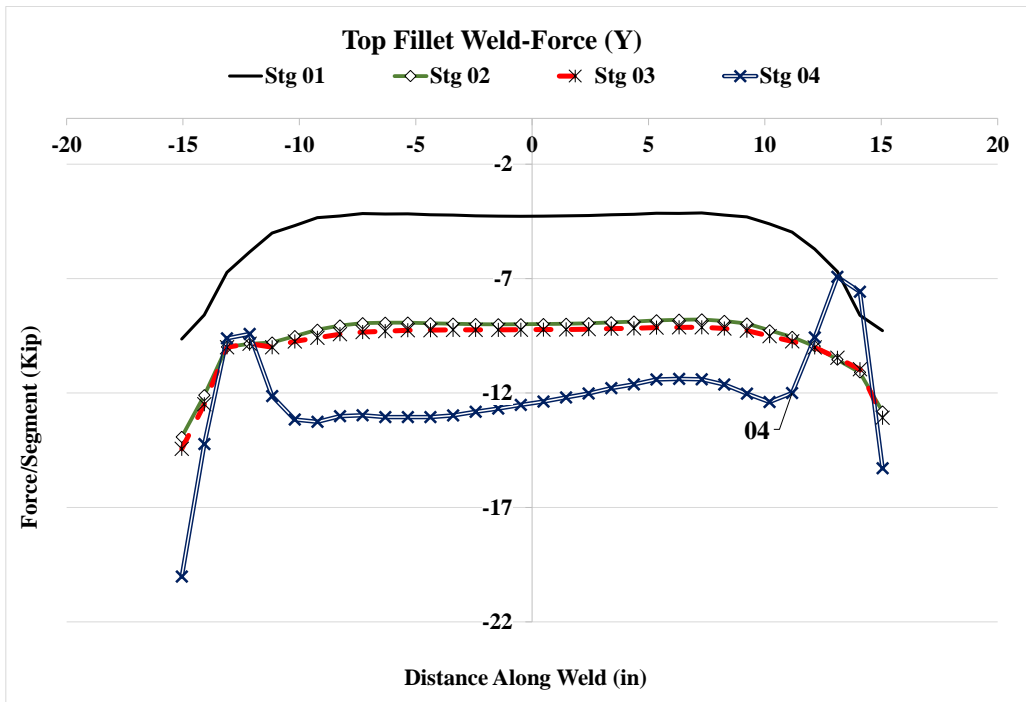


Figure 5.71: Forces and stresses in horizontal weld, (Y) Case 7C1

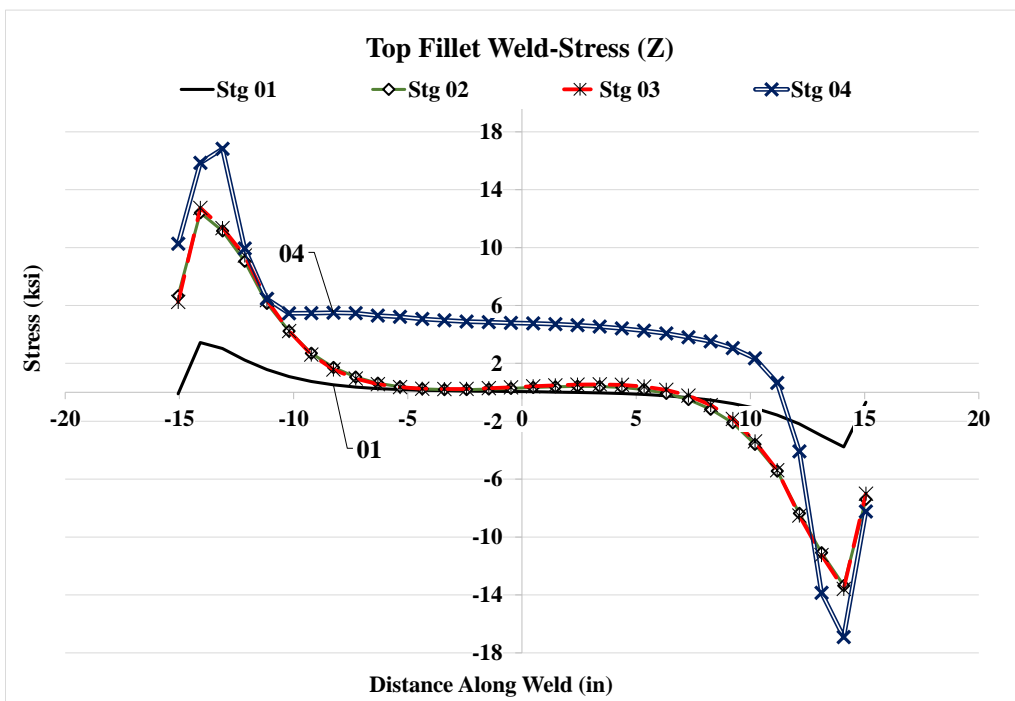
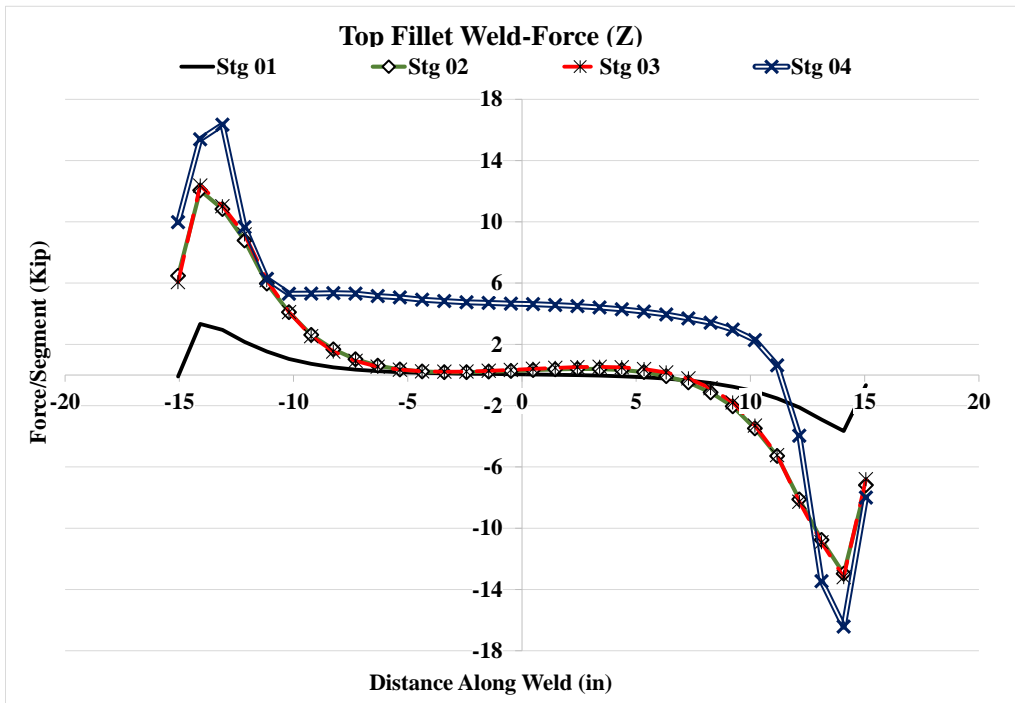


Figure 5.72: Forces and stresses in horizontal weld, (Z) Case 7C1

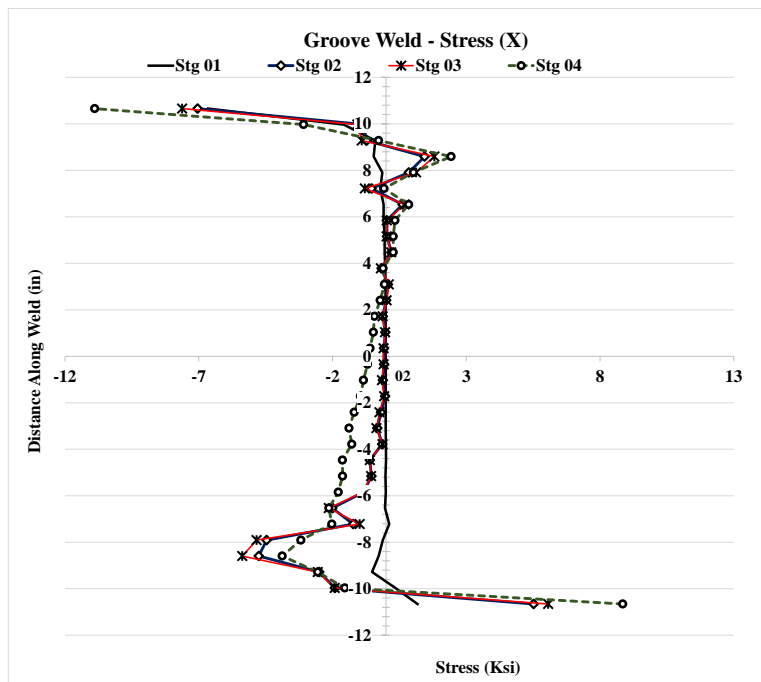
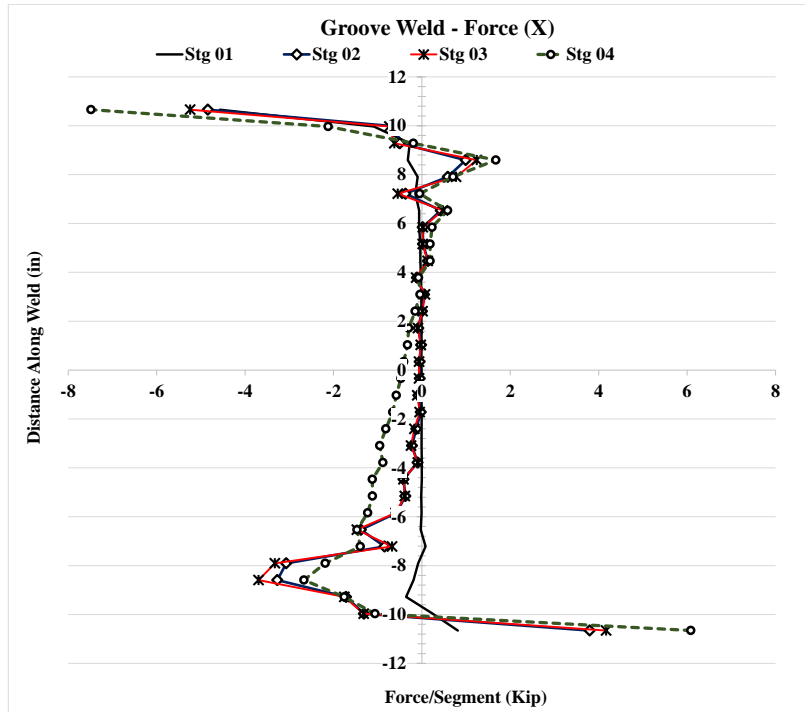


Figure 5.73: Forces and stresses in vertical weld, (X) Case 7C1

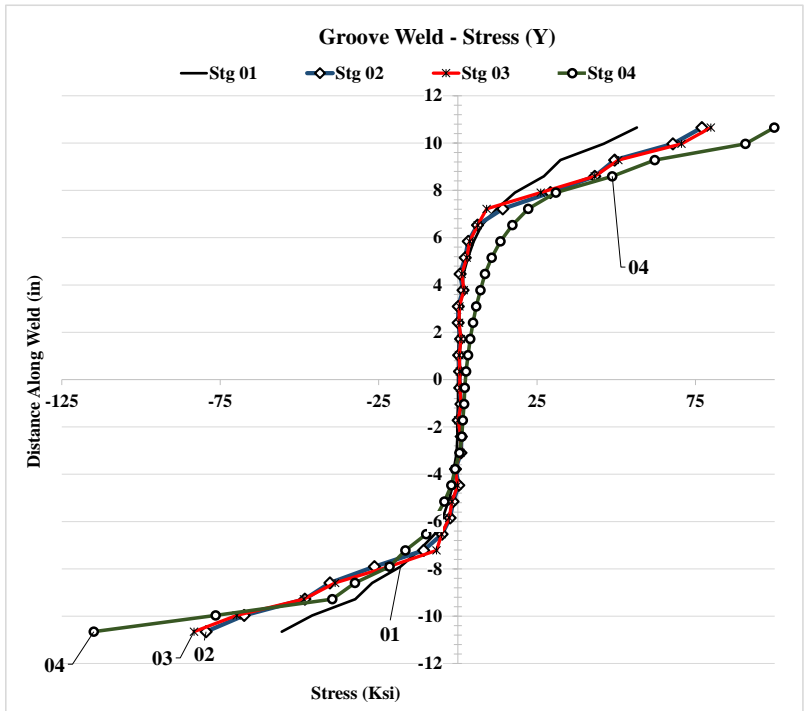
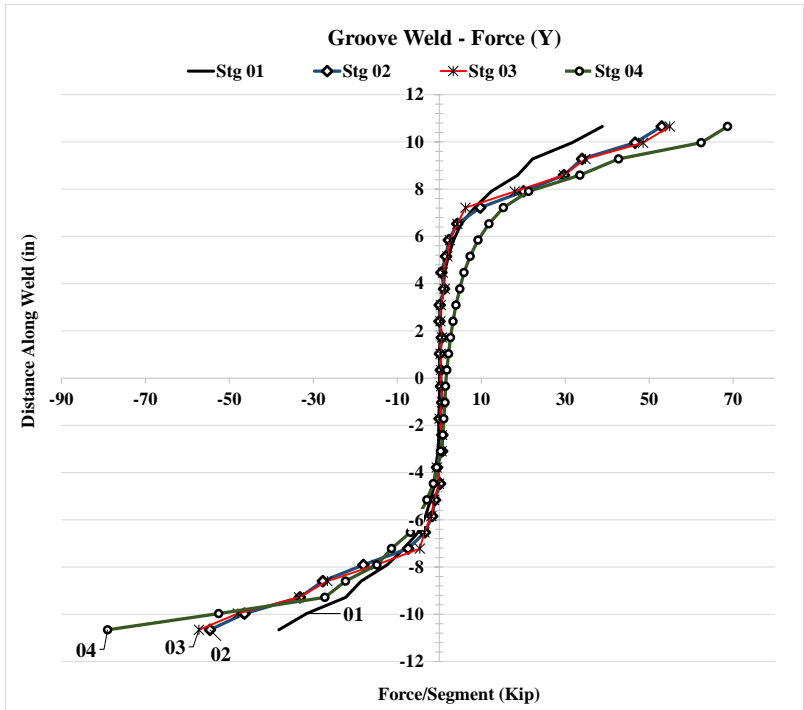


Figure 5.74: Forces and stresses in vertical weld, (Y) Case 7C1

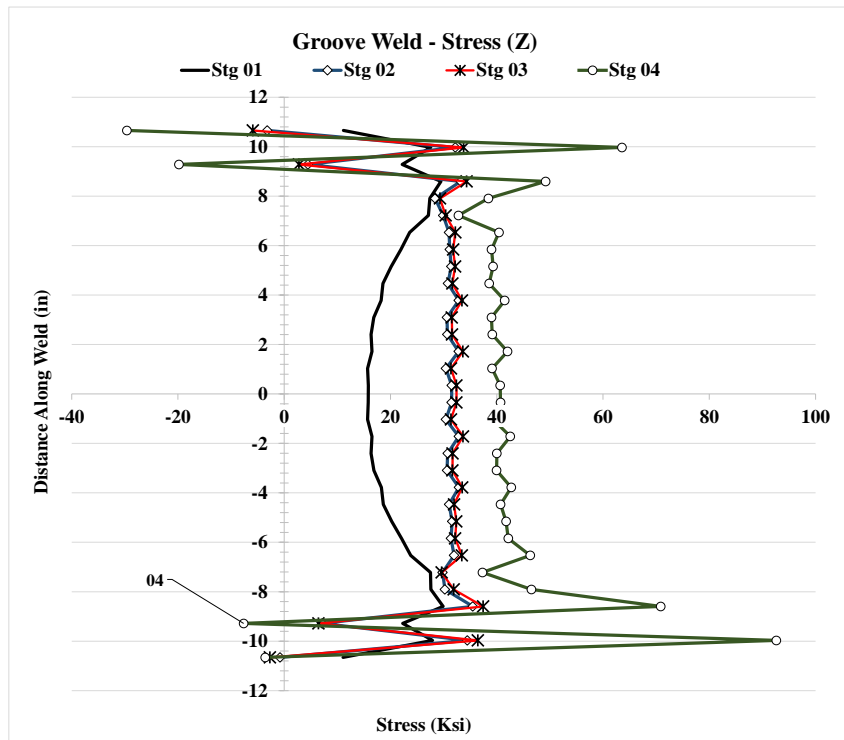
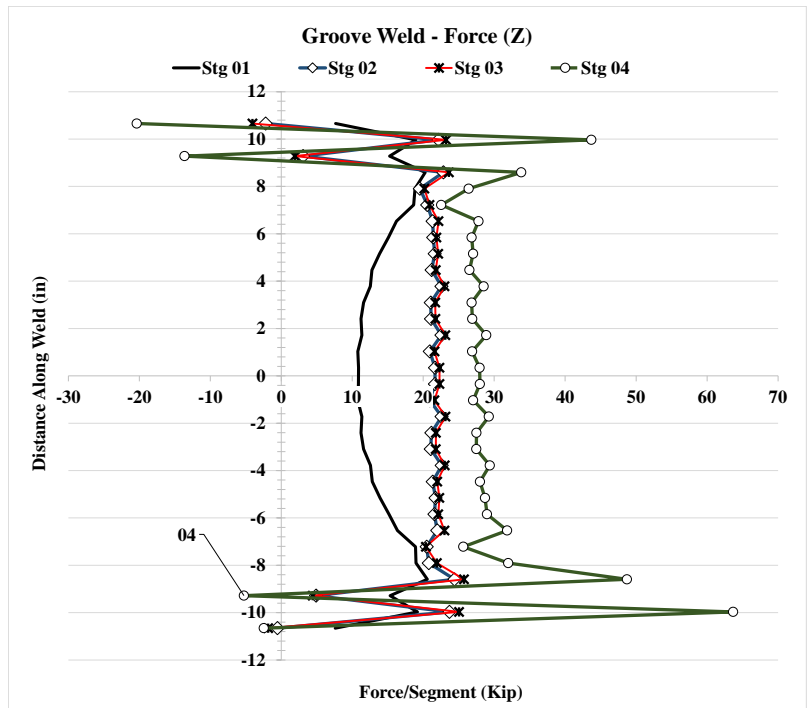


Figure 5.75: Forces and stresses in vertical weld, (X) Case 7C1

### 5.2.8 Analysis Case 8A

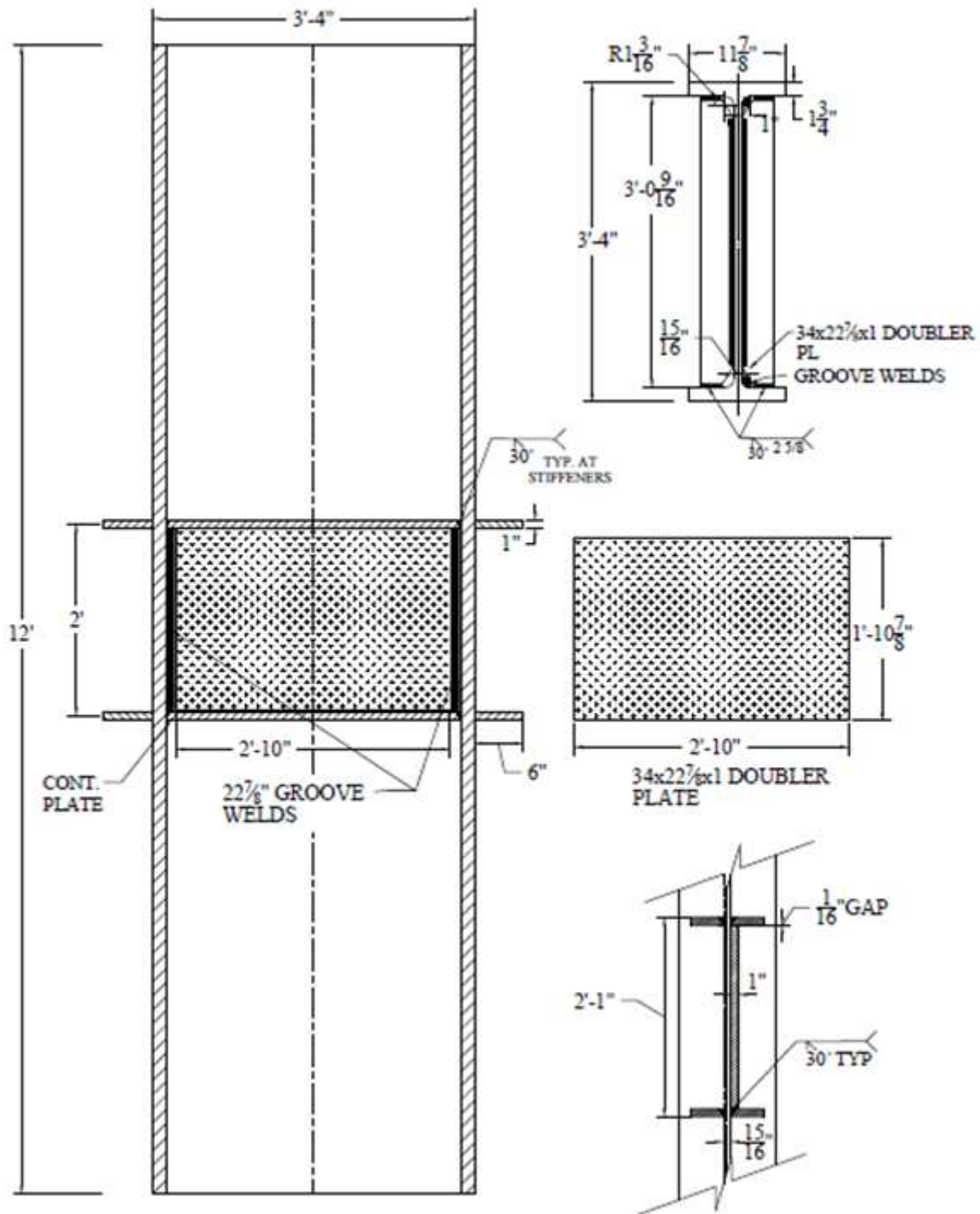


Figure 5.76: W40x264 Analysis case 8A



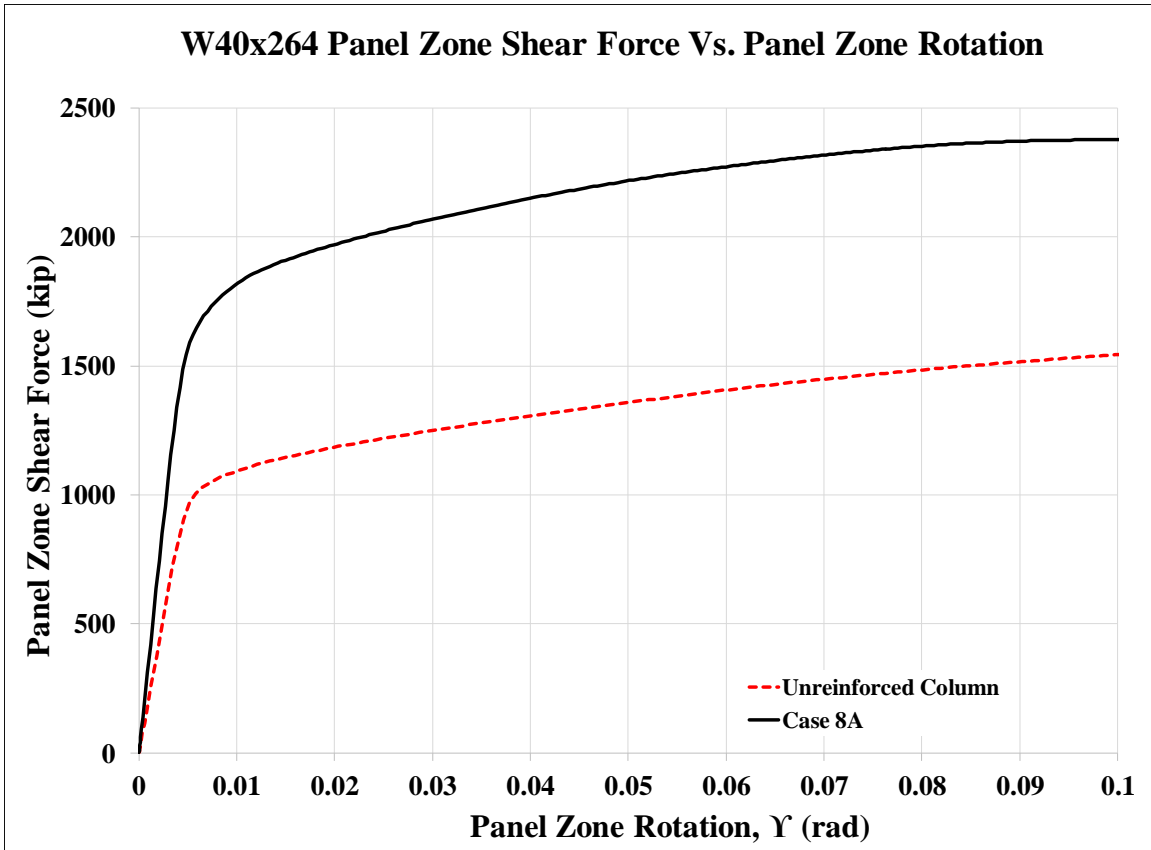


Figure 5.77: Panel zone shear vs. panel zone rotation Case 8A

Stage	Applied Force/Loading Plate (Kip)	Panel Shear Force (Kip)	% Higher Than Unreinforced Col.	Panel Zone Rotation (rad)
1	926	1,544	159%	0.005
2	1,164	1,941	172%	0.017
3	1,184	1,974	166%	0.020
4	1,426	2,377	154%	0.100

Table 5.9: Panel zone shear and force on loading plate Case 8A

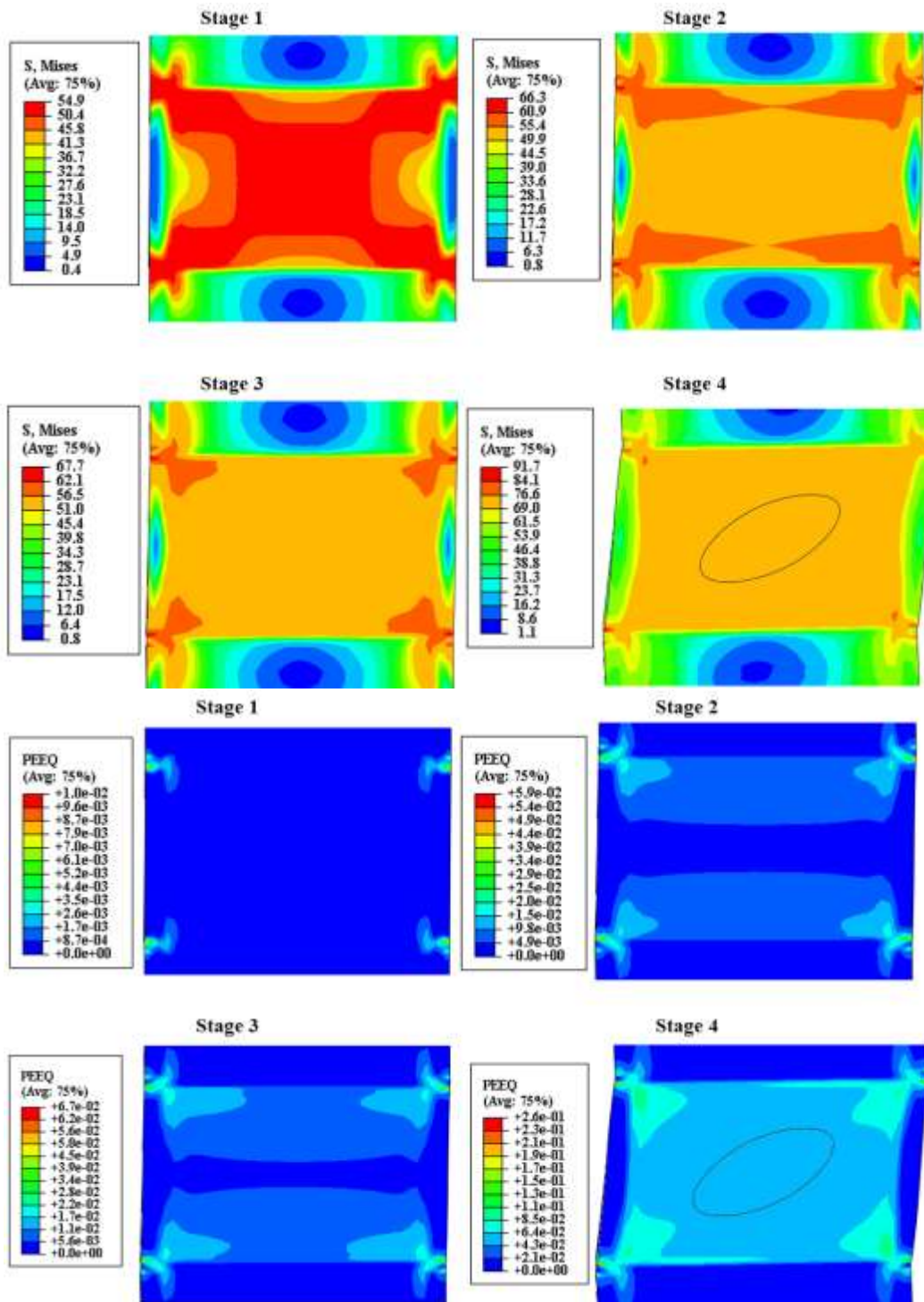


Figure 5.78: VMS and PEEQ in the column Case 8A

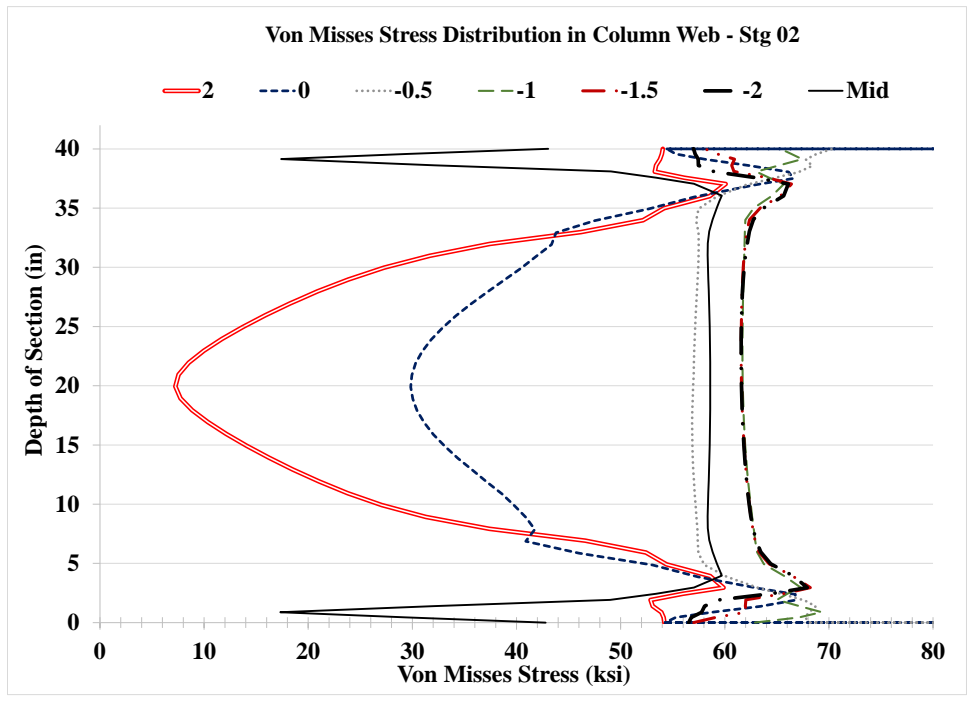
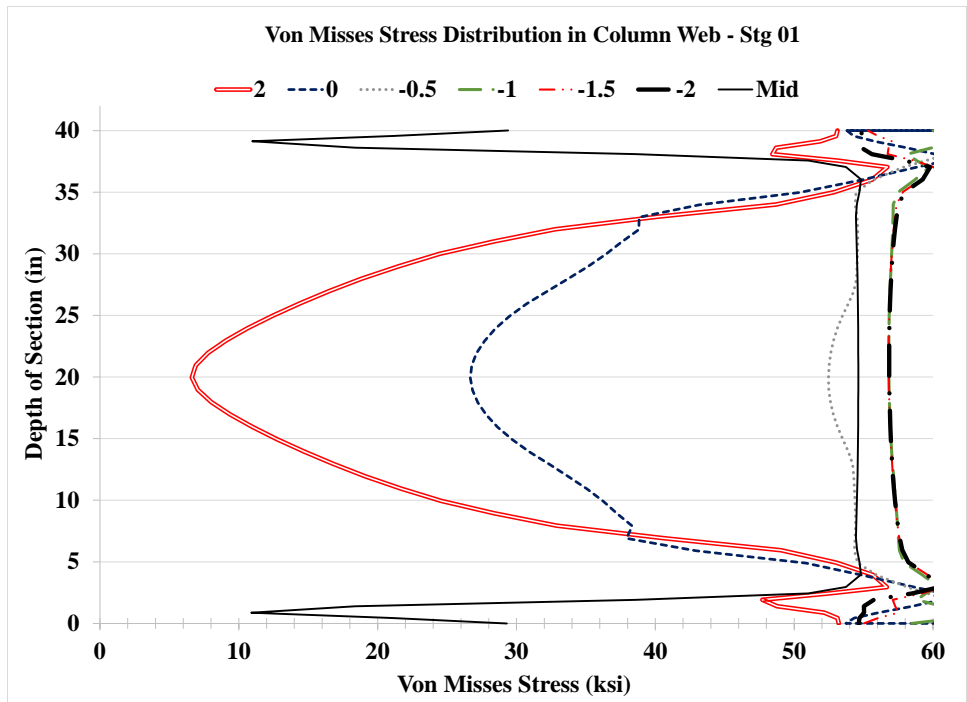


Figure 5.79: VMS distribution in column web at different heights Stg. 01-04 Case 8A

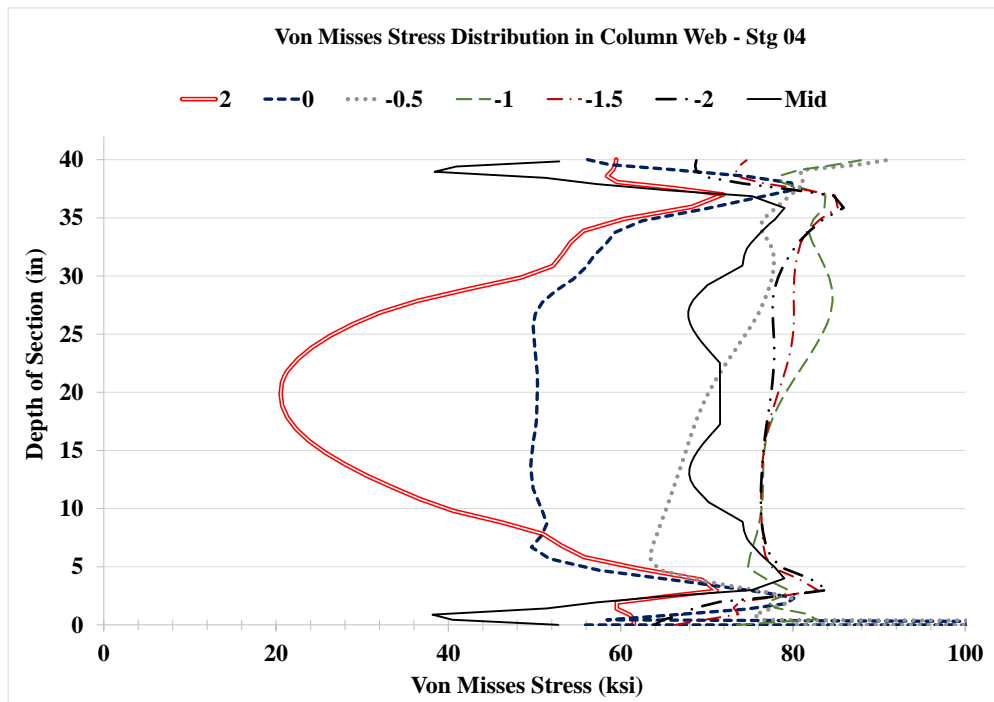
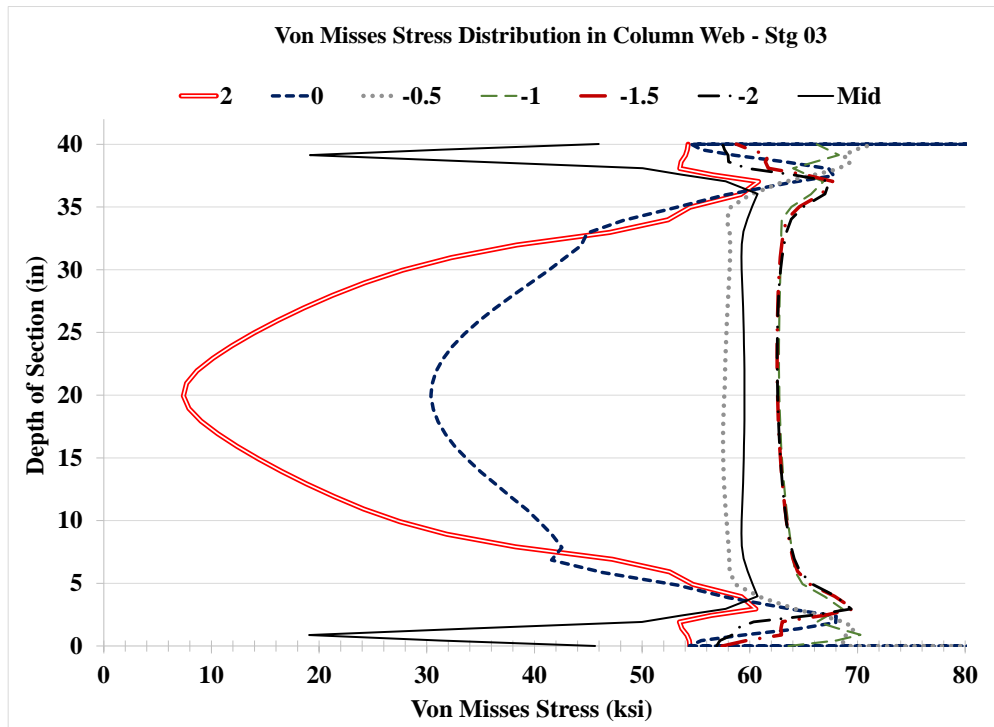


Figure 5.79: VMS distribution in column web at different heights Stg. 01-04 Case 8A

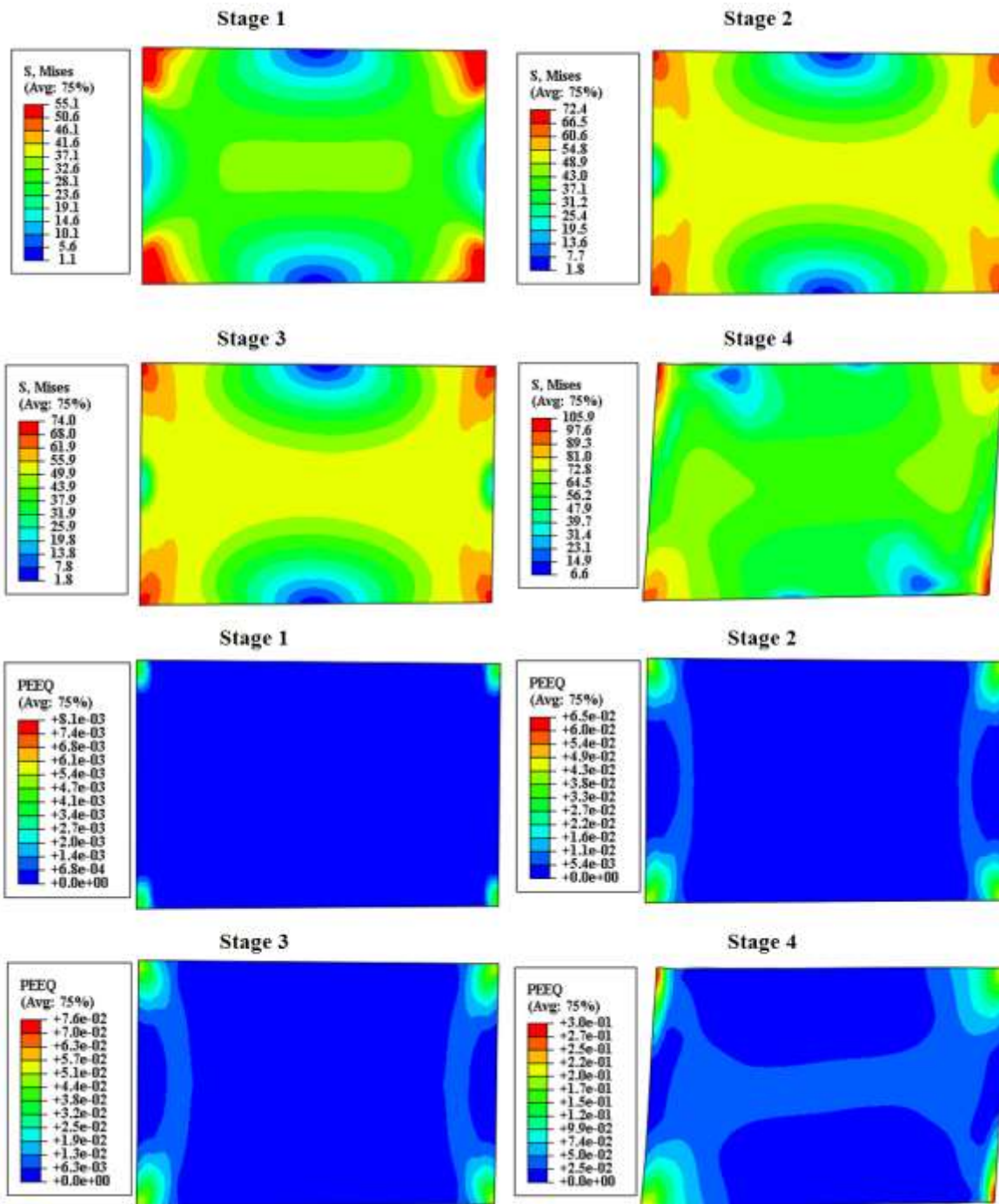


Figure 5.80: VMS and PEEQ in the DP Case 8A

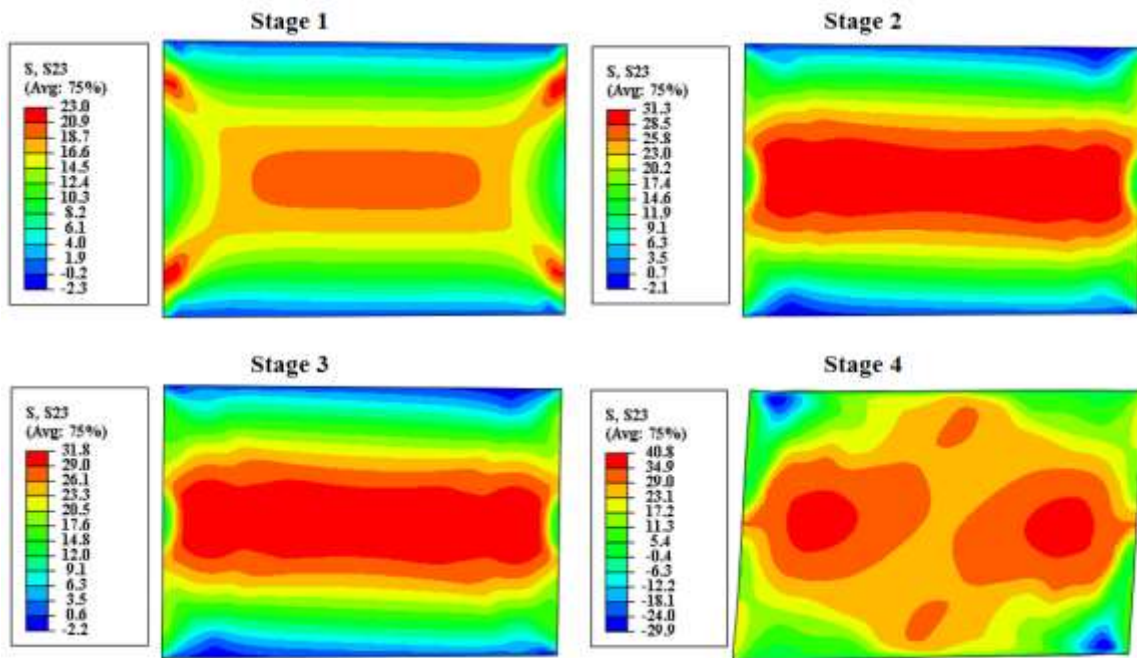


Figure 5.81: Shear stress, S23 in the DP Case 8A

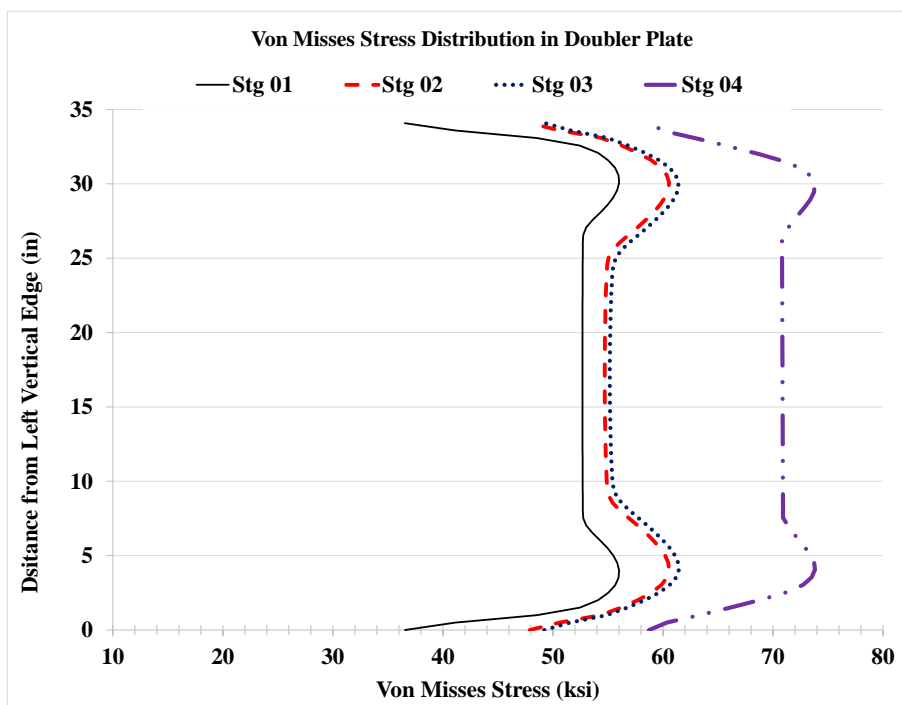


Figure 5.81: VMS distribution at mid-depth of DP Case 8A

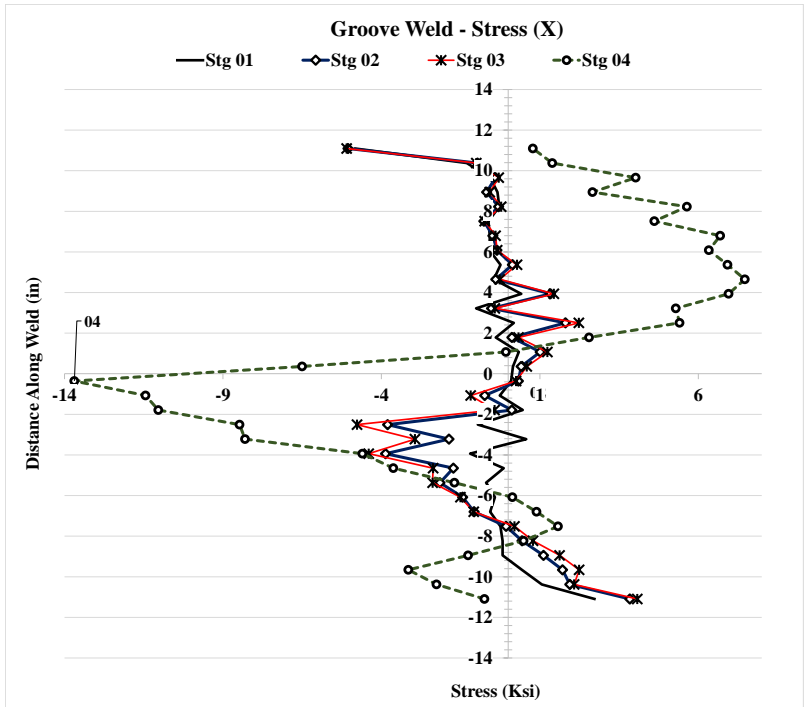
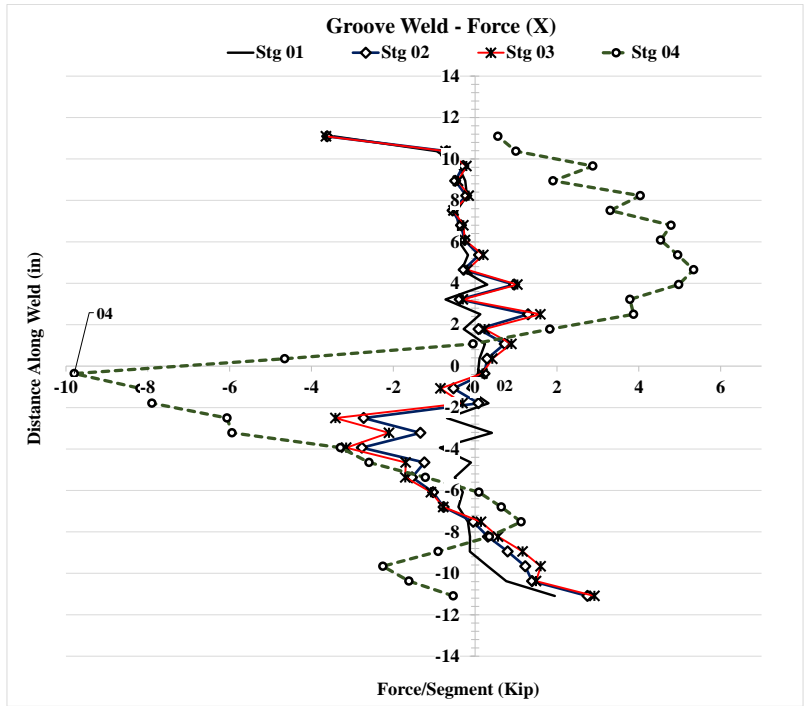


Figure 5.82: Forces and stresses in vertical weld, (X) Case 8A

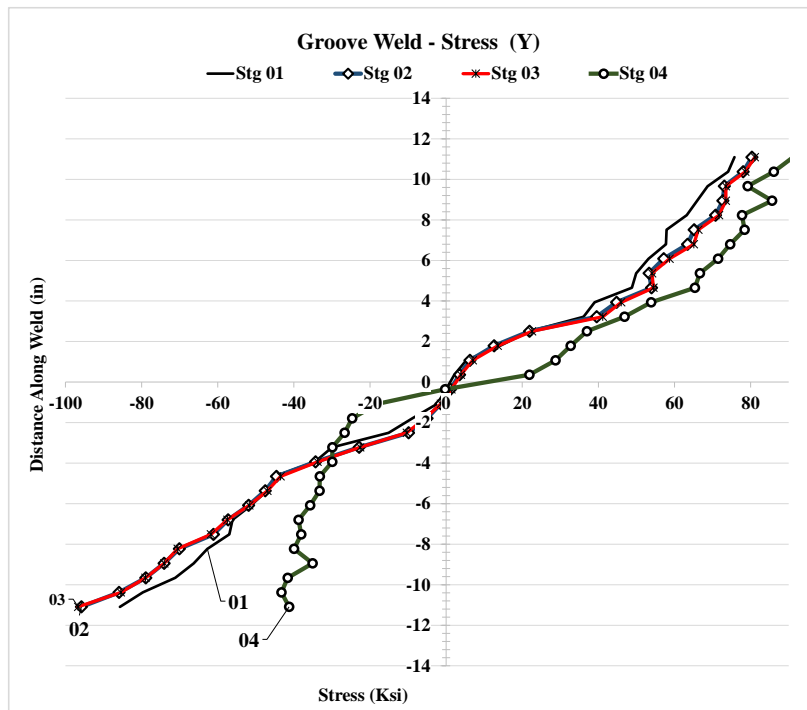
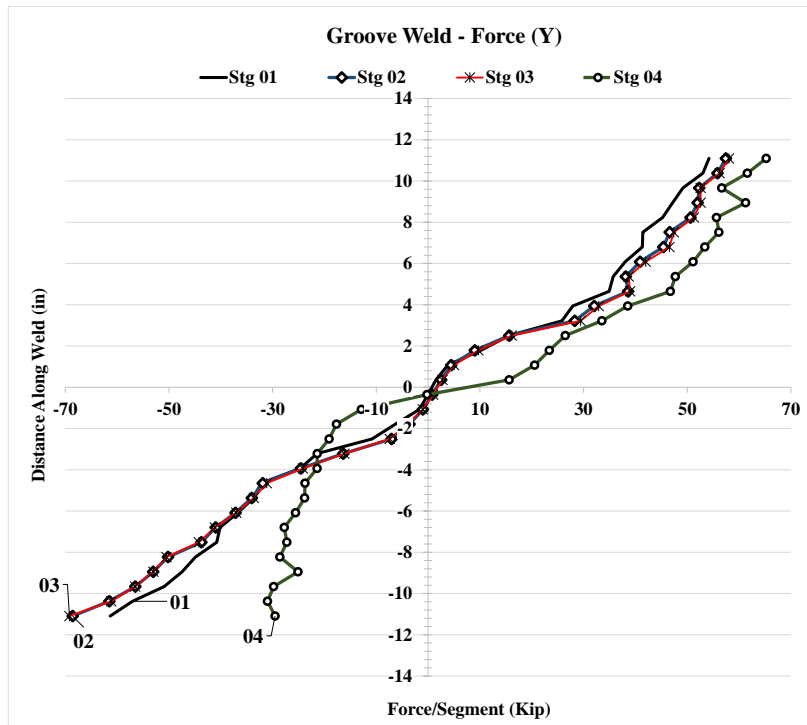


Figure 5.83: Forces and stresses in vertical weld, (Y) Case 8A



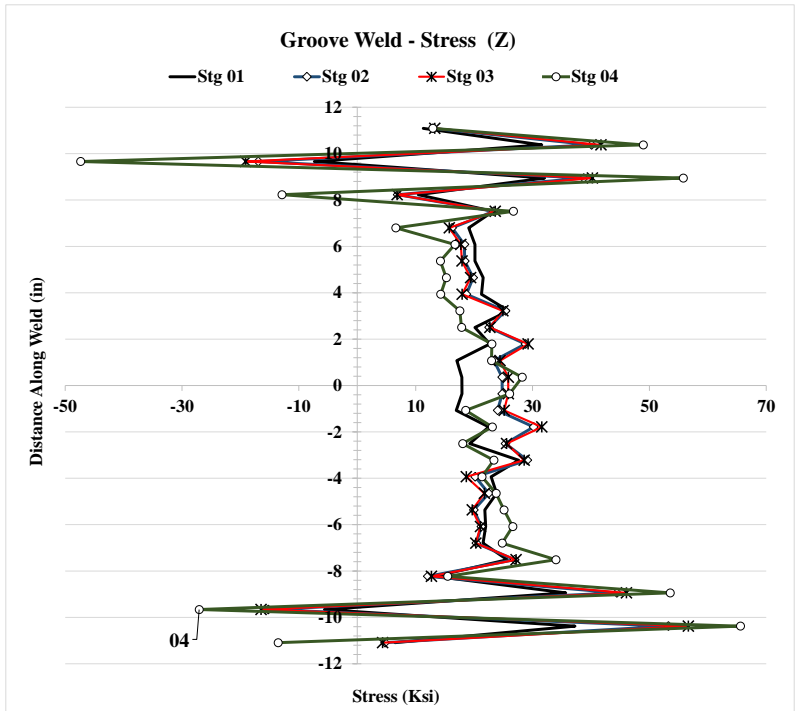
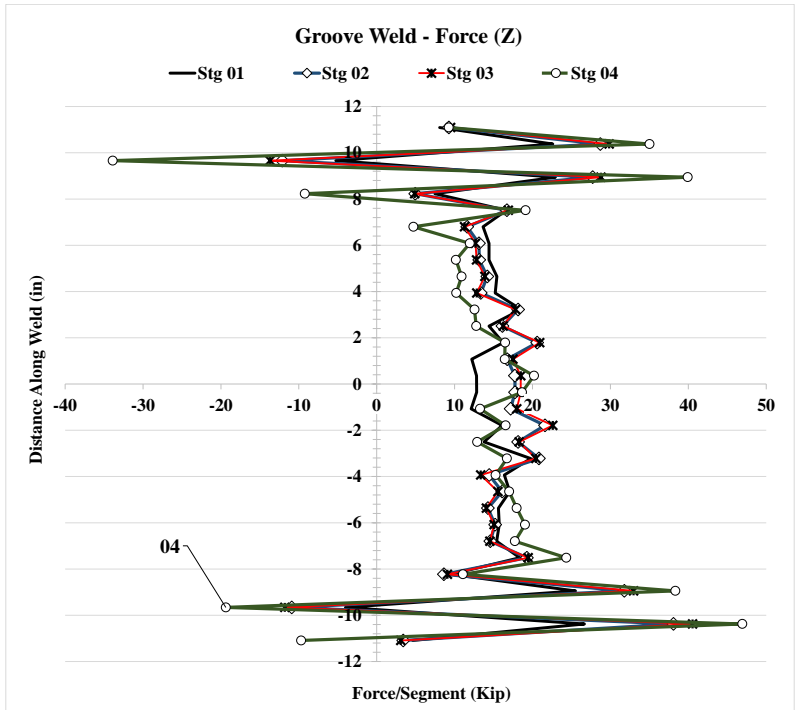


Figure 5.84: Forces and stresses in vertical weld, (Z) Case 8A

### 5.2.9 Analysis Case 8A1

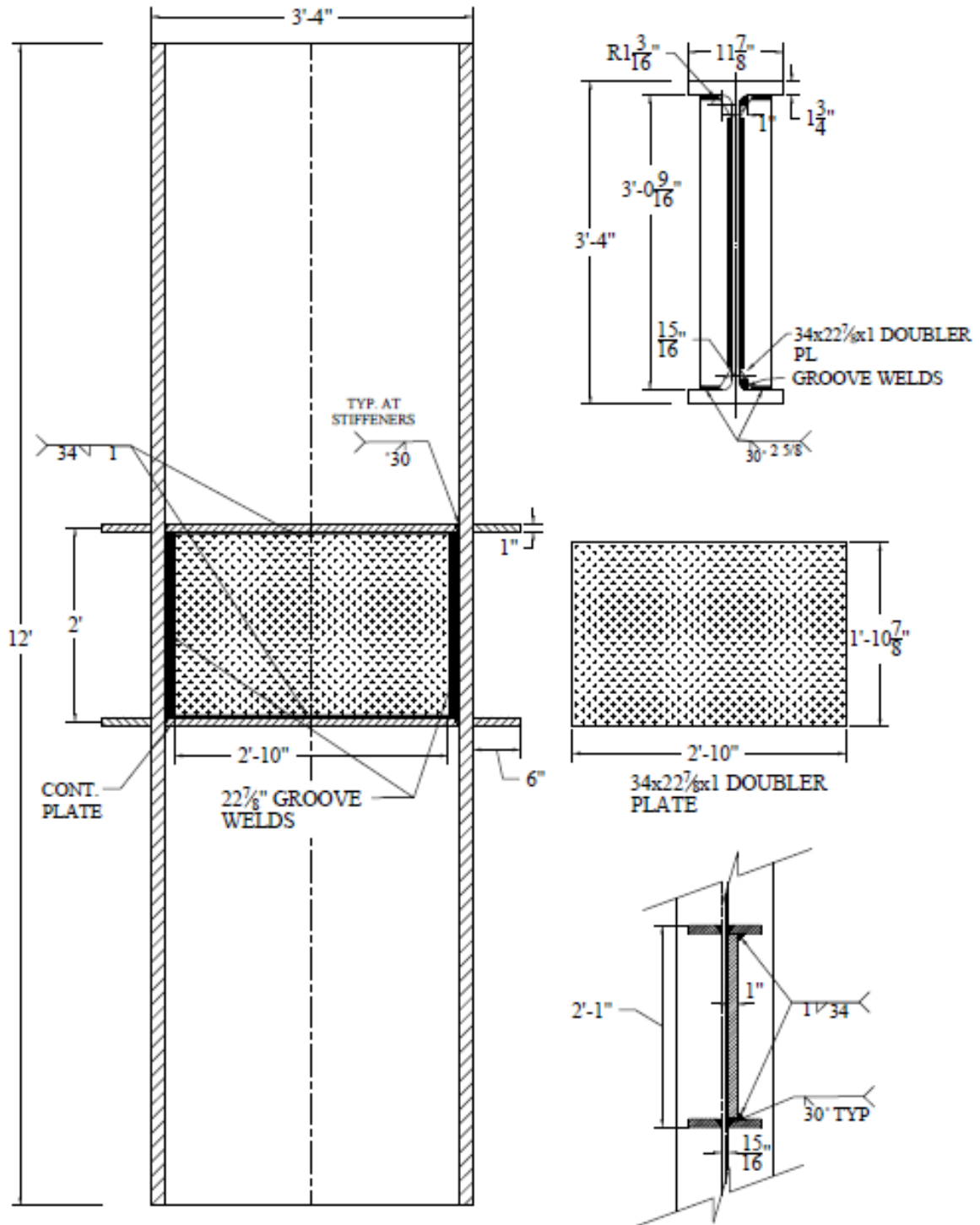


Figure 5.85: W40x264 Analysis case 8A1

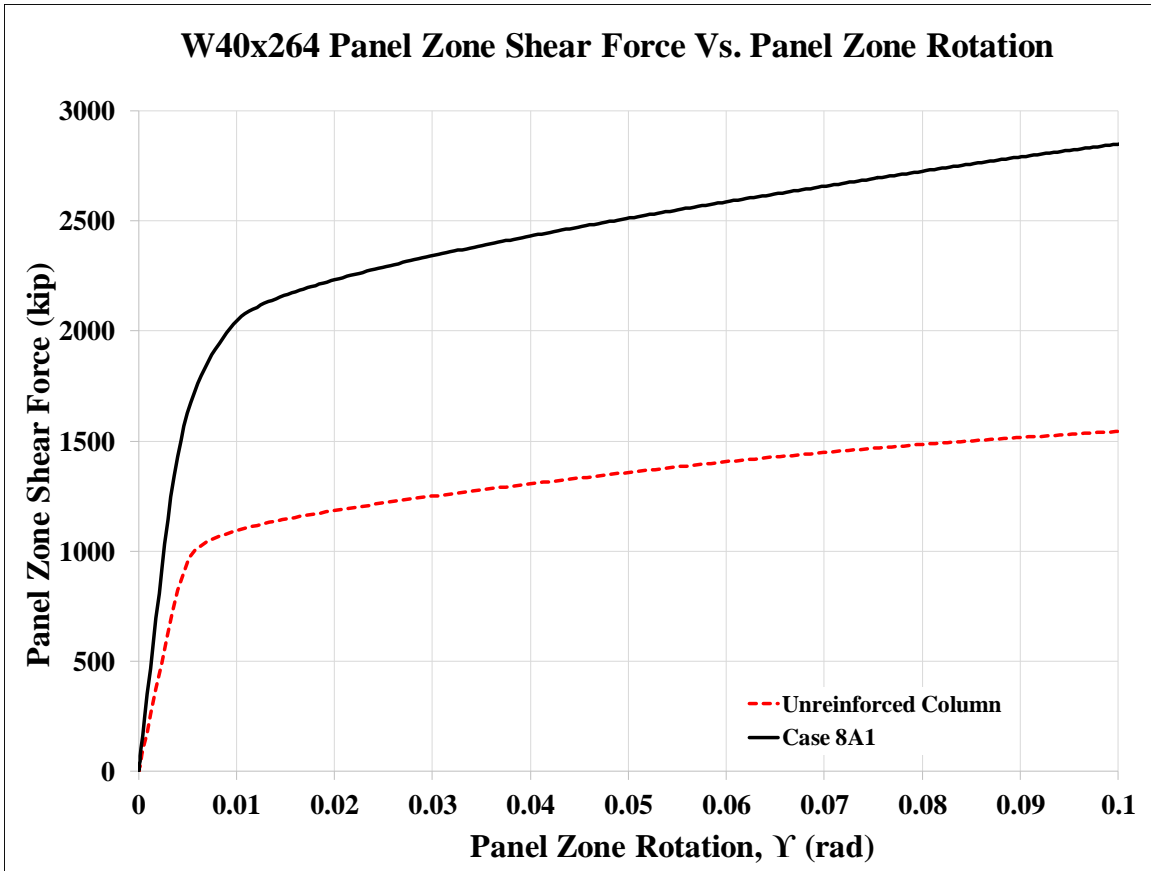


Figure 5.86: Panel zone shear vs. panel zone rotation Case 8A1

Stage	Applied Force/Loading Plate (Kip)	Panel Shear Force (Kip)	% Higher Than Unreinforced Col.	Panel Zone Rotation (rad)
1	941	1,568	162%	0.005
2	1,300	2,167	192%	0.015
3	1,340	2,233	188%	0.020
4	1,711	2,851	185%	0.100

Table 5.10: Panel zone shear and force on loading plate Case 8A1

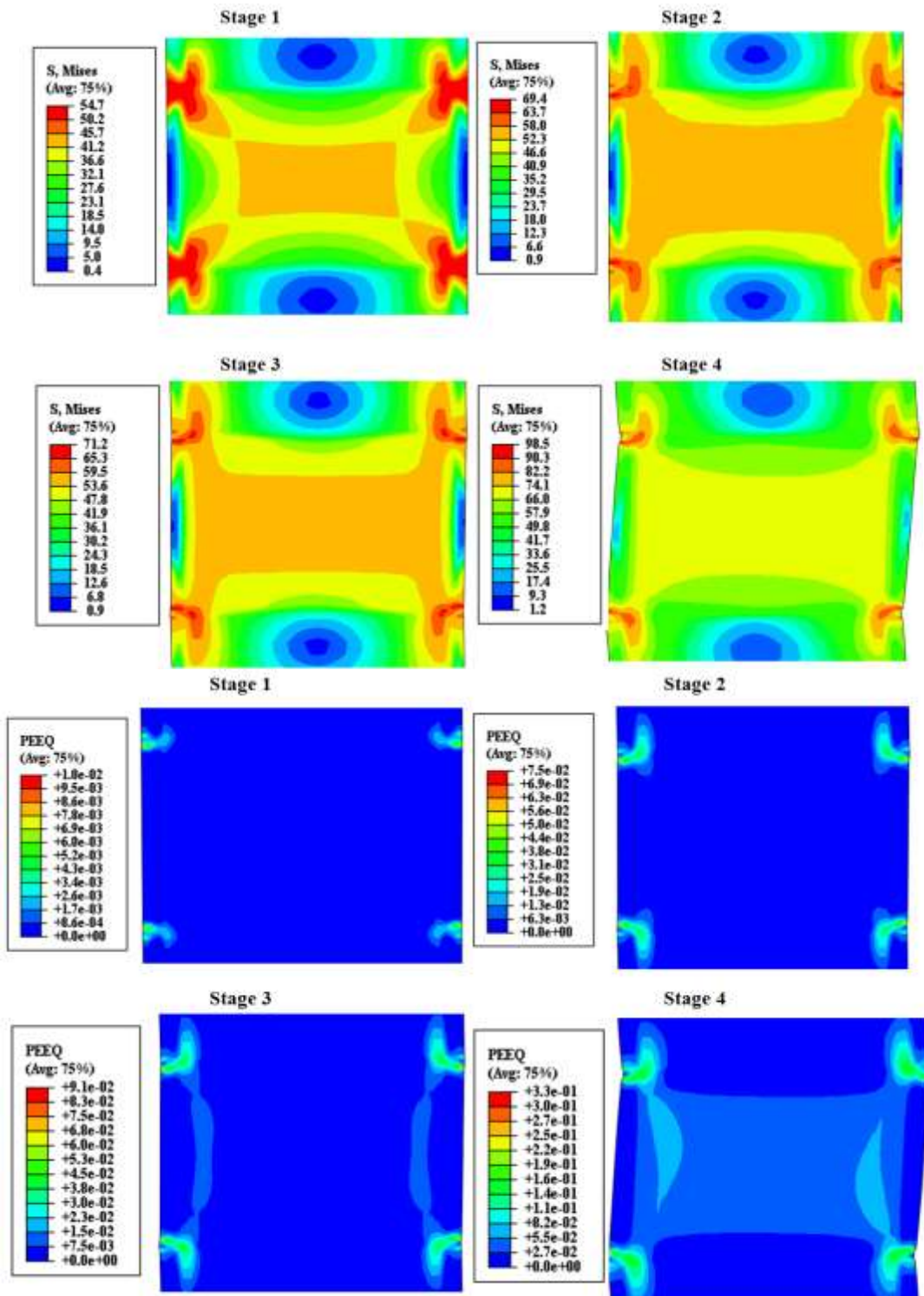


Figure 5.87: VMS and PEEQ in the column Case 8A1

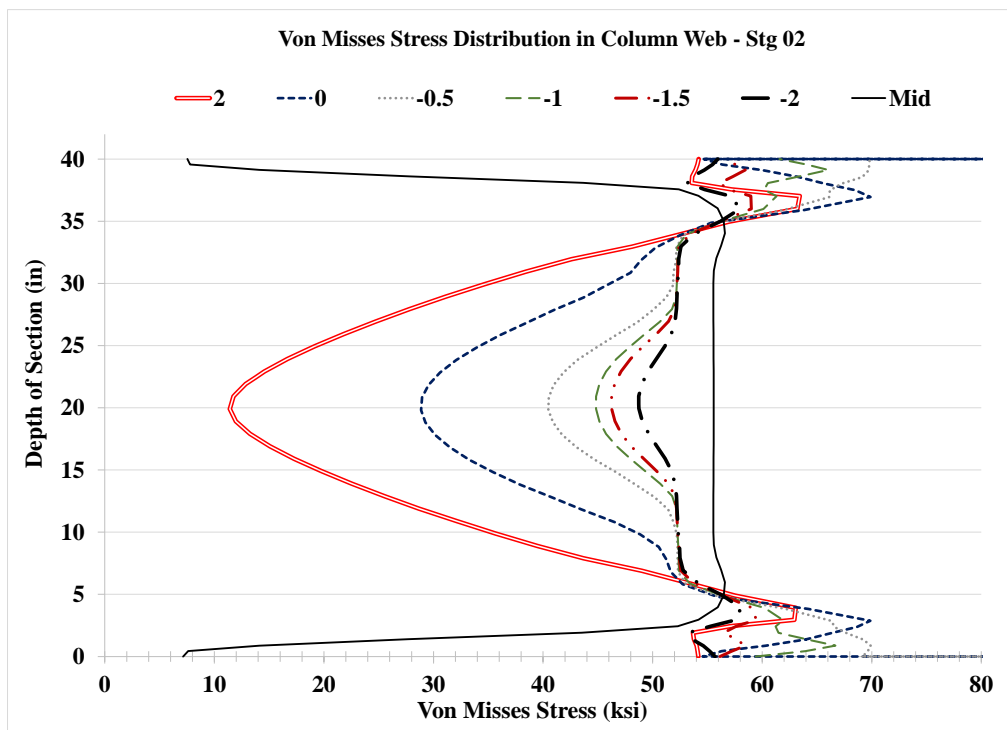
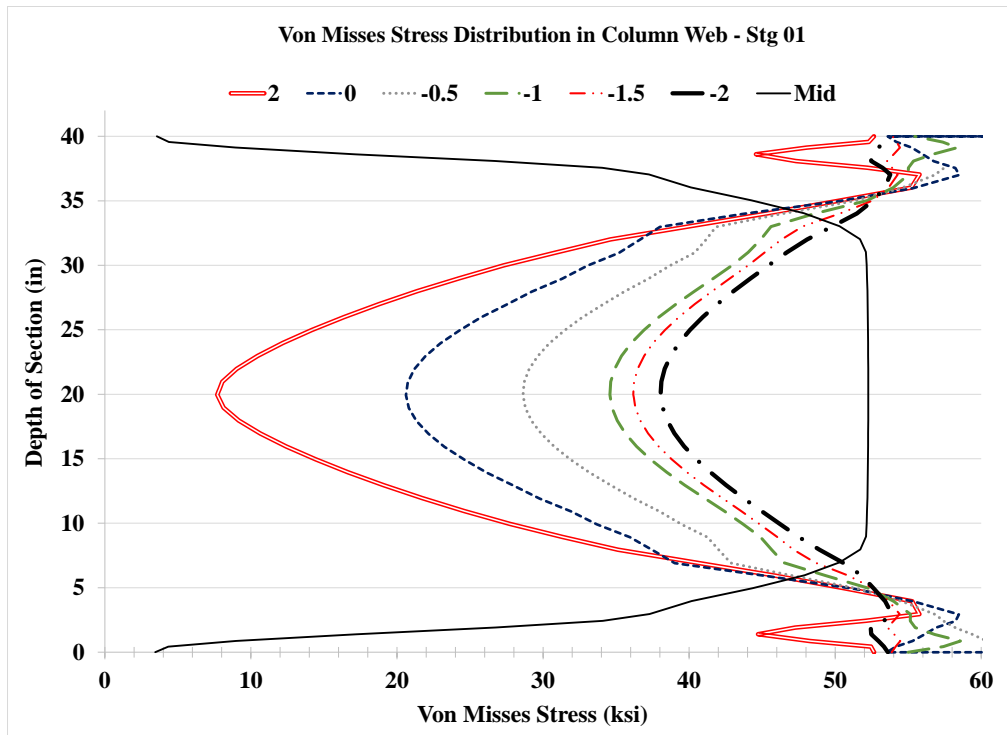


Figure 5.88: VMS distribution in column web at different heights Stg. 01-04 Case 8A1

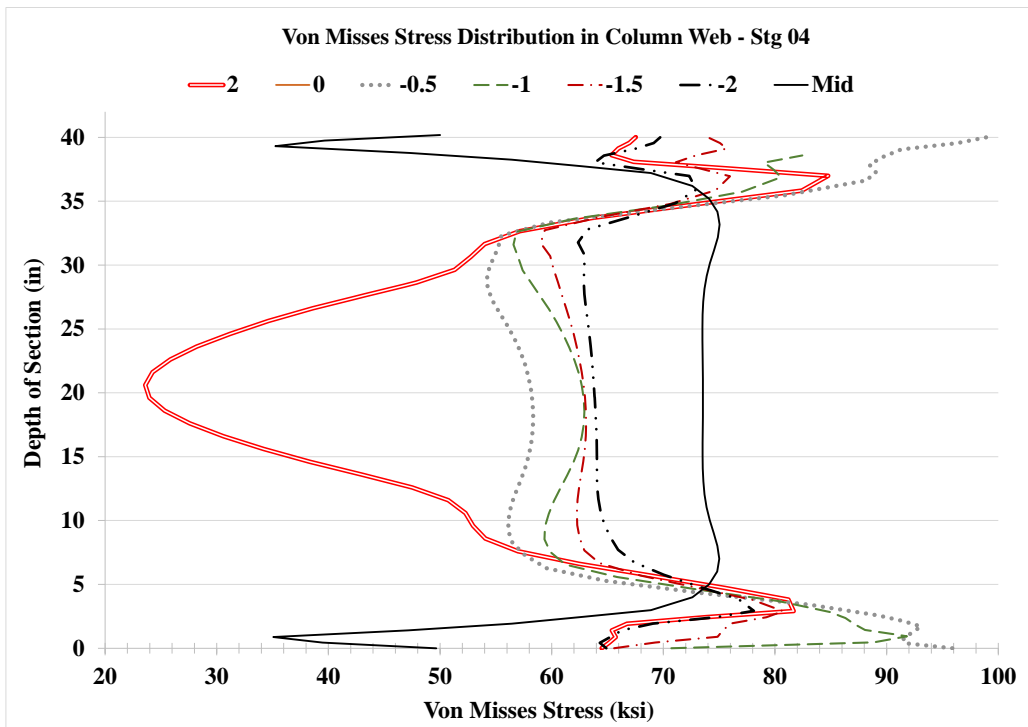
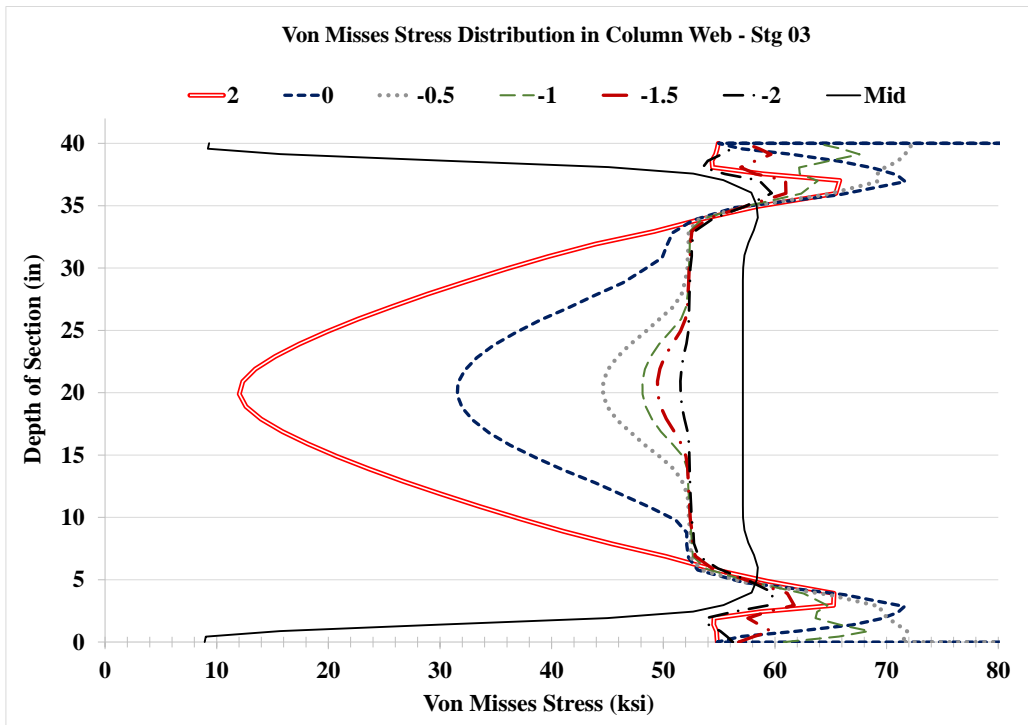


Figure 5.88: VMS distribution in column web at different heights Stg. 01-04 Case 8A1

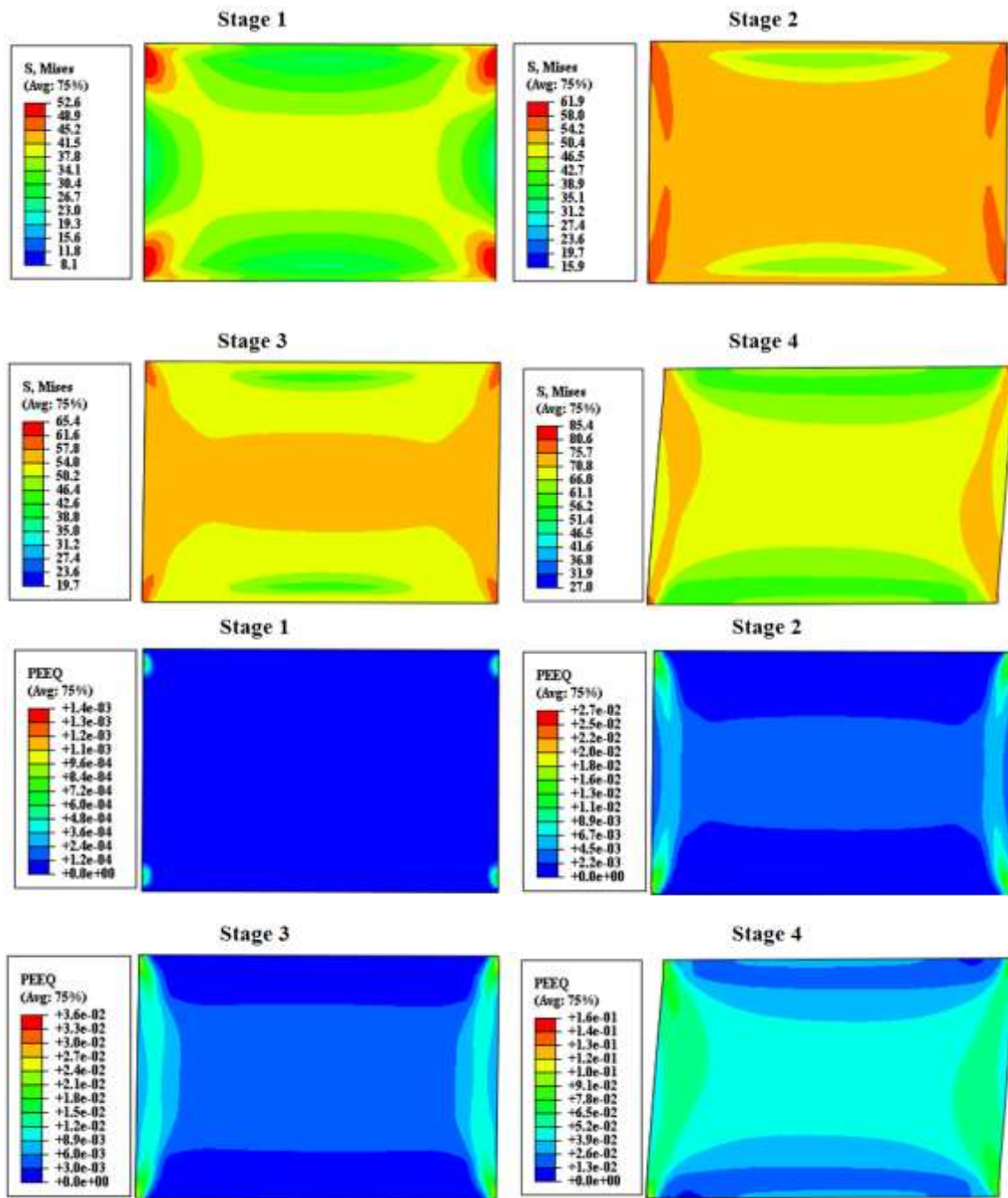


Figure 5.89: VMS and PEEQ in the DP Case 8A1

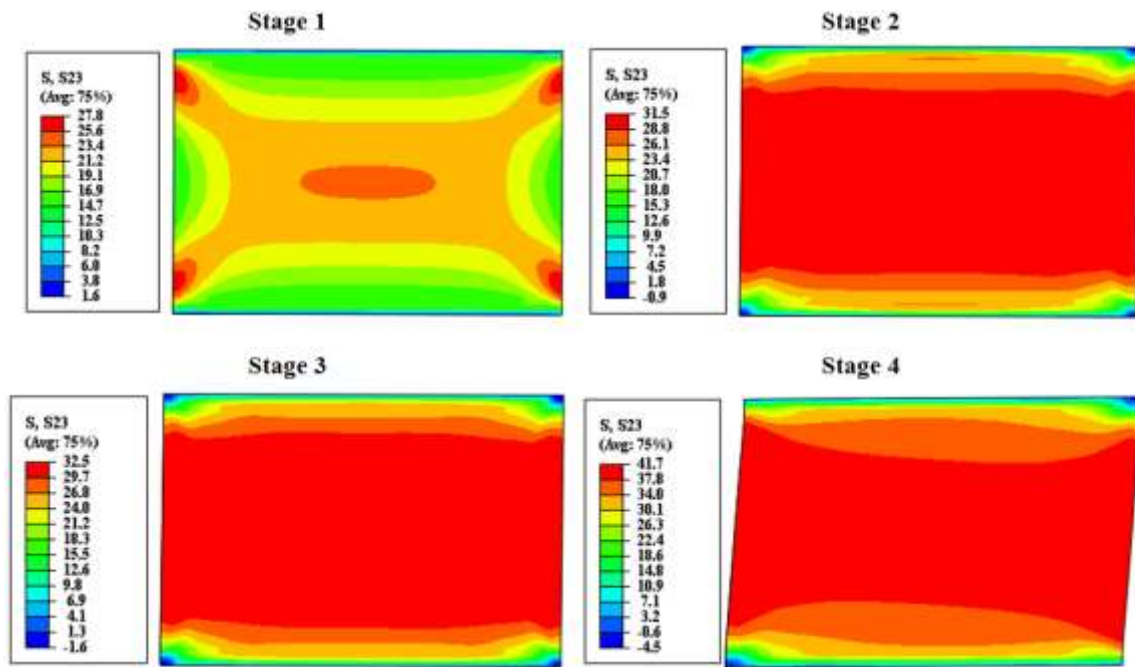


Figure 5.90: Shear stress, S23 in the DP Case 8A1

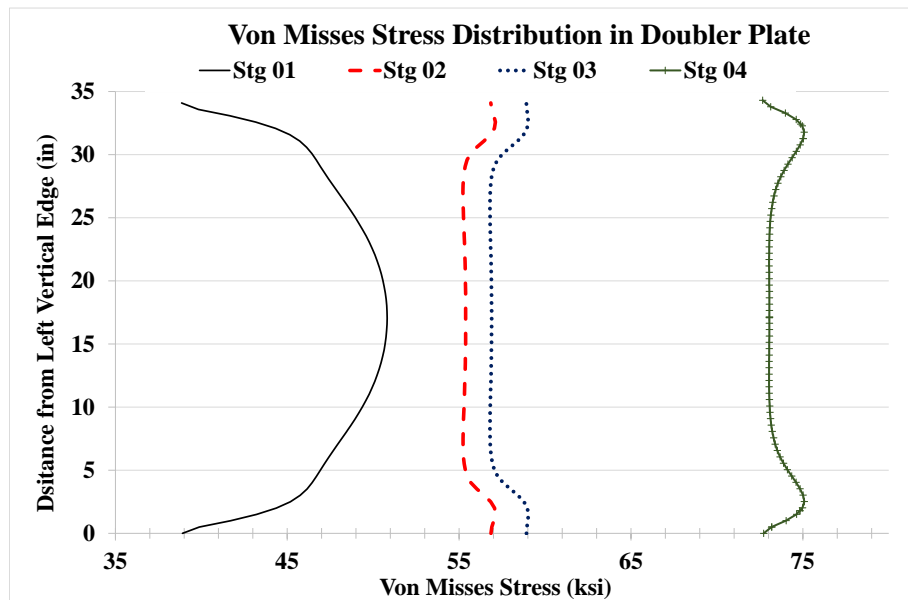


Figure 5.91: VMS distribution at mid-depth of DP Case 8A1



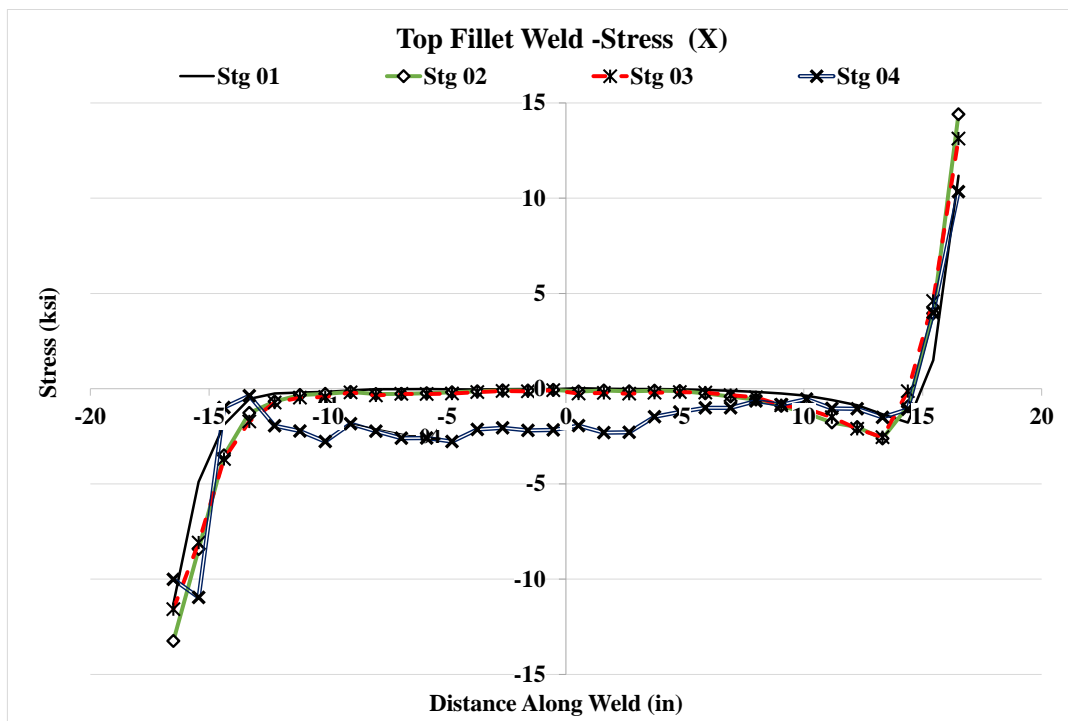
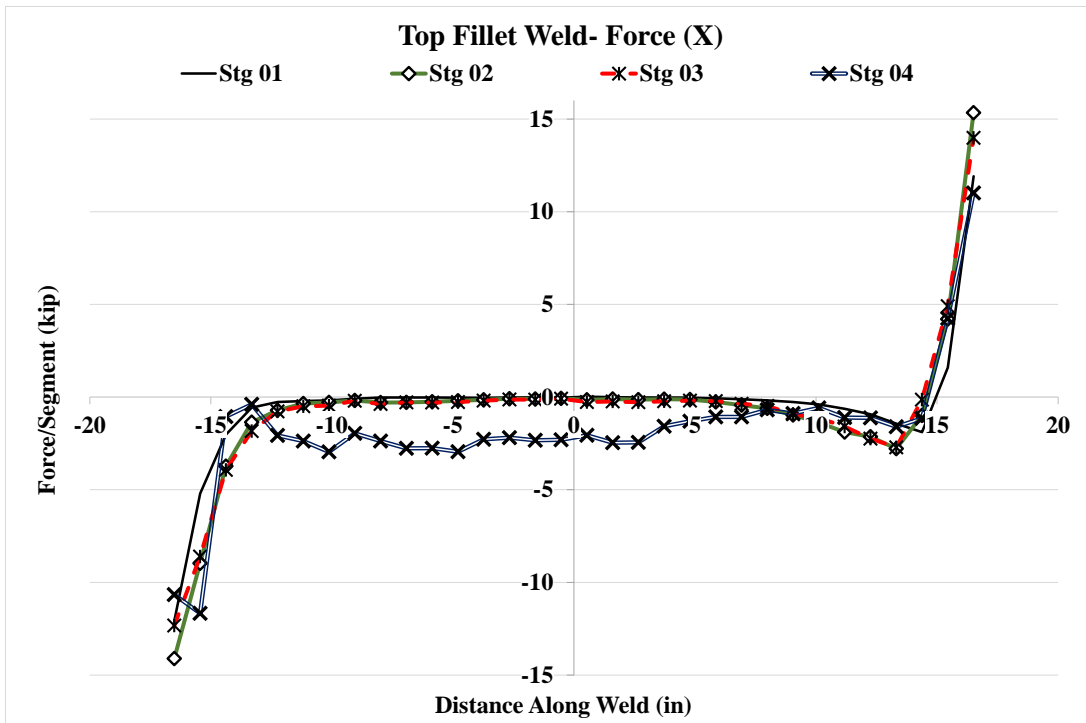


Figure 5.92: Forces and stresses in horizontal weld, (X) Case 8A1

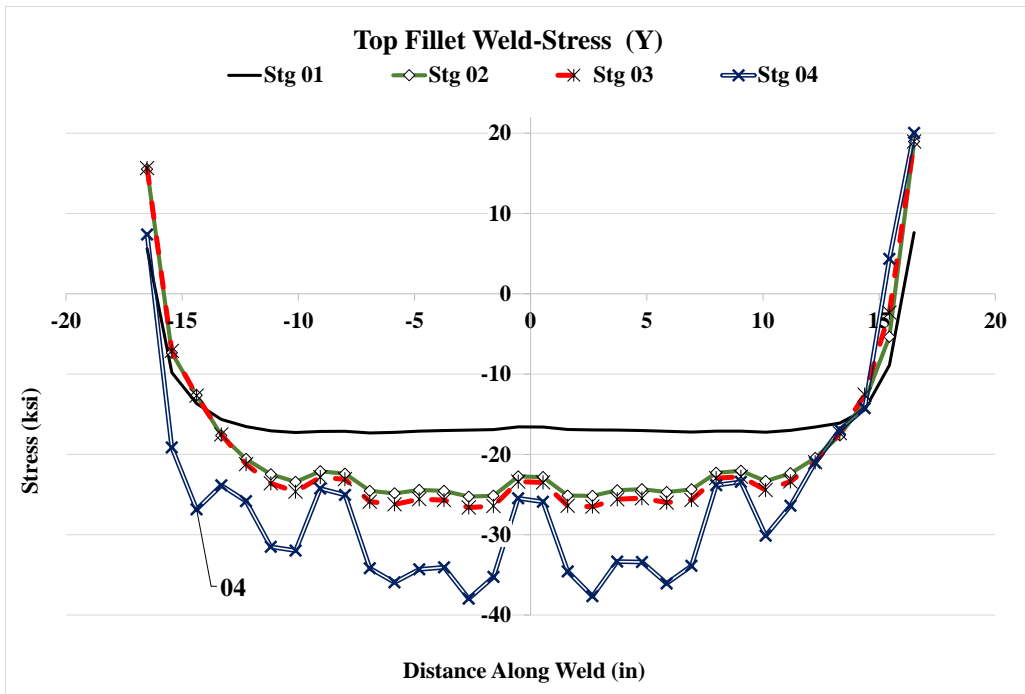
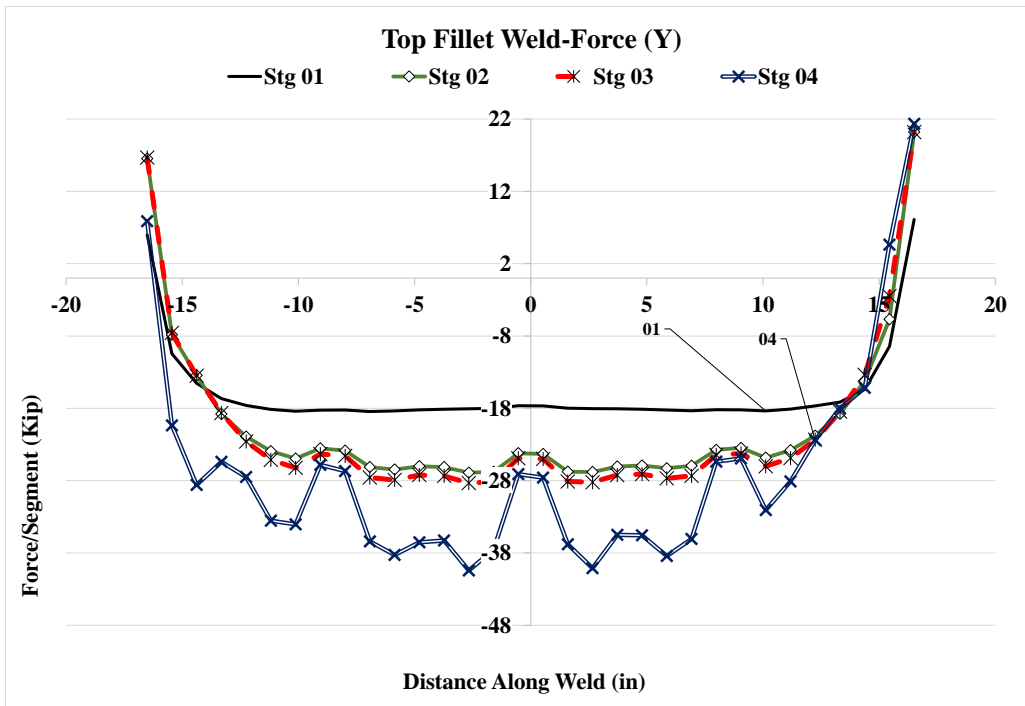


Figure 5.93: Forces and stresses in horizontal weld, (Y) Case 8A1

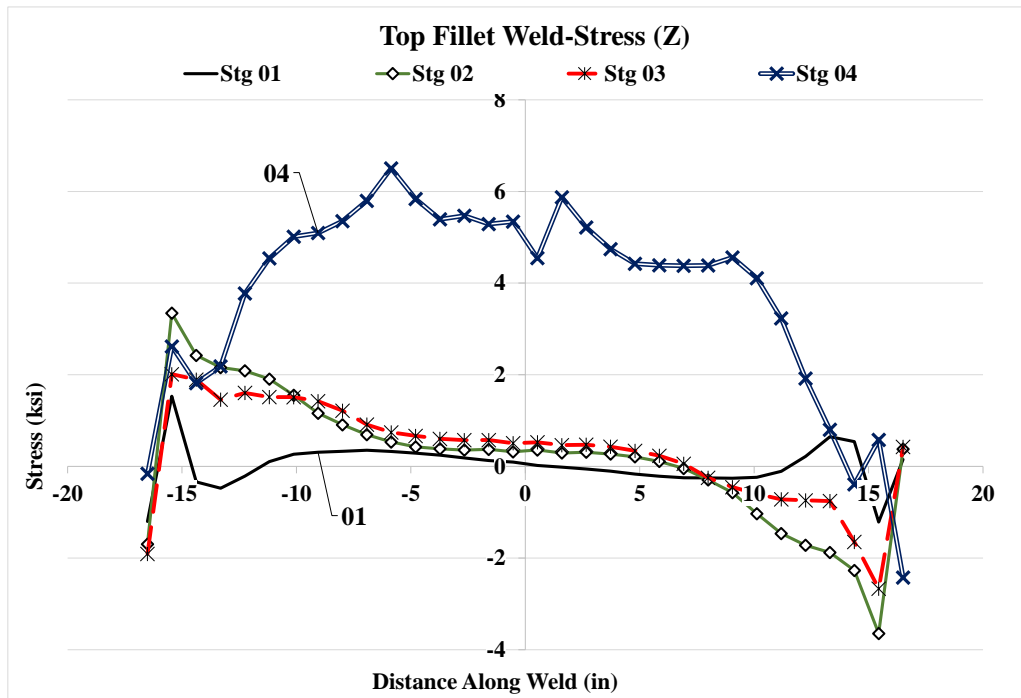
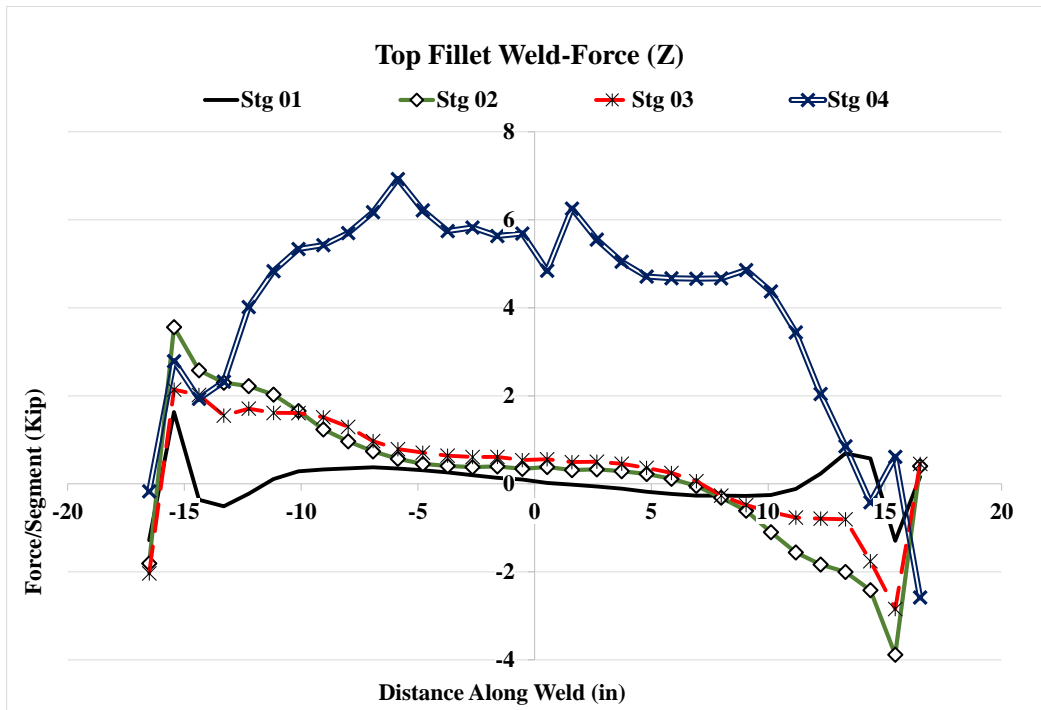


Figure 5.94: Forces and stresses in horizontal weld, (Z) Case 8A1

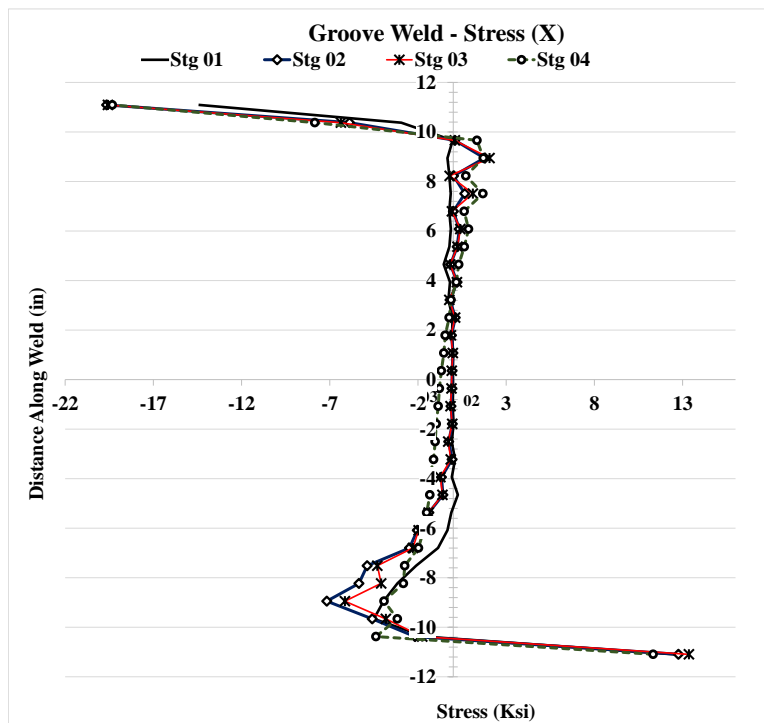
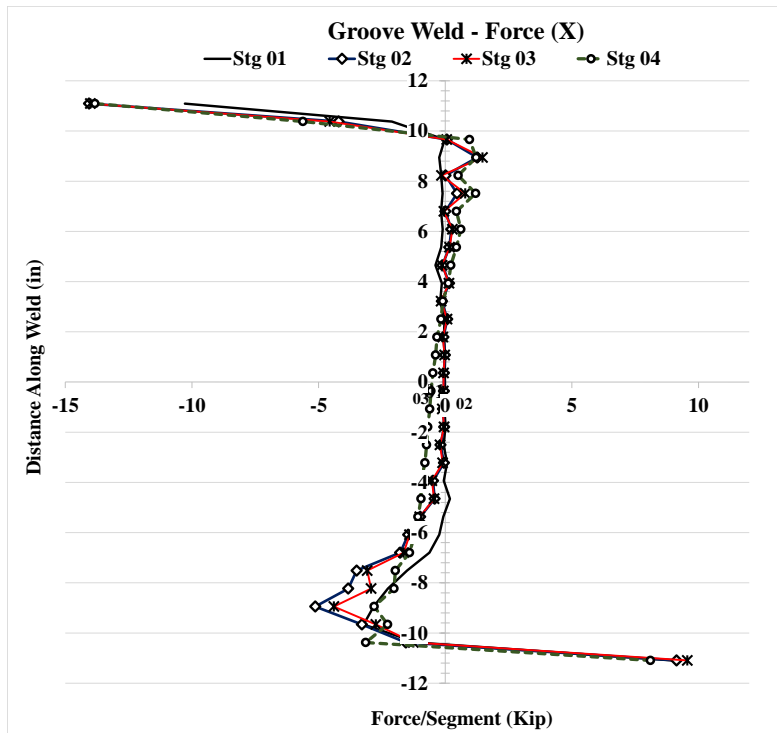


Figure 5.95: Forces and stresses in vertical weld, (X) Case 8A1

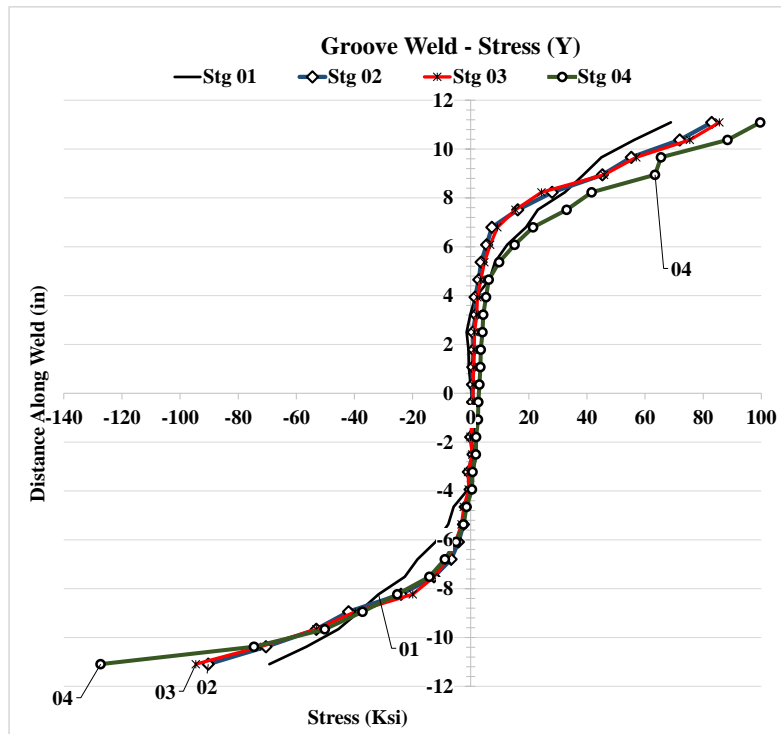
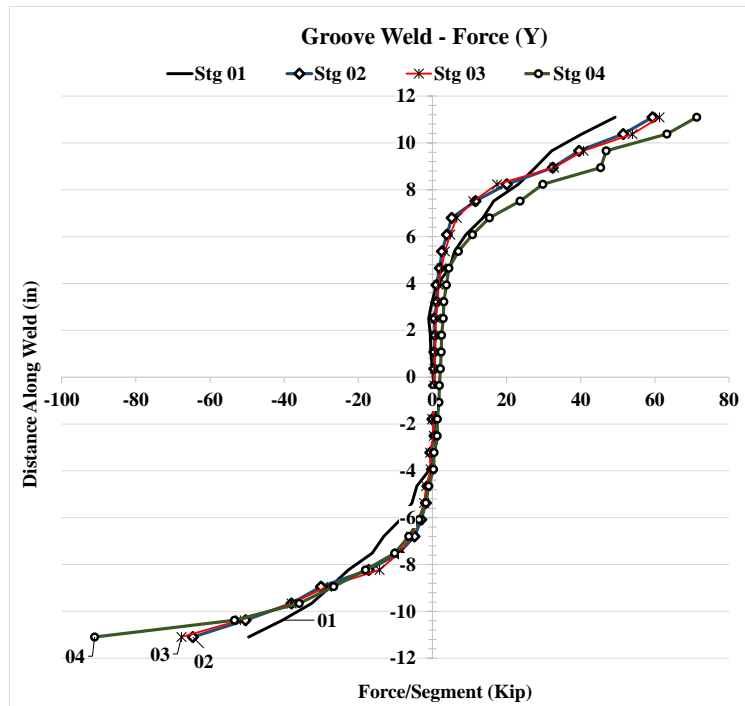


Figure 5.96: Forces and stresses in vertical weld, (Y) Case8A1

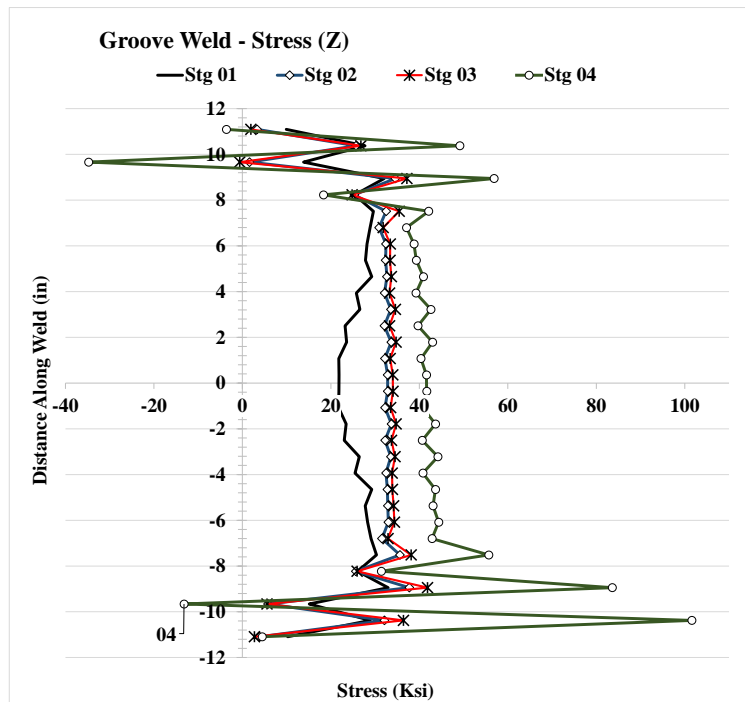
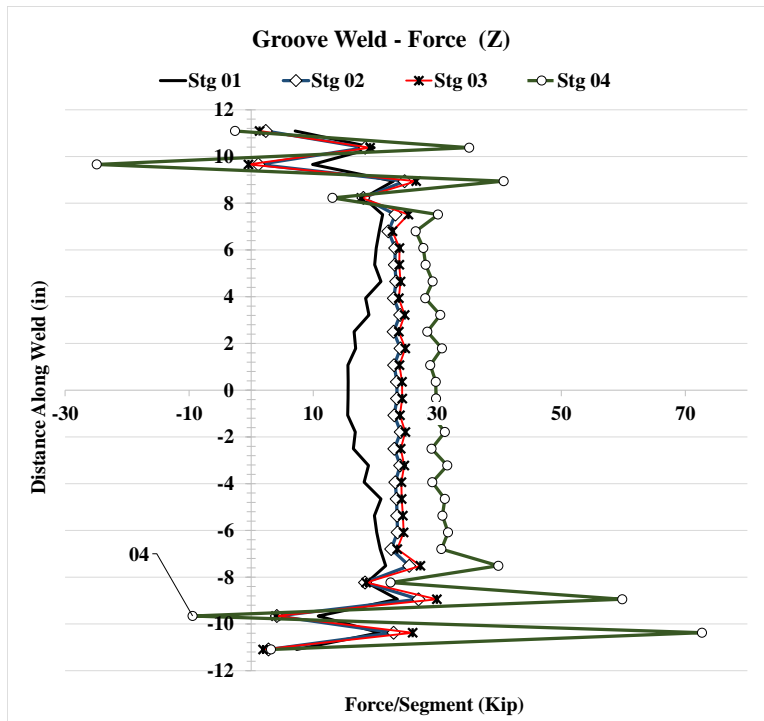


Figure 5.97: Forces and stresses in vertical weld, (Z) Case 8A1

### 5.2.10 Analysis Case 8C

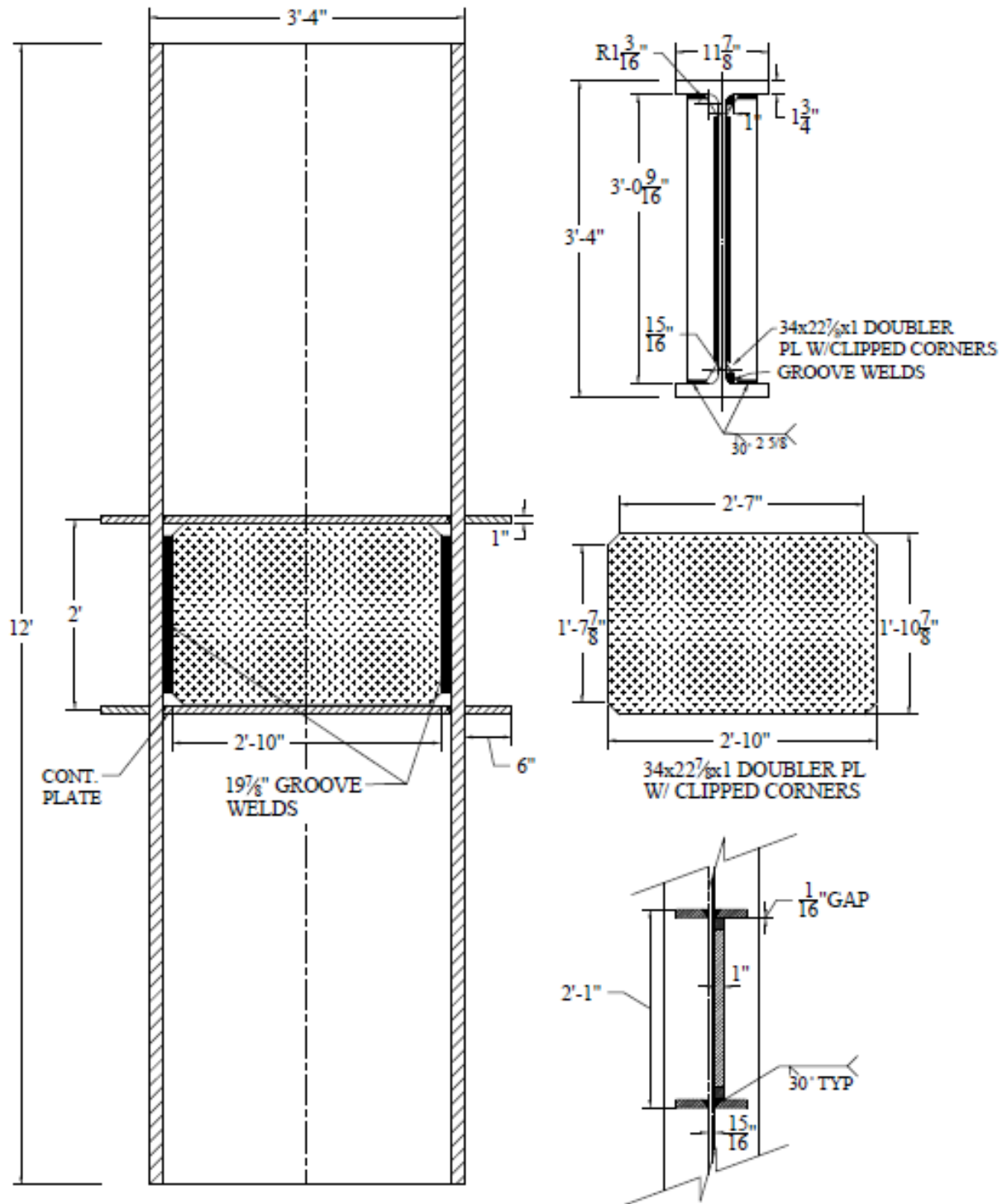


Figure 5.98: W40x264 Analysis case 8C

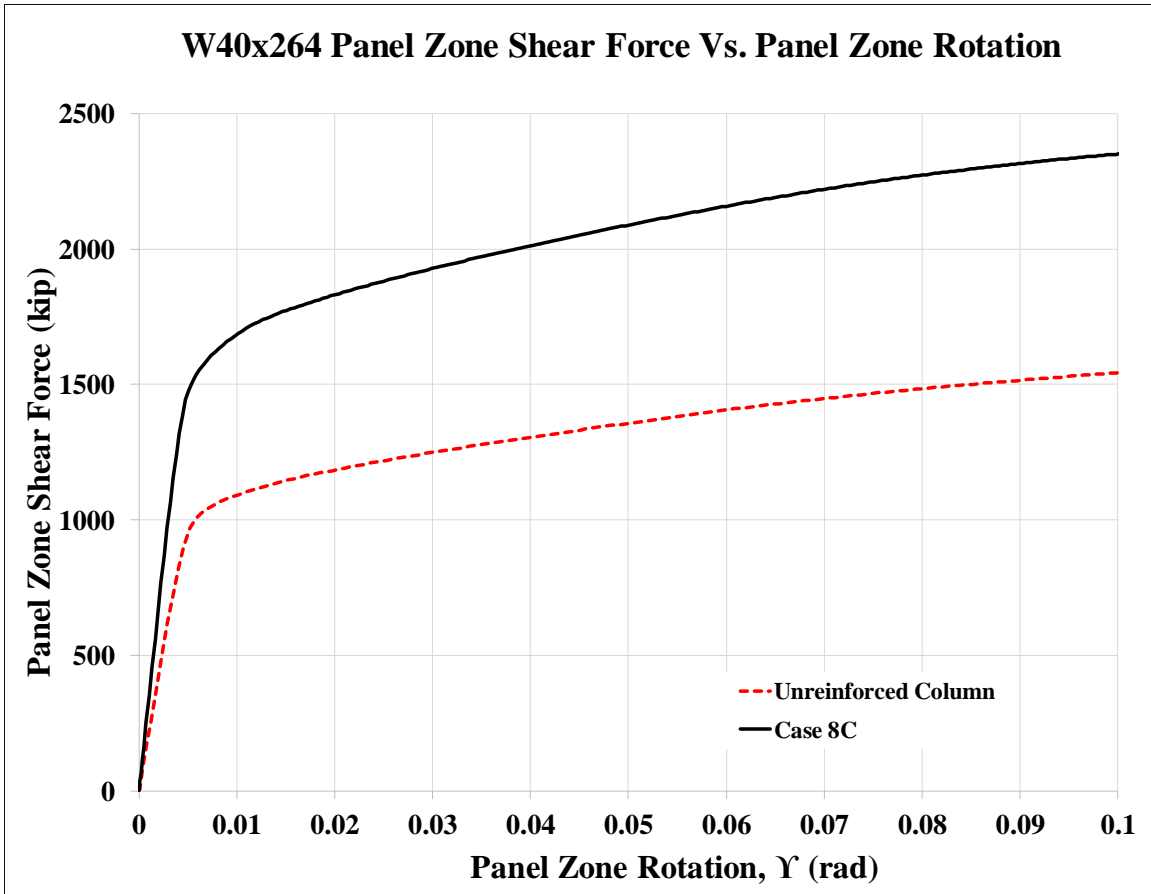


Figure 5.99: Panel zone shear vs. panel zone rotation Case 8C

Stage	Applied Force/Loading Plate (Kip)	Panel Shear Force (Kip)	% Higher Than Unreinforced Col.	Panel Zone Rotation (rad)
1	889	1,481	153%	0.005
2	1,067	1,779	157%	0.015
3	1,099	1,831	154%	0.020
4	1,411	2,351	152%	0.100

Table 5.11: Panel zone shear and force on loading plate Case 8C



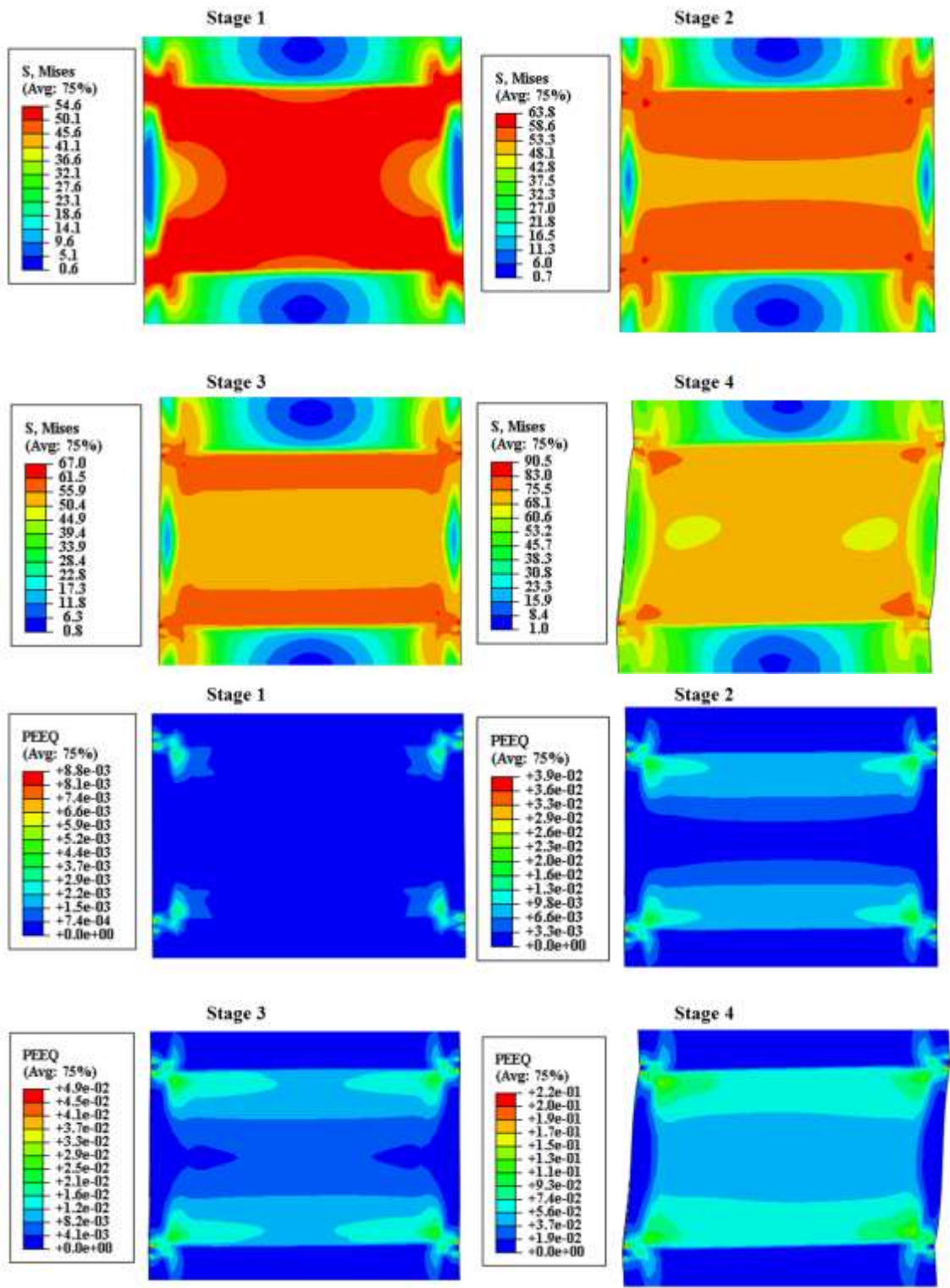


Figure 5.100: VMS and PEEQ in the column Case 8C

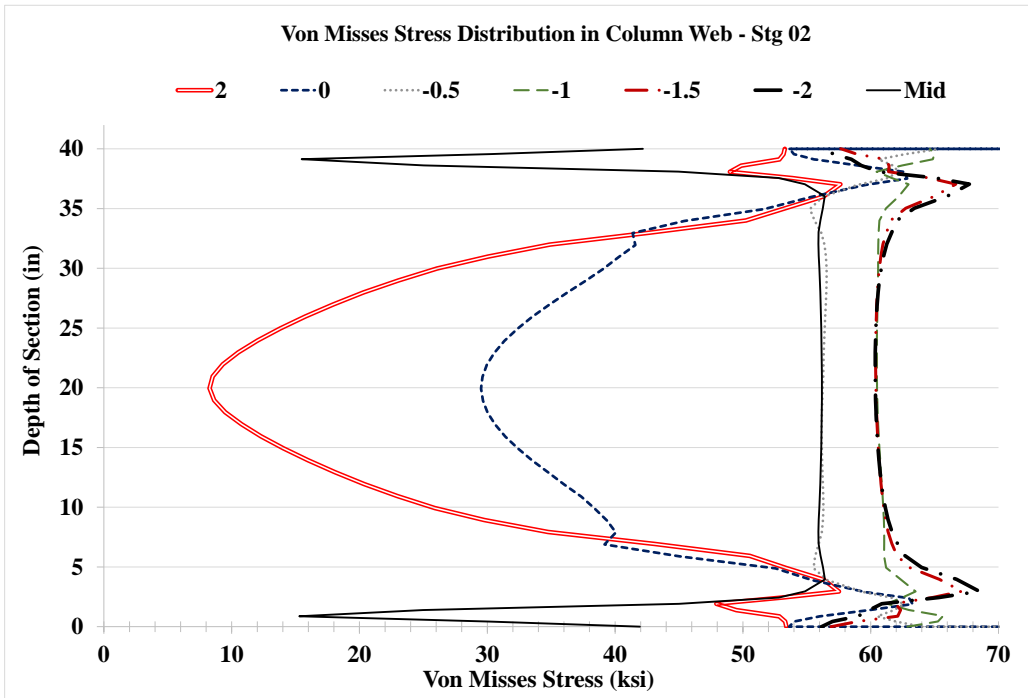
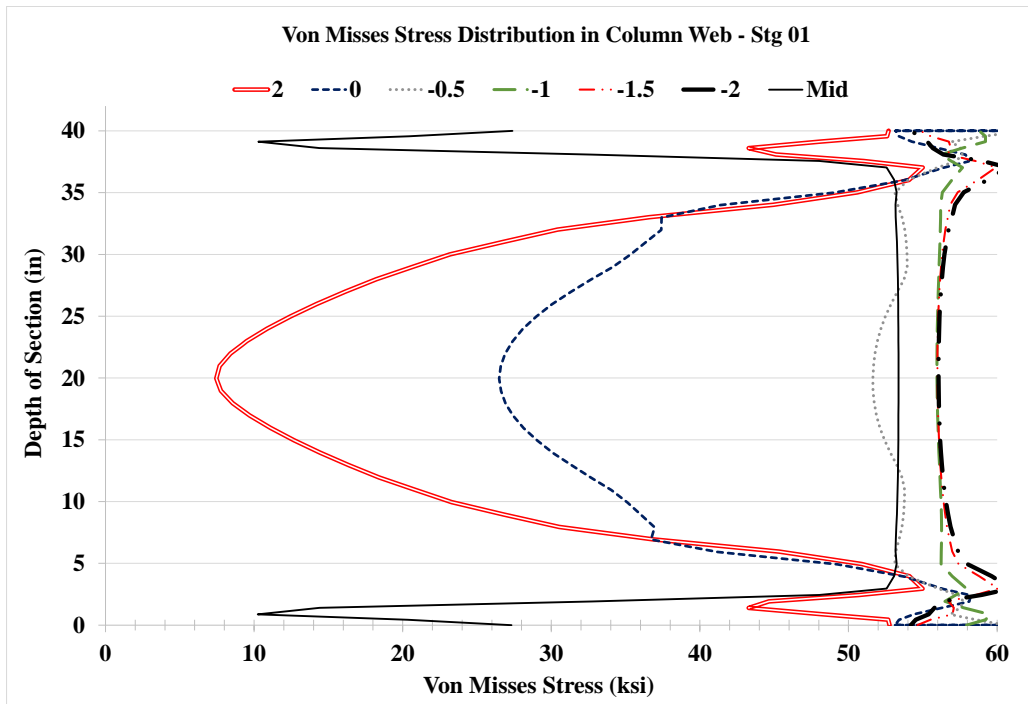


Figure 5.101: VMS distribution in column web at different heights Stg. 01-04 Case 8C

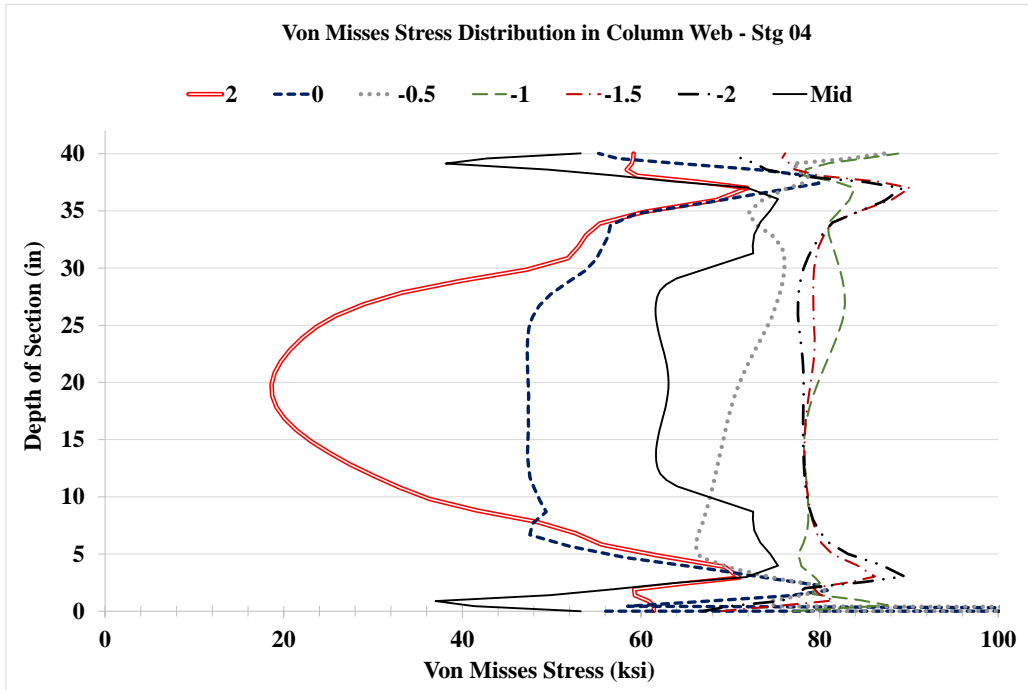
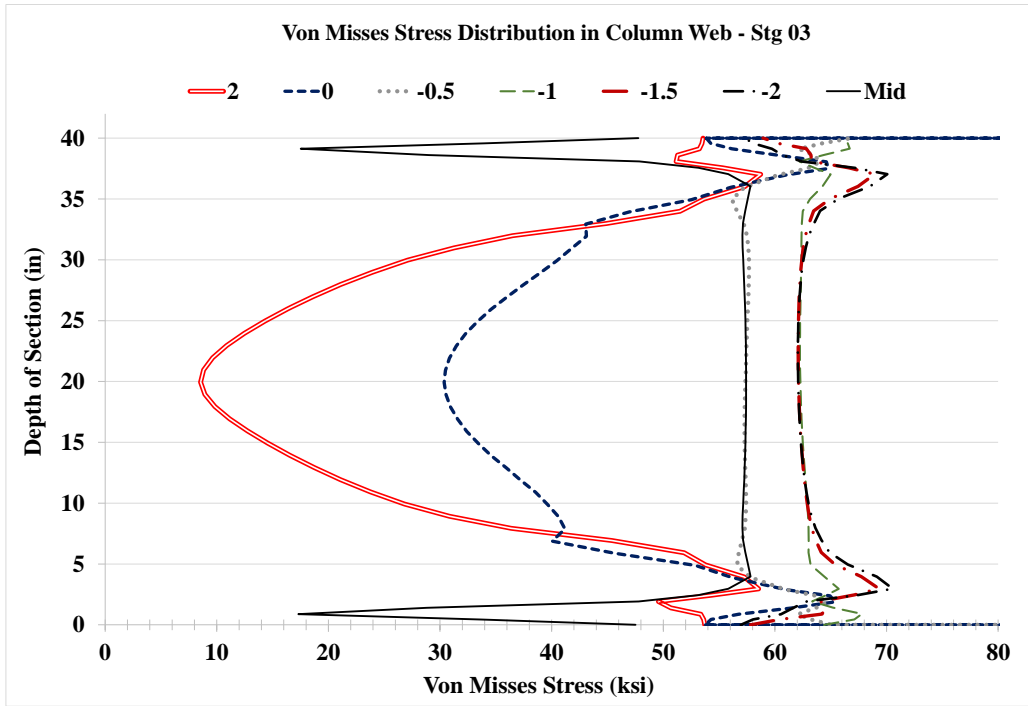


Figure 5.101: VMS distribution in column web at different heights Stg. 01-04 Case 8C

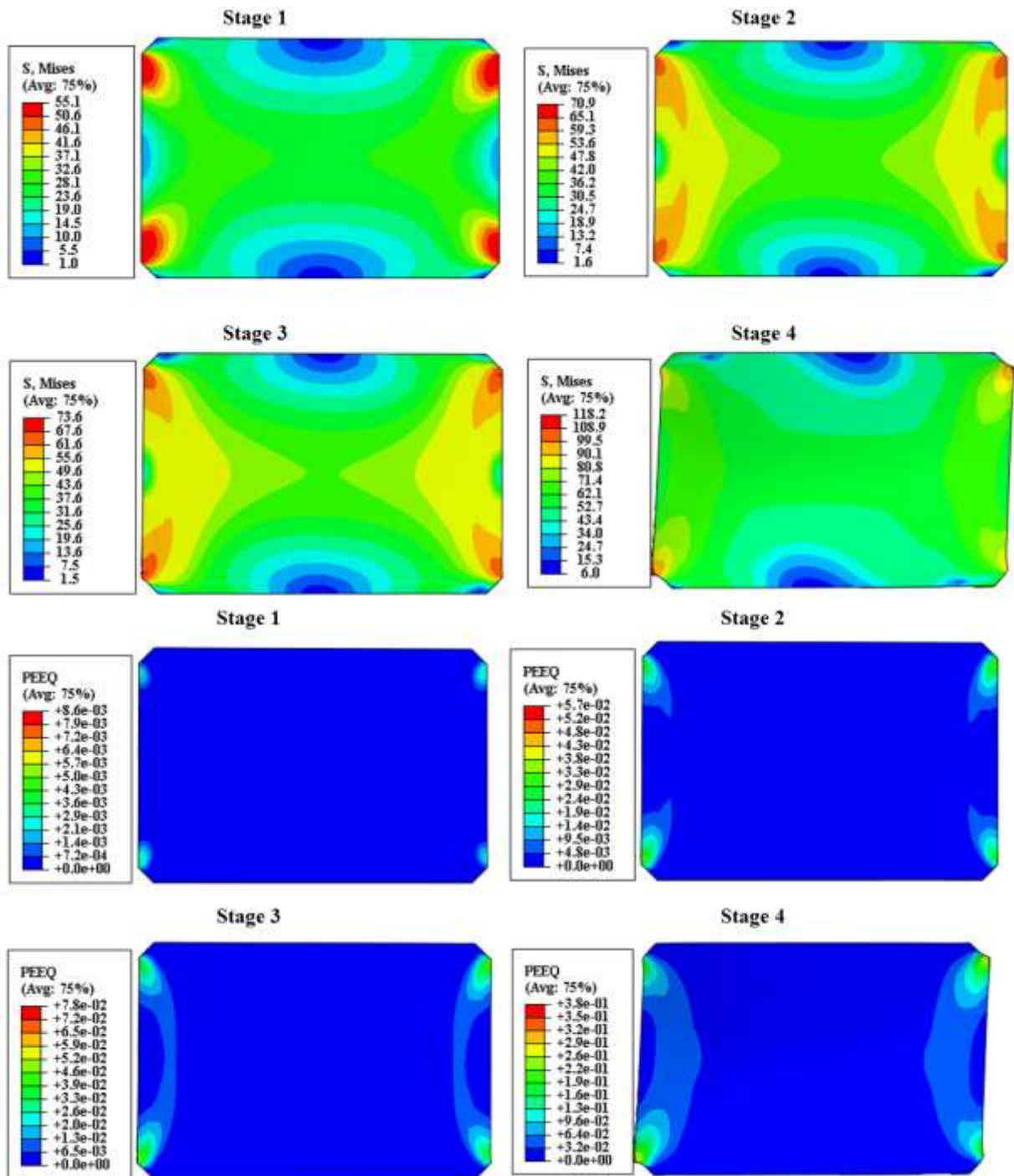


Figure 5.102: VMS and PEEQ in the DP Case 8C

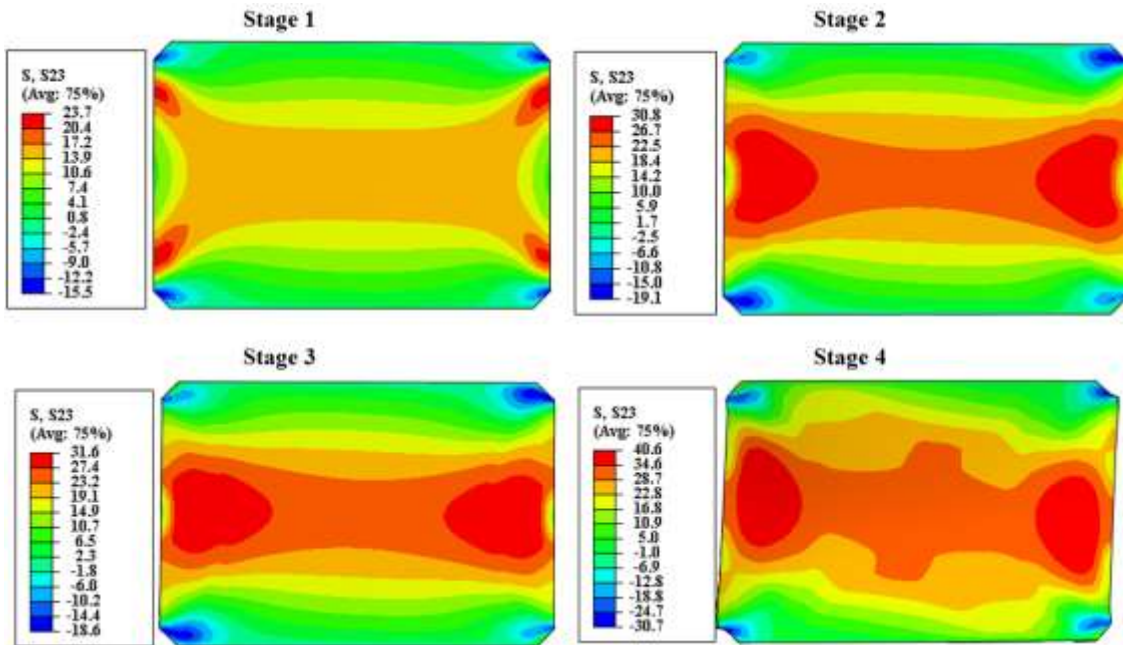


Figure 5.103: Shear stress, S<sub>23</sub> in the DP Case 8C

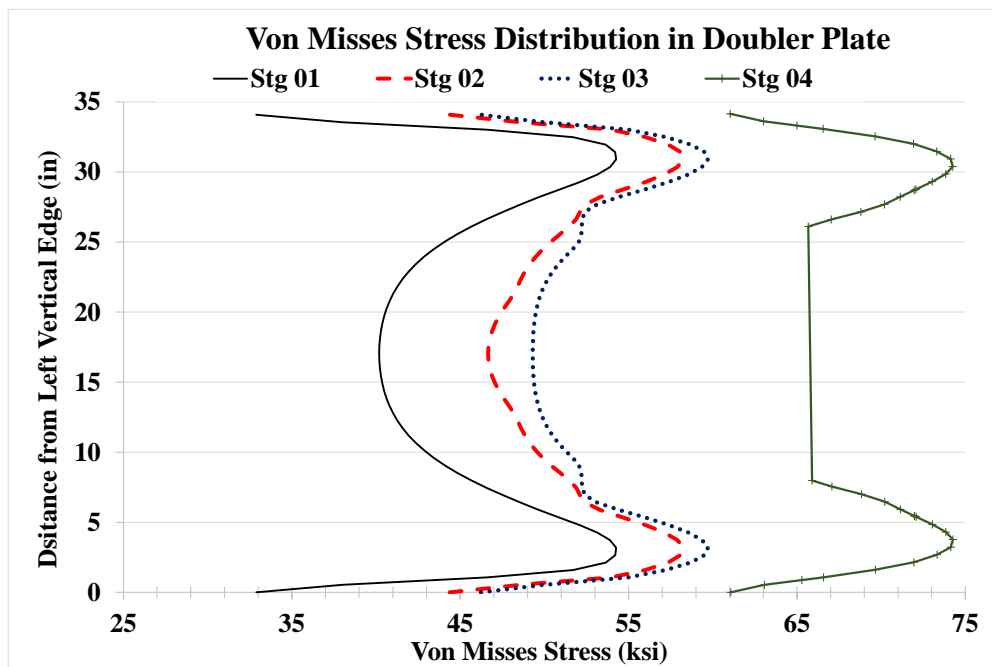


Figure 5.104: VMS distribution at mid-depth of DP Case 8C

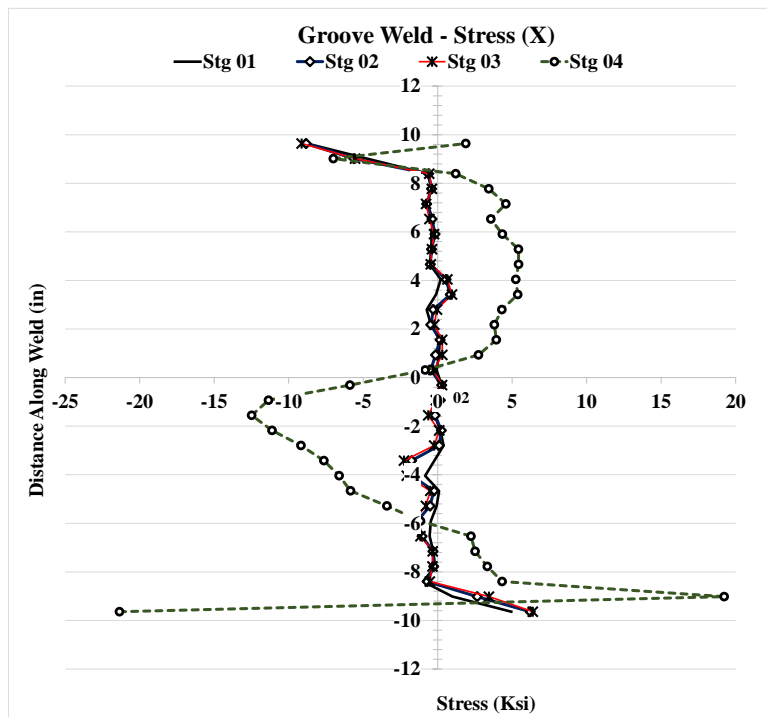
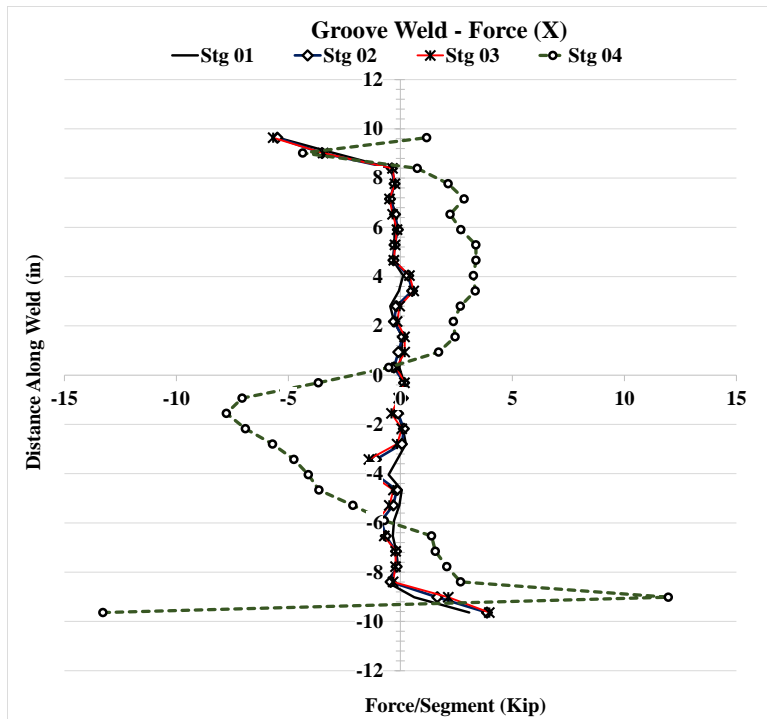


Figure 5.105: Forces and stresses in vertical weld, (X) Case 8C

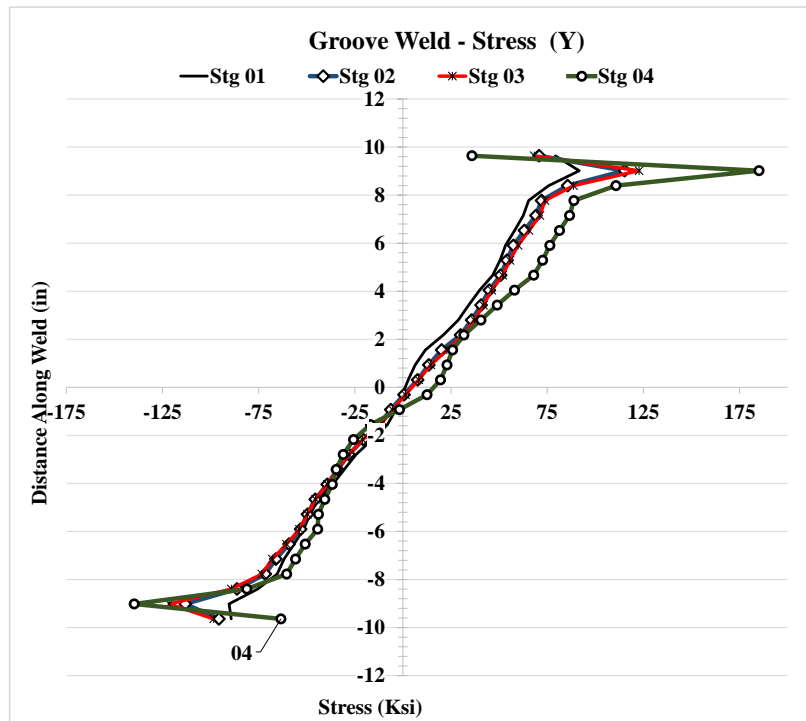
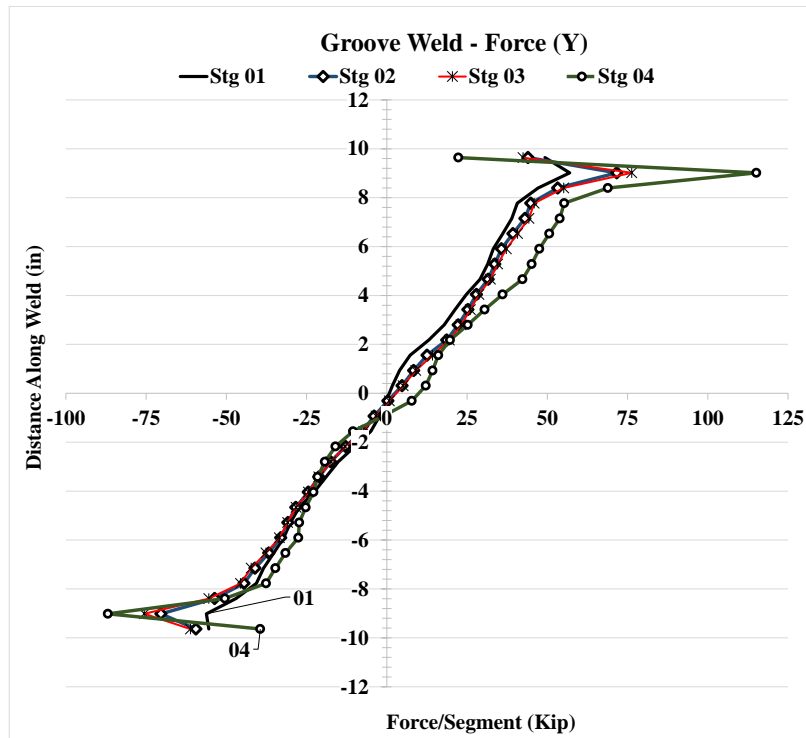


Figure 5.106: Forces and stresses in vertical weld, (Y) Case 8C

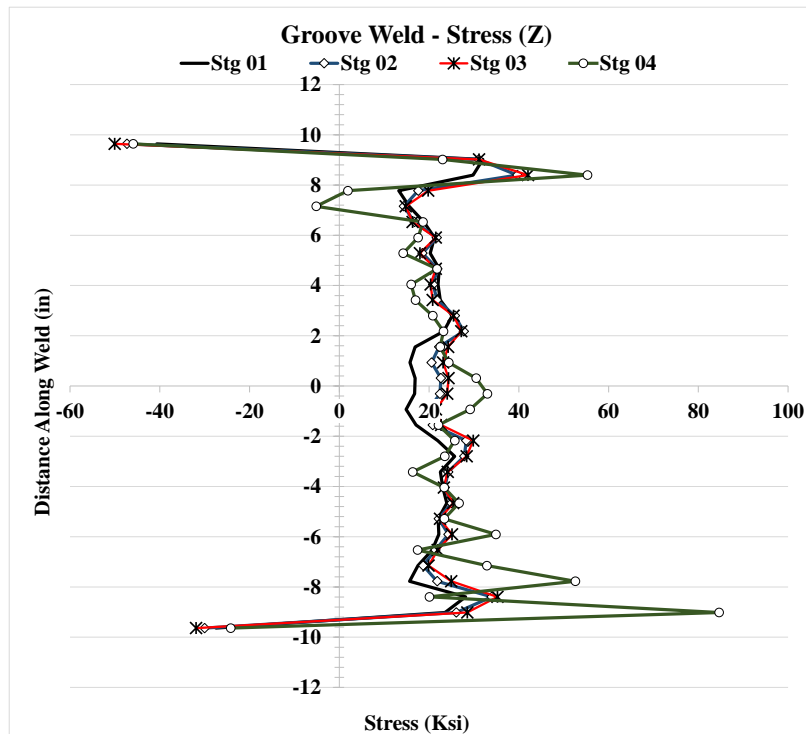
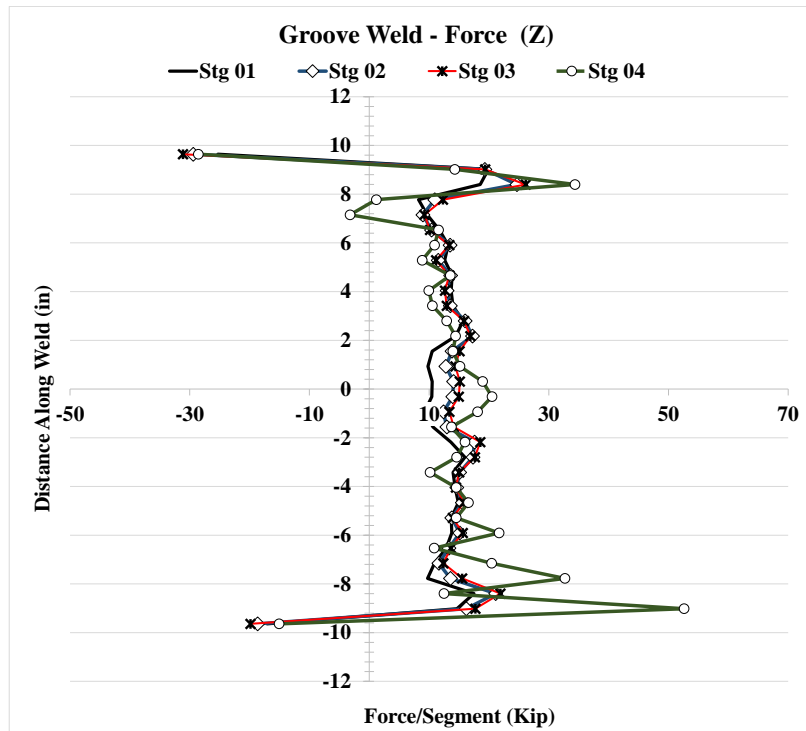


Figure 5.107: Forces and stresses in vertical weld, (Z) Case 8C



### 5.2.11 Analysis Case 8C1

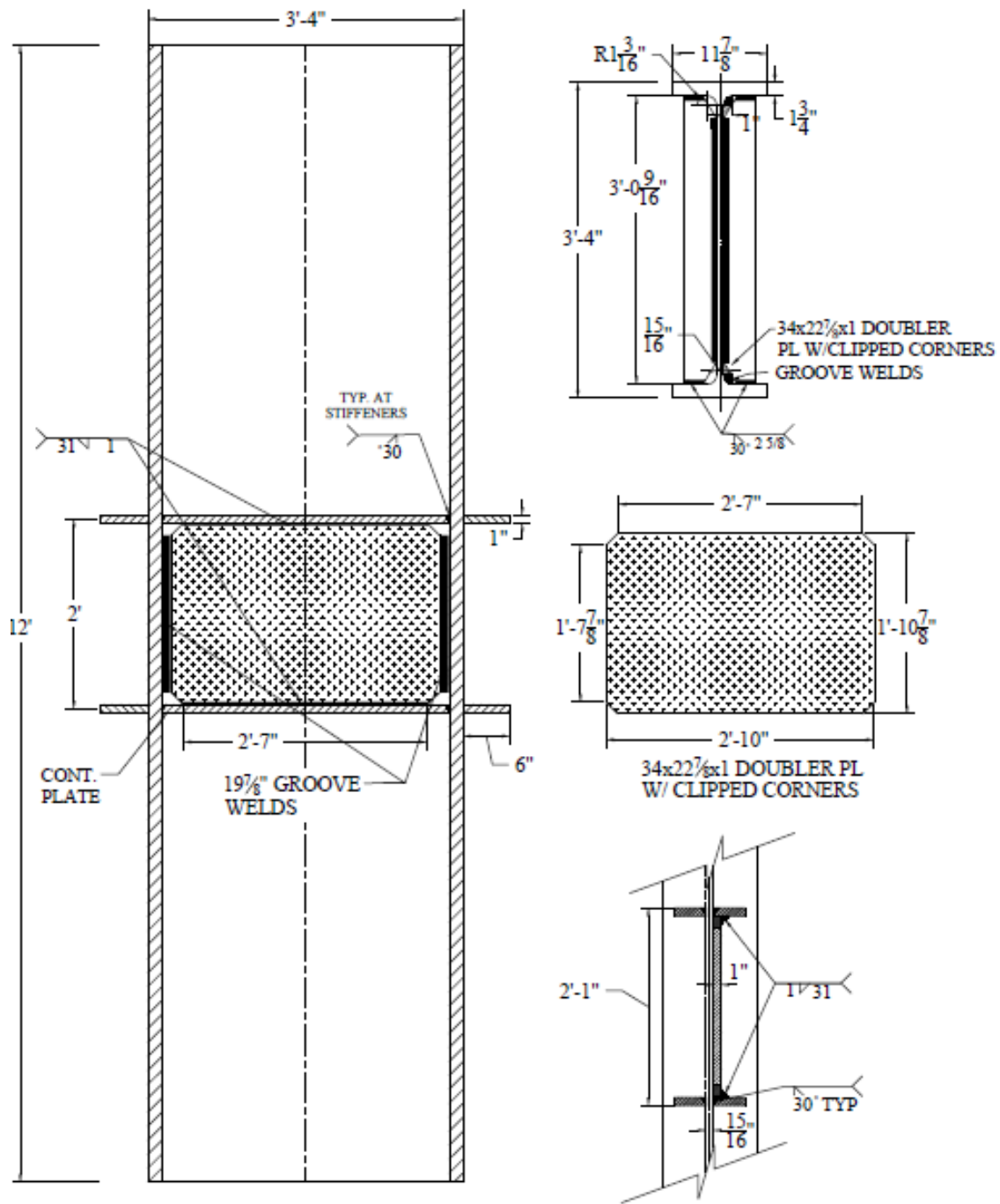


Figure 5.108: W40x264 Analysis case 8C1

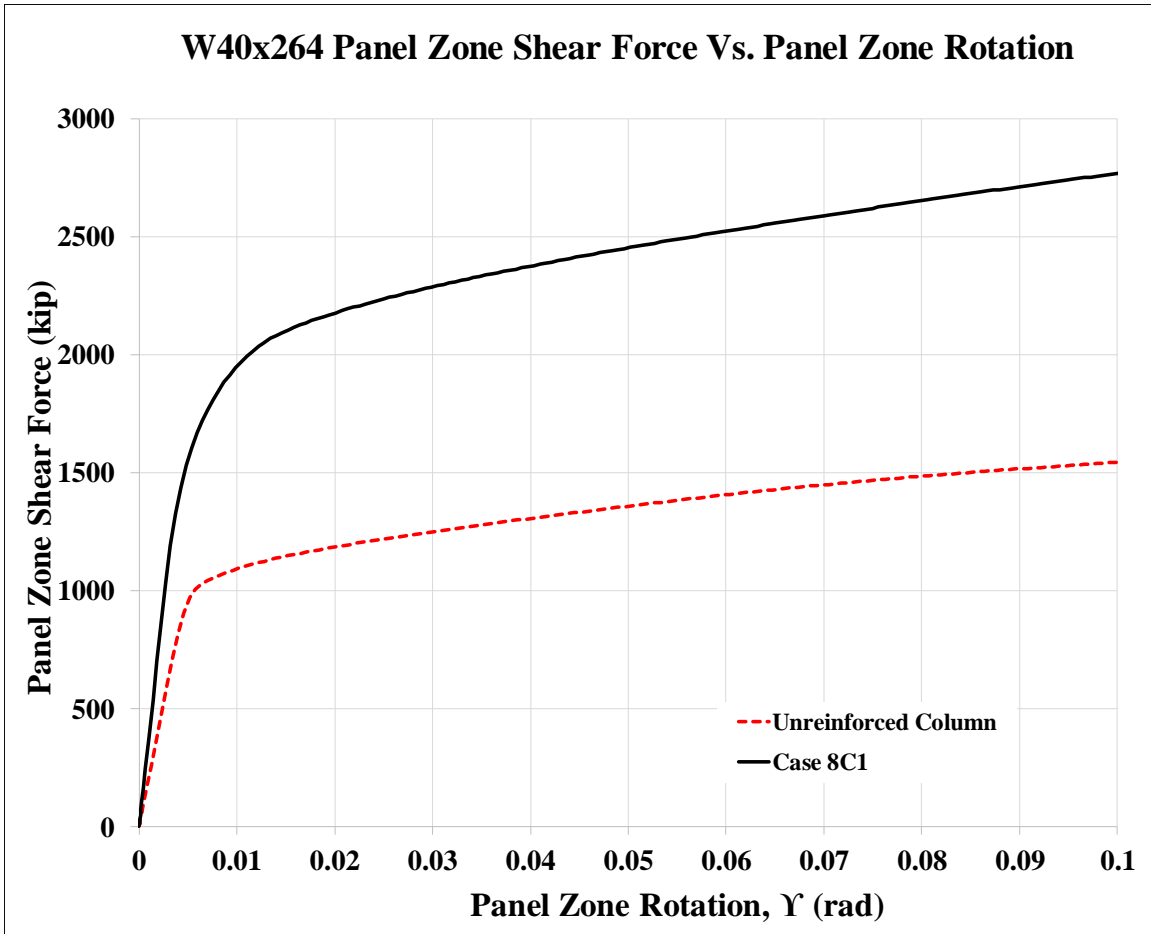


Figure 5.109: Panel zone shear vs. panel zone rotation Case 8C1

Stage	Applied Force/Loading Plate (Kip)	Panel Shear Force (Kip)	% Higher Than Unreinforced Col.	Panel Zone Rotation (rad)
1	918	1,530	158%	0.005
2	1,269	2,115	187%	0.016
3	1,306	2,177	183%	0.020
4	1,662	2,770	179%	0.100

Table 5.12: Panel zone shear and force on loading plate Case 8C1

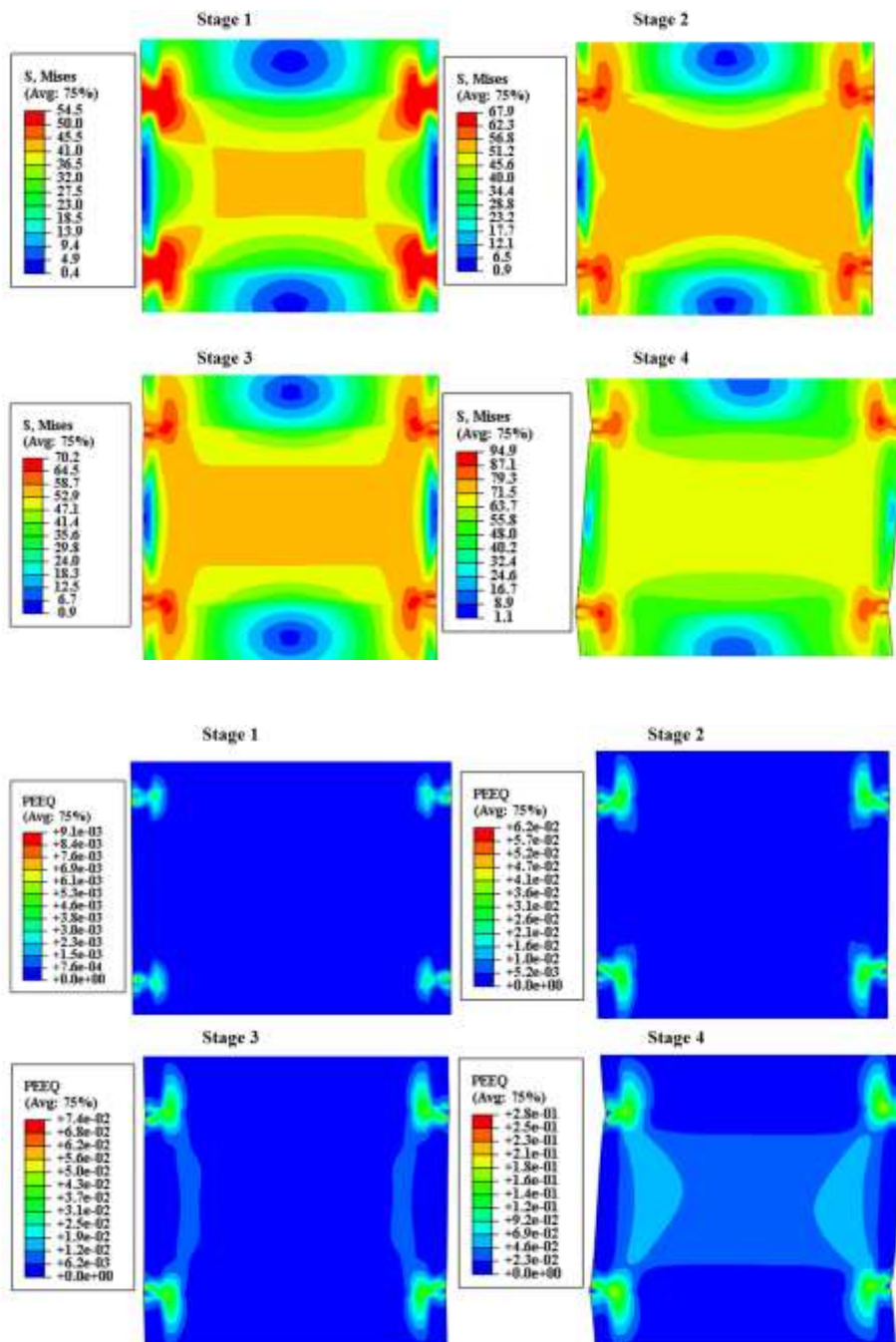


Figure 5.110: VMS and PEEQ in the column Case 8C1

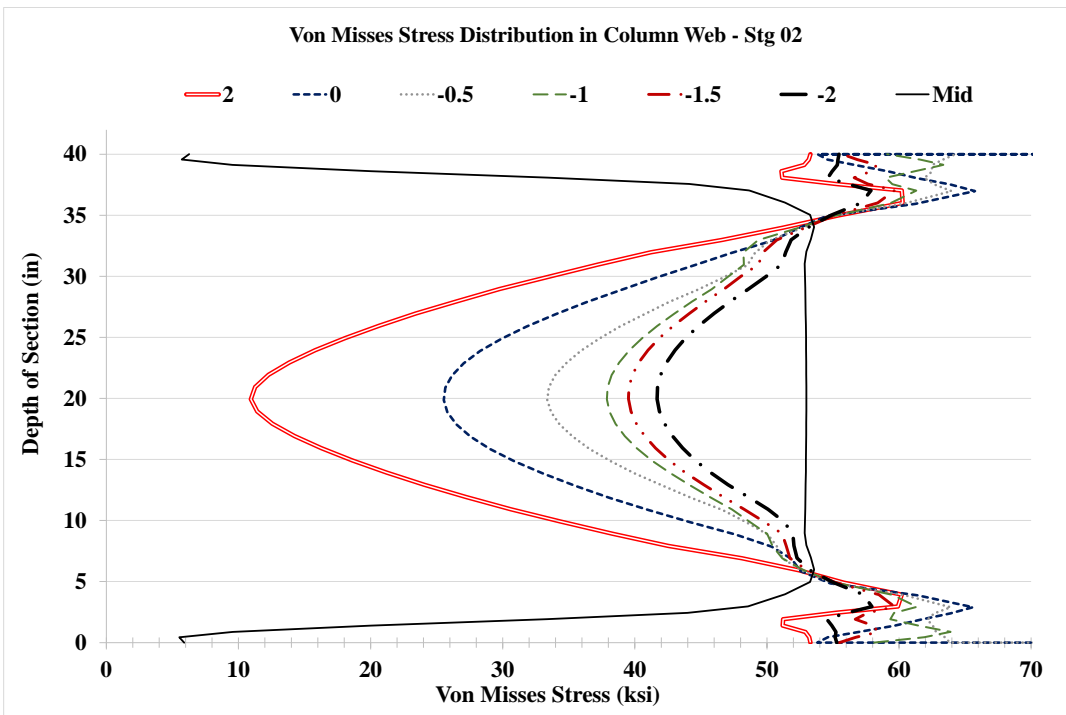
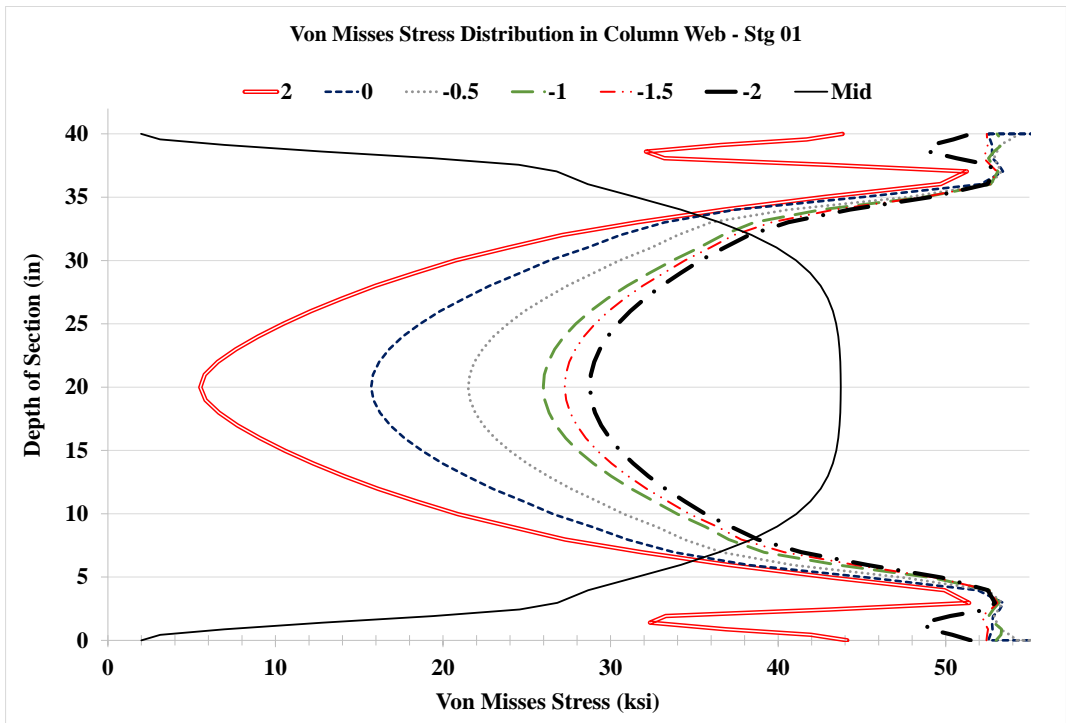


Figure 5.111: VMS distribution in column web at different heights Stg. 01-04 Case 8C1

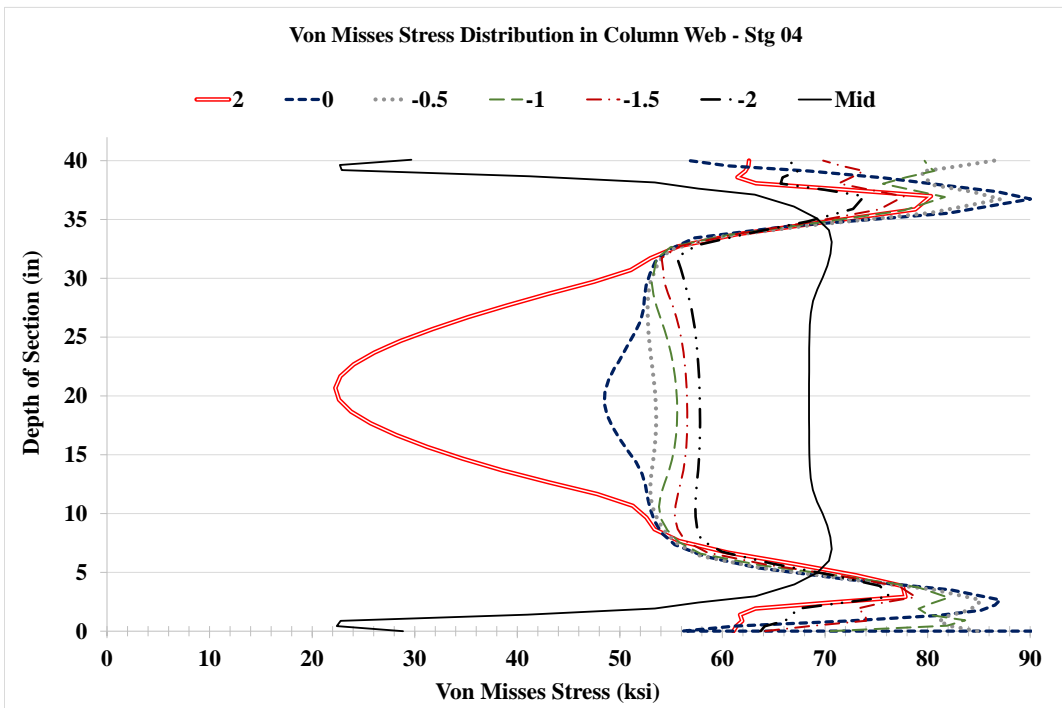
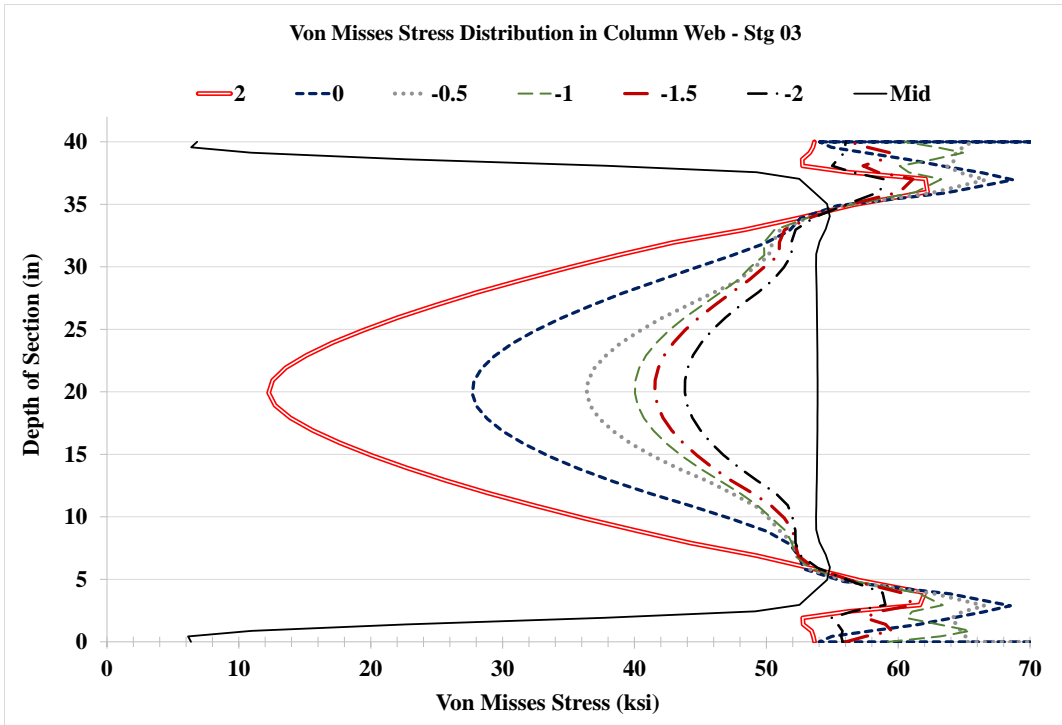


Figure 5.111: VMS distribution in column web at different heights Stg. 01-04 Case 8C1

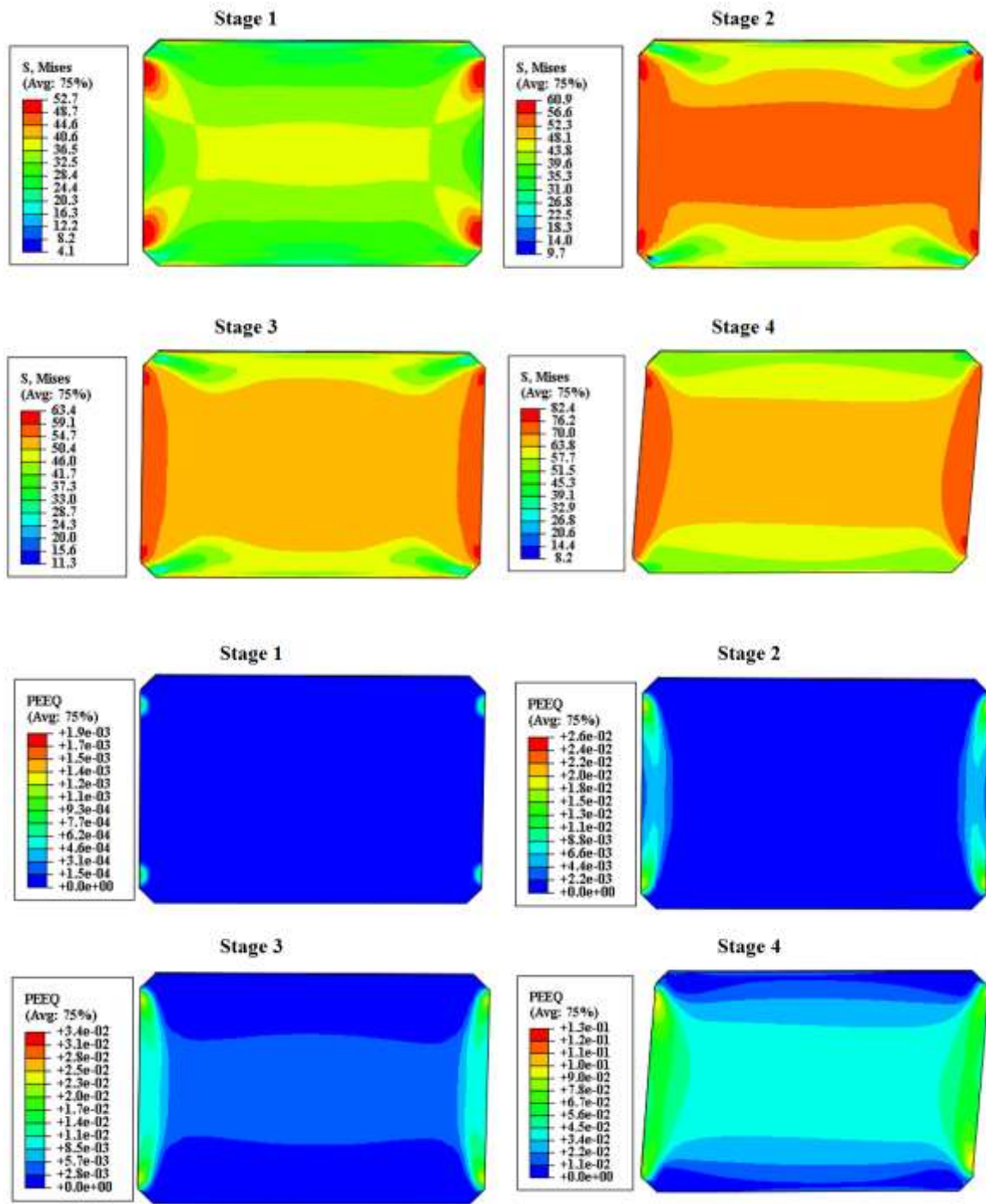


Figure 5.112: VMS and PEEQ in the DP Case 8C1

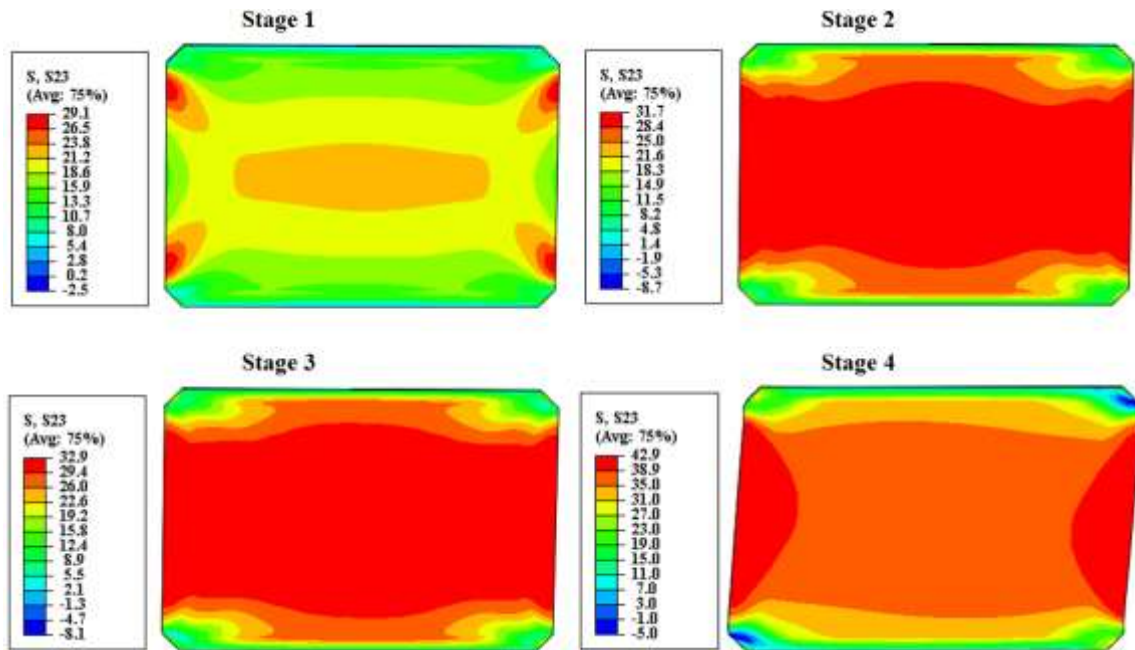


Figure 5.113: Shear stress, S23 in the DP Case 8C1

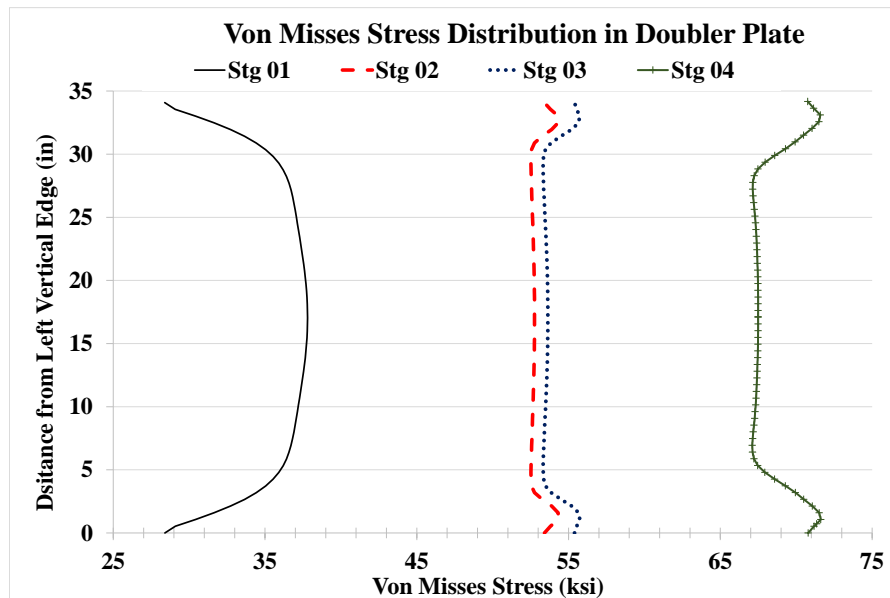


Figure 5.114: VMS distribution at mid-depth of DP Case 8C1

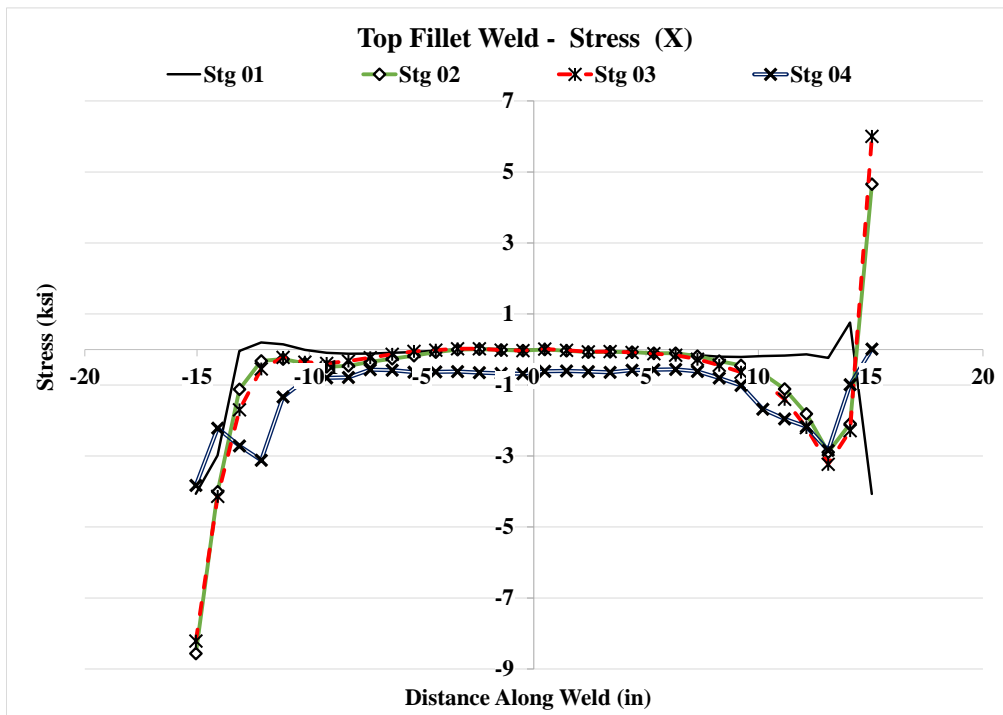
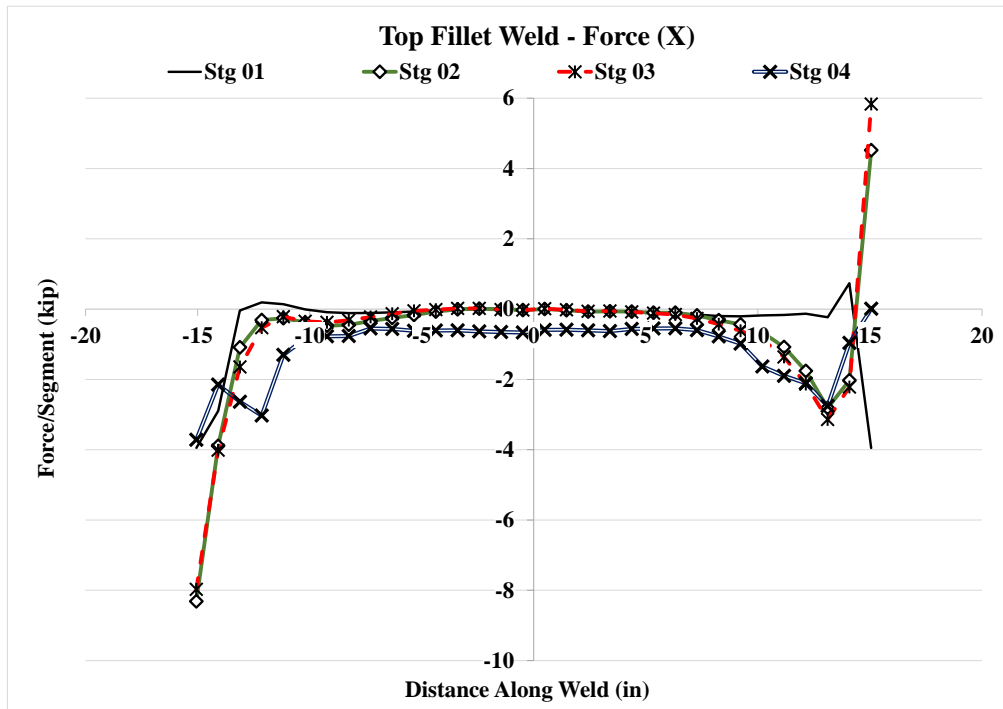


Figure 5.115: Forces and stresses in horizontal weld, (X) Case 8C1



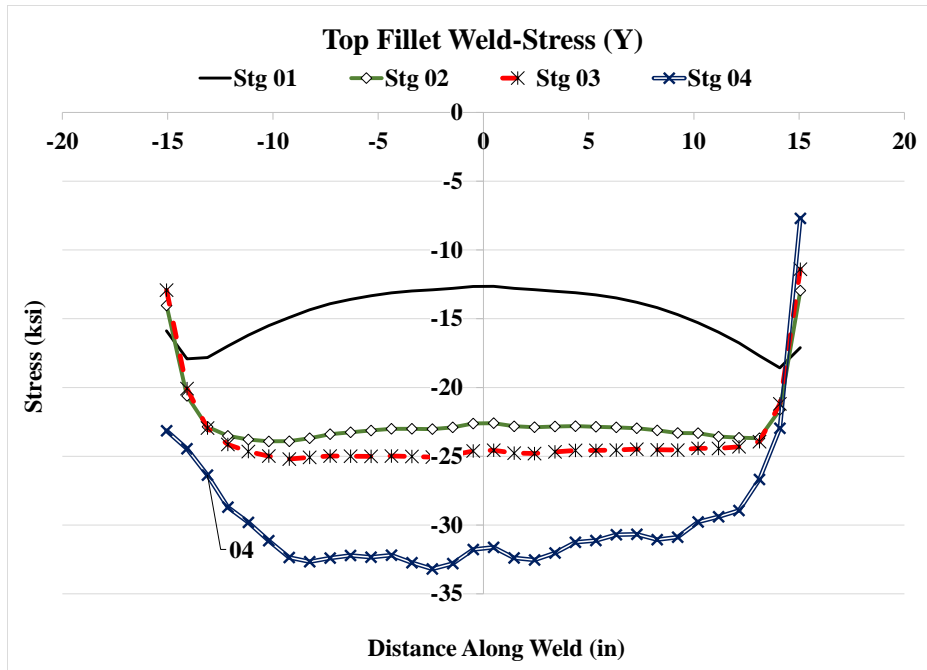
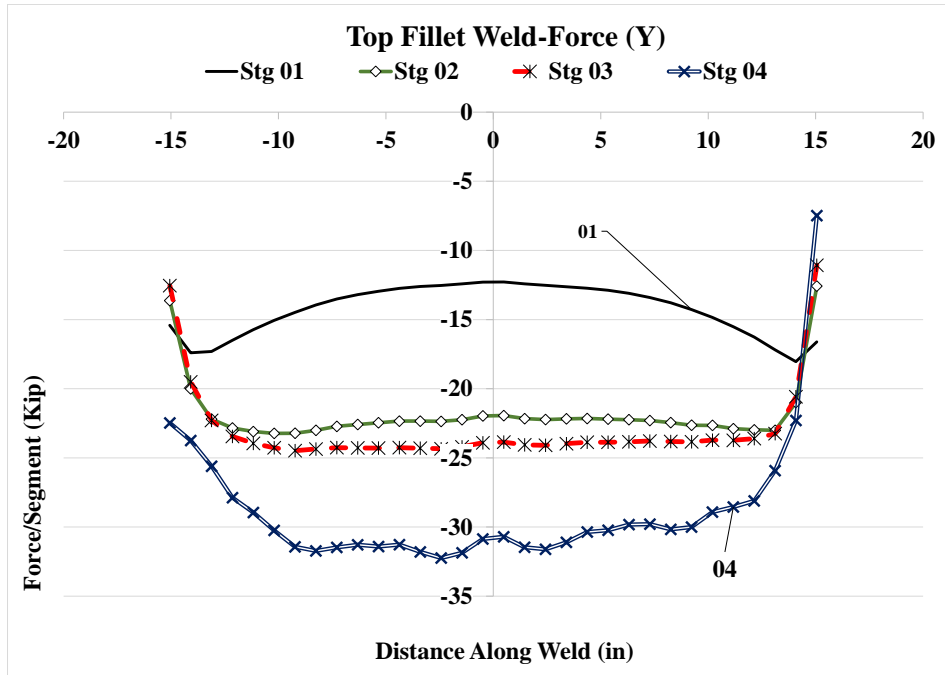


Figure 5.116: Forces and stresses in horizontal weld, (Y) Case 8C1

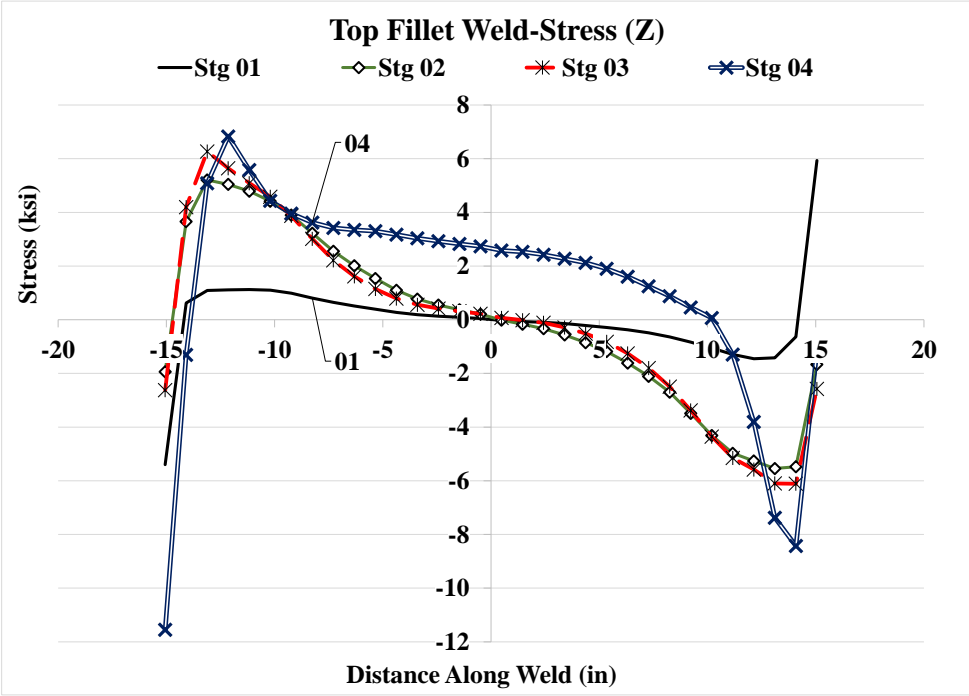
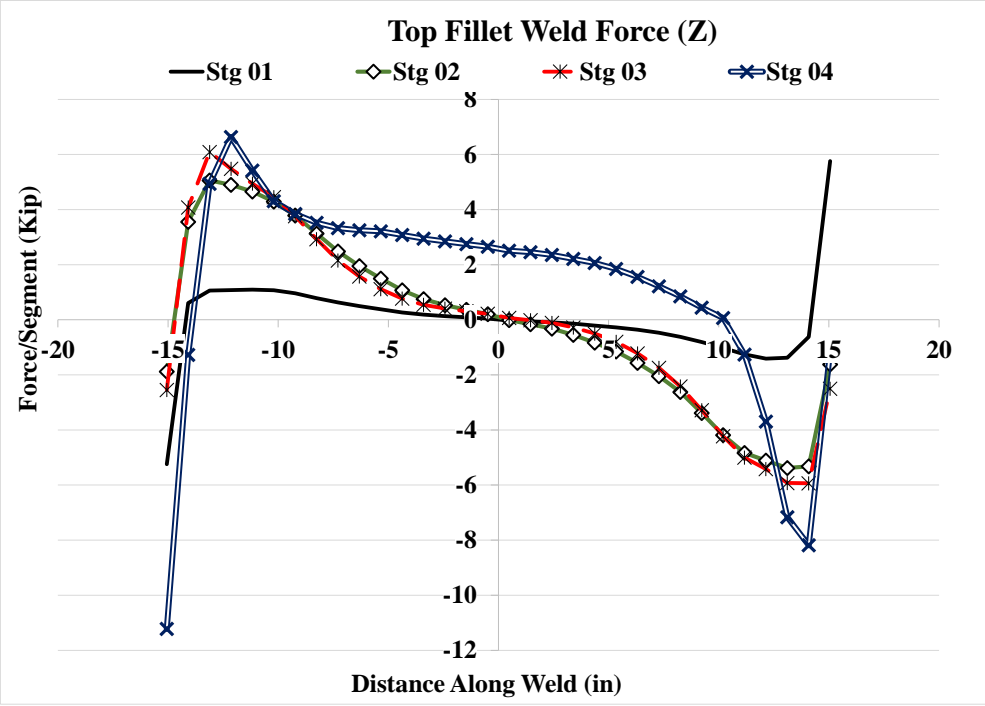


Figure 5.117: Forces and stresses in horizontal weld, (Z) Case 8C1

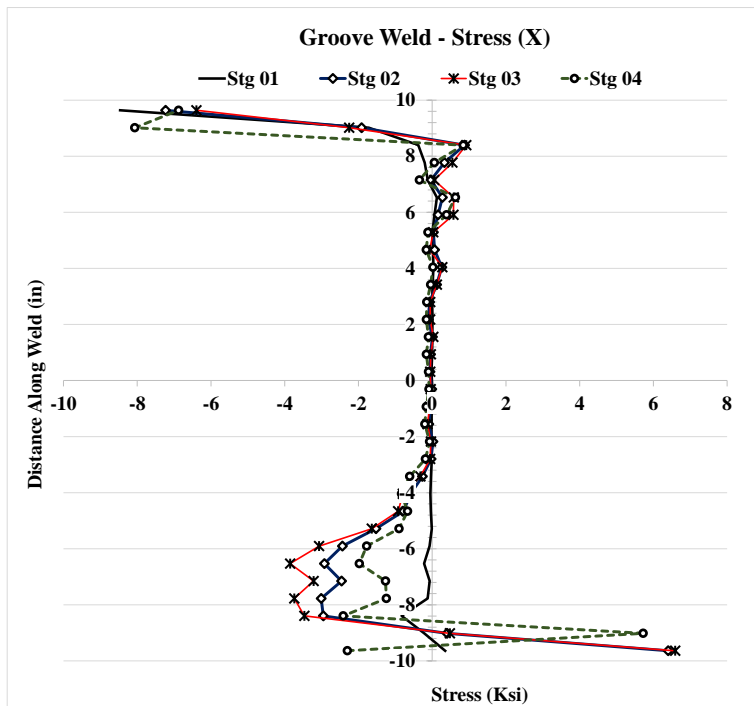
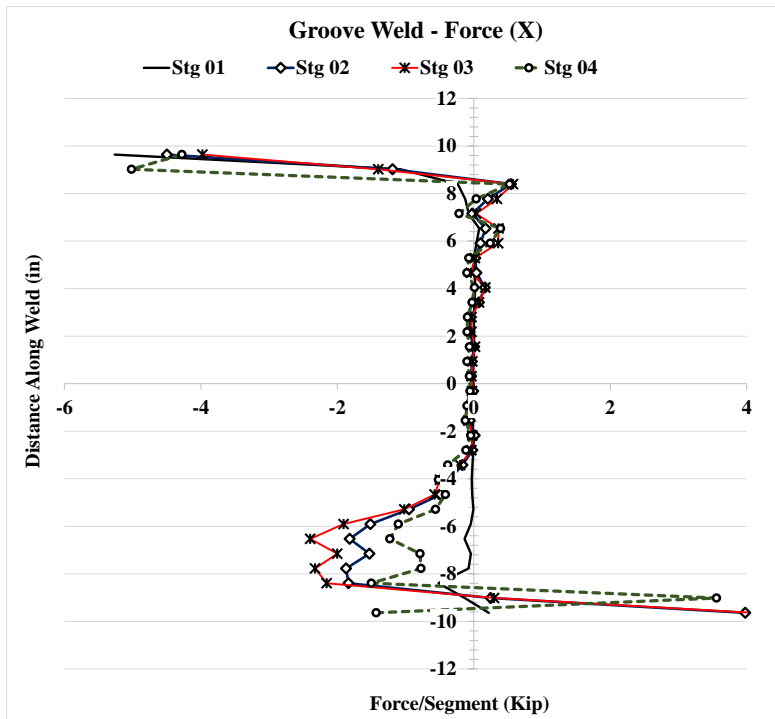


Figure 5.118: Forces and stresses in vertical weld, (X) Case 8C1

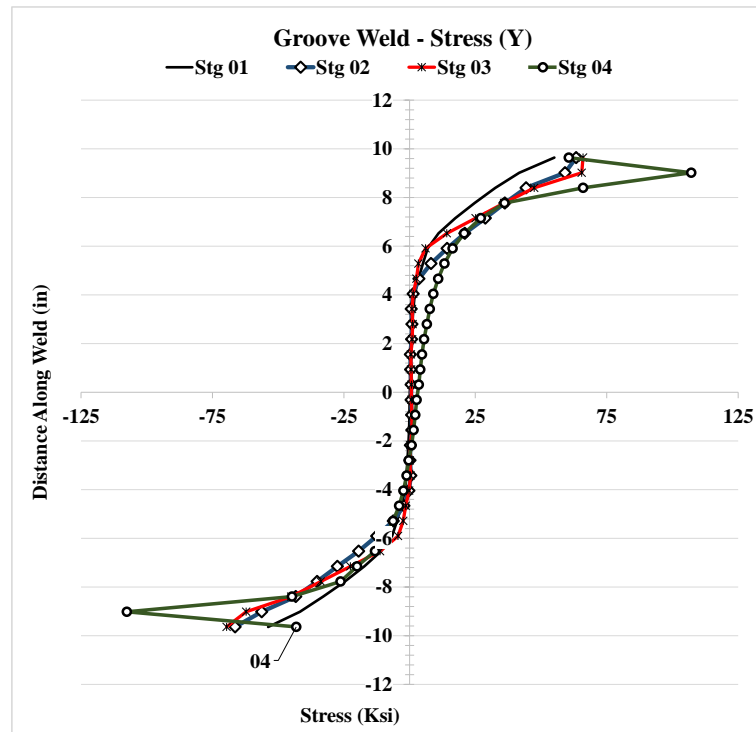
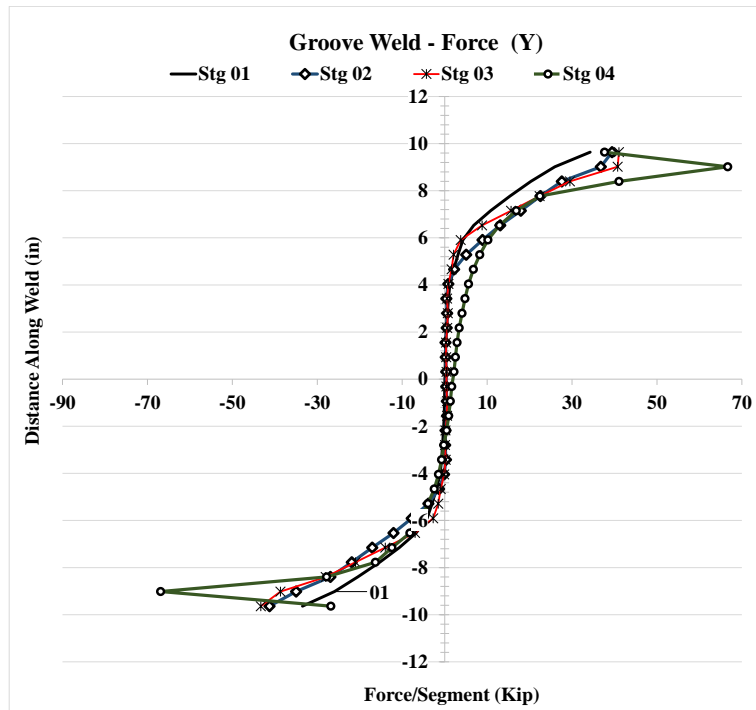


Figure 5.119: Forces and stresses in vertical weld, (X) Case 8C1

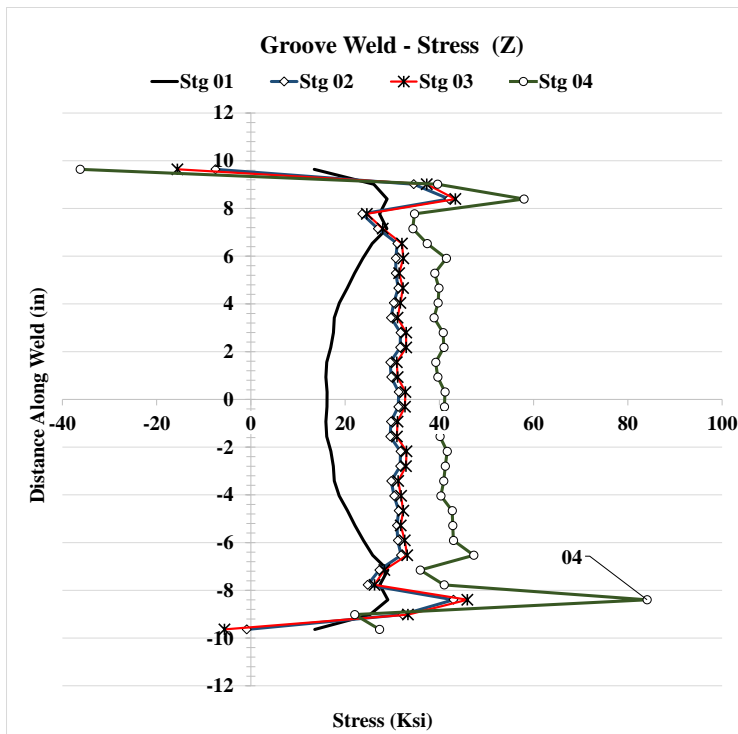
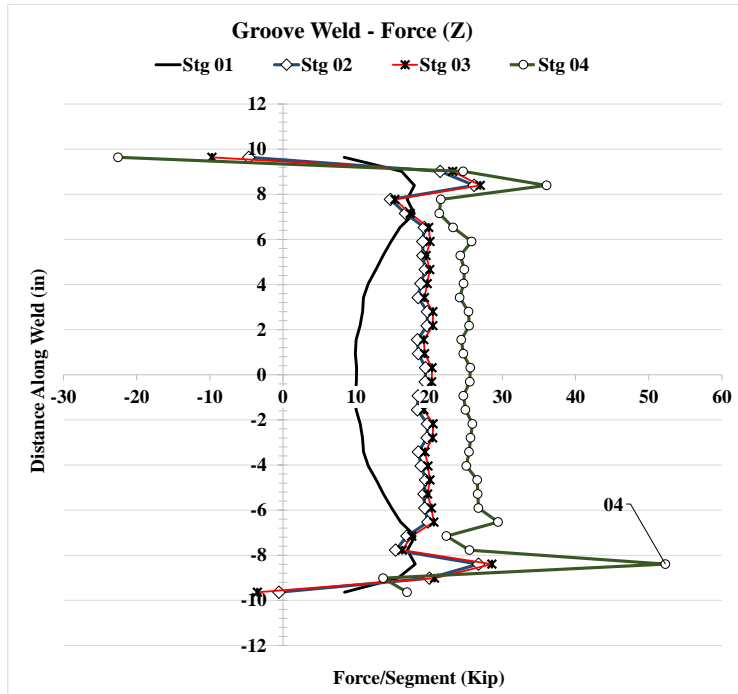


Figure 5.120: Forces and stresses in vertical weld, (Z) Case 8C1



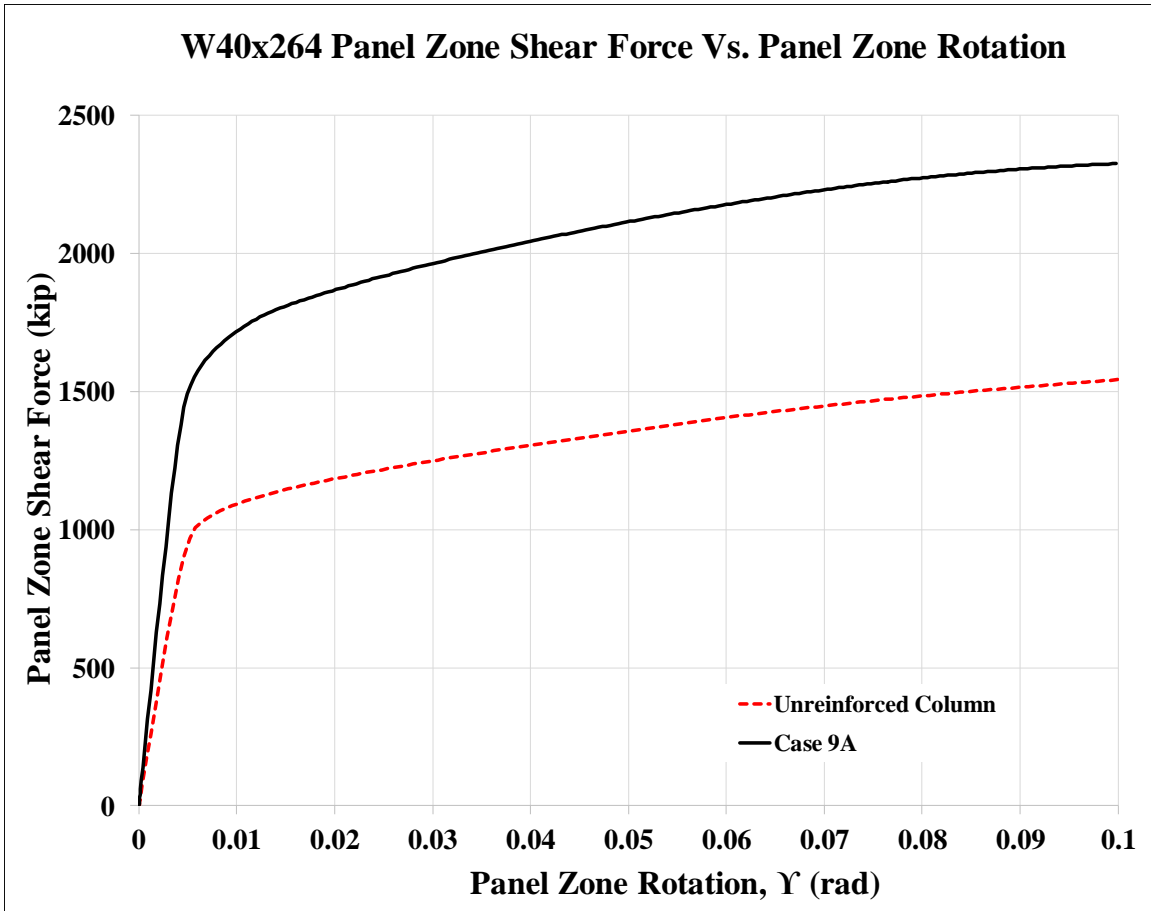


Figure 5.122: Panel zone shear vs. panel zone rotation Case 9A

Stage	Applied Force/Loading Plate (Kip)	Panel Shear Force (Kip)	% Higher Than Unreinforced Col.	Panel Zone Rotation (rad)
1	895	1,492	154%	0.005
2	1,114	1,856	164%	0.019
3	1,122	1,870	158%	0.020
4	1,396	2,326	151%	0.100

Table 5.13: Panel zone shear and force on loading plate Case 9A

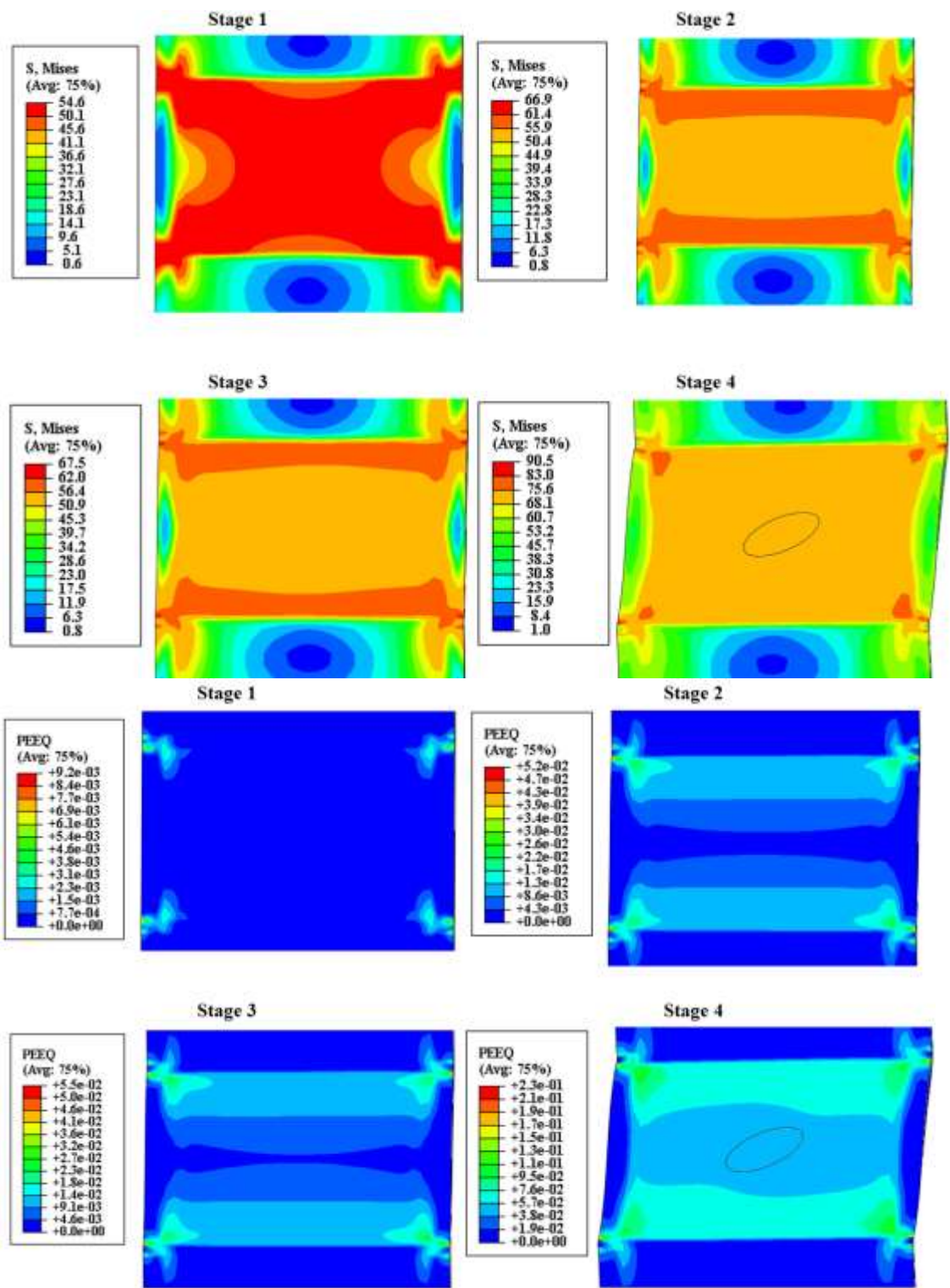


Figure 5.123: VMS and PEEQ in the column Case 9A



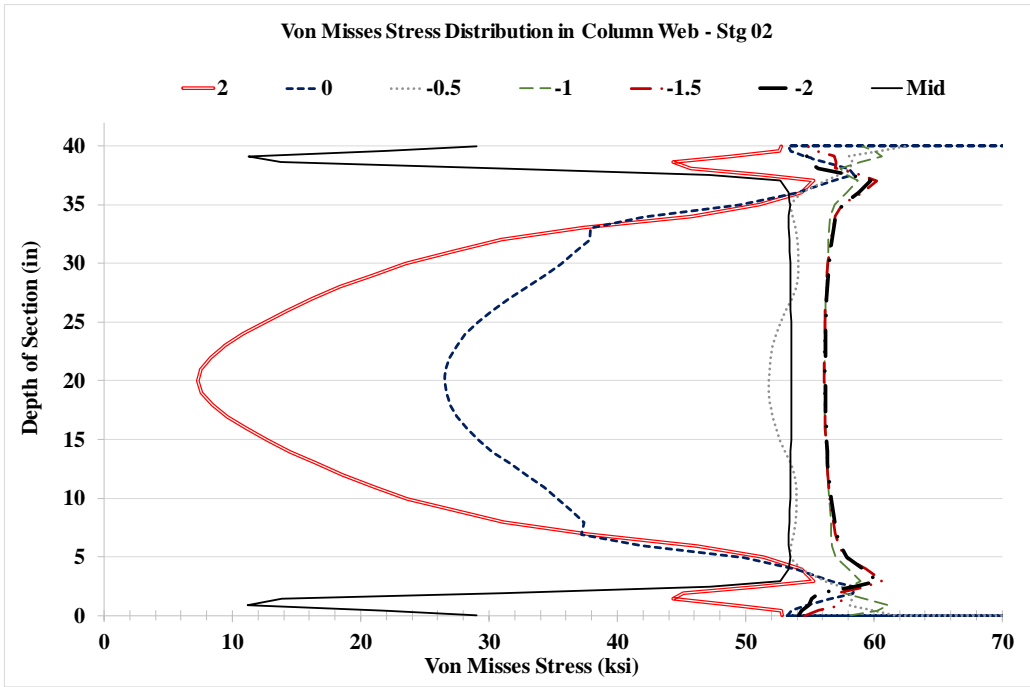
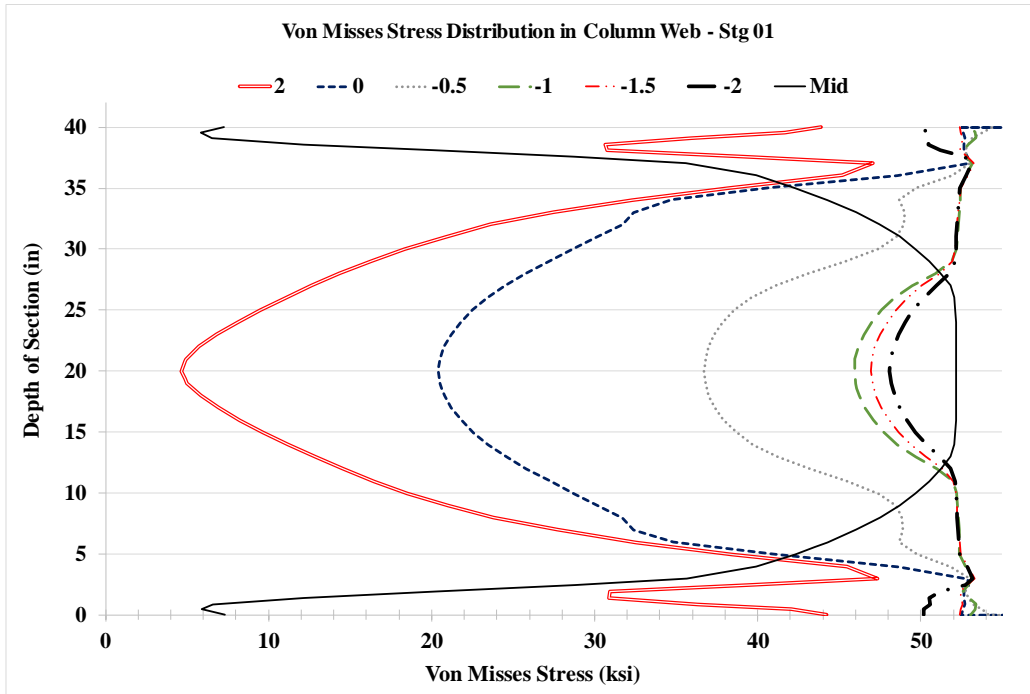


Figure 5.124: VMS distribution in column web at different heights Stg. 01-04 Case 9A

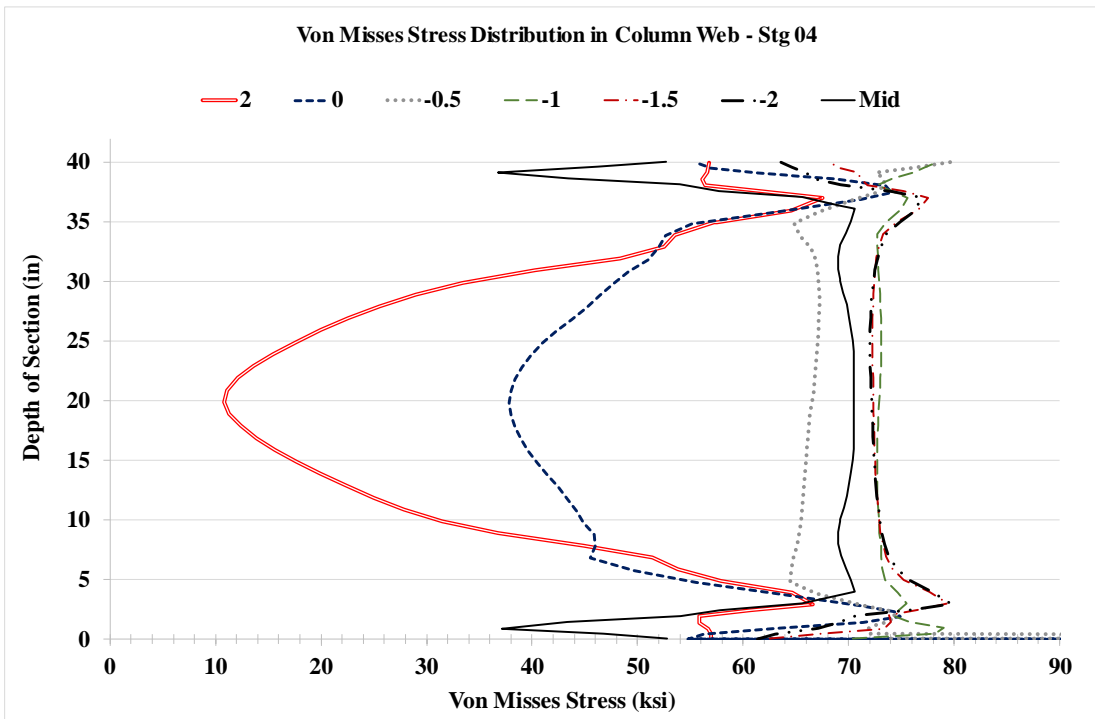
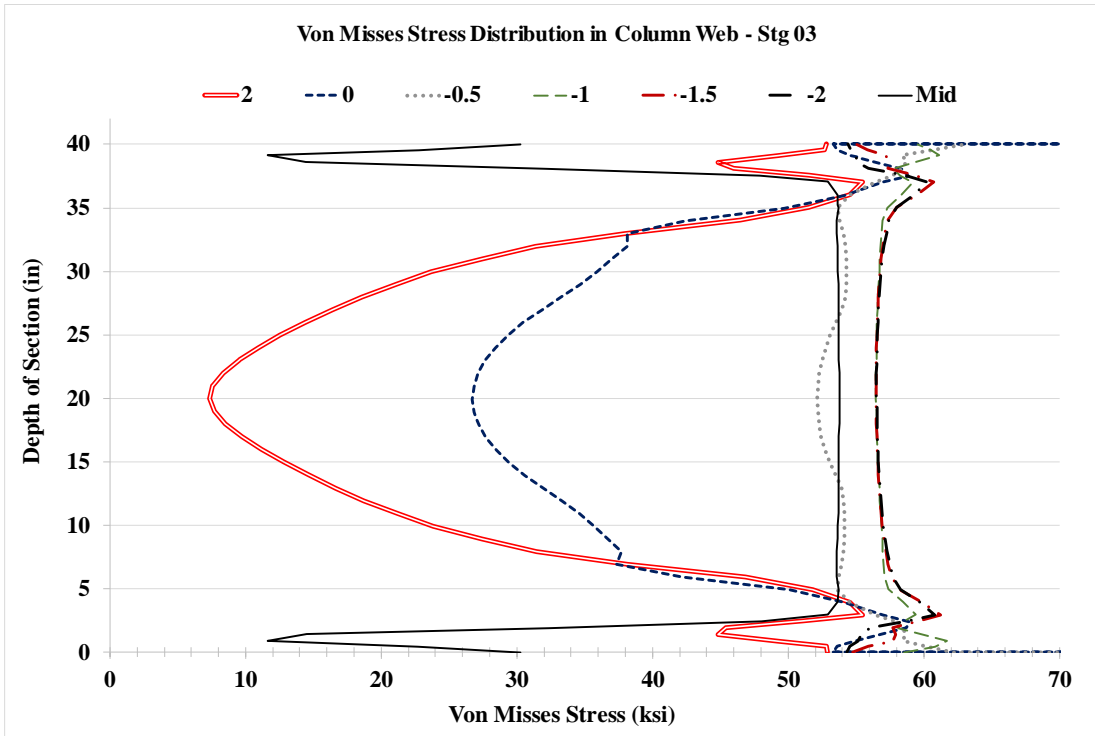


Figure 5.124: VMS distribution in column web at different heights Stg. 01-04 Case 9A

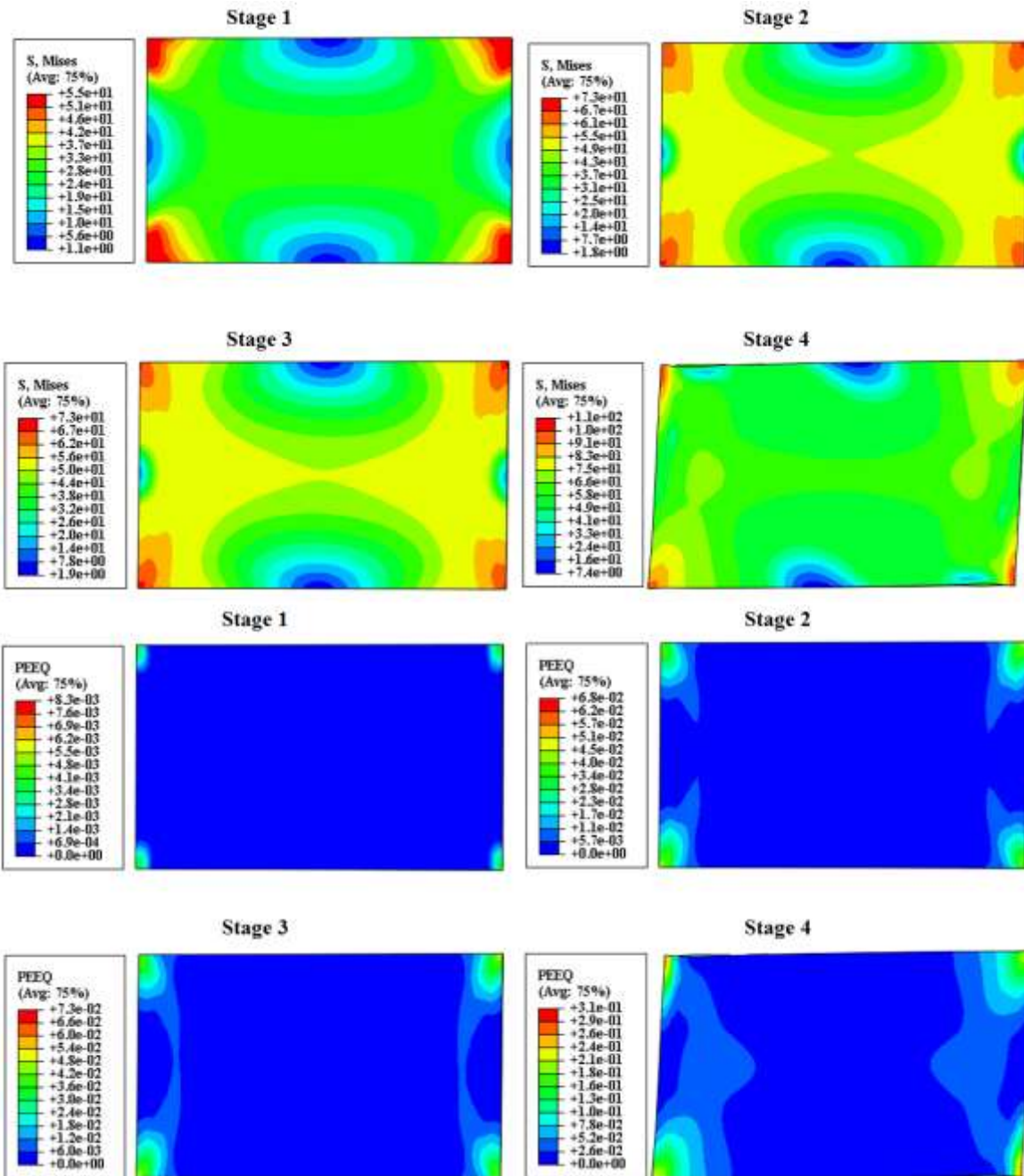


Figure 5.125: VMS and PEEQ in the DP Case 9A

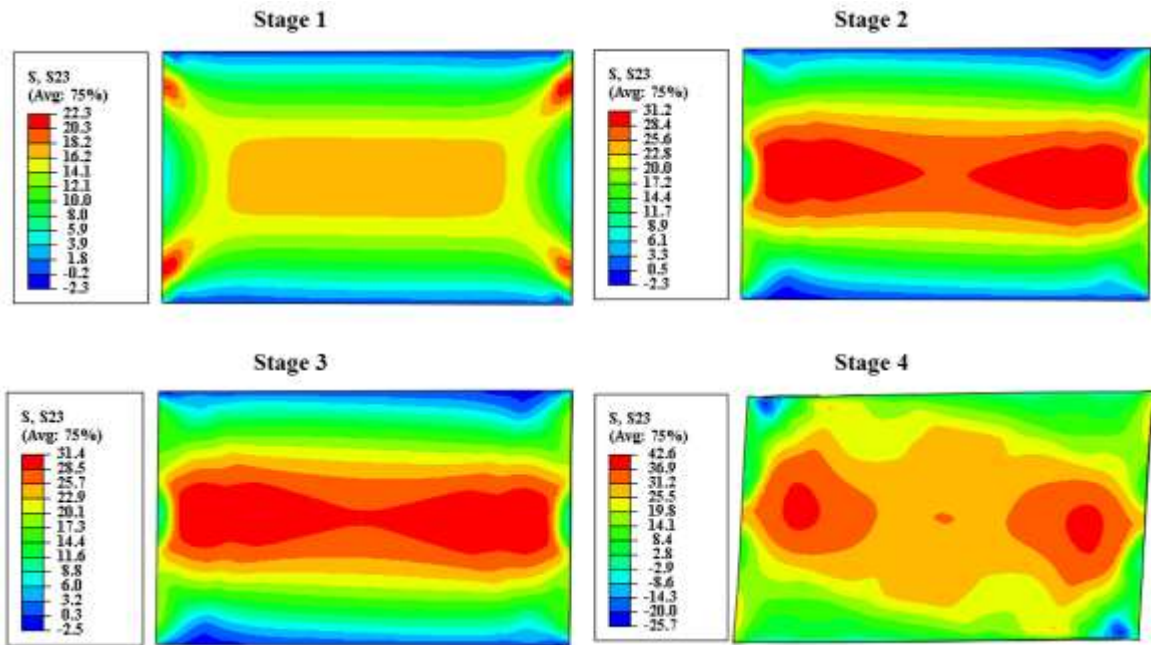


Figure 5.126: Shear stress, S23 in the DP Case 9A

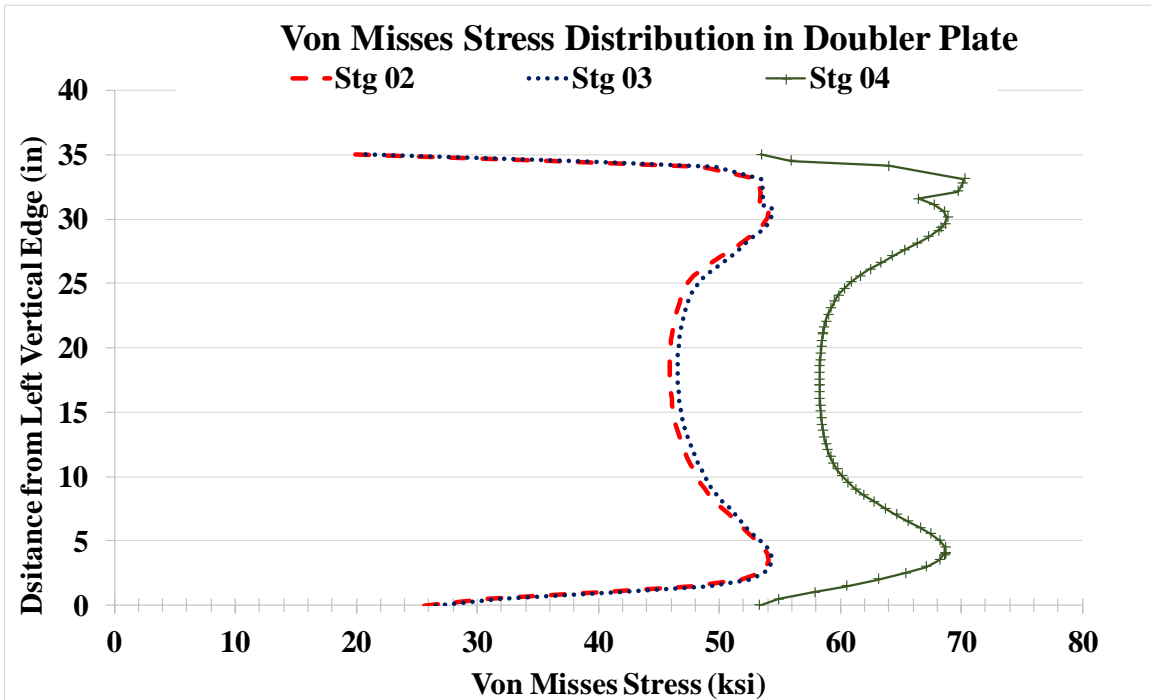


Figure 5.127: VMS distribution at mid-depth of DP Case 9A

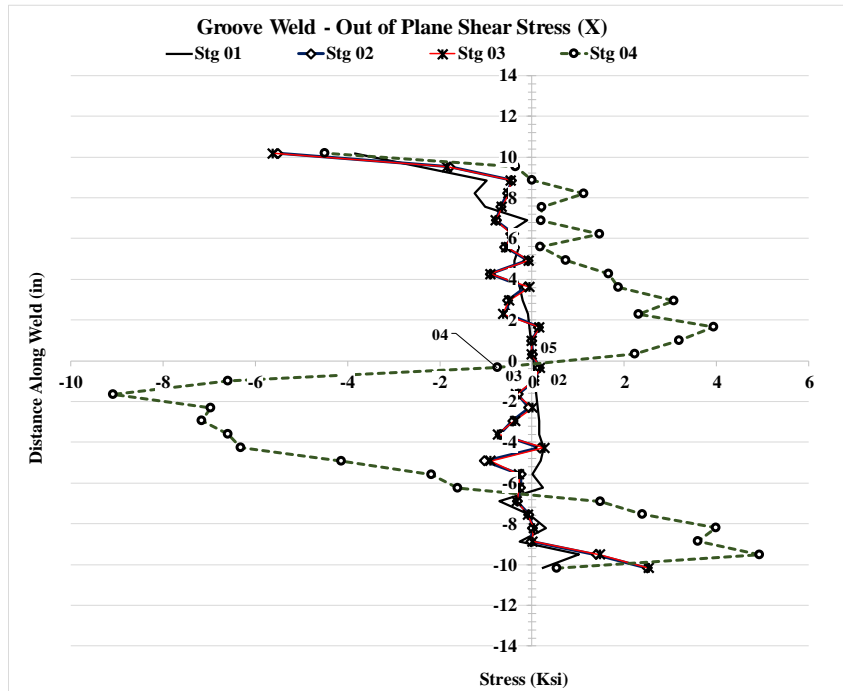
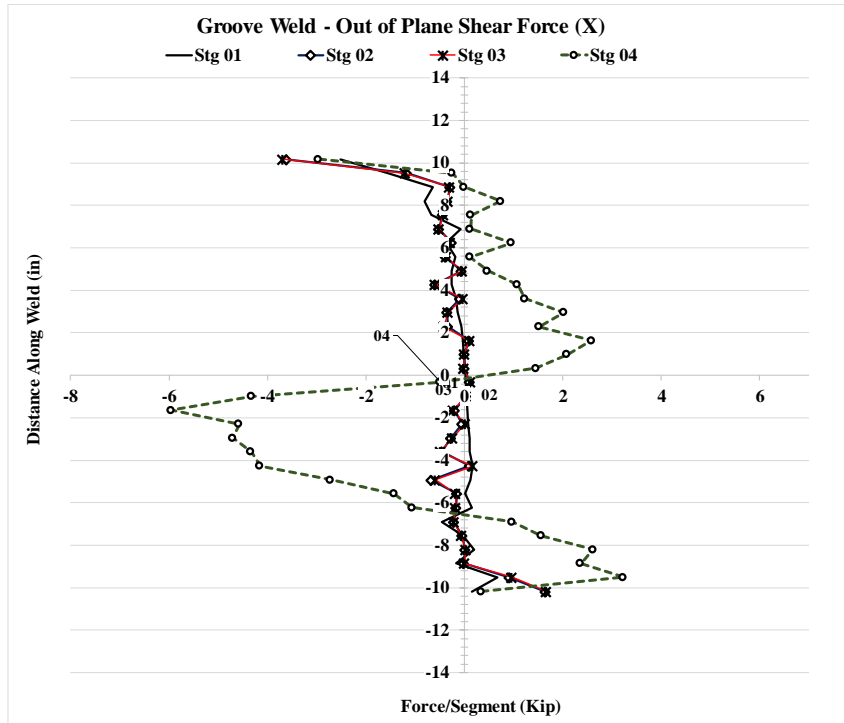


Figure 5.128: Forces and stresses in vertical weld, (X) Case 9A

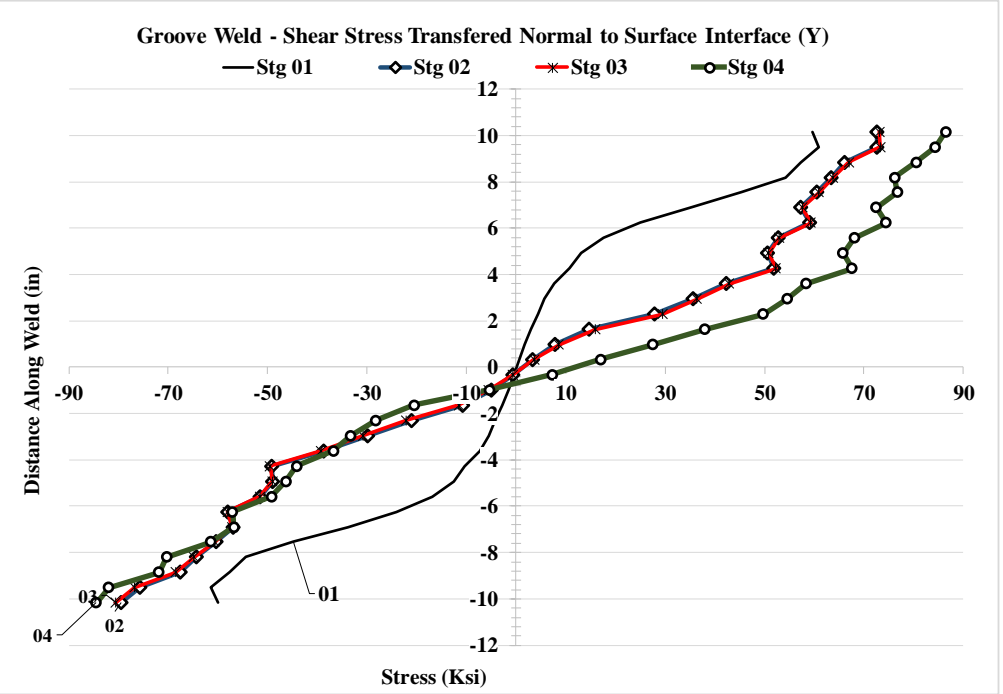
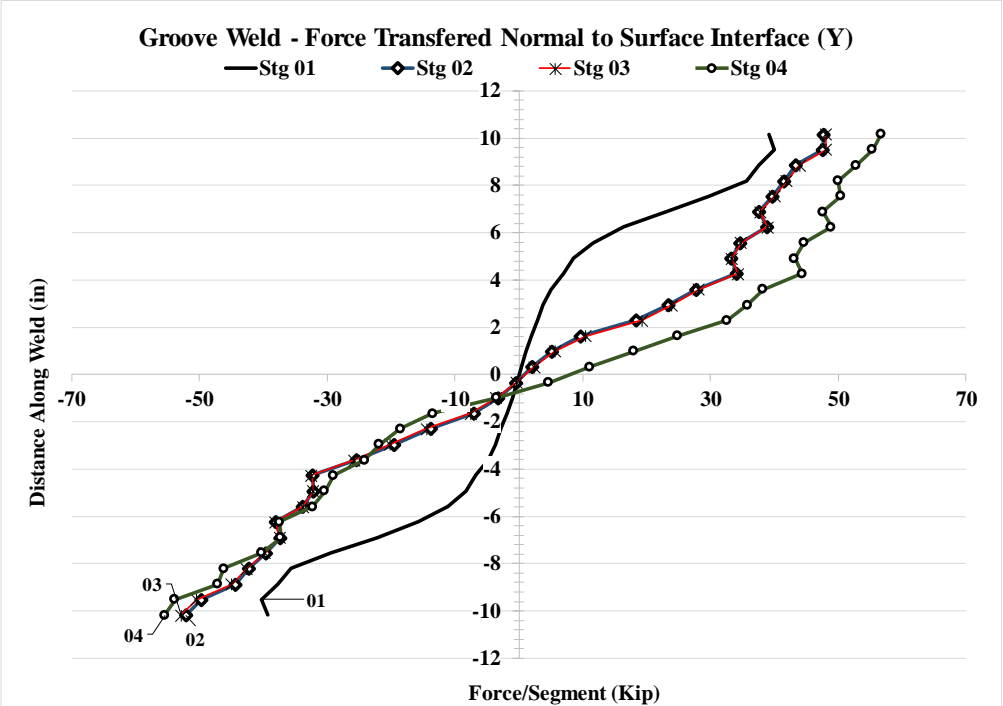


Figure 5.129: Forces and stresses in vertical weld, (Y) Case 9A

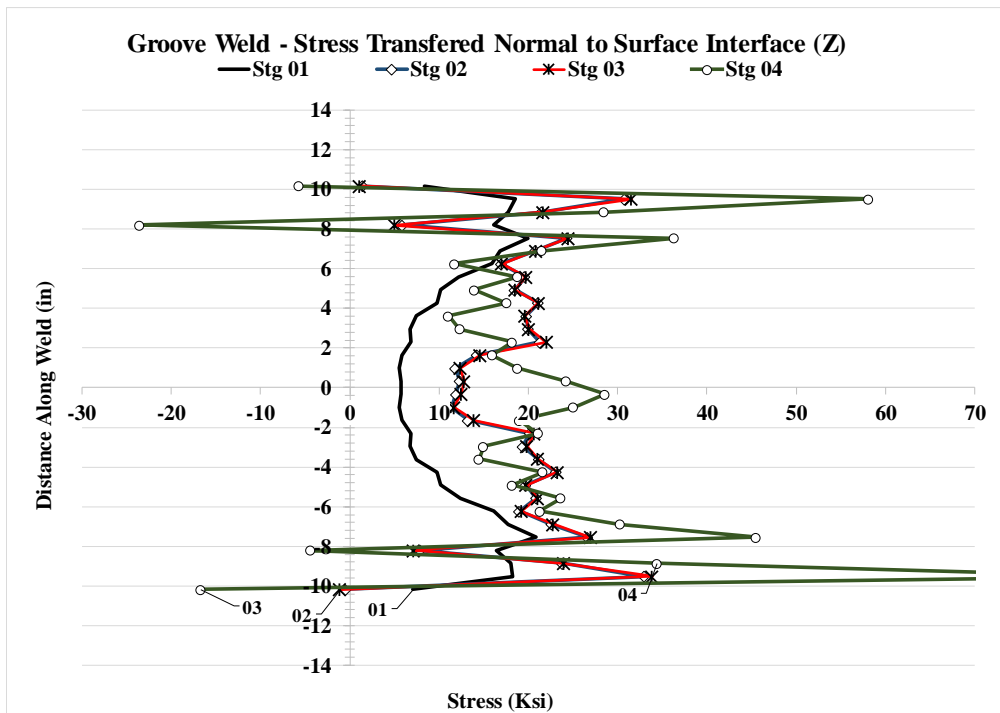
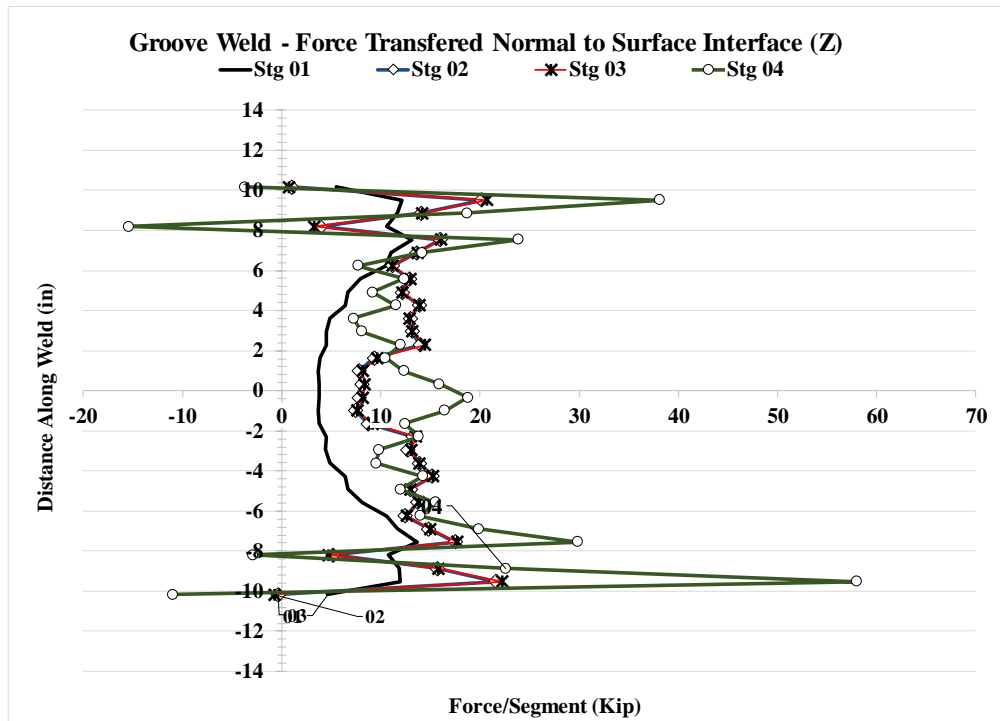


Figure 5.130: Forces and stresses in vertical weld, (Z) Case 9A

5.2.13 Analysis Case 9C

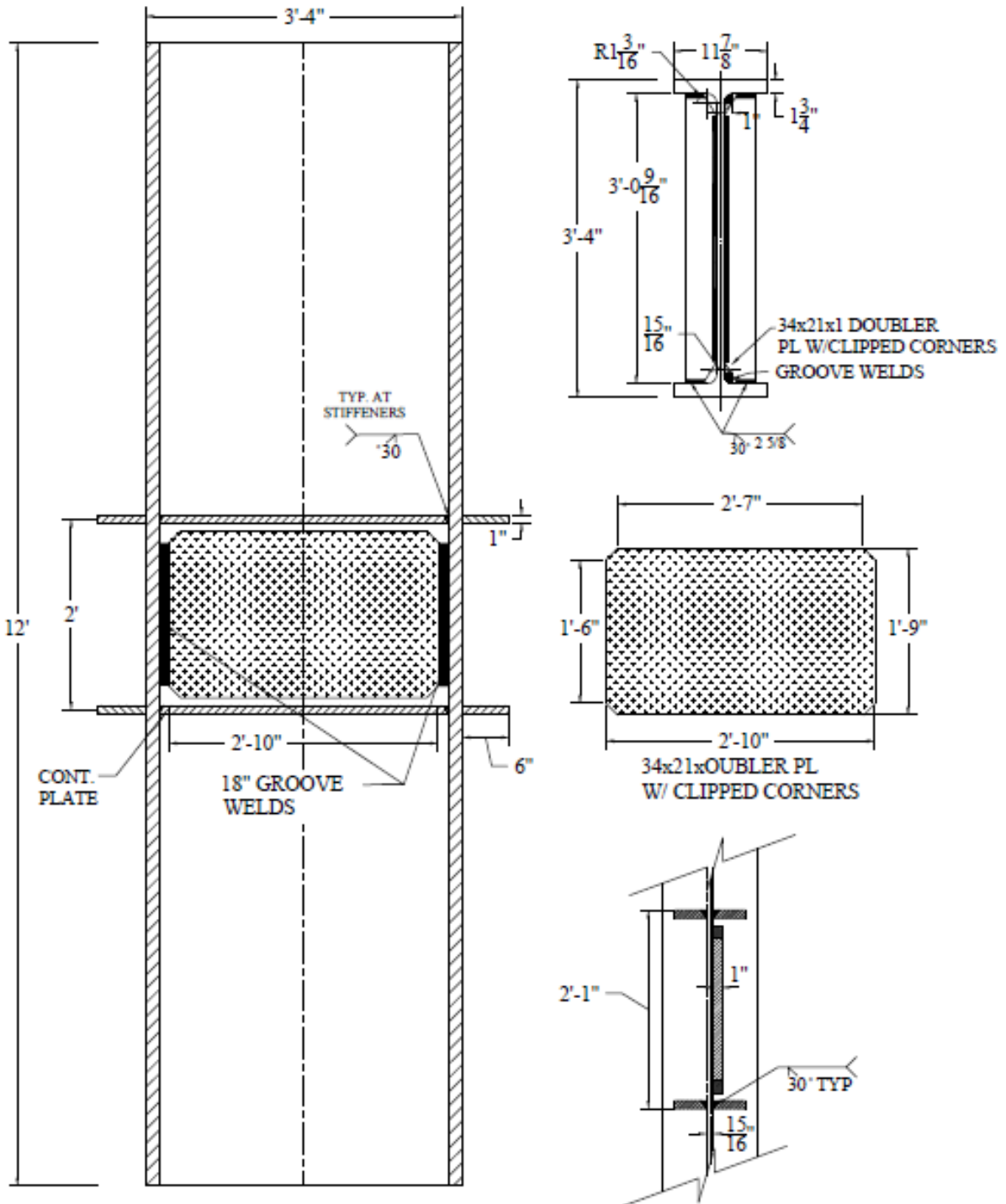


Figure 5.131: W40x264 Analysis case 9C



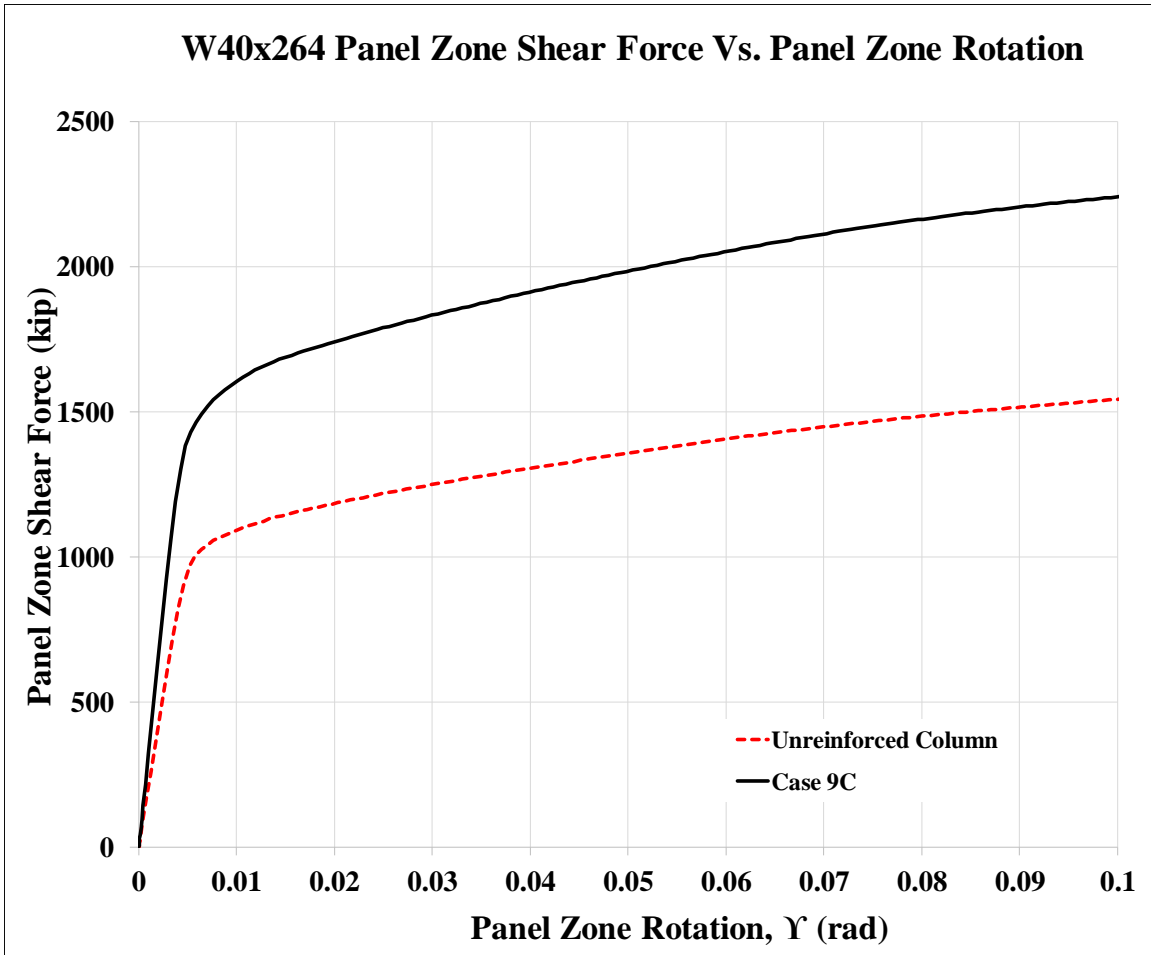


Figure 5.132: Panel zone shear vs. panel zone rotation Case 9C

Stage	Applied Force/Loading Plate (Kip)	Panel Shear Force (Kip)	% Higher Than Unreinforced Col.	Panel Zone Rotation (rad)
1	830	1,384	143%	0.005
2	1,026	1,709	151%	0.017
3	1,049	1,748	147%	0.021
4	1,346	2,243	145%	0.101

Table 5.14: Panel zone shear and force on loading plate Case 9C

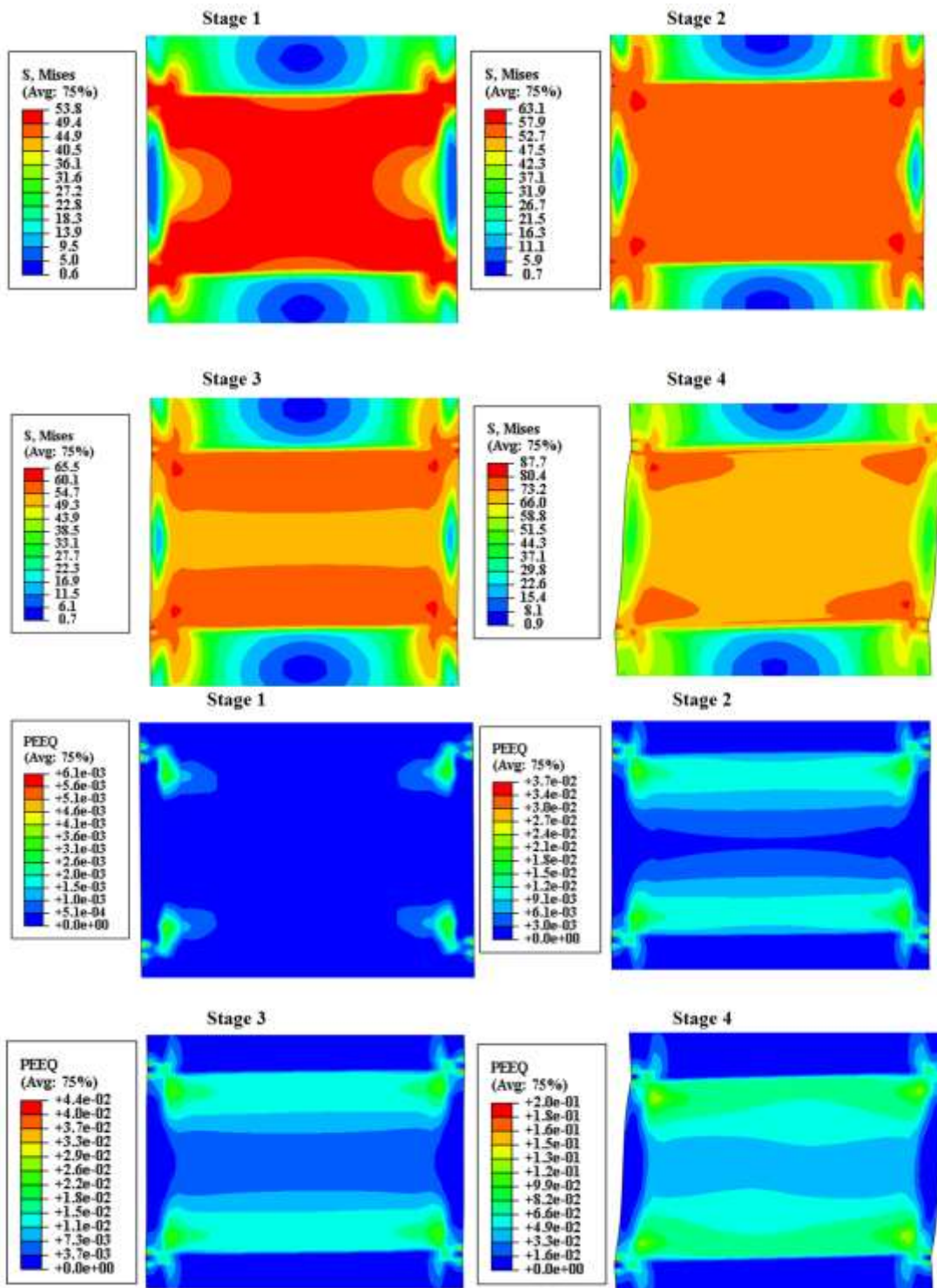


Figure 5.133: VMS and PEEQ in the column Case 9C

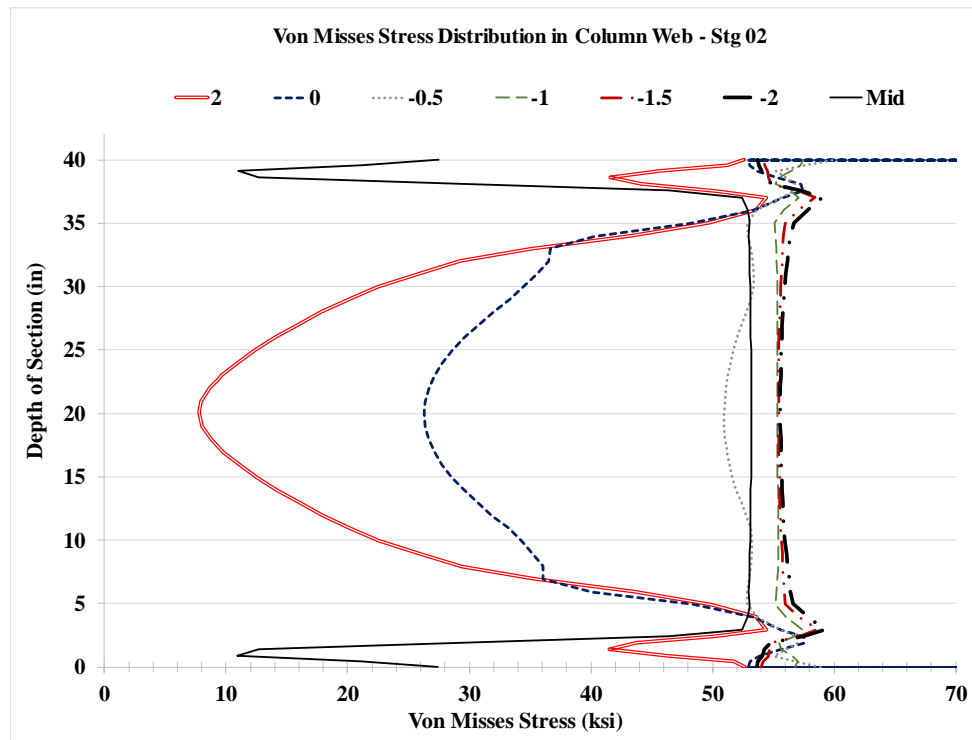
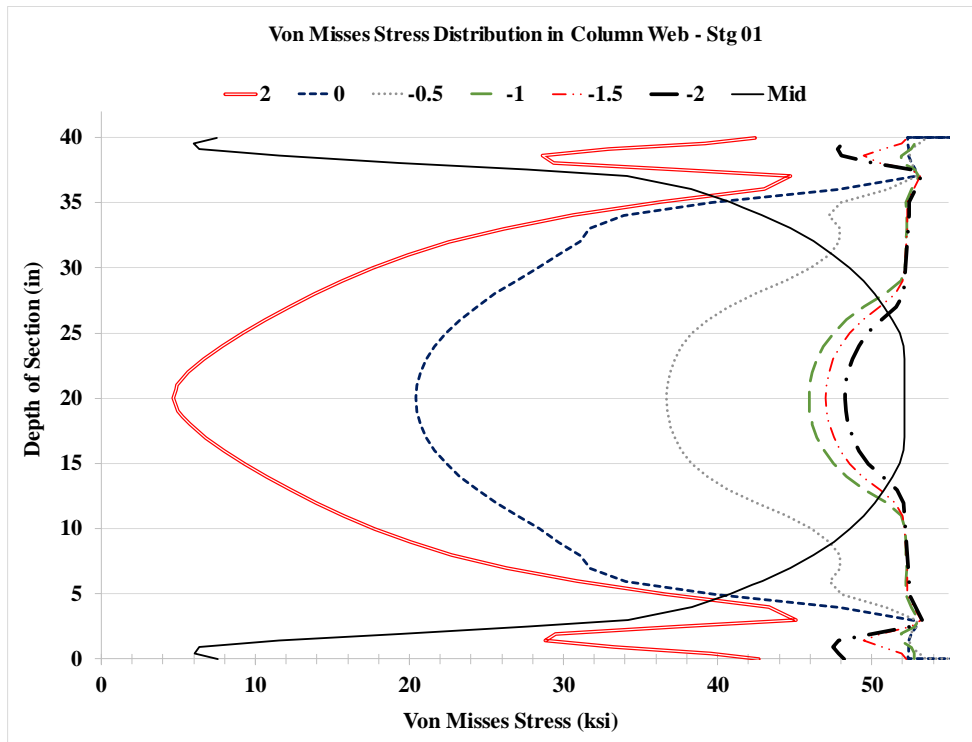


Figure 5.134: VMS distribution in column web at different heights Stg. 01-04 Case 9C

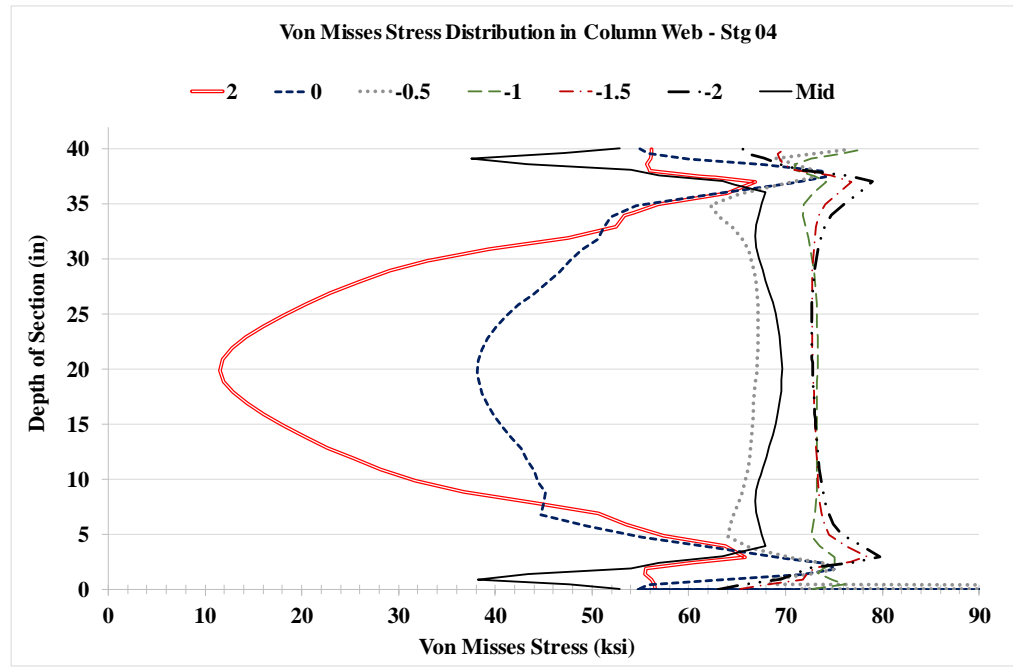
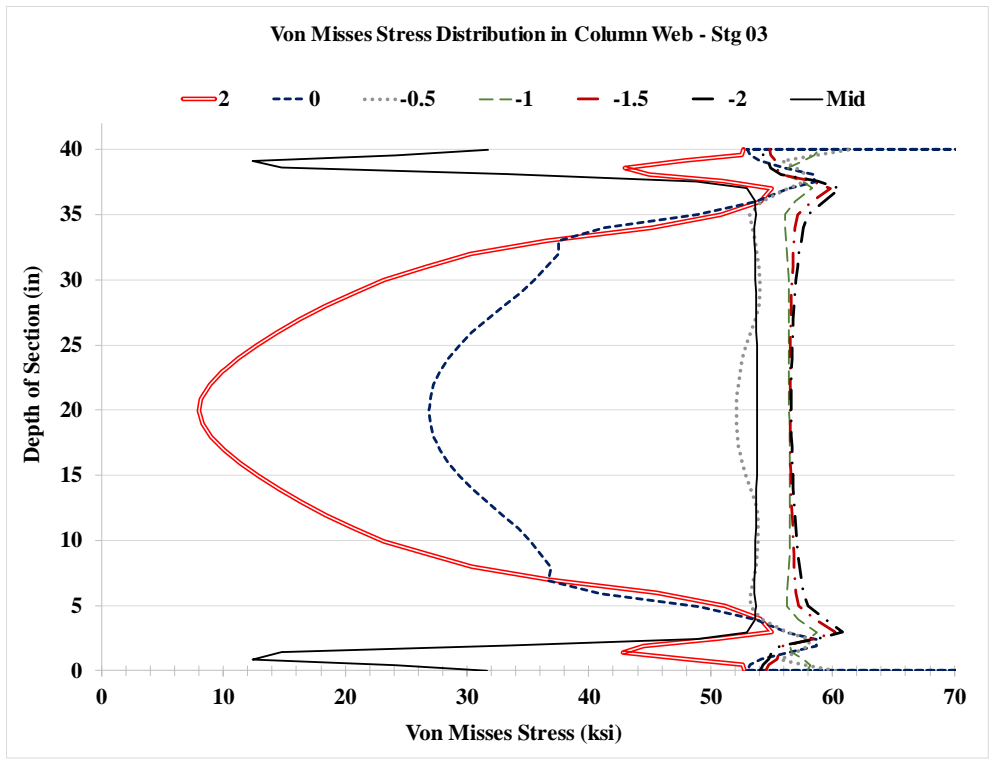


Figure 5.134: VMS distribution in column web at different heights Stg. 01-04 Case 9C

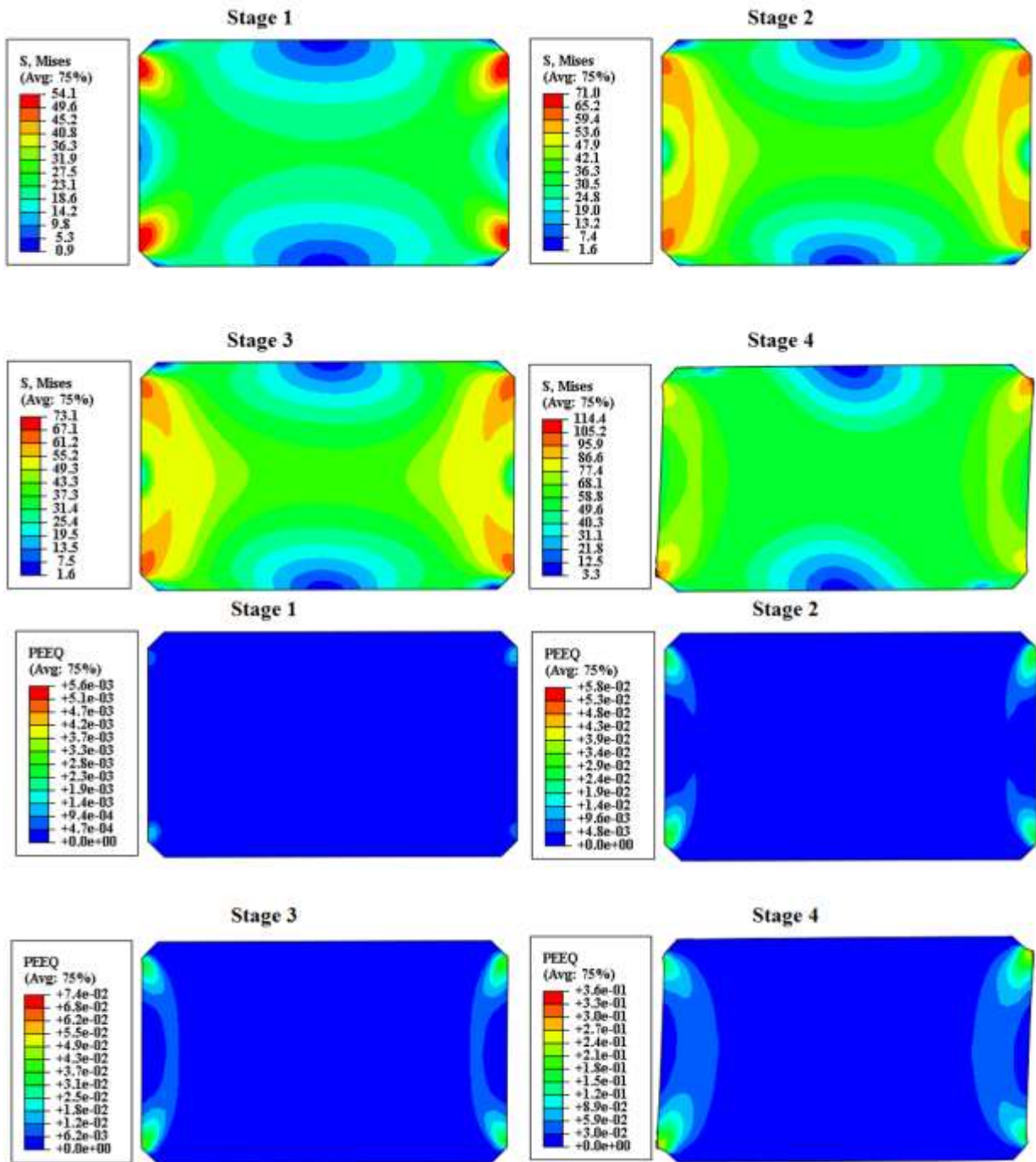


Figure 5.135: VMS and PEEQ in the DP Case 9C

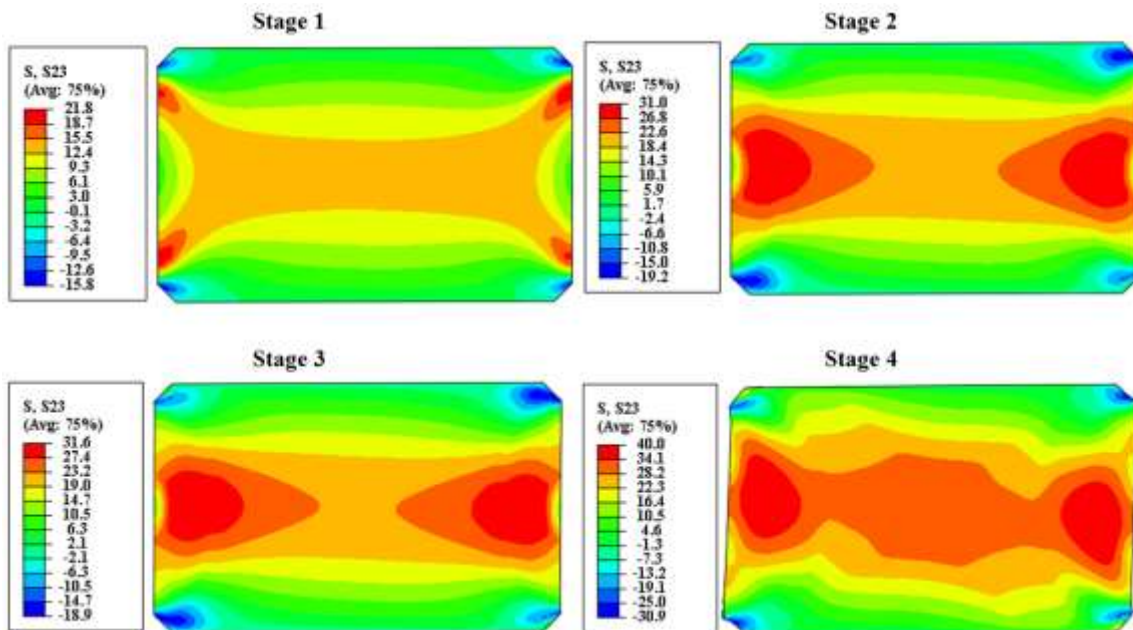


Figure 5.136: Shear stress, S23 in the DP Case 9C

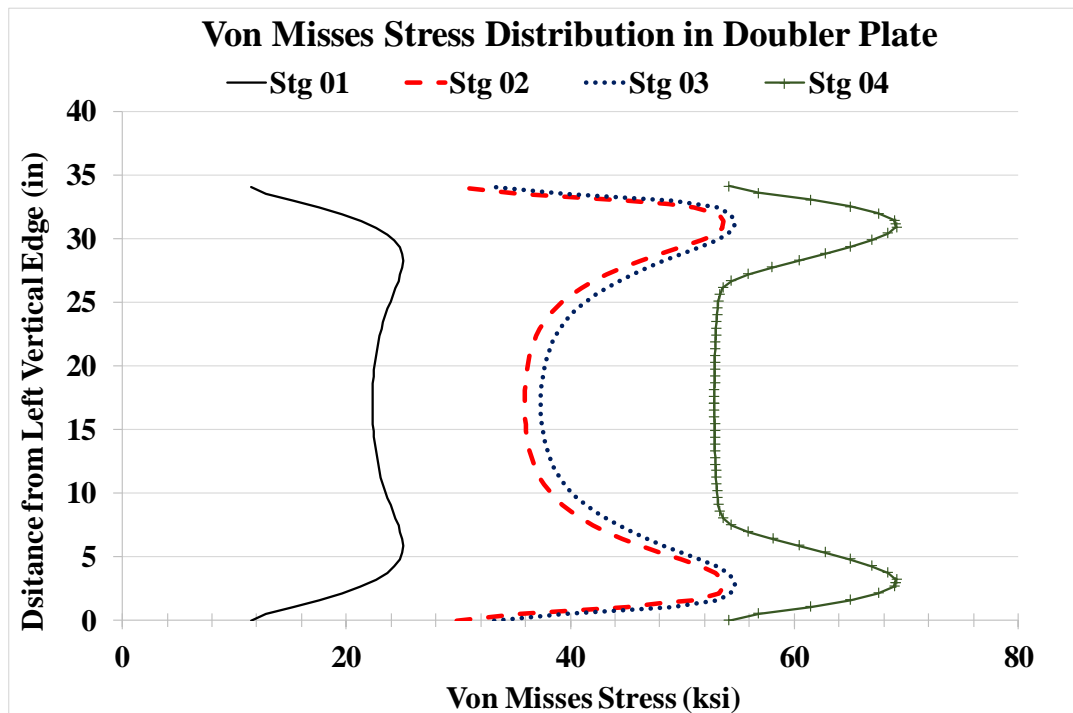


Figure 5.137: VMS distribution at mid-depth of DP Case 9C

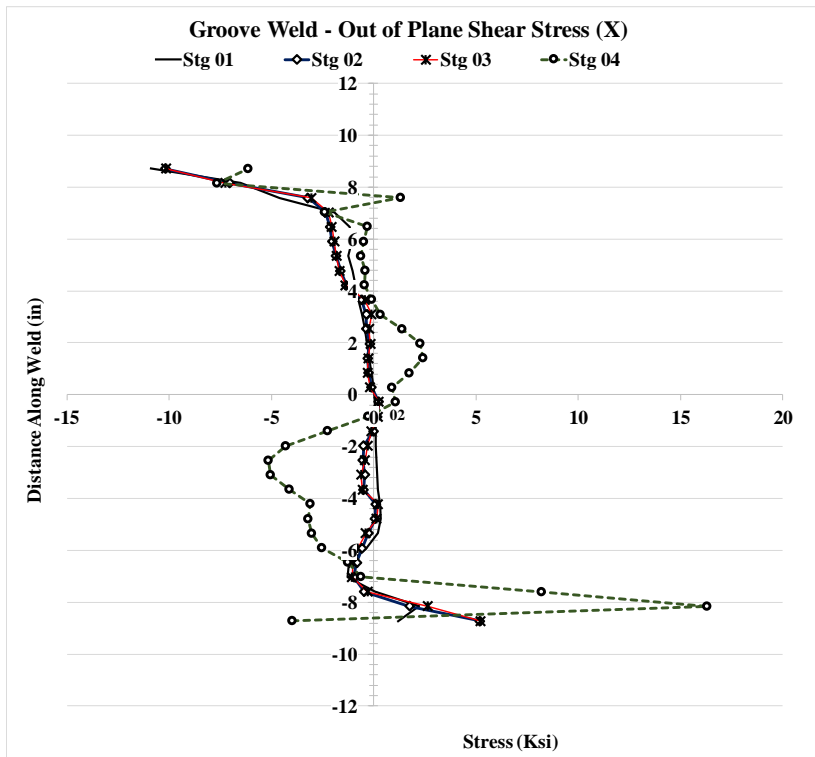
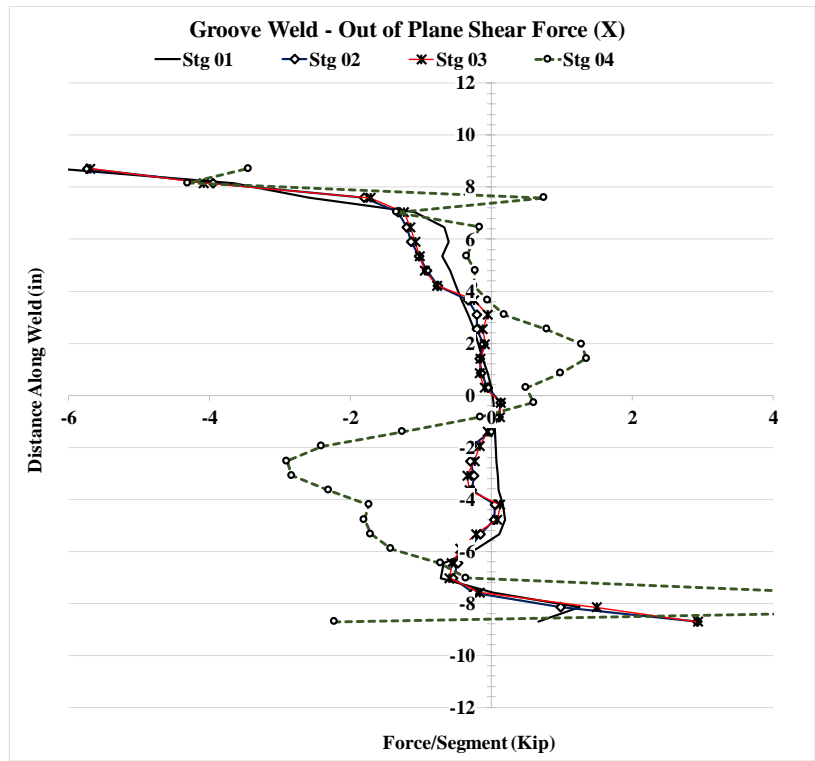


Figure 5.138: Forces and stresses in vertical weld, (X) Case 9C

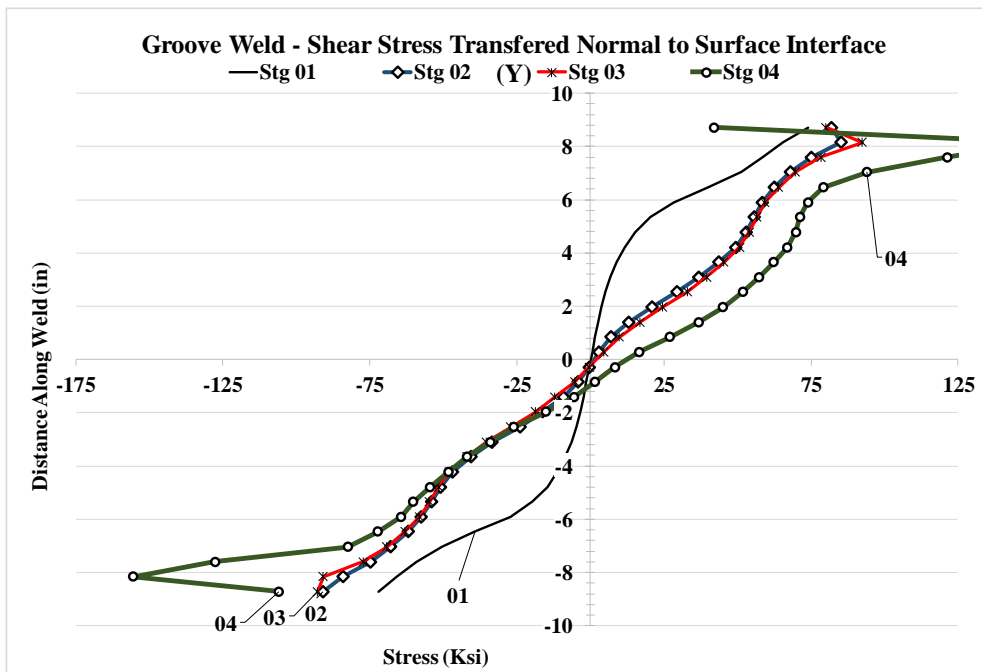
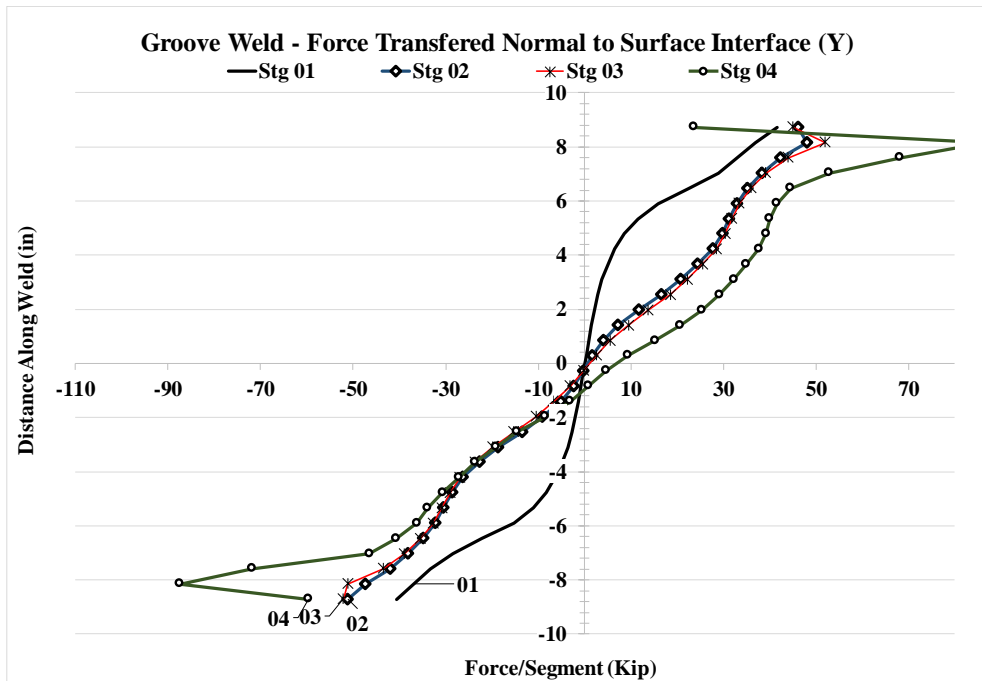


Figure 5.139: Forces and stresses in vertical weld, (Y) Case 9C



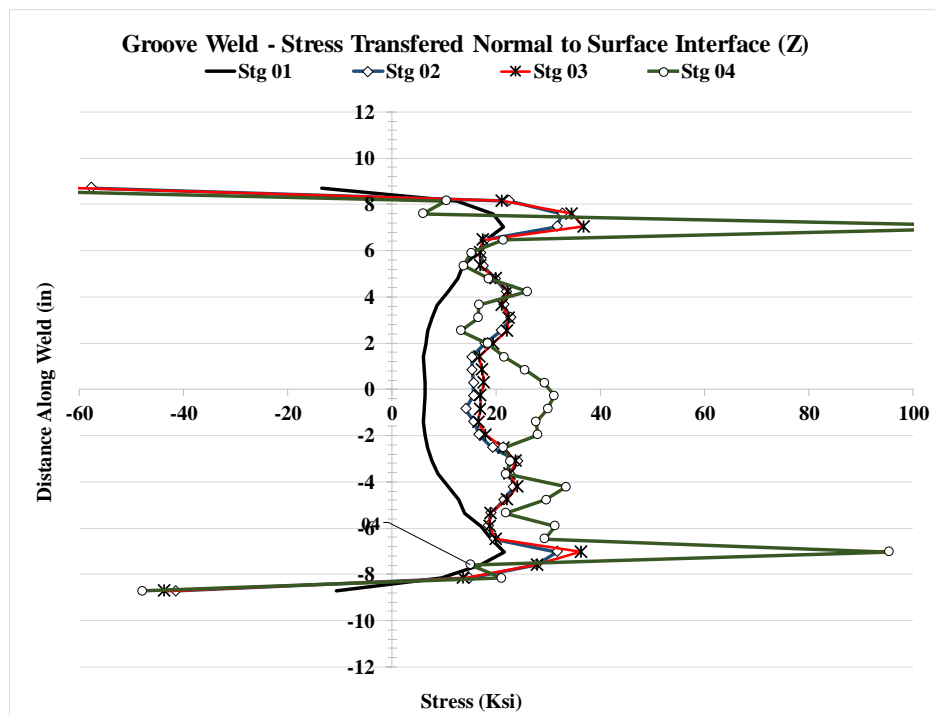
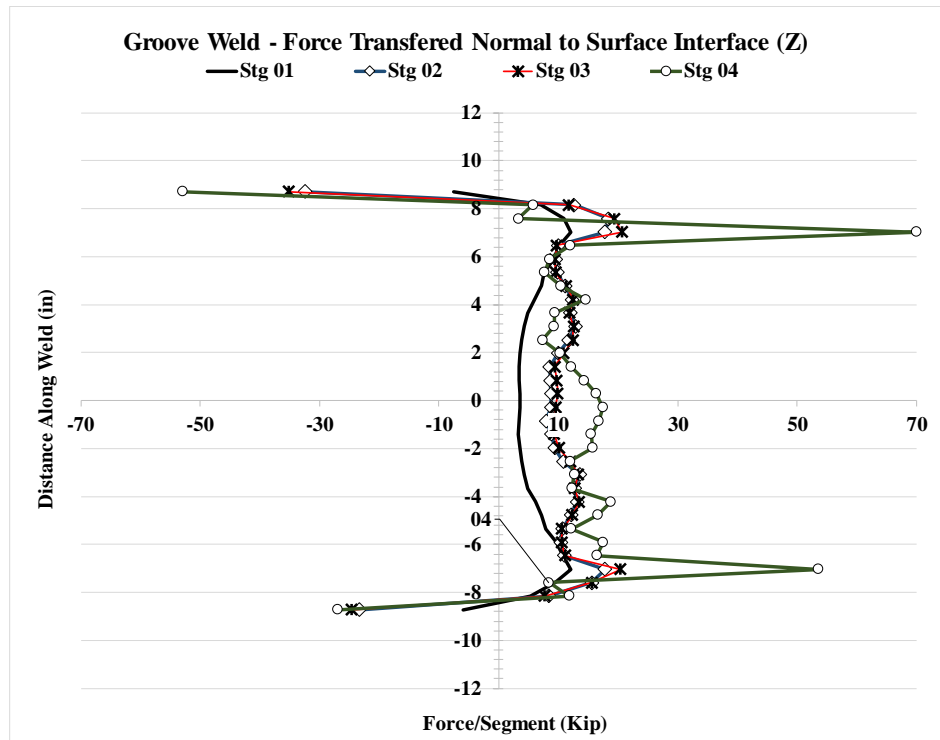


Figure 5.140: Forces and stresses in vertical weld, (Z) Case 9C

### 5.2.14 Analysis Case 10A1

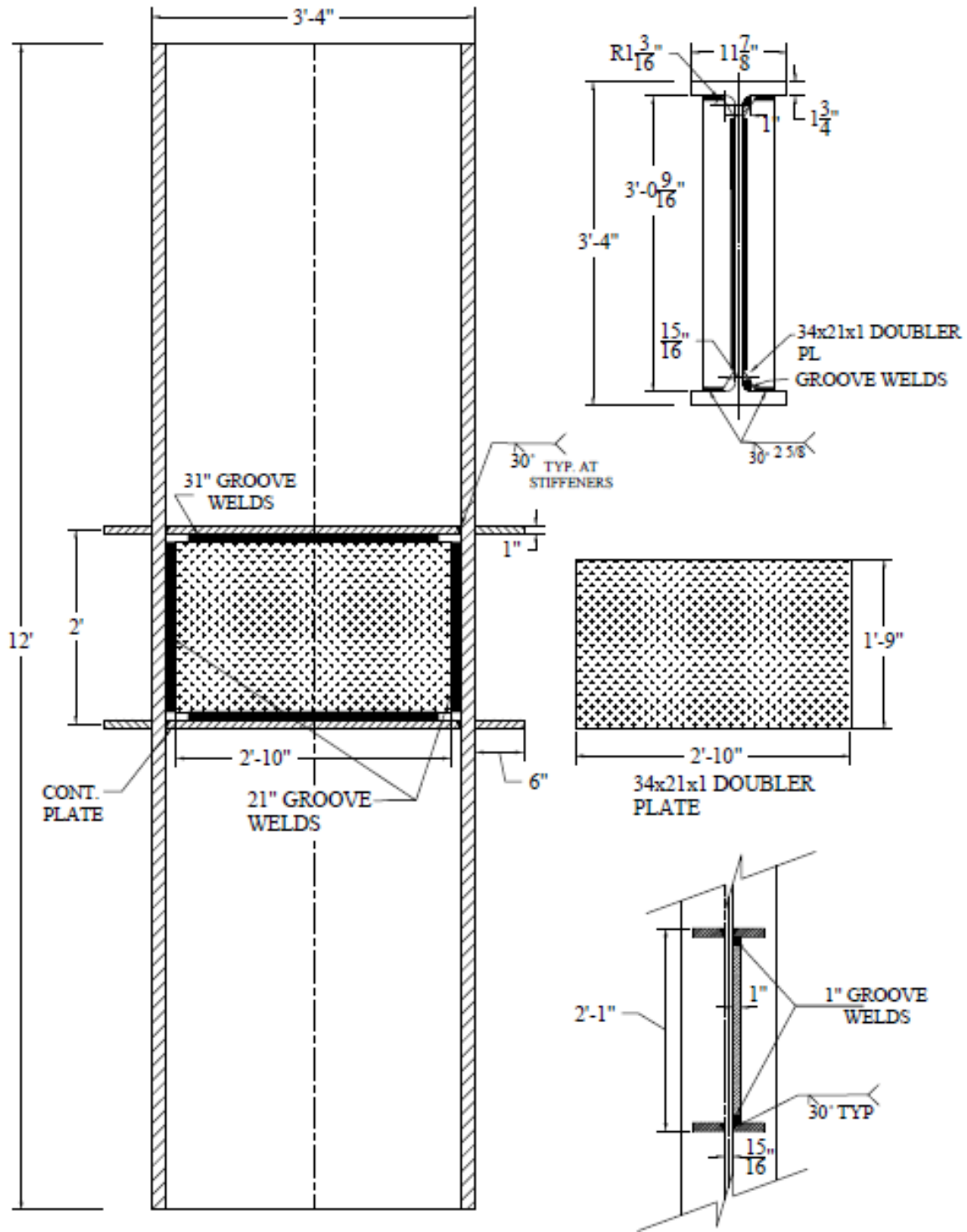


Figure 5.141: W40x264 Analysis case 10A1

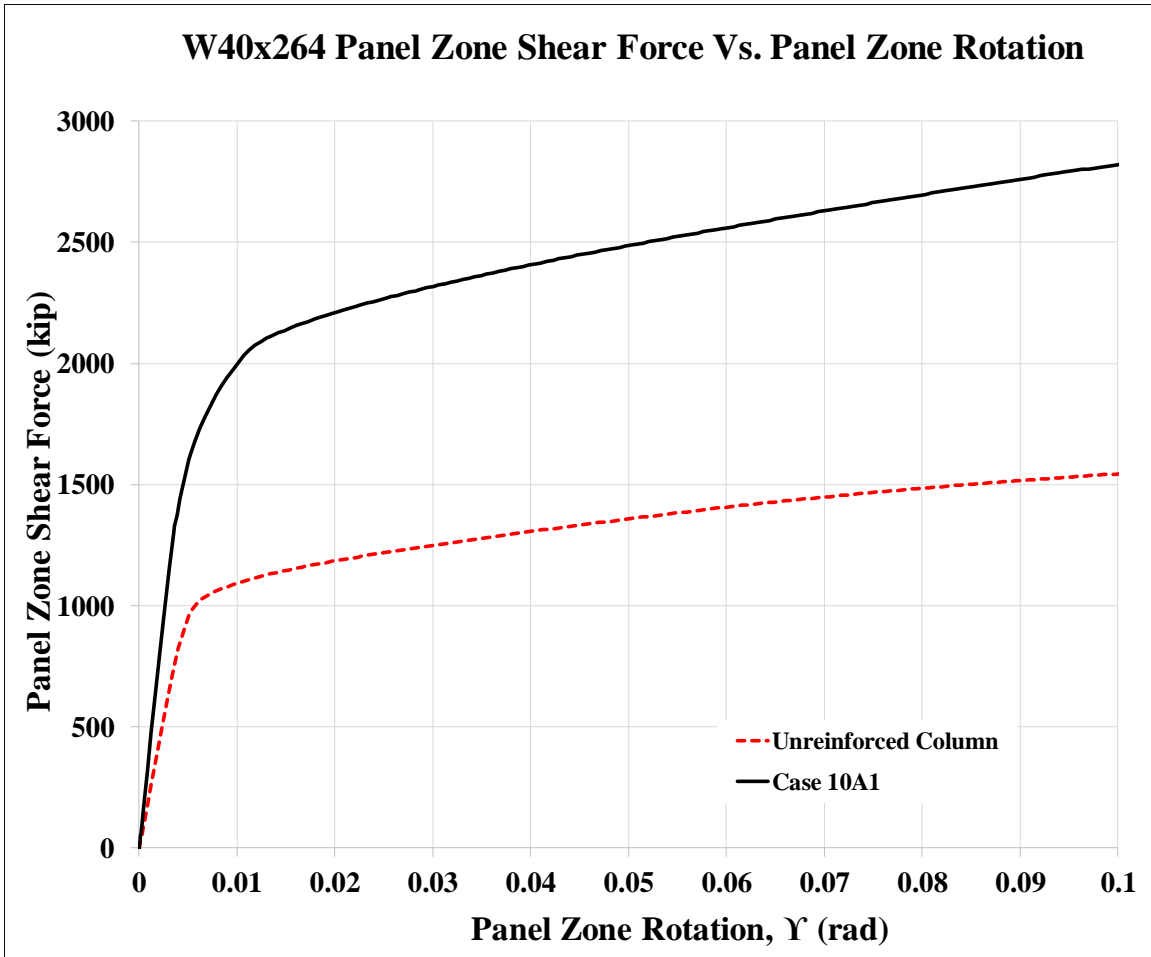


Figure 5.142: Panel zone shear vs. panel zone rotation Case 10A1

Stage	Applied Force/Loading Plate (Kip)	Panel Shear Force (Kip)	% Higher Than Unreinforced Col.	Panel Zone Rotation (rad)
1	913	1,522	157%	0.005
2	1,308	2,181	193%	0.018
3	1,327	2,212	186%	0.020
4	1,693	2,821	183%	0.100

Table 5.15: Panel zone shear and force on loading plate Case 10A1

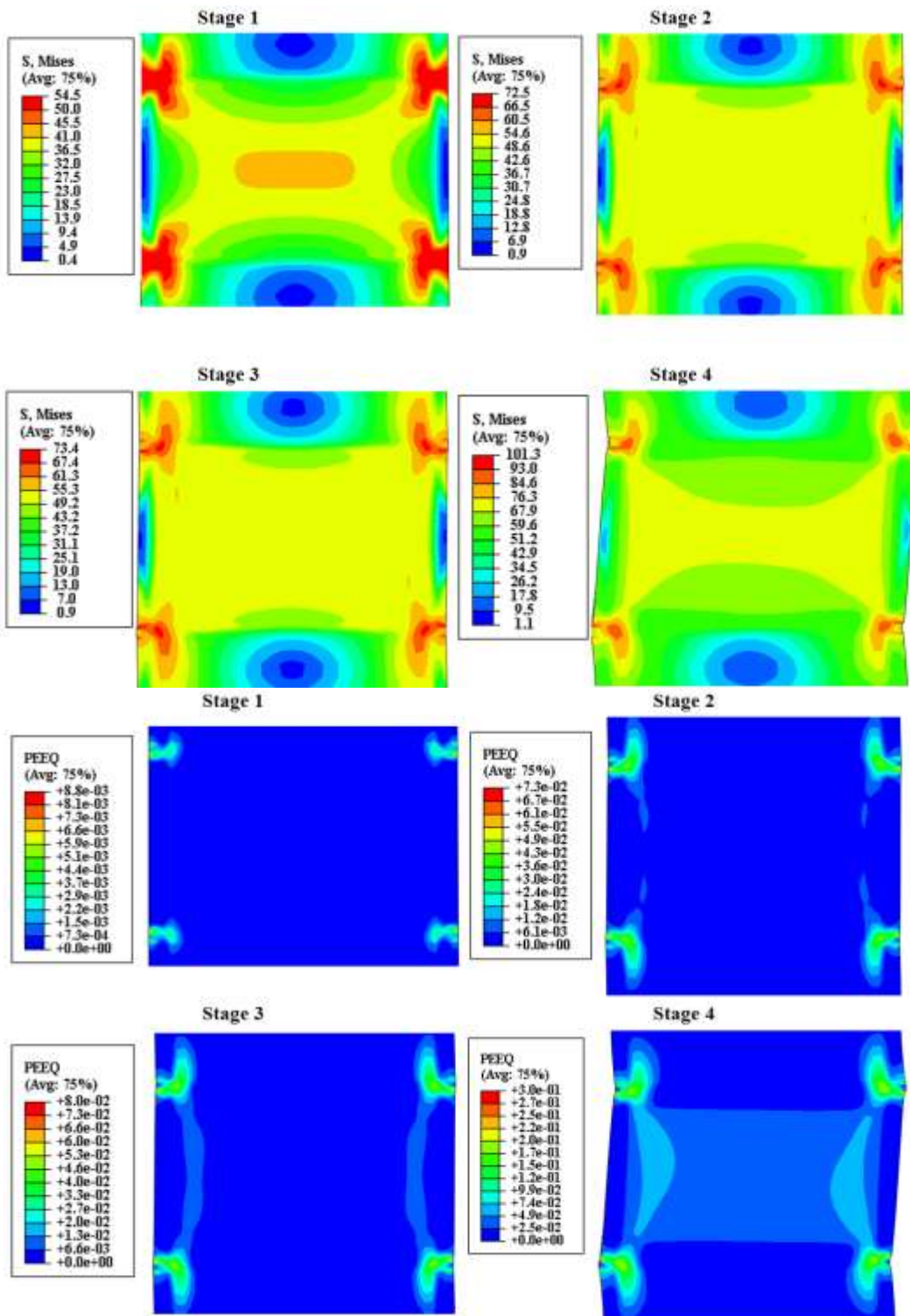


Figure 5.143: VMS and PEEQ in the column Case 10A1

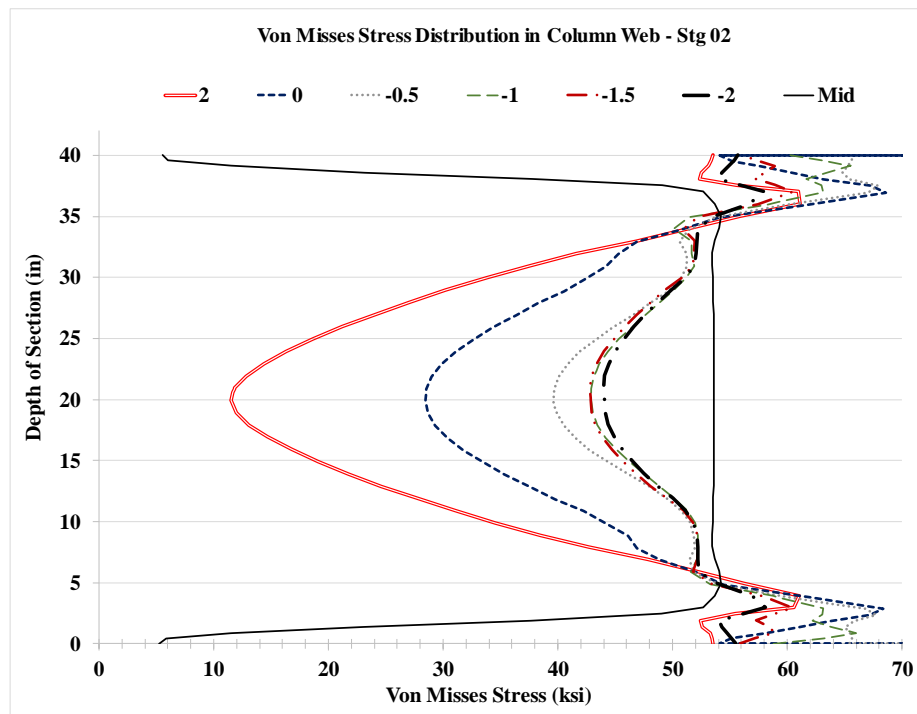
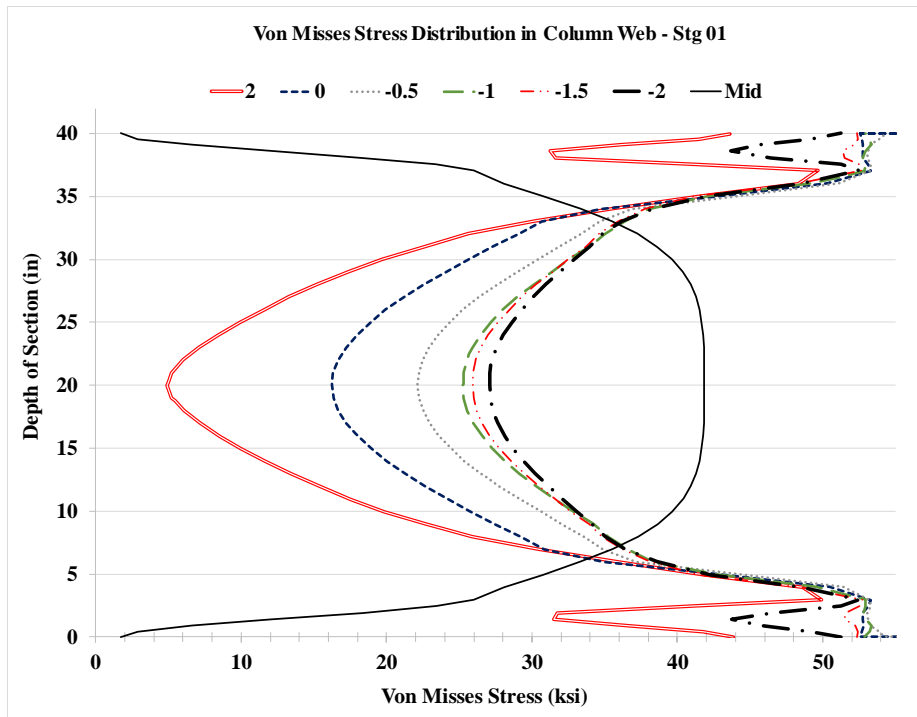


Figure 5.144: VMS distribution in column web at different heights Stg. 01-04 Case 10A1

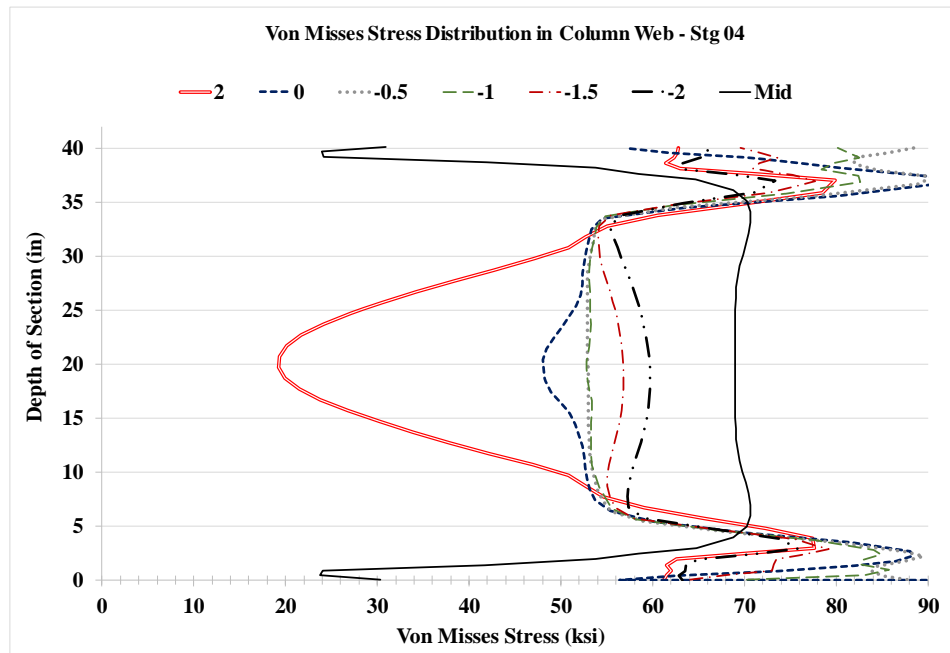
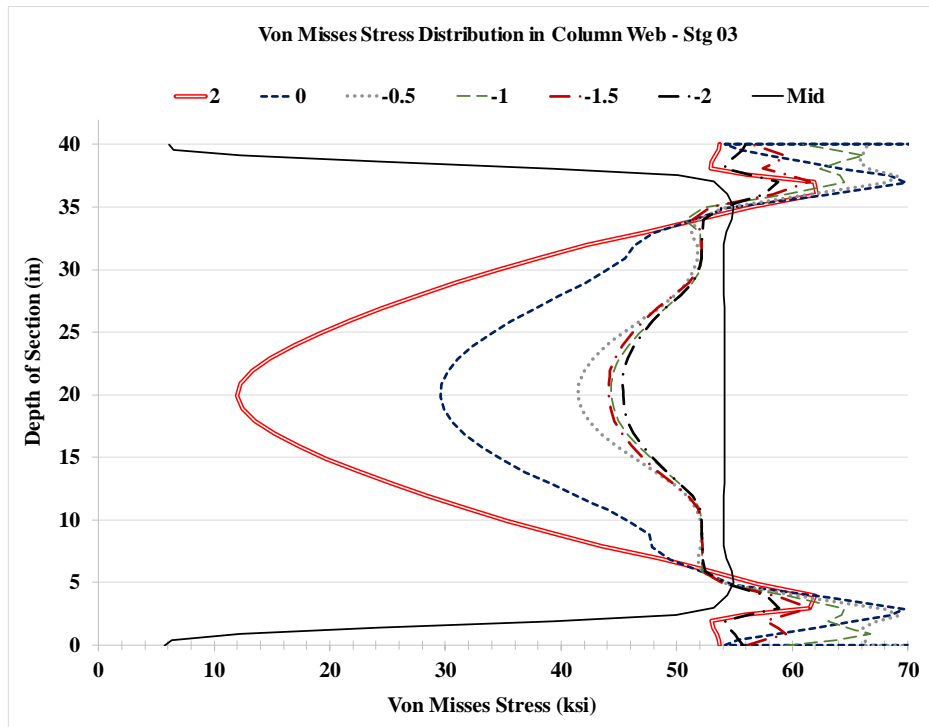


Figure 5.144: VMS distribution in column web at different heights Stg. 01-04 Case 10A1

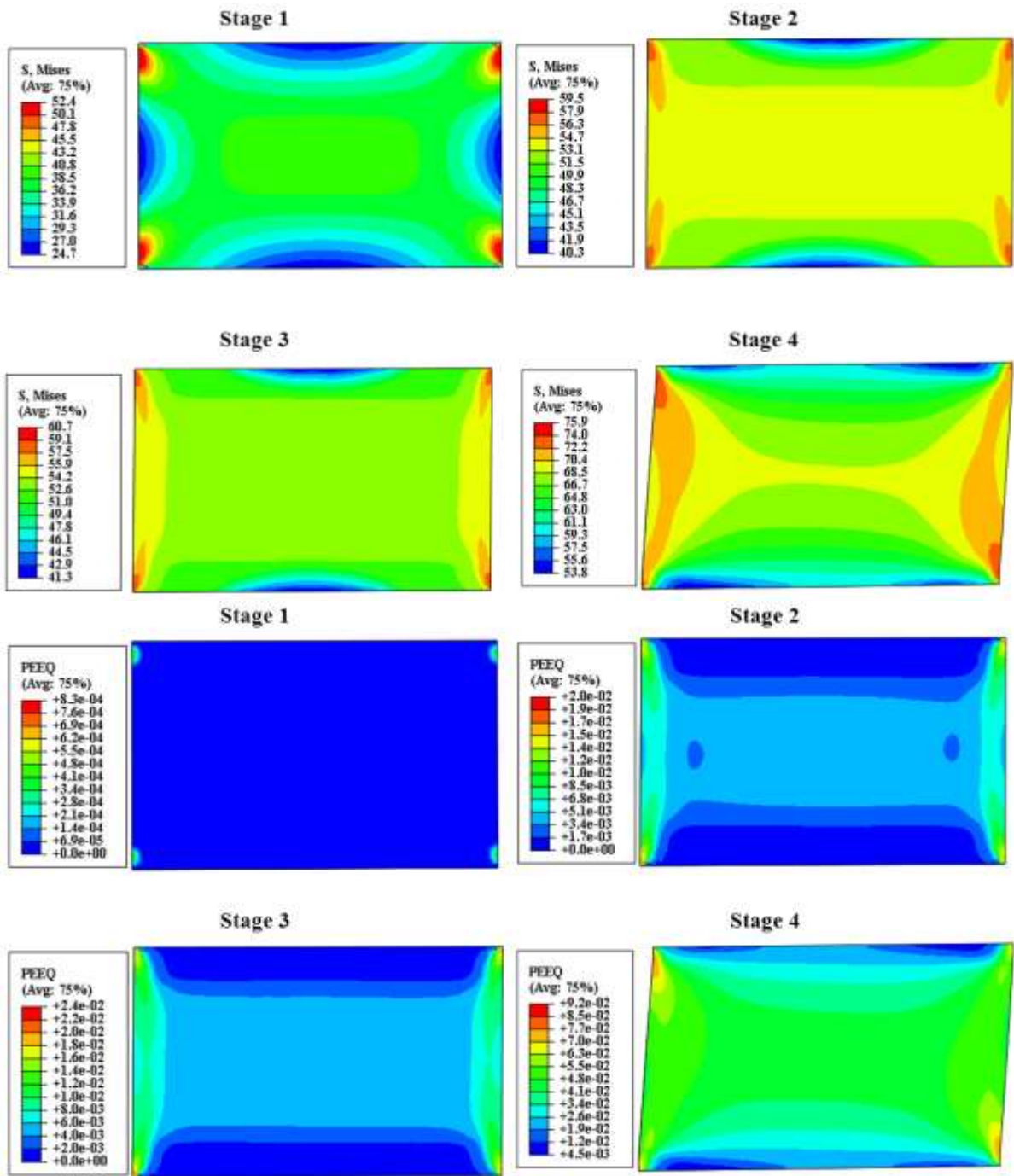


Figure 5.145: VMS and PEEQ in the DP Case 10A1

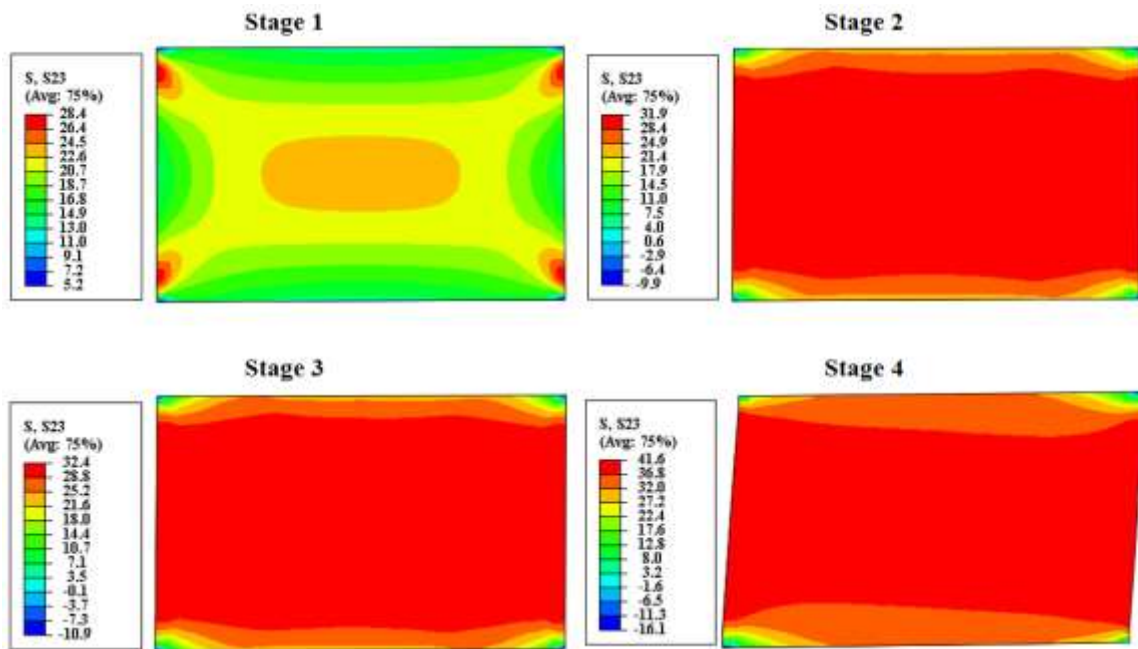


Figure 5.146: Shear stress, S23 in the DP Case 10A1

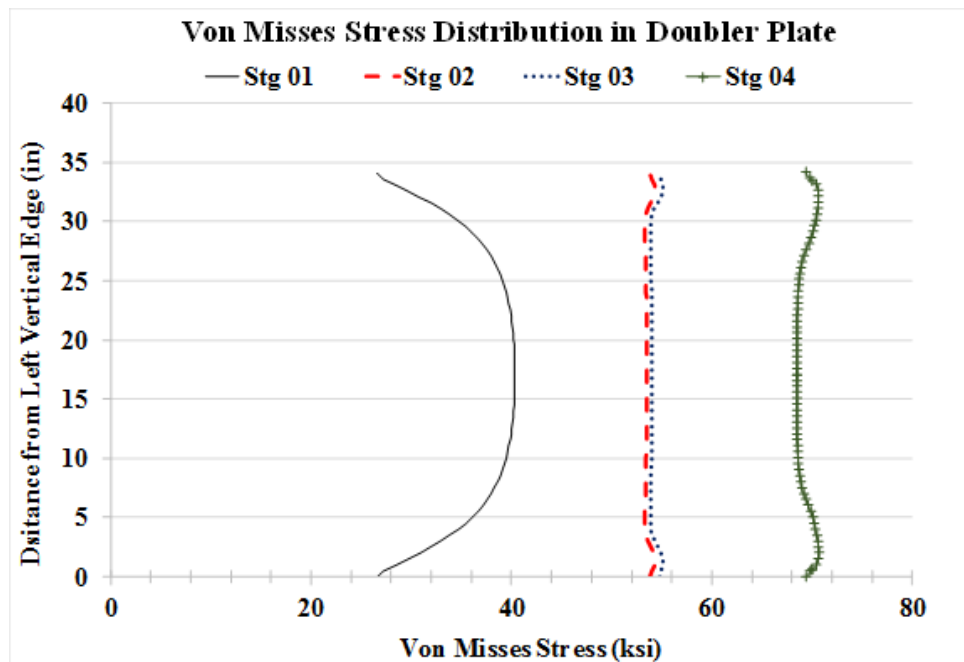


Figure 5.147: VMS distribution at mid-depth of DP Case 10A1



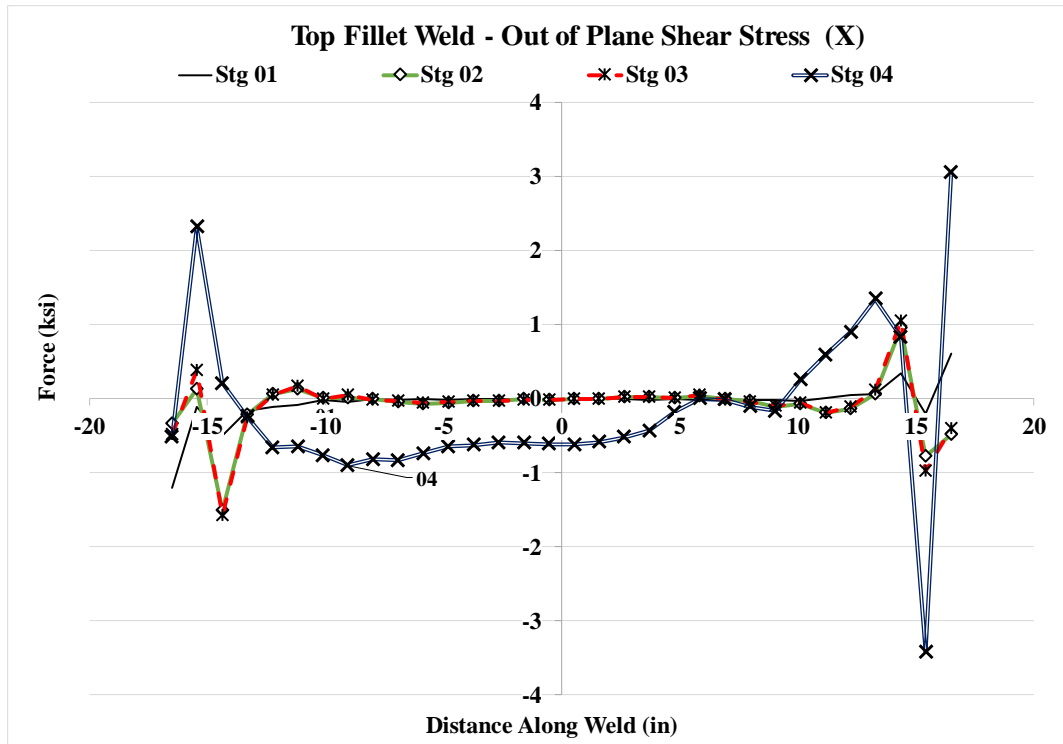
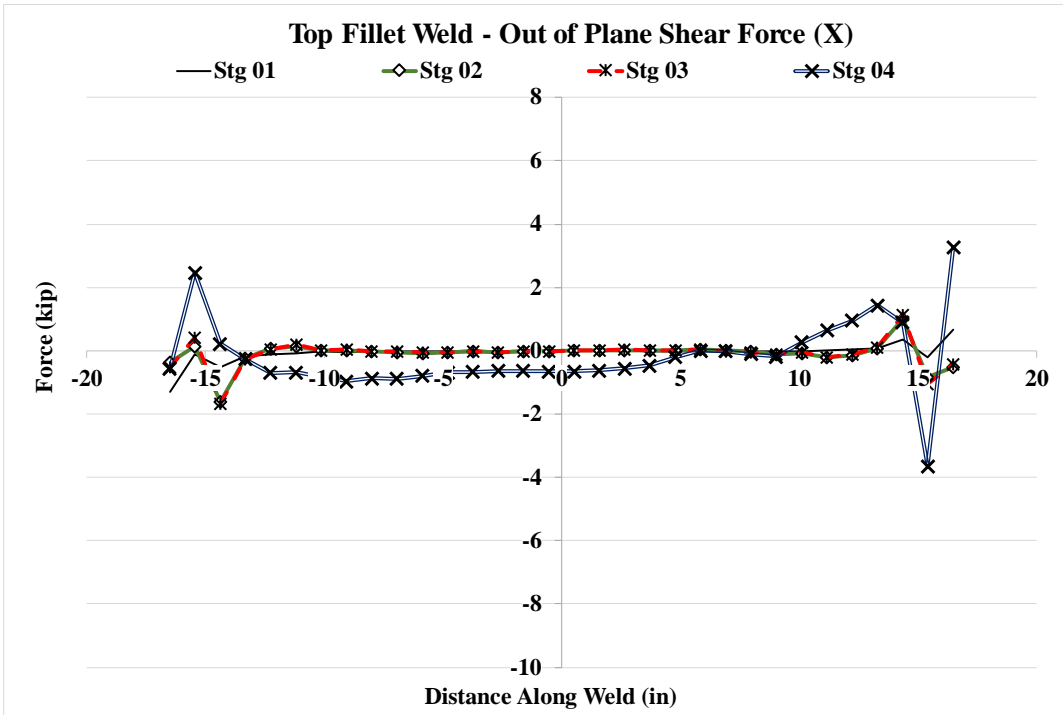


Figure 5.148: Forces and stresses in horizontal weld, (X) Case 10A1

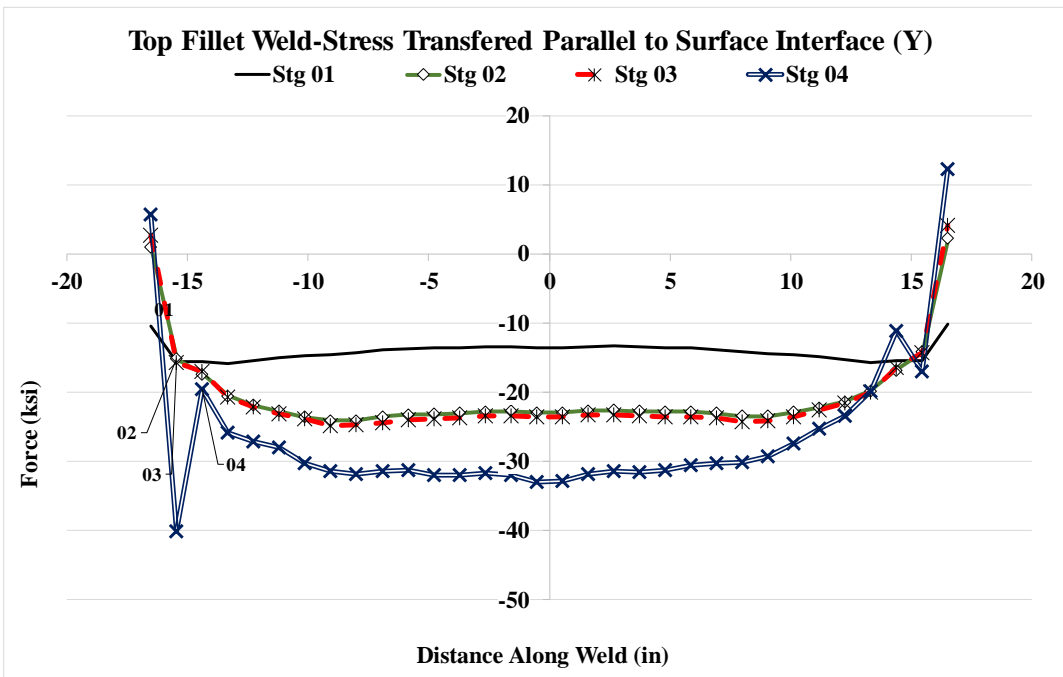
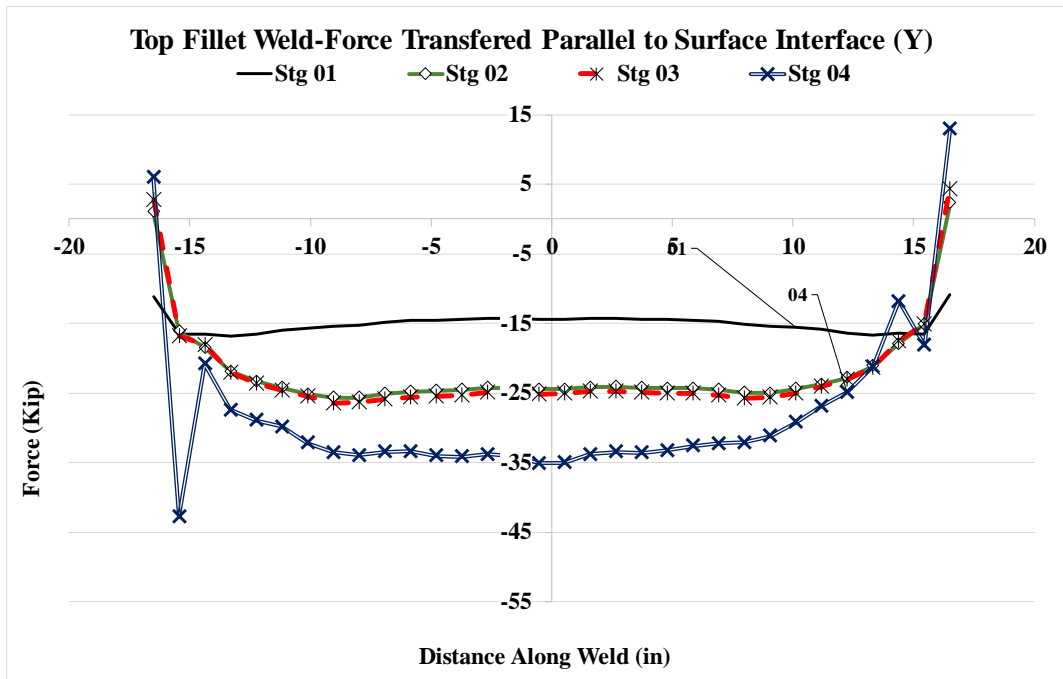


Figure 5.149: Forces and stresses in horizontal weld, (Y) Case 10A1

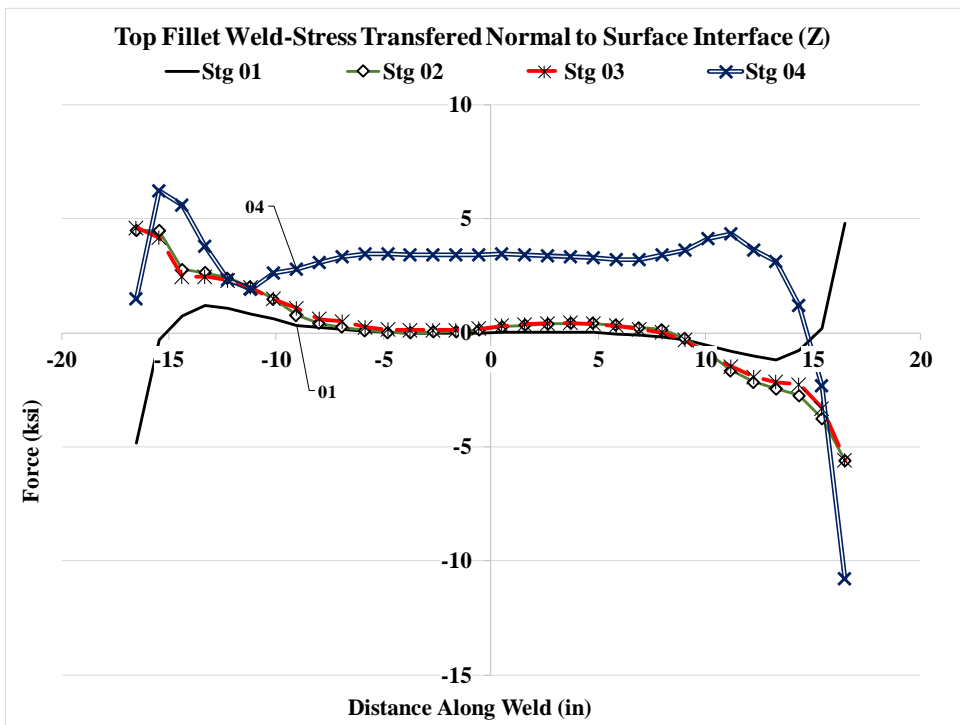
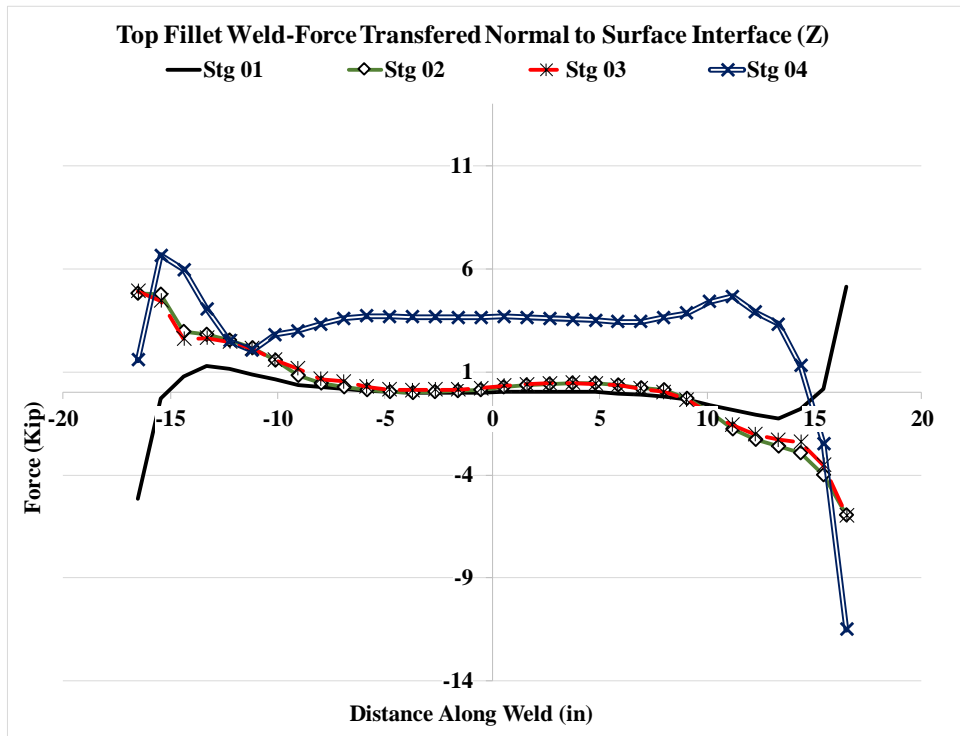


Figure 5.150: Forces and stresses in horizontal weld, (Z) Case 10A1

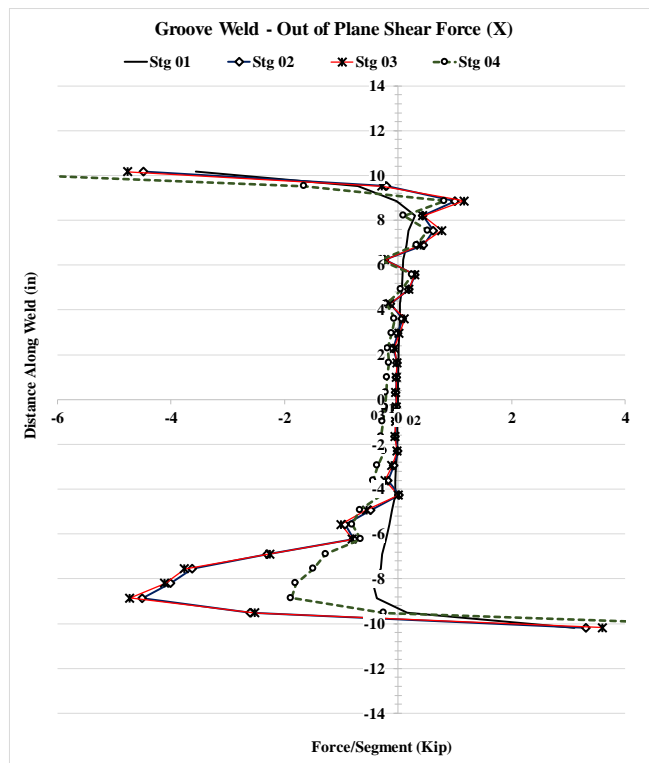
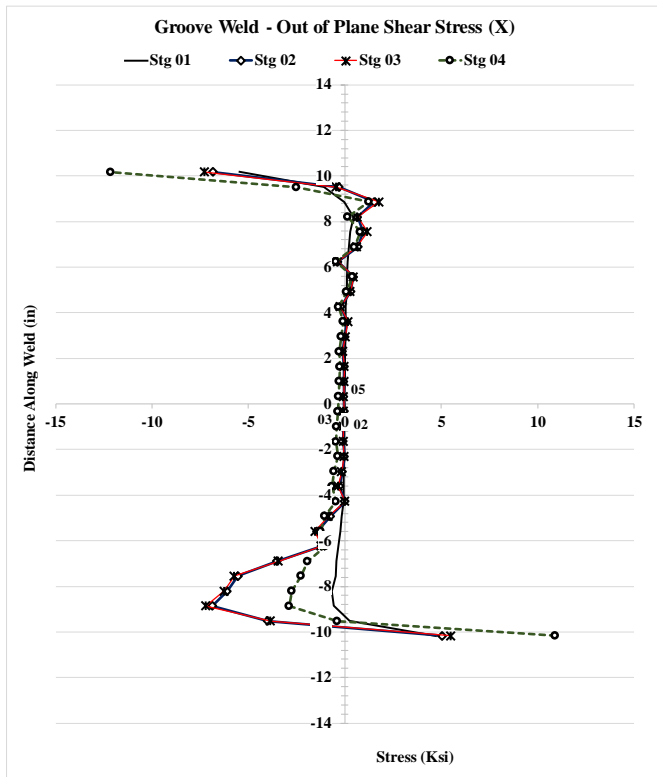


Figure 5.151: Forces and stresses in vertical weld, (X) Case 10A1

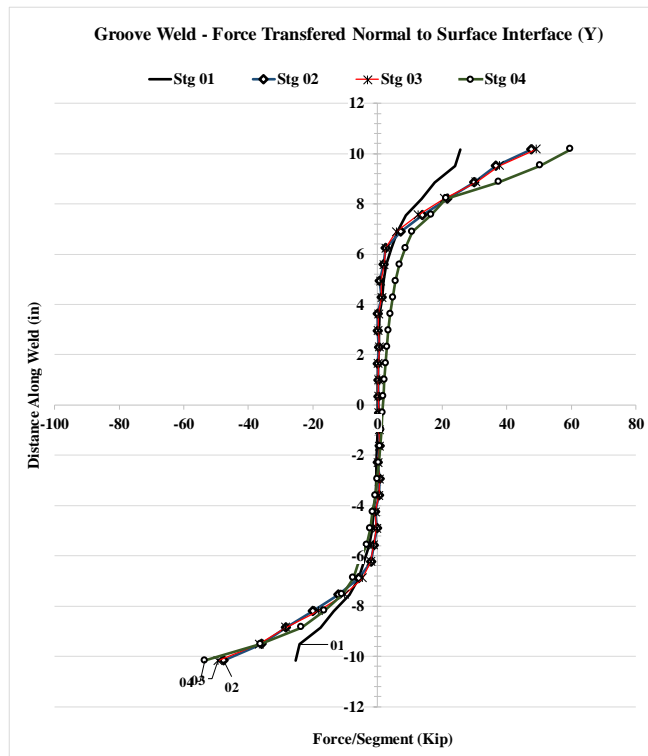
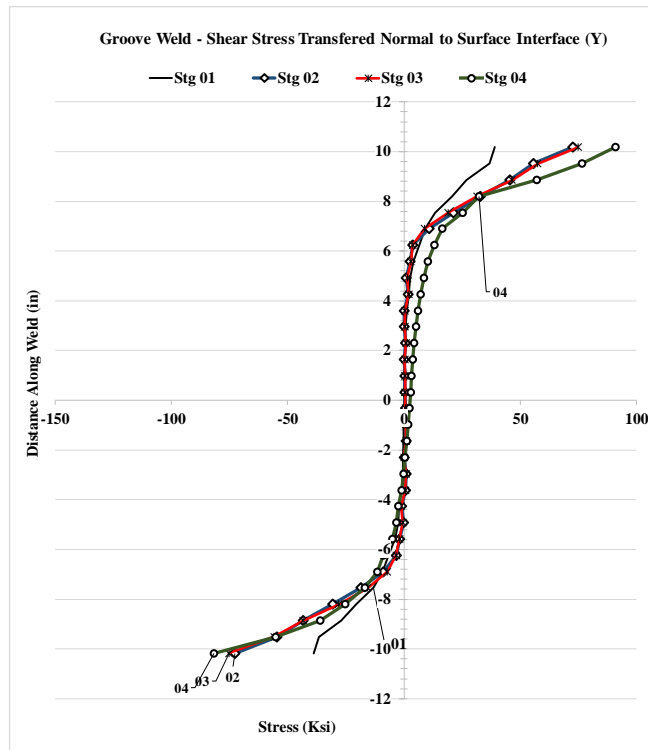


Figure 5.152: Forces and stresses in vertical weld, (Y) Case 10A1

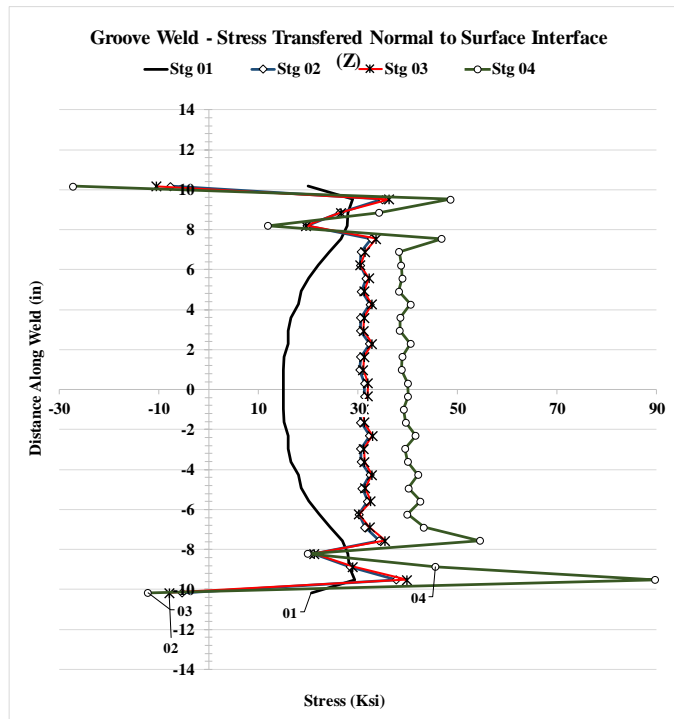
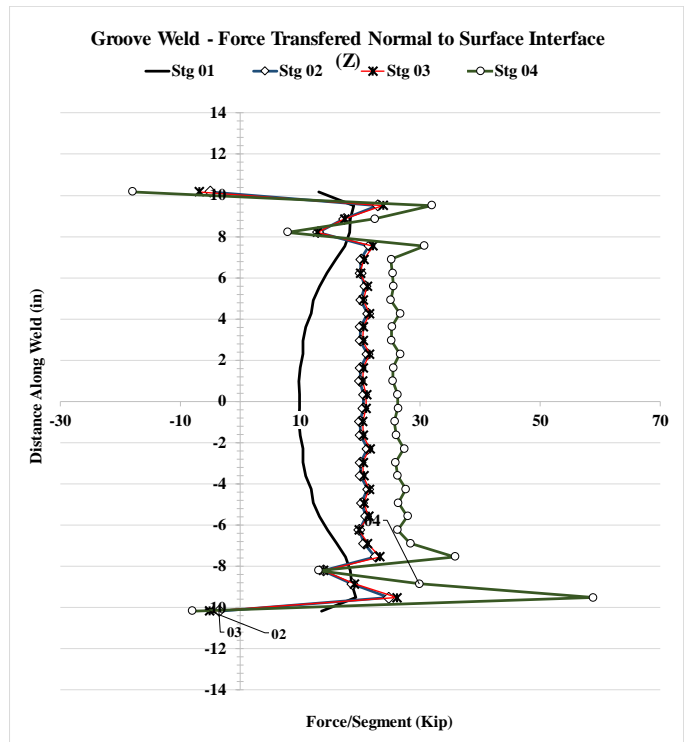


Figure 5.153: Forces and stresses in vertical weld, (Z) Case 10A1

5.2.15 Analysis Case 10C1

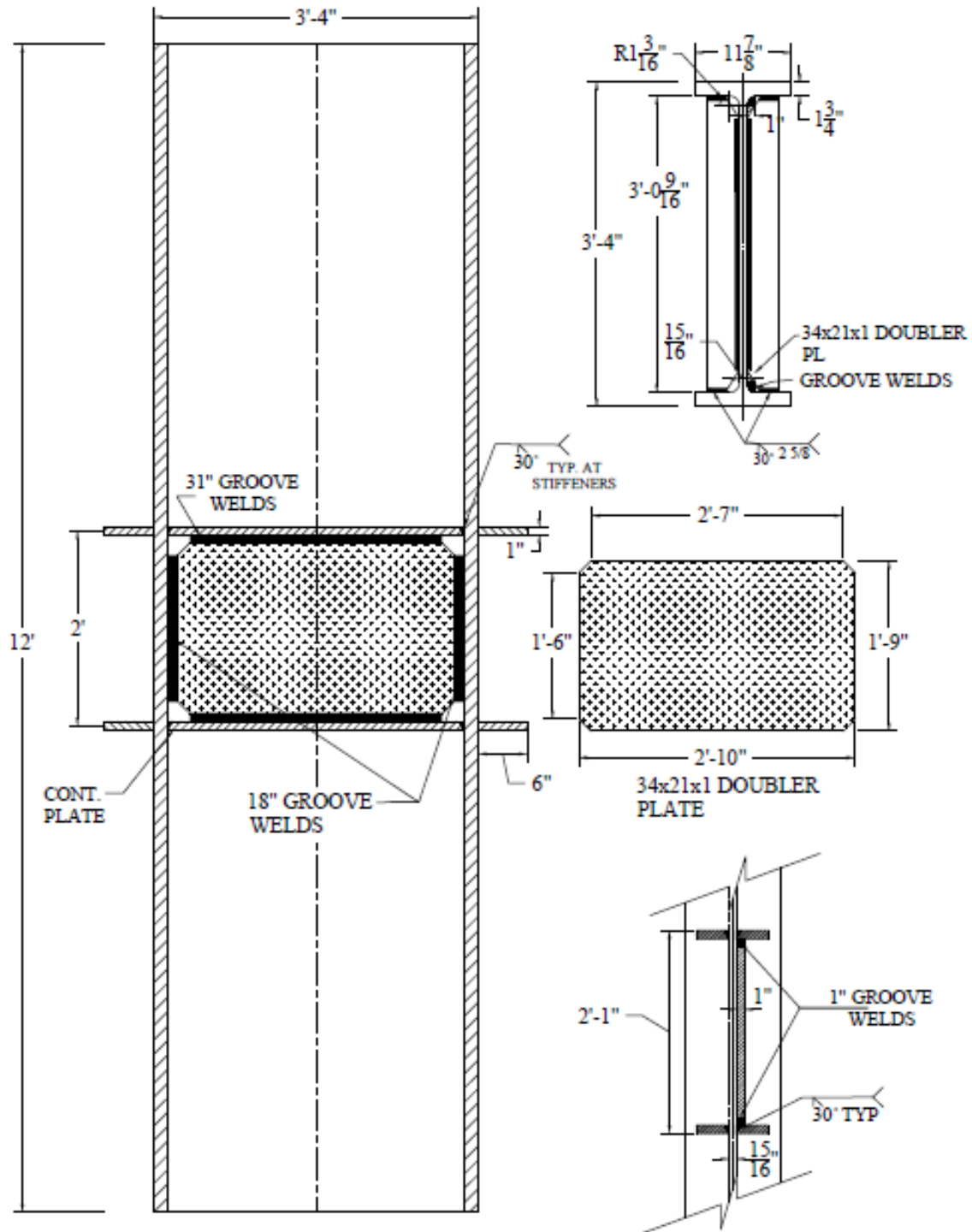


Figure 5.154: W40x264 Analysis case 10C1

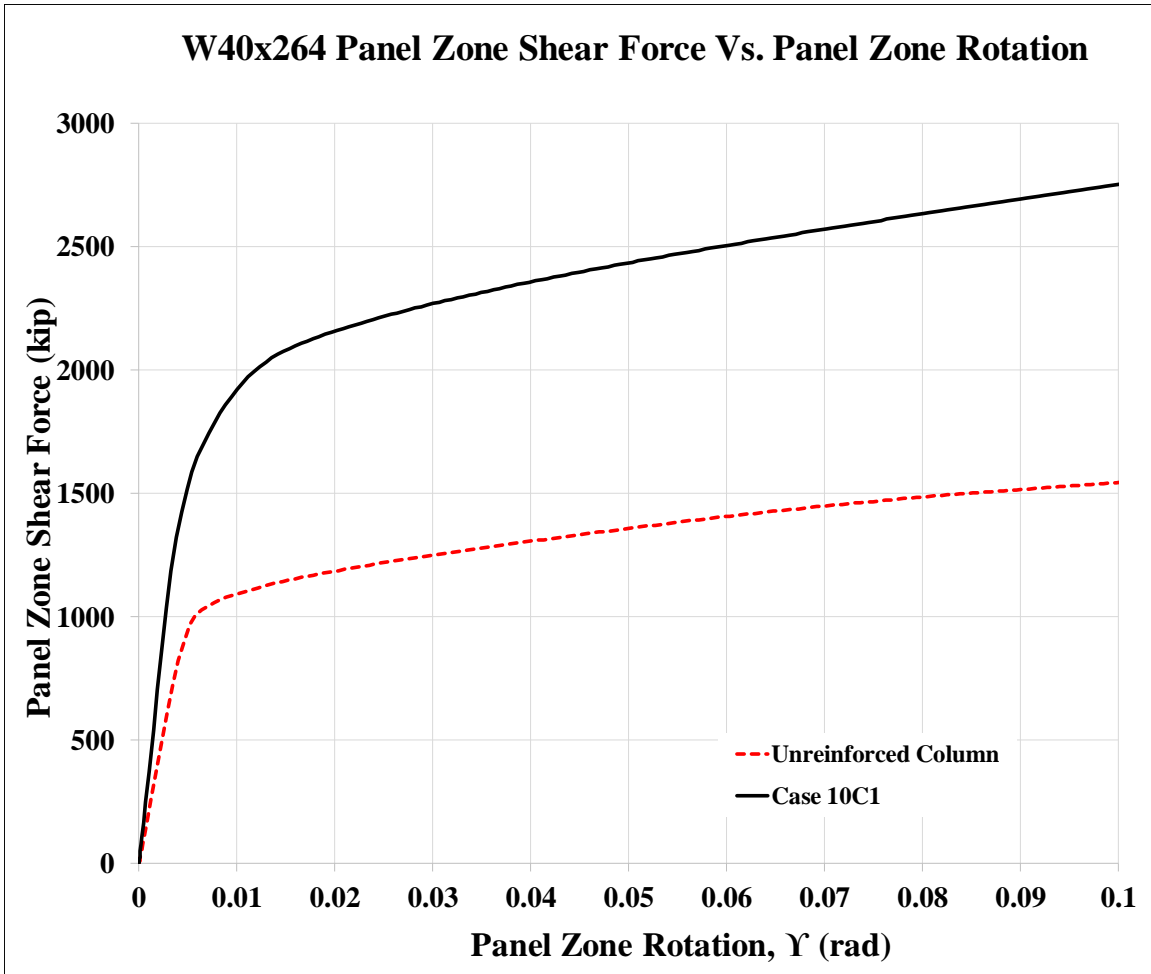


Figure 5.155: Panel zone shear vs. panel zone rotation Case

Stage	Applied Force/Loading Plate (Kip)	Panel Shear Force (Kip)	% Higher Than Unreinforced Col.	Panel Zone Rotation (rad)
1	856	1,426	147%	0.004
2	1,270	2,117	187%	0.017
3	1,296	2,161	182%	0.020
4	1,653	2,755	178%	0.101

Table 5.16: Panel zone shear and force on loading plate Case 10C1



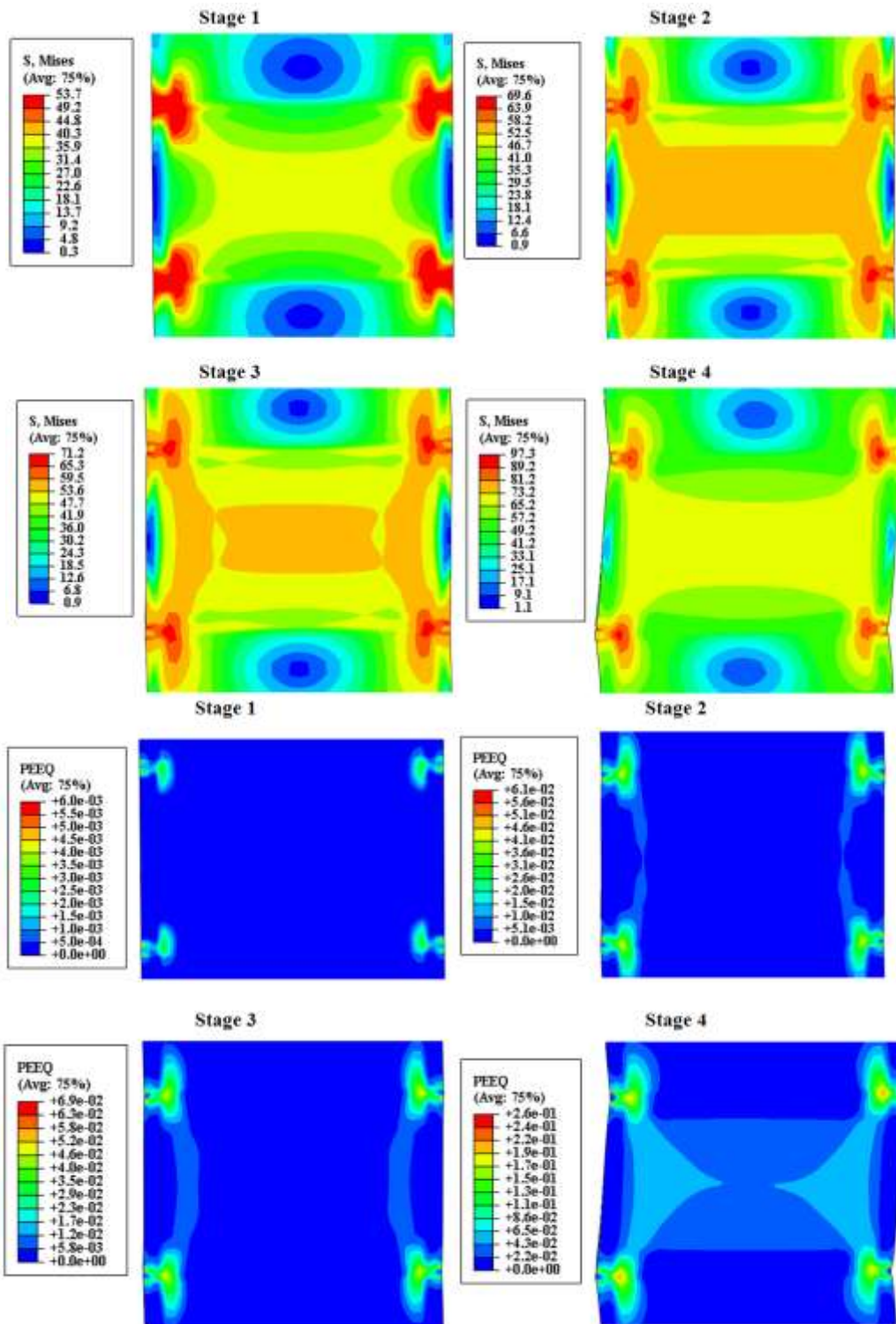


Figure 5.156: VMS and PEEQ in the column Case 10C1

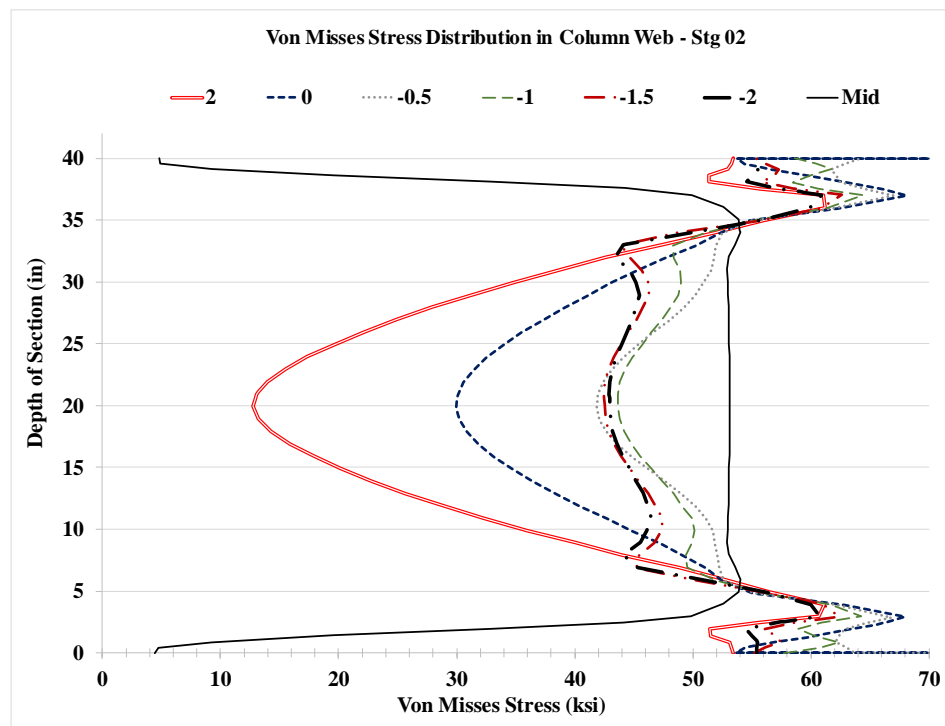
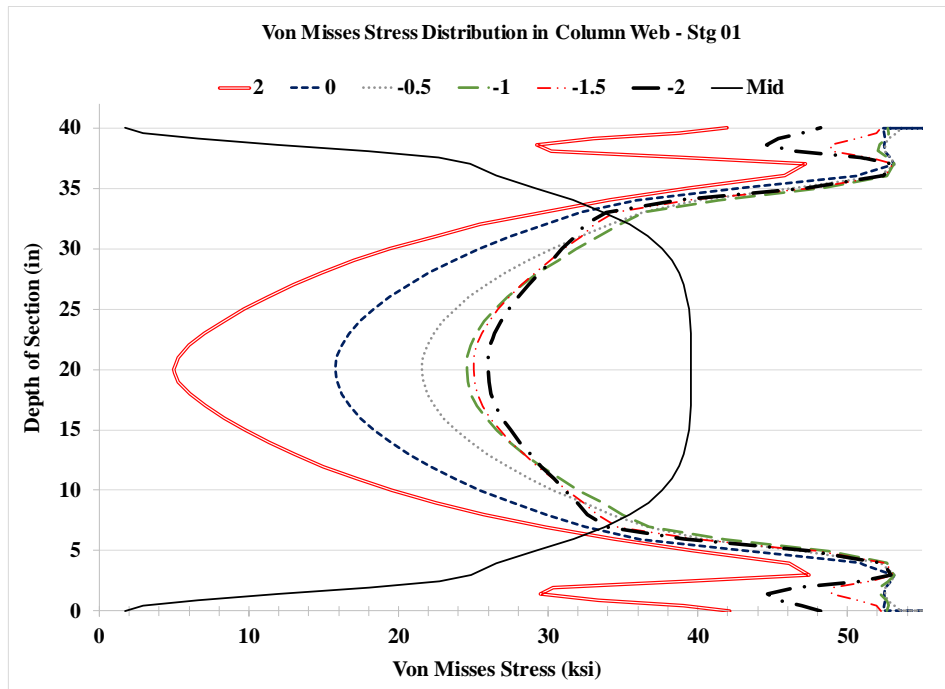


Figure 5.157: VMS distribution in column web at different heights Stg. 01-04 Case 10C1

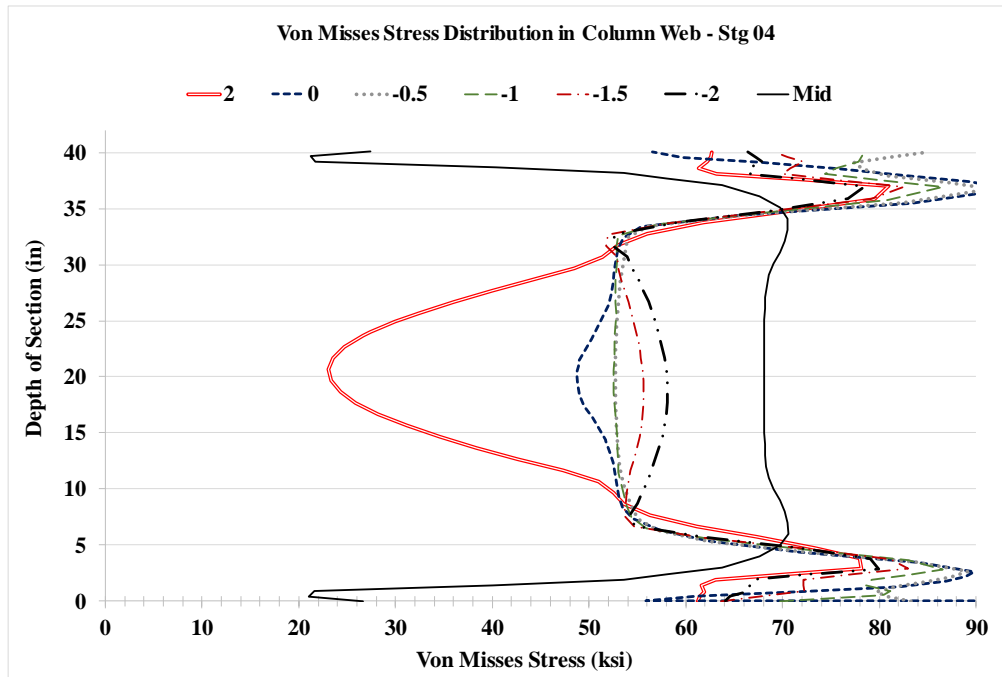
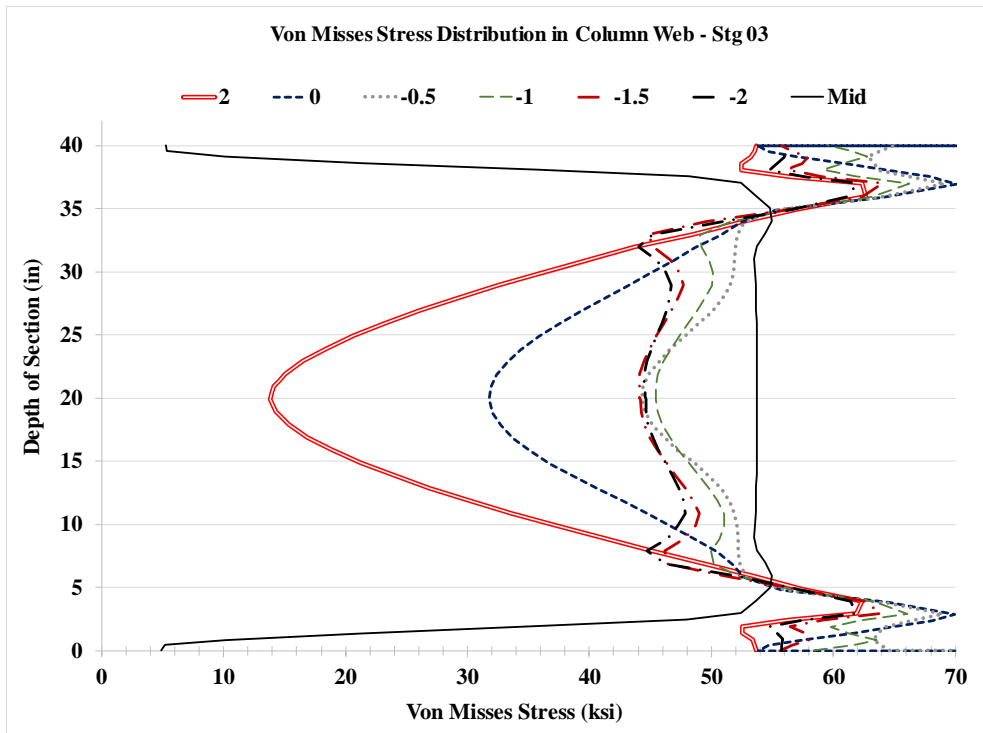


Figure 5.157: VMS distribution in column web at different heights Stg. 01-04 Case 10C1

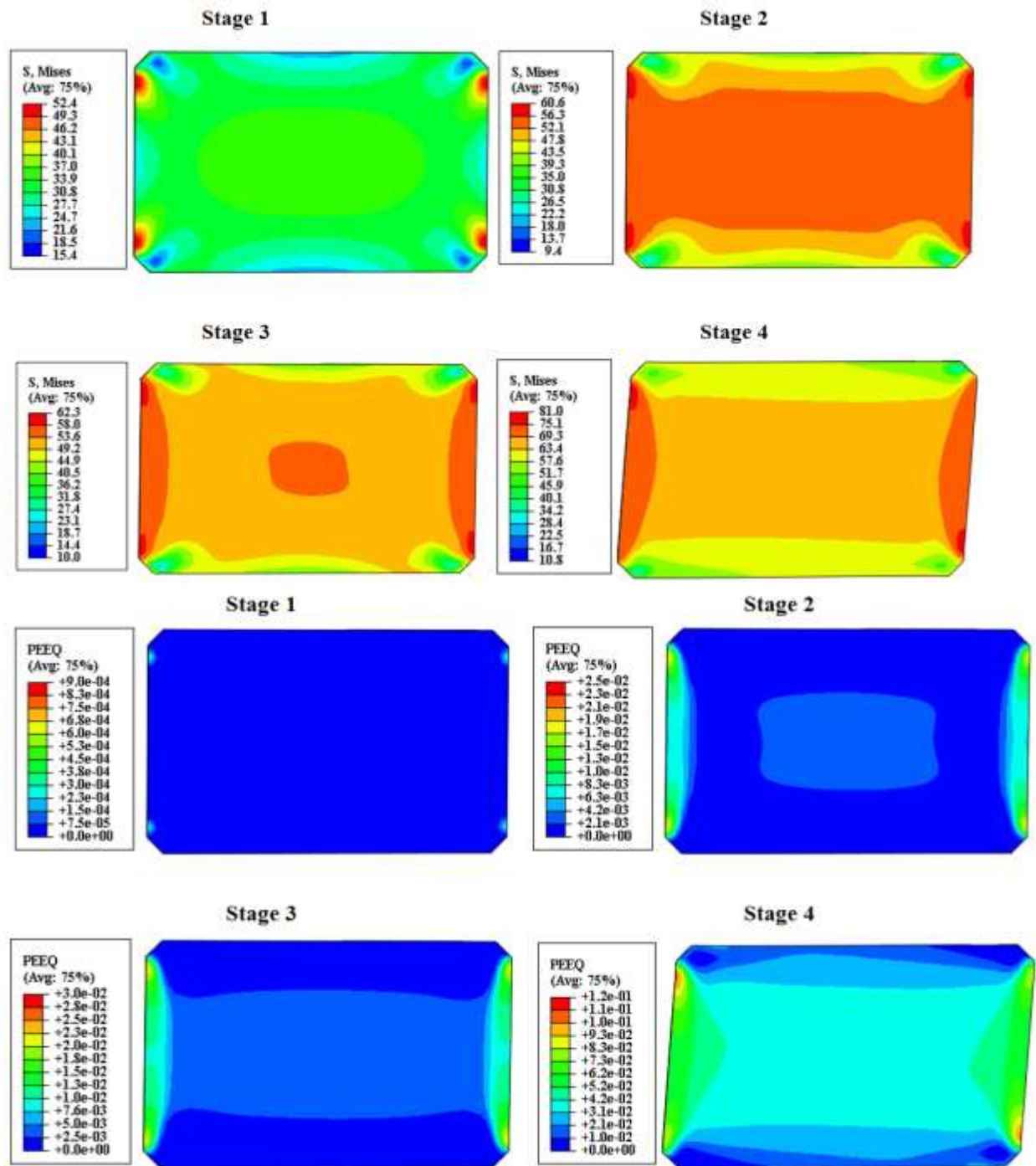


Figure 5.158: VMS and PEEQ in the DP Case 10C1

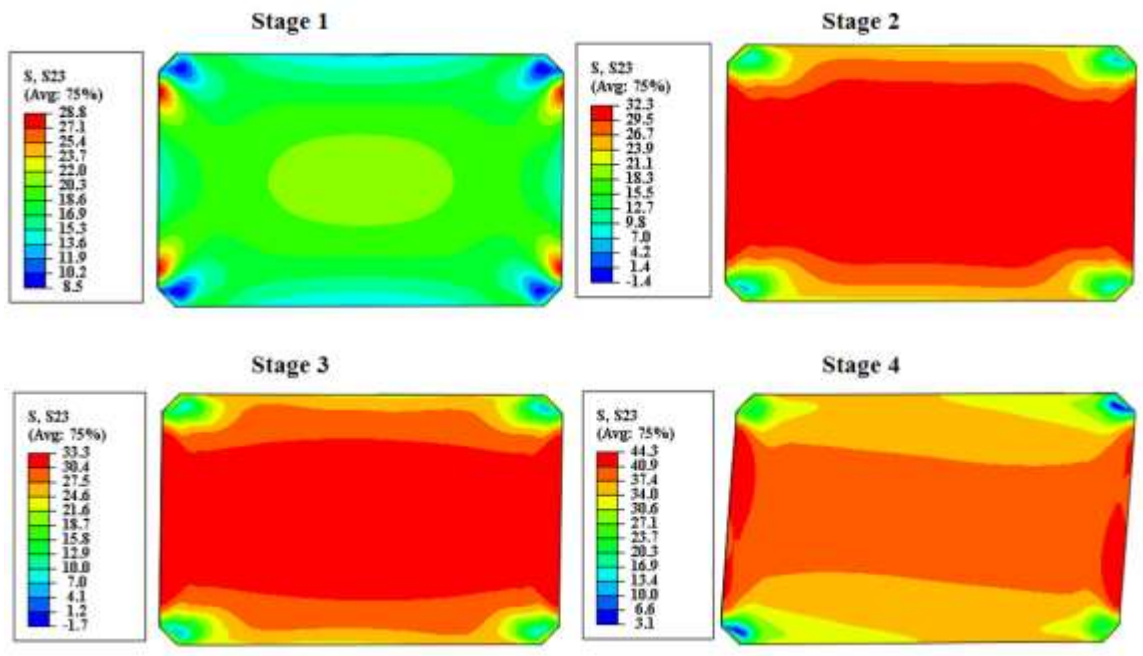


Figure 5.159: Shear stress, S23 in the DP Case 10C1

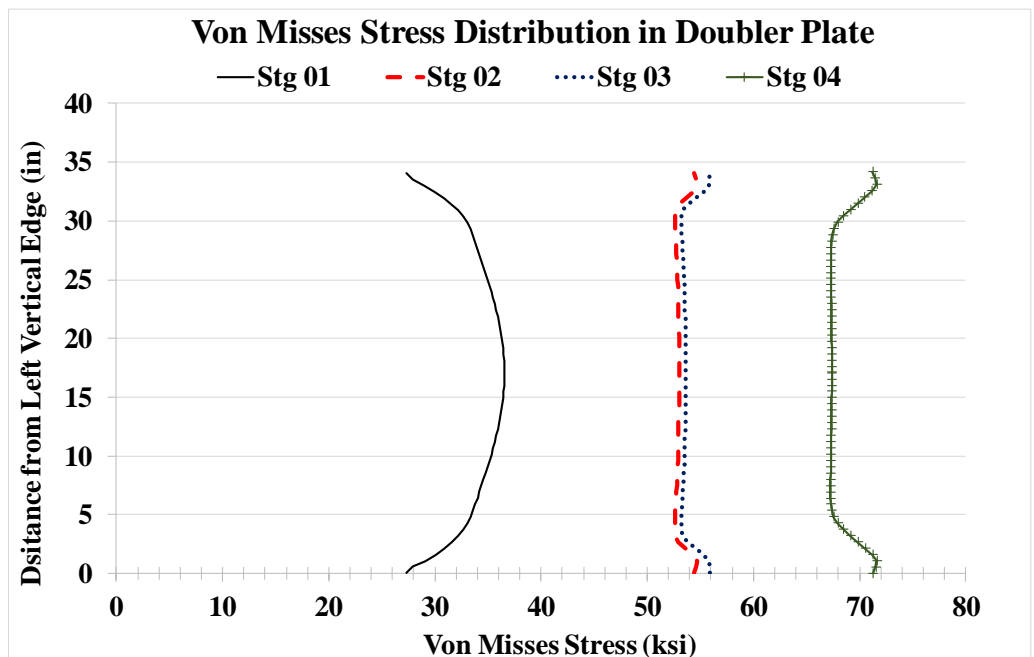


Figure 5.160: VMS distribution at mid-depth of DP Case 10C1

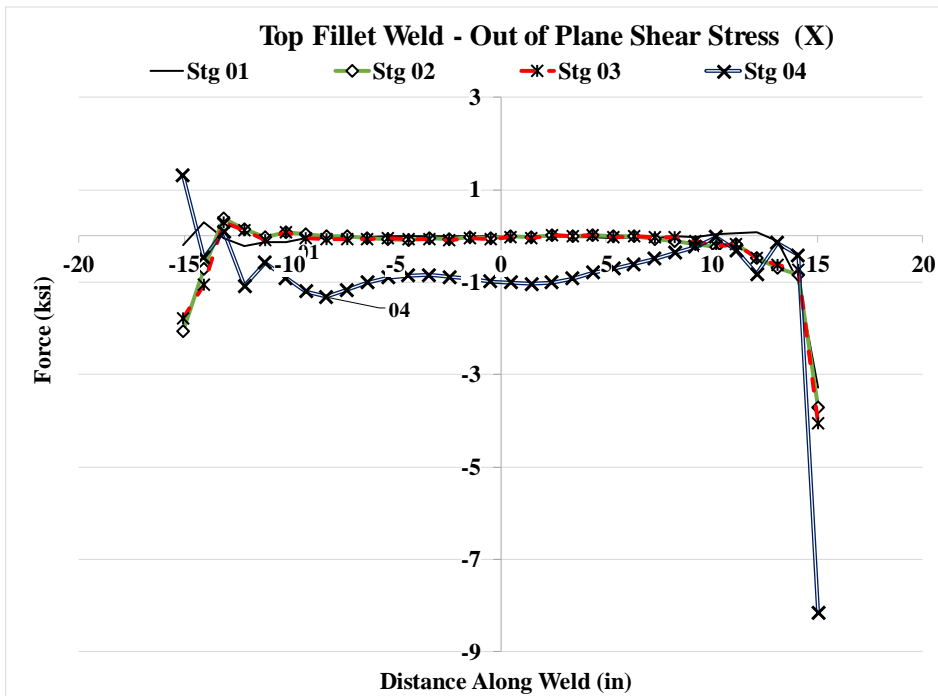
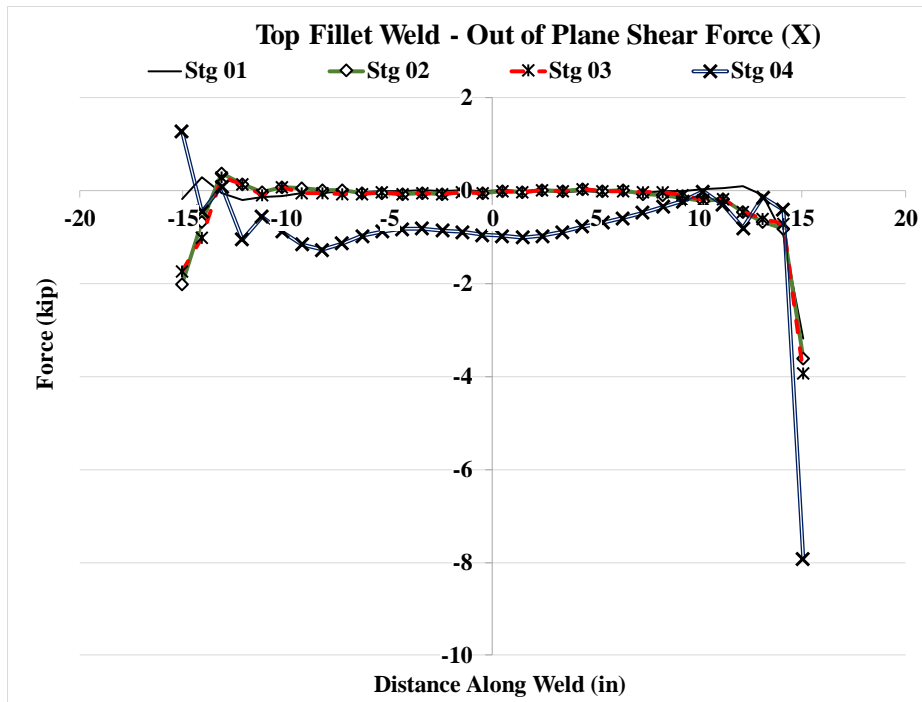


Figure 5.161: Forces and stresses in horizontal weld, (X) Case 10C1

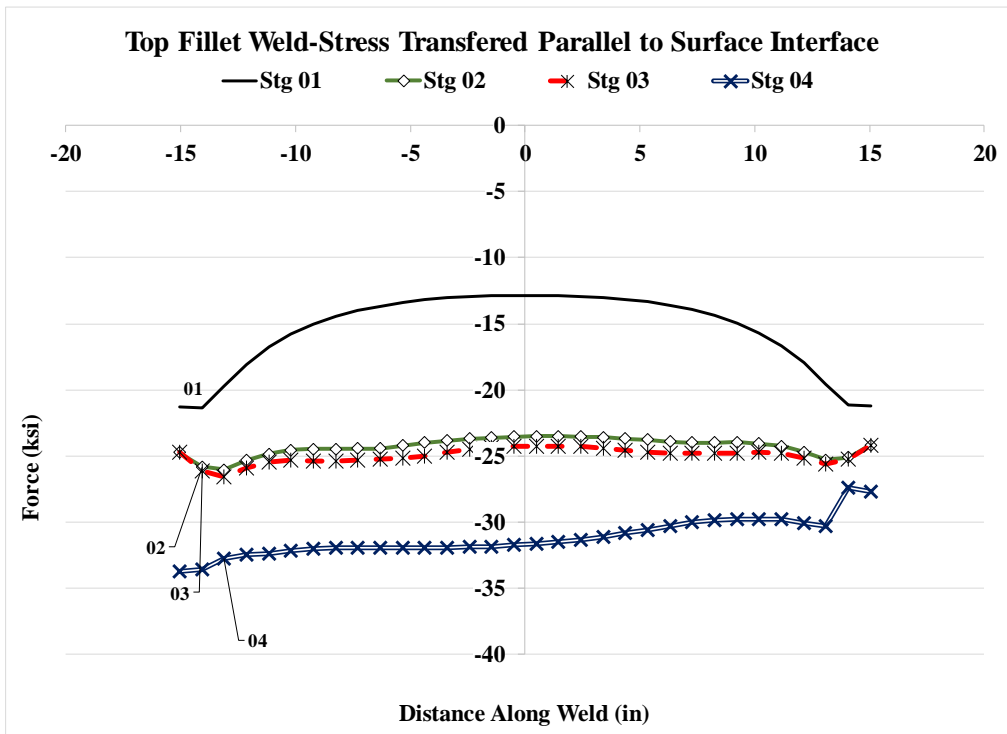
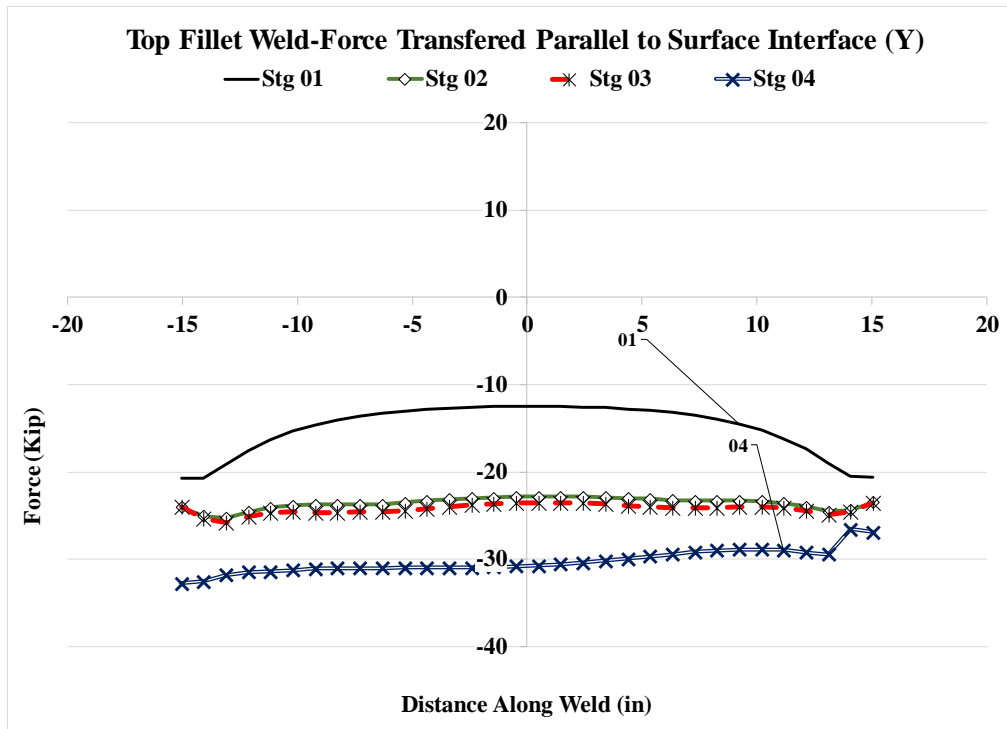


Figure 5.162: Forces and stresses in horizontal weld, (Y) Case 10C1

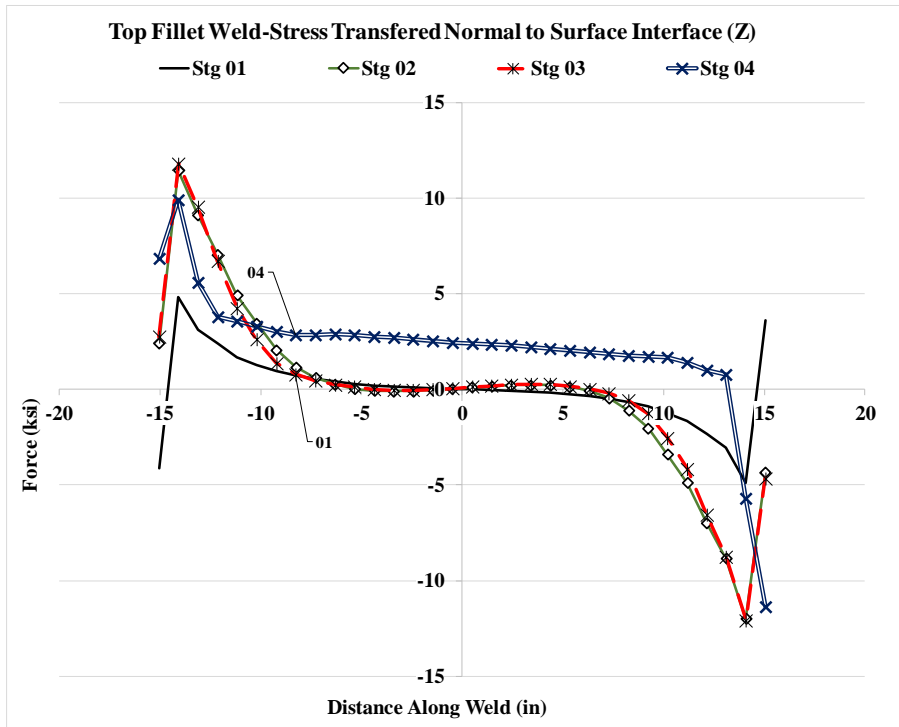
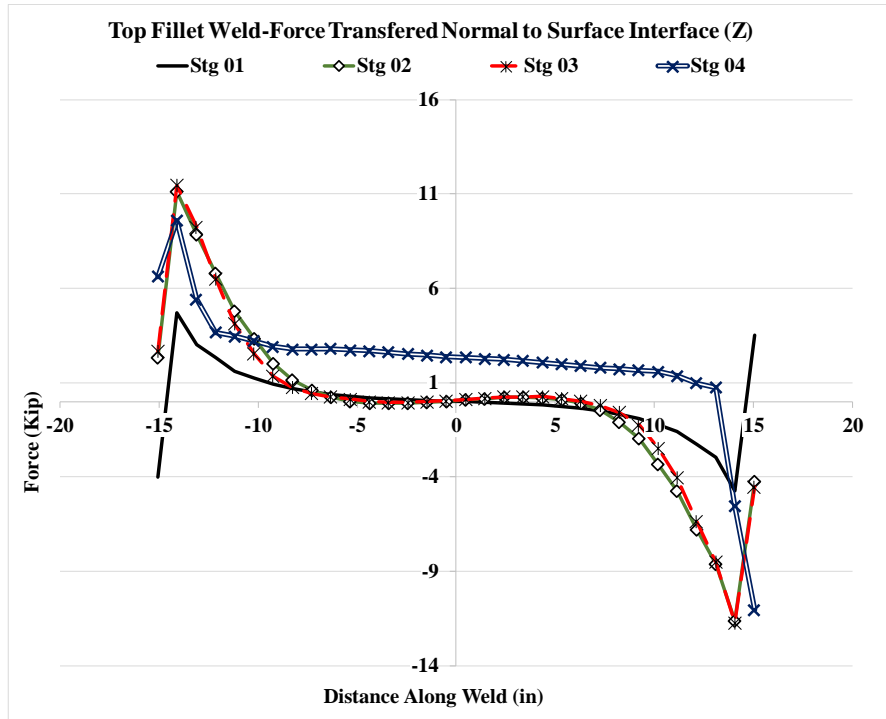


Figure 5.163: Forces and stresses in horizontal weld, (Z) Case 10C1



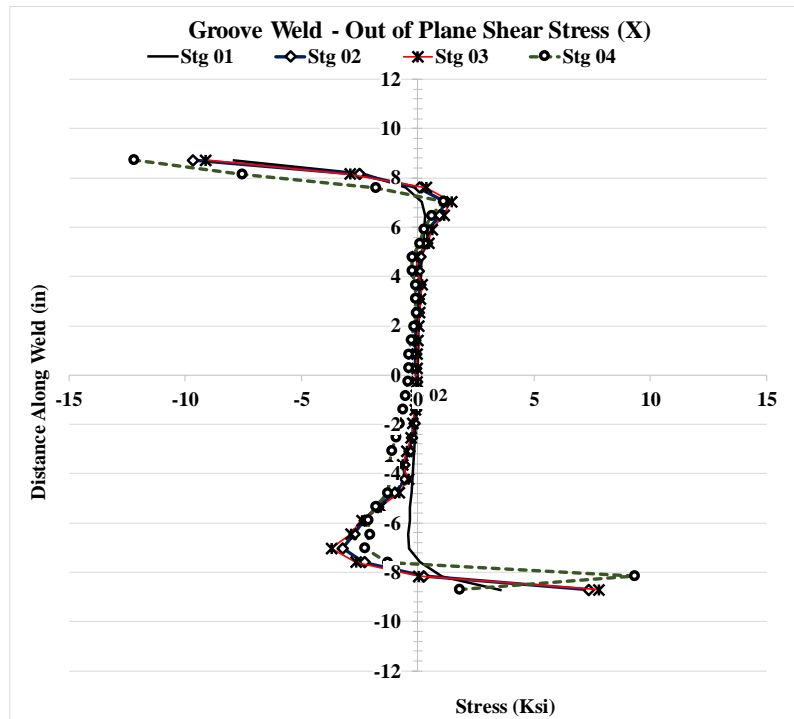
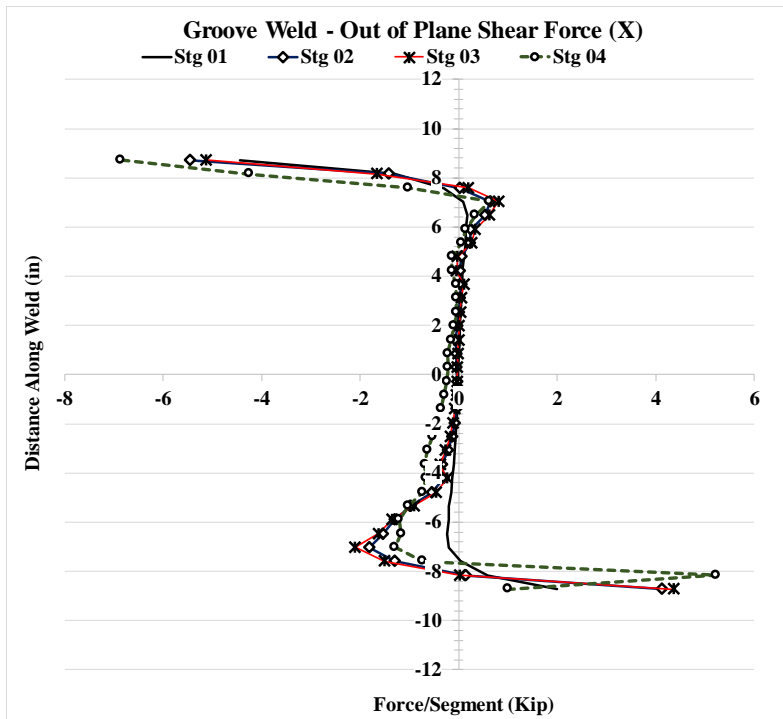


Figure 5.164: Forces and stresses in vertical weld, (X) Case 10C1

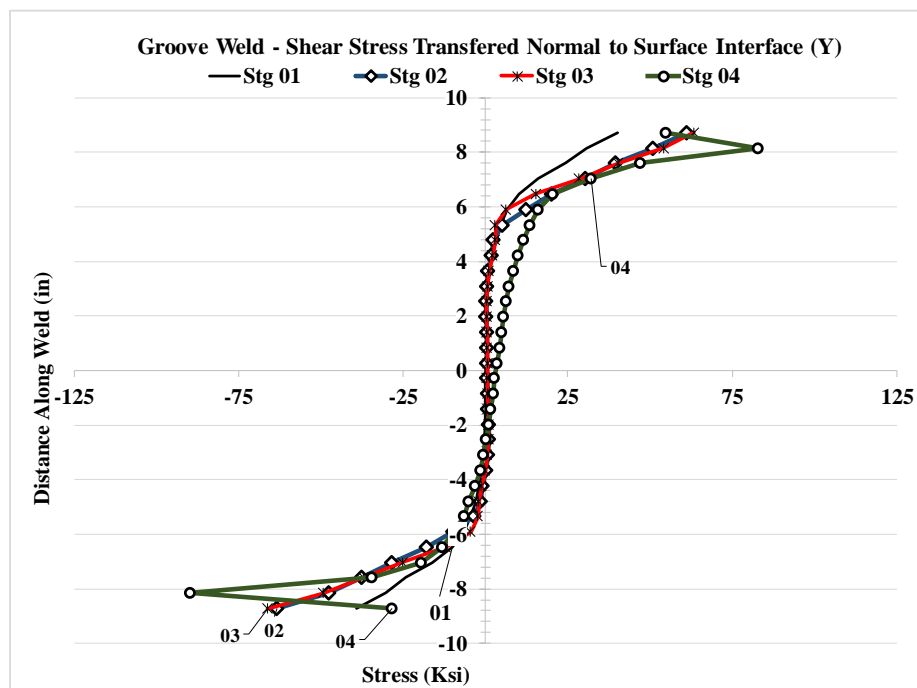
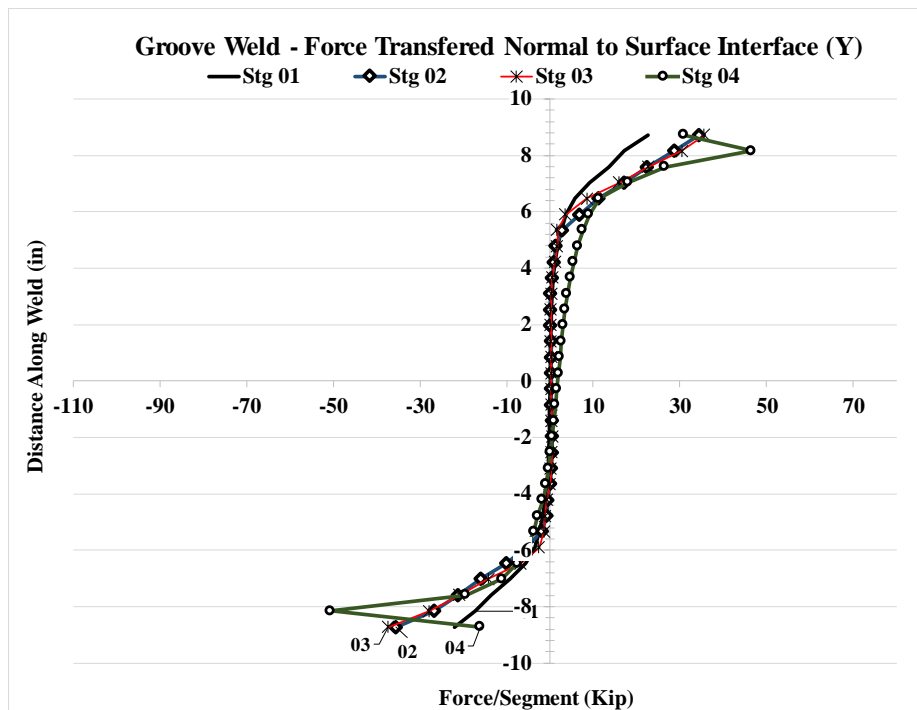


Figure 5.165: Forces and stresses in vertical weld, (Y) Case 10C1

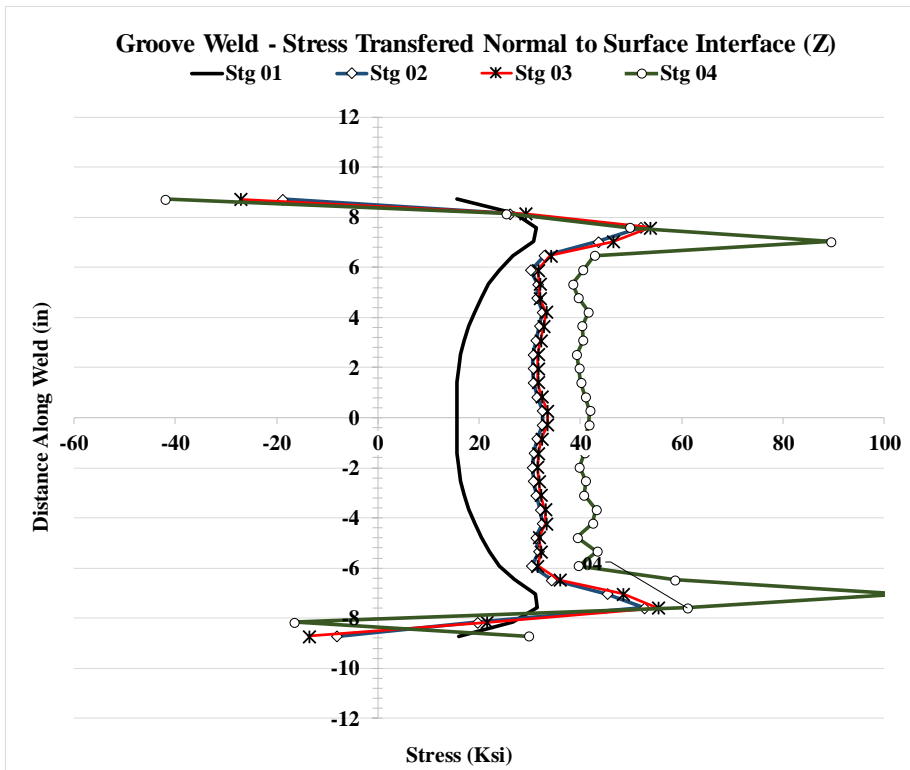
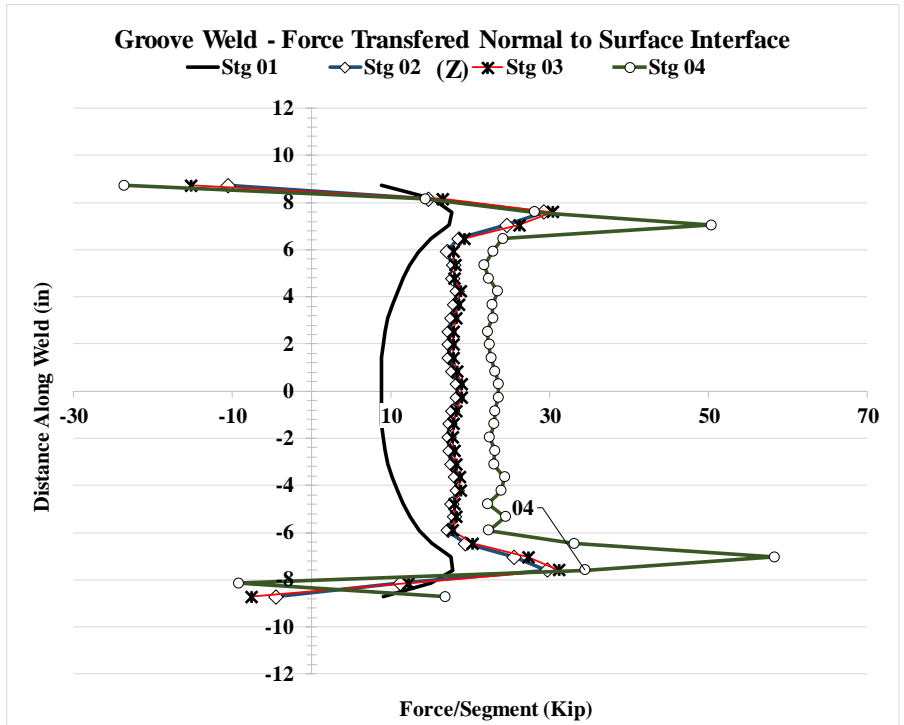


Figure 5.166: Forces and stresses in vertical weld, (Z) Case 10C1

### 5.3 DISCUSSION OF ANALYSIS RESULTS

Case	VMS in Column Web (ksi)		VMS in DP (ksi)		Shear Stress, S23 in DP (ksi)		Shear at mid-height of DP (kip)		Total PZ shear (kip)	
	Stg 01	Stg 04	Stg 01	Stg 04	Stg 01	Stg 04	Stg 01	Stg 04	Stg 01	Stg 04
<b>6</b>	53.8	79.1							970	1,545
<b>6A</b>	54.8	85.6	54.0	70.9	22.1	40.9	563	1,098	1,262	2,246
<b>6A1</b>	56.2	80.8	53.5	81.9	26.9	38.5	674	<b>1,259</b>	1,378	2,497
<b>6C</b>	55.0	87.0	54.1	81.6	22.6	38.5	493	1,122	1,195	2,211
<b>6C1</b>	56.3	89.7	53.3	85.0	27.2	38.2	618	<b>1,200</b>	1,285	2,378
<b>7A1</b>	56.3	83.7	52.8	84.3	29.0	42.5	830	<b>1,391</b>	1,736	<b>2,953</b>
<b>7C1</b>	55.0	84.5	52.7	84.3	28.7	42.8	738	<b>1,376</b>	1,564	<b>2,876</b>
<b>8A</b>	54.9	76.6	55.1	97.6	23.0	40.8	1,035	1,075	1,544	2,377
<b>8A1</b>	54.7	82.2	52.6	75.7	27.8	41.7	943	<b>1,430</b>	1,568	<b>2,851</b>
<b>8C</b>	54.6	83.0	55.1	90.1	23.7	40.6	889	1,098	1,481	2,351
<b>8C1</b>	54.5	87.1	52.7	76.2	29.1	42.9	707	<b>1,336</b>	1,530	2,770
<b>9A</b>	54.6	83.0	55.0	83.0	22.3	42.6	525	1,138	1,492	2,326
<b>9C</b>	53.8	80.4	54.1	86.6	21.8	40.0	439	1,097	1,384	2,243
<b>10A1</b>	54.5	84.6	52.4	75.9	28.4	41.6	729	<b>1,356</b>	1,522	<b>2,821</b>
<b>10C1</b>	53.7	81.2	52.4	81.0	28.8	44.3	671	<b>1,333</b>	1,426	<b>2,755</b>

Table 5.17: Summary of VMS stresses and forces on column web and DP at Stg. 01 and Stg. 04

This chapter reports the results from a variety of analysis performed on a “deep” W40x264 column. Table 5.17 is a summary of the peak forces and stresses from the results. It should be noted that peak stress values for this column are not the best indicators of performance of the different cases. Large forces were applied by the loading plates due to the large size of the column and the 1 inch thickness of the DP. As expected this resulted in areas of high stress concentrations near the point where the loading is being applied on the column. An attempt was made to report stress values that represented the overall cross section better than these localized stress levels. A key observation that can be seen in Table 5.17 is the higher levels of shear force recorded at the mid-height cross section of the DPs with horizontal welds at the top. Shear values for the DPs with horizontal welds at stg 4, (PZ rotation of 0.01), ranged from 1200 to 1430 kips whereas those without ranged from 1070-1122 kips, an average 20% difference between these. This can also be observed in the values for the total PZ shear required to rotate 0.1 radians.

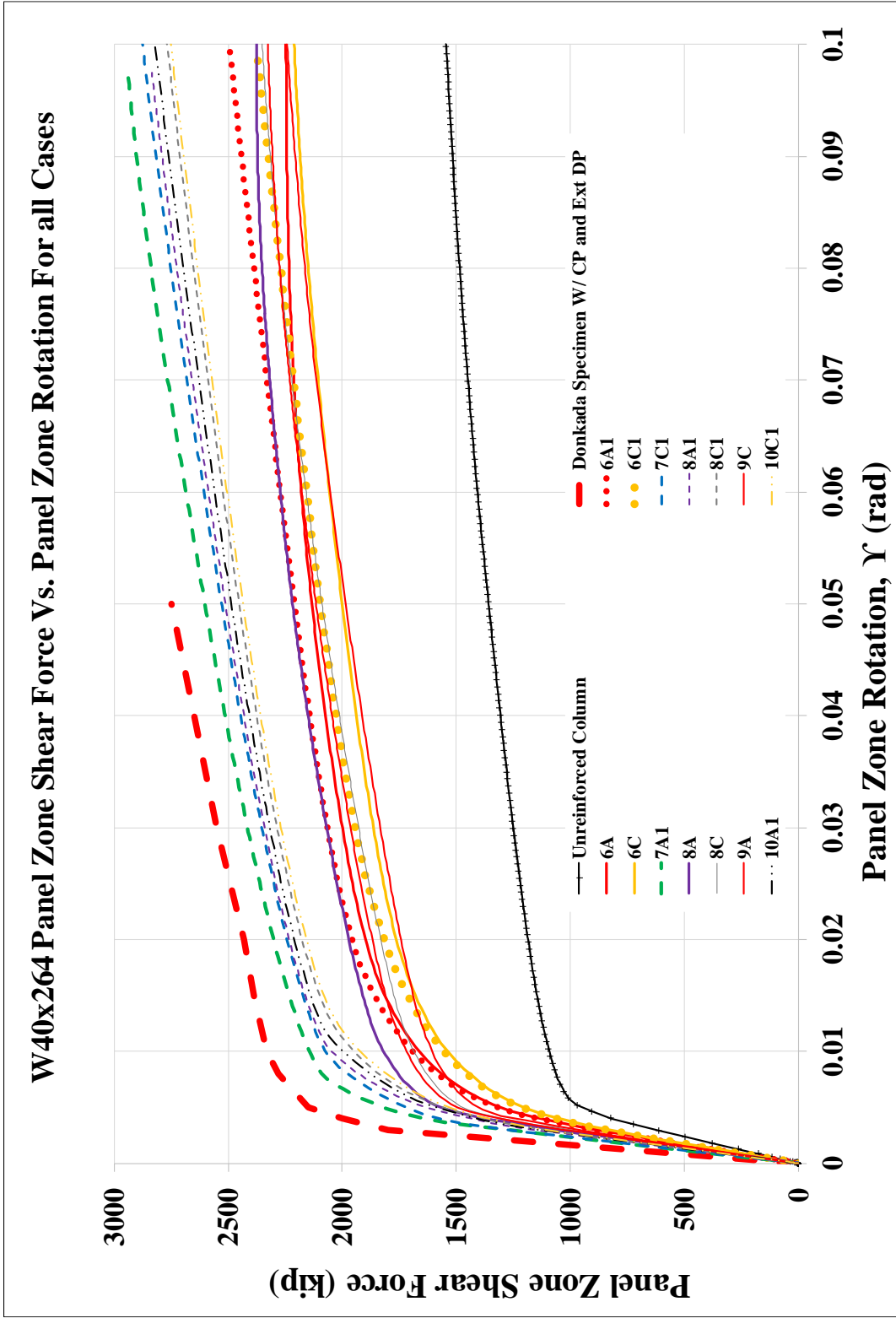


Figure 5.167: PZ Shear force vs PZ rotation plots for cases using a “deep” W40x264 column

Five different case series were modeled in order to see how different arrangements of the PZ attachments improved overall performance. Some of the values that were considered when evaluating the performance of the different cases included: stresses on the column and DP, PZ rotation vs. PZ shear force comparisons, and weld force transfer. Figure 5.167 is a plot of the PZ shear force vs. PZ rotation for all the models considered in Chapter 5. The values for an unreinforced column are also plotted in order to show the improved performance that these arrangements have on the performance of the PZ. Case 5 from Donkada (2012) is also plotted in order to provide another source for comparison. Case 5 can be used to compare the difference in performance between a “fitted” DP and an “extended” DP since the main difference between the cases in this chapter and Case 5 is the use of a DP that is extended 6 inches above and below the beam flanges. It should be noted that Case five does not use welds at the top of the column. Although the values reported only reached 0.05 radians of PZ rotation a comparison between Case 5 and all other cases in this chapter might indicate that a PZ with an extended DP is both stronger and stiffer. It should be noted that almost all the stress values reported at a height of 2 inches above the loading plates are far lower than those inside the PZ. This is due to the shear stress traveling “into” the PZ rather than away. This might explain why Case 5 which does not use a weld at the top of the DP outperforms all cases modeled in this chapter. Plot 5.167 also shows the improvement that using a horizontal weld to attach the top and bottom of the DP provides. In order to make this observation obvious all cases with a weld at the top were plotted using dashed lines.

Attention should also be brought to the 6A1 and 6C1 in this plot. Case series 6 did not have CPs but 6A1 and 6C1 differed in that they were welded all around. This seems to point to an increase in performance of the whole specimen due to the addition of CPs. Donkada

(2012) concludes that “Continuity plates appear to contribute to panel zone strength in columns with thinner flanges by resisting local flange bending, local web yielding, web compression buckling and web crippling which result in lower design strengths”. Figure 5.168 is a plot of the principal stress flow in a column with continuity plates and one without at a PZ rotation close to 0.1 radians. Notice that not only does the lack of a CPs result in local buckling of the flanges but also affects how the stresses are distributed in the entire column once this “kinking” of the flanges occurs. Another observation that cases 6A1 and 6C1 help point out is that that all the other specimens which used CPs but no horizontal weld performed similarly to the cases that were welded all around but used no CPs.

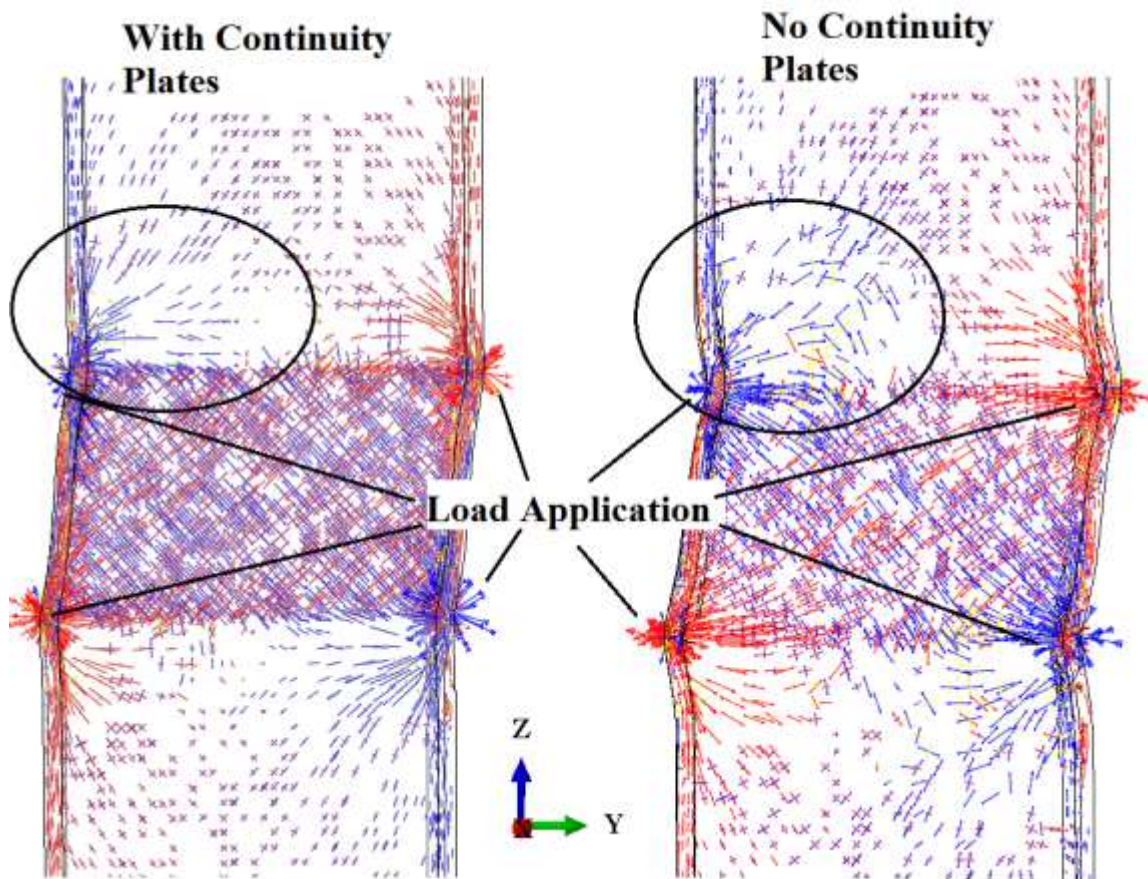


Figure 5.168: Principal stress flow in column with and without CPs, near 0.1 PZ rotation

Figure 5.167 also showed that the differences in performance of the different specimens can be seen before the yield point of the curve, stg. point 01. For this reason case comparisons of were done at the first two stage points selected rather than at peak load 1 rotation levels. A sum of the weld forces for the different cases is reported on Tables 5.18 – 5.21, and were used in the comparisons between the different arrangements.

### 5.3.1 Case Comparisons

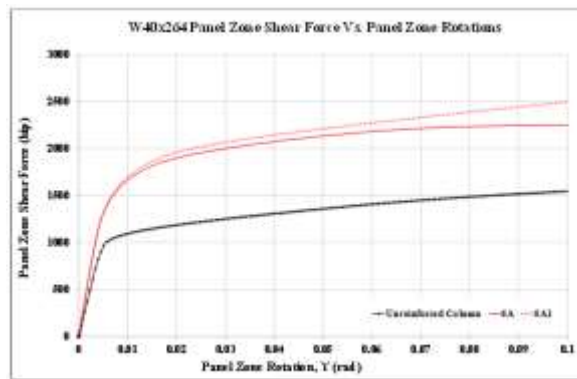


Figure 5.169: PZ and PZ shear force vs PZ rotation between Case 6A and 6A1

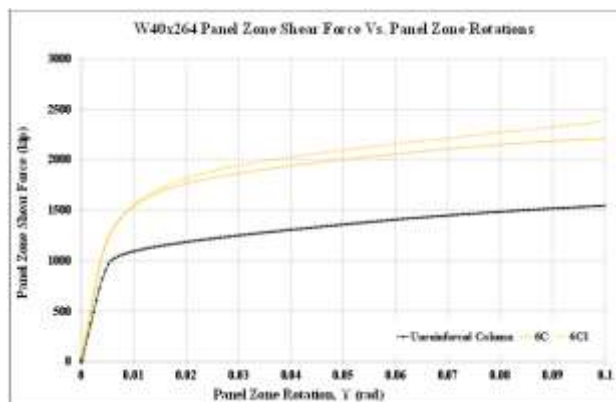


Figure 5.170: PZ and PZ shear force vs PZ rotation between Case 6C and 6C1



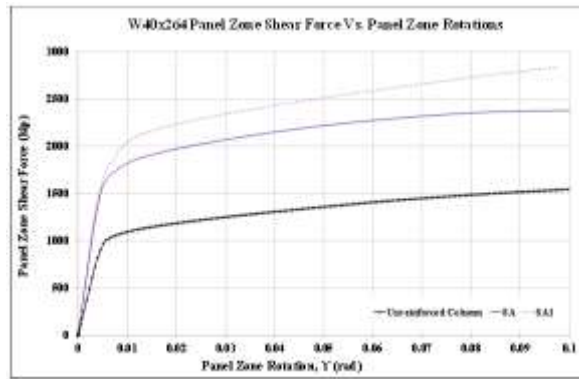


Figure 5.171: PZ and PZ shear force vs PZ rotation between Case 8A and 8A1

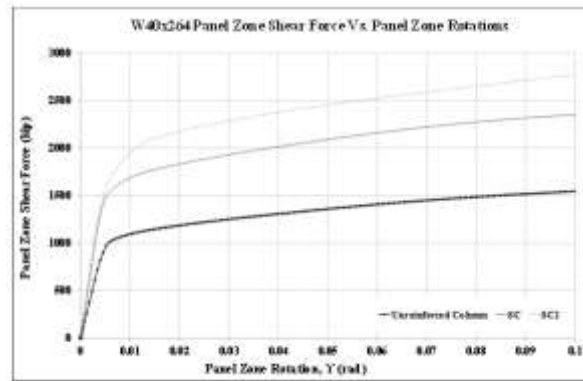


Figure 5.172: PZ shear force vs PZ rotation between Case 8C and 8C1

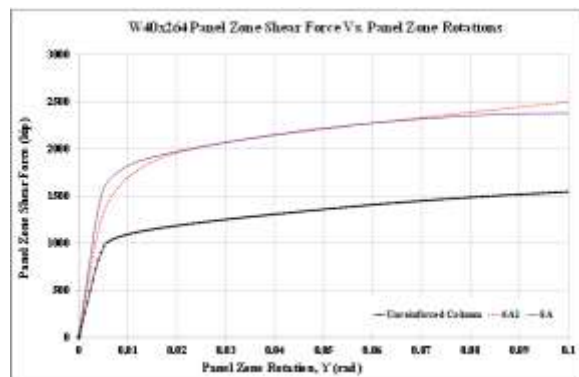


Figure 5.173: PZ and PZ shear force vs PZ rotation between 6A1 and 8A

When looking at the performance of case series 6, 8 and 9 for the deep column specimen no insightful observations were seen besides the obvious improvement that the use of a weld at the top of the DP provided, Figures 5.169 – 5.72. Case series 6 was used to determine how the performance of the PZ would vary when no CPs were used. A small increase in performance can be seen relative to the amount of force required for a PZ rotation of 0.1 radians when welds are used at the top and bottom of the DP. Table 5.19 shows that the use of a fillet weld at the top of the DP increased the vertical forces transferred by more than 100 kips. This did not improve the performance of the PZ drastically. As mentioned above the large DP used in the deep W40x264 buckles when no welds are used all the way around. Figure 5.174 illustrates the shear stress in the DPs of specimens with and without welds at the top. It can be seen that the entire area of the DPs that were welded all the way around is effectively being used to resist the PZ shear. Whereas the ones without a weld at the top used about a third of the DP and once the 0.1 PZ rotation was reached the area resisting shear had substantially decreased due to buckling of the DP.

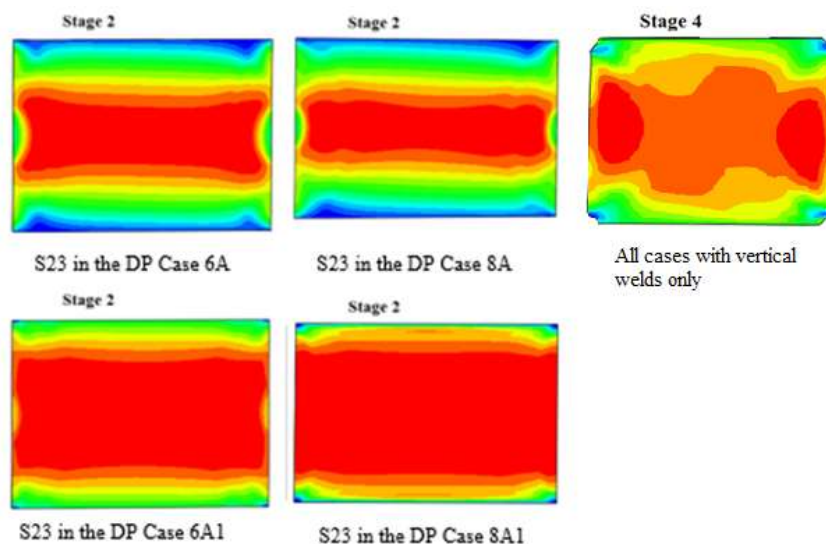


Figure 5.174 Difference in shear stresses in DPs with horizontal welds and without

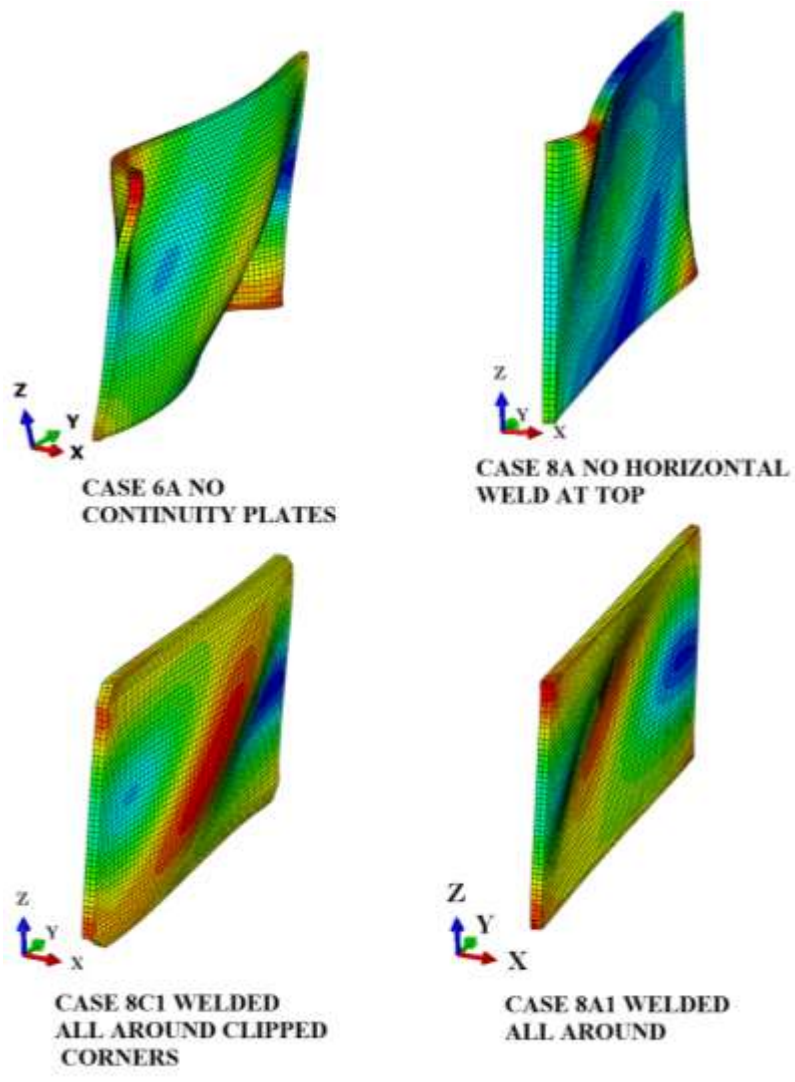


Figure 5.175: Buckling of DPs at 0.1 radians (scaled 3 times)

Figure 5.173 which compares the performance of a DP that was welded all the way around to that of one that used vertical welds alone but CPs, shows that the use of continuity plates does not improve the performance of the DP when resisting PZ rotation.

Case series 7 which used a doubler plate that was extended all the way to the same height of the loading plates and had the continuity plates welded onto them were the specimens that showed the greatest PZ strength. Cases 7A1 and 7C1, required 2,953 and 2876 kips of PZ shear respectively, to reach a rotation of 0.1 radians. The benefits of this arrangement were also seen in the “shallow” column discussed in Chapter 4. The increase in stiffness is likely due to the same reasons that an extended DP substantially increases performance in a deep column. One key observation that mirrors that of Donkada (2012) is the decrease in force requirement from horizontal welds as the DP extends away from the PZ. The benefit of an extension of ½ inch above the center of the loading plate is shown in Figure 5.176. Cases 7 required an average of 20% more force to rotate 0.1 radians than cases 6A1 and 6C1 which were welded all around, even though the welds at the top of the plated transferred less force.

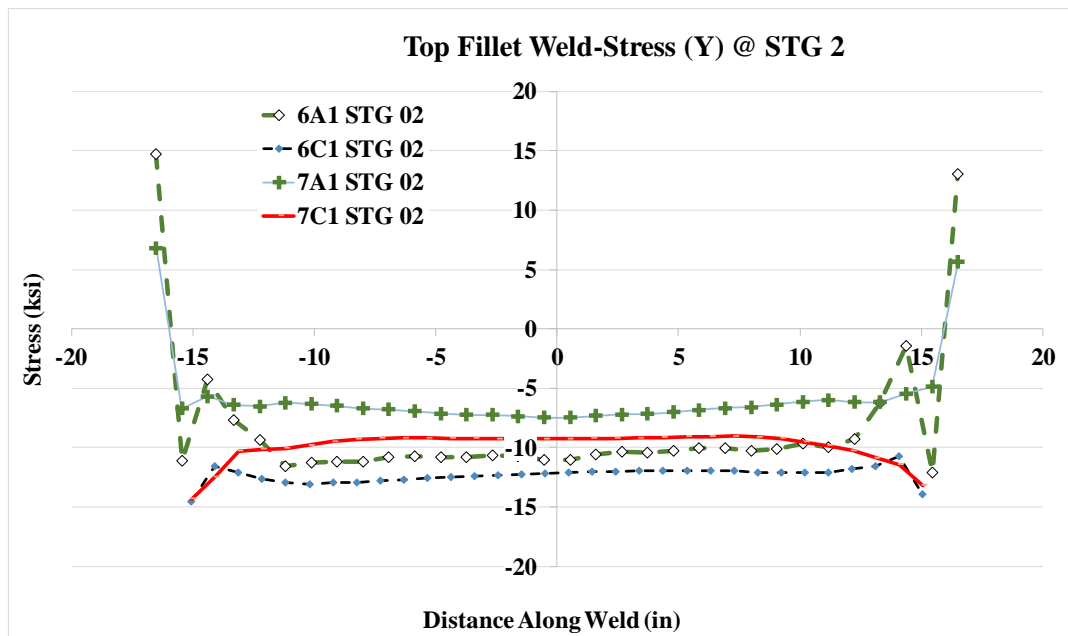


Figure 5.176: Weld stresses on case series 6 and 7

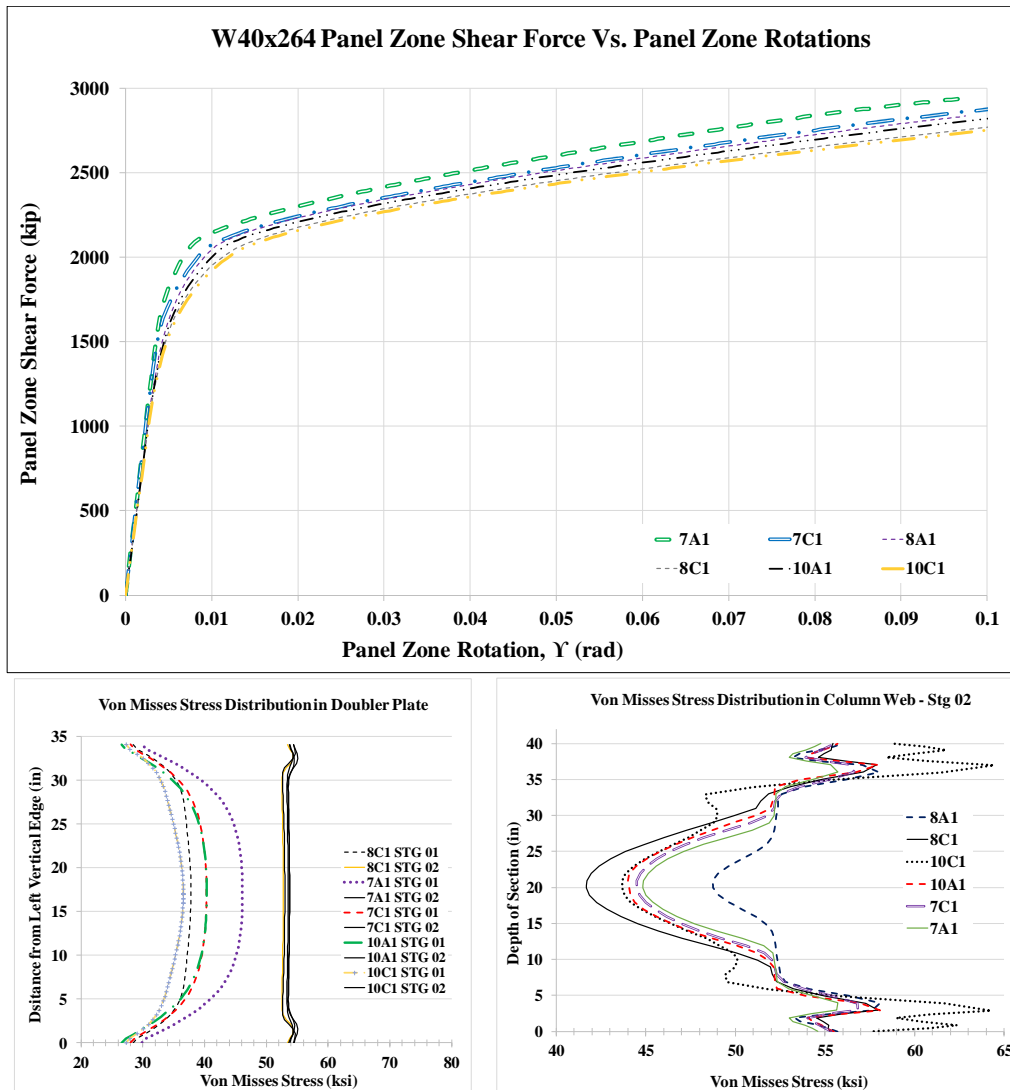


Figure 5.177: Stress distributions for cases with highest PZ strength

With the exception to case series 7 which seems to benefit from a slight extension of the DP, the other two case series which showed the highest PZ strength were case series 8 (with horizontal welds) and 10. Figure 5.177 illustrates the observation that as long as a weld is provided at the top of the doubler plate the DP will effectively increase the PZ shear force. When looking at the VMS stress levels in the DP in cases 8 (with horizontal welds) and 10, the values are the same by stg. 02 of the loading which is PZ rotation of .02 radians.

Even though the weld modeled in case 10 was a groove weld and in case 8 a fillet weld, Figure 5.178 shows that the force transferred parallel to the weld at the top is almost the same. In cases 8A1, 8C1, 10A1 and 10C1 the weld at the top transferred 59%, 69%, 66% and 70% of the shear force at mid-height of the DP.

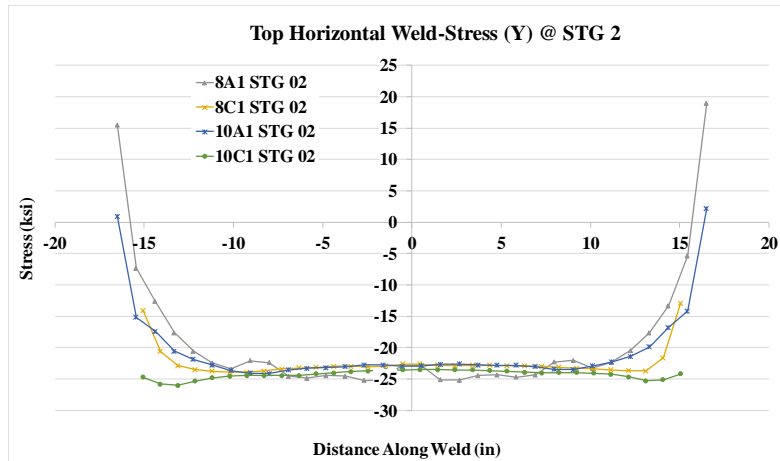


Figure 5.178: Stress on horizontal weld segments due to horizontal forces

Case 9A and 9C were determined to provide no benefits to the strength of the PZ. The DP height was decreased to accommodate a 1 inch gap between the DP and the CPs. This case resulted in high stress concentrations and plastic strains column web area were the gap was. Clearly the reduction of area of the DP, results in lower performance in both “shallow” and “deep” column specimens.

### 5.3.2 Forces in the Welds

The total forces applied by both vertical and horizontal welds were divided by the DP shear strength and presented in Tables 4.25 and 4.26. The average segment weld forces were also reported for the two outer most segments of weld on tables 5.20 and 5.21. Unlike the

W14x398 column the outer segments of the vertical welds in the W40x264 column did not show a substantial decrease in force in the Y direction when a weld was used at the top of the doubler plate. Figure 5.179 illustrates the how the horizontal load being applied by a vertical weld in cases without a weld at the top and bottom of the DP is more linear than that of the smaller column. This could be due to the use of the larger vertical weld used for the inch thick doubler plate.

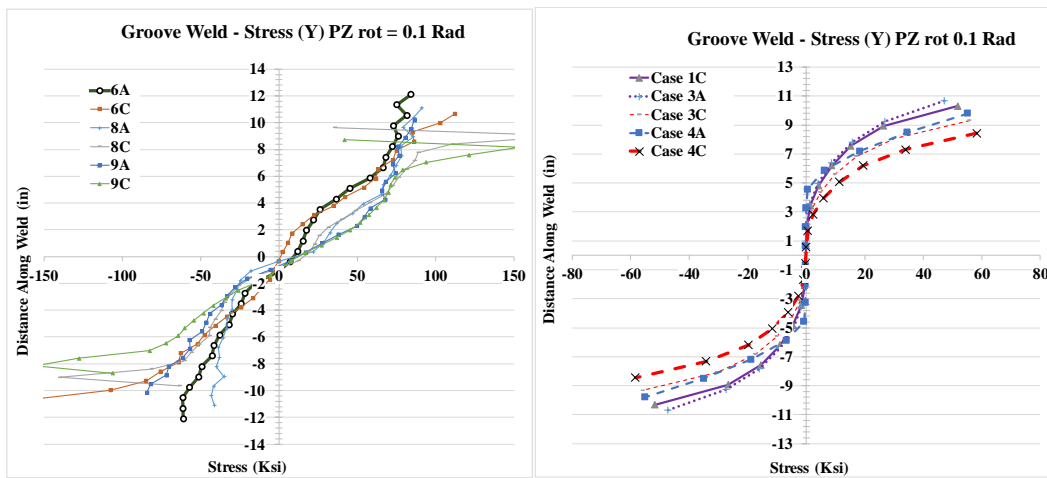
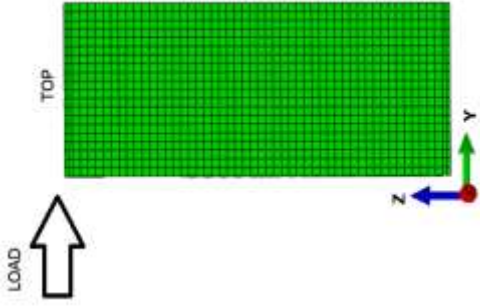


Figure 5.179: Vertical weld transfer of forces for “deep” (Left) and “shallow” (Right) columns

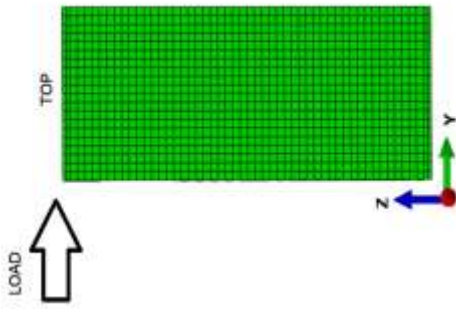
The forces transferred onto the DP by either weld were similar in all the cases modeled with the exception of the case where the DP was extended 1/2 inch beyond the center of the loading plate. A substantial reduction of force in the outer segments of the vertical weld was not seen in the cases when a horizontal weld was used in conjunction, which was an obvious observation in the W14x398. The use of a horizontal weld allowed an increase in vertical load that the vertical weld applied to DP which resulted in a stronger PZ. This also kept the DP from buckling.



Sum of Load Transferred by all Horizontal Weld Segments												
Case	Stage 01			Stage 02			Stage 03			Stage 04		
	X	Y	Z	X	Y	Z	X	Y	Z	X	Y	Z
6												
6A												
6A1	-3.3	-173	1.0	-5.7	-285	12.3	-5.8	-283	11.5	-5.9	-343	91.2
6C												
6C1	-4.5	-233	1.3	-11.5	-384	14.0	-8.8	-356	10.2	-22.8	-481	144.0
7A1	-10.9	-121	0.5	-21.2	-199	7.3	-24.8	-207	12.0	-27.7	-261	135.8
7C1	-17.2	-165	-0.6	-25.4	-307	6.1	-27.9	-315	8.5	-24.8	-390	114.6
8A												
8A1	-13.3	-504	0.7	-23.7	-643	6.3	-22.6	-664	11.1	-57.0	-857	128.0
8C												
8C1	-12.0	-457	0.6	-21.2	-698	-2.8	-21.5	-734	-3.1	-35.9	-921	36.3
9A												
9C												
10A1	-1.7	-481	0.3	-2.9	-694	5.4	-2.7	-706	7.6	-6.1	-898	93.4
10C1	-4.9	-481	-0.1	-8.9	-755	-0.8	-9.3	-776	0.9	-28.0	-969	66.9

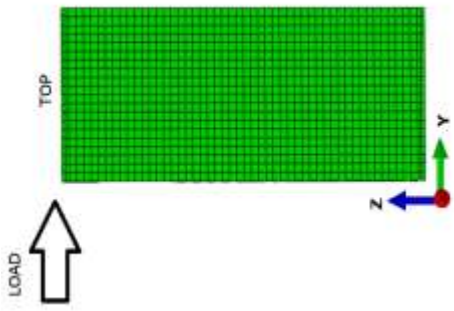
Table 5.18: Total force transferred to DP by top horizontal weld





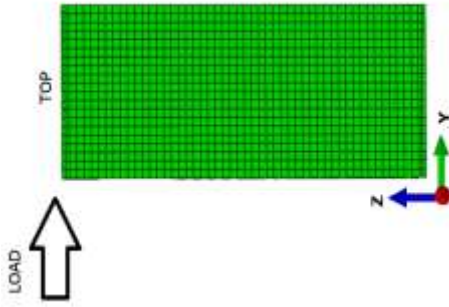
Sum of Load Transferred by all Vertical Weld Segments												
Case	Stage 01			Stage 02			Stage 03			Stage 04		
	X	Y	Z	X	Y	Z	X	Y	Z	X	Y	Z
6												
6A	-4.3	1.0	319	-8.5	5.3	483	-6.7	6.0	491	0.5	196	522
6A1	-11.6	1.0	426	-19.3	3.5	562	-19.8	3.3	560	-36.8	24	703
6C	-6.5	2.4	252	-7.4	11.8	389	-7.4	12.6	394	-5.5	38	514
6C1	-5.6	1.9	377	-12.6	15.1	517	-13.4	11.6	512	-25.0	52	628
7A1	-8.4	1.3	523	-23.4	6.0	635	-24.9	8.4	660	-33.0	42	865
7C1	-6.3	2.1	453	-14.1	13.0	612	-14.9	15.3	626	-19.9	78	815
8A	-6.9	15.1	455	-8.9	40.5	490	-9.4	51.2	494	-5.0	349	443
8A1	-17.0	4.4	569	-29.9	13.6	655	-26.6	18.5	681	-28.3	94	873
8C	-9.3	15.5	350	-9.9	31.0	389	-10.5	38.2	402	-10.6	210	433
8C1	-7.5	2.2	417	-11.0	11.2	574	-12.5	14.1	592	-14.5	80	771
9A	-6.5	3.2	242	-7.8	13.8	377	-7.7	14.7	380	-11.2	169	435
9C	-16.6	4.0	179	-17.6	14.3	290	-16.8	17.7	300	-12.0	104	390
10A1	-2.2	2.0	432	-18.4	13.3	595	-18.7	15.1	604	-12.7	81	781
10C1	-3.9	1.8	373	-9.6	12.6	545	-9.3	14.7	558	-15.8	71	730

Table 5.19: Total force transferred to DP by vertical weld



Average Force Transferred by Each of the 2 Outermost Horizontal Weld Segments (kip)													
Case	Segment Length (in)	Stage 01			Stage 02			Stage 03			Stage 04		
		X	Y	Z	X	Y	Z	X	Y	Z	X	Y	Z
6													
6A													
6A1	1 1/16	-1.6	0.9	1.0	-0.7	1.9	7.3	-0.6	1.6	7.7	-2.1	7.5	6.9
6C													
6C1	1	-1.6	-9.8	-1.0	-2.4	-12.7	6.8	-2.3	-11.6	4.3	-2.7	-15.8	8.2
7A1	1 1/16	-2.5	-0.1	2.3	1.3	0.0	7.0	2.7	0.0	6.4	-1.6	-0.1	4.8
7C1	1	-5.0	-9.1	1.6	-3.5	-13.0	9.3	-3.0	-13.5	9.2	-3.8	-17.1	12.7
8A													
8A1	1 1/16	-8.6	-2.2	0.2	-11.5	4.4	0.9	-10.5	4.5	0.1	-11.2	-6.3	1.3
8C													
8C1	1	-3.4	-16.4	-2.3	-6.1	-16.8	0.8	-6.0	-16.0	0.8	-2.9	-23.1	-6.2
9A													
9C													
10A1	1 1/16	-0.7	-13.9	-2.7	-0.1	-7.6	4.8	-0.1	-7.0	4.7	1.0	-18.4	4.1
10C1	1	0.0	-20.7	0.4	-1.3	-24.5	6.7	-1.4	-24.7	7.1	0.4	-32.7	8.1

Table 5.20: Average force transferred by two outermost horizontal weld segments



		Average Force Transferred by Each of the 2 Outermost Vertical Weld Segments (kip)															
Case	Segment Length (in)	Stage 01			Stage 02			Stage 03			Stage 04						
		X	Y	Z	X	Y	Z	X	Y	Z	X	Y	Z				
6																	
6A	13/16	-0.1	-46.2	6.9	0.5	-58.7	7.8	0.6	-60.1	7.4	-1.1	-47.8	5.7				
6A1	13/16	0.2	-48.2	6.6	-0.3	-62.9	2.7	-0.2	-62.3	3.0	-3.0	-89.3	1.9				
6C	11/16	0.6	-47.9	2.5	1.2	-59.3	6.6	1.3	-60.1	6.8	2.3	-91.4	22.5				
6C1	11/16	2.1	-43.6	8.5	2.9	-57.7	11.4	2.8	-54.9	10.4	4.7	-85.2	21.2				
7A1	13/16	0.6	-45.1	8.8	-1.3	-57.0	0.6	-1.3	-60.0	0.1	-1.8	-83.7	3.1				
7C1	11/16	0.5	-34.9	13.4	1.2	-50.5	11.6	1.4	-52.6	11.6	2.5	-65.8	30.6				
8A	11/16	1.4	-59.2	15.6	2.1	-65.0	20.8	2.2	-65.2	21.8	-1.1	-30.2	18.6				
8A1	11/16	3.9	-45.0	14.0	3.8	-57.5	12.9	4.1	-59.7	14.0	2.5	-72.2	37.9				
8C	10/16	1.8	-55.9	-1.2	2.8	-64.9	-1.2	3.1	-68.4	-1.1	-0.7	-63.2	18.8				
8C1	10/16	0.0	-29.7	12.1	2.1	-38.1	9.7	2.2	-41.0	8.6	1.1	-46.9	15.3				
9A	11/16	0.4	-39.8	8.3	1.3	-50.9	10.7	1.3	-51.7	10.8	1.8	-54.6	23.5				
9C	9/16	1.0	-38.8	-0.3	2.0	-49.3	-7.5	2.2	-51.6	-8.5	3.5	-73.5	-7.6				
10A1	11/16	1.6	-24.7	16.4	0.4	-41.8	10.6	0.5	-43.0	10.5	3.5	-44.9	25.4				
10C1	9/16	1.3	-19.6	12.0	2.1	-31.2	3.3	2.2	-32.5	2.2	3.1	-33.2	3.7				

Table 5.21: Average force transferred by two outermost vertical weld segments

In order to understand the forces that the welds attaching the DP to the column must provide the total force transferred by the welds in each case was divided by the shear strength of the DP. Although key observations were seen for case series 6, this arrangement is impractical since no CPs were used. Case 7 also shows low force requirements on 30% to 40% of DP strength, Table 5.22. This however is believed to be due to the length of the DP and the fact that the fillet weld at the top of the DP sits at a height of about 1 inch above the center of the loading plate. Case series 8 and 10 show that for the top weld 80% to 100% of the DP shear strength is required at PZ rotation levels of 0.1 radians. This observation was also seen in the “shallow” column cases.

$$S_v = .6F_y t_{dp} l_{dpv} = .6 * 50ksi * 1inch * 24 inch = 720 kip$$

$$S_h = .6F_y t_{dp} l_{dph} = .6 * 50ksi * 1inch * 34 inch = 1020 kip$$

Case	Horizontal Weld Force in Y direction/DP shear strength, $S_h$			
	Stage 01	Stage 02	Stage 03	Stage 04
	Y	Y	Y	Y
6				
6A				
6A1	0.2	0.3	0.3	0.3
6C				
6C1	0.2	0.4	0.3	0.5
7A1	0.1	0.2	0.2	0.3
7C1	0.2	0.3	0.3	0.4
8A				
8A1	0.5	0.6	0.7	0.8
8C				
8C1	0.4	0.7	0.7	0.9
9A				
9C				
10A1	0.5	0.7	0.7	0.9
10C1	0.5	0.7	0.8	1.0

Table 5.22: Relation between the horizontal force in the horizontal weld and shear strength of DP

A similar comparison was conducted in the vertical weld for all cases including the ones not using a horizontal weld. It can be seen that when the DP is welded onto the column using both horizontal and vertical welds, the vertical load being applied by the vertical weld increases substantially. The values reported on tables 5.22 and 5.23 might seem to indicate that the welds used to attach a DP should be designed for the full shear strength of the DP. This assumes that the DP sized properly and that the thickness is enough to keep it from buckling. An appropriate recommendation and one that case 10 seems to verify is the use of a groove weld for both vertical and horizontal edges of a DP.

Case	Vertical Weld Force in Z direction/DP shear strength, $S_v$			
	Stage 01	Stage 02	Stage 03	Stage 04
	Z	Z	Z	Z
<b>6</b>				
<b>6A</b>	0.4	0.7	0.7	0.7
<b>6A1</b>	0.6	0.8	0.8	1.0
<b>6C</b>	0.4	0.5	0.5	0.7
<b>6C1</b>	0.5	0.7	0.7	0.9
<b>7A1</b>	0.7	0.9	0.9	1.2
<b>7C1</b>	0.6	0.8	0.9	1.1
<b>8A</b>	0.6	0.7	0.7	0.6
<b>8A1</b>	0.8	0.9	0.9	1.2
<b>8C</b>	0.5	0.5	0.6	0.6
<b>8C1</b>	0.6	0.8	0.8	1.1
<b>9A</b>	0.3	0.5	0.5	0.6
<b>9C</b>	0.2	0.4	0.4	0.5
<b>10A1</b>	0.6	0.8	0.8	1.1
<b>10C1</b>	0.5	0.8	0.8	1.0

Table 5.23: Relation between the vertical force in the vertical weld and shear strength of DP

### 5.3.3 Summary

Key observations from this chapter can be summarized as follows:

- The “deep” column specimen had a higher propensity to have buckling issues. It is due to this that continuity plates assisted in the increase of PZ strength. By keeping the flanges and web from buckling the shear force was effectively transferred to the DP by the welds.
- The use of a weld at the top and bottom of the DP increased the strength of the PZ substantially. This was due to two separate reasons. One of them was that it kept the DP from buckling at PZ rotations lower than 0.1 radians. Figure 5.175 shows some of these buckling issues for the various models which did not use a weld at the top of the flange. It should also be mentioned that this issue increased the complexity of the modeling substantially.
- Except for case series 7 the weld at the top and bottom of the DP transferred between 60 to 70 % of the shear force reported at mid-height of the DP at a PZ rotation of 0.1 radians. This reduced the demand on the vertical weld and as a result the vertical weld was able to transfer more vertical load to the DP. Poisson’s effect might help explain this observation.
- Besides case series 7 no particular arrangement was clearly observed to be the best performance wise. Some of the plots presented, might indicate that as long as welds are provided and DP is thick enough the performance of the different arrangements would be similar. This could be due to the length of the welds being used. The horizontal welds at the top and bottom of the DPs in the “deep” column were more than 3 times the length of those in the “shallow” column.

- Because the intent of the thesis was to understand the behavior of “fitted” DPs case series 7 bordered the definition of such. The top of the DP was at the same level as that of the top of the loading plate. The benefits from this arrangement were substantial and the force requirements of the fillet weld at the top of the DP were lower. Unlike the comparison of an extended DP in the “shallow” column, the PZ shear strength reported in Case 5 from Donkada (2012) was the highest.

## CHAPTER 6

### Summary and Conclusions

#### 6.1 SUMMARY

One of the methods used to resist seismic loads in steel structures is the use of special moment frames. These systems are exposed to large lateral forces resulting from seismic events. In cases when the column cannot provide adequate shear strength to resist the high levels of shear in the panel zone, a doubler plate is used to increase strength by increasing the area of the PZ. This thesis focused in the case where a “fitted” doubler plate is used to increase the PZ strength. The program Abaqus was used to analyze two simplified models of a W14x398 shallow column and a W40x264 deep column. The objectives of the analyses were as follows:

- 1) Gain a better understanding of the performance of different attachment details for fitted DPs.
- 2) Study the effects that clipped corners on fitted doubler plates have in the PZ and the welds attaching it and gain a perspective of the force flow through the panel zone.
- 3) Report the forces and stresses that both horizontal and vertical welds transfer to the fitted DP and determine if both welds are necessary. Obtain a range of forces for which the welds attaching the plates should be designed for.



## 6.2 CONCLUSIONS

The following conclusions were drawn from the results of this study:

- The use of “fitted” DPs in the “shallow” column does not appear to affect the overall load-deformation response of the panel zone compared to the case where the doubler plate is extended 6-inches above and below the panel zone. Extended doubler plates were investigated by Donkada (2012). This study on fitted doubler plates showed essentially the same panel zone load-deformation response as that reported by Donkada.
- The use of the clipped corners did not result in performance deficits for either the “shallow” or “deep” column specimens. A slight increase in force levels in the welds within the first 2 inches away from the loading plates was noticed in the W14x398 column.
- In the W14x398 “shallow” column, the outermost segments of the welds transfer much higher forces than those near the center of the weld. This was evident in all variations of the “fitted” DP especially in the vertical weld when no weld was used to attach the top and bottom of the DP. The use of a weld at the top of a “fitted” DP seems to alleviate the demand on the vertical groove weld reducing these stresses substantially.
- The reduction in load that the use of a horizontal weld provides to a vertical weld results in an increase of the force applied to the DP in the direction parallel to the

weld. This results in higher PZ strengths on both “shallow” and “deep” column cases

- Because a the DP in a deep column has higher propensity to buckle when no horizontal weld is used to attach the DP, the use of horizontal welds at the top and bottom of the fitted DP are recommended
- Tables 4.25, 4.26, 5.22, and 5.23 which show the relation between the forces transferred by the welds and the shear strength of the DP would seem to indicate that the top weld in a “fitted” DP should be designed to provide more than 80% of the shear strength of the DP. This does not mean that a weld designed for lower strength will necessarily fail but that if properly sized, the performance of a “fitted” DP would likely improve with an increase in strength capacity in the welds used. Based on this, the use of groove welds to attach all sides of a “fitted” DP is recommended.

### **6.3 FUTURE WORK**

This work used simplifications in order to reduce computing expense, an example of this is the use of loading plates to represent the beam flanges. Monotonic and cyclic loading was utilized in this and the previous work by Shirsat, Donkada, and Gupta. Some recommendations for furthering the understanding of the panel zone region of special moment frames and the attachments that reinforce it include:

- The results from the series of thesis with extended and fitted DPs should be reworked in a detailed study using beams instead of loading plates, Figures 6.1 and 6.2. Because beams of different depths are often attached to in SMFs, a study of a model using these might be insightful.
- Shell elements are often used along with brick elements. A verification study that explores the results from this and the previous studies might reveal that using shells might speed up analysis while producing the same results.
- The stresses and plastic strains reported in this thesis might be reported more accurately if a local model of the welds alone with a dense mesh was used.
- Buckling of the DP greatly influenced the time spent analyzing the “deep” column modeled in this thesis. Additional work is needed to investigate the stability of doubler plates and validate E3-7 from *Provisions for Steel Structural Buildings* (AISC 2010).

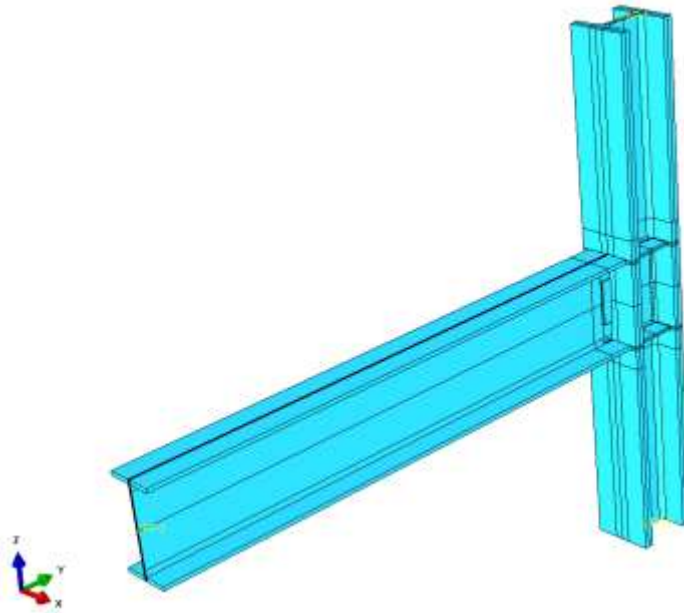


Figure 6.1: Abaqus PZ model with one beam attached

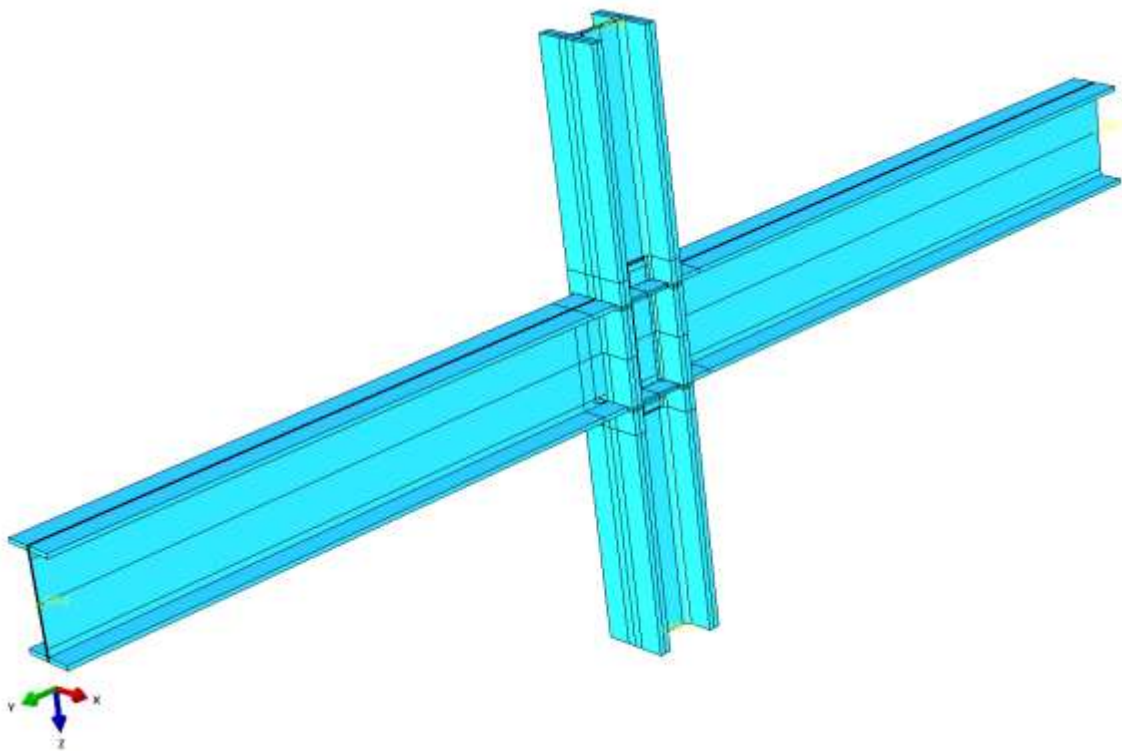


Figure 6.2: Abaqus PZ model with two beams attached

## Appendix A: Sample Abaqus Input File for W40x264 Column Case 8C1

```
**
** PARTS
**
*Part, name=CJP-CPFlange
*Element, type=C3D8R
** Section: Okazaki Trilinear Weld
*Solid Section, elset=_PickedSet12, material="Okazaki Trilinear Weld"
,
*End Part
**
*Part, name=CJP-CPWeb
*Element, type=C3D8R
** Section: Okazaki Trilinear Weld
*Solid Section, elset=_PickedSet12, material="Okazaki Trilinear Weld"
,
*End Part
**
*Part, name="Continuity Plate"
*Element, type=C3D8R
** Section: Okazaki Trilinear Steel
*Solid Section, elset=_PickedSet25, material="Okazaki Trilinear Steel"
,
*End Part
**
*Part, name=Doubler
*Element, type=C3D8R
** Section: Okazaki Trilinear Steel
*Solid Section, elset=_PickedSet3, material="Okazaki Trilinear Steel"
,
*End Part
**
*Part, name=Fillet
*Element, type=C3D8R
** Section: Okazaki Trilinear Weld
*Solid Section, elset=_PickedSet14, material="Okazaki Trilinear Weld"
,
*End Part
**
*Part, name="Groove Weld"
*Element, type=C3D8R
** Section: Okazaki Trilinear Weld
*Solid Section, elset=_PickedSet14, material="Okazaki Trilinear Weld"
,
```

```

*End Part
**
*Part, name="Loading Plate"
*Element, type=C3D8R
** Section: Elastic
*Solid Section, elset=_PickedSet6, material="Elastic Steel"
,
*End Part
**
*Part, name=W40X264
*Element, type=C3D8R
** Section: Okazaki Trilinear Steel
*Solid Section, elset=_PickedSet39, material="Okazaki Trilinear Steel"
,
*End Part
**
**
** ASSEMBLY
**
*Assembly, name=Assembly
**
*Instance, name=W40X264-1, part=W40X264
*End Instance
**
*Instance, name="Loading Plate-TL", part="Loading Plate"
*End Instance
**
*Instance, name="Loading Plate-TR", part="Loading Plate"
*End Instance
**
*Instance, name="Loading Plate-BR", part="Loading Plate"
*End Instance
**
*Instance, name="Loading Plate-BL", part="Loading Plate"
*End Instance
**
*Instance, name=Doubler-1, part=Doubler
*End Instance
**

```

```
*End Instance
**
*Instance, name="Groove Weld-2", part="Groove Weld"
*End Instance
**
*Instance, name=Fillet-1, part=Fillet
*End Instance
**
*Instance, name=Fillet-2, part=Fillet
*End Instance
**
*Instance, name=CJP-CPFlange-1, part=CJP-CPFlange
*End Instance
**
*Instance, name=CJP-CPWeb-1, part=CJP-CPWeb
*End Instance
**
*Instance, name="Continuity Plate-1", part="Continuity Plate"
*End Instance
**
*Instance, name=CJP-CPFlange-2, part=CJP-CPFlange
*End Instance
**
*Instance, name=CJP-CPFlange-3, part=CJP-CPFlange
*End Instance
**
*Instance, name=CJP-CPWeb-2, part=CJP-CPWeb
*End Instance
**
*Instance, name="Continuity Plate-2", part="Continuity Plate"
*End Instance
**
*Instance, name=CJP-CPFlange-4, part=CJP-CPFlange
*End Instance
**
*Instance, name=CJP-CPFlange-5, part=CJP-CPFlange
*End Instance
**
*Instance, name=CJP-CPWeb-3, part=CJP-CPWeb
*End Instance
**
```

```

*Instance, name=CJP-CPFlange-6, part=CJP-CPFlange
*End Instance
**
*Instance, name=CJP-CPFlange-7, part=CJP-CPFlange
*End Instance
**
*Instance, name=CJP-CPWeb-4, part=CJP-CPWeb
*End Instance
**
*Instance, name="Continuity Plate-4", part="Continuity Plate"
*End Instance
**
*Instance, name=CJP-CPFlange-8, part=CJP-CPFlange
*End Instance
**
*Nset, nset=BLDisp, instance=W40X264-1
*Nset, nset=BRDisp, instance=W40X264-1
*Nset, nset=RollerReact
*Nset, nset=TLDisp, instance=W40X264-1
*Nset, nset=TRDisp, instance=W40X264-1
*Nset, nset=TieReact
*Surface, type=ELEMENT, name=ColBott
*Surface, type=ELEMENT, name=ColMid
*Surface, type=ELEMENT, name=ColTop
*Surface, type=ELEMENT, name=DBL1
*Surface, type=ELEMENT, name=DBL2
*Surface, type=ELEMENT, name=DBL3
*Surface, type=ELEMENT, name=DBL4
*Surface, type=ELEMENT, name=DBL5
*Surface, type=ELEMENT, name=DBL6
*Surface, type=ELEMENT, name=DBL7
*Surface, type=ELEMENT, name=DBL8
*Surface, type=ELEMENT, name=FL1
*Surface, type=ELEMENT, name=FL2
*Surface, type=ELEMENT, name=FL3
*Surface, type=ELEMENT, name=FL4
*Surface, type=ELEMENT, name=FL5
*Surface, type=ELEMENT, name=FL6
*Surface, type=ELEMENT, name=FL7
*Surface, type=ELEMENT, name=FL8
*Surface, type=ELEMENT, name=FL9

```



\*Surface, type=ELEMENT, name=FL10  
\*Surface, type=ELEMENT, name=FL11  
\*Surface, type=ELEMENT, name=FL12  
\*Surface, type=ELEMENT, name=FL13  
\*Surface, type=ELEMENT, name=FL14  
\*Surface, type=ELEMENT, name=FL15  
\*Surface, type=ELEMENT, name=FL16  
\*Surface, type=ELEMENT, name=FL17  
\*Surface, type=ELEMENT, name=FL18  
\*Surface, type=ELEMENT, name=FL19  
\*Surface, type=ELEMENT, name=FL20  
\*Surface, type=ELEMENT, name=FL21  
\*Surface, type=ELEMENT, name=FL22  
\*Surface, type=ELEMENT, name=FL23  
\*Surface, type=ELEMENT, name=FL24  
\*Surface, type=ELEMENT, name=FL25  
\*Surface, type=ELEMENT, name=FL26  
\*Surface, type=ELEMENT, name=FL27  
\*Surface, type=ELEMENT, name=FL28  
\*Surface, type=ELEMENT, name=FL29  
\*Surface, type=ELEMENT, name=FL30  
\*Surface, type=ELEMENT, name=FL31  
\*Surface, type=ELEMENT, name=FL32  
\*Surface, type=ELEMENT, name=GR1  
\*Surface, type=ELEMENT, name=GR2  
\*Surface, type=ELEMENT, name=GR3  
\*Surface, type=ELEMENT, name=GR4  
\*Surface, type=ELEMENT, name=GR5  
\*Surface, type=ELEMENT, name=GR6  
\*Surface, type=ELEMENT, name=GR7  
\*Surface, type=ELEMENT, name=GR8  
\*Surface, type=ELEMENT, name=GR9  
\*Surface, type=ELEMENT, name=GR10  
\*Surface, type=ELEMENT, name=GR11  
\*Surface, type=ELEMENT, name=GR12  
\*Surface, type=ELEMENT, name=GR13  
\*Surface, type=ELEMENT, name=GR14  
\*Surface, type=ELEMENT, name=GR15  
\*Surface, type=ELEMENT, name=GR16

\*Surface, type=ELEMENT, name= GR11  
\*Surface, type=ELEMENT, name= GR12  
\*Surface, type=ELEMENT, name= GR13  
\*Surface, type=ELEMENT, name= GR14  
\*Surface, type=ELEMENT, name= GR15  
\*Surface, type=ELEMENT, name= GR16  
\*Surface, type=ELEMENT, name= GR17  
\*Surface, type=ELEMENT, name= GR18  
\*Surface, type=ELEMENT, name= GR19  
\*Surface, type=ELEMENT, name= GR20  
\*Surface, type=ELEMENT, name= GR21  
\*Surface, type=ELEMENT, name= GR22  
\*Surface, type=ELEMENT, name= GR23  
\*Surface, type=ELEMENT, name= GR24  
\*Surface, type=ELEMENT, name= GR25  
\*Surface, type=ELEMENT, name= GR26  
\*Surface, type=ELEMENT, name= GR27  
\*Surface, type=ELEMENT, name= GR28  
\*Surface, type=ELEMENT, name= GR29  
\*Surface, type=ELEMENT, name= GR30  
\*Surface, type=ELEMENT, name= GR31  
\*Surface, type=ELEMENT, name= GR32  
\*Surface, type=ELEMENT, name= Stiff01  
\*Surface, type=ELEMENT, name= Stiff02  
\*Surface, type=ELEMENT, name= Stiff03  
\*Surface, type=ELEMENT, name= Stiff04  
\*Surface, type=ELEMENT, name= Stiff05  
\*Surface, type=ELEMENT, name= Stiff06  
\*Surface, type=ELEMENT, name=\_PickedSurf18, internal  
\*Surface, type=ELEMENT, name=\_PickedSurf19, internal  
\*Surface, type=ELEMENT, name=\_PickedSurf20, internal  
\*Surface, type=ELEMENT, name=\_PickedSurf21, internal  
\*Surface, type=ELEMENT, name=\_PickedSurf22, internal  
\*Surface, type=ELEMENT, name=\_PickedSurf23, internal  
\*Surface, type=ELEMENT, name=\_PickedSurf24, internal  
\*Surface, type=ELEMENT, name=\_PickedSurf25, internal

---

```

** Constraint: BL Load
*Tie, name="BL Load", adjust=yes
_PickedSurf23, _PickedSurf22
** Constraint: BLP01
*Tie, name=BLP01, adjust=yes
_PickedSurf219, _PickedSurf218
** Constraint: BLP02
*Tie, name=BLP02, adjust=yes
_PickedSurf221, _PickedSurf220
** Constraint: BLP03
*Tie, name=BLP03, adjust=yes
_PickedSurf223, _PickedSurf222
** Constraint: BLP04
*Tie, name=BLP04, adjust=yes, type=NODE TO SURFACE
_PickedSurf225, _PickedSurf224
** Constraint: BLP05
*Tie, name=BLP05, adjust=yes, type=NODE TO SURFACE
_PickedSurf227, _PickedSurf226
** Constraint: BLP06
*Tie, name=BLP06, adjust=yes
_PickedSurf229, _PickedSurf480
** Constraint: BLP07
*Tie, name=BLP07, adjust=yes
_PickedSet282_CNS, _PickedSurf278
** Constraint: BLP08
*Tie, name=BLP08, adjust=yes
_PickedSet281_CNS, _PickedSurf280
** Constraint: BLP21
*Tie, name=BLP21, adjust=yes
_PickedSurf262, _PickedSurf261
** Constraint: BLP22
*Tie, name=BLP22, adjust=yes
_PickedSurf264, _PickedSurf263
** Constraint: BLP23
*Tie, name=BLP23, adjust=yes
_PickedSurf266, _PickedSurf265
** Constraint: BLP24
*Tie, name=BLP24, adjust=yes
_PickedSurf268, _PickedSurf267
** Constraint: BLP25
*Tie, name=BLP25, adjust=yes
_PickedSurf270, _PickedSurf269
** Constraint: BLP26
*Tie, name=BLP26, adjust=yes
_PickedSurf272, _PickedSurf271
** Constraint: BLP27

```

\_PickedSurf270, \_PickedSurf269  
 \*\* Constraint: BLP26  
 \*Tie, name=BLP26, adjust=yes  
 \_PickedSurf272, \_PickedSurf271  
 \*\* Constraint: BLP27  
 \*Tie, name=BLP27, adjust=yes  
 \_PickedSet284\_CNS, \_PickedSurf283  
 \*\* Constraint: BLP28  
 \*Tie, name=BLP28, adjust=yes  
 \_PickedSet291\_CNS, \_PickedSurf285  
 \*\* Constraint: BR Load  
 \*Tie, name="BR Load", adjust=yes  
 \_PickedSurf25, \_PickedSurf24  
 \*\* Constraint: Col01  
 \*Tie, name=Col01, adjust=yes, type=NODE TO SURFACE  
 \_PickedSurf438, \_PickedSurf471  
 \*\* Constraint: Col02  
 \*Tie, name=Col02, adjust=yes, type=NODE TO SURFACE  
 \_PickedSurf439, \_PickedSurf176  
 \*\* Constraint: Col03  
 \*Tie, name=Col03, adjust=yes, type=NODE TO SURFACE  
 \_PickedSurf440, \_PickedSurf472  
 \*\* Constraint: Col04  
 \*Tie, name=Col04, adjust=yes, type=NODE TO SURFACE  
 \_PickedSurf441, \_PickedSurf473  
 \*\* Constraint: DbIBott  
 \*Tie, name=DbIBott, adjust=yes  
 \_PickedSurf442, \_PickedSurf474  
 \*\* Constraint: DbILeft  
 \*Tie, name=DbILeft, adjust=yes  
 \_PickedSurf444, \_PickedSurf458  
 \*\* Constraint: DbIRight  
 \*Tie, name=DbIRight, adjust=yes  
 \_PickedSurf445, \_PickedSurf460  
 \*\* Constraint: DbITop  
 \*Tie, name=DbITop, adjust=yes  
 \_PickedSurf443, \_PickedSurf475  
 \*\* Constraint: Roller  
 \*Rigid Body, ref node=\_PickedSet6, tie nset=\_PickedSet7  
 \*\* Constraint: TL Load  
 \*Tie, name="TL Load", adjust=yes  
 \_PickedSurf19, \_PickedSurf18  
 \*\* Constraint: TLP01  
 \*Tie, name=TLP01, adjust=yes  
 \_PickedSurf191, \_PickedSurf190  
 \*\* Constraint: TLP02

---

\*Tie, name=TLP02, adjust=yes  
\_PickedSurf193, \_PickedSurf192  
\*\* Constraint: TLP03

\*Tie, name=TLP03, adjust=yes  
\_PickedSurf195, \_PickedSurf194  
\*\* Constraint: TLP04

\*Tie, name=TLP04, adjust=yes  
\_PickedSurf197, \_PickedSurf196  
\*\* Constraint: TLP05

\*Tie, name=TLP05, adjust=yes  
\_PickedSurf199, \_PickedSurf198  
\*\* Constraint: TLP06

\*Tie, name=TLP06, adjust=yes  
\_PickedSurf201, \_PickedSurf479  
\*\* Constraint: TLP07

\*Tie, name=TLP07, adjust=yes  
\_PickedSet203\_CNS\_, \_PickedSurf202  
\*\* Constraint: TLP08

\*Tie, name=TLP08, adjust=yes  
\_PickedSet205\_CNS\_, \_PickedSurf204  
\*\* Constraint: TLP21

\*Tie, name=TLP21, adjust=yes  
\_PickedSurf241, \_PickedSurf240  
\*\* Constraint: TLP22

\*Tie, name=TLP22, adjust=yes  
\_PickedSurf243, \_PickedSurf242  
\*\* Constraint: TLP23

\*Tie, name=TLP23, adjust=yes  
\_PickedSurf245, \_PickedSurf244  
\*\* Constraint: TLP24

\*Tie, name=TLP24, adjust=yes  
\_PickedSurf247, \_PickedSurf246  
\*\* Constraint: TLP25

\*Tie, name=TLP25, adjust=yes  
\_PickedSurf249, \_PickedSurf248  
\*\* Constraint: TLP26

\*Tie, name=TLP26, adjust=yes  
\_PickedSurf251, \_PickedSurf252  
\*\* Constraint: TLP27

\*Tie, name=TLP27, adjust=yes  
\_PickedSet288\_CNS\_, \_PickedSurf287  
\*\* Constraint: TLP28

\*Tie, name=TLP28, adjust=yes  
\_PickedSet292\_CNS\_, \_PickedSurf289  
\*\* Constraint: TR Load

\*Tie, name="TR Load", adjust=yes  
\_PickedSurf21, \_PickedSurf20

\*Tie, name="TR Load", adjust=yes  
\_PickedSurf21, \_PickedSurf20

\*\* Constraint: Tie

\*Rigid Body, ref node=\_PickedSet8, tie nset=\_PickedSet9

\*End Assembly

\*Amplitude, name=Amp-1

0,	0,	1,	0.045,	2,	0,	3,	-0.045
4,	0,	5,	0.045,	6,	0,	7,	-0.045
8,	0,	9,	0.045,	10,	0,	11,	-0.045
12,	0,	13,	0.045,	14,	0,	15,	-0.045
16,	0,	17,	0.045,	18,	0,	19,	-0.045
20,	0,	21,	0.045,	22,	0,	23,	-0.045
24,	0,	25,	0.06,	26,	0,	27,	-0.06
28,	0,	29,	0.06,	30,	0,	31,	-0.06
32,	0,	33,	0.06,	34,	0,	35,	-0.06
36,	0,	37,	0.06,	38,	0,	39,	-0.06
40,	0,	41,	0.06,	42,	0,	43,	-0.06
44,	0,	45,	0.06,	46,	0,	47,	-0.06
48,	0,	49,	0.09,	50,	0,	51,	-0.09
52,	0,	53,	0.09,	54,	0,	55,	-0.09
56,	0,	57,	0.09,	58,	0,	59,	-0.09
60,	0,	61,	0.09,	62,	0,	63,	-0.09
64,	0,	65,	0.09,	66,	0,	67,	-0.09
68,	0,	69,	0.09,	70,	0,	71,	-0.09
72,	0,	73,	0.12,	74,	0,	75,	-0.12
76,	0,	77,	0.12,	78,	0,	79,	-0.12
80,	0,	81,	0.12,	82,	0,	83,	-0.12
84,	0,	85,	0.12,	86,	0,	87,	-0.12
88,	0,	89,	0.18,	90,	0,	91,	-0.18
92,	0,	93,	0.18,	94,	0,	95,	-0.18
96,	0,	97,	0.24,	98,	0,	99,	-0.24
100,	0,	101,	0.24,	102,	0,	103,	-0.24
104,	0,	105,	0.36,	106,	0,	107,	-0.36
108,	0,	109,	0.36,	110,	0,	111,	-0.36
112,	0,	113,	0.48,	114,	0,	115,	-0.48

\*Amplitude, name=Amp-2

0,	0,	1,	0.025,	2,	0.05,	3,	0.075
4,	0.1,	5,	0.125,	6,	0.15,	7,	0.175
8,	0.2,	9,	0.225,	10,	0.25,	11,	0.275
12,	0.3,	13,	0.325,	14,	0.35,	15,	0.375
16,	0.4,	17,	0.425,	18,	0.45,	19,	0.475
20,	0.5,	21,	0.525,	22,	0.55,	23,	0.575
24,	0.6,	25,	0.625,	26,	0.65,	27,	0.675
28,	0.7,	29,	0.725,	30,	0.75,	31,	0.775
32,	0.8,	33,	0.825,	34,	0.85,	35,	0.875
36,	0.9,	37,	0.925,	38,	0.95,	39,	0.975
40,	1,	41,	1.025,	42,	1.05,	43,	1.075
44,	1.1,	45,	1.125,	46,	1.15,	47,	1.175
48,	1.2,	49,	1.225,	50,	1.25,	51,	1.275
52,	1.3,	53,	1.325,	54,	1.35,	55,	1.375
56,	1.4,	57,	1.425,	58,	1.45,	59,	1.475
60,	1.5						

```

**
** MATERIALS
**
*Material, name="Elastic Steel"
  *Elastic
  29000., 0.3
*Material, name="Okazaki Multi Steel"
  *Elastic
  29000., 0.3
  *Plastic, hardening= COMBINED, datatype= STABILIZED, number backstresses=6
  0.001, 0.
  17.8433, 0.00135927
  37.2603, 0.00410534
  55.2118, 0.0131522
  64.5, 0.0358959
  70.2, 0.07492
*Material, name="Okazaki Multi Weld"
  *Elastic
  29000., 0.3
  *Plastic, hardening= COMBINED, datatype= STABILIZED, number backstresses=6
  0.001, 0.
  19.7558, 0.000463528
  49.8417, 0.0036715
  71.54, 0.0154504
  76.23, 0.025441
  86.32, 0.0743642
*Material, name="Okazaki Trilinear Steel"
  *Elastic
  29000., 0.3
  *Plastic
  52.09, 0.
  69.94, 0.04808
  125.7, 0.43508
*Material, name="Okazaki Trilinear Weld"
  *Elastic
  29000., 0.3
  *Plastic
  65.15, 0.
  83.65, 0.04804
  145.91, 0.43467
**
** INTERACTION PROPERTIES
**
*Surface Interaction, name=IntProp-1
1,
  *Surface Behavior, pressure-overclosure= HARD
**

```

```

** BOUNDARY CONDITIONS
**
** Name: Roller Type: Displacement/Rotation

*Boundary
_PickedSet174, 1, 1
_PickedSet174, 2, 2
_PickedSet174, 5, 5
_PickedSet174, 6, 6

** Name: Tie Type: Displacement/Rotation

*Boundary
_PickedSet173, 1, 1
_PickedSet173, 2, 2
_PickedSet173, 3, 3
_PickedSet173, 5, 5
_PickedSet173, 6, 6

**
** INTERACTIONS
**
** Interaction: Int-1

*Contact Pair, interaction=IntProp-1, type=SURFACE TO SURFACE, adjust=0.0
_PickedSurf469, _PickedSurf171

-----
**
** STEP: Loading
**

*Step, name=Loading, nlgeom=YES, inc=70000

*Static
1e-08, 60., 1e-35, 0.1

**
** BOUNDARY CONDITIONS
**
** Name: BotDisp Type: Displacement/Rotation

*Boundary, amplitude=Amp-2
_PickedSet120, 1, 1
_PickedSet120, 2, 2, -3.

** Name: TopDisp Type: Displacement/Rotation

*Boundary, amplitude=Amp-2
_PickedSet118, 1, 1
_PickedSet118, 2, 2, 3.

**
** OUTPUT REQUESTS
**

*section print,name=DBL1, surface=DBL1
SOF

*section print,name=DBL2, surface=DBL2
SOF

*section print,name=DBL3, surface=DBL3
SOF

*section print,name=DBL4, surface=DBL4
SOF

*section print,name=DBL5, surface=DBL5
SOF

```



\*\* OUTPUT REQUESTS

\*\*

\*section print,name=DBL1, surface=DBL1  
SOF

\*section print,name=DBL2, surface=DBL2  
SOF

\*section print,name=DBL3, surface=DBL3  
SOF

\*section print,name=DBL4, surface=DBL4  
SOF

\*section print,name=DBL5, surface=DBL5  
SOF

\*section print,name=DBL6, surface=DBL6  
SOF

\*section print,name=DBL7, surface=DBL7  
SOF

\*section print,name=DBL8, surface=DBL8  
SOF

\*section print,name=FL1, surface=FL1  
SOF

\*section print,name=FL2, surface=FL2  
SOF

\*section print,name=FL3, surface=FL3  
SOF

\*section print,name=FL4, surface=FL4  
SOF

\*section print,name=FL5, surface=FL5  
SOF

\*section print,name=FL6, surface=FL6  
SOF

\*section print,name=FL7, surface=FL7  
SOF

\*section print,name=FL8, surface=FL8  
SOF

\*section print,name=FL9, surface=FL9  
SOF

\*section print,name=FL10, surface=FL10  
SOF

\*section print,name=FL11, surface=FL11  
SOF

\*section print,name=FL12, surface=FL12  
SOF

\*section print,name=FL13, surface=FL13  
SOF

\*section print,name=FL14, surface=FL14  
SOF

\*section print,name=FL15, surface=FL15  
SOF

\*section print,name=FL16, surface=FL16  
SOF

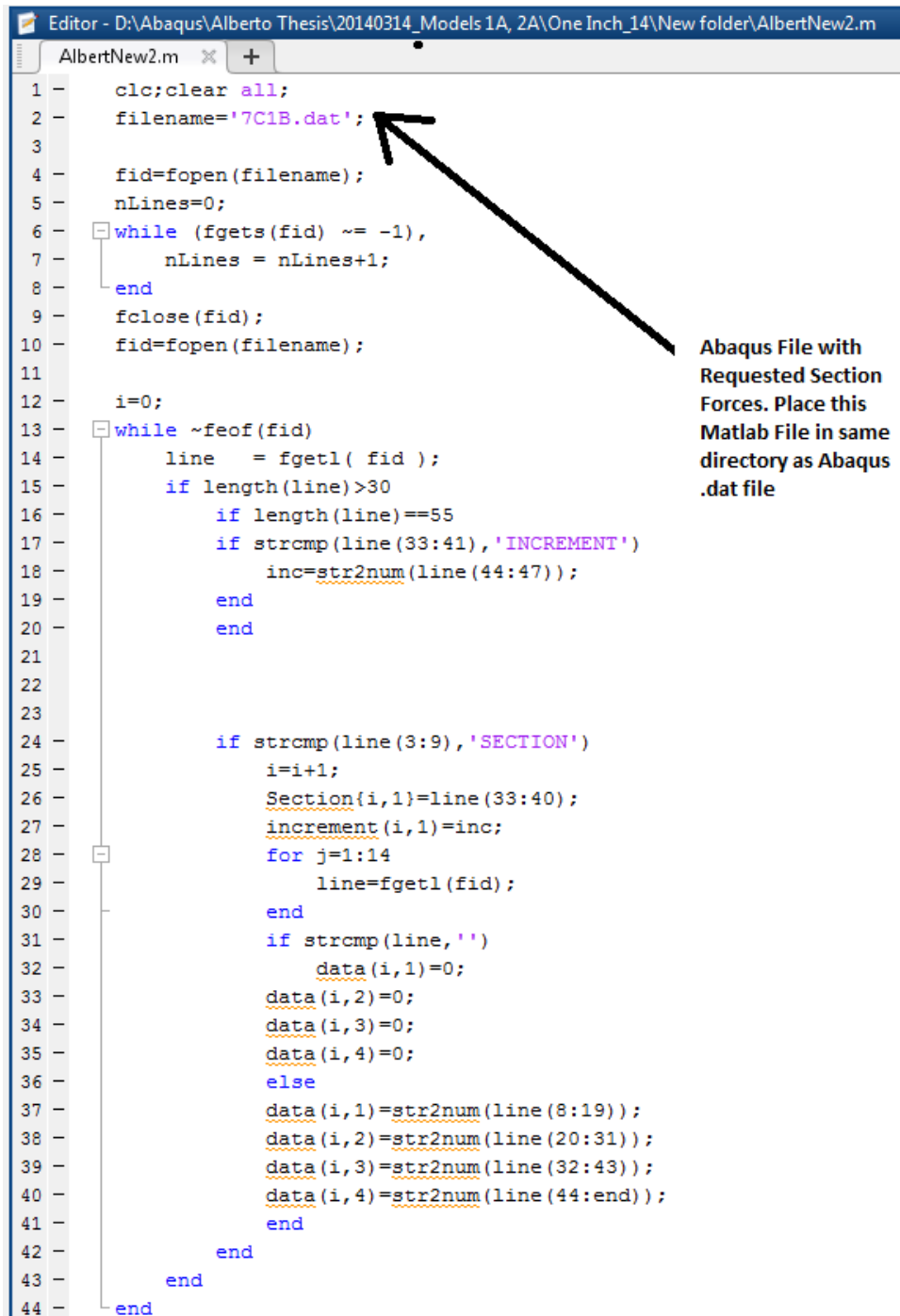
```

*section print,name=Stiff01,surface=Stiff01
SOF
*section print,name=Stiff02,surface=Stiff02
SOF
*section print,name=Stiff03,surface=Stiff03
SOF
*section print,name=Stiff04,surface=Stiff04
SOF
*section print,name=Stiff05,surface=Stiff05
SOF
*section print,name=Stiff06,surface=Stiff06
SOF
*Restart, write, frequency=0
**
** FIELD OUTPUT: F-Output-1
**
*Output, field, variable=PRESELECT
**
** HISTORY OUTPUT: BL
**
*Output, history
  *Node Output, nset=BLDisp
  U1, U2, U3
**
** HISTORY OUTPUT: BR
**
  *Node Output, nset=BRDisp
  U1, U2, U3
**
** HISTORY OUTPUT: Roller
**
  *Node Output, nset=RollerReact
  RF2,
**
** HISTORY OUTPUT: TL
**
  *Node Output, nset=TLDisp
  U1, U2, U3
**
** HISTORY OUTPUT: TR
**
  *Node Output, nset=TRDisp
  U1, U2, U3
**
** HISTORY OUTPUT: Tie
**
  *Node Output, nset=TieReact
  RF2,
*End Step

```

## Appendix B: Matlab Code for Parsing of Large Section Force Data File

```
Editor - D:\Abaqus\Alberto Thesis\20140314_Models 1A, 2A\One Inch_14\New folder\AlbertNew2.m
AlbertNew2.m x +
1 -   clc;clear all;
2 -   filename='7C1B.dat';
3 -
4 -   fid=fopen(filename);
5 -   nLines=0;
6 -   while (fgets(fid) ~= -1),
7 -       nLines = nLines+1;
8 -   end
9 -   fclose(fid);
10 -  fid=fopen(filename);
11 -
12 -  i=0;
13 -  while ~feof(fid)
14 -      line = fgetl( fid );
15 -      if length(line)>30
16 -          if length(line)==55
17 -              if strcmp(line(33:41),'INCREMENT')
18 -                  inc=str2num(line(44:47));
19 -              end
20 -          end
21 -
22 -
23 -
24 -          if strcmp(line(3:9),'SECTION')
25 -              i=i+1;
26 -              Section{i,1}=line(33:40);
27 -              increment(i,1)=inc;
28 -              for j=1:14
29 -                  line=fgetl(fid);
30 -              end
31 -              if strcmp(line,'')
32 -                  data(i,1)=0;
33 -                  data(i,2)=0;
34 -                  data(i,3)=0;
35 -                  data(i,4)=0;
36 -              else
37 -                  data(i,1)=str2num(line(8:19));
38 -                  data(i,2)=str2num(line(20:31));
39 -                  data(i,3)=str2num(line(32:43));
40 -                  data(i,4)=str2num(line(44:end));
41 -              end
42 -          end
43 -      end
44 -  end
```



Abaqus File with Requested Section Forces. Place this Matlab File in same directory as Abaqus .dat file

	Name	value	MIN	MAX
DATA	ans	0	0	0
	data	51759x4 double	-1440	1595
	fid	3	3	3
Abaqus Loading Increment	filename	'7C1B.dat'		
	i	51759	51759	51759
	inc	639	639	639
	increment	51759x1 double	1	639
Section	j	14	14	14
	line	' WALLCLOCK TI...		
	nLines	896665	896665	896665
	Section	51759x1 cell		

SOF 1, X axis    SOF 2, Y axis    SOF 3, Z axis

	1	2	3	4
1	6.0937e-06	-3.7184e-10	-6.0937e-06	8.1353e-12
2	4.0175e-07	-3.8259e-08	-3.5179e-07	1.9022e-07
3	6.3709e-06	-1.0494e-10	6.3709e-06	-1.4220e-11
4	4.0180e-07	3.8189e-08	-3.5188e-07	-1.9018e-07
5	6.2822e-07	1.3114e-08	-2.1832e-07	-5.8892e-07
6	2.2331e-06	-2.4649e-09	-7.4828e-07	2.1040e-06
7	7.8675e-06	-1.2919e-10	-7.8675e-06	7.7406e-10
8	6.0913e-06	-4.0756e-10	6.0913e-06	2.6268e-10
9	2.7991e-07	5.9369e-08	-2.7078e-07	3.8807e-08
10	2.6566e-07	7.2582e-09	-2.5586e-07	7.1116e-08
11	2.3309e-07	-1.3858e-09	-2.2983e-07	3.8803e-08
12	2.0916e-07	-1.8726e-09	-2.0736e-07	2.7360e-08
13	1.9153e-07	-1.5281e-09	-1.9073e-07	1.7474e-08
14	1.7896e-07	-7.2417e-10	-1.7849e-07	1.2925e-08
15	1.6953e-07	-2.9904e-10	-1.6929e-07	8.8881e-09
16	1.6266e-07	-1.0002e-10	-1.6253e-07	6.5553e-09
17	1.5732e-07	1.3387e-10	-1.5725e-07	4.5820e-09

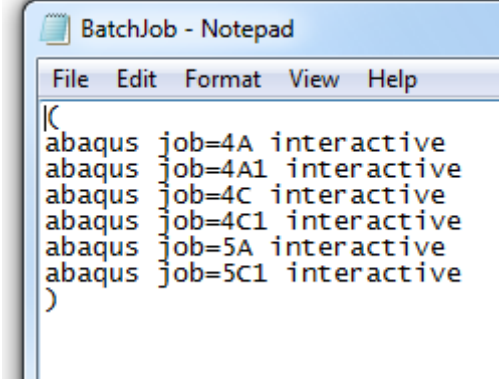
## Appendix C: Abaqus Batch Job Instructions

Instructions:

- 1) Write the following text file in notepad

And save as .bat file. Job= filename

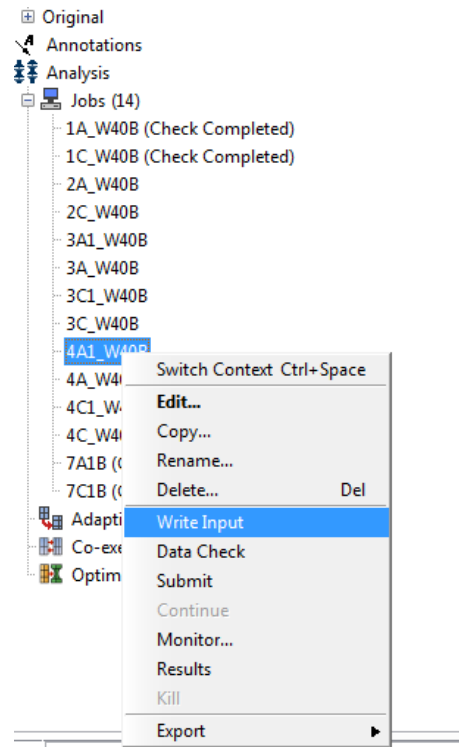
Save this file in the same directory as that which Abaqus saves input files for analysis.



```
(  
abaqus job=4A interactive  
abaqus job=4A1 interactive  
abaqus job=4C interactive  
abaqus job=4C1 interactive  
abaqus job=5A interactive  
abaqus job=5C1 interactive  
)
```

- 2) Write input file for all jobs you request and double click .odb notepad file. Abaqus CAE does not need to be open to run jobs, and job monitor will not show progress but DOS prompt will show start and stop of each analysis case.

- 3) Remove any other job files other than the .imp file otherwise DOS prompt will ask if they should be deleted and will not start analysis on its own.



## References

- Abaqus Analysis User's Manual*. (2014). Dassault Systèmes Simulia Corp., Providence, RI.
- Abaqus/CAE User's Manual*. (2014). Dassault Systèmes Simulia Corp., Providence, RI.
- AISC. (2010a). AISC/ANSI 360-10. *Specification for Structural Steel Buildings*. American Institute of Steel Construction, Inc., Chicago, IL.
- AISC. (2010b). AISC/ANSI 341-10. *Seismic Provisions for Structural Steel Buildings*. American Institute of Steel Construction, Inc., Chicago, IL.
- AISC. (2010c). AISC/ANSI 360-10. *Steel Construction Manual*, 14th ed. American Institute of Steel Construction, Inc., Chicago, IL.
- Becker, R. (1975). "Panel Zone Effect on the Strength and Stiffness of Steel Rigid Frames." *Engineering Journal*, **First Qtr.**, 19-29. American Institute of Steel Construction.
- Brown, S., Song, H. (1992). "Finite Element Simulation of Welding of Large Structures." *Journal of Engineering for Industry*, Vol. 114, 441-451, November. American Society of Mechanical Engineers.
- Cofie, N. G., Krawinkler, H. (1985). "Uniaxial Cyclic Stress-Strain Behavior of Structural Steel." *Journal of Engineering Mechanics*. American Society of Civil Engineers.
- Donkada, S. (2012). "Finite Element Analysis of Doubler Plate Attachment Details and Load Paths in Continuity Plates for Steel Moment Frames." M.S. thesis, The University of Texas at Austin, Austin, TX.
- El-Tawil, S. (2000). "Panel Zone Yielding in Steel Moment Connections." *Engineering Journal*, **Third Qtr.**, 120-131. American Institute of Steel Construction.
- El-Tawil, S., Vidarsonn, E., Mikesell, T., Kunnath, S. K. (1999). "Inelastic Behavior and Design of Steel Panel Zones." *Journal of Structural Engineering*, **Vol.** 125, 183-193, February. American Society of Civil Engineers.
- El-Tawil, S., Mikesell, T., Kunnath, S. K. (2000). "Effect of Local Details and Yield Ratio on Behavior of FR Steel Connections." *Journal of Structural Engineering*, **Vol.** 126, 79-87, January. American Society of Civil Engineers.
- Engelhardt, M. D., Venti, M. J., Fry, G. T., Holliday, S. D. (2000). *Behavior and Design of Radius Cut Reduced Beam Section Connections*. Rep. No. SAC/BD-00/17. SAC Joint Venture.

- Getting Started with Abaqus: Interactive Edition.* (2014). Dassault Systèmes Simulia Corp., Providence, RI.
- Kaufmann, E. J., Metrovich, B. R., Pense, A. W. (2001). *Characterization of Cyclic Inelastic Strain Behavior on Properties of A572 Gr. 50 and A913 Gr. 50 Rolled Sections. Final Rep. to American Institute of Steel Construction. ATLSS Report No. 01-13.* Lehigh University, Bethlehem, PA.
- Krawinkler, H. (1978). “Shear in Beam-Column Joints in Seismic Design of Steel Frames.” *Engineering Journal*, Third Qtr., 82-91. American Institute of Steel Construction.
- Mays, T. W. (2000). “Application of the Finite Element Method to the Seismic Design and Analysis of Large Moment End-Plate Connections”. Ph.D. diss., Virginia Polytechnic Institute and State University.
- Okazaki, T. (2004). “Seismic Performance of Link-to-Column Connections in Steel Eccentrically Braced Frames.” Ph.D. diss., The University of Texas at Austin.
- Popov, E. P. (1987). “Panel Zone Flexibility in Seismic Moment Joints.” *Journal of Constr. Steel Research*, 8, 91-118. Elsevier Applied Science Publishers Ltd, England.
- Ricles, J. M., Zhang, X., Lu, L. -W., Fisher, J. (2004). *Development of Seismic Guidelines for Deep-Column Steel Moment Connections. ATLSS Report No. 04-13.* Lehigh University, Bethlehem, PA.
- Ryu, H. -C. (2005). “Effect of Loading History on the Behavior of Links in Seismic-Resistant Eccentrically Braced Frames.” M.S. thesis, The University of Texas at Austin.
- Shirsat, P. S. (2011). “Preliminary Analysis of Doubler Plate Attachment Details for Steel Moment Resisting Frames.” M.S. thesis, The University of Texas at Austin, Austin, TX.
- Slutter, R. G. (1982). *Test of Panel Zone Behavior in Beam-Column-Connections. Report No. 200.81.403.1.* Fritz Engineering Laboratory. Lehigh University, Bethlehem, PA.